Stereotactic and Functional Neurosurgery

Principles and Applications

Nader Pouratian
Sameer A. Sheth
Editors

Springer

Stereotactic and Functional Neurosurgery

Nader Pouratian • Sameer A. Sheth
Editors

Stereotactic and Functional Neurosurgery

Principles and Applications

Springer

Editors
Nader Pouratian
Department of Neurosurgery
David Geffen School of Medicine at UCLA
Los Angeles, CA
USA

Sameer A. Sheth
Department of Neurosurgery
Baylor College of Medicine
Houston, TX
USA

ISBN 978-3-030-34905-9 ISBN 978-3-030-34906-6 (eBook)
https://doi.org/10.1007/978-3-030-34906-6

This Springer imprint is published by the registered company Springer Nature Switzerland AG
The registered company address is: Gewerbestrasse 11, 6330 Cham, Switzerland

To my family – Talia, Lylah, Noa, and Ari – who encourage and support my drive to understand patients, therapies, and the brain, one patient at a time. – Nader Pouratian

To my family, for always reminding me what is most important in life, and to my patients, for the privilege of being a part of theirs. – Sameer A. Sheth

Preface

Stereotactic and functional neurosurgery is one of the most quickly evolving fields within neurosurgery. The field developed more than half a century ago as a means of performing targeted ablations for a relatively limited set of conditions. Over the decades, the field has broadened to include treatments for a much wider array of disorders of brain function using an assortment of delivery techniques. Today, the field continues to grow extremely rapidly, accumulating an ever-increasing armamentarium of therapeutic modalities for an ever-expanding number of disorders. This expansion has been fueled by an infusion of basic science research, in terms of both the diseases we seek to treat and the mechanisms of the therapies that we employ. As our understanding of the mechanistic basis of neurologic and psychiatric disorders continues to improve, our ability to precisely and effectively target nodes in well-defined dysfunctional networks has accelerated in tandem, benefiting an even wider array of patients. These expanding opportunities, indications, and treatment options necessitate close collaboration and mutual understanding of diseases and techniques with other clinical specialties, including Neurology, Pain Medicine, Psychiatry, Physiatry, Rehabilitation Medicine, and others. Our field will continue to expand yet further as we gain an even greater appreciation of brain-body interactions once considered beyond the scope of neurosurgical intervention, such as with the cardiovascular or gastrointestinal systems.

This book is thus targeted at the wide audience of influencers of this field. This audience certainly includes the modern practitioner of stereotactic and functional neurosurgery, who must be able to fluidly traverse decades worth of surgical techniques, a dynamic research landscape, and a multitude of fields of expertise. The target audience also includes those who are interested in advancing the field from other clinical and basic science perspectives, including neurologists, psychiatrists, neuroscientists, physiologists, and engineers. Part I of the book focuses on Achieving Stereotactic Precision, reviewing the techniques and principles used to deliver therapies in a targeted and precise manner. Part II is devoted to Defining Trajectories and Targets, discussing the various techniques across brain mapping modalities to define appropriate brain targets and to plan optimal approaches. This step is crucial, as the field increasingly recognizes that target identification and engagement define our success. Part III, The Biophysics of Functional Neurosurgical Therapy, provides the most up-to-date summary of the therapeutic mechanisms of the techniques employed in our field, evaluating how our interventions

interact with neural tissue, from neurons to networks. This understanding is critical and is also the most quickly evolving aspect of the field. Part IV (Diseases and Targets) builds on the principles delivered in the prior parts, providing a deep dive into a detailed treatment of the most common disorders using the different techniques available in the field, to bring the reader up to speed on each in turn. The final part (Part V: The Future of Functional Neurosurgery) provides a glimpse of future areas of research and growth within this field.

Our aim with this book is to provide a thorough introduction to stereotactic and functional neurosurgery for the new practitioner while also providing a useful reference for the experienced practitioner seeking to expand into new avenues within the field. Equally important, we invite the multidisciplinary field of clinical and basic neurosciences to use this book to gain a better understanding of the principles and applications of stereotactic and functional neurosurgery to identify opportunities for even further advancement in this exciting and continually evolving field.

Los Angeles, CA, USA — Nader Pouratian
Houston, TX, USA — Sameer A. Sheth

Contents

Contributors

Nzhde Agazaryan, MS, PhD Department of Radiation Oncology, University of California, Los Angeles, Los Angeles, CA, USA

Ellen L. Air, MD, PhD, FAANS Functional Neurosurgery, Department of Neurosurgery, Henry Ford Health System, Detroit, MI, USA

Harith Akram, MBChB, PhD, FRCS Unit of Functional Neurosurgery, UCL Queen Square Institute of Neurology and the National Hospital for Neurology and Neurosurgery, London, UK

Ahmad Alhourani, MD Department of Neurological Surgery, University of Louisville, Louisville, KY, USA

Rushna Ali, MD Restorative and Functional Neurosurgery, Division of Neurosurgery, Spectrum Health Medical Group, Grand Rapids, MI, USA

William Stanley Anderson, MA, PhD, MD Department of Neurological Surgery, Johns Hopkins University, Baltimore, MD, USA

John P. Andrews, MD Department of Neurological Surgery, University of California, San Francisco, San Francisco, CA, USA

Wael F. Asaad, MD, PhD Neurosurgery, Neuroscience, and the Carney Institute for Brain Science, Brown University Alpert Medical School and the Norman Prince Neurosciences Institute of Rhode Island Hospital, Providence, RI, USA

Ausaf A. Bari, MD, PhD Department of Neurosurgery, David Geffen School of Medicine at UCLA, Los Angeles, CA, USA

Adriel Barrios-Anderson, BSc, BA Psychiatric Neurosurgery Program at Butler Hospital, Providence, RI, USA

Anita P. Bhansali, MD Department of Neurosurgery, Texas Health Harris Methodist Hospital Fort Worth, Fort Worth, TX, USA

Robert W. Bina, MD, MS Division of Neurosurgery, Banner University Medical Center, Tucson, AZ, USA

Daniel M. Blumberger, MD, MSc, FRCP(C) Temerty Centre for Therapeutic Brain Intervention, Centre for Addiction and Mental Health, Toronto, ON, Canada

Department of Psychiatry, Institute of Medical Science, University of Toronto, Toronto, ON, Canada

Andrea A. Brock, MD, MSCI Department of Neurosurgery, Clinical Neurosciences Center, University of Utah, Salt Lake City, UT, USA

Ankur Butala, MD Departments of Neurology, Psychiatry & Behavioral Sciences, Johns Hopkins University, Baltimore, MD, USA

Edward F. Chang, MD, PhD Department of Neurological Surgery, University of California, San Francisco, San Francisco, CA, USA

Witney Chen, BS Department of Neurological Surgery, University of California, San Francisco, San Francisco, CA, USA

Srinivas Chivukula, MD Department of Neurosurgery, David Geffen School of Medicine at UCLA, Los Angeles, CA, USA

Catherine Catlett Christian, BS(Eng) Menninger Department of Psychiatry & Behavioral Sciences, Baylor College of Medicine, Houston, TX, USA

G. Rees Cosgrove, MD, FRCSC Epilepsy and Functional Neurosurgery, Department of Neurosurgery, Brigham and Women's Hospital, Boston, MA, USA

Donald J. Crammond, PhD Department of Neurological Surgery, University of Pittsburgh School of Medicine, Pittsburgh, PA, USA

Pierre-François D'Haese, PhD Department of Electrical Engineering and Computer Science, Vanderbilt University, Nashville, TN, USA

Zafiris J. Daskalakis, MD, PhD, FRCP(C) Temerty Centre for Therapeutic Brain Intervention, Centre for Addiction and Mental Health, Toronto, ON, Canada

Department of Psychiatry, Institute of Medical Science, University of Toronto, Toronto, ON, Canada

Coralie de Hemptinne, PhD Department of Neurological Surgery, University of California, San Francisco, San Francisco, CA, USA

Sonja Dieterich, PhD, MBA, FAAPM Department of Radiation Oncology, University of California, Davis, Sacramento, CA, USA

W. Jeffrey Elias, MD Departments of Neurological Surgery and Neurology, University of Virginia, Charlottesville, VA, USA

Jay R. Gavvala, MD, MSCI Department of Neurology – Neurophysiology, Baylor College of Medicine, Houston, TX, USA

Jason L. Gerrard, MD, PhD Department of Neurosurgery, Yale School of Medicine, New Haven, CT, USA

Yale-New Haven Hospital, New Haven, CT, USA

Thierry Gevaert, PhD Department of Radiotherapy, Universitair Ziekenhuis Brussel (UZB), Brussels, Belgium

Vrije Universiteit Brussel (VUB), Brussels, Belgium

Nisha Giridharan, MD Department of Neurosurgery, Baylor College of Medicine, Houston, TX, USA

Steven J. Goetsch, PhD Medical Physics, San Diego Gamma Knife Center, La Jolla, CA, USA

Jorge Gonzalez-Martinez, MD, PhD Department of Neurosurgery, University of Pittsburgh, Pittsburgh, PA, USA

Wayne K. Goodman, MD Menninger Department of Psychiatry & Behavioral Sciences, Baylor College of Medicine, Houston, TX, USA

Robert E. Gross, MD, PhD Department of Neurosurgery, Emory University, Atlanta, GA, USA

Abhijeet Gummadavelli, MD Department of Neurosurgery, Yale School of Medicine, New Haven, CT, USA

Yale-New Haven Hospital, New Haven, CT, USA

Ryder P. Gwinn, MD Center for Neurologic Restoration, Swedish Neuroscience Institute, Swedish Medical Center, Seattle, WA, USA

Casey Halpern, MD Department of Neurosurgery, Stanford University, Palo Alto, CA, USA

Dominique M. O. Higgins, MD, PhD Department of Neurosurgery, Columbia University Irving Medical Center, New York, NY, USA

Jeanette Hui, BSc, MSc Temerty Centre for Therapeutic Brain Intervention, Centre for Addiction and Mental Health, Toronto, ON, Canada

Institute of Medical Science, University of Toronto, Toronto, ON, Canada

Patrick J. Hunt, BS Molecular and Human Genetics, Baylor College of Medicine, Houston, TX, USA

A. Umair Janjua, MD Department of Psychiatry and Behavioral Sciences, Emory University School of Medicine, Atlanta, GA, USA

Joohi Jimenez-Shahed, MD Medical Director, Movement Disorders Neuromodulation, Department of Neurology, Icahn School of Medicine at Mount Sinai, New York, NY, USA

Tania Kaprealian, MD, MBA Department of Radiation Oncology, University of California, Los Angeles, Los Angeles, CA, USA

Patrick J. Karas, MD Department of Neurosurgery, Baylor College of Medicine, Houston, TX, USA

Alon Kashanian, BS Department of Neurosurgery, David Geffen School of Medicine at UCLA, Los Angeles, CA, USA

Omaditya Khanna, MD Department of Neurological Surgery, Thomas Jefferson University Hospital, Philadelphia, PA, USA

Douglas Kondziolka, MD, MSc, FRCSC, FACS Department of Neurosurgery, NYU Langone Health, New York, NY, USA

Department of Radiation Oncology, New York University, New York, NY, USA

Vibhor Krishna, MD, SM Departments of Neurosurgery and Neuroscience, Center for Neuromodulation, The Ohio State University, Columbus, OH, USA

Bornali Kundu, MD, PhD Department of Neurosurgery, Clinical Neurosciences Center, University of Utah, Salt Lake City, UT, USA

Jean-Philippe Langevin, MD Department of Neurosurgery, David Geffen School of Medicine at UCLA, Los Angeles, CA, USA

Neurosurgery Service, Greater Los Angeles VA Healthcare System, Los Angeles, CA, USA

Peter M. Lauro, BA Department of Neuroscience, Warren Alpert Medical School, Brown University, Providence, RI, USA

Shane Lee, PhD Neurosurgery, Neuroscience, and the Carney Institute for Brain Science, Brown University and the Norman Prince Neurosciences Institute of Rhode Island Hospital, Providence, RI, USA

Eric J. Lehrer, MD, MS Department of Radiation Oncology, Icahn School of Medicine at Mount Sinai, New York, NY, USA

Pantelis Lioumis, PhD Temerty Centre for Therapeutic Brain Intervention, Centre for Addiction and Mental Health, Toronto, ON, Canada

Caio Matias, MD, PhD Department of Neurological Surgery, Thomas Jefferson University Hospital, Philadelphia, PA, USA

Abigail McCallum, MD Department of Neurological Surgery, University of Louisville, Louisville, KY, USA

Nicole C. R. McLaughlin, PhD Psychiatric Neurosurgery Program at Butler Hospital, Providence, RI, USA

Psychiatry and Human Behavior, The Warren Alpert Medical School of Brown University, Providence, RI, USA

Matthew K. Mian, MD Department of Neurosurgery, Emory University, Atlanta, GA, USA

Charles B. Mikell, MD Department of Neurosurgery, Stony Brook University Hospital, Stony Brook, NY, USA

Alon Y. Mogilner, MD, PhD Department of Neurosurgery, NYU Langone Medical Center, New York, NY, USA

Shayan Moosa, MD Department of Neurological Surgery, University of Virginia, Charlottesville, VA, USA

Joseph S. Neimat, MD, MS Department of Neurological Surgery, University of Louisville, Louisville, KY, USA

Neepa J. Patel, MD Department of Neurology, Parkinson Disease and Movement Disorders Clinic, Henry Ford Hospital, West Bloomfield, MI, USA

Francisco A. Ponce, MD Department of Neurosurgery, Barrow Neurological Institute, St. Joseph's Hospital and Medical Center, Phoenix, AZ, USA

Michael H. Pourfar, MD Department of Neurosurgery, NYU Langone Medical Center, New York, NY, USA

Marc A. Prablek, MD Department of Neurosurgery, Baylor College of Medicine, Houston, TX, USA

Imran H. Quraishi, MD, PhD Yale-New Haven Hospital, New Haven, CT, USA

Department of Neurology, Yale School of Medicine, New Haven, CT, USA

Ahmed M. Raslan, MD Department of Neurological Surgery, Oregon Health & Science University, Portland, OR, USA

R. Mark Richardson, MD, PhD Department of Neurosurgery, Massachusetts General Hospital, Harvard Medical School, Boston, MA, USA

Patricio Riva-Posse, MD Department of Psychiatry and Behavioral Sciences, Emory University School of Medicine, Atlanta, GA, USA

Pratik Rohatgi, MD Department of Neurosurgery, David Geffen School of Medicine at UCLA, Los Angeles, CA, USA

John D. Rolston, MD, PhD Department of Neurosurgery, Clinical Neurosciences Center, University of Utah, Salt Lake City, UT, USA

Department of Biomedical Engineering, University of Utah, Salt Lake City, UT, USA

Juliana Rotter, MD Department of Neurologic Surgery, Mayo Clinic, Rochester, MN, USA

Francesco Sammartino, MD Center for Neuromodulation, The Ohio State University, Columbus, OH, USA

Akshay V. Save, BS Department of Neurosurgery, Columbia University Irving Medical Center, New York, NY, USA

Himanshu Sharma, MD, PhD Medical Scientist Training Program, Stony Brook University School of Medicine, Stony Brook, NY, USA

Jason P. Sheehan, MD, PhD Department of Neurological Surgery, University of Virginia, Charlottesville, VA, USA

Sameer A. Sheth, MD, PhD Department of Neurosurgery, Baylor College of Medicine, Houston, TX, USA

Philip A. Starr, MD, PhD Department of Neurological Surgery, University of California, San Francisco, San Francisco, CA, USA

Eric A. Storch, PhD Menninger Department of Psychiatry & Behavioral Sciences, Baylor College of Medicine, Houston, TX, USA

Geoffrey P. Stricsek, MD Department of Neurological Surgery, Thomas Jefferson University Hospital, Philadelphia, PA, USA

Stephen Tenn, PhD Department of Radiation Oncology, University of California, Los Angeles, Los Angeles, CA, USA

Zoe E. Teton, BS Department of Neurological Surgery, Oregon Health & Science University, Portland, OR, USA

John A. Thompson, PhD Department of Neurosurgery, University of Colorado School of Medicine, Aurora, CO, USA

Daniel M. Trifiletti, MD Department of Radiation Oncology, Mayo Clinic, Jacksonville, FL, USA

Ashwin Viswanathan, MD Department of Neurosurgery, Baylor College of Medicine, Houston, TX, USA

Doris D. Wang, MD, PhD Department of Neurological Surgery, University of California, San Francisco, San Francisco, CA, USA

Howard L. Weiner, MD Department of Neurosurgery, Baylor College of Medicine, Houston, TX, USA

Division of Pediatric Neurosurgery, Department of Surgery, Texas Children's Hospital, Houston, TX, USA

Christopher J. Winfree, MD Department of Neurosurgery, Columbia University Irving Medical Center, New York, NY, USA

Teresa Wojtasiewicz, MD Department of Neurological Surgery, Johns Hopkins University, Baltimore, MD, USA

Adela Wu, MD Department of Neurosurgery, Stanford University, Palo Alto, CA, USA

Chengyuan Wu, MD, MSBME Department of Neurological Surgery, Thomas Jefferson University Hospital, Philadelphia, PA, USA

Daniel Yoshor, MD Department of Neurosurgery, Baylor College of Medicine, Houston, TX, USA

Nicole A. Young, PhD Department of Neuroscience, The Ohio State University Wexner Medical Center, Columbus, OH, USA

Xuefeng Zhang, MD, PhD Menninger Department of Psychiatry & Behavioral Sciences, Baylor College of Medicine, Michael E. DeBakey VA Medical Center, Houston, TX, USA

Ludvic Zrinzo, MD, PhD, FRCSEd Unit of Functional Neurosurgery, UCL Queen Square Institute of Neurology and the National Hospital for Neurology and Neurosurgery, London, UK

Part I

Achieving Stereotactic Precision

Traditional and Mini-Frames

1

Ahmad Alhourani, Abigail McCallum, and Joseph S. Neimat

Background

The introduction of stereotaxis transformed neurosurgical practice by allowing precise minimally invasive localization of previously inaccessible regions of the human cerebrum. Initial prototypes and experiments by Zernov [1] in 1889 followed by Clarke and Horsley [2] in 1906 provided the groundwork for the first stereotactic system routinely used in humans by Spiegel and Wycis [3] in 1947. However, widespread adoption of the stereotactic method started with the introduction of improved frame designs, specifically the popular Leksell frame, integrating Cartesian targeting and polar trajectory selection [4]. While the traditional frames underwent several modifications up to their current form, they rely on the same basic principle. The frame has a self-contained coordinate system that is registered to reference points of the patient and their imaging. This relationship is calculated by acquiring patient imaging while in the frame. Initial work used ventriculography to find fiducial points like the anterior-posterior commissural line and then used standard coordinates derived from atlases for targeting. As neuroimaging improved to allow direct visualization of target structures, target coordinates are directly transformed into frame coordinates. This approach requires the patient to be rigidly fixed in the frame from the time of imaging and throughout the procedure to maintain a constant relationship. Such a constraint can be cumbersome for awake movement disorder patients as the patient and the frame are bolted to the operative table to support the weight of the frame.

As technologies enabled increased alternatives, several stereotactic systems have been developed to allow greater patient comfort with equivalent accuracy and precision. We describe in this chapter the three most commonly used systems, the theoretical basis for their design, and their practical workflow. We also describe the clinical results from reported experience with each system.

Frame Versus Imaging-Based Coordinate Systems

Imaging technologies have improved to allow volumetric acquisition of both CT and MRI scans. This generates a three-dimensional volume with a set coordinate system where every point or voxel has a distinct X, Y, and Z value. Since the voxel dimensions are known and set by the scanner, different volumes can be fused using simple mathematical transformations. Additionally, their coordinates can be used in calculations to navigate through the volume and target structures. This innovation eliminated the

A. Alhourani · A. McCallum · J. S. Neimat (✉)
Department of Neurological Surgery, University of Louisville, Louisville, KY, USA
e-mail: joseph.neimat@louisville.edu

N. Pouratian, S. A. Sheth (eds.), *Stereotactic and Functional Neurosurgery*,
https://doi.org/10.1007/978-3-030-34906-6_1

need for frames to provide an independent Cartesian coordinate system that was critical when using X-ray ventriculography or 2D CT slice acquisitions. Instead, several new frame systems were developed by essentially co-opting the 3D CT space as their implicit coordinate system. The targeting of platforms and trajectories within this system is based on simple mathematical transforms relating points of attachment and registration to targets and trajectories in the same three-dimensional space. The different systems described below use a different version of the same principle, each with their advantages and disadvantages.

Traditional Frames

Several stereotactic frames are currently utilized in neurosurgical practice; however, the Leksell frame remains the most commonly used frame. It is also regarded for its transformative effect on the field since its introduction in 1949. The main innovation behind it was using the center-of-arc principle instead of a pure Cartesian system used in previous frames. It employs a stereotactic arc on which the targeting probe is mounted perpendicular to the arc. It is the equivalent of the radius of a semicircular arc which would reach the center of the arc when introduced perpendicular to any point along the arc. Targeting a location becomes a matter of translating the center of the arc to line up with the target in three-dimensional space. This allows for great versatility in choosing the trajectory needed.

Other frame models employ the same principle but differ in how the frame is applied or how the coordinate space is described. For example, the Leksell frame uses the posterior superior corner of its 3D space as the zero-reference point, making all values on its axes positive values. On the other hand, the CRW frame uses the center of the frame as the zero point, so it has positive and negative values.

The frame is comprised of several parts: (1) a fixation instrument consisting of four fixation points for rigid fixation into the skull that connect to a graduated frame, (2) the coordinate frame that mounts on the fixation device and contains six radiopaque posts (four vertical posts in each corner and two diagonal in the shape of an N on each side), and (3) the stereotactic arc. The general method for registering the patient space with the frame stereotactic frame relies on defining the geometric center of the frame using the coordinate frame as depicted in Fig. 1.1. The patient needs to be imaged after applying the frame. The four vertical posts help define the center in the X and Y directions, while the diagonal posts define the center in the Z direction. After finding the geometric center, the distance from the target location can be calculated to translate the center of the arc to that location.

The workflow of frame-based targeting typically occurs in a single day. The fixation frame is applied to the patient to maintain a rigid relationship between the patient space and the stereotactic device. The patient is imaged using a stereotactic/volumetric CT or MRI scan to register the frame with the patient space. The stereotactic coordinate system is therefore established on this image set. If this frame-based scan is a CT, which is more common given its speed

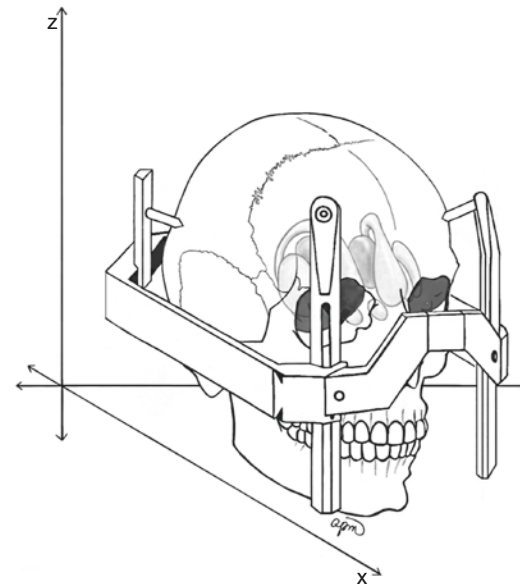

Fig. 1.1 Traditional stereotactic frames and methodology. The base of a Leksell frame applied to a model with basal ganglia rendered showing the coordinate system inherent in the frame

advantage over MRI, then the CT is fused with the preoperative MRI using the surgeon's navigation software of choice. This fusion transfers the coordinate system from CT to MRI. This step is not necessary if the frame-based scan is performed using an MRI. Either way, the stereotactic planning of the trajectory is performed on the MRI, which provides the best anatomical detail. The trajectory is defined by two points: the target and the entry. The planning software provides the coordinates to place the target at the geometric arc center. The target point is thus defined in terms of these three coordinates: X (usually left-right), Y (usually anterior-posterior), and Z (usually superior-inferior). The entry point is defined by an additional three coordinates: sagittal angle ("ring" angle), coronal angle ("arc" angle), and depth of trajectory (usually frame center: 160 mm for CRW and 190 mm for Leksell).

The workflow afterward from burr hole creation, microelectrode mapping, electrode implantation, and macrostimulation is described in more detail in a later chapter.

The main advantages of frame-based systems are their reliability and versatility. The trajectory can be changed to any point within the confines of the stereotactic space. This allows for numerous diverse applications across the whole patient population which led to their widespread adoption. However, they carry several limitations. First, they should be recalibrated periodically due to changes to the metal frame during sterilization procedures. Second, they can only be applied to one trajectory at a time. Also, the substantial weight of the instrument requires fixing the patient to the operative table, thus eliminating the patient's ability to move. Patients with larger head sizes can be limited within the fixation frame. Defining the trajectory is susceptible to human error by entering the wrong coordinates. Finally, the frame and stereotactic arc occupy a large portion of the surgical field and have to periodically be moved or swung out of the way to avoid hampering surgical access.

For applications in DBS surgery, a wide range of accuracy has been reported for these traditional frames, ranging from 1.3 to 1.7 mm [5–7].

STarFix (Surgical Targeting Fixture) Platform

The STarFix system is an alternative method of stereotaxis that relies on custom microtargeting platforms (MTP). The MTP is a lightweight fixture that can incorporate one or more trajectories and is directly attached to the skull; a model of a bilateral DBS platform is depicted in Fig. 1.2a. This process became feasible in the clinical setting with the emergence of rapid prototyping technology where an MTP can be manufactured and delivered in a relatively short time (as little as 3 days, although 7 are usually recommended). The frame is made of DuraForm polyamide, a durable thermoplastic. Each MTP is individualized to both the patient and the target trajectory unlike other systems that can be used across different patients and trajectories. The complete system includes planning software, bone fiducial markers, and a drive and reducer set that allows trajectory adjustments. While the planning software for other frame systems generates frame settings corresponding to the selected entry point and trajectory, the STarFix planning software generates the instruction file for manufacturing an MTP. Finally, the frames are intended for single use but can be reused for the same target as long as the bone markers used for registration are retained.

The STarFix system relies on several basic principles shared with traditional stereotactic frames. First, it uses several fiducial points that are incorporated into the platform itself. Additionally, there is a rigid relationship between the registration points and the trajectory fixture. To incorporate the patient's imaging, the system relies on three key data points: the bone fiducial anchor locations (made more accurate by recording bone fiducial anchor orientation), the target location, and the trajectory to target. Those data points are used to calculate a mathematical transform that translates the imaging space to the patient's physical space. Additional data points such as the orientation of the trajectory with respect to the AC-PC line and midline are incorporated so that trajectory adjustments occur in

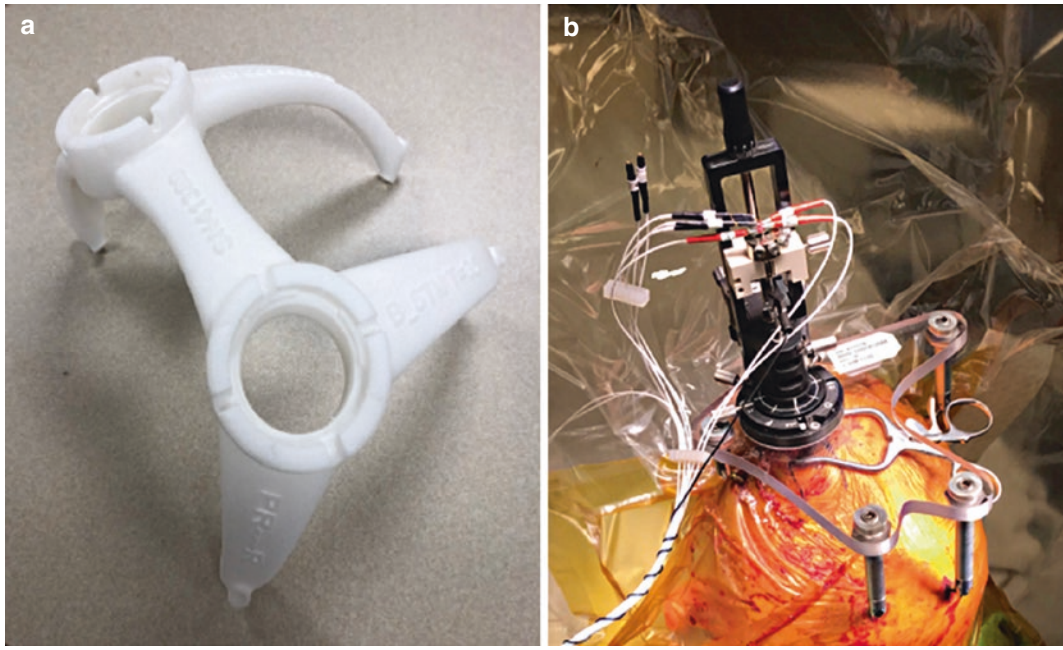

Fig. 1.2 Custom microtargeting platforms. (**a**) A sample of the STarFix frame for a bilateral DBS target. (**b**) A unilateral VIM trajectory targeted using the Microtable with the microdrive mounted

orientations that allow precise anterior-posterior and medial-lateral movements.

The STarFix system has a unique workflow as it is an individualized system requiring frame manufacturing. The general workflow of the STarFix system is broken into two discrete steps over a period of 1–2 weeks. The workflow starts with implantation of the bone fiducial markers which is usually termed Step 1 (termed Step 0 at some centers) in a minor surgical procedure. This can be performed under local or general anesthesia and is sometimes performed in an office setting. The number of fiducial markers varies based on the number of trajectories. At least three are required for unilateral cases and four are typically used for bilateral frames. Of note, larger frames with more than two trajectories that are used for specialized applications such as stereo-EEG require up to six anchors for appropriate rigidity. The bone anchors serve a dual purpose: (1) they serve as a rigid reference point for image registration and (2) rigid physical attachment for the MTP to be mounted on during the targeting procedure. Therefore, the fiducials must remain fixed in the same location between procedures. The bony anchors went through several versions from externalized MRI-detectable posts and caps to the current internalized hex nuts that are buried completely under the scalp. Anchor placement only requires simple stab incisions to allow placement into the outer table of the skull. The incisions are closed with a single suture or staples. A postoperative CT imaging for image registration can be obtained immediately following the procedure while the patient is still under general anesthesia or during the same day. A high-resolution MRI for target identification is typically used and can be obtained under the same general anesthesia (if used) for outstanding motion-free images. Patients are usually discharged home with the simple instruction to keep the anchor sites clean.

Surgical planning follows similar steps to traditional frames where the CT and MR images are co-registered, identifying the target locations and selecting the optimal entry points. However, instead of generating coordinates, the planning software creates a customized MTP design. The design file is sent to the manufacturer, and the MTP is delivered to the hospital

within several days. Several compatible planning software are available to generate the design files such as Voxim, WayPoint Planner/Navigator, and StimPilot.

Stage 2 can be performed any time after the frame is manufactured, but it is usually performed a week after stage 1 in our institution. We prefer electrode placement using microelectrode recordings, so this stage is commonly performed under local anesthesia, with IV sedation. The bone marker incisions are opened after infiltration with local anesthesia. The MTP is rigidly connected to the bone anchors using couplers with submillimetric tolerance. This obviates the need to lock the patient's head to the operating Table. A guide is used to mark the entry point on the scalp and skull through the ring opening of the MTP. The steps afterward from burr hole creation, microelectrode mapping, electrode implantation, and macrostimulation are done in a standard fashion that is essentially the same as that used in frame cases.

The STarFix system offers several advantages for DBS surgery. First, both trajectories can be mounted and mapped simultaneously through separate microdrives, unlike traditional frames than can perform one trajectory at a time. This can potentially provide significant time savings as both sides are explored and recorded at once. Second, the patient is free to move during the procedure providing superior patient comfort especially in patients with severe tremors or dyskinesias. This mobility can help patients overcome the anxiety of being in a rigid frame for extended periods of time. Workflow on the day of surgery typically proceeds more expeditiously, as no scan is needed on the day of procedure. Additionally, there is no limitation on head size to fit inside the frame. A recent iteration of the device termed the Microtable that employs the same strategy of bone marker insertion and subsequent fixture application but can be manufactured on the same day. The fixture is a Lexan plate that has holes of various depths drilled into it to hold legs of different length (Fig. 1.2b). The resulting geometry can reproduce any single stereotactic trajectory with accuracy equivalent to the STarFix platform. The advantage of the Microtable is that the fixture can be created in just a few minutes and therefore be available for same-day surgeries. To date, it has been utilized in more than 20 surgeries, and publications on safety and accuracy are anticipated in the coming year.

Limitations include the fact that the frame is non-deformable around the planned trajectory, limiting the ability to perform changes to the trajectory. However, the trajectory can be adjusted using various offset adapters for the drive assembly allowing for a maximum offset of 11 mm from the central target in all directions. Additionally, no final confirmation fluoroscopic imaging is used due to the lack of stable reference imaging (i.e., the ring and bull's-eye markers of a traditional frame). From a cost point of view, the initial overhead is much lower than purchasing a traditional frame, but the per-case cost is higher because of the need to produce a new frame for every case. Finally, the STarFix system is compatible with most microdrives and cannula systems; however, the frame height from the skull is different from the Leksell frame, and that difference needs to be accounted for when the microelectrodes and cannulas are mounted to calculate the correct distance to target.

The STarFix system was FDA approved in 2001, and the largest reported experience comes from Vanderbilt University, where it has been adopted since 2002. Their case series of 265 patients describes cases performed between 2002 and 2008 using several iterations of the system including its current mature form [8]. The system showed high accuracy with a targeting error of 1.99 ± 0.9 mm across 75 patients. The targeting error was further reduced to 1.24 ± 0.4 mm when accounting for brain shift. The case series demonstrated the safety of the system with a less than 0.2% complication rate across the entire cohort. Earlier versions of the system that had externalized posts and caps suffered from dislodgement of the bony fiducials occurring in 0.1% of patients, especially in patients with severe dyskinesia. This complication has not been seen in the current internalized version of the bony fiducials. The multistep nature of the workflow and the multiple operations raises the concern for

increased infection risk. However, the authors reported only one case of bone marker infection (0.004%) that was simply treated by removal of the fiducials and a short course of antibiotics.

NexFrame

The NexFrame was the first true frameless system used for DBS, as it lacks rigid attachment between the reference points and the trajectory. It utilizes infrared (IR) optical guidance similar to other frameless neuronavigation systems. However, it relies on rigid registration markers and more tightly controlled guide tower allowing for the precision required for DBS lead implantation. It commonly uses bone fiducial markers for image registration; however, they are used as markers for optical tracking to manually register and align the trajectory during surgery [9] and are not incorporated in the fixture itself.

Unlike the STarFix system, the NexFrame tower is a standardized frame that is adjusted during targeting, so it does not require the overhead in time required to manufacture the STarFix frame. Also, it is comprised of disposable components and therefore does not require the need to be recalibrated like traditional frames after repeated use.

The workflow follows a similar, albeit shorter, timeframe to the STarFix system. In stage I, the patient undergoes implantation of four to six bone fiducial markers that are used for rigid registration. This can be performed on the day of surgery or 1–2 days prior. CT images with the fiducials in place are obtained and merged with the preoperative MRI on the StealthStation. Target selection is performed in a standard fashion relative to the AC-PC landmarks. The centers of the fiducials are then marked, and the entry point is selected. A standard burr hole is created overlying the entry point, and the burr hole cover base is attached to the skull to act as a base for the NexFrame and the reference arc. The fiducial markers are then used to register the patient space using optical tracking. The tower is assembled and attached to the base to align with the target. The NexDrive is then attached with light-emitting diodes to track the electrodes' location. The final tract can still be adjusted but is limited by the excursion of the tower. The base allows for two possible movements: 360° of rotation and 25° of angling in any two directions.

The largest case series using the NexFrame included 60 patients with 119 electrode implantations over an 18-month period [10]. In this case series, both stages were done in the same setting and under general anesthesia. The mean targeting error was 1.24 ± 0.87 mm across all targets (STN, GPi, and VIM) and was correlated with the distance from the ventricle. No frame-related complications were reported.

The NexFrame shares similar advantages with the STarFix system in terms of patient comfort and bilateral simultaneous trajectories. Additionally, it does not require the manufacturing time required for the STarFix system with a significantly shorter workflow that can be done in the same day. Although accuracy in experienced hands is comparable to other framed and frameless systems, there is a learning curve to pointing and tightening the frame to secure the trajectory. This can lead to a lack of reproducible precision in less-experienced hands.

System Comparison

The aim of stereotaxis is to reach the intended target with minimal error. This is usually measured by accuracy and precision. Accuracy measures how far the trajectory was from the intended target, while precision measures how wide the variation in the trajectories is. Accuracy can be measured through the targeting error, while precision relates to the standard deviation of that targeting error. Both systems show comparable accuracy to each other and to traditional frames (Table 1.1). There is a wide variation on the reported accuracy of each system, but there is a clear trend in improved accuracy across time as groups become more familiar and adapt at their use [11].

Conceptually, the mini-frame systems use the coordinate system in the patient's imaging rather than having an internal coordinate system as seen

Table 1.1 Comparison between traditional and mini-frame accuracy and application

Category	Traditional frames (Leksell and CRW)	NexFrame	STarFix frame
Targeting error in phantom models (mm)	1.7 ± 1, 1.8 ± 1.1 [12]	1.25 ± 0.6 [12]	0.42 ± 0.15
Targeting error in cases series (mm)	1.4 [13], 1.03 ± 0.76 [6]	1.24 ± 0.87 [10]	1.24 ± 0.4 [8]
Registration method	Fixed	Fixed or deformable	Fixed
Targeting method	Structural	Virtual	Structural
Targeting limitation	Unlimited	Adjustment limited by tower excursion	Adjustments limited
Multiple trajectories	Only one	2 are possible	Limited to number of towers
Coordinate system	Inherent to the frame	Borrowed from imaging	Borrowed from imaging

in traditional frames affording more flexibility. Both the STarFix and NexFrame systems offer better patient comfort by obviating the need for rigid fixation to the table. However, robotic systems still require the patient to remain in a rigid head clamp even if frameless registration is used. All systems use skull-mounted fiducials for registration, but the NexFrame and robotic system offer the option of surface-based deformable registration. Finally, all systems except for the STarFix system can be deployed in the same day.

Conclusion

Overall, the advent of these novel systems has provided a variety of solutions to improve patient comfort and surgical efficiency while maintaining accuracy and precision. They have grown to comprise a substantial percentage of DBS surgeries nationally, and their application to other stereotactic surgeries like LITT and SEEG may expand their utilization in the future. The increasing availability of volumetric imaging and robotic or rapid manufacture techniques has enabled these stereotactic approaches and may provide further novel solutions as underlying technologies continue to improve. Under this influence, the traditional definitions of "framed" and "frameless" strategies are becoming less meaningful. The comfort and precision of stereotactic surgery are continuing to improve as such innovative technologies are applied.

References

1. Kandel' EI, Shchavinskii YV. First stereotaxic apparatus created by Russian scientists in the 19th century. Biomed Eng. 1973;7(2):121–4.
2. Clarke RH, Horsley V. On a method of investigating the deep ganglia and tracts of the central nervous system (cerebellum). Br Med J. 1906:1799–800.
3. Spiegel EA, Wycis HT, Marks M, Lee AJ. Stereotaxic apparatus for operations on the human brain. Science. 1947;106(2754):349–50.
4. Leksell L, Leksell D, Schwebel J. Stereotaxis and nuclear magnetic resonance. J Neurol Neurosurg Psychiatry. 1985;48(1):14–8.
5. Foltynie T, Zrinzo L, Martinez-Torres I, Tripoliti E, Petersen E, Holl E, et al. MRI-guided STN DBS in Parkinson's disease without microelectrode recording: efficacy and safety. J Neurol Neurosurg Psychiatry. 2011;82(4):358–63.
6. Pollo C, Vingerhoets F, Pralong E, Ghika J. Localization of electrodes in the subthalamic nucleus on magnetic resonance imaging. J Neurosurg. 2007;106(1):36–44.
7. Holl EM, Petersen EA, Foltynie T, Martinez-Torres I, Limousin P, Hariz MI, et al. Improving targeting in image-guided frame-based deep brain stimulation. Neurosurgery. 2010;67(2 Suppl Operative):437–47.
8. Konrad PE, Neimat JS, Yu H, Kao CC, Remple MS, D'Haese PF, Dawant BM. Customized, miniature rapid-prototype stereotactic frames for use in deep brain stimulator surgery: initial clinical methodology and experience from 263 patients from 2002 to 2008. Stereotact Funct Neurosurg. 2011;89(1):34–41.
9. Holloway KL, Gaede SE, Starr PA, Rosenow JM, Ramakrishnan V, Henderson JM. Frameless stereotaxy using bone fiducial markers for deep brain stimulation. J Neurosurg. 2005;103(3):404–13.
10. Burchiel KJ, Shirley M, Lee A, Raslan AM. Accuracy of deep brain stimulation electrode placement using

intraoperative computed tomography without microelectrode recording. J Neurosurg. 2013;119(2):301–6.
11. Li Z, Zhang J-G, Ye Y, Li X. Review on factors affecting targeting accuracy of deep brain stimulation electrode implantation between 2001 and 2015. Stereotact Funct Neurosurg. 2016;94(6):351–62.
12. Henderson JM, Holloway KL, Gaede SE, Rosenow JM. The application accuracy of a skull-mounted trajectory guide system for image-guided functional neurosurgery. Comput Aided Surg. 2004;9(4):155–60.
13. Starr PA, Christine CW, Theodosopoulos PV. Implantation of deep brain stimulators into subthalamic nucleus: technical approach and magnetic imaging—verified electrode locations. J Neurosurg. 2002 Aug;97(2):370–87.

Stereotactic Robots

2

Omaditya Khanna, Caio Matias,
Geoffrey P. Stricsek, and Chengyuan Wu

Introduction

The Robot Institute of America defines robots as a "reprogrammable, multifunctional manipulator designed to move materials, parts, tools, or other specialized devices through various programmed motions for the performance of a variety of tasks." The use of robotics in functional neurosurgery holds large promise: robots have the potential to increase the accuracy and precision of targeting miniscule lesions and provide surgeons with increased dexterity via minimally invasive techniques to access important deep-seated anatomic structures in the brain in a safe and effective way. Robots confer the ability to perform complicated, often repetitive tasks, with great precision; it is for this reason that robots have garnered more widespread use in the subspecialty of functional neurosurgery. Given the increasing complexity of surgical procedures performed, the need for a high degree of accuracy in stereotaxy is well addressed by robotic solutions, which has led to their increased use in modern neurosurgical practice.

The use of robotic stereotaxy is the latest technology that builds on the historical trend of the need for improved anatomic and radiographic accuracy in the field of neurosurgery. Early forays into stereotaxy, dating back to the late 1800s, were constrained by the wide variability between bony landmarks and intracranial targets. Frame-based stereotaxy (detailed extensively in Chap. 1) dates back to the late nineteenth century, when it was first used by Gaston Contremoulins, a self-educated scientist, to remove two intracranial bullets [1]. Spiegel and Wycis further improved the use of stereotactic approaches for intracranial surgery in 1947, by pairing pneumoencephalograms with intracranial reference points [2]. The need for a reliable accuracy in stereotaxy naturally lends itself to the use of surgical robots. Nowadays, three-dimensional imaging is obtained that, in conjunction with stereotactic systems, is used to devise trajectories that allow for the precise targeting of intracranial structures. Robots can supplement the surgical workflow by having the surgical plan programmed into the machine, to be subsequently executed with robotic precision during the course of the surgery.

Robots may be integrated into a surgical workflow as either an active or passive system. An *active system* is one in which the robot can be manipulated in real time and interacts with the patient throughout the course of surgery as it is being wielded by the surgeon. A *passive system*, on the contrary, functions to hold a surgical tool in a predetermined fixed position in order to provide improved stability to the surgeon, with the

O. Khanna (✉) · C. Matias · G. P. Stricsek · C. Wu
Department of Neurological Surgery, Thomas Jefferson University Hospital, Philadelphia, PA, USA
e-mail: Omaditya.Khanna@jefferson.edu

N. Pouratian, S. A. Sheth (eds.), *Stereotactic and Functional Neurosurgery*,
https://doi.org/10.1007/978-3-030-34906-6_2

surgeon ultimately actually carrying out the movements directly.

In addition to describing robotic systems as either active or passive, there are three broad categories which robotic systems may be categorized. A *telesurgical system* is one where the surgeon directly controls each movement of the machine; the robotic arm acts as a conduit for each manipulation performed by its user. The most well-known telesurgical system is the da Vinci system (Intuitive Surgical, Inc.; Sunnyvale, CA), which has garnered use across multiple surgical disciplines. The second type of system is a *supervisory controlled system*, in which the machine is pre-programmed with actions which are autonomously performed by the robot, under the close supervision of the surgeon. Lastly, *shared-control models* are systems that allow the surgeon and the robot to concurrently control the motions carried out during an operation [3].

The first use of a robot for a neurosurgical procedure was in 1985, via the Programmable Universal Machine for Assembly (PUMA) device, which represented a passive robotic system. A patient with an intracranial lesion was placed in a stereotactic head frame and underwent target localization using a CT scan. The target coordinates were programmed into the PUMA robot, aiding the surgeon to devise an accurate trajectory to the target lesion and also avoid critical structures along the biopsy path [4]. The MINERVA system, introduced in the 1990s, offered integration of a robotic system with CT guidance to allow a surgeon to monitor instrument position and progress in real time [5]. Although both of these early systems have since been discontinued, the last two decades have brought about an increasing number of innovative robotics designed to help carry out complex neurosurgical procedures.

Integration of robots into the neurosurgical operating room offers many benefits, but also has inherent limitations, for both the patient and the surgeon. This chapter will provide an overview of the use of robotics in the field of stereotactic and functional neurosurgery, including various types of robotic systems available for commercial use, its benefits and disadvantages, and its current and future applications for use in neurosurgical procedures.

Workflow of a Robotic Neurosurgical Procedure

The integration of robotic systems into the neurosurgical workflow presents both opportunities and challenges to the surgeon. Navigated and robotic systems achieve accuracy and workflow benefits using a series of accurate alignments between preoperative images, intraoperative tracking tools, and the patient's relevant anatomy. The following is an overview of the various stages of robot-assisted neurosurgical procedures, each of which must be carried out carefully in order to achieve accuracy and success.

Preoperative Three-Dimensional Imaging

The basis of image-guided procedures is the acquisition of a high-resolution three-dimensional (3D) image to delineate the relevant anatomy. This can be achieved via a CT scan, MRI, angiogram, an intraoperative tomographic scan, or a combination of these images fused together. It is important to note that the overall efficacy of a robotic system is limited by the quality and accuracy of preoperative imaging obtained: if slice thickness is too coarse or if there are significant imaging artifacts, both of which can limit the quality of 3D reconstruction, the achievable accuracy rendered by the robot may be compromised. Indeed, the capabilities offered by robotics and its ever-increasing use in neurosurgery have followed technical advancements in the quality of imaging surgeons are able to obtain.

Trajectory Planning

Based on the 3D anatomical image, the surgeon determines a desired trajectory, which encompasses the tract between the entry point and set

target point. The planned trajectory should ideally avoid traversing through, or abutting, critical structures (such as blood vessels), sulci and ventricular system when possible, and important white matter tracts (see Chap. 5 for a more in-depth description). The preoperative imaging obtained allows the surgeon to devise trajectories using a probe's eye view, providing a view of the devised tract(s) in a reconstructed plane along the cross section of the trajectory. In the case of stereoelectroencephalography (sEEG), multiple trajectories have to be carefully planned to ensure that each one can be inserted safely and still be efficacious (see Chap. 23 for a more detailed discussion of planning invasive monitoring for epilepsy).

Registration

This is the key step that aligns the preoperative 3D imaging and planned trajectories with the actual patient position in the OR, by co-localizing a mutually reliable landmark appreciable on imaging and the patient's body itself. There are a number of different ways of achieving this registration, each with workflow and accuracy tradeoffs. Options include mechanical based surface registration using facial features or bone fiducial registration (where a surgeon uses a probe to specify the location of anatomy, which is co-localized on the preoperative image). The use of frame-based or bone fiducial-based registration confers a higher degree of accuracy between preoperative imaging and intraoperative position [6].

Delivery

Once the preoperative plan has been registered to the intraoperative patient anatomy and position, the robot is used to execute the preplanned trajectory by moving its surgical arm into the correct position. Accuracy of the overall operation also relies on the accuracy of all prior steps and the precision in this step – ensuring the robot is holding the guide in the proper position relative to the plan. This is especially true when multiple trajectories are being executed for the placement of several leads, where each subsequent one is subject to small changes in cerebral surface locations (brain shift) [7], owing factors such as cerebrospinal fluid egress, pneumocephalus, and gravitational effect.

Postoperative Verification

After completion of the surgical procedure, it is important to verify the accuracy of the delivered plan, not only to evaluate the accuracy and efficacy of the surgery itself but also to quantify any errors with the intent to correct for them in future procedures. Systematic errors within an institutional system (which can be different based on target and application) can and should be recognized and compensated for based on continuous assessment and implementation of corrective measures.

Clinical Applications of Robotic Stereotaxy

Recent technological advances in surgical robotics have heralded its use for a wide range of neurosurgical procedures, including stereotactic biopsies of tumors [5], deep brain stimulation (DBS) electrode placement [8], placement of sEEG electrodes for evaluation of medically intractable epilepsy [9], ventricular catheter placement [10], and laser ablation procedures [11]. This section provides an overview of the various stereotactic procedures that have successfully incorporated the use of robots into neurosurgical workflow with excellent results.

Stereotactic Biopsies

Frame-based stereotactic biopsies have been the gold standard for deep-seated lesions that are not amenable to open surgical biopsy or resection, in order to provide a histopathologic diagnosis that is used to guide further treatment. Over the past decade, stereotactic robots have been used to

perform these biopsies, using both frame-based and frameless methods.

One study of 15 biopsies of brain stem lesions using frameless robotic stereotaxy yielded an 87% success rate of histopathological diagnosis on the first attempt. Out of the adults who underwent robotic-guided biopsy, two experienced transient neurological deficits, and one patient suffered permanent deficit [12]. A separate study found a diagnostic yield of 99% for pineal-area lesions [13]. In recent systematic review of 15 publications encompassing a total of 328 robotic brain biopsies performed, Marcus et al. found a diagnostic yield of 75–100%, with a target-point accuracy ranging from 0.9 to 4.5 mm. Taken together, these findings give credence to the use of robots to safety and efficiently perform intracranial biopsies, with or without the use of frame-based systems [14].

DBS Electrode Implantation

The targeted ablation and implantation of electrodes into deep-seated brain nuclei have significantly impacted the treatment of movement and neuropsychiatric disorders such as Parkinson's disease, essential tremor, and medically refractory depression. The efficacy of DBS treatment is predicated upon the accurate placement of leads within the target brain nuclei, with a target-point error of under 3 mm that is often required [15]. Robots are uniquely suited to help carry out placement of DBS leads, primarily owing to its ability to modify the entry and target points without onerous manipulation associated with utilizing frame-based systems.

Frame-based stereotaxy has historically been the gold standard for achieving accuracy in DBS electrode implantation [16]. Differences in stereotactic accuracy and methodology between frame and frameless systems are discussed in Chap. 1. One should be cognizant though that while there may be differences in stereotactic accuracy, these differences may not translate into clinically meaningful differences [17]. Still, as a principle, stereotactic surgeons strive to achieve stereotactic accuracy under all circumstances.

Robots may offer specific advantages for implantation of DBS leads because of their fidelity to carry out planned trajectories whether using frame-based or frameless system. In a study that evaluated the accuracy of DBS lead placement in 30 basal ganglia targets, the in vivo accuracy using a robotic system was found to be within 1 mm of the intended target, comparable to the accuracy conferred with using stereotactic frames [18]. Varma et al. published a single-institution case series of 113 DBS lead placements using a robotic system, reporting a mean error of 1.7 mm from the intended target-point placement, and only in three cases was the deviation greater than 3 mm. Highlighting the importance of assessing functional differences that may result from differences in stereotactic accuracy, patients undergoing DBS placement using a robot were found to have improved activity of daily living (ADL) scores and significant improvement in their motor fluctuations that persisted at 18 months follow-up, results similar to those reported previously using traditional frame-based stereotaxy [19].

sEEG Electrode Placement

The placement of sEEG electrodes serves as an option for the workup of drug-resistant epilepsy when the epileptogenic focus cannot be identified via noninvasive approaches and when invasive monitoring is necessary. The ability to place multiple sEEG electrodes helps encompass both cortical surface and deep matter structures, from which real-time electrophysiological activity can be recorded. The need to place multiple leads within deep-seated areas of the brain while avoiding critical structures along each planned trajectory is repetitive, time-consuming, and prone to error due to the need for constant human intervention and adjustments of frame coordinates. This presents a challenge that robotic systems are uniquely well-suited to help address. Robots are indefatigable; the ability for them to execute trajectories that have been planned by the surgeon in advance of the day of surgery carries a lower chance of misplaced leads, thereby decreasing the risk of perioperative complications and

operative times. As such, the placement of sEEG electrodes represents the most commonly performed functional neurosurgical procedure for which robots are utilized [20].

The earliest reported use of robotic-assisted implantation of sEEG electrodes was in 2005 by Cossu et al.: 17 out of 211 patients underwent placement of sEEG electrodes using a robot, and the remainder were implanted manually using the traditional stereotactic frame-based methodology, with similar rates of seizure freedom between the two groups [21]. In a separate study evaluating placement of 1050 sEEG leads using robotic assistance in 81 patients showed a 6% risk of perioperative minor complications without any mortalities, comparable to manual lead implantation. The median target-point error was found to be 1.77 mm for robotic cases, significantly lower compared to those inserted manually (2.69 mm) [22]. Given the similar accuracy and rates of complications, these early case series gave credence to the use of robotics for sEEG placement, prompting more surgeons to adopt its use in the operating room.

Abhinav et al. chronicled their initial experience after adopting the use of a robotic system for implanting sEEG leads in five adults and found that their total operative time was higher (mean 5.6 hours compared to 3.1 hours), owing to the implementation of an entirely new surgical workflow [23]. A more recent study that evaluated the efficacy of implanting sEEG leads using the ROSA robot found similar rates of complications between the robotic-assisted patient cohort (4%) compared to leads inserted manually using a frame-based technique (3%); however, the use of the robot resulted in markedly decreased surgical times by a mean of 222 minutes. Of the patients who subsequently underwent resection of seizure foci based on their sEEG findings, 66% were seizure-free at 18 months follow up [24]. Taken together, these results, along with other case series that have showcased similar results, demonstrate that robotic-assisted sEEG lead placement is a safe, effective, and efficient technique for evaluation of epileptogenic foci and accounts for the most commonly performed robotic procedure in the field of functional neurosurgery.

Laser Ablation of Intracranial Lesions

Stereotactically applied laser interstitial thermal therapy (LITT) using real-time MRI guidance has been used to treat a wide variety of pathology, including epileptogenic foci and deep-seated intracranial lesions [25]. The success of these procedures necessitates accurate placement of the focus of the laser treatment within the core of the intended target. As such, the use of robotic systems has been shown to be a safe, efficient, and minimally invasive treatment to achieve surgical success.

Calisto et al. published their short case series on robotic-guided LITT of hypothalamic hamartomas. Although the study did not discuss the accuracy of lesion targeting, they found the procedure to be a safe and effective means of achieving seizure freedom, with 15.4% of patients having mild memory impairment postoperatively [26]. Gonzalez-Martinez et al. published their operative technique whereby they utilized a robotic system to guide placement of a laser catheter into the target epileptogenic lesion located adjacent to the right frontal horn and caudate nucleus. Interestingly, this proof of concept arose from the authors' familiarity and success of using a robotic system for placement of sEEG electrodes at their institution [11]. Thus, it is feasible that as robots gain more widespread use and surgeons become more familiar with its use, robots will become more frequently used in a wider variety of stereotactic procedures.

Robotic Systems

Three major robotic systems are used commonly for intracranial applications. This section will focus on providing a brief overview of the workflow and capabilities of each robotic system intended for intracranial use.

Neuromate Robot (Renishaw)

The Neuromate robotic system by Renishaw (Wotton-under-Edge, UK) gained FDA approval

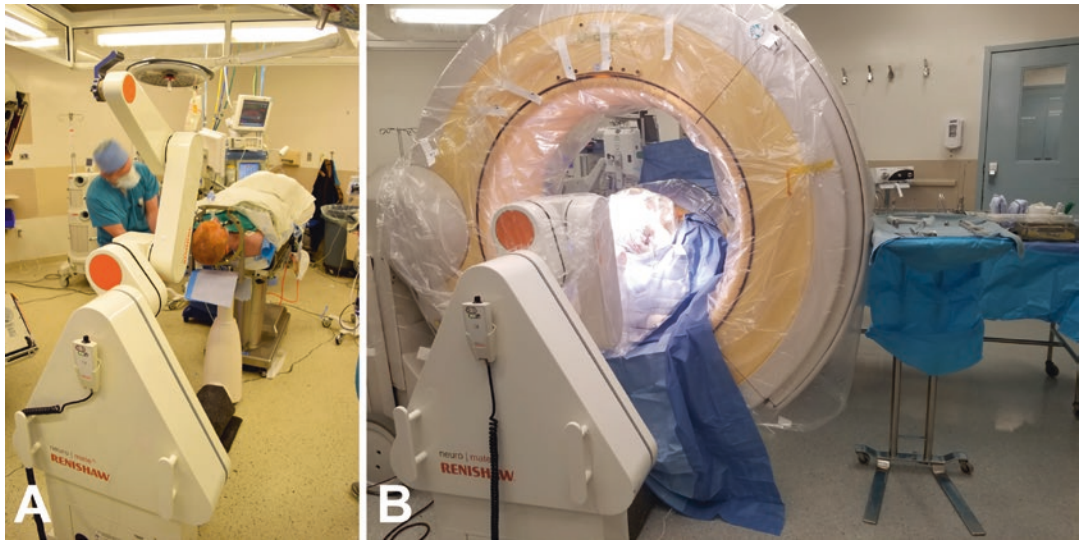

Fig. 2.1 The Neuromate robot gained FDA approval for intracranial procedures in 2014. (**a**) The patient is affixed to the robotic platform at a fixed length, and registration can be performed via frame-based or frameless applications. (**b**) An O-arm is often used in conjunction with the robotic system, which requires copious operating room space, and limits the space available for surgical staff while carrying out the procedure

for cranial procedures in 2014. The Neuromate robot provides surgeons five degrees of freedom and serves as a platform to carry out a broad range of intracranial stereotactic applications (Fig. 2.1).

Preoperative MRI scans, which may be supplemented with functional, vascular, or bone imaging, are used to plan trajectories to intracranial structures/lesions of interest in advance of the date of surgery. Registration can be performed using a conventional stereotactic frame fiducial box or a frameless registration module. When a fiducial box is utilized, the workflow consists of the following steps: the frame is affixed to the patient's head; a volumetric CT scan is acquired with the fiducial box on (usually in a diagnostic CT suite); the fiducial rods are automatically or manually localized using the planning software; once in the operating room, the patient's head is fixed directly to the base of the robot via the stereotactic frame, thereby securing the cranium at a fixed and predetermined length from the base of the robotic arm. The workflow for the frameless method is somewhat different. The frameless registration module consists of five synthetic round fiducial markers and carbon fiber rods that are attached to the laser holder and the robot arm. Once the patient is in the operating room, these fiducial markers are positioned closely to the head and an intraoperative CT scan is acquired. Finally, the stereotactic planning software identifies the center of each fiducial mark and registration is complete. When the robot is activated by the surgeon, the pre-entered coordinates direct the robotic arm into the correct entry point and target angle. The surgeon then inserts the leads to the targeted depth (this has also been calculated during preoperative planning, based on the distance from the target that the robotic arm is set), with the robotic arm providing improved control and stability. This process can be repeated, as necessary, for all leads that are intended to be implanted.

The entry- and target-point error rendered by the Neuromate robot has been studied and corroborated in a several studies investigating its use. In one study, entry-point error for frame-based application using the Neuromate robot was found to be 2 mm or less [22]. Frame-based target-point error has been reported to be between 0.86 and 1.77 mm, conferring a slightly higher accuracy compared to frameless application [18, 19, 27].

Renaissance Guidance System (Mazor Robotics)

The Renaissance guidance system from Mazor (Caesarea, Israel) provides the surgeon with six degrees of freedom. It was initially designed for use in spine surgery, gaining FDA approval for this application in 2004, before it was expanded for use for intracranial stereotactic procedures in 2012 (Fig. 2.2).

The Renaissance robot cannot be used in conjunction with traditional frame-based stereotaxy. Instead, a platform marker is mounted to the skull to serve as a surface marker, and an intraoperative CT scan is obtained. These images are then co-registered with a preoperative MRI, thereby allowing the software to interpret planned trajectories devised preoperatively in conjunction with the reference platform. Then, the guidance unit, which is the size of a beverage can, is affixed to the platform; the Renaissance system provides 360° working volume to access and execute various entry- and target-point trajectories, as needed. At the same time, this design serves as a limitation of the Renaissance system, as it cannot be used for sEEG implantation, owing to the limited reach of its robotic arm.

At the time of publication, there have been no peer-reviewed articles published on the accuracy of the Renaissance robotic system; however, in a white paper published in 2014 that outlined a retrospective case series of 20 subthalamic nucleus (STN) implants at a single institution, the mean target-point error was found to be 0.7 +/− 0.36 mm, lower than using a Leksell frame (1.7 +/− 0.6 mm) [28].

ROSA (Zimmer Biomet)

The ROSA robot from Zimmer Biomet (Warsaw, Indiana, USA) gained FDA approval for cranial surgery in 2010. The ROSA affords the surgeon six degrees of freedom. The ROSA robot is the only available system that can be used for endoscopy procedures in the United States, thereby

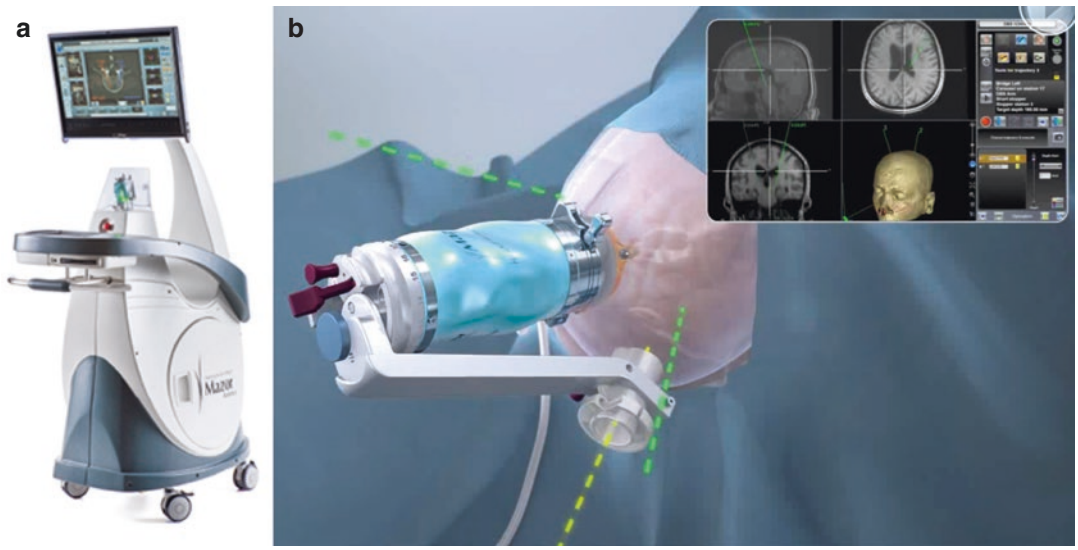

Fig. 2.2 The Renaissance robotic platform robot gained FDA approval for cranial surgery in 2012. (**a**) The Renaissance robotic platform provides its own software which can be used to co-register preoperative imaging with an intraoperative CT scan. (**b**) A small reference frame is affixed to the patient's skull, and then a guidance unit, which contains the robotic arm, is secured to the base. The small, frameless platform utilized by the Renaissance robot provides a 360 degree working volume, allowing for the execution of a wide range of planned trajectories

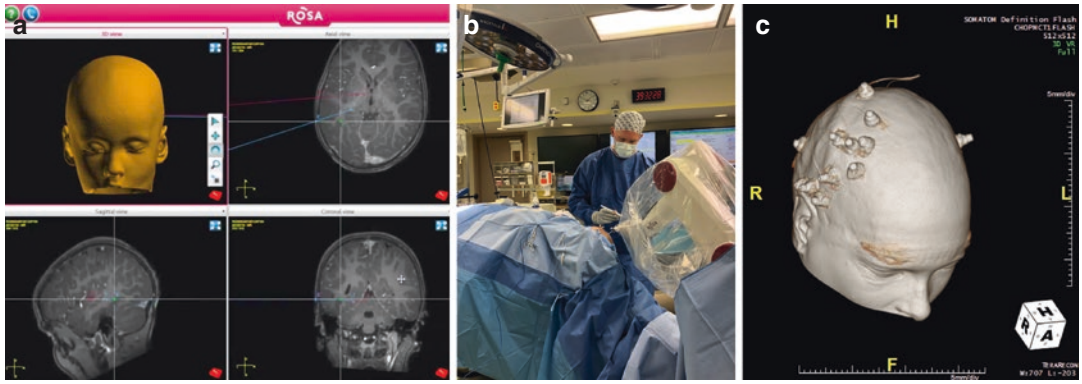

Fig. 2.3 The ROSA robot gained FDA approval for cranial surgery in 2010 and exists as a free-standing system. (**a**) The ROSA robotic system provides its own software that can be used to plan trajectories preoperatively. (**b**) In the operating room, the ROSA system provides haptic feedback while carrying out the surgical procedures, affording the surgeon to manipulate the arm directly to its desired location. (**c**) The ROSA robot has been used extensively for placement of sEEG leads

reducing the risk of traction-related injuries by providing a stable mechanical holder for the endoscope [29] (Fig. 2.3).

Like the other robotic systems, the surgeon plans entry-point and target trajectories preoperatively. The ROSA system also offers frame and frameless registration methods. For the frame-based approach, the robot captures points on a specific case that is attached to the frame. For the frameless approach, the ROSA system offers its own unique laser registration system that automatically captures individual points on the patient's face and forehead. After registration is complete, the robot can be locked in position at a fixed distance from the patient's skull, in order to maintain accuracy throughout the duration of the surgery. The ROSA system is the only robot that provides haptic feedback to the operator, thereby allowing the surgeon to directly manipulate the robotic arm in any desired direction, in a manner analogous to a stereotactic arc.

The ROSA robotic system has been shown to be a highly effective stereotactic system with a wide range of clinical applications, including LITT, responsive neurostimulation, and sEEG [30]. In one study evaluating sEEG electrode implantation, entry-point error was shown to be less than 2 mm in more than 90% of cases, and targeting error is less than 2 mm in 83% of cases [24]. Another single-institution case series evaluating placement of 222 sEEG leads in pediatric patients (mean 11.1 leads per patient) reported a mean radial error of 1.75 +/− 0.74 mm, with no associated postoperative complications from lead placement and monitoring. The mean total case time was 297.95 ± 52.96 minutes, and the mean operating time per lead was 10.98 minutes, with improvements in total (33.36 minutes per lead vs 21.76 minutes per lead) and operative (13.84 minutes vs 7.06 minutes per lead) case times/lead over the course of the study [31].

Advantages of Robots

The integration of robots into neurosurgical procedures offers many benefits for both the patient and the surgeon. Robots inherently provide their operator the ability to carry out repetitive tasks in a safe and efficient manner, provided that the plan programmed into the system is accurate. In a stereotactic surgery, each trajectory employed requires adjusting and conforming various coordinates in order to ensure its correct placement. As the number of trajectories increases, so, too, does the opportunity for error. Robots can decrease this risk of error by limiting the amount of human manipulation and transposition of the operator arm. Furthermore, by setting up the workflow such that the entry- and target-point

coordinates are entered into the robot preoperatively, the error associated with interpretation of frame coordinates during the surgical procedure itself is reduced as well.

The use of frame- and arc-based systems for stereotactic localization of target points does, in fact, confer a high degree of submillimeter precision, and this system has been used widely prior to the advent and adoption of surgical robots. However, their existing design in which the entry point of a trajectory is determined by the less precise arc and ring coordinates serves as a major limitation, owing to the higher degree of human interpretation inherently present while adjusting settings. There are a few studies that have compared the accuracy of entry-point error between frame-based systems and robotic systems, each of which has shown a comparable error rate (less than 2 mm in most cases), thereby showing its reliability in executing the planned trajectories [32].

Current frame- and arc-based systems limit the surgeon's choice of entry points. In sEEG implantations, for example, in which the trajectories are oriented in a lateral to medial, there is a need to be able to plan trajectories that start from a more caudal position. The Leksell frame offers an entry point within an arc of 170°, slightly better than utilizing a CRW frame, which confers an arc range of 120°. Depending on the configuration of the arc of the frame, collisions between the platform and the frame base limit the extent of trajectories that can be planned compared to those feasible with a robot.

Once a surgical team has learned how to effectively employ robotic systems to their surgical workflow, this should lead to decreased total surgical times. Indeed, the value of decreased OR time is not insignificant; one study cited an average decrease in OR time of over 3 hours when compared with traditional stereotactic frames [24]. Decreased length of surgery also serves to reduce surgeon fatigue and, ultimately, to minimize the risk of incurring adverse events, including postoperative infections.

An additional advantage to adopt robotics into neurosurgical practice is the ability to boost the commercial appeal of the hospital and perception of the procedure itself. The term "robot" leads patients to perceive that the procedure itself is cutting edge and to the reckoning that the hospital must be on the forefront of innovation and technology. A recent study quantified the effect of marketing robotic surgery as "innovative" or "state of the art" and found that greater than 30% of patients would choose to undergo a novel procedure over a conventional alternative if it was framed in this manner [33]. As such, if the safety and efficacy of both conventional and novel techniques are at least equal, providing the "state-of-the-art" robotic alternative may provide not only a marketing advantage but also greater confidence in the surgeon's capabilities.

Disadvantages of Robots

Although robots have been utilized with increased prevalence in neurosurgical practice, adopting their use presents its own set of challenges. The operating room itself has to be spacious enough to house the robot system and to accommodate the surgeons, anesthesiologists, nurses, techs, and company representatives involved in the case. Furthermore, there is a learning curve associated with the adoption of the robotic system in the operating room. For intracranial procedures such as DBS and sEEG electrode placement, the surgeons and the support staff must be familiar with the nuances of incorporating the robot into the surgical procedure, which includes sterile draping of the robot, understanding when and where the robotic arm should and should not move, and how to preserve efficient instrument passing between the operator and assistant(s) within the constraints of the limited workspace around the patient and robot position. Like any piece of complex machinery, robots are susceptible to malfunctioning, which can occur at any stage during a procedure. Furthermore, its calibration may become less precise over time, compromising its accuracy. As such, regular servicing and maintenance must be scheduled.

Frame-based systems offer a real-time verification of target engagement through the use of cross hairs and fluoroscopy. Robotic systems do not have similar accessories; thus, unless an

intraoperative CT scan is obtained, the plan executed by the robot is inherently reliant on the accurate imaging fusion and registration. Indeed, one may utilize a frame in conjunction with the use of a robot, thereby affording the surgeon to corroborate the target point manually by setting the coordinates of the frame, but doing so negates the increased efficiency conferred by utilizing a robotic system.

Purchasing a robotic system for use at a hospital carries a steep expenditure upfront and subsequent costs for proper maintenance and servicing of the robot and its software [34]. These costs, however, must be weighed against the savings achieved by reducing total operating room time. Three years after adopting a robot at our institution, our surgical time for placement of bilateral DBS leads and battery typically spans just over 2 hours, and the placement of 10–16 sEEG leads clocks in at around 3 hours, considerably shorter than when these procedures were carried out manually using frame systems. Thus, it is our belief that the adoption of robotic systems into an established neurosurgical practice confers a wide range of benefits and, despite the financial costs associated with it, provides great potential for its use in a variety of procedures.

Conclusions and Future Directions

In recent years, an increasing number of robotic systems have been designed for and integrated into neurosurgical practice. In the field of functional neurosurgery, which has historically relied on the use of stereotaxy for the localization of intracranial targets, the implementation of robotics in the operating room has provided surgeons the advantage of improved accuracy and safety, with less damage to critical surrounding structures, and, ultimately, favorable clinical outcomes.

As more neurosurgeons adopt the use of robotics, new advancements in the technology available will continue to take shape based on refinements and suggestions that serve to improve surgical workflow. As technology continues to improve, combined with the feedback provided by a larger cohort of neurosurgeons using robotic systems, the overall user experience will also continue to improve. For example, miniaturization of components will lead to a decreased robotic footprint and increased portability; and improved sensors and applicators will further enhance the capabilities and skills of surgeons using these systems. Such advancements will also improve the reliability and longevity of robotics, thereby reducing overall costs. Furthermore, improved user interfaces will make integrating robotics into neurosurgical practice more intuitive, with improved automation of perioperative tasks.

Finally, ongoing development may also push robots into a greater role in surgical education as robots with improved visual and haptic feedback can be used to create realistic surgical stimulators. There are a few published studies that suggest that training with robotic technology may shorten the learning curve for surgeon trainees and decreases the learning curve for the acquisition of new surgical skills [35]. The ability to use traditional frame-based methods in conjunction with certain robotic systems also ensures that trainees are still taught how to carry out procedures without robotic assistance and may lead to a greater appreciation of the benefits robots provide. Indeed, the integration of robots into the neurosurgical operating room offers many benefits for both the patient and the surgeon, albeit it requires the development of a new operative workflow. We believe that continued innovation and technical advancements will make robots more prevalent for use in a variety of surgical procedures and foresee its use becoming more mainstream in the field of functional neurosurgery.

References

1. Bourdillon P, Apra C, Leveque M. First clinical use of stereotaxy in humans: the key role of x-ray localization discovered by Gaston Contremoulins. J Neurosurg. 2018;128(3):932–7.
2. Gildenberg PL. Spiegel and Wycis - the early years. Stereotact Funct Neurosurg. 2001;77(1–4):11–6.
3. Nathoo N, Cavusoglu MC, Vogelbaum MA, Barnett GH. In touch with robotics: neurosurgery for the future. Neurosurgery. 2005;56(3):421–33; discussion −33.

4. Kwoh YS, Hou J, Jonckheere EA, Hayati S. A robot with improved absolute positioning accuracy for CT guided stereotactic brain surgery. IEEE Trans Biomed Eng. 1988;35(2):153–60.
5. Glauser D, Fankhauser H, Epitaux M, Hefti JL, Jaccottet A. Neurosurgical robot Minerva: first results and current developments. J Image Guid Surg. 1995;1(5):266–72.
6. Sharma M, Rhiew R, Deogaonkar M, Rezai A, Boulis N. Accuracy and precision of targeting using frameless stereotactic system in deep brain stimulator implantation surgery. Neurol India. 2014;62(5):503–9.
7. D'Haese PF, Pallavaram S, Konrad PE, Neimat J, Fitzpatrick JM, Dawant BM. Clinical accuracy of a customized stereotactic platform for deep brain stimulation after accounting for brain shift. Stereotact Funct Neurosurg. 2010;88(2):81–7.
8. Lozano AM, Mayberg HS, Giacobbe P, Hamani C, Craddock RC, Kennedy SH. Subcallosal cingulate gyrus deep brain stimulation for treatment-resistant depression. Biol Psychiatry. 2008;64(6):461–7.
9. Serletis D, Bulacio J, Bingaman W, Najm I, Gonzalez-Martinez J. The stereotactic approach for mapping epileptic networks: a prospective study of 200 patients. J Neurosurg. 2014;121(5):1239–46.
10. Lollis SS, Roberts DW. Robotic catheter ventriculostomy: feasibility, efficacy, and implications. J Neurosurg. 2008;108(2):269–74.
11. Gonzalez-Martinez J, Vadera S, Mullin J, Enatsu R, Alexopoulos AV, Patwardhan R, et al. Robot-assisted stereotactic laser ablation in medically intractable epilepsy: operative technique. Neurosurgery. 2014;10 Suppl 2:167–72; discussion 72–3.
12. Haegelen C, Touzet G, Reyns N, Maurage CA, Ayachi M, Blond S. Stereotactic robot-guided biopsies of brain stem lesions: experience with 15 cases. Neurochirurgie. 2010;56(5):363–7.
13. Lefranc M, Touzet G, Caron S, Maurage CA, Assaker R, Blond S. Are stereotactic sample biopsies still of value in the modern management of pineal region tumours? Lessons from a single-department, retrospective series. Acta Neurochir. 2011;153(5):1111–21; discussion 21–2.
14. Marcus HJ, Vakharia VN, Ourselin S, Duncan J, Tisdall M, Aquilina K. Robot-assisted stereotactic brain biopsy: systematic review and bibliometric analysis. Childs Nerv Syst. 2018;34:1299.
15. Holl EM, Petersen EA, Foltynie T, Martinez-Torres I, Limousin P, Hariz MI, et al. Improving targeting in image-guided frame-based deep brain stimulation. Neurosurgery. 2010;67(2 Suppl Operative):437–47.
16. Maciunas RJ, Galloway RL Jr, Latimer JW. The application accuracy of stereotactic frames. Neurosurgery. 1994;35(4):682–94; discussion 94–5.
17. Bjartmarz H, Rehncrona S. Comparison of accuracy and precision between frame-based and frameless stereotactic navigation for deep brain stimulation electrode implantation. Stereotact Funct Neurosurg. 2007;85(5):235–42.
18. von Langsdorff D, Paquis P, Fontaine D. In vivo measurement of the frame-based application accuracy of the Neuromate neurosurgical robot. J Neurosurg. 2015;122(1):191–4.
19. Varma TR, Eldridge P. Use of the NeuroMate stereotactic robot in a frameless mode for functional neurosurgery. Int J Med Robot. 2006;2(2):107–13.
20. Cardinale F, Casaceli G, Raneri F, Miller J, Lo Russo G. Implantation of stereoelectroencephalography electrodes: a systematic review. J Clin Neurophysiol. 2016;33(6):490–502.
21. Cossu M, Cardinale F, Colombo N, Mai R, Nobili L, Sartori I, et al. Stereoelectroencephalography in the presurgical evaluation of children with drug-resistant focal epilepsy. J Neurosurg. 2005;103(4 Suppl):333–43.
22. Cardinale F, Cossu M, Castana L, Casaceli G, Schiariti MP, Miserocchi A, et al. Stereoelectroencephalography: surgical methodology, safety, and stereotactic application accuracy in 500 procedures. Neurosurgery. 2013;72(3):353–66; discussion 66.
23. Abhinav K, Prakash S, Sandeman DR. Use of robot-guided stereotactic placement of intracerebral electrodes for investigation of focal epilepsy: initial experience in the UK. Br J Neurosurg. 2013;27(5):704–5.
24. Gonzalez-Martinez J, Bulacio J, Thompson S, Gale J, Smithason S, Najm I, et al. Technique, results, and complications related to robot-assisted stereoelectroencephalography. Neurosurgery. 2016;78(2):169–80.
25. Shukla ND, Ho AL, Pendharkar AV, Sussman ES, Halpern CH. Laser interstitial thermal therapy for the treatment of epilepsy: evidence to date. Neuropsychiatr Dis Treat. 2017;13:2469–75.
26. Calisto A, Dorfmuller G, Fohlen M, Bulteau C, Conti A, Delalande O. Endoscopic disconnection of hypothalamic hamartomas: safety and feasibility of robot-assisted, thulium laser-based procedures. J Neurosurg Pediatr. 2014;14(6):563–72.
27. Li QH, Zamorano L, Pandya A, Perez R, Gong J, Diaz F. The application accuracy of the NeuroMate robot–a quantitative comparison with frameless and frame-based surgical localization systems. Comput Aided Surg. 2002;7(2):90–8.
28. D V. Accuracy of Robotic Guided Subthalamic Nucleus Deep Brain Stimulation for Parkinson's Disease [White Paper]. 2014 [Available from: http://cdn2.hubspot.net/hub/276703/file-2632119232-pdf/docs/RoboticDBSWhitePaper.pdf?__hssc=245777499.12.1432246476596&__hstc=245777499.6da3b5cc931fc9e8e0fbe4303cef9c82.1398801594641.1432062359210.1432246476596.128&hsCtaTracking=7515dbde-0116-4cca-8d14-1c48129738e0%-7C5900ad8d-fe55-4f82-aecd-22c598c7d06b&t=1506606759766.
29. Hoshide R, Calayag M, Meltzer H, Levy ML, Gonda D. Robot-assisted endoscopic third ventriculostomy: institutional experience in 9 patients. J Neurosurg Pediatr. 2017;20(2):125–33.

30. Brandmeir NJ, Savaliya S, Rohatgi P, Sather M. The comparative accuracy of the ROSA stereotactic robot across a wide range of clinical applications and registration techniques. J Robot Surg. 2018;12(1):157–63.
31. Ho AL, Muftuoglu Y, Pendharkar AV, Sussman ES, Porter BE, Halpern CH, et al. Robot-guided pediatric stereoelectroencephalography: single-institution experience. J Neurosurg Pediatr. 2018:1–8.
32. Neudorfer C, Hunsche S, Hellmich M, El Majdoub F, Maarouf M. Comparative study of robot-assisted versus conventional frame-based deep brain stimulation stereotactic neurosurgery. Stereotact Funct Neurosurg. 2018;96(5):327.
33. Dixon PR, Grant RC, Urbach DR. The impact of marketing language on patient preference for robot-assisted surgery. Surg Innov. 2015;22(1):15–9.
34. Fiani B, Quadri SA, Farooqui M, Cathel A, Berman B, Noel J, et al. Impact of robot-assisted spine surgery on health care quality and neurosurgical economics: a systemic review. Neurosurg Rev. 2018;
35. Di Lorenzo N, Coscarella G, Faraci L, Konopacki D, Pietrantuono M, Gaspari AL. Robotic systems and surgical education. JSLS. 2005;9(1):3–12.

3 Intraoperative Magnetic Resonance Imaging and Computed Tomography

Francisco A. Ponce

Abbreviations

ANT	Anterior nucleus of the thalamus
CT	Computed tomography
DBS	Deep brain stimulation
FGATIR	Fast gray matter acquisition T1 inversion recovery
GPe	Globus pallidus externa
GPi	Globus pallidus interna
MER	Microelectrode recording
MRI	Magnetic resonance imaging
MTT	Mammillothalamic tract
STN	Subthalamic nucleus
UPDRS	Unified Parkinson's Disease Rating Scale
VIM	Ventral intermediate nucleus

Introduction

In most deep brain stimulation (DBS) centers today, the surgical approach toward appropriate lead placement has remained largely unchanged over the past two and a half decades. For the most part, the accuracy of lead placement is confirmed by intraoperative test stimulation and microelectrode recording (MER) based on the notion of neurophysiologically defined targets. Aspects of stereotactic surgery that have evolved include surgical planning using high-field preoperative magnetic resonance imaging (MRI) and confirmation of stereotactic accuracy using intraoperative imaging. With the use of surgical navigation for various neurosurgical procedures, intraoperative computed tomographic (CT) and magnetic resonance platforms have become increasingly ubiquitous. Such technologies have been increasingly adopted for surgical guidance and accuracy verification in stereotactic surgery, especially DBS implantation. This chapter reviews the basic principles of the use of intraoperative imaging for verification of stereotactic accuracy in deep brain stimulation surgery.

MRI-Based Anatomical Targeting

The identification of the stereotactic target in DBS surgery has traditionally been performed using Cartesian coordinates of the targeted structure relative to the midcommissural point on the basis of stereotactic atlases. Stereotactic reference imaging initially consisted of ventriculography [1]. Initial targeting was then adjusted for potential inaccuracies and intraoperative brain shift using MER to map the electrophysiological target, followed by test stimulation. Ventriculography has been largely supplanted by MRI, with associated adoption of "direct" targeting, wherein stereotactic targeting is based on direct visualization of the targeted structure on MRI.

The presumption that stereotactic accuracy can be used as a surgical end point that supersedes

F. A. Ponce (✉)
Department of Neurosurgery, Barrow Neurological Institute, St. Joseph's Hospital and Medical Center, Phoenix, AZ, USA
e-mail: Neuropub@barrowneuro.org

N. Pouratian, S. A. Sheth (eds.), *Stereotactic and Functional Neurosurgery*,
https://doi.org/10.1007/978-3-030-34906-6_3

awake testing or electrophysiological mapping is based on the following conditions: (1) the accurate and precise target can be identified on MRI, (2) there is little to no brain shift, and (3) registration and fusion software are accurate. There are many reasons why MER and test stimulation are useful. The brain may shift within the calvarium such that the area being targeted on MRI shifts relative to the skull in surgery. Pneumocephalus or head position may contribute to this. The degree to which brain shift occurs is not completely understood; however, if the brain does shift, then the benefit of demonstrating the lead accuracy on the basis of relative position to the skull using CT intraoperatively may be limited. Another factor is whether the target can be reliably identified purely with MRI; that is, is the target an anatomical or electrophysiological target? Several studies have demonstrated that anatomical location indeed matters, and experience over the past several decades has informed MRI targeting. The expanded use of MRI-based anatomical targeting in the 1990s was followed by the development of high-field MRI and the identification of specific sequences on which the targeted nuclei can be visualized. Four standard targets will be discussed here. Please refer to Chaps. 6 and 7 for more in-depth discussions of target imaging, including use of additional non-traditional sequences and network-based and connectomic target definition.

Subthalamic Nucleus

With subthalamic nucleus (STN) targeting, in particular, there is a growing body of literature reporting that with use of postoperative imaging after MER-based DBS, the optimal target for the clinically effective lead location is the dorsolateral portion of the STN volume [2–7]. Common sequences used for STN visualization include fluid-attenuated inversion recovery, T2-weighted fast spin echo, and susceptibility-weighted imaging (SWI) (Fig. 3.1). Sequences have been obtained in the coronal as well as the axial plane. On the axial plane, the STN can be visualized at the same plane as the red nucleus, lateral to the anterior border of the red nucleus. For targeting in the axial plane, the use of the red nucleus as an internal fiducial has been reported [8], whereby the anterior-posterior position is set at the anterior border of the red nucleus and the lateral position is set 3 mm lateral to the lateral border of the red nucleus. The position of the target can be further refined on the basis of direct visualization of the STN. Rather than targeting in the middle of the structural signal, the report on postoperative motor outcomes by Wodarg et al. [9] found that the lead location within the anterior or lateral quadrants of the MRI-defined STN was predictive of motor response.

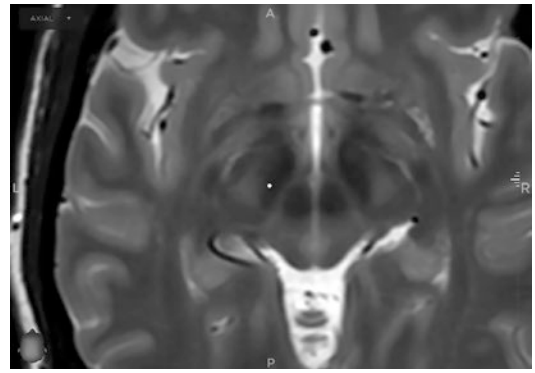

Fig. 3.1 T2-weighted fast spin echo magnetic resonance imaging sequence obtained on a GE 3-Tesla scanner shows the subthalamic nucleus (STN) at the level of the red nucleus. Stereotactic coordinates of the left STN target (marker) are (−10.75, −2.25, −4). (*Used with permission from Barrow Neurological Institute, Phoenix, Arizona*)

Globus Pallidus Interna

Sequences that delineate the globus pallidus interna (GPi) should clearly demonstrate the borders of the internal capsule and capture the gray-white matter differentiation that separates the GPi from the globus pallidus externa (GPe) as well as the internal laminae of the GPi. The proton density [10] and the fast gray matter acquisition T1 inversion recovery (FGATIR) [11] are two MRI sequences on which GPi is well visualized due to the clear demarcation between gray and white matter tracts (Fig. 3.2a). The study by

Starr et al. [2] reported motor outcomes following GPi DBS for dystonia and reported the electrode locations at the level of the intercommissural plane relative to the pallidocapsular border. By stratifying electrode location by extent of motor improvement, they reported a mean (standard deviation) distance from the lead to the pallidocapsular border of 3.6 (±1.2) mm in patients with greater than 70% improvement in the Burke-Fahn-Marsden Dystonia Rating Scale. This position typically falls between the GPe border and a visible internal lamina within the GPi (Fig. 3.2a) and approximately 4.5 mm anterior to the midcommissural point. Once a trajectory is set (starting with a parasagittal trajectory, or 0° from the midsagittal plane, and then moving lateral as needed to avoid a sulcus or the ventricle), the target may be projected to the bottom of the GPi, at the level of the dorsal surface of the optic tract (Fig. 3.2b).

Ventral Intermediate Nucleus

Currently, ventral intermediate nucleus (VIM) cannot be visualized on most MRI sequences. However, there have been reports of VIM visualization, including one that used proton density sequences [12] to identify an ovoid hypointensity as the VIM (Fig. 3.3). A combination of direct and indirect methods can be used for VIM DBS. Targeting at the midcommissural plane, the anterior-posterior distance is often selected as 25% of the distance from the posterior commissure to

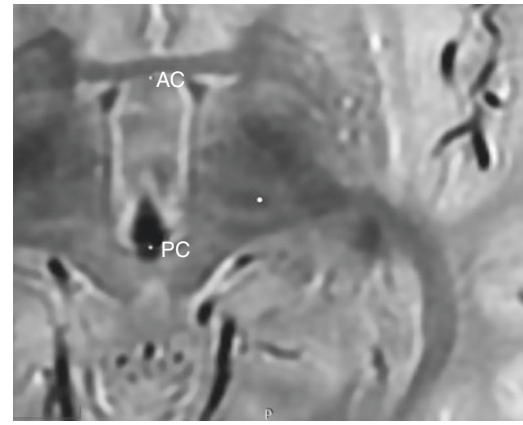

Fig. 3.3 Proton density magnetic resonance imaging sequence obtained on a GE 3-Tesla scanner shows the ventral intermediate nucleus (VIM). The lateral aspect of the VIM signal is targeted. The stereotactic coordinates at the marker are (15, −5.25, 0). This image shows a relatively wide third ventricle, and the target is approximately 4 mm from the internal capsule and 11.5 mm from the wall of the third ventricle. (*Used with permission from Barrow Neurological Institute, Phoenix, Arizona*)

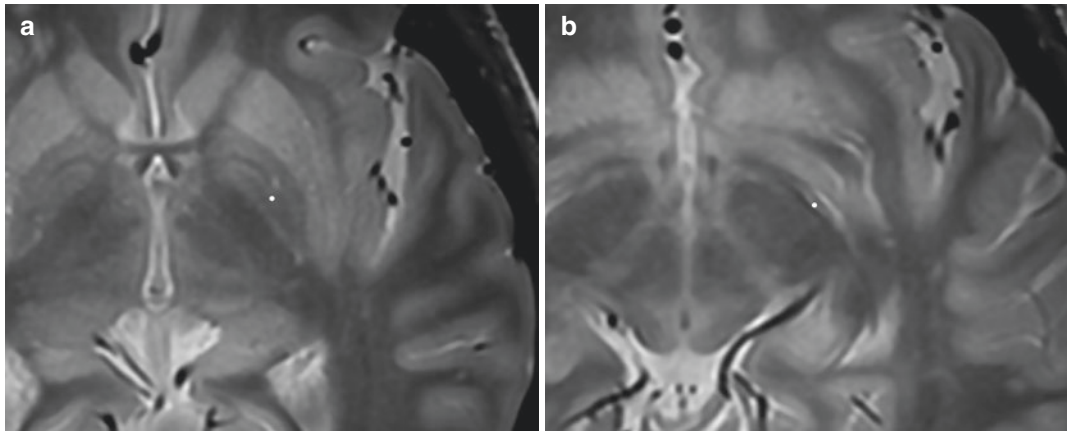

Fig. 3.2 (**a**) Proton density magnetic resonance imaging sequence obtained on a GE 3-Tesla scanner showing the borders of the globus pallidus interna, globus pallidus externa, and internal capsule. The marker is the target and the stereotactic coordinates are (21, 5, 1). (**b**) Following targeting at (or near) the midcommissural plane and setting the trajectory through the appropriate gyrus, the surgical plan is projected 6 mm, to the level of the optic tract; the stereotactic coordinates are (21.08, 2.1, −4.25). (*Used with permission from Barrow Neurological Institute, Phoenix, Arizona*)

the anterior commissure. Next, the lateral distance is approximately 10.5 to 11.5 mm from the wall of the third ventricle. Given that the upper extremities are represented in the lateral aspect of the thalamus, abutting the internal capsule, another measurement can be to ensure that one is 3–4 mm posteromedial to the internal capsule so as to avoid capsular adverse effects but not be too far away from the internal capsule. These steps can be combined with direct visualization for final target selection.

Anterior Nucleus of the Thalamus

The target most commonly used routinely for DBS for epilepsy is the anterior nucleus of the thalamus (ANT), which is part of the circuit of Papez and is connected to the mammillary bodies via the mammillothalamic tract (MTT). Similar to the GPi, the MTT is well visualized on MRI sequences with distinct gray-white matter differentiation, such as proton density and the FGATIR (Fig. 3.4a–c). ANT is located at the dorsal anterior medial corner of the thalamus, which becomes visible as one scrolls to the top of the MTT, and a surrounding lamina can be seen (Fig. 3.4d). The ANT abuts the ventricle so the trajectory is typically transventricular. Care must be taken to place all contact into the parenchyma, and the top of the MTT target is often selected as the target [13].

Brain Shift

Pneumocephalus and variations in head position are two factors that may contribute to the target moving from where it appeared to be when the surgical plan was made. Preoperative imaging is used in conjunction with MER and test stimulation to correct for this error [14].

The brain is floating in the calvarium in a pool of cerebrospinal fluid. Therefore, there is a concern that the position of the brain relative to the skull may change between the time that preoperative imaging used for stereotactic targeting is obtained and the time when the leads are surgically placed. Over the duration of a DBS operation, cerebrospinal fluid egress through the burr hole can result in pneumocephalus and brain shift (Fig. 3.5). This shift can result in the stereotactic target moving from where it appeared on preoperative imaging. One study of 20 patients undergoing DBS with intraoperative MRI reported on the extent of brain shift in deep structures and pneumocephalus, finding significant displacement of the anterior commissure but not of the posterior commissure with significant displacement of anatomical landmarks, although not in a consistent manner across patients [15].

Another factor that may influence brain shift is head position. During the preoperative imaging, the head is typically flat, whereas the head may be raised during the operation for the purpose of patient comfort or because of factors related to respiration. Elevation of head position may result in downward brain shift [16]. It is most likely that any phenomenon of brain shift is a function of the patient undergoing an operation and occurs due to factors such as pneumocephalus and head position. This implies that there may be steps that can be taken in surgery to minimize brain shift. In particular, the degree of pneumocephalus that has been seen in DBS surgery can be quite extensive (Fig. 3.5). However, in contrast with the experience with standard non-image-verified DBS surgery, where brain shift is accepted as a matter of course, pneumocephalus and associated brain shift of deep brain structures have been reported to be minimal when MRI-guided and MRI- and CT-verified DBS techniques are used [17–19]. A study of the use of intraoperative CT without test stimulation or MER among 371 patients showed that when compared with surgery without intraoperative CT and with test stimulation and MER, pneumocephalus was noted in 66% of patients who underwent DBS while awake (31 of 47 patients) and 15.6% of patients who underwent DBS with a general anesthetic (51 of 324 patients). The average volume of air was significantly higher among patients who underwent DBS while awake than among those who underwent DBS with a general anesthetic (8.0 vs. 1.8 mL). In addition, undergoing DBS while awake was

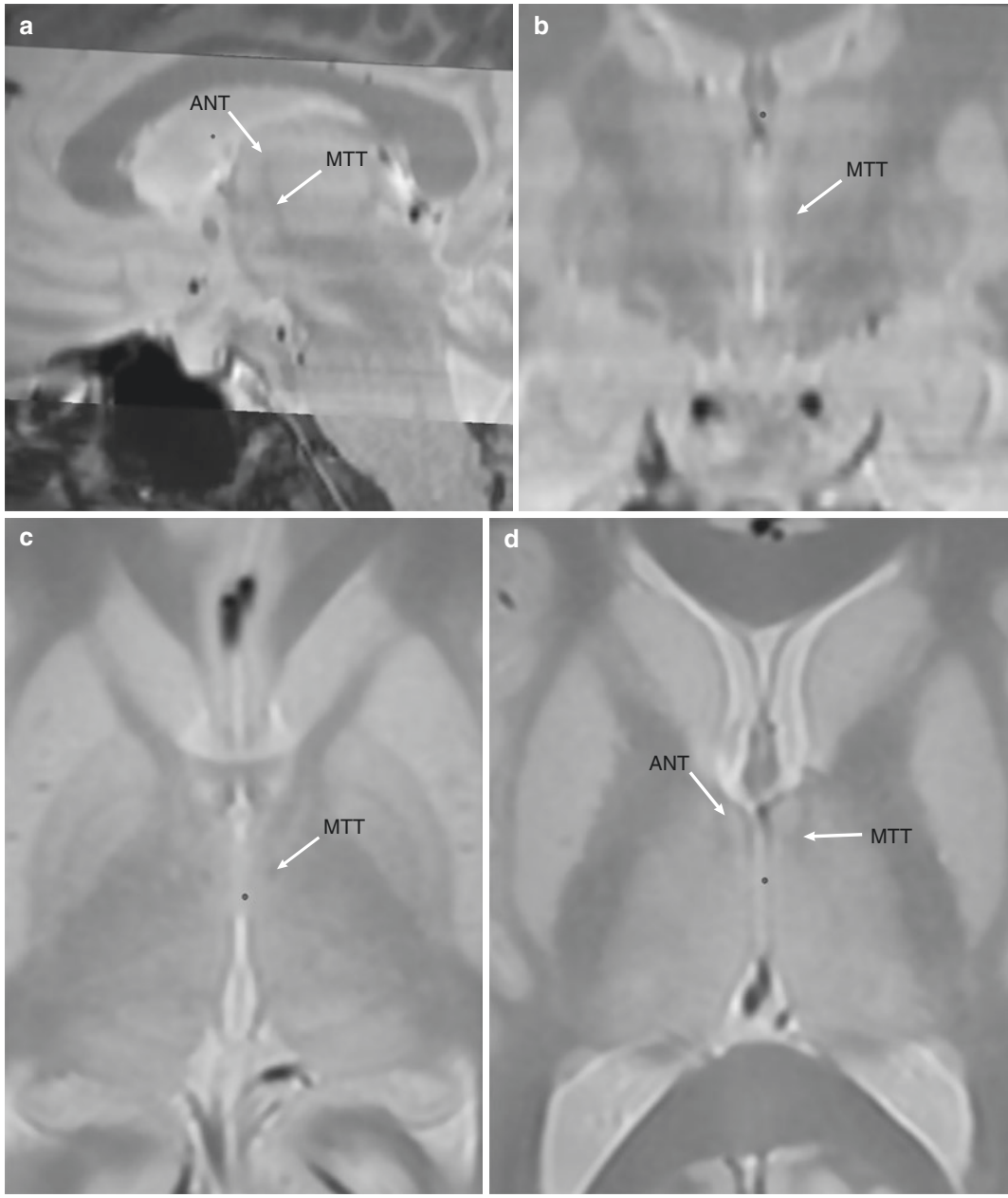

Fig. 3.4 Proton density magnetic resonance imaging sequence obtained on a GE 3-Tesla scanner showing sagittal (**a**), coronal (**b**), and axial (**c**) images of the mammillothalamic tract (MTT), which extends from the mammillary bodies to the anterior nucleus of the thalamus (ANT). The ANT is surrounded by a laminar border (**d**) and is located at the anterior, dorsal, and medial corner of the thalamus, abutting the lateral ventricle. (*Used with permission from Barrow Neurological Institute, Phoenix, Arizona*)

associated with significantly larger cortical brain shifts (5.8 vs. 1.2 mm) [1]. This may be related to longer durations of surgery when using MER and awake test stimulation as surgical end points for verification of target acquisition compared with when stereotactic accuracy is used as an end point. This may also relate to differential impact on CSF loss of spontaneous respiration compared

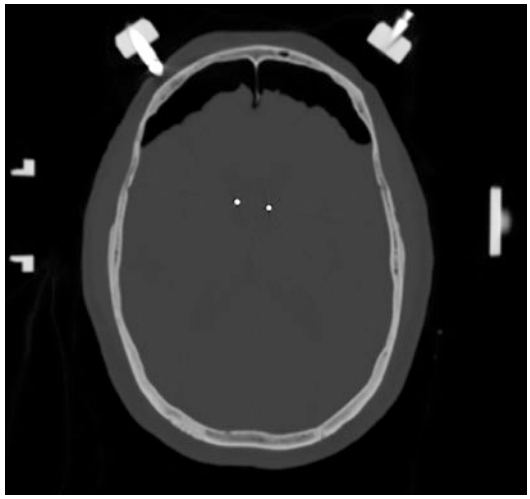

Fig. 3.5 Intraoperative computed tomography showing extensive pneumocephalus following bilateral deep brain stimulation lead placement. The arc supports are seen laterally and the pins are seen anteriorly. (*Used with permission from Barrow Neurological Institute, Phoenix, Arizona*)

to positive pressure ventilation, the latter of which is used with "asleep" DBS implantation.

If the targeted structures are directly visualized on intraoperative MRI, the need to factor in brain shift when assessing stereotactic error intraoperatively may be reduced. If image fusion is performed with the preoperative MRI, then brain shift becomes a factor because, although the calvarium may have accurately fused between the two data sets, the fusion algorithms do not account for changes in the brain tissue itself that may occur in the setting of brain shift.

Fusion Algorithms

The image registration (also referred to as fusion) software is critical in stereotactic neurosurgery. Even when a patient undergoes a preoperative MRI with the stereotactic frame and fiducial box in place, (1) coregistration is used to overlay the target-specific sequences (e.g., T2-weighted fast spin echo, proton density) onto the three-dimensional (3-D) reference sequence (e.g., SPGR or CT), or (2) if a higher-definition 3-Tesla MRI scan is desired for target visualization, it is often obtained prior to frame placement because most stereotactic frames are only approved for use in a 1.5-Tesla scanner, and pre- to post-frame placement MRI fusion is required. While a benefit of the use of MRI for the registration scan is that the image that is being used for formatting (i.e., delineating anterior commissure, posterior commissure, and orientation) is the same scan on which the stereotactic fiducials appear, the use of CT for the registration scan has certain advantages. The most noticeable advantage may be improved workflow on the day of surgery, because the duration of a registration CT is much shorter than the duration of a registration and planning MRI. There may also be some magnetic distortion when using an MRI for registration, although the effect of this distortion on accuracy has not been fully evaluated. It is important, however, for each institution to evaluate distortions and how this may impact systematic errors in stereotactic planning.

The registration scan is the image to which all other images are coregistered. This includes the targeting sequences as well as the intraoperative imaging to verify lead placement. Therefore, for this technology to be reliable, it is important that (1) the position of the lead in the brain is actually where the surgeon measures it to be on the intraoperative imaging and (2) if the lead appears to be off target, it is indeed off target. Otherwise, surgical decisions will be made on the basis of erroneous intraoperative data. Furthermore, every step in surgery has associated errors (e.g., frame error, coregistration error), such that there can be an additive effect of these errors whereby what one sees is not accurate.

There have been a number of studies that have evaluated the reliability of image coregistration, validating the accuracy of what one sees, and these have supported the reliability of fusion technology [20, 21]. A similar study validating lead placement as interpreted on a postoperative MRI has also been reported [22].

Of note, one purported advantage of interventional MRI, or placing the leads under direct MRI visualization, is that the influence of brain shift can be factored in because the position of the targeted structure is seen in real time. A distinction between MRI-guided versus MRI- or CT-verified DBS surgery has thus been made. Still, one must

consider potential advantages of each approach, including the quality of target visualization with constraints in imaging protocols imposed by intraoperative imaging.

Intraoperative MRI and CT

The global intraoperative imaging market is growing, largely because of increasing demand for this technology in spine surgery [23]. Many stereotactic surgeons may therefore already have intraoperative imaging available at their surgical center for other applications. Surgical planning using anatomical targeting depends on high-quality MRI, preferably on a high-field 3-Tesla MRI.

Intraoperative imaging can potentially be used for both the stereotactic registration scan and the scan with which to verify stereotactic accuracy. Stereotactic frame error is one factor that can influence stereotactic accuracy. An advantage of the use of intraoperative imaging modalities for obtaining the registration scan is that the patient does not need to move after the scan, which reduces the risk that the frame or trajectory device may move after image acquisition. The trajectory device, whether frame based or frameless, is placed, and the trajectory is set using stereotactic coordinates or navigation. This process depends on coregistration of the MRI on which the surgical plan was established with a stereotactic image used to register the patient. The reliability of coregistration depends on the internal algorithm of the software being used as well as the quality of the imaging. Additional error can come from motion artifact during the preoperative MRI, which may affect the quality of the fusion of the various image sets. There are various options for MRI or CT currently on the market for intraoperative use, some of which are described below.

Intraoperative CT

In the case of CT, there are many options for portable imaging modalities, and this portable imaging has translated to intraoperative imaging. The cross-utilization of CT imaging in spinal surgery and cranial surgery makes the availability of such imaging modalities at a given surgical center more likely. While intraoperative CT requires coregistration with preoperative images, there are studies that have shown noninferiority of CT to MRI for assessment of lead position [21, 24]. Several systems are commercially available, including those discussed below.

O-arm (Medtronic)

The Medtronic O-arm (Medtronic Inc., Minneapolis, Minnesota) is a mobile cone beam image acquisition system that is widely used in spinal surgery for stereotactic navigation of instrumentation. There are a number of studies in the literature reporting on the use of O-arm with DBS [25–28]. CT images are transferred directly to the surgical planning station, on which coregistration with a preoperative CT scan can be performed. That same preoperative CT scan will be coregistered to preoperative MRIs. The need for a preoperative CT scan is due in part to the lower image quality when visualizing the soft-tissue intracalvarial anatomy. While the O-arm is useful for bone-to-bone fusion and visualization of electrodes, verification that coregistration correctly matched the soft tissue or the ability to visualize an early hemorrhage intraoperatively may be suboptimal [29], although improved soft-tissue visualization has become available with the newest generation device. The current version of the O-arm has a high-definition 3D volumetric mode that allows for both 20-cm and 40-cm fields of view, the latter being capable of including the fiducial box for frame-based registration imaging (Fig. 3.6a) and the ability to leave the arc on the stereotactic frame when scanning after lead placement (Fig. 3.6b).

CereTom/BodyTom (Samsung)

The CereTom is an 8-slice small-bore portable CT scanner for the head that is 32 cm in diameter, and it has a 25-cm field of view. The BodyTom is

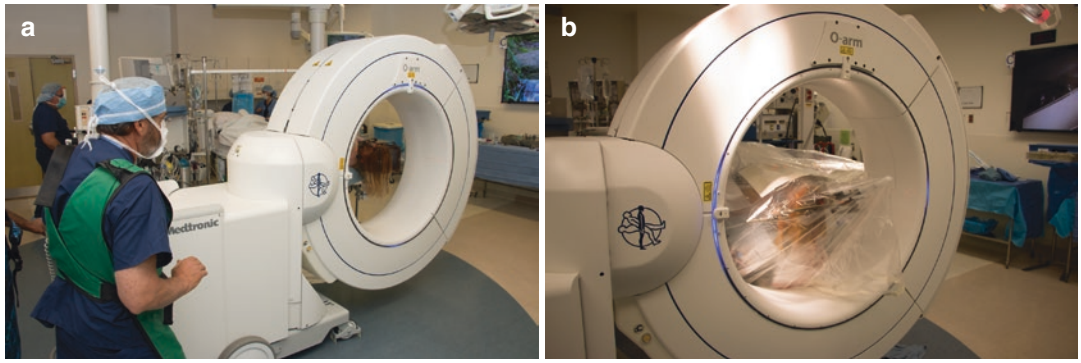

Fig. 3.6 (**a**) O-arm (Medtronic) used intraoperatively with the Leksell stereotactic frame with the fiducial box in place for acquisition of the stereotactic registration scan. (**b**) The O-arm is positioned for acquisition of the post-lead placement computed tomography. A transparent drape is placed over the sterile field, and the arc is still in place on the stereotactic frame. (*Used with permission from Barrow Neurological Institute, Phoenix, Arizona*)

a portable 32-slice full-body scanner with an 85-cm gantry and 60-cm field of view. The CereTom was initially introduced as an imaging option for hospitals without a CT scanner, to image patients in the intensive care unit who are too medically unstable for transport to the radiology department. It has recently also been placed into ambulances to create a mobile stroke unit. The use of the CereTom for DBS has been reported with frameless skull-mounted trajectory devices [30] and with the Leksell stereotactic frame [21]. In both of these settings, the CereTom was used for both the registration scan (Fig. 3.7a, c) and the verification scan following lead placement (Fig. 3.7b, d). While the bore accommodates the hardware used for DBS, it does so with very little room to spare. It can be a challenge to scan below the orbits, and this limit in the intracranial volume that can be scanned may also affect fusion accuracy. An advantage with the BodyTom is the larger gantry, which makes it usable in spinal surgery, therefore increasing the applications for its use in the operating room. It also creates more working area for intraoperative scans; in particular, the surgeon does not need to disassemble the lead delivery systems to fit the patient into the bore (Fig. 3.7e, f). However, the BodyTom has a much larger footprint, which may affect surgical workflow.

Airo (Brainlab)

The Airo has a 107-cm gantry opening with a 32-slice helical scan detector array. Similar to the BodyTom and the O-arm, the Airo is frequently used for spinal instrumentation. This system comes with an integrated base that includes an operating bed, and it is designed specifically for surgical applications. Similar to the O-arm, the manufacturer of the Airo also has a surgical planning navigation platform that is used for stereotactic neurosurgery and which is incorporated with the CT scanner in an integrated manner, as has been done for the spine. To date, no published reports of the use of the Airo for DBS have been identified, although the value and workflow should not fundamentally differ from those of other intraoperative CT imaging systems.

Intraoperative CT "on Rails" (IMRIS, Siemens)

In addition to the use of portable CT scanners as intraoperative CT scanners, there are also integrated systems that are built into the operating room. The CT is brought to the patient by sliding along rails that are mounted on the ceiling or embedded in the floor.

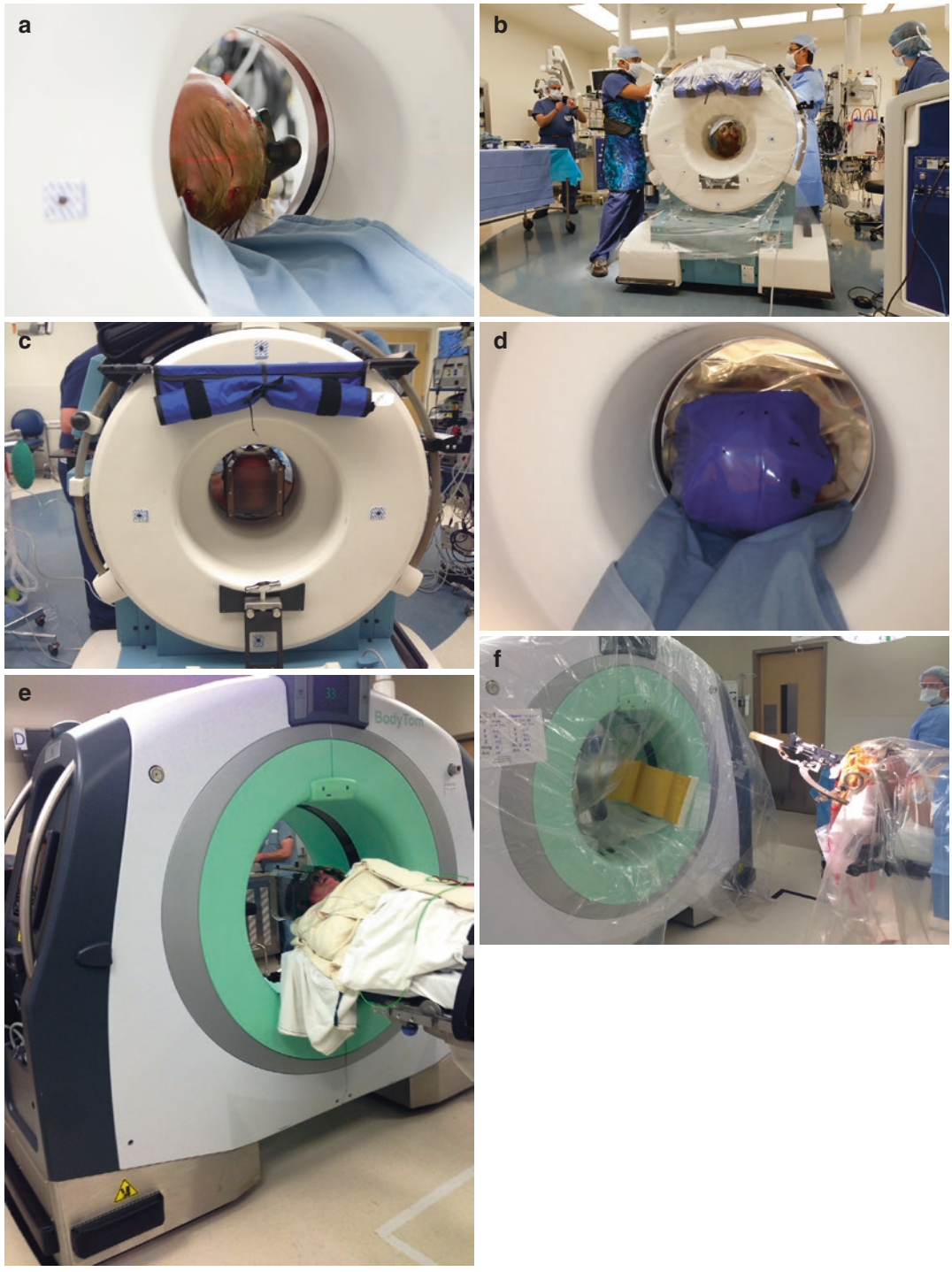

Fig. 3.7 CereTom (Samsung) being used with the NexFrame (Medtronic) for registration scan acquisition (**a**) and verification of stereotactic accuracy of lead placement (**b**). The CereTom can also be used with the Leksell frame for both registration (**c**) and lead verification scans (**d**). The BodyTom has a larger gantry and is also used for (**e**) registration scan and (**f**) lead verification scan. (*Used with permission from Barrow Neurological Institute, Phoenix, Arizona*)

Intraoperative MRI

MRI has also become more available in the neurosurgical operating suite and is primarily used for intraoperative imaging in the setting of neurooncology for intraoperative assessment of tumor resection. The typical setup includes either the patient being moved to the magnet for imaging or the magnet being moved along ceiling-mounted rails into the operating room to the patient (similar to the aforementioned CT systems). In both scenarios, the magnet is kept in a room adjacent to the operating suite. One of the purported advantages of the latter system (intraoperative MRI system; IMRIS) is that the patient need not be moved from the operating room during surgery, thus potentially enhancing workflow and safety [7]. A recent study reported on the use of the IMRIS for 33 patients and found that "frame-based DBS implantation under general anesthesia with intraoperative MRI verification of lead location is safe, accurate, precise, and effective compared with standard implantation performed using awake intraoperative physiology" [31].

Alternatively, DBS surgery has been performed with the patient in the bore of a diagnostic MRI, away from the operating room. Many of the initial reports of the use of the ClearPoint skull-mounted trajectory system for DBS lead placement describe procedures that were performed in this setting (i.e., "interventional" MRI rather than "intraoperative" MRI). Logistical issues here include the opportunity cost of using a diagnostic scanner for a surgical procedure (i.e., not being able to use the scanner for diagnostic purposes during the case and the subsequent limited accessibility of the scanner due to this limitation). In contrast to preoperative MRI (which cannot account for brain shift due to pneumocephalus) or intraoperative CT images (which need to be fused to the preoperative image sets, which is a step that may introduce fusion errors), the ClearPoint system uses real-time MRI to perform target selection and monitor lead placement [32]. So-called MRI-guided lead placement therefore has the advantage of detecting lead placement errors as well as other intraoperative complications, such as hemorrhages, at the time of lead placement, rather than after the lead has already been placed.

Stereotactic Accuracy as an End Point of Surgery

DBS surgery commonly consists of placing a lead through a 14-mm burr hole to a target approximately 75–85 mm deep into the skull. Typically, a stereotactic error of less than 2 mm is deemed to be necessary for successful therapeutic stimulation. A study reporting the management of referred DBS failures found that when lead location was judged quantitatively, 46% of referred patients had misplaced electrodes [33]. An earlier study [34] reported that in a review of the literature, the inaccurate placement of MER-guided lesions or DBS electrodes, as assessed on published MRI figures, was common. Quantitative analysis of the precise location of the lead following placement using postoperative imaging requires the surgeon to complete the operation and later return to the operating room, load the imaging onto the planning station, and merge the images before being able to document the stereotactic error. This is not a common practice; that is, before the adoption of intraoperative CT and MRI in the DBS surgery workflow, it was not a standard step to document stereotactic error intraoperatively on the basis of analysis of a post-implant image on a surgical planning station and compare final lead placement to the intended target. However, given the increasing availability and adoption of such technology, the standardization of this step into DBS surgery is possible and may offer advantages.

Regarding the growing use of intraoperative CT in spinal surgery for verification of hardware placement, one surgeon wrote that, "It is intuitive that our intraoperative threshold for revising a less than ideally placed implant would be much lower compared with when we are faced with the same information postoperatively" [35]. Were a misplaced lead to be identified on a postoperative CT or MRI, the surgeon would have to take the patient back to the operating room and reopen the

incision, whereas with an intraoperative CT or MRI, the incision is already open and the stereotactic devices are already in place for repositioning of the lead; intuitively, the surgeon is therefore more likely to correct for the error. The use of intraoperative imaging for verification of stereotactic accuracy is therefore important because (1) stereotactic accuracy matters and (2) the likelihood of correcting for an error is higher when such imaging is obtained and analyzed during the operation rather than after the operation.

Implications

The increased availability of intraoperative imaging in the neurosurgical operating room in the United States has provided a tool for the DBS surgeon to verify that the lead is indeed where the surgeon believes it to be. Earlier literature highlights that this is not a trivial point and that highly experienced surgeons at high-volume surgical centers send patients out of the operating room with leads that are not positioned where they were intended to be positioned despite the use of MER and test stimulation.

The reliability of acute intraoperative findings is unclear. With regard to MER, Bour et al. [36] found that the site of best MER activity did not necessarily correlate with the site that showed the best clinical response on intraoperative macrostimulation testing, and Wodarg et al. [9] found that MER was unable to distinguish differences in long-term clinical outcomes among patients but that lead location within the MRI-defined STN was predictive of motor response. Due to the acute microlesion effects that occur at the time of lead placement, a surgeon may observe a symptomatic response despite the lead not being at target, and this becomes evident when benefits wear off and become refractory to programing. Similarly, the surgeon may overinterpret the implications of observed side effects, reposition the lead away from the source of the side effects, and in the process reposition the lead away from the most efficacious area for symptomatic control. There may also be confounders, such as patient cooperation in surgery, including patients who do not fully wean from conscious sedation to the point where they can cooperate in surgery. This variability in the performance and interpretation of MER and test stimulation between surgeons and across surgical centers may limit the ability to standardize DBS surgery.

Stereotactic location of a lead matters and is used to evaluate DBS failures. Combining the importance of stereotactic location and the incidence of lead repositioning following awake surgery has led the field to consider the role of stereotactic accuracy as an end point, without the use of intraoperative awake test stimulation or MER. The decades of evaluating lead position coupled with high-field MRI that clearly delineates the borders of subcortical structures have increased the confidence in direct targeting and, when coupled with intraoperative imaging for verification of accuracy, make the assessment of stereotactic accuracy as a surgical end point feasible. If a surgeon hits his or her target but picks the wrong target, motor outcomes will be suboptimal. Therefore, a critical requirement is that, in addition to hitting the target, the surgeon is able to pick the right target on high-quality MR images.

Many studies over the past decade have assessed functional outcomes following image-verified DBS surgery without MER or test stimulation under general anesthesia (“asleep”) and shown good outcomes [37–39]. Other studies have compared outcomes to the standard (“awake”) technique and have not shown any difference [40, 41].

In one study, the investigators conducted a long-term and detailed follow-up study on the clinical effectiveness of treatment among 82 patients with Parkinson’s disease who were subjected to asleep STN-DBS treatment [37]. The results indicated that the total Unified Parkinson’s Disease Rating Scale III (UPDRS-III) score, without medication, improved from 68.78 before the operation to 45.89 at 1 year after the operation. Similarly, another study followed a cohort of 213 patients with Parkinson’s disease who underwent DBS surgery [42]. One-year follow-up data were obtained for 188 patients, and 5-year follow-up data were obtained for 65 patients.

The results indicated that the UPDRS-III score improved by 61% at 1 year and by 37% at 5 years. In a recent study, the efficacy of DBS surgeries performed by the same surgeon in the same surgical center under MER guidance with patients in the awake condition and with iCT guidance with patients in the asleep condition was reported [40]. The study showed that the UPDRS-III score improvement with stimulation did not differ between awake and asleep groups for the GPi or STN target. The percentage improvement in Parkinson's Disease Questionnaire 39 score and levodopa equivalent doses was similar for awake and asleep groups for both the GPi and STN cohorts. In another surgical center, the authors analyzed the outcomes of 30 patients who underwent asleep DBS and 39 patients who underwent awake DBS. The results demonstrated no difference in improvement of UPDRS-III or UPDRS-II [41].

In general, on the basis of the published results discussed above, the clinical outcomes for patients with Parkinson's disease are similar when final lead position is determined on the basis of test stimulation and MER versus stereotactic accuracy. Given factors such as surgical efficiency, patient comfort, and the variability in outcomes associated with the standard awake technique, reliance on intraoperative MRI and CT for verification of lead placement is likely to grow.

Conclusions

The growing availability of intraoperative MRI and CT in neurosurgery has implications for DBS surgery. Over the past 15 years, more surgical centers have incorporated intraoperative 3D imaging to assess stereotactic error at the time of lead placement, and the published reports of these practices have highlighted the importance of stereotactic accuracy in motor outcomes following surgery. Additional benefits include the use of intraoperative 3D imaging to obtain the stereotactic registration scan as well as improved surgical workflow. As intraoperative CT and MRI continue to be adopted in DBS surgery, surgical centers will continue to evaluate the question of whether stereotactic error is an additional data point to be considered intraoperatively along with MER and test stimulation, or whether stereotactic accuracy alone is sufficiently predictive of motor outcomes, such that intraoperative imaging may diminish the need for MER and test stimulation.

Acknowledgments The authors thank the staff of Neuroscience Publications at Barrow Neurological Institute for assistance with manuscript preparation.

Disclosures FAP is a consultant for Medtronic and Boston Scientific.

Financial Support Barrow Center for Neuromodulation

References

1. Ko AL, Magown P, Ozpinar A, Hamzaoglu V, Burchiel KJ. Asleep deep brain stimulation reduces incidence of intracranial air during electrode implantation. Stereotact Funct Neurosurg. 2018;96(2):83–90. Epub 2018/05/31.
2. Starr PA, Turner RS, Rau G, et al. Microelectrode-guided implantation of deep brain stimulators into the globus pallidus internus for dystonia: techniques, electrode locations, and outcomes. J Neurosurg. 2006;104(4):488–501. Epub 2006/04/20.
3. Saint-Cyr JA, Hoque T, Pereira LC, et al. Localization of clinically effective stimulating electrodes in the human subthalamic nucleus on magnetic resonance imaging. J Neurosurg. 2002;97(5):1152–66. Epub 2002/11/27.
4. McClelland S 3rd, Ford B, Senatus PB, et al. Subthalamic stimulation for Parkinson disease: determination of electrode location necessary for clinical efficacy. Neurosurg Focus. 2005;19(5):E12. Epub 2006/01/10.
5. Zonenshayn M, Sterio D, Kelly PJ, Rezai AR, Beric A. Location of the active contact within the subthalamic nucleus (STN) in the treatment of idiopathic Parkinson's disease. Surg Neurol. 2004;62(3):216–25; discussion 25–6. Epub 2004/09/01.
6. Lanotte MM, Rizzone M, Bergamasco B, Faccani G, Melcarne A, Lopiano L. Deep brain stimulation of the subthalamic nucleus: anatomical, neurophysiological, and outcome correlations with the effects of stimulation. J Neurol Neurosurg Psychiatry. 2002;72(1):53–8. Epub 2002/01/11.
7. Maks CB, Butson CR, Walter BL, Vitek JL, McIntyre CC. Deep brain stimulation activation volumes and their association with neurophysiological mapping and therapeutic outcomes. J Neurol Neurosurg Psychiatry. 2009;80(6):659–66. Epub 2008/04/12.

8. Andrade-Souza YM, Schwalb JM, Hamani C, et al. Comparison of three methods of targeting the subthalamic nucleus for chronic stimulation in Parkinson's disease. Neurosurgery. 2005;56(2 Suppl):360–8; discussion −8. Epub 2005/03/30.
9. Wodarg F, Herzog J, Reese R, et al. Stimulation site within the MRI-defined STN predicts postoperative motor outcome. Mov Disord. 2012;27(7):874–9. Epub 2012/04/21.
10. O'Gorman RL, Shmueli K, Ashkan K, et al. Optimal MRI methods for direct stereotactic targeting of the subthalamic nucleus and globus pallidus. Eur Radiol. 2011;21(1):130–6. Epub 2010/07/24.
11. Sudhyadhom A, Haq IU, Foote KD, Okun MS, Bova FJ. A high resolution and high contrast MRI for differentiation of subcortical structures for DBS targeting: the Fast Gray Matter Acquisition T1 Inversion Recovery (FGATIR). NeuroImage. 2009;47(Suppl 2):T44–52. Epub 2009/04/14.
12. Spiegelmann R, Nissim O, Daniels D, Ocherashvilli A, Mardor Y. Stereotactic targeting of the ventrointermediate nucleus of the thalamus by direct visualization with high-field MRI. Stereotact Funct Neurosurg. 2006;84(1):19–23. Epub 2006/04/26.
13. Cukiert A, Lehtimaki K. Deep brain stimulation targeting in refractory epilepsy. Epilepsia. 2017;58 Suppl 1:80–4. Epub 2017/04/08.
14. Montgomery EB Jr. Microelectrode targeting of the subthalamic nucleus for deep brain stimulation surgery. Mov Disord. 2012;27(11):1387–91. Epub 2012/04/18.
15. Matias CM, Frizon LA, Asfahan F, Uribe JD, Machado AG. Brain shift and pneumocephalus assessment during frame-based deep brain stimulation implantation with intraoperative magnetic resonance imaging. Oper Neurosurg (Hagerstown). 2018;14(6):668–74. Epub 2017/10/04.
16. Alterman RL, Weisz D. Microelectrode recording during deep brain stimulation and ablative procedures. Mov Disord. 2012;27(11):1347–9. Epub 2012/08/29.
17. Petersen EA, Holl EM, Martinez-Torres I, et al. Minimizing brain shift in stereotactic functional neurosurgery. Neurosurgery. 2010;67(3 Suppl Operative):ons213–21; discussion ons 21. Epub 2010/08/04.
18. Khan MF, Mewes K, Gross RE, Skrinjar O. Assessment of brain shift related to deep brain stimulation surgery. Stereotact Funct Neurosurg. 2008;86(1):44–53. Epub 2007/09/21.
19. Ivan ME, Yarlagadda J, Saxena AP, et al. Brain shift during bur hole-based procedures using interventional MRI. J Neurosurg. 2014;121(1):149–60. Epub 2014/05/03.
20. Shin M, Penholate MF, Lefaucheur JP, Gurruchaga JM, Brugieres P, Nguyen JP. Assessing accuracy of the magnetic resonance imaging-computed tomography fusion images to evaluate the electrode positions in subthalamic nucleus after deep-brain stimulation. Neurosurgery. 2010;66(6):1193–202; discussion 202. Epub 2010/05/25.
21. Mirzadeh Z, Chapple K, Lambert M, Dhall R, Ponce FA. Validation of CT-MRI fusion for intraoperative assessment of stereotactic accuracy in DBS surgery. Mov Disord. 2014;29(14):1788–95. Epub 2014/11/08.
22. Hyam JA, Akram H, Foltynie T, Limousin P, Hariz M, Zrinzo L. What you see is what you get: Lead location within deep brain structures is accurately depicted by stereotactic magnetic resonance imaging. Neurosurgery. 2015;11 Suppl 3:412–9; discussion 9. Epub 2015/06/19.
23. Grand View Research. Intraoperative imaging market size worth $4.2 billion by 2025; 2017. Available from: https://www.grandviewresearch.com/press-release/global-intraoperative-imaging-market.
24. Kremer NI, DLM O, van Laar PJ, et al. Accuracy of intraoperative computed tomography in deep brain stimulation-A prospective noninferiority study. Neuromodulation. 2019;22(4):472–7. Epub 2019/01/11.
25. Katati MJ, Jover VA, Ianez VB, et al. An initial experience with intraoperative O-Arm for deep brain stimulation surgery: can it replace post-operative MRI? Acta Neurol Belg. 2018. Epub 2018/11/09.
26. Frizon LA, Shao J, Maldonado-Naranjo AL, et al. The safety and efficacy of using the O-arm intraoperative imaging system for deep brain stimulation lead implantation. Neuromodulation. 2018;21(6):588–92. Epub 2017/12/22.
27. Carlson JD, McLeod KE, McLeod PS, Mark JB. Stereotactic accuracy and surgical utility of the O-arm in deep brain stimulation surgery. Oper Neurosurg (Hagerstown). 2017;13(1):96–107. Epub 2017/09/22.
28. Shahlaie K, Larson PS, Starr PA. Intraoperative computed tomography for deep brain stimulation surgery: technique and accuracy assessment. Neurosurgery. 2011;68(1 Suppl Operative):114–24; discussion 24. Epub 2011/01/06.
29. Servello D, Zekaj E, Saleh C, Pacchetti C, Porta M. The pros and cons of intraoperative CT scan in evaluation of deep brain stimulation lead implantation: a retrospective study. Surg Neurol Int. 2016;7(Suppl 19):S551–6. Epub 2016/09/02.
30. Burchiel KJ, McCartney S, Lee A, Raslan AM. Accuracy of deep brain stimulation electrode placement using intraoperative computed tomography without microelectrode recording. J Neurosurg. 2013;119(2):301–6. Epub 2013/06/04.
31. Matias CM, Frizon LA, Nagel SJ, Lobel DA, Machado AG. Deep brain stimulation outcomes in patients implanted under general anesthesia with frame-based stereotaxy and intraoperative MRI. J Neurosurg. 2018;129(6):1572–8. Epub 2018/01/27.
32. Ostrem JL, Ziman N, Galifianakis NB, et al. Clinical outcomes using ClearPoint interventional MRI for deep brain stimulation lead placement in Parkinson's disease. J Neurosurg. 2016;124(4):908–16. Epub 2015/10/27.
33. Okun MS, Tagliati M, Pourfar M, et al. Management of referred deep brain stimulation

failures: a retrospective analysis from 2 movement disorders centers. Arch Neurol. 2005;62(8):1250–5. Epub 2005/06/16.
34. Hariz MI, Fodstad H. Do microelectrode techniques increase accuracy or decrease risks in pallidotomy and deep brain stimulation? A critical review of the literature. Stereotact Funct Neurosurg. 1999;72(2–4):157–69. Epub 2000/06/15.
35. Rampersaud YR. Computed tomography and pedicle screws. J Neurosurg Spine. 2014;21(3):317–8. Epub 2014/06/14.
36. Bour LJ, Contarino MF, Foncke EM, et al. Long-term experience with intraoperative microrecording during DBS neurosurgery in STN and GPi. Acta Neurochir (Wien). 2010;152(12):2069–77. Epub 2010/10/16.
37. Harries AM, Kausar J, Roberts SA, et al. Deep brain stimulation of the subthalamic nucleus for advanced Parkinson disease using general anesthesia: long-term results. J Neurosurg. 2012;116(1):107–13. Epub 2011/10/18.
38. Hertel F, Zuchner M, Weimar I, et al. Implantation of electrodes for deep brain stimulation of the subthalamic nucleus in advanced Parkinson's disease with the aid of intraoperative microrecording under general anesthesia. Neurosurgery. 2006;59(5):E1138; discussion E. Epub 2006/12/05.
39. Chen SY, Tsai ST, Lin SH, et al. Subthalamic deep brain stimulation in Parkinson's disease under different anesthetic modalities: a comparative cohort study. Stereotact Funct Neurosurg. 2011;89(6):372–80. Epub 2011/11/23.
40. Chen T, Mirzadeh Z, Chapple KM, et al. Clinical outcomes following awake and asleep deep brain stimulation for Parkinson disease. J Neurosurg. 2018;130(1):109–20. Epub 2018/03/17.
41. Brodsky MA. Author response: clinical outcomes of asleep vs awake deep brain stimulation for Parkinson disease. Neurology. 2018;91(5):241–2. Epub 2018/08/01.
42. Fluchere F, Witjas T, Eusebio A, et al. Controlled general anaesthesia for subthalamic nucleus stimulation in Parkinson's disease. J Neurol Neurosurg Psychiatry. 2014;85(10):1167–73. Epub 2013/11/20.

Frameless Image Guidance in Stereotactic Radiosurgery

4

Nzhde Agazaryan, Stephen Tenn, Sonja Dieterich, Thierry Gevaert, Steven J. Goetsch, and Tania Kaprealian

Introduction

The principles of stereotactic radiosurgery (SRS) were developed by Dr. Lars Leksell and a group of colleague physicians and physicists in Sweden starting in the 1950s. SRS allows for the accurate and precise delivery of focused beams resulting in high doses of radiation at the focal volume. Early in the development of SRS, rigid frames fixed to skeletal anatomy served both to immobilize the patient and to localize the target with respect to the delivery of radiation treatment [1]. With this frame-based technique, target localization accuracy and precision relies critically on the geometric accuracy and the mechanical rigidity of the frames as well as the reliability of their fixation to patient anatomy. Once the frame is attached to the patient, the stereotactic coordinates of the target are determined from simulation CT or MRI scans. Treatment coordinates are then subsequently transferred to the treatment machine via the stereotactic frame.

An alternate approach to the frame-based stereotactic alignment employs imaging systems to detect the patients' position relative to the radiation treatment fields. Misalignments, when detected, are corrected prior to delivering the treatment or portions of the treatment. Although the term stereotaxy, which comes from the terms *stereo* meaning "solidity" and *tactile* meaning "touch," used to refer to techniques with geometrically fixed frames with known relationship with the internal anatomy of the patients, this term continues to be used with the methods employing image guidance as the means for localization. Within radiation oncology, the use of imaging to guide and verify placement of treatment fields is not a new concept. In the early 1980s, Verhey and coauthors described the use of pretreatment and posttreatment radiographs of patients in the treatment position to analyze intra-treatment movement during proton radiotherapy [2]. More recently, the advent of electronic X-ray image detection, such as electronic portal megavoltage (MV) imaging and planar kilovoltage (kV) imaging, has made nearly real-time automatic detection and correction of patient position with image guidance feasible. The real-time image guidance process typically goes as follows: initial patient alignment to the treatment

N. Agazaryan (✉) · S. Tenn · T. Kaprealian
Department of Radiation Oncology, University of California, Los Angeles, Los Angeles, CA, USA
e-mail: nagazaryan@mednet.ucla.edu

S. Dieterich
Department of Radiation Oncology, University of California Davis, Sacramento, CA, USA

T. Gevaert
Department of Radiotherapy, Universitair Ziekenhuis Brussel (UZB), Brussels, Belgium

Vrije Universiteit Brussel (VUB), Brussels, Belgium

S. J. Goetsch
Medical Physics, San Diego Gamma Knife Center, La Jolla, CA, USA

N. Pouratian, S. A. Sheth (eds.), *Stereotactic and Functional Neurosurgery*,
https://doi.org/10.1007/978-3-030-34906-6_4

isocenter is performed based on external landmarks, and this is followed by imaging that can detect either the target directly or surrogate anatomy closely associated with the target. These "real-time" or "on-line" images are then compared to reference images that would be expected when the patient is perfectly aligned. The reference images are referred to as digitally reconstructed radiographs (DRR). The comparison, or image registration, procedure detects and quantifies any misalignment between the two sets of images and consequently determines patient misalignment from correct treatment position. Target misalignment can then be corrected by adjusting the patient position or by moving the treatment beam.

Image guidance technologies decouple the patient alignment process from the immobilization devices. Because of this, patients can be immobilized with more comfortable and noninvasive methods. Examples are molded thermoplastic mask in the treatment of cranial targets and vacloc bags for spine targets. While these devices are less rigid and allow more patient movement than a traditional localization frame, this disadvantage can be partially compensated by more frequent imaging and repositioning of the patient during treatment delivery. On the other hand, these devices can be reused for multiple treatments (fractions) following a single planning CT or MRI scan facilitating multisession radiosurgery, more readily allowing for multifraction radiosurgery or staged radiosurgery.

In this chapter, we consider frameless treatment and imaging technologies associated with three widely used radiosurgery treatment delivery systems: CyberKnife, Leksell Gamma Knife Perfexion, and gantry-mounted linac technologies. There exist other commercial frameless SRS and IGRT systems (e.g., MVCT on Tomotherapy and MRI on ViewRay and Elekta Unity). However, they are not routinely used for cranial stereotactic therapy, and the paucity of experience with these systems specific to radiosurgery at the time this is written leads us to exclude them from extensive discussion in this chapter.

CyberKnife Technology

From its inception, the CyberKnife (CK) system was developed as a dedicated frameless image-guided radiosurgery system [3]. With this system, the therapeutic radiation is delivered to the patient with a compact 6 MV linear accelerator that is mounted to a robotic arm (Fig. 4.1). Gross patient positioning is performed via a movable couch top. Minor corrections for small patient and organ movements are subsequently accomplished by the robotic arm, adjusting the position of the treatment beams. The robot can correct for patient misalignment up to ±10 mm in translation, ±1.5° in pitch and roll, and ±3° in yaw. Image guidance is foundational to this system, and the use of the robotic arm allows correction to the treatment beams if patient misalignment is detected via stereoscopic X-ray imaging.

Description of Imaging System

The CyberKnife imaging system consists of two oil-cooled X-ray cameras mounted to the ceiling and two complimentary image detectors mounted to the floor. The X-ray cameras operate within an energy range of 80 kV–120 kV. In clinical practice, cranial imaging is typically performed at 100 kV, and spine imaging is typically performed approximately 120 kV. The image detectors are amorphous silicon flat panels. In the current configuration, they are installed below the floor with a flush cover (Fig. 4.1). The central axes of each X-ray camera cross at a 90-degree angle, and the crossing point is within ±1 mm tolerance from a physical point in the room defined as the machine's isocenter.

Tracking Algorithms

Several imaging and registration algorithms are available to detect and track the target position. The cranial tracking algorithm is used for SRS targets inside the cranium, as well as C1 to C2 spine levels. The spine tracking algorithm is used for all spine targets starting approximately at C3

Fig. 4.1 CyberKnife system configuration showing the two X-ray cameras mounted on the ceiling. The two amorphous silicon detector imagers are embedded in the floor. (Image courtesy of Accuray Incorporated – © 2019 Accuray Incorporated. All Rights Reserved)

to C4 and inferior. If the skeletal anatomy is too severely eroded to clearly detect in the X-ray images, the cranial or spine tracking algorithms may fail to reliably localize the targets. In these cases, metal fiducial markers can be implanted near the target tissue, and a fiducial tracking algorithm is available for tracking these markers.

Cranial Tracking Algorithm

The cranial tracking algorithm was developed specifically to align cranial targets to the treatment beams. The algorithm automatically registers stereoscopic X-rays of the patient's head with DRRs prospectively generated to represent possible patient setup translational and rotational deviations from the planned treatment position. To generate the DRRs, the treatment planner will select an imaging isocenter location within the simulation CT. This point represents an ideal alignment location for the patient's head within the field of view of the image guidance X-ray cameras. Once the imaging isocenter has been selected, the software creates a matrix of DRR images to represent a range of potential positions the patient's head may be in at the time of treatment. This includes in-plane translations and out-of-plane rotations. The matrix contains fewer DRRs for positions far away from the setup goal. Once the patient has been grossly aligned to the image isocenter, a set of orthogonal images is acquired. The 2D-3D registration algorithm performs an iterative registration of these X-ray images to DRRs from the matrix library to find the closest match. In this way, patient's offset in both translation and rotation is determined from the best matched DRR. Phantom studies have shown that this method can align a rigid phantom within approximately 0.3 mm and 0.3 degrees of an alignment performed with fiducial alignment, considered as the gold standard for comparison purposes [4].

With the CyberKnife system, the position of the imaging isocenter is independent of the target's location. This is due to the robot's freedom of movement in directing treatment beams. For cranial tracking, the patient is typically positioned such that the isocenter is located along the patient's midline axis to maximize the projected field of view around the cranium. This position provides about 10–20 mm of margin, or what is known as "flash," anteriorly and superiorly around the patient's head in the images. For adults, this isocenter location is located along the cranial midline at the superior aspect of the hypothalamus, approximately 3 cm superior to the pituitary gland. This placement of the isocenter maximizes imaging and localization accuracy and robustness. For pediatric patients, it is important to set the inferior border of the images no lower than the upper incisors. Because the mandible is a mobile structure relative to the rest of the cranium, if too much of the mandible is

visible in the image, especially for anesthetized pediatric patients, its change in position relative to the target location may affect image registration accuracy which in turn will affect beam positioning accuracy.

Spine Tracking Algorithm

In the early days of CK spinal radiosurgery, gold fiducials were implanted in the spine as localization surrogates [5, 6]. While accurate spinal target alignment can be achieved with this method, it required invasive placement of the fiducial markers in the vertebral bodies close to the target location. The introduction of high-density fiducial markers can also cause artifacts on the simulation CT that hinder target identification. In 2006, Fu and Kuduvalli described an image processing method to enhance skeletal features in DRRs of the spine [7]. Generation of these enhanced DRRs enabled the development of a robust spine tracking algorithm which eliminated the need for fiducial placement in most patients. The spine tracking algorithm generates the enhanced DRRs followed by an iterative 2D-3D registration of X-rays to DRR as described for the cranial tracking algorithm. This algorithm has replaced fiducial tracking for spine SRS except in cases where the vertebral body bone density is extremely low and skeletal features are compromised in DRR generation.

Image Guidance Quality Assurance Tests

During installation, the imaging system is mechanically aligned and calibrated using a special jig. The precision of the imager alignment ability is then tested using the CyberKnife robot itself as a high-precision phantom positioning device. An anthropomorphic head and cervical spine SRS phantom (CIRS, Norfolk, Virginia) is mounted to the robot collimator assembly. The robot then positions the phantom according to three test motion tables, which the imaging system has to accurately identify [4].

Imaging Frequency and Clinical Accuracy

The thermoplastic masks used to immobilize patients with cranial targets and the vacloc moldable cushions used to immobilize patients with spinal targets allow small amounts of patient movement (typically up to 3 mm). This movement can occur during treatment and can affect dose placement. In order to mitigate the negative effect of patient movement on the dose placement, the patient is imaged during treatment. If movement from the ideal treatment position is detected, the treatment is corrected. A study of patient motion during CyberKnife treatments for cranial and spinal targets was performed by Murphy and coworkers [8]. They found that imaging approximately once per minute would result in less than 2% of the dose to be misdirected by more than 2 mm for the patients they studied.

On the CyberKnife imaging frequency can be set by the treatment team for each patient treatment. The treatment delivery software allows images to be taken every n-th beam, with typical imaging frequencies being every 3–5 beams in clinical practice. Factors determining the image frequency for a given patient include proximity of the target to critical structures, patient-specific tendencies to move, length of treatment, and imaging dose.

In-Room and Gantry-Mounted Imaging Technology

The development of localization methods using optical image guidance [9], stereoscopic X-ray imaging [10], optical guidance in combination with stereoscopic X-ray images [11–13], or cone-beam CT (CBCT) [14, 15] has provided the foundation for frameless stereotactic radiosurgery deliveries on traditional gantry-mounted linear accelerators. In this section, we discuss the ExacTrac system and CBCT as they relate to SRS treatment alignment.

ExacTrac

The current ExacTrac system (Brainlab AG, Munich, Germany) integrates infrared (IR) tracking with oblique stereoscopic kV X-ray imaging for fast and accurate patient positioning [12, 16]. The IR component consists of an IR illuminator and a camera mounted to the ceiling above the distal end of the treatment couch. IR reflective marker balls attached to the patient or to the treatment couch via arrays can be tracked by the cameras with positioning uncertainty of 0.3 mm and 20 Hz sampling frequency [17]. It is used for initial patient positioning and also for tracking and guiding couch movement when adjustments to patient position are required. It can also be used for real-time monitoring of patient position if markers are placed on the patient. The stereoscopic X-ray imaging component utilizes dual kilovolt (kV) X-ray cameras (each composed of a source and a flat panel imager). On the ExacTrac system, the X-ray sources are located in the floor next to the linac gantry, and the flat panel imagers are mounted to the ceiling above the treatment couch. The camera axes are not orthogonal as with the CyberKnife system, but intersect at isocenter with a 62° angle. Similar to the CyberKnife X-ray cameras, these are used for position detection and verification. Unlike CyberKnife, corrections to target position on gantry-mounted linac delivery systems are made by shifting the patient via the treatment couch. The IR system guides these movements more accurately than the couch motors can by themselves.

The ExacTrac system calculates an image registration that corrects for all six degrees of freedom (DOF) (three translations and three rotations) of the patient's current position to the planned position. The ExacTrac method does not require pre-generated DRRs. Instead, the registration process proceeds in nearly real time with the reference 3D image set being iteratively translated and rotated by small amounts [18]. During each iteration, a pair of DRRs is generated and compared with the acquired images. The algorithm proceeds until the generated DRRs match the acquired images within a tolerance limit. The orientation of the CT set that generated the matching DRRs represents the current orientation of the patient, and the set of translations and rotations needed to bring the patient into correct alignment are fully determined. Because the algorithm registers two-dimensional (2D) localization X-ray images to 3D CT images, it is described as a 2D-3D image registration technique.

The accuracy of registration is influenced by image quality and differences in anatomy at the time of treatment. Therefore, the registration result must be carefully reviewed (visual inspection) by the treatment team before delivering the treatment. Tools to increase the robustness and accuracy of the registration include restricting the registration to a specific region of interest (ROI) by masking areas of the planar images to exclude potentially confusing structures (e.g., the mandible, upper cervical spine, or IR reflectors) that may not correlate as well with the target position (Fig. 4.2). Alternately, the volume from which the DRR is generated can be limited to exclude these structures from appearing in the DRRs themselves. Ideally, regions in close proximity to the target location will be used for the registration, and those further away, especially mobile structures, can be excluded [19].

Next-Generation ExacTrac® Dynamic

Next-generation ExacTrac is named ExacTrac® Dynamic and combines surface, thermal, and X-ray-based tracking (Fig. 4.3). A new thermal-surface camera technology is implemented in parallel with the real-time X-ray tracking. This system enables nearly real-time internal anatomy verification at wide range of couch position and gantry angles. It allows for immediate and accurate shift calculation, beam hold, and repositioning anytime during treatment.

The 4D thermal camera creates an accurate and reliable hybrid thermal surface by correlating the 3D heat signature to the reconstructed 3D surface of the patient. The system appears to be resistant to issues caused by room lighting, reflections, skin tone, or clothing. Additionally, incorporating it with a single camera mount eliminates gantry-related blocking.

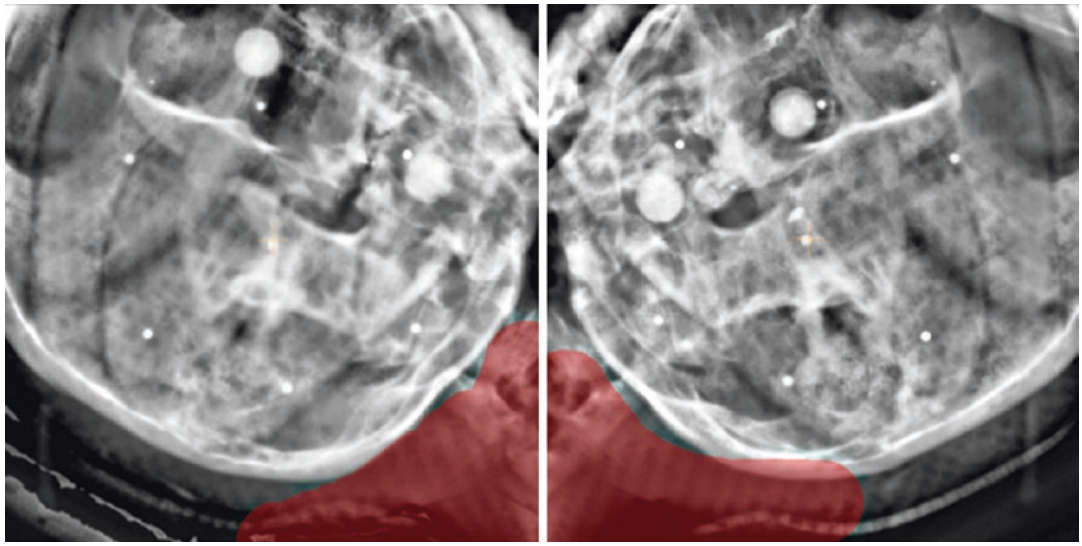

Fig. 4.2 2D-3D registration of X-rays with dynamically generated DRR. The cervical spine is masked (*red*) to exclude from the registration process

Fig. 4.3 Next-generation ExacTrac® Dynamic combines surface, thermal, and X-ray-based tracking. (Image courtesy of Brainlab AG, Munich, Germany)

ExacTrac Dynamic imaging is specifically designed to address the challenges associated with motion management by using X-ray technology to track moving targets. It has larger panels to visualize larger area and more intuitively interpret X-ray images.

Accuracy Assessment

The accuracy of the ExacTrac image registration algorithm has been investigated by performing registration calculations after introducing known translational (up to 30.0 mm) and rotational (up to 4.0°) errors on anthropomorphic phantoms [12]. Hidden target tests have also been used to assess the setup accuracy potential of the system [16]. In this test, a high density target embedded in an anthropomorphic phantom is aligned to the treatment machine isocenter via the IGRT system while masking the target itself from the registration procedure. The treatment beam is then used to image the target and thus determine how accurately the target is placed. Average deviations between known translational displacements and calculated displacements varied from 0.3 to 0.6 mm, while the average deviation between rotations was less than 0.2 degrees.

Image-guided beam alignment accuracy can be significantly influenced by the spatial resolution of the reference CT study. Yan et al. [13] reported that the CT slice thickness has a significant effect on the positioning accuracy of the ExacTrac system and stated that a thin-slice CT image enhances the positional accuracy. Murphy et al. [20] have also demonstrated that the precision of image-guided head localization improves by a factor of two when the CT slice thickness is reduced from 3.0 to 1.5 mm. Clinically, the CT image resolution used for generating treatment plans and subsequently for generating DRRs used in the image guidance process is not coarser than 1.5 mm in the slice thickness direction.

Gantry-Mounted Cone-Beam CT

Another commonly employed image-guided positioning approach used with gantry-mounted linacs for radiosurgical procedures is cone-beam CT (CBCT) (Fig. 4.4). With this technique, the kV X-ray source and flat panel imager are both mounted to the gantry, and the image reconstruction data are acquired in the form of a sequence of planar images as the gantry rotates around the patient. Because the image data comes from a wide flat panel detector, the X-ray beam generating the images is in the geometry of a cone beam rather than the fan beam of a traditional CT scanner. A cone-beam reconstructed image will therefore have worse image quality when compared to a traditional CT. However, the advantage of the gantry-mounted CBCT is that a high-resolution three-dimensional set of information is acquired with the patient on the treatment machine immediately prior to treatment delivery. In certain cases, for example, lytic spinal lesions, the increased tissue contrast over planar kV imaging can make this technique ideal for aligning the target to the treatment beams with little ambiguity in the registration.

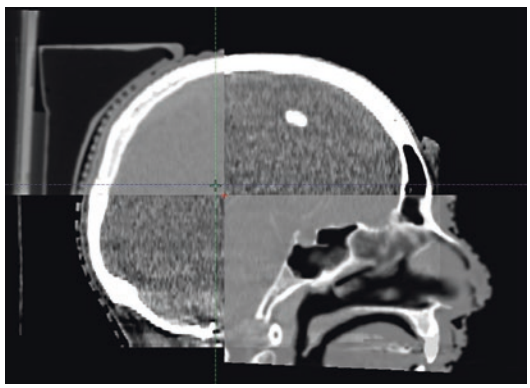

Fig. 4.4 3D-3D matching of the CBCT image with the simulation CT

Image registration between the planning CT and the CBCT is able to make use of 3D information from both image sets regarding the difference in patient position. This is, therefore, known as 3D/3D image registration. Because of its increased ability to visualize soft tissue contrast CBCT is able to more directly detect the tumor and therefore to detect difference in tumor position between the planning CT and the position at the time of treatment than 2D planar imaging. Sub-pixel size setup errors can be correctly determined, which makes it suitable for treatments where high precision is indispensable, such as stereotactic treatments [21]. The implementation of CBCT is particularly favorable as anatomical structures and soft tissues are often better visualized on axial cross-sectional images than on planar radiographic images [22, 23].

Compared to CBCT imaging, the ExacTrac system offers several advantages, including faster patient setup time, motion tracking capability, real-time imaging during treatment delivery, the ability to acquire images when the treatment couch is rotated (as is typical during a cranial treatment delivery), and less radiation exposure to the patient [17, 24, 25].

Since many linacs that have the ExacTrac system also have CBCT, it is interesting to investigate whether localization accuracy is comparable between these two imaging systems. Ma et al. [26] compared these two modalities on a Novalis Tx treatment unit and found a modest difference (root-mean-square translations <0.5 mm for phantom and <1.5 mm for patients) in localization accuracy for phantom and patient measurements between stereoscopic X-ray imaging and CBCT. Therefore, the 2D/3D registration approach of the ExacTrac system (planar imaging) has comparable localization accuracy to a 3D/3D registration approach

using CBCT. However, anatomic structures are better visualized with the use of axial CT images. The author also investigated whether there was any benefit to applying both imaging modalities prior to treatment, but did not find relevant improvement in accuracy. In terms of geometrical accuracy using either stereoscopic images (ExacTrac) or CBCT for IGRT purposes, a submillimeter accuracy (0.6 mm ± 0.4 mm) can be expected [27].

Patient Immobilization Devices

In order to maintain accurate alignment during the treatment, various devices (i.e., thermoplastic masks or bite-block systems) have been designed to immobilize patients undergoing radiosurgery treatment delivery. However, as noted previously in the CyberKnife section above, patient movement during treatment is still a possibility with these noninvasive devices. Hoogeman et al. [28] studied the time dependence of patient motion and showed that despite application of thermoplastic masks and vacuum bags, patients still tend to drift away from their initial setup during treatment. The ExacTrac IGRT approach can mitigate intrafraction motion effects through a process of repeat imaging and setup correction performed intermittently during the treatment delivery. Frequent verification imaging during treatment delivery has shown a significant reduction in target position uncertainty from intrafraction motion (13%), compared to verification images taken only at the end of treatment [29]. Moreover, the standard deviation in movement errors becomes much smaller (38% reduction), which means that fewer large movements can be expected during treatment delivery. By applying verification images during treatment, reduction of setup inaccuracies and correction of intrafraction motion are possible, allowing reduction or even omission of "traditional" setup planning margins in the treatment portals.

As an additional step forward in the quest for patient comfort, a new radiotherapy procedure that is both frameless and maskless has been proposed based on minimal patient immobilization and patient monitoring with a surface imaging system [30, 31]. The minimal immobilization system consists of a patient-specific head mold made out of expandable foam that conforms to the back of the patient's head. A custom headrest can be added in order to provide more comfort to the patient. With this system, the patient's face is left uncovered to provide maximal comfort. A region of interest, consisting of the forehead, nose, eyes, and temporal bones, is monitored during treatment using a video surface imaging system. The system consists of three ceiling-mounted optical stereo camera pods. The images from these cameras are combined to build a composite three-dimensional surface image of the patient. The system can track real-time surface position with respect to a reference surface image. The reference image can be extracted from the patient's planning CT image, or a surface image of the patient acquired previously at the correct treatment position. The topology of the surface is reconstructed by identifying the pattern reflected from the projector or flash in the stereo images. The system then detects patient motion by comparing the live images with the reference image. Deviation from the reference (body contour extracted from the planning CT) is shown on the screen, and shifts and rotations can be applied until this deviation is as close to 0 as possible. Next, a CBCT image is acquired to refine the setup based on internal anatomy, and immediately afterward, a new reference surface image will be acquired for detecting motion during the treatment delivery.

Leksell Gamma Knife Technology

Elekta Corporation (Stockholm, Sweden) was founded in 1972 by Swedish neurosurgeon Lars Leksell and his two sons. Leksell had introduced the concept of stereotactic radiosurgery in a historic paper published in 1951 [32]. In 1967, Larsson and Leksell devised the "Gamma Unit," containing 179 cobalt-60 sealed radiation sources, in static locations, carefully focused on a single point in space. The first commercial Leksell Gamma Knife (later designated as the Model U) was installed at the University of

Pittsburgh Medical Center in 1987 [33]. This unit included interchangeable source collimators capable of creating a nearly spherical treatment zone of 4, 8, 14, or 18 mm in diameter.

The Elekta Gamma Knife evolved substantially over the years. A complete redesign of the Gamma Knife concept was introduced with the Gamma Knife Perfexion (PFX) in 2006 [34]. The PFX used the same cobalt-60 sealed source design, but replaced the nearly hemispherical fixed array of sources with 8 rods containing 24 sources each. Each movable rod could be configured over a blocked, 4-mm-, 8-mm-, or 16-mm-diameter collimator, yielding nearly 65,000 possible irradiation configurations. A very sophisticated computer algorithm (Leksell GammaPlan 10.0) was supplied with the unit to assist in treatment planning and to communicate with the computer which actually operates the treatment unit.

New Icon Fractionated Treatment System

Traditionally, the Gamm Knife has been used with frame-based localization and immobilization. However, an upgrade for the Gamma Knife Perfexion system was introduced in 2015 based on a prototype created at Princess Margaret Hospital in Toronto [35, 36]. The upgrade includes a couch-mounted cone-beam computed tomography (CBCT) system, a High Definition Motion Management System (HDMM), and a supply of relocatable thermoplastic facemasks (Fig. 4.5). The integrated PFX Icon system can be used for traditional single-dose stereotactic intracranial radiosurgery using the Leksell Model G docking stereotactic frame, or it can be used in multi-fraction treatments.

The CBCT device is mounted on the Leksell Gamma Knife Perfexion patient couch so that it can image the patient's head while in treatment position. The X-ray tube has an energy range of 70–120 kVp. There are two preset imaging modes: Preset 1 uses 0.4mAs per projection at 90kVp, with a voxel size of 0.5 mm and a resolution of 7 line pairs/cm. Preset 2 uses 1.0mAs per projection with the same voxel size and a resolution of 8 line pairs/cm. The manufacturer specifies a CTDI is 2.5 mGy and 6.3 mGy, and the contrast-to-noise ratio (CNR) is 1.0 and 1.5, respectively. The detector is amorphous silicon with 780 by 710 pixels and fixed resolution of 0.368 mm.

Fig. 4.5 Gamma Knife Perfexion Icon with High Definition Motion Management (HDMM) system that includes infrared camera, attachment to the couch, four immobile reflective makers, and Icon head support. (Image courtesy of Elekta AB)

The HDMM utilizes an infrared stereoscopic camera mounted at the foot of the bed on a popup frame. The camera tracks the motion of four reference markers and one patient marker placed on the patient's nose tip. A CT scan of the patient in the thermoplastic mask "zeroes" the system so that motion can be detected. Once treatment begins, patient motion is monitored and the treatment can be paused if the vector deviation exceeds a present limit (typically 1.0 millimeter).

A number of centers have reported on their early experience with the Gamma Knife Perfexion Icon. Zeverino et al. [35] reported on the alignment of the CBCT imager coordinates with the Leksell stereotactic coordinate system. This is a vital evaluation since the CBCT image space is directly converted to Leksell stereotactic space. The authors report use of the Ball Cube phantom (Accuray Inc., Sunnyvale, CA) with Gafchromic EBT3 films (Ashland Inc., Wayne, NJ). The films were placed along the axial and then the sagittal planes machined into the cube, allowing an image to be formed with a single exposure of the Gamma Knife Perfexion 16-mm collimators after

alignment using the CBCT imaging system. The CBCT center of rotation agreed with the Unit Center Point (UCP) of the Gamma Knife Perfexion within 0.13 mm.

Two early reports, one by AlDahlawi et al. [37] and another by Chung et al. [38], evaluated the stability of the CBCT stereotactic coordinate space with respect to the standard frame-based system. AlDahlawi and coworkers found that over a 6-week period of multiple measurements, the difference between the frame-based and the CBCT-based stereotactic space ranged from 0.21 to 0.33 mm. Chung and coworkers reported results of an end-to-end test using the CIRS 605 phantom (CIRS Inc., Norfolk, VA) with radiochromic film. Irradiation was repeated four times over 18 months. The overall deviation between radiation isocenter (UCP) and center of the patient positioning system was 0.09 ± 0.03 mm.

Quality Assurance

Elekta provides a test tool (QA Tool) which measures the spatial accuracy (Focus Precision Test) of the patient positioning system using the 4-mm collimator for the Gamma Knife Perfexion [34]. The American Association of Physicists in Medicine (Task Group 178, pre-publication document 2018) recommends that the vector error along the three orthogonal coordinates be less than 0.4 mm. The US Nuclear Regulatory Commission (NRC) recommends in its Licensing Guidance [39] that this test tool be employed at least monthly. The Gamma Knife Icon™ has a similar tool called the QA Tool Plus specifically for cone-beam CT QA [38]. The NRC licensing guidance recommends the use of this QA Tool Plus each day before the use of the cone-beam CT. The NRC further recommends testing the HDMM system each day before use.

Clinical Results

The Leksell Gamma Knife Society published a report in 2018 based on user surveys of clinical indication and patterns of use in Calendar Year 2017. They found that Leksell Gamma Knife centers who had adopted the Perfexion Icon™ system use the frameless mask system for 26.7% of single-session treatments and 77.3% of the multi-session treatments. A report from a Korean group [40] accumulated statistics from 41 patients regarding co-registration accuracy from one treatment to another, using CBCT registration. They found a mean three-dimensional deviation of 0.2 ± 0.1 mm. The co-registration of stereotactic CT images with CBCT was 0.5 ± 0.1 mm, and the co-registration of MR images with CBCT was 0.8 ± 0.1 mm.

Finally, a combined group from Great Britain, Switzerland, and Australia published a report on the simulated fractionated treatment of five large brain mets [41]. Each clinical case was previously treated with a Leksell Gamma Knife in a single fraction with stereotactic frame. To simulate three or five fraction treatments, a "worst-case scenario" was simulated with displacements of 0.0, 0.5, 1.0, and 2.0 mm. A "sumPlan" was computed from the individual treatments. They found that for a plan prescribed at the 50% isodose line, the margin necessary would be 0.2 to 0.5 mm for a three-fraction plan and 0.0 mm for a five-fraction plan.

Conclusions and Future Directions

Image guidance is now a mainstay of stereotactic radiosurgery and radiotherapy deliveries. It facilitates highly accurate target alignment without the need for an invasive head ring making multi-session SRS deliveries available to patients that may not be able to tolerate a single SRS delivery. Accuracy is similar to traditional frame-based alignment methods. This technology has also made stereotactic accuracy and precision available for treatment of sites outside of the cranial vault such as the spine.

The spectrum of IGRT technologies employed in radiation therapy continues to expand. Magnetic resonance imaging has recently been integrated into the treatment processes, providing the advantages of combining the real-time soft

tissue imaging and concurrent radiation treatments. Benefits of MR-guided radiation therapy (MRgRT) include superior soft tissue imaging, the ability to track tumors and gate treatment delivery, and the opportunity to adapt for interfraction and intra-fraction anatomical variations. MRgRT also offers the potential for providing sophisticated biomarker-guided treatments.

Additionally, MRgRT allows for better offline and online adaptive MRI-guided radiotherapy, where variations detected with MRI can be used to adapt the treatment plans. As clinical adoption of MRgRT expands, there is a need to develop work flows and quality assurance techniques, innovate imaging science, and assess clinical outcome benefits. While there is relatively little experience using this technique for stereotactic deliveries at this point, this will surely change as more units are brought to market and more institutions gain experience with them. MRgRT with unsurpassed soft tissue contrast and possibility to perform functional studies are tools that will continue to advance the field of radiotherapy and radiosurgery for our patients.

References

1. Leksell L. Stereotactic radiosurgery. J Neurol Neurosurg Psychiatry. 1983;46(9):797–803.
2. Verhey LJ, Goitein M, McNulty P, Munzenrider JE, Suit HD. Precise positioning of patients for radiation therapy. Int J Radiat Oncol Biol Phys. 1982;8(2):289–94.
3. Adler JR, Murphy MJ, Chang SD, Hancock SL. Image-guided robotic radiosurgery. Neurosurgery. 1999;44(6):1299–306.
4. Fu DS, Kuduvalli G. A fast, accurate, and automatic 2D-3D image registration for image-guided cranial radiosurgery. Med Phys. 2008;35(5):2180–94.
5. Murphy MJ. Fiducial-based targeting accuracy for external-beam radiotherapy. Med Phys. 2002;29(3):334–44.
6. West JB, Fitzpatrick JM, Toms SA, Maurer CR Jr, Maciunas RJ. Fiducial point placement and the accuracy of point-based, rigid body registration. Neurosurgery. 2001;48(4):810–6; discussion 6–7.
7. Fu D, Kuduvalli G, Maurer CR, Allision JW, Adler JR. 3D target localization using 2D local displacements of skeletal structures in orthogonal X-ray images for image-guided spinal radiosurgery. Int J Comput Assist Radiol Surg. 2006;1:198–200.
8. Murphy MJ, Chang SD, Gibbs IC, Le QT, Hai J, Kim D, et al. Patterns of patient movement during frameless image-guided radiosurgery. Int J Radiat Oncol Biol Phys. 2003;55(5):1400–8.
9. Ryken TC, Meeks SL, Pennington EC, Hitchon P, Traynelis V, Mayr NA, et al. Initial clinical experience with frameless stereotactic radiosurgery: analysis of accuracy and feasibility. Int J Radiat Oncol Biol Phys. 2001;51(4):1152–8.
10. Chang SD, Main W, Martin DP, Gibbs IC, Heilbrun MP. An analysis of the accuracy of the CyberKnife: a robotic frameless stereotactic radiosurgical system. Neurosurgery. 2003;52(1):140–6; discussion 6–7.
11. Gevaert T, Verellen D, Engels B, Depuydt T, Heuninckx K, Tournel K, et al. Clinical evaluation of a robotic 6-degree of freedom treatment couch for frameless radiosurgery. Int J Radiat Oncol Biol Phys. 2012;83(1):467–74.
12. Verellen D, Soete G, Linthout N, Van Acker S, De Roover P, Vinh-Hung V, et al. Quality assurance of a system for improved target localization and patient set-up that combines real-time infrared tracking and stereoscopic X-ray imaging. Radiother Oncol. 2003;67(1):129–41.
13. Yan H, Yin FF, Kim JH. A phantom study on the positioning accuracy of the Novalis Body system. Med Phys. 2003;30(12):3052–60.
14. Groh BA, Siewerdsen JH, Drake DG, Wong JW, Jaffray DA. A performance comparison of flat-panel imager-based MV and kV cone-beam CT. Med Phys. 2002;29(6):967–75.
15. Thilmann C, Nill S, Tucking T, Hoss A, Hesse B, Dietrich L, et al. Correction of patient positioning errors based on in-line cone beam CTs: clinical implementation and first experiences. Radiat Oncol. 2006;1:16.
16. Gevaert T, Verellen D, Tournel K, Linthout N, Bral S, Engels B, et al. Setup accuracy of the Novalis ExacTrac 6DOF system for frameless radiosurgery. Int J Radiat Oncol Biol Phys. 2012;82(5):1627–35.
17. Jin JY, Yin FF, Tenn SE, Medin PM, Solberg TD. Use of the BrainLAB ExacTrac X-Ray 6D system in image-guided radiotherapy. Med Dosim. 2008;33(2):124–34.
18. Agazaryan N, Tenn SE, Desalles AA, Selch MT. Image-guided radiosurgery for spinal tumors: methods, accuracy and patient intrafraction motion. Phys Med Biol. 2008;53(6):1715–27.
19. Zhang L, Garden AS, Lo J, Ang KK, Ahamad A, Morrison WH, et al. Multiple regions-of-interest analysis of setup uncertainties for head-and-neck cancer radiotherapy. Int J Radiat Oncol Biol Phys. 2006;64(5):1559–69.
20. Murphy MJ. The importance of computed tomography slice thickness in radiographic patient positioning for radiosurgery. Med Phys. 1999;26(2):171–5.
21. Oldham M, Letourneau D, Watt L, Hugo G, Yan D, Lockman D, et al. Cone-beam-CT guided radiation therapy: a model for on-line application. Radiother Oncol. 2005;75(3):271–8.

22. van Herk M. Different styles of image-guided radiotherapy. Semin Radiat Oncol. 2007;17(4):258–67.
23. Verellen D, De Ridder M, Tournel K, Duchateau M, Reynders T, Gevaert T, et al. An overview of volumetric imaging technologies and their quality assurance for IGRT. Acta Oncol. 2008;47(7):1271–8.
24. Lee SW, Jin JY, Guan H, Martin F, Kim JH, Yin FF. Clinical assessment and characterization of a dual tube kilovoltage X-ray localization system in the radiotherapy treatment room. J Appl Clin Med Phys. 2008;9(1):2318.
25. Walter C, Boda-Heggemann J, Wertz H, Loeb I, Rahn A, Lohr F, et al. Phantom and in-vivo measurements of dose exposure by image-guided radiotherapy (IGRT): MV portal images vs. kV portal images vs. cone-beam CT. Radiother Oncol. 2007;85(3):418–23.
26. Ma J, Chang Z, Wang Z, Jackie Wu Q, Kirkpatrick JP, Yin FF. ExacTrac X-ray 6 degree-of-freedom image-guidance for intracranial non-invasive stereotactic radiotherapy: comparison with kilo-voltage cone-beam CT. Radiother Oncol. 2009;93(3):602–8.
27. Rahimian J, Chen JC, Rao AA, Girvigian MR, Miller MJ, Greathouse HE. Geometrical accuracy of the Novalis stereotactic radiosurgery system for trigeminal neuralgia. J Neurosurg. 2004;101 Suppl 3:351–5.
28. Hoogeman MS, Nuyttens JJ, Levendag PC, Heijmen BJ. Time dependence of intrafraction patient motion assessed by repeat stereoscopic imaging. Int J Radiat Oncol Biol Phys. 2008;70(2):609–18.
29. Gevaert T, Boussaer M, Engels B, Litre CF, Prieur A, Wdowczyk D, et al. Evaluation of the clinical usefulness for using verification images during frameless radiosurgery. Radiother Oncol. 2013;108(1):114–7.
30. Cervino LI, Detorie N, Taylor M, Lawson JD, Harry T, Murphy KT, et al. Initial clinical experience with a frameless and maskless stereotactic radiosurgery treatment. Pract Radiat Oncol. 2012;2(1):54–62.
31. Mancosu P, Fogliata A, Stravato A, Tomatis S, Cozzi L, Scorsetti M. Accuracy evaluation of the optical surface monitoring system on EDGE linear accelerator in a phantom study. Med Dosim. 2016;41(2):173–9.
32. Leksell L. The stereotaxic method and radiosurgery of the brain. Acta Chir Scand. 1951;102(4):316–9.
33. Wu A, Lindner G, Maitz AH, Kalend AM, Lunsford LD, Flickinger JC, et al. Physics of gamma knife approach on convergent beams in stereotactic radiosurgery. Int J Radiat Oncol Biol Phys. 1990;18(4):941–9.
34. Lindquist C, Paddick I. The Leksell Gamma Knife Perfexion and comparisons with its predecessors. Neurosurgery. 2007;61(3 Suppl):130–40; discussion 40–1.
35. Zeverino M, Jaccard M, Patin D, Ryckx N, Marguet M, Tuleasca C, et al. Commissioning of the Leksell Gamma Knife((R)) Icon. Med Phys. 2017;44(2):355–63.
36. Ruschin M, Komljenovic PT, Ansell S, Menard C, Bootsma G, Cho YB, et al. Cone beam computed tomography image guidance system for a dedicated intracranial radiosurgery treatment unit. Int J Radiat Oncol Biol Phys. 2013;85(1):243–50.
37. AlDahlawi I, Prasad D, Podgorsak MB. Evaluation of stability of stereotactic space defined by cone-beam CT for the Leksell Gamma Knife Icon. J Appl Clin Med Phys. 2017;18(3):67–72.
38. Chung HT, Park WY, Kim TH, Kim YK, Chun KJ. Assessment of the accuracy and stability of frameless gamma knife radiosurgery. J Appl Clin Med Phys. 2018;19(4):148–54.
39. Leksell Gamma Knife Perfexion and Leksell Gamma Knife Icon Licensing Guidance. In: Commission UNR, editor. Bethesda, MD; 2016.
40. Chung HT, Kim JH, Kim JW, Paek SH, Kim DG, Chun KJ, et al. Assessment of image co-registration accuracy for frameless gamma knife surgery. PLoS One. 2018 Mar 2;13(3):e0193809.
41. Reiner B, Bownes P, Buckley DL, Thwaites DI. Quantifying the effects of positional uncertainties and estimating margins for Gamma-Knife fractionated radiosurgery of large brain metastases. J Radiosurg SBRT. 2017;4(4):275–87.

Part II

Defining Trajectories and Targets

Principles of Safe Stereotactic Trajectories

5

Rushna Ali and Ellen L. Air

Introduction

Since Horsley and Clark published their seminal work in 1906 [1], numerous technological advancements have been adopted to improve safety, accuracy, and precision of stereotactic interventions. Ventriculography was combined with stereotactic technique by Spiegel and Wycis to estimate the location of specific intracranial structures in patients [2]. Various surrogate markers were then introduced in an effort to refine initial surgical targeting. These included recognition of neural firing patterns recorded with microelectrode techniques [3] as well as characteristic electrical impedance patterns recorded from the tip of a probe as it traveled through different brain structures [4]. Through the course of these experiences, key principles of safe stereotactic trajectories have been identified.

R. Ali
Restorative and Functional Neurosurgery, Division of Neurosurgery, Spectrum Health Medical Group, Grand Rapids, MI, USA

E. L. Air (✉)
Functional Neurosurgery, Department of Neurosurgery, Henry Ford Health System, Detroit, MI, USA
e-mail: eair1@hfhs.org

Preoperative Considerations

As with any neurosurgical procedure, patient selection and medical optimization are critical. Despite their relatively low incidence, hemorrhagic complications carry by far the highest risk of devastating neurological outcome in functional neurosurgery, with an overall bleeding rate ranging from 1.4% to 3.4% for asymptomatic and 0.4% to 2.1% for symptomatic bleeding [5]. Age, male gender, chronic hypertension, the number of microelectrode passes, a diagnosis of Parkinson's disease, and the anatomic target have all been associated with increased hemorrhage rates [6]. Given that many stereotactic procedures are performed via a small opening with limited hemostatic control, particular attention should be paid to modifiable risks of hemorrhage.

The most commonly encountered situation is that of patients taking antiplatelet or anticoagulation medication preoperatively, accounting for approximately 1 in 10 surgical patients [7]. The indication for such treatment should be confirmed with the prescribing physician so the risks of discontinuation are clear and the timing of therapy resumption determined. As neurosurgeons, the immediacy of a major bleeding complication weighs heavier than the risk of thrombotic event. Unlike other surgical specialties, all neurosurgical procedures are considered to have a high risk of bleeding (>1.5%) [8]. However, the true annual risk and associated

N. Pouratian, S. A. Sheth (eds.), *Stereotactic and Functional Neurosurgery*,
https://doi.org/10.1007/978-3-030-34906-6_5

morbidity of a thrombotic event should be determined for each patient [9]. Several guidelines have been published regarding the cessation and restarting of specific anticoagulation agents [8, 10–13].

Another key preoperative decision is the selection of stereotactic system appropriate to the procedure. Frame-based, frameless, and robotic systems are available, each with unique advantages and disadvantages (see Chap. 1). For neurosurgeons with more than one type of system available, the size and location of the target, as well as the goal of the procedure, should guide the approach. For example, navigation systems such as StealthStation™ (Medtronic, Minneapolis, MN, USA) and Brainlab Stereotaxy (Brainlab AG, Munich, Germany) can be used for both frameless and frame-based stereotaxy. Needle biopsy of a 3-cm lesion may be more amenable to the frameless approach than DBS implantation into the subthalamic nucleus, a target of less than 1 cm in any dimension [14, 15]. The full spectrum of anticipated surgical procedures should similarly be considered prior to investing in any stereotactic system.

Preoperative Imaging

Once the patient has been appropriately optimized and the broader surgical approach determined, preoperative volumetric imaging is obtained. Far past the days of Spiegel and Wycis [2], technological advances have culminated in stereotactic computed tomography (CT) and magnetic resonance imaging (MRI). These tools permit in vivo stereotactic localization of visualized pathological and anatomical structures, both before and after the surgical intervention. As will be discussed in more detail elsewhere, each has its pros and cons. Regardless, it is important to identify key structures on the imaging to plan optimal stereotactic trajectories, particularly the target and the vasculature.

MRI is the imaging modality of choice for most situations as it provides the greatest anatomic detail. MRI is limited by image distortion due to both susceptibility artifact and field inhomogeneity. Gradient field inhomogeneity is related to the magnet itself and can be reduced by acquiring 3-D scans [16]. It is also consistent and can be mathematically corrected [17]. Susceptibility artifact is due to tissue density itself and is therefore unavoidable. It is important to note that susceptibility artifact, and therefore spatial distortion, increases with magnet strength [18]. For the vast majority of stereotactic procedures, these issues are small in practicality, but should be kept in mind as higher field strengths gain prominence in clinical settings [19].

CT imaging is well-documented as geometrically reliable, though it lacks the delineation of brain structures [20]. CT angiogram combines the advantages of precise visualization of blood vessels (especially arteries) with the spatial accuracy of a CT scan. For invasive EEG electrode placement, this method is frequently used with good results [21, 22]. Newer MR imaging sequences, such as a 3-T time of flight (TOF), have been utilized to improve the safety of stereotactic trajectory by allowing better visualization, and therefore avoidance, of deep perforating vessels [23].

Image Fusion and Registration

In order to avoid issues of MR distortion, fusing non-stereotactic MR data onto stereotactic CT images was initially considered. This idea suggested that contrast-rich MR data at the center of the field could be supplemented with accurate fiducial localization with CT at the field periphery [24]. Numerous commercially available software packages were developed and provide this function. However, magnetic inhomogeneities are nonlinear, whereas most fusion algorithms are linear [25]. In addition, fusion between CT and MR images may result in fusion errors that often go undetected. Fusion algorithms are found to introduce mean errors of between 1.2 and 1.7 mm; larger errors of close to 4.0 mm have been reported in individual patients [26]. Anatomical targeting on stereotactic MR images that visualize the fiducials and target on the same image eliminate fusion errors. Detailed surgical planning will require import of the images to a

dedicated software platform that allows image manipulation and precise planning of both target and trajectory. The default on some software platforms is to minimize registration error across the volume of the acquired images. However, the aim of stereotactic surgery is to maximize accuracy at the target level. Therefore, accuracy of registration at the level of the target is more desirable.

Contemporary stereotactic frames are based on the arc-centered principle that maximizes surgical precision at the target, irrespective of the surgical trajectory. Mini-frame or frameless navigation boasts maximum precision at the entry point and then endeavors to replicate the planned virtual trajectory during surgery. However, small errors in trajectory can translate into significant errors at the target level.

Trajectory Planning

A surgical trajectory that avoids sulci has been shown to reduce the incidence of hemorrhagic complications, presumably by avoiding the enclosed vessels [27]. Planning an entry point to penetrate the crest of a gyrus is not sufficient to avoid sulci en route to the target. The individual complexity of the sulcal pattern and obliquity of the surgical trajectory require the image manipulation of the acquired stereotactic images with commercially available planning software that allows reconstruction along the proposed trajectory. Entry through the crest of a gyrus helps to limit excessive cerebrospinal fluid (CSF) loss when opening the dura during surgery (Fig. 5.1). Moreover, avoiding stiff anatomical barriers, such as the pia and ependyma, minimizes brain shift, thus improving surgical accuracy and minimizing risk of hemorrhage [6]. Coagulating the pia using bipolar cautery prior to insertion is also prudent to avoid inadvertent bleeding from pial vessels.

Transventricular trajectories are normally avoided in stereotaxis as minor displacement while traversing the ventricle can result in significant deviation from the planned trajectory [28]. Brain deformation from cerebrospinal fluid loss during ventricular puncture may also contribute to inaccuracy of electrode/biopsy needle placement [29]. However, there is evidence that transventricular trajectories do not increase the risk of complications while maintaining stereotactic accuracy at the target [30]. This particularly applies to very medial targets [31] and may be

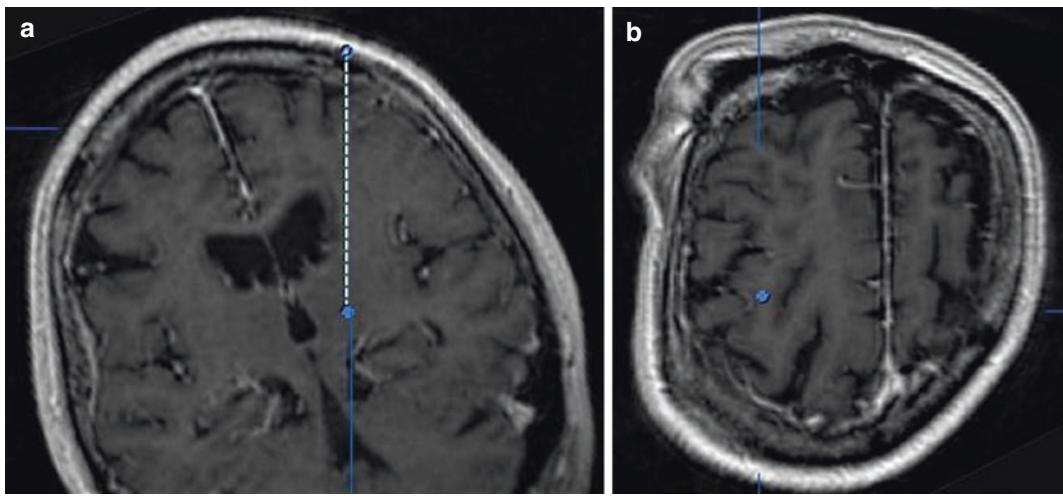

Fig. 5.1 Example trajectory. (**a**) Coronal view along the trajectory. The entry point is at the apex of a gyrus and avoids crossing sulci or entering the ventricle. (**b**) Probe's-eye view of the trajectory near the entry into the brain. The blue dot (trajectory) is central within the gyrus. Care was taken to avoid the sulcal vessel just to the left

due to taking a perpendicular approach to the ventricular wall (Fig. 5.2).

Patient Positioning

As with other forms of surgery, patient positioning is a vital part of the surgical procedure. A balance must be achieved between access to the surgical site and visibility of appropriate anatomical or fiducial markers for image registration. Most planning images are obtained in the supine position, incorporating the facial structures which are often used for registration. However, only a subset of stereotactic procedures is performed in the supine position. While head position during image acquisition, on its own, has not been shown to affect stereotactic accuracy [32], relative shift of the skull and intracranial structures to the facial structures or fiducials used for registration can negatively impact accuracy [33–35]. Obtaining stereotactic images once the patient has been positioned, as when using intraoperative CT or MRI, may increase accuracy. Alternatively, the use of bone fiducials or registration of the bony contours of the skull (e.g., mastoid region) in the region of surgery has been shown to increase accuracy [36–38]. It is also important to have full access to every entry point. This can be a challenge when performing multi-electrode implantations, such as for sEEG. Preoperative planning should anticipate trajectory entry sites relative to head fixation (Fig. 5.3).

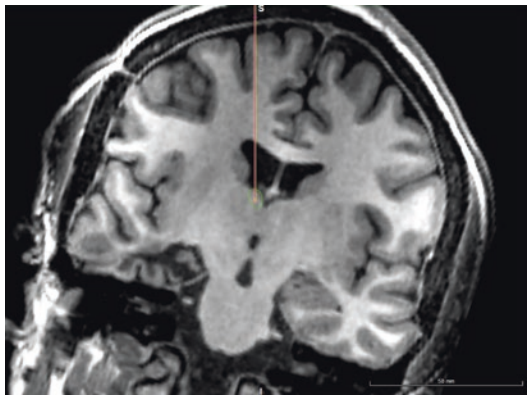

Fig. 5.2 Example of transventricular trajectory. Note the entry and exit points are steep with respect to the wall of the ventricle, diminishing the chance of deflection off the ventricular wall

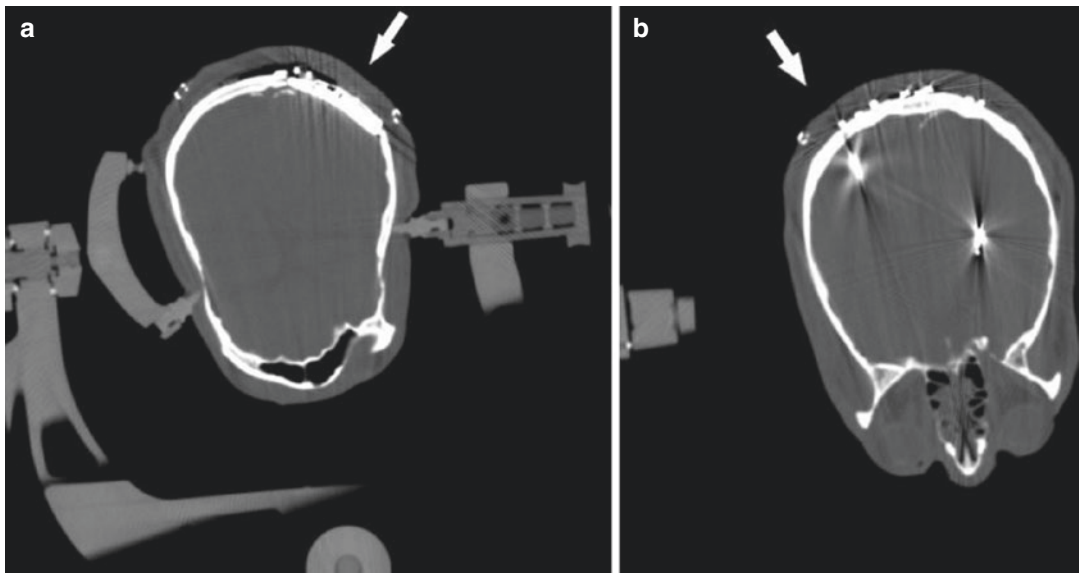

Fig. 5.3 Example of surgical positioning to allow for full surgical access. (**a**) Note the headholder pins are situated to allow sufficient room for implantation of a pulse generator into the skull (*arrow*), as well as to access the entry points for depth electrode placement (**b**). Arrow denotes left entry point

Special Considerations for Deep Brain Stimulation

The use of microelectrode recordings (MER) to guide lead placement in DBS surgery in the current era of advanced neuroimaging has led to significant debate. Proponents of MER claim that it increases targeting accuracy [39] without significantly increasing risk [40], whereas others claim intraoperative test stimulation alone is sufficient to ensure target accuracy [41, 42]. Advancements in neuroimaging have precipitated a trend toward direct, image-based targeting under general anesthesia without the use of microelectrode recording or intraoperative test stimulation, also referred to as "asleep" deep brain stimulation surgery. Asleep DBS, utilizing imaging in the form of intraoperative computed tomography (iCT) or magnetic resonance imaging (iMRI), has demonstrated reliable targeting accuracy of DBS leads implanted within the globus pallidus and subthalamic nucleus while also improving clinical outcomes. These studies suggest that increased risk of intracranial hemorrhage (ICH) and cognitive decline may be related to the use of MER [43]. However, in the absence of conclusive evidence, the general consensus is that it is acceptable to continue using MER since the risk profile continues to be low. With regard to target-specific risk for hemorrhage, some studies have reported increased hemorrhage rates with globus pallidus interna (GPi) target [44], whereas other authors have found a trend toward increased hemorrhages when the ventralis intermedius nucleus (VIM) of the thalamus was targeted. On the other hand, other studies have shown VIM to be associated with the least incidence of hemorrhages [43]. Due to conflicting evidence and since both GPi and VIM have small perforating vessels in their vicinity, a determination cannot be made about which target is more prone to hemorrhagic complications.

Use of Robotic Assistance

Robotic assistance has been increasingly used in stereotactic procedures because of its potential for improving accuracy and precision [45]. Neurosurgical robots have assisted in a number of cranial procedures, including ablation of epileptogenic lesions, biopsies, and deep brain stimulation. The use of robots is not only considered to increase accuracy but is also deemed safe for the patient [46]. The robot provides a technical advantage compared to a traditional arc-based frame especially when an unusually low trajectory is planned that falls near or below the arc of a Leksell or CRW frame. Another advantage of using the robot is improved efficiency since minor adjustments can be made to the entry point without the need for complete readjustment for movements outside of a singular fixed plane as with arc-based frames, and the surgeon can quickly move from one trajectory to the next. For procedures performed in the prone position, skull fiducials are preferred for registration, which improves accuracy and precision over other laser-guided navigational systems that are routinely used in stereotactic procedures. Laser-guided registration and navigation can be performed using the robot when patients are supine so that facial bony landmarks can be utilized for registration.

Special Circumstances

When considering stereotactic approaches to the brainstem, transgression of pial, ependymal, or tentorial surfaces can be avoided by considering ipsilateral transfrontal or contralateral transfrontal entry points; the latter allows access to more laterally placed pontine lesions [47]. Both approaches allow the patient to remain supine during surgery, in a similar position to that in which images are traditionally acquired, thus preventing error due to positional brain shift. The transtentorial route is less favorable because of the increased risk of hemorrhage and trajectory deviation. The suboccipital, transcerebellar approach is often used to access brainstem lesions. Care must be taken to ensure that the frame is placed low enough to allow the lesion to be visualized and to physically allow the required trajectory with a particular frame. Semi-recumbent, lateral, and prone positions have been described to provide access, some of

which may limit the possibility of surgery under local anesthesia. The suboccipital approach provides the shortest distance to the brainstem target [48]. One study compared the two approaches and found an improved rate of successful diagnostic biopsy in patients undergoing the transfrontal approach compared to the suboccipital, transcerebellar approach, without any significant difference in rate of complications [49].

When performing biopsy of a partially solid, partially cystic lesion, the solid portion should be targeted first to prevent targeting errors that would occur with significant brain shift after cyst aspiration.

Conclusion

With careful planning and preparation, stereotaxis can be performed safely for a wide range of indications.

References

1. Clarke RH, Horsley V. THE CLASSIC: On a method of investigating the deep ganglia and tracts of the central nervous system (cerebellum). Br Med J. 1906;1799–1800.
2. Spiegel EA, Wycis HT, Marks M, Lee AJ. Stereotaxic apparatus for operations on the human brain. Science. 1947;106(2754):349–50.
3. Guiot G, Hardy J, Albe-Fessard D. Precise delimitation of the subcortical structures and identification of thalamic nuclei in man by stereotactic electrophysiology. Neurochirurgia (Stuttg). 1962;5:1–18.
4. Zrinzo LU, Hariz MI. Recording in functional neurosurgery. In: Lozano AM, Gildenberg PL, Tasker RR, editors. Textbook of stereotactic and functional neurosurgery. 2nd ed. Berlin: Springer; 2009. p. 1325–30.
5. Krüger MT, Coenen VA, Jenkner C, Urbach H, Egger K, Reinacher PC. Combination of CT angiography and MRI in surgical planning of deep brain stimulation. Neuroradiology. 2018;60(11):1151–8.
6. Ben-Haim S, Asaad WF, Gale JT, Eskandar EN. Risk factors for hemorrhage during microelectrode-guided deep brain stimulation and the introduction of an improved microelectrode design. Neurosurgery. 2009;64(4):754–62; discussion 762–3.
7. Roger VL, Go AS, Lloyd-Jones DM, Benjamin EJ, Berry JD, Borden WB, et al. Heart disease and stroke statistics-2012 update: a report from the American Heart Association. Circulation. 2012;125(1):e2–e220.
8. Baron TH, Kamath PS, McBane RD. Management of antithrombotic therapy in patients undergoing invasive procedures. N Engl J Med. 2013;368(22):2113–24.
9. Hornor MA, Duane TM, Ehlers AP, Jensen EH, Brown PS, Pohl D, et al. American College of Surgeons' Guidelines for the Perioperative Management of Antithrombotic Medication. J Am Coll Surg. 2018;227(5):521–536.e1.
10. Douketis JD, Spyropoulos AC, Spencer FA, Mayr M, Jaffer AK, Eckman MH, et al. Perioperative management of antithrombotic therapy: antithrombotic therapy and prevention of thrombosis: American College of Chest Physicians evidence-based clinical practice guidelines. Chest. 2012;141(2suppl):e326–50.
11. Doherty JU, Gluckman TJ, Hucker WJ, Januzzi JL, Ortel TL, Saxonhouse SJ, et al. 2017 ACC expert consensus decision pathway for periprocedural management of anticoagulation in patients with nonvalvular atrial fibrillation: a report of the American College of Cardiology Clinical Expert Consensus Document Task Force. J Am Coll Cardiol. 2017;69:871–98.
12. Kearon C, Akl EA, Ornelas J, Blaivas A, Jimenez D, Bounameaux H, et al. Antithrombotic therapy for VTE disease: CHEST guideline and expert panel report. Chest. 2016;149:315–52.
13. Fleisher LA, Fleischmann KE, Auerbach AD, Barnason SA, Beckman JA, Bozkurt B, et al. 2014 ACC/ AHA guideline on perioperative cardiovascular evaluation and management of patients undergoing noncardiac surgery: a report of the American College of Cardiology/American Heart Association Task Force on practice guidelines. J Am Coll Cardiol. 2014;64:77–137.
14. Roth A, Buttrick SS, Cajigas I, Jagid JR, Ivan ME. Accuracy of frame-based and frameless systems for deep brain stimulation: a meta-analysis. J Clin Neurosci. 2018;57:1–5.
15. Mavridis I, Boviatsis E, Anagnostopoulou S. Anatomy of the human subthalamic nucleus: a combined morphometric study. Anat Res Int. 2013;2013:319710.
16. Walton L, Hampshire A, Forster DM, Kemeny AA. Stereotactic localization with magnetic resonance imaging: a phantom study to compare the accuracy obtained using two-dimensional and three-dimensional data acquisitions. Neurosurgery. 1997;41(1):131–7; discussion 137–9.
17. Sumanaweera TS, Glover GH, Hemler PF, van den Elsen PA, Martin D, Adler JR, Napel S. MR geometric distortion correction for improved frame-based stereotaxic target localization accuracy. Magn Reson Med. 1995;34(1):106–13.
18. Sumanaweera TS, Adler JR Jr, Napel S, Glover GH. Characterization of spatial distortion in magnetic resonance imaging and its implications for stereotactic surgery. Neurosurgery. 1994;35(4):696–703; discussion 703–4.
19. Abosch A, Yacoub E, Ugurbil K, Harel N. An assessment of current brain targets for deep brain stimulation surgery with susceptibility-weighted imaging at 7 tesla. Neurosurgery. 2010;67(6):1745–56.

20. Bucholz RD, Ho HW, Rubin JP. Variables affecting the accuracy of stereotactic localization using computerized tomography. J Neurosurg. 1993;79(5):667–73.
21. Nowell M, Rodionov R, Diehl B, Wehner T, Zombori G, Kinghorn J, et al. A novel method for implementation of frameless StereoEEG in epilepsy surgery. Neurosurgery. 2014;10:525–34.
22. Gilard V, Proust F, Gerardin E, Lebas A, Chastan N, Fréger P, et al. Usefulness of multidetector-row computerized tomographic angiography for the surgical planning in stereoelectroencephalography. Diagn Interv Imaging. 2016;97:333–7.
23. Sato S, Dan M, Hata H, Miyasaka K, Hanihara M, Shibahara I, et al. Safe stereotactic biopsy for basal ganglia lesions: avoiding injury to the basal perforating arteries. Stereotact Funct Neurosurg. 2018;96(4):244–8.
24. Yu C, Petrovich Z, Apuzzo ML, Luxton G. An image fusion study of the geometric accuracy of magnetic resonance imaging with the Leksell stereotactic localization system. J Appl Clin Med Phys. 2001;2(1):42–50.
25. Sankar T, Lozano AM. Magnetic resonance imaging distortion in functional neurosurgery. World Neurosurg. 2011;75:29–31.
26. O'Gorman RL, Jarosz JM, Samuel M, Clough C, Selway RP, Ashkan K. CT/MR image fusion in the postoperative assessment of electrodes implanted for deep brain stimulation. Stereotact Funct Neurosurg. 2009;87(4):205–10.
27. Elias WJ, Sansur CA, Frysinger RC. Sulcal and ventricular trajectories in stereotactic surgery. J Neurosurg. 2009;110(2):201–7.
28. Zrinzo L, van Hulzen AL, Gorgulho AA, Limousin P, Staal MJ, De Salles AA, et al. Avoiding the ventricle: a simple step to improve accuracy of anatomical targeting during deep brain stimulation. J Neurosurg. 2009;110(6):1283–90.
29. Khan MF, Mewes K, Gross RE, Skrinjar O. Assessment of brain shift related to deep brain stimulation surgery. Stereotact Funct Neurosurg. 2008;86(1):44–53.
30. Lehtimäki K, Coenen VA, Gonçalves Ferreira A, Boon P, Elger C, Taylor RS, et al. The surgical approach to the anterior nucleus of thalamus in patients with refractory epilepsy: experience from the International Multicenter Registry (MORE). Neurosurgery. 2019;84(1):141–50.
31. Khan S, Javed S, Park N, Gill SS, Patel NK. A magnetic resonance imaging-directed method for transventricular targeting of midline structures for deep brain stimulation using implantable guide tubes. Neurosurgery. 2010;66(6 Suppl Operative):234–7; discussion 237.
32. Reinges MH, Krings T, Nguyen HH, Hans FJ, Korinth MC, Holler M, et al. Is the head position during preoperative image data acquisition essential for the accuracy of navigated brain tumor surgery? Comput Aided Surg. 2000;5(6):426–32.
33. Marmulla R, Mühling J, Lüth T, Hassfeld S. Physiological shift of facial skin and its influence on the change in precision of computer-assisted surgery. Br J Oral Maxillofac Surg. 2006;44(4):273–8.
34. Smith TR, Mithal DS, Stadler JA, Asgarian C, Muro K, Rosenow JM. Impact of fiducial arrangement and registration sequence on target accuracy using a phantom frameless stereotactic navigation model. J Clin Neurosci. 2014;21(11):1976–80.
35. Rohlfing T, Maurer CR Jr, Dean D, Maciunas RJ. Effect of changing patient position from supine to prone on the accuracy of a Brown-Roberts-Wells stereotactic head frame system. Neurosurgery. 2003;52(3):610–8; discussion 617–8.
36. Zhou C, Anschuetz L, Weder S, Xie L, Caversaccio M, Weber S. Surface matching for high-accuracy registration of the lateral skull base. Int J Comput Assist Radiol Surg. 2016;11(11):2097–103.
37. Salma A, Makiese O, Sammet S, Ammirati M. Effect of registration mode on neuronavigation precision: an exploration of the role of random error. Comput Aided Surg. 2012;17(4):172–8.
38. Ammirati M, Gross JD, Ammirati G, Dugan S. Comparison of registration accuracy of skin- and bone-implanted fiducials for frameless stereotaxis of the brain: a prospective study. Skull Base. 2002;12(3):125–30.
39. Alterman RL, Sterio D, Beric A, Kelly PJ. Microelectrode recording during posteroventral pallidotomy: impact on target selection and complications. Neurosurgery. 1999;44:315–23.
40. Rezai AR, Kopell BH, Gross RE, Vitek JL, Sharan AD, Limousin P, Benabid AL. Deep brain stimulation for Parkinson's disease: surgical issues. Mov Disord. 2006;21(Suppl 14):197–218.
41. Palur RS, Berk C, Schulzer M, Honey CR. A meta-analysis comparing the results of pallidotomy performed using microelectrode recording or macroelectrode stimulation. J Neurosurg. 2002;96:1058–62.
42. Hariz MI, Fodstad H. Do microelectrode techniques increase accuracy or decrease risks in pallidotomy and deep brain stimulation? A critical review of the literature. Stereotact Funct Neurosurg. 1999;72:157–69.
43. Binder DK, Rau GM, Starr PA. Risk factors for hemorrhage during microelectrode-guided deep brain stimulator implantation for movement disorders. Neurosurgery. 2005;56(4):722–32.
44. Obeso JA, Olanow CW, Rodriguez-Oroz MC, Krack P, Kumar R, Lang AE. The Deep-Brain Stimulation for Parkinson's Disease Study Group: Deep-brain stimulation of the subthalamic nucleus or the pars interna of the globus pallidus in Parkinson's disease. N Engl J Med. 2001;345:956–63.
45. Mattei TA, Rodriguez AH, Sambhara D, Mendel E. Current state-of-the-art and future perspectives of robotic technology in neurosurgery. Neurosurg Rev. 2014;37:357–66.
46. Lefranc M, Le Gars D. Robotic implantation of deep brain stimulation leads, assisted by intra-operative, flat-panel CT. Acta Neurochir. 2012;154:2069–74.

47. Amundson EW, McGirt MJ, Olivi A. A contralateral, transfrontal, extraventricular approach to stereotactic brainstem biopsy procedures. Technical note. J Neurosurg. 2005;102(3):565–70.
48. Gonçalves-Ferreira AJ, Herculano-Carvalho M, Pimentel J. Stereotactic biopsies of focal brainstem lesions. Surg Neurol. 2003;60(4):311–20.
49. Dellaretti M, Reyns N, Touzet G, Dubois F, Gusmão S, Pereira JL, et al. Stereotactic biopsy for brainstem tumors: comparison of transcerebellar with transfrontal approach. Stereotact Funct Neurosurg. 2012;90(2):79–83.

Structural Imaging and Target Visualization

6

Himanshu Sharma and Charles B. Mikell

Abbreviations

ADC	Apparent diffusion coefficient
ALS	Amyotrophic lateral sclerosis
BOLD	Blood oxygen level dependent
CSF	Cerebrospinal fluid
CT	Computed tomography
DBS	Deep brain stimulation
DWI	Diffusion-weighted imaging
EPI	Echo-planar imaging
FDA	Food and Drug Administration
FDG	2[18]F-fluoro-2-deoxy-D-glucose
FLAIR	Fluid-attenuated inversion recovery
fMRI	Functional magnetic resonance imaging
FSE	Fast spin echo
GPi	Globus pallidus internus
GRE	Gradient recalled echo
LITT	Laser interstitial thermal therapy
MRI	Magnetic resonance imaging
OCD	Obsessive-compulsive disorder
PET	Positron emission tomography
RF	Radiofrequency
SE	Spin echo
SN	Substantia nigra
STIR	Short tau inversion recovery
STN	Subthalamic nucleus
SWI	Susceptibility-weighted imaging
T	Tesla
TE	Echo time
TR	Repetition time

H. Sharma
Medical Scientist Training Program, Stony Brook University School of Medicine,
Stony Brook, NY, USA

C. B. Mikell (✉)
Department of Neurosurgery, Stony Brook University Hospital, Stony Brook, NY, USA
e-mail: charles.mikell@stonybrookmedicine.edu

Introduction and Context

Targeting brain structures deep in the brain without direct visualization was first described in 1908 by Clarke and Horsley who, by electrolytically generating cerebellar lesions in a rhesus monkey, first established the practical principles of stereotaxy [1]. The first attempt at stereotaxy in humans, however, was not attempted until 40 years later, when Spiegel et al. performed a stereotactic thermocoagulation of the thalamus [2], which was followed within a few years by the development of Leksell's arc-radius stereotactic frame system [3].

Through the twentieth century, in order to improve targeting of relevant anatomic structures, early stereotactic practitioners developed a multimodal combination of physiologic testing, atlas-based coordinate systems generated from cadaveric specimens (e.g., the Talairach coordinate system [4]), and ventriculographic guidance [5]. However, these systems have their own intrinsic limitations. In particular, atlas-

N. Pouratian, S. A. Sheth (eds.), *Stereotactic and Functional Neurosurgery*,
https://doi.org/10.1007/978-3-030-34906-6_6

based coordinate systems were particularly susceptible to the inherent subcortical anatomical variation between individuals [6–8]. Indeed, even in a relatively recent study, purely atlas-based coordinates failed to accurately target the subthalamic nucleus (STN) as defined by microelectrode recording on the first pass in over half of trials [9].

The variability giving rise to this difficulty arises not only due to normal anatomic variation but also by disease (e.g., atrophy, mass effect), age, and other physiologic characteristics such as gender [10, 11].

In the 1970s, the introduction of computed tomography (CT) allowed for visualization of intracranial structures, followed within the decade by the advent of magnetic resonance imaging (MRI) which provided even greater resolution and soft-tissue discrimination. The advent of the ability to radiologically visualize targets for surgical planning in the 1970s and 1980s was a momentous development in the field, as it allowed surgeons to adapt targets to each patient. This advance not only improved the efficacy and off-target effect profiles of functional interventions, but can also reduce the duration of surgery and number of passes needed to reach the intended target.

Practically, the advent of neuroimaging modified the derivation of stereotactic coordinates and stereotactic coordinate systems of the past, for example, by enabling the creation of probabilistic rather than anatomic mappings of targeted regions [12, 13]. It has also enabled direct targeting of structures, particularly those characterized by low functional but significant anatomic variability across individuals, obviating the need for anatomic atlases entirely in some cases.

Structural Imaging

MRI

Almost immediately after its widespread clinical introduction in the 1980s, MRI became the predominant imaging modality for use in functional neurosurgery. It is particularly valued for preoperative target localization as well as operative planning in large part because MR images are characterized by excellent tissue resolution, the ability to easily distinguish gray and white matter junctions, and the ability to clearly visualize vasculature both at the cortical surface as well as deep within the brain parenchyma [14]. Research and development in this field has continued to rapidly advance, with key advances in the operative arena arising through the development of higher field-strength machines, intraoperative and interventional MRI (discussed at greater length in Chaps. 3 and 4), computational improvements, and novel methods of image analysis such as diffusion imaging and connectivity-based segmentation (Chap. 7).

Imaging Workflow

With the proliferation in technological advances over the last few decades, the workflow for MRI-based target identification and planning is often highly variable and depends in many ways on clinical context, equipment availability, and surgeon preference. Doubtless, with the continued advance of intraoperative MRI systems including robotic guided tools, this workflow will continue to evolve over the coming years. Generally, however, the role of neuroimaging in stereotactic surgery begins with preoperative imaging to identify the target and region of interest and to define the coordinates of the target(s) within a stereotactic reference system (e.g., Talairach, MNI). In invasive procedures (unlike, e.g., focused ultrasound), this imaging is also used to plot a 3D trajectory that allows for a safe and efficient approach to the target. The use of intraoperative imaging (in conjunction with other techniques) to adjust and confirm target engagement is often critical and is covered elsewhere in this textbook. Finally, postoperative imaging confirms proper target engagement, identifies potential complications, and helps to limit the necessity of reoperation later.

Some key determinations relevant to structural imaging that need to be made preoperatively include (1) whether to use MRI alone for stereotactic images or whether to fuse these images

with those from a CT scan, (2) whether to use stereotactic frame guidance or frameless stereotaxy, and (3) whether to use real-time interventional MRI guidance, in which case preoperative MR imaging for guidance purposes may be dispensed with entirely. There are benefits and drawback to each of these approaches, but all of these options have been clinically validated.

Fusion of MR images with preoperative CT scans is a method developed to overcome some of the geometric distortion inherent to MRI (discussed below). In this approach, MR images are used primarily to determine target coordinates and identify the outlines of the regions and structures of interest. Rather than being used as a standalone reference, however, these images are fused to a preoperative CT scan which serves as the stereotactic reference image [15]. It should be noted, however, that while the MRI-CT fusion process has been demonstrated to reduce error and improve outcomes in stereotactic radiosurgery [16–18], the issue has not yet been fully resolved for deep brain stimulation (DBS). There are some data to indicate that MRI-CT fusion shows promise in this regard, but definitive evidence requires larger-scale clinical validation [19]. It is likely, however, that as susceptibility to this specific form of geometric distortion inherent to MR imaging increases with field strength, this approach may become more relevant with the continued expansion of the use of 7 T MRI machines in clinical practice. It can also be advantageous to perform other image fusions such as fusion of multiple MR image sequences, or fusion of MRI with other modalities such as positron emission tomography (PET) for preoperative planning, depending on the target(s) to be visualized [20].

Frameless stereotaxy in the context of conventional stereotactic functional neurosurgery involves the use of stereotaxy devices designed specifically for these purposes. Each clinical goal may have its own device-specific requirements relevant to target and trajectory choice, and this decision can impose additional restrictions on operative planning. For example, with one effective and commonly used device, the STarFix system (FHC Inc., Bowdoin, ME), the trajectory is built into the custom device shipped to the clinic and therefore cannot be changed intraoperatively. As a general principle, the use of frameless stereotaxy allows for (and indeed, in some cases, requires) target imaging and trajectory planning to be done independently of the operation. This can be advantageous for planning purposes and reduces intraoperative time but may increase targeting errors due to brain shift. The effect of this trade-off is still under investigation, with some studies indicating about a 2-mm shift between framed and frameless stereotaxy, while others suggest that the two are functionally equivalent [21–23]. The surgeon's preference may also be impacted by the requirement for intraoperative imaging which can be complicated by CT/MRI artifact or the requirement for MRI-compatible stereotactic devices. One notable exception to the requirement for preoperative stereotactic imaging is with the frameless stereotaxy used in interventional MRI, in which case the imaging for stereotactic guidance is performed intraoperatively.

Intraoperative integration of MRI in the neurosurgical suite, initially introduced in the mid-1990s [24], is also experiencing rapid evolution, and while an in-depth discussion is deferred to other chapters in this text, a few key points bear mentioning here. There exist two broad categories of intraoperative MR for stereotactic neurosurgery: the first involves the use of MRI intraoperatively to refine, correct, and/or verify the trajectory taken and target reached. The second, termed interventional MRI, uses images taken after dural opening for target coordinate derivation and stereotactic guidance through a frameless stereotaxy device. This allows for CSF drainage and brain shift to occur before imaging is to be taken, with average vector accuracy reported at 0.6–0.8 mm through this method [14, 25]. Limitations to this technique include the fact that introduction of mobile MRI can lead to significant OR workflow alterations, while nonmobile MRI techniques generally preclude intraoperative microelectrode recording.

After preoperative images are obtained, the target of interest is identified on imaging, and the coordinates that identify the structural target are

derived in the coordinate system of choice. These values will be used intraoperatively as the end point of the trajectory, and deriving them may be accomplished in a number of ways. First, coordinates may be taken directly from stereotactic atlases that exist for this purpose, from personal experience, or from the literature. These coordinates are generally described in reference to the anterior and posterior commissures, and for common targets, a rich literature usually exists to guide coordinate choice. A second option is to use stereotactic atlases that can be directly fused with the preoperative CT or MR imaging and thus overlaid on the imaging with fiducial placement to allow for targeting. Finally, depending on the target and the imaging modalities available, the target in question and its boundaries may be directly identifiable on preoperative imaging. These strategies are not mutually exclusive, and in many cases, the approach used depends on the context, preference, and prior experience. As general principles, there is literature to support the use of direct targeting over atlas-based coordinates [26] and the use of 3D reconstruction over 2D images [27] where feasible.

Postoperatively, imaging is important to verify correct lead and contact positioning and may be done by postoperative stereotactic MRI or fusion of the preoperative stereotactic MRI with postoperative stereotactic CT. There remains some debate on the relative merits of each approach [28], but the error generated in either case is likely less than 0.7 mm [29]. It is important to be cognizant of the specific DBS system used as well as the MRI parameters to ensure patient safety if postoperative MRI is chosen, as not each DBS system has only been validated under all imaging conditions. Please see the section on the role of CT imaging for further discussion.

Imaging Principles

Regardless of the imaging modality and operative workflow used, in the preoperative period, the acquisition of MR images with particular focus on the region of interest is the first step in operative planning. At this stage, factors identified on these images may help predict outcomes [30], and certainly, identification of specific abnormalities may delay or preclude surgery (e.g., upon visualization of severe atrophy or severe leukoencephalopathy when planning for DBS to treat Parkinson's disease) [31]. Therefore, appropriate image sequence selection is important in not only target visualization but, in some cases, ruling out other subtle pathology (e.g., tumor as opposed to cortical dysplasia as an epileptogenic focus). Due to the tremendous number of specialized imaging options available for individual cases, a comprehensive overview of MRI sequences is beyond the scope of this chapter. However, certain basic principles apply to the approach to standard MRI for target visualization which will be covered here at the risk of oversimplification.

Underlying MR imaging is the concept that different tissue types can be distinguished by the specific physical characteristics of their atoms (i.e., T1 recovery, T2 decay, and T2$*$ decay times). These values describe how the magnetization vectors in the tissue realign with a magnetic field after being excited. In order to detect this realignment (and therefore localize and characterize a tissue region of interest), MRI exposes the patient to a magnetic field and then excites the tissue with a radiofrequency (RF) pulse. The subsequent changes in magnetization vectors are detected by measuring the induced current in a receiver coil.

In MR imaging, tissue contrast is generated by detecting and displaying these values and their differences. By weighing different values (e.g., T1 recovery time) more or less heavily, different types of tissue (or disease process) may be accentuated. For example, T2 weighting shows greater signal in tissue with higher water content. To weigh a specific value more heavily, one can vary parameters of the RF pulse sequence used. Two basic pulse sequence parameters to be familiar with are TR (repetition time) and TE (echo time), which denote the time between pulses (TR) and the time between the pulse and the center of the echo received (TE). The pulse sequences themselves can be generally described by the RF pulses and the magnetic field gradients applied.

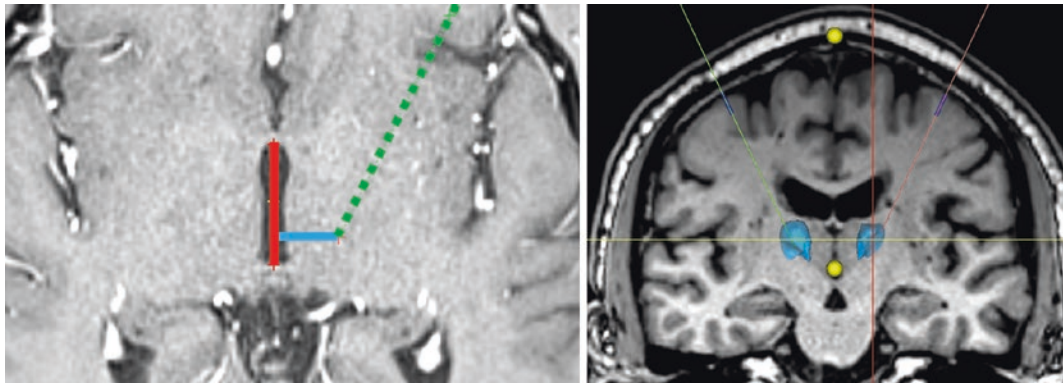

Fig. 6.1 Targeting VIM thalamus on T1 images. The AC-PC (anterior commissure-posterior commissure) coordinate system still furnishes remarkable reproducibility on T1-weighted images. In targets such as VIM thalamus that are not easily identified radiographically, AC-PC coordinates are useful (left panel). In this example, the stereotactic target (VIM nucleus) is 11 mm lateral to the wall of the third ventricle. The trajectory is shown in green. The AC-PC line is shown in red. It is also possible to target based off an atlas, which can be co-registered to the T1 preconstrast image (right panel). In this case, the hand-sensory area of the ventral posterior lateral nucleus is targeted for mapping, with a plan to place the final electrode anterior to this area

Two basic pulse sequences exist: spin echo (SE) and gradient recalled echo (GRE), with all other currently used sequence variations on these.

SE-based sequences include fast SE (FSE), STIR (short tau inversion recovery, in which fat signal is cancelled out), and FLAIR (fluid-attenuated inversion recovery, in which CSF signal is cancelled out). Generally, due to bright cerebrospinal fluid (CSF) signal, SE sequences other than FLAIR may be less well-suited to examining periventricular structures [32]. T1 FLAIR sequences can be useful in the examination of gray/white matter interfaces.

GRE-based sequences include coherent (including partially refocused or fully refocused GRE), incoherent (spoiled) GRE, echo-planar imaging (EPI), and diffusion-weighted imaging, with applications of these sequences including MR angiographic techniques (time of flight, contrast-enhanced, etc.). GRE sequences are excellent at detecting tissue with magnetic susceptibility differences (e.g., iron from hemorrhage or identifying tissues with high iron content such as the caudate, red nucleus, or the substantia nigra). In general, however, it is important to note that GRE sequences are particularly susceptible to field inhomogeneity and geometric distortion and generate artifact at air/bone tissue interfaces [33].

Among other uses, incoherent GRE (e.g., SPGR, FLASH, T1-FFE) can be used to generate high-resolution T1-weighted images, including 3D images (e.g., VIBE, LAVA, THRIVE) (Fig. 6.1) [33]. Similar ultrafast GRE (MP RAGE, BRAVO) protocols generate high-quality 3D T1-weighted images often used in epilepsy protocols to detect subtle cortical dysplasias [34]. Coherent GRE has many subtypes and are usually T2 or T2∗ weighted. Postexcitation sequences (FISP, GRASS, FFE) generate high signal-to-noise ratio images, while preexcitation sequences (PSIF, SSFP, T2-FFE) are often used for imaging of the inner ear and CSF flow studies. To generate high-resolution 3D T2-weighted images, however, fully refocused GRE (e.g., CISS, FIESTA) is often ideal.

EPI sequences are characterized by extremely short acquisition times and have better tissue contrast than other GRE sequences. Thus, applications include diffusion and perfusion imaging [35]. EPI also forms the basis of blood-oxygen-level-dependent (BOLD) imaging, which itself is the predominant sequence used as the basis of functional MRI (discussed below). With these sequences, motion artifact is minimized, but spatial resolution is limited, and EPI shares the other weaknesses of GRE-based sequences discussed above.

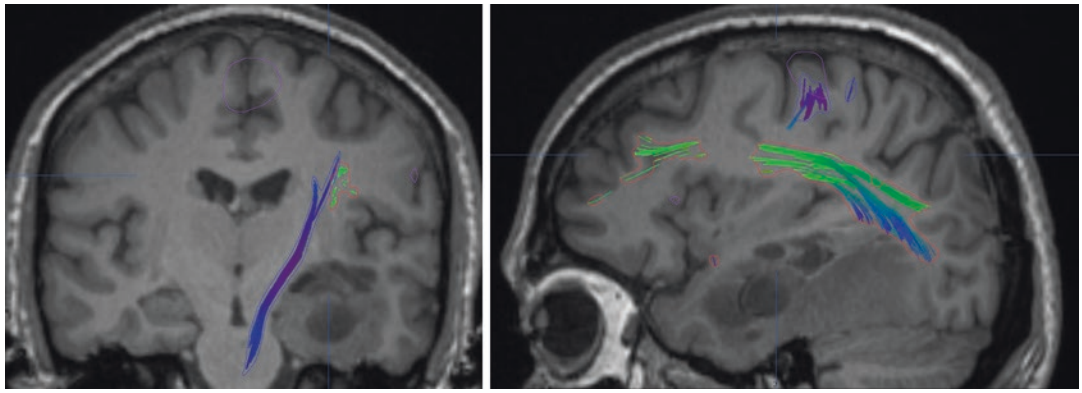

Fig. 6.2 Diffusion tensor imaging for critical white matter tracts. Diffusion tensor imaging can be used to identify and avoid critical structures during surgery, including the internal capsule (left panel, blue fibers) and frontotemporal association fibers including the arcuate fasciculus (right panel, in green)

Diffusion-weighted imaging (DWI) is an MRI modality based on the principle of detecting the anisotropy in the diffusion of water molecules. Often (but not always) generated through single-shot EPI [36], DWI allows for fine discrimination of white matter tracts which tend to strongly restrict water diffusion in a single direction (Fig. 6.2). Diffusion imaging gained widespread application in neuroimaging for its early detection of cerebral ischemia, but also is characterized by a superior ability to detect subtle structural changes within white and gray matter and resistance to motion artifact. Changes in diffusivity can also be used to help delineate subtle borders of nuclei and white matter tracts in subcortical regions [37]. Tissue with high T2 relaxation times can create a false-positive signal on DWI (i.e., T2 shine-through), however, and so correlation with apparent diffusion coefficient (ADC) imagery derived from the DWI sequence is required.

One application of DWI is known as connectivity-based segmentation (discussed in Chap. 7) which can help overcome limitations of structural imaging in certain regions that cannot be easily discriminated by the techniques discussed here. Targets that lie in the thalamus, cingulate, and cortex, for example, may all be candidates for this approach which uses tractography to segment targets that may be functionally connected via white matter tracts [38–40]. Sources of error are similar to other MRI sequences and are related to aberrations in the ability to detect subtle changes in water molecule diffusion including patient movement, cardiac pulsations, and CSF signal contamination [37]. Diffusion imaging has a lower resolution when compared to T1/T2-weighted imaging, generating approximately 2-mm isotropic voxels [5].

The specific sequences and protocols used for any particular case therefore depend on the target and application. As an example, the use of multi-gradient echo T2-weighted sequences for regions with high iron content such as the STN has been shown to improve visualization of these structures when combined with simultaneously acquired T1-weighted images (Fig. 6.3) [41]. The use of susceptibility-weighted imaging (SWI) can also be crucial in target identification. When compared with T1- and T2- weighted images, SWI produces higher levels of tissue contrast, which is often critical in identifying the anatomic borders of specific targets often used in DBS.

It behooves the surgeon to become familiar with the often rapidly evolving protocols and sequences relevant to specific surgical indications and targets, as they may significantly improve target visualization.

MR Thermometry

One benefit of MRI is that it can be used to monitor temperature in real time through the use of MR

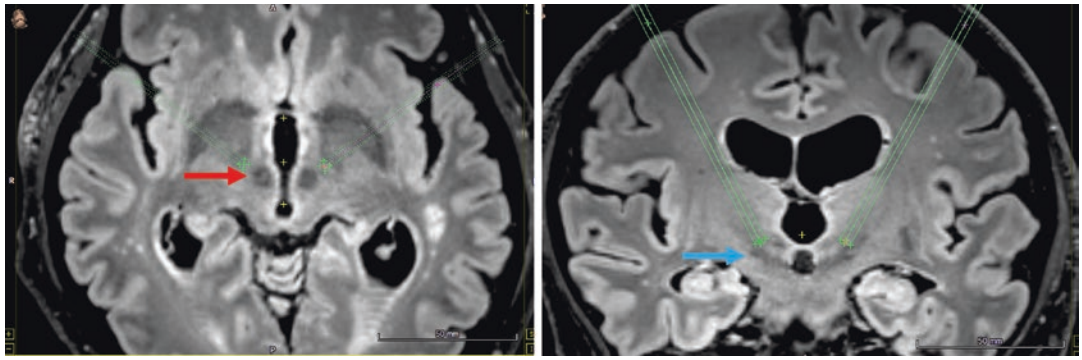

Fig. 6.3 MRI-based targeting of the subthalamic nucleus. The subthalamic nucleus can be directly visualized using T2-weighted MRI for deep brain stimulation surgery. In this case, a FLAIR image shows the red nucleus (left panel, red arrow), which serves as an internal fiducial for locating the subthalamic nucleus. Subthalamic nucleus can often be directly visualized lateral to the red nucleus, in the same plane as the red nucleus's anterior border (right panel). A hazy, T2-dark, almond-shaped area can be appreciated representing the subthalamic nucleus (blue arrow)

thermometry. Real-time MRI can therefore also help observe and guide procedures that take advantage of thermocoagulation or heat-activated therapies to achieve their effects. Many of these procedures have relevance to functional neurosurgery. One such example is the use of MRI to guide focused ultrasound to noninvasively ablate specific intracranial targets. This strategy has been approved for essential tremor, Parkinson's disease, obsessive-compulsive disorder (OCD), and neuropathic pain, with ongoing clinical trials for indications ranging from major depressive disorder to Alzheimer's disease and ALS [42]. Another example is the use of laser interstitial thermal therapy (LITT), which, in addition to tumor ablations, has been used to treat epilepsy arising from various structural abnormalities [43].

Drawbacks and Considerations

There are also significant weaknesses and sources of error inherent to MRI-based target and structure identification that one must be cognizant of during operative planning. As MR images take several minutes to acquire, these images can be significantly compromised by motion artifact – particularly in patient populations with tremor or other causes of involuntary movement [44]. Several strategies have been developed to ameliorate motion artifact, including head pads and chin-strap fixation [45] and varying degrees of sedation up to and including general anesthesia, which should be considered in the context of the risks of sedation including seizure and autonomic instability [46]. Tracking and computational correction of both macroscopic and microscopic motion is a major area of study, and several techniques exist to address this issue, some of which are very commonly used (e.g., PROPELLER) [47–49]. More sophisticated correction systems can be expensive and complex, which limits their widespread clinical adoption [50]. These systems demonstrate great technical potential, particularly when used with higher field-strength systems, but large cost-benefit analyses remain to be conducted.

Another weakness that must be considered during preoperative planning is the phenomenon of distortion. Distortion arises from several factors, including field inhomogeneity (for which correctional algorithms may be able to at least partially compensate), the fact that different regions of the brain have different susceptibilities to magnetic alignment, and the distance of the region being mapped from the isocenter of the machine bore [14]. Susceptibility to geometric distortion increases with the strength of the magnetic field and tends to be greatest in the peripheral parts of the brain, particular around bone-brain interfaces [51]. Correction algorithms and fusion with CT can help address this geometric distortion (discussed below).

Currently, specific precautions as specified by manufacturer guidelines need to be taken in order to safely perform MRI in patients with implanted DBS systems, which include not using an MRI machine with greater than 1.5 T field strength, using specific head coils (transmit-receive-type radiofrequency head coil), and imaging parameters with a specific absorption rate (the rate at which energy from the RF pulse is deposited in the patient [52]) no greater than 0.1 W/kg in the head [53]. Implications of these restrictions include the fact that imaging any other part of the body with MRI is contraindicated. There are ongoing research and significant debate in this field, however, with data indicating that 3 T systems may be safe for use with at least some DBS systems [54].

Current and Future Directions

There has been significant interest in the development of higher field-strength MRI machines as increased field strength improves the signal-to-noise ratio in the resultant images. This, therefore, allows for higher resolution (i.e., lower voxel size) and tissue contrast. For example, 7 T machines have generated 120-μm isotropic resolution in human brain MRI scans and 150-μm isotropic voxels for angiographic studies [55, 56]. This distinction is not merely academic; clinically relevant tasks such as discrimination between internal thalamic nuclei, distinction between the lateral and medial GPi, and separating out the anterior STN from the SN are significantly improved at 7 T [57, 58]. Focal cortical dysplasia can be more easily detected at these field strengths, and further improvements are likely to arise as new sequences are developed specifically for neuroimaging with 7 T MRI machines [59, 60]. Higher field strengths, however, are more susceptible to many of the artifacts inherent to MRI, including geometric distortion [51] and motion error [55]. Limited availability of 7 T machines for clinical use can also be a factor, as the first FDA-approved 7 T machines have only been clinically available for a few years as of this writing. As such, there exists some difference of opinion about the role of 7 T MRI in clinical practice.

The Role of CT Imaging

CT, while a critical element of structural imaging in stereotactic and functional neurosurgery, is largely used in conjunction with MRI to take advantage of the unique strengths of CT imaging. CT's advantages lie in its excellent visualization of bone and implanted hardware as well as its high geometric accuracy due to the inherent nature of its line-of-sight mode of image acquisition. Indeed, MR images alone may distort the AC-PC landmarks critical for atlas-based strategies to a clinically significant degree. Fusion with CT imagery along with computational correctional methods can help correct for this distortion [61, 62]. CT methods with current fusion algorithms provide good spatial validity necessary for accurate coordinate derivation [19, 63].

Postoperative imaging to verify electrode placement may be done by fusing preoperative MRI scans with a postoperative CT scan. One significant advantage of this strategy is that it is only through CT imaging that leads can be directly visualized. The metallic electrode contact creates an eccentric signal void on MRI, precluding direct visualization of the contact [64]. One group also noted that when the preoperative scan used as the reference scan was a CT scan (as opposed to a preoperative MRI), the resultant preoperative/postoperative fusion images were more accurate [65]. Proponents of postoperative stereotactic MRI, however, note that the fusion algorithm itself can be a source of error, although this error appears to be shrinking with advances in fusion algorithms [66–68]. Other benefits of postoperative CT imaging include reduced time and cost with the concomitant effects on availability as well as patient comfort and safety.

With regard to vascular imaging in surgical planning, both contrast-enhanced MRI and CT angiography can visualize vessels, although interestingly, vessel location was not identical in the majority of vessels when the two modalities were compared head-to-head. In these cases, CTA localization is considered more accurate. Furthermore, 22% of all vessels were seen only in MRI, while another 13% of vessels were seen only by CTA, raising the prospect that both

imaging modalities may be necessary to minimize the risk of hemorrhage [69].

Disadvantages to the use of CT imaging include the fact that it must be performed in conjunction with MRI to generate sufficient soft-tissue contrast, the risks associated with the fusion process as discussed above, and exposure to ionizing radiation, which is proportional to the resolution achieved.

Functional Imaging

While the primary focus of this chapter is structural neuroimaging, there are aspects of functional imaging that can be used in conjunction with structural neuroimaging to help identify targets for functional neurosurgery, and so a few pertinent topics will be discussed here.

Functional neuroimaging, which in the context of functional neurosurgery can be thought of as a subset of the technical arsenal used for functional brain mapping, differs from structural neuroimaging in that it seeks primarily to ascertain the underlying patterns of neuronal activity that correspond to brain activity associated with specific tasks or functions. Generally, functional neuroimaging techniques use hemodynamic or metabolic changes as surrogates for the underlying neuronal and glial activity. Functional neuroimaging helps improve personalization of targets in the setting of interindividual variability and can particularly be a critical adjunct to structural imaging in the context of disease and structural changes leading to plasticity and/or mass effect.

Two widely used forms of functional neuroimaging are functional MRI (fMRI) and PET imaging.

Functional MRI

fMRI takes advantage of the fact that neuronally active areas of the brain induce increased local blood flow and perfusion. As oxyhemoglobin and deoxyhemoglobin have distinct magnetic properties, increased blood flow to a region can be detected by the influx of oxyhemoglobin, leading to a shorter T2 signal which is termed blood-oxygen-level-dependent (BOLD) signal [70].

The spatial resolution of fMRI is relatively high at approximately 1 mm, but when interpreting such images, it is important to consider that the underlying perfusion changes themselves may not functionally have such high resolution. Similar constraints underlie the functional temporal resolution of approximately 3 seconds [71]. Advantages over other methods of brain mapping include its noninvasive nature, repeatability, safety, and no need for radiation or exogenous contrast agents. fMRI can be used in patients with implanted DBS systems [72]. Disadvantages include difficulty imaging tissue-air interfaces, regions with neovasculature proliferation and/or certain tumors, and significant sensitivity to motion error, including head movement, cardiac pulsations, etc., which can induce systemic effects [73–75].

fMRI has been validated as a method to map eloquent cortex in the preoperative planning for tumor resection throughout the brain [76, 77] and is now widely used to determine language lateralization in preoperative planning for epilepsy surgery [78]. Some advocate for its use (along with magnetoencephalography or transcranial magnetic stimulation) over the Wada test in routine preoperative planning for these surgeries given its noninvasive nature and comparable efficacy with the Wada test [79].

Behaviorally, fMRI has been traditionally measured in paradigms involving responses to a specific stimulus or task in order to identify regions activated by discrete stimuli. However, resting state fMRI has started to move from research to clinical application in specific scenarios and can be particularly relevant to functional neurosurgery in certain cases such as the identification of epileptogenic zones [80]. For example, resting state fMRI has been successfully used to identify sub-centimeter epilepsy foci for the treatment of hypothalamic hamartomas. While the surgical treatment of these hamartomas is notorious for high morbidity, this approach to target identification significantly improved functional outcomes compared with patients who had a standard battery of MRI, and

in the 36 patients tested, this was associated with no neurologic, psychiatric, or endocrinologic morbidity [81].

PET Imaging

PET imaging takes advantage of positron-emitting radioisotopes that generate gamma rays when their emitted positron collides with local electrons. These radioisotopes can be used to create specific compounds, or tracers, that are taken up in specific circumstances which can thereby be used to map different metabolic events. As many different tracers can be made, the phenomena and structures defined by PET imaging are extremely flexible and broad, including blood flow, glucose or amino acid metabolism, and receptor occupancy [70]. As an example, one commonly used tracer is 2[18] F-fluoro-2-deoxy-D-glucose (FDG). FDG is a glucose analog that is taken up by cells and trapped inside the cells by phosphorylation by hexokinase [82]. Thus, FDG can be used as a proxy measure for brain metabolism. Much like with fMRI, FDG is generally used in task-specific paradigms which are compared to baseline metabolism to identify regions associated with specific activities. FDG-PET can also be used to identify epileptogenic foci, especially if MRI studies are negative or inconclusive [83].

Benefits of PET include extremely high sensitivity [71], albeit at the cost of signal-to-noise ratio [84]. PET imaging can provide quantitative results in a variety of contexts as it is also very flexible and applicable to a wide variety of functional and behavioral tasks. Given the questions that still exist regarding the safety of high-strength fMRI fields with DBS systems, PET can provide an alternative means to study structural functionality in this patient population. PET is used extensively translationally to help visualize and validate new structural targets as well as identify responsiveness to intervention. For example, in 1999, based on previous PET imaging, activation of the subgenual cingulate was theorized to play a role in both acute sadness and depression [85]. Furthermore, fluoxetine therapy for depression was shown to decrease the activity of this region [86]. By 2005, these data were used to guide the placement of stimulation leads into the subgenual ACC white matter in 20 patients with treatment-resistant depression. Follow-up PET scans showed reversal of preoperative PET findings of decreased blood flow to the subgenual ACC and related regions specifically in those who demonstrated sustained clinical response to stimulation [87].

Downsides include poor spatial resolution (approximately 4 mm), invasiveness, and radioactivity, precluding its use in children. With regard to spatial resolution, one should be aware of the "partial volume effect" which can cause spillover into adjacent areas, misrepresenting the size of certain phenomena (reviewed in [88]).

Current and Future Directions

Neuroimaging has heralded significant improvement in the ability to directly view and target regions once estimated based on atlas-based methods. While neuroimaging techniques are used extensively in research and have demonstrated reproducible findings, clinical validation still lags behind in many cases. As such, validating some of the approaches and strategies discussed in this chapter remains a major source of ongoing effort. As functional and structural neuroimaging continue to advance, prospective identification of efficacious targets and prediction of response is expected to improve patient outcomes and increase tolerability. Indeed, coupled with advances in our understanding of the neural circuitry underlying various disorders, functional and structural neuroimaging will likely continue to play an ever-more critical role in guiding neurosurgical therapies in the years to come.

References

1. Horsley V, Clarke RH. The structure and functions of the cerebellum examined by a new method. Brain. 1908;31(1):45–124.

2. Spiegel EA, Wycis HT, Marks M, Lee AJ. Stereotaxic apparatus for operations on the human brain. Science. 1947;106(2754):349–50.
3. Leksell L. The stereotaxic method and radiosurgery of the brain. Acta Chir Scand. 1951;102(4):316–9.
4. Talairach J, Tournoux P. Co-planar stereotaxic atlas of the human brain: 3-dimensional proportional system: an approach to cerebral imaging. Stuttgart: Thieme; 1988.
5. Downes A, Pouratian N. Advanced neuroimaging techniques for central neuromodulation. Neurosurg Clin N Am. 2014;25(1):173–85.
6. Littlechild P, Varma TRK, Eldridge PR, Fox S, Forster A, Fletcher N, et al. Variability in position of the subthalamic nucleus targeted by magnetic resonance imaging and microelectrode recordings as compared to atlas co-ordinates. Stereotact Funct Neurosurg. 2003;80(1–4):82–7.
7. Pouratian N, Bookheimer SY. The reliability of neuroanatomy as a predictor of eloquence: a review. Neurosurg Focus. 2010;28(2):E3.
8. Daniluk S, Davies K, Ellias SA, Novak P, Nazzaro JM. Assessment of the variability in the anatomical position and size of the subthalamic nucleus among patients with advanced Parkinson's disease using magnetic resonance imaging. Acta Neurochir. 2010;152(2):201–10; discussion 210.
9. Patel NK, Khan S, Gill SS. Comparison of atlas and magnetic-resonance-imaging-based stereotactic targeting of the subthalamic nucleus in the surgical treatment of Parkinson's disease. Stereotact Funct Neurosurg. 2008;86(3):153–61.
10. Ballmaier M, Sowell ER, Thompson PM, Kumar A, Narr KL, Lavretsky H, et al. Mapping brain size and cortical gray matter changes in elderly depression. Biol Psychiatry. 2004;55(4):382–9.
11. Im K, Lee JM, Lee J, Shin YW, Kim IY, Kwon JS, et al. Gender difference analysis of cortical thickness in healthy young adults with surface-based methods. NeuroImage. 2006;31(1):31–8.
12. Nowinski WL, Belov D, Thirunavuukarasuu A, Benabid AL. A probabilistic functional atlas of the VIM nucleus constructed from pre-, intra- and post-operative electrophysiological and neuroimaging data acquired during the surgical treatment of Parkinson's disease patients. Stereotact Funct Neurosurg. 2005;83(5–6):190–6.
13. Nowinski WL, Belov D, Benabid AL. An algorithm for rapid calculation of a probabilistic functional atlas of subcortical structures from electrophysiological data collected during functional neurosurgery procedures. NeuroImage. 2003;18(1):143–55.
14. Vega RA, Holloway KL, Larson PS. Image-guided deep brain stimulation. Neurosurg Clin N Am. 2014;25(1):159–72.
15. Liu X, Rowe J, Nandi D, Hayward G, Parkin S, Stein J, et al. Localisation of the subthalamic nucleus using radionics image fusion™ and Stereoplan™ combined with field potential recording. Stereotact Funct Neurosurg. 2001;76:63–73.
16. Cohen D, Lustgarten J, Miller E, Khandji A, Goodman RR. Effects of coregistration of MR to CT images on MR stereotactic accuracy. J Neurosurg. 1995;82(5):772–9.
17. Watanabe Y, Perera GM, Mooij RB. Image distortion in MRI-based polymer gel dosimetry of Gamma Knife stereotactic radiosurgery systems. Med Phys. 2002;29(5):797–802.
18. Pollock BE, Link MJ, Foote RL. Failure rate of contemporary low-dose radiosurgical technique for vestibular schwannoma. J Neurosurg. 2009;111(4):840–4.
19. Chen SY, Tsai ST, Hung HY, Lin SH, Pan YH, Lin SZ. Targeting the subthalamic nucleus for deep brain stimulation – a comparative study between magnetic resonance images alone and fusion with computed tomographic images. World Neurosurg. 2011;75(1):132–7; discussion 22–4, 29–31.
20. Jonker B. Image fusion pitfalls for cranial radiosurgery. Surg Neurol Int. 2013;4(Suppl 3):S123–8.
21. Kelman C, Ramakrishnan V, Davies A, Holloway K. Analysis of stereotactic accuracy of the cosman-robert-wells frame and nexframe frameless systems in deep brain stimulation surgery. Stereotact Funct Neurosurg. 2010;88(5):288–95.
22. Holloway K, Docef A. A quantitative assessment of the accuracy and reliability of O-arm images for deep brain stimulation surgery. Neurosurgery. 2013;72(1 Suppl Operative):47–57.
23. Burchiel KJ, McCartney S, Lee A, Raslan AM. Accuracy of deep brain stimulation electrode placement using intraoperative computed tomography without microelectrode recording. J Neurosurg. 2013;119(2):301–6.
24. Black PML, Moriarty T, Alexander E, Stieg P, Woodard EJ, Gleason PL, et al. Development and implementation of intraoperative magnetic resonance imaging and its neurosurgical applications. Neurosurgery. 1997;41(4):831–42; discussion 842–5.
25. Ostrem JL, Galifianakis NB, Markun LC, Grace JK, Martin AJ, Starr PA, et al. Clinical outcomes of PD patients having bilateral STN DBS using high-field interventional MR-imaging for lead placement. Clin Neurol Neurosurg. 2013;115(6):708–12.
26. Schlaier J, Schoedel P, Lange M, Winkler J, Warnat J, Dorenbeck U, et al. Reliability of atlas-derived coordinates in deep brain stimulation. Acta Neurochir. 2005;147(11):1175–80.
27. Andrade-Souza YM, Schwalb JM, Hamani C, Hoque T, Saint-Cyr J, Lozano AM. Comparison of 2-dimensional magnetic resonance imaging and 3-planar reconstruction methods for targeting the subthalamic nucleus in Parkinson disease. Surg Neurol. 2005;63(4):357–62.
28. Ellenbogen JR, Tuura R, Ashkan K. Localisation of DBS electrodes post-implantation, to CT or MRI? Which is the best option? Stereotact Funct Neurosurg. 2018;96(5):347–8.
29. Hyam JA, Akram H, Foltynie T, Limousin P, Hariz M, Zrinzo L. What you see is what you get: Lead location within deep brain structures is accurately

depicted by stereotactic magnetic resonance imaging. Neurosurgery. 2015;11 Suppl 3:412–9; discussion 419.
30. Bonneville F, Welter ML, Elie C, du Montcel ST, Hasboun D, Menuel C, et al. Parkinson disease, brain volumes, and subthalamic nucleus stimulation. Neurology. 2005;64(9):1598 LP–1604.
31. Welter ML, Houeto JL, Tezenas du Montcel S, Mesnage V, Bonnet AM, Pillon B, et al. Clinical predictive factors of subthalamic stimulation in Parkinson's disease. Brain. 2002;125(3):575–83.
32. Kates R, Atkinson D, Brant-Zawadzki M. Fluid-attenuated inversion recovery (FLAIR): clinical prospectus of current and future applications. Top Magn Reson Imaging. 1996;8(6):389–96.
33. Mohindra N, Neyaz Z. Magnetic resonance sequences: Practical neurological applications. Neurol India. 2015;63(2):241–9.
34. Hartman LA, Nace SR, Maksimovic JH, Rusinak D, Rowley HA. Epilepsy imaging: approaches and protocols. Appl Radiol. 2015;44(5):8–20.
35. Poustchi-Amin M, Mirowitz SA, Brown JJ, McKinstry RC, Li T. Principles and applications of echo-planar imaging: a review for the general radiologist. Radiographics. 2001;21(3):767–79.
36. Pipe J. Pulse sequences for diffusion-weighted MRI. In: Diffusion MRI: from quantitative measurement to in vivo neuroanatomy. 2nd ed: Elsevier Inc; 2013. p. 11–34.
37. Nucifora PGP, Verma R, Lee S-K, Melhem ER. Diffusion-tensor MR imaging and tractography: exploring brain microstructure and connectivity. Radiology. 2007;245(2):367–84.
38. Johansen-Berg H, Gutman DA, Behrens TEJ, Matthews PM, Rushworth MFS, Katz E, et al. Anatomical connectivity of the subgenual cingulate region targeted with deep brain stimulation for treatment-resistant depression. Cereb Cortex. 2008;18(6):1374–83.
39. Rushworth MFS, Behrens TEJ, Johansen-Berg H. Connection patterns distinguish 3 regions of human parietal cortex. Cereb Cortex. 2006;16(10):1418–30.
40. Lenglet C, Abosch A, Yacoub E, de Martino F, Sapiro G, Harel N. Comprehensive in vivo mapping of the human basal ganglia and thalamic connectome in individuals using 7T MRI. PLoS One. 2012;7(1):e29153.
41. Elolf E, Bockermann V, Gringel T, Knauth M, Dechent P, Helms G. Improved visibility of the subthalamic nucleus on high-resolution stereotactic MR imaging by added susceptibility (T2∗) contrast using multiple gradient echoes. Am J Neuroradiol. 2007;28(6):1093–4.
42. Jung NY, Chang JW. Magnetic resonance-guided focused ultrasound in neurosurgery: taking lessons from the past to inform the future. J Korean Med Sci. 2018;33(44):e279.
43. Grewal SS, Zimmerman RS, Worrell G, Brinkmann BH, Tatum WO, Crepeau AZ, et al. Laser ablation for mesial temporal epilepsy: a multi-site, single institutional series. J Neurosurg. 2018:1–8.
44. Richter EO, Hoque T, Halliday W, Lozano AM, Saint-Cyr JA. Determining the position and size of the subthalamic nucleus based on magnetic resonance imaging results in patients with advanced Parkinson disease. J Neurosurg. 2004;100(3):541–6.
45. Schlösser R, Hutchinson M, Joseffer S, Rusinek H, Saarimaki A, Stevenson J, et al. Functional magnetic resonance imaging of human brain activity in a verbal fluency task. J Neurol Neurosurg Psychiatry. 1998;64(4):492–8.
46. Venkatraghavan L, Manninen P, Mak P, Lukitto K, Hodaie M, Lozano A. Anesthesia for functional neurosurgery: review of complications. J Neurosurg Anesthesiol. 2006;18(1):64–7.
47. Jenkinson M, Bannister P, Brady M, Smith S. Improved optimization for the robust and accurate linear registration and motion correction of brain images. NeuroImage. 2002;17(2):825–41.
48. Rohde GK, Barnett AS, Basser PJ, Marenco S, Pierpaoli C. Comprehensive approach for correction of motion and distortion in diffusion-weighted MRI. Magn Reson Med. 2003;51(1):103–14.
49. Forbes KPN, Pipe JG, Bird CR, Heiserman JE. PROPELLER MRI: clinical testing of a novel technique for quantification and compensation of head motion. J Magn Reson Imaging. 2001;14(3):215–22.
50. Godenschweger F, Kägebein U, Stucht D, Yarach U, Sciarra A, Yakupov R, et al. Motion correction in MRI of the brain. Phys Med Biol. 2016;61(5):R32–56.
51. Duchin Y, Abosch A, Yacoub E, Sapiro G, Harel N. Feasibility of using ultra-high field (7 T) MRI for clinical surgical targeting. PLoS One. 2012;7(5):e37328.
52. Adair ER, Berglund LG. On the thermoregulatory consequences of NMR imaging. Magn Reson Imaging. 1986;4(4):321–33.
53. Dormont D, Seidenwurm D, Galanaud D, Cornu P, Yelnik J, Bardinet E. Neuroimaging and deep brain stimulation. AJNR Am J Neuroradiol. 2010;31(1):15–23.
54. Sammartino F, Krishna V, Sankar T, Fisico J, Kalia SK, Hodaie M, et al. 3-Tesla MRI in patients with fully implanted deep brain stimulation devices: a preliminary study in 10 patients. J Neurosurg JNS. 2017;127(4):892–8.
55. Stucht D, Danishad KA, Schulze P, Godenschweger F, Zaitsev M, Speck O. Highest resolution in vivo human brain MRI using prospective motion correction. PLoS One. 2015;10(7):1–17.
56. Mattern H, Sciarra A, Godenschweger F, Stucht D, Lüsebrink F, Rose G, et al. Prospective motion correction enables highest resolution time-of-flight angiography at 7T. Magn Reson Med. 2018;80(1):248–58.
57. Abosch A, Yacoub E, Ugurbil K, Harel N. An assessment of current brain targets for deep brain stimulation surgery with susceptibility-weighted imaging at 7 Tesla. Neurosurgery. 2010;67(6):1745–56.
58. Duyn JH, van Gelderen P, Li T-Q, de Zwart JA, Koretsky AP, Fukunaga M. High-field MRI of brain cortical substructure based on signal phase. Proc Natl Acad Sci. 2007;104(28):11796–801.

59. Lupo JM, Li Y, Hess CP, Nelson SJ. Advances in ultra-high field MRI for the clinical management of patients with brain tumors. Curr Opin Neurol. 2011;24(6):605–15.
60. Vargas MI, Martelli P, Xin L, Ipek O, Grouiller F, Pittau F, et al. Clinical neuroimaging using 7 T MRI: challenges and prospects. J Neuroimaging. 2018;28(1):5–13.
61. Menuel C, Garnero L, Bardinet E, Poupon F, Phalippou D, Dormont D. Characterization and correction of distortions in stereotactic magnetic resonance imaging for bilateral subthalamic stimulation in Parkinson disease. J Neurosurg. 2005;103(2):256–66.
62. Alexander E 3rd, Kooy HM, van Herk M, Schwartz M, Barnes PD, Tarbell N, et al. Magnetic resonance image-directed stereotactic neurosurgery: use of image fusion with computerized tomography to enhance spatial accuracy. J Neurosurg. 1995;83(2):271–6.
63. Kooy HM, Van Herk M, Barnes PD, Alexander E, Dunbar SF, Tarbell NJ, et al. Image fusion for stereotactic radiotherapy and radiosurgery treatment planning. Int J Radiat Oncol Biol Phys. 1994;28(5):1229–34.
64. Pinsker MO, Herzog J, Falk D, Volkmann J, Deuschl G, Mehdorn M. Accuracy and distortion of deep brain stimulation electrodes on postoperative MRI and CT. Zentralbl Neurochir. 2008;69(3):144–7.
65. Yoshida F, Miyagi Y, Morioka T, Hashiguchi K, Murakami N, Matsumoto K, et al. Assessment of contact location in subthalamic stimulation for Parkinson's disease by co-registration of computed tomography images. Stereotact Funct Neurosurg. 2008;86(3):162–6.
66. Geevarghese R, Ogorman Tuura R, Lumsden DE, Samuel M, Ashkan K. Registration accuracy of CT/MRI fusion for localisation of deep brain stimulation electrode position: an imaging study and systematic review. Stereotact Funct Neurosurg. 2016;94(3):159–63.
67. O'Gorman RL, Jarosz JM, Samuel M, Clough C, Selway RP, Ashkan K. CT/MR image fusion in the postoperative assessment of electrodes implanted for deep brain stimulation. Stereotact Funct Neurosurg. 2009;87(4):205–10.
68. Bot M, Van Den Munckhof P, Bakay R, Stebbins G, Verhagen Metman L. Accuracy of intraoperative computed tomography during deep brain stimulation procedures: comparison with postoperative magnetic resonance imaging. Stereotact Funct Neurosurg. 2017;95(3):183–8.
69. Krüger MT, Coenen VA, Jenkner C, Urbach H, Egger K, Reinacher PC. Combination of CT angiography and MRI in surgical planning of deep brain stimulation. Neuroradiology. 2018;60(11):1151–8.
70. Tharin S, Golby A. Functional brain mapping and its applications to neurosurgery. Neurosurgery. 2007;60(4 Suppl 2):185–201; discussion 201–2.
71. Volkow ND, Rosen B, Farde L. Imaging the living human brain: magnetic resonance imaging and positron emission tomography. Proc Natl Acad Sci. 1997;94(7):2787–8.
72. Rezai AR, Lozano AM, Crawley AP, Joy MLG, Davis KD, Kwan CL, et al. Thalamic stimulation and functional magnetic resonance imaging: localization of cortical and subcortical activation with implanted electrodes. J Neurosurg. 1999;90(3):583–90.
73. Power JD, Barnes KA, Snyder AZ, Schlaggar BL, Petersen SE. Spurious but systematic correlations in functional connectivity MRI networks arise from subject motion. NeuroImage. 2012;59(3):2142–54.
74. Krings T, Reinges MHT, Erberich S, Kemeny S, Rohde V, Spetzger U, et al. Functional MRI for presurgical planning: problems, artefacts, and solution strategies. J Neurol Neurosurg Psychiatry. 2001;70(6):749–60.
75. Devlin JT, Russell RP, Davis MH, Price CJ, Wilson J, Moss HE, et al. Susceptibility-induced loss of signal: comparing PET and fMRI on a semantic task. NeuroImage. 2000;11(6 Pt 1):589–600.
76. Tyndall AJ, Reinhardt J, Tronnier V, Mariani L, Stippich C. Presurgical motor, somatosensory and language fMRI: technical feasibility and limitations in 491 patients over 13 years. Eur Radiol. 2017;27(1):267–78.
77. Tieleman A, Deblaere K, Van Roost D, Van Damme O, Achten E. Preoperative fMRI in tumour surgery. Eur Radiol. 2009;19(10):2523–34.
78. Rosazza C, Ghielmetti F, Minati L, Vitali P, Giovagnoli AR, Deleo F, et al. Preoperative language lateralization in temporal lobe epilepsy (TLE) predicts perictal, pre- and post-operative language performance: an fMRI study. Neuroimage Clin. 2013;3:73–83.
79. Papanicolaou AC, Rezaie R, Narayana S, Choudhri AF, Wheless JW, Castillo EM, et al. Is it time to replace the Wada test and put awake craniotomy to sleep? Epilepsia. 2014;55(5):629–32.
80. Lee HW, Arora J, Papademetris X, Tokoglu F, Negishi M, Scheinost D, et al. Altered functional connectivity in seizure onset zones revealed by fMRI intrinsic connectivity. Neurology. 2014;83(24):2269–77.
81. Boerwinkle VL, Foldes ST, Torrisi SJ, Temkit H, Gaillard WD, Kerrigan JF, et al. Subcentimeter epilepsy surgery targets by resting state functional magnetic resonance imaging can improve outcomes in hypothalamic hamartoma. Epilepsia. 2018;59(12):2284–95.
82. Farwell MD, Pryma DA, Mankoff DA. PET/CT imaging in cancer: current applications and future directions. Cancer. 2014;120(22):3433–45.
83. Yang PF, Pei JS, Zhang HJ, Lin Q, Mei Z, Zhong ZH, et al. Long-term epilepsy surgery outcomes in patients with PET-positive, MRI-negative temporal lobe epilepsy. Epilepsy Behav. 2014;41:91–7.
84. Petrirena GJ, Goldman S, Delattre JY. Advances in PET imaging of brain tumors: a referring physician's perspective. Curr Opin Oncol. 2011;23(6):617–23.
85. Mayberg HS, Liotti M, Brannan SK, McGinnis S, Mahurin RK, Jerabek PA, et al. Reciprocal limbic-cortical function and negative mood: converging PET findings in depression and normal sadness. Am J Psychiatry. 1999;156(5):675–82.

86. Mayberg HS, Brannan SK, Tekell JL, Silva JA, Mahurin RK, McGinnis S, et al. Regional metabolic effects of fluoxetine in major depression: serial changes and relationship to clinical response. Biol Psychiatry. 2000;48(8):830–43.
87. Lozano AM, Mayberg HS, Giacobbe P, Hamani C, Craddock RC, Kennedy SH. Subcallosal cingulate Gyrus deep brain stimulation for treatment-resistant depression. Biol Psychiatry. 2008;64(6):461–7.
88. Soret M, Bacharach SL, Buvat I. Partial-volume effect in PET tumor imaging. J Nucl Med. 2007;48(6):932–45.

Network-Based Imaging and Connectomics

7

Harith Akram and Ludvic Zrinzo

Introduction

The study of brain networks using advanced MRI techniques is a rapidly developing field within the wide-ranging discipline of neuroscience [1, 2]. In 2009, the US National Institutes of Health (NIH) announced funding for the 5-year Human Connectome Project (HCP) [3]. Since then, 1200 healthy subjects have had their connectomes mapped as part of the Young Adult Human Connectome Project using state-of-the-art anatomical, diffusion and functional MRI scans [3]. This eventually led the HCP consortium to produce an updated map of the human cerebral cortex, published in the journal *Nature* under the title 'The Brain Redefined' in 2016. One hundred eighty cortical areas per hemisphere were mapped using multimodal, advanced MRI connectivity data and cutting-edge machine learning algorithms [4].

Since then, smaller disease-specific connectomes have also been developed focusing on various brain diseases such as Alzheimer's disease, blindness, anxiety, depression, epilepsy and early psychosis to shed light on the brain network dysfunction associated with these conditions. Similar initiatives have been undertaken in Europe under the premise of the Human Brain Project (HBP) and the Virtual Brain neuroinformatics platform [5]. The importance of this field was highlighted again by the announcement of 110 million USD funding for the BRAIN initiative (Brain Research through Advancing Innovative Neurotechnologies) by the Office of Science and Technology Policy at the White House in 2013. This initiative had, at its heart, the objective of supporting the development and application of innovative technologies to create a dynamic understanding of human brain function focusing on studying neural networks [6].

These advances have been received with enthusiasm by the field of stereotactic and functional neurosurgery. This was not surprising considering that progress in functional neurosurgery has been inextricably linked to progress in neuroimaging techniques. Advances in MRI techniques have made it possible to directly target deep brain structures with deep brain stimulation (DBS) or ablative surgery and improve safety based on improved visualisation of trajectories [7, 8]. Current models of the basal ganglia take into account the functionally distinct cortico-subcortical loops that form elements of the motor, associative and emotive systems, passing through the basal ganglia and thalamic nuclei, creating functional subregions within these structures with various degrees of overlap [9]. Localising these subregions (e.g. the sensorimotor subthalamic nucleus [STN]) is not possible using

H. Akram (✉) · L. Zrinzo
Unit of Functional Neurosurgery, UCL Queen Square Institute of Neurology and the National Hospital for Neurology and Neurosurgery, London, UK
e-mail: harith.akram@ucl.ac.uk

N. Pouratian, S. A. Sheth (eds.), *Stereotactic and Functional Neurosurgery*,
https://doi.org/10.1007/978-3-030-34906-6_7

conventional magnetic resonance imaging [9, 10]. This underlying relationship between structure and function suggests that the efficacy of DBS and the prevention of unwanted side effects are influenced by the precise stimulation site within the anatomical target. Those functional subregions often show distinct electrophysiological features. This has been exploited with the use of microelectrode recording (MER) to refine the final electrode location. However, the use of MER to refine the surgical target has several drawbacks. Conventionally, surgery will need to be carried out awake and off medications which can be arduous to some patients. Furthermore, there is a growing body of evidence suggesting that the use of electrophysiological markers is by no means a guarantee of a good long-term outcome. Location of the best MER activity has been shown not to necessarily correlate with the best clinical response on macro-electrode testing intraoperatively [11]. It has been demonstrated that a better predictor of a good long-term clinical outcome may be the DBS lead position within the MRI-defined STN [12, 13]. At some centres, MER also commonly involves the insertion of two to five sharp microelectrodes into the target. This is likely associated with an increased risk of intracranial haemorrhage, which can in rare cases lead to devastating complications and even death [14, 15].

Image-guided and image-verified approach reduces the operative time and patient discomfort as surgery can be carried out under general anaesthesia [14], it allows for relocation of electrodes when results are suboptimal [15], and anatomical targeting errors can be detected and addressed before completing the procedure [16–18]. This approach provides the ability to carry out audit of contact locations leading to a positive impact on future DBS procedures. There are no facile means to replicate an 'ideal MER recording' in subsequent procedures. However, MRI-verified surgery allows for constructing a 'DBS functional map' within the targeted structure through studying correlations between the contact location, side effects and efficacy across a group. The data can then be replicated in future patients to improve targeting [19, 20]. Please refer to Chap. 3 for a more detailed discussion of the advantages and opportunities of intraoperative imaging in stereotactic surgery.

Using an image-guided and image-verified approach thus carries numerous advantages; however, conventional MRI does not provide information on functional mapping within the brain target in a way that MER does. Structural and functional connectivity studies have therefore aimed to provide the opportunity to examine the concept of 'noninvasive' functional mapping against 'invasive' mapping with MER. This can provide new ways to define the subregions in target nuclei, such as the STN in which stimulation in the sensorimotor area gives the optimal results in PD patients [12, 21, 22]. These novel imaging methods also open the door to defining new targets based on innumerable brain mapping studies that have begun to define disease-specific connectomes and enhanced understanding of the pathophysiological basis of an array of neurological and psychiatric diseases.

Structural and Functional MR Connectivity

The science of mapping out brain connections is not new. The structural connectivity of the human brain has been studied for centuries, employing various techniques to define neural connections. Gross anatomical studies in the sixteenth century carried out by the anatomist Andreas Vesalius defined various major white matter tracts. Centuries later, the development of the microscope opened up the door for exploring the microstructural architecture of neural tissue. Tracer studies in nonhuman primates (NHP) allow scientists to make some inferences about the human brain, whilst brain lesion studies in humans similarly allow for mapping out anatomical connections; however, diffusion MRI is the only noninvasive technique currently used to study the brain's structural connectivity.

Functional Connectivity

Functional connectivity is characterised by synchronisation in neural activity between different regions in the brain. These regions might be directly (monosynaptically) or indirectly (polysynaptically) connected. Imaging of neuronal activity was originally studied using positron emission tomography (PET) and single-photon emission computerised tomography (SPECT) techniques. Over the last decade, resting state fMRI has been used to study functional connectivity by examining synchronicity in the haemodynamic response (HDR) on blood-oxygen-level-dependent (BOLD) and other perfusion-sensitive (such as arterial spin labelling) sequences, thus determining correlations between different brain regions [19]. Functional connectivity mapping offers a relatively simple, noninvasive, and fast approach to mapping normal and pathological neural network changes. Resting state fMRI does not rely on an experimental task design, making data analysis streamlined and less vulnerable to experimental bias [20]. Multiple statistical modelling techniques, such as seed-based correlation mapping, principal component analysis (PCA) and independent component analysis (ICA), can then be used to examine this functional connectivity [20, 23]. Networks can also be mapped using graph theory analysis exploring local small world network hubs as well as global connectivity measures. Resting state functional connectivity (fcMRI) has been used in various clinical applications [24]. For example, selective changes were found in individuals at risk of Alzheimer's disease [25] and also documented in patients with major depression [26]. Statistically significant positive correlations have been found between fcMRI and structural connectivity [27–30].

The underlying basis for this modality stems from the observation that the time course of low-frequency (<0.1 Hz) fluctuations in blood-oxygen-level-dependent (BOLD) signal has a high degree of temporal correlation in functionally connected brain areas or 'nodes' [31]. Moreover, this slow frequency signal may correlate with neural electrophysiological activity at higher frequencies [32], in the alpha band range [33], in the gamma band range [34] and in the beta band range [35], thus providing inference between networks identified using fcMRI and their underlying neurophysiological correlates. This relationship can be very useful in studying and understanding Parkinson's disease (PD) neurophysiology as functional connectivity changes may reflect the abnormal synchronised oscillations in PD. Functional connectivity has been used to differentiate PD patients from controls [36] as well as to explore the cognitive deficit associated with PD [37]. It has been shown that differences in functional connectivity patterns of the basal ganglia, as mapped using resting state fMRI, are associated with different degrees of response to L-DOPA therapy in patients with advanced PD. This is consistent with the hypothesis that the clinical effects of dopamine are a result of remapping of functional connectivity [38]. Further studies have examined the functional connectivity changes in relation to STN DBS producing new models of mechanism of action [39] and outcome prediction [40]. A useful guide to network modelling and fMRI acquisition can be found in a review by Smith et al. [41].

Structural Connectivity

Structural connectivity defines direct (monosynaptic) anatomical connections via axonal bundles between different brain regions. This can be assessed using MR diffusion connectivity.

There is no 'standard' approach to acquiring and processing diffusion MRI data. This is partly due to the mixture of applications of diffusion imaging and the restraints associated with acquiring and processing high-quality data. As a result, a plethora of specialised software platforms have been developed, each offering different ways of data processing and visualisation.

The domain of diffusion MRI can be broadly divided into two categories: (1) the study of the scale, density and organisation of brain tissue microstructure, e.g. fractional anisotropy (FA), mean diffusivity (MD), neurite orientation dispersion and density imaging (NODDI) and

(2) the study of macrostructural connectivity by means of tractography. The latter can be mostly subdivided into deterministic, probabilistic and global approaches [42].

An Introduction to Diffusion MRI Acquisition.

MRI is highly sensitive to water tissue content. As a result of Brownian motion, water molecules are mobile and not static. This motion can be random in isotropic environments (e.g. grey matter or CSF) or directional in anisotropic environments (e.g. axonal fibre bundles or blood vessels). A directional displacement of sensitised water molecules (phase shift) can result in a detectable MRI signal loss. This outlines the basic principle of diffusion imaging. In areas of restricted water diffusion, the orientation of white matter tracts can be inferred from the signal loss incurred due to phase shift along the diffusion direction. This conventionally involves the use of a pulse-gradient spin echo sequence, where gradient pulses are applied on both ends of the 180° refocusing pulse. The signal is then acquired using a single-shot rapid image acquisition method such as echo-planar imaging (EPI). The strength and duration of the gradient pulse are directly related to signal loss along the diffusion direction or to the 'diffusion effect'. The factor that reflects the strength and timing of the gradients is termed the *b-value* (s/mm^2). Each diffusion direction is encoded in x, y and z coordinates of the corresponding gradients. Acquiring more diffusion directions results in higher angular resolution. This, however, comes at the expense of increased scanning time [42].

Other factors can influence the way diffusion MRI data is acquired. These include the static magnetic field strength, spatial resolution (voxel size), number of diffusion shells, number of averages acquired, phase encoding direction, the quality and number of channels in the receive head coil, the use of in-plane acceleration or multi-slice acquisition, etc.

At the centre of any MRI acquisition, there is a central trade-off between signal-to-noise ratio (SNR), image spatial resolution and scanning time. With an increase in the static magnetic field comes an increase in the intrinsic SNR (7 T > 3 T > 1.5 T) but not without drawbacks, mainly increased inhomogeneity of both the main field (B0) and the RF transmit field (B1), resulting in worsening geometrical distortion, in addition to the increased specific absorption rate (SAR) resulting in safety implications [43], which is of particular concern in stereotactic and functional neurosurgery where MR safety in the setting of implants is paramount. Diffusion sequences are therefore highly customisable. Careful attention to optimising the scanning parameters should be sought to ensure that the appropriate sequences are acquired.

Modelling Diffusion in a Voxel

Several diffusion methods have been developed, each with its strengths and limitations. These include *diffusion kurtosis imaging* (DKI) [44]; *Q-space imaging* such as diffusion spectral imaging (DSI) [45] and hybrid diffusion imaging (HYDI) [46]; and *model-based approaches* such as the composite hindered and restricted model of diffusion (CHARMED) [47], NODDI [48] and diffusion basis spectral imaging (DBSI) [49]. The most popular diffusion models by far are diffusion tensor imaging (DTI) and high angular resolution diffusion imaging (HARDI).

Diffusion Tensor Imaging (DTI)

DTI is one of the simplest models used to describe the anisotropic diffusion phenomenon in brain tissue. The use of the term is so ubiquitous it has become – wrongly – synonymous with DWI and with tractography. DTI was first described in 1994 [50] as a three-dimensional model of Gaussian diffusion displacements in a voxel, depicted in a 3 × 3 covariance matrix:

$$D = \begin{pmatrix} D_{xx} & D_{xy} & D_{xz} \\ D_{yx} & D_{yy} & D_{yz} \\ D_{zx} & D_{zy} & D_{zz} \end{pmatrix}$$

In order to visualise the tensor as an ellipsoid (Fig. 7.1), the covariance matrix can be diagonalised to yield three eigenvalues ($\lambda 1 > \lambda 2 > \lambda 3$) and their corresponding eigenvectors ($\varepsilon 1$, $\varepsilon 2$ and $\varepsilon 3$).

Several scalar matrices, to describe tissue diffusion properties on the microstructural level,

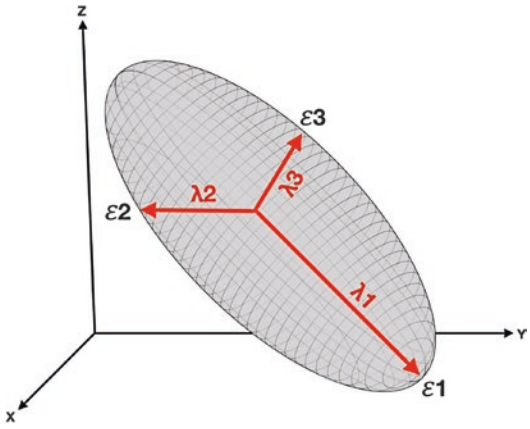

Fig. 7.1 The DTI ellipsoid. (© 2019 Harith Akram)

can be derived from this tensor model such as FA, axial diffusivity, radial diffusivity and MD.

The DTI model has several limitations nonetheless, mainly its inability to resolve multiple fibre orientations in a voxel. Furthermore, the assumption of a Gaussian diffusion profile, which is at the heart of the DTI model, fails at higher b-values. This has necessitated the introduction of more complex models to describe the diffusion signal beyond the simple tensor [42].

High Angular Resolution Diffusion Imaging (HARDI)

In this diffusion method, higher b-values (1000–3000 s/mm^2) and number of diffusion directions (in a single shell) are needed when data is acquired. An ensemble of a finite number of diffusion tensors is modelled in each voxel [51]. This is a more complex model of diffusion than DTI, and it allows for the resolution of multiple crossing fibres (e.g. in spherical deconvolution) [42].

MR Diffusion Tractography

Tractography is a technique used to study white matter pathways and structural connectivity in brain tissue. It is employed after diffusion modelling at the voxel level described in the prior section. Tractography relies on indirect measurements to create 'tracts' through brain voxels. Inferences can be made from these tracts to represent white matter pathways [52]. These pathways have been validated in histological studies, correlating well with known anatomy [53]. The connectivity profile of a region of interest can be used to segment this region according to the maximum probability of connection to the cortex and or to other regions in the brain [54, 55]. This technique has been applied to segment structures within the basal ganglia network [56–58].

Tractography is error prone and has several limitations; however, it remains the only noninvasive method available to measure the structural connectivity in the human brain tissue in vivo. Tractography algorithms can be local or global, deterministic or probabilistic, model based or model-free.

Deterministic Versus Probabilistic Tractography

Deterministic tractography is a technique that involves the creation of streamlines starting from a seed region of interest in white matter and passing through voxels by following the first eigenvector of the diffusion tensor (i.e. the principal direction of diffusion), effectively connecting the arrows in each voxel. Streamlines are then terminated when they reach a target seed or fall below a set curvature or FA value (e.g. in areas of low anisotropy). Deterministic tractography has been very successful in white matter pathway delineation [59]. Since this method usually relies on the DTI model, diffusion data acquisition and processing are relatively fast. Despite its success in visualising large white matter tracts, deterministic tractography has significant drawbacks. These include the inability to accurately visualise tracts in areas of low anisotropy (e.g. thalamus) or high noise (e.g. brainstem) and modelling errors in areas of high anatomical complexity (e.g. crossing or kissing fibres). Moreover, errors incurred during streamline visualisation can get easily propagated resulting in anatomically erroneous connections [60], resulting in white matter pathways that are implausible or known not to exist. Concerns regarding 'accuracy' and 'reproducibility' have also been recently raised

[61]. Overall, deterministic tractography tends to 'underestimate' the number of streamlines in a pathway [62].

Probabilistic tractography does not utilise 'streamlining'. Instead, a function of uncertainty of the fibre orientation measurement is created in each voxel. This is often referred to as the orientation density function or ODF. Once fibre modelling is carried out in each brain voxel, tracts can be generated by the propagation of uncertainty over multiple iterations [52].

In contrast to deterministic tractography, probabilistic tractography can generate tracts in areas of low certainty (low anisotropy, high noise, etc.). It can also provide statistical metrics of connectivity. This method requires higher-quality data (in a single shell, i.e. HARDI, or in a multi-shell form). It is also computationally demanding. These factors translate to relatively long acquisition and processing times. Having said that, with advancements in MR image acquisition (e.g. multiband acquisition) and processing (e.g. GPU processing), these approaches are becoming more feasible in a clinical setting [63], although not regularly deployed at time of publication. In a recent comparison of different tractography techniques, probabilistic tractography was shown to produce results closest to the ground truth; however, it also resulted in more false positives than deterministic approaches (Fig. 7.2) [62].

Applications of MRI Connectivity in Functional Neurosurgery

The applications of MRI structural and functional connectivity can be broadly divided into at least five main categories: (1) the visualisation of surgical targets not readily identifiable on conventional imaging techniques, e.g. the ventrointermedialis (Vim) nucleus of the thalamus and the dentato-rubro-thalamic tract, used in

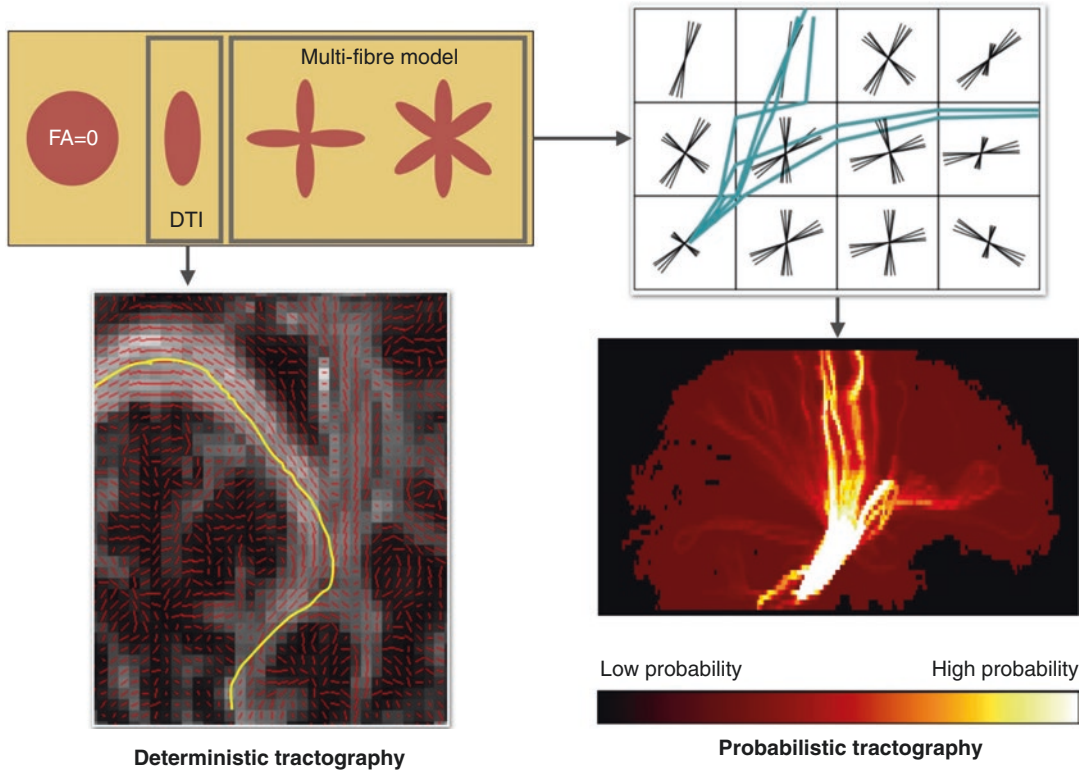

Fig. 7.2 Diffusion modelling and deterministic vs. probabilistic tractography

the treatment of tremor; (2) the refinement of the surgical target within the functional subzones of basal ganglia structures, e.g. the STN [64]; (3) the building of treatment predictive models [38, 40]; (4) the identification of new targets such as the ventral tegmental area (aka the posterior hypothalamic region) for the treatment of cluster headache [65] and CG25 as an experimental target for the treatment of depression [66]; and (5) the investigation of the underlying pathophysiology and the treatment mechanism of action [67]. Other applications may emerge with even more experience and evolution of the field.

Presently, the main application of connectivity in functional neurosurgery has been in thalamic surgery for tremor. Individualised, image-guided and image-verified targeting of the Vim has been a quest for many in the field. Inter-individual variability in the Vim's location has been illustrated in several studies. This was clearly shown in a functional connectivity study that analysed resting state fMRI scans in 58 healthy subjects [68]. Considerable individual variability of atlas-based Vim targeting was again demonstrated in a study that examined the Vim's relation to surrounding major fibre tracts using deterministic tractography in 10 patients with thalamic DBS for ET [69]. The interest in mastering the application of connectivity in defining the thalamic target for tremor serves as proof of principle of the value of connectivity-based targeting and the potential of this approach for other diseases and other applications. The next section therefore focuses on this new and emerging translational application of connectivity.

The Application of MR Connectivity in Tremor Surgery

The Vim of the thalamus is an established surgical target for stereotactic ablation and DBS in the treatment of tremor in PD, essential tremor (ET) and multiple sclerosis [70–77]. A subjacent area, the caudal zona incerta (cZI), is another effective DBS target for the treatment of tremor [78–82].

The Vim is centrally placed on a cerebello-thalamo-cortical network in which pathological oscillations, possibly triggered by pallidal dysfunction in the case of PD, are thought to be culpable for tremor [83]. The cortical focus in this tremor network is in the primary motor cortex, connected to the dentate nucleus of the contralateral cerebellum through the dentato-rubro-thalamic tract (DRT) via the Vim [84–89].

The Vim is not readily visible on conventional, stereotactic MR imaging sequences used in image-guided and image-verified surgery [90–93], although it may be visible on some MR sequences as described in Chap. 3. Identifying the nucleus traditionally involves indirect targeting relying on atlas-defined coordinates in relation to the anterior commissure (AC)–posterior commissure (PC) points as landmarks, along with other identifiable structures such as the lateral thalamic/internal capsule border [94]. Needless to say, this approach does not fully account for individual variability. Furthermore, surgery often needs to be performed with the patient awake to allow for intraoperative confirmation of targeting, which can be a source of discomfort for patients [95]. Moreover, intraoperative confirmation is not always readily feasible, e.g. when performing a thalamotomy using Gamma Knife [96].

To overcome this, various imaging techniques have been proposed to identify the Vim. Ultra-high field MRI provides high contrast-to-noise ratio between thalamic nuclei, better segmenting the nucleus. However, this modality is not readily available in a clinical setting [97]. Another technique relies on contrast in coloured fractional anisotropy (FA) maps, a product of diffusion tensor imaging (DTI) [98, 99]. Simple visualisation of the first-order tensor fields in DTI has also been used to generate deterministic tractography models of the DRT, which is then targeted by DBS [100–103]. This modality is commonly accessible in clinical settings, and imaging is relatively swift to acquire and process. However, it carries limitations related to disentangling crossing fibres, tracking in areas of low anisotropy (e.g. the thalamus) [19] and overall accuracy [61].

An emerging modality utilises high angular resolution diffusion imaging (HARDI) and probabilistic connectivity-based segmentation of the thalamus [25, 53, 103–106]. This technique

successfully models crossing fibres and grey matter (low anisotropy) connectivity and achieves high signal-to-noise ratio but requires prolonged image acquisition and large computational resources which are impractical in clinical practice. Novel MRI acquisition techniques, such as simultaneous multi-slice imaging and multi-band imaging [104], have reduced scanning time. Furthermore, advances in computer processing techniques and relying on graphical processing units to carry out diffusion analysis have facilitated the use of this modality in clinical practice [105, 106]. The first study that developed this approach was carried out by Behrens et al. in 2003. Probabilistic tractography was used to delineate the boundaries between different thalamic nuclei, based on connectivity patterns between the thalamus and various cortical areas [55]. This was the first time probabilistic tractography was used to parcellate grey matter structures, obtaining the quality of results that traditional maximum-likelihood or streamline approaches have failed to produce [107]. The resulting thalamic segmentation corresponded relatively well with previous histological findings [108] and tracer studies in nonhuman primates but was not perfectly equivalent [109–116]. This technique was further validated in another study in 2004 [54]. Other grey matter structures have also been segmented with a similar approach [57, 58, 117] (Fig. 7.3).

Several studies have since used probabilistic tractography to examine Vim connectivity to cortical and cerebellar areas [118–120], or to segment the Vim based on said connectivity [106, 121]. The first of such studies to apply this approach to patients with DBS was presented in a pioneering study by Pouratian et al. in a post hoc analysis of six patients with bilateral Vim DBS and validated in four additional patients from a secondary institution [122].

Since the publication of the study by Behrens et al. in 2003 [55], several studies have set out to replicate these results using hard-segmentation algorithms to form boundaries between thalamic nuclei [122–124]. Although the results of these studies show similar patterns of segmentations, they all have individual inconsistencies. This can be explained by the high variability in dMRI acquisition and processing; the known susceptibility to geometrical distortion leading to registration inaccuracies; and the variability in the cortical seed region of interest definition. Furthermore, tractography has inherent limitations related to the laterality of the seed region whereby medially located regions of interest (i.e. the supplementary motor area (SMA)) will have stronger connectivity to the thalamus when compared to a more laterally located region (i.e. the cortical hand area). This can result in an erroneously large thalamic-SMA region. For these reasons, meaningful and anatomically accurate in vivo segmentation of the human thalamic nuclei continues to be a challenge in the field of neuroimaging. Lack of contrast between these nuclei on conventional MRI [90] is potentially a consequence of the lack of distinct anatomical borders between these structures in the first place [121]. Complicating things further, the disparities between the various histological and cytochemical classification systems have led to a diverse range of grouping and naming conventions [121, 125, 126].

The thalamic nuclei, constructed with diffusion connectivity to cortical areas and demarcated with a hard-segmentation algorithm, differ in their neuroanatomical orientation, shapes and relative sizes when compared to a ground truth model [121]. The biggest differences are seen in the lack of overlap between the nuclei and in the mediolateral orientation which is almost perpendicular to the midsagittal plane as opposed to the expected 45° orientation [121].

These inaccuracies in diffusion connectivity-based segmentation may not be significant for illustration purposes but are detrimental when using these maps in surgical targeting where a good outcome may hinge on submillimetric accuracy. Therefore, in order to rely on these computational models in surgery, multiple validation methods are required (e.g. the overlapping of the M1-thalamic segment with the cerebellar input into the thalamus [127]). Segmenting the thalamic area connected to the contralateral cerebellar dentate nucleus is further representative of the actual Vim. This area was traditionally harder to

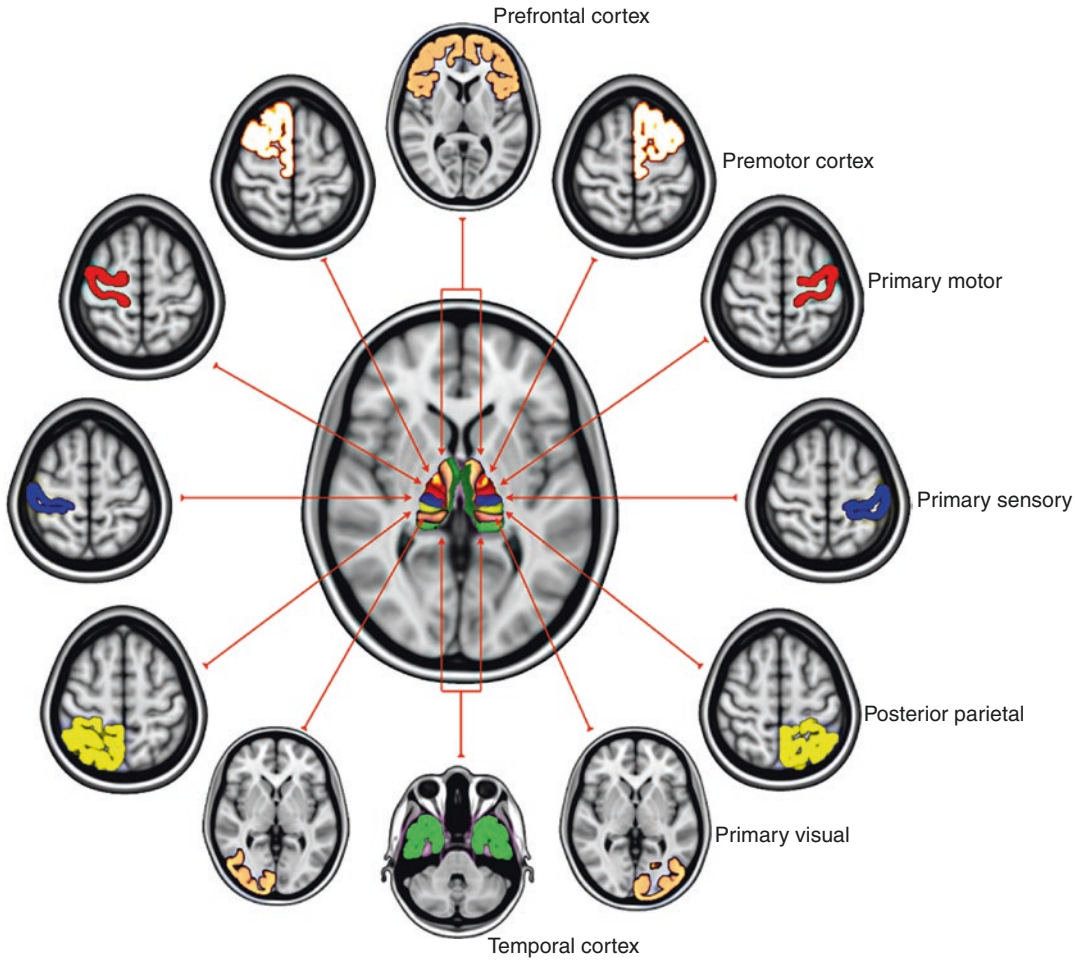

Fig. 7.3 The use of cortical connectivity to segment the thalamus. (© 2019 Harith Akram)

segment due to inherent difficulties in diffusion connectivity techniques highlighted above, but with advances in MRI and computer power, this aim has become more achievable. Connectivity-based segmentation of the Vim can be performed in individual patients in a clinically feasible timescale, using HARDI and high-performance computing with parallel GPU processing [127]. The thalamic area with highest connectivity to the contralateral dentate nucleus has been shown to lie within the much larger area with the highest connectivity to M1 in a ventrolateral position. The area with highest connectivity to the SMA and PMC lies anterior to the M1 area. The area with highest connectivity to S1 lies posterior to the M1 area. This is in keeping with known anatomical information [128]. The ventral posterior (VP) thalamic nuclear complex relays impulses of sensory systems to S1, whilst ventral lateral (VL) nuclear complex relays information from the cerebellum, basal ganglia and substantia nigra (SN) [128]. The VL complex is generally subdivided into the pars anterior (VLa), pars posterior (VLp) and pars medialis (VLm). The VLa relays afferents from the globus pallidus interna (GPi) to the PMC and SMA [94, 129–134], whilst the VLm relays input from the SN to the PMC and prefrontal cortex [109, 135, 136]. The VLp receives a large, topographically organised input from the cerebellar nuclei, projecting principally to M1 [128, 130, 132, 137, 138]. The Vim corresponds to the inferior part of the VLp [109] (Fig. 7.4).

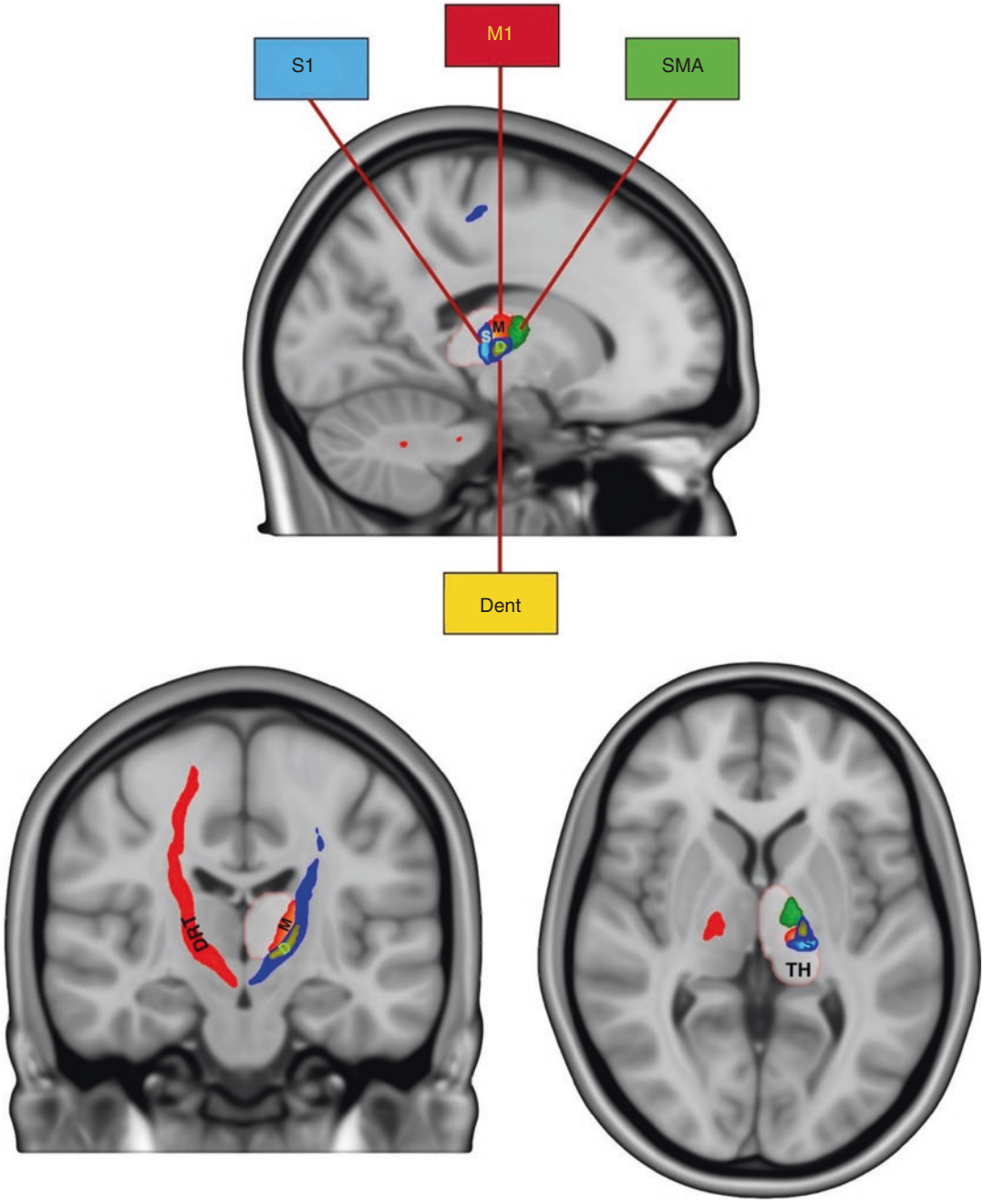

Fig. 7.4 Connectivity-derived thalamic template. (© 2019 Harith Akram)

It is important to bear in mind that the traditional subdivisions of the thalamus [128, 129] are primarily based on histochemical staining of serial sections of human thalami, rather than anatomical connectivity. It is entirely possible that the optimal 'functional' target straddles these subdivisions. Moreover, it is mechanistically likely that network connectivity of the target area will be a better predictor of efficacy than its histochemical properties.

Choosing the appropriate diffusion imaging parameters is paramount to achieving accurate segmentation of grey matter structures [139–141]. In vivo probabilistic tractography studies in the cerebellum, brainstem and diencephalon carry significant challenges. Motion artefacts, caused by the highly pulsatile nature of the region, can degrade the MRI signal during diffusion image acquisition, reducing the signal-to-noise ratio (SNR). This is complicated by the presence of myriad criss-crossing axons and reticular brain regions [142, 143]. One way of dealing with this is by using pulse-gating and respiratory rate monitoring during diffusion imaging. Likewise, by acquiring multiple diffusion scans, at a high angular resolution (increasing acquisition time), SNR is improved [50, 106, 143].

Deterministic approaches have generally failed to produce anatomically accurate representations of the DRT tract, generally showing the tract to arise from the ipsilateral, not the contralateral dentate nucleus [101–103], or stopping at the upper brainstem decussation level [100]. This may not be problematic when the DRT tract itself is being targeted, as it is the case in these reports; however, to accurately segment the Vim based on cerebellar connectivity, the crossing cerebellar streamlines must be mapped. Clear crossing of the DRT tract can be shown from the contralateral dentate nucleus, which passes through the segmented dentate area in the thalamus all the way to M1 using probabilistic tractography [127].

Challenges and Limitations of Current MR Connectivity Techniques

In order to explore the utility of MR connectivity in functional neurosurgery, it is essential to first understand the limitations of these techniques. Tractography makes inferences from water diffusion direction to produce models of white matter bundles. This is a gross representation of neural axons and is highly dependent on voxel size (spatial resolution), number of diffusion directions (directional resolution), field strength and many more highly customisable parameters from sequence acquisition to pre-processing, post-processing and study design, all of which can affect the results. Tractography does not provide information on directionality and struggles in regions with crossing or kissing fibres [144]. Furthermore, tractography has a propensity for favouring short, mesial and straight streamlines over long, lateral and tortuous ones [144] (Fig. 7.5).

Resting state functional MR connectivity can be heavily influenced by motion artefact and medications. The spatial resolution is usually considerably poor. Moreover, these techniques are largely limited to group-level analysis. Whilst this is useful in exploring group-wise changes, inferences on the individual level cannot be readily made, especially on a diagnostic/predictive capacity. This may limit the clinical application of the technique in individual patients. Both structural and functional MR studies rely on image registration which can introduce errors that are unacceptable in stereotactic surgery.

A recurrent concern with MR connectivity studies is that of reproducibility. In contrast to studies that explore a therapeutic intervention, whether pharmacological or surgical where the treatment can often be standardised and verified, connectivity imaging studies are inherently difficult to reproduce. This is attributed to the diversity of MRI acquisition and processing techniques. Furthermore, by employing multiple registration steps, errors are introduced to the system. Nonetheless, meticulous confirmation of registration accuracy at each step can alleviate the impact of this issue.

Scanning time can also pose a big challenge especially in non-academic centres. Long scans can also result in difficulties for many patients undergoing DBS surgery, mainly those undergoing surgery for movement disorders; however, novel MRI acquisition techniques, such as simultaneous multi-slice imaging and multi-band imaging [104], have greatly reduced acquisition times without compromising the SNR.

Another limitation of connectivity studies is often caused by the reliance on DBS volumes of tissue-activated (VTA) models [145]. These are

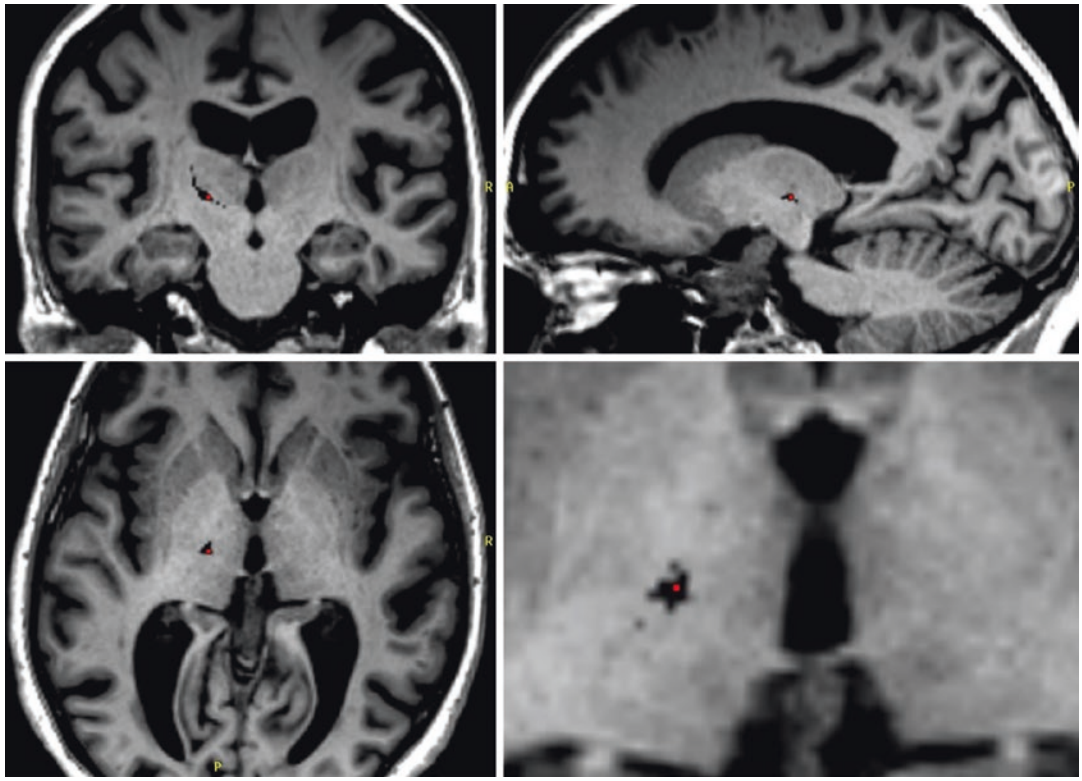

Fig. 7.5 Operative targeting of the connectivity-derived Vim. Black area represents voxels with maximum connectivity to the contralateral dentate nucleus

mostly simplified, finite element linear models that do not account for local impedance inhomogeneity. Indeed, various models over- or underestimate the VTA [146]. The presence of axons of different diameters and cell bodies, with variable action-potential thresholds, in the DBS region, complicates matters further. Ultimately, if a lead is optimally placed in a sweet spot of the functional target, lower currents should be required to achieve therapeutic responses, and VTA models should be less of a concern.

Standardisation of Methods

Method standardisation is by far the biggest challenge facing the field. Diffusion data are noisy and the sequences are highly variable and configurable. Moreover, data analysis is based on statistics and has many options and alternatives with more than one 'right' way (but many wrong ways) of analysis [19]. This, combined with the relative paucity of patients undergoing connectivity studies and functional neurosurgery, makes it essential rather than desirable to have standardised imaging paradigms and processing in order to reproduce and validate the results of these studies.

Quantification of Connectivity

A real challenge in connectivity studies, especially in measuring grey matter connectivity, is coming up with a quantifiable measure of connectivity [63]. Various connectivity indices have been proposed using normalised streamline count [64]. These are by no means perfect. Tractography has many biases and can result in false-positive/negative tracts. Connectivity measures can also be affected by crossing fibres, distance, size of seed/target masks and the straightness/curvature of the streamlines.

DBS Volume of Tissue Activation

This is certainly a challenging area that will require further development. The available models are oversimplified and often do not consider inhomogeneity in local impedance [147]. Improving the existing models cannot, however, rely only on improving the mathematical model but also on a better understanding of the mechanism of action of DBS therapy itself [148]. It is likely that the emergence of more 'steered' stimulation with directional electrodes will enrich the available models by providing more specific efficacy and side-effect data to correlate with virtual stimulation models.

Conclusion and Future Directions

Continuous advances in MRI techniques may lead to improvements in structural, diffusion or functional imaging. Higher spatial resolution and SNR with shorter acquisition times are bound to provide better data and applicability in clinical settings. Furthermore, machine learning and artificial intelligence (AI) are likely to change the way multimodal data are analysed [149]. Multivariate pattern analysis of neuroimaging data achieves increased sensitivity in detecting spatially distributed effects not usually detected by univariate analysis [149]. Using machine learning algorithms will allow for the use of data from group studies to apply to individual datasets. This can significantly increase the clinical applicability of connectivity studies, which often require large groups to overcome biases from the spatial reconstruction of connections resulting in false-positive and/or false-negative results [63, 150].

Another important development will come from further advances in computational power and GPU parallel processing techniques. This has already led to substantial reductions in big dataset processing time, allowing the use of connectivity studies in clinical settings [105].

The use of advanced MRI connectivity studies takes our understanding of brain networks to the next level and provides us with new tools to refine targeting and patient selection, as well as to better understand the treatment mechanisms of action and disease pathophysiology.

The use of these techniques should come with caution. Heavy reliance on complex statistical methods and variability in image acquisition and analysis pose real challenges. Clinicians delving into this world ought to have a good understanding of the science and the methods in order to achieve accurate results and meaningful outcomes rather than relying on a black box approach. Doing otherwise will not only result in erroneous interpretations of the data, thus potentially harming patients, but can also cause harm to the reliability of the techniques themselves, jeopardising progress in this exciting field.

References

1. Hagmann P, Cammoun L, Gigandet X, Gerhard S, Grant PE, Wedeen V, et al. MR connectomics: principles and challenges. J Neurosci Methods. 2010;194(1):34–45.
2. Marcus DS, Harwell J, Olsen T, Hodge M, Glasser MF, Prior F, et al. Informatics and data mining tools and strategies for the human connectome project. Front Neuroinform. Frontiers;. 2011;5:4.
3. Van Essen DC, Ugurbil K, Auerbach E, Barch D, Behrens TEJ, Bucholz R, et al. The human connectome project: a data acquisition perspective. NeuroImage. 2012;62(4):2222–31.
4. Glasser MF, Coalson TS, Robinson EC, Hacker CD, Harwell J, Yacoub E, et al. A multi-modal parcellation of human cerebral cortex. Nature. 2016;536(7615):171–8.
5. Markram H. The human brain project. Sci Am. 2012;306(6):50–5.
6. Mott MC, Gordon JA, Koroshetz WJ. The NIH BRAIN initiative: advancing neurotechnologies, integrating disciplines. PLoS Biol. 2018;16(11):e3000066.
7. Foltynie T, Zrinzo L, Martinez-Torres I, Tripoliti E, Petersen E, Holl E, et al. MRI-guided STN DBS in Parkinson's disease without microelectrode recording: efficacy and safety. J Neurol Neurosurg Psychiatry. 2011;82(4):358–63.
8. Zrinzo L, Yoshida F, Hariz MI, Thornton J, Foltynie T, Yousry TA, et al. Clinical safety of brain magnetic resonance imaging with implanted deep brain stimulation hardware: large case series and review of the literature. World Neurosurg. 2011;76(1–2):164–72.
9. Haber SN, Fudge JL, McFarland NR. Striatonigrostriatal pathways in primates form an

ascending spiral from the shell to the dorsolateral striatum. J Neurosci. 2000;20(6):2369–82.
10. Yelnik J, Bardinet E, Dormont D, Malandain G, Ourselin S, Tandé D, et al. A three-dimensional, histological and deformable atlas of the human basal ganglia. I. Atlas construction based on immunohistochemical and MRI data. NeuroImage. 2007;34(2):618–38.
11. Bour LJ, Contarino MF, Foncke EMJ, Bie RMA, Munckhof P, Speelman JD, et al. Long-term experience with intraoperative microrecording during DBS neurosurgery in STN and GPi. Acta Neurochir. 2010;152(12):2069–77.
12. Wodarg F, Herzog J, Reese R, Falk D, Pinsker MO, Steigerwald F, et al. Stimulation site within the MRI-defined STN predicts postoperative motor outcome. Mov Disord. 2012;27(7):874–9.
13. Aviles-Olmos I, Kefalopoulou Z, Tripoliti E, Candelario J, Akram H, Martinez-Torres I, et al. Long-term outcome of subthalamic nucleus deep brain stimulation for Parkinson's disease using an MRI-guided and MRI-verified approach. J Neurol Neurosurg Psychiatry. 2014;85(12):1419–25.
14. Nakajima T, Zrinzo L, Foltynie T, Olmos IA, Taylor C, Hariz MI, et al. MRI-guided subthalamic nucleus deep brain stimulation without microelectrode recording: can we dispense with surgery under local anaesthesia. Stereotact Funct Neurosurg. 2011;89(5):318–25.
15. Richardson RM, Ostrem JL, Starr PA. Surgical repositioning of misplaced subthalamic electrodes in Parkinson's disease: location of effective and ineffective leads. Stereotact Funct Neurosurg. 2009;87(5):297–303.
16. Van Horn G, Hassenbusch SJ, Zouridakis G, Mullani NA, Wilde MC, Papanicolaou AC. Pallidotomy: a comparison of responders and nonresponders. Neurosurgery. 2001;48(2):263–71; discussion 271–3.
17. Schiff SJ, Dunagan BK, Worth RM. Failure of single-unit neuronal activity to differentiate globus pallidus internus and externus in Parkinson disease. J Neurosurg. 2002;97(1):119–28.
18. Rodriguez-Oroz MC, Rodriguez M, Leiva C, Rodriguez-Palmero M, Nieto J, Garcia-Garcia D, et al. Neuronal activity of the red nucleus in Parkinson's disease. Mov Disord. 2008;23(6):908–11.
19. Ramnani N, Behrens TEJ, Penny W, Matthews PM. New approaches for exploring anatomical and functional connectivity in the human brain. BPS. 2004;56(9):613–9.
20. Zhang D, Raichle ME. Disease and the brain's dark energy. Nat Rev Neurol. Nature Publishing Group;. 2010;6(1):15–28.
21. Weise LM, Seifried C, Eibach S, Gasser T, Roeper J, Seifert V, et al. Correlation of active contact positions with the electrophysiological and anatomical subdivisions of the subthalamic nucleus in deep brain stimulation. Stereotact Funct Neurosurg. Karger Publishers;. 2013;91(5):298–305.
22. Johnsen EL, Sunde N, Mogensen PH, Østergaard K. MRI verified STN stimulation site – gait improvement and clinical outcome. Eur J Neurol. 2010;17(5):746–53.
23. Rogers BP, Morgan VL, Newton AT, Gore JC. Assessing functional connectivity in the human brain by fMRI. Magn Reson Imaging. 2007;25(10):1347–57.
24. Fox MD, Greicius M. Clinical applications of resting state functional connectivity. Front Syst Neurosci. Frontiers;. 2010;4:19.
25. Sorg C, Riedl V, Mühlau M, Calhoun VD, Eichele T, Läer L, et al. Selective changes of resting-state networks in individuals at risk for Alzheimer's disease. Proc Natl Acad Sci U S A. 2007;104(47):18760–5.
26. Greicius MD, Flores BH, Menon V, Glover GH, Solvason HB, Kenna H, et al. Resting-state functional connectivity in major depression: abnormally increased contributions from subgenual cingulate cortex and thalamus. BPS. 2007;62(5):429–37.
27. van den Heuvel M, Mandl R, Luigjes J, Hulshoff Pol H. Microstructural organization of the cingulum tract and the level of default mode functional connectivity. J Neurosci. Society for Neuroscience;. 2008;28(43):10844–51.
28. Greicius MD, Supekar K, Menon V, Dougherty RF. Resting-state functional connectivity reflects structural connectivity in the default mode network. Cereb Cortex. Oxford University Press;. 2009;19(1):72–8.
29. Honey CJ, Sporns O, Cammoun L, Gigandet X, Thiran JP, Meuli R, et al. Predicting human resting-state functional connectivity from structural connectivity. Proc Natl Acad Sci U S A. National Acad Sciences;. 2009;106(6):2035–40.
30. Zhang D, Snyder AZ, Shimony JS, Fox MD, Raichle ME. Noninvasive functional and structural connectivity mapping of the human thalamocortical system. Cereb Cortex. Oxford University Press;. 2010;20(5):1187–94.
31. Biswal B, Yetkin FZ, Haughton VM, Hyde JS. Functional connectivity in the motor cortex of resting human brain using echo-planar MRI. Magn Reson Med. 1995;34(4):537–41.
32. Leopold DA, Murayama Y, Logothetis NK. Very slow activity fluctuations in monkey visual cortex: implications for functional brain imaging. Cereb Cortex. 2003;13(4):422–33.
33. Laufs H, Kleinschmidt A, Beyerle A, Eger E, Salek-Haddadi A, Preibisch C, et al. EEG-correlated fMRI of human alpha activity. NeuroImage. 2003;19(4):1463–76.
34. He BJ, Snyder AZ, Zempel JM, Smyth MD, Raichle ME. Electrophysiological correlates of the brain's intrinsic large-scale functional architecture. Proc Natl Acad Sci U S A. National Acad Sciences;. 2008;105(41):16039–44.

35. de Munck JC, Gonçalves SI, Mammoliti R, Heethaar RM, Lopes da Silva FH. Interactions between different EEG frequency bands and their effect on alpha-fMRI correlations. NeuroImage. 2009;47(1):69–76.
36. Szewczyk-Krolikowski K, Menke RAL, Rolinski M, Duff E, Salimi-Khorshidi G, Filippini N, et al. Functional connectivity in the basal ganglia network differentiates PD patients from controls. Neurology. 2014;83(3):208–14.
37. Baggio H-C, Sala-Llonch R, Segura B, Martí MJ, Valldeoriola F, Compta Y, et al. Functional brain networks and cognitive deficits in Parkinson's disease. Hum Brain Mapp. 2014;35(9):4620–34.
38. Akram H, Wu C, Hyam J, Foltynie T, Limousin P, De Vita E, et al. l-Dopa responsiveness is associated with distinctive connectivity patterns in advanced Parkinson's disease. Mov Disord. 2017;32(6):874–83.
39. Kahan J, Urner M, Moran R, Flandin G, Marreiros A, Mancini L, et al. Resting state functional MRI in Parkinson's disease: the impact of deep brain stimulation on 'effective' connectivity. Brain. Oxford University Press;. 2014;137(Pt 4):1130–44.
40. Horn A, Reich M, Vorwerk J, Li N, Wenzel G, Fang Q, et al. Connectivity Predicts deep brain stimulation outcome in Parkinson disease. Ann Neurol. 2017;82(1):67–78.
41. Smith SM, Miller KL, Salimi-Khorshidi G, Webster M, Beckmann CF, Nichols TE, et al. Network modelling methods for FMRI. NeuroImage. 2011;54(2):875–91.
42. Hoy AR, Alexander AL. Diffusion MRI, Brain mapping an encyclopedic reference, vol. 1: Elsevier; 2015. 6 p.
43. van der Kolk AG, Hendrikse J, Zwanenburg JJM, Visser F, Luijten PR. Clinical applications of 7 T MRI in the brain. Eur J Radiol. 2013;82(5):708–18.
44. Jensen JH, Helpern JA, Ramani A, Lu H, Kaczynski K. Diffusional kurtosis imaging: the quantification of non-Gaussian water diffusion by means of magnetic resonance imaging. Magn Reson Med. 2005;53(6):1432–40.
45. Wedeen VJ, Wang RP, Schmahmann JD, Benner T, Tseng WYI, Dai G, et al. Diffusion spectrum magnetic resonance imaging (DSI) tractography of crossing fibers. NeuroImage. 2008;41(4):1267–77.
46. Wu Y-C, Alexander AL. Hybrid diffusion imaging. NeuroImage. 2007;36(3):617–29.
47. Assaf Y, Freidlin RZ, Rohde GK, Basser PJ. New modeling and experimental framework to characterize hindered and restricted water diffusion in brain white matter. Magn Reson Med. Wiley-Blackwell;. 2004;52(5):965–78.
48. Zhang H, Schneider T, Wheeler-Kingshott CA, Alexander DC. NODDI: practical in vivo neurite orientation dispersion and density imaging of the human brain. NeuroImage. 2012;61(4):1000–16.
49. Wang X, Cusick MF, Wang Y, Sun P, Libbey JE, Trinkaus K, et al. Diffusion basis spectrum imaging detects and distinguishes coexisting subclinical inflammation, demyelination and axonal injury in experimental autoimmune encephalomyelitis mice. NMR Biomed. Wiley-Blackwell;. 2014;27(7):843–52.
50. Basser PJ, Mattiello J, LeBihan D. Estimation of the effective self-diffusion tensor from the NMR spin echo. J Magn Reson B. 1994;103(3):247–54.
51. Tuch DS, Reese TG, Wiegell MR, Makris N, Belliveau JW, Wedeen VJ. High angular resolution diffusion imaging reveals intravoxel white matter fiber heterogeneity. Magn Reson Med. 2002;48(4):577–82.
52. Behrens TEJ, Woolrich MW, Jenkinson M, Johansen-Berg H, Nunes RG, Clare S, et al. Characterization and propagation of uncertainty in diffusion-weighted MR imaging. Magn Reson Med. Wiley Subscription Services, Inc., A Wiley Company;. 2003;50(5):1077–88.
53. Dyrby TB, Søgaard LV, Parker GJ, Alexander DC, Lind NM, Baaré WFC, et al. Validation of in vitro probabilistic tractography. NeuroImage. 2007;37(4):1267–77.
54. Johansen-Berg H. Functional-anatomical validation and individual variation of diffusion tractography-based segmentation of the human thalamus. Cereb Cortex. 2004;15(1):31–9.
55. Behrens TEJ, Johansen-Berg H, Woolrich MW, Smith SM, Wheeler-Kingshott CAM, Boulby PA, et al. Non-invasive mapping of connections between human thalamus and cortex using diffusion imaging. Nat Neurosci. 2003;6(7):750–7.
56. Draganski B, Kherif F, Klöppel S, Cook PA, Alexander DC, Parker GJM, et al. Evidence for segregated and integrative connectivity patterns in the human basal ganglia. J Neurosci. 2008;28(28):7143–52.
57. Lambert C, Zrinzo L, Nagy Z, Lutti A, Hariz M, Foltynie T, et al. Confirmation of functional zones within the human subthalamic nucleus: patterns of connectivity and sub-parcellation using diffusion weighted imaging. NeuroImage. Elsevier B.V;. 2012;60:83–94.
58. Chowdhury R, Lambert C, Dolan RJ, Düzel E. Parcellation of the human substantia nigra based on anatomical connectivity to the striatum. NeuroImage. 2013;81:191–8.
59. Catani M, Howard RJ, Pajevic S, Jones DK. Virtual in vivo interactive dissection of white matter fasciculi in the human brain. NeuroImage. 2002;17(1):77–94.
60. Behrens TEJ, Jbabdi S. MR diffusion tractography. In: Diffusion MRI: Elsevier; 2009. p. 333–51.
61. Petersen MV, Lund TE, Sunde N, Frandsen J, Rosendal F, Juul N, et al. Probabilistic versus deterministic tractography for delineation of the cortico-subthalamic hyperdirect pathway in patients with Parkinson disease selected for deep brain stimulation. J Neurosurg. 2017;126:1657–68.
62. Maier-Hein KH, Neher PF, Houde J-C, Côté M-A, Garyfallidis E, Zhong J, et al. The challenge of mapping the human connectome based on diffusion

tractography. Nat Commun. Nature Publishing Group;. 20177;8(1):1349.
63. Sotiropoulos SN, Jbabdi S, Xu J, Andersson JL, Moeller S, Auerbach EJ, et al. Advances in diffusion MRI acquisition and processing in the human connectome project. NeuroImage. 2013;80:125–43.
64. Akram H, Sotiropoulos SN, Jbabdi S, Georgiev D, Mahlknecht P, Hyam J, et al. Subthalamic deep brain stimulation sweet spots and hyperdirect cortical connectivity in Parkinson's disease. NeuroImage. 2017;158:332–45.
65. May A. A review of diagnostic and functional imaging in headache. J Headache Pain. 2006;7(4):174–84.
66. Mayberg HS, Lozano AM, Voon V, McNeely HE, Seminowicz D, Hamani C, et al. Deep brain stimulation for treatment-resistant depression. Neuron. 2005;45(5):651–60.
67. Tyagi H, Apergis-Schoute AM, Akram H, Foltynie T, Limousin P, Drummond LM, et al. A randomised trial directly comparing ventral capsule and anteromedial subthalamic nucleus stimulation in obsessive compulsive disorder: clinical and imaging evidence for dissociable effects. Biol Psychiatry. Elsevier;. 2019;85(9):726–34.
68. Anderson JS, Dhatt HS, Ferguson MA, Lopez-Larson M, Schrock LE, House PA, et al. Functional connectivity targeting for deep brain stimulation in essential tremor. Am J Neuroradiol. American Society of Neuroradiology;. 2011;32(10):1963–8.
69. Anthofer J, Steib K, Fellner C, Lange M, Brawanski A, Schlaier J. The variability of atlas-based targets in relation to surrounding major fibre tracts in thalamic deep brain stimulation. Acta Neurochir. Springer Vienna; 2014;156(8):1497–504; discussion 1504.
70. Pahwa R, Lyons KE, Wilkinson SB, Tröster AI, Overman J, Kieltyka J, et al. Comparison of thalamotomy to deep brain stimulation of the thalamus in essential tremor. Mov Disord. 2001;16(1):140–3.
71. Berk C, Carr J, Sinden M, Martzke J, Honey CR. Assessing tremor reduction and quality of life following thalamic deep brain stimulation for the treatment of tremor in multiple sclerosis. J Neurol Neurosurg Psychiatry. BMJ Group; 2004;75(8):1210; authorreply 1210–1.
72. Benabid AL, Pollak P, Hommel M, Gaio JM, de Rougemont J, Perret J. [Treatment of Parkinson tremor by chronic stimulation of the ventral intermediate nucleus of the thalamus]. Rev Neurol (Paris). 1989;145(4):320–3.
73. Benabid AL, Pollak P, Gervason C, Hoffmann D, Gao DM, Hommel M, et al. Long-term suppression of tremor by chronic stimulation of the ventral intermediate thalamic nucleus. Lancet. 1991;337(8738):403–6.
74. Pollak P, Benabid AL, Gervason CL, Hoffmann D, Seigneuret E, Perret J. Long-term effects of chronic stimulation of the ventral intermediate thalamic nucleus in different types of tremor. Adv Neurol. 1993;60:408–13.
75. Benabid AL, Pollak P, Seigneuret E, Hoffmann D, Gay E, Perret J. Chronic VIM thalamic stimulation in Parkinson's disease, essential tremor and extra-pyramidal dyskinesias. Acta Neurochir Suppl (Wien). 1993;58:39–44.
76. Schuurman PR, Bosch DA, Merkus MP, Speelman JD. Long-term follow-up of thalamic stimulation versus thalamotomy for tremor suppression. Mov Disord. 2008;23(8):1146–53.
77. Hariz MI, Krack P, Alesch F, Augustinsson L-E, Bosch A, Ekberg R, et al. Multicentre European study of thalamic stimulation for parkinsonian tremor: a 6 year follow-up. J Neurol Neurosurg Psychiatry. 2007;79(6):694–9.
78. Murata J-I, Kitagawa M, Uesugi H, Saito H, Iwasaki Y, Kikuchi S, et al. Electrical stimulation of the posterior subthalamic area for the treatment of intractable proximal tremor. J Neurosurg. 2003;99(4):708–15.
79. Blomstedt P, Sandvik U, Fytagoridis A, Tisch S. The posterior subthalamic area in the treatment of movement disorders: past, present, and future. Neurosurgery. 2009;64(6):1029–38; discussion 1038–42.
80. Blomstedt P, Sandvik U, Tisch S. Deep brain stimulation in the posterior subthalamic area in the treatment of essential tremor. Mov Disord. 2010;25(10):1350–6.
81. Blomstedt P, Hariz GM, Hariz MI, Koskinen LOD. Thalamic deep brain stimulation in the treatment of essential tremor: a long-term follow-up. Br J Neurosurg. 2007;21(5):504–9.
82. Plaha P, Khan S, Gill SS. Bilateral stimulation of the caudal zona incerta nucleus for tremor control. J Neurol Neurosurg Psychiatry. 2008;79(5):504–13.
83. Helmich RC, Janssen MJR, Oyen WJG, Bloem BR, Toni I. Pallidal dysfunction drives a cerebellothalamic circuit into Parkinson tremor. Ann Neurol. 2011;69(2):269–81.
84. Gallay MN, Jeanmonod D, Liu J, Morel A. Human pallidothalamic and cerebellothalamic tracts: anatomical basis for functional stereotactic neurosurgery. Brain Struct Funct. 2008;212(6):443–63.
85. McIntyre CC, Hahn PJ. Network perspectives on the mechanisms of deep brain stimulation. Neurobiol Dis. 2010;38(3):329–37.
86. Jörntell H, Ekerot CF. Topographical organization of projections to cat motor cortex from nucleus interpositus anterior and forelimb skin. J Physiol. Wiley-Blackwell;. 1999;514(Pt 2):551–66.
87. Dum RP, Strick PL. An unfolded map of the cerebellar dentate nucleus and its projections to the cerebral cortex. J Neurophysiol. 2003;89(1):634–9.
88. Helmich RC, Hallett M, Deuschl G, Toni I, Bloem BR. Cerebral causes and consequences of parkinsonian resting tremor: a tale of two circuits? Brain. Oxford University Press;. 2012;135(Pt 11):3206–26.
89. Baker KB, Schuster D, Cooperrider J, Machado AG. Deep brain stimulation of the lateral cerebellar nucleus produces frequency-specific alterations

in motor evoked potentials in the rat in vivo. Exp Neurol. Elsevier Inc;. 2010;226(2):259–64.
90. Lemaire J-J, Sakka L, Ouchchane L, Caire F, Gabrillargues J, Bonny J-M. Anatomy of the human thalamus based on spontaneous contrast and microscopic voxels in high-field magnetic resonance imaging. Neurosurgery. 2010;66(3 Suppl Operative):161–72.
91. Deistung A, Schäfer A, Schweser F, Biedermann U, Turner R, Reichenbach JR. Toward in vivo histology: a comparison of quantitative susceptibility mapping (QSM) with magnitude-, phase-, and $R2_*$-imaging at ultra-high magnetic field strength. NeuroImage. Elsevier Inc;. 2013;65(C):299–314.
92. Traynor CR, Barker GJ, Crum WR, Williams SCR, Richardson MP. Segmentation of the thalamus in MRI based on T1 and T2. NeuroImage. 2011;56(3):939–50.
93. Vassal F, Coste J, Derost P, Mendes V, Gabrillargues J, Nuti C, et al. Direct stereotactic targeting of the ventrointermediate nucleus of the thalamus based on anatomic 1.5-T MRI mapping with a white matter attenuated inversion recovery (WAIR) sequence. Brain Stimul. 2012;5(4):625–33.
94. Schaltenbrand G, Wahren W, Hassler R. Atlas for stereotaxy of the human brain: Thieme Medical Publishers; 1977. 1 p.
95. Gross RE, Krack P, Rodriguez-Oroz MC, Rezai AR, Benabid AL. Electrophysiological mapping for the implantation of deep brain stimulators for Parkinson's disease and tremor. Mov Disord. 2006;21(S14):S259–83.
96. Witjas T, Carron R, Krack P, Eusebio A, Vaugoyeau M, Hariz M, et al. A prospective single-blind study of Gamma Knife thalamotomy for tremor. Neurology. 2015;85(18):1562–8.
97. Spiegelmann R, Nissim O, Daniels D, Ocherashvilli A, Mardor Y. Stereotactic targeting of the ventrointermediate nucleus of the thalamus by direct visualization with high-field MRI. Stereotact Funct Neurosurg. 2006;84(1):19–23.
98. Lefranc M, Carron R, Régis J. Prelemniscal radiations: a new reliable landmark of the thalamic nucleus ventralis intermedius location. Stereotact Funct Neurosurg. 2015;93(6):400–6.
99. Sedrak M, Gorgulho A, Frew A, Behnke E, DeSalles A, Pouratian N. Diffusion tensor imaging and colored fractional anisotropy mapping of the ventralis intermedius nucleus of the thalamus. Neurosurgery. 2011;69(5):1124–9; discussion 1129–30.
100. Sammartino F, Krishna V, King NKK, Lozano AM, Schwartz ML, Huang Y, et al. Tractography-based ventral intermediate nucleus targeting: novel methodology and intraoperative validation. Mov Disord. 2016;31(8):1217–25.
101. Coenen VA, Rijntjes M, Prokop T, Piroth T, Amtage F, Urbach H, et al. One-pass deep brain stimulation of dentato-rubro-thalamic tract and subthalamic nucleus for tremor-dominant or equivalent type Parkinson's disease. Acta Neurochir. Springer Vienna;. 2016;158(4):773–81.
102. Coenen VA, Allert N, Paus S, Kronenburger M, Urbach H, Mädler B. Modulation of the cerebello-thalamo-cortical network in thalamic deep brain stimulation for tremor: a diffusion tensor imaging study. Neurosurgery. 2014;75(6):657–69; discussion 669–70.
103. Coenen VA, Mädler B, Schiffbauer H, Urbach H, Allert N. Individual fiber anatomy of the subthalamic region revealed with diffusion tensor imaging: a concept to identify the deep brain stimulation target for tremor suppression. Neurosurgery. 2011;68(4):1069–75; discussion 1075–6.
104. Feinberg DA, Setsompop K. Ultra-fast MRI of the human brain with simultaneous multi-slice imaging. J Magn Reson. 2013;229:90–100.
105. Hernandez M, Guerrero GD, Cecilia JM, García JM, Inuggi A, Jbabdi S, et al. Accelerating fibre orientation estimation from diffusion weighted magnetic resonance imaging using GPUs. Yacoub E, editor. PLoS One. 2013;8(4):e61892.
106. Hernandez-Fernandez M, Reguly I, Giles M, Jbabdi S, Smith S, Sotiropoulos S. A fast and flexible toolbox for tracking brain connections in diffusion MRI datasets using GPUs. Geneva, Switzerland; 2016.
107. Jones DK, Simmons A, Williams SC, Horsfield MA. Non-invasive assessment of axonal fiber connectivity in the human brain via diffusion tensor MRI. Magn Reson Med. 1999;42(1):37–41.
108. Morel A, Magnin M, Jeanmonod D. Multiarchitectonic and stereotactic atlas of the human thalamus. J Comp Neurol. 1997;387(4):588–630.
109. Jones EG. The thalamus: Springer Science & Business Media; 2012. 1 p.
110. Tanaka D. Thalamic projections of the dorsomedial prefrontal cortex in the rhesus monkey (Macaca mulatta). Brain Res. 1976;110(1):21–38.
111. Tobias TJ. Afferents to prefrontal cortex from the thalamic mediodorsal nucleus in the rhesus monkey. Brain Res. 1975;83(2):191–212.
112. Markowitsch HJ, Irle E, Emmans D. Cortical and subcortical afferent connections of the squirrel monkey's (lateral) premotor cortex: evidence for visual cortical afferents. Int J Neurosci. 1987;37(3–4):127–48.
113. Yarita H, Iino M, Tanabe T, Kogure S, Takagi SF. A transthalamic olfactory pathway to orbitofrontal cortex in the monkey. J Neurophysiol. 1980;43(1):69–85.
114. Russchen FT, Amaral DG, Price JL. The afferent input to the magnocellular division of the mediodorsal thalamic nucleus in the monkey, Macaca fascicularis. J Comp Neurol. 1987;256(2):175–210.
115. Jones EG, Powell TP. Connexions of the somatic sensory cortex of the rhesus monkey. 3. Thalamic connexions. Brain. 1970;93(1):37–56.
116. Jones EG, Wise SP, Coulter JD. Differential thalamic relationships of sensory-motor and

parietal cortical fields in monkeys. J Comp Neurol. 1979;183(4):833–81.
117. Johansen-Berg H, Gutman DA, Behrens TEJ, Matthews PM, Rushworth MFS, Katz E, et al. Anatomical connectivity of the subgenual cingulate region targeted with deep brain stimulation for treatment-resistant depression. Cereb Cortex. 2008;18(6):1374–83.
118. Klein JC, Barbe MT, Seifried C, Baudrexel S, Runge M, Maarouf M, et al. The tremor network targeted by successful VIM deep brain stimulation in humans. Neurology. 2012;78(11):787–95.
119. Groppa S, Herzog J, Falk D, Riedel C, Deuschl G, Volkmann J. Physiological and anatomical decomposition of subthalamic neurostimulation effects in essential tremor. Brain. Oxford University Press;. 2014;137(Pt 1):109–21.
120. Hyam JA, Owen SLF, Kringelbach ML, Jenkinson N, Stein JF, Green AL, et al. Contrasting connectivity of the ventralis intermedius and ventralis oralis posterior nuclei of the motor thalamus demonstrated by probabilistic tractography. Neurosurgery. 2012;70(1):162–9.
121. Ilinsky I, Horn A, Paul-Gilloteaux P, Gressens P, Verney C, Kultas-Ilinsky K. Human motor thalamus reconstructed in 3D from continuous sagittal sections with identified subcortical afferent territories. eNeuro. 2018;5(3)
122. Pouratian N, Zheng Z, Bari AA, Behnke E, Elias WJ, Desalles AAF. Multi-institutional evaluation of deep brain stimulation targeting using probabilistic connectivity-based thalamic segmentation. J Neurosurg. 2011;115(5):995–1004.
123. Middlebrooks EH, Tuna IS, Almeida L, Grewal SS, Wong J, Heckman MG, et al. Structural connectivity-based segmentation of the thalamus and prediction of tremor improvement following thalamic deep brain stimulation of the ventral intermediate nucleus. Neuroimage Clin. 2018;20:1266–73.
124. Kim W, Chivukula S, Hauptman J, Pouratian N. Diffusion tensor imaging-based thalamic segmentation in deep brain stimulation for chronic pain conditions. Stereotact Funct Neurosurg. 2016;94(4):225–34.
125. Hassler R. [Anatomy of the thalamus]. Arch Psychiatr Nervenkr Z Gesamte Neurol Psychiatr. 1950;184(3–4):249–56.
126. Hirai T, Jones EG. A new parcellation of the human thalamus on the basis of histochemical staining. Brain Res Brain Res Rev. 1989;14(1):1–34.
127. Akram H, Dayal V, Mahlknecht P, Georgiev D, Hyam J, Foltynie T, et al. Connectivity derived thalamic segmentation in deep brain stimulation for tremor. Neuroimage Clin. 2018;18:130–42.
128. Nieuwenhuys R, Voogd J, van Huijzen C. The human central nervous system: Springer Science & Business Media; 2013. 1 p.
129. Parent A, De Bellefeuille L. Organization of efferent projections from the internal segment of globus pallidus in primate as revealed by fluorescence retrograde labeling method. Brain Res. 1982;245(2):201–13.
130. Sakai ST, Stepniewska I, Qi HX, Kaas JH. Pallidal and cerebellar afferents to pre-supplementary motor area thalamocortical neurons in the owl monkey: a multiple labeling study. J Comp Neurol. 2000;417(2):164–80.
131. DeVito JL, Anderson ME. An autoradiographic study of efferent connections of the globus pallidus in Macaca mulatta. Exp Brain Res. 1982;46(1):107–17.
132. Sakai ST, Inase M, Tanji J. Pallidal and cerebellar inputs to thalamocortical neurons projecting to the supplementary motor area in Macaca fuscata: a triple-labeling light microscopic study. Anat Embryol. 1999;199(1):9–19.
133. Nauta HJ. Projections of the pallidal complex: an autoradiographic study in the cat. NSC. 1979;4(12):1853–73.
134. Kuo JS, Carpenter MB. Organization of pallidothalamic projections in the rhesus monkey. J Comp Neurol. Wiley Subscription Services, Inc., A Wiley Company;. 1973;151(3):201–36.
135. Schell GR, Strick PL. The origin of thalamic inputs to the arcuate premotor and supplementary motor areas. J Neurosci. 1984 Feb;4(2):539–60.
136. Strick PL. Light microscopic analysis of the cortical projection of the thalamic ventrolateral nucleus in the cat. Brain Res. 1973;55(1):1–24.
137. Asanuma C, Thach WT, Jones EG. Distribution of cerebellar terminations and their relation to other afferent terminations in the ventral lateral thalamic region of the monkey. Brain Res. 1983;286(3):237–65.
138. Percheron G, François C, Talbi B, Meder JF, Fénelon G, Yelnik J. The primate motor thalamus analysed with reference to subcortical afferent territories. Stereotact Funct Neurosurg. 1993;60(1–3):32–41.
139. Lambert C, Simon H, Colman J, Barrick TR. Defining thalamic nuclei and topographic connectivity gradients in vivo. NeuroImage. 2017;158:466–79.
140. Calabrese E, Hickey P, Hulette C, Zhang J, Parente B, Lad SP, et al. Postmortem diffusion MRI of the human brainstem and thalamus for deep brain stimulator electrode localization. Hum Brain Mapp. 2015;36(8):3167–78.
141. Miller KL, Stagg CJ, Douaud G, Jbabdi S, Smith SM, Behrens TEJ, et al. Diffusion imaging of whole, post-mortem human brains on a clinical MRI scanner. NeuroImage. Elsevier Inc;. 2011;57(1):167–81.
142. Lambert C, Chowdhury R, Fitzgerald THB, Fleming SM, Lutti A, Hutton C, et al. Characterizing aging in the human brainstem using quantitative multimodal MRI analysis. Front Hum Neurosci. Frontiers;. 2013;7:462.
143. Lambert C, Lutti A, Helms G, Frackowiak R, Ashburner J. Multiparametric brainstem segmentation using a modified multivariate mixture of Gaussians. Neuroimage Clin. 2013;2:684–94.

144. Behrens TEJ, Berg HJ, Jbabdi S, Rushworth MFS, Woolrich MW. Probabilistic diffusion tractography with multiple fibre orientations: what can we gain? NeuroImage. 2007;34(1):144–55.
145. Åström M, Zrinzo LU, Tisch S, Tripoliti E, Hariz MI, Wårdell K. Method for patient-specific finite element modeling and simulation of deep brain stimulation. Med Biol Eng Comput. 2008;47(1):21–8.
146. Maks CB, Butson CR, Walter BL, Vitek JL, CC MI. Deep brain stimulation activation volumes and their association with neurophysiological mapping and therapeutic outcomes. J Neurol Neurosurg Psychiatry. BMJ Publishing Group Ltd;. 2009;80(6):659–66.
147. Åström M, Lemaire J-J, Wårdell K. Influence of heterogeneous and anisotropic tissue conductivity on electric field distribution in deep brain stimulation. Med Biol Eng Comput. 2012;50(1):23–32.
148. Åström M, Diczfalusy E, Martens H, Wårdell K. Relationship between neural activation and electric field distribution during deep brain stimulation. IEEE Trans Biomed Eng. 2015;62(2):664–72.
149. Schrouff J, Rosa MJ, Rondina JM, Marquand AF, Chu C, Ashburner J, et al. PRoNTo: pattern recognition for neuroimaging toolbox. Neuroinformatics. 2013;11(3):319–37.
150. Jbabdi S, Johansen-Berg H. Tractography: where do we go from here? Brain Connect. 2011;1(3):169–83.

Microelectrode Recording in Neurosurgical Patients

8

Bornali Kundu, Andrea A. Brock, John A. Thompson, and John D. Rolston

Abbreviations

AC-PC	Anterior commissure–posterior commissure
CT	Computed tomography
DBS	Deep brain stimulation
DSP	Digital signal processing
EMG	Electromyography
GPe	Globus pallidus externus
GPi	Globus pallidus internus
LFP	Local field potential
MER	Microelectrode recording
MRI	Magnetic resonance imaging
PD	Parkinson disease
SNr	Substantia nigra pars reticulate
STN	Subthalamic nucleus
UPDRS	Unified Parkinson's Disease Rating Scale
Vc	Ventrocaudalis
Vim	Ventral intermediate nucleus of the thalamus
Voa	Ventralis oralis anterior
Vop	Ventralis oralis posterior

B. Kundu · A. A. Brock
Department of Neurosurgery, Clinical Neurosciences Center, University of Utah, Salt Lake City, UT, USA

J. A. Thompson
Department of Neurosurgery, University of Colorado School of Medicine, Aurora, CO, USA

J. D. Rolston (✉)
Department of Neurosurgery, Clinical Neurosciences Center, University of Utah, Salt Lake City, UT, USA

Department of Biomedical Engineering, University of Utah, Salt Lake City, UT, USA
e-mail: john.rolston@hsc.utah.edu

Physical Principles of Microelectrode Recording

Microelectrode recording (MER) is the technique of inserting a small, high-impedance electrode into the brain parenchyma and recording spontaneous and evoked neural activity. This activity takes the form of both single-neuron activity ("spiking") and local field potential (LFP) activity. The patterns of recorded activity differ in predictable ways depending on the anatomical location and disease state. These differentiable patterns in MER allow the physician to infer the anatomical location of the electrode, which can then be used to map deep brain structures.

In design, a microelectrode consists of a conducting metal filament (often tungsten, platinum–iridium, stainless steel, or other rigid metal) fit inside a separate shielding cannula (Fig. 8.1). The electrode is insulated with a nonconductive material such as Parylene C or glass, with only the sharpened electrode tip deinsulated. The ability of a microelectrode to record single neurons is dependent on the surface area of its exposed tip. The exposed area should be commensurate with the size of a cell, ~15–25 μm in diameter [1].

N. Pouratian, S. A. Sheth (eds.), *Stereotactic and Functional Neurosurgery*,
https://doi.org/10.1007/978-3-030-34906-6_8

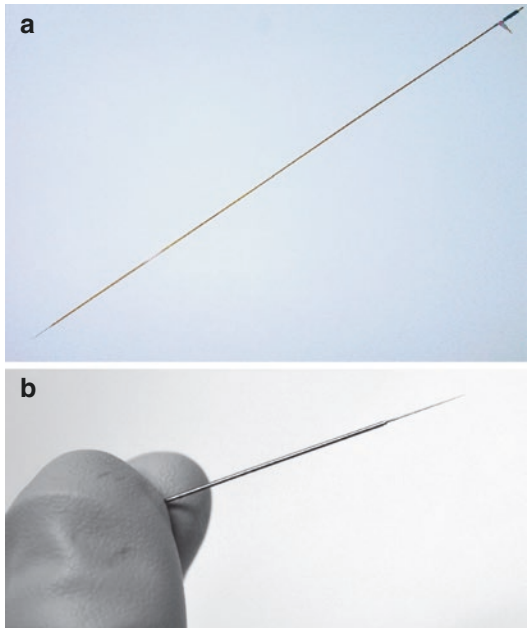

Fig. 8.1 Photographs of a microelectrode. (**a**) The D.ZAP microelectrode made by FHC. (**b**) A microelectrode tip. (Images courtesy of FHC, Inc.)

Electrodes with larger exposed surfaces tend to record from larger populations of cells and are termed macroelectrodes. With a large enough macroelectrode, thousands to millions of cells are recorded simultaneously such that individual cells are no longer discernible, as is the case for intracranial electrocorticography or scalp electroencephalography.

Typical microelectrodes have impedances in the range of 500 kΩ to 1 MΩ. In comparison, deep brain stimulation (DBS) macroelectrodes have impedances nearly 1000 times smaller, between 1 kΩ and 2 kΩ [2]. The high impedance of microelectrodes is directly related to the surface area of the microelectrode: The smaller the surface area for a given material, the higher the impedance. Large changes in electrode impedance during recording sessions thereby suggest damage to the electrode's insulation.

It is a common misconception that only high-impedance electrodes can record single cells. The ideal electrode for single units would in fact have as small an impedance as possible, coupled with a very small exposed surface area (commensurate with the size of a single neuron, as noted earlier). Low impedance is desirable because thermal noise in the electrode is proportional to the square root of electrode impedance—known as Johnson–Nyquist noise [3], $V_{RMS} = \sqrt{4k_B TZ\Delta f}$, where V_{RMS} is the root-mean-squared voltage (noise), k_B is Boltzmann's constant, Z is the impedance, and Δf is the frequency band of interest in Hz. As an example, if the impedance of an electrode increases fourfold, the thermal noise affecting the recordings doubles.

In general, small electrodes have high impedance, so "high impedance" has become interchangeable with "small diameter"; however, many materials can be electroplated or otherwise coated with more conductive substances to decrease impedance while leaving the exposed surface area unchanged. Alternatively, surfaces can be made "rougher" by techniques like platinum black pulsed plating, increasing the effective surface area while keeping the electrode diameter near constant [4]. These methods help lower electrode noise while not compromising the ability to record single cells.

The microelectrode is attached to a preamplifier (sometimes called a "headstage") that is mounted on the stereotactic frame (Fig. 8.2). The headstage converts the high-impedance signal of the microelectrode to a buffered low-impedance signal, which is far less susceptible to noise [1]. Because all electrical voltages are potential *differences* between two points, the voltage recorded by the microelectrode must always be obtained in comparison with another electrode elsewhere. This is often done by "grounding" the patient and using this ground as the reference. To accomplish this, most recording systems have an alligator clip or other system with which to connect the recording system's ground via a low-impedance connection to the patient. This can be done, for example, by connecting the implanted guide tube to the ground, which acts as a large, low-impedance connection with the patient. This also permits the guide tube to act as a Faraday cage for the microelectrode, reducing noise [5].

To provide additional recording options, most microelectrodes also have another exposed surface (e.g., at the end of the protecting sheath) that can act as an indifferent or reference electrode (Fig. 8.1). Using this reference electrode can help

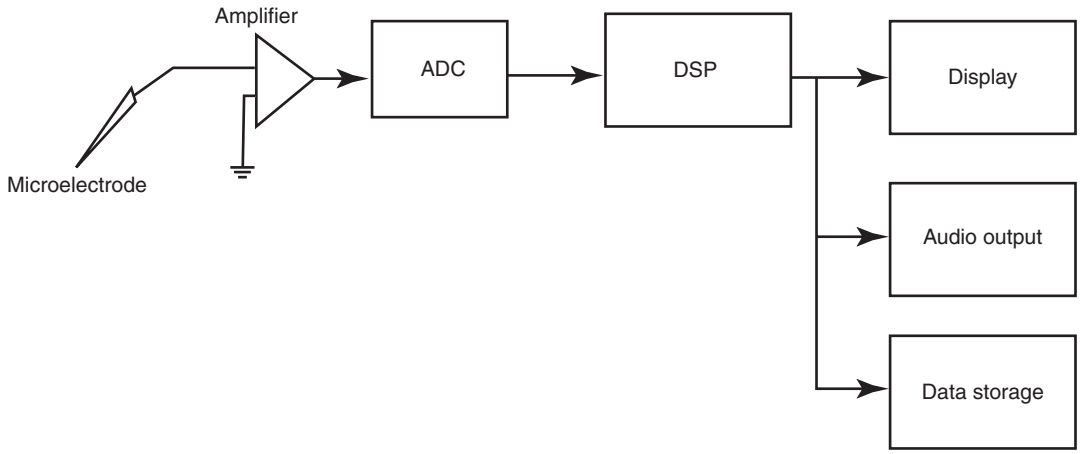

Fig. 8.2 MER acquisition setup. The microelectrode is mounted to the headstage, and the signal is filtered through the preamplifier. Data are then digitized in the analog-to-digital converter (ADC) and recorded by the digital signal processing (DSP). The signal is then displayed and can be projected as audio output for the clinician. Data are stored in a range of sampling rates from 30 KHz for single-unit activity to 256 Hz for LFP recordings

reduce common-mode noise, which is shared between the microelectrode and reference (e.g., 50- or 60-Hz line noise). However, if there is a true signal at the reference electrode (e.g., a large LFP), this signal will then contaminate the MER.

All modern recording systems take the analog signal from the headstage and digitize it for recording and display (Fig. 8.2). Because action potentials last only a few milliseconds, the recording system must digitize at a rate that preserves the action potential waveform. By Nyquist's theorem, the maximum frequency a system can confidently reproduce is half the sampling rate. For example, if an action potential has energy at 5 kHz, the minimum sampling rate to faithfully reproduce this waveform is 10 kHz. Current systems therefore typically oversample at 20–40 kHz.

The recorded signal is displayed in close to real time on a monitor and directly sonified. Serendipitously, the frequency of neural signals (~20 Hz for the beta frequency band and <20 kHz for action potentials) and the frequency range that humans can hear (20 Hz to 20 kHz) overlap significantly, so the recorded waveforms can be directly played by a speaker. The sound of an action potential is often a "pop," which is distinguishable from the recorded background noise. Multiunit activity (the cacophonous overlapping of numerous nearby cells that are not individually identifiable) can make the background signal louder, a phenomenon useful, for example, for determining when dense nuclei, like the subthalamic nucleus (STN), are entered. The recording system detects individual spikes by thresholding the signal. A few milliseconds before and after these threshold crossings are saved and displayed so the user can judge the quality of the waveform.

MER in Practice

Modern stereotactic surgery using MER combines traditional stereotactic neurosurgery—pioneered by Spiegel and Wycis and relying on pneumoencephalograms [6, 7]—with MER recordings, which were historically done in the neocortex for epilepsy surgery [8]. The motivation was to reduce error from individual differences in subcortical neuroanatomy when targeting these areas in patients with movement disorders. In the 1940s, Meyers [9] was the first to report LFP data showing tremor-related brain activity from striatum and motor cortex during open surgery for treatment of Parkinson disease

(PD). In 1958, Wetzel and Snider [10] performed some of the first macroelectrode recordings in patients, in the context of pallidotomy for treatment of PD. At that same time, MER techniques to record single-unit activity from human thalamus and other subcortical structures were reported by Albe-Fessard and Guiot [8]. In this work, they describe single units in the ventral nuclear group of the thalamus showing coherent activity with the patient's tremor. Work by Benabid and colleagues showed that stimulation of the ventral intermediate nucleus (Vim) of the thalamus using the aforementioned technique treats tremor symptoms of PD [11, 12]. Following this, the globus pallidus internal (GPi) and STN were also described as targets for DBS stimulation to treat PD [13, 14].

Our protocol for performing MER is as follows. The patient is placed in a stereotactic frame, and then a computed tomography (CT) scan is obtained. This scan serves as a reference for coregistering the patient's preoperative magnetic resonance imaging (MRI) scans. This imaging set can then be used to perform indirect targeting, based on visualization of the anterior commissure–posterior commissure (AC-PC) plane, or direct targeting, visualizing the target structures directly. The burr hole location is determined based on this initial trajectory, taking care to avoid blood vessels, sulci, and the ventricles when possible. Once the burr hole has been made, the patient is awakened from anesthesia, and a guide tube is advanced down the planned trajectory to a point 10–25 mm above the target, depending on the trajectory. Guide tubes are more rigid than the microelectrodes and reduce the risk of electrode deflection. Guide tube distances are chosen to ensure some portion of tissue can be sampled by the microelectrode before reaching the target. Note that there are cases where MER is done in an asleep patient, but the quality of the recording is not as readily interpretable in that case [15, 16]. In some pediatric patients or patients with severe anxiety or dystonia, the surgery must be performed under anesthesia. In this case, MER can confirm the final position in the GPi or STN. Importantly, capsular side effects but not sensory side effects can be sufficiently mapped under general anesthesia. In the case of PD, the STN can be identified with MER sufficiently under general anesthesia, and using this method, others have shown comparable long-term outcomes to awake DBS in case series [16].

Once the guide tube is in position, the microelectrode is introduced and extended a few millimeters past the guide tube's terminus. The impedance should be checked at this point to ensure the microelectrode was not damaged. The electrode is then advanced with a microdrive in submillimeter steps to the target. The recordings are monitored for changes in the background intensity and the presence or absence of single units. Larger step sizes can be used initially, ~0.5 mm, although smaller step sizes, ~0.1 mm, should be used once single units are identified in mapped structures.

Aside from recording spontaneous activity, recorded neurons can be monitored for evoked responses. For example, in the STN, movement-sensitive cells can be identified by listening for their modulation during passive or active joint movements. Additionally, microstimulation of the electrode can be used to confirm electrode location or test for side effects. Microstimulation is delivered at 1–100 μA (300- to 330-Hz trains; 100- to 700-μs pulse widths) [17, 18]. The effects of stimulation depend on nearby structures, such as the internal capsule or sensory thalamus, when targeting the Vim. When microstimulation evokes paresthesias, for instance, this suggests that the electrode is near the sensory thalamus. This can be used to map the electrode's position.

After a suitable recording is obtained, followed by favorable stimulation, the permanent macroelectrode is placed along the final guide cannula trajectory. The location of the base of the electrode within the target depends on the target. If one is using directional leads, the middle two contacts are generally placed at the target location (because these are the segmented contacts with directional capabilities in currently commercially available systems). Macrostimulation is done to confirm there are no limiting side effects. If optimal responses are not acquired, it is appropriate to try a new trajectory 2 mm away

from the first. This trajectory is built into the "Ben gun" head mount (named after Benabid), which has five possible trajectories for the guide cannula organized in a "plus" or "x" configuration. There is also the method of recording simultaneously from multiple, planned, parallel tracks via the Ben gun [19, 20]. The advantage here is to have the option to choose the best trajectory based on more complete localization information. Some advocate using all 5 tracks simultaneously to map a cylindrical volume of tissue and assess effects without having to account for post-lesion decrement of tremor that might occur with serial insertions [19]. Whether an increased number of lead placements results in increased rate of hemorrhage is controversial [21–23].

Targeting GPi

The GPi is a common target for PD and dystonia treatment [24]. It is targeted through a frontal approach and is located roughly 2–3 mm anterior to the midcommissural point (MCP), 5–6 mm below the intercommissural line, and 20–21 mm from the midline [25], specifically targeting the posteroventral portion of the nucleus. For direct targeting, we find the pallidocapsular border at the axial level of the AC-PC line, divide that line into thirds, and take a point 3 mm perpendicular to that line at the junction of the anterior 2/3 and posterior 1/3 divisions [25]. The GPi can also be targeted based on the optic tract's lateral border (19–21 mm lateral from midline and 2–3 mm superolateral to the tract) [25]. The angles of approach are ~60 degrees from the AC-PC plane and along the vertical in the coronal plane.

Along the approach trajectory, the microelectrode encounters several critical structures that help confirm electrode location (Fig. 8.3). The cells of the striatum fire at relatively low frequency (0–10 Hz). Deeper, the globus pallidus external (GPe) segment contains cells that show either "bursting" or "pausing" activity. Bursters in the GPe fire at a mean rate of 50 Hz, whereas pausing cells fire at a mean rate of 20 Hz [26]. Border cells of the white laminae mark the border between the external segment of the GPe and the GPi. These cells have a regular firing rate at 20–40 Hz and span 1–2 mm [27]. Border cells can also occasionally be encountered between the external and internal segments of the GPi (respectively denoted as GPi,e and GPi,i).

Upon entering the GPi, there is an increase in the background activity and increased uniformity of the firing rate. The GPi fires at 60–100 Hz in patients with PD and at a lower rate in dystonic patients (~50 Hz) [24]. Firing rates for Tourette disease have been described as intermediate between these two ranges [28]. Under anesthesia, the rate of firing of all cell groups is lower [28]. In the GPi, there are also tremor cells that fire in correlation with the physical tremor (as can be confirmed with electromyography (EMG) recordings) and are generally located in the ventral portion of the GP [28]. The rate is modulated by movement of the contralateral arm or leg. Generally, 4–8 mm of GPe and 5–12 mm of GPi may be encountered on a single tract [28].

The somatotopy within the GPi is somewhat variable. In general, leg representation is dorsal and lateral, while arm representation is caudal and medial, although in some cases leg representation is central and arm representation flanks this area medially and laterally [29]. This is tested by passive or active joint movement in the patient while listening for modulation. After the electrode exits the GPi, there is a quiet period as it passes through the ansa lenticularis. Finally, the optic tract is encountered below the inferior margin of GPi, which is marked by high-frequency activity and light-evoked electrical activity, thus marking the lower bound of the electrode trajectory. This is approximately at 22–24 mm along the parasagittal plane [30]. Behaviorally, the patient may see stimulation-induced phosphenes in the contralateral visual field. The recording is stopped 1 mm past the last GPi cells to avoid injury to vessels within the choroidal fissure. This technique is no different when performing pallidotomy except the DBS target may be 2 mm more anterior to avoid stimulating the internal capsule [28].

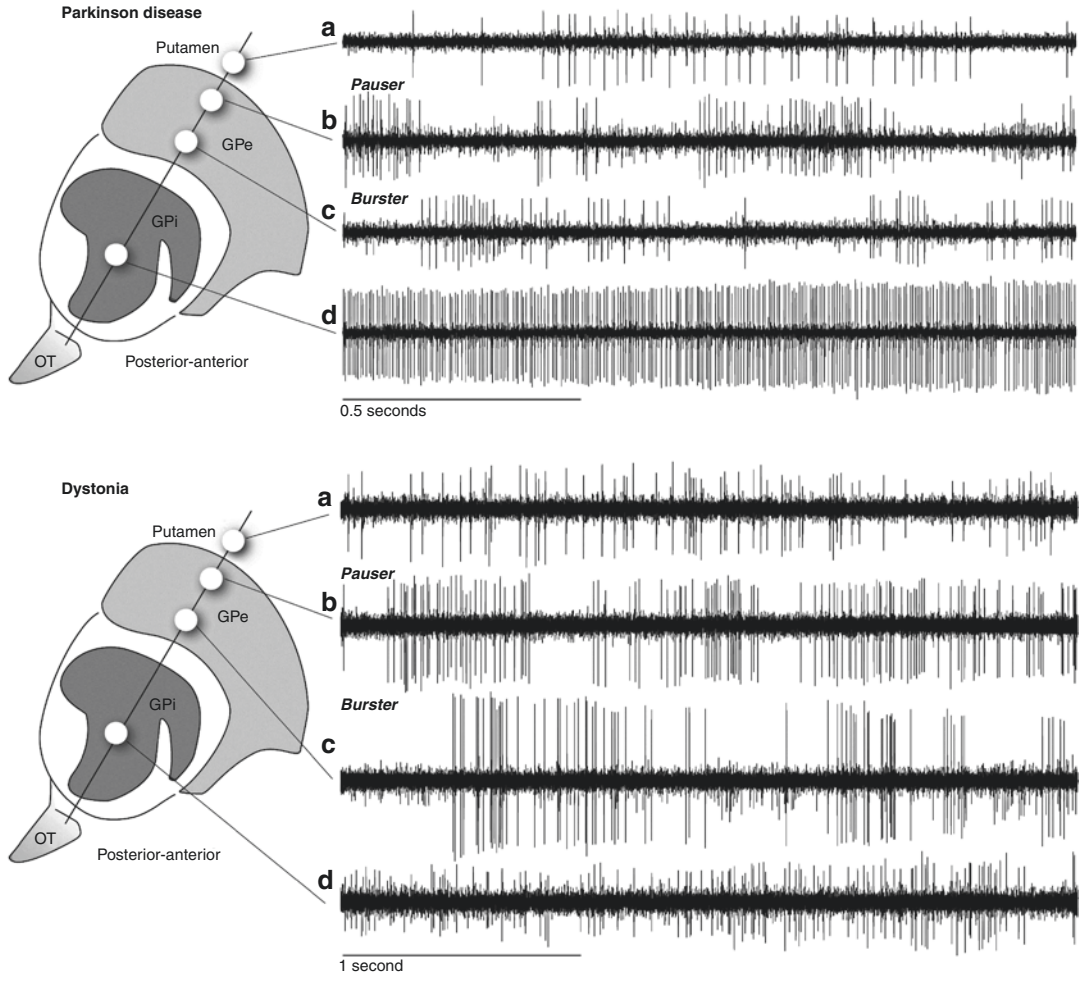

Fig. 8.3 GPi MER. (*Top*) Representative MER traces from typical structures traversed on descent to the GPi from a surgical subject with Parkinson disease. A: Caudate nucleus; B: pausing type neuron, GPe; C: bursting type neuron, GPe; D: GPi. (*Bottom*) Representative MER traces from typical structures traversed on descent to the GPi from a surgical subject with dystonia. A: Caudate nucleus; B: pausing type neuron, GPe; C: bursting type neuron, GPe; D: GPi

Targeting the STN

Although targeting of the STN or the GPi has comparable efficacy in treating the symptoms of PD [31, 32], STN targeting has been associated with more neurocognitive changes [33]. The nucleus is bordered rostrally by the zona incerta followed by field of Forel (H2 sector) in the rostrocaudal direction. The zona incerta is roughly 2.5–4 mm in thickness. This area is quiet, thus marking the border before entry into the STN and increased background activity. The third cranial nerve lies anterior and medially to the STN, the red nucleus lies posteromedially, the cerebellar peduncle is medial, and the medial lemniscus is posterior. The frontopontine bundle is located anteromedially, and stimulation can cause contralateral gaze deviation, as opposed to medial and downward gaze deviation of the ipsilateral eye with stimulation of the ipsilateral third cranial nerve. The STN is 11–12 mm lateral to midline, 3–4 mm posterior to the MCP, and 4 mm ventral to the MCP. The nucleus can be visualized on a T2-weighted MRI scan that is aligned to

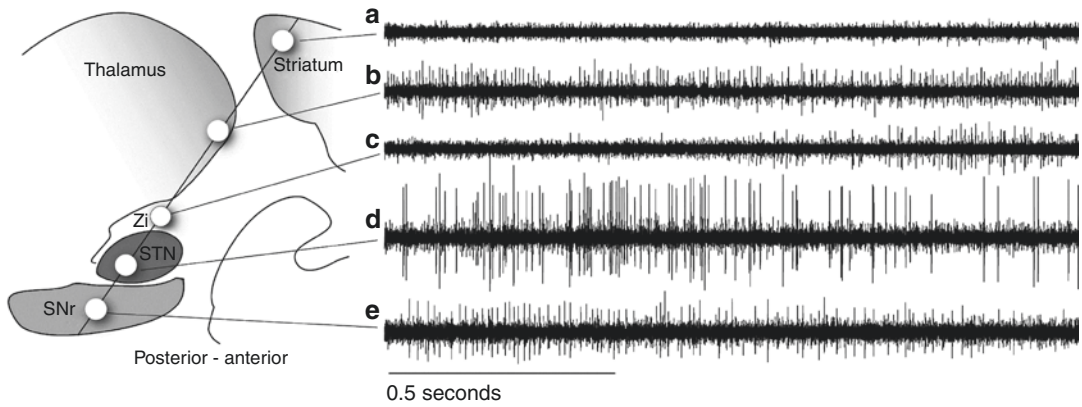

Fig. 8.4 STN MER. Representative MER traces from typical structures traversed on descent to the STN from a surgical subject with Parkinson's disease. A: Striatum; B: thalamus; C: zona incerta (Zi); D: STN; E: SNr

the AC-PC line. The AP angle of the trajectory is similar to that of the GPi and is roughly 70 degrees from the AC-PC line and 10–20 degrees lateral in the coronal plane, at the vertical from target. In an ideal trajectory, one would initially traverse the dorsal thalamus before entering the STN [18]. Cells in the STN have variable firing rates, ranging from 20 to 50 Hz with high background activity (Fig. 8.4). The sound of background activity is sometimes referred to by clinicians as "raindrops on a tin roof." There are kinesthetic cells here that will respond to passive limb movement. Beyond the STN is the substantia nigra pars reticulata (SNr), within which cells fire at a higher rate of 50–70 Hz and there is significantly less background activity. The distance between the two structures is ~2–3 mm. We typically seek a trajectory through STN >5 mm in thickness.

Side effects are defined by the location of the lead. Stimulation of the SNr may lead to feelings of fear and anxiety. Mood changes may also be seen with stimulation of the anterior portion of the STN's limbic division. The internal capsule is located laterally, and its stimulation can cause muscle contraction. If no effect is seen with stimulation, the lead may be dorsal in the thalamus. Stimulation posteromedial to the target can stimulate the medial lemniscus, causing paresthesias. Corticobulbar fibers lie lateral to the target, and their stimulation can cause facial contractions and dysarthria. The oculomotor nerve also passes medially, and its stimulation would cause ipsilateral eye adduction; however, contralateral gaze deviation is a result of stimulation of the frontopontine bundle. Direct stimulation of the STN can cause dyskinesia. Some physicians approach the STN with a parallel lead configuration through the Ben gun to optimize targeting [34]. It is not clear whether multiple passes increases the risk of hemorrhage because the number of reported procedures comparing the two is low [34, 35]. Typical microstimulation parameters are currents of 100 mA, pulse trains of 0.2–0.7 ms, at 330 Hz. Macrostimulation is delivered at much higher amplitudes, on the order of milliamperes or volts.

Targeting the Vim of the Thalamus

The tremor component of essential tremor and tremor-dominant PD can be treated with stimulation of the Vim nucleus of the thalamus. The location of the Vim nucleus varies from 1 to 7 mm posterior to the MCP (or 20% of the length of AC-PC line anterior to the PC), 14–15 mm lateral from midline, and 0–3 mm above the AC-PC line [1, 12]. The angles are 60 degrees from the AC-PC plane and 5–10 degrees in the coronal plane from the true vertical at target. Targeting the Vim requires the trajectory of the electrode to traverse near the caudate into the thalamus. En route, it is important to identify the sensory

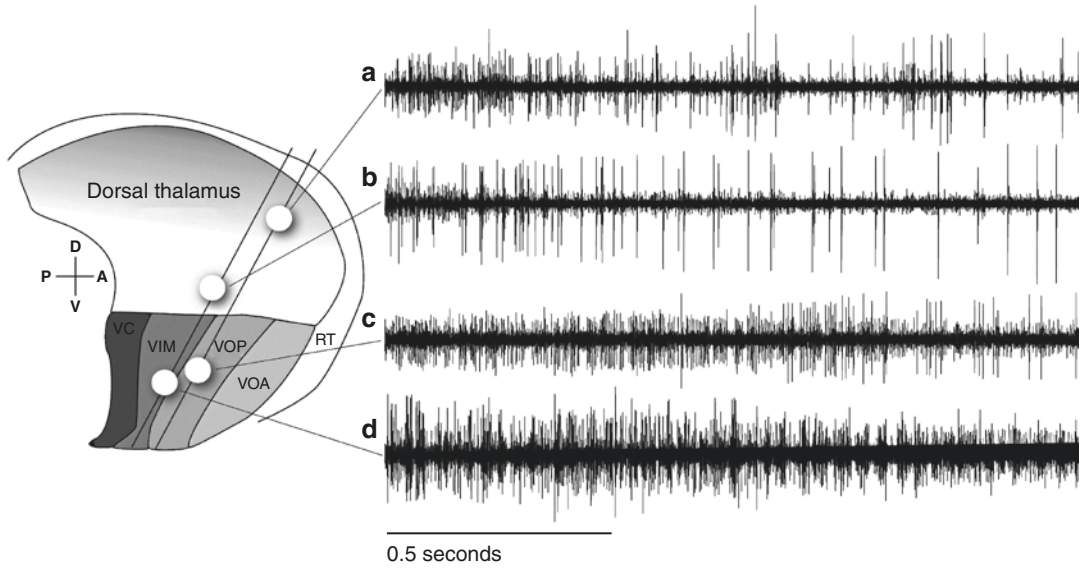

Fig. 8.5 Vim MER. Representative MER traces from typical structures traversed on descent to the Vim of the thalamus from a surgical subject with essential tremor. A: Anterior trajectory dorsal tier of thalamus; B: posterior trajectory dorsal tier of thalamus; C: Vop nucleus of the thalamus; D: Vim of the thalamus.VC ventrocaudalis nucleus, Voa ventralis oralis anterior, RT reticular nucleus

thalamus (ventrocaudalis or Vc nucleus), which marks the posterior boundary of motor thalamus (Fig. 8.5). The Vc is roughly 4 mm anterior to the PC along the intercommissural line [36] and 11 mm lateral for oral responses versus 18 mm lateral for responses in the legs [37]. The "tactile neurons" in that area can be identified by stimulating the corresponding receptive field on the body through light touch. "Deep tactile cells" in the sensory thalamus respond to pressure or squeezing of the tendons and mark the anterior boundary of the Vc nucleus before transition into the Vim nucleus [17]. The receptive field will be on the contralateral side of the body, with possible additional ipsilateral representation of the lips [38]. There should be reasonably good concordance with projected (as determined by electrical stimulation) and receptive (as determined by touch) fields [37]. Microstimulation evokes paresthesias in the corresponding body area.

The Vim nucleus is characterized by the presence of "kinesthetic cells," which normally respond to changes in joint position, but in essential tremor often fire in time with the tremor frequency, as reflected by EMG. Microstimulation (constant current, pulse width 100 μsec, frequency 300 Hz [28]) causes the tremor cells to stop firing, and the electromyographic activity quiets as well [39]. The mean firing rate of tremor cells is about 7–14 Hz, which is the mean tremor frequency in patients with essential tremor. Tremor cells may also be seen in the caudal ventralis oralis posterior (Vop), STN, and GP [28, 40, 41]. The mediolateral position is defined by the body part being treated: Oral and facial representation is roughly 12–14 mm from midline, upper limb representation is 14–16 mm, and leg representation is lateral to this [17]. The location must also not cause side effects such as muscle contraction or paresthesia. A rule of thumb is that side effects caused at or below 20 μA suggest the electrode needs to be moved anteriorly. The most ventral contact of the DBS lead is typically targeted at the base of the nucleus.

The pallidal receiving area of the thalamus (ventralis oralis anterior/posterior (Voa/Vop) in the terminology of Hassler) is further anterior to the Vim nucleus (the cerebellar receiving area) and contains "voluntary cells," which are activated during the motor preparation period [37].

Again, the somatotopy is roughly face/jaw medially and leg laterally [42]. This somatotopy can be distorted in stroke or other lesion patients [43]. In contrast to tremor cells in the Vim nucleus, voluntary cells also fire at the tremor frequency but continue to fire when the tremor has stopped with stimulation. Lidocaine injection to the site will quiet the cells, but this practice is no longer used to confirm target location because of time constraints in the operating room [44]. The current thought is that both cell types may be involved with tremor generation [45]. The internal capsule lies laterally and is relatively quiet electrically. Microstimulation will result in paresthesias (Vc stimulation) or muscle contraction (internal capsule stimulation).

Accuracy of MER Versus Imaging

MER was initially used to allow for the necessary spatial resolution of stereotactic surgery with the original metal frames. The mean vector error with the use of MER ranged from 0.9 mm to 2.8 mm [46–49]. Additionally, Brahimaj et al. [50] reported an average radial error of 1.2 mm for all targets. For protocols relying on imaging, error between the final location of the electrode tip and the proposed target based on stereotactic coordinates was 2.2 mm [51]. The radial error for the left and right sides are reportedly 0.8 and 0.7 mm, respectively; and these were not statistically different between locations [48].

When comparing asleep DBS with traditional MER-guided placement, one group retrospectively reviewed 21 patients who underwent asleep DBS and compared them with 24 patients who underwent routine placement that included MER. In addition to showing statistically small radial error with asleep DBS, patients who underwent MER showed lower side-effect thresholds [48]. However, multiple studies have found no difference in the Unified Parkinson's Disease Rating Scale (UPDRS) III scores or levodopa dosing equivalents between the groups [48, 52, 53]. Additionally, a meta-analysis to compare these two groups also did not find a difference between UPDRS III scores or levodopa-equivalent doses [54]. However, these results are confounded by including studies where the asleep cohorts also had MER intraoperatively.

LFP Applications

Aside from single-unit and multiunit recordings, intracranial electrodes can also be used to measure LFP. LFPs are extracellular measures of voltage differences between a large neuronal ensemble (including components of axons, dendrites, soma) and a reference. LFP measurement does not differentiate incoming versus outgoing signal direction as would single-cell action potentials. LFP recordings are useful for seizure focus localization and can also be decomposed into their spectral counterparts (e.g., the spectral coefficients associated with the short-time Fourier transform or continuous wavelet transform algorithms [55, 56]) to discern whether neuronal ensembles are oscillating at a particular frequency with significant power and at particular phases. For example, the beta frequency band (13–30 Hz) power is elevated in PD patients in both STN [57, 58] and Vim and has a complex relationship with tremor frequency and amplitude [55].

Coordinated firing at particular frequencies is thought to be a mode of communication and information transfer between neural ensembles, much like a particular radio frequency can be used to transmit information along that bandwidth. This activity is lowered with DBS and levodopa [57, 58]. Importantly, beta activity is highest in the dorsal region of the STN [59]. The physical distance spanned in the nucleus by this beta power is related to best PD control with DBS (specifically bradykinesia and rigidity) and not the actual anatomical center of the nucleus [60]. This makes beta band power a potentially powerful biomarker and target for stimulation and adaptive, closed-loop stimulation paradigms.

Recently, studies have shown that there is a complex substructure to beta band activity such that beta activity appears to come in bursts in time and to predict performance on a motor task in nonhuman primates [61]. In PD patients,

sustained bursts occur with concurrent interhemispheric synchronization (i.e., phase coupled) between bilateral STNs. The theory here is that aberrant coupling of the motor system is disrupting normal motor function. Longer bursts are related to the clinical symptoms of rigidity and bradykinesia [62]. Levodopa causes the bursts to become shorter and have lower amplitude. Finally, gamma band (60–90 Hz) power has also been shown to be elevated in the STN and GP of PD patients treated with levodopa [63, 64]. Broad band gamma power is thought to reflect cortical neuronal activity itself [65]. Coupling between beta phase in M1 and gamma amplitude in M1 is exaggerated in PD compared with dystonia and epilepsy patients, although all those patients show similar beta band power in motor cortex [66]. Cross-structural coupling between STN beta and M1 gamma is increased in PD [66], and this coupling is decreased with DBS [67].

In dystonia, there is excessive drive of the motor control circuits leading to abnormal antagonist/agonist muscle co-contractions. There is lower beta power and greater theta power in the pallidum in dystonic patients compared with PD [68], and there is greater phase coherence between motor cortex and pallidum that is disrupted by DBS [69]. Finally, in essential tremor, Vim LFP power in beta band is coherent with tremor frequency, as measured with EMG [68].

Conclusion

Further research is needed using MER to identify LFP-based biomarkers of movement disorders and use them for diagnosis, targeting, and designing better stimulation treatment regimens, perhaps via adaptive closed-loop DBS. However, the realm of MER for research is vast, spanning applications in brain machine interfaces [70–74], consciousness [75], cognition [76–80], memory [81–85], and psychiatric disorders [86–88]. Microelectrode arrays such as the Utah array have allowed single-unit recordings from a cortical patch and thus afford high-resolution population activity recordings to power brain machine interfaces [70] or study epileptic events [89, 90]. MER remains an important technique in the repertoire of a functional neurosurgeon. This chapter covers the basics of performing this technique. On the basis of current research, we foresee a future need to refine the ability to measure LFP-based oscillations to guide targeting particular areas of the traditional target nuclei and tracts.

References

1. Starr PA. Technical considerations in movement disorder surgery. In: Schulder M, Gandhi C, editors. Handbook of stereotactic and functional neurosurgery. 1st ed. New York: Marcel Decker Inc; 2003.
2. Satzer D, Lanctin D, Eberly LE, Abosch A. Variation in deep brain stimulation electrode impedance over years following electrode implantation. Stereotact Funct Neurosurg [Internet]. 2014 [cited 2018 Dec 12];92(2):94–102. Available from: https://www.ncbi.nlm.nih.gov/pmc/articles/PMC4531050/pdf/nihms554312.pdf.
3. Johnson JB. Thermal agitation of electricity in conductors. Phys Rev [Internet]. 1928 [cited 2018 Dec 12];32(1):97–109. Available from: https://link.aps.org/doi/10.1103/PhysRev.32.97.
4. Desai SA. Improving impedance of implantable microwire multi-electrode arrays by ultrasonic electroplating of durable platinum black. Front Neuroeng [Internet]. 2010;3(May):1–11. Available from: http://journal.frontiersin.org/article/10.3389/fneng.2010.00005/abstract.
5. Shils JL, Patterson T, Stecker MM. Electrical properties of metal microelectrodes. Am J Electroneurodiagnostic Technol [Internet]. 2000 [cited 2018 Dec 14];40(2):143–53. Available from: https://www.tandfonline.com/doi/full/10.1080/1086508X.2000.11079297.
6. Spiegel EA, Wycis HT. Ansotomy in paralysis agitans. Arch Neurol Psychiatry [Internet]. 1954 [cited 2018 Dec 14];71(5):598. Available from: http://archneurpsyc.jamanetwork.com/article.aspx?doi=10.1001/archneurpsyc.1954.02320410060005.
7. Spiegel E, Wycis T. Stereoencephalotomy. Part II. Clinical and physiological application. In: Clinical and physiological applications. New York: Grune and Straton; 1962.
8. Albe-Fessard D, Arfel G, Guiot G, Derome P, Hertzog E, Vourc'h G, et al. Electrophysiological studies of some deep cerebral structures in man. J Neurol Sci [Internet]. 1966 [cited 2018 Nov 14];3(1):37–51. Available from: http://www.ncbi.nlm.nih.gov/pubmed/5331941.
9. Meyers R. Surgical procedure for postencephalitic tremor, with notes on the physiology of the premotor fibers. Arch Neurol Psychiatr. 1940:455–9.

10. Wetzel N, Snider R. Neurophysiological correlates in human stereotaxis. Q Bull Northwest universirty Med Sch. 1958;32(4):386–92.
11. Benabid AL, Pollak P, Louveau A, Henry S, de Rougemont J. Combined (thalamotomy and stimulation) stereotactic surgery of the VIM thalamic nucleus for bilateral Parkinson disease. Stereotact Funct Neurosurg [Internet]. 1987 [cited 2018 Dec 14];50(1–6):344–6. Available from: https://www.karger.com/Article/FullText/100803.
12. Benabid AL, Pollak P, Gao D, Hoffmann D, Limousin P, Gay E, et al. Chronic electrical stimulation of the ventralis intermedius nucleus of the thalamus as a treatment of movement disorders. J Neurosurg [Internet]. 1996;84(2):203–14. Available from: http://thejns.org/doi/abs/10.3171/jns.1996.84.2.0203.
13. Siegfried J, Lippitz B. Bilateral chronic electrostimulation of ventroposterolateral pallidum: a new therapeutic approach for alleviating all parkinsonian symptoms. Neurosurgery [Internet]. 1994;35(6):1126–9; discussion 1129–30. Available from: http://www.ncbi.nlm.nih.gov/pubmed/7885558.
14. Limousin P, Pollak P, Benazzouz A, Hoffmann D, Le Bas J-F, Perret JE, et al. Effect on parkinsonian signs and symptoms of bilateral STN stimulation. Lancet [Internet]. 1995 [cited 2018 Dec 14];345(8942):91–5. Available from: https://www.sciencedirect.com/science/article/pii/S0140673695900624?via%3Dihub.
15. Pinsker MO, Volkmann J, Falk D, Herzog J, Steigerwald F, Deuschl G, et al. Deep brain stimulation of the internal globus pallidus in dystonia: target localisation under general anaesthesia. Acta Neurochir. 2009;151(7):751–8.
16. Harries AM, Kausar J, Roberts SAG, Mocroft AP, Hodson JA, Pall HS, et al. Deep brain stimulation of the subthalamic nucleus for advanced Parkinson disease using general anesthesia: long-term results. J Neurosurg [Internet]. 2012;116(1):107–13. Available from: http://thejns.org/doi/10.3171/2011.7.JNS11319.
17. Schwalb J, Hamani C, Lozano A. Thalamic deep brain stimulation for the control of tremor. In: Starr P, Barbaro N, Larson P, editors. Neurosurgical operative atlas: functional neurosurgery. 2nd ed. New York: Thieme; 2009.
18. Kopell B, Machado A, Rezai A. Chronic subthalamic nucleus stimulation for Parkinson's disease. In: Starr P, Barbaro N, Larson P, editors. Neurosurgical operative atlas: functional neurosurgery. 2nd ed. New York: Thieme; 2009.
19. Pollak P, Krack P, Fraix V, Mendes A, Moro E, Chabardes S, et al. Intraoperative micro- and macrostimulation of the subthalamic nucleus in Parkinson's disease. Mov Disord. 2002;17(SUPPL. 3)
20. Bejjani B-P, Dormont D, Pidoux B, Yelnik J, Damier P, Arnulf I, et al. Bilateral subthalamic stimulation for Parkinson's disease by using three-dimensional stereotactic magnetic resonance imaging and electrophysiological guidance. J Neurosurg [Internet]. 2000 [cited 2018 Dec 13];92(4):615–25. Available from: http://www.ncbi.nlm.nih.gov/pubmed/10761650.
21. Binder DK, Rau GM, Starr PA. Risk factors for hemorrhage during microelectrode-guided deep brain stimulator implantation for movement disorders. Neurosurgery. 2005;56(4):722–8.
22. Sansur CA, Frysinger RC, Pouratian N, Fu K-M, Bittl M, Oskouian RJ, et al. Incidence of symptomatic hemorrhage after stereotactic electrode placement. J Neurosurg [Internet]. 2007;107(5):998–1003. Available from: http://thejns.org/doi/10.3171/JNS-07/11/0998.
23. Zrinzo L, Foltynie T, Limousin P, Hariz MI. Reducing hemorrhagic complications in functional neurosurgery: a large case series and systematic literature review. J Neurosurg [Internet]. 2012;116(1):84–94. Available from: http://thejns.org/doi/10.3171/2011.8.JNS101407.
24. Starr PA, Rau GM, Davis V, Marks WJ, Ostrem JL, Simmons D, et al. Spontaneous pallidal neuronal activity in human dystonia: comparison with Parkinson's disease and normal macaque. J Neurophysiol [Internet]. 2005;93(6):3165–76. Available from: http://www.physiology.org/doi/10.1152/jn.00971.2004.
25. Panov F, Larson P, Martin A, Starr P. Deep brain stimulation for Parkinson's disease. In: Winn H, editor. Youman's neurological surgery. 7th ed. Philadelphia: Elsevier; 2016. p. 619–26.
26. Anderson WS, Winberry J, Liu CC, Shi C, Lenz FA. Applying microelectrode recordings in neurosurgery. Contemp Neurosurg [Internet]. 2010 [cited 2018 Dec 19];32(3):1–7. Available from: http://www.ncbi.nlm.nih.gov/pubmed/28316357.
27. Hutchison WD, Lozano AM, Davis KD, Saint-Cyr JA, Lang AE, Dostrovsky JO. Differential neuronal activity in segments of globus pallidus in Parkinson's disease patients. Neuroreport [Internet]. 1994 [cited 2018 Oct 31];5(12):1533–7. Available from: http://www.ncbi.nlm.nih.gov/pubmed/7948856.
28. Shils J, Arle J. Neurophysiologic monitoring for movement disorders surgery. In: Winn H, editor. Youman's neurological surgery. 7th ed. Philadelphia: Elsevier; 2016. p. 654–76.
29. Taha JM, Favre J, Baumann TK, Burchiel KJ. Characteristics and somatotopic organization of kinesthetic cells in the globus pallidus of patients with Parkinson's disease. J Neurosurg [Internet]. 1996 [cited 2018 Nov 14];85(6):1005–12. Available from: http://thejns.org/doi/10.3171/jns.1996.85.6.1005.
30. Hamani C, Schwalb J, Hutchinson W, Lozano A. Microelectrode-guided pallidotomy. In: Starr PA, Barbaro N, Larson P, editors. Neurosurgical operative atlas: functional neurosurgery. 2nd ed. New York: Thieme; 2009.
31. Follett KA, Weaver FM, Stern M, Hur K, Harris CL, Luo P, et al. Pallidal versus subthalamic deep-brain stimulation for Parkinson's disease. N Engl J Med [Internet]. 2010 [cited 2018 Dec

14];362(22):2077–91. Available from: http://www.nejm.org/doi/abs/10.1056/NEJMoa0907083.
32. Anderson VC, Burchiel KJ, Hogarth P, Favre J, Hammerstad JP. Pallidal vs subthalamic nucleus deep brain stimulation in Parkinson disease. Arch Neurol [Internet]. 2005 [cited 2018 Dec 14];62(4):554. Available from: http://archneur.jamanetwork.com/article.aspx?doi=10.1001/archneur.62.4.554.
33. Okun MS, Wu SS, Fayad S, Ward H, Bowers D, Rosado C, et al. Acute and chronic mood and apathy outcomes from a randomized study of unilateral STN and GPi DBS. PLoS One. 2014;9(12):1–16.
34. Temel Y, Wilbrink P, Duits A, Boon P, Tromp S, Ackermans L, et al. Single electrode and multiple electrode guided electrical stimulation of the subthalamic nucleus in advanced Parkinson's disease. Oper Neurosurg [Internet]. 2007 [cited 2018 Nov 11];61(5 Suppl 2):346–57. Available from: http://www.ncbi.nlm.nih.gov/pubmed/18091250.
35. Bjerknes S, Toft M, Konglund AE, Pham U, Waage TR, Pedersen L, et al. Multiple microelectrode recordings in STN-DBS surgery for Parkinson's disease: a randomized study. Mov Disord Clin Pract. 2018;5(3):296–305.
36. Kutz S, Bakay R. Thalamotomy for tremor. In: Starr PA, Barbaro N, Larson PS, editors. Neurosurgical operative atlas: functional neurosurgery. 2nd ed. New York: Thieme; 2009.
37. Hutchinson W, Dostrovsky J, Hodaie M, Cavis K, Lozano A, Tasker R. Microelectrode recoding in functional neurosurgery. In: Lozano A, Gildernberg P, Tasker R, editors. Textbook of stereotactic and functional neurosurgery. 2nd ed. Berlin: Springer; 2009. p. 1283–323.
38. Lenz FA, Dostrovsky JO, Tasker RR, Yamashiro K, Kwan HC, Murphy JT. Single-unit analysis of the human ventral thalamic nuclear group: somatosensory responses. J Neurophysiol [Internet]. 1988;59(2):299–316. Available from: http://www.ncbi.nlm.nih.gov/entrez/query.fcgi?cmd=Retrieve&db=PubMed&dopt=Citation&list_uids=3351564.
39. Lenz F, Kwan HC, Martin R, Tasker R, Dostrovsky J, Lenz YE. Single unit analysis of the human ventral thalamic nuclear group: tremor-related activity in fucntionally identified cells. Brain. 1994;117:531–43.
40. Lenz FA, Dostrovsky JO, Tasker RR, Yamashiro K, Kwan HC, Murphy JT. Single-unit analysis of the human ventral thalamic nuclear group: somatosensory responses. J Neurophysiol [Internet]. 1988 [cited 2018 Oct 31];59(2):299–316. Available from: http://www.ncbi.nlm.nih.gov/pubmed/3351564.
41. Levy R, Hutchison WD, Lozano AM, Dostrovsky JO. High-frequency synchronization of neuronal activity in the subthalamic nucleus of parkinsonian patients with limb tremor. J Neurosci [Internet]. 2000;20(20):7766–75. Available from: http://www.ncbi.nlm.nih.gov/pubmed/11027240.
42. Lenz FA, Kwan HC, Dostrovsky JO, Tasker RR, Murphy JT, Lenz YE. Single unit analysis of the human ventral thalamic nuclear group. Activity correlated with movement. Brain [Internet]. 1990 [cited 2018 Oct 31];113(Pt 6):1795–821. Available from: http://www.ncbi.nlm.nih.gov/pubmed/2276045.
43. Lenz FA, Kwan HC, Martin R, Tasker R, Richardson RT, Dostrovsky JO. Characteristics of somatotopic organization and spontaneous neuronal activity in the region of the thalamic principal sensory nucleus in patients with spinal cord transection. J Neurophysiol [Internet]. 1994 [cited 2018 Oct 31];72(4):1570–87. Available from: http://www.physiology.org/doi/10.1152/jn.1994.72.4.1570.
44. Dostrovsky JO, Sher GD, Davis KD, Parrent AG, Hutchison WD, Tasker RR. Microinjection of lidocaine into human thalamus: a useful tool in stereotactic surgery. Stereotact Funct Neurosurg [Internet]. 1993 [cited 2018 Dec 14];60(4):168–74. Available from: http://www.ncbi.nlm.nih.gov/pubmed/8327796.
45. Jones MW, Tasker RR. The relationship of documented destruction of specific cell types to complications and effectiveness in thalamotomy for tremor in Parkinson's disease. Stereotact Funct Neurosurg [Internet]. 1990 [cited 2018 Oct 31];54(1–8):207–11. Available from: http://www.ncbi.nlm.nih.gov/pubmed/2080337.
46. Fiegele T, Feuchtner G, Sohm F, Bauer R, Anton JV, Gotwald T, et al. Accuracy of stereotactic electrode placement in deep brain stimulation by intraoperative computed tomography. Parkinsonism Relat Disord [Internet]. 2008 [cited 2018 Nov 14];14(8):595–9. Available from: http://linkinghub.elsevier.com/retrieve/pii/S1353802008000308.
47. Kelman C, Ramakrishnan V, Davies A, Holloway K. Analysis of stereotactic accuracy of the cosman-robert-wells frame and nexframe frameless systems in deep brain stimulation surgery. Stereotact Funct Neurosurg [Internet]. 2010 [cited 2018 Nov 14];88(5):288–95. Available from: https://www.karger.com/Article/FullText/316761.
48. Lee PS, Weiner GM, Corson D, Kappel J, Chang YF, Suski VR, et al. Outcomes of interventional-MRI versus microelectrode recording-guided subthalamic deep brain stimulation. Front Neurol. 2018;9(APR):1–8.
49. Nowacki A, Debove I, Fiechter M, Rossi F, Oertel MF, Wiest R, et al. Targeting accuracy of the subthalamic nucleus in deep brain stimulation surgery: comparison between 3 T T2-weighted magnetic resonance imaging and microelectrode recording resultEs. Oper Neurosurg (Hagerstown, Md) [Internet]. 2018 [cited 2018 Nov 14];15(1):66–71. Available from: https://academic.oup.com/ons/article/15/1/66/4060570.
50. Brahimaj B, Kochanski RB, Sani S. Microelectrode accuracy in deep brain stimulation surgery. J Clin Neurosci [Internet]. 2018 [cited 2018 Nov 14];50:58–61. Available from: https://linkinghub.elsevier.com/retrieve/pii/S0967586817312377.
51. Starr PA, Martin AJ, Ostrem JL, Talke P, Levesque N, Larson PS. Subthalamic nucleus deep brain stimulator placement using high-field interventional magnetic resonance imaging and a skull-mounted

aiming device: technique and application accuracy. J Neurosurg [Internet]. 2010 [cited 2018 Nov 14];112(3):479–90. Available from: http://thejns.org/doi/10.3171/2009.6.JNS081161.
52. Saleh S, Swanson KI, Lake WB, Sillay KA. Awake neurophysiologically guided versus asleep MRI-guided STN DBS for Parkinson disease: a comparison of outcomes using levodopa equivalents. Stereotact Funct Neurosurg [Internet]. 2015 [cited 2018 Nov 14];93(6):419–26. Available from: https://www.karger.com/Article/FullText/442425.
53. Brodsky MA, Anderson S, Murchison C, Seier M, Wilhelm J, Vederman A, et al. Clinical outcomes of asleep vs awake deep brain stimulation for Parkinson disease. Neurology [Internet]. 2017 [cited 2018 Nov 14];89(19):1944–50. Available from: http://www.neurology.org/lookup/doi/10.1212/WNL.0000000000004630.
54. Ho AL, Ali R, Connolly ID, Henderson JM, Dhall R, Stein SC, et al. Awake versus asleep deep brain stimulation for Parkinson's disease: a critical comparison and meta-analysis. J Neurol Neurosurg Psychiatry [Internet]. 2018 [cited 2018 Nov 14];89(7):687–91. Available from: http://jnnp.bmj.com/lookup/doi/10.1136/jnnp-2016-314500.
55. Wang SY, Aziz TZ, Stein JF, Liu X. Time-frequency analysis of transient neuromuscular events: dynamic changes in activity of the subthalamic nucleus and forearm muscles related to the intermittent resting tremor. J Neurosci Methods. 2005;145(1–2):151–8.
56. Bakstein E, Burgess J, Warwick K, Ruiz V, Aziz T, Stein J. Parkinsonian tremor identification with multiple local field potential feature classification. J Neurosci Methods [Internet]. 2012;209(2):320–30. Available from: https://doi.org/10.1016/j.jneumeth.2012.06.027.
57. Kühn AA, Williams D, Kupsch A, Limousin P, Hariz M, Schneider G-H, et al. Event-related beta desynchronization in human subthalamic nucleus correlates with motor performance. Brain [Internet]. 2004 [cited 2018 Nov 7];127(Pt 4):735–46. Available from: https://academic.oup.com/brain/article-lookup/doi/10.1093/brain/awh106.
58. Brown P. Oscillatory nature of human basal ganglia activity: relationship to the pathophysiology of Parkinson's disease. Mov Disord [Internet]. 2003 [cited 2018 Nov 7];18(4):357–63. Available from: http://doi.wiley.com/10.1002/mds.10358.
59. Weinberger M, Mahant N, Hutchison WD, Lozano AM, Moro E, Hodaie M, et al. Beta oscillatory activity in the subthalamic nucleus and its relation to dopaminergic response in Parkinson's disease. J Neurophysiol [Internet]. 2006;96(6):3248–56. Available from: http://jn.physiology.org/cgi/doi/10.1152/jn.00697.2006.
60. Zaidel A, Spivak A, Grieb B, Bergman H, Israel Z. Subthalamic span of β oscillations predicts deep brain stimulation efficacy for patients with Parkinson's disease. Brain. 2010;133(7):2007–21.
61. Feingold J, Gibson DJ, DePasquale B, Graybiel AM. Bursts of beta oscillation differentiate postperformance activity in the striatum and motor cortex of monkeys performing movement tasks. Proc Natl Acad Sci [Internet]. 2015;112(44):13687–92. Available from: http://www.pnas.org/lookup/doi/10.1073/pnas.1517629112.
62. Tinkhauser G, Pogosyan A, Tan H, Herz DM, Kühn AA, Brown P. Beta burst dynamics in Parkinson's disease off and on dopaminergic medication. Brain. 2017;140(11):2968–81.
63. Brown P, Oliviero A, Mazzone P, Insola A, Tonali P, Di Lazzaro V. Dopamine dependency of oscillations between subthalamic nucleus and pallidum in Parkinson's disease. J Neurosci [Internet]. 2001;21 [cited 2018 Dec 14]. Available from: http://www.jneurosci.org/content/jneuro/21/3/1033.full.pdf.
64. Brown P, Williams D. Basal ganglia local field potential activity: Character and functional significance in the human. Clin Neurophysiol [Internet]. 2005 [cited 2018 Dec 14];116(11):2510–9. Available from: https://www.sciencedirect.com/science/article/pii/S1388245705002142?via%3Dihub.
65. Manning JR, Jacobs J, Fried I, Kahana MJ. Broadband shifts in local field potential power spectra are correlated with single-neuron spiking in humans. J Neurosci [Internet]. 2009 [cited 2012 Mar 10];29(43):13613–20. Available from: http://www.pubmedcentral.nih.gov/articlerender.fcgi?artid=3001247&tool=pmcentrez&rendertype=abstract.
66. de Hemptinne C, Ryapolova-Webb ES, Air EL, Garcia PA, Miller KJ, Ojemann JG, et al. Exaggerated phase-amplitude coupling in the primary motor cortex in Parkinson disease. Proc Natl Acad Sci U S A [Internet]. 2013 [cited 2014 May 27];110(12):4780–5. Available from: http://www.pubmedcentral.nih.gov/articlerender.fcgi?artid=3606991&tool=pmcentrez&rendertype=abstract.
67. de Hemptinne C, Swann NC, Ostrem JL, Ryapolova-Webb ES, San Luciano M, Galifianakis NB, et al. Therapeutic deep brain stimulation reduces cortical phase-amplitude coupling in Parkinson's disease. Nat Neurosci [Internet]. 2015;18(5):779–86. Available from: https://doi.org/10.1038/nn.3997.
68. Marsden JF, Ashby P, Limousin-Dowsey P, Rothwell JC, Brown P. Coherence between cerebellar thalamus, cortex and muscle in man: cerebellar thalamus interactions. Brain [Internet]. 2000 [cited 2018 Dec 14];123(Pt 7:1459–70. Available from: http://www.ncbi.nlm.nih.gov/pubmed/10869057.
69. Wang DD, de Hemptinne C, Miocinovic S, Ostrem JL, Galifianakis NB, San Luciano M, et al. Pallidal deep-brain stimulation disrupts pallidal beta oscillations and coherence with primary motor cortex in Parkinson's disease. J Neurosci [Internet]. 2018;38(19):4556–68. Available from: http://www.jneurosci.org/lookup/doi/10.1523/JNEUROSCI.0431-18.2018.
70. Velliste M, Perel S, Spalding MC, Whitford AS, Schwartz AB. Cortical control of a prosthetic arm for self-feeding. Nature. 2008;453(7198):1098–101.

71. Collinger JL, Wodlinger B, Downey JE, Wang W, Tyler-Kabara EC, Weber DJ, et al. High-performance neuroprosthetic control by an individual with tetraplegia. Lancet [Internet]. 2013 [cited 2014 Jan 26];381(9866):557–64. Available from: http://www.ncbi.nlm.nih.gov/pubmed/23253623.
72. Nicolelis MA, Lebedev MA. Principles of neural ensemble physiology underlying the operation of brain-machine interfaces. Nat Rev Neurosci [Internet]. 2009;10(7):530–40. Available from: http://www.ncbi.nlm.nih.gov/pubmed/19543222.
73. O'Doherty JE, Lebedev MA, Ifft PJ, Zhuang KZ, Shokur S, Bleuler H, et al. Active tactile exploration using a brain–machine–brain interface. Nature [Internet]. 2011 [cited 2018 Dec 18];479(7372):228–31. Available from: http://www.nature.com/articles/nature10489.
74. Shanechi M, Rollin R, Powers M, Wornell G, Brown E, Williams Z. Neural population partitioning and a concurrent brain-machine interface for sequential motor function. Nat Neurosciu. 2012;15(12):1–23.
75. Kundu B, Brock AA, Englot DJ, Butson CR, Rolston JD. Deep brain stimulation for the treatment of disorders of consciousness and cognition in traumatic brain injury patients: a review. Neurosurg Focus. 2018;45(August):1–8.
76. Engel AK, Moll CKE, Fried I, Ojemann GA. Invasive recordings from the human brain: clinical insights and beyond. Nat Rev Neurosci [Internet]. 2005 [cited 2014 Jul 19];6(1):35–47. Available from: http://www.ncbi.nlm.nih.gov/pubmed/15611725.
77. Canolty RT, Ganguly K, Kennerley SW, Cadieu CF, Koepsell K, Wallis JD, et al. Oscillatory phase coupling coordinates anatomically dispersed functional cell assemblies. Proc Natl Acad Sci [Internet]. 2010;107(40):17356–61. Available from: http://www.pnas.org/cgi/doi/10.1073/pnas.1008306107.
78. Hipp JF, Engel AK, Siegel M. Oscillatory synchronization in large-scale cortical networks predicts perception. Neuron [Internet]. 2011 [cited 2013 Jan 30];69(2):387–96. Available from: http://www.ncbi.nlm.nih.gov/pubmed/21262474.
79. Kreiman G, Koch C, Fried I. Imagery neurons in the human brain. Nature [Internet]. 2000;408(6810):357–61. Available from: http://www.ncbi.nlm.nih.gov/pubmed/11099042.
80. Sheth SA, Mian MK, Patel SR, Asaad WF, Williams ZM, Dougherty DD, et al. Human dorsal anterior cingulate cortex neurons mediate ongoing behavioural adaptation. Nature. 2012;488(7410):218–21.
81. Kamiński J, Sullivan S, Chung JM, Ross IB, Mamelak AN, Rutishauser U. Persistently active neurons in human medial frontal and medial temporal lobe support working memory. Nat Neurosci. 2017;20(4):590–601.
82. Ezzyat Y, Kragel JE, Burke JF, Levy DF, Lyalenko A, Wanda P, et al. Direct brain stimulation modulates encoding states and memory performance in humans. Curr Biol [Internet]. 2017;27(9):1251–8. Available from: https://doi.org/10.1016/j.cub.2017.03.028.
83. Ojemann GA, Dodrill CB. Verbal memory deficits after left temporal lobectomy for epilepsy. Mechanism and intraoperative prediction. J Neurosurg [Internet]. 1985;62(1):101–7. Available from: http://www.ncbi.nlm.nih.gov/pubmed/3964840.
84. Watrous AJ, Tandon N, Conner CR, Pieters T, Ekstrom AD. Frequency-specific network connectivity increases underlie accurate spatiotemporal memory retrieval. Nat Neurosci [Internet]. 2013 [cited 2014 Jul 11];16(3):349–56. Available from: http://www.pubmedcentral.nih.gov/articlerender.fcgi?artid=3581758&tool=pmcentrez&rendertype=abstract.
85. Mukamel R, Fried I. Human intracranial recordings and cognitive neuroscience. Annu Rev Psychol [Internet]. 2012;63(1):511–37. Available from: http://www.annualreviews.org/doi/10.1146/annurev-psych-120709-145401.
86. Neumann WJ, Huebl J, Brücke C, Gabriëls L, Bajbouj M, Merkl A, et al. Different patterns of local field potentials from limbic DBS targets in patients with major depressive and obsessive compulsive disorder. Mol Psychiatry. 2014;19(11):1186–92.
87. Dyster TG, Mikell CB, Sheth SA. The co-evolution of neuroimaging and psychiatric neurosurgery. Front Neuroanat [Internet]. 2016;10(June):1–12. Available from: http://journal.frontiersin.org/Article/10.3389/fnana.2016.00068/abstract.
88. Cash SS, Hochberg LR. The emergence of single neurons in clinical neurology. Neuron [Internet]. 2015;86(1):79–91. Available from: https://doi.org/10.1016/j.neuron.2015.03.058.
89. Smith EH, Liou J-Y, Davis TS, Merricks EM, Kellis SS, Weiss SA, et al. The ictal wavefront is the spatiotemporal source of discharges during spontaneous human seizures. Nat Commun [Internet]. 2016;7:11098. Available from: http://www.scopus.com/inward/record.url?eid=2-s2.0-84962683987&partnerID=tZOtx3y1.
90. Weiss SA, Banks GP, McKhann GM, Goodman RR, Emerson RG, Trevelyan AJ, et al. Ictal high frequency oscillations distinguish two types of seizure territories in humans. Brain [Internet]. 2013 [cited 2018 Dec 18];136(12):3796–808. Available from: https://academic.oup.com/brain/article-lookup/doi/10.1093/brain/awt276.

Local Field Potentials and ECoG

9

Doris D. Wang, Witney Chen, Philip A. Starr, and Coralie de Hemptinne

Abbreviations

BG	Basal ganglia
BGTC	Basal ganglia thalamocortical
DBS	Deep brain stimulation
ECoG	Electrocorticography
EEG	Electroencephalography
GP	Globus pallidus
GPi	Globus pallidus interna
HFO	High-frequency oscillations
LFP	Local field potentials
M1	Primary motor cortex
PAC	Phase amplitude coupling
PD	Parkinson's disease
STN	Subthalamic nucleus

Introduction

The ability to directly measure brain activity at the macroscopic level offers a tremendous opportunity to investigate neural network functions. Extracellular activity generated by a population of neurons can be measured in the form of field potentials, which encompass a range of signals including local field potentials (LFPs) recorded using depth electrodes, electrocorticography (ECoG) potentials using subdural strips or grids, as well as electroencephalography (EEG) potentials using scalp electrodes. All field potential recordings have temporal resolutions in the millisecond range and differ in their spatial resolution and invasiveness, depending on the type of electrodes used [1].

In humans, one of the first applications of invasive field potential recording was for localization of epileptic foci using temporarily placed depth and subdural electrodes. These allowed clinicians to more accurately pinpoint areas of seizure focus, with higher spatial resolution that is possible using noninvasive methods. For patients with movement disorders undergoing deep brain stimulation (DBS) surgery, it is also possible to record LFP from the basal ganglia (BG) using implanted DBS electrodes (Fig. 9.1a, b). Simultaneous recordings of BG LFPs from deep brain leads and cortical field potentials from ECoG electrodes temporarily placed over the cortex (Fig. 9.1c) has allowed researchers to further characterize cortical–subcortical network activity in patients with movement disorders [2]. Although these recordings were initially limited to using externalized electrodes in the intraoperative and the perioperative period, technological advances in implantable neural interfaces now allow for chronic, multisite brain recordings in

D. D. Wang · W. Chen · P. A. Starr
C. de Hemptinne (✉)
Department of Neurological Surgery, University of California, San Francisco, San Francisco, CA, USA
e-mail: Coralie.Dehemptinne@ucsf.edu

N. Pouratian, S. A. Sheth (eds.), *Stereotactic and Functional Neurosurgery*,
https://doi.org/10.1007/978-3-030-34906-6_9

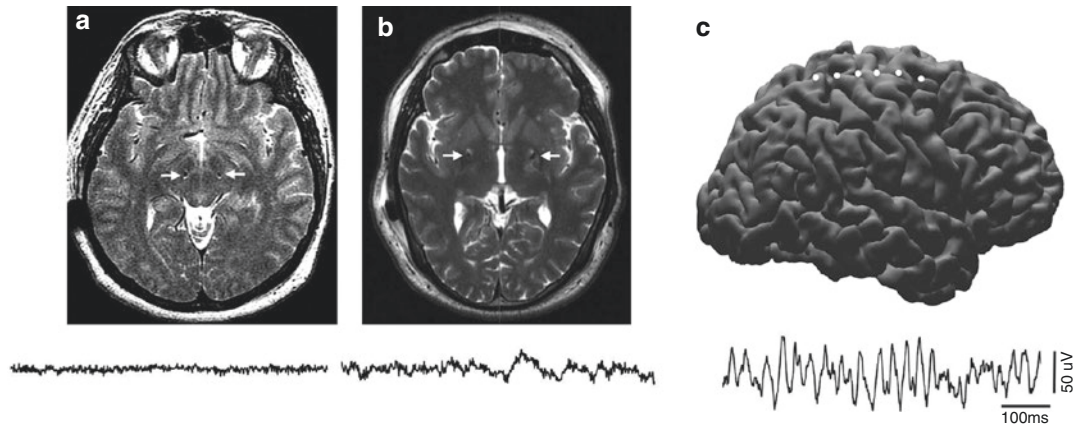

Fig. 9.1 Subcortical and cortical electrode localization (top panels) and example of their respective field potentials (lower panels). (**a**) Subthalamic (STN) and (**b**) GP leads are shown on postoperative axial MRIs at the approximate plane of the active contacts (*white arrows*). (**c**) ECoG strip overlying the sensorimotor cortex. Each ECoG contact (*white dot*) was identified on an intraoperative CT scan and plotted on the patient's MRI-derived 3D reconstruction

the ambulatory setting [3–5]. These new research platforms are opening new avenues for understanding brain functions and diseases.

Based on these field potential recordings, activity from these neural ensembles appears to oscillate. Oscillations represent rhythmic, synchronized sub- or supra-threshold neural activities from groups of neurons near the recording electrode [6]. Neural networks can oscillate across many frequency ranges from 0.5 to 500 Hz, and different oscillatory frequencies have been linked to different behavioral states [7, 8]. Brain oscillations provide one of the key mechanisms for the encoding, storage, and processing of information across different regions of the neural network by biasing the probability of neuronal spiking activity [9, 10]. Synchronization of oscillatory activity across brain regions is often thought of as a means of network-based coordination or communication. Additionally, oscillatory activity has shed light on the pathophysiology of neurological diseases and holds the potential to improve and refine existing treatments [11].

In this chapter, we discuss recent findings regarding the role of network oscillatory activities in movement disorders, based on studies from LFP and ECoG potentials. We also discuss how this knowledge is relevant for clinical practice, both in understanding the mechanism of existing DBS therapy as well as designing closed-loop therapy.

Oscillatory Signatures of Movement Disorders

Human LFPs and ECoG potentials have given us immense insight into the pathophysiology of movement disorders and mechanisms of therapies. Based on these bodies of work, excessive synchronization of the motor network in different frequency bands may be phenomenologically associated with diverse motor symptoms of movement disorders. Here, we summarize some of the evidence supporting this framework.

Beta Oscillations in Hypokinetic States

BG LFP and cortical ECoG recordings in humans have led to the advent of the "oscillatory hypothesis" of the hypokinetic symptoms in Parkinson's disease (PD), which posits that bradykinesia arises from excessively synchronized beta activity (13–30 Hz) in the BG thalamocortical (BGTC) motor loop [12, 13]. Importantly, beta rhythms

themselves are not necessarily pathological. In healthy subjects, cortical beta is modulated during movement [14, 15] and may play a role in maintaining a motor state [16]. Given its role in posture maintenance and fluid motor control [17–19], exaggerated synchronous beta activity could lead to the inability to switch between different states and may account for the akinetic state in PD [16].

The initial evidence for the oscillatory hypothesis indicated that beta modulation could be an indicator of therapeutic efficacy. In the subthalamic (STN) of PD patients, reduction in beta amplitude by dopaminergic medications (Fig. 9.2a) or DBS was correlated with reduction in hypokinetic symptoms [20–22]. However, presence of a spectral power peak in the beta band within the STN LFP is not, in itself, pathognomonic of PD, since it is also present in isolated dystonia [23] and obsessive compulsive disorder [24]. Nonetheless, the view that dopamine depletion causes excessive beta synchrony in BG nuclei has been supported in several rodent models of Parkinsonism [20, 21] as well as in dystonia patients after taking dopamine antagonists [25]. Other sites of the BG, namely, the globus pallidus (GP), also demonstrate elevated resting beta band oscillations compared to non-Parkinsonian movement disorders [26–29]. Elevated beta synchrony in PD may also present in the form of cross-structure coherence, and this has been demonstrated between cortico-cortical areas [30] and between the GP and primary motor cortex (M1) [26, 31] in humans. Cortico-cortical beta coherence can be reduced by therapeutic levodopa and STN stimulation [30] and cortico-pallidal beta coherence by pallidal DBS [26, 31], adding to the growing body of evidence that akinesia in PD is correlated with excessive beta synchrony in the brain and that therapeutic DBS works by disrupting this abnormal synchrony.

In addition to beta band amplitude and coherence, other metrics of beta synchronization, such as cross-frequency interactions between beta phase and gamma activity coupling, appear to be elevated in the Parkinsonian state as well. In normal physiology, phase amplitude coupling (PAC) is an important mechanism for communication within and between neuron ensembles in different brain regions by coordinating timing of neuronal activity in connected networks [32, 33]. Excessive coupling may entrain neuronal firing in an inflexible pattern that limits information encoding by spatiotemporal selectivity [34]. In the Parkinsonian BG, the coupling of beta phase to the amplitude of high-frequency oscillations (HFO, 200–400 Hz) has been seen in STN LFPs and can be modulated by dopaminergic state [35]. A recent study also reported the presence of coupling between low beta phase to low gamma (50–80 Hz) and HFO activity in the GP, which were both attenuated with movement [36]. Beta-HFO PAC throughout

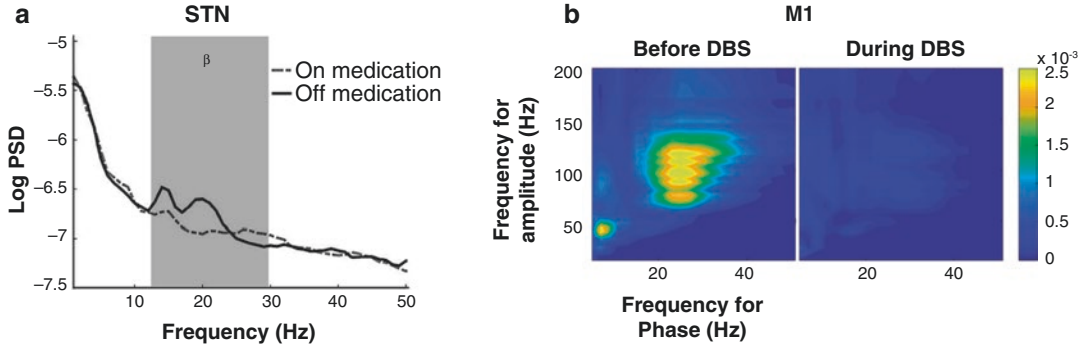

Fig. 9.2 Effect of PD treatments on cortical and subcortical field potentials. (**a**) Dopaminergic medication is associated with a reduction in beta oscillatory activity (13–30 Hz, *grey rectangle*) in the STN (*dashed line*: spectral power in the on-medication state; *black line:* spectral power in the off-medication state). (**b**) Therapeutic DBS reduces the excessive cortical beta-broadband gamma PAC (left panel: before DBS; right panel: during DBS). Color bar represents amplitude of PAC

the BGTC could be an important marker of the Parkinsonian state, supported by nonhuman primate model of Parkinsonism showing emergence of beta-HFO coupling in the pallidum in the mild state that increased with symptom severity [37]. This excessive neuronal synchronization to beta oscillations extends beyond the BG, and it exists both within the M1 and between the M1 and BG [38, 39]. Cortical PAC between beta oscillatory phase and broadband gamma activity (50–200 Hz) is reversibly suppressed by DBS (Fig. 9.2b) [39]. PAC may be measurable in the time domain by the "sharpness" of the maxima or minima in the voltage time series [40]. These abnormally synchronized activities throughout the motor network may result in hypokinesia by prohibiting the natural, dynamic neural modulation required to initiate and execute fluid movements, and DBS provides a mechanism to reduce these excessive synchronizations.

Gamma Oscillations and Hyperkinetic State

Narrowband gamma oscillations (60–90 Hz) have been observed in the subcortical structures such as the thalamus and BG, as supported by recordings from the lateral geniculate nucleus and visual cortex [41], as well as the striatum [42] and STN [43] of healthy awake rodents. In patients with PD, dopamine medication and movement both increase the amplitude of the narrowband gamma oscillations within the BG as well as its coherence with the M1 [44, 45]. Additionally, thalamic recordings from patients with other types of movement disorders also reveal the presence of movement-modulated gamma oscillations sharply tuned to frequencies of ~70 Hz range [46], suggesting that these subcortical gamma oscillations may transiently become coherent with the motor cortex to create a "prokinetic" state during normal movement. In the diseased state, hyperkinetic phenotypes may arise via appropriation and exaggeration of normal gamma oscillations. For instance, dyskinesia is associated with a narrowband increase in gamma power between 60 and 90 Hz. This oscillation is found in both in the M1 and the STN, with a strong phase coherence between the two regions [3] (Fig. 9.3). Similarly, M1 ECoG recordings from patients with isolated generalized dystonia have also demonstrated this increase in narrowband gamma power at ~80 Hz during movements that trigger dystonic posturing [47]. This suggests that when gamma oscillations become excessively or pathologically synchronized with the motor cortex, they create a "hyperkinetic" state, manifesting as dyskinesia in PD [3] or dystonic posturing in isolated dystonia [47].

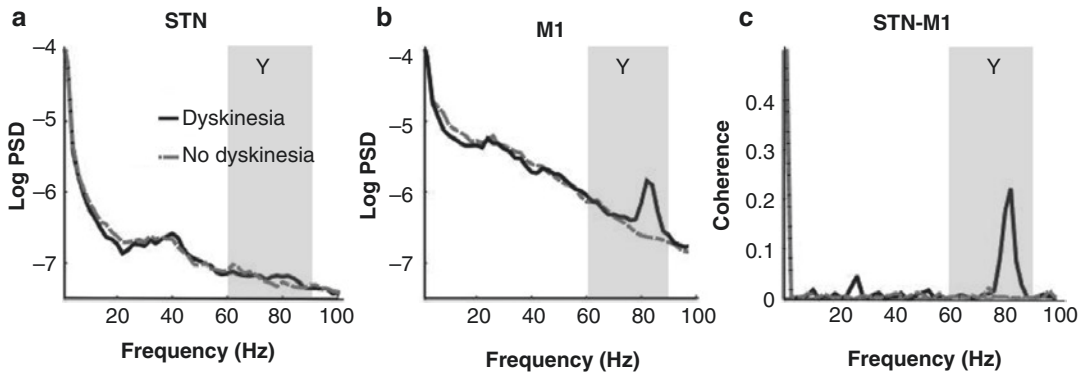

Fig. 9.3 Physiological marker of dyskinesia in the BG cortical network in an individual patient with PD in the on-medication state. (**a**) A slight increase in gamma band (60–90 Hz) amplitude is found in the STN during episode of dyskinesia (*black solid line*) compared to the non-dyskinetic state (*gray dash line*). (**b**) Dyskinesia is associated with a large increase in gamma oscillation power in the motor cortex (M1). (**c**) A large increase in STN-M1 coherence in the gamma band is also associated with dyskinesia

Theta–Alpha Oscillations in Tremor

Tremor is a common feature of several movement disorders: resting tremor in PD, postural tremor in essential tremor (ET), and dystonic tremors in isolated dystonia. Despite their phenomenological differences, studies based on field potential characteristics associated with tremors show that there may share similar physiological characteristics. STN LFP recordings from PD patients demonstrated that onset of resting tremor is associated with beta band suppression and increase in tremor frequency amplitude (~5 Hz) in both STN LFPs and surface EMGs [48]. This was confirmed in another study using MEG combined with STN LFP recording, where tremor was associated with increased amplitudes at both the tremor and double-tremor (~10 Hz) frequency within the STN, as well as in cortico-cortical coherence [49]. We also found similar increases in theta and alpha amplitudes in the globus pallidus interna (GPi) LFP of PD patients with onset of tremor (unpublished data, Fig. 9.4). Similarly, LFP recorded from the thalamic nuclei of ET patients has been compared to those of patients with multiple sclerosis or chronic pain undergoing DBS; ET patients exhibited enhanced coherence of 5–15 Hz oscillation when the electrodes were placed in the ventral intermediate and ventral oral posterior nuclei of the thalamus [50]. Together, these findings suggest that excessive narrowband synchrony in the theta and alpha frequency ranges may be a marker of tremor in the BGTC circuit.

Theta Oscillations in Dystonia

Several studies have examined LFP characteristics in patients with isolated dystonia undergoing GPi DBS implantation and found enhanced oscillatory activity in the low-frequency band (4–12 Hz) [26–28, 51–54]. Such synchronization correlates with involuntary EMG activity, indicating that it may contribute to the pathophysiology of dystonia and may be a biomarker for isolated dystonia [52, 53, 55]. Pallidal low-frequency oscillations temporally lead similar oscillations in dystonic muscle activity based on directed transfer function computations, suggesting that they may play a causal role [55]. Furthermore, high-frequency stimulation of the GPi, a highly effective therapy for improving dystonia, has been shown to suppress low-frequency activity and phasic dystonic movements in patients with dystonia [56]. However,

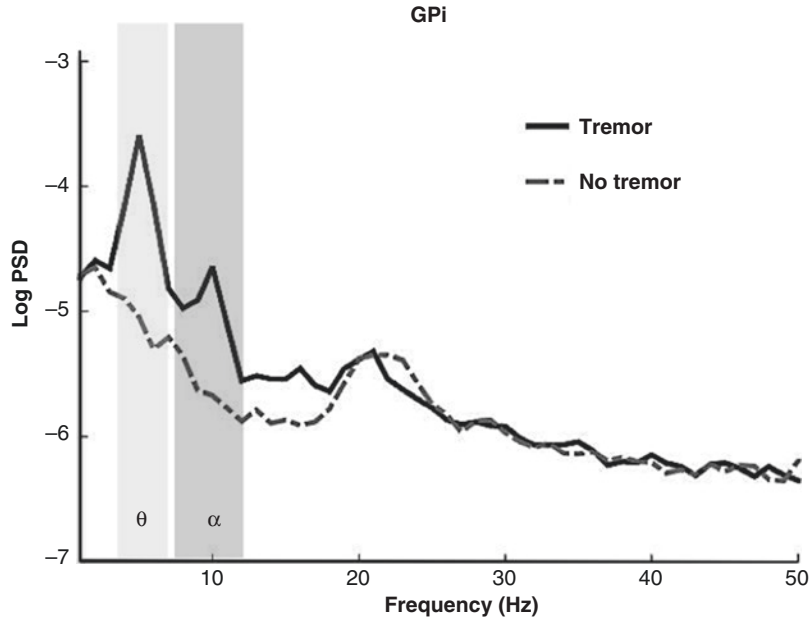

Fig. 9.4 Physiological marker of tremor in the GP of a patient with PD. Spectral power peaks at tremor frequency (5 Hz, theta band, *light grey rectangle*) and double tremor frequency (10 Hz, alpha band, *dark grey rectangle*) were seen when patient was experiencing tremor (*black curve*) but not in the absence of tremor (*dashed grey curve*). Both recordings were performed in the off-medication state

the elevated resting low-frequency oscillation may not be pervasive through other BG structures, as one comparison between STN LFPs of dystonia and PD patients did not show this increased theta power in the STN of dystonia patients [23]. This could be due to differences in inputs between the GPi and STN.

Relevance for Clinical Practice

Informing DBS Targeting in the STN

Characterization of cortico-basal ganglia oscillatory signatures through invasive recording can be applied in the clinical setting to aid DBS targeting. The boundaries of sensorimotor STN are most commonly determined using microelectrode recordings with identification of movement-related single units [57]. Although this method has high spatial resolution, it relies on the ability to isolate high signal-to-noise single units and can be highly subjective. Spectral analyses of LFPs, which represent robust population activity, are therefore more quantitative and possibly more objective. The sensorimotor region of the STN is characterized by increased amplitude of beta oscillations in the 13–30 Hz range [58–61], but the dorsal and ventral borders of the nucleus are better delineated by the higher frequency range of the beta band (21–35 Hz) in PD patients [62]. Although LFP-based identification of STN borders is an objective measure, oscillatory activity, particularly in lower frequencies, is not as spatially focal as single unit activity. Additionally, the frequency limits for beta and high beta oscillations are defined arbitrarily, and there may be patient-specific frequency limits that best characterize their BG nuclei. Thus, LFPs are most likely to serve as an adjunct to traditional MER STN mapping [63] in cases where physiological target identification is performed.

LFPs and ECoG may also be valuable tools in establishing predictive measures of therapeutic stimulation location. Beta oscillations, which are localized to the dorsolateral region of the STN, may predict the active contact location of effective DBS stimulation [61]. Additionally, M1 ECoG can be jointly used to map the topography of the M1-STN hyperdirect pathway. It has been suggested that effective STN DBS is mediated by antidromic propagation of stimulation through the hyperdirect pathway to M1 [64–66]. In a pilot study, STN electrodes that elicited the largest amplitude evoked potentials in M1 were found to be the most clinically effective DBS electrodes [67]. As DBS electrode designs get more complex with segmented directional leads, we need better predictive tools to help define the spatial topography of stimulation and to assess the effect of stimulation on cortico-BG circuitry.

Towards Adaptive Brain Stimulation

Understanding the neural signatures of motor symptoms in PD—both in the cortex and in the BG—are critical for the development of better stimulation technologies. Currently, DBS functions in "open loop" fashion, meaning that stimulation is delivered constantly according to settings manually set by a clinician, without any feedback or modulation of output. Stimulation parameters are manually adjusted to optimize symptom management against stimulation-induced side effects, which can be a time-intensive and cumbersome process. "Closed-loop" DBS aims to introduce feedback signals that reflect the patients' symptomatic state, in order to automatically adjust stimulation output. These feedback signals can be derived from multiple sources: directly from the brain, using BG LFP, cortical ECoG, or a combination of the two; peripheral sensors worn by the patient such as accelerometers and EMG sensors; or patient subjective reports on symptoms severity. Identification of personalized physiological biomarkers for particular symptoms as well as patient-specific stimulation algorithms are critical to tailor DBS to optimally treat each symptom. Initial pilot studies have implemented close d-loop algorithms using single unit recordings in nonhuman primates [68], LFP in Parkinson's patients [69–71], and peripheral sensors in essential tremor patients [72, 73]. These proof-of-principle studies establish the feasibility and potential benefits of closed-loop DBS over open loop DBS. The advent of LFP

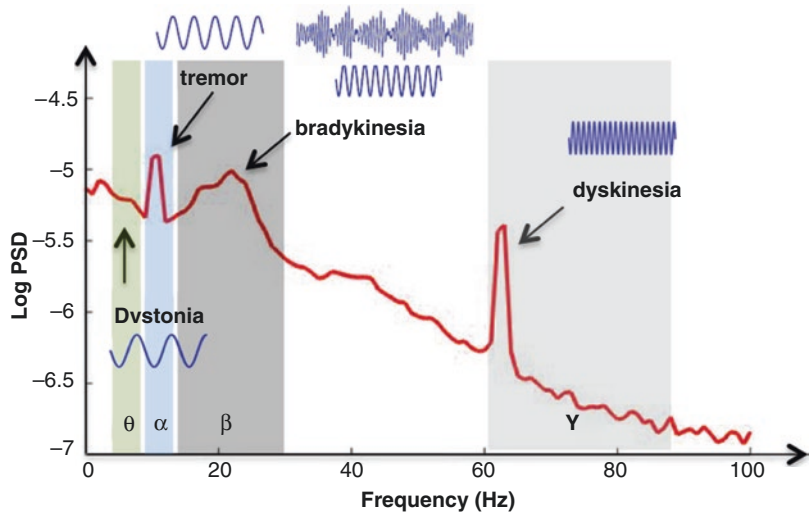

Fig. 9.5 Schematic illustrating markers of symptom identified either in the cortex or in BG nuclei. Dystonia is associated with theta power (5 Hz, *green rectangle*), tremor is associated with increase in alpha power (10 Hz, *blue rectangle*), rigidity and bradykinesia are associated with excessive beta power and PAC (13–30 Hz), dyskinesia is associated with increased gamma oscillations (60–90 Hz)

and ECoG as research tools will advance the clinical field towards more advanced stimulation technologies.

Understanding Non-motor Networks

Deep brain stimulation has been used as a potential treatment for psychiatric conditions such as depression, anxiety, anorexia, obsessive compulsive disorder, Tourette's syndrome, and chronic pain [74]. However, the efficacy across patients varies [75] and the early randomized trials have failed to underscore the complexities of psychiatric disorders. There is an unmet need to understand the underlying pathophysiology on a circuit level using high-resolution recording techniques. While multisite LFP and ECoG recordings have largely been implemented to understand motor networks, these powerful research tools can similarly be used to study nonmotor circuits. Impletmenting of these techniques would advance our understanding of neuropsychiatric diseases and drive the development of more informed models of DBS targeting and therapeutic mechanisms for novel neurological and psychiatric applications. Using these tools, we might improve neuromodulation therapy for other neurological and psychiatric disorders by (1) better characterizing the neural circuits and associated symptom- and disease-specific biomarkers, (2) validating target choices and the effects of stimulation on network activity, and (3) reassessing the use of universal therapeutic approaches to treat heterogeneous phenotypes across patients [76].

Conclusion

Direct brain recordings of BG LFP and ECoG potentials have greatly informed our understanding of cortico-BG network activity in movement disorders. These high spatiotemporal resolution metrics of population activity have launched the "oscillatory hypothesis" of movement disorders, placing an emphasis on pathological synchronization in the motor network that contributes to diseased state (Fig. 9.5). From these evolving models, we can devise new ways to advance DBS targeting, clinical programming, and stimulation paradigms. Future application of these invasive recording techniques to study non-motor brain networks reflects the power of these tools in advancing our understanding of the human brain.

References

1. Pesaran B, Vinck M, Einevoll GT, Sirota A, Fries P, Siegel M, Truccolo W, Schroeder CE, Srinivasan R. Investigating large-scale brain dynamics using field potential recordings: analysis and interpretation. Nat Neurosci. 2018;21(7):903–19. Epub 2018/06/27.

https://doi.org/10.1038/s41593-018-0171-8. PubMed PMID: 29942039.
2. Panov F, Levin E, de Hemptinne C, Swann NC, Qasim S, Miocinovic S, Ostrem JL, Starr PA. Intraoperative electrocorticography for physiological research in movement disorders: principles and experience in 200 cases. J Neurosurg. 2017;126(1):122–31. Epub 2016/02/27. https://doi.org/10.3171/2015.11.JNS151341. PubMed PMID: 26918474; PMCID: PMC5001942.
3. Swann NC, de Hemptinne C, Miocinovic S, Qasim S, Wang SS, Ziman N, Ostrem JL, San Luciano M, Galifianakis NB, Starr PA. Gamma oscillations in the hyperkinetic state detected with chronic human brain recordings in Parkinson's Disease. J Neurosci. 2016;36(24):6445–58. https://doi.org/10.1523/JNEUROSCI.1128-16.2016. PubMed PMID: 27307233; PMCID: PMC5015781.
4. DiLorenzo DJ, Mangubat EZ, Rossi MA, Byrne RW. Chronic unlimited recording electrocorticography-guided resective epilepsy surgery: technology-enabled enhanced fidelity in seizure focus localization with improved surgical efficacy. J Neurosurg. 2014;120(6):1402–14. Epub 2014/03/25. https://doi.org/10.3171/2014.1.JNS131592. PubMed PMID: 24655096.
5. Swann NC, de Hemptinne C, Miocinovic S, Qasim S, Ostrem JL, Galifianakis NB, Luciano MS, Wang SS, Ziman N, Taylor R, Starr PA. Chronic multisite brain recordings from a totally implantable bidirectional neural interface: experience in 5 patients with Parkinson's disease. J Neurosurg. 2018;128(2):605–16. Epub 2017/04/15. https://doi.org/10.3171/2016.11.JNS161162. PubMed PMID: 28409730; PMCID: PMC5641233.
6. Buzsaki G, Draguhn A. Neuronal oscillations in cortical networks. Science. 2004;304(5679):1926–9. Epub 2004/06/26. https://doi.org/10.1126/science.1099745. PubMed PMID: 15218136.
7. Csicsvari J, Jamieson B, Wise KD, Buzsaki G. Mechanisms of gamma oscillations in the hippocampus of the behaving rat. Neuron. 2003;37(2):311–22. Epub 2003/01/28. PubMed PMID: 12546825.
8. Hammond C, Bergman H, Brown P. Pathological synchronization in Parkinson's disease: networks, models and treatments. Trends Neurosci. 2007;30(7):357–64. PubMed PMID: 17532060.
9. Llinas RR. The intrinsic electrophysiological properties of mammalian neurons: insights into central nervous system function. Science. 1988;242(4886):1654–64. Epub 1988/12/23. PubMed PMID: 3059497.
10. Fries P. A mechanism for cognitive dynamics: neuronal communication through neuronal coherence. Trends Cogn Sci. 2005;9(10):474–80. Epub 2005/09/10. https://doi.org/10.1016/j.tics.2005.08.011. PubMed PMID: 16150631.
11. Thompson JA, Lanctin D, Ince NF, Abosch A. Clinical implications of local field potentials for understanding and treating movement disorders. Stereotact Funct Neurosurg. 2014;92(4):251–63. Epub 2014/08/30. https://doi.org/10.1159/000364913. PubMed PMID: 25170784.
12. Brown P. Oscillatory nature of human basal ganglia activity: relationship to the pathophysiology of Parkinson's disease. Mov Disord. 2003;18(4):357–63. PubMed PMID: 12671940.
13. Oswal A, Brown P, Litvak V. Synchronized neural oscillations and the pathophysiology of Parkinson's disease. Curr Opin Neurol. 2013;26(6):662–70. https://doi.org/10.1097/WCO.0000000000000034. PubMed PMID: 24150222.
14. Doyle LM, Yarrow K, Brown P. Lateralization of event-related beta desynchronization in the EEG during pre-cued reaction time tasks. Clin Neurophysiol. 2005;116(8):1879–88. Epub 2005/06/28. https://doi.org/10.1016/j.clinph.2005.03.017. PubMed PMID: 15979401.
15. van Wijk BC, Beek PJ, Daffertshofer A. Neural synchrony within the motor system: what have we learned so far? Front Hum Neurosci. 2012;6:252. Epub 2012/09/13. https://doi.org/10.3389/fnhum.2012.00252. PubMed PMID: 22969718; PMCID: PMC3432872.
16. Engel AK, Fries P. Beta-band oscillations--signalling the status quo? Curr Opin Neurobiol. 2010;20(2):156–65. PubMed PMID: 20359884.
17. Sanes JN, Donoghue JP. Oscillations in local field potentials of the primate motor cortex during voluntary movement. Proc Natl Acad Sci U S A. 1993;90(10):4470–4. PubMed PMID: 8506287; PMCID: PMC46533.
18. Klostermann F, Nikulin VV, Kuhn AA, Marzinzik F, Wahl M, Pogosyan A, Kupsch A, Schneider GH, Brown P, Curio G. Task-related differential dynamics of EEG alpha- and beta-band synchronization in cortico-basal motor structures. Eur J Neurosci. 2007;25(5):1604–15. https://doi.org/10.1111/j.1460-9568.2007.05417.x. PubMed PMID: 17425586.
19. Chakarov V, Naranjo JR, Schulte-Monting J, Omlor W, Huethe F, Kristeva R. Beta-range EEG-EMG coherence with isometric compensation for increasing modulated low-level forces. J Neurophysiol. 2009;102(2):1115–20. https://doi.org/10.1152/jn.91095.2008. PubMed PMID: 19458142.
20. Priori A, Foffani G, Pesenti A, Tamma F, Bianchi AM, Pellegrini M, Locatelli M, Moxon KA, Villani RM. Rhythm-specific pharmacological modulation of subthalamic activity in Parkinson's disease. Exp Neurol. 2004;189(2):369–79. PubMed PMID: 15380487.
21. Bronte-Stewart H, Barberini C, Koop MM, Hill BC, Henderson JM, Wingeier B. The STN beta-band profile in Parkinson's disease is stationary and shows prolonged attenuation after deep brain stimulation. Exp Neurol. 2009;215(1):20–8. PubMed PMID: 18929561.
22. Kuhn AA, Kempf F, Brucke C, Gaynor Doyle L, Martinez-Torres I, Pogosyan A, Trottenberg T, Kupsch A, Schneider GH, Hariz MI, Vandenberghe W, Nuttin B, Brown P. High-frequency stimulation

of the subthalamic nucleus suppresses oscillatory beta activity in patients with Parkinson's disease in parallel with improvement in motor performance. J Neurosci. 2008;28(24):6165–73. PubMed PMID: 18550758.
23. Wang DD, de Hemptinne C, Miocinovic S, Qasim SE, Miller AM, Ostrem JL, Galifianakis NB, San Luciano M, Starr PA. Subthalamic local field potentials in Parkinson's disease and isolated dystonia: an evaluation of potential biomarkers. Neurobiol Dis. 2016;89:213–22. Epub 2016/02/18. https://doi.org/10.1016/j.nbd.2016.02.015. PubMed PMID: 26884091.
24. Rappel P, Marmor O, Bick AS, Arkadir D, Linetsky E, Castrioto A, Tamir I, Freedman SA, Mevorach T, Gilad M, Bergman H, Israel Z, Eitan R. Subthalamic theta activity: a novel human subcortical biomarker for obsessive compulsive disorder. Transl Psychiatry. 2018;8(1):118. Epub 2018/06/20. https://doi.org/10.1038/s41398-018-0165-z. PubMed PMID: 29915200; PMCID: PMC6006433.
25. Kuhn AA, Brucke C, Schneider GH, Trottenberg T, Kivi A, Kupsch A, Capelle HH, Krauss JK, Brown P. Increased beta activity in dystonia patients after drug-induced dopamine deficiency. Exp Neurol. 2008;214(1):140–3. Epub 2008/09/02. https://doi.org/10.1016/j.expneurol.2008.07.023. PubMed PMID: 18760276.
26. Wang DD, de Hemptinne C, Miocinovic S, Ostrem JL, Galifianakis NB, San Luciano M, Starr PA. Pallidal deep-brain stimulation disrupts pallidal beta oscillations and coherence with primary motor cortex in Parkinson's disease. J Neurosci. 2018;38(19):4556–68. Epub 2018/04/18. https://doi.org/10.1523/JNEUROSCI.0431-18.2018. PubMed PMID: 29661966; PMCID: PMC5943981.
27. Weinberger M, Hutchison WD, Alavi M, Hodaie M, Lozano AM, Moro E, Dostrovsky JO. Oscillatory activity in the globus pallidus internus: comparison between Parkinson's disease and dystonia. Clin Neurophysiol. 2012;123(2):358–68. Epub 2011/08/17. https://doi.org/10.1016/j.clinph.2011.07.029. PubMed PMID: 21843964.
28. Silberstein P, Kuhn AA, Kupsch A, Trottenberg T, Krauss JK, Wohrle JC, Mazzone P, Insola A, Di Lazzaro V, Oliviero A, Aziz T, Brown P. Patterning of globus pallidus local field potentials differs between Parkinson's disease and dystonia. Brain. 2003;126(Pt 12):2597–608. PubMed PMID: 12937079.
29. Jimenez-Shahed J, Telkes I, Viswanathan A, Ince NF. GPi oscillatory activity differentiates tics from the resting state, voluntary movements, and the unmedicated Parkinsonian state. Front Neurosci. 2016;10:436. https://doi.org/10.3389/fnins.2016.00436. PubMed PMID: 27733815; PMCID: PMC5039204.
30. Silberstein P, Pogosyan A, Kuhn AA, Hotton G, Tisch S, Kupsch A, Dowsey-Limousin P, Hariz MI, Brown P. Cortico-cortical coupling in Parkinson's disease and its modulation by therapy. Brain. 2005;128(Pt 6):1277–91. PubMed PMID: 15774503.
31. Malekmohammadi M, Shahriari Y, AuYong N, O'Keeffe A, Bordelon Y, Hu X, Pouratian N. Pallidal stimulation in Parkinson disease differentially modulates local and network beta activity. J Neural Eng. 2018;15(5):056016. Epub 2018/07/05. https://doi.org/10.1088/1741-2552/aad0fb. PubMed PMID: 29972146; PMCID: PMC6125208.
32. Canolty RT, Ganguly K, Kennerley SW, Cadieu CF, Koepsell K, Wallis JD, Carmena JM. Oscillatory phase coupling coordinates anatomically dispersed functional cell assemblies. Proc Natl Acad Sci U S A. 2010;107(40):17356–61. https://doi.org/10.1073/pnas.1008306107. PubMed PMID: 20855620; PMCID: PMC2951408.
33. Canolty RT, Knight RT. The functional role of cross-frequency coupling. Trends Cogn Sci. 2010;14(11):506–15. PubMed PMID: 20932795.
34. Litvak V, Jha A, Eusebio A, Oostenveld R, Foltynie T, Limousin P, Zrinzo L, Hariz MI, Friston K, Brown P. Resting oscillatory cortico-subthalamic connectivity in patients with Parkinson's disease. Brain. 2011;134(Pt 2):359–74. PubMed PMID: 21147836.
35. Lopez-Azcarate J, Tainta M, Rodriguez-Oroz MC, Valencia M, Gonzalez R, Guridi J, Iriarte J, Obeso JA, Artieda J, Alegre M. Coupling between beta and high-frequency activity in the human subthalamic nucleus may be a pathophysiological mechanism in Parkinson's disease. J Neurosci. 2010;30(19):6667–77. PubMed PMID: 20463229.
36. AuYong N, Malekmohammadi M, Ricks-Oddie J, Pouratian N. Movement-modulation of local power and phase amplitude coupling in bilateral globus pallidus interna in Parkinson disease. Front Hum Neurosci. 2018;12:270. Epub 2018/07/25. https://doi.org/10.3389/fnhum.2018.00270. PubMed PMID: 30038563; PMCID: PMC6046436.
37. Connolly AT, Jensen AL, Bello EM, Netoff TI, Baker KB, Johnson MD, Vitek JL. Modulations in oscillatory frequency and coupling in globus pallidus with increasing parkinsonian severity. J Neurosci. 2015;35(15):6231–40. https://doi.org/10.1523/JNEUROSCI.4137-14.2015. PubMed PMID: 25878293; PMCID: PMC4397612.
38. de Hemptinne C, Ryapolova-Webb ES, Air EL, Garcia PA, Miller KJ, Ojemann JG, Ostrem JL, Galifianakis NB, Starr PA. Exaggerated phase-amplitude coupling in the primary motor cortex in Parkinson disease. Proc Natl Acad Sci U S A. 2013;110(12):4780–5. Epub 2013/03/09. https://doi.org/10.1073/pnas.1214546110. PubMed PMID: 23471992; PMCID: 3606991.
39. de Hemptinne C, Swann NC, Ostrem JL, Ryapolova-Webb ES, San Luciano M, Galifianakis NB, Starr PA. Therapeutic deep brain stimulation reduces cortical phase-amplitude coupling in Parkinson's disease. Nat Neurosci. 2015;18(5):779–86. https://doi.org/10.1038/nn.3997. PubMed PMID: 25867121; PMCID: PMC4414895.
40. Cole SR, van der Meij R, Peterson EJ, de Hemptinne C, Starr PA, Voytek B. Nonsinusoidal beta oscillations reflect cortical pathophysiology in Parkinson's disease.

J Neurosci. 2017;37(18):4830–40. Epub 2017/04/19. https://doi.org/10.1523/JNEUROSCI.2208-16.2017. PubMed PMID: 28416595; PMCID: PMC5426572.
41. Saleem AB, Lien AD, Krumin M, Haider B, Roson MR, Ayaz A, Reinhold K, Busse L, Carandini M, Harris KD. Subcortical source and modulation of the narrowband gamma oscillation in mouse visual cortex. Neuron. 2017;93(2):315–22. Epub 2017/01/20. https://doi.org/10.1016/j.neuron.2016.12.028. PubMed PMID: 28103479; PMCID: PMC5263254.
42. Berke JD, Okatan M, Skurski J, Eichenbaum HB. Oscillatory entrainment of striatal neurons in freely moving rats. Neuron. 2004;43(6):883–96. Epub 2004/09/15. https://doi.org/10.1016/j.neuron.2004.08.035. PubMed PMID: 15363398.
43. Brown P, Kupsch A, Magill PJ, Sharott A, Harnack D, Meissner W. Oscillatory local field potentials recorded from the subthalamic nucleus of the alert rat. Exp Neurol. 2002;177(2):581–5. PubMed PMID: 12429204.
44. Cassidy M, Mazzone P, Oliviero A, Insola A, Tonali P, Di Lazzaro V, Brown P. Movement-related changes in synchronization in the human basal ganglia. Brain. 2002;125(Pt 6):1235–46. PubMed PMID: 12023312.
45. Williams D, Tijssen M, Van Bruggen G, Bosch A, Insola A, Di Lazzaro V, Mazzone P, Oliviero A, Quartarone A, Speelman H, Brown P. Dopamine-dependent changes in the functional connectivity between basal ganglia and cerebral cortex in humans. Brain. 2002;125(Pt 7):1558–69. PubMed PMID: 12077005.
46. Kempf F, Brucke C, Salih F, Trottenberg T, Kupsch A, Schneider GH, Doyle Gaynor LM, Hoffmann KT, Vesper J, Wohrle J, Altenmuller DM, Krauss JK, Mazzone P, Di Lazzaro V, Yelnik J, Kuhn AA, Brown P. Gamma activity and reactivity in human thalamic local field potentials. Eur J Neurosci. 2009;29(5):943–53. PubMed PMID: 19291224.
47. Miocinovic S, Swann NC, de Hemptinne C, Miller A, Ostrem JL, Starr PA. Cortical gamma oscillations in isolated dystonia. Parkinsonism Relat Disord. 2018. https://doi.org/10.1016/j.parkreldis.2018.01.017. PubMed PMID: 29371063.
48. Wang SY, Aziz TZ, Stein JF, Liu X. Time-frequency analysis of transient neuromuscular events: dynamic changes in activity of the subthalamic nucleus and forearm muscles related to the intermittent resting tremor. J Neurosci Methods. 2005;145(1–2):151–8. Epub 2005/06/01. https://doi.org/10.1016/j.jneumeth.2004.12.009. PubMed PMID: 15922033.
49. Hirschmann J, Hartmann CJ, Butz M, Hoogenboom N, Ozkurt TE, Elben S, Vesper J, Wojtecki L, Schnitzler A. A direct relationship between oscillatory subthalamic nucleus-cortex coupling and rest tremor in Parkinson's disease. Brain. 2013;136(Pt 12):3659–70. Epub 2013/10/25. https://doi.org/10.1093/brain/awt271. PubMed PMID: 24154618.
50. Kane A, Hutchison WD, Hodaie M, Lozano AM, Dostrovsky JO. Enhanced synchronization of thalamic theta band local field potentials in patients with essential tremor. Exp Neurol. 2009;217(1):171–6. Epub 2009/02/24. https://doi.org/10.1016/j.expneurol.2009.02.005. PubMed PMID: 19233174.
51. Liu X, Griffin IC, Parkin SG, Miall RC, Rowe JG, Gregory RP, Scott RB, Aziz TZ, Stein JF. Involvement of the medial pallidum in focal myoclonic dystonia: a clinical and neurophysiological case study. Mov Disord. 2002;17(2):346–53. PubMed PMID: 11921122.
52. Liu X, Wang S, Yianni J, Nandi D, Bain PG, Gregory R, Stein JF, Aziz TZ. The sensory and motor representation of synchronized oscillations in the globus pallidus in patients with primary dystonia. Brain. 2008;131(Pt 6):1562–73. https://doi.org/10.1093/brain/awn083. PubMed PMID: 18487278.
53. Chen CC, Kuhn AA, Hoffmann KT, Kupsch A, Schneider GH, Trottenberg T, Krauss JK, Wohrle JC, Bardinet E, Yelnik J, Brown P. Oscillatory pallidal local field potential activity correlates with involuntary EMG in dystonia. Neurology. 2006;66(3):418–20. https://doi.org/10.1212/01.wnl.0000196470.00165.7d. PubMed PMID: 16476944.
54. Chen CC, Kuhn AA, Trottenberg T, Kupsch A, Schneider GH, Brown P. Neuronal activity in globus pallidus interna can be synchronized to local field potential activity over 3-12 Hz in patients with dystonia. Exp Neurol. 2006;202(2):480–6. Epub 2006/08/26. S0014-4886(06)00428-6 [pii]. https://doi.org/10.1016/j.expneurol.2006.07.011. PubMed PMID: 16930593.
55. Sharott A, Grosse P, Kuhn AA, Salih F, Engel AK, Kupsch A, Schneider GH, Krauss JK, Brown P. Is the synchronization between pallidal and muscle activity in primary dystonia due to peripheral afferance or a motor drive? Brain. 2008;131(Pt 2):473–84. https://doi.org/10.1093/brain/awm324. PubMed PMID: 18178569.
56. Barow E, Neumann WJ, Brucke C, Huebl J, Horn A, Brown P, Krauss JK, Schneider GH, Kuhn AA. Deep brain stimulation suppresses pallidal low frequency activity in patients with phasic dystonic movements. Brain. 2014;137(Pt 11):3012–24. https://doi.org/10.1093/brain/awu258. PubMed PMID: 25212852; PMCID: PMC4813762.
57. Starr PA, Christine CW, Theodosopoulos PV, Lindsey N, Byrd D, Mosley A, Marks WJ, Jr. Implantation of deep brain stimulators into the subthalamic nucleus: technical approach and magnetic resonance imaging-verified lead locations. J Neurosurg. 2002;97(2):370–87. Epub 2002/08/21. https://doi.org/10.3171/jns.2002.97.2.0370. PubMed PMID: 12186466.
58. Chen CC, Pogosyan A, Zrinzo LU, Tisch S, Limousin P, Ashkan K, Yousry T, Hariz MI, Brown P. Intra-operative recordings of local field potentials can help localize the subthalamic nucleus in Parkinson's disease surgery. Exp Neurol. 2006;198(1):214–21. PubMed PMID: 16403500.
59. Trottenberg T, Kupsch A, Schneider GH, Brown P, Kuhn AA. Frequency-dependent distribution of local field potential activity within the subthalamic nucleus

in Parkinson's disease. Exp Neurol. 2007;205(1):287–91. PubMed PMID: 17336961.
60. Zaidel A, Spivak A, Shpigelman L, Bergman H, Israel Z. Delimiting subterritories of the human subthalamic nucleus by means of microelectrode recordings and a hidden Markov model. Mov Disord. 2009;24(12):1785–93. PubMed PMID: 19533755.
61. Zaidel A, Spivak A, Grieb B, Bergman H, Israel Z. Subthalamic span of beta oscillations predicts deep brain stimulation efficacy for patients with Parkinson's disease. Brain. 2010;133(Pt 7):2007–21. PubMed PMID: 20534648.
62. Miyagi Y, Okamoto T, Morioka T, Tobimatsu S, Nakanishi Y, Aihara K, Hashiguchi K, Murakami N, Yoshida F, Samura K, Nagata S, Sasaki T. Spectral analysis of field potential recordings by deep brain stimulation electrode for localization of subthalamic nucleus in patients with Parkinson's disease. Stereotact Funct Neurosurg. 2009;87(4):211–8. Epub 2009/07/03. https://doi.org/10.1159/000225974. PubMed PMID: 19571612.
63. Telkes I, Jimenez-Shahed J, Viswanathan A, Abosch A, Ince NF. Prediction of STN-DBS electrode implantation track in Parkinson's disease by using local field potentials. Front Neurosci. 2016;10:198. Epub 2016/06/01. https://doi.org/10.3389/fnins.2016.00198. PubMed PMID: 27242404; PMCID: PMC4860394.
64. Gradinaru V, Mogri M, Thompson KR, Henderson JM, Deisseroth K. Optical deconstruction of parkinsonian neural circuitry. Science. 2009;324(5925):354–9. Epub 2009/03/21. https://doi.org/10.1126/science.1167093. PubMed PMID: 19299587.
65. Li Q, Ke Y, Chan DC, Qian ZM, Yung KK, Ko H, Arbuthnott GW, Yung WH. Therapeutic deep brain stimulation in parkinsonian rats directly influences motor cortex. Neuron. 2012;76(5):1030–41. Epub 2012/12/12. https://doi.org/10.1016/j.neuron.2012.09.032. PubMed PMID: 23217750.
66. Anderson RW, Farokhniaee A, Gunalan K, Howell B, McIntyre CC. Action potential initiation, propagation, and cortical invasion in the hyperdirect pathway during subthalamic deep brain stimulation. Brain Stimul. 2018;11(5):1140–50. Epub 2018/05/22. https://doi.org/10.1016/j.brs.2018.05.008. PubMed PMID: 29779963; PMCID: PMC6109410.
67. Miocinovic S, de Hemptinne C, Chen W, Isbaine F, Willie JT, Ostrem JL, Starr PA. Cortical potentials evoked by subthalamic stimulation demonstrate a short latency hyperdirect pathway in humans. J Neurosci. 2018;38(43):9129–41. Epub 2018/09/12. https://doi.org/10.1523/JNEUROSCI.1327-18.2018. PubMed PMID: 30201770; PMCID: PMC6199405.
68. Rosin B, Slovik M, Mitelman R, Rivlin-Etzion M, Haber SN, Israel Z, Vaadia E, Bergman H. Closed-loop deep brain stimulation is superior in ameliorating parkinsonism. Neuron. 2011;72(2):370–84. Epub 2011/10/25. https://doi.org/10.1016/j.neuron.2011.08.023. PubMed PMID: 22017994.
69. Little S, Pogosyan A, Neal S, Zavala B, Zrinzo L, Hariz M, Foltynie T, Limousin P, Ashkan K, FitzGerald J, Green AL, Aziz TZ, Brown P. Adaptive deep brain stimulation in advanced Parkinson disease. Ann Neurol. 2013;74(3):449–57. Epub 2013/07/16. https://doi.org/10.1002/ana.23951. PubMed PMID: 23852650; PMCID: 3886292.
70. Rosa M, Arlotti M, Marceglia S, Cogiamanian F, Ardolino G, Fonzo AD, Lopiano L, Scelzo E, Merola A, Locatelli M, Rampini PM, Priori A. Adaptive deep brain stimulation controls levodopa-induced side effects in Parkinsonian patients. Mov Disord. 2017;32(4):628–9. Epub 2017/02/18. https://doi.org/10.1002/mds.26953. PubMed PMID: 28211585; PMCID: PMC5412843.
71. Swann NC, de Hemptinne C, Thompson MC, Miocinovic S, Miller AM, Gilron R, Ostrem JL, Chizeck HJ, Starr PA. Adaptive deep brain stimulation for Parkinson's disease using motor cortex sensing. J Neural Eng. 2018;15(4):046006. Epub 2018/05/10. https://doi.org/10.1088/1741-2552/aabc9b. PubMed PMID: 29741160; PMCID: PMC6021210.
72. Herron JA, Thompson MC, Brown T, Chizeck HJ, Ojemann JG, Ko AL. Chronic electrocorticography for sensing movement intention and closed-loop deep brain stimulation with wearable sensors in an essential tremor patient. J Neurosurg. 2017;127(3):580–7. Epub 2016/11/20. https://doi.org/10.3171/2016.8.JNS16536. PubMed PMID: 27858575.
73. Haddock A, Mitchell KT, Miller A, Ostrem JL, Chizeck HJ, Miocinovic S. Automated deep brain stimulation programming for tremor. IEEE Trans Neural Syst Rehabil Eng. 2018;26(8):1618–25. Epub 2018/07/12. https://doi.org/10.1109/TNSRE.2018.2852222. PubMed PMID: 29994714.
74. Roy HA, Green AL, Aziz TZ. State of the art: novel applications for deep brain stimulation. Neuromodulation. 2018;21(2):126–34. Epub 2017/05/19. https://doi.org/10.1111/ner.12604. PubMed PMID: 28516669.
75. Holtzheimer PE, Mayberg HS. Deep brain stimulation for psychiatric disorders. Annu Rev Neurosci. 2011;34:289–307. Epub 2011/06/23. https://doi.org/10.1146/annurev-neuro-061010-113638. PubMed PMID: 21692660; PMCID: PMC4413475.
76. Ramirez-Zamora A, Giordano JJ, Gunduz A, Brown P, Sanchez JC, Foote KD, Almeida L, Starr PA, Bronte-Stewart HM, Hu W, McIntyre C, Goodman W, Kumsa D, Grill WM, Walker HC, Johnson MD, Vitek JL, Greene D, Rizzuto DS, Song D, Berger TW, Hampson RE, Deadwyler SA, Hochberg LR, Schiff ND, Stypulkowski P, Worrell G, Tiruvadi V, Mayberg HS, Jimenez-Shahed J, Nanda P, Sheth SA, Gross RE, Lempka SF, Li L, Deeb W, Okun MS. Evolving applications, technological challenges and future opportunities in neuromodulation: proceedings of the fifth annual deep brain stimulation think tank. Front Neurosci. 2017;11:734. Epub 2018/02/09. https://doi.org/10.3389/fnins.2017.00734. PubMed PMID: 29416498; PMCID: PMC5787550.

Awake Testing to Confirm Target Engagement

10

Neepa J. Patel, Jay R. Gavvala, and Joohi Jimenez-Shahed

Abbreviations

ALIC	Anterior limb of the internal capsule
CM–Pf	Centromedian–parafascicular complex
DBS	Deep brain stimulation
EEG	Electroencephalogram
FDG	Fluorodeoxyglucose
FUS	Focused ultrasound
GPi	Globus pallidus interna
Hz	Hertz
mA	Milliamperes
MEG	Magnetoencephalography
MER	Microelectrode recording
MRI	Magnetic resonance imaging
OCD	Obsessive compulsive disorder
PD	Parkinson's disease
PET	Positron emission tomography
RNS	Responsive neurostimulation
SCG	Subcallosal cingulate gyrus
SEEG	Stereo-encephalography
SISCOM	Subtraction ictal SPECT co-registered to MRI
SPECT	Single-photon emission computed tomography
SPM	Statistical parametric mapping
STN	Subthalamic nucleus
TS	Tourette syndrome
Usec	Microseconds
V	Volts
Vc	Ventral caudal nucleus
VC/VS	Ventral caudate/ventral striatum
ViM	Ventral intermediate nucleus
VNS	Vagal nerve stimulation

Introduction

Stereotactic functional neurosurgery requires both accuracy and precision to achieve targeted treatment to eloquent and deep structures of the brain. Awake testing to confirm target engagement is an important component of the intraoperative evaluation. General anesthesia is not recommended in neurosurgical procedures requiring neurophysiological monitoring as it is difficult to gather key functional anatomical information such as neuronal firing patterns and patient feedback on neurological symptoms which can aide with localization during the

N. J. Patel
Department of Neurology, Parkinson Disease and Movement Disorders Clinic, Henry Ford Hospital, West Bloomfield, MI, USA

J. R. Gavvala
Department of Neurology – Neurophysiology, Baylor College of Medicine, Houston, TX, USA

J. Jimenez-Shahed (✉)
Medical Director, Movement Disorders Neuromodulation, Department of Neurology, Icahn School of Medicine at Mount Sinai, New York, NY, USA
e-mail: Joohi.Jimenez-shahed@mountsinai.org

N. Pouratian, S. A. Sheth (eds.), *Stereotactic and Functional Neurosurgery*,
https://doi.org/10.1007/978-3-030-34906-6_10

surgery. Many neurosurgeons will utilize short-acting anesthesia during frame placement and creation of the burr hole; however, this is discontinued promptly after the procedure is completed. Identification of specific neuronal signatures and intraoperative testing ensure accurate localization and aide in ensuring there are no unintended neurological sequelae from the procedure. Sedation of the patient will reduce responsiveness and neurological evaluations in the operating room and more importantly can dampen neuronal firing. The previous chapters discussed strategies for intraoperative monitoring to identify and localize the target of interest in detail. In this section, we will review the role of awake testing procedures to confirm appropriate target engagement for deep brain stimulation (DBS), high-frequency ultrasound, and epilepsy surgeries.

Deep Brain Stimulation for Movement Disorders

Deep brain stimulation (DBS) was first approved for the treatment of tremor in 1997. Since its original approval, this therapy is being utilized for the treatment of a variety of neurological and psychiatric disorders [1]. Attenuation of symptoms is achieved by introducing stimulation within specific brain structures. In order to ensure accurate placement of the DBS electrode, surgery is traditionally performed while the patient is awake in order to assess neurophysiological characteristics of the structures along the electrode trajectory. Once the optimal trajectory and location for implantation is identified, the DBS electrode is inserted and the patient undergoes clinical testing of stimulation. It is important to confirm clinical response and identify side effects from stimulation prior to securing the lead to ensure usability of the electrode and sufficient response to therapy. Newer strategies such as image-guided techniques do not utilize intraoperative test stimulation and will not be discussed in this chapter [2–4].

Presently, there are three DBS systems available in the US market which offer unique options for stimulation delivery (Fig. 10.1). The neurosurgeon and treating neurologist must consider the anatomy of the target structure, electrode design, and desired stimulation programming options when selecting a specific device for indi-

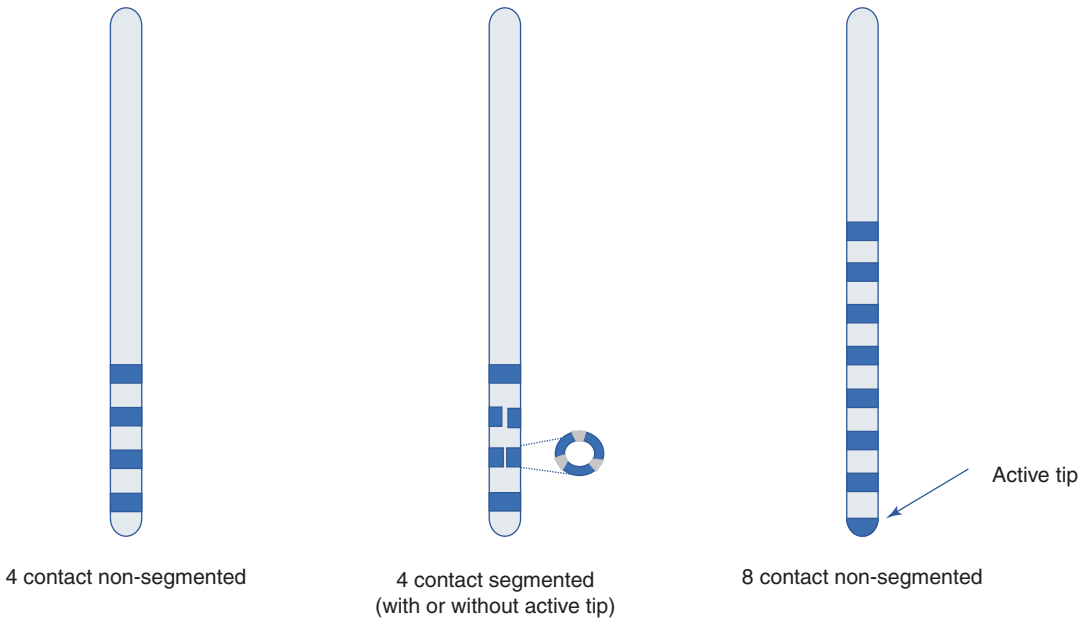

Fig. 10.1 Comparison of deep brain stimulation electrodes. Current deep brain stimulation leads available in the United States in 2019. The electrode contacts are typically 1.5 mm in width and are typically spaced 1.5 or 0.5 mm apart

vidual patients. For the purposes of this chapter, we will provide a general overview based on a 4-contact electrode with whole ring activation for intraoperative testing.

A standardized and methodical approach for intraoperative testing is recommended. Utilizing the same protocol for testing with standard settings is important to ensure appropriate response to stimulation. In this chapter, we will discuss test stimulation in the monopolar configuration; however, bipolar stimulation is used by some centers during intraoperative testing. A standard pulse width (60 μs) and frequency (130 Hz) should be set for all surgeries.

Stimulation is introduced with incremental increases in amplitude to a maximum of 5 V or 4 mA (assuming impedance measurements between 1000 and 1200 Ω). In the operating room, the awake patient is encouraged to communicate any unusual sensations or symptoms he/she may experience during the testing procedures. As the stimulation is increased, the patient may experience transient side effects, which often resolve within a few seconds or minutes. If these symptoms are not distressing, we recommend allowing at least 1 minute for the patient to adapt to these side effects prior to deciding to abort further testing of that contact. However, if side effects are persistent or amplify with higher amplitudes, testing of that specific electrode should be discontinued and the next electrode should be engaged. Formal testing of disease-specific symptoms such as tremor, rigidity, and bradykinesia as well as evaluation for common side effects such as speech changes, facial spasms, and abnormalities in eye movements should be performed at every 0.5–1.0 V or mA change. Key region-specific elements of the examination will be discussed subsequently.

When the electrode is not implanted in the optimal trajectory, the degree of symptom benefits, side effects, or lack of clinical response aids in identifying the location of the electrode in space. The following sections will serve as a guide for the direction to move the electrode based on the side effects elicited. If an electrode position varies from the optimal target by a substantial amount (e.g., more than 3–4 mm), the presence or absence of stimulation-induced side effects may no longer hold relevance.

Ventral Intermediate Nucleus of the Thalamus

The ventral intermediate nucleus (ViM) is used for the treatment of medication refractory tremor disorders such as essential, parkinsonian, or dystonic tremor. It is a 4 × 4 × 6 mm nucleus that receives projections from the contralateral dentate nucleus of the cerebellum [5]. Posterior to the ViM is the ventral caudal nucleus (Vc) of the thalamus, the sensory relay system that receives fibers from the medial lemniscus. If microelectrode recordings (MER) are performed, typical thalamic firing patterns are heard along the trajectory and tremor cells are also identified along the track. Kinesthetic and tactile sensory responses are tested along the trajectory toward the target in order to ensure accurate placement during the MER portion of the evaluation which assist in distinguishing the ViM from Vc.

During awake testing, sensory paresthesias are commonly seen with stimulation of the ventral contacts, which are closer to Vc. These paresthesias may increase in intensity with amplitude titration and should be less intense or eliminated during testing of more proximal contacts. Additionally, tremors in the contralateral arm are expected to reduce with higher amplitudes of stimulation. At least 2–3 contacts should demonstrate marked reduction of tremors without causing side effects in a well-placed electrode. At low-amplitude thresholds (e.g., 2–3 V or 1.5–2 mA) for sensory paresthesias, speech changes and facial pulling indicate the need for alternate electrode positioning (Table 10.1).

Subthalamic Nucleus

The subthalamic nucleus (STN) is primarily targeted for the treatment of Parkinson's disease (PD); however, newer studies also support utilizing this target for the treatment of dystonia [6–8].

Table 10.1 Determination of lead location based on clinical response to stimulation: ventral intermediate nucleus of the thalamus

Direction from ViM	Structure(s) activated	Symptoms
Anterior	Voa	Minimal side effects, suboptimal tremor reduction seen at higher thresholds
Posterior	Vc	Sensory paresthesias (typically focal area)
Medial	Medial ViM, CM/Pf	Dysarthria
Lateral	Internal capsule	Facial contractions, dysarthria, and limb spasms at similar amplitude thresholds
Ventral	Vc, internal capsule	Sensory paresthesias and facial contractions, dysarthria, and limb spasms at low thresholds for ventral contacts higher thresholds for dorsal contacts

Voa ventral oralis anterior, *Vc* ventral caudal, *ViM* ventral intermediate, *CM/Pf* centromedian–perifascicular complex

Table 10.2 Determination of lead location based on clinical response to stimulation: subthalamic nucleus

Direction from STN	Structure(s) activated	Symptoms
Anterior	Internal capsule	Dysarthria, facial pulling, limb spasms
Posterior	Medial lemniscus	Sensory paresthesias (typically hemibody)
Medial	Oculomotor nerve, ventromedial STN (affective)	Diplopia and skew deviation of the ipsilateral eye, mood effects (depression, euphoria, inappropriate laughing)
Lateral	Internal capsule, frontal eye fields	Dysarthria, facial pulling, limb spasms, and conjugate gaze deviation
Ventral	Substantia nigra, internal capsule, frontal eye fields	Akinesia and mood changes, facial pulling, conjugate gaze deviation

STN subthalamic nucleus

The STN is an important nucleus within the indirect pathway of the basal ganglia that is located caudal to the thalamus. The sensorimotor area of the STN is the region of interest for stimulation in movement disorders which is identified by 4–5 mm length of characteristic STN firing on MER. Important structures near the STN are the substantia nigra located ventrally and the red nucleus located medially. Additionally, the frontal eye fields of the internal capsule and oculomotor nucleus are in close proximity to the STN and may be activated if the electrode is too lateral (Table 10.2). Awake testing of a well-placed electrode will result in reduction of parkinsonian symptoms with minimal to no side effects at high thresholds.

Globus Pallidus Internus

The posterolateral portion of the globus pallidus internus (GPi) is commonly targeted for the treatment of PD and dystonia. Dystonia is a heterogeneous disorder associated with both tonic and phasic muscle contractions that result in posturing and spasms of the affected body regions when engaged in activity. The majority of dystonia patients undergo DBS surgery under general anesthesia because of the difficulty with positioning the patient comfortably in the frame for extended periods of time. In those dystonia patients where surgery is being performed in the awake state, a reduction in phasic dystonia symptoms may be observed; however, the tonic dystonic posturing may remain unchanged in the operating room [9]. Thus, stimulation through the DBS electrode is primarily performed to identify the thresholds for side effects to ensure a reasonable therapeutic window for the electrode. Neurophysiologic recordings can identify regional anatomy to ensure appropriate location for implantation. The neurosurgeon will typically implant the electrode dorsal to the optic tract when targeting the posterolateral GPi. In the operating room, microstimulation through the MER electrode that induces phos-

Table 10.3 Determination of lead location based on clinical response to stimulation: globus pallidus internus

Direction from GPi	Structure(s) activated	Symptoms
Anterior	GPe, putamen	No effect or partial benefit to PD symptoms
Posterior	Internal capsule	Facial pulling or limb spasms
Medial	Internal capsule, medial GPi	Facial pulling or muscle contractions, feeling "strange"
Lateral	GPe, putamen	No effect or partial benefit to PD symptoms
Ventral	Optic tract	Phosphenes in contralateral visual field

GPi globus pallidus interna, *GPe* globus pallidus externa

phenes (a sparkle or flashing of lights) indicates that it is implanted too deeply (Table 10.3). In a well-placed electrode, one can expect to find an improvement of parkinsonian symptoms such as tremor, rigidity, and bradykinesia with minimal to no side effects at higher amplitudes; partial to complete reduction of phasic dystonic movements may also be observed in the awake patient.

Other Targets to Treat Neuropsychiatric Conditions with Deep Brain Stimulation

Aside from Parkinson's disease and tremor disorders, DBS is approved by the Food and Drug Administration in the United States for the management of obsessive compulsive disorder (OCD), though the stimulation target is quite different given the circuitry involved. There is also increasing interest in the use of DBS to treat Tourette syndrome (TS) and depression with multiple targets, which remain investigational treatments at this time (Table 10.4). Targeting methods for these structures vary between image-guided and neurophysiology-guided techniques, and as a consequence awake testing is not always used or described in published reports.

Table 10.4 Other neuropsychiatric conditions for DBS and usual or proposed targets

Disease State	Targets
Obsessive compulsive disorder (OCD)[a]	Nucleus accumbens Anterior limb of the internal capsule Ventral capsule/ventral striatum Bed nucleus of the stria terminalis/internal capsule Ventromedial STN
Tourette syndrome (TS)	Posteroventral GPi Anteromedial GPi CM–Pf thalamus[b]
Depression	Subcallosal cingulate gyrus Ventral capsule/ventral striatum Medial forebrain bundle

[a]OCD is the only psychiatric condition currently FDA-approved for treatment with DBS under a humanitarian device exemption (HDE)

[b]Centromedian–parafascicular complex of the thalamus

Obsessive Compulsive Disorder

The most consistent results of intraoperative stimulation effects relate to treatment for OCD. Targeting for this disorder has evolved over time from the original target in the anterior limb of the internal capsule (ALIC) to a more posterior position in the ventral caudate/ventral striatum (VC/VS) and more recently includes interest in the bed nucleus of the stria terminalis [10]. Clinically effective stimulation in this condition is often at higher pulse width (e.g., 210 usec) and amplitude (up to 8 V), and these are replicated in the operating room. Generally, 130 Hz is used during test stimulation. Stimulation that produces effective results is likely engaging white matter tracts in the ventral capsule, which may in turn beneficially interact with both cortical and subcortical structures of the network [10]. The more inferior contacts are likely to produce the best combination of efficacy and tolerability of stimulation, though higher amplitudes of current are more likely associated with psychiatric adverse effects. Otherwise, during test stimulation, transient muscle contractions, olfactory and gustatory sensations, hypomania, anxiety, and fear may be elicited [11]. A positive indicator of

future benefit is thought to be the induction of mirthful laughter, which may be indicative of a greater chance of a favorable outcome during chronic stimulation [12].

Tourette Syndrome

TS is a neuropsychiatric disorder characterized by the presence of motor and phonic tics and frequent psychiatric comorbidities including OCD and attention-deficit hyperactivity disorder. Multiple targets have been proposed in the treatment of this condition with DBS [13], but the largest experience is with the centromedian–parafascicular complex of the thalamus (CM–Pf), or the globus pallidus interna, both the anteromedial (limbic) and posteroventral (motor) regions. Although randomized clinical trials have been attempted [14–17], their success in blinded phases has not paralleled open label results of this treatment, possibly related to trial design [18]. Published reports offer limited information regarding awake testing protocols or findings.

Targeting of the posteroventral GPi and awake testing should follow what is routinely done for PD and dystonia in this target as described earlier in this chapter, though no formal reports in TS exist. Information regarding the potential for stimulation effects and risk of side effects during awake testing can therefore only be extrapolated from the results of chronic stimulation. In a retrospectively reviewed series of 9 TS patients treated with bilateral posteroventral GPi stimulation and followed for 0.5–10 years [19], we found that the most common stimulation-induced side effects included dysarthria ($n = 6$), dystonia ($n = 4$), bradykinesia ($n = 3$), and dyskinesia ($n = 3$).

In the largest randomized trials of DBS for TS, surgical procedures for stimulation in the anteromedial GPi by one group [16] were performed under general anesthesia, and so awake testing was not performed, while in the other [17], an awake procedure was performed but testing was not mentioned in the report. In these reports, stimulation has been reported to produce anxiety, dysarthria, dyskinetic limb movements, and hypomania, which each resolved with stimulation adjustment.

More detailed reports of awake testing have been provided for a series of TS patients treated with the thalamic target in open label treatment. In early reports of CM–Pf stimulation [20], awake testing was performed using successive amplitude titration at a frequency of 100 Hz and a pulse width of 200 usec. An intense feeling of fear during testing in one patient suggested a position that was too lateral and did not recur after electrode repositioning. Eye deviation occurred in a second patient, suggesting stimulation in the mesencephalon, and corrected after electrode repositioning to a more medial position. By contrast, appropriate electrode positioning was suggested by the occurrence of a pleasant feeling during test stimulation. Similarly, sensations of "well-being" were reported in another series of TS patients during awake testing in the thalamic target [21], which, when coupled with no or minimal side effects, suggested appropriate electrode positioning. Test stimulation was performed at a frequency of 100 Hz, a pulse width of 60 usec, and up to 5 mA of current in a set of 3-track recordings, and the permanent electrode track was chosen based on the results of this testing.

In another series of TS patients treated with CM–Pf stimulation [15], multiple-track microelectrode recording was followed by test stimulation at a frequency of 130 Hz, a pulse width of 60 usec, and up to 6 mA of current. Although the results of this testing guided final electrode positioning, further details are not provided. The authors do note, however, that visual disturbances were reported by some patients during chronic stimulation, the nature of which was not readily identifiable following detailed neuro-ophthalmological evaluation.

Treatment-Resistant Depression

While DBS for treatment-resistant depression remains an investigational indication, considerable interest remains in refining the best target and optimizing chances of a treatment response

[22]. Although several potential targets have emerged, randomized trials have only been performed for the subcallosal cingulate gyrus (SCG) and ventral capsule/ventral striatal (VC/VS) targets. In an initial study of the SCG [23], intraoperative monopolar stimulation was conducted in 6 patients at PW of 60 usec and frequency of 130 hz at each contact. Stimulation was titrated in 1.0 V increments every 30 seconds and acute effects were noted. These included improvements in mood, motor speed, and volume/rate of speech in all subjects and were reproducible. Side effects included lightheadedness and psychomotor slowing at very high voltages and more commonly at the higher stimulation contacts. No electrodes were repositioned, and these effects were used to guide outpatient stimulation settings. Four subjects achieved clinical improvement of depression.

The intraoperative test stimulation findings in the SCG were replicated in a larger study of 20 subjects [24], where acute effects of stimulation in the operating room at 3–6 V led to feelings of calmness, improved mood, and increased interest and motivation at the inferior contacts, while some patients experienced mental slowing at higher voltages (8–10 V) and more commonly when stimulating from the superior contacts. Some patients did not experience any behavioral effects during intraoperative testing and no electrodes were reported to be repositioned on the basis of intraoperative effects, lack of effects, or side effects, since targeting was based on radiographic planning. Intraoperative test results were used to guide outpatient stimulation parameters. In this study, the most distal contacts of the quadripolar DBS electrodes were targeted to be placed adjacent to the ventral bank of gray matter, such that the two central contacts were located within white matter, and the uppermost contacts were located adjacent to the upper bank of gray matter of the SCG. Targeting was achieved using direct visualization of the SCG on magnetic resonance imaging (MRI) and microelectrode recording to identify the gray and white matter regions. Ultimately, 60% of subjects were identified as responders to DBS and 35% achieved remission of depression at 6 months.

Later investigations indicated that the responder rate was improved by using a connectomic approach in targeting this region in which comparison of the postoperative probabilistic tractography map to the presurgical deterministic tractography map was used to identify the optimal contact for chronic stimulation [25]. In 11 subjects studied in this manner, intraoperative test stimulation was used as a confirmatory measure of electrode position and to establish preference in cases where two contacts had similar tractography maps. Methods were reapplied in nonresponders to determine if an alternate contact showed favorable tractography patterns. In this study, 9 of 11 (81.8%) subjects were eventually characterized as responders and 6 subjects achieved remission at 1 year.

The VC/VS region is highly interconnected via a dense collection of nuclei to the orbitofrontal cortex, reward pathways, thalamus, hypothalamus, and amygdala [26]. The goal of test stimulation in patients treated with VC/VS stimulation is to identify contacts that improve mood and anxiety symptoms without causing dose-limiting side effects. In one series [26], common observations during intraoperative awake testing included acute mood improvement, spontaneous smiling, reduced anxiety, and increased energy and awareness. Adverse effects of stimulation included tachycardia, increased anxiety, a sense of warmth/sweating, speech perseveration, and facial motor effects, all of which resolve with stimulation cessation or adjustment. During DBS procedures, if stimulation at least one contact led to subjective improvement and lack of adverse effects, the electrode positioning was felt to be adequate. In this series, lead position was altered in two patients on the basis of results of intraoperative testing.

The stereotactic targeting of the VC/VS intended to place the ventral contact at the ventral striatum and ventral anterior limb of the internal capsule (ALIC), while the more dorsal contacts would be positioned along the main axis of the ALIC. In a subset of bilaterally stimulated patients with adequate postoperative imaging ($n = 6$) and in whom a systematic contact evaluation was performed [27], the majority of improved

mood effects were noted with use of the inferior two contacts. The most inferior contact in the VS region was often accompanied by autonomic effects. The next more dorsal contact (also dorsal to the anterior commissure) was associated with improved mood, greater sense of energy and alertness, laughing, calmness, and talkative behavior without much autonomic effect. The combined concordance between intraoperative stimulation and postoperative programming results was 89% in this series. Minor facial motor and nonspecific sensory adverse effects of stimulation were noted along the trajectory of the ALIC. Stimulation parameters were 90 usec and 130 Hz, and stimulation was titrated in 1–2 V increments in monopolar configurations. Bipolar configurations were tested with a pulse width of 120 usec.

Lastly, two small series of stimulation of the medial forebrain bundle [28, 29] for medication-refractory depression describe the utility of intraoperative testing to confirm adequate electrode positioning. Surrounding structures include the red nucleus, subthalamic nucleus, and mammillary bodies. Monopolar test stimulations from the macroelectrode tip at parameters of 60 usec and 130 Hz were used, while amplitudes were titrated to 2–3 V to determine mood effects and presence of double vision [30]. Three groups of symptoms were appreciated: appetitive motivation (head movement toward the examiner with initiation of visual and social contact), autonomic effects (increased heart rate by about 10 beats/minute), and double or blurred vision due to co-activation of oculomotor pathways. If the oculomotor effects were noted at a low threshold, the electrode position was changed.

Together, the use of awake testing in OCD, TS, and depression can inform clinical decision-making regarding final electrode positioning and in some cases predicting treatment response. In other cases, awake testing does not correlate with individual outcomes and may be more useful to serve as confirmation that electrodes can be titrated in the outpatient settings to clinically relevant parameters.

High-Frequency Ultrasound for the Treatment of Movement Disorders

MRI-guided focused ultrasound (MRgFUS) is a novel approach to movement disorders surgery as a minimally invasive ablative method to target areas of interest. Thus far, the Vim has been studied for tremor control but theoretically this technique may be applied to the GPi and other brain areas previously targeted by traditional lesional approaches such as gamma knife or radiofrequency surgery [31, 32].

The procedure occurs in an interventional radiology suite. A stereotactic frame and elastic water-filled diaphragm are affixed to a fully shaved scalp. A pre-procedure 3 T-MRI is acquired for surgical planning, after which serial sonications are delivered by a transducer with incremental increases in energy, while MRI thermometry monitors tissue temperature to avoid bleeding and cavitation caused by excessive heating. The awake patient undergoes repeated clinical testing during the procedure to identify therapeutic benefits and side effects by disruption of the targeted tissue after which a small lesion is made. Testing for tremor reduction and side effects is similar to the evaluations described in the ViM section for DBS electrode surgery.

Epilepsy

Approximately 30% of patients with epilepsy will have intractable epilepsy, practically defined as a failure of two appropriately chosen and dosed anti-seizure medications [33]. It is statistically unlikely that any new medication trial will offer sustained seizure freedom, and as such patients are generally recommended to undergo evaluation for more invasive options including resective surgery, deep brain stimulation (DBS), responsive neurostimulation (RNS), or vagus nerve stimulation (VNS). Surgical candidacy is assessed utilizing a series of noninvasive studies with the goal being identification of epileptogenic cortex but also assessment of eloquent cortex that should not

be resected. The following sections outline the extent of awake testing in the evaluation of epilepsy patients. In contrast to awake testing during DBS surgeries which are conducted intraoperatively to assess for appropriate therapeutic benefit, these evaluations are conducted prior to the epilepsy surgery itself in order to confirm a patient's candidacy for surgical treatment.

Epileptogenic Cortex Identification

Magnetic Resonance Imaging (MRI)

The standard presurgical epilepsy workup includes an MRI scan of the brain with thin cut slices that are oriented perpendicular to the axis of the hippocampus. Improvements in magnet strength and epilepsy protocol scans have led to improvements in detection rates with rates increasing by 2.5 times with use of a 3 T magnet MRI as compared to a 1.5 T magnet, particularly for subtle pathologies such as heterotopias, focal cortical dysplasia, and hippocampal sclerosis [34, 35].

Epilepsy Monitoring Unit (EMU)

Video EEG monitoring is performed to capture habitual events and to confirm the diagnosis of epilepsy. This is typically performed as an inpatient study under 24-hour supervision to safely wean medications, efficiently capture seizures, and test the patient during the event [36].

Positron Emission Tomography (PET)

Hypometabolism seen on a fluorodeoxyglucose (FDG) positron emission tomography (PET) scan has been postulated to effectively localize the seizure focus or foci. In cases of temporal lobe epilepsy managed surgically, findings of unilateral hypometabolism by PET even in the absence of an MRI abnormality was associated with seizure freedom rates approaching cases of mesial temporal sclerosis, even without additional invasive EEG monitoring [37]. In patients with focal cortical dysplasia, co-registration of PET and MRI findings may help identify subtle areas of focal cortical dysplasia not seen on visual analysis of MRI alone [38].

Single-Photon Emission Computed Tomography (SPECT)

Perfusion studies with injection of radionucleotide tracers obtained in the ictal and interictal states have shown to be helpful in the identification of epileptic foci. Current standard of care involves the utilization of subtraction ictal single-photon emission computed tomography (SPECT) co-registered to MRI (SISCOM) which if localized to the surgical site has a 62.5% chance of seizure freedom compared to 20% if the results are discordant with the surgical site [39]. This procedure is highly dependent on early recognition of a seizure and prompt injection of the radionucleotide, with late injections (greater than 45 seconds after seizure onset) shown to have a higher likelihood of nonlocalizing or equivocal results (47.6% to 10%) [40]. More recently, statistical parametric mapping (SPM) has been validated as a technique to determine the statistical significance of perfusion changes in epilepsy patients by comparing the changes to a control group without epilepsy. In 49 cases of refractory focal epilepsy with normal MRIs, the SPM-processed SPECT scans detected hyperperfusion concordant with the surgical resection site 67% of the time compared to 38% when using SISCOM [41, 42].

Magnetoencephalography (MEG)

MEG is a neurophysiological test measuring magnetic fields generated by the human brain. Magnetic fields have less distortion from the resistive properties of the skull and scalp and provide superior resolution than scalp EEG [43]. Furthermore, MEG systems typically utilize several hundred channels of recording, offering a higher spatial resolution. However, the magnetic fields generated by the brain are very weak and there is a very low signal-to-noise ratio. As a result, sophisticated technology is utilized to amplify the signal and testing must occur in a magnetically shielded room. These requirements make the MEG machine expensive and difficult to maintain, limiting its widespread availability. In patients with refractory epilepsy who undergo surgical intervention, however, having a well-defined cluster of MEG

spikes is shown to be a predictor of seizure freedom [44]. Conversely, incomplete resection of tissue associated with a cluster of MEG spikes in the targeted area is associated with a worse postsurgical outcome [44].

Eloquent Cortex Identification

Functional MRI (fMRI)

Functional MRI is based on use of blood-oxygen-level-dependent (BOLD) contrast imaging, measuring hemodynamic changes in activated areas relative to inactivated areas. This has been shown to be an effective localizing tool for identifying central sulcus and visual cortex when compared to extraoperative cortical stimulation [45]. This has been also showed as a useful tool in lateralizing language activity and has largely replaced Wada as the testing of choice to lateralize language function [46].

Wada Testing

The Wada test (intracarotid amobarbital procedure) utilizes a cerebral angiogram and administration of a barbiturate via an intra-arterial catheter which temporarily impairs function on the side of the injection. This test is performed with the patient awake with language and memory testing performed during the procedure to assess medication effect. Despite the invasiveness of the procedure and the potential risks of an angiogram, it remains the gold standard for memory lateralization prior to resective temporal lobe surgery [47].

Magnetoencephalography (MEG)

In addition to identifying epileptic foci, MEG has been shown to be effective in mapping critical functional cortex. Hand motor responses obtained by MEG and fMRI were shown to be within 10 mm of each other [48]. Similarly, stimulus-evoked responses in the visual auditory or somatosensory cortices can be generated through signal averaging of several trials [48]. MEG can also identify language cortices, although this requires additional modeling and processing in contrast to fMRI which directly measures hemodynamic responses from activated cortex. Even with this, MEG has been shown to be concordant to Wada testing across series on average 70–80% of the time [49].

Phase II Evaluations

Phase II evaluations are performed when noninvasive testing does not provide a clear treatment path. In some cases, a patient's epilepsy surgery evaluation will require intracranial EEG sampling as a necessary diagnostic step before discussing surgical treatment options. Traditional invasive epilepsy surgery evaluations in the United States have been performed with the placement of subdural grids and strips to identify epileptogenic cortex and to define boundaries of functional tissue. However, these electrodes require a craniotomy, posing an increased risk of morbidity and mortality [50]. Stereotactic depth electrodes strategically placed to understand onset and evolution of the patient's seizures have been employed in selected centers across Europe for decades (stereo-encephalography [SEEG]) and have found increasing interest in the United States. Multiple electrodes are placed deep within the substance of the brain through burr holes. This offers the advantage of being a minimally invasive approach while allowing greater precision and extent of coverage including the possibility of bilateral electrode placement. Furthermore, these electrodes enable the identification of deep epileptogenic foci that were previously difficult to identify with subdural electrodes including the insula and cingulate cortices [51].

Phase II Planning

Traditional synthesis of preoperative testing in the workup for epilepsy surgery involves patient management conferences where individual tests are discussed and the epilepsy management team comes to a consensus on type of surgery to perform and the need for phase II coverage. Discussions of intracranial coverage and schemes involve cartoon maps depicted in 2D space.

With increased utilization of SEEG, there is a greater technical requirement. Electrode trajectories must now be visualized and planned in 3D space in order to appropriately target important regions of the brain as well as to avoid injuries secondary to SEEG electrodes. Vessel imaging is now routinely performed through CT angiography or double-contrast MRI without need for cerebral angiography in order to ensure safe placement of SEEG electrodes to avoid traversing vessels.

The benefits of SEEG are further enhanced with the use of recent technologic advances. Planning software allows the treating clinicians to plan depth electrode trajectories in advance using the patient's preoperative MRI scans. Robotic assist devices allow expedited placement of electrodes without the need for stereotactic frames.

The current state of SEEG allows for a robust ability to engage the epileptogenic targets and downstream network hubs. Utilizing clinical semiology and expected propagation of clinical symptoms along epileptogenic networks, functional data, neurophysiologic data, and structural imaging, clinicians can develop an implantation scheme sampling from several of these regions. Software incorporating multimodal co-registration of relevant neurophysiologic, functional, and imaging data including MEG, EEG–fMRI, SISCOM, and other neurophysiologic studies allows tailored planning for depth electrode placement [52].

Resection

Select patients who have readily identifiable epileptogenic networks that do not overlap with eloquent cortex may be candidates for resective surgery. Frequently, prior functional and epileptogenic cortex testing is compiled to devise a resection scheme which can be performed while the patient is asleep. However, in select cases, there is sufficient concern about eloquent cortex in close proximity to the proposed resection. In such cases, direct cortical stimulation is applied while the patient is awake and performing customized tasks to identify eloquent language, motor, speech, or visual cortex, so-called awake craniotomies. In the adult population, resection of tumors near eloquent cortex, particularly the perirolandic cortex, have been shown to be more cost-effective with better immediate and late neurologic outcomes when performed under awake mapping conditions [53].

Summary

The utilization of intraoperative testing for the implantation of DBS electrodes is well established in the treatment of movement disorders targets. This layer of testing is a useful tool in the operating room which provides real-time verification of the symptomatic benefits from stimulation and spatial resolution to assist the neurosurgeon with electrode repositioning should the patient experience excessive side effects or suboptimal therapeutic response from the initial electrode tract.

When neuropsychiatric disorders such as OCD, depression, and TS are being treated with DBS, intraoperative testing can verify appropriate electrode positioning if acute beneficial effects are noted, confirm usability of electrodes at clinically relevant settings, or indicate presence of side effects that may warrant electrode repositioning. In select cases, intraoperative testing results may predict long-term outcome. For patients with intractable epilepsy, presurgical testing as part of an evaluation for epilepsy surgery is necessary to better delineate the extent of epileptogenic cortex and to identify eloquent cortex that should not be included in any resection. Recent advances in technology allow for a greater ability to integrate this information in surgical planning and any possible resection. In cases where there is a concern for a resection that may encroach upon eloquent cortex, an awake craniotomy with direct cortical stimulation can be performed as a means to preserve neurologic function.

References

1. Youngerman BE, Chan AK, Mikell CB, McKhann GM, Sheth SA. A decade of emerging indications: deep brain stimulation in the United States. J Neurosurg. 2016;125(2):461–71.
2. Lee PS, Weiner GM, Corson D, Kappel J, Chang YF, Suski VR, et al. Outcomes of interventional-MRI versus microelectrode recording-guided subthalamic deep brain stimulation. Front Neurol. 2018;9:241.
3. Park SC, Lee CS, Kim SM, Choi EJ, Lee JK. Comparison of the stereotactic accuracies of function-guided deep brain stimulation, calculated using multitrack target locations geometrically inferred from three-dimensional trajectory rotations, and of magnetic resonance imaging-guided deep brain stimulation and outcomes. World Neurosurg. 2017;98:734–49. e7
4. Brodsky MA, Anderson S, Murchison C, Seier M, Wilhelm J, Vederman A, et al. Clinical outcomes of asleep vs awake deep brain stimulation for Parkinson disease. Neurology. 2017;89(19):1944–50.
5. Sammartino F, Krishna V, King NK, Lozano AM, Schwartz ML, Huang Y, et al. Tractography-based ventral intermediate nucleus targeting: novel methodology and intraoperative validation. Mov Disord. 2016;31(8):1217–25.
6. Yao C, Horn A, Li N, Lu Y, Fu Z, Wang N, et al. Postoperative electrode location and clinical efficacy of subthalamic nucleus deep brain stimulation in Meige syndrome. Parkinsonism Relat Disord. 2019;58:40–5.
7. Deng Z, Pan Y, Zhang C, Zhang J, Qiu X, Zhan S, et al. Subthalamic deep brain stimulation in patients with primary dystonia: a ten-year follow-up study. Parkinsonism Relat Disord. 2018;55:103–10.
8. Ostrem JL, San Luciano M, Dodenhoff KA, Ziman N, Markun LC, Racine CA, et al. Subthalamic nucleus deep brain stimulation in isolated dystonia: a 3-year follow-up study. Neurology. 2017;88(1):25–35.
9. Ruge D, Tisch S, Hariz MI, Zrinzo L, Bhatia KP, Quinn NP, et al. Deep brain stimulation effects in dystonia: time course of electrophysiological changes in early treatment. Mov Disord. 2011;26(10):1913–21.
10. Karas PJ, Lee S, Jimenez-Shahed J, Goodman WK, Viswanathan A, Sheth SA. Deep brain stimulation for obsessive compulsive disorder: evolution of surgical stimulation target parallels changing model of dysfunctional brain circuits. Front Neurosci. 2018;12:998.
11. Morishita T, Fayad SM, Goodman WK, Foote KD, Chen D, Peace DA, et al. Surgical neuroanatomy and programming in deep brain stimulation for obsessive compulsive disorder. Neuromodulation. 2014;17(4):312–9; discussion 9.
12. Haq IU, Foote KD, Goodman WG, Wu SS, Sudhyadhom A, Ricciuti N, et al. Smile and laughter induction and intraoperative predictors of response to deep brain stimulation for obsessive-compulsive disorder. NeuroImage. 2011;54 Suppl 1:S247–55.
13. Viswanathan A, Jimenez-Shahed J, Baizabal Carvallo JF, Jankovic J. Deep brain stimulation for Tourette syndrome: target selection. Stereotact Funct Neurosurg. 2012;90(4):213–24.
14. Maciunas RJ, Maddux BN, Riley DE, Whitney CM, Schoenberg MR, Ogrocki PJ, et al. Prospective randomized double-blind trial of bilateral thalamic deep brain stimulation in adults with Tourette syndrome. J Neurosurg. 2007;107(5):1004–14.
15. Ackermans L, Duits A, van der Linden C, Tijssen M, Schruers K, Temel Y, et al. Double-blind clinical trial of thalamic stimulation in patients with Tourette syndrome. Brain. 2011;134(Pt 3):832–44.
16. Kefalopoulou Z, Zrinzo L, Jahanshahi M, Candelario J, Milabo C, Beigi M, et al. Bilateral globus pallidus stimulation for severe Tourette's syndrome: a double-blind, randomised crossover trial. Lancet Neurol. 2015;14(6):595–605.
17. Welter ML, Houeto JL, Thobois S, Bataille B, Guenot M, Worbe Y, et al. Anterior pallidal deep brain stimulation for Tourette's syndrome: a randomised, double-blind, controlled trial. Lancet Neurol. 2017;16(8):610–9.
18. Jimenez-Shahed J. Design challenges for stimulation trials of Tourette's syndrome. Lancet Neurol. 2015;14(6):563–5.
19. Niemann N, Strutt A, Viswanathan A, Jimenez Shahed J. Safety profile of unblinded internal pllidal deep bain stimulation for medically refractory Tourette syndrome (P1.045). Neurology. 2016;86(16 Supplement):P1.045.
20. Visser-Vandewalle V, Temel Y, Boon P, Vreeling F, Colle H, Hoogland G, et al. Chronic bilateral thalamic stimulation: a new therapeutic approach in intractable Tourette syndrome. Report of three cases. J Neurosurg. 2003;99(6):1094–100.
21. Servello D, Porta M, Sassi M, Brambilla A, Robertson MM. Deep brain stimulation in 18 patients with severe Gilles de la Tourette syndrome refractory to treatment: the surgery and stimulation. J Neurol Neurosurg Psychiatry. 2008;79(2):136–42.
22. Drobisz D, Damborska A. Deep brain stimulation targets for treating depression. Behav Brain Res. 2019;359:266–73.
23. Mayberg HS, Lozano AM, Voon V, McNeely HE, Seminowicz D, Hamani C, et al. Deep brain stimulation for treatment-resistant depression. Neuron. 2005;45(5):651–60.
24. Lozano AM, Mayberg HS, Giacobbe P, Hamani C, Craddock RC, Kennedy SH. Subcallosal cingulate gyrus deep brain stimulation for treatment-resistant depression. Biol Psychiatry. 2008;64(6):461–7.
25. Riva-Posse P, Choi KS, Holtzheimer PE, Crowell AL, Garlow SJ, Rajendra JK, et al. A connectomic approach for subcallosal cingulate deep brain stimulation surgery: prospective targeting in treatment-resistant depression. Mol Psychiatry. 2018;23(4):843–9.
26. Malone DA Jr, Dougherty DD, Rezai AR, Carpenter LL, Friehs GM, Eskandar EN, et al. Deep brain stimulation of the ventral capsule/ventral striatum

for treatment-resistant depression. Biol Psychiatry. 2009;65(4):267–75.
27. Machado A, Haber S, Sears N, Greenberg B, Malone D, Rezai A. Functional topography of the ventral striatum and anterior limb of the internal capsule determined by electrical stimulation of awake patients. Clin Neurophysiol. 2009;120(11):1941–8.
28. Schlaepfer TE, Bewernick BH, Kayser S, Madler B, Coenen VA. Rapid effects of deep brain stimulation for treatment-resistant major depression. Biol Psychiatry. 2013;73(12):1204–12.
29. Fenoy AJ, Schulz P, Selvaraj S, Burrows C, Spiker D, Cao B, et al. Deep brain stimulation of the medial forebrain bundle: distinctive responses in resistant depression. J Affect Disord. 2016;203:143–51.
30. Schlaepfer TE, Bewernick BH. Deep brain stimulation for major depression. Handb Clin Neurol. 2013;116:235–43.
31. Elias WJ, Lipsman N, Ondo WG, Ghanouni P, Kim YG, Lee W, et al. A randomized trial of focused ultrasound thalamotomy for essential tremor. N Engl J Med. 2016;375(8):730–9.
32. Schlesinger I, Sinai A, Zaaroor M. MRI-guided focused ultrasound in Parkinson's disease: a review. Parkinsons Dis. 2017;2017:8124624.
33. Kwan P, Arzimanoglou A, Berg AT, Brodie MJ, Allen Hauser W, Mathern G, et al. Definition of drug resistant epilepsy: consensus proposal by the ad hoc Task Force of the ILAE Commission on Therapeutic Strategies. Epilepsia. 2010;51(6):1069–77.
34. Ho K, Lawn N, Bynevelt M, Lee J, Dunne J. Neuroimaging of first-ever seizure: contribution of MRI if CT is normal. Neurol Clin Pract. 2013;3(5):398–403.
35. Von Oertzen J, Urbach H, Jungbluth S, Kurthen M, Reuber M, Fernandez G, et al. Standard magnetic resonance imaging is inadequate for patients with refractory focal epilepsy. J Neurol Neurosurg Psychiatry. 2002;73(6):643–7.
36. Shih JJ, Fountain NB, Herman ST, Bagic A, Lado F, Arnold S, et al. Indications and methodology for video-electroencephalographic studies in the epilepsy monitoring unit. Epilepsia. 2018;59(1):27–36.
37. LoPinto-Khoury C, Sperling MR, Skidmore C, Nei M, Evans J, Sharan A, et al. Surgical outcome in PET-positive, MRI-negative patients with temporal lobe epilepsy. Epilepsia. 2012;53(2):342–8.
38. Salamon N, Kung J, Shaw SJ, Koo J, Koh S, Wu JY, et al. FDG-PET/MRI coregistration improves detection of cortical dysplasia in patients with epilepsy. Neurology. 2008;71(20):1594–601.
39. von Oertzen TJ, Mormann F, Urbach H, Reichmann K, Koenig R, Clusmann H, et al. Prospective use of subtraction ictal SPECT coregistered to MRI (SISCOM) in presurgical evaluation of epilepsy. Epilepsia. 2011;52(12):2239–48.
40. Matsuda H, Matsuda K, Nakamura F, Kameyama S, Masuda H, Otsuki T, et al. Contribution of subtraction ictal SPECT coregistered to MRI to epilepsy surgery: a multicenter study. Ann Nucl Med. 2009;23(3):283–91.
41. McNally KA, Paige AL, Varghese G, Zhang H, Novotny EJ Jr, Spencer SS, et al. Localizing value of ictal-interictal SPECT analyzed by SPM (ISAS). Epilepsia. 2005;46(9):1450–64.
42. Sulc V, Stykel S, Hanson DP, Brinkmann BH, Jones DT, Holmes DR 3rd, et al. Statistical SPECT processing in MRI-negative epilepsy surgery. Neurology. 2014;82(11):932–9.
43. Kharkar S, Knowlton R. Magnetoencephalography in the presurgical evaluation of epilepsy. Epilepsy Behav. 2015;46:19–26.
44. Almubarak S, Alexopoulos A, Von-Podewils F, Wang ZI, Kakisaka Y, Mosher JC, et al. The correlation of magnetoencephalography to intracranial EEG in localizing the epileptogenic zone: a study of the surgical resection outcome. Epilepsy Res. 2014;108(9):1581–90.
45. Beers CA, Federico P. Functional MRI applications in epilepsy surgery. Can J Neurol Sci. 2012;39(3):271–85.
46. Szaflarski JP, Gloss D, Binder JR, Gaillard WD, Golby AJ, Holland SK, et al. Practice guideline summary: use of fMRI in the presurgical evaluation of patients with epilepsy: report of the Guideline Development, Dissemination, and Implementation Subcommittee of the American Academy of Neurology. Neurology. 2017;88(4):395–402.
47. Mansouri A, Fallah A, Valiante TA. Determining surgical candidacy in temporal lobe epilepsy. Epilepsy Res Treat. 2012;2012:706917.
48. Burgess RC, Funke ME, Bowyer SM, Lewine JD, Kirsch HE, Bagic AI, et al. American Clinical Magnetoencephalography Society Clinical Practice Guideline 2: presurgical functional brain mapping using magnetic evoked fields. J Clin Neurophysiol. 2011;28(4):355–61.
49. Papanicolaou AC, Simos PG, Castillo EM, Breier JI, Sarkari S, Pataraia E, et al. Magnetocephalography: a noninvasive alternative to the Wada procedure. J Neurosurg. 2004;100(5):867–76.
50. Wellmer J, von der Groeben F, Klarmann U, Weber C, Elger CE, Urbach H, et al. Risks and benefits of invasive epilepsy surgery workup with implanted subdural and depth electrodes. Epilepsia. 2012;53(8):1322–32.
51. Gonzalez-Martinez JA. The stereo-electroencephalography: the epileptogenic zone. J Clin Neurophysiol. 2016;33(6):522–9.
52. Duncan JS, Winston GP, Koepp MJ, Ourselin S. Brain imaging in the assessment for epilepsy surgery. Lancet Neurol. 2016;15(4):420–33.
53. Taylor MD, Bernstein M. Awake craniotomy with brain mapping as the routine surgical approach to treating patients with supratentorial intraaxial tumors: a prospective trial of 200 cases. J Neurosurg. 1999;90(1):35–41.

11 Cloud-Based Stereotactic and Functional Neurosurgery and Registries

Pierre-François D'Haese

Our healthcare system continually evolves, with three significant forces at work: advancing the quality of care, managing the cost of care, and enhancing engagement and patient relationship. Those forces are transforming healthcare into an "information-driven," "evidence-based," and "outcome-driven" model. Healthcare has experienced a decade of digitizing medical records and aggregating years of research and development data in electronic databases. Following this trend, clinicians and researchers have gathered information about people with certain conditions, both individually and as groups, and over time, to increase our understanding of that condition. Clinical registries have provided information to healthcare professionals to improve the quality and safety of the care they provide to their patients. For example, the use of evidence-based practice guidelines can be evaluated by asking questions like, "How many patients are receiving recommended treatment(s)?" In addition, information from clinical data registries is used to compare the effectiveness of different treatments for the same disease or condition, to evaluate different approaches to a procedure, and to monitor the safety of implanted devices. The information from clinical data registries is also used to support healthcare education, accreditation, and certification. Finally, information from clinical data registries is increasingly used to ensure that payment is adjusted based on the quality of care provided and to give patients the information they need to make better choices.

The primary challenge of any registry remains its sole purpose: gathering meaningful data. A clinical data registry begins by defining a patient population and then recruits healthcare professionals who will submit data on a representative sample of these patients. As data enters the clinical data registry, quality checks are performed to ensure the correctness and completeness of the data. If something is missing or outside of the expected range, the registry staff contacts the submitting healthcare professionals and asks them to review and verify the data. Many registry leaders are overburdened by the challenges that persist when structuring, accessing, standardizing, and managing clinical data between multiple centers within a budget.

Moreover, the sensitivity of data privacy and ownership adds to the challenges of a successful registry. Government agencies have strict privacy requirements set by law such as the Federal Information Security Management Act (FISMA) and the Health Insurance Portability and Accountability Act (HIPAA). Ultimately, gathering data from the clinical flow and sharing it in a de-identified way with a registry has been slow, inefficient, and costly. While registries are by default research initiatives, clinical data is stored

P.-F. D'Haese (✉)
Department of Electrical Engineering and Computer Science, Vanderbilt University, Nashville, TN, USA
e-mail: pf.dhaese@vanderbilt.edu

N. Pouratian, S. A. Sheth (eds.), *Stereotactic and Functional Neurosurgery*,
https://doi.org/10.1007/978-3-030-34906-6_11

in each environment in the electronic medical records (EMRs), a centralized electronic system that archives evidence of care for each patient.

There is evidence of pharmaceutical and some life science companies that have been able to create value by extracting data from EMR systems. For instance, Flatiron, Inc., a Google-funded, New York-based company, has set up a model to extract from EMR patient diagnoses, medications, and their effect on treating a patient's cancer. Flatiron connects a large number of medical centers to harvest data on a large number of patients. Its analysts can mine the data to see what treatments are most useful for particular conditions, identify patterns, and gain knowledge to improve patient care and reduce costs. The industry could indeed benefit from connecting with the clinical flow through EMRs. The conclusion is not so clear for registries. Research and clinical systems are kept in two very distinct siloes for obvious privacy and data ownership reasons. These are not only separated by different IT systems and management teams but by completely different privacy and legal units which makes it extremely difficult to "plug into" a set of EMR systems and exploit the data for population-based analyses. In addition, while it is true that EMR data is exploitable for learning how medications affect patients suffering from cancer, the data involved in treating disorders of the central nervous system (CNS) (e.g., Parkinson disease, Alzheimer's disease, epilepsy, or depression) is less standardized and not usually stored in electronic medical records in an easily usable way across medical centers.

According to the World Health Organization, if left unchecked, 15 years from now, more than 12 million Americans will suffer from neurological diseases. The necessity of finding treatments for neurodegenerative diseases is thus increasing. Neurodegenerative diseases require solutions that involve a broad range of expertise encompassing such different fields as neurology, genetics, brain imaging, drug discovery, electrophysiology, stereotactic neurosurgery, and computer science, all of which generate large datasets related to small targets within the brain. Neuromodulation has emerged as a restorative therapy to treat neurological conditions such as Parkinson disease. As a result of pioneering work by Drs. Benabid and DeLong, deep brain stimulation (DBS) is now a primary surgical technique that reduces tremors and manages motor symptoms in patients with advanced Parkinson disease, dystonia, or essential tremor and shows promise in the treatment of depression or obsessive compulsive disorder. Much of the future potential in precisely focused therapy such as DBS or MR-guided focused ultrasound relies on understanding the exact location of delivered therapy and its impact on circuitry with a millimetric (or even submillimetric) level of precision. DBS is one of the only minimally invasive therapies that allow for the capture of complex data and relate it to an accurate location inside the patient's brain. Recordings during DBS implantation provide access to single neuron activity as well as local field potentials and electrocorticography, in research settings. No other therapy provides such exceptional access to data. Deep brain stimulation is, therefore, a chance for the clinical research community to study electrophysiological brain mechanisms. However, time for intraoperative data collection is limited necessitating aggregation of data from a population of patients. Precise co-localization of population data for DBS therapy can have an enormous impact on our ability to create models and accurately study DBS mechanisms. The variation in human brain anatomy is large enough that a simple aggregation of data without accurate co-representation within a common space leads to vague generalizations and comparisons of treatment modalities and diagnostic capabilities [1].

Responding to the need to collect and share data, a number of research tools have been developed to support registries. In 2003, Neurotargeting created a collaborative system called CranialVault [1–4] which focuses on DBS; in 2005, Marcus et al. [5] offered to the community the XNAT system which has a primary objective of supporting the sharing of clinical images and associated data. This is a goal shared by other successful initiatives such as NiDB [6], LORIS [7], and COINS [8]. The Alzheimer's Disease Neuroimaging Initiative (ADNI) unites researchers with study

data as they work to define the progression of Alzheimer's disease [9]; Ascoli et al. [10, 11] focus on sharing cell data, Kotter [12] on cortical connectivity, and Van Horn on fMRI [13], to give only a few examples. Another example is the Collaborative Research in Computational Neuroscience (CRCNS) program funded by the US National Institutes of Health (NIH) and National Science Foundation which focuses on supporting data sharing. The CRCNS provides a resource for sharing a wide variety of experimental data that are publicly available [14]. In parallel, tools to support structured heterogeneous data acquisition within or across institutions have been developed such as the REDCap [15] system which can claim more than 100,000 projects with over 150,000 users spanning numerous research focus areas across the REDCap consortium.

Historically, registries have been organized by governmental entities or associated with professional societies or the research community, facilitated by systems like REDCap or XNat or through a Data Coordinating Center.

The complexity and heterogeneous nature of the data acquired during neuromodulation procedures have been the main reasons for the difficulty in creating large-scale registries and have limited the global adoption of existing ones. A system that can store and share data efficiently should be able to connect imaging datasets to electrophysiological neuronal signals, patients' responses to stimulation, disease progression and follow-up scores, the amount of medication taken by patients, neuromodulation parameters, and quality of life measures and clinical care. The absence of widespread standards for data acquisition and processing further complicates the task.

Over the last 15 years at Vanderbilt University, our team has studied solutions that could circumvent these challenges while using modern technologies. The rest of this chapter discusses in detail the challenges associated with capitalizing on big data for neuromodulation based on our experiences over the years and through multiple iterations of conception and refinement of a system that is called CranialCloud. The associated research was performed at Vanderbilt University, directed by Dr. Benoit Dawant, PhD, Dr. Pierre-Francois D'Haese, PhD, and Dr. Peter E Konrad, MD, PhD, and funded by 3 R01 (2R01-EB006136 and 9R01-NS095291). The underlying technology was translated to a newly formed company called Neurotargeting using NIH phase I and II STTR funding (R41NS063705, 9R42MH100007). The company's role was to create an independent, legal, and commercial framework for such a solution to be sustainable across institutions. Forming a company was crucial in order to handle the regulatory and privacy requirements related to a system that would collect data from the clinical flow. While this chapter is not intended to promote any concept related to Neurotargeting, some of the following discussion will mention Vanderbilt University and Neurotargeting's data framework, CranialCloud.

Ideally, a registry should provide a patient-centric system, integrated into the clinical flow, that would combine continuous data acquisition during the whole extent of care of the patient with the collection of data from advanced and sometimes homemade research protocols. We envisioned a system that would work as easily as Dropbox but as securely as a vault for storing valuable patient data. This system would allow clinicians and researchers to not only cross the boundaries of interdisciplinary collaborations but also enable researchers to create a collaborative network without breaching any legal aspects, would be able to interconnect with existing devices and data acquisition systems as well as with other existing archives, would allow experts in data analytics to plug-in for expert analyses, would enable research while considering ethical implications, and could validate and disseminate technology once developed.

Creating an SQL-based structure [2, 4] was the clearest starting point, allowing storage for any deep brain stimulation-related data, connection to clinical tools to accumulate data without disrupting the clinical flow, and integration of a processing pipeline used to normalize [4] the data collected from each patient into a standard reference system called the atlas. Most systems are currently developed as centralized archives with virtual private databases in which data from any partnering group can be stored. In its original

iteration, the CranialVault system centralized data at Vanderbilt University. This type of architecture allows easier management and sharing of data across groups, but difficulties arise concerning data ownership, cross-institutional data sharing (such as receiving multiple Institutional Review Board (IRB) approvals for sharing data across universities), and the stability of a resource that is largely sustained by investor-initiated federal grants. The common alternative is to use a set of individual databases connected between each other, known as a distributed database. While used often in the industry, this system also has its drawbacks. It necessitates both local and global management teams operating on one system. The local servers must be maintained while the global team is responsible for managing the interconnection between groups. With the adoption of modern technologies in healthcare, a third alternative has come to light: cloud-based solutions, consisting of a set of interconnected nodes hosted in the cloud, with each institution or group owning its own account.

The following are essential components to fulfill the necessities of a robust, HIPAA-compliant cloud-based archive for neuromodulation data. Incorporated in the reasoning are the pitfalls that can produce a suboptimal design.

- Patient-centric and PHI
- Integration with clinical workflow
- Assuring data quality and completeness
- Integration of spatial and temporal data
- Ready for sensing and clinical surveillance data
- Respecting the privacy and ethical implications of neuroscience research
- Security from the ground up
- Fostering data sharing
- Data normalization
- Custom patient-based medicine

Patient-Centric and PHI

Due to the legal and security requirements, several archives have decided to ban protected health information (PHI) from their system. Avoiding PHI altogether allows for simpler data management, storage, and transfer without the security burden required to satisfy the Office for Civil Rights (OCR) and HIPPA regulations in US policy. However, operating in a fully anonymized setting becomes a limitation when working with longitudinal datasets from patients or subjects that are observed for an extensive period of time. Furthermore, an anonymized system does not integrate easily into the clinical flow. When data is completely de-identified, significant clinical features included in the PHI restricts the ability to trace data from a given patient over a long time or in complex clinical environments. While longitudinal studies are performed with de-identified patients, the study must be designed accordingly to track patients in time.

Integration with Clinical Workflow

For archives that focus on large and complex datasets, such as the one involved in the BRAIN Initiative, ease-of-use and automated, non-disruptive data acquisition are essential. It is crucial for the archive to be integrated with the clinical tools that produce or create application programming interfaces (APIs) and channels for such datasets. This connection demands an extensive understanding of the multidimensional data to be obtained as well as the data acquisition flow.

A useful model of this integration is the collection and use of microelectrode recordings (MER) during deep brain stimulation recordings. MER can produce gigabytes of data on systems that are frequently not connected to the Ethernet and thus necessitate dedicated formats and storage tools. NeurOmega from Alpha Omega (Nazareth, Israel) and the LP+ from FHC (Bowdoin, ME, USA) are both systems that are commonly used to collect MER data from humans. The signals recorded from such systems are not associated with the patient's scans, but rather with a patient, a trajectory, and a position on this trajectory. While this is a relevant aspect, it prevents the MER data from being co-located with the patient's brain. The co-localization of MER information can then only be "estimated" on an MRI through manual transfer to a Cartesian reference system (AC–PC system). In order to

accurately locate the signals from a patient's brain, additional significant data has to be gathered including imaging data (preoperative MRI or CT) and a surgical plan (position of the trajectory, frame coordinates, etc.), all of which are accessible and already structured throughout the clinical flow. Thus, it is imperative to determine the standards and force the industry to open their softwares to acquire data directly from the clinical flow. Our experience has revealed the difficulties in connecting with software from leaders in the industry. While the reasons are numerous, the software for neuromodulation is not their main market and ventures to move toward new technologies are not recognized as a top priority. This disconnection from the leaders drove us to design and create a suite of software dedicated to DBS and connected to our cloud-based archive. The system has since been regulatory cleared [2] for use in the clinical flow, ranging from planning to intraoperative guidance to postoperative programming.

Assuring Data Quality and Completeness

Various datasets are commonly interconnected; missing information can cause misinterpretation when analyzed by researchers, leading many engineers to build archives specifically for their labs. Thus, the development of an archive that will be used in a collaborative environment generates challenges when researchers need to be able to trust the data from others. Therefore, designing the proper methods to filter the data requires an understanding of data complexity. To demonstrate this notion with the example of MER data, the location of the MER signals will only be accurate if the system is designed with a broad perception of factors that can create such inaccuracies. For example, the amount of brain shift in surgery could be an element that would make the location MER in the brain inaccurate and consequently misleading or unusable by others. Thus, it is crucial to create a system that can store information to allow the integration of enough data to evaluate and assure the quality by manual or automated quality checks.

Integration of Spatial and Temporal Data

The brain is a dynamic system and consequently the archive must be able to combine spatial and temporal datasets, allowing for a centralized view of the brain. Spatial data is usually related to the ability to detect recordings or events and relate them to a position or network in a patient's brain. This data requires imaging techniques varying from clinical MRI to advanced diffusion imaging. While spatial data is limited to recordings of brain activity, temporal analysis relates specific events to brain activity, storing a triggering event, and the ensuing activity that can take milliseconds, minutes, or even a lifetime. The archive should have the ability to not only store such data, but it should be able to efficiently query it for data analysis.

Ready for Sensing and Clinical Surveillance Data

Sensing and surveillance systems can be used to monitor daily electronic data streams for abnormal counts of various features. The benefits of such technologies are being evaluated not only by the industry but also by researchers through devices such as sensing DBS generators from Medtronic [16] or wearable sensors like those developed by Fitbit. However, the data that these technologies generate introduces specific challenges when being handled, streamed, and stored. As these technologies become the norm, the archive design must include methods to efficiently handle the storage, processing, and querying of such data.

Respecting the Privacy and Ethical Implications of Neuroscience Research

Brain research may raise important issues about neural enhancement, data privacy, and appropriate use of brain data in law, education, and business. Cloud-based archives must adhere to the highest ethical standards for research with human

subjects under applicable laws. To support these standards, it is important for the user of the system to easily be able to track IRBs and consent forms and respect HIPAA compliance by being able to remove patient data upon an individual's request to be withdrawn from a study.

Security from the Ground Up

As opposed to data stored in the local IT architecture of a medical center, the archives deployed in a public cloud such as the Amazon Cloud are exposed to usual cloud risks including hacking, rogue administrators, accidents, complicit service providers, and snooping governments. Therefore, security needs to be thought through from the ground up in any trans-institutional patient-data management system. Client-side cryptography is a good solution to these issues as it allows users to protect their own data with individual, per-file encryption and protect access to that data with user-controlled keys. The encryption, decryption, and key management are all done on the end user's computer or device, meaning the data in the cloud only exists in its encrypted state.

To remain a completely HIPAA-compliant, cloud-based system, users need to employ multi-level encryption to ensure data integrity, ownership, and security. In addition, the cloud-based archive legal entity needs to maintain a Business Associate Agreement with Amazon AWS as well as with each medical center. The archive also needs to be constantly monitored by a third-party entity to keep the security and ownership control at the highest global standards. In rare cases, some institutions may require the data to be hosted physically at the institution. Therefore, the system should allow for the deployment of a physical node at an institution while keeping it connected to the cloud network.

Fostering Data Sharing

While the concept is accepted by most researchers, open-data sharing remains challenging as it leads to questions of data ownership and issues with IRB, IP, or publishing. However, there is a clear need for data sharing across selected partnering institutions. To foster data sharing, we designed the CranialCloud to allow the creation of "social networks" —research networks that permit researchers to share data selectively with other researchers they want to share data with instead of relying on an open-ended sharing agreement. The researcher or clinician could then share data privately to facilitate collaboration prior to publication. To comply with the NIH vision, a defined period of time could be established before that dataset is shared with the rest of the research community. Publication agreements in advance of sharing can also help mitigate future concerns about necessary and sufficient attributions.

Data Normalization

The impact of data normalization in neuromodulation [1] has often been neglected. Since its pioneering days, DBS researchers have made progress by studying the location of motor and sensorial brain functions from data collected from cohorts of patients. A common approach to study such data has been to build probabilistic maps that represent the likelihood of observing a particular response to the experiment of interest. Such inter-patient studies require a mechanism to compare brains from different patients. While human brains are topologically similar, they are also different in size, shape, and connectivity. Regardless, because of the lack of better tools, the stereotactic or the Talairach coordinate system [17] has found the most widespread acceptance in the clinical community to normalize DBS-related observations for localization and communication of three-dimensional positions in the brain. It uses the anterior and posterior commissures as internal landmarks to define a right-handed coordinate system. Their midpoint typically defines the origin even though either the anterior or posterior commissure is sometimes used instead. A point in the three-dimensional space is then defined as being anterior–posterior, medial–lateral, or dorsal–ventral to this origin. Stereotactic and linear methods used to

match different brains cannot accurately match functional areas across individuals because these are local subregions that are not well predicted by gross anatomical landmarks. The use of Talairach coordinates is often favored over other methods because of its simplicity and its prevalence in the medical literature prior to the availability of more sophisticated normalization schemes. However, the progress made in medical image processing permits volumetric approaches such as nonlinear registration algorithms to align such regions with better accuracy and allowing more focal mapping of data from a population of patients and subsequent analyses as illustrated in Fig. 11.1. In a nutshell, these algorithms use the MRI intensity distribution to find the optimal transform between scans from different patients or between a patient and a volume of reference (often called atlas). Nonlinear registration algorithms have been well known in the imaging community. The algorithm initially used in the CranialCloud is the algorithm designed by Rhode et al. [18] at Vanderbilt University but is one option among other similar algorithms [18–22]. Figure 11.1 shows the effect of normalization on 620 data points showing at least 50% efficacy in tremor reduction (measured subjectively by a neurologist during surgery) from 86 DBS ventral intermediate nucleus (Vim) implantations. One could easily see the dramatic effect of using a suboptimal normalization system on the statistical analysis intended to show optimal location for stimulation to control tremor in patients. The view presents the Vim of the reference MRI volume overlaid with the segmentations of structures and the probabilistic map of tremor control built from a population of patients using (a) Talairach coordinates and (b) nonlinear image normalization. The view shows that statistical maps created by nonlinear normalization of data from several individuals are highly localized, while those created using the Talairach coordinates have a larger spread. This is because nonlinear methods have substantially more degrees of freedom and can thus better account for local anatomical differences. Furthermore, the map built using nonlinear normalization correlates strongly with the anatomical Vim, while the Talairach approach produces scattered results.

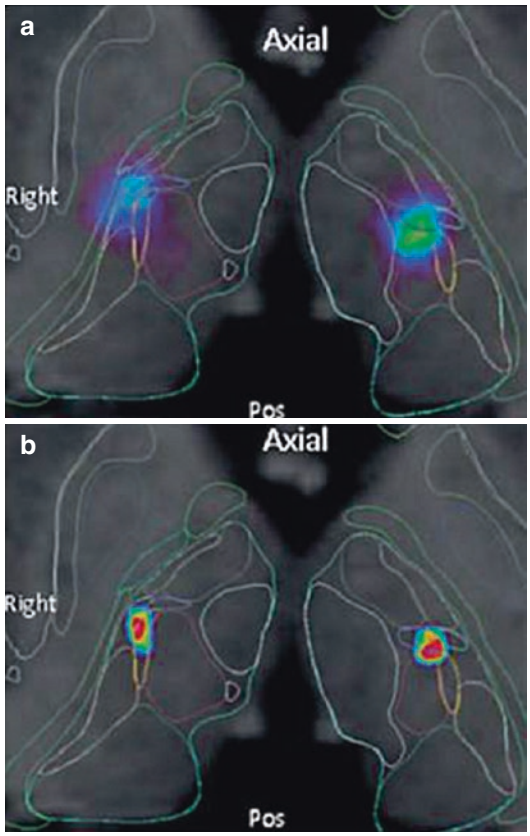

Fig. 11.1 Normalized data of location of optimal tremor control in over 100 patients recorded from intraoperative stimulation overlaid to a reference atlas MRI. (**a**) Points are normalized using Talairach rigid approach. (**b**) Points are normalized using a nonlinear registration approach. One can note how focal the statistical map created from the points is on (**b**) compared to (**a**)

This illustrates the importance of the choice of the normalization scheme when analyzing such data and interpreting the results of such analyses. Even though these new nonlinear methods require more processing than methods that rely on Talairach coordinates, they should be preferred to linear ones in order to accurately and reliably compare functional information across individuals. Recently, nonlinear algorithms have been made more accessible to researchers and clinicians alike in user-friendly software packages and allowing a wider use in clinical analyses. Their use will likely improve the accuracy of statistical studies and clinical conclusions in stereotactic and functional data analyses.

Custom Patient-Based Medicine

DBS requires precise targeting so that the final implant can be placed in an optimal location to achieve therapeutic benefit without causing side effects. Every single patient gets a custom lead placement. Traditionally, this custom position is reached by refining an initial preoperative target based on what his or her doctors are able to test in the operating room. Although this process compensates for initial inaccuracies in preoperative targeting and allows adjustment for the anatomic and physiological variability across patients, it is time consuming and invasive, and it may increase the operative risk when multiple penetrations are required. Given the importance of accurate localization of the optimal target, different approaches have been used to develop preoperative planning methods more adapted to a patient's singular anatomy. Such methods include indirect targeting based on anatomic landmarks and direct targeting using various imaging modalities. An alternative option is to couple functional atlases with nonlinear image registration techniques. Such an approach allows physicians to use a priori information contained in preoperative patient images and deform a physiological atlas to match a patient's anatomy. Given their potential, there has been much effort over the past few decades toward increasing the robustness and accuracy of such nonlinear registration algorithms and validating their use to automatically guide DBS planning.

In the CranialCloud system, the locations of the final DBS implant and the individual contacts are extracted from a postoperative CT or MRI. The individual contacts are projected onto the reference atlas by using fully automatic nonrigid registration between a patient's preoperative MRI and the atlas MRI.

When it is needed to customize the atlas to a new patient's anatomy, the reverse process is used. The atlas MRI is nonlinearly transformed onto the patient's MRI and all the content of the atlas is projected onto the patient. Using outcome measures, the atlas points can be filtered to only show a subset of the cloud of contacts. Filters can be set to select all the points that match global criteria such as a certain percentage of control of the symptoms, a specific change in UPDRS, or similar metrics. We have shown that taking the centroid of a cloud of active contacts associated to patients showing a satisfactory control of their symptoms through stimulation exceeded the precision of the best manual approach to subthalamic DBS targeting for Parkinson disease [23]. Filtering is not limited to using global metrics that can be applied to patients. One could explore the effect of adaptive filtering based on preoperative predictors such as filtering to select patients that would show similar anatomy than the patient to be treated or selecting patients that would show similar disease progression, for example. With access to a large number of patients in the database, these filters would become more and more selective and we would be able to test the effect of such filters on targeting and programming accuracy.

Conclusion

When looking at the amount of existing archives available, one could think that building an archive that can be used to store, normalize, and create predictive models to assist DBS care is a fairly simple task. A deeper analysis shows that this is far from true. Designing a system that can unify a vast range of DBS practices requires a deep understanding of clinical data flow and engineering algorithms and the opportunity to connect to proprietary software from competitive companies without defined data standards. Our attempt to create a system for neuromodulation and in particular for DBS was a crusade of 15 years of research at Vanderbilt University and funded by the NIH through 3 R01 (2R01-EB006136 and 9R01-NS095291) and a phase I and II STTR (R41NS063705, 9R42MH100007). It was clinically evaluated at a number of partnering institutions (Ohio State University, Dr. Ali Rezai M.D.; the VA in Richmond, Dr. Kathryn Holloway, MD; Wake Forest Medical Center, Dr. Stephen Tatter; and Thomas Jefferson University, Dr. Ashwini Sharan, MD) that allowed the testing of the data sharing concepts among a controlled group of neurosurgical users who commonly perform DBS surgery. This allowed toolsets to be

developed and data compatibility to be checked prior to release of any commercial products. This inter-institutional users group has worked for the past 5 years to constantly improve the data streaming concepts and shared best practices, communicated with the engineering team and taken a visionary approach in using state-of-the-art image processing to guide their practice.

Disclosure Dr. D'Haese is the cofounder and shareholders of Neurotargeting, LLC. Neurotargeting has acquired technology developed at Vanderbilt University by Dr. D'Haese related to the management and processing of clinical data generated from neuromodulation. Neurotargeting's role was to create the legal and commercial framework for such a framework to be sustainable. While this chapter is not intended to promote any concept related to Neurotargeting, some of the discussion will mention Vanderbilt University and Neurotargeting data framework called CranialCloud.

References

1. D'Haese P-F, Pallavaram S, Kao C, Neimat JS, Konrad PE, Dawant BM. Effect of data normalization on the creation of neuro probabilistic atlases. Stereotact Funct Neurosurg. 2013;91(3):148–52.
2. D'Haese P-F, et al. CranialVault and its CRAVE tools: a clinical computer assistance system for Deep Brain Stimulation (DBS) therapy. Med Image Anal. 2012;16(3):744–53.
3. Tourdias T, et al. Visualization of intra-thalamic nuclei with optimized white-matter-nulled MPRAGE at 7T. NeuroImage. 2014;84:534–45.
4. D'Haese P-F, Konrad PE, Pallavaram S, Li R, Prasad P, Rodriguez WJ, Dawant BM. CranialCloud: a cloud-based architecture to support trans-institutional collaborative efforts in neuro-degenerative disorders. Int J Comput Assist Radiol Surg. 2015;10:815.
5. Marcus DS, et al. The extensible neuroimaging archive toolkit: an informatics platform for managing, exploring, and sharing neuroimaging data. Neuroinformatics. 2007;5(1):11–34.
6. Book GA, et al. Neuroinformatics database (NiDB)--a modular, portable database for the storage, analysis, and sharing of neuroimaging data. Neuroinformatics. 2013;11(4):495–505.
7. Das S, et al. LORIS: a web-based data management system for multi-center studies. Front Neuroinform. 2011;5:37.
8. Scott A, et al. COINS: an innovative informatics and neuroimaging tool suite built for large heterogeneous datasets. Front Neuroinform. 2011;5:33.
9. Mueller SG, et al. Ways toward an early diagnosis in Alzheimer's disease: the Alzheimer's Disease Neuroimaging Initiative (ADNI). Alzheimers Dement. 2005;1(1):55–66.
10. Ascoli GA. The ups and downs of neuroscience shares. Neuroinformatics. 2006;4(3):213–6.
11. Ascoli GA. A community spring for neuroscience data sharing. Neuroinformatics. 2014;12(4):509–11.
12. Kotter R. Online retrieval, processing, and visualization of primate connectivity data from the CoCoMac database. Neuroinformatics. 2004;2(2):127–44.
13. Van Horn JD, Ishai A. Mapping the human brain: new insights from FMRI data sharing. Neuroinformatics. 2007;5(3):146–53.
14. Teeters JL, et al. Data sharing for computational neuroscience. Neuroinformatics. 2008;6(1):47–55.
15. Harris PA, et al. Research electronic data capture (REDCap)--a metadata-driven methodology and workflow process for providing translational research informatics support. J Biomed Inform. 2009;42(2):377–81.
16. Medtronic Brain Radio. http://www.medtronic.com/us-en/about/news/dbs-brain-radio.html.
17. Talairach J, Tournoux P. Co-planar stereotaxic atlas of the human brain. Stuttgart: Thieme Publishing Group; 1988.
18. Rohde GK, Aldroubi A, Dawant BM. The adaptive bases algorithm for intensity-based nonrigid image registration. IEEE Trans Med Imaging. Nov 2003;22:1470–9.
19. Modat M, Ridgway GR, Taylor ZA, Lehmann M, Barnes J, Hawkes DJ, et al. Fast free-form deformation using graphics processing units. Comput Methods Prog Biomed. 2010;98:278–84.
20. Avants BB, Epstein CL, Grossman M, Gee JC. Symmetric diffeomorphic image registration with cross-correlation: evaluating automated labeling of elderly and neurodegenerative brain. Med Image Anal. 2008;12:26–41.
21. Ardekani BA, Guckemus S, Bachman A, Hoptman MJ, Wojtaszek M, Nierenberg J. Quantitative comparison of algorithms for inter-subject registration of 3D volumetric brain MRI scans. J Neurosci Methods. 2005;142:67–76.
22. Klein A, Andersson J, Ardekani BA, Ashburner J, Avants B, Chiang MC, et al. Evaluation of 14 nonlinear deformation algorithms applied to human brain MRI registration. Neuroimage. 2009;46:786–802.
23. Pallavaram S, D'Haese PF, Lake W, Konrad PE, Dawant B, Neimat JS. Fully automated targeting using nonrigid image registration matches accuracy and exceeds precision of best manual approaches to subthalamic deep brain stimulation targeting in parkinson disease. Neurosurgery. 2015;76(6):756–65.

Suggested Reading

Datteri RD, Dawant BM. Estimation of rigid-body registration quality using registration networks. In: SPIE Medical Imaging 2012; 2012a.

Datteri RD, Dawant BM. Estimation and reduction of target registration error. Med Image Comput Comput Assist Interv. 2012b;15:139–46.

Datteri RD, Dawant BM. Automatic detection of the magnitude and spatial location of error in non-rigid registration. In: Biomedical image registration, 5th international workshop, WBIR 2012, Nashville; 2012c. p. 21–30.

Datteri RD, Liu Y, D'Haese PF, Dawant BM. Validation of a nonrigid registration error detection algorithm using clinical MRI brain data. IEEE Trans Med Imaging. 2015;34:86–96.

D'Haese PF, Cetinkaya E, Konrad PE, Kao C, Dawant BM. Computer-aided placement of deep brain stimulators: from planning to intraoperative guidance. IEEE Trans Med Imaging. 2005;24:1469–78.

Henderson EY, Goble T, D'Haese PF, Pallavaram S, Oluigbo C, Agrawal P, et al. Successful subthalamic nucleus deep brain stimulation therapy after significant lead displacement from a subdural hematoma. J Clin Neurosci. Feb 2015;22:387–90.

Jermakowicz WJ, Kanner AM, Sur S, Bermudez C, D'Haese P-F, Kolcun JPG, Cajigas I, Li R, Millan C, Ribot R, Serrano EA, Velez N, Lowe MR, Rey GJ, Jagid JR. Laser thermal ablation for mesiotemporal epilepsy: analysis of ablation volumes and trajectories. Epilepsia. 2017;58:801.

Kahn E, D'Haese PF, Dawant B, Allen L, Kao C, Charles PD, et al. Deep brain stimulation in early stage Parkinson disease: operative experience from a prospective randomised clinical trial. J Neurol Neurosurg Psychiatry. Feb 2012;83:164–70.

Liu Y, Dawant BM. Automatic detection of the anterior and posterior commissures on MRI scans using regression forests. In: Engineering in Medicine and Biology Society (EMBC), 2014 36th Annual International Conference of the IEEE; 2014. p. 1505–8.

Liu Y, D'Haese P-F, Dawant BM. Effects of deformable registration algorithms on the creation of statistical maps for preoperative targeting in deep brain stimulation procedures. In: SPIE medical imaging 2014: image-guided procedures, robotic interventions, and modeling, San Diego; 2014a.

Liu Y, Konrad PE, Neimat JS, Tatter SB, Yu H, Datteri RD, et al. Multisurgeons, multisite validation of a trajectory planning algorithm for deep brain stimulation procedures. IEEE Trans Biomed Eng. 2014b;61:2479–87.

Liu Y, D'Haese P-F, Newton A, Dawant BM. Thalamic nuclei segmentation in clinical 3T T1- weighted images using high-resolution 7T shape models. Presented at the SPIE medical imaging 2015, Orlando, Florida; 2015.

Newton A, Dawant BM, D'Haese PF. Visualizing Intrathalamic structures with combined use of MPRAGE and SWI at 7T. In: International Society for Magnetic Resonance in Medicine, Milan, Italy; 2014.

Pallavaram S, D'Haese PF, Kao C, Yu H, Remple M, Neimat J, et al. A new method for creating electrophysiological maps for DBS surgery and their application to surgical guidance. Med Image Comput Comput Assist Interv. 2008;5241:670–7 (PMID: 18979804).

Pallavaram S, Dawant BM, Haese M, Remple JS, Neimat C, Kao PEK, et al. A method to correct for brain shift when building electrophysiological atlases for deep brain stimulation (DBS) surgery. Med Image Comput Comput Assist Interv. 2009a;5761:557–64 (PMID: 20426032).

Pallavaram S, Dawant BM, Koyama T, Yu H, Neimat JS, Konrad PE, et al. Validation of a fully automatic method for the routine selection of the anterior and posterior commissures in MR images. Stereotact Funct Neurosurg. 2009b;87:148–54.

Pallavaram S, Phibbs F, Tolleson C, Davis T, Fang J, Hedera P, et al. Neurologist consistency in interpreting information provided by an interactive visualization software for deep brain stimulation postoperative programming assistance. Neuromodulation. 2014;17:11–5.

Phibbs F, Pallavaram S, Tolleson C, D'Haese P-F, Dawant BM. Use of efficacy probability maps for the post-operative programming of deep brain stimulation in essential tremor. Parkinsonism Relat Disord. 2014a;20:1341–4.

Phibbs FT, Pallavaram S, Tolleson C, D'Haese PF, Dawant BM. Use of efficacy probability maps for the post-operative programming of deep brain stimulation in essential tremor. Parkinsonism Relat Disord. 2014b;20:1341–4.

Rezai AR, Kopell BH, Gross RE, Vitek JL, Sharan AD, Limousin P, et al. Deep brain stimulation for Parkinson disease: surgical issues. Mov Disord. 2006;21 Suppl 14:S197–218.

Tolleson C, Pallavaram S, Li C, Fang J, Phibbs F, Konrad P, et al. The optimal pallidal target in deep brain stimulation for dystonia: a study using a functional atlas based on nonlinear image registration. Stereotact Funct Neurosurg. 2014;93:17–24.

Wu C, D'Haese PF, Pallavaram S, Dawant BM, Konrad P, Sharan AD. Variations in thalamic anatomy affect targeting in deep brain stimulation for epilepsy. Stereotact Funct Neurosurg. 2016;94(6):387–96.

Yu H, Hedera P, Fang J, Davis TL, Konrad PE. Confined stimulation using dual thalamic deep brain stimulation leads rescues refractory essential tremor: report of three cases. Stereotact Funct Neurosurg. 2009;87:309–13.

Yu H, Kao C, Pallavaram S, Rodriguez WJ, D'Haese P-F, Davis T, et al. Simultaneous multiple electrode stimulation may be a more effective tremor control therapy. In: North American Neuromodulation Society (NANS), Las Vegas, USA; 2014.

Part III

The Biophysics of Functional Neurosurgical Therapy

Responsive Neurostimulation

12

Abhijeet Gummadavelli, Imran H. Quraishi, and Jason L. Gerrard

An Introduction into Responsive Neurostimulation

Responsive Neurostimulation Introduction and History

As one of the most common neurological disorders, epilepsy affects approximately 1% of the population. Various reports show that between 30% and 40% of epilepsy patients will be drug-resistant, a statistic that has not changed significantly despite the introduction of many new antiepileptic medications. Beginning with the reports of Sir Horsley [1], epilepsy surgery has provided an alternative for those with refractory epilepsy, offering a cure for some cases. The anterior medial temporal lobectomy, for example, offers a 60–75% chance of seizure freedom for properly selected patients with medial temporal lobe (MTL) epilepsy. There are, however, inherent risks with epilepsy surgery, and surgical results for extra-temporal epilepsy are quite variable. In some instances, resective surgery is not feasible due to overlap with functionally eloquent brain tissue and the resulting neurological deficit, and therefore other surgical treatment options are needed.

Responsive neurostimulation (RNS) benefitted from serendipitous clinical observations and the advancement of applied technology. Direct application of electrical current to epileptic cortex was first reported in the 1950s [2]. Targeted cortical stimulation arose from the standard clinical investigations in localizing "eloquent" cortices (i.e., language, motor, sensory) in relation to the epileptogenic zone in surgical candidates. As part of the evaluation, cortical and subcortical electrodes are placed as grids and strip electrodes in the subdural space or depth electrodes into subcortical nuclei. A phenomenon known among clinical electrophysiologists was that cortical stimulation in pre-resection patients with brief bursts of pulse stimulations could stop afterdischarges within seconds [3, 4]. Lesser and colleagues quantified the phenomenon after noting that in 19 patients with subdural electrodes, brief pulse stimulations (0.3–2 s train of 300 μs biphasic pulses at 50 Hz) were able to abort prolonged runs of testing stimulation-induced afterdischarges; they prognosticated that brief pulse stimulations may be able to acutely treat seizures [3].

A. Gummadavelli · J. L. Gerrard (✉)
Department of Neurosurgery, Yale School of Medicine, New Haven, CT, USA

Yale-New Haven Hospital, New Haven, CT, USA
e-mail: jason.gerrard@yale.edu

I. H. Quraishi
Yale-New Haven Hospital, New Haven, CT, USA

Department of Neurology, Yale School of Medicine, New Haven, CT, USA

N. Pouratian, S. A. Sheth (eds.), *Stereotactic and Functional Neurosurgery*,
https://doi.org/10.1007/978-3-030-34906-6_12

The use of neurostimulation for neuromodulation in the treatment of neurological disorders is gaining significant momentum with the recent approval of responsive neurostimulation (RNS) and deep brain stimulation (DBS) for epilepsy. Although both RNS and DBS are neurostimulation-based therapies, there are important differences between these two approaches to neurostimulation in the treatment of epilepsy. There are several theoretical mechanisms by which neurostimulation affects seizures and modulates epileptic networks. The inhibitory hypothesis proposes that neurostimulation causes preferential release of inhibitory neurotransmitters. Depolarization blockade is the hypothesis of the "reversible lesion" approach, in which high-frequency stimulation is presumed to inactivate neurons in the vicinity of the electrode by over-depolarization and failure of voltage-gated ion channels. This "reversible lesion" concept was utilized in the development of DBS for movement disorders. Synaptic inhibition and synaptic depression refer to the presumed effects caused by stimulation-induced depolarization of the distal axon and depletion of neurotransmitters at the axon terminal. In addition, there are slower mechanisms, involving changes in transcription, proteins, and neurotrophic factors that influence network activity over longer time scales.

In general, there are two mechanistic approaches to neuromodulation for network disorders such as epilepsy: network modulation and onset disruption. The first is a "network approach" in which the neurostimulation is designed to treat a particular neurological disorder by overall modulation of a network through either nodal modulation (i.e., depolarization blockade), modulatory effects on fibers of passage, or longer-term changes in the network. The second mechanism involves disruption of a periodic abnormal resonance or synchrony, most commonly via bursts of high-frequency stimulation. Responsive neurostimulation technique utilizes the onset disruption approach to treatment. This approach was translated from the cardiac field with the success of implanted cardiac monitors and defibrillators. Similarly, the RNS device is designed to continuously monitor intracranial EEG (icEEG) activity and then rapidly respond with high-frequency neurostimulation designed to "disrupt" the network synchrony required for seizure progression and propagation. From this concept and early data suggesting that neurostimulation in humans can be antiepileptic [5], the concept of using electrical stimulation to disrupt seizure formation and propagation evolved into studies in the epilepsy monitoring unit. Lesser and colleagues showed that brief bursts of stimulation could shorten or terminate afterdischarges in patients with intracranial electrodes [3, 6] during intracranial recording sessions. Additional work suggested that responsive stimulation suppressed spontaneous seizures in mice [7] and cats [8]. The next logical step included small pilot trials of responsive stimulation for seizures in the epilepsy monitoring unit. In a small series, Peters et al. [9] utilized a bedside external system to detect seizures in the EMU and then deliver short bursts of computer-controlled responsive stimulation to terminate seizures in eight patients [10]. An additional open trial in patients with intracranial electrodes implanted for localization of seizure and functional tissue utilized responsive stimulation triggered by a detection algorithm to disrupt the detected seizure [11]. They reported that responsive cortical stimulation suppressed electrographic seizures in the four reported patients.

From these and other data, the potential utility of seizure detection and responsive neurostimulation was recognized, and a multicenter pivotal trial to show safety and efficacy was designed utilizing the NeuroPace responsive neurostimulation (RNS) device [12]. A total of 191 patients with medically refractory partial-onset epilepsy were enrolled and randomized to either stimulation or control groups for the blinded evaluation phase. Following surgical implantation, all patients had a 1-month recovery period and 1 month of recordings to set the detection algorithm. Next, all patients were studied during the 3-month blinded period with patients randomized in equal number to stimulation on or off. This 3-month blinded period was followed by open-label and long-term evaluation that continued for

several years. Electrode arrays consisting of four-contact strips or depth electrodes were placed into the seizure-onset zone(s), and an array of tools were available for the detection of abnormal electrographic activity. The resulting current-controlled biphasic stimulation could be adjusted to include desired electrode contacts with frequency range of 1–333 Hz, current ranging from 1 to 12 mA and pulse widths between 40 and 1000 μs.

The results of this RNS pivotal trial were published in 2011 [12], and since then longer-term follow-up studies have also been reported, showing continued improvement in seizure reduction outcomes [13, 14]. In the blinded, randomized, and controlled portion of the pivotal study, patients in the treatment arm showed a 37.9% decrease overall during the entire blinded period versus a 17.2% decrease in the control arm. During the final month of the blinded period, patients in the study arm showed a 41.5% decrease in seizures, while the control group reported a 9.4% decrease as the control group drifted back to their pre-op baseline [12] (Fig. 12.1).

Overall, there was a significant difference in the decrease in seizures in the treatment group versus the sham group ($p = 0.012$). In the treatment group (blue), seizure rate continued to decrease during the 3-month blinded period. In the sham group, there was an initial decline in seizures, likely from the implant effect which is well known in movement disorder surgery, that moved back toward baseline seizure frequency during the 3-month blinded period. By the final month, the treatment group showed a 41.5% decrease, while the sham groups showed only a 9.4% decrease in seizure frequency.

During the long-term open-label portion, patients in the study showed a median decrease in seizures of 44% at 1 year and 53% at 2 years. At 2 years, the majority (55%) of patients showed a meaningful improvement in seizures (≥50%) and were labeled as responders [13]. This trend of continued improvement over time continued during the remainder of the long-term follow-up period. The results of the pivotal trial and long-term open-label follow-up lead to approval of the NeuroPace RNS device by the US Food and Drug Administration in November of 2013. More recently, the long-term outcomes were reported showing the responder rate at 57.9% at 3 years, 60.8% at year 4, and 61% at year 5 [14]. The RNS system has rapidly become a mainstay in the treatment of medication refractory complex partial epilepsy with two or fewer identified onset zones. As the first FDA-approved closed-loop neuromodulatory device, the RNS system has provided a new treatment option for patients and new insight from chronic intracranial LFP recordings.

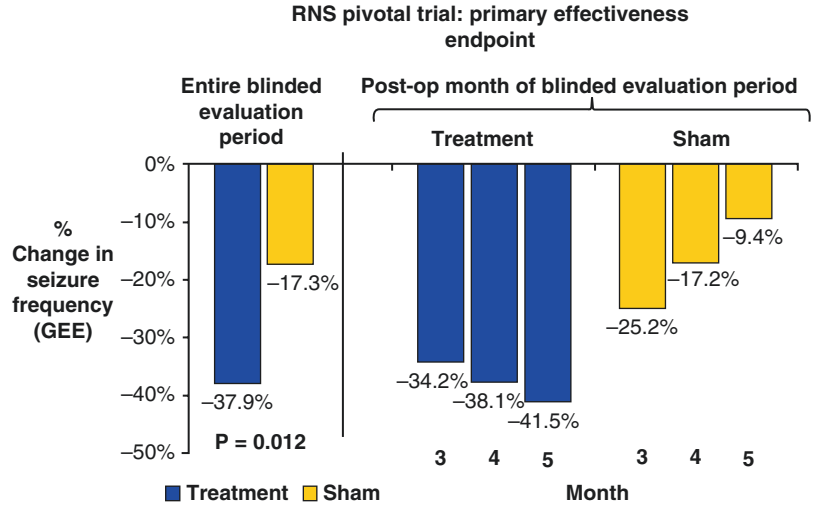

Fig. 12.1 Results of RNS® System Pivotal Study (Morrell et al. [12]). (© 2011 NeuroPace, Inc. Image used with permission from NeuroPace, Inc.)

Comparison to Other Forms of Neurostimulation for Epilepsy

In the United States, there are now three FDA-approved neurostimulation options for the treatment of epilepsy. Vagus nerve stimulation (VNS) has been available the longest and is the only extracranial option. The mechanism of this form of stimulation is not clear. The majority of vagus nerve fibers are afferents including visceral sensory information with cell bodies near the jugular foramen. Afferents bifurcate in the medulla and synapse in the bilateral nucleus solitarius. There are widespread projections from the nucleus solitarius to the reticular formation, pons, midbrain, cerebellum, thalamus, and hypothalamus. VNS increases activity in these projection pathways [15]. The idea that it could inhibit hypersynchronous discharges was proposed in the 1980s [16] and was later supported in animal models with acute abortive effects on seizures and short-term prophylactic effects [17], as well as a chronic progressive prophylactic (neuromodulatory) effect [18]. In the first human trials, no effect was seen on interictal discharges, but the stimulator was observed in some cases to abort seizures [19]. In another case, hippocampal spiking was seen to decrease with 30 Hz vagus nerve stimulation [20], although the effect size was small.

The first randomized controlled trial included 114 patients with focal epilepsy and a median of 0.7 seizures per day [21]. There was, however, no true negative control in which no stimulation was delivered. Patients were randomized to either high or low stimulation settings. Seizure reduction was 24.5% in the high-stimulation group versus 6.1% in the low-stimulation group ($p = 0.01$). Fifty percent or greater response rates were seen in 31% of patients receiving high-stimulation and 6% of the low-stimulation group ($p = 0.02$), respectively. A second study was done on 196 patients with fewer seizures (6/month), again with an active control. Seizure reduction was observed to be 28% in the high-stimulation versus 15% reduction in the low-stimulation group ($p = 0.04$), respectively. Multiple long-term follow-up studies have shown a cumulative effect [22]. Seizure reduction was reportedly increased annually over about 7 years before reaching a plateau.

The second form of stimulation that was developed for epilepsy (though the third to be approved in the United States) was thalamic deep brain stimulation (DBS). As with VNS, the idea was to target a nucleus that would affect large regions of the brain rather than relying on the precise localization of seizure onset zones. Two nuclei have been studied in detail for this purpose. The centromedian nucleus of the thalamus (CMT) is an intralaminar nucleus involved in attention and arousal and receives fibers from widespread cortical regions and the reticular formation among other areas. Stimulation of this nucleus was shown to treat interictal discharges [23]. In early small trials, an external CMT stimulator was demonstrated to reduce tonic-clonic seizures by 80–100% and focal impaired awareness seizures by 60–100% by seizure diaries. These results have not been validated in larger controlled trials to date.

The second nucleus that was evaluated (simultaneously by other groups [24]) was the anterior nucleus of the thalamus (ANT), which forms a node of the limbic network including the hippocampus, often implicated in focal seizures. In an early attempt, stimulation of the anterior nucleus produced a reduction of seizures in four out of six patients [25]. The ANT was selected for more widespread commercialization and tested with the Stimulus of the Anterior Nucleus of the Thalamus in Epilepsy (SANTE) trial, in which patients with focal epilepsy with or without focal to bilateral tonic-clonic seizures were blinded to have stimulation either on or off for 3 months after implantation [26]. The primary efficacy measure was a reduction in seizures in the active group in the blinded phase. Both groups had a reduction in seizure frequency (21–22%) in the postoperative phase that has been termed an implant effect. In the blinded phase, there was no statistically significant difference in overall seizures, though there was a reduction in the prespecified "most severe" seizures (40% vs. 20%, $p < 0.05$) and in seizure injuries (26% vs. 7%, $p = 0.01$), and the difference between groups appeared to have been blunted by the implant effect, such that it was more obvious in the final month of the blinded phase. Long-term response rates have been better; by 3 years post-implantation, 67% of patients ($N = 42$, from an initial 108

patients) had a 50% or greater improvement in seizures. Potential side effects noted in the early trial included depression and memory impairment, but further longer-term evaluation of the cohort did not support a significant change in either memory or depression scores.

In contrast to these other modalities, the current responsive neurostimulation system offers some unique benefits and also challenges, as outlined in the rest of this chapter. One benefit is that stimulation is responsive; in their current incarnations, VNS (with a minor exception of tachycardia-based activation) and DBS use chronic stimulation that does not change in response to epileptiform activity. Another benefit is the availability of electrocortigraphy, which can be used to tailor stimulation and also to monitor response to stimulation or other therapies. A limitation is the need for accurate seizure onset localization [27]. Most of these patients will undergo intracranial EEG prior to implantation of the RNS system. Another limitation is the effort required in programming and long-term follow-up, which vastly exceeds that in the other available modalities.

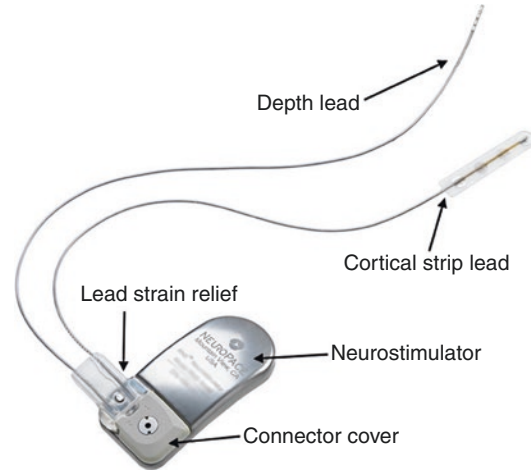

Fig. 12.2 The RNS® System Implantable Hardware. The RNS System includes the RNS® Neurostimulator, the connector cover, and lead strain relief cover. The neurostimulator can be connected to two electrode arrays/leads. Here, it is shown with one cortical strip array/lead and one depth electrode array/lead. Note that each array/lead has four electrode contacts. (© 2019 NeuroPace, Inc. Image used with permission from NeuroPace, Inc.)

RNS Hardware

RNS hardware consists of (1) an implanted stimulator with an on-board computer and (2) one or two electrode arrays consisting of either a subdural strip array or intracranial depth electrode array. Each electrode array typically has four contacts. The stimulator sits within a "ferrule" or housing that is placed within a designed craniectomy and screwed to the skull. As will be later described in the surgical procedure, after lead implantation, a precise craniectomy is performed to fit the ferrule. It is attached to the skull with four microscrews. The RNS system allows a few electrode array configurations, each array having four electrode contacts in either a strip or depth electrode array. The strip electrode arrays all come with the standard circular electrodes with 1 cm spacing between each of the electrode contacts. The strip arrays come with 15, 25, or 35 cm of lead wire connected to the strip. The depth electrode arrays also have four electrode contacts with two spacing configurations. The electrode contacts on the depth array are cylindrical rather than circular and have a smaller surface area. Depth electrode arrays are available with either 3.5 mm electrode spacing for more compact structures or 10 mm spacing between the electrode contacts. Each variety comes with either 30 or 44 cm in total length depending on the length of wire desired to connect to the RNS device (Fig. 12.2).

Advantages of the RNS System Other than Treatment of Seizures

The RNS system has been shown to be a safe and effective therapeutic system for the treatment of medication refractory complex partial epilepsy through the RNS pivotal trial [12] and long-term open-label follow-up [13, 14]. It is FDA approved for the treatment of adults with partial-onset medication refractory seizures. The device can be connected to two electrode arrays through which it monitors intracranial EEG (icEEG), stores

episodes of icEEG data from detections and planned electrocortigrams (ECoGs), and delivers brief neurostimulation in response to epileptiform detections. The parameters of the detections, recordings, and stimulation are individually set for each patient by their epileptologist. In addition to the documented therapeutic effects, the growing use of the RNS product has led to large datasets of long-term ECoG segments during scheduled ECoG storage and device detections. These data have fueled what the senior author has termed the ECoG Revolution, which has led to several new lines of investigation that are validating additional advantages of the RNS system. The most obvious of these is the ability to more objectively evaluate the number of seizures or seizure-like events experienced by patients with epilepsy. Although objective studies have shown that epilepsy patient diaries are not reliable [28, 29] to capture accurate seizure frequency reporting, the patient-reported seizure diary continues to be the cornerstone for controlled trials on epilepsy treatments. For the first time, the RNS system has provided long-term ECoGs that provide objective data on the frequency and duration of epileptiform activity, including seizures. These data are now being utilized for a variety of treatment modifications that can benefit therapy.

The acquisition of long-term ECoG data from patients with implanted RNS systems has led to publications on seizure patterns, prediction of response to antiepileptic medications, and seizure warning systems. Reviewing over the long-term data from RNS patients has identified clear, slow periodicities in seizure occurrence such as circadian, catamenial, and ultradian rhythms. As suggested in some prior publications [30–32], long-term ECoGs from the RNS system have shown that the majority of patients with partial epilepsy have a circadian periodicity in their epileptiform activity (63/65 subjects) [33]. This circadian periodicity could potentially be utilized to tailor the timing of treatment in individual patients. The periodicity of seizures in patients with partial epilepsy is further supported by data from patients with another long-term implanted device designed for seizure prediction (NeuroVista, Melbourne, VIC, Australia). Data reported from patients implanted with the NeuroVista device also show circadian, diurnal, and longer periodicities in seizure activity [34]. The circadian periodicity of seizures has been fairly well known in epilepsy and previously reported and now additionally substantiated by RNS ECoGs. The presence of longer periodicities, however, was reported more recently in a multicenter study of seizure patterns in 37 patients with long-term ECoGs recorded from their RNS system. Baud et al. [35] confirmed the known circadian rhythms previously reported and also showed much slower, multi-day (termed infradian or multidien) rhythms that vary across subjects but are relatively stable for individual patients. The long-term ECoGs from the RNS system are leading to the ability to recognize stable periodicities in a patient's epileptic activity and the potential to better predict seizure activity and tailor individual therapies.

The customization of medication therapies is another good example of the use of these chronic RNS ECoGs. The circadian, diurnal, and slower periodicities in an individual patient's epilepsy can be utilized for customization of their medication treatment program, with "rescue" drugs added into periods of high seizure probability. In addition, it has recently been reported that in patients with RNS and established detection settings, changes in the RNS detections especially the long episodes (detections lasting for a prespecified duration, typically around 30 seconds) can predict the effectiveness of a newly introduced antiseizure medication within 1–2 weeks [36, 37]. These promising data suggest that the chronic ECoGs from RNS can also help to identify the efficacy of medication changes in a short period of time, allowing providers to quickly customize the patient's medication therapy and eliminate long trial periods of medications that are not effective for that individual.

Additionally, the chronic RNS ECoG recordings can also be utilized to assist in seizure-onset lateralization and onset zone prioritization. One group of patients who are excellent candidates for the RNS system are those with bitemporal epilepsy, that is, patients with bilateral medial

temporal lobe (MTL) seizure onset. Although some temporal lobe epilepsy patients are clearly bitemporal on scalp EEG, this is most commonly established with intracranial monitoring including the placement of intracranial electrodes into the bilateral medial temporal lobe structures in addition to other cortical and subcortical locations. Patients with bitemporal epilepsy are often poor candidates for surgical resection, especially in cases when the most common onset zone involves the dominant medial temporal structures. Bilateral temporal resections are not performed due to the high likelihood of memory and cognitive impairment [38]. In patients with bitemporal epilepsy, bilateral longitudinal MTL electrodes are commonly placed with connection to the RNS device (see Fig. 12.5). For many years, epilepsy centers have wondered if patients who are found to have bilateral MTL onset during the limited intracranial monitoring session are truly bitemporal in onset or if one MTL is significantly more crucial in the patient's seizures. The present-day intracranial study has significant limitations that may affect the seizures recorded, which themselves can be limited in number. Patients are most often confined to bed and any movement out of bed must be controlled and supervised. The time frame of intracranial studies is constrained and is most often kept as short as possible while still obtaining the pertinent information needed to localize seizure-onset zone(s) and map functional cortex. To this end, the patient's antiepileptic medications are rapidly weaned off and sometimes additional measures are taken to promote seizure activity during the intracranial study if necessary. Some groups will also include electrical stimulation to induce seizure activity during the intracranial study. Recently, long-term ambulatory ECoGs obtained from patients with RNS showed that 84% of patients believed to have bilateral MTL epilepsy were found to have independent bilateral MTL electrographic seizures [39]. Sixteen percent of the patients had only unilateral electrographic seizures recorded after an average of more than 4 years of intracranial recordings. The average time to record bilateral electrographic seizures in the home, ambulatory setting was 41.6 days [39], much longer than intracranial studies are performed. Those patients with proven unilateral electrographic onset could then go onto resection if this was deemed appropriate.

There are also reports of using these long-term ECoGs for seizure-onset localization from patients with extra-temporal epilepsy, although these reports are not systematic but typically case reports [40]. Some of these patients had two seizure-onset zones identified during their intracranial study and had RNS electrodes implanted in both onset zones. There are now several reports of the long-term ambulatory ECoGs from an RNS device leading to targeted resection after months or years of intracranial recordings showing a crucial or dominant onset zone that is resectable [40].

Finally, the availability of long-term ambulatory ECoGs from electrodes permanently implanted in seizure-onset regions creates the potential to warn patients about seizures and even predict seizure events. We discussed the recognition of patient-specific slow periodicities in seizure events using the aforementioned RNS system. The identification of an individualized periodicity provides vital information for seizure prediction algorithms. These data, combined with additional information, may lead to predication methods that are accurate enough to be useful for assisting patients with epilepsy. Additionally, the RNS system might be utilized to warn patients about impeding seizures. In many, but not all, patients a stimulation paradigm can be identified that illicts a reliable "sensation" for the patient [93]. The sensation can vary from referred dural discomfort to aura-like sensations. There are trials underway to utilize such stimulation paradigms during the fifth and final detection of the RNS system to warn epilepsy patients. The sensation illicited by this fifth detection can warn patients that they are about to experience a seizure event.

Network-Based Targeting

Unlike traditional "open-loop" continuously delivered stimulation, responsive neurostimulation (RNS) is intermittent and reactive to a pathology-specific biomarker. Placement of RNS

electrodes in the pathologic neural circuit, most commonly directly at the site of pathology onset, is critical in its function to modulate the severity of disease. In these sections, we will discuss the network-based pathologies for which RNS has been applied, mostly widely in medically refractory epilepsy as discussed previously. Few cases of RNS for other indications (usually those that are currently treated with deep brain stimulation) have been investigated [41], such as closed-loop deep-brain stimulation paradigms in Parkinson disorder [42] or neuropsychiatric disorders [43, 44], thalamic responsive stimulation in a patient with Tourette syndrome [45], responsive spinal stimulation based on body position for chronic pain patients [46], and status epilepticus [47].

Theory of Seizure Genesis

To understand the biophysics of why RNS can be useful in epilepsy, it is first necessary to discuss the current theories of seizure generation. The prevailing concept in seizure genesis assumed an imbalance between excitation and inhibition, and specifically "runaway" excitation. A crucial addition to this paradigm came with the "network theory" of epilepsies which suggested that network hypersynchrony resulted in seizure generation and propagation [48–50]. Aberrant network properties in a number of circumstances (an aberrant node in a circuit, an aberrant pathway, combined nodal and pathway aberrance, or emergent aberrance from structural abnormality) result in a pathogenic seizure-generating network [51]. A single or multiple such networks may exist in a single patient; moreover, these networks may be dynamic during the duration of the patient's epilepsy to generate multiple independent seizure-onset foci [52, 53]. The phenotypic expression of a seizure (its semiology is the specific instance of network aberrance) is defined by its onset within the seizure-generating network and its subsequent variable propagation [48].

Several human and animal studies have used electrophysiological (scalp EEG, intracranial EEG, MEG, synchrony), metabolic neuroimaging (fMRI, PET, SPECT, functional connectivity), and structural neuroimaging (diffusion tensor imaging, anatomic connectivity) measures to identify ictal and interictal properties of seizure networks (reviewed in Spencer et al. [51]) [54, 55]. It is increasingly being found that individualized modeling of patient data can recreate previously empirically observed networks [56]. Manual and automated classifications of functional connectivity in epilepsy patients have helped identify these networks from intracranial EEG [57] and resting-state functional MRI data [58]. Some distributed brain networks that have been commonly implicated in epilepsies are listed in Table 12.1.

Table 12.1 Five commonly identified network patterns in patients with focal and generalized epilepsies

Network	Anatomy	References
1. Limbic–frontal network	Bilateral hippocampi, amygdalae, entorhinal cortex, lateral temporal cortex, anterior and medial thalamus, cingulate cortex, inferior frontal lobes	[48, 56]
2. Occipi-totemporal network	Lateral temporal cortex, medial occipital cortex	[48]
3. Parietal–frontal network	Superior parietal lobule, medial frontal cortex	[48]
4. Parietotemporal network	Parietal cortex, medial temporal cortex	[48]
5. Frontal–subcortical network	Bifrontal cortex, pons, subthalamic nucleus	[48]

While an individual patient's seizure-generating network is unique, clinical and electrophysiological observations can identify common networks and suggest targets for intervention

Differences in Seizure Patterns Based on Onset

The current state of responsive neurostimulation in epilepsies is limited by its indication for focal onset with or without generalization; thus, it needs adequate localization for its use. It thereby

fits within the maxim of "thinking globally while acting locally"; the sensing and/or stimulating electrodes are placed in the epileptic zone to disrupt the seizure-onset pattern (SOP) before it can propagate to the seizure-generating network. For some patients with temporal lobe epilepsy, whether they are poor candidates for invasive surgery, have localization to dominant temporal lobe, or have bilateral temporal lobe localization, RNS with rostrally directed depth electrodes that traverse the long axis of the hippocampi, or a temporal strip electrode that follows the parahippocampal gyrus may be therapeutically beneficial. RNS can also be used for seizures originating from a neocortical focus. This is particularly relevant when the seizure-onset focus is in eloquent cortex; up to two-thirds of patients undergoing focal resection in extra-temporal cortex have increased neurological deficits [59]. In this case, subdural strip electrodes or cortical depth electrodes over the neocortical focus can sense onset of the seizure and also used for stimulation designed to disrupt seizure propagation. As will be discussed further, in multifocal seizures, RNS in central nodes of distributed circuits, such as in the anterior thalamus [60] or centromedian thalamus (discussed later), have been attempted.

The electrographic seizure pattern (ESP) also termed ictal onset pattern (IOP) or seizure onset pattern (SOP) that is to be disrupted can vary between patients and by seizure-onset regions. The power–frequency or time–frequency spectrum of ESPs can be characteristic of seizure onset and be characteristic to onset location or pathology. For example, mesial temporal onset of seizures is associated with low-frequency high-amplitude repetitive spiking (LFRS; sometimes termed periodic spikes), while neocortical onset zones are typically associated with a low-voltage fast activity (LVFA) pattern [61]. Seizure onsets in focal cortical dysplasia often display polyspikes followed by LVFA while seizures initiated in malformations of cortical development with LVFA alone [62]. High-frequency oscillations (HFOs) are noted to accompany a number of different seizure onset patterns [63]. An important conclusion drawn by the shared electrographic patterns observed again strongly suggests shared focal and distributed networks that are subsumed by the ictal pathology.

Mechanism of RNS

The fundamental mechanistic difference of responsive neurostimulation is that it is a "closed-loop" system; "algorithmic interpretation of electrocorticographic signal results in direct electrical stimulation." Bursts of high-frequency electrical stimulation in a variety of cortical and subcortical structures has been proposed to disrupt seizures during propagation [3, 4]. The exact mechanism of this disruption by high-frequency burst stimulation remains an area of active investigation. Empirical observations have noted direct and indirect effects of stimulation. High-frequency responsive electrical stimulation has been observed to have an acute and direct local inhibitory effect in an epileptogenic zone by modulation of the spectral content of the SOP, as well as indirect amplitude attenuation and frequency modulation of the seizure onset pattern [2, 3, 64–68]. Hypothesized mechanisms of acute electrical stimulation are varied and informed by the literature attempting to understand deep brain stimulation; effects could be dependent on the local composition of the target of stimulation. (1) Inhibitory effects could be from depolarization blockade with high extracellular potassium concentration or inactivation of voltage-gated currents. (2) Inhibitory or excitatory end effects due to synaptic inhibition or excitation by antidromic and/or orthodromic axonal depolarization; orthodromic axonal activation could also lead to synaptic depression by neurotransmitter depletion. (3) Network modulation or desynchronization blocks "abnormal" flow of information [69, 70]. The described direct inhibitory mechanisms of stimulation do not however explain the indirect effects of seizure reduction well beyond the period immediately following responsive neurostimulation. Long-term network effects may be linked to neurotrophic factor expression changes in the local target of stimulation as well as the brain regions to which it projects [64]. A notable

feature of outcomes in patients implanted with responsive neurostimulators that may give insight into the mechanism, as discussed subsequently, is that seizure frequency reduction improves with duration of responsive stimulation [13].

The detection of the seizure occurs with a measurement of voltage at a specific seizure-onset area. That signal is used to train the RNS algorithms to determine what voltage patterns define a patient's epileptiform activity/seizure at that detector site. With clinician-set parameters, the RNS system can deliver a biphasic (charge-balanced) stimulation (1–333 Hz; 1–12 mA; 40–1000 μs pulse width). The specifics of parameter modification in relation to clinical judgment will be discussed later. An interesting and important factor to consider is the inflammatory reaction surrounding the detector/stimulation electrodes that can affect its electrical properties; reactive gliosis surrounding the electrode occurs within weeks of implantation and may alter electrode impedance, which typically stabilizes by 1 year post-implantation [71].

Responsive Neurostimulation (RNS) Device and Initial Outcomes

Device Hardware

As listed previously, the components of responsive neurostimulation devices consist of recording/detection electrodes placed at the seizure-onset site(s), a programmable neurostimulator equipped with algorithms to identify electrographic markers of seizures and several stimulation paradigms, stimulation electrodes that target the seizure-onset site or a node within the seizure circuit, and a wireless programming wand. Electrodes may be subdural strip electrodes or cortical/subcortical depth electrodes. The stimulator device contains a battery, the onboard computer that stores data, contains the algorithms for detection, and stores stimulation paradigms, and a radio-frequency transmitter/receiver for interrogation/programming with the wireless wand. Responsive cortical and subcortical neurostimulation was initially designed and tested with the RNS© System (NeuroPace, Mountain View, CA). While initial studies of RNS were performed with external responsive neurostimulators [11], the RNS System (leads and stimulator) is internalized at the time of implantation; the leads are targeted intracranially in patient-specific manner and the stimulator is placed in a fitted craniectomy. The current RNS System is capable of detecting and/or stimulating from one to two electrode arrays for a total of four bipolar recording channels. It is predicted, however, that future iterations will likely increase the electrode number. To date, the RNS© System is the only FDA-approved responsive stimulation device available for clinical use, although other conceptually similar responsive devices are undergoing clinical trial testing; RNS is approved for focal-onset (1–2 foci) medically refractory epilepsy. Few studies have considered the long-term effects of chronically implanted responsive neurostimulation electrodes. It has been found that with the RNS© System electrodes, there may be some short-term variance of impedence, long-term (over 1 year) impendence was stable both for depth electrodes and subdural electrodes [71, 72]. The RNS device originally required replacement for low battery every 3–5 years. Recently, an updated model was released with a reported doubling of the battery life and data storage capabilities. As in DBS, there are a variety of factors affecting battery life including frequency of therapies, stimulation intensity, electrode impedance, and capacitor mode. Reports vary on the rates of infection after replacement of the cranial stimulator from 3.7% to 10% [73, 74]. Infection is an important issue as it most commonly mandates removal of all cranially and intracranially implanted hardware, which is often difficult.

Initial Trials of RNS in Epilepsy

The primary 2-year open-label safety study that included 65 patients ("feasibility" trial) was deemed successful for delivering safe and effective therapy [75, 76]. Adult patients (18–65 years old) with simple partial, complex partial, or generalized tonic-clonic seizures were implanted,

targeting the seizure focus. They found that median reduction in seizure frequency in the primary evaluation period was greatest for GTC (59%) and 27% for CPS; there was also a significant decrease (29%) of total disabling seizures ($p < 0.0001$). In the secondary evaluation period, the median seizure reduction was 66% for GTC and 34% for CPS; total disabling seizures decreased by 35% [76].

The first randomized controlled trial with RNS system ("pivotal" trial) assessed safety and efficacy. Two hundred forty adults (18–70 years old) with partial seizures and failed 2 or more antiseizure medications and suspected to have 1–2 sites of seizure onset were recruited. One hundred ninety-one adults were implanted and allowed 1 month to recover. Then they were randomized to have responsive stimulation or sham stimulation, with no significant differences in age, gender, number of antiseizure medications, number of seizures per day, temporal lobe onset, multifocal onset, prior epilepsy surgery, or prior intracranial electrocorticography. Outcomes were assessed in two time frames: a 12-week blinded period and an 84-week open-label period. During the randomized period, 96 of 97 patients completed responsive stimulation and 93 of 94 patients completed sham stimulation. In the 84-week open-label responsive stimulation period, 176 of the 187 patients had completed or were yet to complete responsive stimulation. This first study showed that the mean seizure frequency was reduced in all patients (prior to randomization) compared to baseline, suggesting an effect of implantation; this has been noted in anterior thalamic deep brain stimulation for refractory epilepsy as well [26]. Across the entire blinded period, the mean seizure frequency was significantly reduced in the responsive stimulation group by 37.9% compared to 17.3% in the sham stimulation group. Importantly, this reduction remained significant when adjusted for seizure-onset site, multifocality, or prior surgical treatment. In the blinded period, patients with responsive stimulation also had 11% more seizure-free days (27% in responsive stimulation group vs. 16% in sham group). Interestingly, quality of life measures (QOLIE-89) were significantly improved in all patients, both in the blinded period and the open-label period.

The initial study reported a significant adverse event rate of 12% in 28 days postoperatively and 18.3% in 84 days postoperatively. Six patients died, four of which were attributed to sudden unexplained death in epilepsy (SUDEP). Specific reported rates included intracranial hemorrhages 4.7% (9 patients) and implant-related or surgical-site infection 5.2% (10 patients).

Long-term outcomes of patients implanted in the feasibility and pivotal trials were assessed, including 191 patients and mean follow-up of 5.4 years. Long-term seizure reduction rates at the beginning of years 3–6 were 60%, 63%, 65.5%, and 65.7%, respectively. Eighty-four percent of patients showed some improvement in seizure frequency; 60% had seizure frequency reduction by greater than one-half; 12.9% of patients had at least 1 period of seizure freedom lasting ≥1 year. The most recent 9-year follow-up shows a median of 67.2% seizure reduction across 230 patients; one-third of patients achieved over 90% seizure frequency reduction in their most recent 3-month period [77].

RNS Efficacy and Onset Site

RNS appears to be effective for focal epilepsy regardless of the onset lobe. As discussed earlier, the most common sites of RNS placement include temporal lobe structures (including hippocampus) and neocortical targets. Less commonly the insula or other subcortical structures shown to be central nodes in a distributed seizure-generating network. Recently, targeting has included the thalamus in some patients. When subgroup analysis was done specifically on patients with mesial temporal lobe epilepsy, the median seizure reduction was 70% over 6 years of follow-up; 15% of patients had at least 1 period of seizure freedom lasting ≥1 year [78]. Interestingly, lead precision did not seem to affect efficacy; effective leads were found in hippocampal and parahippocampal tissue on postoperative imaging. A prospective randomized controlled trial of 126 patients, pooled from the feasibility and pivotal trials

(described earlier), with partial seizures originating from a neocortical onset trialed with the NeuroPace RNS System found that the median seizure reduction rates for frontal/parietal, temporal, and multi-lobar onsets were 70%, 58%, and 51%, respectively [59]. Responsive insular cortical stimulation shows 50–75% seizure frequency reduction [79].

RNS and SUDEP

Sudden unexplained death in epilepsy (SUDEP) is a significant cause of epilepsy-related mortality, particularly in patients with medically refractory seizures [80]; however, the underlying and likely heterogenous mechanisms are still unknown. By its nature, the continuously recording responsive neurostimulators electrodes might become important tools to evaluate potential mechanisms of SUDEP and efficacy of seizure reduction on SUDEP risk. In one study considering 707 patients implanted with the RNS device, 7 SUDEP events were identified (2 possible, 1 probable, 4 definite), 3/7 had a >50% seizure reduction in the 3 months prior to SUDEP, and 2/7 had the RNS disabled at time of SUDEP [80]. Notably, 3 of the 5 definite or probable cases of SUDEP had increased epileptiform activity on the responsive neurostimulator electrodes just prior to death; however, 1 patient with SUDEP did not have any epileptiform activity on RNS electrodes near the time of death [80]. Responsive neurostimulation, by decreasing seizure frequency, is suggested to confer decreased SUDEP rate (2/1000 patient-stimulation years, CI 0.7–5.2) [80] compared to medication (6.1/1000 patient years, CI 3.3–10.3) [81] or patients that underwent epilepsy surgery but with recurrent seizures (6.3/1000 patient years, CI 3.0–11.6) [82].

Neuropsychiatric Outcomes with RNS

Neuropsychological testing holds a crucial role in evaluation of patients suffering epilepsy, especially because many psychiatric diseases are comorbid with epilepsy. The pathophysiological relationship is unclear, but overlapping network associations have been hypothesized [51]. Neuropsychological evaluation data through 2 years of responsive neurostimulation from 175 of the 191 patients enrolled in the pivotal trial suggests modest but statistically significant benefits in verbal cognition, specifically in (1) the Boston Naming Test specifically for patients with neocortical seizure onset and (2) the learning phase of the Rey Auditory Visual Learning Test specifically in patients with mesial temporal lobe seizure onset [83]. Interestingly, cognitive improvements were not directly correlated with reduction in seizure frequency or changes in antiseizure medications [83]. Analysis of quality of life of the 191 patients from the pivotal trial showed that at 2 years 44% noted improved quality of life, regardless of seizure onset, while only 16% of patients reported quality of life declines [84].

Pediatric Responsive Neurostimulation

Although responsive neurostimulation is not currently approved for medically refractory epilepsy for patients under 18 years old, a number of off-label pediatric cases have been reported [85, 86]. The AAN and ILAE have defined medically refractory epilepsy as the failure to control seizures with 2 or more tolerated and appropriately scheduled antiseizure medications. However, the majority of patients with refractory epilepsy are not appropriately referred for surgical evaluation, despite years of advocacy. Increasing evidence shows that the extended duration before patients with medically refractory epilepsy are referred for surgical evaluation can decrease the odds of successful therapy. Increasing evidence suggest that the longer a patient has refractory epilepsy, the more intractable the seizures become to all treatments, including surgery. It is also established that increased duration of seizures can change the nodes and connectivity in the seizure-generating network. Finally, the risk of SUDEP is highest in patients with medication refractory epilepsy. Thus, the need for early treatment of refractory

seizures in children is becoming increasingly recognized. Case reports of pediatric applications of the NeuroPace responsive neurostimulation have suggested its utility as an "adjuvant" therapy after resection [86], for refractory seizures [85], and over eloquent cortex [85, 86]. The first reports of pediatric RNS were bilateral anterior thalamic RNS and angular/supramarginal gyrus RNS implants improved seizure frequency by 80–90% in two pediatric patients [85]. Similarly, a 16-year-old patient with an incompletely resected left temporal focal cortical dysplasia was treated with an RNS system implanted with a depth electrode in the insula and an angular gyrus/posterior superior temporal gyrus strip electrode; she was found to have reduced seizure intensity and duration at 2 months postoperatively and only auras but no awareness-impairing seizures at 6 months postoperatively [86]. The "immature" seizure-generating network may be particularly susceptible to the desynchronizing effects of responsive neurostimulation, resulting in effective seizure reduction; this hypothesis remains to undergo rigorous scientific testing. However, empirical evidence suggests its validity. One of the unique technical aspects of RNS in children is the placement of the stimulator and ferrule in the required craniectomy; however, no reports of significant difficulties were encountered even the in the youngest reported case of RNS in a 9-year-old child [85].

Surgical Implantation and Techniques

The NeuroPace responsive neurostimulation system (RNS) is an FDA-approved adjunctive therapy in reducing the frequency of seizures in individuals 18 years of age or older with partial-onsent seizures. The labeling for the RNS indicates that the system is used in patients who "have undergone diagnostic testing that localized no more than 2 epileptogenic foci, are refractory to two or more antiepileptic medications, and currently have frequent and disabling seizures." For most patients implanted with the RNS system, the "diagnostic testing" that localizes the seizure-onset zone(s) involves an intracranial study. At our center, it is rare for patients to undergo RNS placement without a preceding intracranial EEG study. There are a few exceptions to this general principle, typically in patients with clear bilateral medial temporal lobe (MTL) epilepsy or unilateral MTL patients with clear, concordant presurgical evaluation who are not candidates for anterior medial temporal lobectomy or unwilling to undergo resection or LITT ablation of the MTL structures. Once the patient's seizure-onset zone or two onset zones are identified, there are a variety of techniques available for the placement of RNS electrode arrays and the RNS device. The major considerations in RNS surgical planning include the following: (1) the electrode arrays to be utilized for maximal coverage of the seizure-onset zone(s), (2) the craniectomy for implantation of the RNS device, (3) stereotactic equipment, devices, and techniques utilized for the placement of the electrode arrays, (4) timing of the RNS implantation in the majority of patients who undergo preceding intracranial EEG study for seizure-onset localization, and (5) incorporation of the incisions and craniotomies/craniectomies that were utilized for the preceding intracranial study.

The RNS system has a few electrode array configurations, each array having four electrode contacts in either a strip or depth electrode array (Fig. 12.3). The strip electrode arrays all come with the standard circular electrodes with 1 cm spacing between each of the electrode contacts. The strip arrays come with 15, 25, or 35 cm of lead wire connected to the strip. The depth electrode arrays also have four cylindrical electrode contacts with two spacing configurations. Depth electrode arrays are available with either 3.5 mm electrode spacing for more compact structures or 10 mm spacing between the electrode contacts. Each variety comes with either 30 or 44 cm in total length depending on the length or wire desired to connect to the RNS device. Cortical onset zones can be covered with either strip or depth electrode arrays. Most commonly, strip electrode arrays are utilized to cover the cortical surface onsets and depth electrodes are utilized for cortical onset zones shown to be deeper, that is, within a sulcus, during intracra-

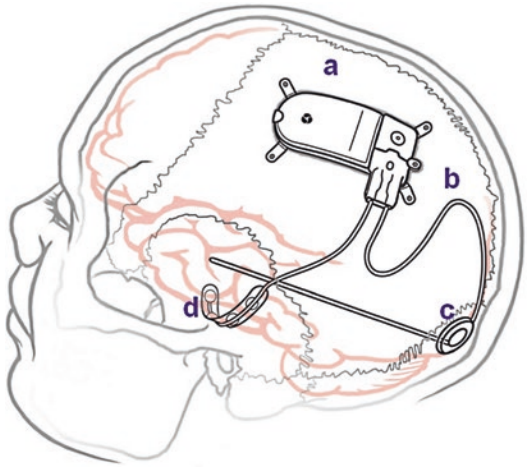

Fig. 12.3 Schematic of the Implanted RNS® System. The RNS® neurostimulator is held within the ferrule/housing implanted in the cranium (**a**). The neurostimulator is connected to two intracranial electrode arrays/leads (**b**). In this example, the RNS System includes a longitudinal depth electrode array within the medial temporal structures (**c**) and a subdural strip electrode array over the parahippocampal and inferior-lateral temporal regions (**d**). (Modified image used with permission from NeuroPace, Inc.)

nial study. Multiple electrode arrays can be combined to enhance coverage of an onset zone with multiple strips for broader coverage or a combination of multiple depths or depth and strip arrays to cover both surface and deeper cortical onsets.

The electrode arrays and onset zone(s) to be covered will dictate the surgical approach or approaches required for implantation of the electrode arrays. For example, in Fig. 12.3, the implant includes a medial temporal longitudinal depth electrode array (hippocampus and amygdala) and a subtemporal and parahippocampal strip electrode array. Each of these arrays will require the planning of incision, burr hole or small craniectomy, and tunneling of electrode array leads to the RNS device. Alternatively, a larger incision can be designed to incorporate the placement of all of the components of the RNS system, including the craniectomy required for placement of the RNS device. This example also includes the use of multiple approaches, which requires stereotactic equipment and potentially multiple patient positionings for successful placement of the electrode arrays and RNS device.

Once the electrode array configurations to be utilized have been determined, the location of the craniectomy for RNS ferrule/housing and device implantation must be incorporated into the surgical plan in addition to the electrode array placements. As there is wide variation in the location of target seizure-onset zones, electrode arrays for covering the onset zone(s), and implantation techniques, there is no "standard" RNS system implantation approach. The RNS housing and device have a subtle curvature, which allows it to fit the general cranial shape in a variety of locations. It has been our experience, however, that whenever possible the craniectomy for RNS implantation should be placed superiorly, above the temporalis muscle. This placement allows for replacement surgery without repeat disruptions of the temporalis muscle, minimizing discomfort and potential cosmetic deformity from temporalis atrophy. In addition, the RNS housing and device produce significant amount of artifact from beam scattering in post-op CT imaging. The more superior placement of the RNS device minimizes the extent of this artifact. There are a few additional general principles to surgical planning for the RNS system. When possible, it is beneficial to plan a separate incision for the craniectomy and placement of the RNS housing and device, especially when using only depth electrode arrays. Also, direct and place the excess lead wire off from the RNS device and away from the incision and future surgical approach for RNS device replacement (see Fig. 12.4, yellow arrow). This approach again makes replacement surgeries more straightforward and lowers the risk of inadvertent lead wire injury during replacement surgery. Electrode lead wire placed on top of the RNS system could potentially interfere with electronic communication for analysis, data offloading, and programing. If the RNS implant design involves all strip electrode arrays, it can be feasible to design the craniectomy for the RNS housing and device such that the strip arrays are placed via this craniectomy. When this single craniectomy approach is utilized, the lead wires should exit through the craniectomy away from

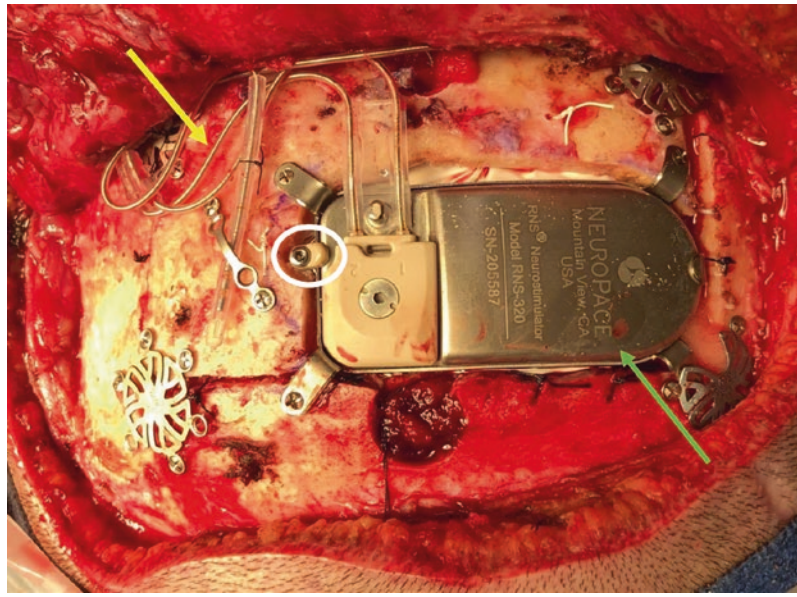

Fig. 12.4 RNS ferrule and device implanted into corner of prior craniotomy. A portion of the bone flap matching the RNS ferrule was removed from the bone flap and the RNS ferrule is attached to both the bone flap and the native skull. Several additional cranial fixation plates and screws are utilized to secure the bone flap with the RNS device. Note that the RNS device is positioned such that only a portion of the incision will be required during replacement surgeries, the lower and right portions of the incision. Once the RNS device is placed within the RNS ferrule, it is held into the ferrule by the set screw with small plastic flange (*white oval*). The RNS device is close to the incision but not directly under the incision. In addition, the RNS electrode array wires and connection to the device is kept away from the incision (*yellow arrow*). During future replacement surgeries, there are no wires between the incision and the RNS device (*green arrow*)

the site of the connector head and as much as possible away from the incision and approach for future device changes.

After the seizure-onset zone(s) have been identified, the electrode arrays determined, and the placement of the RNS housing and device decided, the overall design of the surgical implantation is then tailored to the specific circumstances of the patient and the stereotactic, surgical, and intra-procedural imaging equipment available to the surgeon. Given the variety of targets, electrode arrays, and techniques, any of the widely utilized stereotactic platforms (frameless, fiducial based, frame-based, robotic, or direct image-guided) can be utilized for the placement of electrode arrays within the target seizure-onset zone(s). In general terms, the stereotactic systems utilized will depend on the overall design of the implant, the location of seizure-onset zone(s), and the trajectory length to the targeted seizure-onset zone(s). At our center, we have utilized frameless navigation, a stereotactic robotic system, and direct image-guided systems for placement of depth electrode arrays depending on the trajectory length. We typically utilize a frameless stereotactic system for placement of strip electrodes on the cortical surface and cortical depths placed along with strips during a cortical RNS implant with both electrode array types. When using RNS depth electrode arrays targeting deeper structures with longer trajectory lengths, we prefer the increased accuracy of direct image-guided placement, frame-based, or stereotactic robotic placement of depth electrodes. In fact, with experience, it has become our preference to place depth electrodes separately from the RNS housing and device in depth-only RNS implants (i.e., bilateral MTL). The staging the implant of depth electrodes and the RNS ferrule and device is similar to the commonly used

approach in DBS. The staged approach provides for highly accurate placement of depth electrodes with postimplant imaging that confirms the desired position of the depth electrodes before the imaging limitations and artifacts of the RNS housing and device are introduced. The most crucial element is that neurosurgeons performing RNS implants be familiar and comfortable with the operative environment and the stereotactic and surgical equipment to be utilized in the RNS implant.

RNS Implantation Following Intracranial Electrode Study

As mentioned earlier in this chapter, it is common for epilepsy patients to undergo an intracranial electrode study for localization of seizure-onset zone(s). Thus, there are often additional considerations for the RNS implant surgery, depending on the technique and approach used for the intracranial electrode study. The first of these considerations is the timing of the RNS system implant relative to the intracranial study. Some surgeons have reported implantation of the RNS system in the same setting as removal of the intracranial electrodes in cases when the access needed for implantation of the RNS electrode arrays and device are present from a craniectomy used for the intracranial study. Although it has been suggested that infection rates are acceptable, it has been our practice to delay the implantation of permanent hardware such as the RNS system for a period of 4–6 weeks after the completion of the intracranial study. The majority of surgeons implanting RNS systems following an intracranial study for seizure-onset localization wait for some period of time between the intracranial study and RNS implantation surgery. In fact, over the last two decades, it has become our general practice to defer definitive surgical intervention for a period of 4–6 weeks after the intracranial study, unless the definitive intervention involves cortical resection or multiple subpial transections that can be performed through the craniotomy performed for the intracranial study. Furthermore, in intracranial study cases involving craniectomy for grids and strips, we typically do not replace the bone flap until the definitive surgical treatment when it involves similar cranial access or RNS implantation. This approach has significantly lowered our rate of infection following intracranial studies. In these instances, the cranial defect is covered with a titanium mesh until the definitive surgical treatment. With the growing usage of depth-only intracranial studies, stereoelectroencephalogram (SEEG), it is common to delay the RNS implantation surgery because there are no incisions or craniotomies involved in the SEEG intracranial study.

Given that the majority of RNS implants are delayed following an intracranial study, it is therefore important to store the location of seizure-onset zone(s) to be targeted in the subsequent RNS implant surgery. To this end, all of our patients undergoing intracranial study undergo post-implant volumetric CT and MRI imaging for localization of all implanted electrodes. We utilize an in-house developed program for electrode localization, which interfaces with our frameless stereotactic navigation system. This provides the capability of using stereotactic navigation to return to the location of any electrode contacts found to be critical in the patients' seizure-onset zone(s) during RNS implantation. There are a few software programs available with the capability to localize each implanted electrode. In cases of patients proven to have MTL seizure onset, the long axis of the hippocampus and amygdala are most commonly targeted anatomically from a posterior, occipital–parietal approach. If necessary, the location of the identified onset electrodes from the intracranial study can be colocalized during the trajectory planning for MTL depth electrode implantation.

There are several other considerations for RNS implantation surgery in patients who have undergone prior surgery. In those patients who have undergone a prior craniotomy or craniectomy for resection or intracranial study, the prior approach must be taken into account during RNS implantation surgery. This starts with securing the head for stereotactic navigation. Care must be taken in the attachment of whatever cranial stabilization device is utilized (i.e., MAYFIELD®

skull clamps, Leksell or CRW frame) to avoid pin placement onto the prior craniotomy or craniectomy site. It is best to avoid pin placement over prior craniotomy site, even in cases of remote prior surgery as antiepileptic medications are known to inhibit bone healing. Therefore, it should not be assumed that a remote craniotomy flap will have fused with the native skull. The incision or incisions utilized for RNS implant surgery must take into account any prior incisions utilized for the intracranial study or prior resection. It is critical to design the RNS implantation incision(s) to avoid excessive interruption of scalp vasculature. In general, if the RNS implant is in the same or similar region as the prior intracranial incision, then the prior incision should be utilized with appropriate modifications to provide the exposure required for the RNS implantation. Care should be taken to minimize additional interruption of scalp perfusion and minimize the potential cosmetic impact. Furthermore, when performing an intracranial study with a planned craniotomy in a patient who may be an RNS candidate, the incision utilized for the intracranial implant should anticipate potential future RNS implant surgery. Finally, the incision and RNS placement should be designed to optimize future device replacement surgeries as well, whenever possible.

In addition to any prior incision(s), any prior craniotomies or craniectomies must also be considered. Most commonly, the prior craniotomy/craniectomy site is utilized for the placement of the RNS ferrule and device. In this instance, the RNS ferrule can be placed into the middle of the bone flap or a portion of the craniotomy flap designed to fit the RNS ferrule is removed and at least half of the ferrule is attached to native skull. Often, a considerable amount of design and work is required for optimal placement of the RNS ferrule and device in the setting of a prior craniotomy/craniectomy. Figure 12.4 shows a complex example of an RNS implant following an intracranial study with prior craniotomy. The RNS ferrule and device are positioned in the corner of the craniotomy flap and attached to both the craniotomy flap and the native skull. Several additional standard cranial fixation devices are utilized to ensure security of the bone flap. As previously mentioned, antiseizure medications can inhibit proper bone healing and therefore craniotomy flaps are replaced with several fixation plates. The RNS device and housing is positioned close to a portion of the incision but not directly under the incision. This allows future device change surgeries to utilize only a portion of the incision to access and change the RNS device. In addition, the electrode array lead wires exit through burr holes that are away from the incision and the excess wire is kept away from the incision (Fig. 12.4, yellow arrow), future approach during surgeries to remove and replace the RNS device and away from the lead wires and the connector region of the RNS (Fig. 12.4, green arrow). Alternatively, the craniectomy for the RNS ferrule and device can be designed outside of the craniotomy flap or partially overlapping with the craniotomy flap and the native skull. The first option requires additional exposure for the craniectomy, which can be difficult or impossible within the exposure provided by the incision. The later option requires less additional exposure but requires a new craniectomy and removal of a portion of the craniotomy flap that fits together precisely to accommodate the RNS ferrule.

RNS implantation done following depth-only intracranial studies, commonly referred to as stereoelectroencephalogram (SEEG), is most often done in a delayed fashion. The SEEG technique utilizes placement of depth electrodes through a series of small burr holes and does not utilize any incision. Therefore, RNS implantation following an SEEG study does not have any prior incisions or craniotomies to account for, and the RNS implant can be designed based on optimal positioning of the RNS ferrule and device, the target onset zone(s), and the electrode arrays to be utilized.

Implanting RNS Depth Electrodes

As mentioned, there are a variety of stereotactic techniques that can be utilized for the placement of RNS depth electrodes. Experienced epilepsy surgeons have described the use of frameless ste-

reotactic navigation, frame-based targeting, and stereotactic robotic placement of RNS depth electrodes with adequate accuracy. Our center was the first to describe the use of ClearPoint® for direct image-guided placement of RNS electrodes using intraoperative MRI [87]. In a depth-only RNS implantation, the trajectories are planned using volumetric imaging (MRI and/or CT) and stereotactic targeting software. The entry site burr holes should be kept away from the RNS ferrule craniectomy and clear from the incision that will be used for replacement surgeries. Depending on the design of the implant, the burr holes can be performed within the same incision as the craniectomy for the RNS device or through separate small linear or curvilinear incisions. We prefer to keep the burr holes away from the RNS device and through separate small incisions when possible. This allows the excess lead wire to be kept away from the RNS device. It is recommended that burr holes are utilized and the RNS electrode is secured within the NeuroPace® Burr Hole Cover Model 8110. Other methods for securing the RNS electrode wire are available and effective. It was reported during the pivotal trial that electrode wires secured by a small titanium "dogbone" plate were more likely to break and therefore we avoid this technique whenever possible. Patient positioning depends on the entry sites of the planned trajectories. The head is placed into the MAYFIELD head holder or frame depending on the stereotactic technique utilized for depth electrode placement. Placement of RNS depth electrodes into the MTL structures for patients with MTL epilepsy is most commonly done with a posterior occipital–parietal approach to place the RNS depth electrode along the long axis of the hippocampus. Figure 12.5 shows the use of ClearPoint® and intraoperative MRI for direct image-guided placement of RNS depth electrodes into the MTL structures (hippocampus and amygdala). In some RNS implants, such as those with bilateral MTL electrodes, the placement of the RNS ferrule and device may require a separate positioning of the patient and head. In addition, postoperative imaging is limited to CT imaging as none of the RNS components are MRI compatible, and after placement of the RNS ferrule and device there can be considerable artifact. With experience, it has become the preference at our center to place the depth electrodes in a separate surgery than the RNS ferrule and device, similar to the approach commonly utilized for DBS implantation surgery. We utilize this staged approach most commonly for RNS implantation designs that require different positioning and stereotactic equipment for the two aspects of the procedure. This also allows us to verify that the depth electrodes are optimally positioned before the craniectomy and RNS

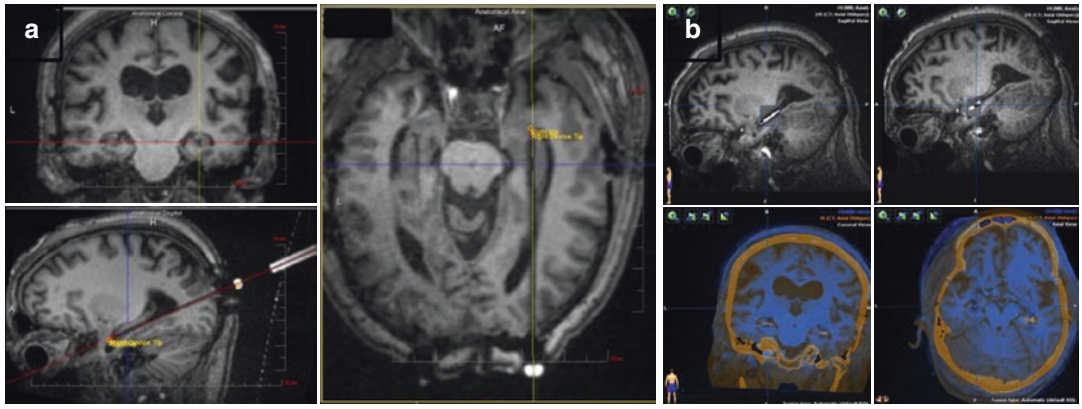

Fig. 12.5 The use of the ClearPoint® system and intraoperative MRI for direct image-guided placement of RNS depth electrode arrays to the bilateral MTL structures (hippocampus and amygdala). (**a**) Intraoperative MRI showing the tower aligned and placement of ceramic stylet and cannula. (**b**) Fusion of intraoperative MRI with post-op CT showing electrode placement directly within the operative trajectory and within the MTL structures

device implantation is completed. Alternatively, the patient can be repositioned and the entire procedure completed in a single two-stage operation.

Implanting RNS Strip Electrodes

For cortical based seizure-onset zones, strip electrodes are commonly utilized. The placement of RNS strip electrode arrays requires small craniectomy and opening of the dura for placement of the strip electrode array(s) into the subdural space. In patients who have prior recent craniotomy for localization of seizure-onset zone(s) via intracranial study, the existing craniotomy can often be utilized for placement of the strip electrode arrays. Again, any of the widely used stereotactic techniques can be utilized to ensure proper placement of the strip electrode arrays. We commonly utilize a frameless stereotactic neuro-navigation system for cortical strip electrode arrays. The prior onset zone electrode locations are stored and colocalized with the volumetric imaging used for registration and stereotactic navigation if necessary. Strip electrode arrays should be secured to the dura once they are in appropriate position. Multiple strip electrode arrays can be sutured together to form grid-shaped coverage when desired.

If there is no prior craniotomy effecting the RNS implant, then the RNS system implant design is tailored as previously described. The strip electrode arrays can sometimes be placed via the craniectomy required for the RNS ferrule and device. This is often utilized with frontal and or parietal cortical locations that are more superior or cortical locations that can be covered by sliding the strip in the subdural space to the desired location from the RNS device craniectomy. Stereotactic neuro-navigation is utilized to ensure that the strip electrode is placed over the desired cortical region. The strip electrode arrays can also be placed via separate small craniectomy, utilizing stereotactic neuro-navigation to ensure the proper placement of the strip electrode arrays. A burr hole is most often insufficient for proper placement of strip electrode arrays unless the craniectomy is widened with high-speed drills and/or kerrisons. This is especially true if more than one strip is to be utilized. When using a separate craniectomy for placement of the strip electrode array(s), it is important to keep the separate craniectomy away from the craniectomy for the RNS ferrule and device and positioned to keep the excess lead wire away from the incision that will be utilized for RNS replacement surgery. This can be achieved through a single larger incision or through a separate incision with craniectomy for the strip electrode arrays. With a separate incision, the lead wire is tunneled under the scalp over to the RNS device, as always, keeping the lead wire away from the incision and approach to be utilized for RNS replacement surgery whenever possible.

Implanting and Connecting the RNS Device

The design principles for placement of the craniectomy to house the RNS ferrule and RNS device have been reviewed in prior sections. Once the location of the RNS ferrule and device has been determined, the provided template is utilized to outline the necessary craniectomy. Once the craniectomy is outlined, burr holes are placed at diagonally opposite corners of the craniectomy. The burr holes are positioned so that the outside edge of the burr hole matches with the edge of the craniectomy. The dura is then stripped underneath the desired craniectomy location. A high-speed drill with cutting blade and footplate is then utilized to complete the craniectomy, following the template line between the two burr holes. The RNS ferrule is then utilized to verify the fit within the craniectomy. Most often, the high-speed drill and kerrisons are utilized to modify the craniectomy until the RNS ferrule has a good fit within the craniectomy.

If the electrode arrays and RNS device are placed within the same incision for a cortical onset target, it can be beneficial to perform the RNS ferrule craniectomy prior to placing the electrode arrays. This decreased the risks of

damaging any electrode wires during drilling for the RNS ferrule craniectomy. Care must be taken to avoid durotomy and CSF loss as this can cause brain shift and inaccuracies in registered stereotactic neuro-navigation systems. If the same craniectomy is utilized for strip array placement, then the dura is opened as needed and the strip electrode arrays are placed. We try not to place the electrode arrays directly under the RNS device if possible as this makes post-op imaging difficult to interpret. Again, if strip electrode arrays are placed through the RNS craniectomy, then care should be taken to have the lead wires exit the cranium away from the RNS connector site and the incision. If depth electrodes targeting deeper structures are utilized through a separate craniectomy, it is recommended to place these electrode arrays before the RNS device craniectomy is performed to minimize the risk of excessive CSF loss and brain shift. Once the RNS ferrule is placed, it is secured into position by four standard titanium skull screws available from any cranial plating system kit.

The RNS device is then placed within the ferrule and the set screw is placed over the RNS device and tightened to the proper torque with the provided screwdriver (Fig. 12.4, white oval). The electrode array leads are then routed to the connector site of the RNS device and placed into the two ports of the RNS connector head. Care must be taken to be sure that the leads are all the way into the RNS connector head. There is a brown marking on the leads that should be just visible at the edge of the connector head when the leads are properly inserted into the RNS connector head. The RNS connector head is then connected to the RNS device by tightening the set screw in the center of the RNS connector head to the RNS device with the same screwdriver until the torque setting of the screwdriver is reached. The lead wires are routed into the grooves of the strain relief section of the device. Finally, the strain relief cover is placed over the lead wires connecting into the RNS connector head and this is snapped into position. Upon completion of the RNS implant, an intraoperative photo can be taken and placed within the patient's electronic medical record. This picture can be useful for any future questions regarding hardware positioning and for planning device replacement surgery. The RNS device is now interrogated and analyzed and ECoG recordings are obtained. The electrode impedances are tested and verified to be in the proper clinical range. Following this, several minutes of ECoG recordings are obtained to verify signal and proper ECoG recordings on the implanted RNS system. Many times, epileptiform activity can be visualized in these short ECoG recordings, which is reassuring for the positioning of the electrodes. The entire field is now irrigated copiously with saline or saline mixed with antibiotic solution once the entire system implant is completed. Vancomycin powder can be utilized over the entire field if desired. The scalp is then closed with standard surgical technique.

RNS System Programming

Introduction

Relative to most other neurostimulation modalities, the RNS system requires a more significant investment in individualizing programming to achieve the goal of responsive therapy. Programming is divided into two major phases, which are optimally performed sequentially. First, detection criteria are established to identify seizure onset patterns as accurately as possible. Once this is done, then stimulations are enabled and titrated. If the desired response is not achieved, more advanced measures may be taken, including varying the electrode contacts, the polarity mode, or even swapping the electrode leads altogether. Since seizure freedom is rare, there may be a continuous process of optimization over the years that a device remains implanted. The device counts seizure onset patterns, which are shown in graphical form in the programming interface and are useful to assess therapeutic response. The detection criteria set the sensitivity and specificity for seizure onsets, so if they are altered after therapy has been enabled the baseline counts will change. Therefore, detection settings are usually kept stable as much as possible after the initial programming.

Detection of Seizure-Onset Patterns

The RNS system provides electrocorticogram (ECoG) data that is used in the initial phase to identify ictal and interictal patterns and guide the programming of detection patterns. These ECoGs are recorded based on programmable triggers. Older models of the device can buffer up to 6 min of ECoG data (typically four 90-s recordings) with a 250-Hz sample rate and frequency response range of 4–90 Hz. As of 2019, the current model RNS-320 allows 12 min of data (e.g., eight 90-s recordings) [88]. The duration of these ECoGs is adjustable, as are the triggers. The most common triggers are "long episodes," which are periods of sustained detections lasting for a user-specified duration (default 30 s); saturations, which are times when the recorded activity in any channel exceeds a threshold (which is adjustable); magnet swipes, when the patient marks an event for recording; and up to four scheduled detections. The scheduled detections are useful to characterize baseline activity. The available ECoG recording slots are limited, so some of them can be reserved for one or more triggers to prevent them from being overwritten by later events. The most useful or accurate trigger varies between patients, but magnet swipes may be particularly useful early on as they are a direct indication of a patient's reported clinical events, serving a similar function as a push button in the epilepsy monitoring unit.

Three types of detection patterns are available in the current devices: a bandpass detector, line-length detector, and area-under-the-curve detector. Bandpass detectors identify power within a specified frequency band over a programmable duration. They can be used in various ways. A spike can be identified by a high frequency within a short time window. Neocortical seizures can often be captured early by beta or gamma range activity over a period of 0.5–1 s. A spectrogram of the ECoG is available in the programming interface to guide frequency-based detection [89]. Line-length detectors (also labeled as "power change" detectors) identify periods of high-voltage oscillations. Line-length measurements are based on a fractal measure [90] that is sensitive to seizure onset [91] and are computationally efficient to calculate. Practically, these can be used to capture polyspike activity, which may occur either at the onset or in the middle of the seizure. Area-under-the-curve detectors are a measure of absolute power based on amplitude-integrated EEG. They are used the least often but can help capture slow waves or, by setting a negative threshold, electrodecremental activity. They can also be helpful to detect activity changes in patients with a highly active background.

Each type of detector has a set of parameters to fine-tune accuracy, including a threshold above which it activates. By default, these detectors evaluate the signal relative to the recent baseline to identify a relative change. The duration of the baseline can be changed, or a detector can be set based on an absolute threshold instead. Within a single detection pattern, the three detector types can be combined by an AND rule. Up to four detection patterns can be programmed on up to two channels. Typically, 1–2 patterns are defined based on one of the electrodes and another 1–2 patterns for the other electrode. In advanced usage, additional Boolean logic can be applied between detections patterns across channels.

Default settings at the time of implantation are line-length detectors with 75% thresholds. These are usually sensitive enough to capture enough electrographic seizures to guide initial programming. By design, these initial detection patterns are sensitive but nonspecific, so they will need to be adjusted or replaced once some ictal ECoG recordings are available. Moreover, many seizures are poorly captured at onset by line-length detectors, so the default patterns will usually fail at the goal of early detections.

In most cases, seizure onset patterns will be detected many more times than clinical seizures. A typical frequency of episode starts (essentially total detections) is 500–1000/day. These appear to represent spontaneously aborted seizure onsets. It is unknown if treating these is necessary or even beneficial, but the prevailing hypothesis is that regularly stimulating these brief onset rhythms has a long-term neuromodulatory effect.

In practice, the detection patterns are never made so specific to treat only sustained or clinical seizures. By the time onset patterns evolve sufficiently to increase specificity to that degree, it is too late to abort them with stimulation.

Stimulation Settings

The currently available RNS system delivers up to five sequential therapies consisting of two bursts of biphasic square wave constant current stimulation (ten bursts total). The waveform is similar to that produced by stimulators used for cortical stimulation mapping. The two bursts in each therapy can be set to have identical parameters or, to save battery life, alternate stimulation between electrode leads. The possible ranges of stimulation are listed in Table 12.2 along with typical settings that have been determined empirically from over 10 years of device trials. If a detection pattern is sustained, stimulation therapies will continue to be delivered up to five times in a row, after which stimulation is exhausted. That is, after five consecutive stimulations with ongoing detection, the stimulation will not return while the device is detecting continuous seizure. Once detection stops, the stimulation resets. Each of the five therapies can be programmed individually. In almost all cases, they are set identically, especially when the device is first programmed, but in some situations certain practitioners assign higher intensities to later therapies to abort seizures better or even to provide patients with a sensation of high activity.

Table 12.2 Typical responsive neurostimulator programming parameters

Parameter	Available range	Typical neocortical	Typical hippocampal
Amplitude	0–12 mA	2–8 mA	1–3.5 mA
Charge density	0–25 μC/cm^2	1–4 μC/cm^2	1–3.5 μC/cm^2
Pulse width per phase	40–1000 μs	160 μs	160 μs
Frequency	1–333 Hz	200 Hz	100 Hz
Burst duration	10 ms–5 s	100 ms	100 ms
Electrode pattern	Each contact and the "can" can be set to +, −, or 0	Monopolar or lead-to-lead bipolar	Bipolar within lead

Lead polarity is conventionally represented in the shorthand (lead 1)(lead 2)(can), and contacts within each lead are labeled from the distal tip. In monopolar stimulation, one or both electrodes is set to anodal (or cathodal) stimulation and the can as the opposite, for example, (++++)(0000)(−) for anodal stimulation of lead 1. Unlike some other neurostimulation systems, the stimulation waveform consists of actively charge-balanced biphasic pulses. Therefore, the selection of anodal or cathodal stimulation may have minimal significance, although there have been anecdotal reports of anodal stimulation (for the first half of the biphasic pulse) being more effective. Monopolar stimulation provides a large field with gradual drop-off. In a lead-to-lead bipolar configuration, the leads are set to opposite polarity, for example, (++++)(−−−−)(0). For parallel electrodes, this method provides a relatively constant field between them. Conventional within-lead bipolar stimulation, for example, (+−+−)(0000)(0) for lead 1, provides focused stimulation with a steep drop-off [92]. This mode is often used in the medial temporal lobe to prevent a more posterior field from causing photopsias. Other much less common modes are guarded cathode (tripole), for example, (+−+0), or a wider bipole, for example, (++−−).

Once a stimulation paradigm is selected, the charge density can be increased incrementally between programming sessions by about 0.5 μC/cm^2 until reaching the target level of stimulation. Estimated charge density (provided in the programming interface) is a much better measure of stimulation intensity than current amplitude since the same current from the device will deliver vastly different charge at each electrode contact depending on the electrode configuration. This process of incremental adjustment typically takes months and may be sufficient to see an initial clinical response. Once the target is reached, the stimulation pattern, frequency, and burst duration can be adjusted, often in that order. If these adjustments fail to achieve the desired response over time, then, if more than two electrodes were

implanted initially, it may be possible to change the connected electrodes at the time of the next device replacement.

New stimulation settings must be tested during a live-streamed ECoG session before being enabled. The first reason is to make sure the stimulation can actually be delivered; if the charge exceeds device capacity or the capacitor mode, then an error will be displayed. The second reason is to make sure the patient can tolerate the setting. Common effects of stimulation at high charge densities are dysesthesias with subdural electrodes or photopsias with occipitotemporal depth electrodes [93]. Photopsias may be best appreciated in a dark room. The third reason is to make sure there are no afterdischarges or provoked seizures. When viewing the ECoG, it will be apparent that the recording is suppressed for a brief period during and after therapy delivery. This is done by the device to prevent stimulation artifact from erroneously triggering another detection.

Older models of device have several levels of battery-saving modes that adjust the number of capacitors used to deliver charge. The battery-saving feature is somewhat hidden in the current programmers (and were in a secret menu in the older model programmers). The lowest number of capacitors that can provide the desired charge density should be used as this can substantially extend battery life and time to device replacement. As of the current generation, RNS-320, capacitor modes are set automatically.

Utility of Data Provided by the RNS System

Assessing Clinical Response to Stimulation

As with antiseizure medications, VNS, and DBS, the conventional means to assess therapeutic response is patient reporting. NeuroPace provides an online diary [94] for this purpose that integrates with their online portal for provider data review. Although they are the current standard in studies of epilepsy patients, the accuracy of diary reports of clinical seizures is known to be poor. Even when diaries are attempted in the controlled environment of an inpatient epilepsy monitoring unit, less than 50% of all seizures (including less than 60% of bilateral tonic-clonic seizures) are reported [28]. Outpatient seizure reporting introduces further variability since diaries may not be at hand, lost, or forgotten [29]. Patient reporting will also miss "subclinical" seizures. One example of the importance of subclinical seizures is their influence on surgical outcomes [95]. Such seizures may have subtle behavioral manifestations that are not recognized, and they may affect cerebral metabolism, partial oxygenation, and blood flow [96]. We argue that these seizures should also be monitored and treated.

The RNS System provides several measures that can be used for a more objective assessment of clinical response, including total detection counts, "long episode" counts, and a subset of electrocorticograms (Table 12.3). These detections are all individualized to a patient's own ictal onset patterns. Long episodes appear to be particularly useful. In one study, long episode-triggered ECoGs were at least 92% specific for electrographic seizures in over half of patients [97]. This accuracy was seen despite only moderate interrater reliability in categorization of RNS-provided ECoGs [98]. Thus, long episode frequency could be considered a surrogate for seizure frequency that is at least as accurate if not better than a seizure diary.

Seizures captured as long episodes, saturations, or particularly as ECoGs may be directly informative to patients. Since many patients are unaware of their seizures, they often question if they have had a seizure. Telling a patient if an event was a seizure or not removes a level of uncertainty and may put them at ease. In cases where an ECoG is not recorded for a clinical event, some details of the detection can still be identified in an "initial interrogation report" that includes the time, detection pattern(s), and duration of each detection, up to a limit of approximately 500–1000 between interrogations (depending on the device model and available memory).

Table 12.3 Key data available from the NeuroPace RNS-320

Type of data	Data available	Approximate buffer limit
Event rates (hourly)	Episode starts Long episodes Saturations Magnet swipes	Several months
Event details	Time Trigger (detection pattern, saturation, magnet, etc.) Number of sequential detections of each pattern Number of stimulations Total event duration	~1000 events (1–2 days)
ECoGs	Scheduled Triggered (by long episode, magnet, or saturation)	12 min (e.g., eight 90-s recordings)
Programming settings history	Detection criteria Stimulation settings Definition of long episode duration	Indefinite (online)

Medication Responses

These measurements of possibly subclinical activity can also be used to assess response to medications [99]. There is no established biomarker to determine the response to antiseizure medications short of waiting to see their effect, often for months. Scalp EEG is a poor biomarker for most medications. In some cases, after medications are started, there is a clear, rapid decline in detection rates. In patients with stable detection settings, changes in detection counts (episode starts or long episodes) within the first 1–2 weeks correlate with eventual clinical efficacy or inefficacy [36, 100]. These data could be used to identify the efficacy of medication trials early to allow more rapid medication adjustments than conventionally possible.

Identification of Dominant Seizure Focus

The RNS System can be used for long-term epilepsy monitoring to lateralize seizures or identify the dominant seizure focus. Conventional epilepsy monitoring of around a week could easily miss seizures from the opposite side. In some patients with bitemporal RNS, the dominant focus will alternate over time [101]. Review of data from the NeuroPace Long-Term Treatment trial shows that this is not uncommon [39, 102]. Electrodes were presumably implanted bilaterally due to confirmed bitemporal disease. The time from the first recorded seizure on either side until the first seizure on the opposite side was measured in each patient. Out of 69 patients, 25 had bilateral seizures within the first week, but 22 had unilateral seizures alone for more than 4 weeks, and 6 had unilateral seizures alone for more than 7 years. If one focus turns out to predominate over a long enough time period, then it might even be amenable to later resection with a potentially good outcome [103].

Temporal Patterns of Epileptiform Activity

The event rates stored by the device provide a convenient means to identify temporal patterns of seizure activity and can be used to guide medication timing, rescue medications, and identify potential precipitants of seizure activity. At the most granular level, essentially all patients display a strong circadian cycle. This is discernible even with a simple line-length detector, which yields a bimodal distribution [31]. These circadian patterns have been shown to differ by seizure-onset location [104, 105]. Understanding of circadian cycles may allow altered medication management and identification of patients at increased risk of sudden unexpected death in epilepsy.

Review of daily event rate graphs often also reveals clear multiday (infradian or multidien) cycles. Such cycles may be on the order of several days, weeks, or longer. The combination of multiple scales of these circadian and infradian cycles has been proposed to modulate seizure risk in a manner useful to develop a seizure forecasting algorithm [97]. At a more practical level, knowledge of seizure cycles may allow behavioral modification or increased medications at peak times of activity.

Future Directions

The RNS device is the first FDA-approved closed-loop or "responsive" neurostimulation device. It has been shown to be a safe and effective therapy for patients with refractory epilepsy who are not candidates for surgical resection. This device has created an entirely new source of long-term intracranial data from patients with chronic, refractory epilepsy and these data have led to new discoveries into epilepsy and epilepsy therapy. At the present time, however, the RNS device and the data acquired are limited in the scale of available neurophysiological data and acquisition and computing hardware. For example, the original RNS device could store only six min of ECOG data and the battery would last on average 3–4 years. Recently, a new model was released, which doubled the battery life and data storage capabilities of the RNS device. The most obvious future directions for responsive neurostimulation and the RNS device is the improvement in the capabilities of the hardware, including electrode arrays, number of channels available, data sampling rate, data storage, and transmission capabilities. Many of our RNS patients have more than two electrode arrays implanted. It is hoped that future RNS devices will provide for the use of more than two electrode arrays. In addition, if the patient does not have a good result with their responsive neurostimulation, the electrode arrays could be changed without additional intracranial surgery, perhaps during device change surgery.

In addition, new targets and techniques of responsive stimulation in the treatment of refractory epilepsy are under investigation. Ongoing research suggests that the epileptic network can be widespread, even in focal-onset epilepsies. Additional subcortical nodes within a patient's seizure-generating network could be targeted for a neuromodulatory and disruptive neurostimulation therapy. For example, several groups have reported implanting RNS depth electrode arrays into the thalamus, using both the anterior nucleus (ANT) and the centromedian nucleus (CMT). Recently, our group reported the first responsive stimulation of the centromedian nucleus of the thalamus, an intralaminar nucleus, known to have input from basal ganglia structures and widespread cortical outputs, was in a patient with multifocal bilateral parietal onsets of seizures [40]. The data from this patient has shown that seizure onsets can be detected in the CMT, providing the first in human data that seizure propagation and perhaps even onset can be recorded and detected in the thalamus, making the thalamus an attractive target for the treatment of patients with multiple or broad cortical seizure-onset zones.

References

1. V H. Paris letter. Science. 1886;7(170):409–12.
2. Penfield W, Jasper HH. Electrocorticography. In: Epilepsy and the functional anatomy of the human brain. Boston: Little Brown; 1954.
3. Lesser RP, Kim SH, Beyderman L, Miglioretti DL, Webber WR, Bare M, et al. Brief bursts of pulse stimulation terminate afterdischarges caused by cortical stimulation. Neurology. 1999;53(9):2073–81.
4. Lesser RP, Luders H, Klem G, Dinner DS, Morris HH, Hahn J. Cortical afterdischarge and functional response thresholds: results of extraoperative testing. Epilepsia. 1984;25(5):615–21.
5. Faber J, Vladyka V. Antiepileptic effect of electric stimulation of the locus coeruleus in man. Act Nerv Super (Praha). 1983;25(4):304–8.
6. Motamedi GK, Lesser RP, Miglioretti DL, Mizuno-Matsumoto Y, Gordon B, Webber WR, et al. Optimizing parameters for terminating cortical afterdischarges with pulse stimulation. Epilepsia. 2002;43(8):836–46.
7. Vercueil L, Benazzouz A, Deransart C, Bressand K, Marescaux C, Depaulis A, et al. High-frequency

stimulation of the subthalamic nucleus suppresses absence seizures in the rat: comparison with neurotoxic lesions. Epilepsy Res. 1998;31(1):39–46.
8. Psatta DM. Control of chronic experimental focal epilepsy by feedback caudatum stimulations. Epilepsia. 1983;24(4):444–54.
9. Peters TE, Bhavaraju NC, Frei MG, Osorio I. Network system for automated seizure detection and contingent delivery of therapy. J Clin Neurophysiol. 2001;18(6):545–9.
10. Osorio I, Frei MG, Manly BF, Sunderam S, Bhavaraju NC, Wilkinson SB. An introduction to contingent (closed-loop) brain electrical stimulation for seizure blockage, to ultra-short-term clinical trials, and to multidimensional statistical analysis of therapeutic efficacy. J Clin Neurophysiol. 2001;18(6):533–44.
11. Kossoff EH, Ritzl EK, Politsky JM, Murro AM, Smith JR, Duckrow RB, et al. Effect of an external responsive neurostimulator on seizures and electrographic discharges during subdural electrode monitoring. Epilepsia. 2004;45(12):1560–7.
12. Morrell MJ, Group RNSSiES. Responsive cortical stimulation for the treatment of medically intractable partial epilepsy. Neurology. 2011;77(13):1295–304.
13. Heck CN, King-Stephens D, Massey AD, Nair DR, Jobst BC, Barkley GL, et al. Two-year seizure reduction in adults with medically intractable partial onset epilepsy treated with responsive neurostimulation: final results of the RNS System Pivotal trial. Epilepsia. 2014;55(3):432–41.
14. Bergey GK, Morrell MJ, Mizrahi EM, Goldman A, King-Stephens D, Nair D, et al. Long-term treatment with responsive brain stimulation in adults with refractory partial seizures. Neurology. 2015;84(8):810–7.
15. Naritoku DK, Terry WJ, Helfert RH. Regional induction of fos immunoreactivity in the brain by anticonvulsant stimulation of the vagus nerve. Epilepsy Res. 1995;22(1):53–62.
16. Zabara J. Inhibition of experimental seizures in canines by repetitive vagal stimulation. Epilepsia. 1992;33(6):1005–12.
17. Takaya M, Terry WJ, Naritoku DK. Vagus nerve stimulation induces a sustained anticonvulsant effect. Epilepsia. 1996;37(11):1111–6.
18. Lockard JS, Congdon WC, DuCharme LL. Feasibility and safety of vagal stimulation in monkey model. Epilepsia. 1990;31(Suppl 2):S20–6.
19. Hammond EJ, Uthman BM, Reid SA, Wilder BJ. Electrophysiological studies of cervical vagus nerve stimulation in humans: I. EEG effects. Epilepsia. 1992;33(6):1013–20.
20. Olejniczak PW, Fisch BJ, Carey M, Butterbaugh G, Happel L, Tardo C. The effect of vagus nerve stimulation on epileptiform activity recorded from hippocampal depth electrodes. Epilepsia. 2001;42(3):423–9.
21. A randomized controlled trial of chronic vagus nerve stimulation for treatment of medically intractable seizures. The Vagus Nerve Stimulation Study Group. Neurology. 1995;45(2):224–30.
22. Ardesch JJ, Buschman HP, Wagener-Schimmel LJ, van der Aa HE, Hageman G. Vagus nerve stimulation for medically refractory epilepsy: a long-term follow-up study. Seizure. 2007;16(7):579–85.
23. Velasco F, Velasco M, Velasco AL, Jimenez F, Marquez I, Rise M. Electrical stimulation of the centromedian thalamic nucleus in control of seizures: long-term studies. Epilepsia. 1995;36(1):63–71.
24. Cooper IS, Upton AR, Amin I. Reversibility of chronic neurologic deficits. Some effects of electrical stimulation of the thalamus and internal capsule in man. Appl Neurophysiol. 1980;43(3-5):244–58.
25. Upton AR, Amin I, Garnett S, Springman M, Nahmias C, Cooper IS. Evoked metabolic responses in the limbic-striate system produced by stimulation of anterior thalamic nucleus in man. Pacing Clin Electrophysiol. 1987;10(1 Pt 2):217–25.
26. Fisher R, Salanova V, Witt T, Worth R, Henry T, Gross R, et al. Electrical stimulation of the anterior nucleus of thalamus for treatment of refractory epilepsy. Epilepsia. 2010;51(5):899–908.
27. David W, Damisah E, Gerrard J, Hirsch LJ, Quraishi I, Duckrow RB, Herlopian A, Spencer DD, Farooque P. Outcomes and predictors of outcome with the use of responsive neurostimulation at a single center. New Orleans: American Epilepsy Society; 2019.
28. Hoppe C, Poepel A, Elger CE. Epilepsy: accuracy of patient seizure counts. Arch Neurol. 2007;64(11):1595–9.
29. Blum DE, Eskola J, Bortz JJ, Fisher RS. Patient awareness of seizures. Neurology. 1996;47(1):260–4.
30. Bazil CW, Walczak TS. Effects of sleep and sleep stage on epileptic and nonepileptic seizures. Epilepsia. 1997;38(1):56–62.
31. Duckrow RB, Tcheng TK. Daily variation in an intracranial EEG feature in humans detected by a responsive neurostimulator system. Epilepsia. 2007;48(8):1614–20.
32. Herman ST, Walczak TS, Bazil CW. Distribution of partial seizures during the sleep--wake cycle: differences by seizure onset site. Neurology. 2001;56(11):1453–9.
33. Anderson CT, Tcheng TK, Sun FT, Morrell MJ. Day-night patterns of epileptiform activity in 65 patients with long-term ambulatory electrocorticography. J Clin Neurophysiol. 2015;32(5):406–12.
34. Karoly PJ, Goldenholz DM, Freestone DR, Moss RE, Grayden DB, Theodore WH, et al. Circadian and circaseptan rhythms in human epilepsy: a retrospective cohort study. Lancet Neurol. 2018;17(11):977–85.
35. Baud MO, Kleen JK, Mirro EA, Andrechak JC, King-Stephens D, Chang EF, et al. Multi-day rhythms modulate seizure risk in epilepsy. Nat Commun. 2018;9(1):88.
36. Imran H. Quraishi, Michael R. Mercier, Tara L. Skarpaas, Lawrence J. Hirsch. Early detection rate changes from a brain-responsive neurostimulation

system predict efficacy of newly added antiseizure drugs. Epilepsia. 2019. https://doi.org/10.1111/epi.16412.
37. Mercier M, Hirsch LJ, Duckrow RB, Quraishi IH. Early changes in responsive neurostimulator detection rates after introduction of anti-seizure drugs predict efficacy. 31st International Congress of Clinical Neurophysiology (ICCN) of the IFCN; Washington, DC, USA. Clin Neurophysiol. 2018;129(Suppl 1):e4.
38. Scoville WB, Milner B. Loss of recent memory after bilateral hippocampal lesions. J Neurol Neurosurg Psychiatry. 1957;20(1):11–21.
39. King-Stephens D, Mirro E, Weber PB, Laxer KD, Van Ness PC, Salanova V, et al. Lateralization of mesial temporal lobe epilepsy with chronic ambulatory electrocorticography. Epilepsia. 2015;56(6):959–67.
40. Gummadavelli A, Zaveri HP, Spencer DD, Gerrard JL. Expanding brain-computer interfaces for controlling epilepsy networks: novel thalamic responsive neurostimulation in refractory epilepsy. Front Neurosci. 2018;12:474.
41. Sun FT, Morrell MJ. Closed-loop neurostimulation: the clinical experience. Neurotherapeutics. 2014;11(3):553–63.
42. Kuo CH, White-Dzuro GA, Ko AL. Approaches to closed-loop deep brain stimulation for movement disorders. Neurosurg Focus. 2018;45(2):E2.
43. Bina RW, Langevin JP. Closed loop deep brain stimulation for PTSD, addiction, and disorders of affective facial interpretation: review and discussion of potential biomarkers and stimulation paradigms. Front Neurosci. 2018;12:300.
44. Widge AS, Malone DA Jr, Dougherty DD. Closing the loop on deep brain stimulation for treatment-resistant depression. Front Neurosci. 2018;12:175.
45. Molina R, Okun MS, Shute JB, Opri E, Rossi PJ, Martinez-Ramirez D, et al. Report of a patient undergoing chronic responsive deep brain stimulation for Tourette syndrome: proof of concept. J Neurosurg. 2018;129(2):308–14.
46. Denison T, Litt B. Advancing neuromodulation through control systems: a general framework and case study in posture-responsive stimulation. Neuromodulation. 2014;17(Suppl 1):48–57.
47. Ernst LD, Krause KL, Kellogg MA, Raslan AM, Spencer DC. Novel use of responsive neurostimulation (RNS system) in the treatment of super refractory status epilepticus. J Clin Neurophysiol. 2019;36(3):242–5.
48. Spencer SS. Neural networks in human epilepsy: evidence of and implications for treatment. Epilepsia. 2002;43(3):219–27.
49. Kramer MA, Cash SS. Epilepsy as a disorder of cortical network organization. Neuroscientist. 2012;18(4):360–72.
50. Scott RC, Menendez de la Prida L, Mahoney JM, Kobow K, Sankar R, de Curtis M. WONOEP APPRAISAL: the many facets of epilepsy networks. Epilepsia. 2018;59(8):1475–83.
51. Spencer DD, Gerrard JL, Zaveri HP. The roles of surgery and technology in understanding focal epilepsy and its comorbidities. Lancet Neurol. 2018;17(4):373–82.
52. Englot DJ, Konrad PE, Morgan VL. Regional and global connectivity disturbances in focal epilepsy, related neurocognitive sequelae, and potential mechanistic underpinnings. Epilepsia. 2016;57(10):1546–57.
53. Farrell JS, Nguyen QA, Soltesz I. Resolving the micro-macro disconnect to address core features of seizure networks. Neuron. 2019;101(6):1016–28.
54. Bartolomei F, Lagarde S, Wendling F, McGonigal A, Jirsa V, Guye M, et al. Defining epileptogenic networks: contribution of SEEG and signal analysis. Epilepsia. 2017;58(7):1131–47.
55. Sobayo T, Fine AS, Mogul DJ. A study of multi-site brain dynamics during limbic seizures. Conf Proc IEEE Eng Med Biol Soc. 2011;2011:7557–9.
56. Jirsa VK, Proix T, Perdikis D, Woodman MM, Wang H, Gonzalez-Martinez J, et al. The Virtual Epileptic Patient: individualized whole-brain models of epilepsy spread. Neuroimage. 2017;145(Pt B):377–88.
57. Marino AC, Yang GJ, Tyrtova E, Wu K, Zaveri HP, Farooque P, et al. Resting state connectivity in neocortical epilepsy: the epilepsy network as a patient-specific biomarker. Clin Neurophysiol. 2019;130(2):280–8.
58. Bharath RD, Panda R, Raj J, Bhardwaj S, Sinha S, Chaitanya G, et al. Machine learning identifies "rsfMRI epilepsy networks" in temporal lobe epilepsy. Eur Radiol. 2019;29(7):3496–505.
59. Jobst BC, Kapur R, Barkley GL, Bazil CW, Berg MJ, Bergey GK, et al. Brain-responsive neurostimulation in patients with medically intractable seizures arising from eloquent and other neocortical areas. Epilepsia. 2017;58(6):1005–14.
60. Elder C, Friedman D, Devinsky O, Doyle W, Dugan P. Responsive neurostimulation targeting the anterior nucleus of the thalamus in 3 patients with treatment-resistant multifocal epilepsy. Epilepsia Open. 2019;4(1):187–92.
61. Singh S, Sandy S, Wiebe S. Ictal onset on intracranial EEG: do we know it when we see it? State of the evidence. Epilepsia. 2015;56(10):1629–38.
62. Lagarde S, Buzori S, Trebuchon A, Carron R, Scavarda D, Milh M, et al. The repertoire of seizure onset patterns in human focal epilepsies: determinants and prognostic values. Epilepsia. 2019;60(1):85–95.
63. Perucca P, Dubeau F, Gotman J. Intracranial electroencephalographic seizure-onset patterns: effect of underlying pathology. Brain. 2014;137(Pt 1):183–96.
64. Kokkinos V, Sisterson ND, Wozny TA, Richardson RM. Association of closed-loop brain stimulation neurophysiological features with seizure control among patients with focal epilepsy. JAMA Neurol. 2019;76(7):800–8.

65. Child ND, Stead M, Wirrell EC, Nickels KC, Wetjen NM, Lee KH, et al. Chronic subthreshold subdural cortical stimulation for the treatment of focal epilepsy originating from eloquent cortex. Epilepsia. 2014;55(3):e18–21.
66. Lundstrom BN, Worrell GA, Stead M, Van Gompel JJ. Chronic subthreshold cortical stimulation: a therapeutic and potentially restorative therapy for focal epilepsy. Expert Rev Neurother. 2017;17(7):661–6.
67. Osorio I, Frei MG, Sunderam S, Giftakis J, Bhavaraju NC, Schaffner SF, et al. Automated seizure abatement in humans using electrical stimulation. Ann Neurol. 2005;57(2):258–68.
68. Bruzzone MJ, Issa N, Rose S, Warnke P, Towle VL, Tao JX, et al. Insights into the therapeutic effect of responsive neurostimulation assessed with scalp EEG recording: a case report. J Clin Neurophysiol. 2018;35(5):438–41.
69. Durand D. Electrical stimulation can inhibit synchronized neuronal activity. Brain Res. 1986;382(1):139–44.
70. Chiken S, Nambu A. Mechanism of deep brain stimulation: inhibition, excitation, or disruption? Neuroscientist. 2016;22(3):313–22.
71. Sillay KA, Rutecki P, Cicora K, Worrell G, Drazkowski J, Shih JJ, et al. Long-term measurement of impedance in chronically implanted depth and subdural electrodes during responsive neurostimulation in humans. Brain Stimul. 2013;6(5):718–26.
72. Wu C, Evans JJ, Skidmore C, Sperling MR, Sharan AD. Impedance variations over time for a closed-loop neurostimulation device: early experience with chronically implanted electrodes. Neuromodulation. 2013;16(1):46–50; discussion.
73. Wei Z, Gordon CR, Bergey GK, Sacks JM, Anderson WS. Implant site infection and bone flap osteomyelitis associated with the NeuroPace responsive neurostimulation system. World Neurosurg. 2016;88:687.e1–6.
74. Weber PB, Kapur R, Gwinn RP, Zimmerman RS, Courtney TA, Morrell MJ. Infection and erosion rates in trials of a cranially implanted neurostimulator do not increase with subsequent neurostimulator placements. Stereotact Funct Neurosurg. 2017;95(5):325–9.
75. Goodman RR, McKhann GM II, Spencer D, Vives KP, Gwinn R, Marsh WR, et al. Safety and preliminary efficacy of a responsive neurostimulator for the treatment of intractable epilepsy in adults 884. Neurosurgery. 2006;59(2):482.
76. Monday, December 4, 2006 Platform Highlights Session A 3:45 p.m.–5:45 p.m. Epilepsia. 2006;47(s4):1–7.
77. Nair D, Morrell M. Nine-year prospective safety and effectiveness outcomes from the long-term treatment trial of the RNS® System (S36.005). Neurology. 2019;92(15 Supplement):S36.005.
78. Geller EB, Skarpaas TL, Gross RE, Goodman RR, Barkley GL, Bazil CW, et al. Brain-responsive neurostimulation in patients with medically intractable mesial temporal lobe epilepsy. Epilepsia. 2017;58(6):994–1004.
79. Chen H, Dugan P, Chong DJ, Liu A, Doyle W, Friedman D. Application of RNS in refractory epilepsy: targeting insula. Epilepsia Open. 2017;2(3):345–9.
80. Devinsky O, Friedman D, Duckrow RB, Fountain NB, Gwinn RP, Leiphart JW, et al. Sudden unexpected death in epilepsy in patients treated with brain-responsive neurostimulation. Epilepsia. 2018;59(3):555–61.
81. Ryvlin P, Cucherat M, Rheims S. Risk of sudden unexpected death in epilepsy in patients given adjunctive antiepileptic treatment for refractory seizures: a meta-analysis of placebo-controlled randomised trials. Lancet Neurol. 2011;10(11):961–8.
82. Sperling MR. Sudden unexplained death in epilepsy. Epilepsy Curr. 2001;1(1):21–3.
83. Loring DW, Kapur R, Meador KJ, Morrell MJ. Differential neuropsychological outcomes following targeted responsive neurostimulation for partial-onset epilepsy. Epilepsia. 2015;56(11):1836–44.
84. Meador KJ, Kapur R, Loring DW, Kanner AM, Morrell MJ, Investigators RNSSPT. Quality of life and mood in patients with medically intractable epilepsy treated with targeted responsive neurostimulation. Epilepsy Behav. 2015;45:242–7.
85. Kokoszka MA, Panov F, La Vega-Talbott M, McGoldrick PE, Wolf SM, Ghatan S. Treatment of medically refractory seizures with responsive neurostimulation: 2 pediatric cases. J Neurosurg Pediatr. 2018;21(4):421–7.
86. Singhal NS, Numis AL, Lee MB, Chang EF, Sullivan JE, Auguste KI, et al. Responsive neurostimulation for treatment of pediatric drug-resistant epilepsy. Epilepsy Behav Case Rep. 2018;10:21–4.
87. Gerrard JL, Goble, TJ, Spencer DD. Placement of responsive neurostimulator depth electrodes with intraoperative MRI and ClearPoint neuronavigation. American Society for Stereotactic and Functional Neurosurgery Annual Meeting. Chicago, IL. 2016.
88. RNS® System Programming Manual. Rev. 2: NeuroPace, Inc.; 2018.
89. Patient Database Management System (PDMS): NeuroPace, Inc. Available from: https://pdms.neuropace.com.
90. Katz MJ. Fractals and the analysis of waveforms. Comput Biol Med. 1988;18(3):145–56.
91. Esteller R, Echauz J, Tcheng T. Comparison of line length feature before and after brain electrical stimulation in epileptic patients. Conf Proc IEEE Eng Med Biol Soc. 2004;7:4710–3.
92. Nathan SS, Sinha SR, Gordon B, Lesser RP, Thakor NV. Determination of current density distributions generated by electrical stimulation of the human cerebral cortex. Electroencephalogr Clin Neurophysiol. 1993;86:183–92.
93. Quraishi IH, Hirsch LJ. Patient-detectable responsive neurostimulation as a seizure-warning system.

American Epilepsy Society Annual Meeting, New Orleans; 2018.
94. My Seizure Diary: NeuroPace, Inc. Available from: https://www.myseizurediary.com.
95. Farooque P, Duckrow R. Subclinical seizures during intracranial EEG recording: are they clinically significant? Epilepsy Res. 2014;108(10):1790–6.
96. Claassen J, Vespa P. Electrophysiologic monitoring in acute brain injury. Neurocrit Care. 2014;21:129–47.
97. Baud MO, Kleen JK, Mirro EA, Andrechak JC, Chang EF, Rao VR, et al. Multi-day rhythms modulate seizure risk in epilepsy. Nat Commun. 2018;9:1–10.
98. Quigg M, Sun F, Fountain NB, Jobst BC, Wong VSS, Mirro E, et al. Interrater reliability in interpretation of electrocorticographic seizure detections of the responsive neurostimulator. Epilepsia. 2015;56:968–71.
99. Skarpaas TL, Tcheng TK, Morrell MJ. Clinical and electrocorticographic response to antiepileptic drugs in patients treated with responsive stimulation. Epilepsy Behav. 2018;83:192–200.
100. Mercier MR, Quraishi IH, Duckrow RB, Hirsch LJ. Early changes in responsive neurostimulator detection rates after introduction of anti-seizure drugs predict efficacy. American Clinical Neurophysiology Society Annual Meeting, Phoenix; 2018.
101. Smart O, Rolston JD, Epstein CM, Gross RE. Hippocampal seizure-onset laterality can change over long timescales: a same-patient observation over 500 days. Epilepsy Behav Case Rep. 2013;1:56–61.
102. King-Stephens D, Mirro EA, Van PC, Salanova V, Spencer DC. Lateralization of temporal lobe epilepsy with long-term ambulatory intracranial monitoring using the RNS system: experience at 4 centers. Epilepsy Curr. 2011;11. https://www.aesnet.org/sites/default/files/file_attach/ProfessionalEducation/Currents/2011/AbstSuppVol11num1/Volume%2011%20Supplement%201%20Abstracts.pdf.
103. Enatsu R, Alexopoulos A, Bingaman W, Nair D. Complementary effect of surgical resection and responsive brain stimulation in the treatment of bitemporal lobe epilepsy: a case report. Epilepsy Behav. 2012;24(4):513–6.
104. Durazzo TS, Spencer SS, Duckrow RB, Novotny EJ, Spencer DD, Zaveri HP. Temporal distributions of seizure occurrence from various epileptogenic regions. Neurology. 2008;70:1265–71.
105. Spencer DC, Sun FT, Brown SN, Jobst BC, Fountain NB, Wong VSS, et al. Circadian and ultradian patterns of epileptiform discharges differ by seizure-onset location during long-term ambulatory intracranial monitoring. Epilepsia. 2016;57:1495–502.

Spinal Stimulation

13

Akshay V. Save, Dominique M. O. Higgins, and Christopher J. Winfree

Introduction

Spinal cord stimulation (SCS), previously known as dorsal column stimulation, refers to the use of implantable electrical generators in the spinal canal to dampen the electrochemical sensation of pain. It was first used clinically in 1967 by Dr. C. Norman Shealy to manage intractable pleural chest pain in a patient with an inoperable bronchogenic carcinoma and diffusely metastatic disease [1]. Despite the patient passing away days later from undiagnosed endocarditis, his pain was successfully managed briefly with spinal cord stimulation at the T2–3 levels with periodic changes in the stimulation frequency. This short experience proved that spinal cord stimulation could be used in the management of localized pain. Further, the need to intermittently change the stimulation frequency highlighted the challenge of neuroplasticity in pain pathways when treating complex intractable pain.

Since then, significant technological advances have changed the face of neurogenic pain management. In 1989, the United States Food and Drug Administration approved spinal cord stimulation for treatment of chronic trunk, back, and limb pain. Today, narrower leads, implantable, rechargeable generators, and varied stimulation algorithms have made spinal cord stimulation a viable option when seeking to manage a variety of chronic intractable pain etiologies.

Types of Spinal Cord Stimulators

Components of spinal cord stimulators consist of electrode leads connected to a pulse generator or battery. Leads are divided broadly into two categories, paddle and percutaneous. Paddle electrodes are generally implanted via an open surgical approach, as they require a laminectomy or laminotomy for access to the epidural space. Percutaneous electrodes, as the name implies, are implanted using fluoroscopy and a large gauge spinal needle (e.g., Touhy). The choice of which electrode to use depends on a variety of factors, including distribution of symptoms, surgical history, and surgeon preference. Paddle electrodes tend to migrate less and may require less power resulting in a longer battery life. Percutaneous electrode placement, on the other hand, is less invasive and more easily allows refinement of the final electrode position in both the rostral–caudal and medial–lateral planes.

The number of contact leads in electrodes used also varies depending on clinical need. Typically, electrodes are available with 4, 8, or 16 contact leads. Greater number of contact leads

A. V. Save (✉) · D. M. O. Higgins · C. J. Winfree
Department of Neurosurgery, Columbia University Irving Medical Center, New York, NY, USA
e-mail: akshay.save@columbia.edu

N. Pouratian, S. A. Sheth (eds.), *Stereotactic and Functional Neurosurgery*,
https://doi.org/10.1007/978-3-030-34906-6_13

allows for postoperative adjustment of the location and direction of stimulation being applied without having to undergo a reoperation for positioning [2]. However, the added complexity of programming is not always required, and thus electrode selection should be tailored to the individual clinical scenario.

The electrode ultimately relies on a power source, which is most commonly an implanted pulse generator or IPG. These are relatively small subcutaneous batteries that are connected to the tunneled electrode prior to implantation. Their lifespan depends to some degree on the stimulator settings used but on average lasts approximately 4–5 years [2]. Newer systems available employ rechargeable IPGs. These are beneficial in that they avoid additional surgeries for battery replacement; however, they have an increased upfront cost to the patient. Older systems used radiofrequency-coupled devices with an implanted receiver and external power source. Despite the ease of changing the batteries in these systems, they have fallen out of favor, in large part due to the patient preference for an entirely internalized system that minimizes the impact of management on daily life.

Mechanism of Action

Spinal cord stimulation has a complex mechanism of action that has not yet been completely understood. In 1965, Melzack and Wall initially proposed a "gate theory" of pain modulation [1, 3–8]. The gate theory of pain explains that the sensation of pain requires transmission of painful stimuli along neurons in the peripheral nervous system across a physiological "gate" into the central nervous system, where it is ultimately experienced. Further, the activation of other sensory nervous pathways may influence the reactivity of this gate and inhibit the transmission of pain along ascending pathways. Smaller A-delta and C fibers that provide nociceptive sensation synapse alongside the larger diameter A-beta fibers that provide tactile sensation in the substantia gelatinosa of the dorsal horn. Stimulation of the larger fibers inhibits the neural signaling from the smaller pain fibers, suppressing the transmission of pain. From this theory sparked the paradigm that nociceptive stimuli would be replaced with more tolerable paresthesias along the same pain distribution, which is consistent with clinical findings [3–6]. While this had been the dominant theory for many years, recent preclinical and clinical data suggest a multifactorial mechanism for pain control [3–6], which may provide insight into why this treatment modality works more effectively in certain patient populations.

Additional mechanisms being considered include the activation of GABA interneurons in the dorsal horn, activation of supraspinal pathways that modulate descending serotonergic and noradrenergic neurons, downregulation of microglial and immune cell markers to suppress immune-modulated pain, suppression of efferent sympathetic fibers, or the local release of vasodilatory and nociceptive molecules peripherally [3–6, 9]. Pain relief from spinal cord stimulation is partially diminished when delivered concurrently with pharmacologic opioid antagonism. This clinical finding suggests that activation of descending opioid pathways and the local release of endogenous opiates likely play a role in pain relief [10]. Functional MRI and PET imaging also showed that electrical stimulation of the dorsal columns with spinal cord stimulators resulted in increased blood flow to not only thalamic and somatosensory pathways but also the anterior cingulate and prefrontal cortices [3–6]. Whereas the thalamic and somatosensory effects are likely to directly modulate neural connectivity with the corresponding nociceptive pathways, it is hypothesized that stimulation of the anterior cingulate and prefrontal cortices plays a role in the emotive, experiential aspects of pain. It should be noted that the various waveforms available for spinal cord stimulation programming likely influence different sensory pathways and different cell types within the nervous system.

The stimulators generate various waveforms that then have an electrophysiologic effect on the segmental sensory fibers, typically of the dorsal column, modulating pain via the mechanisms described earlier. The coverage area of the waveform generated depends on a variety of factors,

including the number of electrodes placed, the number of contact leads, and their interval spacing [5]. These variables should be decided on preoperatively to optimize coverage. For example, two percutaneous electrodes are often placed on either side of midline if there is a concern for electrode migration and bilateral coverage is needed, whereas a single paddle electrode may suffice. The orientation of the contacts also plays an important role in the coverage generated. Original electrodes were monopolar but have since evolved to include bi- and tripolar configurations. The programmer can designate combinations of anodes and cathodes to shape the area of coverage obtained [11, 12]. For instance, transverse tripolar stimulation, which is reported to have increased benefit for axial back pain [13], involves a central cathode contact with flanking anodes that serve to shield the dorsal roots laterally. These are typically done using paddle electrodes, but the effect can also be simulated using three percutaneous electrodes. Similarly, for multicontact electrodes, the distance between contacts should be factored into the choice of electrode because it will affect the area and depth of coverage.

After placement, the electrodes must be programmed with certain electrophysiological parameters that determine the characteristics of the square waveform generated. The most important programming parameters are the pulse frequency (the number of electrical stimuli delivered in unit time), pulse width (the duration of the stimulus), and amplitude of stimulation (the intensity of the current delivered). The most common waveforms used are conventional or tonic, high-frequency, Burst, and high-density stimulation. Tonic stimulators provide electrical pulses at lower frequencies around 40–50 Hz, with a pulse width of 200–500 μs. The amplitude is adjusted based on patient feedback to provide pain relief with a tolerable degree of paresthesias. Approximately 50% of patients have a 50% decrease in their pain levels with this type of waveform stimulation [6, 14, 15]. Some patients, however, find the paresthesias to be intolerable over time. Additionally, others start to have attenuated benefit with chronic stimulation [14]. To address these issues, three paresthesia-free stimulation techniques were developed: high-frequency, Burst, and high-density stimulation [14]. High-frequency stimulation delivers pulses in the range of 10 kilohertz with a much narrower pulse width of 30 μs. Burst frequency stimulation uses serial high-frequency pulses (bursts) with an intervening stimulation-free period. Bursts occur at 40 Hz similar to tonic stimulation, with 5 pulses per burst that each have a pulse width of 1000 μs [3–7]. High-density stimulation also has a higher frequency stimulation ranging from 500 to 1200 Hz, but with a pulse width similar to tonic stimulation, thus increasing the density of stimulation [14].

Both preclinical and clinical research findings suggest that tonic, high frequency, and Burst stimulation likely have slightly differing targets and mechanisms of action [3–6]. The amplitude and pulse width together constitute the charge per electrical pulse, which roughly determines if an action potential will occur as well as the type of neuronal–axonal units that will depolarize [9, 16]. While the frequency of stimulation influences the rate of depolarization, leading to a more synchronized, summative effect, there is also evidence that different frequency ranges activate different receptor pathways. For example, low-frequency stimulation activates μ-opioid systems, whereas higher frequencies preferentially activate the endogenous δ-opioid pathways [9]. Higher frequencies are also thought to affect interneurons that interact with other neurotransmitters such as acetylcholine, adenosine, serotonin, and norepinephrine, resulting in a more complicated method of pain relief [15, 16]. These various electrophysiological parameters should all be finely tuned on an individual patient basis to achieve optimal pain management.

With newer advances in technology, Burst stimulation is becoming more common in clinical practice [3–9, 16]. Preclinical studies suggest that Burst stimulation more closely resembles the depolarization of natural pathways compared to tonic stimulation. Animal studies have shown a greater cortical activation signature with Burst rather than tonic stimulation. EEG recordings in patients receiving Burst stimulation showed

greater activity in the dorsal anterior cingulate cortex compared to patients receiving tonic stimulation. Given the role of the thalamic–cingulate pathway in the emotional perception of pain, it is thought that Burst stimulation may ameliorate the way patients perceive and experience pain [5, 15]. All in all, there are clearly differences between tonic and Burst stimulation, though further research is necessary to understand if certain patient populations would differentially benefit from a particular method.

Initial trials with Burst and high-frequency stimulation showed promising results and increased efficacy [17–20] compared to tonic stimulation. More recent studies have painted a less clear picture, and such stimulation techniques long-term may suffer from similar drawbacks encountered with tonic stimulation [21]. One possibility is that the unregulated firing of the stimulator without feedback into the system results in unwanted or off-target effects that eventually dampen the efficacy. To this end, more recent efforts have been made to develop what are termed "closed-loop" spinal cord stimulators. These function by not only delivering stimulation but also measuring the evoked action potentials. Over time, the amount of stimulation can then be varied to maintain a constant evoked potential rather than a fixed waveform [21]. There are currently ongoing research trials with these novel stimulators to determine their efficacy broadly before they are available for clinical use.

Initial Workup and Assessment

It is important to exclude other treatable causes of pain prior to considering spinal cord stimulation. Further, a thorough history and physical examination to comprehensively localize the distribution of pain is critical. A trial period of 3–7 days with a temporary external battery is recommended prior to permanent implantation [6, 22, 23]. Only patients who respond positively to the trial run should be considered for permanent treatment. A positive response to the trial period is defined as a 50% improvement in pain symptoms as well as functional improvement in activity [6].

Indications

Spinal cord stimulation should be considered in patients with chronic intractable localized pain refractory to conservative medical management. In the United States, postlaminectomy syndrome (PLS) and complex regional pain syndrome (CRPS) are the most common indications for spinal cord stimulation, whereas chronic vascular pain and refractory angina are the most common in Europe [24]. There is a growing body of literature suggesting that spinal cord stimulation may also be effective in treating painful diabetic peripheral neuropathy (PDPN) [17, 25–27]. While there is currently no definitive, class 1 evidence to support its use in patients with post-herpetic neuralgia, cancer-related, or post-amputation pain, it should still be considered in patients suffering from these types of pain syndromes when refractory to other modalities.

Postlaminectomy Syndrome

Postlaminectomy syndrome (PLS), also referred to as failed back surgery syndrome (FBSS), refers to refractory axial back and/or leg pain that persists or worsens following surgical management. Patients with PLS should be carefully evaluated for causes of persistent symptoms, such as residual lateral recess or foraminal stenosis, extraforaminal compression, and spondylolisthesis. In the absence of identifiable surgical pathology amenable to additional decompression and/or instrumentation, PLS patients should be considered candidates for spinal cord stimulation [6, 24, 27–29]. Patients with a chief complaint of axial back pain may respond well to tonic stimulation; however, paresthesia-free stimulation techniques tend to offer better outcomes [27, 30, 31].

Complex Regional Pain Syndrome

Complex regional pain syndrome is characterized primarily by pain, inflammatory changes, decreased mobility, or dermatologic changes affecting an anatomic area that occurs most frequently after trauma

or surgery. The pain does not correspond to any known dermatomal or peripheral nerve distributions and extends beyond the usual healing time course for the initial injury. In type 1 CRPS, there is no damage to peripheral nerves, whereas type 2 CRPS has associated damage along a particular peripheral nerve distribution. This diagnosis is predominantly clinical, with history and physical examination findings consistent with hyperesthesia, temperature differences, unexplained regional swelling, or motor dysfunction along the affected area. Both CRPS 1 and 2 patients may benefit from SCS, though the majority of studies to date have focused on CRPS 1 [32, 33].

Chronic Vascular Ischemia

Claudication and pain from untreatable chronic ischemia can be treated with spinal cord stimulation [6, 25, 33, 34]. This is especially relevant when revascularization cannot be completed due to patient comorbidities or extremely poor disease. Percutaneous coronary intervention, coronary artery bypass graft, and spinal cord stimulation should be considered as complementary procedures based on the extent of vascular disease. Thus, in elderly patients suffering from chronic angina that are not well conditioned for major surgical intervention, thoracic spinal cord stimulation may be considered as a lower morbidity and lower cost option rather than coronary artery bypass grafts [34].

Painful Diabetic Peripheral Neuropathy

Diabetic peripheral neuropathies are common in patients with poorly controlled or long-standing diabetes mellitus. Between 15% and 25% of these patients develop painful neuropathies, usually in the lower extremities, that are often incompletely managed by medical therapy. Medical management consists of trialing multiple drug combinations, which is limited by poor side-effect profiles. Though the role of spinal cord stimulation remains under debate in PDPN, several observational studies have suggested that it may have positive effects on pain management and quality of life [6, 17, 26, 27].

Contraindications/Exclusionary Criteria

Active infection is considered a contraindication for implantation, given the risk of extending infection to the epidural space and subsequently the central nervous system. Presumed infected hardware must likely be explanted. Patients with uncontrolled coagulopathies or clotting dysfunction should not be considered for this procedure because of the risk of spinal epidural hematoma, which requires urgent neurosurgical decompression to avoid permanent neurologic damage [6, 24, 25]. Previously, implanted pacemakers/defibrillators and future anticipated MRI were considered contraindications to implantation. The concern for patients with pacemakers or defibrillators was that the electricity from spinal cord stimulators would inappropriately interfere with cardiac pacing. This interference was initially thought to be voltage and frequency dependent [35] and more likely in patients with unipolar pacers [35, 36]. However, subsequent studies have shown that spinal cord stimulators can safely be implanted and used in patients with advanced heart failure without interfering with implantable cardioverter defibrillators [37]. Further, with the advent of newer, MRI-compatible pulse generators, future MRI is no longer a contraindication, though it remains a concern in patients with older devices.

Psychiatric comorbidities, such as depression, debilitating anxiety, somatization, or psychosis, should be appropriately managed prior to spinal cord stimulation consideration to provide the highest likelihood of success.

The effects of spinal cord stimulation on pregnant patients or developing fetuses have not been fully characterized. Though there is not thorough scientific literature for this clinical situation, physiological anatomic changes during the course of pregnancy may result in damage to the equipment and subsequently the patient [38].

Additionally, the presence of a spinal cord stimulator specifically in the lumbar region has been thought to potentially limit the options for anesthesia during labor and delivery. As such, spinal cord stimulator manufacturers currently do not recommend its use in patients who are currently pregnant or who plan to become pregnant. However, there have been some published case reports and case series that suggest that implantation of spinal cord stimulators in young women of childbearing age can be done safely by coordinating multidisciplinary care with obstetrics, surgical services, anesthesia, and pain management teams [39, 40]. As such, young females with intractable chronic pain should still be considered for spinal cord stimulators. In these cases, electrical stimulation may provide patients with sufficient pain relief to enable them to reduce or eliminate the need for pain medications during pregnancy that are either teratogenic or addictive.

Anatomic Considerations

There are many anatomic considerations that need to be taken into account when considering spinal cord stimulator implantation in different regions of the spine. Stimulation in the cervical spinal cord is predominantly designed to treat pain in the neck and upper extremities. For pain at the neck, shoulder, and hand, spinal cord stimulators should be placed between C1–2, C2–4, and C5–6, respectively [41]. Common indications in this region are CRPS and persistent pain after cervical spine surgery [42]. Implantation can be completed with direct application following a cervical laminectomy or by needle insertion caudally with subsequent advancement to the desired site. As increased distance between insertion and target site increases the risk of failure due to a progressive rise in the resistance experienced, a common technique for cervical percutaneous leads involves introducing the needle in upper thoracic levels, between T1 and T4. Challenges for implantation in the cervical spine include a changing distribution of paresthesias as well as an increased risk of lead migration, which are most likely related to the mobility of the neck at this level [6, 42–44].

Targeted stimulation of the thoracic spinal cord on the other hand is used to treat back, lower limb, and angina. To target the lower back, anterior thigh, posterior thigh, and legs, spinal cord stimulators should be placed at T9–10, T11–12, T11–L1, and L1, respectively [41]. In our experience, the T7–8 levels can be effective targets for low back and leg coverage as well. In a 100 patient study of implantation for refractory angina, spinal cord stimulators were introduced at the level of T5–6 and advanced rostrally until stimulation-evoked paresthesias in the appropriate anginal distribution [45]. At the thoracic level, spinal column mobility is limited by attachment to the ribs, which may be a factor in the low rate of lead migration in this region. However, postural changes are most likely to cause fluctuations in stimulation in the mid-thoracic spine, presumably due to the degree of kyphosis and dorsal CSF diameter [6, 43, 44].

Leads placed in the lumbar spinal levels often lay directly over the conus medullaris and cauda equina as the spinal cord terminates. This has been found to be helpful for pelvic, foot, and sacral pains. However, stimulation in the cauda equina is extremely variable, likely due to how thin the nerves are in the CSF, and maintaining consistent levels of stimulation can be challenging.

Surgical Procedure

All patients should undergo imaging of the spinal canal in the area where the electrodes and/or needles will be placed. Noncontrast MRI or CT myelography can confirm that there is sufficient room in the spinal canal to accommodate the introducer needles in the case of percutaneous leads and the paddle in the case of paddle leads. Neuromonitoring should be used if the patient is either under general anesthesia or sedated to minimize the risks of neurological injury during lead placement.

Percutaneous spinal cord stimulator implantation is performed with the patient in the prone position. Intraoperative fluoroscopy is used to localize the spinal anatomy. Local anesthetic with a vasodilator is administered by the entry

site. A small incision is made off of the midline. A large gauge spinal needle (e.g., Tuohy) is inserted and used to access the epidural space on the midline using a paraspinous loss of resistance technique. After removal of the stylet, the electrode is inserted and steered to the desired location under fluoroscopic guidance. This process is repeated for the opposite side. After the electrode is confirmed to be in the desired location, intraoperative testing can be done by reducing sedation and asking the patient to describe continuing pain or new paresthesia distributions. For newer high-frequency or paresthesia-free stimulation modalities (e.g., HF10), leads are placed anatomically rather than relying on paresthesia mapping. If a single electrode is being placed, mapping may also be useful to determine physiologic midline. Otherwise, this can be determined anatomically or, alternatively two unilateral electrodes, can be placed on either side of midline. For tunneling the wires, another incision is then made between the two needles, through which the electrode wires are tunneled and attached to the anchoring hardware. For the test implantation, the generator remains extracorporeal; however, for the permanent implantation, a subcutaneous pocket is constructed to accommodate the generator. Intraoperative fluoroscopy is used prior to closure to confirm that electrode position has not changed during the anchoring process. Deep tissues and dermis are closed with sutures and a clean dressing is applied.

For insertion of paddle electrodes, the patient is similarly positioned prone. The level of interest is localized with fluoroscopy. A midline incision is made, followed by a sub-periosteal dissection to expose the lamina or laminae of interest. Bony removal can be carried out in standard fashion using a combination of high-speed drills, Rongeurs, and Kerrisons. The extent of bony removal needed will depend on the rostral–caudal exposure needed and the laterality of placement. In some instances, a laminotomy may suffice for exposure. In other cases, an adjacent level laminotomy or even a full laminectomy may be needed to address scarring or soft tissue in the epidural space. The key here is to enable placement of the paddle lead using a gentle technique to avoid spinal cord injury. If unacceptable resistance is met while advancing the electrode, then more bone and/or soft tissue likely needs to be removed. Trial templates and spacers may be used in preparation for implantation although their routine use is not mandatory. If mapping is needed, this may proceed as described earlier. The electrodes can be similarly tunneled to connect to the IPG.

Potential Surgical Complications

While major surgical complications are rare, minor complications are a common cause of failure in spinal cord stimulation, with estimates ranging from 10% to 40%. Surgical complications can be further classified as mechanical and biological.

Device-related mechanical complications are the most common and have occurred in up to 38% patients in recent case series. These are frequently due to lead migration, lead generator disconnection, lead fracture, and pulse generator failure. Lead migration, the most common complication, should be suspected if significant pain relief is achieved initially but suddenly worsens or disappears. In experienced centers, this may still occur in 13–27% of cases. While this can be fixed with reprogramming of the generator, a minor relocation procedure may be necessary. The other mechanical complications require reoperation and replacement of hardware [6, 46, 47].

Biologic complications occur in about 7.5% of cases and include infection, seromas, hematomas, implantation site pain, epidural fibrosis, spinal cord injury, spinal cord compression, and allergic reaction. Infection is the most common biologic complication but can be minimized by appropriate preoperative antimicrobial skin preparation and postoperative antibiotics. Deep infections are frequently associated with abscess formation. Both superficial and deep infections require explantation of hardware and treatment with antibiotics. In some case series, almost 50% of infections are due to staphylococcal species, but frequently no definitive organism is identified. Major surgical complications, including

traumatic spinal cord injury and spinal epidural hematomas resulting in spinal cord compression, are rare in the hands of experienced surgeons [6, 46, 47]. Epidural fibrosis, while uncommon, can occur with chronic implantation, and depending on clinical severity may require stimulator removal. Case reports published on this clinical complication suggest that epidural fibrosis is preceded by the development of tolerance to stimulation. Tolerance is a phenomenon whereby patients with initial improvements in pain symptoms with SCS may experience a progressive loss of pain control efficacy. Epidural fibrosis can occur over a wide time course, with reports as early as 9 months to as late as 17 years postimplantation [48].

Fortunately, despite these potential complications, spinal cord stimulator implantation remains an overall safe procedure, especially considering that implantation is reversible and can be done minimally invasively.

Side Effects

Conventional, low-frequency tonic stimulation almost always results in some degree of paresthesias along the previously painful regions, which can be uncomfortable for some patients. This problem is not observed with high-frequency or Burst stimulation. As briefly described earlier, another important side effect of long-term spinal cord stimulation is the development of tolerance. The phenomenon is not fully understood, but is thought to occur as a result of neuroplasticity diminishing the effects of stimulation on pain pathways over time. Another cause is the development of chronic scarring over time that decreases the efficacy of stimulation by insulation of the electrical signal [48]. It is currently difficult to prospectively predict which patients will develop tolerance, but it occurs in approximately 29% of SCS cases over a 10-year follow-up period. In some cases, increasing the pulse amplitude or allowing for "washout" periods with no stimulation may help counteract the development of tolerance due to neuroplasticity [49, 50].

Efficacy

Spinal cord stimulation is an effective procedure to treat chronic pain from a variety of sources [6, 18, 49, 51, 52]. There is Level I evidence recommending conventional SCS in patients with PLS, CRPS, and chronic pain from vascular disease. A study by North et al. in 2005 compared patients undergoing spinal cord stimulation versus repeated spinal surgery for FBSS [53]. They showed that patients in the spinal cord stimulation cohort had greater satisfaction with treatment and were less likely to require escalating opioid dosage than patients who had repeat surgery. Further, patients who had spinal cord stimulation were unlikely to cross over into the reoperation group [53]. On average, studies have shown a 3-point decrease in patient's visual analog scale (VAS) score and a 41.4% decrease in pain rating with SCS [51]. Large multicenter trials have also demonstrated improvements in quality of life, mood, and satisfaction, which were sustained at 12 months [51].

Within the last 5 years, high-frequency SCS has been approved with Level I evidence for the treatment of chronic refractory pain. A large multicenter study comparing high-frequency stimulation to conventional stimulation showed a larger percentage of responders at 24 months for chronic back (76.5% compared to 49.3%) and leg pain (72.9% vs. 49.3%). This study also found that the degree of pain relief was greater with high-frequency SCS, with an average 5-point decrease in back pain score and corresponding 66.9% decrease in back pain rating, with similar results for leg pain. The absence of paresthesias has also been noted as a very attractive factor of high-frequency SCS, likely contributing to improved patient satisfaction and decreased pain [19].

At present, there is no conclusive Level I evidence for the use of Burst stimulation. However, as the newer Burst stimulation technology has been increasingly implemented, there are now results from trials comparing conventional and Burst stimulation. Burst stimulation was shown to be more effective than conventional stimulation for decreasing VAS pain scores in patients with PLS and PDPN [18, 27]. In 2017, the

SUNBURST (Success Using Neuromodulation with BURST) trial studied the safety and effectiveness of Burst stimulation for patients with chronic trunk or limb pain. SUNBURST was a prospective, multicenter, randomized crossover trial with 100 patients undergoing a 12-week trial period of both Burst and conventional stimulation modalities. This study found that that not only is Burst stimulation safe and effective but also that it provides superior pain relief than tonic stimulation. Furthermore, with Burst stimulation, only 17% of patients experienced paresthesias, compared to 92% with tonic low-frequency stimulation. In this crossover study, 68% of patients preferred Burst stimulation to conventional stimulation, most often citing the decreased extent of paresthesias as the reason [18].

As previously discussed, it is widely accepted that the level of pain relief achieved from spinal cord stimulation diminishes gradually over time, likely due to the development of tolerance. A study comparing the initial trial period to permanent implantation showed that there was a statistically significant difference in subjective pain score and reliance on opioid use for breakthrough pain, though disability indices did not differ. This highlights the importance of setting realistic expectations when discussing potential benefits and risks to potential procedural candidates [23].

Predictors of Success

A meta-analysis of many factors, including location of pain, history of back surgery, initial level of pain, litigation/worker's compensation, age, gender, duration of pain, duration of follow-up, publication year, method of data collection, study design, quality score, method of SCS lead implant, and type of SCS lead, did not find any statistically significant predictors of success [51]. A retrospective study revealed lower rates of 6-month satisfactory pain relief (defined as less than 50% of initial pain) in smokers [49, 50]. This may be due to poor wound healing, higher levels of inflammatory cytokines, or diminished transmission along neural pathways. Patients who had delayed treatment were also observed to have worse outcomes, with as low as 9% of patients achieving durable pain relief when symptoms had presented 15 years prior to treatment. In the context of PDPN, severity of neuropathy at initiation was found to be associated with a greater risk of long-term treatment failure [26].

Cost-Effectiveness

Spinal cord stimulation is a successful and cost-effective intervention for intractable pain. Studies on patients with PLS in the early 2000s found that spinal cord stimulators become cost neutral between 2 and 5 years and cost beneficial afterwards [54, 55]. The PRECISE study in 2015, a large multicenter, longitudinal study in patients with FBSS refractory to conventional medical management, showed that spinal cord stimulation together with conventional medical management was cost-effective in over 80% of cases [56]. Another longitudinal analysis of patients with a history of FBSS between 2000 and 2012 showed that while spinal cord stimulator implantation results in a short-term increase in healthcare costs during the first year, there is a significant decrease in the annual cumulative costs over the following 9 years [55–57]. Since then, multiple follow-up studies have affirmed these improvements in clinical outcomes, quality of life metrics, and cost-effectiveness [58].

For patients with CPRS, SCS with conventional medical management was found to be more cost-effective than conventional medical management alone. In peripheral arterial disease and refractory angina pectoris, Kumar and Rizvi were able to show that SCS with conventional medical management also portended a benefit in terms of quality-adjusted life years [59]. For painful diabetic peripheral neuropathy, the cost-effectiveness analyses suffer from a lack of high-quality randomized controlled studies. Similar to the situation in other indications, the high initial cost of implantation makes SCS not cost-effective for PDPN in the short-term though this may be outweighed by the long-term benefits [60].

Conclusion

Spinal cord stimulator implantation has been shown to be a clinically effective intervention for chronic intractable pain that has been refractory to conventional medical management. The simplicity of the procedure, low complication rates, and ease of reversibility make it an attractive therapeutic option for chronic pain. Additionally, for PLS, CRPS, and pain from vascular disease in particular, the current body of literature has shown it to be a reliable and cost-effective long-term treatment. Additional studies are warranted to determine the efficacy of the newer generation of stimulation techniques and other potential areas of treatment.

References

1. Shealy CN, Mortimer JT, Reswick JB. Electrical inhibition of pain by stimulation of the dorsal columns: preliminary clinical report. Anesth Analg. 1967;46(4):489–91.
2. Bradley K. The technology: the anatomy of a spinal cord and nerve root stimulator: the lead and the power source. Pain Med. 2006;7(suppl 1):S27–34.
3. Chakravarthy K, Kent AR, Raza A, Xing F, Kinfe TM. Burst spinal cord stimulation: review of preclinical studies and comments on clinical outcomes: review of Burst spinal cord stimulation. Neuromodulation. 2018;21(5):431–9.
4. Linderoth B, Foreman RD. Conventional and novel spinal stimulation algorithms: hypothetical mechanisms of action and comments on outcomes: conventional and novel SCS algorithms. Neuromodulation. 2017;20(6):525–33.
5. Dones I, Levi V. Spinal cord stimulation for neuropathic pain: current trends and future applications. Brain Sci. 2018;8(8):138.
6. Deer TR, Mekhail N, Provenzano D, Pope J, Krames E, Leong M, et al. The appropriate use of neurostimulation of the spinal cord and peripheral nervous system for the treatment of chronic pain and ischemic diseases: the neuromodulation appropriateness consensus committee: appropriate use of neurostimulation. Neuromodulation. 2014;17(6):515–50.
7. Moore DM, McCrory C. Spinal cord stimulation. BJA Educ. 2016;16(8):258–63.
8. Sinclair C, Verrills P, Barnard A. A review of spinal cord stimulation systems for chronic pain. J Pain Res. 2016;Volume 9:481–92.
9. Vallejo R, Bradley K, Kapural L. Spinal cord stimulation in chronic pain: mode of action. Spine. 2017;42:S53–60.
10. Gee L, Smith HC, Ghulam-Jelani Z, Khan H, Prusik J, Feustel PJ, et al. Spinal cord stimulation for the treatment of chronic pain reduces opioid use and results in superior clinical outcomes when used without opioids. Neurosurgery. 2019;84(1):217–26.
11. Kaschner AG, Sandmann W, Larkamp H. Percutaneous flexible bipolar epidural neuroelectrode for spinal cord stimulation. J Neurosurg. 1984;60(6):1317–9.
12. Sankarasubramanian V, Buitenweg JR, Holsheimer J, Veltink P. Electrode alignment of transverse tripoles using a percutaneous triple-lead approach in spinal cord stimulation. J Neural Eng. 2011;8(1):016010.
13. Buvanendran A, Lubenow TJ. Efficacy of transverse tripolar spinal cord stimulator for the relief of chronic low back pain from failed back surgery. Pain Physician. 2008;11(3):333–8.
14. Hoydonckx Y, Costanzi M, Bhatia A. A scoping review of novel spinal cord stimulation modes for complex regional pain syndrome. Can J Pain. 2019 Jan;3(1):33–48.
15. De Ridder D, Vanneste S. Burst and tonic spinal cord stimulation: different and common brain mechanisms: Burst and tonic SCS activate descending pain inhibitory pathways. Neuromodulation. 2016;19(1):47–59.
16. Miller JP, Eldabe S, Buchser E, Johanek LM, Guan Y, Linderoth B. Parameters of spinal cord stimulation and their role in electrical charge delivery: a review: SCS parameters and charge delivery. Neuromodulation. 2016;19(4):373–84.
17. Slangen R, Schaper NC, Faber CG, Joosten EA, Dirksen CD, van Dongen RT, et al. Spinal cord stimulation and pain relief in painful diabetic peripheral neuropathy: a prospective two-center randomized controlled trial. Diabetes Care. 2014;37(11):3016–24.
18. Deer T, Slavin KV, Amirdelfan K, North RB, Burton AW, Yearwood TL, et al. Success using neuromodulation with BURST (SUNBURST) study: results from a prospective, randomized controlled trial using a novel burst waveform: results from the SUNBURST study. Neuromodulation. 2018;21(1):56–66.
19. Kapural L, Yu C, Doust MW, Gliner BE, Vallejo R, Sitzman BT, et al. Comparison of 10-kHz high-frequency and traditional low-frequency spinal cord stimulation for the treatment of chronic back and leg pain: 24-month results from a multicenter, randomized, controlled pivotal trial. Neurosurgery. 2016;79(5):667–77.
20. Demartini L, Terranova G, Innamorato MA, Dario A, Sofia M, Angelini C, et al. Comparison of tonic vs. Burst spinal cord stimulation during trial period. Neuromodulation. 2019;22(3):327–32.
21. Levy R, Deer TR, Poree L, Rosen SM, Kapural L, Amirdelfan K, et al. Multicenter, randomized, double-blind study protocol using human spinal cord recording comparing safety, efficacy, and neurophysiological responses between patients being treated with evoked compound action potential–controlled closed-loop spinal cord stimulation or open-loop spinal cord

stimulation (the evoke study). Neuromodulation. 2019;22(3):317–26.
22. Mathew L, Winfree C, Miller-Saultz D, Sonty N. Transcutaneous electrical nerve stimulator trial may be used as a screening tool prior to spinal cord stimulator implantation. Pain. 2010;150(2):327–31.
23. Malige A, Sokunbi G. Spinal cord stimulators: a comparison of the trial period versus permanent outcomes. Spine. 2019;44(11):E687–92.
24. Deer T, Masone RJ. Selection of spinal cord stimulation candidates for the treatment of chronic pain. Pain Med. 2008;9(suppl 1):S82–92.
25. Deer TR, Masone RJ. Spinal cord stimulation: indications and selection. In: Atlas of implantable therapies for pain management [Internet]. New York, NY: Springer New York; 2011. [cited 2018 Dec 10]. p. 9–12. Available from: http://link.springer.com/10.1007/978-0-387-88567-4_2.
26. van Beek M, Geurts JW, Slangen R, Schaper NC, Faber CG, Joosten EA, et al. Severity of neuropathy is associated with long-term spinal cord stimulation outcome in painful diabetic peripheral neuropathy: five-year follow-up of a prospective two-center clinical trial. Diabetes Care. 2018;41(1):32–8.
27. de Vos CC, Bom MJ, Vanneste S, Lenders MWPM, de Ridder D. Burst spinal cord stimulation evaluated in patients with failed Back surgery syndrome and painful diabetic neuropathy: Burst spinal cord stimulation evaluated. Neuromodulation. 2014;17(2):152–9.
28. Devulder J, De Laat M, Van Bastelaere M, Rolly G. Spinal cord stimulation: a valuable treatment for chronic failed back surgery patients. J Pain Symptom Manag. 1997;13(5):296–301.
29. Waszak PM, Modrić M, Paturej A, Malyshev SM, Przygocka A, Garnier H, et al. Spinal cord stimulation in failed back surgery syndrome: review of clinical use, quality of life and cost-effectiveness. Asian Spine J. 2016;10(6):1195–204.
30. Al-Kaisy A, Van Buyten J-P, Smet I, Palmisani S, Pang D, Smith T. Sustained effectiveness of 10 kHz high-frequency spinal cord stimulation for patients with chronic, low back pain: 24-month results of a prospective multicenter study. Pain Med. 2014;15(3):347–54.
31. Van Buyten J-P, Al-Kaisy A, Smet I, Palmisani S, Smith T. High-frequency spinal cord stimulation for the treatment of chronic back pain patients: results of a prospective multicenter European clinical study: high-frequency spinal cord stimulation. Neuromodulation. 2013;16(1):59–66.
32. Shrivastav M, Musley S. Spinal cord stimulation for complex regional pain syndrome. In: 2009 Annual International Conference of the IEEE Engineering in Medicine and Biology Society [Internet]. Minneapolis, MN: IEEE; 2009. [cited 2019 Feb 22]. p. 2033–6. Available from: http://ieeexplore.ieee.org/document/5334418/.
33. Vannemreddy P, Slavin KV. Spinal cord stimulation: current applications for treatment of chronic pain. Anesth Essays Res. 2011;5(1):20–7.
34. Eldabe S, Thomson S, Duarte R, Brookes M, deBelder M, Raphael J, et al. The effectiveness and cost-effectiveness of spinal cord stimulation for refractory angina (RASCAL study): a pilot randomized controlled trial. Neuromodulation. 2016;19(1):60–70.
35. Romanó M, Zucco F, Baldini MR, Allaria B. Technical and clinical problems in patients with simultaneous implantation of a cardiac pacemaker and spinal cord stimulator. Pacing Clin Electrophysiol. 1993;16(8):1639–44.
36. Patel J, DeFrancesch F, Smith C. Spine intervention society's patient safety committee. Spinal cord stimulation patients with permanent pacemakers and defibrillators. Pain Med. 2018;19(8):1693–4.
37. Torre-Amione G, Alo K, Estep JD, Valderrabano M, Khalil N, Farazi TG, et al. Spinal cord stimulation is safe and feasible in patients with advanced heart failure: early clinical experience. Eur J Heart Fail. 2014;16(7):788–95.
38. Saxena A, Eljamel MS. Spinal cord stimulation in the first two trimesters of pregnancy: case report and review of the literature. Neuromodulation. 2009;12(4):281–3.
39. Fedoroff IC, Blackwell E, Malysh L, McDonald WN, Boyd M. Spinal cord stimulation in pregnancy: a literature review. Neuromodulation. 2012;15(6):537–41.
40. Hanson JL, Goodman EJ. Labor epidural placement in a woman with a cervical spinal cord stimulator. Int J Obstet Anesth. 2006;15(3):246–9.
41. Barolat G, Massaro F, He J, Zeme S, Ketcik B. Mapping of sensory responses to epidural stimulation of the intraspinal neural structures in man. J Neurosurg. 1993;78(2):233–9.
42. Deer TR, Skaribas IM, Haider N, Salmon J, Kim C, Nelson C, et al. Effectiveness of cervical spinal cord stimulation for the management of chronic pain: cervical SCS. Neuromodulation. 2014;17(3):265–71.
43. Holsheimer J, Barolat G, Struijk JJ, He J. Significance of the spinal cord position in spinal cord stimulation. Acta Neurochir Suppl. 1995;64:119–24.
44. Holsheimer J, Struijk JJ, Tas NR. Effects of electrode geometry and combination on nerve fibre selectivity in spinal cord stimulation. Med Biol Eng Comput. 1995;33(5):676–82.
45. Gomes B et al. Spinal cord stimulation for refractory angina: 100 case-experience from the National Refractory Angina Service. Br J Cardiol [Internet]. [cited 2019 May 16]. Available from: https://bjcardio.co.uk/2016/07/spinal-cord-stimulation-for-refractory-angina-100-case-experience-from-the-national-refractory-angina-service/.
46. Eldabe S, Buchser E, Duarte RV. Complications of spinal cord stimulation and peripheral nerve stimulation techniques: a review of the literature. Pain Med. 2016;17(2):325–36.
47. Gabriella Gutman JZ. A review of surgical techniques in spinal cord stimulator implantation to decrease the post-operative infection rate. J Spine [Internet]. 2015 [cited 2018 Dec 10];04(01).

Available from: http://www.omicsgroup.org/journals/a-review-of-surgical-techniques-in-spinal-cord-stimulator-implantation-to-decrease-the-postoperative-infection-rate-2165-7939-4-202.php?aid=39053.
48. Al Tamimi M, Aoun SG, Gluf W. Spinal cord compression secondary to epidural fibrosis associated with percutaneously placed spinal cord stimulation electrodes: case report and review of the literature. World Neurosurg. 2017;104:1051.e1–5.
49. Bir SC, Konar S, Maiti T, Nanda A, Guthikonda B. Neuromodulation in intractable pain management: outcomes and predictors of revisions of spinal cord stimulators. Neurosurg Focus. 2016;40:E4.
50. De La Cruz P, Fama C, Roth S, Haller J, Wilock M, Lange S, et al. Predictors of spinal cord stimulation success: predictors of spinal cord stimulation success. Neuromodulation. 2015;18(7):599–602.
51. Grider J, Manchikanti L, Carayannopoulos A, Sharma ML, Balog CC, Harned ME, et al. Effectiveness of spinal cord stimulation in chronic spinal pain: a systematic review. Pain Physician. 2016;19(1):E33–54.
52. Sundaraj SR, Johnstone C, Noore F, Wynn P, Castro M. Spinal cord stimulation: a seven-year audit. J Clin Neurosci. 2005;12(3):264–70.
53. North RB, Kidd DH, Farrokhi F, Piantadosi SA. Spinal cord stimulation versus repeated lumbosacral spine surgery for chronic pain: a randomized, controlled trial. Neurosurgery. 2005;56(1):98–106; discussion 106–107.
54. Budd K. Spinal cord stimulation: cost-benefit study: SCS: cost-benefit study. Neuromodulation. 2002;5(2):75–8.
55. Taylor RS, Taylor RJ, Van Buyten J-P, Buchser E, North R, Bayliss S. The cost effectiveness of spinal cord stimulation in the treatment of pain: a systematic review of the literature. J Pain Symptom Manag. 2004;27(4):370–8.
56. Zucco F, Ciampichini R, Lavano A, Costantini A, De Rose M, Poli P, et al. Cost-effectiveness and cost-utility analysis of spinal cord stimulation in patients with failed back surgery syndrome: results from the PRECISE study: cost-utility of spinal cord stimulation. Neuromodulation. 2015;18(4):266–76.
57. Farber SH, Han JL, Elsamadicy AA, Hussaini Q, Yang S, Pagadala P, et al. Long-term cost utility of spinal cord stimulation in patients with failed back surgery syndrome. Pain Physician. 2017;20(6):E797–805.
58. Hoelscher C, Riley J, Wu C, Sharan A. Cost-effectiveness data regarding spinal cord stimulation for low back pain. Spine [Internet]. 2017 Jul 15 [cited 2018 Dec 10];42. Available from: https://insights.ovid.com/pubmed?pmid=28399549.
59. Kumar K, Rizvi S. Cost-effectiveness of spinal cord stimulation therapy in management of chronic pain. Pain Med. 2013;14(11):1631–49.
60. Slangen R, Faber CG, Schaper NC, Joosten EA, van Dongen RT, Kessels AG, et al. A trial-based economic evaluation comparing spinal cord stimulation with best medical treatment in painful diabetic peripheral neuropathy. J Pain. 2017;18(4):405–14.

Peripheral Nerve Stimulation

14

Pratik Rohatgi, Srinivas Chivukula,
Alon Kashanian, and Ausaf A. Bari

Introduction

In 1967, Wall and Sweet reported the first clinical use of peripheral nerve stimulation (PNS) in the treatment of neuropathic pain. Their hypothesis stemmed from the recently advanced gate control theory of pain perception, namely, that stimulation of large-diameter cutaneous nerves could saturate the transmission of pain impulses by smaller nerve fibers, mitigating the central perception of pain [1, 2]. They applied a square wave of 0.1 msec pulse width at 100 Hz of increasing voltage until paresthesias and/or hypesthesia was produced in the receptive field of the nerve in question. Remarkably, prior to treating patients, the authors tested the technique on themselves by placing needle electrodes near their own infraorbital nerves and described the sensation as "not unpleasant and always tolerable for an indefinite period of time" [1]. In the decades since, peripheral nerve stimulation has become an important tool for the treatment of a variety of disorders including neuropathic pain, visceral referred pain, musculoskeletal pain, and chronic refractory pain [3]. In this in this chapter, we discuss the biology of peripheral nerves with respect to the somatosensory system, biophysics of peripheral nerve stimulation, and the use of PNS for the treatment of neuropathic pain.

P. Rohatgi · S. Chivukula · A. Kashanian
A. A. Bari (✉)
Department of Neurosurgery,
David Geffen School of Medicine at UCLA,
Los Angeles, CA, USA
e-mail: abari@mednet.ucla.edu

The Physiology of the Somatosensory Peripheral Nervous System

In the somatosensory system, information from peripheral cutaneous receptors is converted into electrophysiologic signals that are processed and subsequently transmitted to the central nervous system (CNS) [4]. Somatic sensations are broadly categorized into several distinct modalities. Exteroception is the response of direct interaction with the external world through the sense of touch (including the sensation of contact, pressure, stroking, motion, and vibration), thermal perception, and pain or nociception. Proprioception is the sense of joint and limb position and movement transmitted through receptors in skeletal muscle, joint capsules, and skin. Interoception is a mostly unconscious perception of the major organs and their internal state through receptors in the viscera. Afferent, or sensory, nerve fibers can be categorized by the information they relay to the CNS as either general or specialized and either somatic or visceral [5]. General somatic afferent (GSA) fibers transmit information from exteroceptive

N. Pouratian, S. A. Sheth (eds.), *Stereotactic and Functional Neurosurgery*,
https://doi.org/10.1007/978-3-030-34906-6_14

and proprioceptive receptors. General visceral afferent (GVA) fibers transmit information of interoception and visceral pain. Special somatic afferents (SSA) transmit visual, auditory, and vestibular sensory input. Special visceral afferents (SVA) transmit taste and smell. General somatic afferent information from the trunk and peripheral extremities is transmitted to the CNS via nerve fibers of dorsal root ganglion neurons. Individual neurons in each ganglion are specialized to respond to specific stimuli through differences in morphology and molecular expression at the dendrite [4]. General visceral afferent, SSA, and SVA modalities are mainly transmitted through the cranial nerves of the brain stem.

Dorsal root ganglion neurons originate from neural crest cells [4]. These are pseudo-unipolar neurons that carry primary afferent fibers. The proximal terminal of the neuron synapses with neurons of the CNS in the dorsal horn of the spinal cord. The dorsal horn is divided into functional layers of gray matter termed the laminae of Rexed 1–10, from superficial to deep [6, 7]. Of note, the major nociceptive primary afferents terminate on Rexed laminae I and II [8]. The distal termination of the nerve ends in a specialized receptor type or exists as a free nerve ending that determines the receptive field to which it is tuned and in response to which an action potential is generated. These neurons are bundled in fascicles and joined by efferent motor axons to form a peripheral nerve that travels to a specific anatomical part of the body, defining a sensory dermatome and muscular myotome. The nerve fibers are classified into functional groups by their degree of myelination and diameter, which both influence nerve conduction velocity. Large-diameter axons conduct action potentials more rapidly due to lower internal (longitudinal) resistance. The myelin sheath of a Schwann cell around an axon increases conduction velocity through a process termed saltatory conduction. Group A fibers are the most heavily myelinated, group B fibers are moderately myelinated, and group C fibers are unmyelinated.

Aα, Aβ, and Aγ fibers are large-diameter myelinated fibers that convey sensations of touch and proprioception transduced by cutaneous, subcutaneous, muscle, and skeletal mechanoreceptors. These fibers range in diameter from 6 to 20 μm with conduction velocities ranging from 36 to 120 m/s [4]. Slower smaller-diameter axons that are lightly myelinated or unmyelinated (Aδ and C fibers, respectively) transmit information from chemoreceptors, thermal receptors, and nociceptors. Aδ fibers have a diameter of 1–6 μm and conduction velocities of 4–36 m/s, whereas C fibers have a diameter of 0.2–1.5 μm and conduction velocities ranging from 0.2 to 2.0 m/s. Therefore, the somatosensory system transmits different types of information to the CNS at different rates and temporal resolution. Due to its faster conduction velocity, multiple impulses can be transmitted by an Aδ fiber in the same time a type C fiber transmits the initial stimuli. Consequently, Aδ fibers transmit sensations perceived as pain faster than the type C fibers and can respond to changes in stimuli more rapidly [9]. Nociceptors innervated by Aδ fibers respond to stimuli perceived as sharp, whereas C fibers transmit a dull, burning pain that is diffusely localized.

Properties of peripheral nerves can be measured using cutaneous stimulating and recording electrodes placed both proximally and distally along the course of a peripheral nerve. By stimulating a cutaneous sensory nerve with a distally placed electrode, a proximally placed electrode can measure the resulting compound action potential, a summation of action potentials from each axon within the nerve. An increase in stimulation will result in recruitment of a larger number of axons, and those with the largest diameter are recruited first due to their lower electrical resistance. Therefore, lower stimulation intensities are perceived as tingling through the activation of Aβ fibers while increased stimulation results in pain through the activation of Aδ and C fibers [4].

Theories of Pain Perception

Although significant research has been dedicated to elucidating the mechanisms that underlie pain perception, its physiological basis remains unclear. Most frameworks that have been proposed describe a series of observations about

nociception but fail to adequately account for the multidimensionality and complexity inherent in the experience of pain. In this section, we briefly outline three influential theories of pain perception including (1) the specificity (labeled line) theory, (2) the intensity theory, and (3) the gate control theory. Later, we will focus on the latter, which inspired the development of modern PNS for the treatment of neuropathic pain.

Specificity Theory of Pain Perception

The fundamental tenet of the specificity (labeled line) theory is that each sensory modality has specific specialized receptor end organs and their associated primary afferent sensory fibers that are sensitive to a particular stimulus (or family of stimuli) [10, 11]. Non-noxious mechanical stimuli, for example, are encoded by low threshold mechanoreceptors which project through dedicated afferent fibers to mechanoreceptive neurons in the spinal cord and the brainstem and from there to higher-order "mechanoreceptive" brain regions [11]. Similarly, noxious stimuli activate a nociceptor, which projects through dedicated pain conducting afferent fibers to higher-order pain centers. Such a theory was rooted in a belief that the brain, contrary to the prevailing idea of much of the eighteenth century, is not a "common sensorium," but rather a heterogeneous structure in which nerves with specialized functions convey a perceived stimulus from a sensory organ to a *dedicated* brain region for its perceptual experience [10–12].

The specificity theory of pain perception found validation in the discovery of specific, cutaneous touch receptors including Pacinian corpuscles (1835), Meissner's corpuscles (1853), Merkel's discs (1875), and Ruffini's end organs (1893) [11, 13–15]. These appeared to provide evidence that specific sensory qualities were encoded by dedicated nerve fibers. Moreover, in a series of experiments between 1854 and 1859, Schiff and Woroschiloff identified specific pathways for pain and temperature transmission within the spinal cord (anterolateral pathway) distinct from the posterior columns (for tactile sensation) [12]. This provided further corroboration that various sensory qualities were conducted by dedicated fiber tracts. Through the early twentieth century, validity for the specificity theory in explaining pain perception appeared to grow with the discovery of myelinated fibers (that responded to mechanical noxious stimuli) and unmyelinated nerve fibers (that responded to chemical nociceptive stimuli) [11, 16, 17]. Indeed, it was the prevailing theory of pain perception until the promulgation of the gate control theory by Melzack and Wall in 1965, described below [2].

Intensity and Pattern Theory of Pain Perception

A less popular theory that coexisted with the specificity theory was the intensity theory. In its simplest form, its foundational idea was that pain occurs in any sensory system when sufficient intensity is reached through repeated stimulation, rather than by virtue of the stimulus itself [11, 18]. An early nineteenth century experiment appeared to corroborate this theory by demonstrating that repeated subthreshold tactile stimulation (below the threshold for tactile perception) produced pain in patients with syphilis (with degenerated dorsal columns) [18]. This was interpreted to indicate that repeated subthreshold stimuli were summated in the spinal cord (or elsewhere in the nervous system) to produce the sensation of pain. A self-evident, major shortcoming of this theory is that outside of special circumstances (such as patients with syphilis) it failed to explain the myriad ways in which single (non-summated) stimuli could also elicit pain in animal and human subjects. The theory was occasionally expanded and referred to as the pattern theory – a concept of pain perception in which the experience of pain depended not only on the intensity of the stimulus but also on the specific pattern of neural firing that it elicited within peripheral nerves encoding its transmission [11, 18–20]. Due to a lack of experimental evidence, the theory quickly fell out of favor, especially with the introduction of the gate control theory.

Gate Control Theory of Pain Perception

At its core, the gate control theory was an attempt to bridge the gap between two dominant theories of its era – the "specificity" and the "intensity" theories of pain perception – by delineating a framework derived from aspects of both and based on the then available electrophysiological data [2]. While the specificity theory proposed the presence of dedicated pathways for each somatosensory modality, the intensity theory stated that any sensation could be elicited by producing a specific pattern of neuronal activity within the peripheral nerves. Within this context, the gate control theory accepted that there were at least two fiber types – small fibers (Aδ and C that mediated primarily pain) and touch fibers (Aα and Aβ that mediated primarily touch) [11]. In fact, the difference in small and large fiber inputs played an important role in the elaboration of the theory. It had been demonstrated that large fibers traversed deeper Rexed laminae of the dorsal horn, prior to curving rostrally to enter the substantia gelatinosa (SG), contained in Rexed laminae II, from the ventral side. Small diameter afferents, on the other hand, entered the SG directly from the dorsal side. Moreover, high-frequency stimulation of the large-diameter sensory fibers appeared to enhance negative potentials measured at the dorsal root ganglia, while similar stimulation of small sensory afferents enhanced positive dorsal root potentials [11, 21, 22]. In distilling these complex electrophysiological findings into a unified theory of pain perception, Melzack and Wall assumed that both large and small fibers projected to a common cell population that was termed the "transmission" (or T) cell, which projected to the forebrain for the conscious perception of pain [2]. The output of the T cells was modulated by the balance between small and large fiber input. Selective activation of large fibers was assumed to reduce the net input to T cells, by inhibiting (or closing) a presynaptic gate located in the SG. Conversely, small fiber activity facilitated (or opened) the gate, thereby increasing T cell input. Pain is perceived when T cell output reaches an internal threshold. This occurs when small fiber activation of the T cell overcomes large fiber inhibition.

The fundamental predictions of this seminal theory, namely, that stimulation of large-diameter fibers should close the gate by reducing activity in T cells and thereby diminish pain perception, spurred exploration into peripheral nerve stimulation. In 1967, Wall and Sweet reported on their outcomes from high-frequency, transcutaneous electrical nerve stimulation (TENS) in eight pain patients, four of whom had peripheral nerve damage [1, 2, 23, 24]. In all patients, the stimulation of large-diameter afferents was analgesic. Interestingly, patients with peripheral nerve damage experienced a longer duration of relief after cessation of stimulation than patients without nerve damage. The rationale for the abolition of pain was thought to be the selective Aα and Aβ fiber stimulation, while the reappearance of pain was thought to arise from a gradual reopening of the gate by ongoing small fiber activity. Furthermore, because patients with peripheral nerve damage presumably had fewer preserved small fibers (Aδ and C), the duration of relief following stimulation cessation was longer (or time to reappearance of pain was greater) [21].

Electrical Nerve Stimulation

Nerves transmit cutaneous information by means of propagation of action potentials [25]. When a stimulus sufficiently depolarizes an axon from its resting membrane potential, an action potential is propagated along its long axis. The resting potential across a membrane selectively permeable to a single ion is modeled by the Nernst equation, which was subsequently expanded in by the Goldman equation for the dominant ions influencing the resting potential of the neuron [25–28]. Electrical conduction along an axon is modeled as a series of parallel RC circuits, mathematically modeled by the cable equation [29]. Based on this work, the threshold amplitude for depolarization of myelinated nerves is expected to increase based on electrode distance to the fiber and decrease based on stimulus pulse duration and fiber diam-

eter [29]. This is the basis of the differential activation of recruitment of different cell and axon types, enabling therapeutic PNS.

Paresthesia-Free Stimulation

PNS, like spinal cord stimulation (SCS), has shown great clinical success in recent decades. It has the advantage of being targeted to specific peripheral nerve distributions, with little to no side effects. The stimulation patterns used in PNS, however, have historically predominantly relied on the production of paresthesias, which, based on Melzack and Wall's gate control theory of pain perception, are necessary for analgesia [2]. Until recently, the pattern of stimulation used in PNS (similar to SCS) has been composed of pulse waves at a frequency of 40–50 Hz, a pulse width between 300 and 500 μs, and a peak amplitude between 2 and 4 mA [3, 30, 31]. This paresthesia-generating pattern is known as "tonic" stimulation. In recent years, it has become increasingly clear that paresthesias are not necessary for pain relief in SCS. Effective pain relief in SCS has also been demonstrated with systems delivering pulses in short bursts or continuously but in much higher frequencies, both of which operate without the generation of paresthesias [3, 30]. Such paresthesia-free stimulation is becoming increasingly utilized in PNS, although clinical outcomes data remain limited.

Burst Stimulation

Burst stimulation consists of small bursts of pulses rather than continuous streams of pulses. More specifically, the pulses are delivered in a series of five 1000 μs pulses at a frequency of 500 Hz, with an interspike interval of 1000 μs, and spike trains repeated at a frequency of 40 Hz [30, 32]. The mechanisms by which burst stimulation achieves paresthesia-free stimulation are unknown but are believed to arise through modified neuronal firing. In rodents, increasing the number of pulses in a burst, or their pulse width, led to greater reductions in the firing rate of neurons within the dorsal horn from their baseline [33, 34]. This was especially true for wide dynamic range (WDR) neurons, which appear to function as the T cells (from the gate control theory), and may alter neural transmission from the thalamus to the anterior cingulate cortex and influence the perception of pain [3]. Burst stimulation also appears to differ from tonic stimulation in its effect on dorsal column nuclei (in particular, the gracile nucleus). Tonic stimulation appears to significantly increase spontaneous activity of gracile nucleus neurons (by 20%), compared to no significant change during burst stimulation [30, 33, 34]. Because the gracile nucleus is the tactile sensory receiving area for much of the information ascending within the dorsal columns, this also supports why tonic stimulation results in paresthesias, compared to burst stimulation which does not.

High-Frequency Stimulation

High-frequency (HF) stimulation is a more recent alternative to burst stimulation for the induction of paresthesia-free stimulation. HF stimulation involves the use of kilohertz range tonic stimulation (up to 10 kHz) and has shown success in spinal cord stimulation [30]. Its mechanism of action appears to be a rapid and reversible conduction block of neural activity by inactivation of sodium channels along several nodes of Ranvier [30, 35–40]. HF stimulation appears to *block* paresthesias by inhibiting large-diameter fibers from generating action potentials. Nerve fibers that are greater than 15–18 μm shut down at 4 kHz and those that are smaller (8–9 μm) shut down at frequencies of around 8 kHz [30, 36, 37]. Medium fibers that reduce WDR signaling are activated instead by HF stimulation, which leads to decreased pain stimulus conduction. Indeed, the mechanisms through which HF stimulation mitigates pain may be more complex. Although the effect of pulse rate has not been systematically evaluated, it appears that beyond a certain threshold, pain relief may not be significantly different with further increases in stimulation frequency [30]. For example, in a recent randomized, multicenter, double-blind, crossover clinical study of SCS, 1

kHz stimulation was compared with 10 kHz stimulation and demonstrated no observable differences in clinical outcomes [3, 30, 41]. Future work is necessary to evaluate the role of HF patterns for PNS.

Devices Used for Peripheral Nerve Stimulation

Starting with Wall and Sweet in the 1960s, externalized wire electrodes were percutaneously placed adjacent to nerves but the adoption of this technique was greatly limited by lack of commercialized equipment [1, 42]. By the 1970s and 1980s, implantable cuff-shaped electrodes which were later supplanted by button-shaped and paddle electrodes were used in a number of clinical studies, demonstrating greater than 50% pain relief for some patients [42]. These procedures subsequently fell out of favor and were replaced by a growing interest in SCS, which avoided the challenges at that time of surgical nerve exposure, electrode positioning, and generation of fibrosis around the nerve and electrodes. In 1999, the use of percutaneous SCS leads for PNS described by Weiner and Reed greatly renewed interest in PNS for a variety of pain disorders [43]. Despite growing evidence supporting PNS, the surgical placement of commonly used SCS systems for PNS generally remains "off-label." These companies offer several different features and capabilities on their platform, allowing the surgeon to select an implant that best matches the patient's goals for therapy. These considerations include battery size and recharging ability, whole-body MRI compatibility, the ability implant 1–4 leads with up to 32 active contacts, choice of programing waveforms, and programming interface [44–47]. Each company offers either paddle or percutaneous lead configurations, the latter more commonly used for PNS [42]. Recently, percutaneously inserted electrodes powered by an external, transcutaneous transmitter and battery pack have been introduced by several companies. Examples include the Freedom Stimulator by Stimwave, StimRouter by Bioness, and the SPRINT PNS System by SPR Therapeutics. These stimulator systems have FDA approval for PNS throughout the body but not for craniofacial nerve stimulation at time of publication. This style of stimulator is particularly amenable for placement for and treatment of intercostal nerve pain, shoulder pain, and extremity pain along a specific peripheral nerve distribution [48–52].

Patient Selection

Peripheral nerve stimulation is generally regarded as second-line treatment for chronic pain disorders ranging from localized neuralgias, complex regional pain syndrome, post-traumatic pain, postherpetic pain, and postoperative pain throughout the body [53]. Patients should be co-managed with a pain specialist and keep a pain diary to track their visual analog scores (VAS) for pain. A large portion of the initial patient encounter should be focused on managing expectations and emphasizing that PNS is only one component of a comprehensive pain plan. Pain psychology evaluation is also advised for patients considering implantation of a stimulator [54]. Responses to local blocks or TENS treatment have not predicted how patients respond to PNS [42, 55]. As such, a trial period using externalized leads is first completed before a permanent implant is considered. As a general guide, patients should have a 50% reduction in their VAS scores noted in their diary and reasonable expectations for treatment with a permanent implant. Some of the transcutaneous powered systems described above have options for permanent implantation in one stage, with a second operation reserved for removal if necessary. The duration of a trial varies between institutions, with some concern that short duration trials do not adequately account for early placebo effect. Still, no systematic benefits of longer trial periods have been reported.

Surgical Technique

Placement of a SCS for PNS can be performed as an outpatient procedure [53]. It is important to map and mark the region of the patient's pain prior

to the start of the procedure. Conscious sedation is used for trial placement while general anesthesia is used for permanent implantation. Patient positioning depends on the targeted nerve(s). Ultrasound can be helpful to identify the target nerve or its associated neurovascular bundle [52]. Once the nerve or the region of interest is identified, a small stab incision is made just proximal to the pain region along the course of the nerve. Minimal to no local anesthetic is used to avoid an inadvertent nerve block which will eliminate the utility of intraoperative testing (if planned) or postoperative device programming. Under fluoroscopic guidance, a Tuohy needle is passed subcutaneously along the course of the nerve above deep fascia. A percutaneous lead is introduced through the Tuohy needle which is then removed. It can be useful at this point to awaken the patient and apply paresthesia-inducing stimulation to ensure adequate coverage and make any lead position adjustments as necessary. Fluoroscopy is used to ensure the lead does not migrate while using the Tuohy and to document final lead position. The externalized lead is secured to the skin with suture and sterile dressings. In recovery, the leads are connected to an external generator and initially programmed to provide paresthesia in the distribution of pain without motor contractions. The Neurostimulation Appropriateness Consensus Committee recommends the use of prophylactic antibiotics for no longer than 24 hours after surgery, but studies suggest benefit in using antibiotics during the trial setting for the reduction of permanent implant infection [56, 57].

Patients are informed to keep a daily pain diary to log their VAS. The patient is seen in clinic after 1–2 weeks, during which time stimulation parameters are adjusted. The electrodes are removed in the office and if the patient responds well to PNS and wishes to proceed, permanent implantation is scheduled in a few weeks to allow for wound healing. Images obtained for the trial in addition to insight gained from programming during the trial period guide permanent electrode placement. General anesthesia is recommended mainly due to the pain from tunneling subcutaneous extension cables and placement of the pulse generator. Once the stimulation leads are placed, they should be secured to the fascia and excess cabling should be used to create a strain relief loop. Implantable stimulators are commonly placed in subcutaneous infraclavicular pocket or in the gluteal region below the belt line but above the ischial tuberosity. Each manufacture has guidelines on the acceptable depth of implantation. Lead impedances are interrogated in the OR prior to skin closure. The device is turned on in the recovery area and programmed to settings that provided the best overall pain relief with minimal side effects during the trial period.

Trigeminal Nerve Stimulation for Pain

Peripheral nerve stimulation is a useful alternative option for treating craniofacial pain refractory to pharmacological therapy that is not appropriate for traditional surgical procedures such as microvascular decompression and/or percutaneous trigeminal rhizotomy procedures. PNS for facial pain is addressed briefly in Chap. 32, but discussed in greater detail here. Since the experiments by Wall and Sweet, stimulation of peripheral branches of the trigeminal nerve has been well demonstrated to mitigate certain types of facial pain. Neuropathic and postherpetic neuralgia pain have been the most commonly studied [58–63]. Furthermore, trigeminal nerve stimulation (TNS) has also shown some promise for the treatment of refractory headache disorders [64, 65].

In a case series of TNS published in 2015, 15 out of 35 patients with intractable craniofacial pain trialed with stimulation proceeded to permanent implantation [58]. In this study, indications for peripheral trigeminal branch stimulation included trigeminal neuralgia, trigeminal neuropathic pain, trigeminal deafferentation pain, postherpetic neuralgia, and headache. After a minimum follow-up length of 15 months, 73% of these patients reported "worthwhile" pain relief. Though there were no serious side effects, seven patients underwent 12 revision surgeries related to hardware complications including three total explants. The authors noted that the lancinating pain characteristic of trigeminal neuralgia type 1

did not respond well to neurostimulation and should be managed by traditional treatment options. In addition, stimulation of the mandibular branch for temporomandibular joint was attempted in this study but was not found to be beneficial. Stimulation parameters appear to be patient dependent, as noted in a case series of six patients treated with PNS to the trigeminal nerve, that were programmed with pulse widths from 210 to 450 μsec and frequencies between 16 and 80 Hz [66]. Peripheral nerve stimulation systems implanted for the treatment of ophthalmic postherpetic neuralgia were programmed with similar parameter ranges [61]. Amplitude of stimulation influenced the intensity of the paresthesias elicited by stimulation and was titrated to comfort.

For trigeminal nerve stimulation, a percutaneous SCS lead is placed adjacent to the targeted nerve branch. The patient is positioned supine on the operating table with head turned toward the unaffected side. A small stab incision is made on the lateral side of the face, commonly just anterior the tragus where minimal local anesthetic is injected. To target the supraorbital or infraorbital nerves, the distal tip of a four- or eight-contact percutaneous lead is placed 1 cm away from the orbital rim and medially past the mid-pupillary line (Fig. 14.1). For the mandibular branch, the needle is directed toward the chin. In recovery, the leads are connected to an external generator and initially programmed to provide paresthesia in the distribution of pain without producing facial muscle contraction. Imaging and insight gained from programming during the trial period guide permanent electrode placement. The leads are tunneled behind the ear and secured both at the insertion sites and to the temporalis fascia. Extension cables are tunneled behind the ear and over the clavicle and connected to the pulse generator, placed in an infraclavicular pocket.

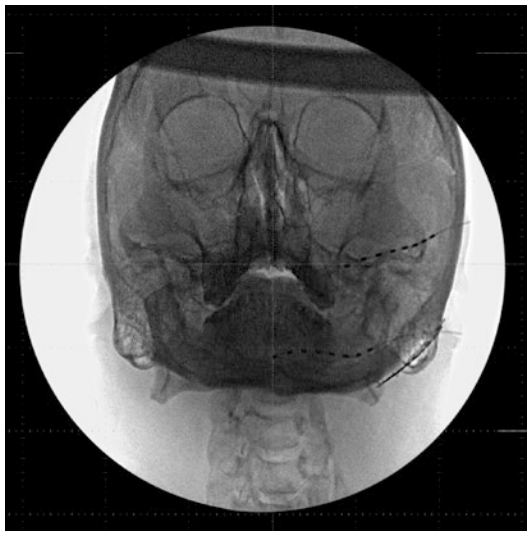

Fig. 14.1 Intraoperative x-ray for placement of leads for infraorbital and mandibular nerve stimulation

Greater and Lesser Occipital Nerve Stimulation for Pain

One of the more common uses of PNS is for the treatment of occipital neuralgia (ON) and related headache disorders. In 1999, Weiner and Reed described percutaneous lead placement for the treatment of intractable ON [43]. They demonstrated that pain relief could be achieved by placing the electrode in proximity to the nerve rather than directly on the nerve with paddle electrodes or cuff electrodes. Their technique was widely adopted and cuff electrodes have largely been abandoned in PNS for the treatment of pain [42].

A number of published case series show excellent results with ONS for the treatment of medically refractory ON, with improvement estimated to be as high as 60–90% [43, 59, 67–71]. One of the larger prospective studies followed 11 patients with occipital headaches over a 12-week period. Following ONS, 64% of patients reported a decreased headache frequency and 91% of patients reduced their medication use [72]. Interestingly, ONS has also been shown to improve pain associated with disorders of the trigeminal nerve, such as cluster headache, which is considered a trigeminal autonomic cephalalgia [73–75]. In a pilot study, ONS reduced the average number of weekly cluster headache attacks by about 80% in eight patients with drug-resistant chronic cluster headache [75].

A large interest in using ONS for the treatment of chronic migraines lead to several large

trials, with a meta-analysis of five randomized controlled trials (total $n = 402$) concluding that ONS reduced mean severe headache frequency by 2.59 days per month after 3 months in comparison to patients undergoing sham stimulation [76]. The Precision Implantable Stimulator for Migraine (PRISM) study compared active bilateral stimulation (stimulation parameters: 250 μs, 60 Hz, 0–12.7 mA) to sham stimulation in 139 out of 179 screened patients with episodic or chronic migraine. Twelve weeks after implantation, patients treated with ONS did not report a statistically significant difference in daily frequency of migraine compared to those treated with sham stimulation, based on daily pain diary entries [77]. The authors hypothesized that the lack of efficacy was due do the heterogenous character of headaches despite using definitions defined in the 2004 International Classification of Headache Disorders. In the Occipital Nerve Stimulation for the Treatment of Chronic Migraine Headache (ONSTIM) study, three-month responder rates were 39% for patients in the adjustable stimulation group, 6% in the sham stimulation group, and 0% for those in the medical management group [78]. A responder was defined as someone who achieved a 50% or greater reduction in number of headache days per month or a three-point or greater reduction in average overall pain *intensity* compared to baseline. In a multicenter study of 157 patients (Clinicaltrials.gov NCT00615342), there was no significant difference between active and control groups with regard to number of responders reaching a 50% reduction in mean daily (VAS) at 12 weeks, but there were significant reductions in pain intensity, headache days, and migraine-related disability [79]. The authors published a 52-week update which reported continued efficacy of ONS for chronic migraine, with intention-to-treat analysis showing a 50% reduction in headache days and/or pain intensity in 48% of patients [80].

The technique for occipital nerve lead implantation is similar to that of TNS and can be performed with the patient in either prone or lateral position. Percutaneous electrodes are introduced at the midline and directed laterally above the nuchal fascia (Fig. 14.2). Eight-contact percutaneous leads span a length long enough to have electrode contacts perpendicularly cross both the greater and lesser occipital nerves. To ensure the distal electrode tip does not pierce the scalp, the hair on the back of the head can be clipped. With the patient prone, the stimulator battery can be easily placed in the gluteal position whereas lateral positioning allows for infraclavicular placement. Surprisingly, in the NCT00615342 study referenced above, 70% of patients experienced an adverse event, totaling 209 with 183 of these device/procedure related [80]. In fact, lead migration or dislodgement appeared to be a common adverse effect associated with implanted ONS, with randomized trials demonstrating an incidence rate of 10–24% [35, 43, 68, 69, 76]. The authors of one series suggest the use of paddle-type leads instead of cylindrical leads to reduce the occurrence of lead migration [69]. Yet others report similar rates of migration with paddle electrodes [75]. Other variations in technique include open placement of a cylindrical electrode, a greater number of strain relief coils with lead cabling, and varying pulse generator placement from a gluteal to infraclavicular location [78, 81]. Infection rates vary from 4% to 30% based on follow-up ranging from 2 months to 6 years [76].

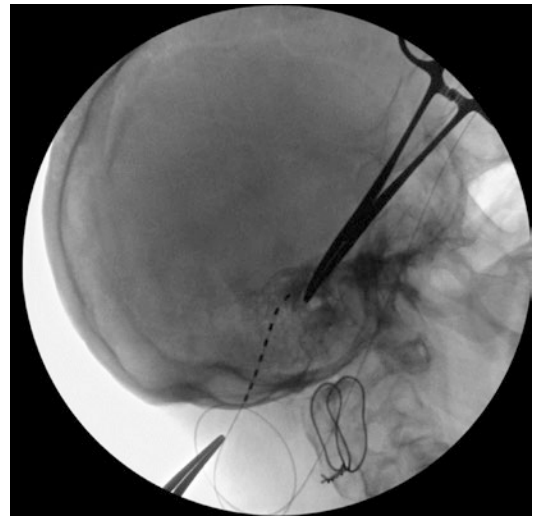

Fig. 14.2 Intraoperative x-ray for placement of lead for unilateral occipital nerve stimulation

Peripheral Nerve Stimulation for Postamputation Pain

Amputation can lead to chronic neuropathic pain that responds poorly to medication and frequently leads to opioid dependence [82–86]. Two types of chronic pain may occur after amputation: phantom limb pain (PLP) and residual limb pain (RLP). Up to 70–80% of patients experience either PLP, RLP, or both [87, 88]. For many amputees, the pain following amputation can impact activities of daily living more than the loss of the limb itself [89–91]. Additionally, poor management of RLP limits the use of prostheses, further impairing function in these patients. Therefore, PNS is an appealing treatment for these conditions. In a study of 16 patients with PLP and/or RLP, 14 patients responded to stimulation with ≥75% paresthesia coverage [92]. Nine of these patients completed a two-week home trial with a percutaneous PNS system and reported a 56 ± 26% reduction in pain at the end of the trial period [92]. In this study, the surgeons used ultrasound to guide percutaneous placement of a monopolar lead near the femoral or sciatic nerve and used stimulation to further validate proximity to the nerve while avoiding local cutaneous stimulation [92]. Once the patient reported limb paresthesia without cutaneous spread, the monopolar lead was replaced with the stimulating electrode, at a depth 0.5–2.0 cm shallower than the monopolar lead. In a pilot trial, using a cuff electrode wrapped around the sciatic or tibial nerve to deliver 10 kHz stimulation, seven patients with postamputation pain experienced a 75% reduction in pain at the three-month endpoint [93].

Peripheral Nerve Field Stimulation

Peripheral nerve stimulation differs in principle from peripheral nerve field stimulation (PNFS) [48]. Peripheral nerve stimulation refers to stimulation of a targeted nerve by an electrode implanted in its proximity. Its mechanism of therapeutic benefit is attributed to direct stimulation of the nerve. Consequently, the patient's pain must be attributed to a specific nerve and the surgeon needs to have a working knowledge of the nerve's anatomical course for proper electrode placement. Conversely, PNFS refers to the placement of subcutaneous electrodes in the region of the patient's pain, thus benefiting patients who have symptoms that may be less well localized [94]. For PNFS, the depth at which the electrode is implanted is critical as a shallow placement can result in stimulation that is perceived as a burning sensation and may lead to skin erosion, whereas insertion that is too deep may trigger muscle contractions. To program PNFS, frequencies between 20 and 50 Hz and pulse widths of 90–250 μsec are best tolerated, with higher settings of either parameter resulting in burning or pinching sensations [94]. For well-placed electrodes, intensities between 1.5 and 2 mA can provide patients with pain relief. PNFS has been used for the treatment of complex regional pain syndrome, neuralgias, post-traumatic pain, and postoperative pain throughout the body [94]. In a study of 100 patients who underwent PNFS for treatment of chronic craniofacial, thorax, lumbosacral, abdominal, pelvic, and groin pain, 72% of patients demonstrated a reduction in analgesic use after surgery and a mean pain reduction of 36% [95]. Although the procedures are similar and use the same implantable hardware, insurance reimbursement and authorization may be more challenging for PNFS than for PNS in the United States [9].

Brain Correlates of Peripheral Nerve Stimulation

As described earlier in this chapter, peripheral nerve stimulation in its earliest use was grounded on the gate control theory of pain perception, in which a non-noxious stimulus interferes with the transmission of pain-related sensory input [21, 96]. Mounting evidence indicates that at least a part of the pain alleviation may stem from central neuromodulation [96]. This may occur on two different timescales – acutely from alterations in network activity between the peripheral and central nervous system and chronically from an integration of modulated neural activity in the

nervous system. Chronic stimulation results in adaptive changes in the brain and contributes to the therapeutic effect of peripheral nerve stimulation [94, 97]. Data regarding central neuromodulation following PNS are limited to functional neuroimaging studies. Most studies that describe the central effects of PNS are from vagus nerve stimulation (VNS) for epilepsy and depression [98–100]. Other peripheral nerve stimulation paradigms in which the brain correlates have been studied include trigeminal nerve stimulation for neuropathic trigeminal pain, occipital nerve stimulation for headaches and occipital neuralgia, and sacral nerve stimulation (SNS) for urinary and fecal incontinence or detrusor hyperactivity [75, 101, 102]. In this section, we briefly highlight brain correlates of VNS and SNS, which may be reflective of patterns of central neuromodulation in response to PNS that will need to be explored further to truly understand the mechanisms by which PNS exerts its effects.

Unlike most PNS, VNS is unique in that the vagus nerve carries sensory afferents belonging to different categories that synapse on the nucleus of the solitary tract (NTS), the dorsal motor nucleus of the vagus nerve, and others [96, 97, 99]. Because the NTS in turn projects diffusely to the reticular formation, hypothalamus, thalamus, and other cortical and subcortical structures, functional neuroimaging studies implicate a major role for the thalamus and limbic structures in the mechanisms of action of VNS [96]. Increased regional cerebral blood flow (rCBF) on positron emission tomography (PET) has been described in regions of the bilateral, anterior thalami, the cingulate gyrus, hypothalamic, and the postcentral gyrus in the acute phase in patients implanted with VNS for epilepsy, for instance [96]. In contrast, single photon emission computed tomography (SPECT) studies suggest that after chronic VNS (at least 6 months of stimulation), there is a general trend toward thalamic and limbic inhibition [96, 99, 100, 102, 103]. This trend of initial increased activity but delayed depression readily explains the efficacy of VNS in the treatment of epilepsy. The thalamus supplies excitatory glutamatergic input to the cortex. The depression that occurs over the long term may not only decrease seizures of limbic origin but may also enable the thalamus to serve as a gating structure for secondary generalization of limbic seizures to the rest of the cortex [96, 103].

VNS is hypothesized to affect clinical depression due to connectivity of the NTS to several regions implicated in the pathogenesis of depression including the prefrontal cortex, cingulate cortex, amygdala, hippocampus, thalamus, and basal forebrain [96, 100, 102, 104, 105]. While mechanisms by which VNS modulates network activity are largely unknown for patients with depression, functional neuroimaging studies definitively indicate that on both acute and chronic timescales they are central to its neuromodulatory effects.

Sacral nerve stimulation differs from vagus nerve stimulation because vagus nerve nuclei are directly located in the brain stem. As such, sacral stimulation can serve as a paradigm to understand how peripheral nerve stimulation modulates targets that are not directly connected within the central nervous system. Chronic stimulation of the sacral S3 nerve is used for urge incontinence and for medically refractory bladder hyperactivity. The urge during bladder distension may involve the periaqueductal gray, anterior cingulate gyrus, insula, thalamus, and cerebellum [96, 106, 107]. In functional imaging studies, in patients implanted with SNS, acute SNS has been found to lead to decreased rCBS in the medial cerebellum, insula, and orbitofrontal cortex [96, 106–109]. After chronic SNS, there is a decreased rCBF in the middle cingulate gyrus, the dorsolateral prefrontal cortex, the thalamus, and the cerebellum, among others. In particular, the difference between the acute and chronic states appears to involve the premotor and the cerebellar regions. This indicates that acute SNS alters structures involved in sensorimotor learning (premotor cortex and cerebellum), while chronic SNS leads to these regions becoming less active while regions involved in central control of micturition becoming more active [96, 106–109].

These two paradigms allow us to conclude that pathologies affect multiple brain structures both primarily and secondarily. Appropriately targeted peripheral nerve stimulation appears to

achieve therapeutic benefits by acutely altering the relative valence of the various brain structures involved through modulating variables such as rCBF. Through chronic stimulation, brain regions appear to develop adaptive strategies that help provide sustained relief. More work is necessary to elucidate the mechanisms by which central neuromodulation relates to PNS, which may ultimately lead to optimized therapies.

Peripheral Nerve Stimulation for Epilepsy and Depression

Concerningly, as many as 20–30% of patients with epilepsy will develop drug-resistant epilepsy and thus remain at risk for seizure-related injury [110]. Similarly, major depressive disorder can become a chronic illness for many patients who become refractory to multiple antidepressant medications [111, 112]. As such, vagus nerve stimulation (VNS) and trigeminal nerve stimulation (TNS) are being studied as treatment adjuncts.

VNS is a neuromodulatory treatment that was approved by the FDA in 1997 as an adjunctive therapy for epilepsy in adults over 12 years of age with partial onset seizures [110]. Treatment consists of chronic intermittent electrical stimulation of the left vagus nerve by a cuff electrode connected to an implanted programmable pulse generator (neurocybernetic prosthesis, Cyberonics, Inc., Houston, TX, USA). Following the observation that stimulation of the vagus nerve of dogs demonstrated an anticonvulsive effect, the first human patients were implanted in 1988 as part of two initial pilot studies [113, 114]. Since then, several controlled studies have demonstrated both short- and long-term improvement in seizure control. A recent review, including both adult and pediatric patients, demonstrated that approximately 60% of individuals receiving VNS have 50% or greater reduction in seizure frequency [110]. As such, VNS has been widely adopted as a treatment of epilepsy and an estimated 100,000 VNS devices have been implanted worldwide as of 2014 [115].

Although VNS was not originally intended for treatment of depression, Elger et al. noted improvement in mood, independent of effects on seizure activity, in patients who received VNS for treatment of drug-resistant epilepsy [116]. Rush et al. conducted the first trial that systematically examined the short-term efficacy (10 weeks) of VNS in 30 patients with major depressive episodes and found that 40% of patients responded favorably (greater than or equal to 50% reduction in baseline 28-item Hamilton Depression Rating Scale ($HDRS_{28}$) to VNS therapy [117]. Likewise, when patients receive long-term treatment (greater than 12 months), studies show that as many as two-thirds of patients respond favorably to VNS therapy [118–120]. However, though VNS received FDA approval in 2005 for the treatment of depression, multiple systemic review studies have concluded that more research, particularly in the form of randomized control studies, are needed to convincingly establish the safety and efficacy of this therapy for the treatment of depression [118, 121].

The ability to neuromodulate brain activity via stimulation of the vagus nerve inspired clinicians and scientists to investigate the therapeutic potential of other cranial nerves, such as the trigeminal nerve. In contrast to the vagus nerve, the trigeminal nerve is located more superficially and is not associated with the adverse autonomic effects potentially seen with VNS [122]. In their animal model study, Fanselow et al. demonstrated that TNS can cause cortical and thalamic desynchronization, resulting in a decrease in the number of seizures in awake rats [123]. Based on this work, DeGiorgio and colleagues evaluated the feasibility of external TNS (eTNS) in adults with drug-resistant epilepsy in a series of early-phase clinical studies [124–126]. Positive results from these studies led this same group to conduct the first double-blind randomized active-control trial of eTNS in 50 patients with drug-resistant epilepsy. Although the responder rate (defined as greater than 50% reduction in seizure frequency) was not statistically significant between the treatment group and controls, 40.5% of the 25 patients that received eTNS responded to treatment upon evaluation at 18 weeks. Similar to findings in VNS studies, the authors also noted significant improvement in

mood, independent of changes in seizure frequency, in those receiving eTNS compared with the control group [116, 127]. Although not FDA approved, recent analyses have observed a significant improvement in both quality of life and mood in those using eTNS, as well as a retention rates that are comparable to commonly prescribed antiepileptic drugs [128, 129].

Considering the known anatomical connections of the trigeminal nerve to structures associated with mood and regulation and the known effects of VNS on both epilepsy and mood, Drs. Cook and Schrader conducted the first proof-of-concept trial of eTNS in 11 adults with unipolar major depressive disorder [130]. Nightly stimulation of the V1 branch was well-tolerated over an 8-week period and resulted in significant improvement in $HDRS_{28}$, which decreased from a score of 28.0 (s.d. = 6.9) to 14.4 (s.d. = 6.5), as well as significant improvement in quality of life [131]. Promising results ultimately motivated randomized, double-blind, sham-controlled clinical trials, in which patients underwent 10 daily 30-minute eTNS sessions for major depressive disorder. Both of these trials demonstrated positive effects of TNS in improving depressive symptoms, with a mean reduction in $HDRS_{28}$ of up to 36.15% [132, 133]. Further studies are currently underway to help establish TNS for depression, including investigation of subcutaneous TNS as an alternative technique [122].

Conclusion

PNS is not a new field, but still evolving likely in large part due to limited regulatory approval for this approach. The biophysical underpinning relies on differential modulation of peripheral nerve fibers of different sizes which convey different aspects of peripheral sensation. Successful applications have been detailed in facial, truncal, and extremity pain suggesting PNS as a useful option for peripheral neuromodulation and treatment for chronic pain. While work to date has largely focused on treatment of chronic pain, there is increasing interest in the role of peripheral neuromodulation to access and modulate the central nervous system in other neurological and psychiatric disorders, such as epilepsy and depression.

References

1. Wall PD, Sweet WH. Temporary abolition of pain in man. Science (80-.). [Internet]. 1967 [cited 2018 Dec 7];155(3758):108–9. Available from: http://www.ncbi.nlm.nih.gov/pubmed/6015561.
2. Melzack R, Wall PD. Pain mechanisms: a new theory. Science [Internet]. 1965 [cited 2018 Dec 4];150 (3699):971–9. Available from: http://www.ncbi.nlm.nih.gov/pubmed/5320816.
3. Burchiel KJ, Raslan AM. Functional neurosurgery and neuromodulation. 1st ed: Elsevier Health Sciences; 2018.
4. Kandel ER. Principles of neural science. 5th ed. Kandel ER, Schwartz JH, Jessell TM, Siegelbaum SA, Hudspeth AJ, editors. McGraw-Hill Education; 2013.
5. Moore SP, Psarros TG. The definitive neurological surgery board review: Blackwell Pub; 2005.
6. Rexed B. A cytoarchitectonic atlas of the spinal cord in the cat. J Comp Neurol. [Internet]. 1954 [cited 2019 Apr 14];100:297–379. Available from: http://www.ncbi.nlm.nih.gov/pubmed/13163236.
7. Rexed B. The cytoarchitectonic organization of the spinal cord in the cat. J Comp Neurol. [Internet]. 1952 [cited 2019 Apr 14];96:414–95. Available from: http://www.ncbi.nlm.nih.gov/pubmed/14946260.
8. Todd AJ. Neuronal circuitry for pain processing in the dorsal horn. Nat Rev Neurosci. [Internet]. Europe PMC Funders; 2010 [cited 2019 Apr 14];11:823–36. Available from: http://www.ncbi.nlm.nih.gov/pubmed/21068766.
9. Burchiel KJ, editor. Surgical management of pain [Internet]. Stuttgart: Georg Thieme Verlag; 2015 [cited 2018 Dec 4]. Available from: http://www.thieme-connect.de/products/ebooks/book/10.1055/b-002-102571.
10. Dubner R, Sessle B, Storey A. The neural basis of oral and facial function. Dubner R, editor. New York: Plenum; 1978.
11. Moayedi M, Davis KD. Theories of pain: from specificity to gate control. J Neurophysiol. 2013;109: 5–12.
12. Rey R. The history of pain. Cambridge: Harvard University Press; 1995.
13. Iggo A, Muir AR. The structure and function of a slowly adapting touch corpuscle in hairy skin. J Physiol. 1969;200:763–96.
14. Cauna N, Ross L. The fine structure of Meissner's touch corpuscles of human fingers. J Biophys Biochem Cytol. 1960;8:467–82.
15. Cauna N, Manna G. The structure of human digital pacinian corpuscles (corpus cula lamellosa) and its functional significance. J Anat. [Internet]. 1958;92:

1–20. Available from: http://www.ncbi.nlm.nih.gov/pubmed/13513492.
16. Burgess PR, Perl ER. Myelinated afferent fibres responding specifically to noxious stimulation of the skin. J Physiol. 1967;190:541–62.
17. Bessou P, Perl ER. Response of cutaneous sensory units with unmyelinated fibers to noxious stimuli. J Neurophysiol. 1969;32:1025–43.
18. Dallenbach KM. Pain: history and present status. Am J Psychol. 1939;52:331.
19. Sinclair DC. Cutaneous sensation and the doctrine of specific energy. Brain [Internet]. 1955;78:584–614. Available from: http://www.ncbi.nlm.nih.gov/pubmed/13293271.
20. Weddell G. Somesthesis and the chemical senses. Annu Rev Psychol. 1955;6:119–36.
21. Mendell LM. Constructing and deconstructing the gate theory of pain. Pain. 2014;155:210–6.
22. Rudomin P, Schmidt RF. Presynaptic inhibition in the vertebrate spinal cord revisited. Exp Brain Res. 1999;129:1–37.
23. Bates JA, Nathan PW. Transcutaneous electrical nerve stimulation for chronic pain. Anaesthesia. 1980;35:817–22.
24. Nathan PW, Wall PD. Treatment of post-herpetic neuralgia by prolonged electric stimulation. Br Med J. 1974;3:645–7.
25. Hodgkin AL, Huxley AF. A quantitative description of membrane current and its application to conduction and excitation in nerve. J Physiol. [Internet]. John Wiley & Sons, Ltd (10.1111); 1952 [cited 2019 Apr 13];117:500–44. Available from: http://doi.wiley.com/10.1113/jphysiol.1952.sp004764.
26. Goldman DE. Potential, impedance, and rectification in membranes. J Gen Physiol. [Internet]. 1943 [cited 2019 Apr 14];27:37–60. Available from: http://www.ncbi.nlm.nih.gov/pubmed/19873371.
27. Hodgkin A, Rushton W. The electrical constants of a crustacean nerve fibre. Proc R Soc Med. [Internet]. 1946 [cited 2019 Apr 14];134:444–79. Available from: http://www.ncbi.nlm.nih.gov/pubmed/20281590.
28. Hodgkin A, Katz B. The effect of sodium ions on the electrical activity of giant axon of the squid. J Physiol. [Internet]. Wiley-Blackwell; 1949 [cited 2019 Apr 14];108:37–77. Available from: http://www.ncbi.nlm.nih.gov/pubmed/18128147.
29. Grill WM. Nerve Stimulation. Wiley Encycl Biomed Eng. [Internet]. Hoboken, NJ, USA: John Wiley & Sons, Inc.; 2006 [cited 2018 Dec 8]. Available from: http://doi.wiley.com/10.1002/9780471740360.ebs0825.
30. Ahmed S, Yearwood T, De Ridder D, Vanneste S. Burst and high frequency stimulation: underlying mechanism of action. Expert Rev Med Devices. 2018;15:61–70.
31. Sdrulla AD, Guan Y, Raja SN. Spinal cord stimulation: clinical efficacy and potential mechanisms. Pain Pract. 2018;18:1048–67.
32. De Ridder D, Perera S, Vanneste S. Are 10 kHz stimulation and burst stimulation fundamentally the same? Neuromodulation. 2017;20:650–3.
33. Chakravarthy K, Nava A, Christo PJ, Williams K. Review of recent advances in Peripheral Nerve Stimulation (PNS) [Internet]. Curr Pain Headache Rep. 2016 [cited 2019 Jan 3]. p. 60. Available from: http://link.springer.com/10.1007/s11916-016-0590-8.
34. Manning A, Ortega RG, Moir L, Edwards T, Aziz TZ, Bojanic S, et al. Burst or conventional peripheral nerve field stimulation for treatment of neuropathic facial pain. Neuromodulation. 2019;22:645.
35. Kapural L, Mekhail N, Hayek SM, Stanton-Hicks M, Malak O. Occipital nerve electrical stimulation via the midline approach and subcutaneous surgical leads for treatment of severe occipital neuralgia: a pilot study. Anesth Analg. [Internet]. 2005 [cited 2018 Dec 11];101:171–4. Available from: http://www.ncbi.nlm.nih.gov/pubmed/15976227
36. Kilgore KL, Bhadra N. Reversible nerve conduction block using kilohertz frequency alternating current. Neuromodulation. 2014;17:242–54; discussion 254–5.
37. Lempka SF, McIntyre CC, Kilgore KL, Machado AG. Computational analysis of kilohertz frequency spinal cord stimulation for chronic pain management. Anesthesiology. 2015;122:1362–76.
38. Arle JE, Mei L, Carlson KW, Shils JL. High-frequency stimulation of dorsal column axons: potential underlying mechanism of paresthesia-free neuropathic pain relief. Neuromodulation. 2016;19:385–97.
39. Cuellar JM, Alataris K, Walker A, Yeomans DC, Antognini JF. Effect of high-frequency alternating current on spinal afferent nociceptive transmission. Neuromodulation. 2013;16:318–27; discussion 327.
40. Shechter R, Yang F, Xu Q, Cheong Y-K, He S-Q, Sdrulla A, et al. Conventional and kilohertz-frequency spinal cord stimulation produces intensity- and frequency-dependent inhibition of mechanical hypersensitivity in a rat model of neuropathic pain. Anesthesiology. 2013;119:422–32.
41. Thomson SJ, Tavakkolizadeh M, Love-Jones S, Patel NK, Gu JW, Bains A, et al. Effects of rate on analgesia in kilohertz frequency spinal cord stimulation: results of the PROCO randomized controlled trial. Neuromodulation. 2018;21:67–76.
42. Slavin K V. History of peripheral nerve stimulation. Prog Neurol Surg. [Internet]. Karger Publishers; 2011 [cited 2018 Dec 4];24:1–15. Available from: http://www.ncbi.nlm.nih.gov/pubmed/21422772.
43. Weiner RL, Reed KL. Peripheral neurostimulation for control of intractable occipital neuralgia. Neuromodulation [Internet]. 1999 [cited 2018 Dec 12];2:217–21. Available from: http://www.ncbi.nlm.nih.gov/pubmed/22151211.
44. Medtronic. Spinal cord stimulation systems | Medtronic [Internet]. [cited 2019 Apr 14]. Available from: https://www.medtronic.com/us-en/healthcare-professionals/products/neurological/spinal-cord-stimulation-systems.html.
45. Nevro. Nevro - offering HF10 therapy for chronic pain relief [Internet]. [cited 2019 Apr 14]. Available

from: https://www.nevro.com/English/Home/default.aspx.
46. Abott. Our products | Abbott Neuromodulation [Internet]. [cited 2019 Apr 14]. Available from: https://www.neuromodulation.abbott/us/en/hcp/products.html.
47. Boston Scientific. Spectra WaveWriterTM SCS System – Pain Management – Boston Scientific - Boston Scientific [Internet]. [cited 2019 Apr 14]. Available from: https://www.bostonscientific.com/en-US/products/spinal-cord-stimulator-systems/spectra-wavewriter-scs.html.
48. Deer TR, Levy RM, Verrills P, Mackey S, Abejon D. Perspective: peripheral nerve stimulation and peripheral nerve field stimulation birds of a different feather. Pain Med. [Internet]. Narnia; 2015 [cited 2019 Apr 11];16:411–2. Available from: https://academic.oup.com/painmedicine/article-lookup/doi/10.1111/pme.12662.
49. Deer T, Pope J, Benyamin R, Vallejo R, Friedman A, Caraway D, et al. Prospective, multicenter, randomized, double-blinded, partial crossover study to assess the safety and efficacy of the novel neuromodulation system in the treatment of patients with chronic pain of peripheral nerve origin. Neuromodulation Technol Neural Interface [Internet]. 2016 [cited 2019 Jan 2];19:91–100. Available from: http://www.ncbi.nlm.nih.gov/pubmed/26799373.
50. Yu DT, Chae J, Walker ME, Fang Z-P. Percutaneous intramuscular neuromuscular electric stimulation for the treatment of shoulder subluxation and pain in patients with chronic hemiplegia: a pilot study. Arch Phys Med Rehabil. [Internet]. 2001 [cited 2019 Apr 15];82:20–5. Available from: http://www.ncbi.nlm.nih.gov/pubmed/11239281.
51. Ilfeld BM, Gilmore CA, Grant SA, Bolognesi MP, Del Gaizo DJ, Wongsarnpigoon A, et al. Ultrasound-guided percutaneous peripheral nerve stimulation for analgesia following total knee arthroplasty: a prospective feasibility study. J Orthop Surg Res. [Internet]. 2017 [cited 2019 Apr 15];12:4. Available from: http://www.ncbi.nlm.nih.gov/pubmed/28086940.
52. Ilfeld BM, Finneran JJ, Gabriel RA, Said ET, Nguyen PL, Abramson WB, et al. Ultrasound-guided percutaneous peripheral nerve stimulation: neuromodulation of the suprascapular nerve and brachial plexus for postoperative analgesia following ambulatory rotator cuff repair. A proof-of-concept study. Reg Anesth Pain Med. [Internet]. 2019 [cited 2019 Apr 15];rapm-2018-100121. Available from: http://www.ncbi.nlm.nih.gov/pubmed/30770421.
53. Eljamel S, Neurostimulation SKV. Principles and practice. Chichester: Wiley Blackwell; 2013.
54. Campbell CM, Jamison RN, Edwards RR. Psychological screening/phenotyping as predictors for spinal cord stimulation. Curr Pain Headache Rep. [Internet]. 2013 [cited 2019 Apr 11];17:307. Available from: http://www.ncbi.nlm.nih.gov/pubmed/23247806.
55. Nayak R, Banik RK. Current innovations in peripheral nerve stimulation. Pain Res Treat. [Internet]. Hindawi; 2018 [cited 2018 Dec 5];2018:1–5. Available from: https://www.hindawi.com/journals/prt/2018/9091216/.
56. Hoelzer BC, Bendel MA, Deer TR, Eldrige JS, Walega DR, Wang Z, et al. Spinal cord stimulator implant infection rates and risk factors: a multicenter retrospective study. Neuromodulation Technol Neural Interface [Internet]. 2017 [cited 2019 Apr 15];20:558–62. Available from: http://www.ncbi.nlm.nih.gov/pubmed/28493599.
57. Deer TR, Provenzano DA, Hanes M, Pope JE, Thomson SJ, Russo MA, et al. The Neurostimulation Appropriateness Consensus Committee (NACC) recommendations for infection prevention and management. Neuromodulation Technol Neural Interface [Internet]. John Wiley & Sons, Ltd (10.1111); 2017 [cited 2019 Apr 15];20:31–50. Available from: http://doi.wiley.com/10.1111/ner.12565.
58. Ellis JA, Mejia Munne JC, Winfree CJ. Trigeminal branch stimulation for the treatment of intractable craniofacial pain. J Neurosurg. [Internet]. 2015;123:283–8. Available from: http://www.ncbi.nlm.nih.gov/pubmed/25635476.
59. Slavin K V., Wess C. Trigeminal branch stimulation for intractable neuropathic pain: technical note. Neuromodulation [Internet]. Wiley/Blackwell (10.1111); 2005 [cited 2018 Dec 10];8:7–13. Available from: http://doi.wiley.com/10.1111/j.1094-7159.2005.05215.x.
60. Slavin K, Colpan M, Munawar N, Wess C. Trigeminal and occipital peripheral nerve stimulation for craniofacial pain: a single-institution experience and review of the literature. Neurosurg Focus [Internet]. 2006 [cited 2018 Dec 19];21:1–5. Available from: http://www.ncbi.nlm.nih.gov/pubmed/17341049.
61. Dunteman E. Peripheral nerve stimulation for unremitting ophthalmic postherpetic neuralgia. Neuromodulation [Internet]. 2002 [cited 2018 Dec 10];5:32–7. Available from: http://www.ncbi.nlm.nih.gov/pubmed/22151779.
62. Johnson MD, Burchiel KJ. Peripheral stimulation for treatment of trigeminal postherpetic neuralgia and trigeminal posttraumatic neuropathic pain: a pilot study. Neurosurgery [Internet]. 2004 [cited 2018 Dec 28];55:135–41. Available from: http://www.ncbi.nlm.nih.gov/pubmed/15214982.
63. Stidd DA, Wuollet AL, Bowden K, Price T, Patwardhan A, Barker S, et al. Peripheral nerve stimulation for trigeminal neuropathic pain. Pain Physician [Internet]. [cited 2018 Dec 28];15:27–33. Available from: http://www.ncbi.nlm.nih.gov/pubmed/22270735.
64. Narouze SN, Kapural L. Supraorbital nerve electric stimulation for the treatment of intractable chronic cluster headache: A case report. Headache [Internet]. John Wiley & Sons, Ltd; 2007 [cited 2018 Dec 10];47:1100–2. Available from: http://doi.wiley.com/10.1111/j.1526-4610.2007.00869.x.

65. Amin S, Buvanendran A, Park K-S, Kroin JS, Moric M. Peripheral nerve stimulator for the treatment of supraorbital neuralgia: a retrospective case series. Cephalalgia [Internet]. 2008 [cited 2018 Dec 10];28:355–9. Available from: https://journals.sagepub.com/doi/pdf/10.1111/j.1468-2982.2008.01535.x.
66. Feletti A, Santi GZ, Sammartino F, Bevilacqua M, Cisotto P, Longatti P. Peripheral trigeminal nerve field stimulation: report of 6 cases. Neurosurg Focus [Internet]. 2013 [cited 2018 Dec 11];35:E10. Available from: http://www.ncbi.nlm.nih.gov/pubmed/23991813.
67. Johnstone CSH, Sundaraj R. Occipital nerve stimulation for the treatment of occipital neuralgia - eight case studies. Neuromodulation [Internet]. 2006 [cited 2018 Dec 11];9:41–7. Available from: http://www.ncbi.nlm.nih.gov/pubmed/22151592.
68. Lorenzo-Martin C, Ajayi O, Erdemir A, Wei R. Tribological performance of quaternary CrSiCN coatings under dry and lubricated conditions. Wear [Internet]. 2017 [cited 2018 Dec 18];376–377:1682–90. Available from: http://www.ncbi.nlm.nih.gov/pubmed/16385335.
69. Oh MY, Ortega J, Bellotte JB, Whiting DM, Aló K. Peripheral nerve stimulation for the treatment of occipital neuralgia and transformed migraine using a C1-2-3 subcutaneous paddle style electrode: a technical report. Neuromodulation [Internet]. 2004 [cited 2018 Dec 17];7:103–12. Available from: http://www.ncbi.nlm.nih.gov/pubmed/22151191.
70. Palmisani S, Al-Kaisy A, Arcioni R, Smith T, Negro A, Lambru G, et al. A six year retrospective review of occipital nerve stimulation practice - controversies and challenges of an emerging technique for treating refractory headache syndromes. J Headache Pain [Internet]. 2013 [cited 2018 Dec 18];14:67. Available from: http://www.ncbi.nlm.nih.gov/pubmed/23919570.
71. Abhinav K, Park ND, Prakash SK, Love-Jones S, Patel NK. Novel use of narrow paddle electrodes for occipital nerve stimulation - technical note. Neuromodulation [Internet]. 2013 [cited 2018 Dec 18];16:607–9. Available from: http://www.ncbi.nlm.nih.gov/pubmed/23106950.
72. Melvin EA, Jordan FR, Weiner RL, Primm D. Using peripheral stimulation to reduce the pain of C2-mediated occipital headaches: a preliminary report. Pain Physician [Internet]. 2007 [cited 2018 Dec 11];10:453–60. Available from: http://www.ncbi.nlm.nih.gov/pubmed/17525779.
73. Schwedt TJ, Dodick DW, Hentz J, Trentman TL, Zimmerman RS. Occipital nerve stimulation for chronic headache – Long-term safety and efficacy. Cephalalgia [Internet]. SAGE PublicationsSage UK: London, England; 2007 [cited 2018 Dec 25];27:153–7. Available from: http://journals.sagepub.com/doi/10.1111/j.1468-2982.2007.01272.x.
74. Dodick DW, Trentman TL, Zimmerman RSEE. Occipital nerve stimulation for intractable chronic primary headache disorders. Cephalalgia. 2003;23:701.
75. Magis D, Allena M, Bolla M, De Pasqua V, Remacle JM, Schoenen J. Occipital nerve stimulation for drug-resistant chronic cluster headache: a prospective pilot study. Lancet Neurol. [Internet]. 2007 [cited 2018 Dec 17];6:314–21. Available from: http://www.ncbi.nlm.nih.gov/pubmed/17362835.
76. Chen YF, Bramley G, Unwin G, Hanu-Cernat D, Dretzke J, Moore D, et al. Occipital nerve stimulation for chronic migraine-A systematic review and meta-analysis. Sommer C, editor. PLoS One [Internet]. Public Library of Science; 2015 [cited 2018 Dec 19];10:e0116786. Available from: http://dx.plos.org/10.1371/journal.pone.0116786.
77. Lipton R, Goadsby PJ, Cady R, Aurora SK, Grosberg BM, et al. PO47 PRISM study: occipital nerve stimulation for treatment-refractory migraine. Cephalalgia [Internet]. Blackwell Publishing Ltd Cephalalgia; 2009;29:30. Available from: http://journals.sagepub.com/doi/pdf/10.1111/J.1468-2982.2009.01960.X.
78. Saper JR, Dodick DW, Silberstein SD, McCarville S, Sun M, Goadsby PJ. Occipital nerve stimulation for the treatment of intractable chronic migraine headache: ONSTIM feasibility study. Cephalalgia [Internet]. SAGE Publications; 2011 [cited 2018 Dec 11];31:271–85. Available from: http://www.ncbi.nlm.nih.gov/pubmed/20861241.
79. Silberstein SD, Dodick DW, Saper J, Huh B, Slavin K V, Sharan A, et al. Safety and efficacy of peripheral nerve stimulation of the occipital nerves for the management of chronic migraine: results from a randomized, multicenter, double-blinded, controlled study. Cephalalgia [Internet]. 2012 [cited 2018 Dec 11];32:1165–79. Available from: http://www.ncbi.nlm.nih.gov/pubmed/23034698.
80. Dodick DW, Silberstein SD, Reed KL, Deer TR, Slavin K V, Huh B, et al. Safety and efficacy of peripheral nerve stimulation of the occipital nerves for the management of chronic migraine: long-term results from a randomized, multicenter, double-blinded, controlled study. Cephalalgia [Internet]. 2015 [cited 2018 Dec 11];35:344–58. Available from: http://www.ncbi.nlm.nih.gov/pubmed/25078718.
81. Magown P, Garcia R, Beauprie I, Mendez IM. Occipital nerve stimulation for intractable occipital neuralgia: an open surgical technique. Clin Neurosurg. [Internet]. 2009 [cited 2018 Dec 17];56:119–24. Available from: https://www.reedmigraine.com/wp-content/uploads/2018/04/Occipital-Nerve-Stimulation-Neuralgia-Magown-2009.pdf.
82. Sherman RA, Sherman CJ. Prevalence and characteristics of chronic phantom limb pain among American veterans. Results of a trial survey. Am J Phys Med. [Internet]. 1983 [cited 2018 Dec 25];62:227–38. Available from: http://www.ncbi.nlm.nih.gov/pubmed/6624883.
83. Sherman RA, Sherman CJ, Parker L. Chronic phantom and stump pain among american veterans: results of a survey. Pain [Internet]. 1984 [cited 2018 Dec

25];18:83–95. Available from: http://www.ncbi.nlm.nih.gov/pubmed/6709380.
84. Sherman RA, Sherman CJ, Gall NG. A survey of current phantom limb pain treatment in the United States. Pain [Internet]. 1980 [cited 2018 Dec 25];8:85–99. Available from: http://www.ncbi.nlm.nih.gov/pubmed/6988765.
85. Jahangiri M, Jayatunga AP, Bradley JWP, Dark CH. Prevention of phantom pain after major lower limb amputation by epidural infusion of diamorphine, clonidine and bupivacaine. Ann R Coll Surg Engl. [Internet]. Royal College of Surgeons of England; 1994 [cited 2018 Dec 25];76:324–6. Available from: http://www.ncbi.nlm.nih.gov/pubmed/7979074.
86. Rosenquist RHN. Phantom limb pain. In: Benzon HT, Rathmell JP, Wu CLT, DC AC, editors. Raj's practical management of pain. Philadelphia: Mosby Elsevier; 2008. p. 445–53.
87. Ehde DM, Czerniecki JM, Smith DG, Campbell KM, Edwards WT, Jensen MP, et al. Chronic phantom sensations, phantom pain, residual limb pain, and other regional pain after lower limb amputation. Arch Phys Med Rehabil. [Internet]. 2000 [cited 2018 Dec 25];81:1039–44. Available from: http://www.ncbi.nlm.nih.gov/pubmed/10943752.
88. Ephraim PL, Wegener ST, MacKenzie EJ, Dillingham TR, Pezzin LE. Phantom pain, residual limb pain, and back pain in amputees: results of a national survey [Internet]. Arch Phys Med Rehabil. 2005 [cited 2018 Dec 25]. p. 1910–9. Available from: http://www.ncbi.nlm.nih.gov/pubmed/16213230.
89. Millstein S, Bain D, Hunter GA. A review of employment patterns of industrial amputees—factors influencing rehabilitation. Prosthet Orthot Int. [Internet]. 1985 [cited 2018 Dec 26];9:69–78. Available from: http://www.ncbi.nlm.nih.gov/pubmed/4047922.
90. Whyte AS, Carroll LJ. A preliminary examination of the relationship between employment, pain and disability in an amputee population. Disabil Rehabil. [Internet]. 2002 [cited 2018 Dec 26];24:462–70. Available from: http://www.ncbi.nlm.nih.gov/pubmed/12097215.
91. Rudy TE, Lieber SJ, Boston JR, Gourley LM, Baysal E. Psychosocial predictors of physical performance in disabled individuals with chronic pain [Internet]. Clin J Pain. The Clinical Journal of Pain; 2003 [cited 2018 Dec 26]. p. 18–30. Available from: https://insights.ovid.com/pubmed?pmid=12514453.
92. Rauck RL, Cohen SP, Gilmore CA, North JM, Kapural L, Zang RH, et al. Treatment of post-amputation pain with peripheral nerve stimulation. Neuromodulation [Internet]. 2014 [cited 2018 Dec 11];17:188–96. Available from: http://www.ncbi.nlm.nih.gov/pubmed/23947830.
93. Soin A, Syed Shah N, Fang ZP. High-frequency electrical nerve block for postamputation pain: a pilot study. Neuromodulation [Internet]. 2015 [cited 2018 Dec 25];18:197–205. Available from: http://www.ncbi.nlm.nih.gov/pubmed/25655583.
94. Deogaonkar M, Slavin K V. Peripheral nerve/field stimulation for neuropathic pain. Neurosurg Clin N Am. [Internet]. 2014 [cited 2019 Apr 11];25:1–10. Available from: http://www.ncbi.nlm.nih.gov/pubmed/24262894.
95. Verrills P, Vivian D, Mitchell B, Barnard A. Peripheral nerve field stimulation for chronic pain: 100 cases and review of the literature. Pain Med. [Internet]. Oxford University Press; 2011 [cited 2018 Dec 5];12:1395–405. Available from: https://academic.oup.com/painmedicine/article-lookup/doi/10.1111/j.1526-4637.2011.01201.x.
96. Bari A, Pouratian N. Brain imaging correlates of peripheral nerve stimulation. Surg Neurol Int. 2012;3:260.
97. Liu W-C, Mosier K, Kalnin AJ, Marks D. BOLD fMRI activation induced by vagus nerve stimulation in seizure patients. J Neurol Neurosurg Psychiatry. 2003;74:811–3.
98. Barnes A, Duncan R, Chisholm JA, Lindsay K, Patterson J, Wyper D. Investigation into the mechanisms of vagus nerve stimulation for the treatment of intractable epilepsy, using 99mTc-HMPAO SPET brain images. Eur J Nucl Med Mol Imaging. 2003;30:301–5.
99. Bertram EH, Mangan PS, Zhang D, Scott CA, Williamson JM. The midline thalamus: alterations and a potential role in limbic epilepsy. Epilepsia. 2001;42:967–78.
100. Bohning DE, Lomarev MP, Denslow S, Nahas Z, Shastri A, George MS. Feasibility of vagus nerve stimulation-synchronized blood oxygenation level-dependent functional MRI. Investig Radiol. 2001;36:470–9.
101. Bosch JL, Groen J. Sacral nerve neuromodulation in the treatment of patients with refractory motor urge incontinence: long-term results of a prospective longitudinal study. J Urol. 2000;163:1219–22.
102. Conway CR, Sheline YI, Chibnall JT, Bucholz RD, Price JL, Gangwani S, et al. Brain blood-flow change with acute vagus nerve stimulation in treatment-refractory major depressive disorder. Brain Stimul. 2012;5:163–71.
103. Garnett ES, Nahmias C, Scheffel A, Firnau G, Upton AR. Regional cerebral blood flow in man manipulated by direct vagal stimulation. Pacing Clin Electrophysiol. 1992;15:1579–80.
104. Nestler EJ, Barrot M, DiLeone RJ, Eisch AJ, Gold SJ, Monteggia LM. Neurobiology of depression. Neuron. 2002;34:13–25.
105. Nahas Z, Marangell LB, Husain MM, Rush AJ, Sackeim HA, Lisanby SH, et al. Two-year outcome of vagus nerve stimulation (VNS) for treatment of major depressive episodes. J Clin Psychiatry. 2005;66:1097–104.
106. Zempleni M-Z, Michels L, Mehnert U, Schurch B, Kollias S. Cortical substrate of bladder control in

SCI and the effect of peripheral pudendal stimulation. NeuroImage. 2010;49:2983–94.
107. Mehnert U, Boy S, Svensson J, Michels L, Reitz A, Candia V, et al. Brain activation in response to bladder filling and simultaneous stimulation of the dorsal clitoral nerve--an fMRI study in healthy women. NeuroImage. 2008;41:682–9.
108. Lundby L, Møller A, Buntzen S, Krogh K, Vang K, Gjedde A, et al. Relief of fecal incontinence by sacral nerve stimulation linked to focal brain activation. Dis Colon Rectum. 2011;54:318–23.
109. DasGupta R. Different brain effects during chronic and acute sacral neuromodulation in urge incontinent patients with implanted neurostimulators. BJU Int. 2007;99:700.
110. Panebianco M, Zavanone C, Dupont S, Restivo DA, Pavone A. Vagus nerve stimulation therapy in partial epilepsy: a review. Acta Neurol Belg. 2016;116:241–8.
111. Kessler RC, Berglund P, Demler O, Jin R, Koretz D, Merikangas KR, et al. The epidemiology of major depressive disorder. JAMA. 2003;289:3095.
112. Rush AJ, Trivedi MH, Wisniewski SR, Nierenberg AA, Stewart JW, Warden D, et al. Acute and longer-term outcomes in depressed outpatients requiring one or several treatment steps: a STAR∗D report. Am J Psychiatry. 2006;163:1905–17.
113. Zabara J. Inhibition of experimental seizures in canines by repetitive vagal stimulation. Epilepsia. 33:1005–12.
114. Uthman BM. Vagus nerve stimulation for seizures. Arch Med Res. Elsevier;. 2000;31:300–3.
115. Chakravarthy K, Chaudhry H, Williams K, Christo PJ. Review of the uses of vagal nerve stimulation in chronic pain management. Curr Pain Headache Rep. Springer US;. 2015;19:54.
116. Elger G, Hoppe C, Falkai P, Rush AJ, Elger CE. Vagus nerve stimulation is associated with mood improvements in epilepsy patients. Epilepsy Res. 2000;42:203–10.
117. Rush AJ, George MS, Sackeim HA, Marangell LB, Husain MM, Giller C, et al. Vagus nerve stimulation (VNS) for treatment-resistant depressions: a multicenter study. Biol Psychiatry. 2000;47:276–86.
118. Carreno FR, Frazer A. Vagal nerve stimulation for treatment-resistant depression. Neurotherapeutics. 2017;14:716–27.
119. Aaronson ST, Sears P, Ruvuna F, Bunker M, Conway CR, Dougherty DD, et al. A 5-year observational study of patients with treatment-resistant depression treated with vagus nerve stimulation or treatment as usual: comparison of response, remission, and suicidality. Am J Psychiatry. 2017;174:640–8.
120. Müller HHO, Lücke C, Moeller S, Philipsen A, Sperling W. Efficacy and long-term tuning parameters of vagus nerve stimulation in long-term treated depressive patients. J Clin Neurosci. 2017;44:340–1.
121. Lv H, Zhao Y-H, Chen J-G, Wang D-Y, Chen H, et al. Front Psychol. Frontiers Media SA;. 2019;10:64.
122. Gorgulho AA, Fernandes F, Damiani LP, Barbosa DAN, Cury A, Lasagno CM, et al. Double blinded randomized trial of subcutaneous trigeminal nerve stimulation as adjuvant treatment for major unipolar depressive disorder. Neurosurgery. 2019;85(5):717–28.
123. Fanselow EE, Reid AP, Nicolelis MA. Reduction of pentylenetetrazole-induced seizure activity in awake rats by seizure-triggered trigeminal nerve stimulation. J Neurosci. 2000;20:8160–8.
124. DeGiorgio CM, Shewmon DA, Whitehurst T. Trigeminal nerve stimulation for epilepsy. Neurology. 2003;61:421–2.
125. DeGiorgio CM, Shewmon A, Murray D, Whitehurst T. Pilot study of Trigeminal Nerve Stimulation (TNS) for epilepsy: a proof-of-concept trial. Epilepsia. 2006;47:1213–5.
126. DeGiorgio CM, Murray D, Markovic D, Whitehurst T. Trigeminal nerve stimulation for epilepsy: long-term feasibility and efficacy. Neurology. 2009;72:936–8.
127. DeGiorgio CM, Soss J, Cook IA, Markovic D, Gornbein J, Murray D, et al. Randomized controlled trial of trigeminal nerve stimulation for drug-resistant epilepsy. Neurology. 2013;80:786–91.
128. Slaght SJ, Nashef L. An audit of external trigeminal nerve stimulation (eTNS) in epilepsy. Seizure. 2017;52:60–2.
129. Olivié L, Giraldez BG, Sierra-Marcos A, Díaz-Gómez E, Serratosa JM. External trigeminal nerve stimulation: a long term follow up study. Seizure. W.B. Saunders;. 2019;69:218–20.
130. DeGiorgio CM, Fanselow EE, Schrader LM, Cook IA. Trigeminal nerve stimulation: seminal animal and human studies for epilepsy and depression. Neurosurg Clin N Am. 2011;22:449–56.
131. Cook IA, Schrader LM, DeGiorgio CM, Miller PR, Maremont ER, Leuchter AF. Trigeminal nerve stimulation in major depressive disorder: acute outcomes in an open pilot study. Epilepsy Behav. 2013;28:221–6.
132. Shiozawa P, da Silva ME, Netto GTM, Taiar I, Cordeiro Q. Effect of a 10-day trigeminal nerve stimulation (TNS) protocol for treating major depressive disorder: a phase II, sham-controlled, randomized clinical trial. Epilepsy Behav. Academic Press;. 2015;44:23–6.
133. Generoso MB, Taiar IT, Garrocini LP, Bernardon R, Cordeiro Q, Uchida RR, et al. Effect of a 10-day transcutaneous trigeminal nerve stimulation (TNS) protocol for depression amelioration: a randomized, double blind, and sham-controlled phase II clinical trial. Epilepsy Behav. 2019;95:39–42.

15

Non-invasive Central Neuromodulation with Transcranial Magnetic Stimulation

Jeanette Hui, Pantelis Lioumis, Daniel M. Blumberger, and Zafiris J. Daskalakis

Introduction

In 1980, Merton and Morton created the first non-invasive technique for focal modulation of the human cortex. They demonstrated that transcranial electrical stimulation (TES) could stimulate motor areas of the brain through the intact scalp by using high-amplitude and short-duration electrical pulses delivered through two surface electrodes [1]. This resulted in the brief activation of peripheral muscles known as motor-evoked potentials (MEPs) that were recorded with electromyography (EMG). Although it was immediately clear that TES could be tremendously useful for research and clinical purposes, the main drawback of TES is that it is painful and poorly tolerated [1]. Five years later, Barker and colleagues developed a stimulating device that overcame many of these technical limitations and showed for the first time that the brain can be stimulated with magnetic pulses through transcranial magnetic stimulation (TMS) [2]. TMS is now routinely used as both a clinical and a research tool to investigate neurophysiology and cortical properties of excitability and connectivity.

Scientific Principles of Non-invasive Neuromodulation

Physical Principles of TMS

The fundamental principles of electromagnetic induction govern the activation of neurons through TMS. In accordance with Faraday's law, a time-varying electrical current $\boldsymbol{I(t)}$ passes through the TMS stimulating coil placed tangentially against the scalp and induces a magnetic field $\vec{\boldsymbol{B}}$ perpendicular to the plane of the coil. The magnetic field, which typically has duration of 100 μs and can reach values up to 4 Tesla, acts according to the Biot-Savart law:

$$\vec{B}(r,t) = \frac{\mu_0}{4\pi} I(t) \oint_C \frac{dl(r') \times (r - r')}{|r - r'|^3} \quad (15.1)$$

J. Hui
Temerty Centre for Therapeutic Brain Intervention, Centre for Addiction and Mental Health, Toronto, ON, Canada

Institute of Medical Science, University of Toronto, Toronto, ON, Canada

P. Lioumis
Temerty Centre for Therapeutic Brain Intervention, Centre for Addiction and Mental Health, Toronto, ON, Canada

D. M. Blumberger · Z. J. Daskalakis (✉)
Temerty Centre for Therapeutic Brain Intervention, Centre for Addiction and Mental Health, Toronto, ON, Canada

Department of Psychiatry, Institute of Medical Science, University of Toronto, Toronto, ON, Canada
e-mail: Jeff.Daskalakis@camh.ca

N. Pouratian, S. A. Sheth (eds.), *Stereotactic and Functional Neurosurgery*,
https://doi.org/10.1007/978-3-030-34906-6_15

where $\boldsymbol{\mu_0}$ is the free space permeability, $\boldsymbol{dl}$ is the vector along the windings of the coil $\boldsymbol{C}$, and $\boldsymbol{r}$ is the point of space where the field is being calculated. $\vec{\boldsymbol{B}}$ induces an electric field $\vec{\boldsymbol{E}}$ in nearby conductors (scalp, skull, and cortical tissue) at a proportional intensity [2]. This relation is described by Maxwell's equation:

$$\nabla \times \vec{\boldsymbol{E}} = -\partial \vec{\mathrm{B}} / \partial t \tag{15.2}$$

The electric field in the cortex will then generate large currents of several kiloamps that set free charges into motion between intracellular and extracellular spaces. When many neurons under the TMS coil reach a sufficient level of depolarization and become simultaneously activated, they generate a highly synchronous burst of neural firing. Note that the strength of electromagnetic fields declines with the fourth power of distance below the coil. Hence, the depth of penetration is limited to the outermost 2–2.5 cm of superficial brain tissue [3]. For this reason, magnetic stimulation is particularly suitable for targeting regions in the cerebral cortex that lie directly below the skull. Magnetic fields readily penetrate the brain without attenuation by the scalp or skull, resulting in minimal to no activation of pain receptors [2, 4]. In contrast, currents induced on the scalp by TES are much stronger than those produced by TMS. The direct application of electrical stimuli through TES is met with high resistivity from the skull and undergoes significant dissipation before it can reach underlying brain tissue. Thus, very high voltage stimulation on the order of 1–1.5 kV is required to induce action potentials in cortical neurons [5]. Due to the strong pain generated at the scalp level, clinical use of TES is restricted to monitoring motor and spinal cord pathways under general anaesthesia [6].

Physiological Mechanisms of TMS

Neurons are excitable at lower thresholds when the induced currents are timed and oriented to match the normal flow of postsynaptic current [7–9]. As current travels from the dendrites, through the soma, and along the axon, it follows a pathway of low resistivity. Similar orientation selectivity has also been observed in TMS. Even the earliest TMS studies have consistently found that maximal MEPs are recorded in the motor cortex when the magnetic coil is oriented 45° to the midsagittal line (Fig. 15.1) [10, 11]. Later studies employing advanced neuronavigation methods have verified these findings and further indicate that the primary motor cortex is optimally stimulated when induced current is perpendicular to the central sulcus [12–14]. Optimal alignment of the TMS coil during stimulation generates an electric field that maximizes the length of neuronal membrane and the number of neurons activated by the stimulus, evoking action potentials at or near the soma [15–18]. In vitro studies indicate that a suprathreshold TMS pulse activates layer 5 pyramidal neurons, which generate a highly synchronous burst of neural firing. These cells can then synapse upon specific microcircuits in the cortex, including GABAergic neurons in layer 1, supporting assumptions that TMS probes both excitatory and inhibitory cortical pathways [19, 20]. In summary, the predominant activation mechanisms of pyramidal tract neurons are related to the trajectories of current propagation along the axon and the alignment of the electric field to cortical columns.

The effects of TMS are highly dependent on the instantaneous states of the stimulated neuronal populations. As all behavioural, perceptual, and physiological outcomes are influenced by neural activation states, studies using brain stimulation methods must account for the initial state of the subject by attempting to maintain consistent stimulation conditions across and within experimental sessions. In a broad sense, state dependence relies on many factors, including: levels of fatigue, wakefulness, TMS priming, drug influence, and the stimulation environment [21]. The effect of state modulation on specific neuronal response properties has been elucidated through studies of single neuronal units. For example, the stimulus-response curve of a motor neuron model changes drastically during onset of firing, responding even to subthreshold stimuli that would not normally reach threshold [22]. When tonic drive exceeds the threshold for firing, the response plateaus for weak stimuli but reaches

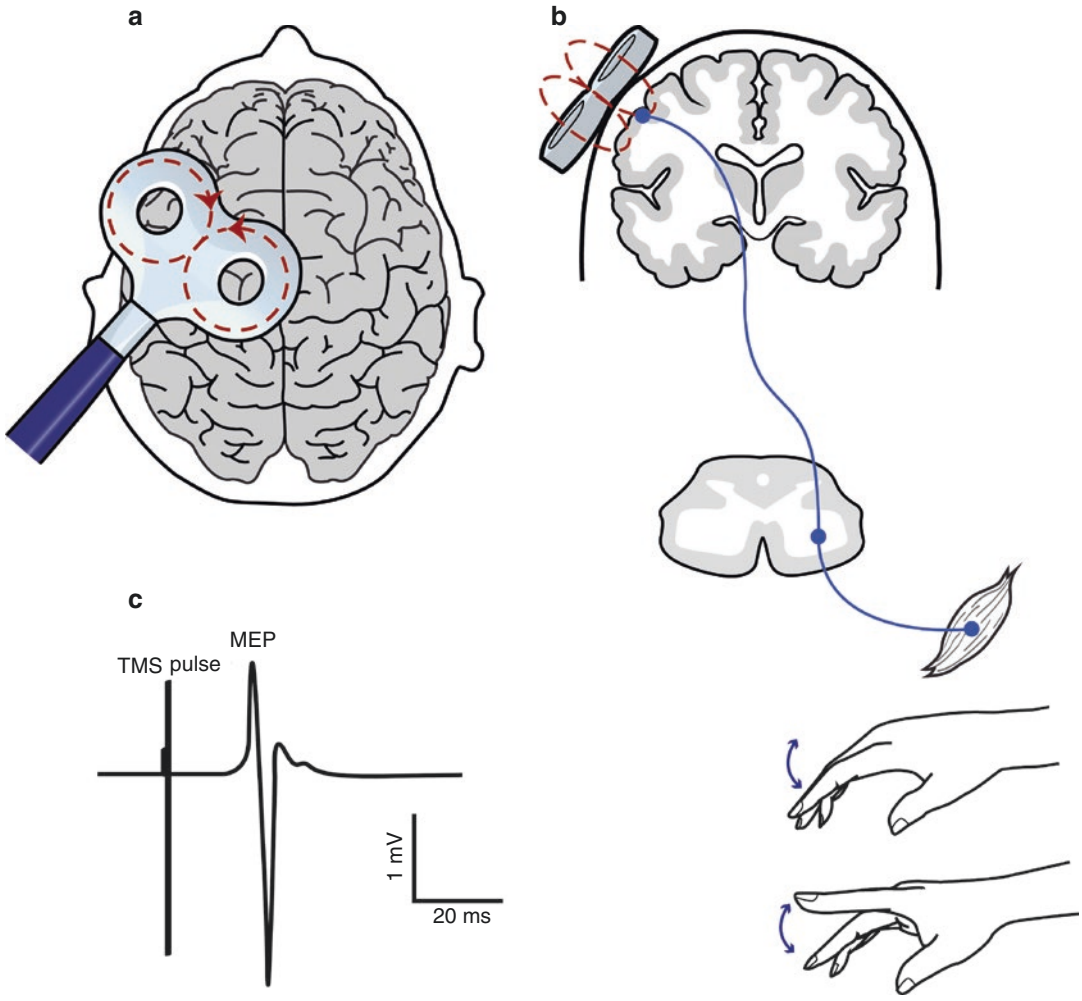

Fig. 15.1 Illustration of TMS-induced current propagation along the corticospinal tract and the corresponding MEP response. (**a**) A figure-of-eight coil is positioned over the left motor cortex, oriented approximately 45° with respect to the midsagittal line. Coil current is depicted by dashed arrows drawn inside coil rim. (**b**) Single-pulse TMS applied over the left motor cortex induces current propagates from pyramidal tract neurons to spinal motor neurons before terminating on peripheral nerves. A pulse with suprathreshold intensity creates a visible muscle twitch in the right first dorsal interosseous muscle. (**c**) Motor-evoked potential (MEP) elicited in target muscle from single-pulse TMS

a maximum for strong stimuli to produce low firing rates [22]. Additionally, the timing of the outcome measure with respect to the TMS pulse modulates single unit activity. While a TMS pulse applied hundreds of milliseconds prior to the onset of activity evoked by a visual stimulus can suppress firing rates, the delivery of the pulse immediately before the visual stimulus can lift subthreshold activity above threshold to facilitate firing [23, 24]. Hence, considerations of initial activation states provide valuable insight upon the dynamics of neuronal interactions and response properties within different brain areas and can also aid in providing optimal interventions for treatment and rehabilitation [21].

Modelling studies have investigated several physiological mechanisms to explain the spatial and temporal pattern of cortical activation observed from TMS [25]. These mechanisms not only rely on the anisotropy and heterogeneity of

conductive brain tissue but also depend on various stimulation parameters, such as the geometry of the magnetic coil, as well as pulse intensity, width, and direction. These factors will be addressed in the next section.

Parameters of Stimulation

The pattern of tissue activation in the cortex can be estimated when properties of the external electric field are closely controlled. The first example is the effect of coil geometry on the shape and depth of the induced current. The earliest TMS studies used circular coils, which produce broad ring-shaped electric fields strongest around the perimeter of the coil and weakest towards the centre [2]. Figure-of-eight-shaped coils were developed to improve the focality of stimulation and have been extremely valuable for the purposes of therapeutic TMS applications and brain mapping. The conventional 70-mm figure-of-eight coils consist of two adjacent circular loops with current flowing in opposite directions. The inductance in the centre of this coil is approximately twice of that in either of the single loops, producing maximal current under the coil centre where the two loops meet [12, 26]. Another configuration is the Hesed (H) coil, which contains complex winding patterns that are contoured to the shape of the skull. At the expense of reduced focality, the H-coil permits a greater depth of penetration to effectively stimulate deeper brain structures [27].

Next, outcomes of TMS depend on a number of stimulation pulse parameters. Stimulation intensity impacts the specific pathways and neuronal populations that are activated by TMS. Subthreshold stimulation preferentially activates trans-synaptic pathways, whereas suprathreshold stimulation excites both trans-synaptic pathways and axonal pathways deeper in the grey matter. With sufficiently high TMS intensities, the cerebellum and subcortical structures can also be targeted. Stimulation paradigms that vary according to the frequency and intensity at which TMS pulses are administered can assess the involvement of specific pathways and neurobiological substrates in cortical excitability, cortical inhibition, and plasticity-like effects. These will be further discussed in subsequent sections. Current elicited by the magnetic field can carry a monophasic configuration, in which a strong initial current is balanced by a dampened return current, or a biphasic configuration, where the initial direction of the current is reversed twice. In general, biphasic stimulation requires lower intensities and produces smaller decay artefacts at the expense of reduced focality. Interestingly, interactive effects have consistently been demonstrated between the stimulus pulse waveform (monophasic vs. biphasic) and directionality of current flow induced in tissue (posterior-anterior (PA) vs. anterior-posterior (AP)). For example, the most effective direction for the initial current is opposite for these two types of stimulation – monophasic pulses evoke stronger responses when administered over the motor cortex in a PA direction, while biphasic pulses provide more efficient motor stimulation when the initial induced current is propagated from the AP direction [17, 26, 28]. However, conventional monophasic and biphasic TMS circuits, induced with damped cosine electric field pulses, can experience significant decay of capacitor voltage over pulse duration [29, 30]. The recent development of controllable pulse parameter TMS (cTMS) devices allows near rectangular electric field pulses to be induced while reducing power consumption and coil overheating [30]. cTMS permits controllability over the width, polarity, number, frequency, and duration of pulses that may permit neuronal populations with distinct strength-duration characteristics to be selectively activated [31].

Enhancing TMS with Neurophysiological and Neural Imaging Modalities

TMS provides a unique paradigm for characterizing neural networks across healthy and disease states. Although behavioural outcomes and phosphenes can be characterized to study the prefrontal and visual cortices, respectively, the literature has

traditionally relied on EMG output to characterize the stimulatory effects of TMS. However, there are rather limited uses for TMS-EMG in basic research and in clinical applications. TMS-EMG is (1) restricted to motor brain areas due to its reliance on motor output and (2) only permits properties of corticospinal excitability to be investigated. These shortcomings limit the application of TMS to motor cortical regions and prevent functional cortico-cortical connectivity and the instantaneous state of the brain from being assessed. To address these issues, neurophysiological modalities such as electroencephalography (EEG) have been used in conjunction with TMS.

Evoked EEG Responses by TMS

EEG non-invasively measures the electric potential difference between electrodes that arise from the induction of an electric field, i.e. through TMS stimulation. The electric activities of tightly packed neurons propagate to the surface of the scalp as quickly as several milliseconds after the induction of an action potential [32, 33]. With a high temporal resolution on the order of milliseconds, EEG is one of the few modalities that can accurately quantify these voltage fluctuations along dimensions of time, frequency, and space. TMS-EEG measures TMS-evoked potentials (TEPs) induced only after the stimulation of functional and intact cortical regions [34]. Mirroring the principles of MEPs, TEPs offer a measure of cortical reactivity and involve the spatial and temporal summation of excitatory postsynaptic potentials (EPSPs) and inhibitory postsynaptic potentials (IPSPs) from a large population of pyramidal neurons and interneurons [32, 33]. Data are typically presented as a waveform of varying amplitude as a function of time. Over the motor cortex, TEPs demonstrate positive peaks at 30 ms (P30), 55 ms (P55), and 180 ms (P180) and negative troughs at 15 ms (N15), 45 ms (N45), 100 ms (N100), and 280 ms (N280) [35].

It is well established that TEPs elicited from the primary motor cortex reliably exhibit higher amplitude responses than TEPs from non-motor cortical regions [35, 36]. This can be explained by the cytoarchitecture of the primary motor cortex, which contains longitudinally oriented pyramidal neurons that propagate electrical activity perpendicular to the cortical surface. Since surface EEG electrodes are aligned tangentially to the scalp, they are highly sensitive to the radially oriented dipoles from motor cortical neurons. TEPs have also been extensively characterized in the dorsolateral prefrontal cortex (DLPFC), showing peaks at P25, N40, P60, N100, and P185 [35], and are highly reproducible within individuals over premotor, occipital, and parietal regions as well [35, 37]. Thus, TMS-EEG is a powerful tool to assess physiological relationships in human brain networks.

Physical Considerations to Prevent TMS-EEG Artefacts

Some of the greatest technological challenges in implementing concurrent TMS-EEG involve the maintenance of high-quality EEG recordings while the TMS coil induces a large, perturbing electromagnetic field in close proximity. The first attempts to combine TMS with EEG suffered from massive electromagnetic artefacts that were several-folds larger in amplitude than that of sensory-evoked potentials [38]. This artefact saturated EEG amplifiers for seconds after the pulse, precluding the detection of underlying neural signal. Several improvements in EEG amplifier technology have helped to reduce this artefact. In a sample-and-hold circuit, electrodes are decoupled from the amplifier immediately before the TMS pulse, allowing EEG recordings to take place as quickly as 2 ms following the pulse [13]. As opposed to traditional alternating current (AC) amplifiers, direct current (DC) coupled amplifiers minimize amplifier saturation and eliminate the prolonged negative deflection caused by the TMS pulse [39]. The development of TMS-compatible EEG electrodes with online and offline noise removal techniques can further assist to minimize the pulse artefact [40–42].

Artefacts secondary to the electromagnetic pulse also contaminate the EEG response. These artefacts result from environmental (i.e. power

line) and physiological noise (i.e. eye movements, cardiac rhythms, muscle contraction) and other TMS-related sources (i.e. TMS-induced activation of nearby cranial nerves and muscle movement, sensory-evoked potentials from the tapping sensation of the coil on the scalp, auditory-evoked potentials caused by the loud click emitted during a TMS pulse, and movement of EEG electrodes) [43]. Careful preparations must be taken to mitigate these effects from masking the TEP response [44]. For example, electrode impedances should be maintained below 5 kΩ throughout recordings. A thin layer of foam attached under the stimulating coil will reduce vibrations and bone conduction. A masking noise containing specific time-varying frequency components of the TMS click played through headphones can prevent contamination of TEPs from auditory responses [45–47]. Finally, implementing a sham condition to mimic the induction of sound and scalp sensations help minimize the impact of auditory and somatosensory-evoked potentials [48].

Overall, TMS-EEG permits the in vivo assessment of neural processes across numerous brain regions and states. Although this combination of methods is technically challenging, its cause-and-effect approach has allowed scientists to expand our collective understanding of numerous cortical processes including: functional cortico-cortical connectivity, state-dependent excitability, and the plastic reorganization of cortical circuitry after therapeutic treatment. The main shortcoming of TMS-EEG methodology is that it offers low spatial resolution on the order of centimetres. Hence, the combination of TMS-EEG with neuroimaging methods (stereotactic MRI) gives rise to a powerful multimodal setup to modulate and characterize neural networks with a high degree of spatial and temporal precision.

Stereotactic Navigation Systems in TMS

Typical TMS methods that use standard coil locations based on cranial landmarks or electrode positions on an EEG cap cannot account for intersubject variability in cortical anatomy or skull sizes [49, 50]. Additionally, subtle changes in coil position and orientation can alter the direction of current flow across neurons [51, 52]. Inconsistent selection of the stimulation site is regarded as one of the highest sources of error in TMS outcomes [10, 53]. These technical and methodological limitations can confound clinical interpretations and obscure the reliability of pre-operative mapping for cortical regions [9]. Many of these fundamental issues historically associated with TMS can be resolved by employing an optical tracking system so that stimulation procedures can reference and adhere to an individual's specific brain anatomy.

Navigated TMS (nTMS) is based on the principles of frameless stereotaxy and is acquired by combining an individual's T1-weighted magnetic resonance imaging (MRI) scan into a 3D reconstruction of their head and brain anatomy. Infrared cameras are placed around the room to detect trackers fixed to the stimulating coil and mounted on the subject's head. The navigation software communicates with these trackers while cranial landmarks are marked with a digitizing pen to align the MRI head model with homologous points on the participant's physical head. Once co-registration is completed, the desired stimulation sites and TMS coil can be visualized over the participant's structural brain image for the duration of stimulation. Now, coil location, coil orientation, and estimates of the induced electric field can be optically tracked and reliably reproduced across several stimulation sessions for the same subject. A nTMS system allows for highly accurate coil placement (position error = 1.2 mm, orientation error = 0.3°) and greater consistency of MEPs recorded during TMS (ICC = 0.97), compared to non-navigated trials (position error = 5.5 mm, orientation error = 3.3°, ICC = 0.93) [54]. This is true even for simple processes, such as locating the motor hand region to determine the motor hotspot [55]. Thus, nTMS offers significantly enhanced spatial accuracy between and within sessions over conventional TMS methods.

TMS as a Research Tool

TMS stimulation paradigms open up the possibility for particular physiological pathways to be probed in vivo for mechanistic investigations of cortical excitability, inhibition, and plasticity. Many of the following paradigms, including short interval cortical inhibition, intracortical facilitation, long interval cortical inhibition, and paired associative stimulation, rely on an outcome measure assessed with EMG, EEG, or both of these methods. Meanwhile, oscillatory activity can only be interpreted from EEG recordings. Of note, all of these protocols first require motor threshold assessments using TMS-EMG to establish the intensity of stimulating pulses.

Motor Threshold

Motor threshold (MT) characterizes an individual's level of corticospinal excitability through glutamatergic neurotransmission and is used as a reference to guide the intensity for any type of TMS paradigm (e.g. paired-pulse TMS to characterize cortical inhibition). MT is determined by applying single-pulse TMS over the motor cortex while the coil is placed at an optimal position to elicit MEPs from the target muscle (i.e. right abductor pollicis brevis (APB) muscle). Resting motor threshold (RMT) is defined as the minimum stimulus intensity to evoke MEPs with peak-to-peak amplitude of over 50 μV in at least 5 out of 10 consecutive trials in the relaxed target muscle. In depression, left hemispheric RMTs are significantly higher than right hemispheric RMTs, signalling frontal interhemispheric asymmetry [56, 57]. We will discuss later in the repetitive TMS section how these observations provided the initial basis for targeting frontal areas to treat depression with TMS. Altered RMT levels have also been reported in patients with stroke or neurodegenerative disorders, including Alzheimer's disease [58] and amyotrophic lateral sclerosis [59]. Most studies report normal RMT in Parkinson's disease [60, 61], although the accuracy of this measurement may be impeded by involuntary contractions caused from tremor and rigidity [62].

Paired-Pulse TMS to Assess Cortical Inhibition and Excitation

TMS applied in a paired-pulse sequence is used to modulate the excitability of cortico-cortical interactions in the human cortex. Paired-pulse TMS (ppTMS) involves the application of a conditioning stimulus (CS) and a subsequent test stimulus (TS). Depending on the inter-stimulus interval (ISI) and CS intensity, an increase or decrease in the conditioned TMS-evoked response can be observed when compared with the unconditioned response (Fig. 15.2) [44].

Short interval cortical inhibition (SICI) involves a subthreshold CS, set at 80% of the RMT intensity, delivered 2–3 ms prior to the suprathreshold TS. SICI is thought to arise due to the activation of low threshold inhibitory interneurons through the CS, which generate IPSPs to inhibit the cortical response to the subsequent TS [63]. SICI is linked to $GABA_A$ receptor-mediated inhibitory neurotransmission, as SICI is increased by medications that facilitate $GABA_A$ receptor activity and decreased by $GABA_A$ reuptake inhibitors [64, 65]. Further supporting a role of GABA, SICI exhibits a similar time course as $GABA_A$ receptor-induced IPSPs [66]. Reduced SICI has been described in schizophrenia patients at varying stages of illness, including: high-risk individuals, first-episode patients, and chronic patients [67–69]. Further, studies have indicated a correlation between SICI strength with positive symptoms of schizophrenia and cognitive dysfunction [67, 70, 71]. The persistence of these deficits at different stages supports the theory of $GABA_A$ergic dysfunction in schizophrenia.

Intracortical facilitation (ICF) is induced using a similar paradigm to SICI but involves longer ISIs between 7 and 30 ms. Excitation indexed by ICF is primarily associated with the activity of NMDA receptors and GABAergic circuits and may arise from the summation of EPSPs from the CS and TS [72]. TMS-EEG studies have demonstrated that SICI and ICF bidirectionally modulate the P60 component of TEPs in both the motor cortex and DLPFC, implying that these two measures rely on similar mechanisms across different cortical regions

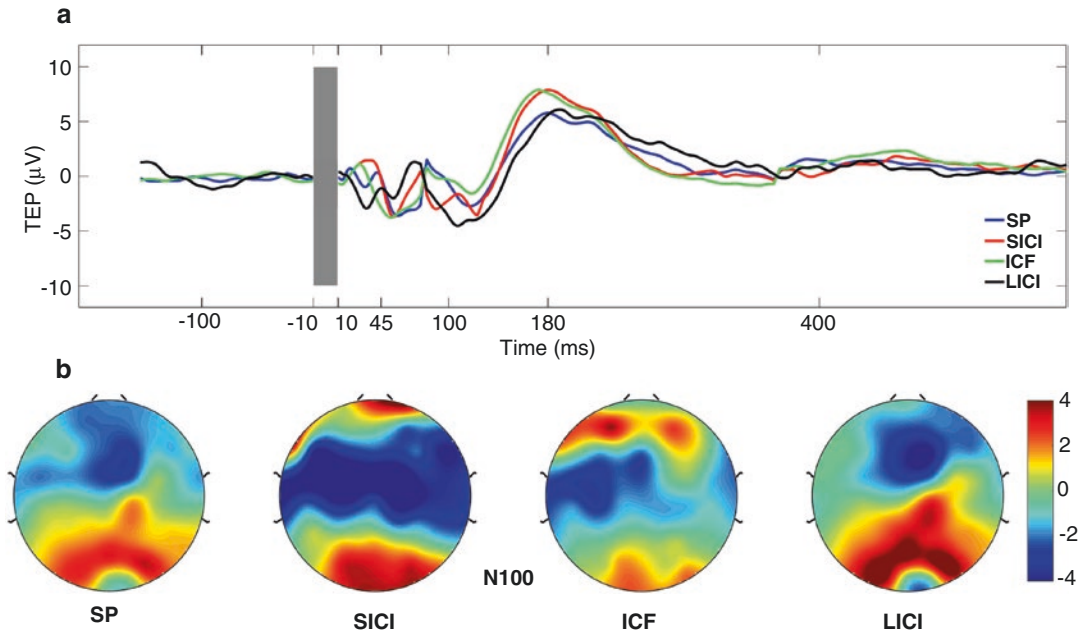

Fig. 15.2 TMS-EEG measures of cortical excitability. (**a**) TMS-evoked potentials after DLPFC stimulation. Traces represent average across 100 trials from the F3 electrode for one healthy volunteer. The effect of the CS on the TS is highlighted here in comparison to the single-pulse condition where TS is administered alone. The CS modulates the N100 deflection in a clear manner. N100 is typically increased in the SICI and LICI conditions and decreased from ICF, when compared against the SP condition. (**b**) The topographical distribution of the N100 component of SP, SICI, and ICF paradigm is localized bilaterally, as demonstrated in previous studies. (Figure adapted with permission from Lioumis et al. [44])

[72, 73]. Similar to SICI, changes in ICF have also been linked to patients with schizophrenia. However, this has only been demonstrated in the DLPFC and is not associated with deficits in cognitive function [71]. Finally, alterations in intracortical excitability may occur in acute stroke that persist into the chronic stage of stroke recovery. Although variable results have been obtained by different groups [74, 75], some researchers report significant differences in the thresholds for contralesional ICF and ipsilesional SICI in chronic stroke patients, correlating to their performance on a motor function task [76]. Following rehabilitation treatment with low frequency repetitive TMS, one study showed an increase in ICF but not SICI [77], perhaps due to the greater contribution of spinal mechanisms to ICF. Hence, ICF as a measure of cortical excitability may carry potential clinical utility for tracking functional improvements in post-stroke recovery.

In long interval cortical inhibition (LICI), a suprathreshold CS is paired with a suprathreshold TS at long ISIs between 50 and 200 ms, inhibiting conditioned MEPs and TEPs [48, 78]. Pharmacological studies have related the neurobiological basis of LICI to slow IPSPs mediated through $GABA_B$ receptors, as LICI is increased by $GABA_B$ receptor agonists in both the motor cortex and DLPFC [79, 80]. Further, maximum inhibition from LICI is achieved when the CS precedes the TS by 100–150 ms, consistent with the time course associated with $GABA_B$ receptor activity [81, 82]. LICI demonstrates high test-retest reliability in both the motor cortex and DLPFC [83], and similar mechanisms likely mediate both EMG and EEG suppression through LICI [48]. LICI-evoked changes in TEP components and oscillatory power are strongly associated with schizophrenia [84, 85] and alcohol dependence [86] and predict treatment response to magnetic seizure therapy in treatment-resistant depression [87].

Plasticity

Paired associative brain stimulation (PAS) provides a reliable and non-invasive method to assess long-term potentiation (LTP)-like or long-term depression (LTD)-like plasticity. In the human cortex, PAS involves the pairing of a suprathreshold electrical stimulus applied to a peripheral nerve (i.e. median nerve) with a suprathreshold TMS pulse applied to the contralateral cortex. The ISI is selected according to effects evoked by spike-timing-dependent plasticity, whereby synaptic transmission is facilitated when presynaptic input precedes postsynaptic excitation (via longer ISIs of 21.5–25 ms) and inhibited if postsynaptic excitation precedes presynaptic input (via shorter ISIs ~10 ms) [88]. Of note, the modulatory effects of PAS are specific to the region of stimulation and can be used to explore cortico-cortical connectivity across different frequency bands with EEG [89, 90]. Plasticity can also be evoked at the level of the spinal cord with limb-specific ISIs, whereby orthodromic volleys induced via TMS travel down through the corticospinal tract and meet with antidromic volleys induced by peripheral nerve stimulation in lower motor neurons [91]. Recently, spinal PAS has been shown to enhance recovery of function in individuals with incomplete spinal cord injuries [92, 93]. In general, the utility of PAS in clinical populations can help elucidate biomarkers of abnormal synaptic plasticity, which is a pathophysiological feature of a number of psychiatric and neurological disorders, including: major depressive disorder [94], schizophrenia [95, 96], Alzheimer's disease [97], Huntington's disease [98], and Parkinson's disease [99]. Other plasticity-inducing brain stimulation protocols, such as repetitive transcranial magnetic stimulation and theta burst stimulation, are increasingly being used for therapeutic purposes and will be discussed later.

Cortical Oscillations

Oscillatory activity (discussed in detail in Chap. 9) reflects momentary brain states and is associated with specific behavioural and cognitive functions. The most studied frequency bands include: delta (1–3 Hz), theta (4–7 Hz), alpha (8–12 Hz), beta (12–28 Hz), and gamma (30–50 Hz). Lower-frequency oscillations are traditionally associated with different stages of the sleep cycle, while those in the higher frequency range are more closely related to motor and cognitive control. Although the mechanisms underlying the generation of cortical oscillations are still under investigation, TMS-EEG can elucidate the functional specificity of brain rhythms through network effects [46, 100] and carries a potential role in the diagnosis of clinical disorders. TMS evokes a brief period of phase alignment in EEG oscillatory activity, which can be decomposed into time and frequency components through offline data analysis [43]. Under this approach, abnormal amplitude and synchronization of gamma oscillations have been identified in frontal regions of schizophrenia patients [47] that relate to the severity of positive symptoms and performance in a verbal memory task [101]. Meanwhile, Parkinson's disease patients display a specific TMS-induced increase in beta oscillations [102]. Alpha asymmetry has been established as a marker for cortical hypoactivity in depression [103, 104]. A recent longitudinal study revealed significant increases of TMS-evoked alpha oscillations in ischemic subcortical stroke patients at baseline, correlating with clinical improvements during follow-up evaluations 40 and 60 days later [105]. These findings suggest that alpha activity may be used as a predictor for motor recovery in stroke. In summary, TMS-EEG research has provided new views on brain oscillations as potential physiological biomarkers for clinical disorders.

Clinical Applications of TMS

Repetitive TMS

While a single TMS pulse produces short-lived effects on neural activation, repetitively applied pulses can induce neural modulation that outlasts the period of stimulation [106]. In this

regard, repetitive TMS (rTMS) carries tremendous potential in therapeutic applications. Currently, rTMS is an FDA-approved treatment to alleviate symptoms of medication-resistant depression. Three of the most common protocols employed to treat depression include: low-frequency rTMS (<1 Hz) applied over the right DLPFC to reduce cortical excitability [107], high-frequency rTMS (5–20 Hz) targeting the left DLPFC to facilitate cortical excitability [108], or both stimuli applied in a sequential bilateral fashion [109]. These paradigms typically involve suprathreshold pulses administered for long durations (10–40 min) and are thought to modulate metaplasticity by inducing complex changes in gene regulation, de novo protein expression, and morphology [110]. Many sham-controlled studies support the antidepressant efficacy of rTMS, as depressive symptoms are significantly reduced after 2–4 weeks of treatment [111, 112] and the odds of retaining remission are improved by several-fold with rTMS [113, 114]. TMS investigations have not provided clear evidence for a systematic influence of non-motor rTMS on RMT of MEPs [115–117], suggesting that stimulation intensity for rTMS need not be adjusted over the course of treatment to improve efficacy. On the other hand, EEG studies have consistently demonstrated that high frequency rTMS applied to the left DLPFC increases alpha band power when depressed patients are in the awake state [118–120], while decreases in alpha power during rapid eye movement (REM) sleep correlate with treatment outcome [121]. The neurobiological underpinnings of the antidepressant effects from rTMS currently remain under investigation.

Overall, rTMS has yielded promising results to ameliorate depressive symptoms and holds potential for treating other disorders including: anxiety, post-traumatic stress disorder, stroke, pain, and schizophrenia. Unfortunately, rTMS involves long session lengths that are repeated over several weeks, which restrict treatment capacity and increase cost per session. Hence, researchers are exploring novel methods of applying rTMS that can help improve accessibility and cost-effectiveness of treatment.

Theta Burst Stimulation

Theta burst stimulation (TBS) is a rTMS protocol that involves bursts of subthreshold pulses applied with high frequency (50 Hz) at an interburst interval of 200 ms [122]. By mimicking endogenous theta rhythms, TBS improves induction of long-term synaptic potentiation effects and requires lower intensities and duration of stimulation in comparison with other rTMS protocols [122, 123]. One form of TBS, known as intermittent TBS (iTBS), delivers 600 pulses in only 3 min and is superior to sham treatment for medication-resistant depression [124, 125]. Recently, a large multicentre, randomized, non-inferiority clinical trial demonstrated that iTBS reduces symptoms of depression on a level equivalent to standard rTMS procedures [126]. These findings suggest that widespread incorporation of iTBS in rTMS clinics could increase the number of patients that can be accommodated for treatment by three- to fourfold. TMS-EEG studies provide direct evidence for a modulatory effect of iTBS on DLPFC cortical reactivity, as later TEP peaks and theta power are increased following iTBS [127, 128]. Pharmacological studies reveal that TBS-induced plasticity may rely on complex interactions between the glutamatergic, dopaminergic, and GABAergic networks. To optimize the therapeutic efficacy of TBS, further research is necessary to identify the neurobiological mechanisms of TBS effects, as well as TMS-EEG biomarkers that can help predict TBS response.

nTMS in Preoperative Mapping

Surgical resection involves a trade-off between preserving brain function and minimizing the presence of residual tumour after treatment. To achieve optimal and safe resections, intraoperative brain mapping through direct cortical stimulation (DCS) is used to obtain the functional and anatomical topography of individual patients. Intraoperative brain mapping is considered the gold standard to obtain this information reliably. However, intracranial recordings require diagnostic surgery and present a high risk of compli-

cations [129]. Thus, functional maps obtained non-invasively and outside of the operating theatre are of great use to assist with neurosurgical procedures. The most widely adopted neuroimaging method for this purpose is functional MRI (fMRI). Yet fMRI carries poor temporal resolution and provides an indirect measure for assessing functional effects from cortical activation [130, 131]. Moreover, with most analytic approaches, fMRI identifies all areas involved in language, but not necessarily brain regions that are essential to language – which is what is important surgically. In recent years, nTMS has been increasingly utilized for pre-surgical functional mapping for brain tumours and epilepsy, as it establishes a causal link between the stimulated section of the brain and observed behavioural responses in a manner analogous to DCS [132]. Reports describe nTMS as a reliable technique to map motor and language processes, which influences preoperative planning and improves surgical outcomes. Furthermore, nTMS is well-tolerated by healthy subjects and neurosurgical patients [133, 134].

Motor Mapping

Conventionally, motor responses are assigned a colour code that represents the MEP amplitude evoked from a specific region of stimulation. nTMS maps are an ensemble of coloured markers that correspond to stimulation spots and are overlaid on the individual's MRI scans. Visual inspection of these maps allows resectable vs. non-resectable areas to be easily identified (Fig. 15.3). These anatomical and functional data can be transferred to the operating room to guide surgery for rolandic lesions and intraoperative mapping procedures.

In mapping the motor cortex, a strong correlation exists between the spatial accuracy of nTMS with that provided by intraoperative DCS. Very low discrepancies (5–10 mm) occur when nTMS and DCS are used to locate the motor hotspot [135, 136]. Compared to fMRI, nTMS has more precise spatial resolution and can be implemented preoperatively with greater ease [137].

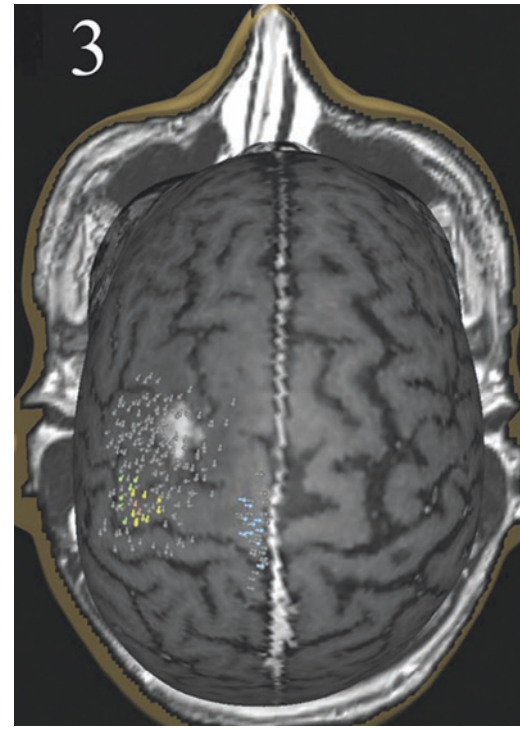

Fig. 15.3 nTMS somatotopic mapping for a rolandic tumour patient (patient #3). Each stimuli point is coloured according to the EMG channel with the highest amplitude MEP output. The peeling depth of the 3D magnetic resonance imaging was set to 25 mm to visualize the tumour (red arrow) with the central sulcus. Green, abductor pollicis brevis; yellow, abductor digiti minimi; pink, first dorsal interosseous; blue, tibialis anterior; grey, no response. (Original figure obtained from Picht et al. [152], with permission from Oxford University Press)

Interestingly, nTMS is more accurate than fMRI for mapping cortical areas (i.e. upper extremities), but less accurate for subcortical regions (i.e. lower extremities) [138]. Overall, the results of nTMS mapping induce modifications in preoperative planning and lead to a positive effect on clinical outcomes. One study, which assessed the broad impact of nTMS on surgical planning in 73 patients with rolandic brain tumours, reported that nTMS confirmed the expected anatomy in 22% of patients, prompted the identification of high-risk functional cortical areas in 27%, and modified the surgical approach in 16% [139]. In addition, surgical and oncological outcomes are improved when patients receive preoperative nTMS mapping, as demonstrated by a lower

postoperative rate of residual tumour and improved progression-free survival [139–141]. In summary, nTMS provides an accurate method to assess motor topography and identify eloquent motor cortical areas that would otherwise cause permanent neurological deficits if removed.

Speech and Language Mapping

As for preoperative motor mapping, fMRI and nTMS have also been used to study language laterality as an alternative to invasive DCS procedures in awake craniotomy or through an implanted subdural electrode grid. The most commonly used language task is visual object naming, during which the subject is asked to name objects that are presented visually while short trains of repetitive nTMS (rnTMS) pulses are targeted to a specific cortical site to disrupt naming. Offline video analysis of the mapping session can reveal which stimulation sites (i.e. left Brodmann area 44, Broca's area) produce dysarthria, hesitation, anomia, phonological errors, or semantic errors. These data are allocated to their respective anatomical location in MRI scans to produce a language map. This map is particularly useful in guiding neurosurgical planning for patients with focal pathologies located in the perisylvian areas [142].

Both rnTMS and DCS are lesion-based approaches that allow accurate targeting of eloquent speech areas [143]. rnTMS is generally more sensitive but less specific than DCS for detecting classic motor speech areas, as resection of some rnTMS-positive and DCS-negative sites results in no major language complications [144, 145]. The oversensitivity of rnTMS results may be attributed to human error during offline video analysis whereas only very clear responses are kept during online DCS mapping [144]. Meanwhile, rnTMS rarely yields false-negative results. This implies that rnTMS language mapping may be helpful in creating "negative maps" to prescreen for unlikely language sites. Moreover, intra- and interindividual replicability are typically highest for frontal areas identified through rnTMS rather than temporoparietal areas [146]. In comparing preoperative fMRI language mapping to intraoperative DCS mapping, a review of nine studies suggests that fMRI is not a feasible alternative to DCS for analysing brain lesions located in language areas [147]. As outlined above, passive functional imaging methods are unable to differentiate those regions essential for function from those that are merely coactivated, hampering its accuracy when mapping eloquent language areas during language testing [148, 149]. rnTMS has been increasingly used over fMRI in recent years due to its superior sensitivity, already replacing fMRI at several institutions as the primary method for non-invasive preoperative language mapping [142, 150].

In summary, preoperative nTMS holds tremendous promise for accurately mapping eloquent regions to assist with surgical planning and improving patient safety. However, we must emphasize that it is not intended to replace intraoperative DCS procedures. The intrinsic limitations of the navigation system, such as those imposed by co-registration errors, variations in optical tracking of the TMS coil, and variability of brain volumes over time, continue to prevent nTMS from attaining the same degree of spatial accuracy as DCS [142]. Rather, nTMS should be regarded as a helpful adjunct to DCS and improve the reliability of results. The coherency of the two maps can help guarantee the functional organization of the network to extend resections while preserving function in order to maintain patients' quality of life. Future improvements to broaden the application of nTMS may be achieved by implementing complementary diffusion tensor imaging procedures for fibre-tracking data [151] or magnetoencephalography to help detect the sources and spread of epileptic activity [136].

Conclusion

TMS has great promise as a non-invasive neurostimulation technique that can help elucidate the physiological properties of cortical areas. The physical and physiological mechanisms of TMS must be carefully considered when it is used to modulate specific cortical processes and regions.

When combined with EEG, almost the entire cortical mantle can be investigated. This includes the DLPFC, which is implicated in the pathophysiology of many mental disorders and is currently targeted with rTMS and iTBS protocols to ameliorate depressive symptomatology. TMS-EEG can further probe the pharmacological and therapeutic treatment effects on specific TEP components and cortical oscillations. These studies have provided essential insights upon the involvement of the GABAergic inhibitory network and glutamatergic system in neuropsychiatric disorders and can further provide biomarkers that may be crucial in predicting a patient's response to different kinds of therapy. Integration of TMS with MRI-guided neuronavigation allows consistent selection of the stimulation site, which offers a valuable tool to map functionally eloquent areas and improve surgical outcomes. Equally important, MRI-guided TMS-EEG provides an accurate assessment of brain dynamics, potentially serving as a reliable biomarker.

References

1. Merton PA, Morton HB. Stimulation of the cerebral cortex in the intact human subject. Nature. 1980;285(5762):227.
2. Barker AT, Jalinous R, Freeston IL. Non-invasive magnetic stimulation of human motor cortex. Lancet (Lond, Engl). 1985;1(8437):1106–7.
3. Barker AT. The history and basic principles of magnetic nerve stimulation. Electroencephalogr Clin Neurophysiol Suppl. 1999;51:3–21.
4. Rossini PM, Rossi S. Clinical applications of motor evoked potentials. Electroencephalogr Clin Neurophysiol. 1998;106(3):180–94.
5. Merton PA, Morton HB, Hill DK, Marsden CD. Scope of a technique for electrical stimulation of human brain, spinal cord, and muscle. Lancet. 1982;320(8298):597–600.
6. Deletis V, Sala F. Intraoperative neurophysiological monitoring of the spinal cord during spinal cord and spine surgery: a review focus on the corticospinal tracts. Clin Neurophysiol. 2008;119(2):248–64.
7. Schubert D, Kötter R, Zilles K, Luhmann HJ, Staiger JF. Cell type-specific circuits of cortical layer IV spiny neurons. J Neurosci. 2003;23(7):2961–70.
8. Day BL, Dressler D, Maertens de Noordhout A, Marsden CD, Nakashima K, Rothwell JC, et al. Electric and magnetic stimulation of human motor cortex: surface EMG and single motor unit responses. J Physiol. 1989;412:449–73.
9. Ruohonen J, Karhu J. Navigated transcranial magnetic stimulation. Neurophysiol Clin Neurophysiol. 2010;40(1):7–17.
10. Mills KR, Boniface SJ, Schubert M. Magnetic brain stimulation with a double coil: the importance of coil orientation. Electroencephalogr Clin Neurophysiol Potentials Sect. 1992;85(1):17–21.
11. Brasil-Neto JP, McShane LM, Fuhr P, Hallett M, Cohen LG. Topographic mapping of the human motor cortex with magnetic stimulation: factors affecting accuracy and reproducibility. Electroencephalogr Clin Neurophysiol Potentials Sect. 1992;85(1):9–16.
12. Ilmoniemi RJ, Ruohonen J, Karhu J. Transcranial magnetic stimulation--a new tool for functional imaging of the brain. Crit Rev Biomed Eng. 1999;27(3–5):241–84.
13. Ilmoniemi RJ, Virtanen J, Ruohonen J, Karhu J, Aronen HJ, Näätänen R, et al. Neuronal responses to magnetic stimulation reveal cortical reactivity and connectivity. Neuroreport. 1997;8(16):3537–40.
14. Pascual-Leone A, Cohen LG, Brasil-Neto JP, Hallett M. Non-invasive differentiation of motor cortical representation of hand muscles by mapping of optimal current directions. Electroencephalogr Clin Neurophysiol. 1994;93(1):42–8.
15. Rushton WA. The effect upon the threshold for nervous excitation of the length of nerve exposed, and the angle between current and nerve. J Physiol. 1927;63(4):357–77.
16. Silva S, Basser PJ, Miranda PC. Elucidating the mechanisms and loci of neuronal excitation by transcranial magnetic stimulation using a finite element model of a cortical sulcus. Clin Neurophysiol. 2008;119(10):2405–13.
17. Terao Y, Ugawa Y. Basic mechanisms of TMS. J Clin Neurophysiol. 2002;19(4):322–43.
18. Landau WM, Bishop GH, Clare MH. Site of excitation in stimulation of the motor cortex. J Neurophysiol. 1965;28(6):1206–22.
19. Murphy SC, Palmer LM, Nyffeler T, Müri RM, Larkum ME. Transcranial magnetic stimulation (TMS) inhibits cortical dendrites. elife. 2016;5:e13598.
20. Rothwell JC, Day BL, Thompson PD, Kujirai T. Short latency intracortical inhibition: one of the most popular tools in human motor neurophysiology. J Physiol. 2009;587(1):11–2.
21. Silvanto J, Muggleton N, Walsh V. State-dependency in brain stimulation studies of perception and cognition. Trends Cogn Sci. 2008;12:447–54.
22. Matthews PB. The effect of firing on the excitability of a model motoneurone and its implications for cortical stimulation. J Physiol. 1999;518((Pt 3)):867–82.
23. Matheson NA, Shemmell JBH, De Ridder D, Reynolds JNJ. Understanding the effects of repetitive transcranial magnetic stimulation on neuronal circuits. Front Neural Circuits. 2016;10:67.
24. Moliadze V, Zhao Y, Eysel U, Funke K. Effect of transcranial magnetic stimulation on single-unit activity in the cat primary visual cortex. J Physiol. 2003;553(2):665–79.

25. Salvador R, Silva S, Basser PJ, Miranda PC. Determining which mechanisms lead to activation in the motor cortex: a modeling study of transcranial magnetic stimulation using realistic stimulus waveforms and sulcal geometry. Clin Neurophysiol. 2011;122(4):748–58.
26. Ueno S, Tashiro T, Harada K. Localized stimulation of neural tissues in the brain by means of a paired configuration of time-varying magnetic fields. J Appl Phys. 1988;64(10):5862–4.
27. Zangen A, Roth Y, Voller B, Hallett M. Transcranial magnetic stimulation of deep brain regions: evidence for efficacy of the H-coil. Clin Neurophysiol. 2005;116(4):775–9.
28. Lazzaro V, Oliviero A, Mazzone P, Insola A, Pilato F, Saturno E, et al. Comparison of descending volleys evoked by monophasic and biphasic magnetic stimulation of the motor cortex in conscious humans. Exp Brain Res. 2001;141(1):121–7.
29. Jalinous R. Principles of magnetic stimulator design. In: Pascual-Leone A, Davey NJ, Rothwell JC, editors. Handbook of transcranial magnetic stimulation. London: Arnold; 2002. p. 30–8.
30. Peterchev AV, Jalinous R, Lisanby SH. A transcranial magnetic stimulator inducing near-rectangular pulses with controllable pulse width (cTMS). IEEE Trans Biomed Eng. 2008;55(1):257–66.
31. Peterchev AV, Murphy DL, Lisanby SH. Repetitive transcranial magnetic stimulator with controllable pulse parameters. J Neural Eng. 2011;8(3):036016.
32. Kirschstein T, Köhling R. What is the source of the EEG? Clin EEG Neurosci. 2009;40(3):146–9.
33. Hill AT, Rogasch NC, Fitzgerald PB, Hoy KE. TMS-EEG: a window into the neurophysiological effects of transcranial electrical stimulation in non-motor brain regions. Neurosci Biobehav Rev. 2016;64:175–84.
34. Gosseries O, Sarasso S, Casarotto S, Boly M, Schnakers C, Napolitani M, et al. On the cerebral origin of EEG responses to TMS: insights from severe cortical lesions. Brain Stimul. 2015;8(1):142–9.
35. Lioumis P, Kicić D, Savolainen P, Mäkelä JP, Kähkönen S. Reproducibility of TMS-evoked EEG responses. Hum Brain Mapp. 2009;30(4):1387–96.
36. Kähkönen S, Ilmoniemi RJ. Transcranial magnetic stimulation: applications for neuropsychopharmacology. J Psychopharmacol. 2004;18(2):257–61.
37. Casarotto S, Romero Lauro LJ, Bellina V, Casali AG, Rosanova M, Pigorini A, et al. EEG responses to TMS are sensitive to changes in the perturbation parameters and repeatable over time. Valdes-Sosa PA, editor. PLoS One. 2010;5(4):e10281.
38. Ilmoniemi RJ, Karhu J. TMS and Electrocephalography: Methods and Current Advances. In: Epstein CM, Wassermann EM, Ziemann U, editors. Oxford Handbook of Transcranial Stimulation. Oxford: Oxford University Press; 2008:593–608.
39. Daskalakis ZJ, Farzan F, Radhu N, Fitzgerald PB. Combined transcranial magnetic stimulation and electroencephalography: its past, present and future. Brain Res. 2012;1463:93–107.
40. Virtanen J, Ruohonen J, Näätänen R, Ilmoniemi RJ. Instrumentation for the measurement of electric brain responses to transcranial magnetic stimulation. Med Biol Eng Comput. 1999;37(3):322–6.
41. Atluri S, Frehlich M, Mei Y, Garcia Dominguez L, Rogasch NC, Wong W, et al. TMSEEG: a MATLAB-based graphical user interface for processing electrophysiological signals during transcranial magnetic stimulation. Front Neural Circuits. 2016;10:78.
42. Casula EP, Bertoldo A, Tarantino V, Maiella M, Koch G, Rothwell JC, et al. TMS-evoked long-lasting artefacts: a new adaptive algorithm for EEG signal correction. Clin Neurophysiol. 2017;128(9):1563–74.
43. Farzan F, Vernet M, Shafi MMD, Rotenberg A, Daskalakis ZJ, Pascual-Leone A. Characterizing and modulating brain circuitry through transcranial magnetic stimulation combined with electroencephalography. Front Neural Circuits. 2016;10:73.
44. Lioumis P, Zomorrodi R, Hadas I, Daskalakis ZJ, Blumberger DM. Combined transcranial magnetic stimulation and electroencephalography of the dorsolateral prefrontal cortex. J Vis Exp. 2018;138:e57983.
45. Fuggetta G, Fiaschi A, Manganotti P. Modulation of cortical oscillatory activities induced by varying single-pulse transcranial magnetic stimulation intensity over the left primary motor area: a combined EEG and TMS study. NeuroImage. 2005;27(4):896–908.
46. Rosanova M, Casali A, Bellina V, Resta F, Mariotti M, Massimini M. Natural frequencies of human corticothalamic circuits. J Neurosci. 2009;29(24):7679–85.
47. Ferrarelli F, Massimini M, Peterson MJ, Riedner BA, Lazar M, Murphy MJ, et al. Reduced evoked gamma oscillations in the frontal cortex in schizophrenia patients: a TMS/EEG study. Am J Psychiatry. 2008;165(8):996–1005.
48. Daskalakis ZJ, Farzan F, Barr MS, Maller JJ, Chen R, Fitzgerald PB. Long-interval cortical inhibition from the dorsolateral prefrontal cortex: a TMS–EEG study. Neuropsychopharmacology. 2008;33(12):2860–9.
49. Beam W, Borckardt JJ, Reeves ST, George MS. An efficient and accurate new method for locating the F3 position for prefrontal TMS applications. Brain Stimul. 2009;2(1):50–4.
50. Herwig U, Satrapi P, Schönfeldt-Lecuona C. Using the international 10-20 EEG system for positioning of transcranial magnetic stimulation. Brain Topogr. 2003;16(2):95–9.
51. Neggers SFW, Langerak TR, Schutter DJLG, Mandl RCW, Ramsey NF, Lemmens PJJ, et al. A stereotactic method for image-guided transcranial magnetic stimulation validated with fMRI and motor-evoked potentials. NeuroImage. 2004;21(4):1805–17.
52. Schmidt S, Bathe-Peters R, Fleischmann R, Rönnefarth M, Scholz M, Brandt SA. Nonphysiological factors in navigated TMS studies; confounding covariates and valid intracortical estimates. Hum Brain Mapp. 2015;36(1):40–9.
53. Julkunen P, Säisänen L, Danner N, Niskanen E, Hukkanen T, Mervaala E, et al. Comparison of navigated and non-navigated transcranial mag-

netic stimulation for motor cortex mapping, motor threshold and motor evoked potentials. NeuroImage. 2009;44(3):790–5.
54. Rodseth J, Washabaugh EP, Krishnan C. A novel low-cost approach for navigated transcranial magnetic stimulation. Restor Neurol Neurosci. 2017;35(6):601–9.
55. Sparing R, Buelte D, Meister IG, Pauš T, Fink GR. Transcranial magnetic stimulation and the challenge of coil placement: a comparison of conventional and stereotaxic neuronavigational strategies. Hum Brain Mapp. 2008;29(1):82–96.
56. Funk AP, George MS. Prefrontal EEG asymmetry as a potential biomarker of antidepressant treatment response with transcranial magnetic stimulation (TMS): a case series. Clin EEG Neurosci. 2008;39(3):125–30.
57. Concerto C, Lanza G, Cantone M, Pennisi M, Giordano D, Spampinato C, et al. Different patterns of cortical excitability in major depression and vascular depression: a transcranial magnetic stimulation study. BMC Psychiatry. 2013;13(1):300.
58. Di Lazzaro V, Oliviero A, Tonali PA, Marra C, Daniele A, Profice P, et al. Noninvasive in vivo assessment of cholinergic cortical circuits in AD using transcranial magnetic stimulation. Neurology. 2002;59(3):392–7.
59. Eisen A, Shytbel W, Murphy K, Hoirch M. Cortical magnetic stimulation in amyotrophic lateral sclerosis. Muscle Nerve. 1990;13(2):146–51.
60. Ridding MC, Rothwell JC, Inzelberg R. Changes in excitability of motor cortical circuitry in patients with parkinson's disease. Ann Neurol. 1995;37(2):181–8.
61. Ni Z, Bahl N, Gunraj CA, Mazzella F, Chen R. Increased motor cortical facilitation and decreased inhibition in Parkinson disease. Neurology. 2013;80(19):1746–53.
62. Ni Z, Chen R. Transcranial magnetic stimulation to understand pathophysiology and as potential treatment for neurodegenerative diseases. Transl Neurodegener. 2015;4:22.
63. Ilić TV, Meintzschel F, Cleff U, Ruge D, Kessler KR, Ziemann U. Short-interval paired-pulse inhibition and facilitation of human motor cortex: the dimension of stimulus intensity. J Physiol. 2002;545(Pt 1):153–67.
64. Ziemann U, Lönnecker S, Steinhoff BJ, Paulus W. The effect of lorazepam on the motor cortical excitability in man. Exp Brain Res. 1996;109(1):127–35.
65. Werhahn KJ, Kunesch E, Noachtar S, Benecke R, Classen J. Differential effects on motorcortical inhibition induced by blockade of GABA uptake in humans. J Physiol. 1999;517(Pt 2):591–7.
66. Wang XJ, Buzsáki G. Gamma oscillation by synaptic inhibition in a hippocampal interneuronal network model. J Neurosci. 1996;16(20):6402–13.
67. Wobrock T, Schneider M, Kadovic D, Schneider-Axmann T, Ecker UKH, Retz W, et al. Reduced cortical inhibition in first-episode schizophrenia. Schizophr Res. 2008;105(1–3):252–61.
68. Hasan A, Wobrock T, Grefkes C, Labusga M, Levold K, Schneider-Axmann T, et al. Deficient inhibitory cortical networks in antipsychotic-naive subjects at risk of developing first-episode psychosis and first-episode schizophrenia patients: a cross-sectional study. Biol Psychiatry. 2012;72(9):744–51.
69. Hasan A, Nitsche MA, Rein B, Schneider-Axmann T, Guse B, Gruber O, et al. Dysfunctional long-term potentiation-like plasticity in schizophrenia revealed by transcranial direct current stimulation. Behav Brain Res. 2011;224(1):15–22.
70. Daskalakis ZJ, Christensen BK, Chen R, Fitzgerald PB, Zipursky RB, Kapur S. Evidence for impaired cortical inhibition in schizophrenia using transcranial magnetic stimulation. Arch Gen Psychiatry. 2002;59(4):347–54.
71. Noda Y, Barr MS, Zomorrodi R, Cash RFH, Farzan F, Rajji TK, et al. Evaluation of short interval cortical inhibition and intracortical facilitation from the dorsolateral prefrontal cortex in patients with schizophrenia. Sci Rep. 2017;7(1):17106.
72. Cash RFH, Noda Y, Zomorrodi R, Radhu N, Farzan F, Rajji TK, et al. Characterization of glutamatergic and GABAA-mediated neurotransmission in motor and dorsolateral prefrontal cortex using paired-pulse TMS-EEG. Neuropsychopharmacology. 2017;42(2):502–11.
73. Ferreri F, Pasqualetti P, Määttä S, Ponzo D, Ferrarelli F, Tononi G, et al. Human brain connectivity during single and paired pulse transcranial magnetic stimulation. NeuroImage. 2011;54(1):90–102.
74. Swayne OBC, Rothwell JC, Ward NS, Greenwood RJ. Stages of motor output reorganization after hemispheric stroke suggested by longitudinal studies of cortical physiology. Cereb Cortex. 2008;18(8):1909–22.
75. Takeuchi N, Chuma T, Matsuo Y, Watanabe I, Ikoma K. Repetitive transcranial magnetic stimulation of contralesional primary motor cortex improves hand function after stroke. Stroke. 2005;36(12):2681–6.
76. Edwards JD, Meehan SK, Linsdell MA, Borich MR, Anbarani K, Jones PW, et al. Changes in thresholds for intracortical excitability in chronic stroke: more than just altered intracortical inhibition. Restor Neurol Neurosci. 2013;31(6):693–705.
77. Mello EA, Cohen LG, Monteiro Dos Anjos S, Conti J, Andrade KNF, Tovar Moll F, et al. Increase in short-interval intracortical facilitation of the motor cortex after low-frequency repetitive magnetic stimulation of the unaffected hemisphere in the subacute phase after stroke. Neural Plast. 2015;2015:407320.
78. Valls-Solé J, Pascual-Leone A, Wassermann EM, Hallett M. Human motor evoked responses to paired transcranial magnetic stimuli. Electroencephalogr Clin Neurophysiol. 1992;85(6):355–64.
79. McDonnell MN, Orekhov Y, Ziemann U. The role of GABA(B) receptors in intracortical inhibition in the human motor cortex. Exp Brain Res. 2006;173(1):86–93.
80. Salavati B, Rajji TK, Zomorrodi R, Blumberger DM, Chen R, Pollock BG, et al. Pharmacological manipulation of cortical inhibition in the dorsolateral prefrontal cortex. Neuropsychopharmacology. 2018;43(2):354–61.

81. Sanger TD, Garg RR, Chen R. Interactions between two different inhibitory systems in the human motor cortex. J Physiol. 2001;530(Pt 2):307–17.
82. McCormick DA. GABA as an inhibitory neurotransmitter in human cerebral cortex. J Neurophysiol. 1989;62(5):1018–27.
83. Farzan F, Barr MS, Levinson AJ, Chen R, Wong W, Fitzgerald PB, et al. Reliability of long-interval cortical inhibition in healthy human subjects: a TMS–EEG study. J Neurophysiol. 2010;104(3):1339–46.
84. Farzan F, Barr MS, Levinson AJ, Chen R, Wong W, Fitzgerald PB, et al. Evidence for gamma inhibition deficits in the dorsolateral prefrontal cortex of patients with schizophrenia. Brain. 2010;133(5):1505–14.
85. Radhu N, Garcia Dominguez L, Farzan F, Richter MA, Semeralul MO, Chen R, et al. Evidence for inhibitory deficits in the prefrontal cortex in schizophrenia. Brain. 2015;138(2):483–97.
86. Naim-Feil J, Bradshaw JL, Rogasch NC, Daskalakis ZJ, Sheppard DM, Lubman DI, et al. Cortical inhibition within motor and frontal regions in alcohol dependence post-detoxification: a pilot TMS-EEG study. World J Biol Psychiatry. 2016;17(7):547–56.
87. Sun Y, Farzan F, Mulsant BH, Rajji TK, Fitzgerald PB, Barr MS, et al. Indicators for remission of suicidal ideation following magnetic seizure therapy in patients with treatment-resistant depression. JAMA Psychiat. 2016;73(4):337.
88. Stefan K, Kunesch E, Cohen LG, Benecke R, Classen J. Induction of plasticity in the human motor cortex by paired associative stimulation. Brain. 2000;123(Pt 3):572–84.
89. Rajji TK, Sun Y, Zomorrodi-Moghaddam R, Farzan F, Blumberger DM, Mulsant BH, et al. PAS-induced potentiation of cortical-evoked activity in the dorsolateral prefrontal cortex. Neuropsychopharmacology. 2013;38(12):2545–52.
90. Veniero D, Ponzo V, Koch G. Paired associative stimulation enforces the communication between interconnected areas. J Neurosci. 2013;33(34):13773–83.
91. McGie SC, Masani K, Popovic MR. Failure of spinal paired associative stimulation to induce neuroplasticity in the human corticospinal tract. J Spinal Cord Med. 2014;37(5):565–74.
92. Shulga A, Lioumis P, Kirveskari E, Savolainen S, Mäkelä JP, Ylinen A. The use of F-response in defining interstimulus intervals appropriate for LTP-like plasticity induction in lower limb spinal paired associative stimulation. J Neurosci Methods. 2015;242:112–7.
93. Shulga A, Lioumis P, Zubareva A, Brandstack N, Kuusela L, Kirveskari E, et al. Long-term paired associative stimulation can restore voluntary control over paralyzed muscles in incomplete chronic spinal cord injury patients. Spinal Cord Ser Cases. 2016;2:16016.
94. Player MJ, Taylor JL, Weickert CS, Alonzo A, Sachdev P, Martin D, et al. Neuroplasticity in depressed individuals compared with healthy controls. Neuropsychopharmacology. 2013;38(11):2101–8.
95. Frantseva MV, Fitzgerald PB, Chen R, Moller B, Daigle M, Daskalakis ZJ. Evidence for impaired long-term potentiation in schizophrenia and its relationship to motor skill leaning. Cereb Cortex. 2008;18(5):990–6.
96. Daskalakis ZJ, Christensen BK, Fitzgerald PB, Chen R. Dysfunctional neural plasticity in patients with schizophrenia. Arch Gen Psychiatry. 2008;65(4):378.
97. Di Lorenzo F, Ponzo V, Motta C, Bonnì S, Picazio S, Caltagirone C, et al. Impaired spike timing dependent cortico-cortical plasticity in Alzheimer's disease patients. J Alzheimers Dis. 2018:1–9.
98. Orth M, Schippling S, Schneider SA, Bhatia KP, Talelli P, Tabrizi SJ, et al. Abnormal motor cortex plasticity in premanifest and very early manifest Huntington disease. J Neurol Neurosurg Psychiatry. 2010;81(3):267–70.
99. Morgante F, Espay AJ, Gunraj C, Lang AE, Chen R. Motor cortex plasticity in Parkinson's disease and levodopa-induced dyskinesias. Brain. 2006;129(4):1059–69.
100. Thut G, Miniussi C. New insights into rhythmic brain activity from TMS–EEG studies. Trends Cogn Sci. 2009;13(4):182–9.
101. Ferrarelli F, Sarasso S, Guller Y, Riedner BA, Peterson MJ, Bellesi M, et al. Reduced natural oscillatory frequency of frontal thalamocortical circuits in schizophrenia. Arch Gen Psychiatry. 2012;69(8):766–74.
102. Van Der Werf YD, Sadikot AF, Strafella AP, Paus T. The neural response to transcranial magnetic stimulation of the human motor cortex. II. Thalamocortical contributions. Exp Brain Res. 2006;175(2):246–55.
103. Kentgen LM, Tenke CE, Pine DS, Fong R, Klein RG, Bruder GE. Electroencephalographic asymmetries in adolescents with major depression: influence of comorbidity with anxiety disorders. J Abnorm Psychol. 2000;109(4):797–802.
104. Bruder GE, Tenke CE, Warner V, Nomura Y, Grillon C, Hille J, et al. Electroencephalographic measures of regional hemispheric activity in offspring at risk for depressive disorders. Biol Psychiatry. 2005;57(4):328–35.
105. Pellicciari MC, Bonnì S, Ponzo V, Cinnera AM, Mancini M, Casula EP, et al. Dynamic reorganization of TMS-evoked activity in subcortical stroke patients. NeuroImage. 2018;175:365–78.
106. Maeda F, Keenan JP, Tormos JM, Topka H, Pascual-Leone A. Modulation of corticospinal excitability by repetitive transcranial magnetic stimulation. Clin Neurophysiol. 2000;111(5):800–5.
107. Klein E, Kreinin I, Chistyakov A, Koren D, Mecz L, Marmur S, et al. Therapeutic efficacy of right prefrontal slow repetitive transcranial magnetic stimulation in major depression: a double-blind controlled study. Arch Gen Psychiatry. 1999;56(4):315–20.
108. George MS, Nahas Z, Molloy M, Speer AM, Oliver NC, Li XB, et al. A controlled trial of daily left pre-

frontal cortex TMS for treating depression. Biol Psychiatry. 2000;48(10):962–70.
109. Fitzgerald PB, Benitez J, de Castella A, Daskalakis ZJ, Brown TL, Kulkarni J. A randomized, controlled trial of sequential bilateral repetitive transcranial magnetic stimulation for treatment-resistant depression. Am J Psychiatry. 2006;163(1):88–94.
110. Cirillo G, Di Pino G, Capone F, Ranieri F, Florio L, Todisco V, et al. Neurobiological after-effects of non-invasive brain stimulation. Brain Stimul. 2017;10(1):1–18.
111. George MS, Wassermann EM, Kimbrell TA, Little JT, Williams WE, Danielson AL, et al. Mood improvement following daily left prefrontal repetitive transcranial magnetic stimulation in patients with depression: a placebo-controlled crossover trial. Am J Psychiatry. 1997;154(12):1752–6.
112. Fitzgerald PB, Brown TL, Marston NAU, Daskalakis ZJ, de Castella A, Kulkarni J. Transcranial magnetic stimulation in the treatment of depression. Arch Gen Psychiatry. 2003;60(10):1002.
113. Avery DH, Holtzheimer PE, Fawaz W, Russo J, Neumaier J, Dunner DL, et al. A controlled study of repetitive transcranial magnetic stimulation in medication-resistant major depression. Biol Psychiatry. 2006;59(2):187–94.
114. George MS, Lisanby SH, Avery D, McDonald WM, Durkalski V, Pavlicova M, et al. Daily left prefrontal transcranial magnetic stimulation therapy for major depressive disorder. Arch Gen Psychiatry. 2010;67(5):507.
115. Chistyakov AV, Kaplan B, Rubichek O, Kreinin I, Koren D, Feinsod M, et al. Antidepressant effects of different schedules of repetitive transcranial magnetic stimulation vs. clomipramine in patients with major depression: relationship to changes in cortical excitability. Int J Neuropsychopharmacol. 2005;8(2):223–33.
116. Triggs WJ, McCoy KJ, Greer R, Rossi F, Bowers D, Kortenkamp S, et al. Effects of left frontal transcranial magnetic stimulation on depressed mood, cognition, and corticomotor threshold. Biol Psychiatry. 1999;45(11):1440–6.
117. Dolberg OT, Dannon PN, Schreiber S, Grunhaus L. Magnetic motor threshold and response to TMS in major depressive disorder. Acta Psychiatr Scand. 2002;106(3):220–3.
118. Noda Y, Nakamura M, Saeki T, Inoue M, Iwanari H, Kasai K. Potentiation of quantitative electroencephalograms following prefrontal repetitive transcranial magnetic stimulation in patients with major depression. Neurosci Res. 2013;77(1–2):70–7.
119. Valiulis V, Gerulskis G, Dapšys K, Vištartaite G, Šiurkute A, Mačiulis V. Electrophysiological differences between high and low frequency rTMS protocols in depression treatment. Acta Neurobiol Exp (Wars). 2012;72(3):283–95.
120. Spronk D, Arns M, Bootsma A, van Ruth R, Fitzgerald PB. Long term effects of left frontal rTMS on EEG and ERPs in patients with depression. Clin EEG Neurosci. 2008;39(3):118–24.
121. Pellicciari MC, Cordone S, Marzano C, Bignotti S, Gazzoli A, Miniussi C, et al. Dorsolateral prefrontal transcranial magnetic stimulation in patients with major depression locally affects alpha power of REM sleep. Front Hum Neurosci. 2013;7:433.
122. Huang Y-Z, Edwards MJ, Rounis E, Bhatia KP, Rothwell JC. Theta burst stimulation of the human motor cortex. Neuron. 2005;45(2):201–6.
123. Suppa A, Huang Y-Z, Funke K, Ridding MC, Cheeran B, Di Lazzaro V, et al. Ten years of theta burst stimulation in humans: established knowledge, unknowns and prospects. Brain Stimul. 2016;9(3):323–35.
124. Li C-T, Chen M-H, Juan C-H, Huang H-H, Chen L-F, Hsieh J-C, et al. Efficacy of prefrontal theta-burst stimulation in refractory depression: a randomized sham-controlled study. Brain. 2014;137(7):2088–98.
125. Chistyakov AV, Rubicsek O, Kaplan B, Zaaroor M, Klein E. Safety, tolerability and preliminary evidence for antidepressant efficacy of theta-burst transcranial magnetic stimulation in patients with major depression. Int J Neuropsychopharmacol. 2010;13(03):387.
126. Blumberger DM, Vila-Rodriguez F, Thorpe KE, Feffer K, Noda Y, Giacobbe P, et al. Effectiveness of theta burst versus high-frequency repetitive transcranial magnetic stimulation in patients with depression (THREE-D): a randomised non-inferiority trial. Lancet (Lond, Engl). 2018;391(10131):1683–92.
127. Chung SW, Rogasch NC, Hoy KE, Sullivan CM, Cash RFH, Fitzgerald PB. Impact of different intensities of intermittent theta burst stimulation on the cortical properties during TMS-EEG and working memory performance. Hum Brain Mapp. 2018;39(2):783–802.
128. Chung SW, Rogasch NC, Hoy KE, Fitzgerald PB. The effect of single and repeated prefrontal intermittent theta burst stimulation on cortical reactivity and working memory. Brain Stimul. 2018;11(3):566–74.
129. Hamer HM, Morris HH, Mascha EJ, Karafa MT, Bingaman WE, Bej MD, et al. Complications of invasive video-EEG monitoring with subdural grid electrodes. Neurology. 2002;58(1):97–103.
130. Lehéricy S, Duffau H, Cornu P, Capelle L, Pidoux B, Carpentier A, et al. Correspondence between functional magnetic resonance imaging somatotopy and individual brain anatomy of the central region: comparison with intraoperative stimulation in patients with brain tumors. J Neurosurg. 2000;92(4):589–98.
131. Holodny AI, Schulder M, Liu WC, Wolko J, Maldjian JA, Kalnin AJ. The effect of brain tumors on BOLD functional MR imaging activation in the adjacent motor cortex: implications for image-guided neurosurgery. AJNR Am J Neuroradiol. 2000;21(8):1415–22.

132. Takahashi S, Vajkoczy P, Picht T. Navigated transcranial magnetic stimulation for mapping the motor cortex in patients with rolandic brain tumors. Neurosurg Focus. 2013;34(4):E3.
133. Tarapore PE, Picht T, Bulubas L, Shin Y, Kulchytska N, Meyer B, et al. Safety and tolerability of navigated TMS for preoperative mapping in neurosurgical patients. Clin Neurophysiol. 2016;127(3):1895–900.
134. Tarapore PE, Picht T, Bulubas L, Shin Y, Kulchytska N, Meyer B, et al. Safety and tolerability of navigated TMS in healthy volunteers. Clin Neurophysiol. 2016;127(3):1916–8.
135. Krings T, Buchbinder BR, Butler WE, Chiappa KH, Jiang HJ, Rosen BR, et al. Stereotactic transcranial magnetic stimulation: correlation with direct electrical cortical stimulation. Neurosurgery. 1997;41(6):1319–25; discussion 1325–6.
136. Vitikainen A-M, Lioumis P, Paetau R, Salli E, Komssi S, Metsähonkala L, et al. Combined use of non-invasive techniques for improved functional localization for a selected group of epilepsy surgery candidates. NeuroImage. 2009;45(2):342–8.
137. Coburger J, Musahl C, Henkes H, Horvath-Rizea D, Bittl M, Weissbach C, et al. Comparison of navigated transcranial magnetic stimulation and functional magnetic resonance imaging for preoperative mapping in rolandic tumor surgery. Neurosurg Rev. 2013;36(1):65–76.
138. Forster M-T, Hattingen E, Senft C, Gasser T, Seifert V, Szelényi A. Navigated transcranial magnetic stimulation and functional magnetic resonance imaging: advanced adjuncts in preoperative planning for central region tumors. Neurosurgery. 2011;68(5):1317–24; discussion 1324–5.
139. Picht T, Schulz J, Hanna M, Schmidt S, Suess O, Vajkoczy P. Assessment of the influence of navigated transcranial magnetic stimulation on surgical planning for tumors in or near the motor cortex. Neurosurgery. 2012;70(5):1248–57.
140. Krieg SM, Sabih J, Bulubasova L, Obermueller T, Negwer C, Janssen I, et al. Preoperative motor mapping by navigated transcranial magnetic brain stimulation improves outcome for motor eloquent lesions. Neuro-Oncology. 2014;16(9):1274–82.
141. Frey D, Schilt S, Strack V, Zdunczyk A, Rosler J, Niraula B, et al. Navigated transcranial magnetic stimulation improves the treatment outcome in patients with brain tumors in motor eloquent locations. Neuro-Oncology. 2014;16(10):1365–72.
142. Lefaucheur J-P, Picht T. The value of preoperative functional cortical mapping using navigated TMS. Neurophysiol Clin. 2016;46(2):125–33.
143. Lioumis P, Zhdanov A, Mäkelä N, Lehtinen H, Wilenius J, Neuvonen T, et al. A novel approach for documenting naming errors induced by navigated transcranial magnetic stimulation. J Neurosci Methods. 2012;204(2):349–54.
144. Picht T, Krieg SM, Sollmann N, Rösler J, Niraula B, Neuvonen T, et al. A comparison of language mapping by preoperative navigated transcranial magnetic stimulation and direct cortical stimulation during awake surgery. Neurosurgery. 2013;72(5):808–19.
145. Tarapore PE, Findlay AM, Honma SM, Mizuiri D, Houde JF, Berger MS, et al. Language mapping with navigated repetitive TMS: proof of technique and validation. NeuroImage. 2013;82:260–72.
146. Sollmann N, Hauck T, Hapfelmeier A, Meyer B, Ringel F, Krieg SM. Intra- and interobserver variability of language mapping by navigated transcranial magnetic brain stimulation. BMC Neurosci. 2013;14(1):150.
147. Giussani C, Roux F-E, Ojemann J, Sganzerla EP, Pirillo D, Papagno C. Is preoperative functional magnetic resonance imaging reliable for language areas mapping in brain tumor surgery? Review of language functional magnetic resonance imaging and direct cortical stimulation correlation studies. Neurosurgery. 2010;66(1):113–20.
148. Yetkin FZ, Mueller WM, Morris GL, McAuliffe TL, Ulmer JL, Cox RW, et al. Functional MR activation correlated with intraoperative cortical mapping. AJNR Am J Neuroradiol. 1997;18(7):1311–5.
149. FitzGerald DB, Cosgrove GR, Ronner S, Jiang H, Buchbinder BR, Belliveau JW, et al. Location of language in the cortex: a comparison between functional MR imaging and electrocortical stimulation. AJNR Am J Neuroradiol. 1997;18(8):1529–39.
150. Ille S, Sollmann N, Hauck T, Maurer S, Tanigawa N, Obermueller T, et al. Combined noninvasive language mapping by navigated transcranial magnetic stimulation and functional MRI and its comparison with direct cortical stimulation. J Neurosurg. 2015;123(1):212–25.
151. Krieg SM, Buchmann NH, Gempt J, Shiban E, Meyer B, Ringel F. Diffusion tensor imaging fiber tracking using navigated brain stimulation—a feasibility study. Acta Neurochir. 2012;154(3):555–63.
152. Picht T, Schmidt S, Brandt S, Frey D, Hannula H, Neuvonen T, Karhu J, Vajkoczy P, Suess O. Preoperative functional mapping for rolandic brain tumor surgery: comparison of navigated transcranial magnetic stimulation to direct cortical stimulation. Neurosurgery. 2011;69(3):581–9.

Ablation: Radiofrequency, Laser, and HIFU

16

Anita P. Bhansali and Ryder P. Gwinn

Radiofrequency Ablation

History and Development

The first reported neurosurgical application of radiofrequency ablation (RFA) was in the treatment of trigeminal neuralgia in 1931; Kirschner applied the RF electrode to the gasserian ganglion in order to induce thermocoagulation and thus pain relief [1]. Fenelon used RFA in the 1950s to treat the motor symptoms in Parkinson's disease (PD), using an open procedure and lesioning the ansa lenticularis [2]. Others would go on to build on these techniques, eventually settling on lesions in the globus pallidus internus (GPi), thalamus, and the subthalamic nucleus (STN) and using pneumoencephalography to guide a catheter to the target via a burr hole in place of a craniotomy. Spiegel and Wycis would combine pneumoencephalography, an early stereotactic frame called a *stereoencephalotome*, and RFA to perform pallidotomies in a series of PD patients; they published their results in 1957 [3].

A. P. Bhansali
Department of Neurosurgery, Texas Health Harris Methodist Hospital Fort Worth, Fort Worth, TX, USA

R. P. Gwinn (✉)
Center for Neurologic Restoration, Swedish Neuroscience Institute, Swedish Medical Center, Seattle, WA, USA
e-mail: ryder.gwinn@swedish.org

Around the same time that RF lesioning was being explored for movement disorders, similar procedures were being done for behavioral and mental disorders that would go on to shape the field of epilepsy surgery. Stereotactic RF lesioning of the amygdala-hippocampal complex in aggressive patients who also had epilepsy showed a decrease in seizure frequency [4]. The rhinencephalic RFA, in which multiple RF lesions are created in the temporal lobe and its efferents, entered regular use in the 1980s [5]. In 1995, Patil combined serial RF ablations in the treatment of mesial temporal lobe epilepsy (MTLE) with CT scans after each lesion, in order to track the size and trajectory of the ablation [6]. In 1999, Parrent and Blume built on this strategy by using MRI imaging to track the ablation, and they made note that more coagulations led to more consistent tissue ablation within the target complex, which then resulted in better seizure control [7] (Fig. 16.1).

With the advent of the carbidopa-levodopa combination in the 1960s to control the symptoms of PD, neurosurgical procedures for this condition declined, although interest was renewed when the side effects of the medications, particularly the dosing-related motor fluctuations, became apparent [8]. Laitinen et al. published their results replicating Leksell's posteroventral RFA pallidotomy in Parkinson's patients in 1992 [9], done under local anesthetic so that electrical stimulation

N. Pouratian, S. A. Sheth (eds.), *Stereotactic and Functional Neurosurgery*,
https://doi.org/10.1007/978-3-030-34906-6_16

Fig. 16.1 T1-weighted axial MRI brain image 24 hours after left radiofrequency amygdalohippocampectomy. (From Parrent and Blume [7]. Reprinted with permission from John Wiley and Sons)

could be used to guide the targeting before a lesion was created. By 1997, deep brain stimulation was approved by the FDA for the treatment of PD and became the neurosurgical mainstay of treatment, given the reversibility of stimulation effects and the option for bilateral treatment without the side effects attributed to bilateral ablative procedures.

Today, RFA is used in various fields of medicine, most notably cardiology for the treatment of various arrhythmias. It is also used in the treatment of thyroid nodules, uterine fibroids, and hepatocellular carcinoma, in conjunction with other therapies [10]. Technology utilizing RF technology is still used in certain neurosurgical applications, including percutaneous rhizotomies for trigeminal neuralgia, facet rhizotomies for cervicalgia, and even intratumoral coagulation to facilitate resection of a meningioma [10], but its use in stereotactic procedures has been largely replaced by other modalities. However, as discussed below, there are still providers interested in studying RFA for various intracranial pathologies.

Mechanism of Action

Radiofrequency energy is generated by alternating current with a frequency between 10 and 900 kHz. A voltage differential is set up between the RF, or active, electrode and a reference electrode placed on the patient's body, and thermal energy is generated at the electrode-tissue interface. The active electrode is usually placed to target using a stiff guide tube to maintain a straight trajectory [11].

Biological tissue responds to thermal changes in a predictable fashion outlined by Web et al. in 2011 [10] (Fig. 16.2). Above approximately 43 °C, cell membranes are disrupted and proteins denature, leading to cell death and coagulative necrosis if the temperature is sustained for sufficient time. This necrosis happens in a time-dependent fashion with temperatures between 43 and 57 °C, after which necrosis is essentially immediate. One of the advantages of RF technology is that the system records impedance and temperature at the tip of the active RF electrodes, so that lower temperatures from 40 to 50 °C can be used to cause reversible lesions in order to assess for clinical improvement and adverse effects before permanent lesioning at temperatures above 60 °C [12]. This temperature-controlled energy delivery is in contrast to other methods of thermal energy delivery, which are performed in an MRI scanner, because there have been limitations until recently in the ability to monitor temperature or energy output. The RF electrodes are also capable of electrical stimulation as well as ablation, providing another avenue for clinical testing before treatment [12]. One study [11] reported that a string electrode with a 10 mm active tip and extension up to 8 mm laterally from the guide tube was heated to 75 °C and held for 60 seconds, resulting in lesions about 20 mm in diameter on the immediate post-procedure MRI and about 10 mm on the 1-year scan.

Application of RF energy to biological tissue results in defined borders without vaporization, burning, or adherence of the electrodes to the target tissue. If heating within the coagulate exceeds 2–3 minutes, a carbon layer will form around the electrode tip and inhibit thermal energy from reaching and coagulating tissue outside the target

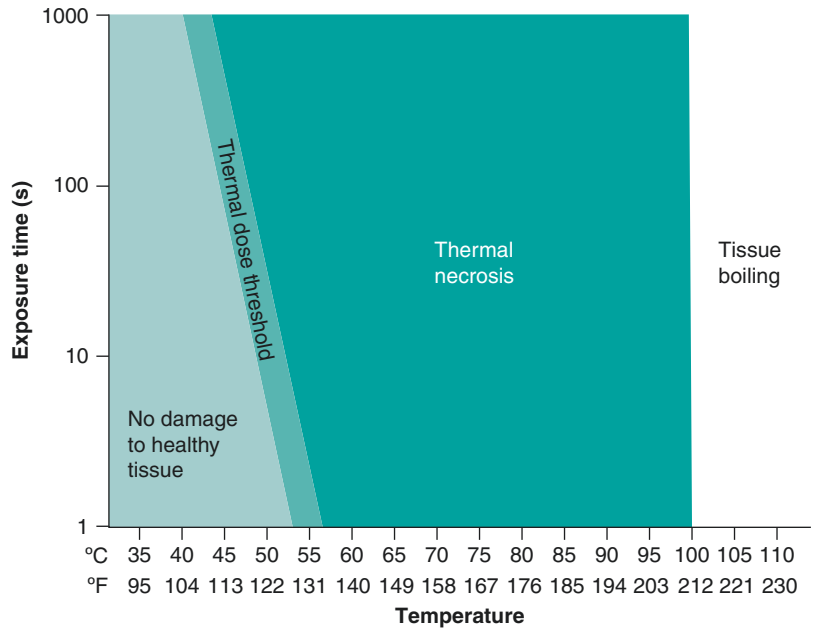

Fig. 16.2 The threshold for thermal necrosis depends on temperature reached in the tissue. As the temperature increases, the exposure time needed to achieve thermal necrosis decreases exponentially. Above 57 °C, thermal necrosis occurs in ≤1 second. Tissue boils above the threshold of 100 °C regardless of the exposure time [10]. (From Foley et al. [55]. Reprinted with permission from Focused Ultrasound Foundation)

area. The RF lesions are generally spherical in shape, but this is subject to some environmental factors, including convective heat loss by nearby heat reservoirs such as CSF spaces or sufficiently large blood vessels [12].

Disadvantages of the system include the necessity to create a cranial defect, inability to control for the heterogeneity of certain brain areas, and inability to control rates of heat absorption and dispersion. While there is a rough correlation between temperature achieved and the volume of coagulated tissue, it is insufficiently precise to predict the exact size and shape of lesions. A specific example is the gray-white junction, which can have unpredictable responses to RFA. In addition, if the target structure is irregularly shaped or larger than 30 mm in diameter, treatment can require repeat ablations and/or repositioning of the electrode, leading to further uncertainty about the lesion created [13].

Clinical Applications and Future Areas of Interest

As noted above, RF technology has been replaced by various techniques in the neurosurgical arsenal in the treatment of functional disorders, particularly in this country. However, there are neurosurgeons outside the USA who continue to explore uses of RFA in conjunction with intracranial stereotaxis.

Combining stereo-EEG (sEEG) with RFA, also called sEEG-guided RF thermocoagulation, has been in use since 2001. Catenoix et al. performed a literature review [14] involving 251 patients treated with this method from 2004 to 2013. While they noted that outcomes overall where not as effective at seizure control as open surgery, it did provide a minimally invasive option with distinct advantages over the original stereotactic RFA procedure for treating epilepsy, namely, having sEEG data to guide lesioning and having multiple sEEG leads and trajectories to use. The group noted that patients with seizure onset zones near eloquent cortical tissue or that are otherwise difficult to access, i.e., nodular heterotopias or focal cortical dysplasia, had an improved risk-to-benefit ratio with this method over conventional methods, and RFA does not preclude further surgery. Voges et al. also published a case report of a patient with nodular heterotopias who was treated with RF thermoablation with a bipolar

electrode of a single seizure onset zone identified by an earlier sEEG monitoring stay; the outcome at the 7-year follow-up was Engel 1B without neuropsychological deficits [12].

A group from the Czech Republic performed selective amygdalohippocampectomy by RFA on 51 patients with mesial temporal lobe epilepsy, some in combination with invasive monitoring with sEEG and others without. Using a Leksell frame, stereotactic planning software, and an occipital approach, they performed thermocoagulation of the amygdalohippocampal complex. Follow-up at 2 years included 32 patients, with 78% achieving Engel class I seizure control and no permanent complications are reported [11]. A follow-up study that looked at 5-year neuropsychological outcomes noted that, like multiple subpial transections, this modality preferentially targeted the longitudinal fibers responsible for seizure spread while reducing the injury-related access to these deep structures via conventional open methods, similar to laser ablation [15].

Hypothalamic hamartomas (HH) are a relatively rare congenital condition that can cause epilepsy – specifically gelastic seizures – as well as endocrinologic and developmental issues. They are a difficult surgical pathology to treat, because of their location and common comorbidities related to open procedures. Minimally invasive stereotactic methods are an option, including radiosurgery, laser interstitial thermal therapy (LITT), and RFA. Homma et al. published results from a 100-patient cohort in 2016 [16], citing a 71% seizure freedom rate at an average of 3 years; however, a follow-up study acknowledged that about 1/3 of these require a second RFA [17]. Because the MR thermography necessary to perform LITT is not widely available, and the laser fiber is disposable and requires financial resources to obtain, RFA for treating hypothalamic hamartomas has been reported recently in several countries outside the USA. One group used robotic guidance to place the RF electrode in five patients and perform an ablative disconnection, resulting in four patients with ILAE class I seizure control and no permanent complications [18]. A second group, citing the potential for mistreatment when relying on radiological abnormality without electrophysiological confirmation of seizure onset, used sEEG-guided RFA to treat nine patients; five patients achieved Engel class I, four patients achieved Engel class II, and one patient developed significant weight gain after surgery [19].

In one of the rarer applications of RFA reported in the literature, DBS electrodes have been used to deliver RF energy to the target area in cases where patients have required removal of the system due to hardware erosion and risk of infection [20]. Two patients with PD underwent RF lesioning based on intraoperative clinical testing to confirm the most effective lead electrodes for symptom control and creating a bipolar lesion between these, before having the system explanted. One patient had the system reimplanted after completing a course of antibiotics, and his team noted his medication requirements and stimulation parameters were lower after the combination of RF lesioning and reimplantation; the other patient declined reimplantation because his results after RF lesioning were good enough.

Laser Interstitial Thermal Therapy

History and Development

The concept of thermal energy generated by laser electromagnetic radiation had been postulated and discussed by the late 1970s; Bown published one of the first papers on the clinical use of this modality in superficial tumors in human patients, as well as data from in vitro and animal models [21]. He broached the subject of laser thermal therapy in the treatment of deeper lesions throughout the body, as well as methods of making this therapy safer and more selective for neoplastic cells.

By 1986, two advances in the burgeoning field of LITT came about: compact laser tips that resisted damage from the high power density at the end of the laser fibers and MRI sequences that allowed almost real-time monitoring of the heat effect in brain and tumor tissue. Ascher and the group in Austria published a case series in 1991 on the use of “interstitial thermotherapy

(ITT)" on patients with centrally located brain tumors [22]. He combined this technology with the use of stereotactic placement to minimize damage to surrounding and overlying structures, and he used local anesthetic to allow assessment of the patient's neurological status throughout the procedure.

While a number of diagnostic methods were tested to allow real-time radiographic monitoring of the thermal ablation, including ultrasound, thermometers, and subcutaneous thermocouple probes, MR thermography was a modality that provided excellent soft tissue resolution without significant artifact from or damage to the fiber-optic laser source [23]. By the mid-1990s, the proton resonance frequency method [24] of MRI sequencing had been developed, which would serve as the predecessor to MR thermography sequences in their current form.

Fig. 16.3 Applicator with diffusing tip. The diode laser fiber is stereotactically inserted into the target tissue using a MRI-compatible applicator with diffusing tip. This creates an ellipsoid distribution of the laser energy across the distal 1 cm tip of the catheter. (Image courtesy of Visualase/Medtronic)

Mechanism of Action

There are two LITT systems that have been in clinical use: the NeuroBlate System from Monteris Medical, Inc., and the Visualase Thermal Therapy System from Medtronic Inc. NeuroBlate uses a 12-W continuous wave neodymium-doped yttrium garnet laser operating at wavelength 1064 nm. Visualase employs a 15-W 980-nm diode laser that has the benefit a local peak in water absorption. This leads to a sharper boundary between ablated tissue and nontarget tissue, as well as shorter depth of penetration that prevents damaging areas outside the region to be treated. The laser fiber has a diffusing tip that creates an ellipsoid area of light distribution into the tissue along the axis of the fiber [25] (Fig. 16.3). A cooling catheter that circulates water to cool the laser fiber tip and prevent carbonization of tissue is a critical safety feature of the system. The MR thermography protocols calculate estimated damage zones approximately every 10 seconds [26].

The effects of thermal energy thus generated are dependent on wavelength, power density, exposure duration, and surface vs interstitial delivery [27]. There are five types of laser-tissue interaction that have been identified [23], and neurosurgical applications rely on photothermal interactions in which light emitted from the laser source is absorbed by the target molecule and then released into the environment to increase the temperature. The heat is then redistributed via convection and conduction into nearby tissue, causing temporary or irreversible damage. Other interactions include photochemical, photoablative, photoplasmic, and photodisruptive effects, but these generally appear at power ranges and frequencies outside of those used for intracerebral lesioning.

An important feature of LITT is the ability to direct thermal energy toward the ablation of pathological tissue while sparing neighboring healthy brain parenchyma. There are three zones of radiographic and histologic change in the area of the laser fiber [28]. The area near the tip of the fiber sees the highest power delivery and thus the greatest temperature increase and tissue destruction. Below 42 °C, thermal energy will lead to local increases in blood flow due to vasodilation; from 42 to 60 °C, protein denaturation and permanent cell damage occurs. At 60 °C, the plasma membrane will be disrupted immediately and the cell will die; if held for 10 minutes at this temperature, coagulation necrosis will occur [25]. Above 100 °C, carbonization and vaporization can occur, the former of which can prevent

penetration of the thermal energy to other target areas, the latter of which can lead to increased ICP. For this reason, the software has a safety shutoff at 90 °C to prevent these processes from taking place, and lower temperature shutoff levels can be set to protect nearby sensitive tissue. The next closest region from the tip also develops tissue necrosis as well as interstitial edema. The marginal zone is the furthest from the fiber tip and features tissue that is damaged, but reversibly [28]. Accounting for large blood vessels and CSF spaces, which act as heat sinks, the laser fiber is able to generate a 2–4 cm circumferential ablation [26]; the lesion can be further elongated by serial withdrawals of the laser fiber with repeated ablations.

Clinical Applications and Future Areas of Interest

While the majority of preliminary research on LITT was for oncologic applications, including intracranial metastases [29], deep-seated recurrent gliomas [30], and treatment of radiation necrosis [31], it has become a mainstay of interventional treatment for epilepsy. The MR-guided stereotactic laser amygdalohippocampectomy is an accepted surgical procedure for the treatment of mesial temporal lobe epilepsy, with a possible advantage of reduced postoperative neuropsychological deficits compared to conventional temporal lobectomy [32] but a concomitant lower rate of seizure freedom. Another application within the epilepsy population is the treatment of hypothalamic hamartomas in pediatric [33] as well as adult populations [26]; they note fewer surgical complications, shorter hospital stays, and the potential for future treatment with repeat LITT or open procedures to complete the disconnection of the hamartoma from the hypothalamus. The largest study to date reported that 14 patients with HH were treated with LITT and 12 were seizure-free at 9 months with no permanent deficits [34], and these results are echoed by other case series. Corpus callosotomy [35], ablation of cavernous malformations [36], and adjunctive ablation of the deeper extensions of a focal cortical dysplasia prior to open resection [37] have been performed with LITT with good early results.

High-Intensity Focused Ultrasound

History and Development

Ultrasound (US) arose out of the study of acoustics in the late nineteenth century, when Pierre and Jacques Curie discovered that the application of high-pressure sound waves could generate electricity when directed toward quartz crystals, a phenomenon known as *piezoelectricity* [38]. The reverse was also true: applying an electrical charge to quartz crystals could generate sound waves. Ultrasonic waves are those with frequencies >20 kHz, above the audible range of human hearing, and their first use as a therapeutic modality in humans was reported in 1960: Meyers and Fry used it to perform pallidotomies and thalamotomies in 48 Parkinson's patients [39]. Because US waves could not penetrate the skull without causing thermal injury to the scalp, the surgeons had to perform craniotomies in order to direct the US waves through the dura and to the target. While the procedure achieved clinical improvement in a number of the patients, the required craniotomy made US lesioning more invasive, and thus less attractive, than other techniques available at the time.

The next advance in the development of therapeutic ultrasound was obviating the need for craniotomy. There were two issues to circumvent: heating of the skull and sufficient energy reaching the target after penetrating the bone. Reducing the frequency of the US waves and using a circulating water bath solved the first issue [40]. Phased array technology, which compensates for US waves that are out of phase because of skull density heterogeneity, was the second innovation that allowed transcranial US treatment [41].

Magnetic resonance (MR) thermometry was the final piece that brought neurosurgical HIFU to its present state. While other organ systems treated with HIFU can be monitored with diagnostic US, the skull prevents real-time monitor-

ing of intracranial tissue with US. MR thermometry sequences allow for visualization of the target areas, surrounding issue, and calculation of the thermal dose delivered, which is dependent on individual skull anatomy and the energy delivered per sonication [42]. By the early 2000s, Jolesz and his group at Brigham and Women's had applied this modern incarnation of HIFU to three patients with inoperable brain tumors [43]. It would take several more years for a transducer powerful enough to reach the temperatures needed for ablation.

Mechanism of Action

The generation of ultrasound waves for clinical use starts with the application of voltage to a piezoelectric (PE) element, which expands and contracts in response, in turn creating the mechanical vibrations that transmit pressure and energy through a given medium. The range of frequencies that most PE transducers operate is 200 kHz to 4 MHz, and modern devices have multiple, i.e., hundreds, of PE sources that can generate ultrasonic waves that are directed in phase to the target after passing through skin and, more significantly, the dense bone of the skull [44]. An early study of US to generate cerebral lesions found that frequencies lower than 835 kHz were less likely to have unfavorable interactions with the skull that generate scalp heating and would deliver energy to the target more efficiently [45].

As noted above, the skull presents a technical challenge for most forms of intracranial treatment, particularly "minimally invasive," non-incisional methods. In the case of US, the skull tends to absorb and reflect US waves before they can reach their target. In doing so, it generates heat in the bone and surrounding skin, which requires active cooling in the form of a circulating water bath [46]. Heterogeneity in the skull itself can also cause the US waves from the individual PE transducers to arrive out of phase such that the energy is not delivered effectively to cause a lesion. In order to account for the variables introduced by individual skull anatomy, a non-contrast head CT is obtained prior to treatment in order to calculate the skull density ratio (SDR) [47]. This value is a global average of the ratio of cancellous to cortical bone Hounsfield units, with a range between 0 and 1. The values of SDR that permit effective lesion are generally >0.4. This pre-procedural imaging also allows identification of frontal air sinuses and other sources of intracranial calcification that can serve to divert or absorb the US waves if not taken into account [48].

Thermal energy is the end result of HIFU therapy, as is the case with the other ablative therapies discussed above. However, there are characteristics unique to this form of energy delivery that provide a more favorable safety profile: namely, performing clinical testing and generating reversible neurological changes to confirm clinical benefit before committing to an irreversible lesion.

The threshold for permanent tissue damage is 56 °C for 1 second [49]. Below this temperature, there is a range of values that permit reversible injury, so that clinical monitoring and repositioning of the target can take place before permanent lesioning occurs. Thus, treatment proceeds in a series of sonications: the first set is done in the 1500–3000 J range, with the goal of reaching 41–46 °C in order to observe changes on MR thermometry scans done roughly every 3 seconds [28] and reposition the coordinates as needed. The next set, with a goal temperature range of 42–50 °C, is done with clinical testing to assess improvement of tremor as well as to observe adverse effects. The final set, once the target has shown clinical benefit without side effects, aims for a range of 50–60 °C to achieve the final lesion at target.

In addition to thermal energy, HIFU also generates mechanical forces in the form of *cavitation*. The US waves cause microbubbles to form that then oscillate; these can then create shock waves with high pressure and shear forces on the target tissue. Modern HIFU systems use transducers with cavitation-detection abilities, which will hold sonications until the cavitation has stopped. Other techniques to reduce the likelihood of cavitation are close-shaving of the head, using degassed water, and ensuring a close fit of

the silicone membrane to the scalp without folds or bubbles in its surface [48]. While cavitation is generally to be avoided during HIFU treatment, there are certain clinical situations, i.e., opening the BBB in tumor treatment (discussed below), that may be able to exploit it in a controlled fashion.

The system approved for use in the USA is the ExAblate 4000 from InSightec Inc., which has a 1024-source phased array transducer which functions at 650 kHz. A 3.0 T MRI is most commonly used in combination for thermographic monitoring, although there are studies [50] that have used 1.5 T magnets (Fig. 16.4).

Clinical Applications and Future Areas of Interest

The only FDA-approved neurosurgical indication for HIFU currently is unilateral ablation of the Vim nucleus for the treatment of essential tremor and tremor-predominant Parkinson's disease. The procedure is done entirely in the MRI suite with the patient awake. Sonications are directed at the Vim contralateral to the side of the body being treated and done in sequential fashion as described above to confirm anatomic location, clinical benefit, and absence of adverse effects before permanent lesioning.

There are several phase I and II studies underway for the use of HIFU in the treatment of rigidity associated with Parkinson's disease. Europe and Israel have already fully approved use of this technology for Parkinson's disease, with both thalamic nuclei and pallidothalamic tracts as targets. Other diseases under consideration include pain, major depression, obsessive compulsive disorder, epilepsy, and breakdown of the blood-brain barrier for the treatment of Alzheimer's disease.

While HIFU has been applied to intracranial tumors in the 2000s [43, 51], sufficiently high temperatures for ablation could not be reached with the technology available at the time without damaging surrounding normal brain parenchyma. With the upgrades available in recent years, several reports have revisited HIFU treatment of tumors. Of particular interest, the controlled use of cavitation by injecting preformed bubbles intravascularly before sonication at the target may induce vessels near by the target tumor to open the BBB without requiring high-power US waves or induction of shock waves [52]. This could be used in the delivery of chemotherapeutic agents that would otherwise be blocked from reaching the abnormal cells, as demonstrated in several animal studies [40].

A unique application of US-generated thermal energy that is being studied is the treatment of ischemic and hemorrhagic strokes. Feasibility studies in animals have shown that HIFU can enhance intravascular thrombolysis when used as an adjunct to t-PA [53]. Cadaveric studies of

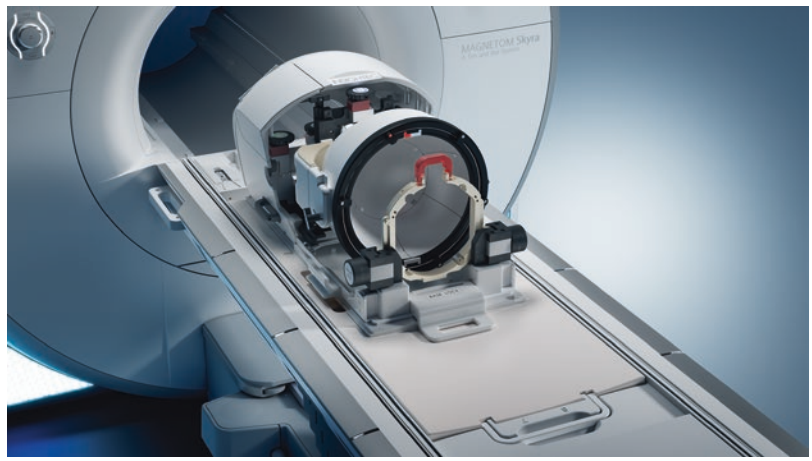

Fig. 16.4 ExAblate 4000 transcranial focused ultrasound system. (ExAblate 4000, InSightec). Patient is fixed to the table by a stereotaxic frame and a membrane holds water between the patient's head and the transducer. This transducer can be moved independently to target brain regions. (Image courtesy of INSIGHTEC)

intraparenchymal hemorrhage have shown enhanced clot liquefaction with HIFU delivery, allowing for needle aspiration [54]. While still in the earliest stages of research, HIFU may prove to be an effective modality for treating the large number of patients who suffer from cerebrovascular pathologies.

Conclusion

There is a rich history of creating and refining new technologies for clinical use in neurosurgery. Each of the three modalities discussed – RFA, LITT, and HIFU – ultimately generates a lesion in brain tissue, but the iterative trajectory that each method followed to reach clinical application was unique and reliant on collaborative interactions between many imaginative scientists and clinicians. Certain quantum leaps in energy delivery, imaging, and monitoring were necessary for these techniques to become clinically meaningful. In the same way, as we explore new intracranial applications for ablative therapies, the advent of new technologies will surely increase our understanding of these modalities and allow us to more fully utilize them in the treatment of neurosurgical diseases.

References

1. Kirschner M. Elektrocoagulation des ganglion gasseri. Zentralbl Chir. 1932;(47):2841–3.
2. Guridi J, Lozano AM. A brief history of pallidotomy. Neurosurgery. 1997;41(5):1169–80; discussion 80–3.
3. Spiegel EA, Wycis HT. Ansotomy in paralysis agitans. AMA Arch Neurol Psychiatry. 1954;71(5):598–614.
4. Narabayashi H, Nagao T, Saito Y, Yoshida M, Nagahata M. Stereotaxic amygdalotomy for behavior disorders. Arch Neurol. 1963;9:1–16.
5. Marossero F, Ravagnati L, Sironi VA, Miserocchi G, Franzini A, Ettorre G, et al. Late results of stereotactic radiofrequency lesions in epilepsy. Acta Neurochir Suppl. 1980;30:145–9.
6. Patil AA, Andrews R, Torkelson R. Stereotactic volumetric radiofrequency lesioning of intracranial structures for control of intractable seizures. Stereotact Funct Neurosurg. 1995;64(3):123–33.
7. Parrent AG, Blume WT. Stereotactic amygdalohippocampotomy for the treatment of medial temporal lobe epilepsy. Epilepsia. 1999;40(10):1408–16.
8. Lozano CS, Tam J, Lozano AM. The changing landscape of surgery for Parkinson's disease. Mov Disord. 2018;33(1):36–47.
9. Laitinen LV, Bergenheim AT, Hariz MI. Leksell's posteroventral pallidotomy in the treatment of Parkinson's disease. J Neurosurg. 1992;76(1):53–61.
10. Webb H, Lubner MG, Hinshaw JL. Thermal ablation. Semin Roentgenol. 2011;46:133–41.
11. Liscak R, Malikova H, Kalina M, Vojtech Z, Prochazka T, Marusic P, et al. Stereotactic radiofrequency amygdalohippocampectomy in the treatment of mesial temporal lobe epilepsy. Acta Neurochir. 2010;152(8):1291–8.
12. Voges J, Buntjen L, Schmitt FC. Radiofrequency-thermoablation: general principle, historical overview and modern applications for epilepsy. Epilepsy Res. 2018;142:113–6.
13. Hirabayashi H, Hariz MI, Wardell K, Blomstedt P. Impact of parameters of radiofrequency coagulation on volume of stereotactic lesion in pallidotomy and thalamotomy. Stereotact Funct Neurosurg. 2012;90(5):307–15.
14. Catenoix H, Bourdillon P, Guenot M, Isnard J. The combination of stereo-EEG and radiofrequency ablation. Epilepsy Res. 2018;142:117–20.
15. Kramska L, Vojtech Z, Lukavsky J, Stara M, Malikova H. Five-year neuropsychological outcome after stereotactic radiofrequency amygdalohippocampectomy for mesial temporal lobe epilepsy: longitudinal study. Stereotact Funct Neurosurg. 2017;95(3):149–57.
16. Homma J, Kameyama S, Masuda H, Ueno T, Fujimoto A, Oishi M, et al. Stereotactic radiofrequency thermocoagulation for hypothalamic hamartoma with intractable gelastic seizures. Epilepsy Res. 2007;76(1):15–21.
17. Kameyama S, Shirozu H, Masuda H, Ito Y, Sonoda M, Akazawa K. MRI-guided stereotactic radiofrequency thermocoagulation for 100 hypothalamic hamartomas. J Neurosurg. 2016;124(5):1503–12.
18. Tandon V, Chandra PS, Doddamani RS, Subianto H, Bajaj J, Garg A, et al. Stereotactic radiofrequency thermocoagulation of hypothalamic hamartoma using robotic guidance (ROSA) coregistered with O-arm guidance-preliminary technical note. World Neurosurg. 2018;112:267–74.
19. Wei PH, An Y, Fan XT, Wang YH, Yang YF, Ren LK, et al. Stereoelectroencephalography-guided radiofrequency thermocoagulation for hypothalamic hamartomas: preliminary evidence. World Neurosurg. 2018;114:e1073–e8.
20. Perez-Suarez J, Torres Diaz CV, Lopez Manzanares L, Navas Garcia M, Pastor J, Barrio Fernandez P, et al. Radiofrequency lesions through deep brain stimulation electrodes in movement disorders: case report and review of the literature. Stereotact Funct Neurosurg. 2017;95(3):137–41.
21. Bown SG. Phototherapy in tumors. World J Surg. 1983;7(6):700–9.
22. Ascher PW, Justich E, Schrottner O. A new surgical but less invasive treatment of central brain

tumours preliminary report. Acta Neurochir Suppl. 1991;52:78–80.
23. Stafford RJ, Fuentes D, Elliott AA, Weinberg JS, Ahrar K. Laser-induced thermal therapy for tumor ablation. Crit Rev Biomed Eng. 2010;38(1):79–100.
24. De Poorter J. Noninvasive MRI thermometry with the proton resonance frequency method: study of susceptibility effects. Magn Reson Med. 1995;34(3):359–67.
25. Kang JY, Sperling MR. Magnetic resonance imaging-guided laser interstitial thermal therapy for treatment of drug-resistant epilepsy. Neurotherapeutics. 2017;14(1):176–81.
26. Du VX, Gandhi SV, Rekate HL, Mehta AD. Laser interstitial thermal therapy: a first line treatment for seizures due to hypothalamic hamartoma? Epilepsia. 2017;58(Suppl 2):77–84.
27. Missios S, Bekelis K, Barnett GH. Renaissance of laser interstitial thermal ablation. Neurosurg Focus. 2015;38(3):E13.
28. Norred SE, Johnson JA. Magnetic resonance-guided laser induced thermal therapy for glioblastoma multiforme: a review. Biomed Res Int. 2014;2014:761312.
29. Carpentier A, McNichols RJ, Stafford RJ, Itzcovitz J, Guichard JP, Reizine D, et al. Real-time magnetic resonance-guided laser thermal therapy for focal metastatic brain tumors. Neurosurgery. 2008;63(1 Suppl 1):ONS21–8; discussion ONS8–9.
30. Schwarzmaier HJ, Eickmeyer F, von Tempelhoff W, Fiedler VU, Niehoff H, Ulrich SD, et al. MR-guided laser-induced interstitial thermotherapy of recurrent glioblastoma multiforme: preliminary results in 16 patients. Eur J Radiol. 2006;59(2):208–15.
31. Rahmathulla G, Recinos PF, Kamian K, Mohammadi AM, Ahluwalia MS, Barnett GH. MRI-guided laser interstitial thermal therapy in neuro-oncology: a review of its current clinical applications. Oncology. 2014;87(2):67–82.
32. Bezchlibnyk YB, Willie JT, Gross RE. A neurosurgeon's view: laser interstitial thermal therapy of mesial temporal lobe structures. Epilepsy Res. 2018;142:135–9.
33. Southwell DG, Birk HS, Larson PS, Starr PA, Sugrue LP, Auguste KI. Laser ablative therapy of sessile hypothalamic hamartomas in children using interventional MRI: report of 5 cases. J Neurosurg Pediatr. 2018;21(5):460–5.
34. Wilfong AA, Curry DJ. Hypothalamic hamartomas: optimal approach to clinical evaluation and diagnosis. Epilepsia. 2013;54(Suppl 9):109–14.
35. Ho AL, Miller KJ, Cartmell S, Inoyama K, Fisher RS, Halpern CH. Stereotactic laser ablation of the splenium for intractable epilepsy. Epilepsy Behav Case Rep. 2016;5:23–6.
36. Drane DL, Loring DW, Voets NL, Price M, Ojemann JG, Willie JT, et al. Better object recognition and naming outcome with MRI-guided stereotactic laser amygdalohippocampotomy for temporal lobe epilepsy. Epilepsia. 2015;56(1):101–13.
37. Ellis JA, Mejia Munne JC, Wang SH, McBrian DK, Akman CI, Feldstein NA, et al. Staged laser interstitial thermal therapy and topectomy for complete obliteration of complex focal cortical dysplasias. J Clin Neurosci. 2016;31:224–8.
38. Curie PJ, Curie J. Crystal physics: development by pressure of polar electricity in hemihedral crystals with inclined faces. C R Hebd Seances Acad Sci. 1880;91(291).
39. Fry WJ, Fry FJ. Fundamental neurological research and human neurosurgery using intense ultrasound. IRE Trans Med Electron. 1960;Me-7:166–81.
40. Harary M, Segar DJ, Huang KT, Tafel IJ, Valdes PA, Cosgrove GR. Focused ultrasound in neurosurgery: a historical perspective. Neurosurg Focus. 2018;44(2):E2.
41. Hynynen K, Jolesz FA. Demonstration of potential noninvasive ultrasound brain therapy through an intact skull. Ultrasound Med Biol. 1998;24(2):275–83.
42. Damianou C, Hynynen K. The effect of various physical parameters on the size and shape of necrosed tissue volume during ultrasound surgery. J Acoust Soc Am. 1994;95(3):1641–9.
43. McDannold N, Clement GT, Black P, Jolesz F, Hynynen K. Transcranial magnetic resonance imaging- guided focused ultrasound surgery of brain tumors: initial findings in 3 patients. Neurosurgery. 2010;66(2):323–32; discussion 32.
44. Tempany CM, McDannold NJ, Hynynen K, Jolesz FA. Focused ultrasound surgery in oncology: overview and principles. Radiology. 2011;259(1):39–56.
45. Lynn JG, Zwemer RL, Chick AJ, Miller AE. A new method for the generation and use of focused ultrasound in experimental biology. J Gen Physiol. 1942;26(2):179–93.
46. Mohammed N, Patra D, Nanda A. A meta-analysis of outcomes and complications of magnetic resonance-guided focused ultrasound in the treatment of essential tremor. Neurosurg Focus. 2018;44(2):E4.
47. Chang WS, Jung HH, Zadicario E, Rachmilevitch I, Tlusty T, Vitek S, et al. Factors associated with successful magnetic resonance-guided focused ultrasound treatment: efficiency of acoustic energy delivery through the skull. J Neurosurg. 2016;124(2):411–6.
48. Wang TR, Bond AE, Dallapiazza RF, Blanke A, Tilden D, Huerta TE, et al. Transcranial magnetic resonance imaging-guided focused ultrasound thalamotomy for tremor: technical note. Neurosurg Focus. 2018;44(2):E3.
49. Zaaroor M, Sinai A, Goldsher D, Eran A, Nassar M, Schlesinger I. Magnetic resonance-guided focused ultrasound thalamotomy for tremor: a report of 30 Parkinson's disease and essential tremor cases. J Neurosurg. 2018;128(1):202–10.
50. Iacopino DG, Gagliardo C, Giugno A, Giammalva GR, Napoli A, Maugeri R, et al. Preliminary experience with a transcranial magnetic resonance-guided focused ultrasound surgery system integrated with a 1.5-T MRI unit in a series of patients with essential tremor and Parkinson's disease. Neurosurg Focus. 2018;44(2):E7.

51. Ram Z, Cohen ZR, Harnof S, Tal S, Faibel M, Nass D, et al. Magnetic resonance imaging-guided, high-intensity focused ultrasound for brain tumor therapy. Neurosurgery. 2006;59(5):949–55; discussion 55–6.
52. Hynynen K, McDannold N, Vykhodtseva N, Jolesz FA. Noninvasive MR imaging-guided focal opening of the blood-brain barrier in rabbits. Radiology. 2001;220(3):640–6.
53. Tsivgoulis G, Eggers J, Ribo M, Perren F, Saqqur M, Rubiera M, et al. Safety and efficacy of ultrasound-enhanced thrombolysis: a comprehensive review and meta-analysis of randomized and nonrandomized studies. Stroke. 2010;41(2):280–7.
54. Monteith SJ, Kassell NF, Goren O, Harnof S. Transcranial MR-guided focused ultrasound sonothrombolysis in the treatment of intracerebral hemorrhage. Neurosurg Focus. 2013;34(5):E14.
55. Foley JL, Eames M, Snell J, Hananel A, Kassell N, Aubry JF. Image-guided focused ultrasound: state of the technology and the challenges that lie ahead. Imaging Med. 2013;5(4):357–70.

Radiosurgery

17

Daniel M. Trifiletti, Eric J. Lehrer, and Jason P. Sheehan

Abbreviations

^{60}Co	Cobalt-60
AVM	Arteriovenous malformation
BRW	Brown-Roberts-Wells
CT	Computerized tomography
CTV	Clinical target volume
DNA	Deoxyribonucleic acid
DPL	Dynamically penalized maximum likelihood
FSE	Fast spin echo
GTV	Gross target volume
Gy	Gray
IMRS	Intensity-modulated radiosurgery
LINAC	Linear accelerator
MLCs	Multileaf collimators
MR	Magnetic resonance
MRI	Magnetic resonance imaging
PTC	Planned target volume
SRS	Stereotactic radiosurgery
US	United States
VP	Ventriculoperitoneal

D. M. Trifiletti
Department of Radiation Oncology, Mayo Clinic, Jacksonville, FL, USA

E. J. Lehrer
Department of Radiation Oncology, Icahn School of Medicine at Mount Sinai, New York, NY, USA

J. P. Sheehan (✉)
Department of Neurological Surgery, University of Virginia, Charlottesville, VA, USA
e-mail: jps2f@hscmail.mcc.virginia.edu

The History of Radiosurgery

Lars Leksell first devised the concept of radiosurgery in 1951 [1]. The initial concept involved using an orthovoltage x-ray tube to focus radiation on the trigeminal ganglion for the treatment of facial pain. He then investigated the different sources of radiation: cross-fired protons, x-rays from an early-generation linear accelerator (LINAC), and ultrasound for radiosurgery. Finally, Leksell and Larsson chose Cobalt-60 (^{60}Co) as the ideal photon radiation source, because of the cost of photon beams, poor skull penetration of ultrasound, and imprecision of LINACs in 1960s. Therefore, the Gamma Knife (Elekta AB, Stockholm), which consisted of 179 ^{60}Co sources in a hemispherical array, was born at the Queen Sofia Hospital in Stockholm in 1968.

In parallel with these developments, clinicians at the University of California, Berkeley, implemented a cyclotron in 1954, and the other stereotactic treatments were performed with particle accelerators built for physics research at Uppsala in Sweden in 1957. While charged particles have been used for radiation therapy and radiosurgery for more than 50 years, the vast majority of radiosurgery is currently performed with Gamma Knife® and LINAC-based radiosurgery platforms because particle accelerators such as cyclotron or synchrotrons have significantly higher cost, require more space, and are significantly more complex than photon-based radiosurgery.

N. Pouratian, S. A. Sheth (eds.), *Stereotactic and Functional Neurosurgery*,
https://doi.org/10.1007/978-3-030-34906-6_17

However, proton radiosurgery offers a theoretical improvement in dose uniformity within large targeted volumes and reduced doses to normal tissues when compared with its photon counterparts due to the presence of a sharp Bragg peak. These unique physical properties of protons have stimulated a great deal of interest and continue to motivate the construction and development of large proton therapy centers. Presently, the majority of proton therapy applications are in treating extracranial malignancies over a prolonged radiotherapy course (e.g., prostate cancer).

The diligence of a multitude of pioneers facilitated advancements in intracranial radiosurgery. Ladislau Steiner, Georg Noren, Christer Lindquist, and other contemporaries of Leksell diligently explored specific indications for Gamma Knife radiosurgery. Federico Colombo in Italy and Osvaldo Betti in Buenos Aires both used modified LINACs to recreate the principle of the Gamma Knife. Jacob Fabrikant and Raymond Kjellberg in the United States (US) utilized the Bragg peak of protons in the delivery of radiosurgery. The efforts of all of these individuals have expanded the principles of non-invasive intracranial surgery.

In 1987, L. Dade Lunsford at the University of Pittsburgh acquired the first dedicated clinical Gamma Knife in the US. In 1989, the Gamma Knife was installed at the University of Virginia. In short order, several radiosurgery platforms were installed in the US, South America, and Asia. As of 2016, more than 300 Gamma Knife machines and more than one million patients have been treated with Gamma Knife radiosurgery, of which 44% for malignant tumors, 36% for benign tumors, 12% with vascular lesions, and 7% with functional disorders [2]. Many hundreds of thousands of additional patients have been treated with Cyberknife (Accuray, Sunnyvale, CA), LINAC, and charged particle systems; furthermore, there has been a recent increased trend in utilization of LINAC-based radiosurgery [3].

In the past 50 years, there have been dramatic advances in radiosurgery techniques. Presently, radiosurgery has played a critical role in various neurosurgical diseases, and radiosurgery keeps advancing its capabilities with more accurate radiation delivery, more convenient radiosurgical planning software, and multiple choices of immobilization tools.

Types of Ionizing Radiation

The term “ionizing radiation” refers to radiation of sufficiently high enough energy to dislodge electrons from atoms or disrupt chemical bonds between atoms and molecules. Two radiation sources are utilized in radiosurgery – artificially generated radiation from man-made machines and spontaneously generated radiation from radionuclides. Two basic forms of radiation are produced from the aforementioned sources, which can include electromagnetic radiation and particle radiation.

Electromagnetic Radiation

Electromagnetic radiation carries energy via oscillating magnetic and electric properties. The electromagnetic spectrum spans a range from radio waves, to infrared waves, through the visible light spectrum, to high-energy x-rays and gamma rays. Radiotherapy and radiosurgery most commonly utilizes high-energy x-rays and gamma rays. These rays exhibit a dual nature; they can be described as waves or as energy packets known as photons.

Another difference between x-rays and gamma rays is their manner of production. X-rays are produced either as a result of the interaction between a high-speed electron and a nucleus (Bremsstrahlung x-rays) or when electrons in the outer shell of an ionized atom fall from a high to a low energy level to fill a vacancy created by an ejected electron (characteristic x-rays). X-rays may either be the product of radioactivity or created by human intervention. For example, linear accelerators generate x-rays through the acceleration of electrons and directing them to strike a target comprised of a substance with a high atomic number. The interactions between the electrons and target nuclei generate primarily Bremsstrahlung and secondarily characteristic x-rays.

In contrast, gamma rays are photons from the nucleus of a radioactive atom when it undergoes decay and emits a photon, for instance, Cobalt-60, which is the source of gamma rays utilized in the Gamma Knife. High-energy photons are indirectly ionizing; therefore, when interacting with tissue, photons cause the liberation of charged particles (electrons) which then proceed to cause the majority of the ionization and, thus, the biological effect observed with radiation treatment. High-energy photons exhibit a property called the "buildup region" when entering tissues. This occurs because the electrons near the surface of the skin are scattered in a mostly forward direction and deposit their energy deeper in the tissue. This gives photons an advantage known as the "skin-sparing" effect, allowing for dose escalation within the deep-seated target.

Charged Particle Radiation

Charged particle radiation differs from photon radiation in that the energy of the radiation propagates as the kinetic energy of the particle itself. This is due to the fact that these particles have a mass. High-energy charged particles such as electrons and protons are directly ionizing forms of radiation and have sufficient kinetic energy to ionize atoms as they interact in tissue. Unlike high-energy photons, which tend to sparsely interact with matter and can travel long distances before being absorbed, high-energy particles tend to have predictable ranges of tissue penetration. The particles most routinely used for therapeutic purposes are electrons and protons. There are a select few centers which employ heavy ions, and, occasionally, attempts have been made to use neutrons.

High-energy electrons are commonly produced in linear accelerators by replacing the target used for x-ray production. Electrons begin depositing appreciable dose near the tissue surface, have a predictable range where they deposit the majority of their energy, and exhibit a rapid dose falloff. This gives electron therapy a particular advantage in the treatment of cutaneous or subcutaneous lesions (e.g., mycosis fungoides).

Proton particles are produced in particle accelerators such as cyclotrons and are over 1500 times heavier than electrons. Therefore, at a particular velocity, protons exhibit a much greater kinetic energy and do not scatter as easily. Hence, protons can potentially cause less damage to surrounding tissues when compared to electrons. Also, most of the energy absorption from protons occurs at the distal end (over the last few millimeters) of the track; this precisely defined area of intense ionization at the end of the track following the passage of protons is called a Bragg peak. Protons have a defined range in tissue, resulting in little to no exit dose. The proton beam may be altered to spread the Bragg peak to conform to the thickness and depth of the volume to be treated. Taking advantage of the Bragg peak effect as well as cross firing of a number of proton beams, a well localized volume of high radiation delivery can be produced and has been applied in a radiosurgical setting, albeit much less frequently than photons.

Radiation Biology

Free Radicals

When cells undergo irradiation with ionizing radiation, photons interact with water molecules in the cytoplasm by stripping an electron from a hydrogen atom, resulting in an energetic electron and an ionized water molecule. The resulting fast electrons continue to interact with water molecules through additional ionizing events. The positively charged water molecule exhibits a short half-life before it undergoes dissociation to an H^+ ion and an OH^- free hydroxyl radical. The hydroxyl radical is extremely reactive and is capable of breaking chemical bonds in nearby molecules. This indirect effect of radiation through free radical intermediaries is responsible for the majority of radiation-induced damage, which is further enhanced by the presence of oxygen. At lower radiation doses, tissue hypoxia (partial oxygen pressure less than 30 mmHg) inhibits the production of free radicals and, thereby, lessens the damaging effects of radiation.

Radiation Injuries to DNA

There is a large body of evidence that suggests that DNA is the most important target for cellular damage by ionizing radiation. Reactive water derivatives may interact with DNA, which creates the potential for permanent cell injury or death. Additionally, radiation is also capable of interacting directly with DNA. Damage to DNA can take on multiple forms, such as (1) single-strand breaks, where one of the two intertwined helices is broken, and (2) double-strand breaks where both helices are broken. Single-strand breaks are the more common of the two and can potentially be repaired by DNA repair enzymes, which use the intact strand as a template. Double-strand breaks are more difficult if not impossible to repair and cause the most deleterious biological damage. Double-strand breaks may be a result of a single particle or the interaction of two single-strand breaks caused by separate particles occurring at close temporal and spatial distances from one another. Cell culture studies on dividing cells have demonstrated that cells in the G2 and M phases of the cell cycle are the most susceptible to double-strand DNA breaks.

Radiation Biology of Conventional Radiation

Radiation causes damage to the DNA of tumor cells as well as the DNA of normal cells in its path. Normal tissue, however, tends to be more capable of DNA repair than tumors. This is partly due to aberrant cell cycle control mechanisms within tumors as well as differences in genetic features that permit damages to the abnormal tumor phenotype. Additionally, aberrations in metabolic patterns may also make tumors more susceptible to increased oxidative stress compared to normal cells.

In order to repair DNA damage, cells require an adequate amount of time. Therefore, normal cellular response to irradiation is to delay the cell cycle. Interestingly, the length of the G2 phase delay positively correlates with radiation resistance. Therefore, the radiobiology of differential cell repair is of great importance for conventional radiotherapy. Conversely, repair plays a less critical role as the number of fractions decreases and the dose per fraction increases (as in radiosurgery).

Cell survival after single doses of radiation is a probability function of the absorbed dose, measured in the unit gray (Gy). Typical mammalian cell survival curves obtained after single-dose radiation treatments in culture have a characteristic shape including a low-dose shoulder region followed by a steeply sloped portion at higher doses [4, 5]. The shoulder region is interpreted as the accumulation of sublethal damage at low doses with lethality resulting from the interaction of two or more of these events. For instance, due to the ability to repair single-strand DNA breaks, such damage would be considered sublethal. However, double-strand breaks may result in permanent cellular changes, which may culminate in cell death. Such a model can be described by the following probabilistic equation in which probability (cure or complication):

$$e^{-K*e^{\left(-\alpha D-\beta D^2\right)}}$$

where K is equal to the number of clonogens and α and β are constants related to single-event cell killing and cell killing through the interaction of sublethal events, respectively, and D represents the radiation dose.

The α/β ratio is the single dose at which overall cell killing is equally attributable to both components of cell killing, such that [6]:

$$\alpha D = \beta D^2 \text{ or } D = \frac{\alpha}{\beta}$$

This model, known as "the linear-quadratic model," has some limitations when applied for radiosurgery as compared to conventional radiation therapy [7]. Nevertheless, it still provides a meaningful method to compare radiosurgery to fractionated radiation schemes. The α/β ratio varies and is dependent on the tumor and tissue type being treated. Late responding tissues (e.g., prostate) have an α/β ratio of approximately 3, whereas many tumors have an α/β ratio of nearly 10. The α/β ratios for skin or mucous membranes range from 5 to 8. Tumors with low α/β ratios

(i.e., a small alpha or single hit component for radiation kinetics) will have less of a desired effect when a low radiation dose per fraction scheme is used than when comparable tissues with a high α/β ratio are treated identically. The radiation dose may be normalized to an equivalent 2 Gy per fraction dose (NTD2Gy) via the following formula [8]:

$$\text{NTD2Gy} = D * \left(d + \frac{\alpha}{\beta} \right) / \left(2Gy + \frac{\alpha}{\beta} \right)$$

where D is the total dose, d is the dose per fraction, and α/β is an intrinsic property of the irradiated tissue.

Conventionally fractionated radiation therapy relies on the four Rs of radiobiology, which are as follows: (1) repair of nonlethal injury, (2) reoxygenation of hypoxic tumor cells, (3) repopulation of tumor cells, and (4) reassortment of tumor cells into more susceptible phases of the cell cycle. Both conventional radiation therapy and radiosurgery have their advantages and disadvantages. The chosen modality is dependent on the clinical scenario; for instance, fractionated regimens are not efficacious when treating functional lesions (e.g., secretory pituitary adenomas) [7].

As mentioned previously, tissue hypoxia at a PaO_2 <30 mmHg inhibits the development of DNA damaging free radicals, thereby minimizing the degree of radiation damage. Experimental studies and clinical experience have suggested that aerated cells become nonviable following irradiation and that the site of irradiation is dominated by hypoxic cells. Consequently, substantial radiation dose escalation of a tumor may prove to have diminishing returns, as hypoxic cells are not adequately depopulated. However, reoxygenation, whereby tumors, may reestablish their oxygenated state between sessions if the radiation is delivered in fractions, making them more susceptible to radiation-induced damage. Reoxygenation is dependent on a variety of factors, such as the reduction of oxygen consumption by dead cells and the reduction in number of cells in relation to capillary blood supply.

Malignant tumors typically fall into the category of early-responding tissues mainly comprised of hypoxic cells, whereas normal brain and spinal cord tissue consists primarily of late-responding tissues comprised of mainly well-aerated cells. When treating malignant tumors, an argument can be made both in favor and against fractionation. While fractionation does increase the cell kill of a tumor for a given total radiation dose, it also reduces the damage to critical late-responding normal tissues (normal brain). However, fractionation permits malignant tumor cells to repopulate between fractions. This phenomenon is in stark contrast to the treatment of many benign tumors and arteriovenous malformations with radiosurgery, in which both targeted abnormal tissue and normal brain tissue consist of late-responding tissue of similar radiological types. In these situations, there is very little gain to be made with fractionation.

The standard approach to conventional radiotherapy involves treatment 5 days per week in 1.8–2 Gy fractions. This dose is most commonly used, as it has been shown to be well-tolerated in multiple different tissue types. For practical purposes, the radiation tolerance of the whole brain is considered to be 45–50 Gy in 20–25 fractions. However, this dose still may result in neurocognitive decline over time.

Radiation Biology of Radiosurgery

A therapeutic advantage may also be achieved by depositing more radiation dose in the tumor than in the surrounding normal tissue, which is the fundamental radiobiologic rationale of radiosurgery. A single radiation beam entering a patient begins with a region of low dose that progressively increases at the target where multiple radiation beams are cross-fired. As a result, the surrounding normal nervous tissue is spared from the high doses of radiation. This rapid dose falloff is the basic principle employed to spare normal tissue in radiosurgery. Although the characteristics of cross-firing are also used in conventional radiotherapy, the practical limits in conventional radiotherapy are two to four treatment fields, and delivery accuracy is on the order of 1 cm or more in

many anatomic sites. In the case of radiosurgery, since hundreds of beams are added together, the isodose lines take on the tumor configuration and deliver a highly conformal radiation field corresponding to the tumor while the steep falloff of dose prevents exposure of surrounding tissues to high doses and damage. In 1951, Lars Leksell at the Karolinska Institute in Stockholm, Sweden, utilized these principles and first described the concept of radiosurgery. He described the use of radiation therapy as a means of replacing the scalpel or electrode for functional neurosurgery.

The initial radiosurgery concept of Leksell was for the treatment of functional neurological disorders (e.g., trigeminal neuralgia), but it now has expanded to become a standard treatment option for numerous benign and malignant central nervous system conditions. When performing radiosurgery, the surgeon does not attempt to spare certain tissues and treat others; rather the goal is to achieve inactivation or destruction within the targeted volume. The obliteration of vascular supply with resultant endothelial dysfunction of tumor vasculature also appears to play a much more significant role in radiosurgery than radiation therapy.

Common Radiosurgery Platforms

Gamma Knife

The Gamma Knife (Elekta AB, Stockholm, Sweden) operates by precisely aligning the gamma-ray emissions from an array of ^{60}Co sources so they all intersect at a single point, which is known as the focus point (Fig. 17.1). Individually, each beam has a comparably low dose rate. However, the summation of the beams at the focus point creates a highly concentrated dose. By spreading the energy of a treatment out among the beams (current models use either 201 or 192 beams, depending on the type of unit), it is possible to achieve a highly conformal radiation dose within the target volume while largely sparing normal brain tissue because the dose rapidly falls to a low level as the distance from the focus (or isocenter) increases. Dosimetry in Gamma Knife radiosurgery is quite different from that of conventionally fractionated radiation therapy which focuses on dose homogeneity within the target volume; however, the steep dose gradient and isocentric plane achieved by the Gamma Knife means that dose within the target is inhomogeneous (Fig. 17.2) [9].

Fig. 17.1 The modern Gamma Knife Icon, a radiosurgical platform utilizing Cobalt-60 and allowing for frame-based and frameless intracranial radiosurgery

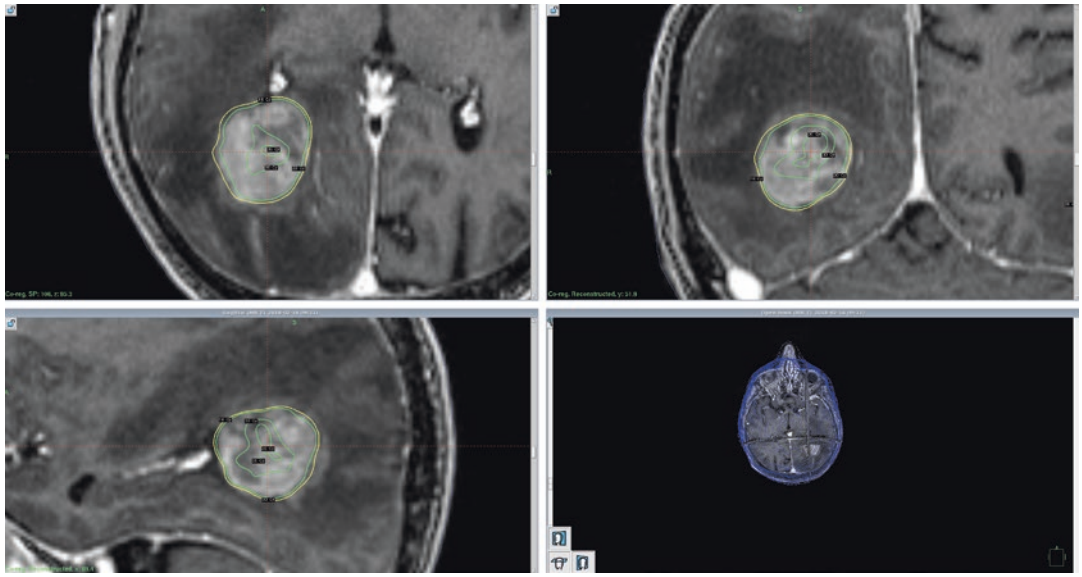

Fig. 17.2 Example of the dose heterogeneity used in radiosurgery. While 18 Gy is prescribed to the tumor margin, a much higher dose can be safely allowed within the tumor

As previously described, radiosurgery is dependent upon on the synthesis of stereotaxis and 3D imaging. The Gamma Knife accomplishes this by using the Leksell frame-based stereotactic system for localization and associated fiducial systems for imaging and treatment planning. The surgeon plans a treatment by defining one or more isocenters (commonly called "shots") which is a location within the brain that will be placed in the focus point of the Gamma Knife unit for a specified period of time. By carefully manipulating the location of the isocenters, the dwell time at each location, and blocking shot apertures, a highly conformal treatment plan can be generated.

The Gamma Knife unit consists of several main components: a large spherical shield (the bulk of the unit) which contains the array of ^{60}Co sources and protects the patient and operational staff from gamma radiation emissions, a central body which holds the source array and contains the primary collimation system that is responsible for directing the gamma rays to the focus point, a treatment table which moves the patient's head in and out of the unit (and in more recent units precisely positions the head so the target is at the focus point), a control suite to allow operational control of the unit, and a treatment planning system which allows the neurosurgeon in conjunction with a radiation oncologist and medical physicist to create appropriate dose distributions.

Older Gamma Knife units (models B, C, U, and 4C) use an external, helmet-based system for final beam collimation. Each helmet contains multiple removable collimators machined to result in a particular field size (4 mm, 8 mm, 14 mm, or 18 mm). Individual collimators may be replaced with solid "plugs" to achieve particular beam-shaping effects, used mainly for the protection of critical structures proximal to the target volume and enhancing the conformality of the beams. Dose plans which make use of more than one field size or which use plugs require the operator to change helmets/plugs during radiosurgery session. In more recent Perfexion and Icon Gamma Knife models, the external collimation system has been replaced by a single, internal collimating structure with precisely machined individual collimators (4 mm, 8 mm, and 16 mm). The Cobalt-60 source array has been split into eight separate sectors with source holders which can slide on linear bearings driven by motors at the rear of the unit to align

the sector with any of the available collimator sizes or a "blocked" position. Thus, each of the eight sectors may be independently configured, leading to the possibility of a "composite" isocenter which is composed of multiple field sizes. In the Perfexion and Icon, shielding with plugs (a highly manual process) has similarly been replaced by the fully automated process of setting a sector to the blocked position. The Icon also adds the flexibility of a mask-based system, cone beam CT, and infrared tracking for hypofractionated radiosurgery.

LINAC-Based Radiosurgery

Linear accelerators were first proposed radiosurgery platforms by Larson et al. in 1974. The earliest reports on clinical LINAC-based radiosurgery were published in 1984 by Betti and Derechinsky and in 1985 by Colombo et al. and Hartmann et al. The linear accelerators used for radiosurgery are typically modified from the machine that used for routine cancer therapy to achieve smaller beam sizes and more precise positioning specifications.

Various approaches have been developed to utilize LINACs as a radiosurgical tool. However, most approaches follow the same basic fundamental technique. Combinations of treatment table, gantry rotations, and collimator rotations are employed to direct the photon beams to the intracranial target from many different angles (instead of the 1–5 beams used in traditional radiation therapy, more than five beams can and are often used). By making use of two intersecting axes of rotation and by putting the center of the target at this intersection point, beam entry points over the entire upper hemisphere of the skull can be targeted. Multileaf collimators (MLCs) are employed to shape the treatment field at each location and may be modulated to achieve particular dose distributions. If x-rays are directed into the head while the gantry is rotating, the central line of the beam might trace out paths, known as arcs. Combinations of arcs and modulating MLCs can aid in achieving conformal dose distributions. Finally, there exist on the market a number of dedicated LINAC-based radiosurgery platforms (Fig. 17.3), including Varian's Edge (Palo Alto), Elekta's Versa HD (Elekta AB, Stockholm), Tomotherapy© Hi-Art© (Tomotherapy Inc., Madison), the Cyberknife (Accuray® Inc., Sunnyvale), and Novalis (BrainLab, Germany).

Fig. 17.3 The Varian Truebeam linear accelerator, one of many LINAC-based radiosurgical platforms

Another LINAC-based radiosurgery modality that has been gaining traction in recent years is magnetic resonance (MR)-based LINACs [10]. These devices are unique in that they are a hybrid LINAC and magnetic resonance imaging (MRI) scanner. The major advantage of these devices is that MRI is capable of providing superior soft tissue contrast throughout the body, both prior to and during treatment sessions. MR LINACs are also discussed at the conclusion of Chap. 4. This stands in stark contrast to cone beam CT, which is employed by most LINACs, can only be used before treatment sessions, and does not offer the enhanced delineation of soft tissues that MRI does. Therefore, MR LINACs may be able to deliver treatment with narrower margins, result-

ing in less exposure of radiation to healthy tissues and minimization of the risk of toxicity. The first MR LINAC was installed in 2008 at UMC Utrecht in the Netherlands. Since that time, an international consortium has been organized to further explore this technology with multiple devices installed throughout the United States and Europe.

Proton Radiosurgery

To utilize a charged particle beam for radiosurgery, several device modifications are required. Since proton beams travel to different depths according to their energy, to provide the best match of Bragg peak effect to the target tissue, energy of the beams and spreading of the Bragg peak need to be adjusted during treatments. A common way of accomplishing this is through the addition of variable thickness absorbers to adjust the energy range of the particles. For instance, if four beams from different directions are used to treat a target, it is likely that the target is shaped differently from the perspective of each beam. In order to treat patients with charged particles, very detailed information about the target from the perspective of each beam is essential. Each beam requires a customized range-modifying absorber, a variable thickness rotating absorber, and a beam-shaping aperture. Charged particle radiosurgery can produce excellent dose distributions, but the treatment process is generally more time-consuming, expensive, and difficult than the Gamma Knife or LINAC platforms.

Gamma Knife Frame-Based Radiosurgery Workflow

Stereotactic Frame Placement and Imaging

Target immobilization and tracking is a fundamental aspect of radiosurgery. Historically, this has been achieved with frame placement, although alternatives have emerged as detailed in Chap. 4. When used, stereotactic frames are usually placed with local anesthesia and intravenous sedation. Prior to frame placement, the scalp is cleansed in a standard fashion and the areas of the pin placements are infiltrated with a long-acting local anesthetic. The clinicians and technicians should preview the pre-SRS MR images and appreciate the location and the nature of the lesions and choose a frame placement strategy which keeps the target near the center of the frame, allowing for optimal dosimetry and avoidance of collisions. Collisions typically occur with the base ring, the post/pin assembly, and the patient's head with the collimator helmet during treatment. It is important to avoid placement of a pin in the flexible or hemi-flexible bone flap in patients who underwent prior craniotomies or have cranial hardware (e.g., a VP shunt). The MRI or CT fiducial should be tried on the frame before transferring the patient to the MRI unit. If the fiducial box does not fit on the frame because of excessive shifting, the frame may need to be repositioned. Confirming that the frame adaptor fits on the patient's head frame is a vital step. If the frame is shifted too anteriorly and the back of the head ring is too close to the neck, the adaptor may not fit and the radiosurgery treatment cannot be carried out. Tight fitting of the adaptor may cause neck discomfort, particularly during a long treatment. The frame cap check provides information about the geometry of all stereotactic frame parts, including posts and screws, as well as information about patient head geometry and positioning in relation to the treatment planning system. This information is required for prediction of potential collisions or close contract with the Gamma Knife collimator system. If the frame cap does not fit, exact post and screw geometry measurements must be entered into the treatment planning system to avoid the possibility of a potential collision.

Typically, with frame-based radiosurgery, patients undergo some form of a dedicated near-imaging study such as a thin-sliced stereotactic MRI with and without intravenous contrast administration. Sequences used depend on the pathology being targeted. For certain lesions, other imaging modalities may be employed, such as CT angiography or stereotactic angiography in the case of arteriovenous malformations. Regular quality control

checks of the MRI unit are performed to ensure image accuracy. A special frame holder is utilized to avoid head movement during MRI. Additionally, accuracy is checked for each image sequence by comparing the known frame measurement with image measurements, in addition to the distance from the posterior fiducials to the middle fiducials. Images are defined with the SRS planning software after being transferred to local computers. The measurements are again checked and compared with known frame measurements and also the distance to the middle fiducial to confirm the absence of any distortion during image transfer.

Treatment Planning

Regardless of the radiosurgical platform being utilized, stereotactic radiosurgery requires clear and accurate imaging of the target. Advances in neuroimaging over the past 25 years have resulted in increased efficacy and safety of radiosurgery for intracranial lesions. The current treatment planning for an intracranial lesion is usually performed on a computer-based software package, where the target volume and the surrounding structures are contoured. A dose plan can be generated to deliver an ideal dose to the target and a safe dose to adjacent critical structures. Various parameters such as dose-volume histograms for the target volume and critical structures can be obtained as well. Also, conformality, dose uniformity, and gradient index can be assessed and adjustments made so as to optimize the treatment plan.

Target volume can be outlined with SRS software manually; some software packages also offer automated contouring. However, care must be taken, as careful examination of a lesion boundary usually demonstrated that it is not always a distinct, sharp line but is rather a smudge of transition between enhancement and non-enhancement. Certain optical illusions, such as the Cornsweet effect, mislead neurosurgeon into prescribing high radiation doses to inappropriate lesion contours. It is not uncommon for one to notice that the isodose lines always seem to "magically" fit the tumor perfectly (illusion of perfection). The visual system can be deceptive by causing us to perceive many different isodose lines as perfect fits to the same tumor. Therefore, some experienced neurosurgeons and radiation oncologists generate conformal dose plans without outlining the target. The absence of a marked lesion boundary allows the clinician to assess the degree of boundary confusion on each image slice, avoids the error of thinking that a particular boundary is the only correct boundary, and reduces the confusion inherent in a display of too many lines. Of course, parameters including dose-volume histograms, conform index, and gradient index can be still obtained retrospectively after a radiosurgical plan is complete.

Dose Prescription

Typically, single-session radiosurgical margin doses may vary from 10 to 15 Gy for meningiomas, schwannomas, and other common benign intracranial tumors, 15–30 Gy for functioning pituitary adenomas [11], 18–30 Gy for arteriovenous malformation, and 16–24 Gy for cerebral metastases and other intracranial malignancies. In the case of trigeminal neuralgia, a maximum dose of 70–90 Gy is prescribed. Care should be taken to avoid high doses or "hot spots" residing on critical neurovascular structures, such as cranial nerves, brainstem, or carotid artery. Radiosurgery can be hypofractionated, typically with the creation of a stereotactic mask (Fig. 17.4), across two to five sessions to deliver a more optimal dose plan tailored to the constraints of a particular case.

Dose Limitations to Critical Structures: Shielding and Plugging Technique

Visual deterioration following SRS is rare and can be avoided if the dose to the optic apparatus is restricted to $\leqq$ 8Gy; however, reports of 10–12 Gy have been described by some groups [12]. Typically, a distance of 3 mm or more between the tumor margin and the optic apparatus is desired. If an acceptable gradient meeting these parameters cannot be constructed, an alternative treatment option should then be considered. Modern radiosurgery platforms may allow

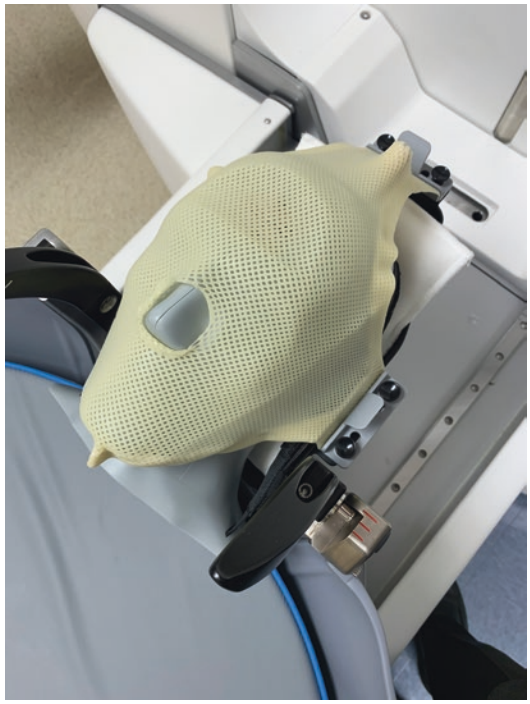

Fig. 17.4 An example of an Aquaplast mask created for custom head immobilization during intracranial stereotactic radiosurgery

for distances as short as 1–2 mm. Ultimately, the tolerable absolute dose permitted likely varies from patient to patient and is likely affected by factors, such as previous damage to the optic apparatus by tumor compression, ischemic changes, type and timing of previous interventions (e.g., fractionated radiation therapy and surgery), patient age, and the presence or absence of other comorbidities (e.g., diabetes).

The majority of the cranial nerves appear to be more resistant to radiation effects than the optic nerve; however, reports of cranial neuropathy, particularly after repeat radiosurgery, are well documented. Although the tolerable limit to the cranial nerves is unknown, reports have detailed effective radiosurgical doses of between 19 and 30 Gy to this region with a low risk of clinically appreciable side effects [13, 14]. Injury to the intracranial great vessels such as the carotid artery is rare after SRS. In cases where the tumor extends into an eloquent area, shielding and plugging techniques can be used to lower radiation doses to critical structures.

For sellar lesions, there does appear to be a direct correlation between the effect on tumor volume and the endocrine remission rate following radiosurgery [15]. Fortunately, since most of these lesions are small enough to be well suited for stereotactic radiosurgery, dose-volume considerations are not usually a limiting factor. Additionally, since the systemic effects of functioning pituitary adenomas can be so devastating, it seems intuitive to deliver a reasonably high dose (≥20Gy to the tumor margin) to allow earlier hormonal normalization although control of tumor growth can usually be achieved with just 16–18 Gy. For improved rates of hormonal normalization in functioning adenomas, a margin dose of 25 or 30 Gy may even be chosen. However, it is fully not known to what degree a higher margin dose will result in delayed hypopituitarism. In cases of functioning adenomas with radiologically identifiable targets in the cavernous sinus, treatment plans can be devised with higher range treatment doses while shielding much of the normal stalk, gland, and optic apparatus.

For brainstem lesions, such as brainstem AVM, metastases, or tumors, dose-volume effects can dramatically affect dose selection. When post-SRS edema presents, patients can suffer from brainstem dysfunction, which can ultimately lead to death. At the University of Virginia, doses up to 14–20 Gy to the tumor margin, which are also received by the brainstem parenchyma, have generally been safe. While a 20 Gy dose did not cause deficits in our patients with brainstem metastases, we generally lower our radiation dose and/or consider fractionated radiosurgery when irradiating near or within the brainstem.

Stereotactic Delivery of Radiation to the Target Volume Inside the Collimator System

The current radiosurgery procedure is a fully automated process in every aspect of the treatment process, including setup of the stereotactic coordinates, setup of different sector positions defining collimator size or blocked beams, and setup of exposure times. All radiosurgical data are exported to the operating console, which is used to control and continuously monitor patient treat-

ment. For Gamma Knife radiosurgery, the only manual aspect is the positioning of the patient's head in the docking device in a selected angle and adjusting the treatment bed height for optimal patient comfort. However, a clearance check for shots that involves close contact with the collimator system needs to be performed, and the setup for coordinates, exposure times, and sectors for different isocenter on the control computer of the operating console should be checked. To perform a clearance check, a special test tool simulating the shape and dimensions of the inner collimator is attached and rotated around the patient's head for various positions. This situation usually occurs in patients with multiple intracranial metastatic lesions. During the radiosurgery treatment, the patient can also be monitored by audio and visual communications. Monitoring of vital signs can also be performed, and the treatment can be also interrupted if deemed necessary.

Removal of the Stereotactic Guiding Device

The final step of the procedure is to remove the pins and frame from patient's head. The pin wound may be oozing, and frequently, bleeding can be stopped by simple compression although sometimes suturing is needed. Pin site infection can be avoided by administering neomycin, bacitracin, or other topical antibiotics. After radiosurgery, the patient is monitored for a few hours and then discharged if in stable condition. However, admission is permitted if the patient experiences unexpected events, such as seizure, nausea, severe pain, anesthetic complications, or new onset neurologic deficits.

The LINAC-Based Radiosurgery Workflow

Immobilization of the Target

The accuracy of frame-based radiosurgery (e.g., Gamma Knife) is usually considered to be less than 1 mm. In recent years, physicians have made great efforts in designing frameless immobilization tools, such as mouth pieces and masks, to enhance patient comfort. In addition to being an invasive procedure, frame placement is also a complicated process for an extracranial and multi-fraction treatment. In the field of LINAC-based radiosurgery, some devices use frameless immobilization techniques (e.g., a thermoplastic mask or bite block relocatable frame) for the entire treatment (see Chap. 4). Intraprocedural imaging (e.g., orthogonal x-rays or cone beam CT) during delivery of radiosurgery can also be performed to confirm appropriate localization or make adjustments for errors. This approach allows for the administration of hypofractionated radiosurgery. However, the accuracy of this approach is a subject of some debate. The issue of precision was initially resolved with the description of a gantry correction device by two University of Florida scientists and more recently by the development of radiosurgery dedicated LINACs. This resulted in LINAC radiosurgery becoming a competitive technique, not only for lesions but also for functional disorders of the brain, such as trigeminal neuralgia and Parkinsonism. In recent medical physics reports, the accuracy of LINAC-based radiosurgery with a localizing mask can approach 1 mm [16, 17].

Dosimetry, Prescribing to a Target Volume

When designing treatment plans for intracranial lesions, the multiple radiation fields enter through the top of the head. Although rarely used in Gamma Knife, LINAC-based radiosurgery more frequently applies the concepts of conventional radiation therapy, including gross target volume (GTV), clinical target volume (CTV), and planned target volume (PTV). The minimal radiation dose thought to be clinically safe and efficacious is prescribed to the PTV. The dose that adequately covers the target is designated as the prescription radiation dose. Typically, in LINAC-based radiosurgery the prescription isodose line is high (70–90%), which means that the maximal dose is 10–30% larger than the dose at margin of the lesion, and the dose distribution is more homogenous than

with the Gamma Knife where the margin isodose is typically at the 50% isodose line.

In similar fashion to the Gamma Knife, the dose falloff in LINAC-based radiosurgery is also steep. There is some variation according to the collimator size and the type of planning used, such as multiple isocenter, dynamic arcs, or static beams. The area of radiation dose falloff is known as the penumbra. Similar to the Gamma Knife, radiation dose in the penumbra may be sufficiently high enough to cause toxicity. When treating lesions adjacent to an eloquent area, such as brainstem, motor area, and spinal cord, it is absolutely necessary to consider the dosimetric consequences of the penumbra. Although it is attractive to cover the lesion with an additional 1 or 3 mm expansile margins, the risk of radiation-induced damage is not always justifiable. However, modern techniques available in LINAC radiosurgery (e.g., intensity modulation) can be used to optimize dose falloff in the vicinity of critical structures.

The different weighting and length of the arcs to achieve asymmetric dose falloff around a lesion can lead to some heterogeneity. Using a multiple isocenter technique usually brings a more heterogenous plan, compared to a shaped beamed technique. A major advantage of heterogenous plans is that you can move the "hot spot" to the necessary area (e.g., the most enhanced area or most diffusion-restricted area of the target). The clinical consequences of sparing normal tissue with multiple isocenter prescriptions at the 50% isodose line versus LINAC shaped beam prescriptions at the 90% IDL are not well understood. The gradient index is device dependent and is not fixed to a particular isodose line. Optimization of the conformality and gradient indices should always be considered with each unique dose plan.

Methods of Conformality in LINAC Machine

Significant development of the techniques of LINAC conformal radiation therapy, including multiple isocenter, shaped beams, and pencil beam approaches, was afforded by the computerized imaging, 3D treatment planning software, and fast-delivery LINACs. Shaped beam radiosurgery is possible with LINACs equipped with a multileaf collimator. Such a collimator automatically changes the shape of the radiation beam, depending on the information obtained by the beam eye's view (BEV) representation of the target lesion. This is possible because of the availability of 3D reconstruction of the target volume in modern planning software. Dynamic arcs and static beams are the two approaches for contemporary shaped beam radiosurgery.

With technical advances, intensity-modulated radiosurgery (IMRS) is a strategy to enhance the efficacy of radiation delivery; this concept was first described by Anders Brahme. In 1988, he proposed that the conventional trial-and-error paradigm for treatment planning be reversed and that one derive the optimal beam intensities from the desired dose distribution by using deterministic techniques. Since that time, several methods have been developed in both planning and delivery technology to allow the optimal intensity to be delivered. With the advent of micro-multileaf collimators, it is now possible to perform IMRS. The success of IMRS hinges on the development and implementation of three components: (1) inverse planning, (2) leaf sequencing, and (3) delivery with a tightly integrated accelerator and a multileaf collimator.

Inverse planning technique is an optimization process whereby one specifies a desired dose distribution and searches for the beam intensity distribution that will satisfy these specifications. This is generally accomplished with an objective function that is then minimized through a mathematical operation. In theory and practice, there are many functions, both physically and biologically based, that can be applied as the objective functions. The physical method called the dynamically penalized maximum likelihood (DPL) algorithm has been integrated into many commercial treatment planning systems for inverse planning of intracranial lesions. An advantage of the DPL approach is the ability to compute a multitude of inverse plans simultaneously. This allows for varying levels of emphasis

to be placed on the target and organs at risk, with the clinical team selecting the appropriate plan for the individual lesion on the basis of the dose-volume histogram and dose distribution information.

Another important advancement in LINAC-based radiosurgery is the volumetric radiation technique, which can result in comparable or improved dose conformity while significantly shortening treatment times. RapidArc is an example of a volumetric arc therapy that delivers a radiation dose with a single or several gantry rotations of the LINAC. It is made possible by a treatment planning algorithm that simultaneously changes three parameters during treatment: (1) rotation speed of the gantry, (2) shape of the treatment aperture with a multileaf collimator, and (3) radiation dose rate. This allows for the delivery of treatment several times faster than with other dynamic treatments. The treatment time with RapidArc is often shorter than with other dynamic treatments.

Frameless Radiosurgery and the Spine

In recent years, frameless, image-guided radiosurgery has gained a great deal of traction and has emerged as a new tool to overcome some of the limitations of frame-based treatments. Characterizing the patient's movement and, in turn, the target and adjacent critical structures during image-guided radiosurgery is crucial, particularly in spinal radiosurgery. Highly conformal delivery, such as with multiple circularly collimated beams, dynamic conformal arcs, and IMRS, has even been used to achieve the prescribed tumor dose. Presently, multiple frameless radiosurgery platforms exist and are widely employed for both intracranial and extracranial targets. The Gamma Knife Icon radiosurgery platform utilizes the same basic core principles as the classic Gamma Knife but is able to achieve adequate immobilization with the use of a mask and not a stereotactic frame (Figs. 17.1 and 17.4).

Image landmarks with either radiopaque fiducials implanted in the vertebrae or direct imaging of vertebral anatomy have been used to localize spinal anatomy and associated tumors [18]. Immobilization is typically accomplished by using moldable cushions with the patient lying in the supine position to reduce target movement as a result of respiration. Yin and colleagues observed <1 mm of respiratory-induced motion in vertebral bodies during fluoroscopic studies of patients lying in the supine position [18]. Another report demonstrated that spinal anatomy may move >2 mm during the radiosurgery treatment [19]. Agazaryan et al. [20] observed that vertebral anatomy movements which vary as much as 3 mm and could occur in as little as 5 minutes. These results suggest a need for intrafraction patient monitoring/imaging and correctional shifts, even for patients whose overall treatment times are expected to be relatively short.

However, several studies have demonstrated an uncertainty of the spinal cord dose associated with simulated patient positioning errors and the need for an accurate understanding of uncertainty in setup and movement. Additionally, post-SRS myelitis has also seen albeit rarely. For spinal radiosurgery, spinal cord tolerance, measurement of patient translations and rotations during SRS delivery, and analyzing post-SRS complications are being further investigated.

Exponential growth of the extracranial applications of radiosurgery is likely to be observed in the coming years, and it can be expected that radiosurgery will play an expanding role in the setting of spinal metastasis.

Proton Beam Radiosurgery

There are two approaches when performing proton radiosurgery. The first approach is using proton cross-fire, and the second one is using the effect of Bragg peak. The idea of "cross-fire" comes from Lawrence in 1954 and Leksell in 1957, who used protons as their radiation source. Lawrence et al. at University of California, Berkeley, treated targets with multiple proton cross-fire arcs from each side of the head, with the beams being oriented to avoid dose overlap in normal tissue but intersecting at the center of the

target [21]. Leksell used the same principles with a 185-MeV proton beam and targeted a lesion through stereotactic fixation [22]. Subsequently, this approach was refined using the high energy of a cyclotron [23].

The second approach is utilizing the effect of the Bragg peak, which was developed from the team at the Harvard Cyclotron Laboratory in 1961. The facility was limited to a 160-MeV proton beam that had an insufficient beam range to use the cross-fire approach; however, the Bragg peak can be applied in such a setting. Unlike the cross-fire approach, proton beams aimed from the vertex of the head toward the feet could be utilized with no downstream dose to the thorax because of the finite range of protons, which were calculated to stop within the target. Although the technical challenge remained the ability to precisely stop the protons at the desired location, several improvements such as lamination planning, and combined peak called the spread-out Bragg peak (SOBP), were established.

Currently, proton beams are delivered through fixed-horizontal-beam rooms or rotational-beam rooms. The STAR system, a stereotactic intracranial beam line equipment, is located at the Massachusetts General Hospital in Boston. Using the STAR system, patients can be treated by position on the couches or specific chairs, and the procedure involved in proton radiosurgery is similar to those for photon-based SRS mentioned above.

The STAR device utilizes the Brown-Roberts-Wells (BRW) coordinate system. Using BRW frames with local anesthesia, patients were secured with bolsters within the STAR system so that they could be rolled on their side as needed to treat with oblique fields. At the hospital-based proton therapy facility, radiosurgery is performed with both the gantry units and the STAR system. The gantry units employ non-isocentric 4-axis robotic patient positioning and amorphous silicon panels for digital imaging rather than film. Final proton beam shaping is achieved with custom brass apertures for each treatment beam and lucite compensators to create the distal shape of the beam. However, the fixed beam line of the STAR system has fewer degrees of freedom of treatment positions but has the advantage of more conformal delivery of treatment. The beam is transported from cyclotron at 185 MeV and reduced to the necessary energy and depth with the appropriate combination of absorbers in the form of a single scattering system. The resulting lateral dose uniformity of ±2.5% at the isocenter depth produces a sharper lateral dose falloff than can be achieved with the gantry field, which is particularly favorable for radiosurgery, where short dose gradients between target and nontarget tissues are desirable.

Proton radiosurgery costs are higher and require more complicated approaches than photon radiosurgery. Theoretically, the physical characteristics of protons should make them an effective modality for stereotactic radiosurgery, although small and conformal proton beam fields are very difficult to accurately model, and extraordinary care should be taken to avoid patient injury. The future of proton radiosurgery promises to be more cost-effective, easier to use, more reliable, and able to deliver more precise doses. Compact proton systems such as one by Mevion are now being utilized; additionally, other charged particles (e.g., carbon ion) are being explored for stereotactic use as well.

Conclusion

Stereotactic radiosurgery is a minimally invasive technique that can be used to treat a multitude of pathologies of the central nervous system (both benign and malignant). While there are fundamental principles of physics and radiation biology that hold true for radiosurgical treatments, there are several important differences depending on the energy source and platform being utilized. Since the Gamma Knife was first introduced in 1968, there has been a myriad of advances in the field, which have resulted in improved safety and efficacy. The field of radiosurgery continues to move forward with greater indications, expansion to particle-based delivery, and the adoption of frameless methods.

References

1. Leksell L. The stereotaxic method and radiosurgery of the brain. Acta Chir Scand. 1951;102(4):316–9.
2. Elekta surpasses one million patients treated with Leksell Gamma Knife [press release]. Stockholm, SE2016.
3. Park HS, Wang EH, Rutter CE, Corso CD, Chiang VL, Yu JB. Changing practice patterns of Gamma Knife versus linear accelerator-based stereotactic radiosurgery for brain metastases in the US. J Neurosurg. 2016;124(4):1018–24.
4. Dale RG. The application of the linear-quadratic dose-effect equation to fractionated and protracted radiotherapy. Br J Radiol. 1985;58(690):515–28.
5. Fowler JF. The linear-quadratic formula and progress in fractionated radiotherapy. Br J Radiol. 1989;62(740):679–94.
6. Hall EJ, Giaccia A. Radiobiology for the radiologist. 6th ed. Philadelphia: Lipincott Williams & Wilkins; 2006.
7. Hall EJ, Brenner DJ. The radiobiology of radiosurgery: rationale for different treatment regimes for AVMs and malignancies. Int J Radiat Oncol Biol Phys. 1993;25(2):381–5.
8. Flickinger JC, Kalend A. Use of normalized total dose to represent the biological effect of fractionated radiotherapy. Radiother Oncol. 1990;17(4):339–47.
9. Wu A. Physics and dosimetry of the gamma knife. Neurosurg Clin N Am. 1992;3(1):35–50.
10. Kerkmeijer LG, Fuller CD, Verkooijen HM, Verheij M, Choudhury A, Harrington KJ, et al. The MRI-linear accelerator consortium: evidence-based clinical introduction of an innovation in radiation oncology connecting researchers, methodology, data collection, quality assurance, and technical development. Front Oncol. 2016;6:215.
11. Sheehan JP, Starke RM, Mathieu D, Young B, Sneed PK, Chiang VL, et al. Gamma Knife radiosurgery for the management of nonfunctioning pituitary adenomas: a multicenter study. J Neurosurg. 2013;119(2):446–56.
12. Leber KA, Bergloff J, Pendl G. Dose-response tolerance of the visual pathways and cranial nerves of the cavernous sinus to stereotactic radiosurgery. J Neurosurg. 1998;88(1):43–50.
13. Kuo JS, Chen JC, Yu C, Zelman V, Giannotta SL, Petrovich Z, et al. Gamma knife radiosurgery for benign cavernous sinus tumors: quantitative analysis of treatment outcomes. Neurosurgery. 2004;54(6):1385–93; discussion 93–4.
14. Liu AL, Wang C, Sun S, Wang M, Liu P. Gamma knife radiosurgery for tumors involving the cavernous sinus. Stereotact Funct Neurosurg. 2005;83(1):45–51.
15. Sheehan JP, Pouratian N, Steiner L, Laws ER, Vance ML. Gamma Knife surgery for pituitary adenomas: factors related to radiological and endocrine outcomes. J Neurosurg. 2011;114(2):303–9.
16. Minniti G, Scaringi C, Clarke E, Valeriani M, Osti M, Enrici RM. Frameless linac-based stereotactic radiosurgery (SRS) for brain metastases: analysis of patient repositioning using a mask fixation system and clinical outcomes. Radiat Oncol. 2011;6:158.
17. Khoshbin Khoshnazar A, Bahreyni Toossi MT, Hashemian A, Salek R. Development of head docking device for linac-based radiosurgery with a Neptun 10 PC linac. Physica medica: PM: an international journal devoted to the applications of physics to medicine and biology: official journal of the Italian Association of Biomedical. Physics. 2006;22(1):25–8.
18. Yin FF, Ryu S, Ajlouni M, Yan H, Jin JY, Lee SW, et al. Image-guided procedures for intensity-modulated spinal radiosurgery. Technical note. J Neurosurg. 2004;101(Suppl 3):419–24.
19. Murphy MJ, Chang SD, Gibbs IC, Le QT, Hai J, Kim D, et al. Patterns of patient movement during frameless image-guided radiosurgery. Int J Radiat Oncol Biol Phys. 2003;55(5):1400–8.
20. Agazaryan N, Tenn SE, Desalles AA, Selch MT. Image-guided radiosurgery for spinal tumors: methods, accuracy and patient intrafraction motion. Phys Med Biol. 2008;53(6):1715–27.
21. Lawrence JH, Tobias CA, Born JL, Mc CR, Roberts JE, Anger HO, et al. Pituitary irradiation with high-energy proton beams: a preliminary report. Cancer Res. 1958;18(2):121–34.
22. Larsson B, Leksell L, Rexed B, Sourander P, Mair W, Andersson B. The high-energy proton beam as a neurosurgical tool. Nature. 1958;182(4644):1222–3.
23. Boone ML, Lawrence JH, Connor WG, Morgado R, Hicks JA, Brown RC. Introduction to the use of protons and heavy ions in radiation therapy: historical perspective. Int J Radiat Oncol Biol Phys. 1977;3:65–9.

Part IV

The Future of Functional Neurosurgery

Parkinson's Disease: Deep Brain Stimulation

18

Donald J. Crammond and R. Mark Richardson

Introduction

Modern deep brain stimulation (DBS) for Parkinson's disease (PD) was developed in the 1980s, based on the discoveries of Benabid and colleagues [1], and then further refined in the 1990s [2]. DBS for PD is now the most common surgical treatment for PD, largely replacing ablative therapies, because of its clinical efficacy, reversibility, and adjustability. Currently, besides the ventral intermediate nucleus (Vim) of the thalamus which is used only for tremor-dominant PD, there are two basal ganglia target nuclei for DBS implantation in PD, the subthalamic nucleus (STN) and the pars interna of the globus pallidus (GPi).

The basal ganglia are components in a complex motor system affected by PD via decreased dopaminergic transmission in the putamen secondary to progressive loss of dopaminergic innervation from the substantia nigra pars compacta. Thus, best medical therapy with levodopa results in resolution of many PD motor symptoms. However, the dose escalation required to counter the progressive dopaminergic loss eventually leads to levodopa-induced dyskinesia and to large "on-off" medication motor fluctuations. DBS was first popularized in the treatment of PD patients with these motor complications, since it can increase medication "on-time" and, depending on target, reduce medication dosage. Research has consistently demonstrated the benefits of DBS for PD patients.

Outcomes

The first multicenter and highly influential study of the application of DBS in the United States was the Veterans Affairs (VA) Cooperative Studies Program [3]. This study demonstrated a significant increase in "on-time" without troubling dyskinesia for patients with either STN DBS or GPi DBS as compared to best medical therapy. In addition, the DBS group showed greater improvement in UPDRS scores, levodopa dosing, and quality of life measures than the best medical therapy group. Since then, similar findings of significant motor benefit beyond that of medication alone have unequivocally been consistently replicated in PD patients undergoing DBS: Jiang et al. [4] found at 5 years that STN DBS improved UPDRS scores in the "*off*" state

D. J. Crammond
Department of Neurological Surgery, University of Pittsburgh School of Medicine, Pittsburgh, PA, USA

R. M. Richardson (✉)
Department of Neurosurgery, Massachusetts General Hospital, Harvard Medical School, Boston, MA, USA
e-mail: mark.richardson@mgh.harvard.edu

N. Pouratian, S. A. Sheth (eds.), *Stereotactic and Functional Neurosurgery*,
https://doi.org/10.1007/978-3-030-34906-6_18

by 35% while Merola et al. [5] found similar "*off*" state improvements in UPDRS as well as ADL scores compared to best medical therapy.

Other studies have demonstrated the efficacy of STN DBS for PD over the long term. The VA Cooperative study followed patients for 2 years and demonstrated that clinical efficacy was maintained for both STN DBS and GPi DBS over that time [6]. Other studies have followed PD patients at longer intervals and have demonstrated stable improvement in motor symptoms, improved quality of life measures, and decreases in levodopa equivalent daily dose, with STN DBS at 4 years [7], 5 years [4], 6–9 years [8–10], and 10 years [11–13]. At longer follow-up intervals, it does appear that STN DBS efficacy is somewhat diminished [4] and that axial symptoms, i.e., postural instability gait difficulties, become the dominant symptoms [8] as well as worsening bradykinesia [13]. Limousin and Foltynie [14] reviewed 15 studies using similar criteria of STN DBS after 5 years and UPDRS Part III studied during off-medication periods which demonstrated substantial DBS-induced improvements in rigidity and tremor at 5 years and longer, with declining benefit for bradykinesia and axial signs, compared to 1 year. Although only two long-term outcome studies (>5 years) in GPi DBS have been published [15, 16], GPi DBS significantly improves UPDRS III scores after 5 years with the greatest benefit to rigidity and dyskinesia.

Patient Selection for DBS

Most centers that perform DBS have a dedicated multidisciplinary movement disorders team, consisting of movement disorder neurologists, neurophysiologists, neurosurgeons, and neuropsychologists and including physician assistants and/or nurse practitioners. Each member plays a unique role in the evaluation, selection, implantation, programming, and follow-up of PD patients undergoing DBS. Early patient selection criteria at most centers were based on Core Assessment Program for Surgical Interventional Therapies in PD (CAPSIT-PD) guidelines, which were established in 1999 [17] and were based on the STN as the primary target for DBS therapy. These initial guidelines included age criteria (i.e., <70 years of age), minimal duration of PD since diagnosis (>7 years), as well as guidelines for on-off medication UPDRS ratings and absence of contraindications such as significant cognitive deficits, dementia, and certain psychiatric and medical comorbidities.

At our center, patients are typically referred for initial evaluation to a movement disorder neurologist. Patients complete a thorough evaluation to confirm their PD diagnosis and are excluded as surgical candidates if they have not been adequately medically optimized or if they have significant comorbidities that would preclude them from surgery. Those patients who pass through the initial evaluation are then presented at a multidisciplinary conference to determine their eligibility for DBS. Patients who are deemed potential surgical candidates then undergo a high-resolution MRI scan to exclude structural abnormalities, on-off UPDRS testing, and a thorough neuropsychological evaluation to identify any relevant cognitive or psychiatric concerns.

A 30% improvement in UPDRS motor symptoms from the off to on medication state, which predicts a good response to DBS [18], is a typical inclusion criterion at most centers. Although some argue that selection of patients for DBS should be more rigorous given the risks of surgery and development of newer dopaminergic agents [19], the field as a whole has been moving toward increasing the availability of DBS treatment to a wider range of PD patients.

Historically, referral for DBS is made when patients with PD develop medication-related side effects (i.e., dyskinesias), experience large on/off fluctuations throughout the day, or cannot tolerate medication side effects. The initial CAPSIT-PD criteria, developed two decades ago, are now widely acknowledged as too restrictive, for instance, recommending implantation only for patients who have had symptoms for >5 years and who are <70 years of age. At many centers, the time and age recommendations have been gradually expanded to include patients with symptoms of a shorter duration and to include older patients. However, a recent review of

patients in the UK between 1997 and 2012 found that timing of DBS implantation for patients with PD has remained relatively stable, with a mean age for implantation of 60 years and a mean time from PD diagnosis of 11 years [20]. One concern in the implantation of DBS in older patients is that there may be higher rates of more serious complications. However, a recent retrospective study of over 1700 patients with Parkinson's disease undergoing DBS up to age 90 did not find a significant increase in complication rate (i.e., intracranial hemorrhage, infection, pulmonary embolism, or pneumonia) or length of hospital stay, as age increased [21]. Thus, DBS appears to be just as safe for older patients with PD, although a long-term outcome study that parsed PD patients into three age groups found that after 5 years of DBS, the older patients (aged 65 and older) had less benefit of DBS, as significantly worse axial scores and no improvement in mood and cognition scores were reported, compared to younger PD patients with DBS [22].

Should Patients Be Referred Earlier for DBS?

Due to the successful DBS treatment of multiple PD motor symptoms in patients with advanced PD, there has been a push toward implantation at earlier ages in the disease or soon after the appearance of motor complications. The EARLYSTIM trial was the first randomized control trial examining early implantation of DBS [23]. PD patients were implanted in the STN after carrying a diagnosis for at least 4 years; mean duration of disease was approximately 7.5 years, with dyskinesias and motor fluctuations present in patients for approximately 1.5 years. In addition, patients were only included in the study if they had a minimum 50% dopamine response. The results of this study demonstrated a significantly greater improvement in off-medication UPDRS-III motor scores of 53% for the DBS group, compared to no change for best medical therapy alone.

Smaller studies have also shown the potential benefits of earlier DBS implants. For instance, a retrospective study comparing early STN DBS (i.e., <3 years of symptoms) to late STN DBS (i.e., >3 years of symptoms) demonstrated a sustained improvement in activities of daily living at 8-year follow-up for the early stimulation patients who never reached the severe levels of disability reported by the late STN group [5]. A different study of early onset PD <4 years also showed that STN DBS is well tolerated and associated with lower medication requirements in the DBS + best medical therapy group as compared to best medical therapy alone [24]. Although there is no evidence that human DBS in PD is a restorative treatment through a regenerative process, studies in rodent models of nigrostriatal dysfunction suggest that DBS has effects on growth factor release and signaling that could potentially have clinical benefit if achieved at an earlier stage of the disease, when less nigrostriatal dopaminergic degeneration has occurred [25, 26]. A study using transcranial motor evoked potentials suggested that DBS may produce clinical benefit through restoring cortical plasticity in motor cortex [27]. This suggestion aligns with evidence that STN DBS works, in part, by reducing pathological levels of phase-amplitude coupling in motor cortex [28]. The field is still at an early stage in terms of understanding how measurable changes in physiology during DBS may impact functional connectivity across the basal ganglia-thalamocortical circuit over time [29].

In contrast to the growing evidence in support of early DBS treatment, there is limited evidence to consider deselecting patients with very advanced pathology. Vasques et al. [30] examined long-term outcomes of GPi DBS in patients with severe dystonodyskinetic syndrome at up to 8-year follow-up. When patients were separated according to the GPi volume at the time of surgery, they found that patients showing less response to DBS had significantly smaller GPi volumes. This finding suggests that the mechanisms of DBS action may require a certain minimum volume of unaffected neural tissue to be present to allow the direct effects of basal ganglia-cortical circuit neuromodulation from DBS to occur. To extend this argument, the benefits of early DBS implantation may be related to several factors related to the remaining volume of

healthy DA neurons in the substantia nigra soon after PD diagnosis, including direct symptom relief through DBS therapy, reduced LEDD over the long term, which will prolong the efficacy of levodopa, and the preserved potential for restorative processes acting throughout the cortical-basal ganglia motor circuitry. Of note, Ngoga et al. [31] reported that DBS improves survival in severe PD patients as compared to similar PD patients who declined DBS therapy, though the underlying reason for this improved survival was not be determined.

Cost-Effectiveness of DBS

One criticism of DBS therapy is related to its perceived cost-effectiveness compared to best medical therapy alone. DBS therapy does cost more than best medical therapy alone, at least up front, most of which is accounted for by the cost of the device and the implantation surgery. Several studies of cost analyses of DBS implantation in Europe [32–34], however, have shed light on the long-term costs of DBS that are favorable toward DBS, when accounting for the value of improved quality of life factors, increased productivity, reduced medication costs, and decreased PD-related injuries. For instance, Dams et al. [34] found that within the German health system, implantation according to the EARLYSTIM criteria resulted in an incremental increased cost of 22,700 EUR per quality-adjusted life year (QALY = 1 year of life × 1 utility value) for STN DBS. They concluded that the additional cost of DBS was cost-effective for the benefit in QALY, given that it was below a derived cutoff of 50,000 EUR per QALY. The United Kingdom and Swedish studies concurred and concluded that the initial costs of DBS are offset by the long-term medication savings.

Target Selection: STN vs. GPi

The majority of a now large collection of studies examining STN and GPi DBS in PD have overall demonstrated similar motor outcomes up to 6 months postoperatively. A meta-analysis of six publications involving 563 patients followed for 6–12 months [35] did not find differences in therapeutic efficacy between targets. However, STN DBS was associated with reduced medication while GPi DBS provided greater relief of psychiatric symptoms. A meta-analysis of STN DBS versus GPi DBS with multiple inclusion and exclusion criteria that assessed UPDRS III and PDQ-39 ADL scores longer than 2 years [36] showed no differences in total UPDRS III scores, no difference in motor subtypes, greater improvements in PDQ-39 ADL for GPi DBS, and greater decreases in LED scores for STN DBS. A literature review of both STN and GPi DBS therapy for PD with at least 3-year [37] and 5-year [38] outcome data concluded that DBS therapy in both targets is effective at controlling the primary motor symptoms of PD (tremor, rigidity, dystonia and on-medication dyskinesias, and motor fluctuations).

Longer-term follow-up studies suggest that the effects of stimulation at these two targets are not wholly equivalent. For instance, Rodriguez-Oroz and colleagues [7] followed patients for 4 years after implantation with STN or GPi DBS. They found that while both targets resulted in stable motor improvement, only STN DBS was associated with significant decreases in dopaminergic medication, while GPi was not. On the other hand, STN DBS was associated with worsening speech side effects and postural stability. The Netherlands SubThalamic and Pallidal Stimulation (NSTAPS) study compared symptom response and level of disability for the STN and GPi [39]. Overall, there were no differences in UPDRS scores and severity of disability during the on state. However, there were larger improvements in these domains during the off state for STN patients as well as a greater reduction in levodopa dosing. This finding suggests that the STN may be a better target than the GPi for patients with advanced PD. This finding persisted at 3-year follow-up [40]. In addition, this study did not find any differences in cognition, mood, or behavioral indices at long-term follow-up between STN and GPi DBS. However, patients in the GPi group were more likely to have a

second operation (8 patients out of 65, versus 1 patient out of 63 in the STN group) due to unsatisfactory or waning clinical effect; for those initial GPi patients, placement in the STN produced a satisfactory clinical benefit.

STN and GPi stimulation appear to result in subtle differences in motor outcomes and may also result in different non-motor effects, such as changes in neurocognitive performance and mood. The VA Cooperative study demonstrated statistically significant worsening of working memory, processing speed, phonemic fluency, and delayed visual memory in patients undergoing STN or GPi DBS versus medical management [3]. However, the magnitude of the relative impact of DBS on function must be noted. For instance, on the working memory measure, there was a 1-point improvement in the standard score for the medical management group from 97.3 to 98.3 and a 1.6-point decline in standard score for the DBS group from 101.2 to 99.6. Thus, the scores for either group are all essentially at mean values both before and after treatment. One influential finding from the subgroup analysis of the VA Cooperative study suggested differential effects of target location of DBS on cognition. Specifically, STN DBS was associated with a decline in processing speed, compared to GPi DBS [6]. Differential effects were also noted in the Cognition and Mood in Parkinson's Disease (COMPARE) trial, which was a randomized, prospective clinical trial designed to evaluate non-motor symptom change following either unilateral GPi or STN DBS [41]. This trial found no overall difference between GPi and STN DBS in motor outcomes, though there was a greater improvement in rigidity for STN DBS. However, STN DBS was associated with worsening cognitive function, a trend toward worse letter verbal fluency following STN DBS; this trend persisted despite whether the DBS was on or off. Interestingly, this worse performance in STN versus GPi implanted patients was only in letter verbal fluency, as there was no difference in semantic verbal fluency between the groups. In addition, results of the COMPARE trial suggest that stimulation of the STN may be associated with greater mood and behavioral effects. This is based on a trend toward worsening self-reported feelings of anger in STN patients, as well as a greater number of mood or behavioral postoperative complications (though GPi and STN had equivalent numbers of overall complications).

The mood changes noted in the COMPARE trial echo prior concerns that STN DBS may be associated with depression and suicidality. Indeed, one large study surveying multiple centers and encompassing over 5000 PD patients found that STN DBS was associated with a significantly increased likelihood of suicidal ideation and completed suicide than expected, based on comparison to age-matched population rates [42]. This study found that risk factors for suicide in the STN DBS PD population were being single, having a history of impulse control disorders or compulsive use of medication, and postoperative depression or apathy. Although one limitation was that there was no control group of PD patients who did not receive DBS, prior research has demonstrated that baseline suicide rates in the PD population are the same or even lower than that observed in the general population. The concern for mood changes and suicidality in PD patients undergoing STN DBS has not been supported by all studies. For instance, the VA Cooperative study demonstrated that, first and foremost, the rates of depression and suicidality were very low for PD patients out to 2 years who were treated with either DBS or best medical therapy. In addition, they found that DBS patients were more likely to feel happy, energetic, and full of life, compared to PD patients treated with best medical therapy alone [43].

It is unclear why earlier studies found an increased rate of mood disturbance and suicidality with STN DBS implantation. One hypothesis is that these changes may be the product of a rapid reduction in dopaminergic agents, following improvement in motor control with DBS. For instance, the large multicenter survey that demonstrated increased suicidality with DBS notably reported an approximately 50–60% reduction in levodopa equivalent daily dose, while the VA Cooperative study had an approximately 25% reduction. Furthermore, a study designed specifically to examine STN DBS for treating PD

patients with hyperdopaminergic profiles (e.g., impulsivity, risk-taking, compulsions, hypersexuality, etc.) accomplished a 73% reduction in levodopa dose [44]. However, they found that of the 30 patients in this study with a hyperdopaminergic profile, 18 developed apathy with DBS and concomitant levodopa reduction. Moreover, two of the patients attempted suicide. Finally, the hypothesis that mood dysregulation may be more closely tied to changes in chronic dopaminergic medication dosing is consistent with some findings that linked STN DBS to mood dysregulation, since STN stimulation results in a greater ability to decrease medications than GPi stimulation.

Subcortical Mapping Using Microelectrode Recording for DBS Placement

Precise, submillimeter targeting within the STN and GPi is critical for obtaining the best possible therapeutic effect on PD motor symptoms and for minimizing adverse motor and non-motor side effects. The 2004 book on the subject of microelectrode recording (MER) in movement disorder surgery [45] documented various opinions at that time on the arguments for and against utilizing MER to improve targeting for DBS that was based on class III evidence with no long-term outcome data to support the value of MER/neurophysiological mapping for target localization. The arguments for MER mapping to identify the borders and dimensions of the functional target include the relatively small size of the STN and GPi of around ~5 mm in the *X*-, *Y*-, and *Z*-dimensions, their depth in the brain that demands long trajectories where a small angular deviation will miss the target completely, target proximity to neighboring structures that do not tolerate current spread of more than a few millimeters such as the corticospinal and corticobulbar tracts of the internal capsule, the ascending medial lemniscus, cranial nerve III and optic tract, established brain shift that accompanies CSF egress after the dura is opened that may amount to several millimeters of shift, and, finally, the fact that for both targets, the optimal target for DBS is actually a small, sensorimotor subregion within the larger STN and GPi nuclei. Other sources of targeting errors include the settings of all hardware components which are cumulative and radiographic and software errors related to MR and CT image resolution and fusion. These collective errors were studied by Brahimaj et al. [46] who measured the final coordinates of a single MER tract at "target" with intraoperative CT and measured the radial distance error from the coordinates of the intended target location. They found a mean error of 1.23 mm from a total of 150 STN targets and a mean error of 1.10 mm from a total of 27 GPi targets. Note that these were microelectrodes placed at target coordinates determined by the initial planning that had not been adjusted based on the results of the MER and document the inherent measured and mechanical errors that arise from simply following the plan.

MER requires the isolation of single-unit action potentials generated by the cell bodies of neurons within target nuclei as the recorded unit activity reveals the frequency and pattern of single neuron activity, which, with multiple unit recordings from a small volume of target tissue, will uniquely identify one nucleus from adjacent nuclei or the functional target within a larger nucleus. Such detailed functional intranuclear mapping at ~50-micron resolution is not possible with any form of direct anatomic targeting. Characteristic patterns of unit discharge at distinct frequencies mostly have been studied to define the functional target of the STN, as the STN was initially approved as the primary target for DBS in PD. MER initially used a single tract that identified the superior and inferior boundaries of the target along the *Z*-dimension or depth within stereotactic space. The combination of a span of ~5 mm of unit activity and the recording of expected "signature" patterns of unit activity within the target defined the "gold standard" for MER to confirm an optimal tract through the center core of the functional target. The goal to maximize the span of target was mostly based on the fact that the span of the four contacts of the first approved DBS electrode is 7.5 mm, and an MER span of ~5 mm with the lowest DBS contact

placed at the inferior target border ensured that the lowest three DBS contacts were located within the functional target. Should a single MER tract not achieve this neurophysiologic and geometric definition of the optimal target, sequential single MER tracts would be performed with the *X*- or *Y*-coordinate adjusted by 2.0 mm serially until the desired targeting was achieved.

Prior to the advent of intraoperative MRI and CT use in DBS surgery, there was evidence that STN DBS placement with MER achieves more accurate targeting and improved motor outcomes compared to DBS electrodes placed without MER [47]. Specifically, they found a 25% reduction in selective components of the UPDRS III scores in 32 patients with STN DBS with MER compared to no change in postoperative UPDRS scores in ten patients with STN DBS without MER. Simultaneous MER from up to five multiple microelectrodes and the associated mapping in three dimensions further appears to improve targeting. For STN targeting, Temel et al. [48] compared two groups of patients with either sequential, single tract MER or simultaneous MER in five tracts and found significant difference in UPDRS motor score reduction at 3 months and 1 year postoperatively of 41% and 55%, respectively. Bjerknes et al. [49] compared single sequential MER to simultaneous 3-tract MER in two groups of patients in a double-blind, randomized study of two groups of 30 patients and noted a 35-point UPDRS III decrease at 12 months postoperatively in patients with multiple MER, compared to a 26-point decrease in patients randomized to sequential single tract MER. In both studies, there was no difference in the occurrence of adverse events, including hemorrhage, between single tract versus multiple simultaneous tract groups.

A large body of literature has detailed intraoperative adjustments made to the initial stereotactic plan, based on MER and macrostimulation to assess stimulation-induced side effects. Bour et al. [50] used simultaneous MER in four or five tracts and found that the targeted, center tract was used for final DBS implantation in only 50% of patients for STN and in only 57% of GPi targeted cases. Indeed, they reported that the center tract had no recorded MER activity in 9% of all STN cases. Based on MER mapping, the final position of the DBS electrode was an average of 2.1 mm below the MRI-based target for STN cases which meant that without MER mapping, only two DBS electrode contacts would have been placed within the STN as compared to three DBS electrode contacts for cases mapped with MER. A recent study reported an average error of 2.2 mm in the *X*-coordinate and of 2.0 mm in the *Y*-coordinate that would have corresponded to misplaced DBS electrode placement in ~20% of all DBS implants, had MER not been performed [51], but this study was poorly controlled. Although Shenai et al. [52] found a 58% improvement in post-op UPDRS scores with MER mapping, no statistical difference was found for STN spans of <4.8 mm as compared to >5.6 mm. However, in all 73 cases, MER did confirm that the target was within the dorsolateral STN. On the other hand, Boës et al. [53] found a highly significant correlation between MER recorded STN span (trajectory length) and 12-month improvement in UPDRS motor scores of approximately 16 points for an increase in STN span of 2 mm. Interestingly, this study found no correlation between MER-based STN span and macrostimulation threshold levels for decreases in joint rigidity or for motor tract activation.

Defining the STN "Functional" Target

Single-Unit Activity

The issue of identifying the appropriate "functional" target for DBS therapy was surveyed across PD specialists who reported a large variability in the stereotactic coordinates that were used to define the STN location for indirect targeting of the STN [54]. Further, Garcia-Garcia et al. [55] applied a novel volumetric analysis of DBS electrodes implanted in STN in 40 patients that was registered to a standardized 3D atlas which normalized the DBS electrode locations in the postoperative MRI within an ellipsoid representation of the STN. Interestingly, when the UPDRS and LED scores at 6 months were

evaluated according to the normalized location of the active DBS contact within the STN, there was a variation of DBS effects by location with the "sweet spot" for maximum clinical DBS efficacy located at the rostral and most lateral parts of the dorsolateral motor region of the STN and at the interface between the STN, zona incerta, and thalamic fasciculus. On the other hand, Bot et al. [56] found that the STN "hot spot" for optimal postoperative DBS outcomes was better localized using the medial STN border as compared to the midcommissural point. These studies and the related practice survey suggest that more research is needed to characterize and define the "functional" target *within* the sensorimotor division of the STN for optimal DBS therapy.

In addition to improving clinical outcomes in DBS therapy, MER mapping has also improved our understanding of basal ganglia physiology that in turn has produced a clear physiological definition of the optimal STN functional target which is leading to a defined neurophysiological biomarker that is specific to PD and is being used to physiologically define DBS targets and to provide a feedback measure of the efficacy of DBS therapy. Early MER studies, e.g., Hutchison et al. [57], identified unique characteristics of unit activity that was characteristic of the dorsolateral sensorimotor region of STN that included high frequencies (mean 37 Hz), bursting patterns of unit activity together with unit responsiveness to active and passive movements including so-called "tremor" cells. Seifried et al. [58] reported average STN unit frequencies of ~51 Hz that were similar in all subregions of STN. However, they also examined the patterns of unit discharge and found irregular discharge to be most common followed by burst patterns and oscillatory discharge and that the latter two patterns were far more common in the dorsal STN. Lourens et al. [59] mapped STN unit discharge frequencies and burst patterns from coherence analysis onto a generic atlas representation of the STN and confirmed a higher discharge frequency (~30 Hz) and higher incidence of bursting activity patterns to the dorsal sensorimotor STN as compared to unit activity recorded in adjacent STN regions. These unit discharge characteristic frequencies and patterns were assumed to be a marker of the functional STN target in PD based on MER studies of induced Parkinsonian NHP's before and after MPTP treatment and were confirmed in human PD patients by Steigerwald et al. [60] who recorded from the STN in both PD and ET patients undergoing MER mapping and found significantly higher STN unit discharge frequencies in PD compared to ET (40.5 Hz vs. 19.3 Hz) and that significantly more units in PD exhibited bursting activity (70% vs. 36%). Deffains et al. [61] confirmed higher unit frequencies in the dorsolateral STN compared to the ventrolateral STN (44.5 Hz vs. 39.9 Hz) and further added that unit activity in the dorsolateral STN had a higher correlation to beta-band oscillatory activity. Pozzi et al. [62] also found regional variations of pathologic bursting activity patterns and discharge rates that were more prevalent within the dorsolateral STN as compared to adjacent regions of the STN.

Within the dorsolateral STN, Guo et al. [63] recorded unit activity and determined the spectral content of the spontaneous unit neuronal discharge when there was no artefact and no movement for 17 awake, akinetic-rigid PD patients. They found the mean spontaneous firing rate was 42.0 Hz and that 56 neurons exhibiting beta-band oscillatory activity (mean 18.9 Hz) had a higher mean firing rate of 48.4 Hz compared to a firing rate of 38.9 Hz for 99 neurons with no oscillatory activity, thus specifically associating high-frequency unit discharge to beta-band activity. Guo et al. [64] further differentiated STN unit high-frequency bursting activity by the measured oscillatory activity from the same 188 STN neurons. Three patterns were found: tremor frequency band oscillations at a mean of 4.9 Hz, beta frequency-band oscillations at a mean of 21.5 Hz, and non-oscillatory units. The majority (92.2%) of the oscillatory neurons were localized in the dorsal half of the STN although the two populations were not spatially separated. Clinically, the best DBS contacts that achieved the greatest and statistically significant reductions in UPDRS III sub-scores at 12 months postoperatively (tremor 3.4 to 0.7, rigidity 4.4 to 1.6, bradykinesia 8.6 to 3.2) were localized to the

same dorsolateral STN regions that contained the greatest oscillatory firing pattern activity.

To conclude this section, there is now a large body of literature that supports the use of MER to localize PD-specific patterns of unit activity and theta-band and beta-band oscillatory activity, linked to tremor-dominant and akinetic-rigid PD subtypes, to the dorsolateral STN. Because of the design and spacing of clinical, multi-contact DBS electrodes, the submillimeter resolution of MER mapping allows mapping of the boundaries and dimensions of the posterior sensorimotor STN to achieve a minimum span of mapped STN of ~5 mm which will localize three DBS contacts to within the posterior and sensorimotor STN and achieve the greatest flexibility in utilizing monopolar or bipolar DBS from three available contacts.

Population Neuronal Discharge and Oscillatory Activity

Following from the localization of high-frequency MER unit activity in the dorsolateral STN, Brown et al. [65] found that the presence of low-frequency, beta-band (<30 Hz) oscillatory activity in STN local field potentials (LFP) was reduced by the administration of levodopa, which shifted the spectrum of oscillatory activity up to the high-frequency band at ~70 Hz. When levodopa and DBS were compared in nine PD patients, Giannicola et al. [66] found that whereas levodopa abolished STN beta LFP oscillations, DBS only decreased beta oscillations, suggesting that the two therapies modulate STN beta oscillations in different ways. Eusebio et al. [67] subsequently verified that DBS suppresses beta-band oscillations.

Levy et al. [68] found the same effect of levodopa on beta-band oscillations and additionally demonstrated that active movement also suppressed these oscillations. Cassidy et al. [69] studied the effect of movement for both STN and GPi beta-band oscillatory activity and showed that active movement reduces beta-band activity both prior to and during movement. However, in a more detailed study, Tan et al. [70] found that higher low-beta power was associated with abnormal force decrements or measures of motor impairment. Beta oscillations studied in freely moving PD subjects are not altered when subjects transition between different postures but are reduced during walking and are significantly reduced with DBS turned on at 1V and 3V stimulation [71]. In a large cohort of 63 STN implanted PD patients, Neumann et al. [72] found a significant correlation of relative spectral beta power to total UPDRS scores in the *off* state and that such correlations require akinetic symptoms to be significant [73]. Beudel et al. [74] performed the same analysis in 39 PD patients with STN DBS and also found a specific correlation of beta-band power to akinetic-rigid UPDRS sub-scores. Geng et al. [75] found that with movement-related decreases of beta-band oscillatory activity there was a concomitant increase in gamma-band oscillations and that these effects were localized more dorsally, compared to ventral regions for alpha-band modulation. Beta-band oscillatory activity is clearly associated with akinetic-rigid PD subtypes but is not sufficient to identify dyskinesia symptoms which are also associated with both low-frequency (4–8 Hz) and high-frequency synchronization [76]. Finally, tremor-dominant PD is further distinguished by the presence of gamma-band HFO which is modulated by levodopa medication [77] and by movement [78].

These studies illustrate that oscillatory activity profiles can be used in isolation or combination as electrophysiological "signatures" for refining DBS therapy for various PD symptom subtypes. As STN functional targeting is optimized using the submillimeter resolution of unit recordings in MER, an important question is to determine the link between unit activity, which has MER-base characteristics associated with localization of the STN "functional" target, and oscillatory activity that is also recorded in the dorsolateral STN. This link between unit activity and LFPs was established by the work of Kuhn et al. [79] and Weinberger et al. [80] using spike-triggered averaging to show that unit neuronal discharges locked to beta oscillations have the strongest coherence in the dorsal STN. Moran et al. [81], using similar approaches, found two distinct dominant oscillatory frequencies, at 3–7 Hz (the tremor frequency

band) and at 8–20 Hz, which varied independently, suggesting two distinct neuronal populations. The possibility of further defining the "functional" STN target using beta-band LFP activity was studied by Zaidel et al. [82] who differentiated the dorsolateral and ventromedial STN based on the association of the root mean square and power spectral density of the MER signals, coining the term dorsolateral oscillatory region. Zaidel et al. [82] further linked the best DBS contact for clinical improvement (based on postoperative UPDRS scores at an average of 16 months) to the recording span of the dorsolateral oscillatory region. Verhagen et al. [83] reported that calculating beta power only over the specific frequencies that show a significant coherence between LFP and neuronal spiking may be beneficial in discriminating the sensorimotor STN. Their results suggest that due to volume conduction of beta frequency oscillations, proper localization of the sensorimotor STN with only LFP recordings is difficult. In fact, LFP recordings of beta-band oscillatory activity alone and based on monopolar recordings may fail to localize the optimal STN target [84].

Machine learning approaches increasingly are being applied in attempts to automatically discriminate the STN. Kostoglou et al. [85] used a machine learning approach to model the correlation of various MER and LFP characteristics and improved UPDRS scores and found that five variables that corresponded to different measures of oscillatory activity were positively correlated while other measures of non-oscillatory features were anticorrelated to reduced UPDRS scores with DBS therapy. A review of ten other machine learning studies of optimizing MER characteristics [86] found that though these approaches are rigorous and quantitative, the authors felt that none were sufficiently robust to be used in clinical practice.

Circuit Analysis

Anatomic studies in nonhuman primates have shown that the major cortical connection to the dorsolateral STN is from the primary motor cortex [87]. More recently, Miocinovic et al. [88] provided evidence for the presence of a monosynaptic, hyperdirect pathway in human PD subjects from antidromic stimulation of this pathway from implanted STN electrodes to primary motor cortex recorded via electrocorticography. One study illustrated this functional connection by showing that DBS attenuates both STN and motor cortical beta-band oscillatory activity in a graded manner such that DBS neuromodulation involves cortico-basal ganglia circuitry or networks and not the basal ganglia alone [89]. Two different NHP studies have shown that both GPi [90] and STN [91] stimulation results in modulation of both oscillatory activity and single-unit discharge in primary motor cortex. Clearly, the mechanisms underlying DBS neuromodulation therapy act at the level of complex basal ganglia-cortical network circuitry.

The search for a clear functional biomarker pathognomonic for PD that could be identified intraoperatively and used to confirm optimal lead placement is complex, as it involves many different characteristics of signals that may not interact in a linear fashion and may be conditional on the state of the patient. Yang et al. [92] and Wang et al. [93] found that phase-amplitude coupling (PAC) in the STN was specific to beta phase and HFO amplitude and was strongest at the dorsal STN border involving locations where DBS contacts were most clinically effective. Additionally, excessive PAC between the STN beta phase and gamma amplitude in primary motor cortex [94] is an interaction that has been demonstrated to be reversibly reduced by therapeutic DBS of the subthalamic nucleus [28], although PAC calculations are computationally intensive, making them difficult to accomplish intraoperatively for directing targeting adjustments. Simultaneous cortical and STN LFP recordings during performance of behavioral tasks also have established the conditional nature of cortico-basal ganglia functional connectivity. For example, PD patients exhibit reductions in the high beta sensorimotor cortical PAC that is not found in non-movement disorder patients studied performing the same visually cued handgrip task [95]. However, the same study found that beta-band oscillatory activity

also is recorded in essential tremor patients, suggesting that the presence of beta-band oscillations is not exclusive to PD pathophysiology. Lipski et al. [96] recorded STN unit activity and sensorimotor LFPs in PD subjects performing a hand movement task and found that STN firing demonstrated phase synchronization to both low and high beta frequency cortical oscillations that was modulated at certain phases of movement and that was not correlated with changes in neuronal firing rate, per se. This behavioral study of basal ganglia and cortical network interactions confirms that biomarkers for PD are dynamic and conditional on the behavioral state of the patient. Indeed, it has been long known that movement itself is therapeutic in Parkinsonian patients, for instance, as shown for the effect of exercise on gait in the PRET-PD randomized trial [97], as if movement facilitates modulation of the basal ganglia cortical circuitry.

Defining the GPi "Functional" Target

Early targeting of the GPi for PD and dystonia patients was based upon nonhuman primate MER mapping studies of the sensorimotor region of the GPi which is located in the caudal region and which includes neurons shown to have altered neuronal discharge patterns in the Parkinsonian animals [98, 99]. MER mapping of the GP combined with microstimulation during pallidotomy in PD [100] further refined the optimal target by localizing the sensorimotor representation of GP and defining stimulation territories that were too close to the internal capsule and optic tracts that would result in adverse side effects of current spread from misplaced pallidotomy targets. The targeting for DBS electrodes in GP used MER to map the sensorimotor region localized to the posterolateroventral region of the GPi [101, 102]. Baker et al. [103] compiled MER mapping results from 299 patients of the unit neuronal response to active and passive movements of the face, arm, and leg. 1767 of 3183 recorded neurons that responded to a single contralateral body region were mapped according to their stereotactic coordinates to produce a three-dimensional map of the somatotopy: leg-related neurons were located dorsal, medial, and anterior to arm-related neurons which were located dorsal and lateral to orofacial-related neurons.

These mapping studies defined a relatively large volume of tissue as the sensorimotor target for GPi DBS which perhaps explains the requirement to use higher stimulation voltages for GPi DBS as compared to STN DBS [104]. However, it is possible that different regions of this large sensorimotor representation within GPi subserve different functional targets for different PD subtypes and for dystonia alone. For example, an MER mapping study of GPi and GPe unit discharge characteristics in 44 children involving 3 distinct dystonia types (14 primary, 22 secondary static, and 8 progressive secondary) found that both GPi and GPe unit neuronal discharge frequencies and discharge patterns differed significantly with dystonia etiology [105]. Interestingly, although the report does not provide maps of DBS electrode locations, the GPi discharge frequency was found to be positively correlated with DBS outcomes at 1 year, which was strongest for the secondary static group. This detailed study suggests that MER mapping is important for locating the highest frequency unit activity within GPi. Although fewer clinical outcome studies have looked at pallidal targeting with MER, Bour et al. [50] reported small but consistent targeting adjustments of the GPi target with MER. In summary, there is strong evidence to support the value of subcortical MER mapping in defining the dimensions of the functional target in STN and GPi for DBS therapy which results in greater efficacy of DBS therapy with the fewest possible side effects.

Placement of DBS Leads in the Asleep Patient with Intraoperative Imaging

Despite the progress in using MER to map and define the optimal placement of DBS electrodes, being awake during brain surgery for several hours is not possible or desirable for every PD patient. Indeed, patient selection strategies need

to be used to only perform awake DBS surgery in the most suitable patients. For patients who would be best served by asleep surgery, several approaches that reduce patient discomfort, anxiety, and fatigue may be used including implanting DBS electrodes under general anesthesia with [106] and without MER [107] and in awake patients without MER [108]. The advent of interventional MRI DBS, where a skull-mounted aiming device is combined with specialized software to enable real-time visualization of target nuclei and lead implantation [109], has been well described elsewhere [110–112]. We feel that if one forgoes MER guidance, the optimal method for targeting the correct functional subregion of each target is real-time guidance with MRI, given that years of experience using MER and numerous studies that have collectively determined and refined the functional targets within STN and GPi for optimal DBS therapy, which can be visualized on MRI. In addition, multiple studies now have provided evidence for equipoise between iMRI-guided and MER-guided lead implantation [113–116]. A more comprehensive consideration of factors, opportunities, and limitations of DBS implantation with a general anesthetic is addressed in Chap. 3.

Stimulation Programming

Clinically, DBS usually involves a very narrow set of stimulation parameters, in addition to the choice of contact(s) used for stimulation, that are known to be effective based on improvements of UPDRS scores, avoiding side effects and subjective reports. Typical parameters are frequency of 130 Hz, pulse duration of 60 microseconds, and 2–4 mA amplitude. Conway et al. [117] undertook a meta-analysis of 21 published reports that manipulated DBS parameters and assessed at least one motor symptom. Seventeen studies investigated alternate stimulation frequencies while five examined alternate stimulus amplitudes and two studied alternate pulse durations. Overall, the meta-analysis reported a low quality of evidence in support of low-frequency DBS and found that low stimulation amplitudes could lead to the reemergence of motor symptoms. Perhaps the typical high-frequency DBS is sufficient for most PD patients. Another aspect of DBS that can be adjusted is the pattern of the delivered stimulation pulses which all current DBS devices maintain at a constant frequency for the duration of the chronic stimulation train, which makes altering the pattern of stimulation very difficult to study in situ. However, work from Grill and colleagues [118] has examined the effect of using irregular stimulation pulse patterns and has shown that three non-regular patterns of stimulation performed better at improving the performance of an alternating finger tapping task in PD subjects compared to regular DBS. Other groups are working on clinical validation of the effects of coordinated reset stimulation, following remarkable results in one study of Parkinsonian nonhuman primates [119, 120]. Research on non-regular stimulation patterns thus holds much promise.

The recent advent of segmented DBS contacts already has affected how stimulation is programmed [121]. In addition, two studies have shown that LFPs can predict the most efficient stimulation contacts for therapeutic benefit and may ultimately serve as a tool for choosing the optimal contact for directional DBS [122, 123]. Given the current knowledge of several potential electrophysiological signals that may be useful biomarkers for specific movement disorder subtypes, the future of DBS is clearly moving to the utilization of closed-loop DBS based on the "sensing" of specific biomarker signals that are used to modify and adapt the delivery of stimulation. Closed-loop DBS is also referred to as adaptive DBS (aDBS), the feasibility of which has already been demonstrated [124, 125]. A recent review by Habets et al. [126] suggested the need for aDBS systems to be highly individualized due to the multitude of PD symptom phenotypes and the fact that currently available aDBS systems sense only a single electrophysiological biomarker signal that may not be representative of most patients' phenotype. To that end, Neumann et al. [127] have proposed electrophysiology-based intelligent aDBS systems that require the sensing of multiple biomarker signals that have so many combinations

and permutations that a machine learning approach would be necessary for the system to learn how to optimize feedback control over DBS to both individualize and optimize aDBS settings for optimal control of PD symptoms.

Conclusion

Modern STN and GPi DBS for PD were introduced over 20 years ago. Since then, our understanding of the pathophysiology of PD has vastly improved through the use of neurophysiological mapping of the basal ganglia which has led to increasingly better-defined functional targets for optimal DBS therapy. Electrophysiological biomarkers that are pathognomonic for PD subtypes have been identified that can be used to study the effects of various treatment modalities. The application of DBS therapy has the potential to become even smarter as individualized biomarker signals may be used as feedback signals for aDBS devices that in turn may use directional current steering to focus therapy on smaller volumes of target tissue, thus minimizing current spread and adverse side effects. Further research on the use of non-regular stimulation patterns could lead to a higher resolution of individualized neuromodulation therapy. Despite this remarkable success at controlling the primary motor symptoms of PD, long-term outcome research studies have raised some concerns over adverse non-motor symptoms associated with STN DBS, which may be avoided by improved targeting of the optimal functional STN target, or by selecting the GPi as an equivalent alternate target for certain patients with cognitive or neuropsychological comorbidities, or perhaps by using additional DBS electrodes placed in other nodes of this complex circuit not discussed in this chapter. Nonetheless, expansion of patient selection criteria to include younger and older patients, earlier use of DBS, and expanding our knowledge of basal ganglia physiology and the functional organization of basal ganglia circuits are likely to make this life-changing treatment even more effective and available to greater numbers of appropriate patients.

References

1. Benabid A, Pollak P, Louveau A, Henry S, de Rougemont J. Combined (thalamotomy and stimulation) stereotactic surgery of the VIM thalamic nucleus for bilateral Parkinson disease. Appl Neurophysiol. 1987;50:344–6.
2. Limousin P, Pollak P, Benazzouz A, Hoffmann D, Bas LJ, Broussolle E, et al. Effect of parkinsonian signs and symptoms of bilateral subthalamic nucleus stimulation. Lancet (London, England). 1995;345:91–5.
3. Weaver FM, Follett K, Stern M, Hur K, Harris C, Marks WJ, et al. Bilateral deep brain stimulation vs best medical therapy for patients with advanced Parkinson disease: a randomized controlled trial. JAMA. 2009;301:63–73.
4. Jiang L-LL, Liu J-LL FX-LL, Xian W-BB GJ, Liu Y-MM, et al. Long-term efficacy of subthalamic nucleus deep brain stimulation in Parkinson's disease: a 5-year follow-up study in China. Chin Med J. 2015;128:2433–8.
5. Merola A, Romagnolo A, Bernardini A, Rizzi L, Artusi CA, Lanotte M, et al. Earlier versus later subthalamic deep brain stimulation in Parkinson's disease. Parkinsonism Relat Disord. 2015;21:972–5.
6. Follett KA, Weaver FM, Stern M, Hur K, Harris CL, Luo P, et al. Pallidal versus subthalamic deep-brain stimulation for Parkinson's disease. N Engl J Med. 2010;362:2077–91.
7. Rodriguez-Oroz M, Obeso J, Lang A, Houeto J-LL, Pollak P, Rehncrona S, et al. Bilateral deep brain stimulation in Parkinson's disease: a multicentre study with 4 years follow-up. Brain J Neurol. 2005;128:2240–9.
8. Lilleeng B, Gjerstad M, Baardsen R, Dalen I, Larsen J. The long-term development of non-motor problems after STN-DBS. Acta Neurol Scand. 2015;132:251–8.
9. Zibetti M, Merola A, Rizzi L, Ricchi V, Angrisano S, Azzaro C, et al. Beyond nine years of continuous subthalamic nucleus deep brain stimulation in Parkinson's disease. Mov Disord. 2011;26:2327–34.
10. Lin HY, Hasegawa H, Mundil N, Samuel M, Ashkan K. Patients' expectations and satisfaction in subthalamic nucleus deep brain stimulation for Parkinson disease: 6-year follow-up. World Neurosurg. 2019;121:e654–60.
11. Castrioto A, Lozano AM, Poon Y-YY, Lang AE, Fallis M, Moro E. Ten-year outcome of subthalamic stimulation in Parkinson disease: a blinded evaluation. Arch Neurol. 2011;68:1550–6.
12. Henriksen BM, Johnsen E, Sunde N, Vase A, Gjelstrup M, Østergaard K. Surviving 10 years with deep brain stimulation for Parkinson's disease – a follow-up of 79 patients. Eur J Neurol. 2016;23:53–61.
13. Janssen ML, Duits AA, Turaihi AH, Ackermans L, Leentjens AF, Leentjes AF, et al. Subthalamic

nucleus high-frequency stimulation for advanced Parkinson's disease: motor and neuropsychological outcome after 10 years. Stereotact Funct Neurosurg. 2014;92:381–7.
14. Limousin P, Foltynie T. Long-term outcomes of deep brain stimulation in Parkinson disease. Nat Rev Neurol. 2019;15:234–42.
15. Volkmann J, Albanese A, Kulisevsky J, Tornqvist A-LL, Houeto J-LL, Pidoux B, et al. Long-term effects of pallidal or subthalamic deep brain stimulation on quality of life in Parkinson's disease. Mov Disord. 2009;24:1154–61.
16. Moro E, Lozano AM, Pollak P, Agid Y, Rehncrona S, Volkmann J, et al. Long-term results of a multicenter study on subthalamic and pallidal stimulation in Parkinson's disease. Mov Disord. 2010;25:578–86.
17. Defer G, Widner H, Marié R, Rémy P, Levivier M. Core assessment program for surgical interventional therapies in Parkinson's disease (CAPSIT-PD). Mov Disord. 1999;14:572–84.
18. Kleiner-Fisman G, Herzog J, Fisman DN, Tamma F, Lyons KE, Pahwa R, et al. Subthalamic nucleus deep brain stimulation: summary and meta-analysis of outcomes. Mov Disord. 2006;21(Suppl 14):S290–304.
19. Galati S, Stefani A. Deep brain stimulation of the subthalamic nucleus: all that glitters isn't gold? Mov Disord. 2015;30:632–7.
20. deSouza R, Akram H, Low H, Green A, Ashkan K, Schapira A. The timing of deep brain stimulation for Parkinson disease in the UK from 1997 to 2012. Eur J Neurol. 2015;22:1415–7.
21. DeLong MR, Huang KT, Gallis J, Lokhnygina Y, Parente B, Hickey P, et al. Effect of advancing age on outcomes of deep brain stimulation for Parkinson disease. JAMA Neurol. 2014;71:1290–5.
22. Shalash A, Alexoudi A, Knudsen K, Volkmann J, Mehdorn M, Deuschl G. The impact of age and disease duration on the long term outcome of neurostimulation of the subthalamic nucleus. Parkinsonism Relat Disord. 2014;20:47–52.
23. Schuepbach WMM, Rau J, Knudsen K, Volkmann J, Krack P, Timmermann L, et al. Neurostimulation for Parkinson's disease with early motor complications. N Engl J Med. 2013;368:610–22.
24. Charles D, Konrad PE, Neimat JS, Molinari AL, Tramontana MG, Finder SG, et al. Subthalamic nucleus deep brain stimulation in early stage Parkinson's disease. Parkinsonism Relat Disord. 2014;20:731–7.
25. Spieles-Engemann AL, Steece-Collier K, Behbehani MM, Collier TJ, Wohlgenant SL, Kemp CJ, et al. Subthalamic nucleus stimulation increases brain derived neurotrophic factor in the nigrostriatal system and primary motor cortex. J Park Dis. 2011;1:123–36.
26. Fischer D, Kemp CJ, Cole-Strauss A, Polinski NK, Paumier KL, Lipton JW, et al. Subthalamic nucleus deep brain stimulation employs trkB signaling for neuroprotection and functional restoration. J Neurosci Off J Soc Neurosci. 2017;37:6786–96.
27. Kim SJ, Udupa K, Ni Z, Moro E, Gunraj C, Mazzella F, et al. Effects of subthalamic nucleus stimulation on motor cortex plasticity in Parkinson disease. Neurology. 2015;85:425–32.
28. de Hemptinne C, Swann NC, Ostrem JL, Ryapolova-Webb ES, Luciano M, Galifianakis NB, et al. Therapeutic deep brain stimulation reduces cortical phase-amplitude coupling in Parkinson's disease. Nat Neurosci. 2015;18:779–86.
29. Alhourani A, Well MM, Randazzo MJ, Wozny TA, Kondylis ED, Lipski WJ, et al. Network effects of deep brain stimulation. J Neurophysiol. 2015;114:2105–17.
30. Vasques X, Cif L, Hess O, Gavarini S, Mennessier G, Coubes P. Prognostic value of globus pallidus internus volume in primary dystonia treated by deep brain stimulation. J Neurosurg. 2009;110:220–8.
31. Ngoga D, Mitchell R, Kausar J, Hodson J, Harries A, Pall H. Deep brain stimulation improves survival in severe Parkinson's disease. J Neurol Neurosurg Psychiatry. 2014;85:17–22.
32. Eggington S, Brandt A, Rasmussen RE, Grifi M, Nyberg J. Cost-effectiveness of deep brain stimulation (Dbs) in the management of advanced Parkinson's disease: a Swedish Payer Perspective. Value Health. 2015;18:A352.
33. Eggington S, Valldeoriola F, Chaudhuri K, Ashkan K, Annoni E, Deuschl G. The cost-effectiveness of deep brain stimulation in combination with best medical therapy, versus best medical therapy alone, in advanced Parkinson's disease. J Neurol. 2014;261:106–16.
34. Dams J, Balzer-Geldsetzer M, Siebert U, Deuschl G, Uepbach W, Krack P, et al. Cost-effectiveness of neurostimulation in Parkinson's disease with early motor complications. Mov Disord. 2016;31:1183–91.
35. Liu Y, Li W, Tan C, Liu X, Wang X, Gui Y, et al. Meta-analysis comparing deep brain stimulation of the globus pallidus and subthalamic nucleus to treat advanced Parkinson disease. J Neurosurg. 2014;121:709–18.
36. Peng L, Fu J, Ming Y, Zeng S, He H, Chen L. The long-term efficacy of STN vs GPi deep brain stimulation for Parkinson disease: a meta-analysis. Medicine. 2018;97:e12153.
37. Mansouri A, Taslimi S, Badhiwala JH, Witiw CD, Nassiri F, Odekerken VJ, et al. Deep brain stimulation for Parkinson's disease: meta-analysis of results of randomized trials at varying lengths of follow-up. J Neurosurg. 2018;128:1199–213.
38. Rodriguez-Oroz MC, Moro E, Krack P. Long-term outcomes of surgical therapies for Parkinson's disease. Mov Disord. 2012;27:1718–28.
39. Odekerken VJ, van Laar T, Staal MJ, Mosch A, Hoffmann CF, Nijssen PC, et al. Subthalamic nucleus versus globus pallidus bilateral deep brain stimulation for advanced Parkinson's disease (NSTAPS

study): a randomised controlled trial. Lancet Neurol. 2013;12:37–44.
40. Odekerken VJ, Boel JA, Schmand BA, de Haan RJ, Figee M, van den Munckhof P, et al. GPi vs STN deep brain stimulation for Parkinson disease: three-year follow-up. Neurology. 2016;86:755–61.
41. Okun MS, Fernandez HH, Wu SS, Kirsch-Darrow L, Bowers D, Bova F, et al. Cognition and mood in Parkinson's disease in subthalamic nucleus versus globus pallidus interna deep brain stimulation: the COMPARE trial. Ann Neurol. 2009;65:586–95.
42. Voon V, Krack P, Lang AE, Lozano AM, Dujardin K, Schüpbach M, et al. A multicentre study on suicide outcomes following subthalamic stimulation for Parkinson's disease. Brain J Neurol. 2008;131:2720–8.
43. Weintraub D, Duda JE, Carlson K, Luo P, Sagher O, Stern M, et al. Suicide ideation and behaviours after STN and GPi DBS surgery for Parkinson's disease: results from a randomised, controlled trial. J Neurol Neurosurg Psychiatry. 2013;84:1113–8.
44. Lhommée E, Klinger H, Thobois S, Schmitt E, Ardouin C, Bichon A, et al. Subthalamic stimulation in Parkinson's disease: restoring the balance of motivated behaviours. Brain J Neurol. 2012;135:1463–77.
45. Israel Z, Burchiel KJ. Microelectrode recording in movement disorders surgery. New York: Thieme; 2004.
46. Brahimaj B, Kochanski RB, Sani S. Microelectrode accuracy in deep brain stimulation surgery. J Clin Neurosci. 2018;50:58–61.
47. Reck C, Maarouf M, Wojtecki L, Groiss SJ, Florin E, Sturm V, et al. Clinical outcome of subthalamic stimulation in Parkinson's disease is improved by intraoperative multiple trajectories microelectrode recording. J Neurol Surg A Cent Eur Neurosurg. 2012;73:377–86.
48. Temel Y, Wilbrink P, Duits A, Boon P, Tromp S, Ackermans L, et al. Single electrode and multiple electrode guided electrical stimulation of the subthalamic nucleus in advanced Parkinson's disease. Neurosurgery. 2007;61:346–55; discussion 355–7.
49. Bjerknes S, Toft M, Konglund AE, Pham U, Waage TR, Pedersen L, et al. Multiple microelectrode recordings in STN-DBS surgery for Parkinson's disease: a randomized study. Mov Disord Clin Pract. 2018;5:296–305.
50. Bour LJ, Contarino M, Foncke EM, de Bie RM, van den Munckhof P, Speelman JD, et al. Long-term experience with intraoperative microrecording during DBS neurosurgery in STN and GPi. Acta Neurochir. 2010;152:2069–77.
51. Lozano CS, Ranjan M, Boutet A, Xu DS, Kucharczyk W, Fasano A, et al. Imaging alone versus microelectrode recording-guided targeting of the STN in patients with Parkinson's disease. J Neurosurg. 2018:1–6.
52. Shenai MB, Patel DM, Romeo A, Whisenhunt J, Walker HC, Guthrie S, et al. The relationship of electrophysiologic subthalamic nucleus length as a predictor of outcomes in deep brain stimulation for Parkinson disease. Stereotact Funct Neurosurg. 2017;95:341–7.
53. Boëx C, Tyrand R, Horvath J, Fleury V, Sadri S, Corniola M, et al. What is the best electrophysiologic marker of the outcome of subthalamic nucleus stimulation in Parkinson disease? World Neurosurg. 2018;120:e1217–24.
54. Hamel W, Köppen JA, Alesch F, Antonini A, Barcia JA, Bergman H, et al. Targeting of the subthalamic nucleus for deep brain stimulation: a survey among Parkinson disease specialists. World Neurosurg. 2017;99:41–6.
55. Garcia-Garcia D, Guridi J, Toledo JB, Alegre M, Obeso JA, Rodríguez-Oroz MC. Stimulation sites in the subthalamic nucleus and clinical improvement in Parkinson's disease: a new approach for active contact localization. J Neurosurg. 2016;125:1068–79.
56. Bot M, Schuurman P, Odekerken VJ, Verhagen R, Contarino FM, Bie RM, et al. Deep brain stimulation for Parkinson's disease: defining the optimal location within the subthalamic nucleus. J Neurol Neurosurg Psychiatry. 2018;89:493–8.
57. Hutchison W, Allan R, Opitz H, Levy R, Dostrovsky J, Lang A, et al. Neurophysiological identification of the subthalamic nucleus in surgery for Parkinson's disease. Ann Neurol. 1998;44:622–8.
58. Seifried C, Weise L, Hartmann R, Gasser T, Baudrexel S, Szelényi A, et al. Intraoperative microelectrode recording for the delineation of subthalamic nucleus topography in Parkinson's disease. Brain Stimul. 2012;5:378–87.
59. Lourens M, Meijer H, Contarino M, van den Munckhof P, Schuurman P, van Gils S, et al. Functional neuronal activity and connectivity within the subthalamic nucleus in Parkinson's disease. Clin Neurophysiol. 2013;124:967–81.
60. Steigerwald F, Pötter M, Herzog J, Pinsker M, Kopper F, Mehdorn H, et al. Neuronal activity of the human subthalamic nucleus in the parkinsonian and nonparkinsonian state. J Neurophysiol. 2008;100:2515–24.
61. Deffains M, Holland P, Moshel S, de Noriega F, Bergman H, Israel Z. Higher neuronal discharge rate in the motor area of the subthalamic nucleus of Parkinsonian patients. J Neurophysiol. 2014;112:1409–20.
62. Pozzi NG, Arnulfo G, Canessa A, Steigerwald F, Nickl R, Homola GA, et al. Distinctive neuronal firing patterns in subterritories of the subthalamic nucleus. Clin Neurophysiol. 2016;127:3387–93.
63. Guo S, Zhuang P, Zheng Z, Zhang Y, Li J, Li Y. Neuronal firing patterns in the subthalamic nucleus in patients with akinetic-rigid-type Parkinson's disease. J Clin Neurosci. 2012;19:1404–7.
64. Guo S, Zhuang P, Hallett M, Zheng Z, Zhang Y, Li J, et al. Subthalamic deep brain stimulation for Parkinson's disease: correlation between locations

of oscillatory activity and optimal site of stimulation. Parkinsonism Relat Disord. 2013;19:109–14.
65. Brown P, Oliviero A, Mazzone P, Insola A, Tonali P, Lazzaro DV. Dopamine dependency of oscillations between subthalamic nucleus and pallidum in Parkinson's disease. J Neurosci Off J Soc Neurosci. 2001;21:1033–8.
66. Giannicola G, Marceglia S, Rossi L, Mrakic-Sposta S, Rampini P, Tamma F, et al. The effects of levodopa and ongoing deep brain stimulation on subthalamic beta oscillations in Parkinson's disease. Exp Neurol. 2010;226:120–7.
67. Eusebio A, Thevathasan W, Gaynor DL, Pogosyan A, Bye E, Foltynie T, et al. Deep brain stimulation can suppress pathological synchronisation in parkinsonian patients. J Neurol Neurosurg Psychiatry. 2011;82:569.
68. Levy R, Ashby P, Hutchison WD, Lang AE, Lozano AM, Dostrovsky JO. Dependence of subthalamic nucleus oscillations on movement and dopamine in Parkinson's disease. Brain J Neurol. 2002;125:1196–209.
69. Cassidy M, Mazzone P, Oliviero A, Insola A, Tonali P, Lazzaro V, et al. Movement-related changes in synchronization in the human basal ganglia. Brain J Neurol. 2002;125:1235–46.
70. Tan H, Pogosyan A, Anzak A, Foltynie T, Limousin P, Zrinzo L, et al. Frequency specific activity in subthalamic nucleus correlates with hand bradykinesia in Parkinson's disease. Exp Neurol. 2013;240:122–9.
71. Quinn EJ, Blumenfeld Z, Velisar A, Koop MM, Shreve LA, Trager MH, et al. Beta oscillations in freely moving Parkinson's subjects are attenuated during deep brain stimulation. Mov Disord. 2015;30:1750–8.
72. Neumann W-JJ, Degen K, Schneider G-HH, Brücke C, Huebl J, Brown P, et al. Subthalamic synchronized oscillatory activity correlates with motor impairment in patients with Parkinson's disease. Mov Disord. 2016;31:1748–51.
73. Neumann W-JJ, Kühn AA. Subthalamic beta power-Unified Parkinson's disease rating scale III correlations require akinetic symptoms. Mov Disord. 2017;32:175–6.
74. Beudel M, Oswal A, Jha A, Foltynie T, Zrinzo L, Hariz M, et al. Oscillatory beta power correlates with akinesia-rigidity in the parkinsonian subthalamic nucleus. Mov Disord. 2017;32:174–5.
75. Geng X, Xu X, Horn A, Li N, Ling Z, Brown P, et al. Intra-operative characterisation of subthalamic oscillations in Parkinson's disease. Clin Neurophysiol. 2018;129(5):1001–10.
76. Alegre M, López-Azcárate J, Alonso-Frech F, Rodríguez-Oroz MC, Valencia M, Guridi J, et al. Subthalamic activity during diphasic dyskinesias in Parkinson's disease. Mov Disord. 2012;27:1178–81.
77. Hirschmann J, Butz M, Hartmann CJ, Hoogenboom N, Özkurt TE, Vesper J, et al. Parkinsonian rest tremor is associated with modulations of subthalamic high-frequency oscillations. Mov Disord. 2016;31:1551–9.
78. Lofredi R, Neumann W-JJ, Bock A, Horn A, Huebl J, Siegert S, et al. Dopamine-dependent scaling of subthalamic gamma bursts with movement velocity in patients with Parkinson's disease. elife. 2018;7.
79. Kühn AA, Trottenberg T, Kivi A, Kupsch A, Schneider G-HH, Brown P. The relationship between local field potential and neuronal discharge in the subthalamic nucleus of patients with Parkinson's disease. Exp Neurol. 2005;194:212–20.
80. Weinberger M, Mahant N, Hutchison WD, Lozano AM, Moro E, Hodaie M, et al. Beta oscillatory activity in the subthalamic nucleus and its relation to dopaminergic response in Parkinson's disease. J Neurophysiol. 2006;96:3248–56.
81. Moran A, Bergman H, Israel Z, Bar-Gad I. Subthalamic nucleus functional organization revealed by parkinsonian neuronal oscillations and synchrony. Brain. 2008;131:3395–409.
82. Zaidel A, Spivak A, Grieb B, Bergman H, Israel Z. Subthalamic span of beta oscillations predicts deep brain stimulation efficacy for patients with Parkinson's disease. Brain J Neurol. 2010;133:2007–21.
83. Verhagen R, Zwartjes DG, Heida T, Wiegers EC, Contarino M, de Bie RM, et al. Advanced target identification in STN-DBS with beta power of combined local field potentials and spiking activity. J Neurosci Methods. 2015;253:116–25.
84. Telkes I, Ince N, Onaran I, Abosch A. Spatiospectral characterization of local field potentials in the subthalamic nucleus via multitrack microelectrode recordings. Conference proceedings: Annual International Conference of the IEEE Engineering in Medicine and Biology Society IEEE Engineering in Medicine and Biology Society Annual Conference. 2015;2015:5561–4.
85. Kostoglou K, Michmizos KP, Stathis P, Sakas D, Nikita KS, Mitsis GD. Classification and prediction of clinical improvement in deep brain stimulation from intraoperative microelectrode recordings. IEEE Trans Biomed Eng. 2017;64:1123–30.
86. Wan KR, Maszczyk T, See AA, Dauwels J, King NK. A review on microelectrode recording selection of features for machine learning in deep brain stimulation surgery for Parkinson's disease. Clin Neurophysiol. 2019;130:145–54.
87. Nambu A, Takada M, Inase M, Tokuno H. Dual somatotopical representations in the primate subthalamic nucleus: evidence for ordered but reversed body-map transformations from the primary motor cortex and the supplementary motor area. J Neurosci Off J Soc Neurosci. 1996;16:2671–83.
88. Miocinovic S, de Hemptinne C, Chen W, Isbaine F, Willie JT, Ostrem JL, et al. Cortical potentials evoked by subthalamic stimulation demonstrate a short latency hyperdirect pathway in humans. J Neurosci Off J Soc Neurosci. 2018;38:9129.

89. Whitmer D, de Solages C, Hill B, Yu H, Henderson JM, Bronte-Stewart H. High frequency deep brain stimulation attenuates subthalamic and cortical rhythms in Parkinson's disease. Front Hum Neurosci. 2012;6:155.
90. McCairn KW, Turner RS. Deep brain stimulation of the globus pallidus internus in the parkinsonian primate: local entrainment and suppression of low-frequency oscillations. J Neurophysiol. 2009;101:1941–60.
91. Johnson LA, Xu W, Baker KB, Zhang J, Vitek JL. Modulation of motor cortex neuronal activity and motor behavior during subthalamic nucleus stimulation in the normal primate. J Neurophysiol. 2015;113:2549–54.
92. Yang AI, Vanegas N, Lungu C, Zaghloul KA. Beta-coupled high-frequency activity and beta-locked neuronal spiking in the subthalamic nucleus of Parkinson's disease. J Neurosci Off J Soc Neurosci. 2014;34:12816–27.
93. Wang DD, de Hemptinne C, Miocinovic S, Qasim SE, Miller AM, Ostrem JL, et al. Subthalamic local field potentials in Parkinson's disease and isolated dystonia: an evaluation of potential biomarkers. Neurobiol Dis. 2016;89:213–22.
94. de Hemptinne C, Ryapolova-Webb ES, Air EL, Garcia PA, Miller KJ, Ojemann JG, et al. Exaggerated phase-amplitude coupling in the primary motor cortex in Parkinson disease. Proc Natl Acad Sci U S A. 2013;110:4780–5.
95. Kondylis ED, Randazzo MJ, Alhourani A, Lipski WJ, Wozny TA, Pandya Y, et al. Movement-related dynamics of cortical oscillations in Parkinson's disease and essential tremor. Brain J Neurol. 2016;139:2211–23.
96. Lipski WJ, Wozny TA, Alhourani A, Kondylis ED, Turner RS, Crammond DJ, et al. Dynamics of human subthalamic neuron phase-locking to motor and sensory cortical oscillations during movement. J Neurophysiol. 2017;118:1472–87.
97. Rafferty MR, Prodoehl J, Robichaud JA, David FJ, Poon C, Goelz LC, et al. Effects of 2 years of exercise on gait impairment in people with Parkinson disease: the PRET-PD randomized trial. J Neurol Phys Ther. 2017;41:21–30.
98. DeLong M, Crutcher MD, Georgopoulos A. Primate globus pallidus and subthalamic nucleus: functional organization. J Neurophysiol. 1985;53:530–43.
99. Bergman H, Wichmann T, Karmon B, MR DL. The primate subthalamic nucleus. II. Neuronal activity in the MPTP model of parkinsonism. J Neurophysiol. 1994;72(2):507–20.
100. Vitek J, Bakay R, Hashimoto T, Kaneoke Y, et al. Microelectrode-guided pallidotomy: technical approach and its application in medically intractable Parkinson's disease. J Neurosurg. 1998;88(6):1027–43.
101. Vayssiere N, van der Gaag N, Cif L, Hemm S, et al. Deep brain stimulation for dystonia confirming a somatotopic organization in the globus pallidus internus. J Neurosurg. 2004;101(2):181–8.
102. Chang EF, Turner RS, Ostrem JL, Davis VR, Starr PA. Neuronal responses to passive movement in the globus pallidus internus in primary dystonia. J Neurophysiol. 2007;98:3696–707.
103. Baker KB, Lee JY, Mavinkurve G, Russo GS, Walter B, DeLong MR, et al. Somatotopic organization in the internal segment of the globus pallidus in Parkinson's disease. Exp Neurol. 2010;222:219–25.
104. Ostrem JL, Starr PA. Treatment of dystonia with deep brain stimulation. Neurotherapeutics. 2008;5:320–30.
105. McClelland V, Valentin A, Rey H, Lumsden D, Elze M, Selway R, et al. Differences in globus pallidus neuronal firing rates and patterns relate to different disease biology in children with dystonia. J Neurol Neurosurg Psychiatry. 2016;87:958–67.
106. Harries AM, Kausar J, Roberts SA, Mocroft A, Hodson JA, Pall HS, et al. Deep brain stimulation of the subthalamic nucleus for advanced Parkinson disease using general anesthesia: long-term results. J Neurosurg. 2012;116:107–13.
107. Burchiel KJ, McCartney S, Lee A, Raslan AM. Accuracy of deep brain stimulation electrode placement using intraoperative computed tomography without microelectrode recording. J Neurosurg. 2013;119:301–6.
108. Aviles-Olmos I, Kefalopoulou Z, Tripoliti E, Candelario J, Akram H, Martinez-Torres I, et al. Long-term outcome of subthalamic nucleus deep brain stimulation for Parkinson's disease using an MRI-guided and MRI-verified approach. J Neurol Neurosurg Psychiatry. 2014;85:1419–25.
109. Larson PS, Starr PA, Bates G, Tansey L, Richardson R, Martin AJ. An optimized system for interventional magnetic resonance imaging-guided stereotactic surgery: preliminary evaluation of targeting accuracy. Neurosurgery. 2012;70:95–103. discussion 103
110. Larson PS, Starr PA, Martin AJ. Deep brain stimulation: interventional and intraoperative MRI approaches. Prog Neurol Surg. 2018;33:187–97.
111. Lee PS, Richardson RM. Interventional MRI–guided deep brain stimulation lead implantation. Neurosurg Clin N Am [Internet]. 2017;28:535–44. Available from: http://www.sciencedirect.com/science/article/pii/S1042368017300657.
112. Richardson RM, Golby AJ. Chapter 13: Functional neurosurgery: deep brain stimulation and gene therapy. In: Image guided neurosurgery [Internet]. Cambridge, Massachusetts, USA: Academic Press; 2015. p. 297–323. Available from: https://www.sciencedirect.com/science/article/pii/B9780128008706000133.
113. Lee PS, Weiner GM, Corson D, Kappel J, Chang Y-FF, Suski VR, et al. Outcomes of interventional-MRI versus microelectrode recording-guided subthalamic deep brain stimulation. Front Neurol. 2018;9:241.

114. Ostrem JL, Ziman N, Galifianakis NB, Starr PA, Luciano MS, Katz M, et al. Clinical outcomes using ClearPoint interventional MRI for deep brain stimulation lead placement in Parkinson's disease. J Neurosurg. 2016;124:908–16.
115. Ostrem JL, Galifianakis NB, Markun LC, Grace JK, Martin AJ, Starr PA, et al. Clinical outcomes of PD patients having bilateral STN DBS using high-field interventional MR-imaging for lead placement. Clin Neurol Neurosurg. 2013;115:708–12.
116. Sidiropoulos C, Rammo R, Merker B, Mahajan A, LeWitt P, Kaminski P, et al. Intraoperative MRI for deep brain stimulation lead placement in Parkinson's disease: 1 year motor and neuropsychological outcomes. J Neurol. 2016;263:1226–31.
117. Conway ZJ, Silburn PA, Thevathasan W, Maley KO, Naughton GA, Cole MH. Alternate subthalamic nucleus deep brain stimulation parameters to manage motor symptoms of Parkinson's disease: systematic review and meta-analysis. Mov Disord Clin Pract. 2019;6:17–26.
118. Brocker DT, Swan BD, Turner DA, Gross RE, Tatter SB, Koop MM, et al. Improved efficacy of temporally non-regular deep brain stimulation in Parkinson's disease. Exp Neurol. 2013;239:60–7.
119. Tass PA, Qin L, Hauptmann C, Dovero S, Bezard E, Boraud T, et al. Coordinated reset has sustained aftereffects in Parkinsonian monkeys. Ann Neurol. 2012;72:816–20.
120. Adamchic I, Hauptmann C, Barnikol UB, Pawelczyk N, Popovych O, Barnikol TT, et al. Coordinated reset neuromodulation for Parkinson's disease: proof-of-concept study. Mov Disord. 2014;29:1679–84.
121. Dembek TA, Reker P, Visser-Vandewalle V, Wirths J, Treuer H, Klehr M, et al. Directional DBS increases side-effect thresholds-A prospective, double-blind trial. Mov Disord. 2017;32:1380–8.
122. Tinkhauser G, Pogosyan A, Debove I, Nowacki A, Shah S, Seidel K, et al. Directional local field potentials: a tool to optimize deep brain stimulation. Mov Disord. 2018;33(1):159–64.
123. Bour L, Lourens M, Verhagen R, de Bie R, van den Munckhof P, Schuurman P, et al. Directional recording of subthalamic spectral power densities in Parkinson's disease and the effect of steering deep brain stimulation. Brain Stimul. 2015;8:730–41.
124. Velisar A, Syrkin-Nikolau J, Blumenfeld Z, Trager MH, Afzal MF, Prabhakar V, et al. Dual threshold neural closed loop deep brain stimulation in Parkinson disease patients. Brain Stimul. 2019;12(4):868–76.
125. Arlotti M, Marceglia S, Foffani G, Volkmann J, Lozano AM, Moro E, et al. Eight-hours adaptive deep brain stimulation in patients with Parkinson disease. Neurology. 2018;90:e971–6.
126. Habets JG, Heijmans M, Kuijf ML, Janssen ML, Temel Y, Kubben PL. An update on adaptive deep brain stimulation in Parkinson's disease. Mov Disord. 2018;33:1834–43.
127. Neumann W-JJ, Turner RS, Blankertz B, Mitchell T, Kühn AA, Richardson R. Toward electrophysiology-based intelligent adaptive deep brain stimulation for movement disorders. Neurotherapeutics. 2019;16:105–18.

Parkinson's Disease: Lesions

19

Juliana Rotter and G. Rees Cosgrove

Historical Background

Rest tremor, bradykinesia, postural instability, and rigidity have remained the principle diagnostic criteria for Parkinson disease (PD) since James Parkinson's early description in 1817 [1]. Leriche performed the earliest known PD surgery in 1912—a bilateral posterior cervical rhizotomy for rigidity [2]. For the next several decades, surgeons began experimenting with lesioning the pyramidal tracts: motor cortectomy [3], midbrain pedunculotomy [4], cerebellar dentatectomy [5], anterolateral cordotomy [6], lateral pyramidal tractotomy [7], posterolateral chordotomy [8], sympathetic ramicotomy, and ganglionectomy [9]. After an inadvertent anterior choroidal artery occlusion during a midbrain pedunculotomy arrested a patient's tremor without hemiplegia, Cooper went on to perform planned surgical ligations of the anterior choroidal artery to alleviate tremor and rigidity. As expected due to the variable distribution of the anterior choroidal artery, surgical results were less than predictable [10, 11]. In 1939, Meyers performed the first surgery targeting the basal ganglia by ablating 2/3 of the caudate nucleus head to induce tremor cessation [12]. With the goal of identifying the optimal target, he subsequently designed a series of experimental surgeries in the extrapyramidal structures, the internal capsule, and pallidofugal fibers using local anesthesia to be able to correlate incremental lesions with clinical response in real time. His systematic approach led him to conclude that pallidofugal targets were superior in reducing tremor and rigidity [13].

Spiegel and Wycis revolutionized functional neurosurgery in 1947 by introducing stereotactic equipment to enable accurate and reproducible lesions in deep brain structures. Numerous stereotactic atlases were subsequently published using the intercommissural line to define the coordinate system [14]. Surgeons favored pallidotomy in parkinsonian patients and experimented not only with novel stereotaxic methods but also with lesioning modalities during both open and closed surgeries—coagulation, chemicals, ultrasound, and electrolysis [15–18]. Patients achieved greatest therapeutic benefit from lesions in the ventral and posterior regions of the globus pallidus interna [19]. After an accidental thalamotomy serendipitously arrested tremor and supported by the meticulous neuroanatomical work by Hassler, pallidotomy fell out of favor even though it produced superior reduc-

J. Rotter
Department of Neurologic Surgery, Mayo Clinic, Rochester, MN, USA

G. R. Cosgrove (✉)
Epilepsy and Functional Neurosurgery, Department of Neurosurgery, Brigham and Women's Hospital, Boston, MA, USA
e-mail: rees.cosgrove@gmail.com

N. Pouratian, S. A. Sheth (eds.), *Stereotactic and Functional Neurosurgery*,
https://doi.org/10.1007/978-3-030-34906-6_19

tions in rigidity and bradykinesia scores [20]. The next technical advance, microelectrode recordings, allowed electrophysiologists to rigorously analyze the anatomic components integral to movement disorders and enabled surgeons to more precisely define thalamic borders in the operating room. With these methods, surgeons were able to identify the optimal thalamic target for tremor control: the ventral intermediate nucleus. However, these lesions provided little relief of akinesia and rigidity [21]. The subthalamic region was also explored during this period as a method to interrupt pallidofugal and rubrothalamic fibers [22].

Although over 37,000 stereotactic neurosurgical operations had been performed for movement disorders predominately for PD, the introduction of levodopa led to a near-complete abandonment of neurosurgical interventions for PD [23]. Several factors accounted for the eventual resurgence of surgical management of the disease: levodopa's diminished effectiveness over time, the development of medically refractory symptoms (flexed posture, freezing, loss of reflexes), and disabling side effects that significantly impaired quality of life (dyskinesias, motor fluctuations, psychiatric conditions) [24]. Laitinen's 1992 landmark paper reintroduced posteroventral pallidotomy as an effective tool for managing advanced PD; his lesions produced excellent and durable reductions in tremor, rigidity, bradykinesia, and medication-induced dyskinesias with few side effects [25, 26]. Bilateral pallidotomies were trialed, and though patients experienced greater benefit than after unilateral operations, many reported greater risk of severe complications including dysarthria, gait disturbance, and swallowing difficulties [27]. Both unilateral and bilateral subthalamotomies were also revisited as lesioning targets in PD with improvements in all cardinal symptoms and reductions in levodopa-induced dyskinesias; however, improvements in tremor and dyskinesias seemed to be temporary and side effects more apparent [28, 29].

The introduction of deep brain stimulation (DBS) in the 1990s relegated lesioning to second-line therapy once again. The observation that high-frequency macrostimulation abolished tremor and predicted successful surgical outcome during thalamotomy served as the foundation for DBS technology. In DBS, the stimulation from a permanently implanted electrode was found to produce similar functional improvements as ablation and with an improved safety profile [30]. Lesioning became reserved for patients with contraindications to DBS, who did not achieve sufficient improvement from DBS, or for whom the cost of DBS and associated medical follow-up would prove too burdensome [31].

Advances in neuroimaging have improved visualization of target nuclei and enabled the introduction of two noninvasive lesioning methods—Gamma Knife (GK) and MRI-guided focused ultrasound (MRgFUS). Although radiosurgery's delayed response and lack of real-time patient assessment for lesional effects make it less predictable than radiofrequency ablation, MRgFUS has shown promise in relieving parkinsonian symptoms with minimal side effects and the ability to monitor the patient during the procedure [32–34].

Functional Anatomy

A generalized model of basal ganglia (BG) circuitry provides sufficient context to understand both the hypoactive parkinsonian symptoms and the clinical response from ablating specific nuclei. In PD, alterations to these circuits change a patient's ability to start and continue motion. Motor symptoms are generally divided into two categories: positive and negative. Positive symptoms are tremor, rigidity, and dystonia, while negative symptoms are bradykinesia (slowed movement), akinesia (absent movement), and loss of postural reflexes. Another major source of disability in PD patients arises after years of levodopa use: involuntary and often painful muscle contractions known as dyskinesias develop in 40% of patients after 4–6 years of medical therapy and in 90% after 9–15 years [35].

As the main BG input source, the striatum incorporates projections from the substantia nigra pars compacta (SNc), the intralaminar nuclei of the thalamus, and widespread cortical

areas including the motor cortex, premotor cortex, and supplementary motor area [36, 37]. With the exception of projections from the subthalamus (STN), most BG connections are inhibitory. Two distinct pathways connect the input (striatum) to the two output nuclei (globus pallidus interna, GPi, and SN pars reticulata, SNr). The "direct" pathway facilitates motion through a monosynaptic connection from the striatum to GPi/SNr, while the "indirect" pathway diminishes unwanted or excessive motion through a polysynaptic relay from the striatum through GP external (GPe) and STN before reaching GPi/SNr. Pallidal projections terminate in the ventral oral posterior thalamic nucleus. The other important thalamic nuclei with regard to parkinsonian pathology—the ventral intermediate thalamic nucleus (VIM)—receives projections from the contralateral cerebellum and projects to the ipsilateral primary motor cortex, premotor cortex, and supplementary motor area [38, 39].

This circuit model serves as a simplified framework to explain the development of parkinsonism from the primary neuropathology—connecting the degeneration of SNc neurons to excessive inhibition of the thalamocortical and brainstem motor systems to the symptoms of hypoactive movement. A dopaminergic deficiency results from nigrostriatal neuronal loss. Via the direct pathway, the nigrostriatal dopaminergic deficiency reduces GPi inhibition. Via the indirect pathway, reduced nigrostriatal dopamine overly inhibits GPe, disinhibits STN, and activates GPi/SNr. The additive inhibitory effects from the direct pathway's reduction in GPi inhibition and the indirect pathway's increase in GPi/STN activity collectively reduce activity in thalamocortical and brainstem motor centers to produce the characteristic impoverished movement of bradykinesia and akinesia [40, 41].

Parkinsonian tremor is likely due to abnormal oscillating neuronal networks within the BG circuit appearing where groups of neurons exhibit a discharge pattern whose frequency is synchronized with limb tremor frequency. These so-called tremor cells exist in the ventralis intermedius (VIM) thalamus, STN, and GPi in tremor conditions as diverse as multiple sclerosis, essential tremor, and PD with the exception of cerebellar tremor syndromes [42, 43].

Physiologic Basis for Lesioning

Pallidotomy

In PD, nigrostriatal neuron degeneration and dopamine deficiency induces GPi hyperactivity through the combined effects of the direct and indirect pathways; this leads to excessive thalamic inhibition and reduced cortical activation, which produces hypokinetic parkinsonian symptoms. Metabolic studies have demonstrated that lesioning of the sensorimotor regions of the GPi in pallidotomy modulates this abnormal circuitry. Ablating GPi reduces lentiform metabolism and pathologic thalamic hyperinhibition, which increases frontal and prefrontal cortex metabolism; these metabolic changes have been correlated with symptom reduction [44, 45].

Thalamotomy

In non-cerebellar tremor syndromes, abnormally oscillating neuronal networks comprised of tremor cells in STN, GPi, and VIM thalamus are associated with a rest tremor. Postthalamotomy metabolic and perfusion studies demonstrated network remodulation differences between the resting and active state. The VIM thalamus appeared functionally disconnected from the laterofrontal and parietal association cortices at rest, while the primary motor cortex exhibited decreased perfusion during motion concomitant with tremor relief [45, 46]. Though thalamotomy arrests tremor, its minor impact on other parkinsonian symptoms has reduced the VIM thalamotomy to a more selective one in patients with tremor-predominant PD only.

Subthalamotomy

Subthalamic hyperactivity is one of several physiological manifestations of the dysregulated indi-

rect pathway in PD. The dopaminergic deficit from nigrostriatal neuron degeneration leads to a hyperinhibited GPe, disinhibited STN, hyperactive GPi/SNR, and reduced thalamocortical output that produces the cardinal parkinsonian symptoms [47]. Subthalamotomies in nonhuman primates normalized GPi/SNr outputs and relieved akinesia, bradykinesia, tremor, and rigidity [48]. Metabolic studies confirmed that STN lesions suppress GPi/SNr activity, which influenced downstream pontine and thalamic activity through the first postoperative year [49, 50].

Deep Brain Stimulation Versus Ablation

To select the most appropriate neurosurgical technique to manage parkinsonian patients, the unique risks and benefits of DBS and ablation should guide decision-making. Though unilateral pallidotomy appears as safe and as effective as pallidal DBS, bilateral ablations appear to be less safe than bilateral DBS implantations due to a higher incidence of speech complications [51, 52]. Though both thalamotomy and VIM DBS demonstrated comparable increases in clinician rating scales for PD and quality of life, the improved DBS side effect profile makes it a superior option for most patients [53, 54].

Despite the merits of DBS, ablation remains a viable alternative and may be considered first-line in select patients. For experienced neurosurgeons, ablations are more straightforward procedures of shorter duration. General anesthesia is not required in lesioning, but is needed for DBS pulse generator implantation [55]. DBS implantation also requires significant follow-up for optimal programming, monitoring, and equipment replacement—these combined costs increase the ultimate price of DBS far above ablation [56]. With lesioning, patients need not be concerned with bulky hardware that is susceptible to infection, migration, malfunction, fracture, or failure reported at rates as high as 49% [57, 58]. Patients who required DBS explant due to hardware complications like infection or migration may also be appropriate candidates for ablation after sufficient recovery and appropriate evaluation [59]. Lastly, DBS is contraindicated in patients with immunodeficiency or autoimmune disorders [60].

Indications and Contraindications

The optimal candidate for ablation has had medically refractory idiopathic PD for 5–10 years with levodopa-responsive motor symptoms of tremor, rigidity, bradykinesia, and drug-induced dyskinesias. In practice, these patient's symptoms should be more lateralized since pallidotomy is generally only done unilaterally. Patients should undergo rigorous neurologic and psychologic evaluation by a specialized movement disorders team in order to exclude patients with alternative diagnoses of supranuclear palsy, multiple system atrophy, and parkinsonism secondary to multifocal ischemic white matter disease—conditions with poorer prognoses that demonstrate minimal improvement after an ablation [61–63]. Patients with dementia, severe depression, psychosis, encephalitis, recent neuroleptic exposure, head trauma, or recent vascular disease should also be excluded [64]. Despite evidence that most patients experience only temporary speech disturbances, speech disorders remain a relevant contraindication. Thalamotomy presents a greater risk than pallidotomy for developing speech complications including hypoprosodia, changed enunciation, speech arrest, and lack of initiative to speak. Speech disturbances are much greater after bilateral ablations than unilateral ablations, both of which exceed the incidence after DBS surgeries [65, 66].

Pallidotomy

Asymmetric medically resistant idiopathic non-tremor-dominant PD patients whose motor symptoms had previously been levodopa-responsive achieve the greatest therapeutic benefit [67, 68]. Though painful dystonias, marked ON/OFF fluctuations, and bradykinesia respond very well, the greatest improvement is seen in dyskinesia reduction and OFF-period disability. Tremor may

respond less well to pallidotomy, although most patients are substantially improved [69]. Postural instability and autonomic dysfunction rarely improve and have also worsened occasionally, so severe ataxia, serious gait problems, orthostatic hypotension, or severe gastrointestinal or genitourinary symptoms of autonomic dysfunction are relative contraindications [70]. Younger patients (<60 years old) derive greater benefit than older patients (>70 years old) though pallidotomies have been performed safely on patients from 30 to 82. Increased time since PD diagnosis also predicts poorer response [64]. Structural abnormalities and lentiform hypometabolism on FDG-PET are relative contraindications [58]. Several studies report increased risks in bilateral pallidotomy though others have safely performed staged bilateral pallidotomies without incurring additional complications; therefore, patients with severe bilateral symptoms should undergo bilateral DBS, but can sometimes be considered for staged bilateral pallidotomy [71, 72].

Thalamotomy

Patients with unilateral or asymmetric tremor-dominant medically refractory PD may experience greater benefit from thalamotomy [73]. Thalamotomy produces excellent reductions in tremor and moderate alleviation of rigidity; however, thalamic lesions typically have little to no impact on bradykinesia, micrographia, hypophonia, and gait [49]. Extending the lesion anteriorly to include the ventral oralis posterior can improve rigidity and levodopa-induced dyskinesias [74]. Bilateral thalamotomies have been associated with higher rates of hypophonia, dysarthria, swallowing difficulties, and worsened bradykinesia; so patients with bilateral tremor might benefit more from bilateral DBS [75, 76].

Subthalamotomy

Due to the historical association of STN damage with hemiballismus, subthalamotomies were not considered as a surgical option. This philosophy slowly shifted with increased understanding of the STN's role in PD, due to several case reports of STN strokes improving parkinsonian tremor, and after early success with DBS stimulation to the STN [30, 77, 78]. Still only rarely performed, radiofrequency subthalamotomy may be considered in advanced, medically refractory relatively asymmetrical PD with disabling dyskinesias [79].

Surgical Procedures

Preoperative Evaluation

A comprehensive multidisciplinary movement disorders team of neurosurgeons, neurologists, psychiatrists, psychologists, and neuroradiologists should evaluate all patients. Their screening consists of a brain MRI, neuropsychological and ophthalmologic testing, as well as a thorough discussion of anticipated risks and benefits. The diagnosis of idiopathic PD must be confirmed to prevent ablating patients whose poor prognosis or comorbid conditions would thwart therapeutic benefit. A detailed history and physical examination might include Unified Parkinson's Disease Rating Scale, Schwab and England scale, Hoehn and Yahr scale, and the SF-36 health survey to quantify overall disability. Prior to surgery, medical management should be optimized, mood or psychiatric disorders must be treated, and the cognitive state of the patient should be assessed. Standard preoperative screening and bloodwork is performed, and agents that alter clotting characteristics should be discontinued at least 5 days prior to surgery.

Stereotactic Radiofrequency Lesioning

Radiofrequency ablations of the pallidum, thalamus, and subthalamus share similar procedural steps with the notable exceptions of lesion location and microelectrode recording/macrostimulation characteristics. This overview describes the general technique for any stereotactic radiofrequency lesion [59, 80, 81].

Preparation for Surgery

Antiparkinson and antitremor medications are withheld overnight to facilitate microelectrode mapping, prevent medication-induced dyskinesias from dislodging the frame, and allow for direct assessment of clinical response. Benzodiazepines, anxiolytics, and other sedating agents are avoided to ensure adequate monitoring of motor symptoms and for full patient cooperation during the surgery. Propofol or midazolam can be used sparingly if a head tremor interferes with stereotactic image acquisition. IV access is established ipsilaterally to the side of lesion generation for complete freedom of movement in the extremity of interest. Oxygen is supplied by nasal cannula. EKG, pulse oximetry, and blood pressure are monitored and maintained in the normal range. Bladder catheterization is not routinely performed.

An MRI-compatible stereotactic frame is typically applied under local anesthesia with or without conscious sedation; however, frameless systems have been adapted for these procedures. General anesthesia can be used in patients with severe symptoms or anxiety.

Stereotactic Imaging

Modern imaging techniques have enabled demarcation of GPi and STN borders, but thalamic nuclei are not well visualized on 1.5–3T MRI scanners. There are two main target planning methodologies that utilize different combinations of images—"direct" and "indirect." In "direct" target planning, the patient undergoes a sagittal T1-weighted MRI after frame application to identify the anterior commissure (AC) and posterior commissure (PC) and measure AC-PC length. The basal ganglia and thalamus, which lie in the AC-PC plane, are subsequently imaged using T2 sequences for GPi and SWI sequences for STN. For patients with contraindications to MRI, a stereotactic CT or ventriculography may be used for "indirect" targeting to estimate the AC-PC length and midcommissural points [75]. CT images alone are not suitable for target identification as their anatomical resolution is not sufficient for adequate target identification; however, a volumetric CT scan may be co-registered with a previous MRI without a frame if an MRI cannot be obtained.

Patient-specific atlases or probabilistic atlases based on large previous data sets can also be used as aids in target identification or verification. Furthermore, diffusion tensor imaging studies have been proposed to personalize target identification [82]. Images are imported into a neuronavigation computer workstation with stereotactic targeting software that calculates optimal trajectories as defined by the entry and lesion targets.

The pallidotomy target is typically 2–3 mm anterior to the midcommissural point, 4–6 mm below the intercommissural line, and 19–22 mm lateral to the midline of the third ventricle; however, these measurements are adjusted based on the patient's unique anatomy. The lesion location lies behind the mammillary bodies' posterior margin and superolateral to the optic tract; the limbic and associative territories of the pallidum, the optic tract, and the internal capsule should be avoided (Fig. 19.1) [83, 84].

The thalamotomy target, VIM nucleus, is usually 25% of the AC-PC length anterior to the posterior commissure point, 11 mm lateral to the third ventricle wall and at the level of the AC-PC (Fig. 19.2) [85].

The optimal STN target, dorsolateral motor region, is 2–3 mm posterior to the midcommissural point, 11–12 mm lateral to the AC-PC, and 4–5 mm inferior to the AC-PC plane [86, 87].

Surgical Technique

After prophylactic antibiotic administration, patients are positioned comfortably in a supine semi-sitting position to encourage full cooperation during the procedure. Draping must cover the field sufficiently without interfering with intraoperative assessment. A local anesthetic numbs the scalp, and a parasagittal incision is made to place a pallidotomy burr hole 3 cm from midline in the midpupillary line and 1–2 cm anterior to the coronal suture or a thalamotomy burr hole 3 cm from midline at the level of the coronal suture. An entry point is selected to avoid venous, sulcal, and ventricular penetration. The pallidotomy entry point is placed more anterolaterally in front of the coronal suture, while the thalamotomy

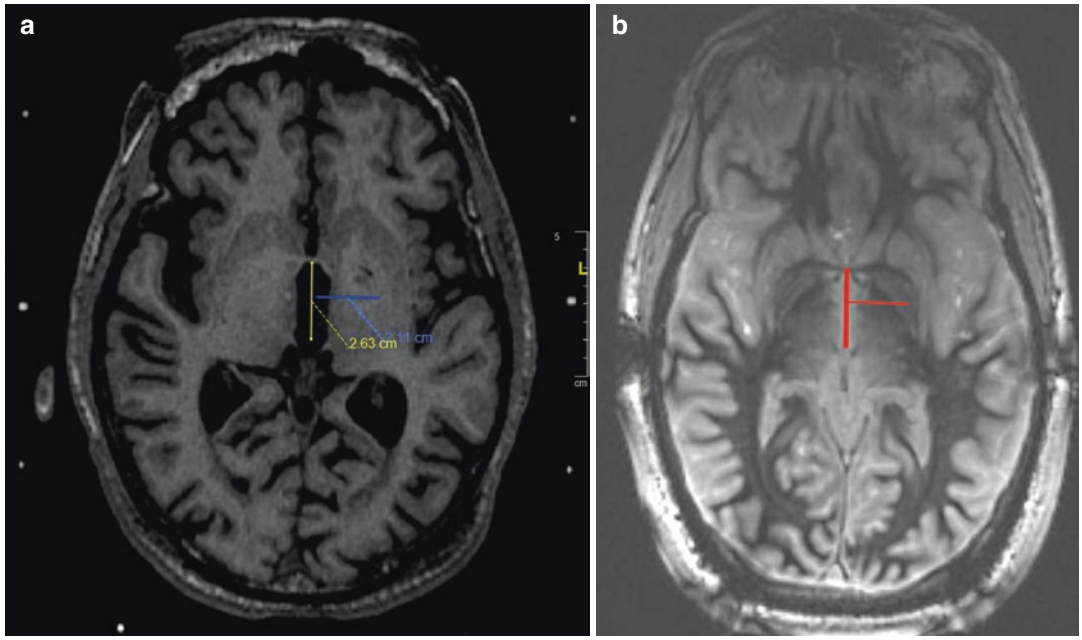

Fig. 19.1 T1-weighted axial MRI demonstrating initial target in GPi at the level of the intercommissural plane 2–3 mm anterior to the midcommissural point and 21 mm lateral (**a**) better seen on axial proton density MR images that better defines GPi anatomy (**b**)

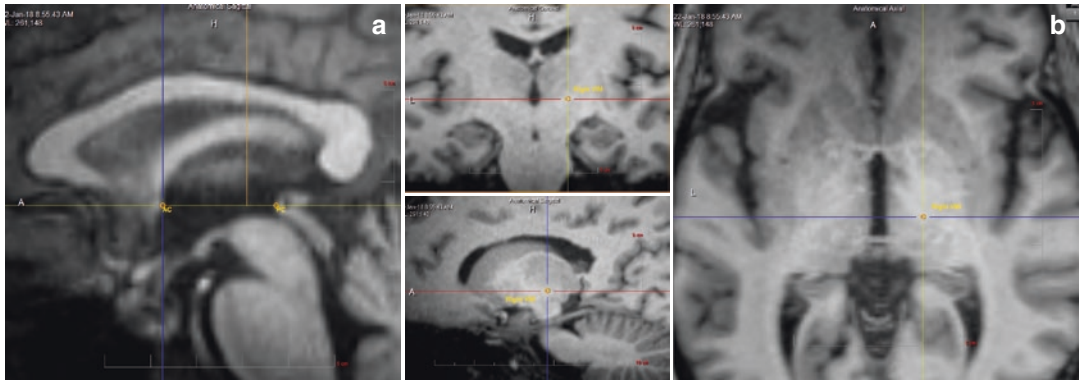

Fig. 19.2 T1-weighted sagittal MRI demonstrating initial targeting of Vim thalamus at the level of the intercommissural plane ¼ the distance anterior to the posterior commissure (**a**) seen on axial, coronal, and sagittal T1-weighted MR images that better defines the location of the internal capsule (**b**)

entry point is about the level of the coronal suture. The dura and pia are coagulated to minimize bleeding during electrode placement. The stereotactic arc is then positioned and the electrode guide tube is lowered into the burr hole. The burr hole is filled with fibrin glue or the skin is temporarily closed with nylon sutures to minimize CSF loss and brain settling.

Microelectrode Recording and Macrostimulation

To confirm the trajectory, define target borders, and refine lesion location, macrostimulation and/or microelectrode recording may be performed. Microelectrode recording was used in 46.2% of pallidotomies, and macroelectrode stimulation was performed in 53.8% of palli-

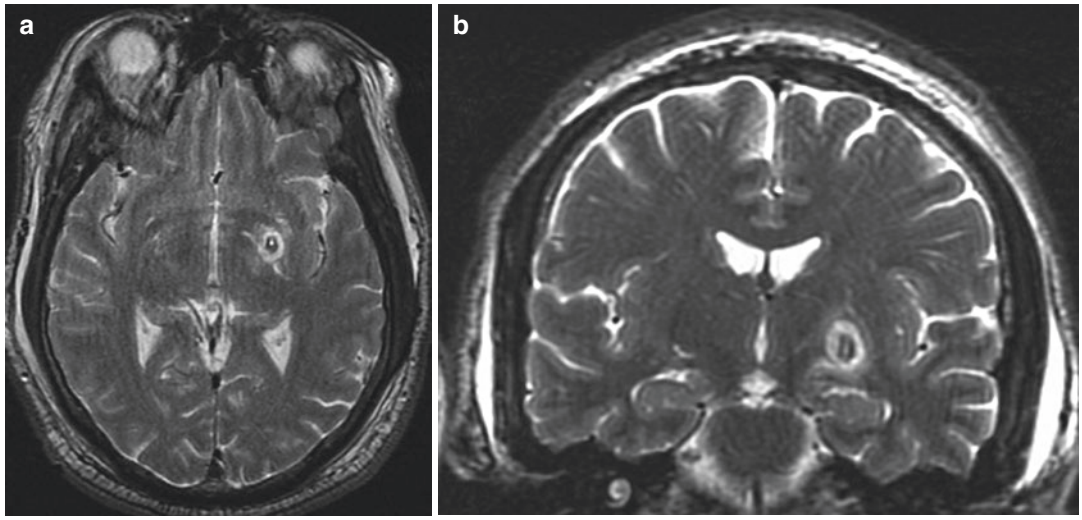

Fig. 19.3 T2-weighted MR images of a radiofrequency pallidotomy 24 hours post-procedure in the axial (**a**) and coronal (**b**) planes. Note the location of the lesion just lateral to the internal capsule and above the optic tract

dotomies from 1992 to 1999 [63]. For microelectrode recording, a microdrive platform is mounted to the frame to precisely drive in a microelectrode, which records activity from individual neurons. Analyzing the neuronal activity of various cell types enables the creation of a detailed map of the basal ganglia and thalamic nuclei for precise targeting; however, specialized expertise, specific equipment, and time for analysis is required. Faster but less precise, a macroelectrode with an exposed tip for stimulation can be used independently or sequentially after microelectrode recording. A square wave pulse is applied at 0–5 volts at 2 Hz for motor thresholds and at 50–75 Hz for visual thresholds, and the patient is monitored for signs of symptom relief, neurologic impairments, or abnormal sensations.

Lesion Generation

The radiofrequency generator conducts heat through a probe with an exposed tip to create a lesion at the target. During both the test lesions and ablation process, speech and sensorimotor functions are continuously monitored. In pallidotomies, visual fields are also monitored. A test lesion is performed at 42–46 °C for 60 seconds, and the permanent lesion is produced by gradually increasing the temperature from 60 to 75 °C for 60 seconds [63]. For pallidotomy, additional lesions are made at 2 mm and 4 mm above the target (Fig. 19.3). For thalamotomy lesions, the initial lesion is placed at the intercomissural plane and a second lesion placed 2 mm superior to the first (Fig. 19.4). A balance must be struck when determining overall lesion size between symptomatic relief and side effects or complications. Lesion size varies also based on procedure type—pallidotomy lesions often measure 6 mm in height and 4 mm in diameter, and thalamotomy lesions measure 4–6 mm in diameter [55, 88]. After ablating the target, the electrode is withdrawn, and the burr hole is filled with Gelfoam and bone dust prior to closing the scalp, removing the frame, and covering with sterile dressing.

Postoperative Care

Patients usually return to their room after a short period of observation. Mild analgesics are typically sufficient to manage postoperative pain though special care is taken to manage blood pressure to minimize hemorrhage risk. Patients are monitored overnight and undergo an MRI prior to discharge to verify lesion location and exclude complications.

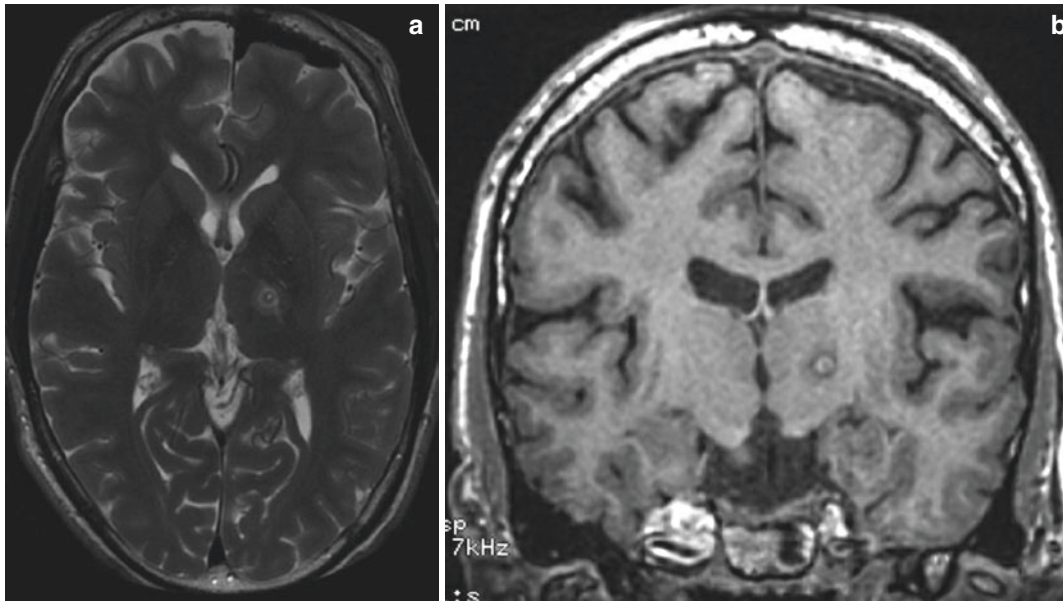

Fig. 19.4 T2-weighted axial MR images of a radiofrequency thalamotomy (**a**) and T1-weighted coronal MR images (**b**) 24 hours post-procedure. Note the location of the lesion just medial to the internal capsule and extending just 1 mm below the intercommissural plane

MRI-Guided Focused Ultrasound (MRgFUS) Lesioning

Although Fry et al. first proposed ultrasound as a surgical option for PD in 1958, his technique required a craniotomy to directly access the site of interest [89]. Since that time, numerous technological discoveries paved the way for the development of the newest noninvasive neurosurgical technique currently undergoing Phase III clinical trials: MRgFUS [90–93]. The physics concept of focused sonication serves as the basis for this therapy: sound energy in the form of an ultrasound wave transmitted through the skull is transformed to thermal energy at the target site. No incisions or burr holes are required to precisely create permanent lesions. A thermal dose of 57 °C for 1 second denatures all proteins and causes death of all cells; the equivalent thermal dose is a function of exposed area and length of exposure [94].

Preoperative screening and surgical preparation remains the same as for radiofrequency ablation. The patient's head is first completely shaved and then fixed in an MRI-compatible stereotactic frame with local anesthetic similarly to radiofrequency ablation procedures. An elastic diaphragm is stretched around the head and connected to the transducer before being filled with degassed and chilled water. Performed in an MRI suite, MRgFUS uses real-time MRI for accurate localization, treatment planning, and thermal dosing control throughout the procedure [95]. Intraoperative MRI scans are fused to the preoperative CT scan for proper skull correction as the skull density alters the thermal energy that reaches the lesion site [96]. The VIM thalamotomy target is one quarter of the AC-PC length anterior to PC, 14 mm lateral to midline or 11 mm from the third ventricle wall if the ventricle is enlarged and 1–2 mm above the AC-PC plane [83]. The pallidotomy target is reported to be 22 mm lateral from midline, 3–4 mm anterior from the AC-PC line midpoint, and 2–3 mm inferior to the intercommissural line [84].

MRgFUS is divided into three phases. During the first stage, MR thermography at lower energies (41–46 °C) is used to confirm the sonication target in sagittal, axial, and coronal planes. In the second stage, energy is gradually

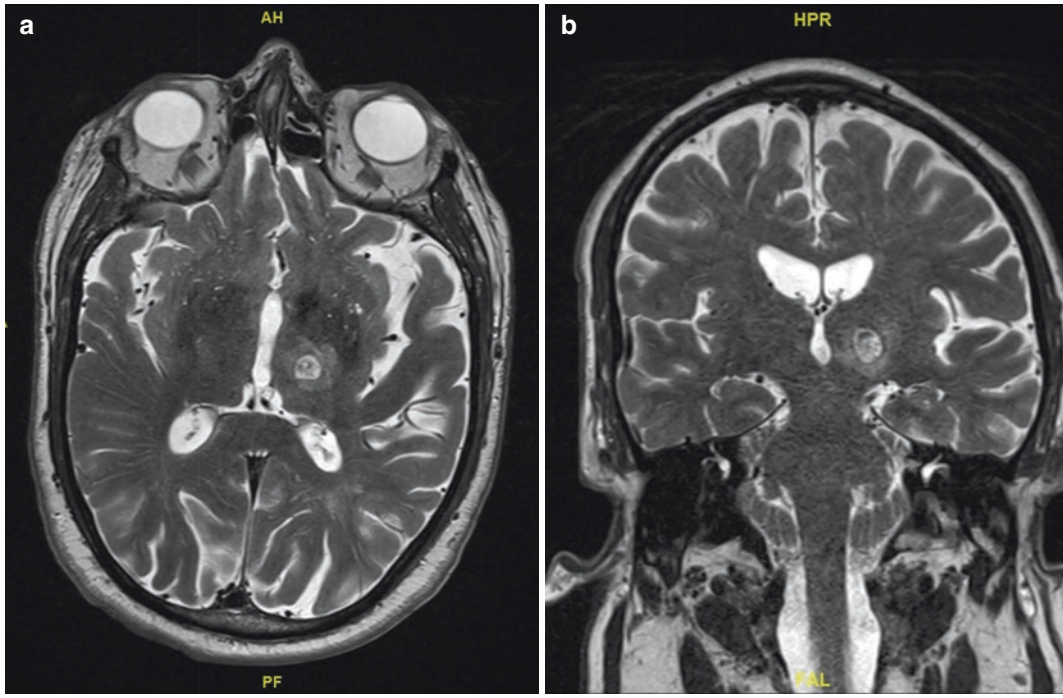

Fig. 19.5 Axial (**a**) and coronal (**b**) thin cut T2-weighted MR images 24 hours post-FUS thalamotomy

increased (46–50 °C) while the patient is monitored for symptom relief and adverse effects. The third and final stage consists of ablation—incrementally, energy is increased through either larger sonication intensity not to exceed 60 °C or prolonged sonication duration (Fig. 19.5). The procedure is typically performed as an outpatient procedure [83, 97].

Gamma Knife (GK) Lesioning

Though introduced as a neurosurgical technique for functional disorders in 1951 by Lars Leksell, stereotactic radiosurgery for PD remains less preferable than DBS and radiofrequency lesioning because of the significant delay in symptomatic improvement and less predictable adverse events [98, 99]. Its application is limited to patient preference and to poor surgical candidates with severe cardiac or respiratory disease, taking chronic anticoagulation, medically noncompliant, and the elderly. Cobalt-60 gamma units produce multiple beams of photon energy that are focused through 4 mm collimator openings. This ionizing radiation produces free radicals; both gamma radiation and free radicals damage tissue and mutate DNA to induce necrosis at the target site [100, 101]. Incisions and burr holes are not required for lesion generation and no head shave is needed.

As described above for radiofrequency ablations, patients should undergo rigorous preoperative screening and surgical preparation; the movement disorders team should also include radiation oncologists and medical physicists. The patient's head is first fixed in a stereotactic frame, and a high-resolution MRI is obtained and then loaded onto a computer with dose-planning software. Individual doses were determined jointly by the neurosurgeon, radiation oncologist, and medical physicist, ranging from 120 to 180 Gy in pallidotomies and 120 to 160 Gy in thalamotomies. Follow-up imaging is performed several months after discharge when the GK results would be visible [91, 92].

Surgical Results

Clinical Outcome

Pallidotomy

Pallidotomy has been evaluated in numerous retrospective case series, several prospective uncontrolled trials, and a few controlled, randomized, blinded clinical trials [102, 103]. Alkhani et al. summarized the results of nearly 2000 PD patients who had received radiofrequency pallidotomies in 40 centers in 12 countries published between 1992 and 1999. In 263 of 1959 patients, pre- and postoperative contralateral dyskinesia scores were documented: mean scores increased by 67.7% from 2.2 +/− 0.6 to 0.71 +/− 0.45 with improvement sustained at 6 months (73.5% of 94 assessed patients) and 12 months (86.4% of 71 assessed patients) [63]. Patients also achieve significant reductions in contralateral symptoms of rigidity, tremor, and bradykinesia during OFF periods with some ipsilateral changes. Changes during the ON periods are less pronounced [26, 78]. Not only are the symptoms better during the OFF periods, but patients report reduced duration of OFF hours per day [65, 95]. The impact on gait remains obscured by conflicting results as some patients describe improved or unchanged gait, while others complain of worsening gait and postural instability [104, 105]. Speech dysfunction worsens in patients with preoperative moderate and severe dysarthria, while mildly dysarthric patients are more likely to experience some benefit to speech after pallidotomy [106].

Thalamotomy

The majority of patients achieve complete or near-complete extremity tremor arrest with little impact on bradykinesia, gait, or executive function [107, 108]. Persistence of tremor relief remains a controversial topic since some patients report sustained benefits over a decade of follow-up, while others have observed a steady decline to preoperative function as compared to baseline. Although the length of benefit from thalamotomy continues to be debated, there does appear to be consensus that thalamotomy does not alter disease progression [109]. Some demonstrate sustained improvements in rigidity opposite to lesion side; however, optimal improvement of rigidity occurs with lesions in the Vop thalamus [59]. Thalamotomy's impact on levodopa-induced dyskinesias was initially controversial with some early publications purported that lesioning prevented their development and others reporting minimal dyskinesia reduction [110]. It appears that the overall dyskinesia reduction was the result of reduced daily levodopa requirements after the surgery. Furthermore, ventralis oralis anterior and posterior have been found to be more appropriate lesioning targets to reduce dyskinesias [111].

MRI-Guided Focused Ultrasound (MRgFUS) Lesioning

Though few case reports of MRgFUS pallidotomy have been published, early results demonstrate similar improvements to radiofrequency pallidotomy in the first 6 months: improved ON and OFF motor scores and reduced levodopa-induced dyskinesias [84, 112]. MRgFUS VIM thalamotomy has been studied more rigorously and been shown to greatly improve tremor in patients with medically refractory tremor-dominant PD in the setting of a placebo response [85]. Alleviating tremor significantly improves quality of life scores through increased ability to complete activities of daily living [113, 114].

Gamma Knife (GK) Lesioning

Elaimy et al. summarized the 14 publications on 79 patients who received GK pallidotomy and 477 patients who received GK thalamotomy for movement disorders. Patients rarely undergo GK pallidotomy due to the controversy surrounding the procedure's efficacy and safety; improvements in bradykinesia, rigidity, and dyskinesia range from 0% to 87%. Although none of the 4 patients in the smallest case series received therapeutic benefit and only 33% of the 18 patients in the intermediate-sized series improved, 2 larger studies of 28 and 29 patients reported 64.3–65.5% reported bradykinesia/rigidity improvements and 85.7–86.8% experienced reduced dyskinesias. GK thalamotomy for tremor has reportedly produced 80–100% improvement in 455 patients with essential tremor, PD, and multiple sclerosis with onset of improvement ranging from 1 week to 1 year [92].

Subthalamotomy

Subthalamotomies produce contralateral tremor arrest, bilateral reductions in bradykinesia and rigidity in the ON and OFF states, and improvements in freezing, postural stability, and facial expression. In comparison with pallidotomy and thalamotomy, subthalamotomy significantly decreases medication needs, which slows medication-induced dyskinesia development and reduces disability [28, 86]. Bilateral procedures demonstrated greater improvements in scores for tremor, bradykinesia, and rigidity on both sides [29].

Complications

Pallidotomy

Alkhani and Lozano's systematic review of 1564 pallidotomy patients provides the most comprehensive analysis of adverse events. Hemorrhage is the most serious complication of radiofrequency pallidotomy and occurs in 1.7% of patients with a mortality rate of 0.4%. It is clear that hemorrhage occurs more commonly with MER-guided procedures. Overall estimated morbidity rate was 23.1% with a 14.3% permanent morbidity rate. The most common complications were (1) weakness that developed in 5.3% and persisted in 2.2%, (2) speech disorders (dysarthria, hypophonia) that occurred in 4.5% and persisted in 2.9%, and (3) visual field deficits that affected 2% and persisted in 1.5% of patients [63]. Most patients do not experience significant cognitive or psychiatric impairment though the elderly are more prone to transient postoperative confusion or somnolence [64, 115]. Several studies indicate temporary mild changes to cognition, memory, and executive function; left-sided lesions may decrease verbal fluency or frontal lobe functions, while right-sided lesions may improve frontal functions [116, 117].

Thalamotomy

As in pallidotomy, mortality rates are low (0.4–9%), and intracranial hemorrhage, which represents the most significant complication of thalamotomy, has been reported in 1.5–6% of patients, again more commonly with MER-guided procedures [118]. Patients report dysarthria, hypophonia, dysphagia, or aphasia with only a subset reporting persistent complications and an even smaller fraction reporting the adverse effects were a source of disability [119]. Historically patients experienced weakness or hemiparesis at rates of 1.7–26% though modern stereotactic techniques seem to have reduced the incidence and most resolve without subsequent treatment [15, 111]. Patients also report temporary perioral or appendicular paresthesias and numbness [120]. Thalamotomy appears to have limited cognitive sequelae of reduced verbal fluency and minor memory impairment; however, some patients experience improvements in verbal memory [121, 122]. Rare complications include infection, thalamic pain syndromes, neglect, dysphagia, sialorrhea, blepharospasm, dystonia, ataxia, hyperkinesia, and hypotonia [111].

MRI-Guided Focused Ultrasound (MRgFUS) Lesioning

The noninvasive technique of MRgFUS represents a major benefit as compared to other neurosurgical interventions for movement disorders—those benefits are most visibly manifested through reduced rates of serious complications. Though larger trials are necessary to confirm the results of the MRgFUS thalamotomy clinical trial, its outcomes are the most current understanding of MRgFUS complication rates in PD. During early trials, internal capsule heating induced mild hemiparesis that eventually improved to near-baseline. The majority of adverse results are temporary and of lower acuity and consist of persistent mild ataxia (5%), orofacial paresthesias (27%), finger paresthesias (5%), and temporary ataxia (35%)—the majority resolved by 12 months. Headache (65%) and dizziness/vertigo (42%) occur only during the procedure with complete resolution upon exiting the MRI suite [85]. Several other minor complications arise at lower rates: nausea, pin-site discomfort, taste disturbances, dyskinesias, subjective speech disturbance, anxiety, fatigue, weight gain, transient hypertension, facial asymmetry, and minor impulsivity [83, 86].

Gamma Knife (GK) Lesioning

In both GK pallidotomy and thalamotomy, a diverse and unpredictable side effects profile develops in the same delayed fashion as clinical benefit with a wide reported range of 0.4–50%. The larger studies of 28 and 29 patients reported complication rates of 3.4–3.6%, the intermediate series of 18 patients reported a 50% complication rate, and the smallest case series of 4 reported 25%. Complications included visual field deficiencies, dysphagia, dysarthria, hemiparesis, hemianesthesia, dementia, and psychosis. In the nine studies on GK thalamotomy, complication rates ranged from 0% to 16.7% though one outlier published a 46.7% complication rate. Complications included hemorrhage, edema, hemiparesis, sensory and motor impairments, dysarthria, dysphagia, and disordered balance [92]. Two hypotheses postulate causes for the increased rates of adverse events in GK pallidotomy versus thalamotomy: (1) pallidal perforating arteries supply more diverse downstream effects than thalamic vessels, and (2) iron accumulates in the pallidum with age, thus increasing the concentration of metallic products susceptible to acting as free radical catalysts that induce greater damage [91, 123].

Subthalamotomy

Subthalamotomies produce contralateral tremor arrest, bilateral reductions in bradykinesia and rigidity in the ON and OFF states, and improvements in freezing, postural stability, and facial expression. In comparison with pallidotomy and thalamotomy, subthalamotomy significantly decreases medication needs, which slows medication-induced dyskinesia development and reduces disability [28, 86]. Bilateral procedures demonstrated greater improvements in scores for tremor, bradykinesia, and rigidity on both sides [29].

A pilot study of ten patients reported results of unilateral MRgFUS subthalamotomy with a lesion target of 3 mm posterior, 12 mm lateral, and 4 mm inferior to the midcommissural point. Results demonstrated improvements of hemibody motor scores for rigidity, akinesia, and tremor by 53% in the OFF state and 47% in the ON state through the first 6 months. Complications included dyskinesias, speech disturbances, anxiety, weight gain, gait ataxia, pin-site pain, transient hypertension, facial asymmetry, and impulsivity [86]. A small case series of 13 patients targeting the pallidothalamic tract guided by tractography also showed equivalent benefit to patients as from radiofrequency lesioning with reduced risk of adverse events—total motor score improvements of 60.9% without postoperative neurologic complications [124].

Conclusion

Radiofrequency ablation procedures have been established as an efficacious and safe surgical option for parkinsonian patients with suboptimal symptom control or levodopa-induced dyskinesias who had previously responded to levodopa therapy. Pallidotomy provides substantial therapeutic relief of tremor, bradykinesia, rigidity, and dyskinesias with some risk of weakness, speech alterations, and visual field deficits. Thalamotomy provides near-complete arrest of tremor with some risk of paresthesias, weakness, and dysarthria. GK has also been shown to effectively produce lesions though in a delayed fashion with less predictable side effects particularly after pallidotomies. Though longer-term and larger studies of MRgFUS lesioning are needed to confirm early results, the novel noninvasive technique's initial experience suggests an important role in the functional neurosurgery armamentarium.

References

1. Parkinson J. An essay on the shaking palsy. J Neuropsychiatry Clin Neurosci. 2002;14(2):223–36.
2. Duker AP, Espay AJ. Surgical treatment of Parkinson disease: past, present, and future. Neurol Clin. 2013;31(3):799–808.
3. Bucy PC, Case TJ. Tremor: physiologic mechanism and abolition by surgical means. Arch Neurol Psychiatr. 1939;41(4):721–46.
4. Walker AE. Cerebral pedunculotomy for the relief of involuntary movements: II. Parkinsonian tremor. J Nerv Ment Dis. 1952;116(6):766–75.

5. Baltuch GH, Stern MB, editors. Deep brain stimulation for Parkinson's disease. Boca Raton: CRC Press; 2007.
6. Putnam TJ. Relief from unilateral paralysis agitans by section of the pyramidal tract. Arch Neurol. 1938;40:1049–50.
7. Oliver L. Surgery in Parkinson's disease division of lateral pyramidal tract for tremor. Lancet. 1949;253(6561):910–3.
8. Puusepp L. Cordotomia posterior lateralis (fasc. Burdachi) on account of trembling and hypertonia of the muscles in the hand. Folia Neuropath Estonia. 1930;10:62–4.
9. Gardner WJ, Williams GH. Interruption of the sympathetic nerve supply to the brain—effect on Parkinson's syndrome. Arch Neurol Psychiatr. 1949;61(4):413–21.
10. Cooper IS. Ligation of the anterior choroidal artery for involuntary movements-parkinsonism. Psychiatry Q. 1953;27(1–4):317–9.
11. Cooper IS. Surgical alleviation of parkinsonism: effects of occlusion of the anterior choroidal artery. J Am Geriatr Soc. 1954;2(11):691–718.
12. Meyers R. Surgical procedure for postencephalitic tremor, with notes on the physiology of premotor fibers. Arch Neurol Psychiatr. 1940;44:455–9.
13. Meyers R. Surgical experiments in the therapy of certain 'extrapyramidal' diseases: a current evaluation. Acta Psychiatr Neurol Suppl. 1951;67:1–42.
14. Spiegel EA, Wycis HT, Marks M, Lee AJ. Stereotaxic apparatus for operations on the human brain. Science. 1947;106(2754):349–50.
15. Waltz JM, Riklan M, Stellar S, Cooper IS. Cryothalamectomy for Parkinson's disease a statistical analysis. Neurology. 1966;16(10):994.
16. Obrador S. A simplified neurosurgical technique for approaching and damaging the region of the globus pallidus in Parkinson's disease. J Neurol Neurosurg Psychiatry. 1957;20(1):47.
17. Fry WJ, Meyers R. Ultrasonic method of modifying brain structures. Stereotact Funct Neurosurg. 1962;22(3–5):315–27.
18. Cooper IS, Bravo G. Chemopallidectomy and chemothalamectomy. J Neurosurg. 1958;15(3):244–50.
19. Guridi J, Lozano AM. A brief history of pallidotomy. Neurosurgery. 1997;41(5):1169–83.
20. Cooper IS. Surgical treatment of parkinsonism. Annu Rev Med. 1965;16(1):309–30.
21. Narabayashi H. Parkinsonian tremor and nucleus ventralis intermedius of the human thalamus. Prog Clin Neurophysiol. 1978;5:165–72.
22. Bertrand CMA. Pneumotaxic technique for producing localized cerebral lesions: and its use in the treatment of Parkinson's disease. J Neurosurg. 1958;15(3):251–64.
23. Speelman JD, Bosch DA. Resurgence of functional neurosurgery for Parkinson's disease: a historical perspective. Mov Disord. 1998;13(3):582–8.
24. Marsden CD, Parkes JD. Success and problems of long-term levodopa therapy in Parkinson's disease. Lancet. 1977;309(8007):345–9.
25. Laitinen LV, Bergenheim AT, Hariz MI. Ventroposterolateral pallidotomy can abolish all parkinsonian symptoms. Stereotact Funct Neurosurg. 1992;58(1–4):14–21.
26. Laitinen LV. Pallidotomy for Parkinson's disease. Neurosurg Clin. 1995;6(1):105–12.
27. Merello M, Starkstein S, Nouzeilles MI, Kuzis G, Leiguarda R. Bilateral pallidotomy for treatment of Parkinson's disease induced corticobulbar syndrome and psychic akinesia avoidable by globus pallidus lesion combined with contralateral stimulation. J Neurol Neurosurg Psychiatry. 2001;71(5):611–4.
28. Obeso JA, Alvarez LM, Macias RJ, Guridi J, Teijeiro J, Juncos JL, Rodriguez MC, Ramos E, Linazasoro GJ, Gorospe A, DeLong MR. Lesion of the subthalamic nucleus (STN) in Parkinson's disease (PD). Neurology. 1997;48(3):12003.
29. Heywood P, Gill SS. Bilateral dorsolateral subthalamotomy for advanced Parkinson's disease. Lancet. 1997;350(9086):1224.
30. Kleiner-Fisman G, Herzog J, Fisman DN, Tamma F, Lyons KE, Pahwa R, Lang AE, Deuschl G. Subthalamic nucleus deep brain stimulation: summary and meta-analysis of outcomes. Mov Disord. 2006;21(S14):S290–304.
31. Tomaszewski KJ, Holloway RG. Deep brain stimulation in the treatment of Parkinson's disease a cost-effectiveness analysis. Neurology. 2001;57(4):663–71.
32. Higuchi Y, Matsuda S, Serizawa T. Gamma knife radiosurgery in movement disorders: indications and limitations. Mov Disord. 2017;32(1):28–35.
33. Christian E, Yu C, Apuzzo ML. Focused ultrasound: relevant history and prospects for the addition of mechanical energy to the neurosurgical armamentarium. World Neurosurg. 2014;82(3–4):354–65.
34. Lozano CS, Tam J, Lozano AM. The changing landscape of surgery for Parkinson's disease. Mov Disord. 2018;33(1):36–47.
35. Ahlskog JE, Muenter MD. Frequency of levodopa-related dyskinesias and motor fluctuations as estimated from the cumulative literature. Mov Disord. 2001;16(3):448–58.
36. Alexander GE, DeLong MR, Strick PL. Parallel organization of functionally segregated circuits linking basal ganglia and cortex. Annu Rev Neurosci. 1986;9(1):357–81.
37. Alexander GE, Crutcher MD. Functional architecture of basal ganglia circuits: neural substrates of parallel processing. Trends Neurosci. 1990;13(7):266–71.
38. Smith Y, Bevan MD, Shink E, Bolam JP. Microcircuitry of the direct and indirect pathways of the basal ganglia. Neuroscience. 1998;86(2):353–87.
39. Crossman AR. Functional anatomy of movement disorders. J Anat. 2000;196(4):519–25.
40. Obeso JA, Rodriguez-Oroz MC, Rodriguez M, Lanciego JL, Artieda J, Gonzalo N, Olanow CW. Pathophysiology of the basal ganglia in Parkinson's disease. Trends Neurosci. 2000;23:S8–19.

41. Miller WC, DeLong MR. Parkinsonian symptomatology an anatomical and physiological analysis. Ann N Y Acad Sci. 1988;515(1):287–302.
42. Jasper HH. Thalamic units involved in somatic sensation and voluntary and involuntary movements in man. Thalamus. 1966:365–90.
43. Deuschl G, Raethjen J, Baron R, Lindemann M, Wilms H, Krack P. The pathophysiology of parkinsonian tremor: a review. J Neurol. 2000;247(5):V33–48.
44. Eidelberg D, Moeller JR, Ishikawa T, Dhawan V, Spetsieris P, Silbersweig D, Stern E, Woods RP, Fazzini E, Dogali M, Beric A. Regional metabolic correlates of surgical outcomes following unilateral pallidotomy for parkinson's disease. Ann Neurol. 1996;39(4):450–9.
45. Henselmans JM, de Jong BM, Pruim J, Staal MJ, Rutgers AW, Haaxma R. Acute effects of thalamotomy and pallidotomy on regional cerebral metabolism, evaluated by PET. Clin Neurol Neurosurg. 2000;102(2):84–90.
46. Boecker H, Wills AJ, Ceballos-Baumann A, Samuel M, Thomas DG, Marsden CD, Brooks DJ. Stereotactic thalamotomy in tremor-dominant Parkinson's disease: an H215O PET motor activation study. Ann Neurol. 1997;41(1):108–11.
47. Bergman H, Wichmann T, DeLong MR. Reversal of experimental parkinsonism by lesions of the subthalamic nucleus. Science. 1990;249(4975):1436–8.
48. Aziz TZ, Peggs D, Sambrook MA, Crossman AR. Lesion of the subthalamic nucleus for the alleviation of 1-methyl-4-phenyl-1, 2, 3, 6-tetrahydropyridine (MPTP)-induced parkinsonism in the primate. Mov Disord. 1991;6(4):288–92.
49. Su PC, Ma Y, Fukuda M, Mentis MJ, Tseng HM, Yen RF, Liu HM, Moeller JR, Eidelberg D. Metabolic changes following subthalamotomy for advanced Parkinson's disease. Ann Neurol. 2001;50(4):514–20.
50. Trošt M, Su PC, Barnes A, Su SL, Yen RF, Tseng HM, Ma Y, Eidelberg D. Evolving metabolic changes during the first postoperative year after subthalamotomy. J Neurosurg. 2003;99(5):872–8.
51. Kumar R, Lozano AM, Montgomery E, Lang AE. Pallidotomy and deep brain stimulation of the pallidum and subthalamic nucleus in advanced Parkinson's disease. Mov Disord. 1998;13:73–82.
52. Blomstedt P, Hariz GM, Hariz MI. Pallidotomy versus pallidal stimulation. Parkinsonism Relat Disord. 2006;12(5):296–301.
53. Tasker RR. Deep brain stimulation is preferable to thalamotomy for tremor suppression. Surg Neurol. 1998;49(2):145–53.
54. Blomstedt P, Hariz MI. Are complications less common in deep brain stimulation than in ablative procedures for movement disorders? Stereotact Funct Neurosurg. 2006;84(2–3):72–81.
55. Gross RE. What happened to posteroventral pallidotomy for Parkinson's disease and dystonia? Neurotherapeutics. 2008;5(2):281–93.
56. McIntosh E, Gray A, Aziz T. Estimating the costs of surgical innovations: the case for subthalamic nucleus stimulation in the treatment of advanced Parkinson's disease. Mov Disord. 2003;18(9):993–9.
57. Hariz MI. Complications of deep brain stimulation surgery. Mov Disord. 2002;17(S3):S162–6.
58. Oh MY, Abosch A, Kim SH, Lang AE, Lozano AM. Long-term hardware-related complications of deep brain stimulation. Neurosurgery. 2002;50(6):1268–76.
59. Lokuketagoda J, Gross R. Thalamotomy and pallidotomy. In: Jandial R, McCormick P, Black PM, editors. Core techniques in operative neurosurgery E-book: expert consult-online. Amsterdam: Elsevier Health Sciences; 2011. p. 290–300.
60. Hooper AK, Okun MS, Foote KD, Fernandez HH, Jacobson C, Zeilman P, Romrell J, Rodriguez RL. Clinical cases where lesion therapy was chosen over deep brain stimulation. Stereotact Funct Neurosurg. 2008;86(3):147–52.
61. Alterman RL, Kelly P, Sterio D, Fazzini E, Eidelberg D, Perrine K, Beric A. Selection criteria for unilateral posteroventral pallidotomy. In: Advances in stereotactic and functional neurosurgery 12. Vienna: Springer; 1997. p. 18–23.
62. Alterman RL, Kelly PJ. Pallidotomy technique and results: the New York University experience. Neurosurg Clin N Am. 1998;9(2):337–44.
63. Tasker RR, Siqueira J, Hawrylyshyn P, Organ LW. What happened to VIM thalamotomy for Parkinson's disease? Stereotact Funct Neurosurg. 1983;46(1–4):68–83.
64. Bronstein JM, DeSalles A, DeLong MR. Stereotactic pallidotomy in the treatment of Parkinson disease: an expert opinion. Arch Neurol. 1999;56(9):1064–9.
65. Alomar S, King NK, Tam J, Bari AA, Hamani C, Lozano AM. Speech and language adverse effects after thalamotomy and deep brain stimulation in patients with movement disorders: a meta-analysis. Mov Disord. 2017;32(1):53–63.
66. Uitti RJ, Wharen RE Jr, Duffy JR, Lucas JA, Schneider SL, Rippeth JD, Wszolek ZK, Obwegeser AA, Turk MF, Atkinson EJ. Unilateral pallidotomy for Parkinson's disease: speech, motor, and neuropsychological outcome measurements. Parkinsonism Relat Disord. 2000;6(3):133–43.
67. Alkhani A, Lozano AM. Pallidotomy for Parkinson disease: a review of contemporary literature. J Neurosurg. 2001;94(1):43–9.
68. Van Horn G, Hassenbusch SJ, Zouridakis G, Mullani NA, Wilde MC, Papanicolaou AC. Pallidotomy: a comparison of responders and nonresponders. Neurosurgery. 2001;48(2):263–73.
69. Iacono RP, Shima F, Lonser RR, Kuniyoshi S, Maeda G, Yamada S. The results, indications, and physiology of posteroventral pallidotomy for patients with Parkinson's disease. Neurosurgery. 1995;36(6):1118–25.
70. Lozano AM, Lang AE. Pallidotomy for Parkinson's disease. Neurosurg Clin N Am. 1998;9(2):325–36.
71. De Bie RM, Schuurman PR, Esselink RA, Bosch DA, Speelman JD. Bilateral pallidotomy in Parkinson's

disease: a retrospective study. Mov Disord. 2002;17(3):533–8.
72. Counihan TJ, Shinobu LA, Eskandar EN, Cosgrove GR, Penney JB Jr. Outcomes following staged bilateral pallidotomy in advanced Parkinson's disease. Neurology. 2001;56(6):799–802.
73. Tasker RR. Thalamotomy. Neurosurg Clin N Am. 1990;1(4):841–64.
74. Narabayashi HI, Yokochi FU, Nakajima YA. Levodopa-induced dyskinesia and thalamotomy. J Neurol Neurosurg Psychiatry. 1984;47(8):831–9.
75. Matsumoto K, Asano T, Baba T, Miyamoto T, Ohmoto T. Long-term follow-up results of bilateral thalamotomy for parkinsonism. Stereotact Funct Neurosurg. 1976;39(3–4):257–60.
76. Hallett M, Litvan I. Evaluation of surgery for Parkinson's disease: a report of the Therapeutics and Technology Assessment Subcommittee of the American Academy of Neurology. Neurology. 1999;53(9):1910.
77. Vidaković A, Dragasević N, Kostić VS. Hemiballism: report of 25 cases. J Neurol Neurosurg Psychiatry. 1994;57(8):945–9.
78. Yamada A, Takeuchi H, Miki H. Unilateral abolition of parkinsonian rigidity after subthalamic nucleus hemorrhage. Clin Neurol. 1992;32(8):887–9.
79. Patel NK, Heywood P, O'Sullivan K, McCarter R, Love S, Gill SS. Unilateral subthalamotomy in the treatment of Parkinson's disease. Brain. 2003;126(5):1136–45.
80. Gross RE, Stern MA, Lazarus JT. Ablative procedures for Parkinson's disease. In: Winn HR, editor. Youmans neurological surgery E-book. Amsterdam: Elsevier Health Sciences; 2011. p. 610–8.
81. Walter BL, Vitek JL. Surgical treatment for Parkinson's disease. Lancet Neurol. 2004;3(12):719–28.
82. See AA, King NK. Improving surgical outcome using diffusion tensor imaging techniques in deep brain stimulation. Front Surg. 2017;4:54.
83. Eskandar EN, Shinobu LA, Penney JB, Cosgrove GR, Counihan TJ. Stereotactic pallidotomy performed without using microelectrode guidance in patients with Parkinson's disease: surgical technique and 2-year results. J Neurosurg. 2000;92(3):375–83.
84. Laitinen LV, Bergenheim AT, Hariz MI. Leksell's posteroventral pallidotomy in the treatment of Parkinson's disease. J Neurosurg. 1992;76(1):53–61.
85. Tasker RR, Yamashiro K, Lenz F, Dostrovsky JO. Thalamotomy for Parkinson's disease: microelectrode technique. In: Modern stereotactic neurosurgery. Boston: Springer; 1988. p. 297–314.
86. Alvarez L, Macias R, Guridi J, Lopez G, Alvarez E, Maragoto C, Teijeiro J, Torres A, Pavon N, Rodriguez-Oroz MC, Ochoa L. Dorsal subthalamotomy for Parkinson's disease. Mov Disord. 2001;16(1):72–8.
87. Rodriguez-Rojas R, Carballo-Barreda M, Alvarez L, Guridi J, Pavon N, Garcia-Maeso I, Macías R, Rodriguez-Oroz MC, Obeso JA. Subthalamotomy for Parkinson's disease: clinical outcome and topography of lesions. J Neurol Neurosurg Psychiatry. 2018;89(6):572–8.
88. Lozano A, Hutchison W, Kiss Z, et al. Methods for microelectrode-guided posteroventral pallidotomy. J Neurosurg. 1996;84(2):194–202. 153.
89. Fry WJ. Use of intense ultrasound in neurological research. Am J Phys Med. 1958;37(3):143–7.
90. Schlesinger I, Sinai A, Zaaroor M. MRI-guided focused ultrasound in Parkinson's disease: a review. Parkinson's Dis. 2017;2017:8124624.
91. Na YC, Chang WS, Jung HH, Kweon EJ, Chang JW. Unilateral magnetic resonance–guided focused ultrasound pallidotomy for Parkinson disease. Neurology. 2015;85(6):549–51.
92. Bond AE, Shah BB, Huss DS, Dallapiazza RF, Warren A, Harrison MB, Sperling SA, Wang XQ, Gwinn R, Witt J, Ro S. Safety and efficacy of focused ultrasound thalamotomy for patients with medication-refractory, tremor-dominant Parkinson disease: a randomized clinical trial. JAMA Neurol. 2017;74(12):1412–8.
93. Martínez-Fernández R, Rodríguez-Rojas R, del Álamo M, Hernández-Fernández F, Pineda-Pardo JA, Dileone M, Alonso-Frech F, Foffani G, Obeso I, Gasca-Salas C, de Luis-Pastor E. Focused ultrasound subthalamotomy in patients with asymmetric Parkinson's disease: a pilot study. Lancet Neurol. 2018;17(1):54–63.
94. Sapareto SA, Dewey WC. Thermal dose determination in cancer therapy. Int J Radiat Oncol Biol Phys. 1984;10(6):787–800.
95. Chung AH, Jolesz FA, Hynynen K. Thermal dosimetry of a focused ultrasound beam in vivo by magnetic resonance imaging. Med Phys. 1999;26(9):2017–26.
96. Chang WS, Jung HH, Zadicario E, Rachmilevitch I, Tlusty T, Vitek S, Chang JW. Factors associated with successful magnetic resonance-guided focused ultrasound treatment: efficiency of acoustic energy delivery through the skull. J Neurosurg. 2016;124(2):411–6.
97. Zaaroor M, Sinai A, Goldsher D, Eran A, Nassar M, Schlesinger I. Magnetic resonance–guided focused ultrasound thalamotomy for tremor: a report of 30 Parkinson's disease and essential tremor cases. J Neurosurg. 2018;128(1):202–10.
98. Duma CM. Movement disorder radiosurgery–planning, physics and complication avoidance. In: Radiosurgery and pathological fundamentals, vol. 20. Basel: Karger Publishers; 2007. p. 249–66.
99. Elaimy AL, Arthurs BJ, Lamoreaux WT, Demakas JJ, Mackay AR, Fairbanks RK, Greeley DR, Cooke BS, Lee CM. Gamma knife radiosurgery for movement disorders: a concise review of the literature. World J Surg Oncol. 2010;8(1):61.
100. Wu A, Lindner G, Maitz AH, Kalend AM, Lunsford LD, Flickinger JC, Bloomer WD. Physics of gamma knife approach on convergent beams in stereotactic radiosurgery. Int J Radiat Oncol Biol Phys. 1990;18(4):941–9.
101. Ganz J. Gamma knife neurosurgery. New York: Springer Science & Business Media; 2010.
102. Merello M, Nouzeilles MI, Cammarota A, Betti O, Leiguarda R. Comparison of 1-year follow-up evalu-

ations of patients with indication for pallidotomy who did not undergo surgery versus patients with Parkinson's disease who did undergo pallidotomy: a case control study. Neurosurgery. 1999;44(3):461–7.
103. de Bie RM, de Haan RJ, Nijssen PC, Rutgers AW, Beute GN, Bosch DA, Haaxma R, Schmand B, Schuurman PR, Staal MJ, Speelman JD. Unilateral pallidotomy in Parkinson's disease: a randomised, single-blind, multicentre trial. Lancet. 1999;354(9191):1665–9.
104. Bastian AJ, Kelly VE, Perlmutter JS, Mink JW. Effects of pallidotomy and levodopa on walking and reaching movements in Parkinson's disease. Mov Disord. 2003;18(9):1008–17.
105. Hagiwara N, Hashimoto T, Ikeda SI. Static balance impairment and its change after pallidotomy in Parkinson's disease. Mov Disord. 2004;19(4):437–45.
106. Schulz GM, Greer M, Friedman W. Changes in vocal intensity in Parkinson's disease following pallidotomy surgery. J Voice. 2000;14(4):589–606.
107. Narabayashi H, Maeda T, Yokochi F. Long-term follow-up study of nucleus ventralis intermedius and ventrolateralis thalamotomy using a microelectrode technique in parkinsonism. Stereotact Funct Neurosurg. 1987;50(1–6):330–7.
108. Kelly PJ, Gillingham FJ. The long-term results of stereotaxic surgery and L-dopa therapy in patients with Parkinson's disease: a 10-year follow-up study. J Neurosurg. 1980;53(3):332–7.
109. Diederich N, Goetz CG, Stebbins GT, Klawans HL, Nittner K, Koulosakis A, Sanker P, Sturm V. Blinded evaluation confirms long-term asymmetric effect of unilateral thalamotomy or subthalamotomy on tremor in Parkinson's disease. Neurology. 1992;42(7):1311.
110. Cardoso F, Jankovic J, Grossman RG, Hamilton WJ. Outcome after stereotactic thalamotomy for dystonia and hemiballismus. Neurosurgery. 1995;36(3):501–8.
111. Guridi J, Obeso JA, Rodriguez-Oroz MC, Lozano AM, Manrique M. L-dopa-induced dyskinesia and stereotactic surgery for Parkinson's disease. Neurosurgery. 2008;62(2):311–25.
112. Chang JW. Magnetic resonance guided focused ultrasound pallidotomy for Parkinson's disease. J Ther Ultrasound. 2015;3(S1):O5.
113. Schlesinger I. MRI guided focused ultrasound thalamotomy for moderate-to-severe tremor in Parkinson's disease. Parkinson's Dis. 2015;2015:219149.
114. Sperling SA, Shah BB, Barrett MJ, Bond AE, Huss DS, Mejia JA, Elias WJ. Focused ultrasound thalamotomy in Parkinson disease: nonmotor outcomes and quality of life. Neurology. 2018;91(14):e1275–84.
115. Lozano AM, Lang AE, Galvez-Jimenez N, Miyasaki J, Duff J, Hutchison WD, Dostrovsky JO. Effect of GPi pallidotomy on motor function in Parkinson's disease. Lancet. 1995;346(8987):1383–7.
116. Demakis GJ, Mercury MG, Sweet JJ, Rezak M, Eller T, Vergenz S. Motor and cognitive sequelae of unilateral pallidotomy in intractable Parkinson's disease: electronic measurement of motor steadiness is a useful outcome measure. J Clin Exp Neuropsychol. 2002;24(5):655–63.
117. Lacritz LH, Cullum CM, Frol AB, Dewey RB Jr, Giller CA. Neuropsychological outcome following unilateral stereotactic pallidotomy in intractable Parkinson's disease. Brain Cogn. 2000;42(3):364–78.
118. Louw DF, Burchiel KJ. Ablative therapy for movement disorders: complications in the treatment of movement disorders. Neurosurg Clin N Am. 1998;9(2):367–74.
119. Bell DS. Speech functions of the thalamus inferred from the effects of thalamotomy. Brain. 1968;91(4):619–38.
120. Wester K, Hauglie-Hanssen E. Stereotaxic thalamotomy--experiences from the levodopa era. J Neurol Neurosurg Psychiatry. 1990;53(5):427–30.
121. Rossitch E Jr, Zeidman SM, Nashold BS Jr, Horner J, Walker J, Osborne D, Bullard DE. Evaluation of memory and language function pre-and postthalamotomy with an attempt to define those patients at risk for postoperative dysfunction. Surg Neurol. 1988;29(1):11–6.
122. Hugdahl K, Wester K. Neurocognitive correlates of stereotactic thalamotomy and thalamic stimulation in parkinsonian patients. Brain Cogn. 2000;42(2):231–52.
123. Duma CM, Deane J. The treatment of movement disorders using gamma knife stereotactic radiosurgery. Neurosurg Clin N Am. 1999;10(2):379–89.
124. Magara A, Bühler R, Moser D, Kowalski M, Pourtehrani P, Jeanmonod D. First experience with MR-guided focused ultrasound in the treatment of Parkinson's disease. J Ther Ultrasound. 2014;2(1):11.

Essential Tremor: Deep Brain Stimulation

20

Adela Wu and Casey Halpern

Introduction

Essential tremor (ET), the most common adult movement disorder and one of the most widely known neurological disorders, affects nearly 1% of the global population and is generally characterized by postural and/or kinetic tremor with variable rates of leg, head, and voice tremors [1]. The symptoms typically cause great distress for patients who have significant decline in function and quality of life [2–4]. Since the era of surgical ablative thalamotomy to treat ET, deep brain stimulation (DBS) has been reported on in more detail in the 1980s as surgeons implanted electrodes in the ventral intermediate thalamic nucleus (VIM) for adjustable electrical stimulation. This induced what has been considered to be a reversible "functional lesion," though the mechanism of action continues to elude understanding. The Federal Drug Administration approved unilateral DBS in 1997, and it is currently considered one of the standards of care for medically refractory ET.

A. Wu (✉) · C. Halpern
Department of Neurosurgery, Stanford University, Palo Alto, CA, USA
e-mail: adelawu@stanford.edu

Patient Selection

Patient evaluation and selection are critical for pursuing DBS intervention for essential tremor. Unfortunately, there are no Class I studies on ET treatment [5]. While the effects of DBS are profound, the prerequisite medical management leading to the determination of medication-refractory tremor must be considered. Prior to referral to neurosurgery, patients are typically trialed on and treated with primidone, propranolol, or a combinatory regimen with possible second-line additions, such as gabapentin or topiramate. Unfortunately, about 50% of ET patients have adequate response to medication [6].

Typically, patients who would benefit from DBS have failed optimized medical therapy and are debilitated in hand or voice communication due to severe intention or voice tremor [7]. Unilateral VIM DBS is indicated for severe hand tremor, while bilateral VIM DBS could be offered to patients with profound bilateral limb, head, voice, or axial tremor [7]. A series of long-term studies with range of follow-up from 0 to 8.5 years demonstrated that ET patients reported high percentages of improvement in their tremor amplitude (82–95%) sustained over time [8]. One report maintains that patients older than age 75 should be excluded from DBS [5], although this is not universally accepted; at many centers, patients over the age of 75 years

N. Pouratian, S. A. Sheth (eds.), *Stereotactic and Functional Neurosurgery*,
https://doi.org/10.1007/978-3-030-34906-6_20

who are functionally debilitated are regularly considered candidates for DBS for tremor control.

While the effects of VIM DBS for ET are excellent, a certain subset of patients develops tolerance to the treatment [9]. Loss of efficacy could be due to several reasons, including inherent limitations of DBS or patient characteristics. Merchant et al. found that patients with primarily intention or proximal postural tremors showed early tolerance to DBS [9]. These patients eventually manifest a pancerebellar syndrome involving persistent ataxia and dysarthria, which can limit overall efficacy and patient satisfaction. In addition, it appears that patients presenting with subtle ataxia and incoordination prior to DBS implantation develop early resistance to treatment as well.

Available Stereotactic Methods

Precise targeting for DBS electrode placement through stereotactic methods is critical for successful treatment effect. Volumetric imaging guidance with both CT and MRI provides anatomical understanding in three dimensions, and often imaging registration is used to combine imaging data into one coordinate system for mapping. Whether with frame or frameless methods, in order to create an accurate aligned targeting system, secured fiducial markers are commonly used to establish a fixed geometric array on the head [10]. These methods are broadly considered in Part I of this book. Fusion of CT, MRI, and sometimes functional imaging is also used for planning of trajectories to the final targets in order to avoid eloquent cortical areas, vasculature, and the ventricles. Frequently, the anterior and posterior commissures (AC-PC) are used as references to produce coordinates to target the VIM, which unfortunately do not take into account anatomic variation in the thalamus and the adjacent third ventricle [11]. Diffusion tensor imaging (DTI) and tractography (discussed in great detail in Chap. 7) provide some confirmation of targeting and good anatomical localization in addition to CT and MRI [12, 13]. DISTINCT is the first randomized controlled trial comparing conventional stereotactic methods against DTI tractography-assisted stereotactic surgery, with final results pending due to its slated completion date in 2020 [14].

In addition to utilizing imaging for localization, electrophysiology also provides useful information for targeting. For example, single-cell recordings and electrical stimulation are nuanced adjunct methods to select electrode placement, especially when even MRI may not differentiate the separate regions of the thalamus [15]. Another method for stereotactic precision involves interventional MRI guidance, which obviates the need for fiducial markers and electrophysiology and can account for potential shifts as the surgeon opens the dura and releases cerebrospinal fluid [16]. Others have tried intraoperative CT with the NexFrame system to successfully implant electrodes in the VIM and GPI with mean vector error 1.59 ± 1.11 mm and mean deviation off trajectory 1.24 ± 0.87 mm [17]. Please refer to Chap. 3 for a more extensive discussion of the role of intraoperative imaging in stereotactic neurosurgery.

Some have investigated an alternative stereotactic method based on a probabilistic map of tremor cells' electrophysiology. Through stimulation of microelectrodes, the investigators selected areas containing single thalamic units firing in bursts (5–10 in a series) at frequencies of 3–10 Hz that matched with elicitation of the patient's tremor [15]. Furthermore, the fornix and posterior commissure (FX-PC) were used as reference for the anteroposterior plane in addition to the AC-PC plane and the boundary between the thalamus and internal capsule. As a result, there appeared to be significantly decreased variation in selection of optimal stimulation target.

Targets

DBS target selection for essential tremor has become more varied. Since its introduction by Benabid et al., the first and most commonly used anatomic target was the thalamic ventral intermedius nucleus (VIM) [18–21]. In a long-term follow-up study on ET patients, subjects underwent assessment by the Fahn, Tolosa, Marin Tremor

Rating Scale (FTMTRS), demonstrating improvement in symptoms at both 1-year and 10-year follow-up following VIM DBS stimulation [20]. Furthermore, an analysis of exact lead position and resultant percent improvement in tremor following DBS stimulation identified the best lead location as the anterior boundary of the VIM [11].

Tolerance to DBS presents a challenge to choosing the VIM as a target. While some long-term studies show that VIM stimulation support sustained efficacy over at least 29–40 months, many studies report decreases in tremor reduction and benefit to daily living activities over time [22–27]. Proximal tremors are also difficult to treat with solely VIM DBS [28].

The posterior subthalamic area (PSA) of the thalamus has recently become a promising alternative target [29]. Murata et al. found that eight patients with severe ET who were treated with PSA DBS had improvements in axial, proximal, and distal tremors [30]. Patients with medically refractory ET had increased symptom relief as well as an 80.1% improvement in FTMTRS scores in the immediate postoperative period and at 1-year follow-up [31].

More precisely, the PSA involves the caudal zona incerta (ZI), prelemniscal radiation, and fasciculus cerebellothalamicus (Fct). The PSA is ventral to VIM and the intercommissural line (ICL). The caudal ZI presents an area with significant therapeutic potential in ET treatment. In fact, the leads associated with large symptom improvement margins in Murata et al.'s study were implanted in the ZI and prelemniscal radiation [30]. Eighteen patients were followed for 4 years following caudal ZI DBS and maintained positive results at their final evaluation with a 52.4% improvement in baseline FTMTRS score as well as improvements in upper extremity tremor, hand function, and activities of daily living [32]. A prospective study by Sandvik et al. reflected the benefits of caudal ZI DBS as well, with improvements in hand tremor, hand function, and activities of daily living on scales measuring tremor rating and quality of life [33]. Further differentiation within the caudal ZI DBS demonstrated that the superior aspect of the PSA, also related to the end of the cerebellothalamic tracts, served as the optimal stimulation location for tremor control [34]. In fact, a recent randomized controlled trial provided Class I evidence that PSA stimulation at comparatively lower stimulation amplitudes was at least equivalent in treatment efficacy as VIM DBS [35, 36]. Overall, the PSA presents an efficacious new DBS target for tremor with significant tremor reduction [37]. Importantly, the PSA can be targeted while preserving a trajectory through VIM.

It is also possible to achieve stimulation of two discrete targets in DBS for ET for presumably maximal treatment effect. For a group of 17 ET patients, all but 4 trajectories that incorporated both the VIM and PSA resulted in optimal intraoperative tremor control [38]. Overall, 69% of study patients had tremor control with postoperative adverse effects including gait ataxia and dysarthria [38].

Nuanced Surgical Methods

Implanted DBS electrodes can prompt further nuance in therapy for ET. While conventional pulse width is 60 μs, a shorter pulse width of 40 μs resulted in a wider therapeutic window and a smaller stimulation energy requirement without sacrificing treatment effect [39]. Likewise, a square biphasic pulse delivered through DBS electrodes demonstrated significant improvement in postural tremor, tremor at rest, and action tremor when compared to conventional DBS settings as well as sustained tremor improvement [40, 41]. Another interesting application involves administering radiofrequency through previously implanted DBS electrodes, with the aim to provide precise ablation localization and success in ET reduction in a limited set of cases [42–44].

Ablative therapies for tremor are discussed in detail in Chap. 20. For reference, a brief overview is provided here. Stereotactic radiosurgery (SRS) to the VIM provides relief from refractory ET symptoms for patients otherwise ineligible for DBS. The International Stereotactic Radiosurgery Society recommends unilateral VIM targeting with dosage between 130 and 150 Gy as an effective option for ET [45]. In a group of essential

tremor ($n = 8$) and Parkinson's disease or multiple sclerosis-related tremors ($n = 2$), bilateral Gamma Knife (GK) thalamotomy in stages was efficacious in most patients who had failed medical treatment in eliminating bilateral tremors and restoring function [46]. A series of 73 ET cases treated with a median dose of 140 Gy for GK thalamotomy demonstrated immediate improvement in preoperative tremor for 93.2% of patients and long-term reduction in ET for 96% of those who already had postoperative tremor relief (median follow-up time, 28 months) [47]. Overall, SRS resulted in an average of 88% reduction in ET for patients [45].

Focused ultrasound (FUS) is a novel option for ET treatment. Through thermal ablation, FUS targets similar anatomical structures as DBS does. Good results and improvement of baseline ET were reported following MRI-guided FUS to the cerebellothalamic tract [48]. In a separate study, FUS-assisted thalamotomy for 18 ET patients provided significant reduction in tremor as well as significant improvement in quality of life at 1 and 6 months postoperatively [49]. Adverse effects from treatment lasted up to 3 months and included headache, vertigo, and gait ataxia as the most common postoperative symptoms [49].

Since the 1980s, surgical thalamotomy was reported as a viable treatment option for medically refractory ET [50, 51]. Now, in some cases, DBS fails to adequately treat ET, and surgical thalamotomy can continue to be considered. In one study on six ET patients and one tremor-dominant PD case, DBS resulted in profound adverse effects, lack of treatment effect, and poor lead positioning. With salvage surgery, six patients (85.7%) reported at least some improvement in their tremors [52].

Clinical Evidence Across Treatment Options

While DBS is the most used treatment for ET, there is an array of alternatives for patients, and the physician plays a significant role in advising patients based on treatment eligibility and treatment outcomes among other factors. Current clinical evidence across ET treatment options depends on retrospective and a few clinical trials. A longitudinal case followed one ET patient over 12 years who experienced immediate postoperative tremor reduction after implantation and programming and had no long-term consequences from her VIM DBS system since 1996 [53]. DBS, the current standard of care for ET, provides the highest percentage of sustained symptom control (84.2%) at 1-year follow-up compared to radiofrequency thalamotomy (70.6%) and MRI-guided FUS (78.3%), although no significant difference in treatment efficacy was ultimately determined among the three modalities [54]. Of note, the FUS treatment group had the lowest complication rate overall [54]. Another systematic review of DBS, radiofrequency thalamotomy, SRS, and FUS revealed that there was no significant difference between unilateral DBS and FUS in terms of health-related quality of life or treatment efficacy by 1-year follow-up [55]. In a recent meta-analysis, FUS is significantly less costly than DBS with significantly greater increases in quality of life and decreased degree of functional disability than either SRS or DBS, which itself is at least 40% more costly than radiosurgery [56, 57].

Conclusion

Essential tremor (ET) is a debilitating and common movement disorder that prevents patients from functioning fully due to kinetic and postural tremors. Deep brain stimulation (DBS) is the current FDA-approved standard of care for medically refractory ET. Electrode placement in the thalamic ventral intermedius nucleus (VIM) with novel targets within the posterior subthalamic area (PSA) relies on stereotactic techniques for precise localization. Current innovations in neurosurgical interventions for ET now include MRI-guided focused ultrasound (FUS), which has been determined to be more cost-effective with similar rates of treatment efficacy as DBS.

References

1. Louis ED, Ferreira JJ. How common is the most common adult movement disorder? Update on the worldwide prevalence of essential tremor. Mov Disord. 2010;25(5):534–41. https://doi.org/10.1002/mds.22838.
2. Chandran V, Pal PK, Reddy JYC, Thennarasu K, Yadav R, Shivashankar N. Non-motor features in essential tremor. Acta Neurol Scand. 2012;125(5):332–7. https://doi.org/10.1111/j.1600-0404.2011.01573.x.
3. Lorenz D, Poremba C, Papengut F, Schreiber S, Deuschl G. The psychosocial burden of essential tremor in an outpatient- and a community-based cohort. Eur J Neurol. 2011;18(7):972–9. https://doi.org/10.1111/j.1468-1331.2010.03295.x.
4. Lorenz D, Schwieger D, Moises H, Deuschl G. Quality of life and personality in essential tremor patients. Mov Disord. 2006;21(8):1114–8. https://doi.org/10.1002/mds.20884.
5. Paschen S, Deuschl G. Patient evaluation and selection for movement disorders surgery: the changing spectrum of indications. Prog Neurol Surg. 2018;33:80–93. https://doi.org/10.1159/000480910.
6. Lyons KE, Pahwa R. Deep brain stimulation and tremor. Neurotherapeutics. 2008;5(2):331–8. https://doi.org/10.1016/j.nurt.2008.01.004.
7. Munhoz RP, Picillo M, Fox SH, et al. Eligibility criteria for deep brain stimulation in Parkinson's disease, tremor, and dystonia. Can J Neurol Sci. 2016;43(4):462–71. https://doi.org/10.1017/cjn.2016.35.
8. Deuschl G, Raethjen J, Hellriegel H, Elble R. Treatment of patients with essential tremor. Lancet Neurol. 2011;10(2):148–61. https://doi.org/10.1016/S1474-4422(10)70322-7.
9. Merchant SH, Kuo S-H, Qiping Y, et al. Objective predictors of "early tolerance" to ventral intermediate nucleus of thalamus deep brain stimulation in essential tremor patients. Clin Neurophysiol. 2018;129(8):1628–33. https://doi.org/10.1016/j.clinph.2018.05.012.
10. Khan FR, Henderson JM. Deep brain stimulation surgical techniques. Handb Clin Neurol. 2013;116:27–37. https://doi.org/10.1016/B978-0-444-53497-2.00003-6.
11. Papavassiliou E, Rau G, Heath S, et al. Thalamic deep brain stimulation for essential tremor: relation of lead location to outcome. Neurosurgery. 2004;54(5):1120–9; discussion 1129–1130. http://www.ncbi.nlm.nih.gov/pubmed/15113466. Accessed 2 Dec 2018.
12. Nowacki A, Schlaier J, Debove I, Pollo C. Validation of diffusion tensor imaging tractography to visualize the dentatorubrothalamic tract for surgical planning. J Neurosurg. 2018;130:1–10. https://doi.org/10.3171/2017.9.JNS171321.
13. Seddighi AS, Seddighi A, Nikouei A. Deep brain nucleus targeting in Parkinson's disease and essential tremor by image guided surgery using neuronavigation system with tractography and volume of tissue of activated assessment. Hell J Nucl Med. 2017;20 Suppl:14–9. http://www.ncbi.nlm.nih.gov/pubmed/29324910. Accessed 1 Dec 2018.
14. Sajonz BEA, Amtage F, Reinacher PC, et al. Deep brain stimulation for tremor tractographic versus traditional (DISTINCT): study protocol of a randomized controlled feasibility trial. JMIR Res Protoc. 2016;5(4):e244. https://doi.org/10.2196/resprot.6885.
15. King NKK, Krishna V, Sammartino F, et al. Anatomic targeting of the optimal location for thalamic deep brain stimulation in patients with essential tremor. World Neurosurg. 2017;107:168–74. https://doi.org/10.1016/j.wneu.2017.07.136.
16. Starr PA, Martin AJ, Ostrem JL, Talke P, Levesque N, Larson PS. Subthalamic nucleus deep brain stimulator placement using high-field interventional magnetic resonance imaging and a skull-mounted aiming device: technique and application accuracy. J Neurosurg. 2010;112(3):479–90. https://doi.org/10.3171/2009.6.JNS081161.
17. Burchiel KJ, McCartney S, Lee A, Raslan AM. Accuracy of deep brain stimulation electrode placement using intraoperative computed tomography without microelectrode recording. J Neurosurg. 2013;119(2):301–6. https://doi.org/10.3171/2013.4.JNS122324.
18. Benabid AL, Pollak P, Louveau A, Henry S, de Rougemont J. Combined (thalamotomy and stimulation) stereotactic surgery of the VIM thalamic nucleus for bilateral Parkinson disease. Appl Neurophysiol. 1987;50(1–6):344–6. http://www.ncbi.nlm.nih.gov/pubmed/3329873. Accessed 1 Dec 2018.
19. Flora ED, Perera CL, Cameron AL, Maddern GJ. Deep brain stimulation for essential tremor: a systematic review. Mov Disord. 2010;25(11):1550–9. https://doi.org/10.1002/mds.23195.
20. Cury RG, Fraix V, Castrioto A, et al. Thalamic deep brain stimulation for tremor in Parkinson disease, essential tremor, and dystonia. Neurology. 2017;89(13):1416–23. https://doi.org/10.1212/WNL.0000000000004295.
21. Crowell JL, Shah BB. Surgery for dystonia and tremor. Curr Neurol Neurosci Rep. 2016;16(3):22. https://doi.org/10.1007/s11910-016-0627-8.
22. Nazzaro JM, Pahwa R, Lyons KE. Long-term benefits in quality of life after unilateral thalamic deep brain stimulation for essential tremor. J Neurosurg. 2012;117(1):156–61. https://doi.org/10.3171/2012.3.JNS112316.
23. Baizabal-Carvallo JF, Kagnoff MN, Jimenez-Shahed J, Fekete R, Jankovic J. The safety and efficacy of thalamic deep brain stimulation in essential tremor: 10 years and beyond. J Neurol Neurosurg Psychiatry. 2014;85(5):567–72. https://doi.org/10.1136/jnnp-2013-304943.
24. Blomstedt P, Hariz G-M, Hariz MI, Koskinen L-OD. Thalamic deep brain stimulation in the

treatment of essential tremor: a long-term follow-up. Br J Neurosurg. 2007;21(5):504–9. https://doi.org/10.1080/02688690701552278.
25. Hariz G-M, Blomstedt P, Koskinen L-OD. Long-term effect of deep brain stimulation for essential tremor on activities of daily living and health-related quality of life. Acta Neurol Scand. 2008;118(6):387–94. https://doi.org/10.1111/j.1600-0404.2008.01065.x.
26. Benabid AL, Pollak P, Gervason C, et al. Long-term suppression of tremor by chronic stimulation of the ventral intermediate thalamic nucleus. Lancet (Lond, Engl). 1991;337(8738):403–6. http://www.ncbi.nlm.nih.gov/pubmed/1671433. Accessed December 15, 2018.
27. Koller WC, Lyons KE, Wilkinson SB, Troster AI, Pahwa R. Long-term safety and efficacy of unilateral deep brain stimulation of the thalamus in essential tremor. Mov Disord. 2001;16(3):464–8. http://www.ncbi.nlm.nih.gov/pubmed/11391740. Accessed 15 Dec 2018.
28. Nguyen JP, Degos JD. Thalamic stimulation and proximal tremor. A specific target in the nucleus ventrointermedius thalami. Arch Neurol. 1993;50(5):498–500. http://www.ncbi.nlm.nih.gov/pubmed/8489406. Accessed 1 Dec 2018.
29. Blomstedt P, Sandvik U, Tisch S. Deep brain stimulation in the posterior subthalamic area in the treatment of essential tremor. Mov Disord. 2010;25(10):1350–6. https://doi.org/10.1002/mds.22758.
30. Murata J, Kitagawa M, Uesugi H, et al. Electrical stimulation of the posterior subthalamic area for the treatment of intractable proximal tremor. J Neurosurg. 2003;99(4):708–15. https://doi.org/10.3171/jns.2003.99.4.0708.
31. Plaha P, Patel NK, Gill SS. Stimulation of the subthalamic region for essential tremor. J Neurosurg. 2004;101(1):48–54. https://doi.org/10.3171/jns.2004.101.1.0048.
32. Fytagoridis A, Sandvik U, Åström M, Bergenheim T, Blomstedt P. Long term follow-up of deep brain stimulation of the caudal zona incerta for essential tremor. J Neurol Neurosurg Psychiatry. 2012;83(3):258–62. https://doi.org/10.1136/jnnp-2011-300765.
33. Sandvik U, Hariz G-M, Blomstedt P. Quality of life following DBS in the caudal zona incerta in patients with essential tremor. Acta Neurochir. 2012;154(3):495–9. https://doi.org/10.1007/s00701-011-1230-z.
34. Fytagoridis A, Åström M, Samuelsson J, Blomstedt P. Deep brain stimulation of the caudal zona incerta: tremor control in relation to the location of stimulation fields. Stereotact Funct Neurosurg. 2016;94(6):363–70. https://doi.org/10.1159/000448926.
35. Barbe MT, Reker P, Hamacher S, et al. DBS of the PSA and the VIM in essential tremor. Neurology. 2018;91(6):e543–50. https://doi.org/10.1212/WNL.0000000000005956.
36. Barbe MT, Liebhart L, Runge M, et al. Deep brain stimulation of the ventral intermediate nucleus in patients with essential tremor: stimulation below intercommissural line is more efficient but equally effective as stimulation above. Exp Neurol. 2011;230(1):131–7. https://doi.org/10.1016/j.expneurol.2011.04.005.
37. Ramirez-Zamora A, Smith H, Kumar V, Prusik J, Phookan S, Pilitsis JG. Evolving concepts in posterior subthalamic area deep brain stimulation for treatment of tremor: surgical neuroanatomy and practical considerations. Stereotact Funct Neurosurg. 2016;94(5):283–97. https://doi.org/10.1159/000449007.
38. Bot M, van Rootselaar F, Contarino MF, et al. Deep brain stimulation for essential tremor: aligning thalamic and posterior subthalamic targets in 1 surgical trajectory. Oper Neurosurg (Hagerstown). 2018;15(2):144–52. https://doi.org/10.1093/ons/opx232.
39. Moldovan A-S, Hartmann CJ, Trenado C, et al. Less is more – pulse width dependent therapeutic window in deep brain stimulation for essential tremor. Brain Stimul. 2018;11(5):1132–9. https://doi.org/10.1016/j.brs.2018.04.019.
40. De Jesus S, Almeida L, Shahgholi L, et al. Square biphasic pulse deep brain stimulation for essential tremor: the BiP tremor study. Parkinsonism Relat Disord. 2018;46:41–6. https://doi.org/10.1016/j.parkreldis.2017.10.015.
41. Akbar U, Raike RS, Hack N, et al. Randomized, blinded pilot testing of nonconventional stimulation patterns and shapes in Parkinson's disease and essential tremor: evidence for further evaluating narrow and biphasic pulses. Neuromodulation. 2016;19(4):343–56. https://doi.org/10.1111/ner.12397.
42. Raoul S, Faighel M, Rivier I, Vérin M, Lajat Y, Damier P. Staged lesions through implanted deep brain stimulating electrodes: a new surgical procedure for treating tremor or dyskinesias. Mov Disord. 2003;18(8):933–8. https://doi.org/10.1002/mds.10457.
43. Oh MY, Hodaie M, Kim SH, Alkhani A, Lang AE, Lozano AM. Deep brain stimulator electrodes used for lesioning: proof of principle. Neurosurgery. 2001;49(2):363–7; discussion 367–369. http://www.ncbi.nlm.nih.gov/pubmed/11504112. Accessed 2 Dec 2018.
44. Pérez-Suárez J, Torres Díaz CV, López Manzanares L, et al. Radiofrequency lesions through deep brain stimulation electrodes in movement disorders: case report and review of the literature. Stereotact Funct Neurosurg. 2017;95(3):137–41. https://doi.org/10.1159/000454891.
45. Martínez-Moreno NE, Sahgal A, De Salles A, et al. Stereotactic radiosurgery for tremor: systematic review. J Neurosurg. 2018;130:1–12. https://doi.org/10.3171/2017.8.JNS17749.
46. Niranjan A, Raju SS, Monaco EA, Flickinger JC, Lunsford LD. Is staged bilateral thalamic radiosurgery an option for otherwise surgically ineligible patients with medically refractory bilateral tremor? J Neurosurg. 2018;128(2):617–26. https://doi.org/10.3171/2016.11.JNS162044.
47. Niranjan A, Raju SS, Kooshkabadi A, Monaco E, Flickinger JC, Lunsford LD. Stereotactic radiosurgery for essential tremor: retrospective analysis of a

19-year experience. Mov Disord. 2017;32(5):769–77. https://doi.org/10.1002/mds.26925.
48. Chazen JL, Sarva H, Stieg PE, et al. Clinical improvement associated with targeted interruption of the cerebellothalamic tract following MR-guided focused ultrasound for essential tremor. J Neurosurg. 2018;129(2):315–23. https://doi.org/10.3171/2017.4.JNS162803.
49. Zaaroor M, Sinai A, Goldsher D, Eran A, Nassar M, Schlesinger I. Magnetic resonance-guided focused ultrasound thalamotomy for tremor: a report of 30 Parkinson's disease and essential tremor cases. J Neurosurg. 2018;128(1):202–10. https://doi.org/10.3171/2016.10.JNS16758.
50. Goldman MS, Ahlskog JE, Kelly PJ. The symptomatic and functional outcome of stereotactic thalamotomy for medically intractable essential tremor. J Neurosurg. 1992;76(6):924–8. https://doi.org/10.3171/jns.1992.76.6.0924.
51. Nagaseki Y, Shibazaki T, Hirai T, et al. Long-term follow-up results of selective VIM-thalamotomy. J Neurosurg. 1986;65(3):296–302. https://doi.org/10.3171/jns.1986.65.3.0296.
52. Bahgat D, Magill ST, Berk C, McCartney S, Burchiel KJ. Thalamotomy as a treatment option for tremor after ineffective deep brain stimulation. Stereotact Funct Neurosurg. 2013;91(1):18–23. https://doi.org/10.1159/000342491.
53. DiLorenzo DJ, Jankovic J, Simpson RK, Takei H, Powell SZ. Long-term deep brain stimulation for essential tremor: 12-year clinicopathologic follow-up. Mov Disord. 2010;25(2):232–8. https://doi.org/10.1002/mds.22935.
54. Kim M, Jung NY, Park CK, Chang WS, Jung HH, Chang JW. Comparative evaluation of magnetic resonance-guided focused ultrasound surgery for essential tremor. Stereotact Funct Neurosurg. 2017;95(4):279–86. https://doi.org/10.1159/000478866.
55. Langford BE, Ridley CJA, Beale RC, Caseby SCL, Marsh WJ, Richard L. Focused ultrasound thalamotomy and other interventions for medication-refractory essential tremor: an indirect comparison of short-term impact on health-related quality of life. Value Health. 2018;21(10):1168–75. https://doi.org/10.1016/j.jval.2018.03.015.
56. Ravikumar VK, Parker JJ, Hornbeck TS, et al. Cost-effectiveness of focused ultrasound, radiosurgery, and DBS for essential tremor. Mov Disord. 2017;32(8):1165–73. https://doi.org/10.1002/mds.26997.
57. McClelland S, Jaboin JJ. Treatment of the ventral intermediate nucleus for medically refractory tremor: a cost-analysis of stereotactic radiosurgery versus deep brain stimulation. Radiother Oncol. 2017;125(1):136–9. https://doi.org/10.1016/j.radonc.2017.07.030.

Essential Tremor: Lesions

21

Shayan Moosa and W. Jeffrey Elias

Abbreviations

AAN	American Academy of Neurology
AC	Anterior commissure
AChA	Anterior choroidal artery
ADC	Apparent diffusion coefficient
ADL	Activities of daily living
CRST	Clinical Rating Scale for Tremor
CSF	Cerebrospinal fluid
CT	Computed tomography
DBS	Deep brain stimulation
DRT	Dentatorubrothalamic tract
DWI	Diffusion-weighted imaging
GK	Gamma Knife
GKRS	Gamma Knife radiosurgery
ICL	Intercommissural line
MCP	Midcommissural point
MER	Microelectrode recording
MPR	MP-RAGE
MRgFUS	Magnetic resonance-guided focused ultrasound
MRI	Magnetic resonance imaging
PC	Posterior commissure
PD	Parkinson's disease
PSA	Posterior subthalamic area
RF	Radiofrequency
SDR	Skull density ratio
SWI	Susceptibility-weighted imaging
Vc	Ventralis caudalis
Vim	Ventral intermediate
VL	Ventrolateral
Vop	Ventralis oralis posterior

S. Moosa
Department of Neurological Surgery, University of Virginia, Charlottesville, VA, USA

W. J. Elias (✉)
Departments of Neurological Surgery and Neurology, University of Virginia, Charlottesville, VA, USA
e-mail: wje4r@virginia.edu

The History of Surgical Lesioning for Tremor

Lesioning of the Pyramidal Tract

The first reported surgical lesion for the treatment of tremor was performed in 1937 by Paul Bucy [1], almost 18 centuries after Galen first identified tremor as a medical disorder [2]. Bucy believed that tremor was derived from the activity of the large pyramidal "Betz" cells and therefore stated that tremor could not be abolished without a corticospinal deficit. Based on this understanding, Bucy extirpated the arm and leg portions of the posterior precentral gyrus with some success in abolishing tremor, but at the cost of considerable hemiparesis.

Surgical lesioning for tremor was performed in other parts of the pyramidal tract as well, including the spinal cord [3], internal capsule, and cerebral peduncle. In 1948, Earl Walker carried out the first pedunculotomy for the treatment of a movement disorder by sectioning the lateral

N. Pouratian, S. A. Sheth (eds.), *Stereotactic and Functional Neurosurgery*,
https://doi.org/10.1007/978-3-030-34906-6_21

two-thirds of the cerebral peduncle [4]. Walker repeated this procedure in patients with Parkinson's disease (PD), reporting significant improvement in tremor at the expense of motor function, with little to no effect on other parkinsonian features [5]. This technique was adopted and further refined by Bucy as it avoided the risk of convulsions associated with cortical resection and resulted in fewer pyramidal deficits with a more substantial recovery of motor function [6, 7]. Despite these improvements, lesioning of the pyramidal tract for tremor fell out of favor in the 1950s and 1960s due to the recognition of the basal ganglia for involuntary movements, the development of stereotactic surgery, and the synthesis of levodopa for the treatment of parkinsonian conditions.

Extrapyramidal Lesioning

In the late 1930s, Russell Meyers postulated that he could achieve improved functional outcomes for patients with PD by lesioning components of the extrapyramidal system such as the caudate nucleus and pallidofugal fibers of the ansa lenticularis. At the time, Walter Dandy had expressed the idea that the ventral striata were necessary for consciousness; however, Meyers had observed a patient struck by a propeller where an open skull fracture revealed bilateral injury to the ventral striata without alteration of consciousness. In 1939, Meyers performed a right transcortical, transventricular resection of the anterior two-thirds of the caudate nucleus for a 26-year-old female with severe left hemiparkinsonism from encephalitis. The patient remained awake for the procedure, and Meyers used cortical stimulation to avoid the motor system. She had immediate relief of tremor following the resection, leading Meyers to perform a total of 58 basal ganglia operations with 69% of his patients exhibiting tremor improvement. While most of Meyers' patients had improvement of tremor and rigidity without expected paralysis, his procedures carried a rate of high morbidity and nearly 15% mortality [8]. Meyers' series inspired Gerard Guiot to lesion the ansa lenticularis from a subfrontal approach, achieving a similar degree of tremor and rigidity relief [9]. Fortunately, Ernest Spiegel and Henry Wycis developed the modern cerebral stereotactic system in 1947 and targeted many of their earliest procedures for tremor [10–12]. Stereotactic lesioning had favorable results for tremor control and decreased rigidity with an improved safety profile.

Irving Cooper performed the first pallidotomy in 1952, which occurred serendipitously when he was forced to occlude the anterior choroidal artery (AChA) during a pedunculotomy for a patient with postencephalitic tremor [13, 14]. Cooper found his patient to be cured of tremor and rigidity without corticospinal deficit, leading him to intentionally occlude the AChA in at least 40 other patients with PD by 1955 [15]. During this time, Cooper also developed a technique involving pneumoencephalography and stereotaxy to lesion the globus pallidus with greater accuracy, reliability, and safety [16]. Ventrolateral (VL) thalamotomy was proposed by Rolf Hassler, who demonstrated that the main outflow tract of the medial globus pallidus is to the VL thalamus [17, 18]. Gonzalo Bravo and Cooper subsequently performed stereotactic lesioning of the VL thalamus, confirming this procedure to be more effective for tremor control with fewer complications as compared to pallidal lesioning [19, 20].

Contemporary methods for creating cerebral lesions for the treatment of tremor have become more precise with the development of computed tomography (CT) in the 1970s and magnetic resonance imaging (MRI) in the 1980s. These methods have also become less invasive with advancements in the field of Gamma Knife radiosurgery (GKRS) and magnetic resonance-guided focused ultrasound (MRgFUS). In the following sections of this chapter, we will review appropriate patient selection for surgical lesioning in the treatment of essential tremor (ET), discuss surgical targets currently used in the ablative treatment of ET, compare and contrast modern lesioning modalities, and highlight upcoming developments in this field. Lesioning for PD and deep brain stimulation (DBS) will be discussed in separate chapters.

Practice Parameters and Patient Selection

Practice Parameters

Essential tremor is the most common movement disorder, affecting up to 5% of the population [21]. Patients with ET typically exhibit postural and kinetic tremor of the upper extremities either unilaterally or bilaterally; however, the axial musculature and lower extremities may also be affected [22]. The first-line medical treatments for ET include propranolol and primidone. Unfortunately, 30–50% of patients with ET will not respond or are intolerant of either drug [23, 24]. Second-line drugs include alprazolam, atenolol, gabapentin, sotalol, and topiramate, but the evidence for their use toward tremor suggests less efficacy [25, 26].

Patients who are refractory to medical therapy for ET may be referred for surgical treatment, which includes cerebral lesioning or neuromodulation with DBS [27]. The clinical evidence for specific lesioning procedures will be reviewed later in this chapter. Current practice parameters published in 2005 and 2011 by the American Academy of Neurology (AAN) describe unilateral thalamotomy as "possibly effective" (Level C evidence) in the treatment of contralateral limb tremor in patients with ET who are refractory to medical treatment. Bilateral thalamotomies are not recommended due to an increased risk for adverse events. DBS is also listed as "possibly effective" (Level C evidence) for the reduction of contralateral limb tremor. While DBS may have a lower risk for adverse events than thalamotomy, specific patient characteristics must be taken into account to determine the best surgical course. According to AAN practice parameters, there is insufficient data to support the use of bilateral DBS for bilateral upper extremity tremor or head/voice tremor, and there is also insufficient evidence (Level U) to support the use of Gamma Knife radiosurgery (GKRS) for the treatment of ET [25, 26].

Patient Selection

The two general categories for the surgical treatment of ET include stereotactic ablation and DBS neuromodulation. DBS is almost always a surgical option, as it is considered safe for both unilateral and bilateral treatment of ET with equal or better efficacy to thalamic ablation. In addition, DBS allows for adjustable and reversible neuromodulation. The DBS procedure requires the implantation of intracranial electrodes and an internal pulse generator, which is generally placed in the chest wall. There is a subset of patients with ET who are not amenable to having implanted hardware due to discomfort, the need for long-term programming adjustments, the potential for repeat surgical operations to address an expired battery or device-related complication, and/or the high cost of the procedure. There are also patients who cannot safely undergo a surgical operation for DBS electrode placement due to severe medical comorbidities and the inability to withhold anticoagulants for the procedure. In addition, patients with a recently infected DBS system, a high risk for hardware infection, or an expected need for cerebral ablation, transcranial magnetic stimulation, or electroconvulsive therapy may be better candidates for cerebral lesioning procedures [27]. Thus, patients with medically refractory ET who are unwilling or unable to undergo DBS may be considered for surgical lesioning. Of note, surgical lesioning is not recommended for the bilateral treatment of tremor due to the increased risk for adverse events; however, ablative and neuromodulatory procedures may be combined for bilateral tremor if necessary [25]. DBS is clearly the best choice for patients with bilateral symptoms and/or significantly bothersome axial tremor.

There are currently three widely accepted modalities for thalamic lesioning: radiofrequency (RF) ablation, GKRS, and MRgFUS. These will be individually described in the ensuing sections of this chapter. Ideal thalamotomy candidates are primarily unilaterally or asymmetrically affected where appendicular tremor of the hand is the primary complaint. The surgeon must be very cautious in cases involving the elderly or those with impaired balance where any degree of ataxia could significantly affect their living situation. In general, patients who are able to safely tolerate an open surgical intervention and prefer not to have or cannot have implanted surgical hardware are

Table 21.1 Comparison of surgical options for essential tremor

–	RF lesion	GKRS lesion	MRgFUS lesion	DBS
Pros	Single operation Intraoperative mapping with MER or stimulation Testing with subtherapeutic lesion No implants	Single operation Less invasive No implants	Single operation Less invasive Testing with subtherapeutic lesion Intraoperative radiographic feedback No implants	Reversible Adjustable Intraoperative mapping with MER or stimulation Safe for bilateral tremor
Cons	Surgical risk Irreversible Transient edema-related side effects Side effects may be permanent	Irreversible Delayed benefit No intraoperative feedback Exposure to radiation Uncomfortable if claustrophobic	Irreversible Transient edema-related side effects Side effects may be permanent Head must be shaved Uncomfortable if claustrophobic	Surgical risk Programming adjustments over time Battery replacements and/or charging Device-related complications (i.e., infection)

DBS deep brain stimulation, *GKRS* Gamma Knife radiosurgery, *MER* microelectrode recording, *MRgFUS* magnetic resonance-guided focused ultrasound, *RF* radiofrequency

considered good candidates for RF ablation [27]. Patients who prefer or require less-invasive lesioning modalities can be considered for MRgFUS or GKRS. Patients who undergo MRgFUS must undergo screening with a head CT, as this procedure can be contraindicated if the skull is unsuitable to transmit acoustic energy (typically in cases where the degree of cancellous bone is elevated in relation to cortical bone). They must also be amenable to undergoing a full head shave. Patients who undergo GKRS or other forms of stereotactic radiosurgery (SRS) must be willing to tolerate delayed benefits from the surgery. Table 21.1 provides a comparison of the current surgical options for medication-refractory ET.

Surgical Targets

Ventral Intermediate Nucleus

The most common surgical target in lesioning procedures for ET is the ventral intermediate (Vim) nucleus of the thalamus. Based on the Schaltenbrand-Wahren atlas, which uses terminology developed by Hassler, the Vim is intermediately located between the motor thalamus anteriorly (ventralis oralis posterior [Vop] nucleus) and sensory thalamus posteriorly (ventralis caudalis [Vc] nucleus) [28]. The medial and lateral borders of the Vim are formed by the central thalamic nucleus and internal capsule, respectively. The Vim measures 1.5–3.5 mm in the anterior-posterior plane, 8–9 mm in the medial-lateral plane, and 8–9 mm in the dorsal-ventral plane [29]. There is a somatotopic organization of the Vim, with the contralateral mouth being represented medially, followed by the contralateral arm and then leg moving laterally. Afferent projections to the Vim carry kinesthetic information and arise from the contralateral spinal cord and deep cerebellar nuclei via the dentatorubrothalamic tract (DRT). The efferent projections from the Vim extend to the ipsilateral primary motor cortex.

Indirect localization of the Vim is based on studies that have examined average distances of successful thalamotomies referenced from the anterior commissure (AC) and posterior commissure (PC). While there is significant variability in Vim targeting among neurosurgeons, lesions are typically placed 25% of the AC-PC distance anterior to PC (typically 7 mm) and approximately 14 mm lateral to midline (or 10–11 mm lateral to the wall of the third ventricle in patients with ventriculomegaly) at the level of the intercommissural line (ICL) [30, 31]. Figure 21.1 provides an example of indirect targeting of the Vim. The neu-

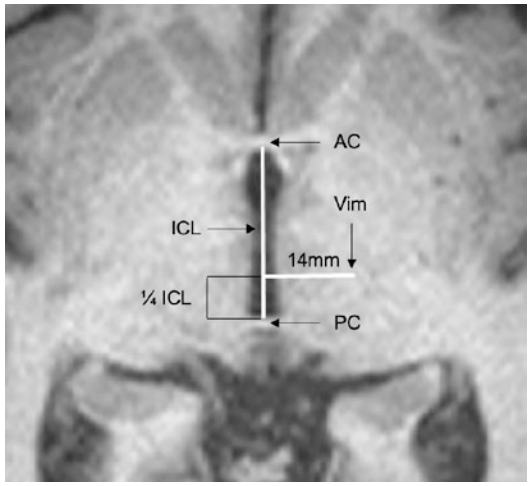

Fig. 21.1 In indirect targeting of the Vim, a straight line is first drawn and measured on an axial plane connecting the ventricular borders of the AC and PC. The y-coordinate is placed ¼ the length of the ICL anterior to the PC. The x-coordinate is placed 14 mm lateral to this point (or 10–11 mm lateral to the wall of the third ventricle in patients with ventriculomegaly). The z-coordinate is the same as the AC-PC plane. AC anterior commissure, ICL intercommissural line, PC posterior commissure, Vim ventral intermediate nucleus

rosurgeon must understand that this is an approximation of the Vim, and care must be taken to adjust the surgical target to avoid lateral deviation into the internal capsule or posterior deviation into the sensory thalamus. This can be performed more easily with the assistance of computer programs that provide an adjusted overlay of a stereotactic atlas on the patient's MRI scan [32]. Since the Vim cannot be directly delineated using current MRI technology, tractography is being investigated as a patient-specific means of localization based on connectivity related to the pyramidal tract, medial lemniscus, DRT, and thalamocortical tracts [33, 34].

Direct mapping of the motor and sensory thalamus can be performed using single-unit microelectrode recording (MER) [35]. Tremor cells, which exhibit bursting activity in synchrony with the patient's extremity tremor, are primarily encountered within the Vim, caudal Vop, and anterior border of Vc [36, 37]. There is evidence that centering a lesion on the cluster of tremor cells improves the efficacy of tremor control [38]. Kinesthetic cells, which may respond to passive joint movements, are also seen within the Vim, while voluntary cells that are responsive to active movement are seen within the Vop. Of note, single-cell recordings from the Vop typically display decreased background activity, frequency, and amplitude in comparison to the Vim [39]. Sensory cells within the Vc respond to light touch and are well localized to a specific body area [32]. Further localization can be performed using micro- or macrostimulation, which commonly result in tremor arrest (Vim), paresthesias (Vc), or facial pulling/dysarthria (internal capsule) based on the location of the electrode.

Posterior Subthalamic Area

While traditionally performed less commonly than Vim thalamotomy, lesioning within the posterior subthalamic area (PSA) and, more specifically, the caudal zona incerta (cZI) are being increasingly considered for both parkinsonian and nonparkinsonian tremor. This technique has been refined over time with an improved understanding of the anatomical location of the pallidothalamic and cerebellothalamic tracts [40]. The PSA is located deep to the motor ventral thalamus, lateral to the red nucleus, and posteromedial to the subthalamic nucleus. The statistical target is typically 10–14 mm lateral to midline, 4.5–7.5 mm posterior to the midcommissural point (MCP), and 2–4 mm inferior to the ICL. This area includes the zona incerta and Forel's fields [41]. Plaha and colleagues have specifically targeted the cZI using the following coordinates: 11–13 mm lateral to midline, 7–8 mm posterior to the MCP, and 4–5 mm inferior to the ICL. Due to variability among lesioning studies of the PSA, it is difficult to draw conclusions as to the efficacy of these procedures [41]. However, lesioning of the PSA appears to provide substantial tremor relief in ET, and bilateral DBS studies involving these areas have demonstrated significant improvement in both distal and axial tremor [42–44].

Radiofrequency Ablation

Surgical Method

Radiofrequency ablation is typically performed with the patient awake in a stereotactic frame. At our institution, we obtain an intraoperative CT after frame placement, which is fused and registered with a preoperative MRI. We use indirect targeting to plan the thalamotomy, taking care to avoid cortical vessels and sulci in order to reduce the risk of hemorrhage. We also avoid traversing the lateral ventricles whenever possible [45]. A burr hole is created at or anterior to the coronal suture, and the dura is sharply opened. Prior to opening the arachnoid, we will typically use bipolar electrocautery to coagulate and fuse the arachnoid to the pia in order to minimize cerebrospinal fluid (CSF) loss and subsequent brain shift. The RF probe has a 1.1 mm outer diameter with a 3 mm exposed tip (Integra Radionics; Burlington, MA). Once the probe is placed at the target, absorbable gelatin sponges or tissue sealant is placed epidurally surrounding the probe to prevent further CSF leak. Stimulation is performed at 150 Hz with gradually increasing voltage, and tremor relief and side effects are continuously monitored. If the probe is placed correctly, patients will typically display significant tremor control with transient paresthesias of the contralateral hand. Persistent paresthesias (suggesting involvement of Vc) may require readjustment of the probe anteriorly, and facial or hand contractions (suggesting involvement of the internal capsule) may require replacement of the probe medially. A test lesion can be performed at 45 °C for 60 seconds. The final therapeutic ablation is performed at 70 °C for 60 seconds while continuously monitoring the motor function of the patient [46]. In most cases, the probe is then withdrawn by 2 mm to perform a second, dorsal ablation. Figure 21.2 provides an example of the evolution of a thermal lesion over time, which is expected to be similar for RF ablation and focused ultrasound.

Clinical Evidence

The majority of initial studies examining the efficacy of RF ablation for tremor were retrospective

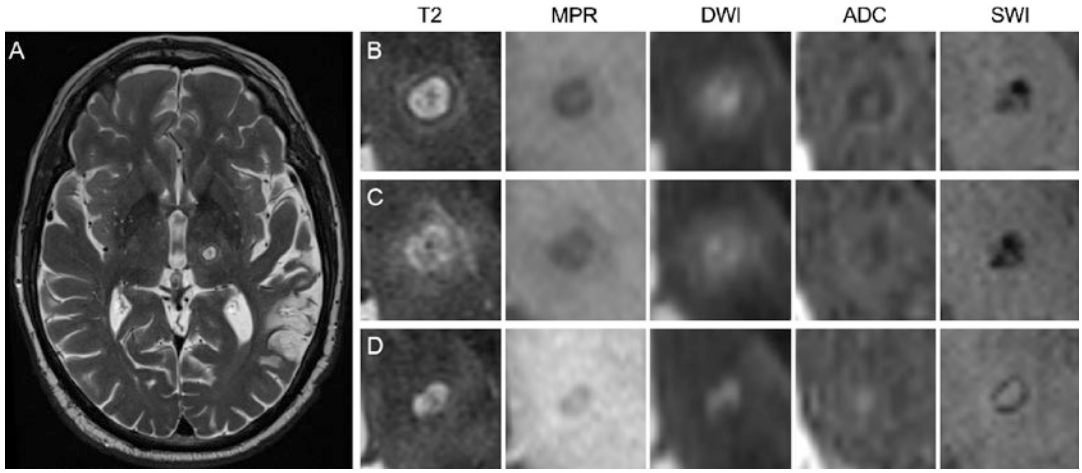

Fig. 21.2 A left thalamic thermal lesion is depicted on the axial T2-weighted MRI (**a**). The evolution of this thermal lesion over 1 month on T2-weighted, MPR, DWI, ADC, and SWI sequences is demonstrated in rows B–D. (**b**) MRI sequences obtained at 1 day postoperatively, (**c**) at 1 week postoperatively, and (**d**) at 1 month postoperatively. Note that, after lesional expansion from 1 day to 1 week postoperatively, the area of cerebral edema significantly declines at 1 month postoperatively. There is also a slight decrease in the size of central coagulative necrosis from 1 week to 1 month postoperatively. ADC apparent diffusion coefficient, DWI diffusion-weighted imaging, MPR MP-RAGE, MRI magnetic resonance imaging, SWI susceptibility-weighted imaging

case series with heterogenous patient populations, surgical targets, and outcome measures [47–51]. Among these studies, moderate to complete tremor improvement at last follow-up ranges from 80% to 100%. There are, however, three studies examining the results of thalamotomy in only patients with ET. In a cohort study of 21 patients who underwent RF thalamotomy for medically refractory ET, Zirh et al. demonstrated a 90% improvement rate from blinded functional assessments at 1 year postoperatively [52]. Akbostanci et al. performed 43 thalamotomies in 37 patients with ET, all of whom had a significant reduction in tremor postoperatively [53]. At last follow-up ranging from 1 to 13 months, 61% of patients had no tremor and 14% had mild tremor. Tremor recurred in five patients, who underwent successful repeat thalamotomies. Sobstyl et al. used the Clinical Rating Scale for Tremor (CRST), a validated and disease-specific measure for tremor [54], to demonstrate ~60% improvement in terms of specific upper extremity motor tasks and functional disabilities [55].

Thalamic lesioning has been directly compared to DBS. Tasker et al. performed a retrospective review of 47 patients with medication-refractory PD or ET who underwent either Vim thalamotomy or DBS placement [56]. Complete or nearly complete abolition of tremor occurred in 69% of patients who underwent thalamotomy, as compared to 79% in the DBS group. In a prospective, randomized comparison of tremor patients treated with either thalamotomy or DBS, Schuurman et al. also demonstrated slightly more improvement in functional ability in the DBS group (90% vs. 79% at 6 months postoperatively) [57]. In contrast, Pahwa et al. report no significant difference in terms of tremor scores or activities of daily living (ADL) scores in their retrospective review of 35 patients with medically refractory ET who underwent either thalamotomy or Vim DBS [58]. Anderson et al. performed a randomized comparison of index finger tapping following unilateral thalamotomy or DBS in 21 subjects with advanced ET. While the clinical improvement in tremor was similar for the two treatments, the thalamotomy group improved the regularity of finger tapping to a greater extent than with DBS [59].

Adverse Events

Radiofrequency thalamotomy results in an irreversible lesion, making DBS a more forgiving procedure. Thalamic lesioning, like all other types of lesioning procedures, involves a balance in terms of lesion size as larger lesions are more effective and durable but more risky. Most transient adverse events following thalamotomy are related to perilesional edema, which subside as the edema decreases over time [27]. Tasker et al. describe transient ataxia, dysarthria, and gait disturbance in 42% of their thalamotomy patients and 26% of DBS patients, which remained permanent in 31% of thalamotomy patients [56]. Schurrman et al. report similar findings with the addition of cognitive deterioration in 9% of the thalamotomy group and none of the DBS group. Of note, two of their patients with DBS implants developed hematoma or infection at the pulse generator site, and there was one mortality after DBS lead placement [57]. Pahwa et al. also describe a higher rate of surgical complications from thalamotomy as compared to DBS; however, more patients in the DBS group required repeat surgery due to device-related complications [58]. RF thalamotomy of course obviates the risks of having surgically implanted devices, including hardware failure and infection. In contrast to thalamic DBS, bilateral RF thalamotomy is not deemed safe due to an increased risk of dysarthria [47, 49, 52]. Overall, the risk of sensory or cerebellar deficit is higher with thalamic lesioning, but these procedures avoid the types of complications (such as infection) that are inherent to implanted neurostimulators.

Stereotactic Radiosurgery

Surgical Method

While Gamma Knife (GK) is more commonly used to treat neuro-oncologic and vascular disorders of the brain, Lars Leksell's original vision for GK was for the treatment of functional disorders [60, 61]. Gamma Knife thalamotomy is performed with the patient awake after placement of

a stereotactic frame. The patient is then sent for a volumetric MRI, or a thin-cut CT scan to fuse to a recent volumetric MRI. The Vim is indirectly targeted on the MRI scan, ensuring that the 20% isodose line remains medial to the internal capsule [62]. After placing the patient into the GKRS unit (Elekta; Stockholm, Sweden), a total of 130–150 Gy is delivered to the Vim using a 4 mm collimator [62–65]. Ionizing radiation is typically administered over approximately 1 hour, although the total time for radiation delivery will depend on the age and half-life of the cobalt source [66]. Figure 21.3 displays an example of a radiosurgical plan for GK thalamotomy. Clinical and radiological effects usually evolve over the course of 1 month to 1 year (mean of 5 months) [63]. Thus, intraoperative testing for tremor relief is not performed, and the target cannot be validated immediately after the procedure.

Clinical Evidence

There are two prospective, blinded, yet uncontrolled, studies of GK thalamotomy designed primarily for the treatment of ET. Witjas et al. report a total of 50 patients (36 ET, 14 PD) who were treated with 130 Gy to the Vim and underwent blinded tremor assessment by expert neurologists over the course of 1 year. Upper limb tremor scores improved by a mean of 54% and ADLs by 72%, although there was a relatively high drop-out rate of 18% [63]. Lim et al. report a similar experimental design for a total of 14 patients (11 ET, 3 PD); however, there was no statistically significant improvement in tremor scores [67]. Of note, two patients in this study had follow-up less than 1 year. There are several retrospective, unblinded reviews related to the efficacy of GK thalamotomy for tremor with varying outcome measures and scales [62, 64, 65, 68, 69]. The largest of these studies, reported by Young et al., evaluated a total of 161 patients with ET who received 140–150 Gy to the Vim with mean follow-up of 33 months. The authors describe that 81% of their patients improved after the treatment, and mean tremor scores improved by 58% [64]. Niranjan et al. describe a retrospective analysis of 73 patients with ET treated with a mean of 140 Gy to the Vim at a single center over 19 years. Using part of the Fahn-Tolosa-Marin clinical tremor rating scale, the authors show that tremor improvement occurred in 93% of their patients, and 96% continued to have tremor relief at last follow-up (mean last follow-up time was 28 months) [68].

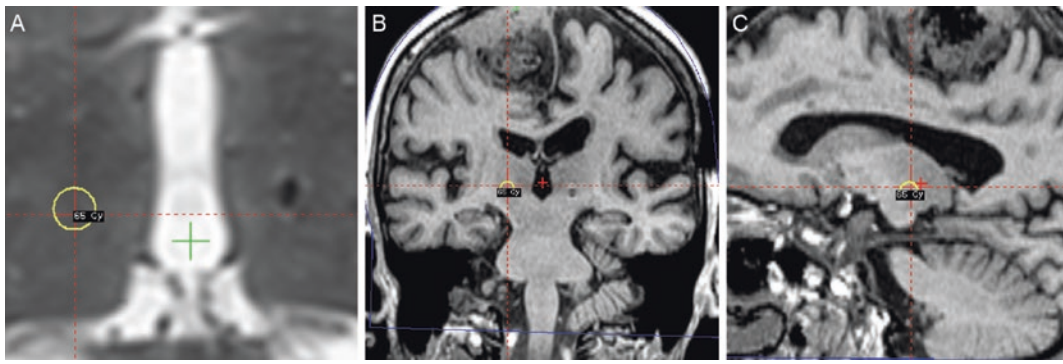

Fig. 21.3 Planning a right-sided GK thalamotomy for a patient with a previously placed left Vim DBS lead, as depicted on (**a**) axial, (**b**) coronal, and (**c**) sagittal MRI sections. The right Vim was treated with a prescription dose of 65.0 Gy to the 50% isodose (yellow circle) with a maximum dose of 130.0 Gy. The coronal and sagittal sections demonstrate a large right posterior frontal extra-axial mass obstructing the typical access point for DBS electrode placement, which was a major determinant in referring the patient for GK thalamotomy. The green and red plus signs indicate the midline. DBS deep brain stimulation, GK Gamma Knife, Vim ventral intermediate nucleus

Adverse Events

The unique issue pertinent to radiosurgical thalamotomy is the delayed and variable response, although some advocate that the latent effects are positive in that there is more time for compensation of brain function. Overall, radiosurgical thalamotomy is well-tolerated with few adverse events. Among the 50 patients treated by Witjas et al., 1 patient developed hemiparesis 12 months postoperatively, and another developed an excessive edematous response observed on MRI, both of which resolved. Of note, 11 patients had minimal to no lesion observed on an MRI performed 1 year postoperatively, indicating high variability of response to ionizing radiation [63]. Similarly, Lim et al. report that 1 of their 14 patients experienced extensive edema surrounding the thalamic lesion. This patient experienced a thalamic hemorrhage 14 months postoperatively while taking anticoagulants. Two other patients experienced mild, delayed finger numbness contralateral to the lesion [67]. Young et al. report mild sensory loss in 4 of 161 patients (2 were permanent) and motor impairment in 10 (6 had permanent contralateral weakness and speech disturbances with progressive improvement). There was a clear correlation between lesion size and the frequency of side effects. Interestingly, none of the 42 patients who underwent staged bilateral lesioning developed a complication [64]. Niranjan et al. report only temporary adverse radiation effects in 3 of 73 patients (4%), including contralateral hemiparesis, facial weakness, dysphagia, and/or numbness [68].

Focused Ultrasound

Surgical Method

There have been significant advancements in the field of stereotactic high-frequency ultrasonography since it was first used to create intracranial lesions in the 1950s by Meyers and William and Francis Fry [70, 71]. Modern MRgFUS utilizes advanced transcranial acoustic delivery of ultrasound, phase correction technology, and MR thermography to achieve cerebral ablation with submillimeter precision [72, 73].

The patient first undergoes preparative imaging, including CT and MRI scans. We use the CT to calculate the skull density ratio (SDR), a predictive measure of skull favorability for the MRgFUS procedure that is based on the Hounsfield unit values of the marrow and cortical bone [74]. On the day of surgery, no pass regions are designated on the CT in the planning software so that the beam paths avoid the frontal sinuses and intracranial calcifications. The hair is clipped and the scalp is shaved to ensure that no microbubbles cavitate during transcranial sonication. The frame is placed low on the head to maximize the available surface area for the ultrasound transducer (NeuroAblate 4000, Insightec; Tirat Carmel, Israel). A silicone membrane is then placed over the scalp, the patient is positioned supine on an MRI table, the membrane is fixed to the transducer, and the space between the membrane and transducer is filled with chilled, degassed water. A reference MRI is acquired, and the Vim is targeted based on the indirect methods described in this chapter. The transducer is adjusted so that its ideal focus matches the thalamic target. A series of test sonications are performed at low temperatures (40–45 °C) to confirm that the heating is occurring at the stereotactic target. Next a series of moderate sonications (50–55 °C) are delivered so that clinical testing of the patient can be performed. Final therapeutic ablations (~60 °C) are prescribed once the targeting is confirmed on thermal images and with a positive clinical tremor response. In our practice, we create an additional therapeutic ablation 2 mm dorsal to the original target in order to enlarge the lesion [75]. As with other thermal lesioning techniques, the clinical effects occur immediately. Postoperative MRI can be obtained after the procedure or on the following day when the lesion has matured. Figure 21.4 further depicts contemporary MRgFUS.

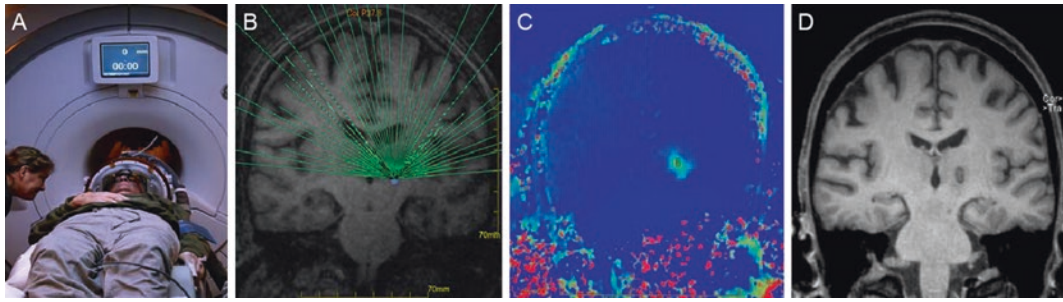

Fig. 21.4 Contemporary MRgFUS. (**a**) Patient supine on MRI table prior to left-sided MRgFUS for ET. A stereotactic frame secures the patient's head to the MRI table and ultrasound transducer. (**b**) A maximum of 1024 individual elements are used to sharply focus the ultrasound beams (*depicted by green lines*) on the target (*blue circle*). (**c**) MR thermometry is used to monitor temperature changes (accurate to ~1 °C) every 3 seconds during a sonication. Temperature changes are mapped in two dimensions in the plane perpendicular to the resonance frequency. On this coronal MRI, the intracranial green area depicts heating at the thalamic target. (**d**) This postoperative coronal T1-weighted MRI demonstrates a left thalamic lesion with less than 1 mm precision. ET essential tremor, MRgFUS magnetic resonance-guided focused ultrasound, MRI magnetic resonance imaging

Clinical Evidence

Focused ultrasound thalamotomy for the treatment of medication-refractory ET was originally explored with 3 uncontrolled pilot studies [76–78], which were followed by a multicenter, randomized, sham-controlled clinical trial of 76 patients with ET [79]. Videotape ratings of tremor and disability scores were performed by independent experts at 3 months and 12 months postoperatively. Mean tremor scores improved by 47% (0.1% in the sham group), and mean disability scores improved by 59% at 3 months in the thalamotomy group. This clinical benefit was sustained at 12 months. A separate follow-up study at 2 years demonstrated sustained clinical benefit in 67 patients who underwent thalamotomy with a mean improvement in tremor score of 56% and disability score of 60% [80]. MRgFUS was subsequently approved by the Food and Drug Administration for the treatment of ET in July 2016.

Adverse Events

The MRgFUS system monitors for cavitation and patient movements in order to prevent unintended tissue destruction. To date, there have been no reported incidences of intracranial hemorrhage or mortality from the use of MRgFUS for movement disorders [81]. Elias et al. report that the most common adverse effects are sensory changes (numbness/paresthesia), which occurred in 38% and persisted in 14%, and gait disturbance (unsteadiness/ataxia), which occurred in 36% and persisted in 9%. Fishman et al. reviewed safety data of 186 patients from five studies who underwent MRgFUS thalamotomy for ET, reporting a 1.6% rate of procedure-related serious adverse events [81]. As with other lesioning modalities, treatment effect may wane over time. DBS salvage and potentially repeat lesioning are possible ways to address the waning efficacy of a thalamic lesion [82].

Future Directions

The field of stereotactic neurosurgery was originally established for intracerebral lesioning. The first era of lesioning ended in the 1960s with the synthesis of L-Dopa [83], and the second era concluded with the advent of DBS in the 1980s [84]. It is important to note, however, that lesioning has not been abandoned because of lack of efficacy. Enthusiasm for lesioning has waned at times, but new advancements in imaging and less-invasive lesioning modalities continue to move this field forward. Currently, high-field MRI [85] and tractography [86, 87] are being

integrated with all lesioning modalities to improve targeting accuracy and precision.

Perhaps the most important clinical issue to address for newer lesioning modalities is the safety of bilateral thalamotomy to treat bilateral and/or axial tremor. As described in this chapter, early ablative studies in the treatment of movement disorders demonstrated a significantly increased risk of dysphagia and disequilibrium in patients with bilateral lesions. However, these studies were performed in a time without the precise stereotactic methods and detailed intracranial imaging techniques available to neurosurgeons today. In addition, the predominant population in these studies were patients with PD and not ET, many of whom had baseline swallowing and balance issues [88]. More recent investigations into bilateral thalamotomy using GKRS to treat ET indicate a comparable risk to unilateral lesioning [64]. Thus, it may be safe to perform bilateral thalamotomies in a staged manner using modern lesioning modalities.

Conclusion

There have been significant advancements in the field of cerebral lesioning for ET since its inception in the 1930s. Surgical teams are able to lesion the Vim or PSA unilaterally in patients with medication-refractory ET using RF ablation, GKRS, and MRgFUS. It is important that these teams take specific patient characteristics and expectations into account in order to determine if cerebral lesioning is appropriate and what method of lesioning should be performed. As surgeons gain access to increasingly accurate, precise, and versatile ablative methods, we expect to bear witness to the rise of a new, third era of cerebral lesioning.

References

1. Bucy PC. Surgical relief of tremor at rest. Ann Surg. 1945;122:933–41.
2. Koehler PJ, Keyser A. Tremor in Latin texts of Dutch physicians: 16th–18th centuries. Mov Disord. 1997;12(5):798–806.
3. Putnam TJ. Relief from unilateral paralysis agitans by section of the pyramidal tract. Arch Neurol Psychiatr. 1938;40:1049–50.
4. Walker AE. Cerebral pedunculotomy for the relief of involuntary movements; hemiballismus. Acta Psychiatr Neurol. 1949;24(3–4):723–9.
5. Walker AE. Cerebral pedunculotomy for the relief of involuntary movements. II. Parkinsonian tremor. J Nerv Ment Dis. 1952;116(6):766–75.
6. Bucy PC, Keplinger JE, Siqueira EB. Destruction of the "pyramidal tract" in man. J Neurosurg. 1964;21:285–98.
7. Jane JA, Yashon D, Becker DP, Beatty R, Sugar O. The effect of destruction of the corticospinal tract in the human cerebral peduncle upon motor function and involuntary movements. Report of 11 cases. J Neurosurg. 1968;29(6):581–5.
8. Abel TJ, Walch T, Howard MA 3rd. Russell Meyers (1905–1999): pioneer of functional and ultrasonic neurosurgery. J Neurosurg. 2016;125(6):1589–95.
9. Guiot G, Brion S. Treatment of abnormal movement by pallidal coagulation. Rev Neurol (Paris). 1953;89(6):578–80.
10. Spiegel EA, Wycis HT. Pallidothalamotomy in chorea. Arch Neurol Psychiatr. 1950;64(2):295–6.
11. Spiegel EA, Wycis HT, Thur C. The stereoencephalotome (model III of our stereotaxic apparatus for operations on the human brain). J Neurosurg. 1951;8(4):452–3.
12. Spiegel EA, Wycis HT. Ansotomy in paralysis agitans. AMA Arch Neurol Psychiatry. 1954;71(5):598–614.
13. Cooper IS. Anterior choroidal artery ligation for involuntary movements. Science. 1953;118(3059):193.
14. Das K, Benzil DL, Rovit RL, Murali R, Couldwell WT. Irving S. Cooper (1922–1985): a pioneer in functional neurosurgery. J Neurosurg. 1998;89(5):865–73.
15. Cooper IS. Surgical alleviation of parkinsonism; effects of occlusion of the anterior choroidal artery. J Am Geriatr Soc. 1954;2(11):691–718.
16. Cooper IS. Chemopallidectomy: an investigative technique in geriatric parkinsonians. Science. 1955;121(3137):217–8.
17. Hassler R, Riechert T. Indications and localization of stereotactic brain operations. Nervenarzt. 1954;25(11):441–7.
18. Hassler R, Riechert T. Symptomatology & surgery of extrapyramidal movement disorders. Med Klin. 1958;53(19):817–24.
19. Bravo GJ, Cooper IS. A clinical and radiological correlation of the lesions produced by chemopallidectomy and thalamectomy. J Neurol Neurosurg Psychiatry. 1959;22(1):1–10.
20. Cooper IS. Results of 1,000 consecutive basal ganglia operations for parkinsonism. Ann Intern Med. 1960;52:483–99.
21. Louis ED, Ferreira JJ. How common is the most common adult movement disorder? Update on the worldwide prevalence of essential tremor. Mov Disord. 2010;25(5):534–41.

22. Deuschl G, Wenzelburger R, Loffler K, Raethjen J, Stolze H. Essential tremor and cerebellar dysfunction clinical and kinematic analysis of intention tremor. Brain. 2000;123(Pt 8):1568–80.
23. Koller WC, Vetere-Overfield B. Acute and chronic effects of propranolol and primidone in essential tremor. Neurology. 1989;39(12):1587–8.
24. Diaz NL, Louis ED. Survey of medication usage patterns among essential tremor patients: movement disorder specialists vs. general neurologists. Parkinsonism Relat Disord. 2010;16(9):604–7.
25. Zesiewicz TA, Elble R, Louis ED, Hauser RA, Sullivan KL, Dewey RB Jr, et al. Practice parameter: therapies for essential tremor (ET): report of the Quality Standards Subcommittee of the American Academy of Neurology. Neurology. 2005;64(12):2008–20.
26. Zesiewicz TA, Elble RJ, Louis ED, Gronseth GS, Ondo WG, Dewey RB Jr, et al. Evidence-based guideline update: treatment of essential tremor (ET): report of the Quality Standards subcommittee of the American Academy of Neurology. Neurology. 2011;77(19):1752–5.
27. Dallapiazza RF, Lee DJ, De Vloo P, Fomenko A, Hamani C, Hodaie M, et al. Outcomes from stereotactic surgery for essential tremor. J Neurol Neurosurg Psychiatry. 2019;90:474–82.
28. Schaltenbrand G, Wahren W. Atlas for stereotaxy of the human brain. New York: Thieme; 1977.
29. Hirai T, Ohye C, Nagaseki Y, Matsumura M. Cytometric analysis of the thalamic ventralis intermedius nucleus in humans. J Neurophysiol. 1989;61(3):478–87.
30. Kelly PJ, Derome P, Guiot G. Thalamic spatial variability and the surgical results of lesions placed with neurophysiologic control. Surg Neurol. 1978;9(5):307–15.
31. Laitinen LV. Brain targets in surgery for Parkinson's disease. Results of a survey of neurosurgeons. J Neurosurg. 1985;62(3):349–51.
32. Hamani C, Dostrovsky JO, Lozano AM. The motor thalamus in neurosurgery. Neurosurgery. 2006;58(1):146–58; discussion −58.
33. Pouratian N, Zheng Z, Bari AA, Behnke E, Elias WJ, Desalles AA. Multi-institutional evaluation of deep brain stimulation targeting using probabilistic connectivity-based thalamic segmentation. J Neurosurg. 2011;115(5):995–1004.
34. Sammartino F, Krishna V, King NK, Lozano AM, Schwartz ML, Huang Y, et al. Tractography-based ventral intermediate nucleus targeting: novel methodology and intraoperative validation. Mov Disord. 2016;31(8):1217–25.
35. Starr PA, Vitek JL, Bakay RA. Ablative surgery and deep brain stimulation for Parkinson's disease. Neurosurgery. 1998;43(5):989–1013; discussion −5.
36. Lenz FA, Kwan HC, Martin RL, Tasker RR, Dostrovsky JO, Lenz YE. Single unit analysis of the human ventral thalamic nuclear group. Tremor-related activity in functionally identified cells. Brain. 1994;117(Pt 3):531–43.
37. Magnin M, Morel A, Jeanmonod D. Single-unit analysis of the pallidum, thalamus and subthalamic nucleus in parkinsonian patients. Neuroscience. 2000;96(3):549–64.
38. Lenz FA, Normand SL, Kwan HC, Andrews D, Rowland LH, Jones MW, et al. Statistical prediction of the optimal site for thalamotomy in parkinsonian tremor. Mov Disord. 1995;10(3):318–28.
39. Vitek JL, Ashe J, Kaneoke Y. Spontaneous neuronal activity in the motor thalamus: alteration in pattern and rate in parkinsonism. Soc Neurosci Abstr. 1994;20:561.
40. Gallay MN, Jeanmonod D, Liu J, Morel A. Human pallidothalamic and cerebellothalamic tracts: anatomical basis for functional stereotactic neurosurgery. Brain Struct Funct. 2008;212(6):443–63.
41. Blomstedt P, Sandvik U, Fytagoridis A, Tisch S. The posterior subthalamic area in the treatment of movement disorders: past, present, and future. Neurosurgery. 2009;64(6):1029–38; discussion 38–42.
42. Plaha P, Patel NK, Gill SS. Stimulation of the subthalamic region for essential tremor. J Neurosurg. 2004;101(1):48–54.
43. Plaha P, Khan S, Gill SS. Bilateral stimulation of the caudal zona incerta nucleus for tremor control. J Neurol Neurosurg Psychiatry. 2008;79(5):504–13.
44. Blomstedt P, Sandvik U, Tisch S. Deep brain stimulation in the posterior subthalamic area in the treatment of essential tremor. Mov Disord. 2010;25(10):1350–6.
45. Elias WJ, Sansur CA, Frysinger RC. Sulcal and ventricular trajectories in stereotactic surgery. J Neurosurg. 2009;110(2):201–7.
46. Vitek JL, Bakay RA, Hashimoto T, Kaneoke Y, Mewes K, Zhang JY, et al. Microelectrode-guided pallidotomy: technical approach and its application in medically intractable Parkinson's disease. J Neurosurg. 1998;88(6):1027–43.
47. Nagaseki Y, Shibazaki T, Hirai T, Kawashima Y, Hirato M, Wada H, et al. Long-term follow-up results of selective VIM-thalamotomy. J Neurosurg. 1986;65(3):296–302.
48. Mohadjer M, Goerke H, Milios E, Etou A, Mundinger F. Long-term results of stereotaxy in the treatment of essential tremor. Stereotact Funct Neurosurg. 1990;54–55:125–9.
49. Goldman MS, Ahlskog JE, Kelly PJ. The symptomatic and functional outcome of stereotactic thalamotomy for medically intractable essential tremor. J Neurosurg. 1992;76(6):924–8.
50. Jankovic J, Cardoso F, Grossman RG, Hamilton WJ. Outcome after stereotactic thalamotomy for parkinsonian, essential, and other types of tremor. Neurosurgery. 1995;37(4):680–6; discussion 6–7.
51. Shahzadi S, Tasker RR, Lozano A. Thalamotomy for essential and cerebellar tremor. Stereotact Funct Neurosurg. 1995;65(1–4):11–7.
52. Zirh A, Reich SG, Dougherty PM, Lenz FA. Stereotactic thalamotomy in the treatment of essential tremor of the upper extremity: reassessment

including a blinded measure of outcome. J Neurol Neurosurg Psychiatry. 1999;66(6):772–5.
53. Akbostanci MC, Slavin KV, Burchiel KJ. Stereotactic ventral intermedial thalamotomy for the treatment of essential tremor (ET): results of a series of 37 patients. Stereotact Funct Neurosurg. 1999;72(2–4):174–7.
54. Fahn S, Tolosa E, Marin C. Clinical rating scale for tremor. In: Jankovic J, Tolosa E, editors. Parkinson's disease and movement disorders. Baltimore/Munich: Urban & Schwarzenberg; 1988. p. 223–34.
55. Sobstyl M, Zabek M, Koziara H, Kadziolka B, Mossakowski Z. Stereotactic ventrolateral thalamotomy in the treatment of essential tremor. Neurol Neurochir Pol. 2006;40(3):179–85.
56. Tasker RR. Deep brain stimulation is preferable to thalamotomy for tremor suppression. Surg Neurol. 1998;49(2):145–53; discussion 53–4.
57. Schuurman PR, Bosch DA, Bossuyt PM, Bonsel GJ, van Someren EJ, de Bie RM, et al. A comparison of continuous thalamic stimulation and thalamotomy for suppression of severe tremor. N Engl J Med. 2000;342(7):461–8.
58. Pahwa R, Lyons KE, Wilkinson SB, Troster AI, Overman J, Kieltyka J, et al. Comparison of thalamotomy to deep brain stimulation of the thalamus in essential tremor. Mov Disord. 2001;16(1):140–3.
59. Anderson VC, Burchiel KJ, Hart MJ, Berk C, Lou JS. A randomized comparison of thalamic stimulation and lesion on self-paced finger movement in essential tremor. Neurosci Lett. 2009;462(2):166–70.
60. Leksell L. Cerebral radiosurgery. I. Gammathalanotomy in two cases of intractable pain. Acta Chir Scand. 1968;134(8):585–95.
61. Steiner L, Forster D, Leksell L, Meyerson BA, Boethius J. Gammathalamotomy in intractable pain. Acta Neurochir. 1980;52(3–4):173–84.
62. Kooshkabadi A, Lunsford LD, Tonetti D, Flickinger JC, Kondziolka D. Gamma Knife thalamotomy for tremor in the magnetic resonance imaging era. J Neurosurg. 2013;118(4):713–8.
63. Witjas T, Carron R, Krack P, Eusebio A, Vaugoyeau M, Hariz M, et al. A prospective single-blind study of Gamma Knife thalamotomy for tremor. Neurology. 2015;85(18):1562–8.
64. Young RF, Li F, Vermeulen S, Meier R. Gamma Knife thalamotomy for treatment of essential tremor (ET): long-term results. J Neurosurg. 2010;112(6):1311–7.
65. Ohye C, Higuchi Y, Shibazaki T, Hashimoto T, Koyama T, Hirai T, et al. Gamma Knife thalamotomy for Parkinson disease and essential tremor (ET): a prospective multicenter study. Neurosurgery. 2012;70(3):526–35; discussion 35–6.
66. Young RF, Shumway-Cook A, Vermeulen SS, Grimm P, Blasko J, Posewitz A, et al. Gamma Knife radiosurgery as a lesioning technique in movement disorder surgery. J Neurosurg. 1998;89(2):183–93.
67. Lim SY, Hodaie M, Fallis M, Poon YY, Mazzella F, Moro E. Gamma Knife thalamotomy for disabling tremor: a blinded evaluation. Arch Neurol. 2010;67(5):584–8.
68. Niranjan A, Raju SS, Kooshkabadi A, Monaco E 3rd, Flickinger JC, Lunsford LD. Stereotactic radiosurgery for essential tremor (ET): retrospective analysis of a 19-year experience. Mov Disord. 2017;32(5):769–77.
69. Kondziolka D, Ong JG, Lee JY, Moore RY, Flickinger JC, Lunsford LD. Gamma Knife thalamotomy for essential tremor. J Neurosurg. 2008;108(1):111–7.
70. Fry WJ, Mosberg WH Jr, Barnard JW, Fry FJ. Production of focal destructive lesions in the central nervous system with ultrasound. J Neurosurg. 1954;11(5):471–8.
71. Jagannathan J, Sanghvi NT, Crum LA, Yen CP, Medel R, Dumont AS, et al. High-intensity focused ultrasound surgery of the brain: part 1--A historical perspective with modern applications. Neurosurgery. 2009;64(2):201–10; discussion 10–1.
72. Clement GT, White PJ, King RL, McDannold N, Hynynen K. A magnetic resonance imaging-compatible, large-scale array for trans-skull ultrasound surgery and therapy. J Ultrasound Med. 2005;24(8):1117–25.
73. Gallay MN, Moser D, Jeanmonod D. Safety and accuracy of incisionless transcranial MR-guided focused ultrasound functional neurosurgery: single-center experience with 253 targets in 180 treatments. J Neurosurg. 2018;1:1–10.
74. Chang WS, Jung HH, Zadicario E, Rachmilevitch I, Tlusty T, Vitek S, et al. Factors associated with successful magnetic resonance-guided focused ultrasound treatment: efficiency of acoustic energy delivery through the skull. J Neurosurg. 2016;124(2):411–6.
75. Wang TR, Bond AE, Dallapiazza RF, Blanke A, Tilden D, Huerta TE, et al. Transcranial magnetic resonance imaging-guided focused ultrasound thalamotomy for tremor: technical note. Neurosurg Focus. 2018;44(2):E3.
76. Chang WS, Jung HH, Kweon EJ, Zadicario E, Rachmilevitch I, Chang JW. Unilateral magnetic resonance guided focused ultrasound thalamotomy for essential tremor (ET): practices and clinicoradiological outcomes. J Neurol Neurosurg Psychiatry. 2015;86(3):257–64.
77. Elias WJ, Huss D, Voss T, Loomba J, Khaled M, Zadicario E, et al. A pilot study of focused ultrasound thalamotomy for essential tremor. N Engl J Med. 2013;369(7):640–8.
78. Lipsman N, Schwartz ML, Huang Y, Lee L, Sankar T, Chapman M, et al. MR-guided focused ultrasound thalamotomy for essential tremor (ET): a proof-of-concept study. Lancet Neurol. 2013;12(5):462–8.
79. Elias WJ, Lipsman N, Ondo WG, Ghanouni P, Kim YG, Lee W, et al. A randomized trial of focused ultrasound thalamotomy for essential tremor. N Engl J Med. 2016;375(8):730–9.
80. Chang JW, Park CK, Lipsman N, Schwartz ML, Ghanouni P, Henderson JM, et al. A prospective trial of magnetic resonance-guided focused ultrasound thalamotomy for essential tremor (ET): results at the 2-year follow-up. Ann Neurol. 2018;83(1):107–14.

81. Fishman PS, Elias WJ, Ghanouni P, Gwinn R, Lipsman N, Schwartz M, et al. Neurological adverse event profile of magnetic resonance imaging-guided focused ultrasound thalamotomy for essential tremor. Mov Disord. 2018;33(5):843–7.
82. Wang TR, Dallapiazza RF, Moosa S, Huss D, Shah BB, Elias WJ. Thalamic deep brain stimulation salvages failed focused ultrasound thalamotomy for essential tremor (ET): a case report. Stereotact Funct Neurosurg. 2018;96(1):60–4.
83. Lanska DJ. Chapter 33: the history of movement disorders. Handb Clin Neurol. 2010;95:501–46.
84. Benabid AL, Chabardes S, Torres N, Piallat B, Krack P, Fraix V, et al. Functional neurosurgery for movement disorders: a historical perspective. Prog Brain Res. 2009;175:379–91.
85. Abosch A, Yacoub E, Ugurbil K, Harel N. An assessment of current brain targets for deep brain stimulation surgery with susceptibility-weighted imaging at 7 tesla. Neurosurgery. 2010;67(6):1745–56; discussion 56.
86. Tian Q, Wintermark M, Jeffrey Elias W, Ghanouni P, Halpern CH, Henderson JM, et al. Diffusion MRI tractography for improved transcranial MRI-guided focused ultrasound thalamotomy targeting for essential tremor. Neuroimage Clin. 2018;19:572–80.
87. Krishna V, Sammartino F, Agrawal P, Changizi BK, Bourekas E, Knopp MV, et al. Prospective tractography-based targeting for improved safety of focused ultrasound thalamotomy. Neurosurgery. 2018;84:160–8.
88. Alshaikh J, Fishman PS. Revisiting bilateral thalamotomy for tremor. Clin Neurol Neurosurg. 2017;158:103–7.

Dystonia

22

Teresa Wojtasiewicz, Ankur Butala, and William Stanley Anderson

Introduction

Dystonia is a heterogenous group of movement disorders characterized by a variety of patterns of abnormal movements and postures, typically patterned and twisting or tremulous, which can affect the head, torso, and limbs. Pooled analysis suggests the prevalence of primary dystonia is 16 per million people, which is likely an underestimate, and the prevalence of secondary dystonia (resulting from a secondary neurological insult) is unknown [1]. As of yet, there is no unifying mechanism to explain the physiology of the constellation of dystonia disorders [2, 3]. Dystonic postures can significantly impair a patient's ability to walk, care for themselves, and work. Over time, dystonic movements can result in musculoskeletal complications including contractures, scoliosis, and bony deformities, and dystonia can be a cause of persistent chronic pain. Neurosurgery can be helpful for patients who do not achieve adequate symptom relief with medical therapy. In the following chapter, we will focus on surgical aspects of dystonia, including preoperative considerations, operative techniques, and postoperative assessment and outcomes.

T. Wojtasiewicz (✉) · W. S. Anderson
Department of Neurological Surgery, Johns Hopkins University, Baltimore, MD, USA
e-mail: twojtas1@jhmi.edu

A. Butala
Departments of Neurology, Psychiatry & Behavioral Sciences, Johns Hopkins University, Baltimore, MD, USA

Classification and Diagnosis of Dystonias

Dystonia is an imprecise diagnosis, comprising a group of disorders. Dystonia is classified using two major axes: clinically (age of onset or anatomical distribution of regions) and etiologically (primary vs. secondary) [4–7].

Clinical Assessment of Dystonia

On clinical assessment of a patient with dystonia, simultaneous activity of muscle agonists and antagonists produces a dystonic contraction. The duration of these contractions may vary considerably, from brief moments to sustained spasms. Rhythmic or semi-rhythmic movements may accompany the contractions, producing a dystonic tremor that can be mistaken for "essential" or a rubral tremor. Dystonic movements may also appear as abnormal twisting or choreiform postures, hence the historical term "torsion dystonia." Dystonias may be segmental (contiguous regions), multifocal (noncontiguous), hemidystonia (hemibody, usually secondary to acquired

N. Pouratian, S. A. Sheth (eds.), *Stereotactic and Functional Neurosurgery*,
https://doi.org/10.1007/978-3-030-34906-6_22

structural pathology), generalized (involving the trunk and two other regions), or multifocal. Many dystonias are now recognized to be task-specific. Task-specific dystonias may develop in parts of the body involved in skilled or repetitive movements such as writing (writer's cramp) or playing a musical instrument (embouchure dystonia) [3, 8, 9]. Dystonia can be associated with overflow movements, where muscles adjacent to those implicated in the dystonia are activated, either ipsilaterally or contralaterally. Mirroring can also be seen, where use of a less severely affected or non-affected limb provokes dystonic movements in the affected area [10]. Some patients may report alleviating maneuvers, such as touching a cheek or chin in cervical torticollis [11, 12]. A wide range of sensory and non-tactile stimuli may alleviate dystonic symptoms [13–16].

Etiology of Dystonia

The etiology of dystonias includes primary dystonias, which typically present early in life and cannot be attributed to an acquired cause, and secondary dystonias which result from a variety of complex triggers. There are many genes implicated in causing different varieties of primary dystonia, including more than 25 monogenic forms of dystonia [17, 18]. Dystonia syndrome may be isolated to dystonic postures (isolated dystonia) or combined with myoclonus, Parkinsonism, or hyperkinetic movements (combined dystonia). The majority of dystonias have an autosomal dominant inheritance albeit variable penetrance, though there are notable exceptions of X-linked, autosomal recessive, and mitochondrial disorders [19]. Secondary dystonias are acquired in the setting of complex genotype-phenotype interactions and often occult environmental triggers. Neoplastic, hemorrhagic, or ischemic insults to the thalamus or basal ganglia may cause focal, segmental, or hemibody dystonias with or without comorbid hyperkinetic movement of choreaballism or myoclonus [20, 21]. Even dystonia-associated perinatal hypoxic-ischemic damage may manifest well into young adulthood [22, 23]. A variety of medications may induce a delayed, tardive, dystonia, including antipsychotics, antiemetics, antidepressants, and anticonvulsants [24].

Rating Scales for Dystonia

Primary and secondary dystonias represent a highly heterogenous group of disorders, both in terms of phenotypic presentation and etiology. Several standardized rating scales have been developed and validated for specific dystonias, including blepharospasm, cervical dystonia, focal dystonia, and generalized dystonias [25–28]. The Movement Disorders Society Task Force on Rating Scales has recommended several scales for preoperative assessment. The Toronto Western Spasmodic Torticollis Rating Scale (TWSTRS) is the most widely used, with good inter-rater reliability, and is an extensive scale with three subscales that measure the clinician-assessed physical severity and response to alleviating maneuvers, as well as patient-informed sections on disability and pain [26]. The Burke-Fahn-Marsden Dystonia Rating Scale (BFMDRS) is another widely used clinician-rating scale in adults and children and assesses generalized dystonia by regional motor manifestation and degree of disability [29, 30].

Medical Management

Many patients with dystonia can have satisfactory control of their symptoms with symptomatic medical management [31]. Symptomatic management is complex and multifaceted and can be broadly divided into three categories: (1) non-pharmacological options, such as physical therapy and bracing, (2) pharmacological treatment, and (3) chemo-denervation (botulinum toxin).

Physical and Supportive Therapy

There are a multitude of non-pharmacological therapies for dystonia, including biofeedback training, postural exercises, bracing, and behavioral therapies with most investigations limited to case series and a few clinical trials [31–34]. Though there is some promising evi-

dence for these physiotherapies, particularly motor retraining and transcutaneous electrical nerve stimulation (TENS) in focal dystonia, these should be adjuvant, not first-line or solitary, treatments [33, 35].

Pharmacological Treatment

Pharmacological management in dystonia consists of symptomatic treatment, as there are no established disease-modifying therapies for any dystonia to date. There are few well-powered blinded clinical trials investigating pharmacological options in dystonia, and existing recommendations are largely based on empirical observations and open-label studies. Some dystonia, such as DYT5a (Segawa disease or dopamine-responsive dystonia, DRD), appears to be rapidly responsive to even low doses of dopamine agonists [36, 37]. Dopamine antagonists, such as clozapine, have also been utilized in the treatment of both acute tardive dystonias and idiopathic dystonias, though efficacy is equivocal and side effects (both immediate and long-term) are notable [38–40]. Dopamine modulation appears to be effective for tardive dystonia [41] and idiopathic dystonia [42], though these medications are not yet widely available [43–45]. Anticholinergic agents have long been observed to improve acute dystonic reactions from antipsychotics [46–48]. Anecdotal evidence suggests that anticholinergic medications appear to be effective for dystonia, particularly in children, who appear to tolerate high doses of anticholinergics better than adults [49, 50]. These medications appear effective in primary dystonia [51] as well as secondary forms of dystonia such as cerebral palsy [52, 53]. However, botulinum toxin has been consistently shown to have superior efficacy and is better tolerated than anticholinergics, and these have been resigned to second- or third-line management options [54].

Botulinum Injections

Intramuscular injection of botulinum toxin is the first-line treatment for dystonia recommended by multiple multidisciplinary societies and national organizations [32, 55–57]. Botulinum injections have been shown to be effective in primary cranial (excluding oromandibular) dystonia, cervical dystonia, and writer's cramp [58–60]. Botulinum is safe in both adults and pediatric patients [61]. The two serotypes of botulinum toxin available in the United States, onabotulinumtoxinA (type A) and rimabotulinumtoxinB (type B), differ in their pharmacological mechanism of action, but have both been shown to be effective in the treatment of dystonia [62, 63].

Surgical Treatment

Surgical treatment for dystonia evolved over the past century from open pallidotomies and thalamotomies [64, 65] to peripheral denervation and modern deep brain stimulation [66, 67], shaped by advances in understanding of pathophysiology, electrophysiology, and functional imaging. Deep brain stimulation (DBS), typically of the pallidum, is the most common surgical procedure used for medically refractory dystonia. As the efficacy of pallidal DBS can vary based on patient characteristics and classification of dystonia, careful preoperative evaluation and counseling about expected outcomes of surgery is critical [68–74]. There are multiple approaches for deep brain stimulation, including a variety of different options for stereotactic localization. We will review both frame-based and intraoperative MRI-guided approaches to the internal globus pallidus (GPi). There are also other techniques that have evolved for treatment of dystonia, including peripheral denervation and new, less invasive methods of performing pallidotomies. We will briefly discuss these techniques.

Deep Brain Stimulation

Deep brain stimulation is beneficial for many dystonia patients resistant to medical therapy and botulinum injections. Multiple randomized controlled trials have shown significant long-term benefit of DBS in primary generalized and cervical dystonia [68–73], and there is also evidence

for use of DBS in patients with certain secondary forms of dystonia [68]. However, not all patients achieve the same degree of benefit, and patients are best managed by an interdisciplinary movement disorders team. A team-based approach should determine whether DBS is the most appropriate therapy, what target is ideal for a given patient, and how a patient should be managed postoperatively. A patient's neurologist begins with a comprehensive neurology assessment to ensure a patient is appropriately diagnosed and appropriately medically optimized and makes a referral for surgical discussion. A potential candidate for DBS is then referred to a neurosurgeon to discuss the procedure, operative risks, and expected benefit. Assessment of medical comorbidities and safety of surgery is important and may require collaboration with other medical specialists. Cognitive assessment with a neuropsychologist and, if appropriate, psychiatrist can ensure no comorbid cognitive impairment or behavioral issues that would reduce a patient's ability to benefit from DBS.

Multidisciplinary team management also includes discussion of the most appropriate target for DBS. Pallidal DBS, targeting the internal globus pallidus (GPi), is the most common approach for dystonia and has been validated with multiple randomized controlled trials [68–73]. However, other targets have shown promise in dystonia, including cortical and thalamic targets [75–77]. The thalamic ventralis intermedius nucleus (Vim) can improve both dystonic and tremor features and can be performed unilaterally [78, 79], bilaterally [80], or in association with GPi DBS [77, 81–83]. Some case series have suggested that the posterior region of the ventrolateral nucleus may also improve dystonic features [84]. The STN and adjacent targets have shown some benefit in secondary dystonia in Parkinson's disease and have also been considered for treatment of dystonia syndromes [76, 85]. Though the GPi is the primary target for dystonia, these other targets may offer promise, and further head-to-head comparison would help establish what target would be ideal for a given individual.

Surgical Procedure: DBS

Many successful, accurate approaches to lead placement exist. Other sections of this text will detail the various options for stereotactic accuracy and the relative benefits and drawbacks of each. We will review the frame-based approach with microelectrode recording and intraoperative testing and the intraoperative MRI-guided approach. Awake DBS using frame stereotaxy and intraoperative testing has been established as a safe, precise technique [86, 87]. However, frame-based approaches and awake testing can be challenging in patients with dystonia, especially those who have cervical dystonia or significant trunk or body movements. Dystonia patients may have so much difficulty with immobilization in a fixed head position that frame-based DBS is not safely possible. A variety of frameless techniques exist for these patients. The outcomes for frameless DBS appear comparable to frame-based techniques, even though clinical studies suggest that frameless technology may not be as accurate [88, 89]. For patients with severe dystonic movements, an awake procedure can be extremely uncomfortable. Furthermore, dystonic symptoms frequently are not alleviated by intraoperative testing, so stimulation can only elicit negative effects. DBS leads can also be accurately placed solely using image guidance [90–92]. This obviates the need for intraoperative testing and allows DBS leads to be placed under general anesthesia, which is very helpful for some dystonia patients who cannot tolerate an awake procedure. There is some controversy over whether current image-guided techniques are as accurate enough for anatomic/image-guided targeting ("asleep" surgery) to be comparable to DBS with microelectrode recording and intraoperative testing ("awake" surgery) [93–95]. However, studies of DBS without microelectrode recording indicate good results, and there is no consensus of whether the revisions in lead location suggested by microelectrode recording lead to improved outcomes [96, 97].

Surgical Procedure: Frame-Based DBS

For a frame-based approach, the patient is preoperatively placed in a stereotactic frame (e.g., Leksell Frame, Elekta, Stockholm, Sweden). The frame is placed parallel to the Frankfort plane. Computed tomography (CT) is performed with the patient in the frame and fused to a preoperative MRI on a computerized planning station. A combination of atlas-based targeting using anterior commissure-posterior commissure (AC-PC) distance and other midline structures (indirect targeting) and MRI-guided targeting (direct targeting) may be performed. Using the Schaltenbrand and Talairach atlases, the globus pallidus interna (GPi) is estimated as 2–3 mm anterior, 3–4 mm inferior, and 20–22 mm lateral to the mid-commissural point stereotactic atlases [98–101]. The coordinates of the GPi can be identified on MRI by finding the junction of the posterior quarters of the GPi and GPe on an axial cut through the anterior commissure [100, 101]. The estimated trajectory of the target is planned, and the X,Y,Z and arc and ring angle coordinates are obtained, using a computerized stereotactic planning station (e.g., Framelink workstation; Medtronic, Minneapolis, MN). In the operating room, the frame is fixed to the operating room table to minimize head movement during surgery (Fig. 22.1). This point can be particularly difficult for patients with dystonia with involuntary head or neck movements. Skin incision is made at the estimated entry point and a burr hole is drilled at each estimated entry point. A DBS electrode fixation device used to anchor the lead at the end of the case is seated securely around each burr hole. The dura is coagulated and incised in a cruciate fashion. The introducer cannula is then placed along the intended trajectory using intraoperative X-ray or CT to guide placement. At this point, if microelectrode recording (MER) is planned, a high-impedance platinum-iridium microelectrode is passed through the cannula (Fig. 22.2). The microelectrode is slowly advanced, while a clinician confirms that the electrode is proceeding along an appropriate tra-

Fig. 22.1 Patient immobilized in Leksell stereotactic frame

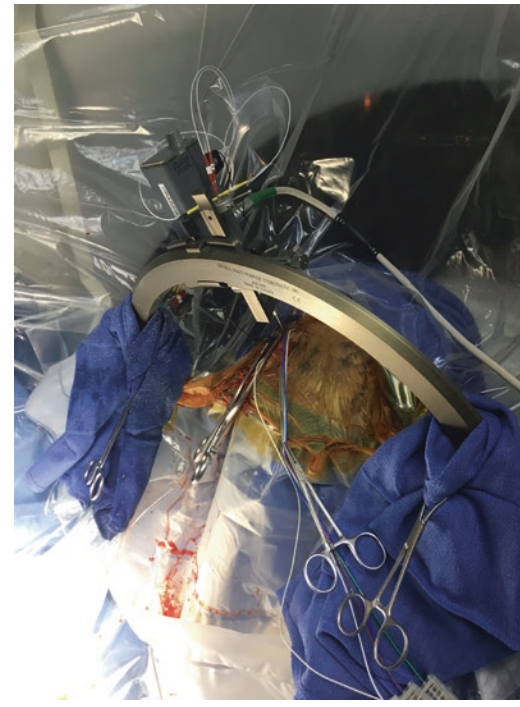

Fig. 22.2 Microelectrode recording apparatus

jectory by monitoring for characteristic neuronal firing patterns and kinesthetic response to movement [102]. The microelectrode is advanced to 4–5 mm below the target, and stimulation is performed while an examiner assesses the patient, monitoring for therapeutic benefit or stimulation-induced side effects. Notably, for dystonia, therapeutic benefit is typically not evident in the operating room. Stimulation-induced side effects can identify the relative positions of the optic tract, internal capsule, and medial lemniscus, and, if needed, the lead trajectory can be revised. After stimulation has been completed, the microelectrodes are removed and the DBS lead is placed. Intraoperative fluoroscopy is used to verify lead location. Stimulation of the lead can be performed at various settings to ascertain symptom relief and any side effects from adjacent structures. Once the lead position is verified, the lead is secured. Once both leads have been placed, temporary lead covers are placed, and the leads are tunneled along the scalp toward the planned pulse generator site.

Surgical Procedure: MRI-Guided DBS [103, 104]

If an MRI-guided approach is deemed appropriate, the patient is brought into the OR suite for induction for endotracheal general anesthesia and then placed into a fixation device. There are a number of options available, depending on what method of stereotactic guidance is chosen. At our institution, we use intraoperative MRI. For this approach, the MRI Interventions (Irvine, CA) ClearPoint head fixation system (Fig. 22.3) and ClearPoint fiducial grids are placed at the estimated scalp entry point for GPi targeting after standard prepping and draping. A standard 3D T1 volumetric acquisition MRI scan with gadolinium is obtained to formulate initial entry points and trajectories. Based on these trajectories, incisions are made. We choose a modified bicoronal incision to facilitate placement of alignment bases. Burr holes are made at each entry point, followed by fixation of the ClearPoint alignment bases (Fig. 22.4). T1 volumetric scans (without contrast) and high-resolution thin-slice biplanar slabs are obtained and repeated as the introducer cannulas are aligned to achieve less than 1 mm radial error in targeting. Once the trajectories have been established, ceramic stylets are inserted through the cannula into the target positions, and another 3D T1-weighted volumetric acquisition scan is obtained to verify good position within the GPi. The stylets are then removed and replaced with two DBS leads after removal from the iMRIS bore. The DBS leads are secured with the burr hole fixation system and tunneled under the scalp in preparation for the implantable pulse generator placement.

Fig. 22.3 Position of patient immobilized in ClearPoint frame

Fig. 22.4 Bilateral ClearPoint navigation towers

Implantation of Pulse Generator

The implantable pulse generator can be placed immediately after the DBS leads or in a delayed fashion at 1 week. The right side is generally preferred to avoid interfering with any potential future need for a cardiac pacemaker. The patient is placed under general anesthesia and an incision is made over the tunneled leads. The leads are tunneled posterior to the pinna and a site is prepared for the connection fixture to the extension cabling. A trough can be drilled in the skull to make the connection fixture less prominent and reduce the tension on the overlying skin. The infraclavicular incision is made and a pocket is prepared above the pectoralis fascia to house the pulse generator. The extension cabling is tunneled to the infraclavicular incision and connected to the pulse generator. The connection fixture and pulse generator are secured with sutures to prevent migration and the incisions are closed.

Postoperative Complications

The complications associated with performing DBS in patients with dystonia are similar to the types of complications seen in performing DBS for other indications [105–119]. Complications from DBS can be procedure-related, hardware-related complications, or stimulation-related. We discuss the risks below.

Procedure-related complications in DBS typically happen immediately during or following surgery. Many of these immediate complications from DBS, including postoperative delirium, seizure, vasovagal response, and headache, are self-limited and do not cause permanent deficits [105–118]. DBS also carries a risk of intracranial hemorrhage, which can cause serious neurological deficits and death [108, 110, 112, 115, 117, 120]. The rate of hemorrhage after DBS is fortunately quite low, ranging from 0.8% to 5%, and only approximately half of these patients are symptomatic [108, 110, 112, 115, 117, 120]. Series of dystonia patients who undergo DBS have shown that dystonia is associated with comparable rates of hemorrhage compared to other groups of patients treated with DBS [117]. Though there has been some concern for a higher rate of hemorrhage in the GPi, the typical target used in dystonia, further analysis has not shown a definitive correlation between hemorrhage risk and anatomical target [119, 121, 122]. The association between hemorrhage and microelectrode recording is controversial. There is some suggestion that microelectrode recording increases the risk of hemorrhage, with a correlation between risk and number of microelectrode passes, but some series have not shown this increased hemorrhage risk [119, 123, 124]. The risks and controversy associated with microelectrode recording are not unique to treatment of dystonia and are covered elsewhere in this text. One postoperative consideration particular to dystonia is status dystonicus, an acute exacerbation of dystonic symptoms that can be triggered by the changes in therapy, infection, or dehydration that can occur in a postoperative setting. Status dystonicus can be severe, leading to life-threatening issues including autonomic instability, respiratory compromise, rhabdomyolysis, or acute renal failure [125–127]. Management of status dystonicus largely consists of supportive medical care, including careful observation in a critical care unit, hydration, benzodiazepines, and antipyretics [125–127].

Hardware-Related Complications

Long-term complications after deep brain stimulation primarily consist of hardware-related complications, including infection, wound breakdown, lead migration, lead fracture, implanted pulse generator (IPG) malfunction, and tethering or pain. These issues can arise even years after initial surgery. The most common complication from DBS is infection [105, 108, 110–113, 115, 116, 128–133]. Infection, either shortly after surgery or many years later, occurs in up to 15.2% of patients, with systemic analysis of multiple trials showing average of approximately 5–6% [105, 108, 110–113, 115, 116, 128–133]. The most common site for infections appears to be the implanted pulse generator (IPG) site [105, 111, 112, 116, 123, 128, 134]. Though infection often necessitates removal of the entire DBS system, superficial infections confined to the implanted pulse generator (IPG) pocket may be amenable to management with antibiotics or removal of the IPG and connections alone [133–135]. In up to 50% of patients treated conservatively, the DBS leads can be preserved [111, 112, 133–135]. Severe infections, or those that have failed conservative management, should be treated with removal of the entire DBS system, followed by antibiotic treatment for several months prior to consideration of reimplantation. Other hardware-related complications, such as lead fracture or other hardware failure, can result in abrupt cessation of therapy delivery. If lead fracture or failure is suspected, initial evaluation consists of interrogating the DBS device to check impedance and current and performing x-ray imaging to assess for hardware disconnection [136]. Patients with dystonia seem to have a slightly higher rate of lead fracture compared to other movement disorders, with up to 5.6% of patients experiencing lead fracture [105, 111, 128, 130, 137, 138]. Dystonic postures of the neck place tension on the extension cabling and may explain this higher rate of lead fracture [105, 111, 128, 130, 137, 138].

Stimulation Side Effects

DBS, even with a well-placed lead, can be associated with neurological side effects related to anatomical regions adjacent to the target chosen. Patients with dystonia seem to tolerate GPi DBS well, with a low incidence of stimulation-induced side effects [139–141]. The most common stimulation side effect in dystonia seems to be dysarthria, which occurs in 4–11% of cases [113, 128, 142]. Though programming can improve or reverse dysarthria, some patients may have persistent symptoms [113, 128, 142]. The GPi is also associated with bradykinesia, and "freezing" of gait, with varying degrees of severity [129, 143–145]. The incidence of bradykinesia is difficult to assess, as there is some indication of slowed motor responses even in patients who do not report symptomatic bradykinesia [73, 146]. There does not seem to be a significant risk of cognitive decline or depression after GPi DBS [139–141].

Outcomes

Primary Generalized Dystonia

Primary, generalized, dystonia is the most studied among dystonia subtypes. There is a suggestion that genetically characterized primary dystonia (such as DYT1) may be particularly responsive to DBS [130]. Early case series of bilateral GPi implantation showed BFMDRS motor score improvements between 22% and 86% over follow-up periods of up to 66 months [84, 147–152]. These encouraging results prompted several prospective, controlled trials of GPi DBS in primary generalized dystonia. One of the seminal prospective studies of GPi stimulation showed robust, >50% improvements in objective motor scores and disabilities domains of BMFDRS a year after implantation [72]. Randomized, sham-controlled data confirmed these results, showing 39.9% improvement in BFMDRS motor score after 3 months compared to 4.5% for sham stimulation [73]. After a year, these patients had a 45% improvement in BFMDRS [73]. Another prospective study, performed in 2010, showed comparable 43.8% improvement in BFMDRS motor score after a year [153]. Long-term follow-up of patients with primary generalized dystonia shows that there is

progressive benefit from GPi DBS, with a range in long-term improvement from preoperative baseline (based on BFMDRS motor score) of 58%–76%, with long-term follow-up ranging from 3 to 20 years [113, 130, 131, 154–156].

Focal Dystonia/Cervical Dystonia

Focal dystonia such as cervical dystonia can also be responsive to DBS. Several retrospective, non-blinded series show that patients with cervical dystonia have outcomes comparable to those with primary generalized dystonia [74]. Other long-term studies demonstrate a wide range of improvements in TWSTRS severity scores, with progressive improvement in TWSTRS severity, disability, and pain scores continuing to improve until 20 months postoperative (severity 38% –> 63%, disability 54% –> 69%, and pain 38% –> 50%) [137, 142, 157–161]. Long-term follow-up suggests that, like primary generalized dystonia, the initial improvement in outcomes persists with 47.6% improvement from baseline TWSTRS score after an average 7.7 years of follow-up [70, 161, 162].

DBS has also been evaluated extensively in idiopathic cranio-cervical dystonia (Meige syndrome), a segmental dystonia involving the periorbital, facial, bucco-oral, and cervical muscles. Meige syndrome is often refractory to pharmacotherapy and chemodenervation, the latter often limited by adverse effects. Bilateral GPi DBS in Meige syndrome has demonstrated efficacy similar to responses in cervical and generalized dystonia; up to 80% improvement in BFMDRS cranial and cervical subscales has been reported up to 10 years postimplantation in case reports and small case series [163–167]. A recent large-scale review, including Meige syndrome treated with GPi or STN DBS, showed a mean improvement of 66.9% in motor scales and 56% in disability scales [168].

Secondary Dystonia

Though anecdotal evidence suggests many types of secondary dystonia improve with DBS, certain subtypes of secondary dystonia appear to be particularly amenable [169]. Of note, the majority of evidence supporting the use of DBS in secondary dystonia is derived from case reports and case series, rather than the blinded, controlled studies, so further study is indicated. Patients with intractable and severe tardive dystonia, a disorder of involuntary muscle contractions and painful spasms as a side effect of dopaminergic antagonist medications, seem to show good response to DBS, with most patients experiencing approximately 50–70% improvement in symptoms over at least 6 months (based on BFMDRS motor score) [69, 76, 170–175]. Cerebral palsy patients generally have more modest improvements, with results ranging from 23.6% to 49.5% improvement on classical dystonia rating scales [176–179]. Importantly, the overall improvement in quality of life for cerebral palsy patients treated with DBS may be significant even in the setting of more meager improvement in their dystonia rating scales [178, 179].

DBS Programming and Stimulation Parameters

The general guiding principle of DBS programming is to improve motor symptoms and minimize adverse stimulation effects. In patients with dystonia, clinical response to changes in DBS settings may not be immediately apparent, which makes programming particularly challenging, and there are currently no set of recommended "ideal" DBS settings for dystonia [180–182]. Programming in dystonia may require several months of continuous stimulation to find optimal settings to achieve global dystonia improvement. The first postoperative programming is typically performed 3–4 weeks after lead placement, allowing any microlesional effects to subside, and performed with the patient in a medication-OFF state allowing the fullest expression of physical symptoms. In rare settings, such as dystonic crisis, this programming may be performed earlier [126, 180]. On initial programming, each lead contact is sequentially activated in a monopolar fashion (case as anode, contact as cathode),

gradually increasing stimulus intensity, voltage, or current amplitude until transient or sustained side effects are obtained [183, 184]. Stimulation of contacts within the posterolateral GPi, typically one contact above that which induces phosphenes, seems to result in the most motor benefit [185–187]. Programming may require many adjustments, including bipolar or double monopolar configurations, high pulse width [188, 189], or frequency modulation [148, 150, 160, 190, 191]. Dystonia DBS programming highlights limitations of open-loop devices and current programming approaches. Emerging lines of inquiry into optimizing treatment of dystonia include modification of the traditional rectangular DBS waveform from passive to active charge balancing [192] and lower-frequency phase-specific stimulation [193]. Perhaps most intriguing is that a wider appreciation of cerebellar contributions to modulating basal ganglia activity opens new treatment avenues and novel targets of stimulation [194–198].

Peripheral Denervation

In patients with cervical dystonia, electromyography can be used to guide denervation of selected muscles involved in the patient's dystonia, providing relief of pain without the need for a permanent implanted device or intracranial manipulation. In the Bertrand procedure, branches of the spinal accessory nerve to the sternocleidomastoid are sectioned, followed by sectioning of the posterior rami of the ipsilateral C1–6 roots to eliminate innervation of ipsilateral paraspinal muscles [199–201]. This technique can improve cervical dystonia symptoms, with a reduction on the TWSTRS severity from 22% to 59% [202–209]. However, there can be significant risks of peripheral denervation, including dysphagia (which may be transient), troubling numbness/paresthesias, and reenervation. Up to 25% of patients can experience troubling reinnervation of the cervical muscles, thought to be a result of incomplete denervation of small branches from the cervical plexus, with recrudescence of symptoms [203, 205]. Though current data suggests that peripheral denervation is likely not as effective or durable as DBS in treatment of cervical dystonia, select patients may still benefit from the procedure [205, 209].

Pallidotomy

Though DBS is currently the primary surgical approach to modulation of the GPi in treatment of dystonia, there is interest in other techniques. For patients who have medical comorbidities that make hardware implantation too risky to consider, patients who require hardware removal due to infection, or patients being treated in settings where DBS hardware and programming support are not available. Radiosurgery began with pallidotomies and thalamotomies [210, 211]. Prior to the advent of DBS, stereotactic pallidotomy, performed with radiofrequency ablation to create lesions, showed promising results in dystonia [212, 213]. With bilateral stereotactic pallidotomy in dystonia, case reports and small case series suggest improvements of an average of 60% in BFMDRS score in primary dystonia, with more mixed and marginal results in secondary dystonia [152, 214–216]. With the advent of DBS, pallidotomy fell out of favor. Recently, pallidal lesioning has regained some interest as a salvage procedure. There are new techniques proposed to perform stereotactic pallidotomy. Some studies suggest radiofrequency ablation can be performed through DBS leads in the pallidum, ideal for a patient with an infection who must have their DBS system removed [217]. Stereotactic radiosurgery, an incision-free approach, has also been used to create pallidal lesions, though the lesions are not as consistent and the results appear to be inferior to those of DBS [218–220]. Laser interstitial therapy (LITT), in which a laser fiber is passed through a burr hole and an ablation trajectory can be defined, has also been used anecdotally for pallidotomy [221]. Finally, MRI-guided focused ultrasound has been used for treatment of essential tremor [222] with low complication rates and may be an option for pallidotomy in the future. Though there is no current procedure that can supplant

deep brain stimulation, these new applications and methods of deep brain stimulation will continue to be an active area of investigation.

Conclusion

In this chapter, we have provided an overview of clinical features of patients with dystonia, who are a heterogenous group of patients with varied responses to treatment. We have provided an overview of preoperative assessment and outlined surgical treatment with deep brain stimulation. We have shown that DBS can be used to treat dystonia with good outcomes for a variety of patients. As in other disorders, there are multiple methods of performing DBS in dystonia. DBS patients require careful follow-up and an experienced programming clinician. Other surgical methods with peripheral denervation or pallidal ablation are areas of continued exploration and research.

References

1. Steeves TD, et al. The prevalence of primary dystonia: a systematic review and meta-analysis. Mov Disord. 2012;27(14):1789–96.
2. Albanese A. How many Dystonias? Clinical evidence. Front Neurol. 2017;8:18.
3. Pirio Richardson S, et al. Research priorities in limb and task-specific Dystonias. Front Neurol. 2017;8:170.
4. Marsden CD. Dystonia: the spectrum of the disease. Res Publ Assoc Res Nerv Ment Dis. 1976;55:351–67.
5. Albanese A, et al. Phenomenology and classification of dystonia: a consensus update. Mov Disord. 2013;28(7):863–73.
6. Morgan VL, Rogers BP, Abou-Khalil B. Segmentation of the thalamus based on BOLD frequencies affected in temporal lobe epilepsy. Epilepsia. 2015;56(11):1819–27.
7. Morgante F, Klein C. Dystonia. Continuum (Minneap Minn). 2013;19(5 Movement Disorders):1225–41.
8. Torres-Russotto D, Perlmutter JS. Task-specific dystonias: a review. Ann N Y Acad Sci. 2008;1142:179–99.
9. Frucht SJ, et al. The natural history of embouchure dystonia. Mov Disord. 2001;16(5):899–906.
10. Sitburana O, et al. Motor overflow and mirror dystonia. Parkinsonism Relat Disord. 2009;15(10):758–61.
11. Patel N, et al. Alleviating manoeuvres (sensory tricks) in cervical dystonia. J Neurol Neurosurg Psychiatry. 2014;85(8):882–4.
12. Broussolle E, et al. Early illustrations of Geste Antagoniste in cervical and generalized dystonia. Tremor Other Hyperkinet Mov (N Y). 2015;5:332.
13. Lee CN, et al. "Visual sensory trick" in patient with cervical dystonia. Neurol Sci. 2012;33(3):665–7.
14. Stojanovic M, et al. Improvement in laryngeal dystonia with background noise. Mov Disord. 1997;12(2):249–50.
15. Asmus F, et al. Reverse sensory geste in cervical dystonia. Mov Disord. 2009;24(2):297–300.
16. Greene PE, Bressman S. Exteroceptive and interoceptive stimuli in dystonia. Mov Disord. 1998;13(3):549–51.
17. Ozelius L, et al. Human gene for torsion dystonia located on chromosome 9q32-q34. Neuron. 1989;2(5):1427–34.
18. Klein C. Genetics in dystonia. Parkinsonism Relat Disord. 2014;20(Suppl 1):S137–42.
19. Phukan J, et al. Primary dystonia and dystonia-plus syndromes: clinical characteristics, diagnosis, and pathogenesis. Lancet Neurol. 2011;10(12):1074–85.
20. Hawker K, Lang AE. Hypoxic-ischemic damage of the basal ganglia. Case reports and a review of the literature. Mov Disord. 1990;5(3):219–24.
21. Lee MS, Marsden CD. Movement disorders following lesions of the thalamus or subthalamic region. Mov Disord. 1994;9(5):493–507.
22. Burke RE, Fahn S, Gold AP. Delayed-onset dystonia in patients with "static" encephalopathy. J Neurol Neurosurg Psychiatry. 1980;43(9):789–97.
23. Hilaire MHS, et al. Delayed-onset dystonia due to perinatal or early childhood asphyxia. Neurology. 1991;41(2, Part 1):216.
24. Zadori D, et al. Drug-induced movement disorders. Expert Opin Drug Saf. 2015;14(6):877–90.
25. Jankovic J, et al. Relationship between various clinical outcome assessments in patients with blepharospasm. Mov Disord. 2009;24(3):407–13.
26. Consky E, Lang A. Clinical assessments of patients with cervical dystonia. In: Jankovic J, Hallett M, editors. Therapy with botulinum toxin. New York: Marcel Dekker; 1994. p. 211–37.
27. Muller J, et al. Craniocervical dystonia questionnaire (CDQ-24): development and validation of a disease-specific quality of life instrument. J Neurol Neurosurg Psychiatry. 2004;75(5):749–53.
28. Comella CL, et al. Rating scales for dystonia: a multicenter assessment. Mov Disord. 2003;18(3):303–12.
29. Krystkowiak P, et al. Reliability of the Burke-Fahn-Marsden scale in a multicenter trial for dystonia. Mov Disord. 2007;22(5):685–9.
30. Burke RE, et al. Validity and reliability of a rating scale for the primary torsion dystonias. Neurology. 1985;35(1):73–7.
31. Jankovic J. Medical treatment of dystonia. Mov Disord. 2013;28(7):1001–12.
32. Albanese A, et al. EFNS guidelines on diagnosis and treatment of primary dystonias. Eur J Neurol. 2011;18(1):5–18.

33. Delnooz CC, et al. Paramedical treatment in primary dystonia: a systematic review. Mov Disord. 2009;24(15):2187–98.
34. De Pauw J, et al. The effectiveness of physiotherapy for cervical dystonia: a systematic literature review. J Neurol. 2014;261(10):1857–65.
35. Tassorelli C, et al. Botulinum toxin and neuromotor rehabilitation: an integrated approach to idiopathic cervical dystonia. Mov Disord. 2006;21(12):2240–3.
36. Nygaard TG, Marsden CD, Duvoisin RC. Dopa-responsive dystonia. Adv Neurol. 1988;50:377–84.
37. Segawa M, et al. Hereditary progressive dystonia with marked diurnal fluctuation. Adv Neurol. 1976;14:215–33.
38. Karp BI, et al. An open trial of clozapine for dystonia. Mov Disord. 1999;14(4):652–7.
39. Jankovic J. Tardive syndromes and other drug-induced movement disorders. Clin Neuropharmacol. 1995;18(3):197–214.
40. Shapleske J, Mickay AP, McKenna PJ. Successful treatment of tardive dystonia with clozapine and clonazepam. Br J Psychiatry. 1996;168(4):516–8.
41. Simpson GM. The treatment of tardive dyskinesia and tardive dystonia. J Clin Psychiatry. 2000;61(Suppl 4):39–44.
42. Jankovic J, Beach J. Long-term effects of tetrabenazine in hyperkinetic movement disorders. Neurology. 1997;48(2):358–62.
43. Chen JJ, et al. Tetrabenazine for the treatment of hyperkinetic movement disorders: a review of the literature. Clin Ther. 2012;34(7):1487–504.
44. Jankovic J. Treatment of hyperkinetic movement disorders with tetrabenazine: a double-blind crossover study. Ann Neurol. 1982;11(1):41–7.
45. Jankovic J, Orman J. Tetrabenazine therapy of dystonia, chorea, tics, and other dyskinesias. Neurology. 1988;38(3):391–4.
46. Boyer WF, Bakalar NH, Lake CR. Anticholinergic prophylaxis of acute haloperidol-induced acute dystonic reactions. J Clin Psychopharmacol. 1987;7(3):164–6.
47. Holloman LC, Marder SR. Management of acute extrapyramidal effects induced by antipsychotic drugs. Am J Health Syst Pharm. 1997;54(21):2461–77.
48. Stern TA, Anderson WH. Benztropine prophylaxis of dystonic reactions. Psychopharmacology (Berl). 1979;61(3):261–2.
49. Fahn S. High dosage anticholinergic therapy in dystonia. Neurology. 1983;33(10):1255–61.
50. Albanese A, et al. A systematic review on the diagnosis and treatment of primary (idiopathic) dystonia and dystonia plus syndromes: report of an EFNS/MDS-ES Task Force. Eur J Neurol. 2006;13(5):433–44.
51. Burke RE, Fahn S, Marsden CD. Torsion dystonia: a double-blind, prospective trial of high-dosage trihexyphenidyl. Neurology. 1986;36(2):160–4.
52. Sanger TD, et al. Prospective open-label clinical trial of trihexyphenidyl in children with secondary dystonia due to cerebral palsy. J Child Neurol. 2007;22(5):530–7.
53. van den Heuvel CNAM, et al. The symptomatic treatment of acquired dystonia: a systematic review. Mov Disord Clin Pract. 2016;3(6):548–58.
54. Brans JW, et al. Botulinum toxin versus trihexyphenidyl in cervical dystonia: a prospective, randomized, double-blind controlled trial. Neurology. 1996;46(4):1066–72.
55. Hallett M, et al. Evidence-based review and assessment of botulinum neurotoxin for the treatment of movement disorders. Toxicon. 2013;67:94–114.
56. Simpson DM, et al. Practice guideline update summary: botulinum neurotoxin for the treatment of blepharospasm, cervical dystonia, adult spasticity, and headache: report of the guideline development Subcommittee of the American Academy of Neurology. Neurology. 2016;86(19):1818–26.
57. Simpson DM, et al. Assessment: botulinum neurotoxin for the treatment of movement disorders (an evidence-based review): report of the therapeutics and technology assessment Subcommittee of the American Academy of Neurology. Neurology. 2008;70(19):1699–706.
58. Kruisdijk JJ, et al. Botulinum toxin for writer's cramp: a randomised, placebo-controlled trial and 1-year follow-up. J Neurol Neurosurg Psychiatry. 2007;78(3):264–70.
59. Bentivoglio AR, et al. Fifteen-year experience in treating blepharospasm with Botox or Dysport: same toxin, two drugs. Neurotox Res. 2009;15(3):224–31.
60. Truong D, et al. Efficacy and safety of botulinum type A toxin (Dysport) in cervical dystonia: results of the first US randomized, double-blind, placebo-controlled study. Mov Disord. 2005;20(7):783–91.
61. Albavera-Hernandez C, Rodriguez JM, Idrovo AJ. Safety of botulinum toxin type A among children with spasticity secondary to cerebral palsy: a systematic review of randomized clinical trials. Clin Rehabil. 2009;23(5):394–407.
62. Pappert EJ, Germanson T. And G. Myobloc/Neurobloc European Cervical Dystonia Study, botulinum toxin type B vs. type A in toxin-naive patients with cervical dystonia: randomized, double-blind, noninferiority trial. Mov Disord. 2008;23(4):510–7.
63. Duarte GS, et al. Botulinum toxin type A versus botulinum toxin type B for cervical dystonia. Cochrane Database Syst Rev. 2016;10:CD004314.
64. Cooper IS. Clinical and physiologic implications of thalamic surgery for disorders of sensory communication. 2. Intention tremor, dystonia, Wilson's disease and torticollis. J Neurol Sci. 1965;2(6):520–53.
65. Cooper IS. 20-year followup study of the neurosurgical treatment of dystonia musculorum deformans. Adv Neurol. 1976;14:423–52.
66. Gildenberg PL. Evolution of basal ganglia surgery for movement disorders. Stereotact Funct Neurosurg. 2006;84(4):131–5.
67. Cif L, Hariz M. Seventy years with the globus pallidus: Pallidal surgery for movement disorders between 1947 and 2017. Mov Disord. 2017;32:972.
68. Pretto TE, et al. A prospective blinded evaluation of deep brain stimulation for the treatment of second-

ary dystonia and primary torticollis syndromes. J Neurosurg. 2008;109(3):405–9.
69. Damier P, et al. Bilateral deep brain stimulation of the globus pallidus to treat tardive dyskinesia. Arch Gen Psychiatry. 2007;64(2):170–6.
70. Kiss ZH, et al. The Canadian multicentre study of deep brain stimulation for cervical dystonia. Brain. 2007;130(Pt 11):2879–86.
71. Diamond A, et al. Globus pallidus deep brain stimulation in dystonia. Mov Disord. 2006;21(5):692–5.
72. Vidailhet M, et al. Bilateral deep-brain stimulation of the globus pallidus in primary generalized dystonia. N Engl J Med. 2005;352(5):459–67.
73. Kupsch A, et al. Pallidal deep-brain stimulation in primary generalized or segmental dystonia. N Engl J Med. 2006;355(19):1978–90.
74. Moro E, et al. Efficacy of pallidal stimulation in isolated dystonia: a systematic review and meta-analysis. Eur J Neurol. 2017;24(4):552–60.
75. Romito LM, et al. Fixed dystonia unresponsive to pallidal stimulation improved by motor cortex stimulation. Neurology. 2007;68(11):875–6.
76. Sun B, et al. Subthalamic nucleus stimulation for primary dystonia and tardive dystonia. Acta Neurochir Suppl. 2007;97(Pt 2):207–14.
77. Woehrle JC, et al. Chronic deep brain stimulation for segmental dystonia. Stereotact Funct Neurosurg. 2009;87(6):379–84.
78. Racette BA, et al. Thalamic stimulation for primary writing tremor. J Neurol. 2001;248(5):380–2.
79. Minguez-Castellanos A, et al. Primary writing tremor treated by chronic thalamic stimulation. Mov Disord. 1999;14(6):1030–3.
80. Kuncel AM, et al. Myoclonus and tremor response to thalamic deep brain stimulation parameters in a patient with inherited myoclonus-dystonia syndrome. Clin Neurol Neurosurg. 2009;111(3):303–6.
81. Hedera P, et al. Surgical targets for dystonic tremor: considerations between the globus pallidus and ventral intermediate thalamic nucleus. Parkinsonism Relat Disord. 2013;19(7):684–6.
82. Morishita T, et al. Should we consider vim thalamic deep brain stimulation for select cases of severe refractory dystonic tremor. Stereotact Funct Neurosurg. 2010;88(2):98–104.
83. Fasano A, Bove F, Lang AE. The treatment of dystonic tremor: a systematic review. J Neurol Neurosurg Psychiatry. 2014;85(7):759–69.
84. Vercueil L, et al. Deep brain stimulation in the treatment of severe dystonia. J Neurol. 2001;248(8):695–700.
85. Ostrem JL, et al. Subthalamic nucleus deep brain stimulation in isolated dystonia: a 3-year follow-up study. Neurology. 2017;88(1):25–35.
86. Kramer DR, et al. Best surgical practices: a stepwise approach to the University of Pennsylvania deep brain stimulation protocol. Neurosurg Focus. 2010;29(2):E3.
87. Machado A, et al. Deep brain stimulation for Parkinson's disease: surgical technique and perioperative management. Mov Disord. 2006;21(Suppl 14):S247–58.
88. Bjartmarz H, Rehncrona S. Comparison of accuracy and precision between frame-based and frameless stereotactic navigation for deep brain stimulation electrode implantation. Stereotact Funct Neurosurg. 2007;85(5):235–42.
89. Bot M, et al. Analysis of stereotactic accuracy in patients undergoing deep brain stimulation using Nexframe and the Leksell frame. Stereotact Funct Neurosurg. 2015;93(5):316–25.
90. Henderson JM, et al. The application accuracy of a skull-mounted trajectory guide system for image-guided functional neurosurgery. Comput Aided Surg. 2004;9(4):155–60.
91. Cheng CY, et al. Deep brain stimulation for Parkinson's disease using frameless technology. Br J Neurosurg. 2014;28(3):383–6.
92. Maciunas RJ, et al. An independent application accuracy evaluation of stereotactic frame systems. Stereotact Funct Neurosurg. 1992;58(1–4):103–7.
93. Hariz MI. Safety and risk of microelectrode recording in surgery for movement disorders. Stereotact Funct Neurosurg. 2002;78(3–4):146–57.
94. Kocabicak E, et al. Is there still need for microelectrode recording now the subthalamic nucleus can be well visualized with high field and ultrahigh MR imaging? Front Integr Neurosci. 2015;9:46.
95. Chen T, Mirzadeh Z, Ponce FA. "Asleep" deep brain stimulation surgery: a critical review of the literature. World Neurosurg. 2017;105:191–8.
96. Kochanski RB, Sani S. Awake versus asleep deep brain stimulation surgery: technical considerations and critical review of the literature. Brain Sci. 2018;8(1):pii: E17.
97. Chen T, et al. Clinical outcomes following awake and asleep deep brain stimulation for Parkinson disease. J Neurosurg. 2018;130(1):109–20. p. 1–12.
98. Schaltenbrand G, Walker AE. Stereotaxy of the human brain. New York: Thieme-Stratton; 1982.
99. Talairach J, Tournoux P. Co-planar stereotaxic atlas for the human brain: 3-D proportional system: an approach to cerebral imaging. New York: Thieme; 1988.
100. O'Gorman RL, et al. Optimal MRI methods for direct stereotactic targeting of the subthalamic nucleus and globus pallidus. Eur Radiol. 2011;21(1):130–6.
101. Vayssiere N, et al. Comparison of atlas- and magnetic resonance imaging-based stereotactic targeting of the globus pallidus internus in the performance of deep brain stimulation for treatment of dystonia. J Neurosurg. 2002;96(4):673–9.
102. Anderson WS, et al. Applying microelectrode recordings in neurosurgery. Contemp Neurosurg. 2010;32(3):1–7.
103. Anderson WS, Lenz FA. Surgery insight: deep brain stimulation for movement disorders. Nat Clin Pract Neuro. 2006;2(6):310–20.
104. Starr PA, et al. Microelectrode-guided implantation of deep brain stimulators into the globus pallidus

internus for dystonia: techniques, electrode locations, and outcomes. Neurosurg Focus. 2004;17(1):E4.
105. Jitkritsadakul O, et al. Systematic review of hardware-related complications of deep brain stimulation: do new indications pose an increased risk? Brain Stimul. 2017;10(5):967–76.
106. Bruggemann N, et al. Short- and long-term outcome of chronic pallidal neurostimulation in monogenic isolated dystonia. Neurology. 2015;84(9):895–903.
107. Romito LM, et al. Pallidal stimulation for acquired dystonia due to cerebral palsy: beyond 5 years. Eur J Neurol. 2014;22(3):426–e32.
108. Beric A, et al. Complications of deep brain stimulation surgery. Stereotact Funct Neurosurg. 2001;77(1–4):73–8.
109. Burdick AP, et al. Relationship between higher rates of adverse events in deep brain stimulation using standardized prospective recording and patient outcomes. Neurosurg Focus. 2010;29(2):E4.
110. Chen T, et al. Complication rates, lengths of stay, and readmission rates in "awake" and "asleep" deep brain simulation. J Neurosurg. 2017;127(2):360–9.
111. Constantoyannis C, et al. Reducing hardware-related complications of deep brain stimulation. Can J Neurol Sci. 2005;32(2):194–200.
112. Fenoy AJ, Simpson RK Jr. Risks of common complications in deep brain stimulation surgery: management and avoidance. J Neurosurg. 2014;120(1):132–9.
113. Isaias IU, Alterman RL, Tagliati M. Deep brain stimulation for primary generalized dystonia: long-term outcomes. Arch Neurol. 2009;66(4):465–70.
114. Kaminska M, et al. Complications of Deep Brain Stimulation (DBS) for dystonia in children – the challenges and 10 year experience in a large paediatric cohort. Eur J Paediatr Neurol. 2017;21(1):168–75.
115. Patel DM, et al. Adverse events associated with deep brain stimulation for movement disorders: analysis of 510 consecutive cases. Neurosurgery. 2015;11(Suppl 2):190–9.
116. Sillay KA, Larson PS, Starr PA. Deep brain stimulator hardware-related infections: incidence and management in a large series. Neurosurgery. 2008;62(2):360–6. discussion 366-7
117. Zrinzo L, et al. Reducing hemorrhagic complications in functional neurosurgery: a large case series and systematic literature review. J Neurosurg. 2011;116(1):84–94.
118. Buhmann C, et al. Adverse events in deep brain stimulation: a retrospective long-term analysis of neurological, psychiatric and other occurrences. PLoS One. 2017;12(7):e0178984.
119. Gorgulho A, et al. Incidence of hemorrhage associated with electrophysiological studies performed using macroelectrodes and microelectrodes in functional neurosurgery. J Neurosurg. 2005;102(5):888–96.
120. Park CK, et al. Analysis of delayed intracerebral hemorrhage associated with deep brain stimulation surgery. World Neurosurg. 2017;104:537–44.
121. Binder DK, Rau GM, Starr PA. Risk factors for hemorrhage during microelectrode-guided deep brain stimulator implantation for movement disorders. Neurosurgery. 2005;56(4):722–32. discussion 722-32
122. Xiaowu H, et al. Risks of intracranial hemorrhage in patients with Parkinson's disease receiving deep brain stimulation and ablation. Parkinsonism Relat Disord. 2010;16(2):96–100.
123. Umemura A, et al. Deep brain stimulation for movement disorders: morbidity and mortality in 109 patients. J Neurosurg. 2003;98(4):779–84.
124. Obeso JA, et al. Deep-brain stimulation of the subthalamic nucleus or the pars interna of the globus pallidus in Parkinson's disease. N Engl J Med. 2001;345(13):956–63.
125. Allen NM, et al. Status dystonicus: a practice guide. Dev Med Child Neurol. 2014;56(2):105–12.
126. Termsarasab P, Frucht SJ. Dystonic storm: a practical clinical and video review. J Clin Mov Disord. 2017;4(10):10.
127. Cheung T, et al. Status dystonicus following deep brain stimulation surgery in DYT1 dystonia patients (P01.227). Neurology. 2012;78(1 Supplement):P01.227.
128. Kenney C, et al. Short-term and long-term safety of deep brain stimulation in the treatment of movement disorders. J Neurosurg. 2007;106(4):621–5.
129. Meoni S, et al. Pallidal deep brain stimulation for dystonia: a long term study. J Neurol Neurosurg Psychiatry. 2017;88(11):960–7.
130. Panov F, et al. Deep brain stimulation in DYT1 dystonia: a 10-year experience. Neurosurgery. 2013;73(1):86–93; discussion 93.
131. Sobstyl M, et al. Long-term outcomes of bilateral pallidal stimulation for primary generalised dystonia. Clin Neurol Neurosurg. 2014;126:82–7.
132. Tagliati M, et al. Long-term management of DBS in dystonia: response to stimulation, adverse events, battery changes, and special considerations. Mov Disord. 2011;26 Suppl 1(26):S54–62.
133. Piacentino M, Pilleri M, Bartolomei L. Hardware-related infections after deep brain stimulation surgery: review of incidence, severity and management in 212 single-center procedures in the first year after implantation. Acta Neurochir (Wien). 2011;153(12):2337–41.
134. Fenoy AJ, Simpson RK Jr. Management of device-related wound complications in deep brain stimulation surgery. J Neurosurg. 2012;116(6):1324–32.
135. Bhatia S, et al. Infections and hardware salvage after deep brain stimulation surgery: a single-center study and review of the literature. Stereotact Funct Neurosurg. 2010;88(3):147–55.
136. Fernandez FS, et al. Lead fractures in deep brain stimulation during long-term follow-up. Parkinsons Dis. 2009;2010(409356):409356.
137. Krauss JK, et al. Pallidal deep brain stimulation in patients with cervical dystonia and severe cervi-

cal dyskinesias with cervical myelopathy. J Neurol Neurosurg Psychiatry. 2002;72(2):249–56.
138. Yianni J, et al. Increased risk of lead fracture and migration in dystonia compared with other movement disorders following deep brain stimulation. J Clin Neurosci. 2004;11(3):243–5.
139. Jahanshahi M, Czernecki V, Zurowski AM. Neuropsychological, neuropsychiatric, and quality of life issues in DBS for dystonia. Mov Disord. 2011;26 Suppl 1(26):S63–78.
140. Halbig TD, et al. Pallidal stimulation in dystonia: effects on cognition, mood, and quality of life. J Neurol Neurosurg Psychiatry. 2005;76(12):1713–6.
141. de Gusmao CM, Pollak LE, Sharma N. Neuropsychological and psychiatric outcome of GPi-deep brain stimulation in dystonia. Brain Stimul. 2017;10(5):994–6.
142. Volkmann J, et al. Pallidal neurostimulation in patients with medication-refractory cervical dystonia: a randomised, sham-controlled trial. Lancet Neurol. 2014;13(9):875–84.
143. Schrader C, et al. GPi-DBS may induce a hypokinetic gait disorder with freezing of gait in patients with dystonia. Neurology. 2011;77(5):483–8.
144. Blahak C, et al. Micrographia induced by pallidal DBS for segmental dystonia: a subtle sign of hypokinesia? J Neural Transm (Vienna). 2011;118(4):549–53.
145. Berman BD, et al. Induction of bradykinesia with pallidal deep brain stimulation in patients with cranial-cervical dystonia. Stereotact Funct Neurosurg. 2009;87(1):37–44.
146. Huebl J, et al. Bradykinesia induced by frequency-specific pallidal stimulation in patients with cervical and segmental dystonia. Parkinsonism Relat Disord. 2015;21(7):800–3.
147. Yianni J, et al. Post-operative progress of dystonia patients following globus pallidus internus deep brain stimulation. Eur J Neurol. 2003;10(3):239–47.
148. Kupsch A, et al. The effects of frequency in pallidal deep brain stimulation for primary dystonia. J Neurol. 2003;250(10):1201–5.
149. Katayama Y, et al. Chronic stimulation of the globus pallidus internus for control of primary generalized dystonia. Acta Neurochir Suppl. 2003;87:125–8.
150. Coubes P, et al. Electrical stimulation of the globus pallidus internus in patients with primary generalized dystonia: long-term results. J Neurosurg. 2004;101(2):189–94.
151. Vayssiere N, et al. Deep brain stimulation for dystonia confirming a somatotopic organization in the globus pallidus internus. J Neurosurg. 2004;101(2):181–8.
152. Eltahawy HA, et al. Primary dystonia is more responsive than secondary dystonia to pallidal interventions: outcome after pallidotomy or pallidal deep brain stimulation. Neurosurgery. 2004;54(3):613–9; discussion 619–21.
153. Valldeoriola F, et al. Efficacy and safety of pallidal stimulation in primary dystonia: results of the Spanish multicentric study. J Neurol Neurosurg Psychiatry. 2010;81(1):65–9.
154. Vidailhet M, et al. Bilateral, pallidal, deep-brain stimulation in primary generalised dystonia: a prospective 3 year follow-up study. Lancet Neurol. 2007;6(3):223–9.
155. Loher TJ, et al. Deep brain stimulation for dystonia: outcome at long-term follow-up. J Neurol. 2008;255(6):881–4.
156. Volkmann J, et al. Pallidal deep brain stimulation in patients with primary generalised or segmental dystonia: 5-year follow-up of a randomised trial. Lancet Neurol. 2012;11(12):1029–38.
157. Cacciola F, et al. Bilateral deep brain stimulation for cervical dystonia: long-term outcome in a series of 10 patients. Neurosurgery. 2010;67(4):957–63.
158. Hung SW, et al. Long-term outcome of bilateral pallidal deep brain stimulation for primary cervical dystonia. Neurology. 2007;68(6):457–9.
159. Krauss JK, et al. Bilateral stimulation of globus pallidus internus for treatment of cervical dystonia. Lancet. 1999;354(9181):837–8.
160. Moro E, et al. Pallidal stimulation in cervical dystonia: clinical implications of acute changes in stimulation parameters. Eur J Neurol. 2009;16(4):506–12.
161. Yamada K, et al. Long disease duration interferes with therapeutic effect of globus pallidus internus pallidal stimulation in primary cervical dystonia. Neuromodulation. 2013;16(3):219–25; discussion 225.
162. Walsh RA, et al. Bilateral pallidal stimulation in cervical dystonia: blinded evidence of benefit beyond 5 years. Brain. 2013;136(Pt 3):761–9.
163. Inoue N, et al. Long-term suppression of Meige syndrome after pallidal stimulation: a 10-year follow-up study. Mov Disord. 2010;25(11):1756–8.
164. Sako W, et al. Bilateral pallidal deep brain stimulation in primary Meige syndrome. Parkinsonism Relat Disord. 2011;17(2):123–5.
165. Lyons MK, et al. Long-term follow-up of deep brain stimulation for Meige syndrome. Neurosurg Focus. 2010;29(2):E5.
166. Reese R, et al. Long-term clinical outcome in meige syndrome treated with internal pallidum deep brain stimulation. Mov Disord. 2011;26(4):691–8.
167. Ostrem JL, et al. Pallidal deep brain stimulation in patients with cranial-cervical dystonia (Meige syndrome). Mov Disord. 2007;22(13):1885–91.
168. Wang X, et al. Deep brain stimulation for Craniocervical dystonia (Meige syndrome): a report of four patients and a literature-based analysis of its treatment effects. Neuromodulation. 2016;19(8):818–23.
169. Vidailhet M, et al. Deep brain stimulation for dystonia. J Neurol Neurosurg Psychiatry. 2013;84(9):1029–42.
170. Chang EF, et al. Long-term benefit sustained after bilateral pallidal deep brain stimulation in patients with refractory tardive dystonia. Stereotact Funct Neurosurg. 2010;88(5):304–10.

171. Sako W, et al. Bilateral deep brain stimulation of the globus pallidus internus in tardive dystonia. Mov Disord. 2008;23(13):1929–31.
172. Trottenberg T, et al. Treatment of severe tardive dystonia with pallidal deep brain stimulation. Neurology. 2005;64(2):344–6.
173. Gruber D, et al. Long-term effects of pallidal deep brain stimulation in tardive dystonia. Neurology. 2009;73(1):53–8.
174. Capelle HH, et al. Chronic deep brain stimulation in patients with tardive dystonia without a history of major psychosis. Mov Disord. 2010;25(10):1477–81.
175. Spindler MA, et al. Globus pallidus interna deep brain stimulation for tardive dyskinesia: case report and review of the literature. Parkinsonism Relat Disord. 2013;19(2):141–7.
176. Marks WA, et al. Dystonia due to cerebral palsy responds to deep brain stimulation of the globus pallidus internus. Mov Disord. 2011;26(9):1748–51.
177. Vidailhet M, et al. Bilateral pallidal deep brain stimulation for the treatment of patients with dystonia-choreoathetosis cerebral palsy: a prospective pilot study. Lancet Neurol. 2009;8(8):709–17.
178. Gimeno H, et al. Beyond the Burke-Fahn-Marsden dystonia rating scale: deep brain stimulation in childhood secondary dystonia. Eur J Paediatr Neurol. 2012;16(5):501–8.
179. Koy A, et al. Effects of deep brain stimulation in dyskinetic cerebral palsy: a meta-analysis. Mov Disord. 2013;28(5):647–54.
180. Kupsch A, et al. Early postoperative management of DBS in dystonia: programming, response to stimulation, adverse events, medication changes, evaluations, and troubleshooting. Mov Disord. 2011;26 Suppl 1:S37–53.
181. Picillo M, et al. Programming deep brain stimulation for tremor and dystonia: the Toronto Western hospital algorithms. Brain Stimul. 2016;9(3):438–52.
182. Isaias IU, et al. Managing dystonia patients treated with deep brain stimulation. In Marks Jr. WJ, editor. Deep brain stimulation management. Cambridge University Press; 2015. p. 108–17.
183. Beaulieu-Boire I, Fasano A. Current or voltage? Another Shakespearean dilemma. Eur J Neurol. 2015;22(6):887–8.
184. Bronstein JM, et al. The rationale driving the evolution of deep brain stimulation to constant-current devices. Neuromodulation. 2015;18(2):85–8; discussion 88–9.
185. Pinsker MO, et al. Deep brain stimulation of the internal globus pallidus in dystonia: target localisation under general anaesthesia. Acta Neurochir (Wien). 2009;151(7):751–8.
186. Cheung T, et al. Defining a therapeutic target for pallidal deep brain stimulation for dystonia. Ann Neurol. 2014;76(1):22–30.
187. Hamani C, et al. Location of active contacts in patients with primary dystonia treated with globus pallidus deep brain stimulation. Neurosurgery. 2008;62(3 Suppl 1):217–23; discussion 223–5.
188. Coubes P, et al. Electrical stimulation of the globus pallidus internus in patients with primary generalized dystonia: long-term results. Journal of neurosurgery. 2004;101(2):189–94.
189. Vercueil L, et al. Effects of pulse width variations in pallidal stimulation for primary generalized dystonia. J Neurol. 2007;254(11):1533–7.
190. Bereznai B, et al. Chronic high-frequency globus pallidus internus stimulation in different types of dystonia: a clinical, video, and MRI report of six patients presenting with segmental, cervical, and generalized dystonia. Mov Disord. 2002;17(1):138–44.
191. Liu LD, et al. Frequency-dependent effects of electrical stimulation in the globus pallidus of dystonia patients. J Neurophysiol. 2012;108(1):5–17.
192. Almeida L, et al. A pilot trial of square biphasic pulse deep brain stimulation for dystonia: the BIP dystonia study. Mov Disord. 2017;32(4):615–8.
193. Cagnan H, et al. Stimulating at the right time: phase-specific deep brain stimulation. Brain. 2017;140(1):132–45.
194. Bologna M, Berardelli A. Cerebellum: an explanation for dystonia? Cerebellum Ataxias. 2017;4:6.
195. Calderon DP, et al. The neural substrates of rapid-onset Dystonia-Parkinsonism. Nat Neurosci. 2011;14(3):357–65.
196. Chen CH, et al. Short latency cerebellar modulation of the basal ganglia. Nat Neurosci. 2014;17(12):1767–75.
197. Shakkottai VG, et al. Current opinions and areas of consensus on the role of the cerebellum in dystonia. Cerebellum. 2017;16(2):577–94.
198. Shaikh AG, et al. Cervical dystonia: a neural integrator disorder. Brain. 2016;139(Pt 10):2590–9.
199. Bertrand C, et al. Technical aspects of selective peripheral denervation for spasmodic torticollis. Appl Neurophysiol. 1982;45:326–30.
200. Bertrand C, et al. Selective peripheral denervation in 111 cases of spasmodic torticollis: rationale and results. Adv Neurol. 1988;50:637–43.
201. Anderson WS, et al. Selective denervation of the levator scapulae muscle: an amendment to the Bertrand procedure for the treatment of spasmodic torticollis. J Neurosurg. 2008;108(4):757.
202. Ford B, et al. Outcome of selective ramisectomy for botulinum toxin resistant torticollis. J Neurol Neurosurg Psychiatry. 1998;65(4):472–8.
203. Münchau A, et al. Prospective study of selective peripheral denervation for botulinum-toxin resistant patients with cervical dystonia. Brain. 2001;124(4):769–83.
204. Cohen-Gadol AA, et al. Selective peripheral denervation for the treatment of intractable spasmodic torticollis: experience with 168 patients at the Mayo Clinic. J Neurosurg. 2003;98(6):1247–54.
205. Bergenheim AT, et al. Selective peripheral denervation for cervical dystonia: long-term follow-up. J Neurol Neurosurg Psychiatry. 2015;86(12):1307–13.

206. Contarino MF, et al. Selective peripheral denervation: comparison with pallidal stimulation and literature review. J Neurol. 2014;261(2):300–8.
207. Meyer CH. Outcome of selective peripheral denervation for cervical dystonia. Stereotact Funct Neurosurg. 2001;77(1–4):44–7.
208. Braun V, Richter HP. Selective peripheral denervation for spasmodic torticollis: 13-year experience with 155 patients. J Neurosurg. 2002;97(2 Suppl):207–12.
209. Ravindran K, et al. Deep brain stimulation versus peripheral denervation for cervical dystonia: a systematic review and meta-analysis. World Neurosurg. 2018;122:e940–6.
210. Laitinen LV. Leksell's unpublished pallidotomies of 1958-1962. Stereotact Funct Neurosurg. 2000;74(1):1–10.
211. Steiner L, et al. Gammathalamotomy in intractable pain. Acta Neurochir (Wien). 1980;52(3–4):173–84.
212. Iacono RP, et al. Simultaneous bilateral pallidoansotomy for idiopathic dystonia musculorum deformans. Pediatric Neurology. 1996;14(2):145–8.
213. Lozano AM, et al. Globus pallidus internus pallidotomy for generalized dystonia. Movement Disorders. 1997;12(6):865–70.
214. Gross RE. What happened to posteroventral pallidotomy for Parkinson's disease and dystonia? Neurotherapeutics. 2008;5(2):281–93.
215. Teive HAG, et al. Bilateral pallidotomy for generalized dystonia. Arquivos de Neuro-Psiquiatria. 2001;59:353–7.
216. Ondo WG, et al. Pallidotomy for generalized dystonia. Movement Disorders. 1998;13(4):693–8.
217. Takeda N, et al. Radiofrequency lesioning through deep brain stimulation electrodes in patients with generalized dystonia. World Neurosurg. 2018;115:220–4.
218. Frighetto L, et al. Stereotactic radiosurgery for movement disorders. Surg Neurol Int. 2012;3(Suppl 1):S10–6.
219. Kondziolka D, Flickinger JC, Lunsford LD. Stereotactic radiosurgery for epilepsy and functional disorders. Neurosurg Clin N Am. 2013;24(4):623–32.
220. Niranjan A, et al. Stereotactic radiosurgery for essential tremor: retrospective analysis of a 19-year experience. Mov Disord. 2017;32(5):769–77.
221. Gross RE, Stern MA. Magnetic resonance-guided stereotactic laser pallidotomy for dystonia. Mov Disord. 2018;33:1502.
222. Elias WJ, et al. A randomized trial of focused ultrasound Thalamotomy for essential tremor. N Engl J Med. 2016;375(8):730–9.

Epilepsy: Invasive Monitoring

23

Jorge Gonzalez-Martinez

Introduction

As originally defined, the main goal of epilepsy surgery is the complete surgical treatment (including resections, disconnections, laser ablation, or neuromodulation) of the cortical and subcortical areas responsible for the initial epileptic activity generation and early spread of seizures. For some, this area is defined as the epileptogenic zone. At times, the epileptogenic zone (EZ) may overlap with functional cortical and subcortical areas. In order to define the anatomical location of the EZ and its proximity with possible cortical and subcortical eloquent areas, a range of noninvasive/less invasive tools are currently available: analysis of seizure semiology through video-scalp electroencephalographic recordings (ictal and interictal recordings), neuropsychological testing, magnetoencephalography (MEG), and MRI [1–3]. Particularly, neuroimaging techniques may provide functional (ictal single-photon emission computed tomography [SPECT] and fMRI) as well as metabolic (magnetic resonance spectroscopy [MRS] and positron emission tomography [PET]) information. These methods are usually complementary and may define cortical zones of interest as the symptomatogenic, irritative, ictal, and functional deficit zones, in addition to the EZ [4]. When (a) the noninvasive data is insufficient to precisely define the location of the hypothetical EZ, when (b) there is suspicion for early involvement of eloquent cortical and subcortical areas, or when (c) there is the possibility for multifocal seizures, invasive monitoring may be indicated [5, 6].

Localizing the Epileptogenic Zone

In most cases of focal medically intractable epilepsy, data generated from noninvasive EEG recordings and other electrophysiologic/neuroimaging techniques are sufficient to approximate the location of the EZ [7–14]. Prolonged video-scalp EEG monitoring, in conjunction with analysis of clinical semiology, remains the gold standard for diagnosis and localization of epileptogenic zone [2]. This noninvasive sampling technique gives an excellent overview of the location and extent of the epileptogenic areas but quite often only approximates the boundaries of both the irritative and EZ. Scalp EEG detects only epileptiform activity that results from EEG synchronization of large areas of the cortex, estimated in some studies to be between 6 and 8 cm^2, and recordings are disturbed by the smearing effect of bone and other high-resistance structures (e.g., meninges and scalp) between the cortical generators and the recording electrodes. MEG may overcome some of these problems, with

J. Gonzalez-Martinez (✉)
Department of Neurosurgery, University of Pittsburgh, Pittsburgh, PA, USA
e-mail: jalmartinez@sbcglobal.net

N. Pouratian, S. A. Sheth (eds.), *Stereotactic and Functional Neurosurgery*,
https://doi.org/10.1007/978-3-030-34906-6_23

better identification of the epileptic activity localized in a tangential orientation (as the interhemispheric fissure, opercular areas, etc.) but still providing limited information regarding the interictal epileptic activity [15, 16]. In specific pathological groups as malformation of cortical development (MCD), between 85% and 100% of patients with MCD exhibit epileptiform discharges on interictal scalp EEG recordings ranging from lobar to lateralized, nonlocalizing to diffuse (including generalized spike-wave patterns in some cases of subependymal heterotopia) [17]. The spatial distribution of interictal spikes is usually more extensive than the structural abnormality as assessed by intraoperative inspection or MRI visual analysis [17]. For these reasons, when subtle forms of cortical dysplasia are suspected as the pathological subtract of medically intractable epilepsy, mainly in patients with extra-temporal epilepsy and non-lesional imaging, extra-operative monitoring is indicated [18–24].

Localization of the Functional/ Eloquent Zone

Localization of functional areas in the brain and the anatomical boundaries of these areas with the EZ is an essential part in the process of developing an adequate and individualized surgical strategy [8, 20, 25–29]. In the particular example of patients with MCD associated with medically intractable epilepsy, because most of the pathological subtract are often localized in the frontal lobe (therefore in potentially eloquent cortex), an understanding of the functional status of the involved region(s) and its anatomical and pathological correlations are essential [1, 2, 30]. In the past, some group assessed the functional status (identified by direct cortical electrical stimulation) of focal MCD and its relationship with imaging and in situ electrocorticographic (ECoG) characteristics in patients who underwent focal neocortical resection for medically intractable epilepsy [31, 32]. Some focal MCD lesions characterized by significant FLAIR signal increase on MRI and located in anatomically functional areas (e.g., primary motor, Broca area) are not functional on direct electrical stimulation, and the same lesions showed no evidence of intrinsic epileptogenicity as assessed through mapping of the ictal onset zones. On the other hand, MCD lesions with mild or no FLAIR signal increase were functional and at times epileptogenic. These results agree with previous observations that eloquent function persisted in MCD devoid of balloon cells [33]. Similar ECoG patterns were reported in patients with low-grade glial tumors (e.g., dysembryoplastic neuroepithelial tumor and ganglioglioma), whereas dysplastic and epileptic cortical areas were found immediately surrounding these lesions. Functional cortex may therefore be displaced within the same hemisphere and have direct implications on the options for epilepsy surgery. Therefore, the precise anatomical location of eloquent cortex located in the vicinity or within the limits of the hypothetical EZ is essential information that will guide the surgeon in performing a safe and efficient surgical strategy, which has, as ultimate goal, a sustained seizure control status with no neurological deficits.

The Subdural Grid Method

Chronic intracranial recordings were initially reported in 1939 when Penfield and colleagues from the Montreal Neurological Institute used epidural single contact electrodes in a patient with an old left temporal-parietal fracture and whose pneumoencephalography disclosed diffuse cerebral atrophy. Subsequently, the use of subdural grid arrays became more popular after multiple publications during the 1980s demonstrated their safety and efficacy [34]. Before that time most invasive techniques involved epidural electrodes or intraoperative recordings.

The most common indications for intracranial electrodes include lateralization or localization of epilepsy and localization of functional/eloquent cortical information. Preoperative noninvasive studies and semiology often suggest focal epilepsy, but scalp electroencephalography is unable to adequately localize or lateralize the epileptogenic zone. Subdural grids have particular advantages in relation to other methods of invasive monitoring. Grids can be placed chroni-

cally, during relative long periods of time (1–2 weeks in average), long enough to record both spontaneous seizures and interictal activity during various stages of arousal. In addition, grids and strips, due to the close proximity and continuity of the electrical contacts, have applicability for mapping of cerebral function extra-operatively. These characteristics allow tailored cortical resections around areas of higher function while minimizing the risk of permanent neurological deterioration. Extra-operative mapping with the subdural method has the main advantage of allowing an optimal coverage of the subdural space adjacent cortex with adequate and continuous superficial functional mapping capabilities [5].

Intraoperative ECoG, as compared with chronically implanted subdural grids, is a limited option because it only provides information restricted to interictal activity. When applied in patients under general anesthesia, it is believed that anesthetic agents may influence EEG activity by altering the thresholds of afterdischarges and motor responses creating a misleading electroencephalographic picture. Additionally, intraoperative functional mapping often requires a cooperative patient that can tolerate being awake during surgery under local anesthesia. This is particularly difficult in the pediatric population.

Subdural grids have considerable disadvantages in relation to other methods of invasive monitoring, including surgical risks, financial costs, and limitations in the ability to access deep cortical regions. Because foreign bodies are inserted into the cranial vault, the risks of the procedure include wound infection, flap osteomyelitis, acute meningitis, cerebral edema, and hemorrhage. Concerns about increased intracranial pressure may reduce the maximal number of electrodes that can be inserted and therefore produce incomplete epileptic mapping from large cortical areas. Other limitations may include the anatomic location of the proposed area of sampling (e.g., mesial orbitofrontal, anterior cingulate gyrus) and "re-do" surgeries with cortical adhesions. Other limitations of subdural grid implantation are the number of available channels for recording with the EEG system in the hospital. Some systems can handle only 64 channels unlike other systems, which can record up to 200 channels, thus allowing the implantation of more electrodes over wider cortical areas. Despite this, only limited coverage of cortical regions can be sampled, and preoperative surgical planning is necessary to maximize the chances of covering the ictal onset zone with the electrodes. One of the main disadvantages of the subdural methodology is the challenge of exploring deep cortical areas, as the depths of sulci, opercular, interhemispheric, mesial temporal structures and insula [35–38]. Depth electrodes implanted using a non- or semi-stereotactic technique can partially compensate these deficiencies.

The Subdural Technique

Subdural electrodes (stainless steel or magnetic resonance-compatible platinum), embedded in strips or grids of polyurethane or other synthetic materials, are implanted over the suspected epileptogenic or functional dysplastic regions (Fig. 23.1). Variability in shape and size of the electrodes permits tailoring their use to the specific clinical situation. Custom-designed arrays of subdural electrodes have been configured for placement in specific anatomical locations. For example, to record from interhemispheric brain regions, rows of electrodes arranged in curvilinear fashion were designed to follow the curvature of the corpus callosum. Subdural grids are inserted through either open craniotomy incisions or burr holes and registered stereotactically for extra-operative mapping. The cortical covering may extend beyond the visualized cortical area, as grids may be slid over the edges of the craniotomy to cover adjacent areas for better ECoG or functional sampling. Besides the ECoG recordings and direct electrical stimulation studies, grids can be used to record somatosensory evoked potentials after stimulation of the trigeminal (lip) or median nerves for central sulcus localization.

All patients that are offered subdural grid electrode implantation for monitoring have previously undergone the standard preoperative evaluation. Decision for invasive monitoring is made during a multidisciplinary meeting, including neurologists, neurosurgeons, neuroradiologists, and neuropsychologists. Areas of coverage are determined based on preoperative noninvasive

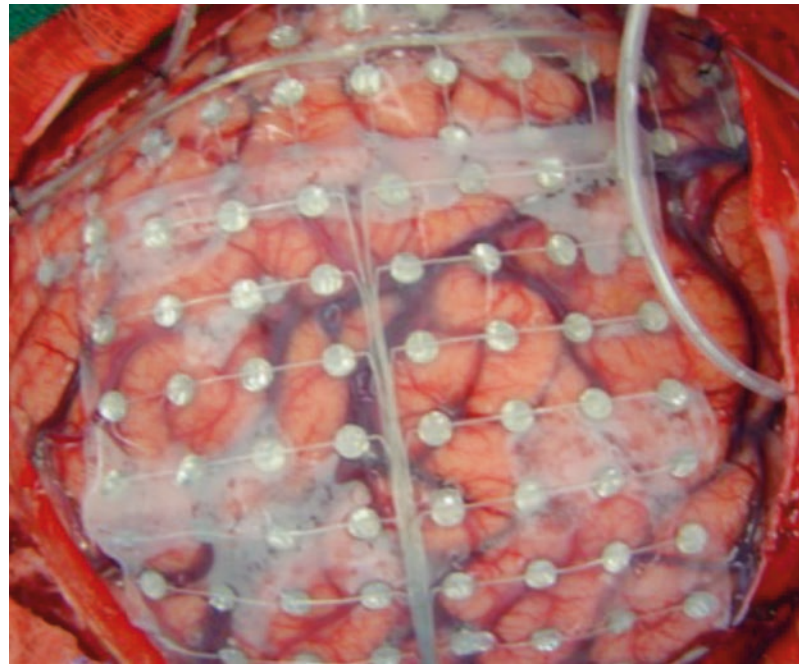

Fig. 23.1 Intraoperative aspect of subdural grid implantation in patient with extra-temporal epilepsy and non-lesional MRI. The picture shows a large right side temporal-parietal occipital craniotomy with placement of large 8X8 subdural grid at the dorsal-lateral convexity of the posterior quadrant region and multiple strips in the subtemporal, frontal, and mesial occipital areas

studies including scalp EEG, ictal SPECT, PET, MEG, and, at times, sphenoidal electrodes. Incision and craniotomy should allow for placement of electrodes in addition to the anticipated area of resection. Positioning of the patient should allow for stereotactic guidance in the event that depth electrodes are to be placed during the same operation. As part of our surgical protocol, perioperatively antibiotics, dexamethasone, and mannitol (0.25 g/kg) are given. The incision should be large enough to allow for a sizable craniotomy. Usually a T-shaped or large question mark incision is used. If basal temporal coverage is needed, the incision should extend down to the zygoma. Orbitofrontal coverage can be easily achieved as long as the incision allows for visualizing the key hole and turning a flap just above this level. Interhemispheric coverage necessitates an incision to midline. In order to facilitate placement of electrodes, the basal and mesial surfaces should be carefully inspected for cortical draining veins that will impede placement of electrodes. Using bayoneted forceps and under a constant stream of irrigation, the grid electrodes can be slid into place. Any resistance likely indicates blockage from a draining vein and the trajectory of the array should be adjusted.

Prior to covering lateral cortex, the depth electrodes are inserted using stereotactic guidance. The entry point should be in the middle of a gyrus, avoiding sulci, with a trajectory that is as perpendicular to the cortical surface as possible. The parenchyma serves to anchor the electrode in place. Using the wand to find the trajectory from the entry point, the pial surface is incised and the electrode inserted. Once the depth electrodes are in place, the grids for lateral coverage can be inserted. Again using bayoneted forceps, the larger grid electrodes are laid over the cortical surface, tucking the edges under the borders of the dural flap. Once in place, each electrode wire is secured to the nearest dural edge with a stitch. The remaining closure is performed using standard neurosurgical technique.

The Stereoelectroencephalography Method

The SEEG method was developed and popularized in France by Jean Talairach and Jean Bancaud during the 1950s and has been mostly used in France and Italy, as the method of choice for invasive mapping in refractory focal epilepsy [8, 26, 27].

The principle of SEEG is based on anatomo-electro-clinical correlations, which takes as the main principle the three-dimensional spatial-temporal organization of the epileptic discharge within the brain in correlation with seizure semiology, and the exploration of the epileptic organization with in situ depth recordings. The implantation strategy is individualized, with electrode placement based on a preimplantation hypothesis that takes into consideration the primary organization of the epileptiform activity and the hypothetical epileptic network involved in the propagation of seizures. For these reasons, the preimplantation hypothesis has a paramount importance in the strategic placement of the electrodes. If the preimplantation hypothesis is incorrect, the placement of the depth electrodes will be likely inadequate and the interpretation of the SEEG recordings misleading. According to several European and recent North-American reports, SEEG methodology enables precise recordings from deep cortical and subcortical structures, multiple noncontiguous lobes, as well as bilateral explorations while avoiding the need for large craniotomies [18–24].

The SEEG methodology was originally described as a multiphase and complex method, using the Talairach stereotactic frame and the double grid system in association with teleangiography. Despite its long reported successful record, with almost 60 years of clinical use, the technical complexity regarding the placement of SEEG depth electrodes may have contributed to the limited widespread application of the technique in centers outside Europe. Taking advantage of new radiological, computational, and robotic innovations, now commonly available in many surgical centers, more modern and less cumbersome methods of stereotactic implantation of SEEG depth electrodes can be applied in routine basis.

In addition to the general indications for invasive monitoring, specific indications can be considered to choose SEEG in detriment to other methods of invasive monitoring. These criteria included:

1. The possibility of a deep-seated or difficult to cover location of the EZ in areas such as the mesial structures of the temporal lobe, opercular areas, cingulate gyrus, interhemispheric regions, posterior orbitofrontal areas, and insula and depths of sulci.
2. A failure of a previous subdural invasive study to clearly outline the exact location of the seizure onset zone.
3. The need for extensive bi-hemispheric explorations.
4. Presurgical evaluation suggestive of a functional network involvement (e.g., limbic system) in the setting of normal MRI.
5. Need for better definition of the EZ in possible candidates for responsive nerve stimulation (RNS).

The SEEG methodology has the advantages of allowing extensive and precise deep brain recordings and stimulations with minimal associated morbidity. In reoperations, mainly in patients who underwent a previous subdural evaluation, possibilities are that the majority of these patients failed epilepsy surgery because of difficulties in accurately localizing the EZ. These patients pose a significant dilemma for further management, having relatively few options available. Further open subdural grid evaluations may carry the risks associated with encountering scar formations and still having limitations related to deep cortical structure recordings. A subsequent evaluation using the SEEG method may overcome these limitations, offering an additional opportunity for seizure localization and sustained seizure freedom. The main disadvantage of the SEEG method is the more restricted capability for performing functional mapping. Due to limited number of contacts located in the superficial cortex, a contiguous mapping of eloquent brain areas cannot be obtained as in the subdural method mapping. In order to overcome this relative disadvantage, the functional mapping information extracted from the SEEG method is frequently complemented with other methods of mapping, as DTI images or awake craniotomies.

Technique of SEEG Implantation: Frame-Based Implantation

The development of an SEEG implantation plan requires the clear formulation of a specific

anatomo-electro-functional hypothesis to be tested. This hypothesis is typically generated during the patient management conference and is based on the results of the various noninvasive evaluation tests. In this decision-making process, the respective significance of presurgical evaluation testing may vary greatly, depending on each patient. After an anatomical and functional localizing hypothesis is formulated, a tailored implantation strategy is planned, with the goal of confirming or rejecting the preimplantation hypothesis. In this phase, the exploration is focused to sample the anatomic lesion (if present), the more likely structure(s) of ictal onset, and the possible pathway(s) of propagation of the seizures (functional networks). The desired targets are reached using commercially available depth electrodes in various lengths and number of contacts, depending on the specific brain region to be explored. The electrodes are implanted using conventional stereotactic technique through small and precisely placed 2.5 mm diameter drill holes. Depth electrodes are inserted using orthogonal or oblique orientation, allowing intracranial recording from lateral, intermediate, or deep cortical and subcortical structures in a three-dimensional arrangement, thus accounting for the dynamic, multidirectional spatiotemporal organization of the epileptic pathways.

The day before surgery, a stereo contrasted volumetric T1 sequence MRI is performed. Images are then transferred to our stereotactic neuronavigation software where trajectories are calculated the following day. The day of surgery, while the patient is under general anesthesia, the stereotactic frame is applied using standard technique. Once the patient is attached to the angiography table with the frame, a stereo-dyna CT and a 3D digital subtracted angiogram (DSA) are performed. The preoperative MR images and the stereo-dyna CT and angiographic images are then digitally processed using dedicated fusion software (syngo XWP, Siemens Healthcare, Forchheim, Germany). These fused images are used during the implantation procedure to confirm the accuracy of the final position of each electrode and to insure the absence of vascular structures along the electrode pathway, which weren't previously noted with the contrasted MRI. Following the planning phase using the stereotactic software, trajectories' coordinates are recorded and transmitted to the operating room. Trajectories are in general planned in orthogonal orientation in relation to the skull's sagittal plane in order to facilitate implantation and later on interpretation of the electrode positions. Using the stereotactic system, coordinates for each trajectory are then adjusted in the stereotactic frame, and a fluoroscopic image, in lateral view, is performed in each new position. Care is taken to assure that the central beam of radiation during fluoroscopy is centered in the middle of the implantation probe in order to avoid parallax errors. If the trajectory is aligned correctly, corresponding to the planned trajectory and passing along an avascular space, the implantation is then continued, with skull perforation, dura opening, placement of the guiding bolt, and final insertion of the electrode under fluoroscopic guidance. If a vessel is recognized along the pathway during fluoroscopy, the guiding tube is manually moved a few millimeters until the next avascular space is recognized and implantation is then continued. The electrode insertion progress is observed under live fluoroscopic control in a frontal view to confirm the straight trajectory of each electrode. For additional guidance a coronal MRI slice corresponding to the level of each electrode implantation is overlaid to the fluoroscopic image. A postimplantation dyna-CT scan is performed while the patient is still anesthetized and positioned in the operating table. The reconstructed images are then fused with the MRI dataset using the previously described fusion software. The resulting merged datasets are displayed and reviewed in axial, sagittal, and coronal planes allowing the verification of the correct placement of the electrodes [18–24].

After surgery, patients are transferred to the epilepsy monitoring unit (EMU). The duration of admission at the epilepsy monitoring unit varies from patient to patient, depending on several factors including number, quality, and ictal and interictal patterns of recordings. The average length of stay of patients in the EMU who underwent SEEG implantation is 7 days (range from 3 to 28 days).

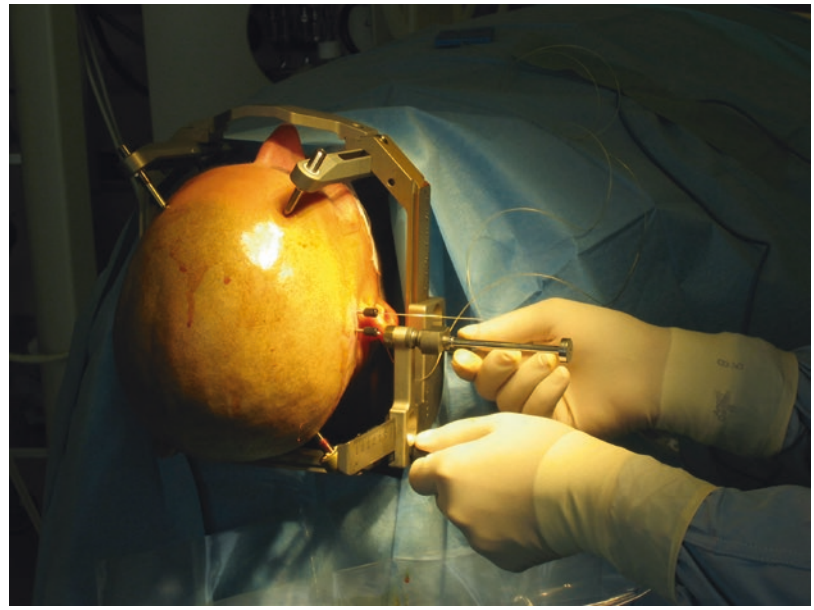

Fig. 23.2 Frame-based SEEG method. Picture showing the SEEG implantation technique using the Leksell frame and lateral implantation device. The figure depicts the adjustments of Y and Z coordinates in a Leksell stereotactic frame system

After obtaining the necessary information, electrodes are removed in the operating room, in a procedure performed under local anesthesia and sedation. Patients are discharged next morning, and resective surgery is scheduled 2–3 months following SEEG electrodes removal (Fig. 23.2).

Robotic-Based Implantation

The day prior to surgery, volumetric preoperative MRIs with contrast are obtained. DICOM format images are then digitally transferred to robotic system native planning software. Three-dimensional volumetric reconstructions are then created (axial, coronal, and sagittal), reformatted based on the topographic location of the AC-PC line. Individual trajectories are planned within the 3D imaging reconstruction according to predetermined target locations and intended trajectories. Trajectories are selected to maximize sampling from superficial and deep cortical and subcortical areas within the preselected zones of interest and are oriented orthogonally in the majority of cases to facilitate the anatomo-electrophysiological correlation during the extra-operative recording phase and to avoid possible trajectories shifts due to excessive angled entry points. Nevertheless, when multiple targets are potentially accessible via a single non-orthogonal trajectory, these multi-target trajectories are selected in order to minimize the number of implanted electrodes per patient.

All trajectories are evaluated for safety and target accuracy in their individual reconstructed planes (axial, sagittal, coronal) and also along the reconstructed "probe's eye view." Any trajectory that appeared to compromise vascular structures is adjusted appropriately without affecting the sampling from areas of interest. A set working distance of 150 mm from the drilling platform to the target is initially utilized for each trajectory, adjusted later to maximally reduce the working distance and, consequently, improve the implantation accuracy. The overall implantation schemas are analyzed using the 3D cranial reconstruction capabilities, and internal trajectories are checked to ensure that no trajectory collisions are present. External trajectory positions are examined for any entry sites that would be prohibitively close (less than 1.5 cm distance) at the skin level.

On the day of surgery, patients are placed under general anesthesia. For each patient, the head is placed into a three-point fixation head holder. The robot is then positioned such that the

working distance (distance between the base of the robotic arm and the midpoint of the cranium) is approximately 70 cm. The robot is locked into position, and the head holder device is secured to the robot. No additional position adjustments are made to the operating table during the implantation procedure. After positioning and securing the patient to the robot, image registrations are performed. Semiautomatic laser-based facial recognition is utilized to register the preoperative volumetric MRI with the patient. The laser is first calibrated using a set distance calibration tool. Preset anatomical facial landmarks are then manually selected with the laser. The areas defined by the manually entered anatomic landmarks subsequently undergo automatic registration using laser-based facial surface scanning. Accuracy of the registration process is then confirmed by correlating additional independently chosen surface landmarks with the registered MRI. After successful registration, the planned trajectories accessibilities are automatically verified by the robot software.

The patients are then prepped and draped in a standard sterile fashion. The robotic working arm is also draped with a sterile plastic cover. A drilling platform, with a 2.5 mm diameter working cannula, is secured to the robotic arm. The desired trajectories are selected on the touch screen interface. After trajectory confirmation, the arm movement is initiated through the use of a foot pedal. The robotic arm automatically locks the drilling platform into a stable position once reaching the calculated position for the selected trajectory. A 2 mm diameter handheld drill is introduced through the platform and used to create a pinhole. Dura is then opened with an insulated dural perforator using monopolar cautery at low settings. A guiding bolt (Ad-Tech, Racine, WI, USA) is screwed firmly into each pinhole. The distance from drilling platform to the retaining bolt is measured. This value is subtracted from the standardized 150 mm platform to target distance. The resulting difference is recorded for later use as the final length of the electrode to be implanted. This process is repeated for each trajectory. All pinholes and retaining bolts are placed prior to beginning electrode insertion. A small stylet (2 mm in diameter) is then set to the previously recorded electrode distance. The stylet is passed gently into the parenchyma, guided by the implantation bolt, followed immediately by the insertion of the pre-measured electrode (Fig. 23.3).

Fig. 23.3 Robotic-based SEEG method. Picture showing the SEEG implantation technique using a robotic assistant device

After implantation of all electrodes, the patient is removed from the fixation device. The head is positioned into a soft foam head holder on a radiolucent table. Fluoroscopy is then utilized in the AP plane to confirm the general accuracy of implanted electrode trajectories. A postimplantation volumetric CT of the brain without contrast, with 1 mm cuts, is obtained. Following SEEG implantation, patients are subjected to clinical monitoring and electrographic recording of all seizure events in the EMU. A second patient management conference is then held, approximately 1 week after implantation, to discuss the results and implications of the SEEG study and to collectively decide upon a plan for surgical resection. Subsequent to this meeting and approximately 6 weeks following removal of the SEEG electrodes, patients undergo a standard craniotomy for tailored resection of the hypothetical epileptogenic zone. Following recovery and discharge from hospital, all patients are followed up with regular visits (6 weeks, 6 months, and every year after resection) to document their seizure outcomes and possible late complications.

Conclusions

The goals of invasive monitoring in refractory focal epilepsy may include (1) the need for better anatomical delineation of the hypothetical epileptogenic zone and (2) the need for the definition of cortical and subcortical functional brain areas. Extra-operative mapping with the subdural method (which here includes subdural grids and strips) has the advantage of allowing an optimal coverage of the subdural space adjacent cortex with adequate and continuous superficial functional mapping capabilities. In addition, from a surgical perspective, subdural implantations are open procedures, with better management of possible intracranial hemorrhagic complications. The disadvantages of the subdural method are related to the incapacity of recording and stimulating from deep cortical and subcortical areas, as the insula, posterior orbitofrontal, cingulate gyrus, depths of sulci, etc. In these scenarios, the SEEG methodology may be considered as a more efficient and safer option. SEEG has the advantages of allowing extensive and precise deep brain recordings and stimulations with minimal associated morbidity.

References

1. Luders H. Epileptic syndromes may be misleading. Epilepsia. 2014;55(10):1677–8.
2. Luders H, Amina S, Bailey C, Baumgartner C, Benbadis S, Bermeo A, et al. Proposal: different types of alteration and loss of consciousness in epilepsy. Epilepsia. 2014;55(8):1140–4.
3. Rosenow F, Klein KM, Strzelczyk A, Hamer HM, Menzler K, Bauer S, et al. New aspects in the field of epilepsy. Nervenarzt. 2014;85(8):955–64.
4. Luders HO, Amina S, Baumgartner C, Benbadis S, Bermeo-Ovalle A, Devereaux M, et al. Modern technology calls for a modern approach to classification of epileptic seizures and the epilepsies. Epilepsia. 2012;53(3):405–11.
5. Jayakar P, Jayakar A, Libenson M, Arzimanoglou A, Rhydenhag B, Cross JH, et al. Epilepsy surgery near or in eloquent cortex in children-practice patterns and recommendations for minimizing and reporting deficits. Epilepsia. 2018;59:1484.
6. Hartlieb T, Winkler P, Coras R, Pieper T, Holthausen H, Blumcke I, et al. Age-related MR characteristics in mild malformation of cortical development with oligodendroglial hyperplasia and epilepsy (MOGHE). Epilepsy Behav. 2018;91:68–74.
7. Cardinale F, Cossu M. SEEG has the lowest rate of complications. J Neurosurg. 2015;122(2):475–7.
8. Cardinale F, Cossu M, Castana L, Casaceli G, Schiariti MP, Miserocchi A, et al. Stereoelectroencephalography: surgical methodology, safety, and stereotactic application accuracy in 500 procedures. Neurosurgery. 2013;72(3):353–66; discussion 66.
9. Cardinale F, Pero G, Quilici L, Piano M, Colombo P, Moscato A, et al. Cerebral angiography for multimodal surgical planning in epilepsy surgery: description of a new three-dimensional technique and literature review. World Neurosurg. 2015;84(2):358–67.
10. Caruana F, Gozzo F, Pelliccia V, Cossu M, Avanzini P. Smile and laughter elicited by electrical stimulation of the frontal operculum. Neuropsychologia. 2016;89:364–70.
11. Cossu M, Cardinale F, Casaceli G, Castana L, Consales A, D'Orio P, et al. Stereo-EEG-guided radiofrequency thermocoagulations. Epilepsia. 2017;58(Suppl 1):66–72.
12. Cossu M, Fuschillo D, Cardinale F, Castana L, Francione S, Nobili L, et al. Stereo-EEG-guided radio-frequency thermocoagulations of epileptogenic

grey-matter nodular heterotopy. J Neurol Neurosurg Psychiatry. 2014;85(6):611–7.
13. Cossu M, Fuschillo D, Casaceli G, Pelliccia V, Castana L, Mai R, et al. Stereoelectroencephalography-guided radiofrequency thermocoagulation in the epileptogenic zone: a retrospective study on 89 cases. J Neurosurg. 2015;123(6):1358–67.
14. Cossu M, Mirandola L, Tassi L. RF-ablation in periventricular heterotopia-related epilepsy. Epilepsy Res. 2018;142:121–5.
15. Kakisaka Y, Alkawadri R, Wang ZI, Enatsu R, Mosher JC, Dubarry AS, et al. Sensitivity of scalp 10-20 EEG and magnetoencephalography. Epileptic Disord. 2013;15(1):27–31.
16. Kakisaka Y, Kubota Y, Wang ZI, Piao Z, Mosher JC, Gonzalez-Martinez J, et al. Use of simultaneous depth and MEG recording may provide complementary information regarding the epileptogenic region. Epileptic Disord. 2012;14(3):298–303.
17. Marnet D, Devaux B, Chassoux F, Landre E, Mann M, Turak B, et al. Surgical resection of focal cortical dysplasias in the central region. Neurochirurgie. 2008;54(3):399–408.
18. Gonzalez-Martinez J, Bulacio J, Alexopoulos A, Jehi L, Bingaman W, Najm I. Stereoelectroencephalography in the "difficult to localize" refractory focal epilepsy: early experience from a North American epilepsy center. Epilepsia. 2013;54(2):323–30.
19. Gonzalez-Martinez J, Bulacio J, Thompson S, Gale J, Smithason S, Najm I, et al. Technique, results, and complications related to robot-assisted stereoelectroencephalography. Neurosurgery. 2016;78(2):169–80.
20. Gonzalez-Martinez J, Lachhwani D. Stereoelectroencephalography in children with cortical dysplasia: technique and results. Childs Nerv Syst. 2014;30(11):1853–7.
21. Gonzalez-Martinez J, Mullin J, Bulacio J, Gupta A, Enatsu R, Najm I, et al. Stereoelectroencephalography in children and adolescents with difficult-to-localize refractory focal epilepsy. Neurosurgery. 2014;75(3):258–68; discussion 67–8.
22. Gonzalez-Martinez J, Mullin J, Vadera S, Bulacio J, Hughes G, Jones S, et al. Stereotactic placement of depth electrodes in medically intractable epilepsy. J Neurosurg. 2014;120(3):639–44.
23. Gonzalez-Martinez J, Najm IM. Indications and selection criteria for invasive monitoring in children with cortical dysplasia. Childs Nerv Syst. 2014;30(11):1823–9.
24. Gonzalez-Martinez JA. The stereoelectroencephalography: the epileptogenic zone. J Clin Neurophysiol. 2016;33(6):522–9.
25. Cardinale F, Casaceli G, Raneri F, Miller J, Lo Russo G. Implantation of Stereoelectroencephalography electrodes: a systematic review. J Clin Neurophysiol. 2016;33(6):490–502.
26. Chauvel P, Rheims S, McGonigal A, Kahane P. French guidelines on stereoelectroencephalography (SEEG): editorial comment. Neurophysiol Clin. 2018;48(1):1–3.
27. Isnard J, Taussig D, Bartolomei F, Bourdillon P, Catenoix H, Chassoux F, et al. French guidelines on stereoelectroencephalography (SEEG). Neurophysiol Clin. 2018;48(1):5–13.
28. Karamanou M, Tsoucalas G, Themistocleous M, Giakoumettis D, Stranjalis G, Androutsos G. Epilepsy and neurosurgery: historical highlights. Curr Pharm Des. 2017;23(42):6373–5.
29. Reif PS, Strzelczyk A, Rosenow F. The history of invasive EEG evaluation in epilepsy patients. Seizure. 2016;41:191–5.
30. Luders H, Amina S, Eccher M, Devereaux M, Lhatoo S. Commentary: should consciousness be used to describe seizures and what terms should be applied: Epilepsia's survey results. Epilepsia. 2015;56(3):344.
31. Najm IM. Mapping brain networks in patients with focal epilepsy. Lancet Neurol. 2018;17(4):295–7.
32. Najm IM, Sarnat HB, Blumcke I. Review: the international consensus classification of focal cortical dysplasia – a critical update 2018. Neuropathol Appl Neurobiol. 2018;44(1):18–31.
33. Ying Z, Wang I, Blumcke I, Bulacio J, Alexopoulos A, Jehi L, et al. A comprehensive clinico-pathological and genetic evaluation of bottom-of-sulcus focal cortical dysplasia in patients with difficult-to-localize focal epilepsy. Epileptic Disord. 2019;21(1):65–77.
34. Wyllie E, Gupta A, Lachhwani DK. The treatment of epilepsy: principles & practice. 4th ed. Philadelphia: Lippincott Williams & Wilkins; 2006. xxi, 1247 pages p
35. Vadera S, Burgess R, Gonzalez-Martinez J. Concomitant use of stereoelectroencephalography (SEEG) and magnetoencephalographic (MEG) in the surgical treatment of refractory focal epilepsy. Clin Neurol Neurosurg. 2014;122:9–11.
36. Vadera S, Chan AY, Mnatsankanyan L, Sazgar M, Sen-Gupta I, Lin J, et al. Strategic hospital partnerships: improved access to care and increased epilepsy surgical volume. Neurosurg Focus. 2018;44(5):E9.
37. Vadera S, Marathe AR, Gonzalez-Martinez J, Taylor DM. Stereoelectroencephalography for continuous two-dimensional cursor control in a brain-machine interface. Neurosurg Focus. 2013;34(6):E3.
38. Vadera S, Mullin J, Bulacio J, Najm I, Bingaman W, Gonzalez-Martinez J. Stereoelectroencephalography following subdural grid placement for difficult to localize epilepsy. Neurosurgery. 2013;72(5):723–9. discussion 9

Epilepsy: Mesial Temporal

24

Patrick J. Karas, Sameer A. Sheth, and Daniel Yoshor

Abbreviations

AChA	Anterior choroidal artery
AED	Antiepileptic drug
ANT	Anterior nucleus of the thalamus
ATL	Anterior temporal lobectomy
C	Caudate
CSF	Cerebrospinal fluid
DBS	Deep brain stimulation
EEG	Electroencephalogram
EMU	Epilepsy monitoring unit
FDG	Fludeoxyglucose
HMPAO	Hexamethylpropyleneamine oxime
IC	Internal capsule
ITG	Inferior temporal gyrus
LITT	Laser interstitial thermal therapy
MEG	Magnetoencephalography
MTLE	Mesial temporal lobe epilepsy
MTG	Middle temporal gyrus
OT	Optic tract
P	Putamen
PCA	Posterior cerebral artery
PET	Positron emission tomography
PHG	Parahippocampal gyrus
RNS	Responsive neurostimulation
SAHC	Selective amygdalohippocampectomy
sEEG	Stereoelectroencephalography
SLAH	Stereotactic laser amygdalohippocampotomy
SOZ	Seizure onset zone
SPECT	Single-photon emission computerized tomography
SRS	Stereotactic radiosurgery
STG	Superior temporal gyrus
SUB	Subiculum
Tc-99m	Technetium-99m
THLV	Temporal horn of the lateral ventricle
VNS	Vagus nerve stimulation

P. J. Karas · S. A. Sheth · D. Yoshor (✉)
Department of Neurosurgery, Baylor College of Medicine, Houston, TX, USA
e-mail: dyoshor@bcm.edu

Introduction

Mesial temporal lobe epilepsy (MTLE) is a common, well-defined focal epilepsy syndrome. The surgical evaluation and treatment of patients with MTLE is also the most extensively studied among focal epilepsy syndromes. Epilepsy affects roughly 1% of the population, and more than 30% of patients with epilepsy have drug-resistant (used interchangeably with medically refractory) epilepsy [1–3]. The International League Against Epilepsy (ILAE) defines drug-resistant epilepsy as failure of adequate trials of two tolerated and appropriately chosen and used antiepileptic drug schedules (whether as monotherapies or in combination) to achieve sustained seizure freedom [4]. Of patients with drug-resistant epilepsy, roughly 25% are candidates for surgical intervention.

N. Pouratian, S. A. Sheth (eds.), *Stereotactic and Functional Neurosurgery*,
https://doi.org/10.1007/978-3-030-34906-6_24

Epilepsy surgery has a long history, with the earliest report from Dudley in the early nineteenth century [5, 6]. However the superiority of surgical resection over continued medical management in properly selected patients with drug-resistant MTLE was only rigorously confirmed in 2001 when Wiebe and colleagues showed 64% freedom from disabling seizures after anterior temporal lobectomy (ATL) compared to only 8% rate with continued medical management [7]. Since that time, epilepsy surgery has become significantly more accepted, leading to advances in patient selection, surgical technique, and technological innovation. Despite these advances, the surgical treatment of epilepsy remains underutilized [8]. Surgical treatment of epilepsy is also more cost-effective compared to continued medial management. While surgery requires a large upfront cost, recurring costs from seizures poorly controlled with medical management build up over time and outrun the cost of surgery within 5–10 years [9–11]. Not only is the cost of epilepsy surgery less than the combined costs of a lifetime of disability from seizures, but many patients continue to suffer from disabling seizures that could be cured or greatly reduced with surgery. Epilepsy surgery requires an interdisciplinary team of neurologists, neurosurgeons, radiologists, and neuropsychologists. This chapter outlines perspectives from many of these parties, reviewing the pathophysiology of MTLE, patient presentation, presurgical evaluation, and evolution of the modern surgical options used to treat MTLE. We also present strategies for preventing harm and achieving maximal efficacy with surgery for patients undergoing MTLE surgery.

The Mesial Temporal Lobe and Mesial Temporal Lobe Epilepsy (MTLE)

Mesial temporal sclerosis (MTS), classically referred to as Ammon's horn sclerosis, is the most common pathology underlying mesial temporal lobe epilepsy, accounting for 50–60% of MTLE cases. Low-grade tumors contribute an additional 20–30% of MTLE cases, and other etiologies including vascular malformations, neuronal loss, or other patterns of gliosis account for the remaining 10–20% [12, 13]. The most common tumors leading to mesial temporal lobe epilepsy include ganglioglioma (40%), dysembryoplastic neuroepithelial tumor (DNET) (20%), and diffuse low-grade glioma (20%). Less common tumors include pilocytic astrocytoma and pleomorphic xanthoastrocytoma [14].

Radiographically, hippocampal sclerosis is exhibited by increased T2 fluid-attenuated inversion recovery (FLAIR) signal in the hippocampus, loss of hippocampal architecture, and sclerosis of the hippocampus (Fig. 24.1). Atrophy of the ipsilateral fornix can also be frequently seen. Histology shows neuronal cell loss with chronic astrogliosis. Gliosis is accompanied by a loss of pyramidal neurons and granule cell dispersion.

The mechanism by which hippocampal sclerosis leads to epilepsy is poorly understood. Hippocampal sclerosis is an acquired lesion, often associated with prolonged febrile seizures in childhood. After significant sclerosis, the hippocampus and surrounding mesial temporal structures can become independent seizure foci capable of generating epileptiform discharges that can spread, manifesting as mesial temporal epilepsy.

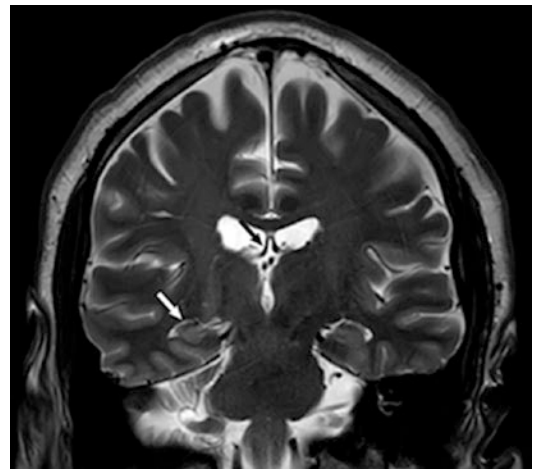

Fig. 24.1 Right mesial temporal sclerosis. T2-weighted coronal image through the bilateral hippocampi illustrates classic findings of mesial temporal sclerosis. Note the sclerotic right hippocampus with loss of internal architecture (*white arrow*). The right hippocampus also appears slightly hyperintense compared to the left, better visualized on T2-FLAIR (not shown). The ipsilateral fornix (*black arrow*) is also small compared to the contralateral fornix

The anatomy of the mesial temporal lobe is complex, and complete understanding of the three-dimensional relationship of mesial temporal structures requires close anatomical study. Mesial temporal structures include the hippocampus, amygdala, subiculum, and entorhinal cortex. The mesial temporal lobe is highly connected to the frontal, temporal, and parietal lobes through Papez's circuit. Working knowledge of the relationships between these structures and their surroundings (Fig. 24.2) is essential to performing mesial temporal surgeries safely. Excellent reviews of mesial temporal anatomy are available [15–17].

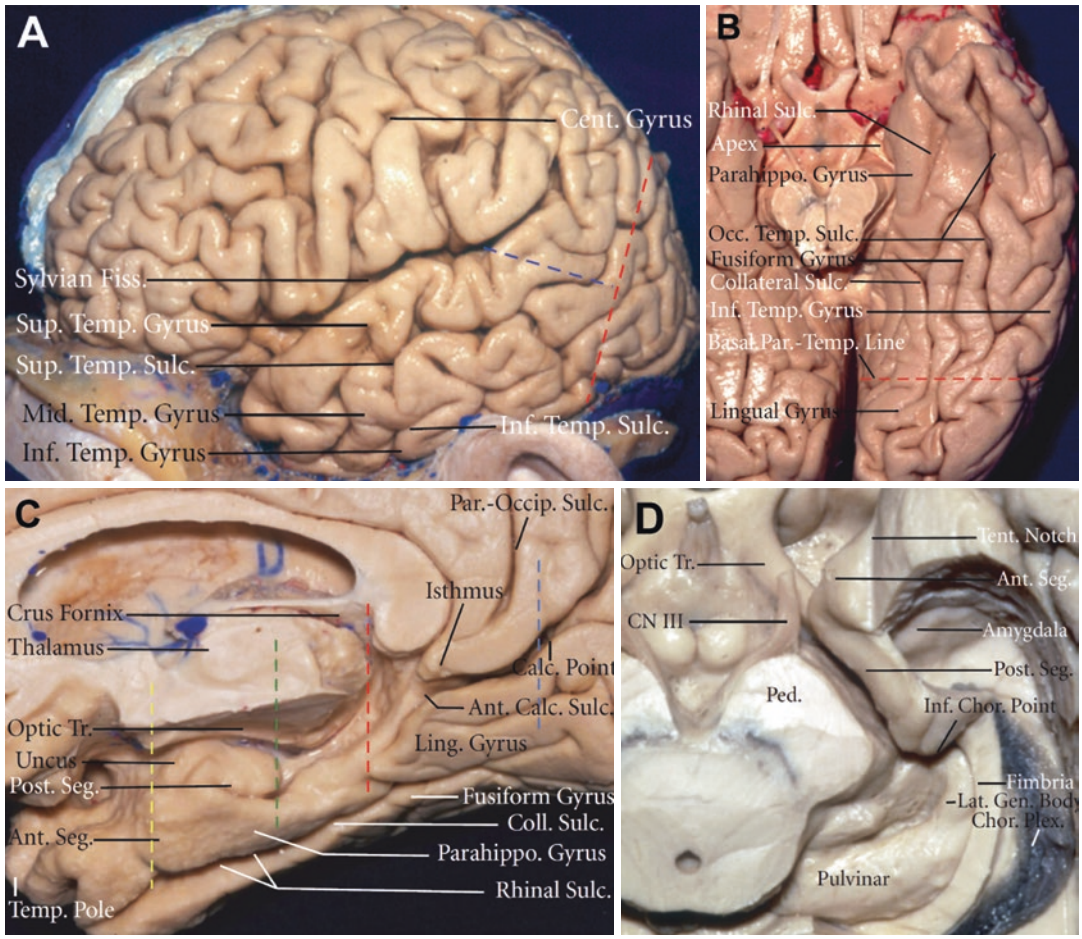

Fig. 24.2 Temporal lobe gross anatomy. Important lateral neocortical landmarks include the superior temporal gyrus, middle temporal gyrus, and inferior temporal gyrus. The Sylvian fissure divides the frontal lobe from the temporal lobe, and the lateral temporal gyri are separated by the superior temporal sulcus and inferior temporal sulcus (**a**). Inferiorly, the fusiform gyrus is medial to the inferior temporal gyrus, separated by the lateral occipital temporal sulcus. The collateral sulcus divides the medial aspect of the fusiform gyrus from the parahippocampal gyrus (**b**). The optic tract, along with other important structures not shown (anterior choroidal artery, posterior cerebral artery, cranial nerve III), runs in the ambient and crural cisterns just medial to the parahippocampus and the uncus (**c**). With the parahippocampal gyrus removed, the proximity of the mesial hippocampal structures (fimbria, hippocampus, amygdala, uncus) to thalamic structures (lateral geniculate nucleus and pulvinar) as well as the cerebral peduncle can be appreciated (**d**). Ant., anterior; Calc., calcarine; Cent., central; Chor., choroidal; Coll., collateral; Fiss., fissure; Gen., geniculate; Inf., inferior; Lat., lateral; Ling., lingual; Occ., occipital; Occip., occipital; Parahippo., parahippocampal; Par., parietal; Ped., peduncle; Post., posterior; Seg., segment; Sulc., sulcus; Sup., superior; Termp., temporal; Tr., tract. (From Kucukyuruk B, et al. [17]. https://creativecommons.org/licenses/by/3.0/)

Semiology of Mesial Temporal Lobe Epilepsy

The semiology of mesial temporal lobe epilepsy is both classic and variable. Isolated seizures of the hippocampus can be clinically silent, often manifesting only as behavioral arrest. Additional symptoms occur with propagation of epileptiform discharges to closely connected structures. Careful attention to the semiology, particularly the temporal progression of the semiology, can help to determine the precise location of the seizure onset zone (SOZ) as well as the path by which the epileptiform activity spreads.

Mesial temporal seizures can be divided into several subtypes based on the SOZ and network of structures involved. These subtypes include mesial (amygdala, hippocampus, parahippocampal gyrus, entorhinal cortex), temporopolar, mesiolateral, lateral, and temporal "plus" subtypes [18]. Isolated mesial temporal seizures often first manifest only as behavioral arrest. Additional signs of amygdala or hippocampal seizures include epigastric discomfort, caused by spread from the amygdala to the posterior insula. Other symptoms include auras of fear, déjà vu or déjà rêvé, and oral or gestural automatisms from early spread to the frontal operculum. Oral automatisms are characterized by lip smacking or chewing. Gestural automatisms include picking, fumbling, and fidgeting with the hands. Contralateral head version often occurs prior to seizure generalization and is also highly suggestive of mesial temporal onset. Patients with seizure onsets within any of the mesial structures often fall into this semiology subtype.

Seizures with temporopolar SOZ have very similar semiology to those of mesial temporal onset but tend to have faster onset of both clinical symptoms and loss of awareness (i.e., impaired consciousness) [19]. The faster loss of awareness likely stems from earlier involvement of the superior temporal gyrus (STG), as the temporal pole is a continuation of the superior temporal gyrus bending inferiorly approaching the lesser wing of the sphenoid. Temporopolar seizures quickly involve the STG, an area of association cortex with robust white matter tract connectivity to a broad array of brain networks, leading to loss of awareness. In contrast, mesial temporal seizures spread first to the temporal pole prior to interacting with the superior temporal gyrus en route to other structures, leading to slower appearance of seizure semiology compared to temporopolar onset seizures.

Mesiolateral temporal onset seizures, like temporopolar onset seizures, also manifest in early loss of awareness. Early vocalizations as well as oral and verbal automatisms are also characteristic. The semiology of these seizures overlaps with the mesial subtype: mesiolateral seizures can start from near simultaneous epileptiform activity from independent mesial and lateral neocortical structures [20, 21].

Lateral temporal onset seizures typically manifest with an auditory aura followed by frequent secondary generalized tonic clonic activity. They are typically of short duration. A lateral temporal SOZ can be secondary to a lesion in the lateral temporal neocortex but can also occur in MRI-negative temporal lobe epilepsy [20, 21]. However there are also rare cases of pure lateral temporal neocortex onset epilepsy with radiographic mesial temporal sclerosis where the only suggestion of neocortical onset is seizure semiology [22]. This highlights the importance of semiology in determination of the SOZ, as performing a selective mesial temporal resection would fail to achieve seizure freedom in such a patient.

Temporal "plus" epilepsy manifests with gustatory, auditory, or vestibular auras, ipsilateral tonic motor signs, contraversion, and postictal dysphoria. This semiology arises from combinations of involvement between the insula, frontal and temporal operculum, orbitofrontal cortex, and temporo-parieto-occipital junction. This complex semiology can arise from fast spread of temporal lobe seizures or from seizure onset zones in the involved epileptic networks [23]. It is imperative that whenever a non-mesial temporal semiology is encountered, the anatomic region responsible for that behavior be investigated in addition to the mesial and neocortical temporal structures prior to consideration for surgery.

Diagnosis and Preoperative Workup

The goals of the presurgical workup are to confirm the diagnosis of epilepsy, identify an epileptogenic lesion if present, determine the size and location of the SOZ, and finally determine the feasibility and safety of resection. Many tools are used to perform this evaluation, and the results from one study can often inform multiple of the above goals. The results from each test must be critically examined for congruous and incongruous findings prior to planning resective surgery.

Confirmation of Epilepsy Diagnosis

Video EEG in an epilepsy monitoring unit remains the gold standard for the diagnosis of epilepsy. Subjective reports from epilepsy monitoring units at busy surgical epilepsy centers suggest that 20–30% of patients referred for surgical epilepsy evaluation have psychogenic nonepileptic seizures (previously referred to as pseudoseizures) and do not in fact have epilepsy [24]. Confirmation of the epilepsy diagnosis by means of video EEG monitoring in an experienced EMU is essential prior to further surgical evaluation. Ictal onset of MTLE is characterized by a diverse set of patterns on scalp EEG, most commonly with cessation of interictal discharges, followed by ipsilateral temporal rhythmic delta-theta activity [25].

Identification of Epileptogenic Lesion

A high-resolution MRI is essential for determining the presence or absence of an intracranial lesion as a source of seizures. This MRI should be reviewed by neurologists, neuroradiologists, and neurosurgeons experienced at diagnosing epileptogenic foci. Diagnoses such as small temporal encephaloceles, cortical dysplasias, or periventricular nodular heterotopias are easy to miss if not explicitly considered. Surgical outcomes are better when an epileptogenic focus is identified, and surgery will fail to achieve seizure freedom if an epileptogenic focus is missed and left in place after surgical resection. Studies using 7T MRI scanners have shown that even in cases of MRI-negative epilepsy (by 3T MRI), there can be epileptogenic lesions visible on 7T MRI thought to be primary epileptogenic foci [26]. The importance of careful scrutiny of MRI scans is emphasized by the fact that after identifying such 3T MRI-negative lesions on 7T MRI, a significant percentage of these lesions can be seen on 3T MRI in retrospect. Preoperative MRI should include T1-weighted, T2-weigted, and susceptibility-weighted images. Some centers routinely obtain CT scans to screen for small bony defects suggestive of encephalocele. The most common etiology of MTLE is mesial temporal sclerosis (Fig. 24.3a).

Determination of Seizure Onset Zone (SOZ)

Determination of the SOZ is essential to achieving seizure freedom; surgical cessation of seizures requires complete removal or disconnection of the entire SOZ. Several tests can help determinate the location and size of the SOZ. An initial hypothesis should be generated based on scalp EEG recordings; however confirmation is necessary due to the poor spatial resolution of scalp EEG.

Fluorodeoxyglucose F 18 (^{18}F-FDG) PET is commonly used for localization. ^{18}F-FDG is a radioactive glucose analog. Like glucose, ^{18}F-FDG is taken up readily by metabolically active cells at a rate proportional to cellular metabolic activity. Also like glucose, after cellular uptake ^{18}F-FDG is phosphorylated and trapped in the cell. ^{18}F-FDG lacks the 2-hydroxyl group present in normal glucose and cannot be further metabolized until after radioactive decay, leading to accumulation of ^{18}F-FDG in proportion to metabolic activity in cells. The PET scan displays the distribution of ^{18}F-FDG throughout the brain. Eventually ^{18}F decays to ^{18}O converting ^{18}F-FDG to glucose-6-phosphate which can then be metabolized just as ordinary glucose. PET scans are typically performed during interictal periods to facilitate easy scheduling. During

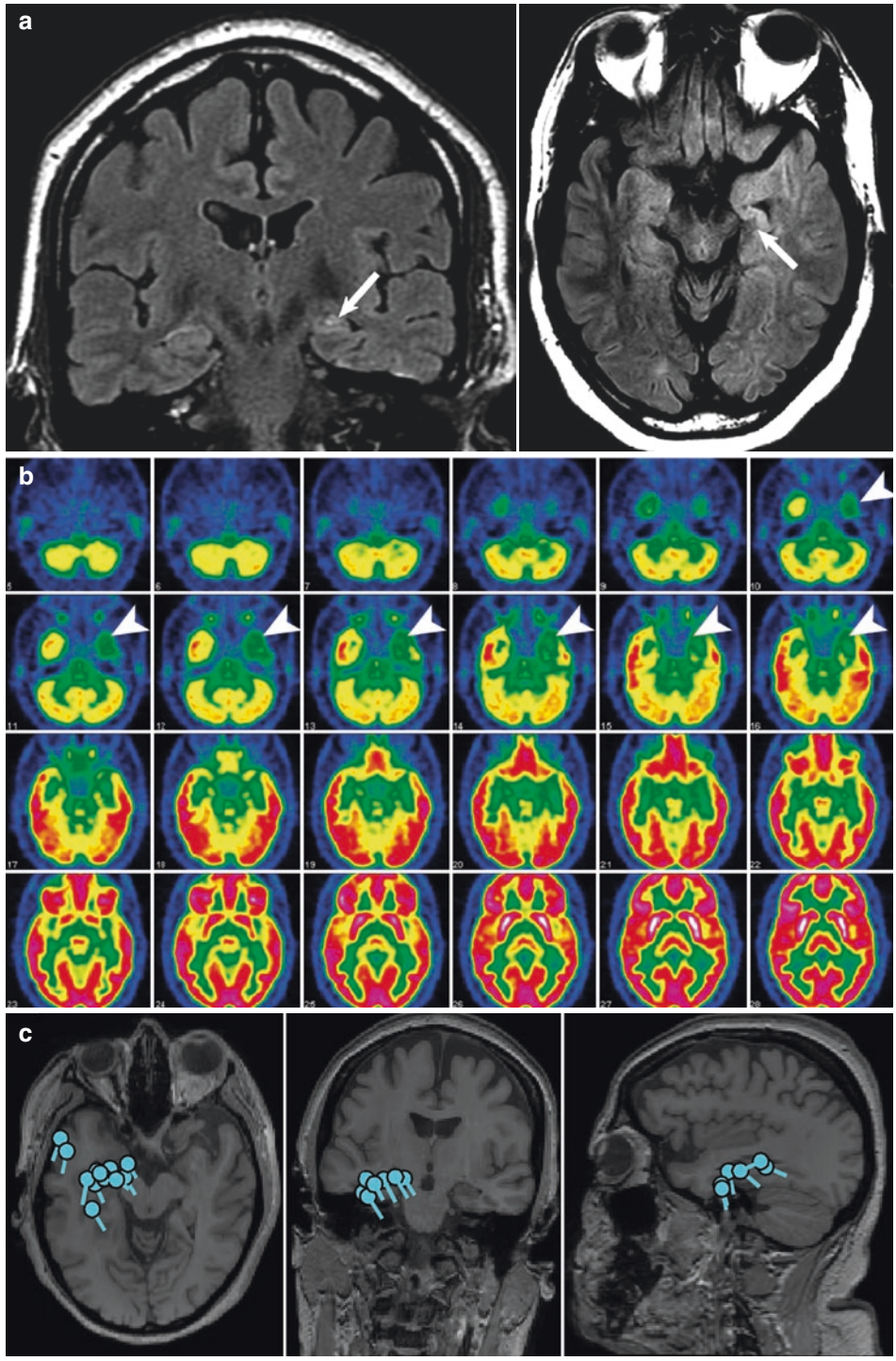

Fig. 24.3 Identification of the seizure onset zone. Coronal (left) and axial (right) cuts through a T2-FLAIR MRI scan show classic left mesial temporal sclerosis (*white arrow)* (**a**). Interictal ^{18}F-FDG PET scan shows hypometabolism in the left temporal pole and mesial temporal region (white arrowheads), corresponding to the region of mesial temporal sclerosis (**b**). Axial, coronal, and sagittal images showing MEG findings suggestive of a left mesial temporal spike cluster. Note the convention for MEG is to display the patient's left on the left side of the screen, the opposite of standard radiographic convention (**c**). (Images courtesy of Dr. Audrey Nath)

ictal periods seizing brain has increased metabolism and increased local cerebral perfusion. In contrast, during interictal periods the seizure onset zone exhibits abnormal hypometabolism. These areas of hypometabolism are readily identifiable by ^{18}F-FDG PET. ^{18}F-FDG PET findings in MTLE often include hypometabolism of the hippocampus and surrounding anterior temporal structures (Fig. 24.3b). Importantly, while an area of hypometabolism often includes the SOZ, this is not always the case. The SOZ may only be a small part of a hypometabolic region seen on ^{18}F-FDG PET.

Ictal SPECT is another nuclear medicine study measuring changes in local cerebral blood flow related to seizures. Ictal SPECT must be performed in a monitored setting with video EEG for confirmation of seizure onset. A tracer, often technetium-99m (Tc-99m) labelled hexamethylpropyleneamine oxime (HMPAO), is injected at the time of seizure onset. In contrast to ^{18}F-FDG PET, the tracer in SPECT distributes according to blood flow, not metabolism. Since blood flow is closely coupled to brain metabolism (flow-metabolism coupling), the tracer distribution closely approximates metabolic activity. Since actively seizing areas of the brain have increased metabolic demand, generally leading to increased local cerebral blood flow, the tracer rapidly distributes in higher quantities to actively seizing locations in the brain where it remains for several hours after the seizure. The ictal SPECT reading is compared to an interictal SPECT in the same patient to determine what areas of the brain have increased local cerebral perfusion during seizures [27], suggestive of the SOZ. Ictal SPECT is most useful in partial epilepsy, and the efficacy decreases with secondarily generalized tonic-clonic activity. Ictal SPECT findings in MTLE generally show increased cerebral blood flow on the side of MTLE in mesial and often lateral anterior temporal structures.

Magnetoencephalography (MEG) localizes the SOZ by measuring changes in the local magnetic field of the brain. In normal brain tissue, populations of axons are roughly aligned in the cerebral mantle. Synchronized firing of populations of neurons changes the current flow leading to the alterations in the magnetic field detected by MEG. Both EEG and MEG are measuring the same neurophysiologic process. Importantly, since magnetic fields are produced tangentially to the direction of current, MEG is best at measuring electrical activity in sulci which produce alterations in the magnetic fields outside the scalp. Magnetic field alterations from electrical activity in gyri often escape detection from the magnetometers arranged around the head since these field alterations occur within the head. EEG, by contrast, detects electrical signal from populations of neurons in both gyri and sulci. The electric fields measured by EEG are heavily distorted by bone and scalp making exact localization of electrical activity difficult. Magnetic fields are not as distorted by these structures, allowing MEG to localize electrical activity with much greater precision than EEG. For this reason, MEG is used for anatomic localization of epileptic populations of neurons, providing additional evidence for the location of the SOZ (Fig. 24.3c). MEG machines are costly and are not widely available. Many busy and successful epilepsy centers do not use MEG in their presurgical epilepsy evaluation.

Neuropsychological Evaluation

A comprehensive neuropsychological evaluation is an essential part of the presurgical evaluation. Specific neuropsychological deficits can suggest involvement of anatomic structures in the epilepsy network. Furthermore, results from neuropsychological testing can also be used to predict the morbidity of different surgical approaches. Neuropsychological deficits from MTLE fall into three predominant categories: memory impairments, executive function impairments, and language impairments [28].

Working memory, including short-term memory, is commonly impaired in patients with MTLE. Severity of working memory impairment is higher with dominant (usually left) temporal lobe epilepsy, earlier age of onset, increased seizure burden, and hippocampal sclerosis [29]. Working memory deficits can further be divided into verbal memory impairment (strongly associated with dominant side MTLE [30, 31]) and spa-

tial memory impairment (more associated with nondominant side MTLE [32]). Deficits in long-term autobiographical memory are also possible, even in cases with intact working memory [33–35]. Such deficits arise from an inability to consolidate episodic memory (context-dependent) despite normal abilities to store semantic knowledge and single items (context-free memory) [36]. Verbal memory function is classically localized to the dominant hippocampus, with spatial memory more associated with the nondominant hippocampus.

Deficits specific to executive function are less well defined. Difficulty forming new associations and registering information [37–40], decreased feedback-based decision-making [41], and poor mental flexibility under high cognitive loads [42] have all been demonstrated in the MTLE population. The mechanism for executive function impairment remains poorly understood but may stem from the high connectivity between mesial temporal and prefrontal structures, frequently involving prefrontal regions in MTLE seizure networks.

Word finding and naming deficits are the most common language impairments in MTLE, present in up to 40% of cases. These deficits are most often present when seizures arise from the language-dominant (usually left) lobe [43, 44]. These language impairments have a significant detrimental impact on daily life [45]. Importantly, auditory naming (by oral definition) is more affected than visual (by picture card) naming [43, 46]; deficits in auditory naming are predictive of seizure focus laterality in 85% of patients [47]. Verbal and auditory naming is classically localized to the dominant lateral temporal neocortex [48, 49]. However, the exact locations are variable and include networks across the anterior temporal, middle temporal, inferior temporal, and posterior superior temporal neocortex [50, 51].

Given the memory and language function of the dominant temporal lobe, determination of language and memory dominance can have a large impact on operative planning and predicting postoperative neuropsychological outcomes. Removing dominant mesial temporal structures often leads to worsening neuropsychological deficits. The intracarotid amobarbital (Wada) test has classically been used to determine language dominance. Over the last decade, language dominance testing with the Wada has slowly been replaced with fMRI, sparing patients periprocedural risk and discomfort associated with catheterization. fMRI has been shown to be a reliable alternative to Wada with similar prediction accuracy for postoperative naming and verbal memory decline after ATL [52].

The most reliable predictors of verbal memory decline after resective surgery for MTLE are dominant lobe temporal epilepsy (dominant side resection), excellent preoperative verbal memory IQ (>120), MRI-negative epilepsy, and late age onset of epilepsy. These risk factors are important in both patient counseling and determination of what surgery to perform.

After confirming the diagnosis of MTLE with video EEG, an interdisciplinary team of neurosurgeons, neurologists, neuroradiologists, and neuropsychologists carefully review and discuss the temporal progression of the seizure semiology; the anatomic findings on MRI, the location of the SOZ as determined by interictal PET, ictal SPECT, and/or MEG; and the neuropsychological testing. The team generates a hypothesis of the seizure focus and seizure network, probing all tests for concordant and discordant data. The multidisciplinary team then makes a decision about invasive monitoring and/or surgical treatment.

Invasive Electroencephalography Monitoring

Invasive monitoring techniques are covered in detail in Chap. 23. A few points specific to MTLE are discussed here. If there is strong concordance between seizure semiology, preoperative MRI with MTS, seizure onset zone studies, and neuropsychological testing, some centers advocate advancing directly to surgical resection without invasive monitoring [53]. If a lesion other than MTS is present on MRI and thought to be the seizure focus, invasive monitoring is also not

required but may be helpful in aiding resection of the entire seizure onset zone to achieve the best seizure freedom outcome. If any of the previously discussed preoperative evaluation is discordant or suggestive of more than one seizure focus, we recommend proceeding with invasive electroencephalography monitoring. Epilepsy monitoring with video and invasive electroencephalography is commonly referred to as phase 2 monitoring.

Effective invasive recordings can be performed with either subdural grids and strips or stereoelectroencephalography (sEEG). The precise location of the implants should be guided by a hypothesis of the seizure onset zone and epileptic networks based on careful consideration of semiology and other aforementioned preoperative test results. For subdural grids and strips, the lateral temporal neocortex is often covered by a grid, while subdural strips can be wrapped around the anterior temporal pole and slid inferiorly to record from fusiform and parahippocampal gyri. Care must be taken when inserting subtemporal strips, as large draining veins from the temporal lobe may traverse this space on their way to the transverse sinus. sEEG electrode trajectories should be planned to sample all suspected anatomic structures under consideration as epileptogenic foci, as well as from the suspected epilepsy network. Particular care must be taken to avoid superficial subdural vascular structures when planning sEEG trajectories to prevent intracranial hemorrhage during electrode placement.

Resective Surgeries for Mesial Temporal Epilepsy

Surgery for the treatment of medically refractory MTLE has evolved significantly over the last two decades. Resective surgery with anterior temporal lobectomy (ATL) remains the gold standard for medically refractory MTLE. Selective amygdalohippocampectomy (SAHC) is an approach that leaves the lateral temporal neocortex in place while removing all mesial temporal structures. Lateral temporal neocortex is preserved with the goal of decreasing postoperative cognitive deficits, particularly naming and language problems.

Anterior Temporal Lobectomy (ATL) Procedure

Anterior temporal lobectomy (ATL) has been the mainstay of treatment for MTLE for half a century. Over time, the amount of lateral neocortex commonly resected has decreased, which has not correlated to loss of efficacy in seizure control when radiographic and electrocorticographic testing colocalizes to the mesial temporal structures. When lateral temporal neocortex is implicated in seizure onset, resection of the mesial temporal structures is also indicated for effective seizure control [54, 55]. There is a wide degree of variation from surgeon to surgeon in how an anterior temporal lobectomy is performed, leading some to conclude that there is no "standard" anterior temporal lobectomy. Here we describe our practice.

Prior to surgery, patients are continued on their current antiepileptic medication regimen. Some surgeons prefer to discontinue valproic acid and its derivatives (e.g., divalproex) 5–7 days prior to surgery due to decreased platelet function, though influence on intraoperative blood loss is debated [56]. Preoperative antibiotics and 10 mg IV dexamethasone are administered just prior to incision. Dexamethasone is tapered over 1 to 2 weeks after surgery. The surgery is usually performed under general anesthesia, as the amount of lateral temporal neocortical resection is small leading to low risk of postoperative language dysfunction. If significant lateral temporal neocortical resection is required for a dominant temporal lobe lesion, surgery can be performed awake to allow for intraoperative language mapping. Speech mapping can also be performed in the epilepsy monitoring unit (EMU) via stimulation with a subcortical grid during phase 2 monitoring allowing for safe dominant lateral temporal neocortical resection under general anesthesia.

In general, our mesial temporal resection which we describe below includes the anterior 3 cm of both the parahippocampal gyrus and hippocampus, the inferior amygdala, and the uncus. The surgery can be divided into four steps: (1) craniotomy, (2) anterolateral neocortical resection, (3) microsurgical resection of mesial

temporal structures (amygdala, hippocampus, and parahippocampal gyrus), and (4) closure.

The patient is positioned on the operating room table supine with a shoulder roll. The head of bed is elevated to bring the head above the level of the heart. The head is placed in a three-point skull pin fixation device, extended slightly, and turned away from the side of surgery. The bed is also rotated to bring the frontotemporal area horizontal to the floor. Cranial navigation can be used but is not necessary, as anatomic landmarks are routinely used to guide the surgery.

A reverse question mark incision is used beginning immediately behind the hairline and extending posteriorly to just superior to the superior temporal line. The incision is taken down just anterior to the ear to the root of the zygoma (Fig. 24.4a), and a myocutaneous flap is elevated and maintained by fish-hook retractors. A modified pterional craniotomy is performed with inferior border at the floor of the middle fossa defined by the root of the zygoma, anterior border at the frontal process of the zygomatic bone, posterior border at approximately the posterior border of the pinna, and superior border at the superior temporal line (Fig. 24.4b). The sphenoid wing should be cut flush with the edge of the craniotomy but does not need to be drilled down further as would be done for exposure of the circle of Willis. The dura is opened in a horseshoe flap and reflected against the temporalis muscle. This exposure should reveal the inferior frontal gyrus, the Sylvian fissure, and the anterior 5–6 cm of superior (STG), middle (MTG), and inferior temporal gyri (ITG) (Fig. 24.5a).

After initial exposure, then next step is lateral temporal neocortical resection. This portion of

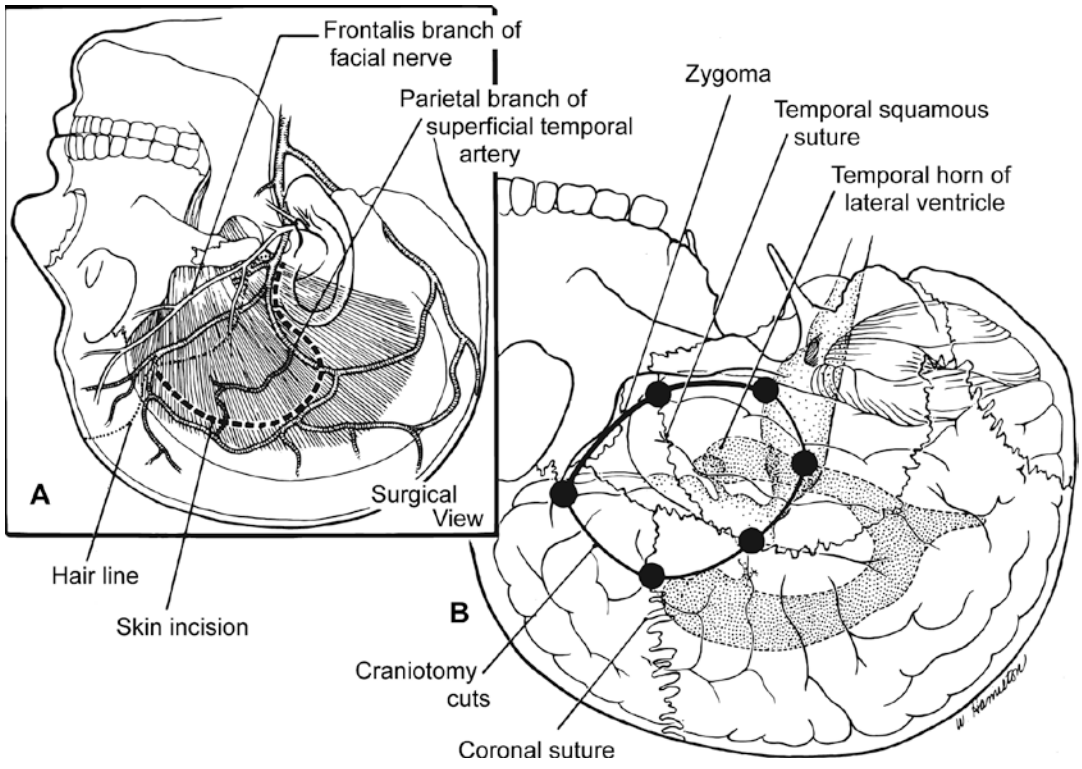

Fig. 24.4 Skin incision and craniotomy for anterior temporal lobectomy. A small reverse question mark incision beginning behind the hairline is used to elevate a myocutaneous flap (**a**). A modified pterional craniotomy is then performed, with special attention to the anterior and inferior cuts to ensure access to the temporal pole, the inferior temporal gyrus, and the floor of the middle fossa (**b**). (Artist: Winifred Hamilton, PhD, Baylor College of Medicine, Houston, TX. From Yoshor D, et al. [57] with permission from Elsevier)

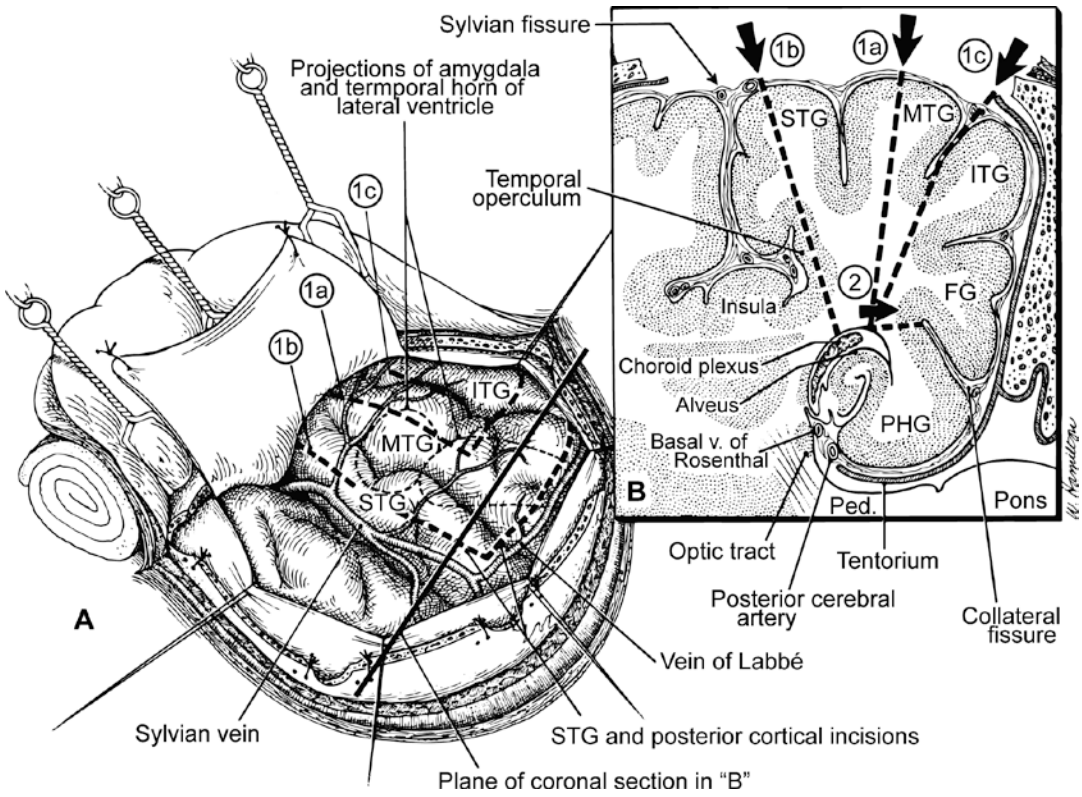

Fig. 24.5 Neocortical incisions for anterior temporal lobectomy and selective amygdalohippocampectomy. Conservative neocortical resection can be achieved by beginning the incision in the middle temporal gyrus parallel to the superior temporal sulcus (incision 1a). The cortical incision is directed slightly posteriorly and inferiorly until the temporal horn of the lateral ventricle is encountered. Alternatively, an incision can be made in the superior temporal gyrus (incision 1b) if language functional cortex is not present. The incision is carried back posteriorly for up to 5 or 6 cm, though the exact amount of neocortical removal is determined on a case-by-case basis. The vein of Labbe represents a firm posterior resection boundary and should always be preserved. Selective amygdalohippocampectomy preserves lateral neocortical structures and is most often performed through a middle or inferior temporal gyrus transcortical corridor (not shown) or via a trans-sulcal approach through the inferior temporal sulcus (incision 1c) (**a**). After entrance into the temporal horn of the lateral ventricle, the collateral eminence is identified just inferior and lateral to the hippocampus, and an incision is carried down from this landmark to the collateral sulcus (incision 2). This step completes the lateral neocortical resection (**b**). FG, fusiform gyrus; ITG, inferior temporal gyrus; MTG, middle temporal gyrus; PHG, parahippocampal gyrus; Ped., peduncle; STG, superior temporal gyrus; v., vein. (Artist: Winifred Hamilton, PhD, Baylor College of Medicine, Houston, TX. From Yoshor D, et al. [57] with permission from Elsevier)

surgery is typically performed under loupe magnification. Preservation of veins, namely, the large Sylvian veins and the vein of Labbe, is of utmost importance to prevent the development of venous infarct. The vein of Labbe runs 4–6 cm posterior to the temporal tip and demarks a posterior limit to resection. Resection is also limited posteriorly by the petrous ridge, but ideally should be only as large as needed to remove epileptogenic temporal neocortex and provide access to the hippocampus in the floor of the temporal horn of the lateral ventricle. To prevent postoperative language deficit, damage to the anterior superior temporal gyrus in the dominant hemisphere must be avoided. Additionally, branches of the middle cerebral artery that perfuse posterior temporal cortex can arise in the anterior Sylvian fissure and pass over the anterior 4 cm of STG and MTG. Damage to these vessels can also lead to language deficits and should be avoided.

The initial entry incision is made parallel to the superior temporal sulcus either in the MTG (Fig. 24.5a, incision 1a) or STG (Fig. 24.5b, incision 1b). The posterior border of the lateral neocortical resection is commonly 3–4 cm for dominant hemisphere and 4–5 cm for nondominant hemisphere resections, though this can be tailored based on the involvement of lateral neocortical structures in the SOZ as determined by the presurgical workup. If an MTG incision is used, dissection is directed orthogonally directly to the temporal horn of the lateral ventricle (Fig. 24.5b, incision 1a). For a STG incision, dissection must be directed slightly inferiorly toward the middle fossa floor to hit the temporal horn and avoid dissecting through the Sylvian fissure into the insula (Fig. 24.5b, incision 1b). Gray matter of the temporal operculum and cerebrospinal fluid (CSF) may be encountered at a depth of 1–2 cm as dissection is carried past the medial aspect of the Sylvian fissure en route to the temporal horn of the lateral ventricle. 2 to 5 cm posterior from the temporal tip, the superficial MTG or STG incision is redirected at a right angle, cutting across the MTG and ITG down to the middle fossa floor creating the posterior border of the lateral neocortical resection. This incision is dissected down, directed in a slightly posterior angle, until entrance into the temporal horn of the lateral ventricle at an average depth of 3–3.5 cm. Measuring this depth on preoperative MRI and using it as a reference during surgery is often helpful.

If difficulty is encountered in locating the temporal horn, frameless stereotaxy can be of use. Alternatively, a careful dissection guided by anatomy is at least as effective as computer-assisted navigation and is not limited by brain shift; the collateral fissure/sulcus can be located medial to the fusiform gyrus and then followed superiorly through the collateral eminence and into the temporal horn just lateral to the hippocampus.

After entering into the temporal horn, the initial STG or MTG incision parallel to the superior temporal sulcus can be carried anteriorly to the temporal tip, taking care to preserve any Sylvian veins draining into the sphenoparietal sinus. The collateral eminence, often seen as a bulge on the floor of the temporal horn running parallel and just lateral to the hippocampus, can then be incised and dissected down to the collateral fissure (Fig. 24.5b, incision 2). Subpial dissection down the collateral fissure on the side of the fusiform gyrus, carried from posterior to anterior, will end at the floor of the middle fossa completing the disconnection and allowing removal of the lateral temporal neocortex.

The microscope is then brought into position for resection of the mesial temporal structures. Traditionally retractors have been used to hold open the anterior portion of the temporal horn. However dynamic retraction with suction and bipolar can be utilized to prevent unnecessary tissue trauma. If retractors are used, it is imperative that the retractor placed on the remaining STG or Sylvian fissure (Fig. 24.6b, retractor R1) does not push too hard or too deep to cause injury to the underlying internal capsule, optic tract, or globus pallidus.

First, we make an incision from the tip of the choroid fissure through the amygdala aiming toward the medial aspect of the greater wing of the sphenoid (Fig. 24.6b, incision 3). This incision is based on an imaginary line connecting the anterior choroidal point to the first segment of the middle cerebral artery (M1), defining the superior border of the amygdala resection. The anterior choroidal point (also referred to as inferior choroidal point or simply choroidal point) is defined as the anterior border of the choroid plexus, where the anterior choroidal artery enters the temporal horn of the lateral ventricle. An alternative landmark to M1 is the limen insulae, defined by the anterior border of the insula, at the lateral limit of the anterior perforating substance where the anterior and posterior stems of the lateral sulcus join. Venturing superior to this line endangers the basal ganglia and can lead to traveling up the temporal stem (see Fig. 24.5b, location of the basal ganglia up the temporal stem).

The amygdala can then be removed with subpial suction aspiration, taking care to preserve the pia overlaying the sphenoid and tentorium. It is imperative that this pial plane is preserved, as it serves as a protective border covering the tento-

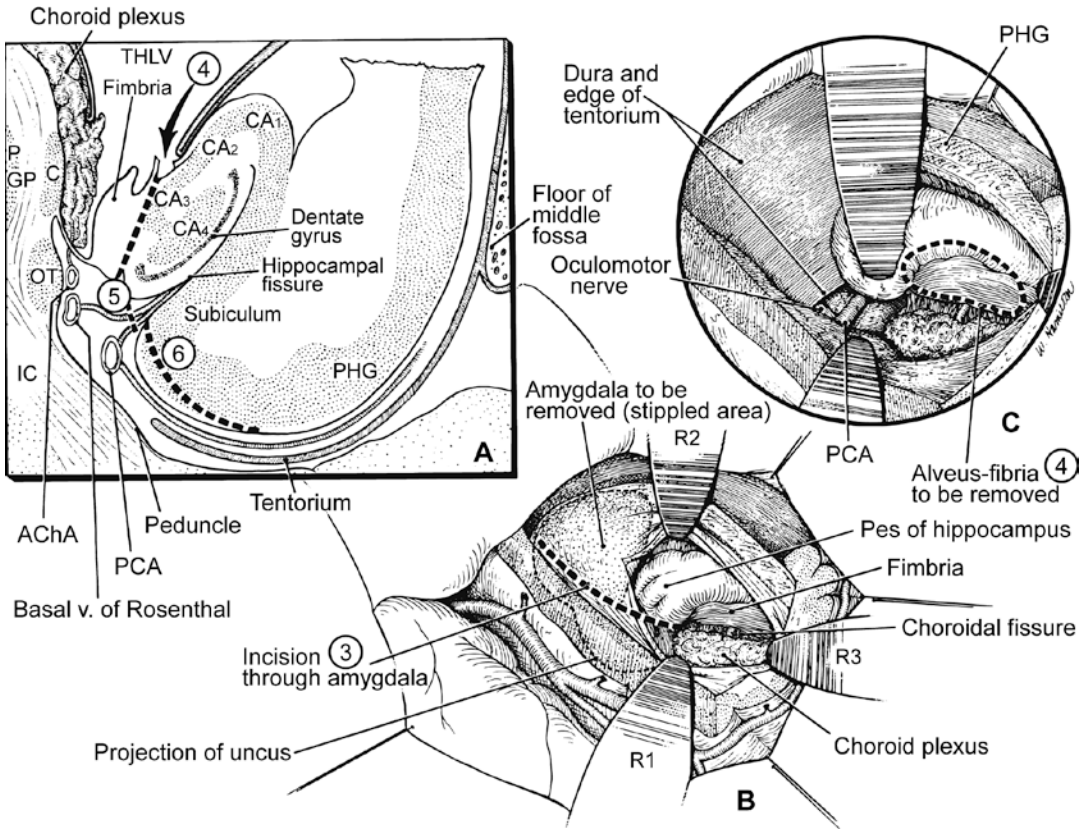

Fig. 24.6 Removal of mesial temporal structures. After removal of lateral neocortical structures, the anterior choroidal point is identified, and the choroid plexus is elevated superiorly and medially. An incision is carried from the anterior choroidal point anteriorly through the amygdala in the direction of M1 (incision 3, panel **b**). Removal of amygdala superior to this plane endangers the basal ganglia. The inferolateral portion of the amygdala can then be removed (**b**). The fimbria and alveus are then disconnected and removed from the hippocampus (incision 4, panels **a** and **c**). Care is taken to preserve mesial pia in order to prevent entry into the ambient and crural cisterns in which travel delicate arterial and venous structures supplying the brainstem. The pia of the hippocampal fissure is identified, and hippocampal feeding arteries are divided freeing the hippocampus from its medial attachments (incision 5, panel **a**). Beginning at the floor of the middle fossa, subpial dissection of the parahippocampal gyrus is performed until the parahippocampal gyrus is freed from its inferior attachments at the inferior side of the hippocampal fissure (incision 6, panel **a**). AChA, anterior choroidal artery; C, tail of the caudate; GP, globus pallidus; IC, internal capsule; OT, optic tract; PCA, posterior cerebral artery; PHG, parahippocampal gyrus; P, putamen; THLV, temporal horn of the lateral ventricle; v., vein. (Artist: Winifred Hamilton, PhD, Baylor College of Medicine, Houston, TX. From Yoshor D, et al. [57] with permission from Elsevier)

rial incisura, beyond which lies the posterior cerebral artery (PCA), basal vein of Rosenthal, anterior choroidal artery (AChA), third and fourth cranial nerves, cerebral peduncle, optic tract, and brainstem. Removal of the amygdala reveals the pia medial to the parahippocampal cortex (Fig. 24.6a, c). The parahippocampal gyrus is then dissected medially in subpial fashion until the subiculum is reached (Fig. 24.6a, incision 6).

More posteriorly, the choroid is gently lifted medially to reveal the underlying choroidal fissure. Just lateral to the choroidal fissure, the fimbria and alveus are removed from the body of the hippocampus with gentle suction aspiration (Fig. 24.6a, c, incision 4) to reveal the edge of the hippocampal fissure (Figs. 24.6a and 24.7a). The hippocampal fissure is comprised of the union of a pia-arachnoid plane, on one side extending down from the choroidal fissure and on the other

side extending up from the medial parahippocampal gyrus. The pia-arachnoid plane extending from the choroidal fissure into the hippocampal fissure often contains a 2–3 mm vein traveling to the hippocampus which must be coagulated and cut (Figs. 24.6a and 24.7a, incision 5), revealing the subiculum underneath. Importantly, posterior to this vein, arterial branches of the AChA anteriorly and PCA posteriorly run through the pia-arachnoid plane of the hippocampal fissure to supply the hippocampus. En passage vessels can also pass through the hippocampal fissure before returning to supply the posterior internal capsule. Arteries must be carefully inspected and en passage vessels preserved to prevent infarction of the posterior capsule and postoperative hemiplegia. Additionally, the course of the PCA may be variable. Occasionally the PCA can be found strongly attached to the subiculum. The PCA must therefore be identified anteriorly as it runs past the tentorial incisura. Its course can be tracked posteriorly prior to incising the subiculum (Fig. 24.7a, b).

The subpial dissection connecting the parahippocampal gyrus to the subiculum can then be continued medially to join the hippocampal fissure (Fig. 24.6a, incision 6). Proceeding in this manner allows for approaching the vessels in the hippocampal fissure from both superomedial and inferolateral angles in order to identify en passage vessels. Alternatively, the pia of the subiculum can be incised from superomedially (Fig. 24.7b, incision 6), which can then be carried subpially to connect with the subpial dissec-

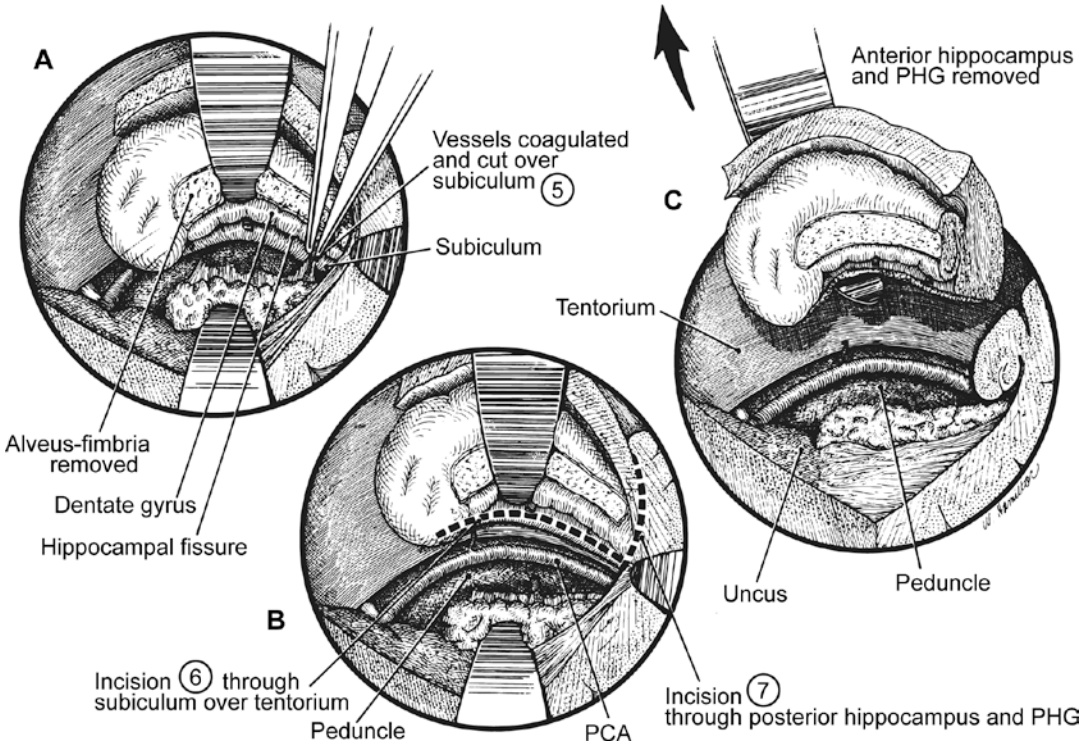

Fig. 24.7 Removal of the hippocampus. Arteries and veins traveling to the hippocampus within the hippocampal fissure are cut to detach the hippocampus (incision 5, panel **a**). Care is taken to preserve en passage vessels within the hippocampal fissure, as branches of the anterior choroidal artery and posterior cerebral artery may traverse the fissure en route to eloquent structures. After devascularization of the hippocampus, careful subpial dissection is used to free the subiculum and parahippocampal cortex from its mesial pia (incision 6, panel **b**). Finally, an incision is made roughly 3 cm posterior from the pes hippocampus through the tail of the hippocampus and the parahippocampal gyrus (incision 7, panel **b**). This allows for en bloc removal of the hippocampus and hippocampal gyrus (**c**). PCA, posterior cerebral artery; PHG, parahippocampal gyrus. (Artist: Winifred Hamilton, PhD, Baylor College of Medicine, Houston, TX. From Yoshor D, et al. [57] with permission from Elsevier)

tion of the medial parahippocampal cortex. An incision through the posterior hippocampus and parahippocampal gyrus is then made roughly 3 cm posterior to the head (pes) of the hippocampus (Fig. 24.7b, incision 7), usually corresponding to 1 cm posterior to the location of the vein traveling into the hippocampal fissure that was previously coagulated and cut. This maneuver frees the hippocampus and parahippocampal gyrus for en bloc removal (Fig. 24.7c). The remainder of the uncus can then be removed with subpial dissection and gentle suction, taking care to preserve small perforating arteries entering the brainstem from the underlying PCA, posterior communicating artery, and AChA. The pial plane covering the crural and ambient cisterns should not be bipolared. Remaining hippocampus can also be removed at this time with gentle suction, following the tail until it curves up and away from the operative field. The hippocampus should be removed posteriorly until at least the coronal plane in line with the lateral mesencephalic sulcus. The lateral geniculate nucleus can sometimes be viewed through the medial pia protecting the ambient cistern and can also serve as a posterior hippocampal resection marker.

Intraoperative recording of the hippocampus can be performed to guide resection. Aggressive resection of spike-generating areas in mesial temporal structures may lead to improved seizure freedom [57]; however this is not well proven and has generally fallen out of practice. If desired, hippocampal recordings are performed after lateral neocortical resection, prior to mesial temporal resection. A strip of four to six electrodes is to be placed through the temporal horn of the lateral ventricle directed posteriorly toward the occipital horn on the ventricular surface of the hippocampus. The use of intraoperative electrocorticography requires strict limitation of inhalational anesthetic use.

Bipolar electrocautery and oxidized regenerated cellulose are used to obtain hemostasis, and the cavity is filled with sterile saline prior to watertight closure of the dura. The bone flap is then replaced, antibiotic irrigation used, and the incision closed in layers.

Selective Amygdalohippocampectomy (SAHC) Procedure

The impetus for developing the selective amygdalohippocampectomy (SAHC) is twofold. First, a convergence of evidence from electrophysiologic, functional imaging, and animal models suggests that resection of mesial temporal structures alone can result in similar seizure outcomes. Second, sparing lateral neocortical structures might spare some of the postoperative neuropsychological deficits associated with ATL. ATL on the other hand allows for better visualization and en bloc resection of mesial temporal structures, as described above.

SAHC can be performed through a variety of approaches. It was first described more than half a century ago via a transcortical approach through the MTG [58]. Other approaches include transsylvian [59, 60] and infratemporal [61] approaches. There are advantages and disadvantages to each approach, but acceptable outcomes can be achieved with all [62]. Here we will briefly describe the transcortical approach, which remains the most popular today.

The patient is positioned similarly as for the ATL, supine and with a large bump allowing the head to be rotated 90 degrees away from the side of surgery, parallel to the floor. The head is placed in a three-point skull pin fixation device, and cranial navigation is used since the limited exposure of the surgery can easily lead to confusion between anatomic landmarks. A linear incision is used just anterior to the ear, running from the level of just superior to tragus, superiorly about 7 cm. The temporalis is incised linearly and retracted laterally, and then a craniotomy is performed roughly 4 cm in diameter. The dura is then opened and flapped inferiorly.

The initial incision for the transcortical approach can be made through the middle or inferior temporal gyrus, or through the inferior temporal sulcus (Fig. 24.5a, b, incision 1c). Bipolar electrocautery is used to create a 1.5–2 cm opening not more than 3.5 cm posterior to the temporal pole. This cortical or sulcal incision is carried down to the temporal horn of

the lateral ventricle using cranial navigation as needed to direct the dissection. A self-retaining retractor is then used to maintain the cortical opening. Resection of the medial temporal structures follows a similar approach to those detailed above for ATL, with some distinctions aimed at maintaining "safe zones" to avoid disorientation. Part of the amygdala is first removed using a combination of electrocautery and suction. This removal is directed to exposing the pia overlying the medial floor of the middle fossa, picking up the pial plane as it travels off the middle fossa floor to protect the surgeon from more medial lying structures in the carotid, crural, and ambient cisterns. Subpial dissection is then continued posteriorly to remove the uncus, taking care to identify the tentorial incisura. Again, the medial pial plane must be carefully preserved to protect cranial nerves III and IV, the PCA and AChA, and the cerebral peduncle.

After removal of the uncus, the choroidal fissure is identified posteriorly within the temporal horn of the lateral ventricle. Again, this fissure marks the superior border of the resection to prevent damage to the optic tract and cerebral peduncle. The choroid can be swept superiorly, protected with a cottonoid and held in place with the tip of a retractor. Retraction posteriorly will reveal the pes hippocampus, and the hippocampus and fimbria are then mobilized off the choroidal fissure in the posterior direction. The posterior border of resection is defined by the plane of the tectal plate seen on neuronavigation, allowing for removal of approximately 2.5 cm of hippocampus. After reaching the posterior border and transecting the hippocampus in this plane, dissection is continued inferiorly from posterior to anterior, freeing the pes hippocampus from the parahippocampal gyrus. The hippocampus is now free except for its attachment on the pia-arachnoid plane of the hippocampal fissure. The hippocampus is freed from the hippocampal fissure in anterior to posterior direction, taking care to only divide arteries feeding the hippocampus and preserving the en passage vessels from AChA anteriorly and PCA posteriorly.

Outcomes for Resective Surgeries

The goal of resective surgery is seizure freedom. While outcomes for clinical trials of antiepileptic medications are often measured by the percent of patients achieving a meaningful reduction in seizure frequency (50% or greater reduction), outcomes for surgical treatment of epilepsy are held to a higher standard and graded using the Engel Classification of Postoperative Outcome (Table 24.1) [63] and/or the ILAE Postoperative Outcome Classification (Table 24.2) [64].

Table 24.1 Engel classification of postoperative outcome

Class	Description
I	Free of disabling seizures
A	*Completely seizure-free since surgery*
B	*Non-disabling simple partial seizures only since surgery*
C	*Some disabling seizures after surgery, but free of disabling seizures for at least 2 years*
D	*Generalized convulsions with AED discontinuation only*
II	Rare disabling seizures (almost seizure-free)
III	Worthwhile improvement[a]
IV	No worthwhile improvement

From Engel J Jr., et al. [63]. Reprinted with permission from John Wiley and Sons

[a]Worthwhile improvement is defined variably. Usages include a range of reduction in seizure frequency ranging from >50% to >90% reduction in seizure frequency

Table 24.2 International League Against Epilepsy (ILAE) postoperative outcome classification

Class	Description
1	Completely seizure-free; no auras[a]
2	Only auras; no other seizures
3	One to 3 seizure days per year; ± auras
4	Four seizure days per year to 50% reduction of baseline seizure days; ± auras
5	Less than 50% reduction of baseline seizure days to 100% increase of baseline seizure days; ± auras
6	More than 100% increase of baseline seizure days; ± auras

From Wieser HG, et al. [64]. Reprinted with permission from John Wiley and Sons

[a]This does not include seizures that occur in the first month after surgery, which do not predict long-term outcome

The first randomized controlled trial of ATL vs. continued medical management in MTLE showed 64% freedom from disabling seizures (58% when including all randomized for consideration for surgery) at 1 year after ATL compared to 8% after continued medical management [7]. The surgical group achieved 38% complete seizure freedom compared to only 3% in the medical group at 1 year. The surgery group also had significantly improved quality of life compared to the medically managed treatment arm. This trial confirmed the role of surgery in medically refractory epilepsy secondary to MTS and helped to popularize the surgery. At the time of publication in 2001, it was estimated that only about 2% of people eligible to undergo surgery for epilepsy actually underwent epilepsy surgery [65].

Additional studies and meta-analyses suggest that 60–90% of patients achieve Engel I outcome after ATL [7, 66–73] and that these outcomes are largely preserved after 5 years. Modern series achieving the highest rates of Engel I outcome after ATL place strong emphasis on the preoperative workup, reporting very high rates of concordance between semiology, MRI findings, and neuropsychological evaluations [73]. Engel I outcome rates of 70–80% can be considered a modern benchmark for seizure reduction after ATL.

Seizure reduction after SAHC is generally compared to outcomes for ATL. No randomized controlled trial comparing SAHC to ATL has been performed, and most single studies have small sample sizes suggesting equivalence or slight superiority of seizure reduction with ATL. A meta-analysis of papers comparing seizure freedom outcomes after ATL and SAHC showed an 8% increased occurrence of freedom from disabling seizures after ATL compared to SAHC [74]. This analysis of 11 studies comparing 1203 participants (620 ATL vs. 583 SAHC) stratified outcomes into freedom from disabling seizures (Engel I) vs. continued seizures (Engel II–IV). The 8% risk difference translates to a number needed to treat of 13 patients for 1 additional patient to achieve seizure freedom following ATL. The superiority of ATL compared to SAHC was maintained when the analysis was limited to only patients with MTS (n = 1092). The superiority of ATL to SAHC for seizure freedom has also been shown in other large meta-analyses [75].

Neuropsychological impairment can increase after ATL. Verbal memory impairment occurs in 25–50% of patients who undergo dominant right side ATL and 30% who undergo left side ATL [76]. Studies examining outcomes of both ATL and SAHC report no difference in verbal memory deficits between the two surgeries, reporting deficits in 40–50% of left-sided surgeries and 30% of right-sided surgeries [77, 78]. Patients at the highest risk for postoperative verbal memory impairment include those with a normal-appearing hippocampus and intact verbal memory on the dominant side, as well as patients with hippocampal sclerosis on the resection side but impaired memory function on the contralateral side. Other risk factors include very high preoperative verbal IQ and late age of epilepsy onset. Spatial memory tends to be more resilient compared to verbal memory after ATL, even when the nondominant hippocampus is resected.

Language deficits, particularly naming difficulty, can appear in up to 25% of patients following dominant side ATL [79]. These deficits can be permanent or transient. Other reports have shown improvement in naming and language corresponding to decrease in seizure frequency [80, 81]. Overall, postoperative language and naming deficits tend to be less severe and rarer compared to memory deficits.

The rationale behind performing SAHC stems from the idea that preservation of non-epileptic lateral temporal neocortex will prevent postoperative neuropsychological decline, specifically in regard to language and naming. Whether patients who undergo SAHC instead of ATL actually have better neuropsychological function remains a subject of debate; some studies show better functional outcomes after SAHC [82–84], while some show equivalence [77, 85]. Variability in neuropsychological batteries among studies has made large meta-analyses difficult.

Postoperative executive function outcomes are not as well defined as memory and language

effects. Most studies suggest that executive function improves after surgery and that this improvement correlates closely with seizure reduction [86–89]. Overall, despite worsening in verbal memory, quality of life measures improve after ATL and SAHC, correlating closely with seizure freedom and reduction in disabling seizure frequency.

Both ATL and SAHC are safe surgeries. Major complications including death, hemiparesis, hemianopsia, and cranial nerve injury resulting in permanent deficit are rare (<1%). New postoperative contralateral superior quadrantanopsia is common and results from interruption of the optic radiations in Meyer's loop as they travel over the temporal horn of the lateral ventricle. Quadrantanopsia occurs in up to 100% of some series but is generally clinically silent.

Psychiatric symptoms after ATL include worsening of depressive symptoms, new-onset depression [90, 91], and occasionally postoperative psychosis [92, 93]. Depression often occurs alongside MTLE [94]. Along with poor postoperative seizure control, depression is a risk factor for postoperative psychiatric symptoms [95].

Stereotactic Laser Amygdalohippocampotomy (SLAH)

Stereotactic laser amygdalohippocampotomy (SLAH) has recently been developed as a "minimally invasive" approach for destroying mesial temporal structures, gaining popularity over the past 5 years. Laser interstitial thermotherapy (LITT) is a thermoablative technique with growing applications, thanks to advances in magnetic resonance thermography allowing real-time monitoring of changes in temperature. Stereotactic laser amygdalohippocampotomy (stereotactic laser amygdalohippocamp*ectomy* is also used interchangeably in literature) is a technique for the treatment of mesial temporal lobe epilepsy in which a laser probe heats the surrounding tissue causing a permanent lesion. Technical details and general principles of LITT are reviewed in Chap. 16.

Stereotactic Laser Amygdalohippocampotomy Procedure

For mesial temporal epilepsy, the procedure is performed after a standard workup as done for ATL or SAHC. The laser fiber assembly is placed using whichever stereotactic platform the surgeon prefers, including standard skull-mounted frame, robotic system, or frameless system. There are currently two commercially available LITT systems: Visualase Thermal Therapy System (Medtronic, Minneapolis, MN, USA) and NeuroBlate Laser Ablation System (Monteris, Plymouth, MN, USA). The details below describe use of the former system.

The trajectory of the laser fiber is along the long axis of the amygdalohippocampal complex beginning from an occipital entry point (Fig. 24.8a). The entry point is chosen to enable safe entry to the pial surface of an occipital gyrus, avoiding vasculature as visualized using a contrast-enhanced MRI. The occipital horn should also be avoided when possible to prevent deflection of the laser cannula off the ependymal surface. Besides standard stereotactic concerns such as vessel avoidance, an additional consideration for these procedures is planning for thermal spread. Heat sinks, including the temporal horn and basal cisterns, prevent heat spread into those structures and limit thermal damage in those directions.

The patient is positioned according to the stereotactic system used. Some use a supine positioned with a head turn, others supine beach-chair with neck flexed (semi-slouched), and yet others a prone position. We use a semi-slouched position with a stereotactic robotic system. After prep and drape of a small region around the planned entry point, a 4 mm stab incision is made, and a 3.2 mm burr hole is drilled along the planned trajectory. We use a titanium anchor bolt affixed with a T-handle wrench to maintain the trajectory. If needed, we pass monopolar cautery through a coated probe to open the dura. We measure and calculate the distance to the planned target from the bolt and pass a guide rod down the trajectory to create a path to target. The 1.6 mm laser cannula is then placed through the anchor

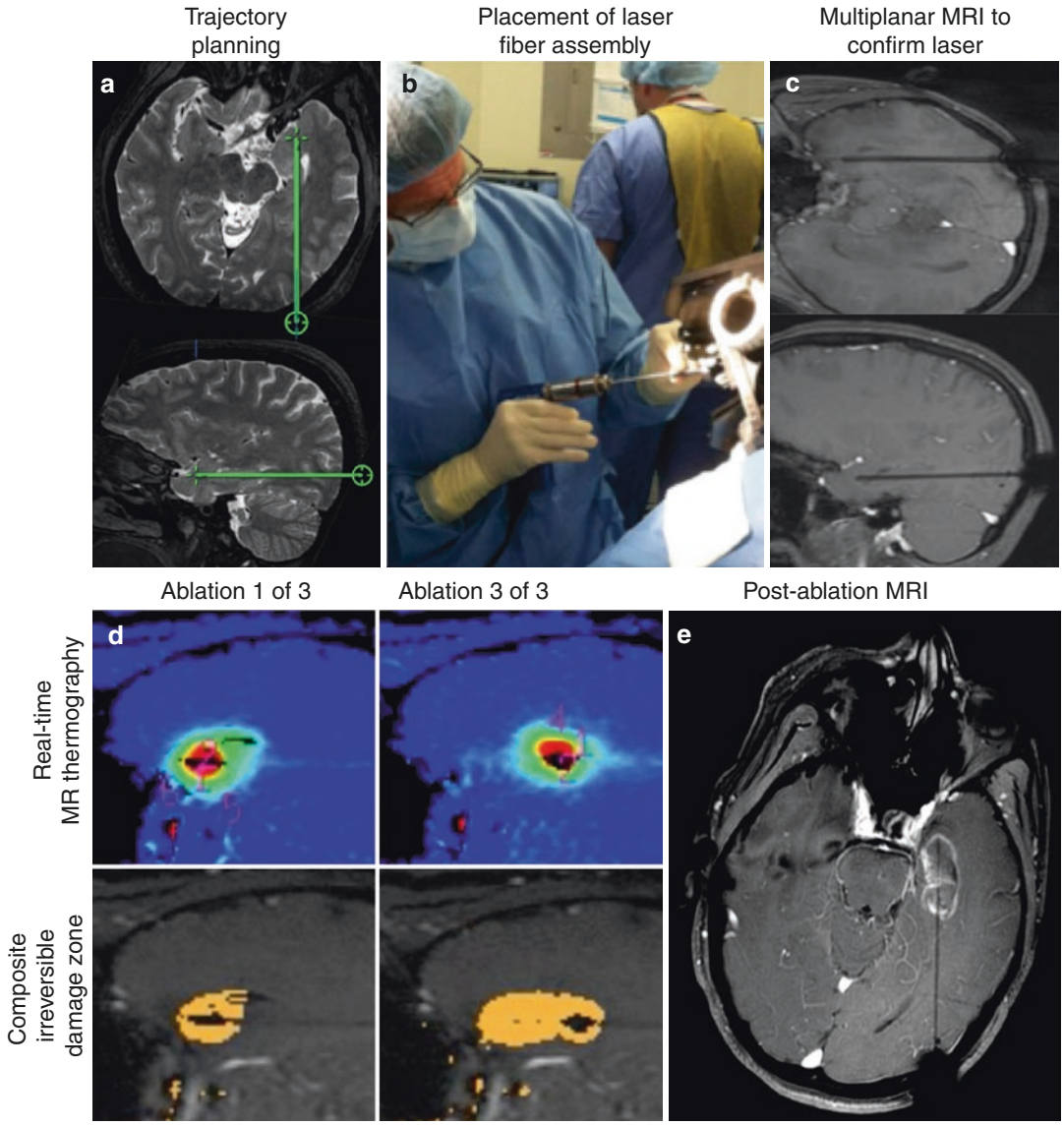

Fig. 24.8 Stereotactic laser amygdalohippocampotomy procedure. The laser cannula trajectory is planned with the laser entering in the occipital lobe and traveling down the long axis of the amygdalohippocampal complex (**a**). The laser fiber assembly is then placed under stereotactic guidance (**b**). The patient is transported to MRI to obtain multiplanar cuts of the laser fiber assembly. This confirms proper placement and defines planes for temperature monitoring (**c**). Ablation is performed under real-time MR thermography monitoring. Composite irreversible damage zones (orange) represent the location of the final lesion. The laser is pulled back 2 times in order to extend the length of the ablation down the long axis of the hippocampus (**d**). A T1-weighted post-contrast MRI is obtained to document the ablation volume and check for intracranial hemorrhage (**e**). (From Youngerman BE, et al. [96]. Reprinted with permission from John Wiley and Sons)

bolt along the trajectory to the distal (closest to temporal pole) part of the planned ablation volume. A laser with 10 mm diffuser tip is then placed into the laser cannula (Fig. 24.8b).

After locking the laser catheter in place with the skull anchor bolt, the patient is transferred to the MRI scanner, and the catheter is visualized with a volumetric scan (Fig. 24.8c). The scanner

is configured to visualize the catheter trajectory in one, two, or three orthogonal planes. The addition of more planes adds time to each thermal image acquisition. We usually use two planes, axial and sagittal. Low-temperature (usually 45–50 C) and high-temperature (usually 90 C) safety points are selected. The low limit is placed near structures at risk such that the laser automatically shuts off before heating those structures beyond the point of irreversible cell death. The high-temperature limit prevents tissue from reaching evaporation temperatures and releasing gas.

Temperature is monitored using fast spoiled gradient-recalled echo at several second intervals (usually 3–8 seconds depending on how many planes are acquired, as mentioned above) to map irreversible and cumulative damage zones (Fig. 24.8d). The most distal ablation volume is performed first, so that subsequent ablations can be achieved by incrementally withdrawing the laser catheter along the trajectory. After ablation of the first volume, the laser cannula is withdrawn in approximately 1 cm increments to perform subsequent ablations. Three to five serial ablations are usually required along the trajectory of the laser to complete the lesion [96]. The posterior extent of the ablation is typically the coronal plane of the lateral mesencephalic sulcus or quadrigeminal plate. Post-ablation T1 post-contrast and diffusion-weighted MRI sequences are obtained to document ablation volume (Fig. 24.8e). The presence of hemorrhage can be assessed with a fast field echo (FFE) or gradient echo sequence. After completion of the ablation, the laser cannula and anchor bolt are removed, and the stab incision is closed with a suture or staple. Most patients can be discharged from the hospital on postoperative day 1.

Both seizure freedom outcomes and operative morbidity are influenced by ablation geometry and extent [97–99]. A recent multicenter study suggests that extent of ablation of the anterior, inferior, and medial structures of the temporal lobe play the largest role in determining seizure freedom [100]. Increasing amygdala ablation volume correlated with improved seizure freedom, as did the inclusion of the hippocampal head, parahippocampal gyrus, and entorhinal and perirhinal cortices. In contrast, ablation of the hippocampal body and tail posteriorly, beyond a coronal plane at the level of the lateral mesencephalic sulcus, was associated with poorer epilepsy control outcomes. Posterior hippocampal ablation likely led to worse outcomes because of the curvature of the amygdalohippocampal complex. A straight laser cannula generally does not allow for both the ablation of the anterior inferior medial structures and the posterior hippocampal body and tail in one trajectory. Failure to ablate enough amygdala is a common pitfall leading to poor postoperative seizure control. Most centers perform the ablation with one laser; however some centers elect to use two laser trajectories in cases of severe mesial temporal sclerosis where a sharp curvature of the amygdala medially from the trajectory of the hippocampus does not allow for ablation of the necessary volumes of both the hippocampus and amygdala.

Importantly, the ablation trajectory must avoid straying too anteriorly putting the trigeminal nerve at risk as it enters Meckel's cave. A superior ablation trajectory, above the level of the choroidal fissure, can cause visual deficit after damage to the optic tract. A more posterior ablation can cause a contralateral superior quadrantanopsia via damage to the optic radiations [101] or contralateral homonymous hemianopsia due to damage to the lateral geniculate body.

Outcomes After Stereotactic Laser Amygdalohippocampotomy

Multiple single-institution series of SLAH suggest that seizure freedom rates are approximately 55–60% (reports range from 38% to 78%) at 1 year after ablation [96, 98–100, 102–107]. These rates improve to 60–89% in patients with radiographic evidence of hippocampal sclerosis. The largest series to date, a multicenter retrospective cohort study of 234 patients who underwent SLAH for MTLE, reported Engel I outcomes in 58% at 1 year and 57.5% at 2 years [100]. This study showed Engel I or II outcomes in 77.1% and 80.2% at 1 and 2 years, respectively. The

presence or absence of radiographic hippocampal sclerosis did not impact outcome, but patients with focal to bilateral tonic-clonic seizures were less likely to achieve Engel I outcomes [96].

Overall complication rates occur in approximately 15–20% of cases [100, 104, 108]. Radiographic rates of hemorrhage are approximately 1–2%, with less than 1% resulting in permanent neurologic injury. Visual complications including quadrantanopsias or cranial nerve III or IV deficits occur in approximately 5% of procedures.

Neurocognitive outcomes have also been reported in many of these series; however definitive outcomes are difficult to generalize due to the small number of patients in each study and the range of different neurocognitive measures used. As with SAHC, SLAH spares lateral neocortical structures. Preliminary direct comparisons of SLAH and ATL suggest that postoperative decline in object recognition and naming are less for SLAH compared to ATL [109]. Surprisingly, selective outcomes suggest that some aspects of verbal memory are spared even with ablation of language-dominant mesial temporal structures. However, the exact nature of the neurocognitive effect (e.g., naming, fluency, verbal memory, learning) varies from series to series. Some, for example, report preservation of verbal memory with decline of learning [108], while others report relative preservation of learning but decline in memory [103]. Larger studies with consistent neurocognitive testing are needed to clarify the neurocognitive effects of SLAH.

To better characterize the efficacy and side effect profile of SLAH, the Stereotactic Laser Ablation for Temporal Lobe Epilepsy (SLATE) study is an industry-sponsored prospective open-label trial of MRI-guided laser ablation using the Visualase system that is currently enrolling. The trial is scheduled to complete in 2022 after enrolling 150 patients. Endpoints including seizure freedom, adverse events, quality of life, and neuropsychological outcomes will be assessed at 12 months [110].

Considering the body of available early data, SLAH appears to be a safe and less invasive approach to the treatment of MTLE in patients with or without mesial temporal sclerosis. SLAH seems to have lower rates of seizure control compared to open surgery (ATL and SAHC). However, the morbidity of SLAH appears to be lower than open surgery. Additionally, the neurocognitive deficits after SLAH may be milder compared to open surgery. The results of the SLATE study will allow for a more definitive comparison of surgical approaches in the future.

Other Procedures

While resection of mesial temporal structures remains the gold standard surgical treatment of MTLE, and ablation continues to gain traction, a number of alternatives are available. Stereotactic radiosurgery has been under investigation and may provide an alternative for patients unable to undergo surgical treatment. Additionally, multiple neuromodulation alternatives are now FDA approved in the United States for treatment of medically refractory epilepsy. These neuromodulation approaches are increasingly used in patients who continue to have disabling seizures despite mesial temporal resection, patients with bilateral mesial temporal epilepsy, and patients who may not be candidates for resective surgery. Finally, hippocampal transection, a surgical technique that attempts to disconnect mesial structures to stop spread of seizures while largely maintaining those mesial structures, was developed as an approach to avoid postoperative cognitive deficit, but has largely been supplanted by ablative and/or neuromodulatory approaches and will not be discussed further.

Stereotactic Radiosurgery

Stereotactic radiosurgery (SRS) can be used as a nonsurgical alternative for the treatment of MTLE caused by mesial temporal sclerosis. Several pilot studies showed remission rates ranging from 47% to 85% after marginal radiation doses ranging from 20 to 29 Gy [111–114], with safety profiles comparable to anterior temporal lobectomy. Specifically, promising verbal

memory outcomes were initially demonstrated and were one initial driver for adoption of SRS [115]. However, seizure remission after SRS is delayed as radiation effects take time, and outcomes were seen gradually over 12–24 months after SRS. Moreover, seizures sometimes get worse before they get better secondary to irritative effects of radiation.

The Radiosurgery versus Open Surgery for Mesial Temporal Lobe Epilepsy (ROSE) trial [116], a multicenter randomized controlled trial comparing 24 Gy SRS versus ATL for medically refractory unilateral mesial temporal lobe epilepsy, failed to show non-inferiority of SRS compared to ATL at 3-year follow-up. The primary outcome of seizure remission rate, defined as freedom from seizures causing impairment of consciousness between months 25 and 36 after treatment, was 52% for SRS (n = 31) compared to 78% for ATL (n = 27). The trial demonstrated immediate efficacy and durability for ATL, with 81% seizure freedom by 3 months maintained at 85% seizure freedom during the final 3-month block (33–36 months after surgery). For SRS, seizure freedom during the first 3 months was only 6%, rising gradually over time to 74% during the last 3-month study period (33–36 months after SRS), re-demonstrating the delayed efficacy of SRS. Neurocognitive outcomes were roughly comparable between the SRS and ATL arms. Importantly, verbal memory outcomes were not statistically different between treatment arms, and overall quality of life outcomes correlated with seizure remission, and therefore quality of life improvement was delayed in the SRS arm compared to the ATL arm. The ROSE trial suggests that ATL should remain the gold standard for treatment of medially refractory MTLE, with SRS a possible alternative in patients unable to tolerate surgery.

Neuromodulation

Neuromodulation for epilepsy is discussed in detail in Chap. 27. Here we present a short summary of neuromodulation specifically for MTLE. Presently, there are three categories of neuromodulation for epilepsy: vagus nerve stimulation (VNS), deep brain stimulation (DBS) of the anterior nucleus of the thalamus, and responsive neurostimulation (RNS). All three of these modalities can be applied to refractory MTLE.

VNS has been approved since 1997 for the treatment of drug-resistant focal epilepsy. VNS is not a first-line treatment for drug-resistant MTLE. However, it can be used in populations of patients with unilateral MTLE unable to undergo mesial temporal resection or ablation, patients with unilateral MTLE who continue to have seizures after ATL or SAHC, or patients with MTLE of bilateral onset. Exact rates of response in this specific population are difficult to determine from the literature, but roughly 50% of patients with focal epilepsy will achieve a decrease of 50% or more in seizure frequency at 1 and 2 years after VNS implantation [117]. When compared to resection, however, these rates are notably inferior, as they are equivalent to an Engel III outcome. This comparison highlights the preference of resection over neuromodulation for those who are candidates.

DBS of the anterior nucleus of the thalamus (ANT) was approved in the United States in 2018 after the Stimulation of the Anterior Nucleus of the Thalamus for Epilepsy (SANTE) trial [118], a multicenter, double-blind randomized trial for focal epilepsy, and 5-year follow-up [119] showed promising results. The ANT is intimately associated with the mesial temporal structures through the medial limbic (Papez) circuit. Efferent projections to the ANT arise from the subiculum and CA1, reaching the ANT through the postcommissural fornix or via the mammillary bodies and mammillothalamic tract. The ANT also sends afferent projections directly and indirectly to the parahippocampal gyrus and hippocampus, leading to a complex network of direct and indirect thalamic-to-mesial cortical loops [120].

The SANTE trial and long-term follow-up reported a median reduction in seizures of 44% at 1 year and 76% at 5 years for the subgroup of patients with seizures of temporal lobe origin. These results appear better than those for VNS, but again, notably worse than those for resective

surgery, as the rate of seizure freedom (Engel I) was very low. While median reduction in seizure frequency was greater compared to placebo, response rate (>50% decrease in seizure frequency) was not significantly different compared to placebo (34% active vs. 25% sham, $p > 0.05$) during the 3-month blinded phase. Patients with a history of prior resective surgery had median seizure reductions of 53% at 1 year and 67% at 5 years. Importantly, both the populations of participants with temporal epilepsy and the population of participants who underwent prior resective surgery contained participants with non-MTLE epilepsies; however these results serve as guidance for subjects with MTLE for future study. Morbidity of ANT DBS include infection (10%), lead misplacement (8%), depression (37%), and memory impairment (27%) [119]. Importantly, the efficacy of DBS appears to increase with time and will hopefully get better as refinements are made in lead placement and stimulation parameters.

The RNS system (NeuroPace Inc., Mountain View, CA) is another neuromodulation alternative for patients with MTLE unable to undergo resective or ablative procedures. In contrast to ANT DBS, which is an open-loop stimulation paradigm applying a constant prescribed dose of stimulation, the RNS system employs a closed-loop paradigm in which brain activity is recorded, and stimulation only occurs if the device detects activity suggestive of an oncoming seizure.

RNS leads for MTLE are most often placed down the long axis of the amygdalohippocampal complex unilaterally or bilaterally. Additional subtemporal strips can be placed, also unilaterally or bilaterally. Only two leads can be connected to the stimulation device in the current version of the system. To date, the strongest data for the use of RNS for MTLE comes from a prospective trial of 111 subjects with MTLE [121]. Seventy-two percent of the subjects had bilateral MTLE, with the remaining 28% with unilateral onset. Twelve percent of these subjects had failed temporal lobectomy. At 6 years, disabling seizures were reduced by median 67%, and 65% of subjects had at least a 50% decrease in seizure frequency (Engel III). During the open-label period, 45% of subjects had seizure-free periods of over 3 months, and 15% had seizure-free periods of at least 1 year (Engel I). No differences were seen between subjects with bilateral vs. unilateral onset, or subjects who had previously undergone resective surgery vs. surgerically naïve subjects. There was also not a statistically significant difference between subjects with depth electrodes in the hippocampus and those with depth electrodes outside placed more laterally outside the hippocampus, although there was a trend toward better seizure control with hippocampal stimulation electrodes. Side effects included implant-site infection (12%) involving superficial soft tissue and necessitating device explant, device lead damage (6%), intracranial hemorrhage (3%), photopsia (14%), transient memory impairment (6%), and depression (5%). As with DBS, seizure control with RNS improves over time after implantation [122] and will likely continue to improve as lead placement and stimulation parameters continue to be refined.

While neuromodulation approaches are becoming increasingly common, they should not be considered replacements for ATL or SAHC. The rates of seizure freedom are significantly higher for ATL and SAHC compared to RNS or ANT DBS. As such, neuromodulation should be reserved for patients who are not candidates for ATL/SAHC, or for patients who have already undergone resective surgery but continue to have uncontrolled seizures.

Conclusions

Mesial temporal lobe epilepsy is a common focal epilepsy syndrome that can be amenable to surgery in properly selected patients. Patient selection is of utmost importance and requires extensive presurgical evaluation by a multidisciplinary team. Anterior temporal resection remains the gold standard operation, achieving freedom from disabling seizures in 70–80% of patients. Selective amygdalohippocampectomy remains a reasonable alternative, though rates of seizure freedom are slightly lower with an unclear neurocognitive advantage over anterior temporal

lobectomy. Stereotactic laser ablation is a new less invasive technique that has the potential to achieve similar outcomes to selective amygdalohippocampectomy. Results of the ongoing trials should help clarify the efficacy and neurocognitive effect of laser ablation. Responsive neurostimulation and anterior nucleus of the thalamus deep brain stimulation are new tools for patients unable to undergo resective surgery and offer an option for patients with bilateral onset mesial temporal epilepsy. Surgical treatments of mesial temporal epilepsy have evolved rapidly over the past two decades, and active research continues to push the boundary forward.

Acknowledgments The authors are grateful to Dr. Winifred Hamilton for her artistic skill in drafting the original versions of Figs. 24.4, 24.5, 24.6, and 24.7 and Dr. Audrey Nath for providing images in Fig. 24.3.

References

1. Cockerell OC, Johnson AL, Sander JW, Hart YM, Shorvon SD. Remission of epilepsy: results from the National General Practice Study of Epilepsy. Lancet. 1995;346(8968):140–4.
2. Kwan P, Brodie MJ. Early identification of refractory epilepsy. N Engl J Med. 2000;342(5):314–9.
3. Mohanraj R, Brodie MJ. Diagnosing refractory epilepsy: response to sequential treatment schedules. Eur J Neurol. 2006;13(3):277–82.
4. Kwan P, Arzimanoglou A, Berg AT, Brodie MJ, Allen Hauser W, Mathern G, et al. Definition of drug resistant epilepsy: consensus proposal by the ad hoc Task Force of the ILAE Commission on Therapeutic Strategies. Epilepsia. 2009;51(6):1069–77.
5. Stone JL, Jensen RL. Benjamin Winslow Dudley and Early American trephination for posttraumatic epilepsy. Neurosurgery. 1997;41(1):263–8.
6. Patchell RA, Young AB, Tibbs PA. Classics in neurology. Benjamin Winslow Dudley and the surgical treatment of epilepsy. Neurology. 1987;37(2):290–1.
7. Wiebe S, Blume WT, Girvin JP, Eliasziw M, Effectiveness and Efficiency of Surgery for Temporal Lobe Epilepsy Study Group. A randomized, controlled trial of surgery for temporal-lobe epilepsy. N Engl J Med. 2001;345(5):311–8.
8. Englot DJ, Ouyang D, Garcia PA, Barbaro NM, Chang EF. Epilepsy surgery trends in the United States, 1990–2008. Neurology. 2012;78(16):1200–6.
9. Wiebe S, Gafni A, Blume WT, Girvin JP. An economic evaluation of surgery for temporal lobe epilepsy. J Epilepsy. 1995;8(3):227–35.
10. Picot M-C, Neveu D, Kahane P, Crespel A, Gélisse P, Hirsch E, et al. Cost-effectiveness of epilepsy surgery in a cohort of patients with medically intractable partial epilepsy – preliminary results. Rev Neurol (Paris). 2004;160 Spec N:5S354–67.
11. Widjaja E, Li B, Schinkel CD, Ritchie LP, Weaver J, Snead OC, et al. Cost-effectiveness of pediatric epilepsy surgery compared to medical treatment in children with intractable epilepsy. Epilepsy Res. 2011;94(1–2):61–8.
12. York MK, Rettig GM, Grossman RG, Hamilton WJ, Armstrong DD, Levin HS, et al. Seizure control and cognitive outcome after temporal lobectomy: a comparison of classic Ammon's horn sclerosis, atypical mesial temporal sclerosis, and tumoral pathologies. Epilepsia. 2003;44(3):387–98.
13. Armstrong DD. The neuropathology of temporal lobe epilepsy. J Neuropathol Exp Neurol. 1993;52(5):433–43.
14. Osborn AG, Hedlund GL, Salzman KL. Osborn's brain. 2nd ed. Philadelphia: Elsevier; 2017.
15. Wen HT, Rhoton AL, de Oliveira E, Cardoso ACC, Tedeschi H, Baccanelli M, et al. Microsurgical anatomy of the temporal lobe: part 1: mesial temporal lobe anatomy and its vascular relationships as applied to amygdalohippocampectomy. Neurosurgery. 1999;45(3):549–92.
16. Wen HT, Rhoton AL, de Oliveira E, Castro LHM, Figueiredo EG, Teixeira MJ. Microsurgical anatomy of the temporal lobe: part 2: Sylvian fissure region and its clinical application. Neurosurgery 2009;65(6 Suppl):1–35.
17. Kucukyuruk B, Richardson RM, Wen HT, Fernandez-Miranda JC, Rhoton AL. Microsurgical anatomy of the temporal lobe and its implications on temporal lobe epilepsy surgery. Epilepsy Res Treat. 2012;2012:1–17.
18. Kahane P, Bartolomei F. Temporal lobe epilepsy and hippocampal sclerosis: lessons from depth EEG recordings. Epilepsia. 2010;51:59–62.
19. Chabardès S, Kahane P, Minotti L, Tassi L, Grand S, Hoffmann D, et al. The temporopolar cortex plays a pivotal role in temporal lobe seizures. Brain. 2005;128(8):1818–31.
20. Bartolomei F, Wendling F, Vignal JP, Kochen S, Bellanger JJ, Badier JM, et al. Seizures of temporal lobe epilepsy: identification of subtypes by coherence analysis using stereo-electro-encephalography. Clin Neurophysiol. 1999;110(10):1741–54.
21. Maillard L, Vignal J-P, Gavaret M, Guye M, Biraben A, McGonigal A, et al. Semiologic and electrophysiologic correlations in temporal lobe seizure subtypes. Epilepsia. 2004;45(12):1590–9.
22. Arzimanoglou A, Kahane P. The ictal onset zone: general principles, pitfalls and caveats. In: Lüders HO, editor. Textbook of epilepsy surgery. London: Informa Healthcare; 2008. p. 597–602.
23. Barba C, Barbati G, Minotti L, Hoffmann D, Kahane P. Ictal clinical and scalp-EEG findings

differentiating temporal lobe epilepsies from temporal "plus" epilepsies. Brain. 2007;130(7):1957–67.
24. Benbadis SR, O'Neill E, Tatum WO, Heriaud L. Outcome of prolonged video-EEG monitoring at a typical referral epilepsy center. Epilepsia. 2004;45(9):1150–3.
25. Dericioglu N, Saygi S. Ictal scalp EEG findings in patients with mesial temporal lobe epilepsy. Clin EEG Neurosci. 2008;39(1):20–7.
26. Feldman RE, Delman BN, Pawha PS, Dyvorne H, Rutland JW, Yoo J, et al. 7T MRI in epilepsy patients with previously normal clinical MRI exams compared against healthy controls. Bernhardt BC, editor. PLoS One. 2019;14(3):e0213642.
27. Varghese GI, Purcaro MJ, Motelow JE, Enev M, McNally KA, Levin AR, et al. Clinical use of ictal SPECT in secondarily generalized tonic-clonic seizures. Brain. 2009;132(Pt 8):2102–13.
28. Zhao F, Kang H, You L, Rastogi P, Venkatesh D, Chandra M. Neuropsychological deficits in temporal lobe epilepsy: a comprehensive review. Ann Indian Acad Neurol. 2014;17(4):374–82.
29. Black LC, Schefft BK, Howe SR, Szaflarski JP, Yeh H, Privitera MD. The effect of seizures on working memory and executive functioning performance. Epilepsy Behav. 2010;17(3):412–9.
30. Wagner DD, Sziklas V, Garver KE, Jones-Gotman M. Material-specific lateralization of working memory in the medial temporal lobe. Neuropsychologia. 2009;47(1):112–22.
31. Düzel E, Hufnagel A, Helmstaedter C, Elger C. Verbal working memory components can be selectively influenced by transcranial magnetic stimulation in patients with left temporal lobe epilepsy. Neuropsychologia. 1996;34(8):775–83.
32. Abrahams S, Morris RG, Polkey CE, Jarosz JM, Cox TCS, Graves M, et al. Hippocampal involvement in spatial and working memory: a structural MRI analysis of patients with unilateral mesial temporal lobe sclerosis. Brain Cogn. 1999;41(1):39–65.
33. Kapur N, Millar J, Colbourn C, Abbott P, Kennedy P, Docherty T. Very long-term amnesia in association with temporal lobe epilepsy: evidence for multiple-stage consolidation processes. Brain Cogn. 1997;35(1):58–70.
34. Blake RV, Wroe SJ, Breen EK, McCarthy RA. Accelerated forgetting in patients with epilepsy: evidence for an impairment in memory consolidation. Brain. 2000;123(3):472–83.
35. Butler CR, Zeman AZ. Recent insights into the impairment of memory in epilepsy: transient epileptic amnesia, accelerated long-term forgetting and remote memory impairment. Brain. 2008;131(9):2243–63.
36. Tramoni E, Felician O, Barbeau EJ, Guedj E, Guye M, Bartolomei F, et al. Long-term consolidation of declarative memory: insight from temporal lobe epilepsy. Brain. 2011;134(3):816–31.
37. Kim C-H, Lee S-A, Yoo H-J, Kang J-K, Lee J-K. Executive performance on the Wisconsin card sorting test in mesial temporal lobe epilepsy. Eur Neurol. 2007;57(1):39–46.
38. Horner MD, Flashman LA, Freides D, Epstein CM, Bakay RAE. Temporal lobe epilepsy and performance on the Wisconsin card sorting test. J Clin Exp Neuropsychol. 1996;18(2):310–3.
39. Oyegbile TO, Dow C, Jones J, Bell B, Rutecki P, Sheth R, et al. The nature and course of neuropsychological morbidity in chronic temporal lobe epilepsy. Neurology. 2004;62(10):1736–42.
40. Hermann B, Seidenberg M, Lee E-J, Chan F, Rutecki P. Cognitive phenotypes in temporal lobe epilepsy. J Int Neuropsychol Soc. 2007;13(01):12–20.
41. Labudda K, Frigge K, Horstmann S, Aengenendt J, Woermann FG, Ebner A, et al. Decision making in patients with temporal lobe epilepsy. Neuropsychologia. 2009;47(1):50–8.
42. McDonald CR, Delis DC, Norman MA, Tecoma ES, Iragui VJ. Discriminating patients with frontal-lobe epilepsy and temporal-lobe epilepsy: utility of a multilevel design fluency test. Neuropsychology. 2005;19(6):806–13.
43. Bell BD, Seidenberg M, Hermann BP, Douville K. Visual and auditory naming in patients with left or bilateral temporal lobe epilepsy. Epilepsy Res. 2003;55(1–2):29–37.
44. Loring DW, Meador KJ, Lee GP. Effects of temporal lobectomy on generative fluency and other language functions. Arch Clin Neuropsychol. 1994;9(3):229–38.
45. Mayeux R, Brandt J, Rosen J, Benson DF. Interictal memory and language impairment in temporal lobe epilepsy. Neurology. 1980;30(2):120–5.
46. Hamberger MJ, Seidel WT. Auditory and visual naming tests: normative and patient data for accuracy, response time, and tip-of-the-tongue. J Int Neuropsychol Soc. 2003;9(3):479–89.
47. Hamberger MJ, Tamny TR. Auditory naming and temporal lobe epilepsy. Epilepsy Res. 1999;35(3):229–43.
48. Price CJ, Devlin JT, Moore CJ, Morton C, Laird AR. Meta-analyses of object naming: effect of baseline. Hum Brain Mapp. 2005;25(1):70–82.
49. Damasio H, Tranel D, Grabowski T, Adolphs R, Damasio A. Neural systems behind word and concept retrieval. Cognition. 2004;92(1–2):179–229.
50. Hamberger MJ, McClelland S, McKhann GM, Williams AC, Goodman RR. Distribution of auditory and visual naming sites in nonlesional temporal lobe epilepsy patients and patients with space-occupying temporal lobe lesions. Epilepsia. 2007;48(3):531–8.
51. Hamberger MJ, Seidel WT, Goodman RR, Perrine K, McKhann GM. Temporal lobe stimulation reveals anatomic distinction between auditory naming processes. Neurology. 2003;60(9):1478–83.

52. Binder JR. Functional MRI is a valid noninvasive alternative to Wada testing. Epilepsy Behav. 2011;20(2):214–22.
53. Diehl B, Lüders HO. Temporal lobe epilepsy: when are invasive recordings needed? Epilepsia. 2000;41(Suppl 3):S61–74.
54. Jooma R, Yeh HS, Privitera MD, Gartner M. Lesionectomy versus electrophysiologically guided resection for temporal lobe tumors manifesting with complex partial seizures. J Neurosurg. 1995;83(2):231–6.
55. Cascino GD, Kelly PJ, Sharbrough FW, Hulihan JF, Hirschorn KA, Trenerry MR. Long-term follow-up of stereotactic lesionectomy in partial epilepsy: predictive factors and electroencephalographic results. Epilepsia. 1992;33(4):639–44.
56. Ward MM, Barbaro NM, Laxer KD, Rampil IJ. Preoperative valproate administration does not increase blood loss during temporal lobectomy. Epilepsia. 1996;37(1):98–101.
57. Yoshor D, Hamilton WJ, Grossman RG. Temporal lobe operations for drug-resistant epilepsy. In: Schmidek HH, Roberts DW, editors. Schmidek and Sweet's operative neurosurgical techniques: indications, methods, and results. 5th ed. Philadelphia: Saunders Elsevier Inc; 2006. p. 1383–93.
58. Niemeyer P. The transventricular amygdalohippocampectomy in temporal lobe epilepsy. In: Baldwin M, Bailey P, editors. Temporal lobe epilepsy. Springfield: Charles C. Thomas; 1958. p. 461–82.
59. Wieser HG, Yaşargil MG. Selective amygdalohippocampectomy as a surgical treatment of mesiobasal limbic epilepsy. Surg Neurol. 1982;17(6):445–57.
60. Yaşargil MG, Wieser HG, Valavanis A, von Ammon K, Roth P. Surgery and results of selective amygdalahippocampectomy in one hundred patients with nonlesional limbic epilepsy. Neurosurg Clin N Am. 1993;4(2):243–61.
61. Park TS, Bourgeois BFD, Silbergeld DL, Dodson WE. Subtemporal transparahippocampal amygdalohippocampectomy for surgical treatment of mesial temporal lobe epilepsy. J Neurosurg. 1996;85(6):1172–6.
62. Hoyt AT, Smith KA. Selective Amygdalohippocampectomy. Neurosurg Clin N Am. 2016;27(1):1–17.
63. Engel J, Van Ness PC, Rasmussen T, Ojemann L. Outcome with respect to epileptic seizures. In: Engel J, editor. Surgical treatment of the epilepsies. New York: Raven Press; 1993. p. 609–21.
64. Wieser HG, Blume WT, Fish D, Goldensohn E, Hufnagel A, King D, et al. Proposal for a new classification of outcome with respect to epileptic seizures following epilepsy surgery. Epilepsia. 2008;42(2):282–6.
65. Engel J Jr. A greater role for surgical treatment of epilepsy: why and when? Epilepsy Curr. 2003;3(2):37–40.
66. Spencer SS, Berg AT, Vickrey BG, Sperling MR, Bazil CW, Shinnar S, et al. Initial outcomes in the Multicenter Study of Epilepsy Surgery. Neurology. 2003;61(12):1680–5.
67. Sperling MR, O'Connor MJ, Saykin AJ, Plummer C. Temporal lobectomy for refractory epilepsy. JAMA. 1996;276(6):470–5.
68. Wyler AR, Hermann BP, Somes G. Extent of medial temporal resection on outcome from anterior temporal lobectomy: a randomized prospective study. Neurosurgery. 1995;37(5):982–90; discussion 990–1.
69. Engel J, Wiebe S, French J, Sperling M, Williamson P, Spencer D, et al. Practice parameter: temporal lobe and localized neocortical resections for epilepsy: report of the Quality Standards Subcommittee of the American Academy of Neurology, in Association with the American Epilepsy Society and the American Association of Neurological Surgeons. Neurology. 2003;60(4):538–47.
70. Cohen-Gadol AA, Wilhelmi BG, Collignon F, White JB, Britton JW, Cambier DM, et al. Long-term outcome of epilepsy surgery among 399 patients with nonlesional seizure foci including mesial temporal lobe sclerosis. J Neurosurg. 2006;104(4):513–24.
71. Elsharkawy AE, Alabbasi AH, Pannek H, Oppel F, Schulz R, Hoppe M, et al. Long-term outcome after temporal lobe epilepsy surgery in 434 consecutive adult patients. J Neurosurg. 2009;110(6):1135–46.
72. Schramm J, Lehmann TN, Zentner J, Mueller CA, Scorzin J, Fimmers R, et al. Randomized controlled trial of 2.5-cm versus 3.5-cm mesial temporal resection in temporal lobe epilepsy—part 1: intent-to-treat analysis. Acta Neurochir. 2011;153(2):209–19.
73. Elliott RE, Bollo RJ, Berliner JL, Silverberg A, Carlson C, Geller EB, et al. Anterior temporal lobectomy with amygdalohippocampectomy for mesial temporal sclerosis: predictors of long-term seizure control. J Neurosurg. 2013;119(2):261–72.
74. Josephson CB, Dykeman J, Fiest KM, Liu X, Sadler RM, Jette N, et al. Systematic review and meta-analysis of standard vs selective temporal lobe epilepsy surgery. Neurology. 2013;80(18):1669–76.
75. Hu W-H, Zhang C, Zhang K, Meng F-G, Chen N, Zhang J-G. Selective amygdalohippocampectomy versus anterior temporal lobectomy in the management of mesial temporal lobe epilepsy: a meta-analysis of comparative studies. J Neurosurg. 2013;119(5):1089–97.
76. Martin RC, Sawrie SM, Roth DL, Gilliam FG, Faught E, Morawetz RB, et al. Individual memory change after anterior temporal lobectomy: a base rate analysis using regression-based outcome methodology. Epilepsia. 1998;39(10):1075–82.
77. Gleissner U, Helmstaedter C, Schramm J, Elger C. Memory outcome after selective amygdalohippocampectomy: a study in 140 patients with temporal lobe epilepsy. Epilepsia. 2002;43(1):87–95.
78. Clusmann H, Schramm J, Kral T, Helmstaedter C, Ostertun B, Fimmers R, et al. Prognostic fac-

tors and outcome after different types of resection for temporal lobe epilepsy. J Neurosurg. 2002;97(5):1131–41.
79. Langfitt JT, Rausch R. Word-finding deficits persist after left anterotemporal lobectomy. Arch Neurol. 1996;53(1):72–6.
80. Davies KG, Maxwell RE, Beniak TE, Destafney E, Fiol ME. Language function after temporal lobectomy without stimulation mapping of cortical function. Epilepsia. 1995;36(2):130–6.
81. Hermann BP, Wyler AR, Somes G. Language function following anterior temporal lobectomy. J Neurosurg. 1991;74(4):560–6.
82. Pauli E, Pickel S, Schulemann H, Buchfelder M, Stefan H. Neuropsychologic findings depending on the type of the resection in temporal lobe epilepsy. Adv Neurol. 1999;81:371–7.
83. Paglioli E, Palmini A, Portuguez M, Paglioli E, Azambuja N, da Costa JC, et al. Seizure and memory outcome following temporal lobe surgery: selective compared with nonselective approaches for hippocampal sclerosis. J Neurosurg. 2006;104(1):70–8.
84. Clusmann H, Kral T, Gleissner U, Sassen R, Urbach H, Blümcke I, et al. Analysis of different types of resection for pediatric patients with temporal lobe epilepsy. Neurosurgery. 2004;54(4):847–60.
85. Jones-Gotman M, Zatorre RJ, Olivier A, Andermann F, Cendes F, Staunton H, et al. Learning and retention of words and designs following excision from medial or lateral temporal-lobe structures. Neuropsychologia. 1997;35(7):963–73.
86. Wachi M, Tomikawa M, Fukuda M, Kameyama S, Kasahara K, Sasagawa M, et al. Neuropsychological changes after surgical treatment for temporal lobe epilepsy. Epilepsia. 2001;42(Suppl 6):4–8.
87. Novelly RA, Augustine EA, Mattson RH, Glaser GH, Williamson PD, Spencer DD, et al. Selective memory improvement and impairment in temporal lobectomy for epilepsy. Ann Neurol. 1984;15(1):64–7.
88. Hermann BP, Wyler AR, Richey ET. Wisconsin card sorting test performance in patients with complex partial seizures of temporal-lobe origin. J Clin Exp Neuropsychol. 1988;10(4):467–76.
89. Rausch R, Crandall PH. Psychological status related to surgical control of temporal lobe seizures. Epilepsia. 1982;23(2):191–202.
90. Naylor AS, Rogvi-Hansen Bá R-H, Kessing L, Kruse-Larsen C. Psychiatric morbidity after surgery for epilepsy: short-term follow up of patients undergoing amygdalohippocampectomy. J Neurol Neurosurg Psychiatry. 1994;57(11):1375–81.
91. Quigg M, Broshek DK, Heidal-Schiltz S, Maedgen JW, Bertram EH. Depression in intractable partial epilepsy varies by laterality of focus and surgery. Epilepsia. 2003;44(3):419–24.
92. Christodoulou C, Koutroumanidis M, Hennessy MJ, Elwes RDC, Polkey CE, Toone BK. Postictal psychosis after temporal lobectomy. Neurology. 2002;59(9):1432–5.
93. Mace CJ, Trimble MR. Psychosis following temporal lobe surgery: a report of six cases. J Neurol Neurosurg Psychiatry. 1991;54(7):639–44.
94. Altshuler L, Rausch R, Delrahim S, Kay J, Crandall P. Temporal lobe epilepsy, temporal lobectomy, and major depression. J Neuropsychiatry Clin Neurosci. 1999;11(4):436–43.
95. Hermann BP, Wyler AR, Ackerman B, Rosenthal T. Short-term psychological outcome of anterior temporal lobectomy. J Neurosurg. 1989;71(3):327–34.
96. Youngerman BE, Oh JY, Anbarasan D, Billakota S, Casadei CH, Corrigan EK, et al. Laser ablation is effective for temporal lobe epilepsy with and without mesial temporal sclerosis if hippocampal seizure onsets are localized by stereoelectroencephalography. Epilepsia. 2018;59(3):595–606.
97. Wu C, Boorman DW, Gorniak RJ, Farrell CJ, Evans JJ, Sharan AD. The effects of anatomic variations on stereotactic laser amygdalohippocampectomy and a proposed protocol for trajectory planning. Neurosurgery. 2015;11:345–57.
98. Jermakowicz WJ, Kanner AM, Sur S, Bermudez C, D'Haese P-F, Kolcun JPG, et al. Laser thermal ablation for mesiotemporal epilepsy: analysis of ablation volumes and trajectories. Epilepsia. 2017;58(5):801–10.
99. Vakharia VN, Sparks R, Li K, O'Keeffe AG, Miserocchi A, McEvoy AW, et al. Automated trajectory planning for laser interstitial thermal therapy in mesial temporal lobe epilepsy. Epilepsia. 2018;59(4):814–24.
100. Wu C, Jermakowicz WJ, Chakravorti S, Cajigas I, Sharan AD, Jagid JR, et al. Effects of surgical targeting in laser interstitial thermal therapy for mesial temporal lobe epilepsy: a multicenter study of 234 patients. Epilepsia. 2019;00:1–13.
101. Yin D, Thompson JA, Drees C, Ojemann SG, Nagae L, Pelak VS, et al. Optic radiation tractography and visual field deficits in laser interstitial thermal therapy for amygdalohippocampectomy in patients with mesial temporal lobe epilepsy. Stereotact Funct Neurosurg. 2017;95(2):107–13.
102. Willie JT, Laxpati NG, Drane DL, Gowda A, Appin C, Hao C, et al. Real-time magnetic resonance-guided stereotactic laser amygdalohippocampotomy for mesial temporal lobe epilepsy. Neurosurgery. 2014;74(6):569–84; discussion 584–5.
103. Donos C, Breier J, Friedman E, Rollo P, Johnson J, Moss L, et al. Laser ablation for mesial temporal lobe epilepsy: surgical and cognitive outcomes with and without mesial temporal sclerosis. Epilepsia. 2018;59(7):1421–32.
104. Le S, Ho AL, Fisher RS, Miller KJ, Henderson JM, Grant GA, et al. Laser interstitial thermal therapy (LITT): seizure outcomes for refractory mesial temporal lobe epilepsy. Epilepsy Behav. 2018;89:37–41.
105. Grewal SS, Zimmerman RS, Worrell G, Brinkmann BH, Tatum WO, Crepeau AZ, et al. Laser ablation for mesial temporal epilepsy: a multi-site, single institutional series. J Neurosurg. 2018:1–8.

106. Tao JX, Wu S, Lacy M, Rose S, Issa NP, Yang CW, et al. Stereotactic EEG-guided laser interstitial thermal therapy for mesial temporal lobe epilepsy. J Neurol Neurosurg Psychiatry. 2018;89(5):542–8.
107. Gross RE, Stern MA, Willie JT, Fasano RE, Saindane AM, Soares BP, et al. Stereotactic laser amygdalohippocampotomy for mesial temporal lobe epilepsy. Ann Neurol. 2018;83(3):575–87.
108. Kang JY, Wu C, Tracy J, Lorenzo M, Evans J, Nei M, et al. Laser interstitial thermal therapy for medically intractable mesial temporal lobe epilepsy. Epilepsia. 2016;57(2):325–34.
109. Drane DL, Loring DW, Voets NL, Price M, Ojemann JG, Willie JT, et al. Better object recognition and naming outcome with MRI-guided stereotactic laser amygdalohippocampotomy for temporal lobe epilepsy. Epilepsia. 2015;56(1):101–13.
110. Stereotactic Laser Ablation for Temporal Lobe Epilepsy (SLATE). Clinical Investigational Plan Study Sponsor: Medtronic Navigation, Inc. [Internet]. 2016 [cited 2019 May 13]. Available from: https://clinicaltrials.gov/ct2/show/NCT02844465.
111. Barbaro NM, Quigg M, Broshek DK, Ward MM, Lamborn KR, Laxer KD, et al. A multicenter, prospective pilot study of gamma knife radiosurgery for mesial temporal lobe epilepsy: seizure response, adverse events, and verbal memory. Ann Neurol. 2009;65(2):167–75.
112. Regis J, Rey M, Bartolomei F, Vladyka V, Liscak R, Schrottner O, et al. Gamma knife surgery in mesial temporal lobe epilepsy: a prospective multicenter study. Epilepsia. 2004;45(5):504–15.
113. Bartolomei F, Hayashi M, Tamura M, Rey M, Fischer C, Chauvel P, et al. Long-term efficacy of gamma knife radiosurgery in mesial temporal lobe epilepsy. Neurology. 2008;70(19):1658–63.
114. Rheims S, Fischer C, Ryvlin P, Isnard J, Guenot M, Tamura M, et al. Long-term outcome of gamma-knife surgery in temporal lobe epilepsy. Epilepsy Res. 2008;80(1):23–9.
115. Quigg M, Broshek DK, Barbaro NM, Ward MM, Laxer KD, Yan G, et al. Neuropsychological outcomes after Gamma Knife radiosurgery for mesial temporal lobe epilepsy: a prospective multicenter study. Epilepsia. 2011;52(5):909–16.
116. Barbaro NM, Quigg M, Ward MM, Chang EF, Broshek DK, Langfitt JT, et al. Radiosurgery versus open surgery for mesial temporal lobe epilepsy: the randomized, controlled ROSE trial. Epilepsia. 2018;59(6):1198–207.
117. Englot DJ, Chang EF, Auguste KI. Efficacy of vagus nerve stimulation for epilepsy by patient age, epilepsy duration, and seizure type. Neurosurg Clin N Am. 2011;22(4):443–8.
118. Fisher R, Salanova V, Witt T, Worth R, Henry T, Gross R, et al. Electrical stimulation of the anterior nucleus of thalamus for treatment of refractory epilepsy. Epilepsia. 2010;51(5):899–908.
119. Salanova V, Witt T, Worth R, Henry TR, Gross RE, Nazzaro JM, et al. Long-term efficacy and safety of thalamic stimulation for drug-resistant partial epilepsy. Neurology. 2015;84(10):1017–25.
120. Child ND, Benarroch EE. Anterior nucleus of the thalamus: functional organization and clinical implications. Neurology. 2013;81(21):1869–76.
121. Geller EB, Skarpaas TL, Gross RE, Goodman RR, Barkley GL, Bazil CW, et al. Brain-responsive neurostimulation in patients with medically intractable mesial temporal lobe epilepsy. Epilepsia. 2017;58(6):994–1004.
122. Nair DR, Morrell MJ. Nine-year prospective safety and effectiveness outcomes from the long-term treatment trial of the RNS® system. In: American Epilepsy Society 2018 Annual Meeting. New Orleans, Louisiana; 2018. p. Abstract 2.075.

Epilepsy: Neocortical

25

John P. Andrews and Edward F. Chang

Surgery for drug-resistant epilepsy of neocortical origin is not as common as is seen for medial temporal lobe epilepsy (mTLE). With more experience, improving diagnostics, and accumulating reports of acceptable rates of seizure control, neocortical epilepsy resections are becoming a more prominent tool in the arsenal of epilepsy treatments. Epilepsy arising from neocortical foci is not rare when all such cases are considered together, and development of surgical expertise in this area is necessary to offer a full range of treatment options to patients with medically refractory disease.

Neocortical seizures have distinct presentations, semiology, and management compared to medial temporal lobe epilepsy, but overlap is also significant. The general principles of drug-resistant epilepsy work-up and treatment, however, hold true: a seizure disorder with a discernable, targetable focus should ideally be clinically recognized, the anatomic origin of seizures should then be reliably localized, and the surrounding indispensable cortex that limits extent of resection must be carefully delineated. These planning steps, followed by the safe execution of a surgical plan, are necessary regardless of the location of seizure focus.

J. P. Andrews · E. F. Chang (✉)
Department of Neurological Surgery, University of California, San Francisco, San Francisco, CA, USA
e-mail: Edward.chang@ucsf.edu

This chapter will review resective surgery for medically intractable seizure disorders arising from the neocortex of the temporal, frontal, occipital, and parietal lobes. While many of these epileptic syndromes do not strictly respect the anatomical borders of lobes, such an organization is helpful from a surgical standpoint, and the semantics of lobular categorization of epilepsy are widely used in the literature. Characteristics of seizure semiology, common diagnostics, and surgical evaluation are considered and presented. Techniques of surgical resection particular to the lobe or syndrome of interest are then reviewed, with a summary of outcomes related to each form of neocortical epilepsy described to conclude each sub-section.

Temporal Neocortical Epilepsy

Expression, Diagnosis, and Evaluation

Epilepsy arising from the neocortex of the temporal lobe may be difficult to distinguish clinically from that originating in mesial temporal structures. The descriptions of semiology and symptomatology, including abdominal auras, rare somatosensory auras, automotor seizures, and progression to tonic-clonic seizures [1–4], have been described similarly between the two entities, with variable distribution. History of febrile seizures may be more common in mTLE than neo-

N. Pouratian, S. A. Sheth (eds.), *Stereotactic and Functional Neurosurgery*,
https://doi.org/10.1007/978-3-030-34906-6_25

cortical temporal lobe epilepsy (ncTLE) [2, 3], and memory may be less likely to lateralize in ncTLE [5]. Sensory hallucinations with visual, auditory, or vestibular features may be more characteristic of lateral-neocortical seizures than those of medial origin [6], but differentiating based on such semiology is inconsistent [1, 2]. The strength of these associations falls short of allowing for definitive diagnosis at the level of individual patients (Fig. 25.1).

The similar semiology may arise from the spatial proximity and dense interconnectivity between the medial and lateral temporal lobe. Seizures arising in temporal neocortex may spread to involve the medial structures early in their evolution, such that unique aspects of a distinct neocortical origin are subsumed by semiology of mTLE, such as abdominal auras. To complicate clinical diagnosis, it has been suggested that in order for certain aspects of auras and temporal semiology to enter into conscious experience, both medial and lateral temporal structures must be involved [1], which may add to the difficulty in untangling ncTLE syndrome from its more common mTLE counterpart.

The dividing line of laterality may not be clear for all ncTLE. The continuum of medial vs lateral or ncTLE has been described in some studies of temporal lobe epilepsy (TLE) as either medial,

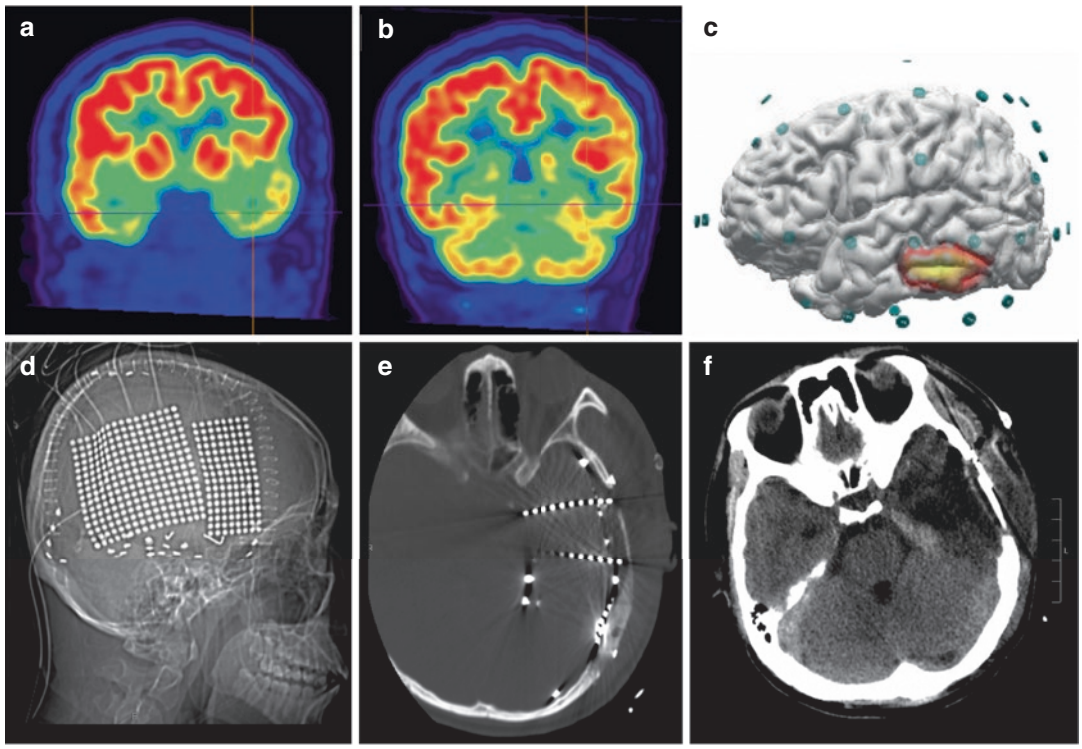

Fig. 25.1 Neocortical temporal lobe epilepsy**.** This 20-year-old man with both partial and generalized seizures had convulsions preceded by an aura of a heavy feeling, sometimes dizziness, before losing consciousness. His MRI was normal. (**a**, **b**) FDG-PET shows reduced radioisotope uptake in the left lateral, posterior inferior temporal lobe. (**c**) The areas of reduced uptake on PET co-localize with a 3D reconstruction of dipole and distributed source estimates from scalp EEG. (**d**, **e**) Two subdural grids were placed over the lateral cortex in combination with depth electrodes placed into the amygdala and hippocampus. Strip electrodes placed under the subtemporal cortex. (**f**) A left anterior temporal lobectomy was carried out with subtemporal extension to include the posterior inferior gyrus of the temporal lobe, to which seizures were localized. The left inferior temporal gyrus showed focal cortical dysplasia type IIa, while no significant pathologic abnormalities were noted in the hippocampus or amygdala. At 1-year follow-up, the patient remains completely seizure-free

lateral-neocortical, or medial-lateral on the basis of stereoelectroencephalography (SEEG) [6]. The study referenced here found that fear and viscerosensory semiologies were significantly more common in medial and medial-lateral epilepsies compared with purely lateral and that sensory hallucinations (visual, auditory, vestibular) were significantly more common in purely lateral TLE. This comes with the caveat that only 13 patients made up the lateral TLE subtype and these features were not absolute (i.e., there was still some crossover in the semiology), except that no purely lateral TLE patients reported fear at seizure onset.

The pathology underlying intractable ncTLE includes lesions of neoplastic origin such as low-grade gliomas, glioneuronal lesions, and dysembryoplastic neuroepithelial tumors [7], as well as non-neoplastic lesions such as cavernomas and vascular malformations, hamartomas, tubers, and cortical dysplasias [8]. In MRI-negative, non-lesional ncTLE, various types of cortical dysplasia or malformations of cortical development and neuronal migration disorders are often detected on pathology, though they may be subtle [9], and unspecified gliosis is still a commonly reported pathology [10–12].

Scalp EEG and MRI may provide the first evidence of cerebral localization pointing to temporal neocortex in a clinical work-up. Scalp EEG cannot provide the detailed margins of epileptic foci needed to make surgical resective decisions in neocortical epilepsies and is limited in spatial recognition to dipoles orthogonal to the surface electrodes and involvement of large amount of cortex. However, despite such limitations, scalp EEG was shown to have localizing value in 74% of ncTLE in a large study of surgically proven ncTLE, more so than in parietal and occipital neocortical epilepsies, while noting that structural lesions interfered with localizing ability in this subset of ncTLE [13].

Multimodal imaging and functional studies can be leveraged to provide the localizing value necessary for an effective surgical work-up. Magnetic source imaging (MSI), 2-[18F]fluoro-2-deoxy-D-glucose-positron emission tomography (FDG-PET), and ictal single-photon emission computed tomography (SPECT) each can contribute value in the non-invasive diagnostic work-up, and MSI may be of particular value in ncTLE [14]. The negative predictive values of each of these modalities in isolation are relatively low, and they have only partial redundancy in patients for whom they will localize epileptic foci, so a negative result in one modality does not mean that an epileptic focus won't be localized effectively by another type of study. While resource allocation may not always allow for it, diagnostic sensitivity and positive predictive values would be maximized through serial acquisition of these studies, beginning with MSI [14, 15].

Intracranial EEG as part of surgical planning and epileptic focus localization is recommended in patients who are surgical candidates for essentially all ncTLE, particularly those without MRI evidence of a structural lesion and those with discordance of localization between an MRI-detectable lesion and surface EEG [1, 11, 16]. Non-invasive imaging studies, including FDG-PET, MSI, or ictal SPECT, may aid in guiding intracranial electrode positioning and coverage to better define ictal-onset zones and prospective margins of resection.

Surgical Resection

The goals of resection in ncTLE are informed by the pathology at hand. Three divisions of pathology that inform both the goals of surgery and the necessary work-up are neoplastic lesional, non-neoplastic lesional, and non-lesional ncTLE. Regarding neoplastic lesional ncTLE, while a patient's original presentation may be for epileptic seizures, with seizure freedom as the presenting goal, a comprehensive work-up may reveal an underlying neoplastic lesion. In such cases, the possibility of tumor recurrence will factor into goals of surgery and inform the approach, usually with the aim of gross total resection in addition to seizure control.

The first step in ncTLE operative planning is distinguishing this form of epilepsy from mTLE. Semiology and non-invasive epilepsy imaging studies are necessary, but may not be suf-

ficient for delineation of ncTLE, and ultimately intracranial monitoring provides the most accurate means of distinguishing ncTLE from mTLE for proper surgical planning. Scalp EEG and non-invasive imaging studies such as SPECT and FDG-PET can miss or falsely localize extratemporal ictal-onset zones [10]. Distinguishing medial from lateral temporal lobe ictal onsets can be carried out through the use of implanted hippocampal electrodes with simultaneous electrode coverage of lateral neocortex. Hippocampal depth electrodes can be inserted either at multiple points from either a lateral approach, orthogonal to the long axis of the hippocampus [6], or as a single electrode down the long axis of the hippocampus from an occipital approach [17]. An anteromedial subdural electrode strip can also be inserted for mesial surface coverage [18]. The relative advantage of stereoelectroencephalography (SEEG) versus a combination of depth electrodes and subdural grids is an ongoing debate. Subdural grids provide excellent spatial resolution to guide neocortical resections and, in combination with depth electrodes in the mesial structures, can provide a detailed mapping of the cortex for surgical decision-making around eloquent cortex [16]. SEEG has the advantage of high accuracy with stereotactic placement and can be particularly useful in patients with dural adhesions that could impede optimal placement of subdural strips or grids [16]. Complication rates are relatively low with both techniques, with SEEG likely being better tolerated by patients [16, 19, 20].

In non-neoplastic lesions and non-lesional epilepsy of temporal neocortex, resection of tissue generating the patient's epileptic seizures is the primary goal. In lesional ncTLE, the degree to which the lesion overlaps with, or abuts, seizure-onset zones will dictate how lesion-focused of a resection to perform. Non-lesional ncTLE will rely on electrophysiologic and functional imaging correlates to delineate the epileptogenic zone for resection.

Lesionectomy, lesionectomy plus corticectomy, tailored lesionectomy/corticectomy plus resection of mesial structures, lateral temporal lobectomy, and multiple subpial transections have all been described for the treatment of ncTLE [21]. One decision point in the surgical treatment of neocortical temporal lobe epilepsy is whether to include medical structures in the resection. Drawing on literature discussing resections for tumor-associated epilepsy of the temporal lobe, outcomes were better with the inclusion of medial structures in tailored resections for ncTLE [7]. However, the contribution of medially associated tumors to these datasets versus more pure populations of lateral temporal neocortical tumors is difficult to tease out. Analyses comparing resective strategies that include medial structures to those that exclude them may be influenced by the inclusion of tumors of medial temporal origin in these datasets, which are more likely to have resections including epileptogenic medial structures [22–25]. Inclusion of medial structures when seizure-onset zones are clearly localized more laterally and there is no lesional component to the medial structures has also been described [2, 5]. Memory deficits are common in surgery for medial temporal lobe epilepsy, particularly verbal memory after surgery on the dominant temporal lobe [26, 27]. Limiting resections to lateral lesions or corticectomy may avoid much of the memory-related morbidity reported with medial resection [28]. This presents an argument to avoid more extended medial resection when there is no evidence of epileptogenicity documented in these structures. In addition, high rates of seizure freedom are documented in focal neocortical temporal lobe resections that spare medial structures to focus definitively on the areas of ictal onset [29, 30].

To access the lateral temporal cortex, a reverse question-mark incision and a temporal craniotomy (in supine positioning with a shoulder bump) can provide adequate exposure. The size of temporal craniotomy must be planned so as to expose cortical areas to be resected. Minimizing craniotomies through keyhole approaches can be limiting when the planned resection extends beyond lesionectomy, and if any intraoperative stimulation techniques will be used, the craniotomy must account for maximal possible resection [31].

Where the boundary of resection must be drawn relative to possible eloquent areas in lateral TLE is another important aspect to incorpo-

rate into surgical planning. Non-lesional resection is best guided by area of ictal onset demonstrated on intracranial EEG. A margin of 1 cm around the cortical onset site, limited by areas of eloquent cortex, can be used to define resective margins [8, 31]. During corticectomy, care should be taken to respect the arachnoid planes of sulci and the traversing sulcal vessels they harbor. In addition, damage to deep white matter tracts should be avoided. Diffusion tensor imaging can be helpful in preoperative planning to avoid these tracts. Corticectomy need not extend deeper than 2.5–3 cm in the absence of a lesion [31], though this is a generality to avoid eloquent white matter tracts, and such specific measurements are not in and of themselves applicable to all neocortical resections nor sufficient to ensure safety of the resection. Language deficits are perhaps the most feared complications of surgery in the dominant temporal neocortex; therefore the utmost caution should be practiced when extending such resections. Because of the variable representation of language in the lateral temporal cortex, cortical language mapping is often necessary for safe, complete resections. Intraoperative direct cortical stimulation techniques may improve safety in resections of lesions that appear intimately associated with eloquent cortex [32, 33]. Intracranial grids have the dual advantage of providing detailed information for seizure-onset localization as well as language mapping when used in a staged fashion.

Approaching lesions or seizure-onset zones in eloquent cortex may necessitate non-resective techniques either to augment or replace resection altogether. Multiple subpial transections is one technique that may provide some improvement in seizure frequency with less risk of compromising indispensable cortex [34, 35]. Responsive neurostimulation of epileptogenic zones is also an evolving technique that has been suggested as a possible adjuvant to resection when epileptogenic zones extend into eloquent cortices [36].

Surgical Outcomes

Seizure freedom rates for ncTLE epilepsy reported in the literature range from 39% to 72% (Table 25.1). This broad range may stem from the heterogenous pathology underlying the syndrome and a lack of standardized resection techniques. An MRI-detectable lesion has been associated with higher rates of seizure freedom when compared to non-lesional ncTLE in the three largest series in the literature [12, 29, 30]. Of these studies, Schramm et al. [29] explicitly note that medial structures were not included in the resection in any of the patients reported. The authors defined neocortical temporal lobe epilepsy through the presence of seizure onset in the temporal lobe, clearly outside mesial structures combined with a lack of MRI-evident mesial temporal abnormalities. Thus, ncTLE was defined anatomically, relative to surgical indications, as opposed to syndromic or semiologic descriptions. The Engel class I outcome of 79% in this study shows that inclusion of medial structures is not a requirement for seizure-free outcome in ncTLE.

The types of resection reported by Schramm and colleagues were anterior 2/3 lateral lobe resection without hippocampectomy (n = 11),

Table 25.1 Neocortical temporal lobe epilepsy surgery series

Author	Year	No. of patients	Engel class I (%)[a]
Burgerman [5]	1995	11	72
Pacia [2]	1996	21	n/a[b]
O'Brien [3]	1996	15	60
Jung [37]	1999	31	68
Lee [8]	2000	23	39[d]
Schramm [29]	2001	62	79
Lee [10]	2003	22	n/a[c]
Maillard [6]	2004	8	75
Lee [11]	2005	31	55
Jansky [38]	2006	29	69[d]
Yun [12]	2006	80	71[d]
Kim [30]	2010	66	42
Dolezolova [39]	2016	7	42

[a] Engel class I or a comparable measure of seizure freedom where designated

[b] Only patients that were seizure-free after anteromedial temporal lobectomy were included in the study, so rates of seizure freedom are not presented

[c] Only patients with "good seizure outcome," defined as seizure-free or > 90% reduction in seizures, were included in the study, so rates of seizure freedom are not presented

[d] "Seizure-free," not explicitly Engel class outcome

corticectomy plus lesionectomy ($n = 50$), and one case of multiple subpial transections (MST). Intracranial EEG (iEEG) was undertaken in 26 of 62 patients reported, with the criteria for an iEEG study being any one of the either lack of an MRI-detectable lesion, inconclusive surface EEG findings, suspicion of bilateral or extratemporal seizure onset, or overlap of suspected epileptogenic zone with cortical language areas. Patients who underwent iEEG studies had worse seizure control as a group after surgery compared with patients who did not undergo invasive monitoring. As with other TLE studies, though, this is almost certainly a result of the high-risk, poorly localized epilepsies making up the population selected for iEEG monitoring and the failure of thorough monitoring to raise otherwise inoperable epilepsies to the seizure freedom rate of patients with better localized seizure foci [36].

Yun et al. [12] report a large study of 193 neocortical epilepsy cases, 80 of which were ncTLE. Of these 80 patients, 57 (71%) were rendered seizure-free at 2-year follow-up. In lesional cases, invasive monitoring was carried out if the lesion was near eloquent cortices, if there was suspicion that the lesion was focal cortical dysplasia, or if preoperative studies showed discordant features. The surgical resections included the ictal-onset zone, areas showing interictal spikes along with pathologic delta waves (even when no ictal onsets occurred in this zone), and excluded eloquent cortex. The study grouped together all types of neocortical epilepsy, which makes for interesting and powerful observations given the high n, but having multiple anatomic constraints and variables changing radically for surgery on different lobes prevents too many conclusions about ncTLE to be drawn. However, it is worthy of note that the positive effect of an MRI-detectable lesion on seizure outcome was consistent across neocortical epilepsies.

Kim et al. [30] report a slightly lower overall seizure-free outcome rate of 42% at 2-year follow-up. Of note, the cohort of 66 ncTLE patients included 9 patients whose ictal intracranial study showed rapid spread of seizure activity to the mesial temporal lobe, leading to tailored resection that included hippocampectomy. Those patients with and without hippocampectomy did not have their respective outcomes reported independently, so whether they faired differently after surgery is uncertain. The finding that outcome was best in patients whose resections included tissue to which seizures spread in the first 3 seconds of ictus is interesting from a surgical planning standpoint and agrees with other studies pointing to seizure spread as a marker of epileptogenicity [36, 40].

In summary, the concept of neocortical temporal lobe epilepsy as a distinct syndrome is continuing to develop, and much progress is still to be made. Surgically, it should be treated as a separate entity from mesial temporal lobe epilepsy, particularly because comparable rates of seizure freedom are obtained without disrupting mesial structures. With the proper work-up and functional mapping, surgery for ncTLE can be carried out with high rates of seizure freedom and low morbidity.

Frontal Lobe Epilepsy

Expression, Diagnosis, and Evaluation

Frontal lobe epilepsy (FLE) is the next most prevalent anatomically localized epilepsy syndrome behind temporal lobe epilepsy [41, 42]. Frameworks for categorization of FLE semiology include breaking FLE into complex partial, focal motor, and supplementary motor seizures, though such divisions are not absolute, and significant overlap exists between these types [43–46]. Focal motor seizures begin with contralateral extremity clonic activity, while consciousness is maintained. Seizures of the supplementary motor area (SMA) are typically characterized by mutism, blank staring, and asymmetric, tonic posturing. Complex partial seizures, sometimes referred to as psychomotor seizures in the literature, consist of unresponsiveness in their early phase, with staring spells and contraversion, during which bipedal movements and vocalization are also described [44, 46] (Fig. 25.2).

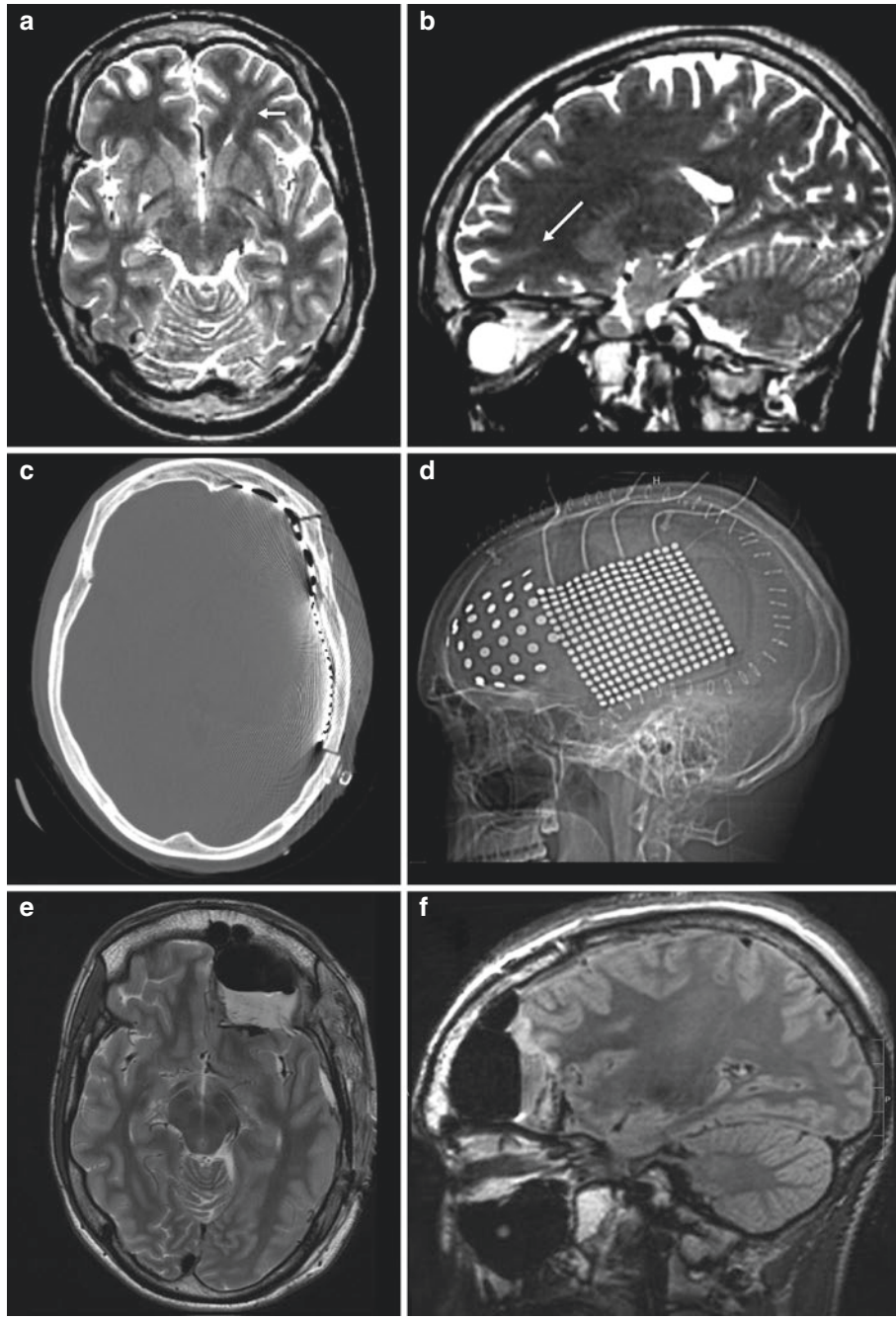

Fig. 25.2 Frontal lobe epilepsy. This 18-year-old man had moderate developmental delay and multiple seizures daily. One type of seizures started with a "fuzzy feeling," and the patient would curl into a ball, making grunting noises. His second type of seizures began with an overwhelming anxiety, sometimes a falling feeling, progressing to loud vocalizations and flinging of arms. Postictally he would be confused and aphasic for hours. (**a**, **b**) T2 MRI sequences showing a transmantle cortical dysplasia (arrows) in the left anterior inferior frontal gyrus, extending toward the frontal horn of the left lateral ventricle. (**c**) Axial CT and (**d**) lateral plain film show two subdural grids placed over the anterolateral cortex of the left frontal lobe. Seizures co-localized with the MRI findings, and subsequently an anterior frontal pole resection was carried out. (**e**) Axial T2 and (**f**) sagittal FLAIR MRI showing adequate resection of the lesion. Intraoperative electrocorticography was placed and monitored for 20 minutes after resection, showing no further evidence of epileptiform discharges. The pathology confirmed focal cortical dysplasia type IIb. The patient has been seizure-free since surgery

A number of anatomic features of the frontal lobe and electrophysiologic features of FLE seizures complicate characterization and localization. Anatomic barriers include the size of the lobe, making up over a third of total cortical volume in humans, such that surface electrodes must draw from deep cortical folds that are densely interconnected. When surgical planning is dependent on localizing discrete epileptic foci, such attributes may contribute to historically lower rates of seizure freedom than temporal lobe epilepsies [42, 47]. The brevity of frontal lobe seizures and their rapid spread are also noted throughout the literature, as well as complex motor movements and more uniquely emotional and sexual semiology [44, 45, 48]. The dense white matter tracts and cortico-cortical connections may serve as the underlying neurophysiology contributing to early descriptions of frontal lobe seizures as rapidly spreading entities. Intuitively, rapidly spreading ictal activity on SEEG has been shown to correlate with poor seizure outcome in surgery for FLE [49].

In regard to classification schemes to correlate semiology with anatomy, one interesting study used SEEG recordings to group semiology to an anatomical rostral-caudal distribution [50]. Semiologic signs were carefully defined, the seizures were reviewed and categorized, and then principle component analysis was used to group together semiology and anatomic localization that appeared to occur together more often than chance. These techniques resulted in four groups of FLE seizures. Seizures of group 1 were most caudal in origin, with involvement of the precentral gyrus and Rolandic operculum. Lateral and medial premotor cortices were also sometimes involved. Group 1 seizures were characterized by elementary motor signs such as contralateral tonic posturing, version, clonic signs, and facial asymmetric contractions. These seizures lacked emotive features or gestural behavior. Group 2 seizures were associated with prefrontal and premotor regions. Elementary motor signs, such as symmetric axial tonic posture and facial contractions, as well as nonintegrated gestural motor behavior were the semiology of this group. Group 3 seizures showed early spread involving rostral prefrontal ventrolateral and rostral cingulate gyrus. Seizure activity simultaneously of both anterior cingulate and prefrontal ventrolateral regions was seen either at onset or as a result of lateral-to-medial seizure spread. Group 3 semiology included nonintegrated gestural motor behavior without elementary motor signs, distal stereotypies. The absence of elementary motor signs was a significant marker of this group. Group 4 seizures presented with gestural motor behavior of fear, sometimes with attempt at escape or physical aggression, as well as screaming, swearing, and autonomic signs. Like group 3, there were no elementary motor signs associated with this group. Anatomic localization of group 4 was orbital and prefrontal, with spread to anterior temporal cortex and amygdala, but not to lateral frontal cortex.

This rostro-caudal axis of semiologic organization is attractive in that it reflects a hierarchical understanding of frontal lobe function [51]. The divisions are less strict categorizations than an organizational gradient, which may nonetheless be helpful in attempts to localize based on semiology. While the rostro-caudal gradient appears robust, the seizure spread along a lateral-to-medial axis makes hard distinctions along this axis less clear, with medial prefrontal cortex possibly acting as a common pathway for seizures of lateral onset.

Surgical Resection

Surgical resection is carried out with the goal of resecting seizure-onset zone. Since semiology can represent either onset or areas of propagation, ignoring areas of cortex with more subtle or silent features, the semiology-based localization described above should not be confused with seizure-onset localization sufficient for guiding surgical resection. While frontal lobectomy is an option, a targeted surgical work-up will often uncover sublobar foci by which to direct surgical management. The lack of standardized frontal lobe resections comparable to anterior temporal lobectomy leads to a more varied approach to frontal lobe epilepsy surgery. The approaches can

be categorized mostly as either medial or lateral, depending on how the epileptic focus can be accessed.

Regarding access to the medial frontal lobe, such as to approach supplementary cortex (SMA), dorsal anterior cingulate gyrus, and pre-SMA targets, a bicoronal incision with unilateral frontal craniotomy may be used, with supine positioning. The cingulate gyrus and corpus callosum can be used to track to ventral cingulate gyrus areas with this approach. A technical note to be aware of is the position of the ventral limit of the falx relative to the corpus callosum. The falx does not lie flush with the corpus callosum. More anteriorly on the falx, there is a significant space between these two structures, and interhemispheric arachnoid adhesions exist. These adhesions necessitate dissection for proper access. These can impede the advancement of subdural strips into these interhemispheric areas. A potential danger of dissection in these interhemispheric cortices is damage to the pericallosal and callosomarginal branches of the anterior cerebral arteries. Direct visualization or meticulous subpial dissection should be utilized to avoid these *en passage* vessels.

Delineating areas of the precentral gyrus corresponding to leg and foot function using motor mapping can aid in avoiding unnecessary morbidity when resections extend near to this region. Just rostral to the leg areas lies the SMA, resection of which leads to an SMA syndrome. The syndrome involves apraxia, or difficulty initiating spontaneous movement in contralateral limbs, and increased or preserved tone. Speech deficits such as akinetic mutism may also present when the lesion involves SMA of the dominant hemisphere. These primary deficits are usually temporary, although they take weeks to resolve, and some exam findings such as alternating bimanual movements can persist [52–55]. Deficits resulting from damage to primary motor cortex, on the contrary, are less likely to recover, so it is important to differentiate between the two possible etiologies for postoperative deficits. Boundaries of the SMA are the cingulate gyrus medial inferiorly and the precentral sulcus posteriorly. While the anterior border lacks easily identifiable anatomic demarcation, the pre-SMA lies at this margin, generally anterior to a vertical plane through the anterior commissure [54]. In contrast to the SMA, the pre-SMA lacks large white matter tract connections to primary motor cortex and is thought to be more involved in cognition and non-motor tasks [52, 56].

Lateral approaches to frontal lobe foci can be taken through a pterional craniotomy for ventral frontal lobe areas. Frontal craniotomy is suited for dorsal lateral frontal areas. The dominant hemisphere's language areas should be identified using language mapping to avoid these eloquent regions. While there is considerable heterogeneity in language localization [33], speech arrest for identifying speech production areas (Broca's) is often localized to pars opercularis or precentral gyrus. Pars triangularis also may localize for naming arrest [57].

Outcomes

Seizure freedom after frontal lobe epilepsy surgery trends lower than that for medial temporal lobe epilepsy, averaging just over 50% in the studies reviewed here (Table 25.2) [47]. Etiologies are similar to other neocortical epilepsies, including focal cortical dysplasia, neoplasms, vascular lesions, and a spectrum of gliotic changes, as well as normal tissue without identifiable pathology. Seizure foci resections in the frontal lobe can be limited by SMA, precentral gyrus, and dominant hemisphere language areas. From a cognitive perspective, aside from short-term deficits from SMA involvement, frontal lobe resections are often well-tolerated [58]. The variety of pathology, variability of follow-up, and differing methods of resection likely contribute to the range of postoperative seizure freedom rates shown in Table 25.2.

As with other neocortical epilepsies, factors that are associated with more localized foci of epileptogenesis are associated with better outcome. The nature of this focality on preoperative assessment is somewhat variable between studies. Most large studies find that an MRI-localizable lesion is associated with better seizure

Table 25.2 Frontal lobe epilepsy surgical series

Author	Year	No of patients	Engel class I (%)[a]
Rasmussen [59]	1991	253	27
Rougier [60]	1992	23	42
Talairach [61]	1992	100	55[b]
Fish [62]	1993	45	20[c]
Laskowitz [43]	1995	16	63
Smith [63]	1997	49	53
Swartz [64]	1998	26	38
Wennberg [65]	1999	25	60
Ferrier [66]	1999	37	32
Mosewich [67]	2000	68	59
Jobst [68]	2000	25	64
Zaatreh [69]	2002	37	35
Kloss [70]	2002	18	78
Luyken [71]	2003	25	80
Tigaran [72]	2003	65	49
Yun [12]	2006	61	39
Jeha [73]	2007	70	30
Lee [74]	2008	71	54
Elsharkawy [75]	2008	97	42
Kim [76]	2010	76	55
Holtkamp [49]	2012	25	60
Lazow [77]	2012	58	55
Ramantani [78]	2017	75	63
Bonini [79]	2017	42	57
Xu [80]	2019	82	52
Morace [81]	2019	44	68

[a] Comparable measure of seizure freedom
[b] "Practically cured" of epilepsy after surgery
[c] Good outcome by Rasmussen score

outcome, but this is not universal. One recent study by Bonini et al. [79] included 42 patients, 38 of whom underwent intracranial monitoring with SEEG. The authors found no difference between seizure outcomes of MRI-negative vs MRI-positive epilepsies, instead stating that completeness of resection of the epileptogenic zone is the most significant marker of outcome. The relevance of this of course depends fully on the preoperative definition of the epileptogenic zone, since theoretically full resection of the epileptogenic zone would by definition render a patient seizure-free. In this study, the authors define the epileptogenic zone visually, as well as using a quantitatively calculated index called the epileptogenicity index, which heavily weights the latency to an area showing ictal activity after ictal onset [82]. Lazow et al. [77] is another study that did not find a MRI localizability of a lesion to be associated with seizure outcome (57% were seizure-free at last follow-up). The relatively high rate of intracranial EEG in the study (89.6%) mirrors that of Bonini et al., which could in theory be affecting the contribution of MRI findings to surgical outcome.

In other large studies of frontal lobe epilepsy surgery with long-term follow-up, lesion on MRI did predict outcome. Elsharkawy et al. [75], in a series of 97 patients operated on for FLE, found a well-circumscribed lesion to be predictive of long-term seizure outcome. The reported seizure outcome at 2, 5, and 14 years in this study was 49.5%, 41.9%, and 41.9%, respectively. Kim et al. [76] also found that MRI localization of the epileptic focus was a predictor of outcome in their series of 76 patients who underwent frontal lobe resection. Jeha et al. [73] and Xu et al. [80] also share the finding correlating MRI abnormalities with seizure control.

Englot et al. [47] performed a systematic review and meta-analysis of frontal lobe epilepsy resections, which took into account 21 studies covering the surgeries of 1199 patients. The overall seizure freedom rate after frontal lobe resections in this meta-analysis was 45.1%. Identification of a focal lesion and abnormality on MRI were predictors of outcome. Within the lesional epilepsy subgroup, gross total resection was a significant predictor of outcome. The running thread through all of these studies is the focality of the epileptic zone is important for surgical planning and guiding resection in this large lobe of the brain with dense interconnectivity. The more complete the resection of the epileptic zone, the more likely such a resection is to achieve stable seizure freedom postoperatively.

Occipital Lobe Epilepsy

Expression, Diagnosis, and Evaluation

The characteristic semiology of occipital lobe epilepsy (OLE) centers around visual symptoms, with the earliest documentation of such seizures

describing shining or flickering lights, as well as loss of sight [83, 84]. Compared with temporal and frontal lobe epilepsy, epilepsy originating from foci in the occipital lobe is relatively rare, commensurate with the smaller size of the occipital lobe. OLE typically makes up a minority when large series of neocortical epilepsies are subdivided anatomically [11, 30]. The pharmacoresistant forms of OLE, with their distinctive visual auras and semiology, are becoming better understood, and patients with this disease may be surgical candidates with good rates of postoperative seizure control.

In a classic series of 25 patients with OLE, Williamson et al. describe the key localizing symptoms and signs as elementary visual hallucinations, ictal amaurosis, sensations of eye movement, and fast, early blinking symptoms [85]. The rapid ictal eye blinking in particular may be a helpful though insensitive clue to suspect occipital lobe epilepsy [86]. The elementary visual hallucinations involved flashing white or colored lights, as well as steady light less commonly. The later characteristics of seizures, occurring longer periods after onset of ictus, and which include visceral epigastric sensations, vertigo, and complex visual hallucinations (faces or scenes), were attributed to seizure spread outside the occipital lobe. This spread can be problematic in skewing the diagnosis of OLE by making these seizures appear as if they are temporal or frontal in origin [85, 87].

The preponderance of visual symptoms, particularly elementary visual hallucinations, continues to be described in more recent series with remarkable similarity to earlier literature [87–89]. If the seizures in questions are complex partial seizures, the impaired awareness or consciousness may interfere with a patient's ability to remember and report accurately on the nature of his or her auras and seizure semiology. Studies have also found that visual hallucinations are not specific to OLE, also being reported in seizures of the temporal-occipital junction and in posterior temporal lobe seizures [90]. Again, spread to nearby contiguous anatomic structures likely plays a part. Complex visual hallucinations such as faces or scenes tend to involve areas outside of the occipital lobe either in addition to or instead of the occipital lobe primarily [90]. Neither surface EEG nor semiology can be relied on for definitive diagnosis of OLE because of these commonly mixed pictures and the dense white matter tracts connecting temporal and occipital lobes. The inferior longitudinal fasciculus likely serves as a tract to spread seizures between occipital and temporal lobes, causing semiology that may be identical to that of temporal lobe epilepsy. The superior white matter tracts provide an easy explanation for motor aspects of seizures in OLE that can mimic frontal lobe epilepsies [85]. Parietal-occipital, temporal-occipital, and purely occipital lobe seizures are sometimes grouped together as "posterior cortex epilepsy" as a means to discuss the similar clinical characteristics and fluid anatomical localization, while elsewhere these entities are referred to as occipital "plus" epilepsies [91–93]. Differentiating OLE from temporal lobe epilepsy is an important part of the diagnostic process, and OLE should be considered and ruled out in any possible surgical candidate with visual symptoms and/or EEG change in the occipital areas [94, 95].

The pathology causing OLE is similar in breadth to other neocortical epilepsies. Neoplasias such as dysembryoplastic neuroepithelial tumors and gangliogliomas, glial scarring, cortical dysplasias, and vascular malformations all appear as players in the underlying histology of larger series of OLE [91, 96, 97]. The more focal, circumscribed of these lesions will be less likely to require as many methods of imaging and evaluation to effectively plan for and diagnose. As mentioned previously, interictal scalp EEG cannot be relied upon for localization because of the high likelihood of appearing temporal in origin, while the information provided on MRI often ends up being the most useful depending on the lesion and pathology. That being said, MRI-negative OLE may still be effectively localized using a combination of techniques. Positron emission tomography (PET) [86] and ictal subtraction single-photon emission computed tomography (SPECT) [98] and magnetoencephalography (MEG)/magnetic source imaging (MSI) [97, 99, 100] are all useful in characterization of possible

epileptogenic foci. Concordance of these studies can effectively guide intracranial electrode placement and may provide non-overlapping information on areas of potential epileptogenicity [100–102].

In addition to visual hallucinations and semiology, visual field deficits are common in patients with OLE. As such, a formal visual field work-up should be assessed prior to any resective surgery. The current state of a patient's visual function must be carefully considered when planning surgery and possibilities of its deterioration discussed and considered between patient and surgeon. When the occipital lobe has been unequivocally localized as the seizure-onset zone and a patient already has a homonymous hemianopia, occipital resection can be pursued with more vigor. When the imaging or functional studies are less convincing as to the location of the lesion, or when there is significant overlap between epileptogenic foci and primary visual cortex in a patient with intact vision, an intracranial study is more likely to provide helpful information in the surgical planning process.

A sound intracranial study is one that answers the questions raised by non-invasive studies, as well as the questions that can be answered in no other way. Questions of laterality or of the involvement of the occipital lobe at all in the epilepsy syndrome must be approached with broad coverage sufficient to rule out either lobe in its entirety. Depth electrodes and SEEG can be useful in capturing information along comparatively large volumes of lobes. MRI-negative OLE often may present an important dilemma where intracranial electrodes should be positioned in a way such that they cross projected resective margins, such as where along the occipital-temporal or occipital-parietal junctions a margin of resection should be drawn. The involvement of mesial temporal structures may be of concern when seizures show elements of temporal lobe origin. The possibility of including medial structures can be evaluated by using hippocampal depth electrodes, either down the long axis of the hippocampus from an occipital approach or laterally at intervals through temporal entry sites [16]. Strips can also be used for medial temporal coverage, depending on the planned approach and coverage necessary for the intracranial study [18]. Extent of coverage involving all three occipital lobe surfaces may contribute to seizure control postoperatively [88]. Subdural strips or grids can offer detailed anatomic distribution along surface cortex. Interhemispheric subdural grids may be most useful in patients with intact vision and questions remaining as to which aspects of the visual cortex are involved in epileptogenesis. Visual function must be addressed with the same rigor that one would address language sites, and many of the same tenets hold true. Stimulation mapping using subdural interhemispheric grids is a useful way to delineate eloquence in visual cortex and optimize functional outcome.

Surgical Resection

A critical aspect of surgical resections in the occipital lobe is the visual status of the patient. This aspect cannot be overemphasized in planning and executions of optimal resection. A balance between optimal seizure control and avoiding new visual deficits can be precarious. While a superior quadrantanopia may be tolerated well in exchange for seizure freedom, inferior quadrantanopia may present a new and ever-present handicap that could detract from quality of life gained in the reduction of seizure rates. In addition, it should be considered that any new deficits in visual function may of course come without seizure freedom. Patients may be under the impression that the more of a deficit to which they are willing to agree, the greater seizure freedom they can expect, but this may not always be the case, as OLE resective seizure outcome is less consistent in comparison to TLE surgery [103]. The prospect of severe visual impairments like a new hemianopia should be enough to discuss withholding resective options in certain cases when the risk-benefit ratio is too high. In any case, the surgeon should be cognizant of visual pathway projections during any occipital resections where preservation of function or any visual quadrant is sought after.

The resection should be tailored to the lesion or epileptic zone delineated in each patient, together with the goals for visual field preservation. Care should be taken to avoid subcortical projections of the visual pathways as well as the superficial primary visual cortex. Intracranial EEG data may be used to guide extension of resections beyond the occipital lobe into temporal or parietal areas. These resections are carried out with standard microsurgical procedure. Electrocorticography can be an effective tool to guide surgical resection, as has been demonstrated in select series [96, 104, 105].

A decision with major impact on surgical planning is that of whether to include mesial temporal structures in an occipital resection. It is not uncommon for resections for OLE to extend into multiple lobes [94], but rigorous comparisons evaluating added benefit of including mesial temporal structures with occipital resections are lacking [88]. Moreover, in contrast to resections of the lateral temporal cortex discussed elsewhere in this chapter, the significant distance between these occipital foci and mesial temporal structures may require staged operations or undue additive technical and morbidity burden. Large occipital-temporal resections that take place in the dominant hemisphere bring language and language-related pathway interconnections into consideration. Alexia without agraphia due to damage to interhemispheric connections in the splenium corpus callosum in patients with dominant temporal lobe damage is another possible deficit that could be precipitated by extending resections. Care should be taken to avoid connections between the occipital lobes and dominant temporal structures that may precipitate such deficits. Image guidance during occipital lobe epilepsy surgery may be a helpful adjunct when working with pathology in this lobe.

Surgical Outcomes

Occipital lobe epilepsy resections are not as common as temporal or frontal lobe epilepsy surgery, nor are there gold standards for resection techniques, so outcomes have more variability and can be predicted with less certainty. Series from the last 10 years, however, tend to average over 50% seizure freedom after at least 1 year of follow-up (Table 25.3). A systematic review and meta-analysis of posterior quadrant epilepsy by Harward et al. [103], which considered data from 584 patients from studies with 6 to 52 patients per study, found that 65% of OLE patients were reported to achieve seizure freedom after surgery. Younger patients and abnormal MRI were both associated with higher likelihood of being seizure-free. Fifty-seven percent of patients showed some degree of visual decline after OLE surgery. These are perhaps the best cumulative representation of OLE outcome data in the literature, but individual studies provide a nuanced look at important aspects of these surgeries, particularly with regard to visual outcome.

A recent series of 42 patients—large with respect to OLE literature—was reported by Heo et al. [116], describing a seizure freedom rate of

Table 25.3 Occipital lobe epilepsy surgical series

Author	Year	No of patients	Engel class I (%)[a]
Rasmussen [106]	1975	25	26
Wyler [107]	1990	14	50
Blume [108]	1991	16	32
Salanova [84]	1992	23	41
Williamson [85]	1992	16	88
Bidzinski [109]	1992	12	83
Aykut-Bingol [110]	1998	35	46
Sturm [111]	2000	6	50
Boesbeck [93]	2002	42	48[b]
Kun Lee [112]	2005	26	62
Dalmagro [91]	2005	44	65
Caicoya [113]	2007	7	71
Binder [96]	2008	52	69
Tandon [86]	2009	21	81
Jehi [114]	2009	11	89
Jobst [88]	2010	14	50
Ibrahim [97]	2012	41	51
Sarkis [115]	2012	35	69[b]
Appel [94]	2015	19	42
Yang [87]	2015	35	71
Marchi [92]	2016	18	55
Heo [116]	2018	42	64

[a] Comparable measure of seizure freedom
[b] Posterior cortex epilepsy, involving overlap with occipital-temporal and occipital-parietal foci

64%. The authors provide a detailed analysis of visual outcomes using a standardized assessment of visual function (the National Eye Institute Visual Function Questionnaire 25 or NEI-VFQ-25) and subsequently correlated these findings with anatomic resection areas [117, 118]. In this study, 61% of patients either developed new visual field defects or had worsening of existing visual field defects. Intuitively, in patients who started with either normal vision or isolated quadrantanopia prior to surgery, resection of primary visual cortices was associated with new or worsening visual defects. Moreover, patients with hemianopia showed significantly worse visual function scores compared to patients in the quadrantanopia or normal vision group. Of the 33 patients who had normal vision or quadrantanopia prior to surgery, 9 patients had normal vision, and 10 had quadrantanopia following occipital resection, suggesting more than half of patients can undergo OLE surgery and have good visual outcome. In addition, the study identified areas of the lateral occipital cortex (LO1 and LO2) [116]—located in the lateral occipital cortex, with LO2 anterior to LO1—whose resection was associated with decline in peripheral vision and vision-specific role difficulties (LO1) and general vision (LO2) through correlating resection maps with the NEI-VFQ-25 visual function questionnaire.

A slightly more cautionary piece of data comes from an earlier series of Kun Lee et al. [112], where of 18 patients who had intact vision preoperatively, only 1 retained normal vision after surgery. These studies from overlapping time points at the same institution may represent a progression toward better preservation of vision over time but also emphasize the range of outcome and comparative paucity of data within the OLE outcome literature. The Binder [96] and Tandon [86] series report roughly half of patients experienced new or worsened visual deficits following OLE surgery.

These data taken together support the role of surgery for OLE for achieving satisfactory rates of seizure freedom. Rates of new or worsened visual deficits are also high, however, and patients should be counseled as to this trade-off.

Parietal Lobe Epilepsy

Expression, Diagnosis, and Evaluation

Parietal lobe epilepsy (PLE) is variable in its presentation and can be difficult to localize because of non-specific semiology. Perhaps for these reasons, PLE resections are the least commonly performed epilepsy resections [119–121]. Descriptions of syndromes of PLE most often center on somatosensory semiology, with other aspects less clearly defined [122]. While the anterior border of the parietal lobe at the central sulcus is clear, the parietal-occipital sulcus is most apparent on the medial aspect of the hemispheres, and laterally the lobe's temporal-parietal junction is anatomically indistinct. Just as the post-central gyrus is perhaps the clearest anatomical margin of the lobe, the somatosensory auras with elementary sensory semiology stemming from that area are the most well-defined characteristics of PLE, while fast spread to other cortical areas elicits symptoms that may falsely localize [122–125]. Primary somatosensory cortex seizures often present with contralateral paresthesias, numbness, and tingling, though many different sensory phenomenon can occur, even within the same patient [124, 126]. The seizures may spread along the affected limb, mimicking the spread of ictal discharges through its homuncular representation on the sensory cortex. Somatosensory areas of the parietal operculum (second sensory area or SII) may also take part in sensory auras of PLE. In contrast to primary somatosensory cortex seizures, which are typified by contralateral focal sensory symptoms, SII seizures are characterized by more widespread, bilateral, axial symptoms of numbness, tingling, or pain [126, 127]. Ictal sensory phenomenon similar to SII semiology has also been described in areas of the parasagittal and inferior parietal cortex [128, 129].

While the sensory aspect of parietal seizures may be the most distinctive element, sensory phenomena do not accompany all PLE seizures, nor is somatosensory semiology specific for parietal lobe localization. In a study of 600 patients with drug-resistant epilepsy who consecutively

underwent video-EEG monitoring, somatosensory auras were reported in 75 (12.5%) [129]. Of those 75 patients reporting somatosensory auras, tingling was the most commonly reported symptom in 58 (77%), with other symptoms described as a sense of pulling in 6 (8%), numbness in 4 (5%), cold/heat in 4 (5%), pain in 2 (3%), and sense of movement in 1 (1%). Parietal lobe was the most common area of localization with a third (32%) of these patients showing MRI localizing in the parietal lobe, but lesions in the frontocentral (22%) and temporal (13%) regions were also found, the rest being non-lesional (20%) and near the vertex (6%) or frontal operculum (5%) [129].

Sensory phenomena are reported in roughly half of patients with drug-resistant PLE [122, 130, 131]. In Williamson et al.'s description of drug-resistant PLE, 4 of 11 patients showed contralateral sensory auras, while in a more recent series of 40 patients with isolated parietal resections, 20/40 patients had somatosensory auras [119]. Multiple types of aura are may be observed, with some patients reporting three or four different types [119, 132].

Different seizure types are reported with variable frequencies, prominent types being focal motor seizures [133] and complex partial seizures [122, 123]. Often more than one type of seizure in a single patient is reported [123, 133]. The largest series of PLE resections is reported from the Montreal Neurological Institute as the experience of the Institute from 1929 to 1988 [134, 135]. In these series, motor characteristics were common, as 57/82 (70%) of patients with non-tumoral and 28/34 (83%) with non-tumoral PLE reported focal motor seizures. Other common seizure characteristics were tonic posturing and oral-gestural automatisms. Todd's paralysis occurred in 22% of non-tumoral and 18% of tumoral PLE. Most patients showing tonic posturing (61%) had epileptogenic zones that included the superior parietal lobule (SPL), suggesting that seizures in the SPL may preferentially spread to supplementary motor cortex. On the other hand, patients with oral or gestural automatism were more likely to have epileptic zones that included the inferior parietal lobule (79% of such patients), suggesting preferential spread to temporal structures and the limbic system from these foci [120, 134, 135].

The localizing ability of scalp EEG in PLE is limited, with falsely localizing or non-localizing commonly reported, while MRI is invaluable for localization of lesions in the parietal lobe [122, 123, 132]. The larger series of PLE since MRI came into clinical use have found the most common pathologies underlying drug-resistant PLE to include low-grade tumors (such as gangliogliomas, dysembryoplastic neuroepithelial tumors, and oligodendrogliomas), cortical dysplasias, non-specific gliosis, and, less commonly, vascular lesions and hamartomas [119, 123, 133, 136]. The role of non-invasive imaging modalities including PET, ictal SPECT, and magnetoencephalography (MEG) or magnetic source imaging (MSI) is similar to that in other neocortical epilepsies [14, 15, 102]. MSI may be particularly valuable in picking up dipoles undetectable by scalp EEG and also has the advantage of being able to be used in conjunction with the measurement of somatosensory evoked potentials to map sensory cortex prior to surgery [137, 138]. Intracranial EEG, whether using subdural grids/strips, SEEG, or a combination of depth and subdural electrodes, remains the gold standard for localization of seizure-onset zone, particularly in cases of non-lesional PLE or when non-invasive imaging studies show discordance or multifocal localization.

Surgical Resection

Surgical resection of parietal lobe epileptogenic foci, like other neocortical epilepsy surgery, typically involves microsurgical removal of a lesion or localized focus in the cortex, as well as conservative corticectomy surrounding the epileptic lesion. The parietal lobe is essentially surrounded by eloquent tissue, which will limit extended resections. Because of the position, both abutting and containing indispensable cortex, the topic of multiple subpial resections (MST) should be addressed as an aspect of surgery in the parietal lobe. MST has been used as an additive technique in conjunction

to traditional resection when the epileptogenic zone extends into primary sensory cortex or language areas [139]. Eleven of 40 patients in the Bonn PLE surgery series and 8/28 in the series out of Yale used MST when lesions extended into eloquent cortex [123, 130]. A recent review of MST for medically refractory epilepsy found that seizure freedom was attained in 55.2% of resections that combined MST with resection and 23.9% of cases where MST was used in isolation [35]. The same study, however, also found a high rate of complications, with mono- or hemiparesis in 20% of patients; transient or permanent dysphagia in 12.3% and 1.9%, respectively; and permanent paresis in 6.6% of patients. This likely stems from the technique being aimed almost exclusively at eloquent cortex.

Intraoperative electrocorticography is used in many centers for evaluation and tailoring of the extent of resection [93, 104, 105, 123, 136]. Functional mapping may also be used as an intraoperative technique to avoid eloquent regions and limit postoperative deficits [140, 141]. The inferior parietal lobule is a tenuous landscape for the neurosurgeon to navigate, and functional stimulation mapping and electrocorticography may supply invaluable information when lesions in this region are excised.

Multilobar epilepsy in the posterior cortex may be approached with disconnective procedures to avoid resection, most often described in pediatric epilepsies. A detailed description of such a technique was published by Dorfer et al. [142]. Neuronavigation was used in all of these procedures; a subdural grid was used to localize the central sulcus using phase reversal for sensory evoked potentials. The disconnection involves corticotomy at the parietal operculum down to the ventricular trigone and then to the interhemispheric fissure and the isthmic splenium of the corpus callosum, where a callosotomy is performed. The fornix is sectioned at the level of the trigone. The corticotomy is then extended subpially through the parietal-temporal opercular cortex, to the posterior aspect of the insula, and then along the inferior insular sulcus through the temporal stem. The temporal stem disconnection is advanced anteriorly to the level of the choroid fissure, and finally the dorsal aspect of the amygdala is suctioned or resected along the border of the middle cerebral artery to complete the disconnection. Dorfer et al. reported seizure freedom in nine of ten patients in which the technique was used, with minimal unexpected complications. Similar techniques and strategies for posterior and multilobar disconnections have since been described [143, 144].

Surgical Outcomes

The largest reported series of parietal lobe epilepsy resections come from the Montreal Neurological Institute, consisting of 34 tumoral and 82 non-tumoral cases, performed in the pre-MRI era [134, 135]. Fifty-three percent of the tumoral and 46% of non-tumoral cases achieved Engel class I seizure freedom. In more recent series, the rates of seizure freedom range from 32% to 91% but are colored by a number of series with relatively few patients (Table 25.4).

Overall, the rates of seizure freedom are favorable, and complications are relatively low. Complications that are reported include Gerstmann syndrome (agraphia, acalculia, finger

Table 25.4 Parietal lobe epilepsy surgical series

Author	Year	No of patients	Engel class I (%)[a]
Williamson [122]	1992	11	91
Cascino [148]	1993	10	90
Salanova [134]	1995	34	75
Salanova [135]	1995	82	65
Boesebeck [93]	2002	21	60[b]
Kasowski [130]	2003	28	55
Kim [146]	2004	38	53
Kim [133]	2004	27	52
Gleissner [147]	2008	15	87
Binder [123]	2009	40	58
Jehi [114]	2009	32	53
Francione [119]	2015	40	75
Liava [149]	2016	59	64
Asadollahi [132]	2017	18	61
Ramantani [136]	2017	34	50

[a] Comparable measure of seizure freedom
[b] Includes temporal-occipital resections in the percent seizure-free, no breakdown

agnosia, and right-left disorientation) and hemisensory syndromes, from encroaching on the angular gyrus posterior laterally or the sensory cortex anteriorly [119, 123, 145]. Visual field deficits make up a considerable portion of the complication burden in some series as well, as it is not uncommon for epileptic zones to extend into the occipital lobe, such as in posterior cortex epilepsies [124, 136, 114, 146]. A study of neuropsychological outcomes in pediatric parietal lobe epilepsy found that between 39% and 66% of pediatric patients with PLE had preoperative cognitive impairments, including 29% with IQ in the range of intellectual disability, and more commonly disorders of attention [147]. Following surgery, the authors found improvements in attention and no significant decline in cognitive function. This same series, though with a small n (15 pediatric patients) reported an excellent seizure outcome, with 87% seizure-free at 1 year and 82% seizure-free at most recent follow-up (Fig. 25.3).

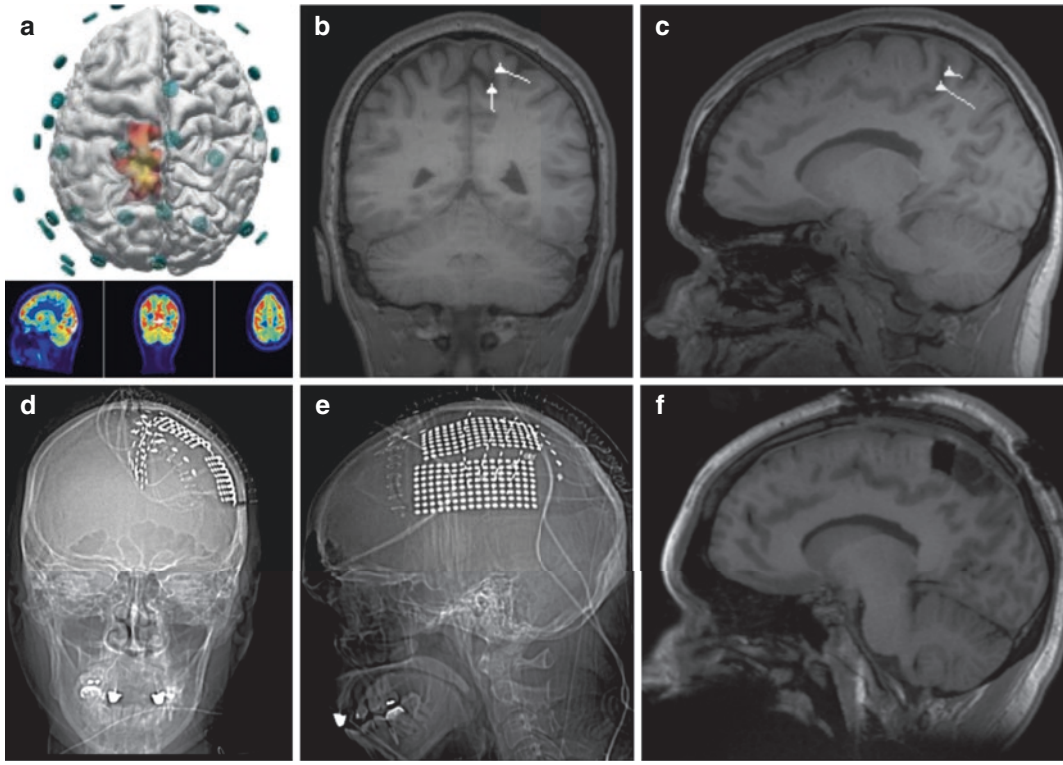

Fig. 25.3 Parietal lobe epilepsy. A 29-year-old woman with left centroparietal lobe seizures, over the somatosensory cortex, based on PET and EEG localization. Her aura consisted of a tingling moving up her right leg, sometimes accompanied by arm pain. This is followed by tonic extension and jerking of the leg. A second seizure type occurs without aura, proceeding from arm flinging directly to generalized tonic-clonic activity. (**a**) 3D reconstruction of dipole and distributed source estimates from scalp EEG show concordance of EEG and reduced radioisotope uptake on PET. (**b**, **c**) Magnetic source imaging (MSI) shows dipoles (*white arrows*) localized the left precuneus. (**d**, **e**) AP and lateral films following placement of intracranial electrodes. Motor mapping was carried out using direct cortical stimulation to find the central Rolandic sulcus. Four 10-contact-depth electrodes were placed under stereotactic guidance to sensory and motor cortices, with strips over the lateral and interhemispheric cortices. Care was taken to slide strips under the dural edge without resistance. Two 128-electrode grids were placed over the lateral cortex. (**f**) Excision of the postcentral gyrus was carried out with the patient awake and cooperating with motor-sensory mapping. Subpial dissection was extended to the pia of the central sulcus. Following surgery, the patient reported mild sensory deficits in her right leg ("5% decreased"). One year after surgery, the patient was seizure-free, and sensory deficits had resolved

Conclusion

Surgery for neocortical epilepsy has broader range of seizure control when compared with mesial temporal lobe resections. As is summarized here, though, advances in diagnostics, imaging, and experience have increased favorable outcomes from these procedures. While each lobe presents unique challenges in diagnostics and surgical technique, certain trends are evident from reviewing the current state of data on neocortical epilepsy. In general, well-circumscribed lesions discernable on MRI are associated with better rates of seizure control. Intracranial monitoring is often helpful or required for delineation of the epileptogenic zone for planning of surgical resection margins, especially when MRI does not reveal an obvious lesion correlating with non-invasive studies. Recording directly from the cortex, either with subdural electrodes, depth electrodes, or SEEG, is especially helpful in discerning involvement of mesial or deep structures. Contemporary series report low complication rates and effective seizure control when intracranial studies are indicated in surgery of the temporal, frontal, occipital, and parietal neocortex.

References

1. Walczak TS. Neocortical temporal lobe epilepsy: characterizing the syndrome. Epilepsia. 1995;36(7):633–5.
2. Pacia SV, Devinsky O, Perrine K, Ravdin L, Luciano D, Vazquez B, et al. Clinical features of neocortical temporal lobe epilepsy. Ann Neurol. 1996;40(5):724–30.
3. O'Brien TJ, Kilpatrick C, Murrie V, Vogrin S, Morris K, Cook MJ. Temporal lobe epilepsy caused by mesial temporal sclerosis and temporal neocortical lesions: a clinical and electroencephalographic study of 46 pathologically proven cases. Brain. 1996;119(6):2133–41.
4. Pfänder M, Arnold S, Henkel A, Weil S, Noachtar S. Findings differentiating mesial from neocortical temporal. Epileptic Disord. 2002;4(3):189–95.
5. Burgerman RS, Sperling MR, French JA, Saykin AJ, O'Connor MJ. Comparison of mesial versus neocortical onset temporal lobe seizures: neurodiagnostic findings and surgical outcome. Epilepsia. 1995;36(7):662–70.
6. Maillard L, Vignal JP, Gavaret M, Guye M, Biraben A, McGonigal A, et al. Semiologic and electrophysiologic correlations in temporal lobe seizure subtypes. Epilepsia. 2004;45(12):1590–9.
7. Englot DJ, Han SJ, Berger MS, Barbaro NM, Chang EF. Extent of surgical resection predicts seizure freedom in low-grade temporal lobe brain tumors. Neurosurgery. 2011;70(4):921–8.
8. Lee SA, Spencer DD, Spencer SS. Intracranial EEG seizure-onset patterns in neocortical epilepsy. Epilepsia. 2000;41(3):297–307.
9. Ochoa JG, Hentgarden D, Paulzak A, Ogden M, Pryson R, Lamle M, et al. Subtle pathological changes in neocortical temporal lobe epilepsy. Epilepsy Behav. 2017;71:17–22.
10. Lee S, Yun C, Oh J, Nam H, Jung S, Paeng J, et al. Intracranial ictal onset zone in nonlesional lateral temporal lobe epilepsy on scalp ictal EEG. Neurology. 2003;61(6):757–64.
11. Lee SK, Lee SY, Kim KK, Hong KS, Lee DS, Chung CK. Surgical outcome and prognostic factors of cryptogenic neocortical epilepsy. Ann Neurol. 2005;58(4):525–32.
12. Yun CH, Lee SK, Lee SY, Kim KK, Jeong SW, Chung CK. Prognostic factors in neocortical epilepsy surgery: multivariate analysis. Epilepsia. 2006;47(3):574–9.
13. Lee SK, Kim JY, Hong KS, Nam HW, Park SH, Chung CK. The clinical usefulness of ictal surface EEG in neocortical epilepsy. Epilepsia. 2000;41(11):1450–5.
14. Knowlton RC, Elgavish RA, Bartolucci A, Ojha B, Limdi N, Blount J, et al. Functional imaging: II. Prediction of epilepsy surgery outcome. Ann Neurol. 2008;64(1):35–41.
15. Knowlton RC, Elgavish RA, Limdi N, Bartolucci A, Ojha B, Blount J, et al. Functional imaging: I. Relative predictive value of intracranial electroencephalography. Ann Neurol. 2008;64(1):25–34.
16. Spencer D, Nguyen DK, Sivaraju A. Invasive EEG in presurgical evaluation of epilepsy. In: Shovon S, Fish D, ed. The Treatment of Epilepsy: second edition. Malden, MA: Blackwell Science Ltd; 2004. 609–35.
17. Van Roost D, Solymosi L, Schramm J, van Oosterwyck B, Eiger CE. Depth electrode implantation in the length axis of the hippocampus for the presurgical evaluation of medial temporal lobe epilepsy: a computed tomography-based stereotactic insertion technique and its accuracy. Neurosurgery. 1998;43(4):819–26.
18. Cohen-Gadol AA, Spencer DD. Use of an anteromedial subdural strip electrode in the evaluation of medial temporal lobe epilepsy. J Neurosurg. 2003;99(5):921–3.
19. Arya R, Mangano FT, Horn PS, Holland KD, Rose DF, Glauser TA. Adverse events related to extraoperative invasive EEG monitoring with subdural grid electrodes: a systematic review and meta-analysis. Epilepsia. 2013;54(5):828–39.

20. Cardinale F, Cossu M, Castana L, Casaceli G, Schiariti MP, Miserocchi A, et al. Stereoelectroencephalography: surgical methodology, safety, and stereotactic application accuracy in 500 procedures. Neurosurgery. 2012;72(3): 353–66.
21. Schramm J, Clusmann H. The surgery of epilepsy. Neurosurgery.2008;62(suppl_2):SHC-463–SHC-81.
22. Ogiwara H, Nordli DR, DiPatri AJ, Alden TD, Bowman RM, Tomita T. Pediatric epileptogenic gangliogliomas: seizure outcome and surgical results. J Neurosurg Pediatr. 2010;5(3):271–6.
23. Giulioni M, Rubboli G, Marucci G, Martinoni M, Volpi L, Michelucci R, et al. Seizure outcome of epilepsy surgery in focal epilepsies associated with temporomesial glioneuronal tumors: lesionectomy compared with tailored resection. J Neurosurg. 2009;111(6):1275–82.
24. Jooma R, Yeh H-S, Privitera MD, Gartner M. Lesionectomy versus electrophysiologically guided resection for temporal lobe tumors manifesting with complex partial seizures. J Neurosurg. 1995;83(2):231–6.
25. Bilginer B, Yalnızoglu D, Soylemezoglu F, Turanlı G, Cila A, Topçu M, et al. Surgery for epilepsy in children with dysembryoplastic neuroepithelial tumor: clinical spectrum, seizure outcome, neuroradiology, and pathology. Childs Nerv Syst. 2009;25(4):485.
26. Jobst BC, Cascino GD. Resective epilepsy surgery for drug-resistant focal epilepsy: a review. JAMA. 2015;313(3):285–93.
27. Téllez-Zenteno JF, Dhar R, Hernandez-Ronquillo L, Wiebe S. Long-term outcomes in epilepsy surgery: antiepileptic drugs, mortality, cognitive and psychosocial aspects. Brain. 2006;130(2):334–45.
28. Helmstaedter C, Elger C, Hufnagel A, Zentner J, Schramm J. Different effects of left anterior temporal lobectomy, selective amygdalohippocampectomy, and temporal cortical lesionectomy on verbal learning, memory, and recognition. J Epilepsy. 1996;9(1):39–45.
29. Schramm J, Kral T, Grunwald T, Blümcke I. Surgical treatment for neocortical temporal lobe epilepsy: clinical and surgical aspects and seizure outcome. J Neurosurg. 2001;94(1):33–42.
30. Kim DW, Kim HK, Lee SK, Chu K, Chung CK. Extent of neocortical resection and surgical outcome of epilepsy: intracranial EEG analysis. Epilepsia. 2010;51(6):1010–7.
31. Clusmann H. Neocortical resections. In: Fountas K, Kapsalaki EZ, editors. Epilepsy surgery and intrinsic brain tumor surgery: a practical atlas. Cham: Springer; 2019. p. 147–63.
32. Chang EF, Clark A, Smith JS, Polley M-Y, Chang SM, Barbaro NM, et al. Functional mapping–guided resection of low-grade gliomas in eloquent areas of the brain: improvement of long-term survival. J Neurosurg. 2011;114(3):566–73.
33. Sanai N, Mirzadeh Z, Berger MS. Functional outcome after language mapping for glioma resection. N Engl J Med. 2008;358(1):18–27.
34. Spencer SS, Schramm J, Wyler A, O'connor M, Orbach D, Krauss G, et al. Multiple subpial transection for intractable partial epilepsy: an international meta-analysis. Epilepsia. 2002;43(2):141–5.
35. Rolston JD, Deng H, Wang DD, Englot DJ, Chang EF. Multiple subpial transections for medically refractory epilepsy: a disaggregated review of patient-level data. Neurosurgery. 2017;82(5):613–20.
36. Andrews JP, Gummadavelli A, Farooque P, Bonito J, Arencibia C, Blumenfeld H, et al. Association of seizure spread with surgical failure in epilepsy. JAMA Neurol. 2019;76(4):462–9.
37. Jung WY, Pacia SV, Devinsky O. Neocortical temporal lobe epilepsy: intracranial EEG features and surgical outcome. J Clin Neurophysiol. 1999; 16(5):419.
38. Janszky J, Pannek H, Fogarasi A, Bone B, Schulz R, Behne F, et al. Prognostic factors for surgery of neocortical temporal lobe epilepsy. Seizure. 2006;15(2):125–32.
39. Doležalová I, Brázdil M, Chrastina J, Hemza J, Hermanová M, Janoušová E, et al. Differences between mesial and neocortical magnetic-resonance-imaging-negative temporal lobe epilepsy. Epilepsy Behav. 2016;61:21–6.
40. Kutsy RL, Farrell DF, Ojemann GA. Ictal patterns of neocortical seizures monitored with intracranial electrodes: correlation with surgical outcome. Epilepsia. 1999;40(3):257–66.
41. Salanova V, Quesney LF, Rasmussen T, Andermann F, Olivier A. Reevaluation of surgical failures and the role of reoperation in 39 patients with frontal lobe epilepsy. Epilepsia. 1994;35(1):70–80.
42. Tellez-Zenteno JF, Dhar R, Wiebe S. Long-term seizure outcomes following epilepsy surgery: a systematic review and meta-analysis. Brain. 2005;128(Pt 5):1188–98.
43. Laskowitz DT, Sperling MR, French JA, O'connor MJ. The syndrome of frontal lobe epilepsy: characteristics and surgical management. Neurology. 1995;45(4):780–7.
44. Hosking PG. Surgery for frontal lobe epilepsy. Seizure. 2003;12(3):160–6.
45. Williamson PD. Frontal lobe seizures. Problems of diagnosis and classification. Adv Neurol. 1992;57:289–309.
46. Salanova V, Morris H, Van Ness P, Kotagal P, Wyllie E, Lüders H. Frontal lobe seizures: electroclinical syndromes. Epilepsia. 1995;36(1):16–24.
47. Englot DJ, Wang DD, Rolston JD, Shih TT, Chang EF. Rates and predictors of long-term seizure freedom after frontal lobe epilepsy surgery: a systematic review and meta-analysis. J Neurosurg. 2012;116(5):1042–8.
48. Williamson PD, Spencer DD, Spencer SS, Novelly RA, Mattson RH. Complex partial seizures of frontal lobe origin. Ann Neurol. 1985;18(4):497–504.

49. Holtkamp M, Sharan A, Sperling MR. Intracranial EEG in predicting surgical outcome in frontal lobe epilepsy. Epilepsia. 2012;53(10):1739–45.
50. Bonini F, McGonigal A, Trébuchon A, Gavaret M, Bartolomei F, Giusiano B, et al. Frontal lobe seizures: from clinical semiology to localization. Epilepsia. 2014;55(2):264–77.
51. Koechlin E, Ody C, Kouneiher F. The architecture of cognitive control in the human prefrontal cortex. Science. 2003;302(5648):1181–5.
52. Nachev P, Kennard C, Husain M. Functional role of the supplementary and pre-supplementary motor areas. Nat Rev Neurosci. 2008;9(11):856.
53. Kim Y-H, Kim CH, Kim JS, Lee SK, Han JH, Kim C-Y, et al. Risk factor analysis of the development of new neurological deficits following supplementary motor area resection. J Neurosurg. 2013;119(1):7–14.
54. Rosenberg K, Nossek E, Liebling R, Fried I, Shapira-Lichter I, Hendler T, et al. Prediction of neurological deficits and recovery after surgery in the supplementary motor area: a prospective study in 26 patients. J Neurosurg. 2010;113(6):1152–63.
55. Duffau H, Lopes M, Denvil D, Capelle L. Delayed onset of the supplementary motor area syndrome after surgical resection of the mesial frontal lobe: a time course study using intraoperative mapping in an awake patient. Stereotact Funct Neurosurg. 2001;76(2):74–82.
56. Bozkurt B, Yagmurlu K, Middlebrooks EH, Karadag A, Ovalioglu TC, Jagadeesan B, et al. Microsurgical and tractographic anatomy of the supplementary motor area complex in humans. World Neurosurg. 2016;95:99–107.
57. Chang EF, Breshears JD, Raygor KP, Lau D, Molinaro AM, Berger MS. Stereotactic probability and variability of speech arrest and anomia sites during stimulation mapping of the language dominant hemisphere. J Neurosurg. 2017;126(1):114–21.
58. Ljunggren S, Andersson-Roswall L, Rydenhag B, Samuelsson H, Malmgren K. Cognitive outcome two years after frontal lobe resection for epilepsy–a prospective longitudinal study. Seizure. 2015;30:50–6.
59. Rasmussen T. Tailoring of cortical excisions for frontal lobe epilepsy. Can J Neurol Sci. 1991;18(S4):606–10.
60. Rougier A, Dartigues J-F, Commenges D, Claverie B, Loiseau P, Cohadon F. A longitudinal assessment of seizure outcome and overall benefit from 100 cortectomies for epilepsy. J Neurol Neurosurg Psychiatry. 1992;55(9):762–7.
61. Talairach J, Bancaud J, Bonis A, Szikla G, Trottier S, Vignal J, et al. Surgical therapy for frontal epilepsies. Adv Neurol. 1992;57:707–32.
62. Fish DR, Smith SJ, Quesney LF, Andermann F, Rasmussen T. Surgical treatment of children with medically intractable frontal or temporal lobe epilepsy: results and highlights of 40 years' experience. Epilepsia. 1993;34(2):244–7.
63. Smith J, Lee M, King D, Murro AM, Park YD, Lee GP, et al. Results of lesional vs. nonlesional frontal lobe epilepsy surgery. Stereotact Funct Neurosurg. 1997;69(1–4):202–9.
64. Swartz B, Delgado-Escueta A, Walsh G, Rich J, Dwan P, DeSalles A, et al. Surgical outcomes in pure frontal lobe epilepsy and foci that mimic them. Epilepsy Res. 1998;29(2):97–108.
65. Wennberg R, Quesney LF, Lozano A, Olivier A, Rasmussen T. Role of electrocorticography at surgery for lesion-related frontal lobe epilepsy. Can J Neurol Sci. 1999;26(1):33–9.
66. Ferrier C, Engelsman J, Alarcon G, Binnie C, Polkey C. Prognostic factors in presurgical assessment of frontal lobe epilepsy. J Neurol Neurosurg Psychiatry. 1999;66(3):350–6.
67. Mosewich R, So EL, O'brien T, Cascino GD, Sharbrough F, Mars W, et al. Factors predictive of the outcome of frontal lobe epilepsy surgery. Epilepsia. 2000;41(7):843–9.
68. Jobst BC, Siegel AM, Thadani VM, Roberts DW, Rhodes HC, Williamson PD. Intractable seizures of frontal lobe origin: clinical characteristics, localizing signs, and results of surgery. Epilepsia. 2000;41(9):1139–52.
69. Zaatreh MM, Spencer DD, Thompson JL, Blumenfeld H, Novotny EJ, Mattson RH, et al. Frontal lobe tumoral epilepsy: clinical, neurophysiologic features and predictors of surgical outcome. Epilepsia. 2002;43(7):727–33.
70. Kloss S, Pieper T, Pannek H, Holthausen H, Tuxhorn I. Epilepsy surgery in children with focal cortical dysplasia (FCD): results of long-term seizure outcome. Neuropediatrics. 2002;33(01):21–6.
71. Luyken C, Blümcke I, Fimmers R, Urbach H, Elger CE, Wiestler OD, et al. The Spectrum of long-term epilepsy–associated tumors: long-term seizure and tumor outcome and neurosurgical aspects. Epilepsia. 2003;44(6):822–30.
72. Tigaran S, Cascino GD, McClelland RL, So EL, Richard MW. Acute postoperative seizures after frontal lobe cortical resection for intractable partial epilepsy. Epilepsia. 2003;44(6):831–5.
73. Jeha LE, Najm I, Bingaman W, Dinner D, Widdess-Walsh P, Lüders H. Surgical outcome and prognostic factors of frontal lobe epilepsy surgery. Brain. 2007;130(2):574–84.
74. Lee JJ, Lee SK, Lee S-y, Park K-I, Kim DW, Lee DS, et al. Frontal lobe epilepsy: clinical characteristics, surgical outcomes and diagnostic modalities. Seizure. 2008;17(6):514–23.
75. Elsharkawy AE, Alabbasi AH, Pannek H, Schulz R, Hoppe M, Pahs G, et al. Outcome of frontal lobe epilepsy surgery in adults. Epilepsy Res. 2008;81(2–3):97–106.
76. Kim CH, Chung CK, Lee SK. Longitudinal change in outcome of frontal lobe epilepsy surgery. Neurosurgery. 2010;67(5):1222–9.
77. Lazow SP, Thadani VM, Gilbert KL, Morse RP, Bujarski KA, Kulandaivel K, et al. Outcome of frontal lobe epilepsy surgery. Epilepsia. 2012;53(10):1746–55.

78. Ramantani G, Kadish NE, Mayer H, Anastasopoulos C, Wagner K, Reuner G, et al. Frontal lobe epilepsy surgery in childhood and adolescence: predictors of long-term seizure freedom, overall cognitive and adaptive functioning. Neurosurgery. 2017;83(1):93–103.
79. Bonini F, McGonigal A, Scavarda D, Carron R, Régis J, Dufour H, et al. Predictive factors of surgical outcome in frontal lobe epilepsy explored with stereoelectroencephalography. Neurosurgery. 2017;83(2):217–25.
80. Xu C, Yu T, Zhang G, Wang Y, Li Y. Prognostic factors and longitudinal change in long-term outcome of frontal lobe epilepsy surgery. World Neurosurg. 2019;121:e32–e8.
81. Morace R, Casciato S, Quarato PP, Mascia A, D'Aniello A, Grammaldo LG, et al. Long-term seizure outcome in frontal lobe epilepsy surgery. Epilepsy Behav. 2019;90:93–8.
82. Bartolomei F, Chauvel P, Wendling F. Epileptogenicity of brain structures in human temporal lobe epilepsy: a quantified study from intracerebral EEG. Brain. 2008;131(7):1818–30.
83. Gowers WR. Cases of cerebral tumour illustrating diagnosis and localisation. Lancet. 1879;i:363–5.
84. Salanova V, Andermann F, Oliver A, Rasmussen T, Quesney L. Occipital lobe epilepsy: electroclinical manifestations, electrocorticography, cortical stimulation and outcome in 42 patients treated between 1930 and 1991: surgery of occipital lobe epilepsy. Brain. 1992;115(6):1655–80.
85. Williamson P, Thadani V, Darcey T, Spencer D, Spencer S, Mattson R. Occipital lobe epilepsy: clinical characteristics, seizure spread patterns, and results of surgery. Ann Neurol. 1992;31(1):3–13.
86. Tandon N, Alexopoulos AV, Warbel A, Najm IM, Bingaman WE. Occipital epilepsy: spatial categorization and surgical management. J Neurosurg. 2009;110(2):306–18.
87. Yang P-F, Jia Y-Z, Lin Q, Mei Z, Chen Z-Q, Zheng Z-Y, et al. Intractable occipital lobe epilepsy: clinical characteristics, surgical treatment, and a systematic review of the literature. Acta Neurochir. 2015;157(1):63–75.
88. Jobst BC, Williamson PD, Thadani VM, Gilbert KL, Holmes GL, Morse RP, et al. Intractable occipital lobe epilepsy: clinical characteristics and surgical treatment. Epilepsia. 2010;51(11):2334–7.
89. Doud A, Julius A, Ransom CB. Visual phenomena in occipital lobe epilepsy: "It's Beautiful!". JAMA Neurol. 2018;75(9):1146–7.
90. Bien CG, Benninger FO, Urbach H, Schramm J, Kurthen M, Elger CE. Localizing value of epileptic visual auras. Brain. 2000;123(Pt 2):244–53.
91. Dalmagro CL, Bianchin MM, Velasco TR, Alexandre V Jr, Walz R, Terra-Bustamante VC, et al. Clinical features of patients with posterior cortex epilepsies and predictors of surgical outcome. Epilepsia. 2005;46(9):1442–9.
92. Marchi A, Bonini F, Lagarde S, McGonigal A, Gavaret M, Scavarda D, et al. Occipital and occipital "plus" epilepsies: a study of involved epileptogenic networks through SEEG quantification. Epilepsy Behav. 2016;62:104–14.
93. Boesebeck F, Schulz R, May T, Ebner A. Lateralizing semiology predicts the seizure outcome after epilepsy surgery in the posterior cortex. Brain. 2002;125(10):2320–31.
94. Appel S, Sharan A, Tracy J, Evans J, Sperling M. A comparison of occipital and temporal lobe epilepsies. Acta Neurol Scand. 2015;132(4):284–90.
95. Yamamoto T, Hamasaki T, Nakamura H, Yamada K. Improvement of visual field defects after focal resection for occipital lobe epilepsy: case report. J Neurosurg. 2018;128(3):862–6.
96. Binder DK, Von Lehe M, Kral T, Bien CG, Urbach H, Schramm J, et al. Surgical treatment of occipital lobe epilepsy. J Neurosurg. 2008;109(1):57–69.
97. Ibrahim GM, Fallah A, Albert GW, Withers T, Otsubo H, Ochi A, et al. Occipital lobe epilepsy in children: characterization, evaluation and surgical outcomes. Epilepsy Res. 2012;99(3):335–45.
98. Desai A, Bekelis K, Thadani VM, Roberts DW, Jobst BC, Duhaime AC, et al. Interictal PET and ictal subtraction SPECT: sensitivity in the detection of seizure foci in patients with medically intractable epilepsy. Epilepsia. 2013 Feb;54(2):341–50.
99. Mamelak AN, Lopez N, Akhtari M, Sutherling WW. Magnetoencephalography-directed surgery in patients with neocortical epilepsy. J Neurosurg. 2002;97(4):865–73.
100. Sutherling W, Mamelak A, Thyerlei D, Maleeva T, Minazad Y, Philpott L, et al. Influence of magnetic source imaging for planning intracranial EEG in epilepsy. Neurology. 2008;71(13):990–6.
101. Knowlton RC, Razdan SN, Limdi N, Elgavish RA, Killen J, Blount J, et al. Effect of epilepsy magnetic source imaging on intracranial electrode placement. Ann Neurol. 2009;65(6):716–23.
102. Knowlton RC. The role of FDG-PET, ictal SPECT, and MEG in the epilepsy surgery evaluation. Epilepsy Behav. 2006;8(1):91–101.
103. Harward SC, Chen WC, Rolston JD, Haglund MM, Englot DJ. Seizure outcomes in occipital lobe and posterior quadrant epilepsy surgery: a systematic review and meta-analysis. Neurosurgery. 2017;82(3):350–8.
104. Chang EF, Christie C, Sullivan JE, Garcia PA, Tihan T, Gupta N, et al. Seizure control outcomes after resection of dysembryoplastic neuroepithelial tumor in 50 patients. J Neurosurg Pediatr. 2010;5(1):123–30.
105. Dorward IG, Titus JB, Limbrick DD, Johnston JM, Bertrand ME, Smyth MD. Extratemporal, nonlesional epilepsy in children: postsurgical clinical and neurocognitive outcomes. J Neurosurg Pediatr. 2011;7(2):179–88.
106. Rasmussen T. Surgery for epilepsy arising in regions other than the temporal and frontal lobes. Adv Neurol. 1975;8:207.
107. Wyler A, Hermann B. Surgical treatment of occipital lobe epileptogenic foci. Epilepsia. 1990;31:638.

108. Blume WT, Whiting SE, Girvin JP. Epilepsy surgery in the posterior cortex. Ann Neurol. 1991;29(6):638–45.
109. Bidziński J, Bacia T, Ruzikowski E. The results of the surgical treatment of occipital lobe epilepsy. Acta Neurochir. 1992;114(3–4):128–30.
110. Aykut-Bingol C, Bronen RA, Kim JH, Spencer DD, Spencer SS. Surgical outcome in occipital lobe epilepsy: implications for pathophysiology. Ann Neurol. 1998;44(1):60–9.
111. Sturm JW, Newton MR, Chinvarun Y, Berlangieri SU, Berkovic SF. Ictal SPECT and interictal PET in the localization of occipital lobe epilepsy. Epilepsia. 2000;41(4):463–6.
112. Kun Lee S, Young Lee S, Kim DW, Soo Lee D, Chung CK. Occipital lobe epilepsy: clinical characteristics, surgical outcome, and role of diagnostic modalities. Epilepsia. 2005;46(5):688–95.
113. Caicoya AG, Macarrón J, Albísua J, Serratosa JM. Tailored resections in occipital lobe epilepsy surgery guided by monitoring with subdural electrodes: characteristics and outcome. Epilepsy Res. 2007;77(1):1–10.
114. Jehi LE, O'Dwyer R, Najm I, Alexopoulos A, Bingaman W. A longitudinal study of surgical outcome and its determinants following posterior cortex epilepsy surgery. Epilepsia. 2009;50(9):2040–52.
115. Sarkis RA, Jehi L, Najm IM, Kotagal P, Bingaman WE. Seizure outcomes following multilobar epilepsy surgery. Epilepsia. 2012;53(1):44–50.
116. Heo W, Kim JS, Chung CK, Lee SK. Relationship between cortical resection and visual function after occipital lobe epilepsy surgery. J Neurosurg. 2018;129(2):524–32.
117. Clemons TE, Chew EY, Bressler SB. McBee W. National Eye Institute visual function questionnaire in the age-related eye disease study (AREDS): AREDS report no. 10. Arch Ophthalmol. 2003;121(2):211–7.
118. Heo JW, Yoon HS, Shin JP, Moon SW, Chin HS, Kwak HW. A validation and reliability study of the Korean version of national eye institute visual function questionnaire 25. J Korean Ophthalmol Soc. 2010;51(10):1354–67.
119. Francione S, Liava A, Mai R, Nobili L, Sartori I, Tassi L, et al. Drug-resistant parietal epilepsy: polymorphic ictal semiology does not preclude good post-surgical outcome. Epileptic Disord. 2015;17(1):32–46.
120. Salanova V. Parietal lobe epilepsy. Handb Clin Neurol. 2018;151:413–25.
121. Salanova V. Parietal lobe epilepsy. J Clin Neurophysiol. 2012;29(5):392–6.
122. Williamson P, Boon P, Thadani V, Darcey T, Spencer D, Spencer S, et al. Parietal lobe epilepsy: diagnostic considerations and results of surgery. Ann Neurol. 1992;31(2):193–201.
123. Binder DK, Podlogar M, Clusmann H, Bien C, Urbach H, Schramm J, et al. Surgical treatment of parietal lobe epilepsy. J Neurosurg. 2009;110(6):1170–8.
124. Sveinbjornsdottir S, Duncan J. Parietal and occipital lobe epilepsy: a review. Epilepsia. 1993;34(3):493–521.
125. Foldvary N, Klem G, Hammel J, Bingaman W, Najm I, Lüders H. The localizing value of ictal EEG in focal epilepsy. Neurology. 2001;57(11):2022–8.
126. Mauguiere F, Courjon J. Somatosensory epilepsy: a review of 127 cases. Brain. 1978;101(2):307–32.
127. Blume WT, Jones DC, Young GB, Gravin JP, Mclachlan RS. Seizures involving secondary sensory and related areas. Brain. 1992;115(5):1509–20.
128. Yamamoto J, Ikeda A, Matsuhashi M, Satow T, Takayama M, Ohara S, et al. Seizures arising from the inferior parietal lobule can show ictal semiology of the second sensory seizure (SII seizure). J Neurol Neurosurg Psychiatry. 2003;74(3):367–9.
129. Tuxhorn IEB. Somatosensory auras in focal epilepsy: a clinical, video EEG and MRI study. Seizure. 2005;14(4):262–8.
130. Kasowski HJ, Stoffman MR, Spencer SS, Spencer DD. Surgical management of parietal lobe epilepsy. Adv Neurol. 2003;93:347–56.
131. Pilipović-Dragović S, Ristić AJ, Bukumirić Z, Trajković G, Sokić D. Long-term seizure outcome following epilepsy surgery in the parietal lobe: a meta-analysis. Epileptic Disord. 2018;20(2):116–22.
132. Asadollahi M, Sperling MR, Rabiei AH, Asadi-Pooya AA. Drug-resistant parietal lobe epilepsy: clinical manifestations and surgery outcome. Epileptic Disord. 2017;19(1):35–9.
133. Kim DW, Lee SK, Yun CH, Kim KK, Lee DS, Chung CK, et al. Parietal lobe epilepsy: the semiology, yield of diagnostic workup, and surgical outcome. Epilepsia. 2004;45(6):641–9.
134. Salanova V, Andermann F, Rasmussen T, Olivier A, Quesney L. Tumoural parietal lobe epilepsy clinical manifestations and outcome in 34 patients treated between 1934 and 1988. Brain. 1995;118(5):1289–304.
135. Salanova V, Andermann F, Rasmussen T, Olivier A, Quesney L. Parietal lobe epilepsy clinical manifestations and outcome in 82 patients treated surgically between 1929 and 1988. Brain. 1995;118(3):607–27.
136. Ramantani G, Stathi A, Brandt A, Strobl K, Schubert-Bast S, Wiegand G, et al. Posterior cortex epilepsy surgery in childhood and adolescence: predictors of long-term seizure outcome. Epilepsia. 2017;58(3):412–9.
137. Roberts TP, Tran Q, Ferrari P, Berger MS. Increased somatosensory neuromagnetic fields ipsilateral to lesions in neurosurgical patients. Neuroreport. 2002;13(5):699–702.
138. Kakisaka Y, Iwasaki M, Alexopoulos AV, Enatsu R, Jin K, Wang ZI, et al. Magnetoencephalography in fronto-parietal opercular epilepsy. Epilepsy Res. 2012;102(1–2):71–7.
139. Morrell F, Whisler WW, Bleck TP. Multiple subpial transection: a new approach to the surgical treatment of focal epilepsy. J Neurosurg. 1989;70(2):231–9.
140. Maldonado IL, Moritz-Gasser S, de Champfleur NM, Bertram L, Moulinie G, Duffau H. Surgery for gliomas involving the left inferior parietal lobule: new insights into the functional anatomy

provided by stimulation mapping in awake patients. J Neurosurg. 2011;115(4):770–9.
141. Rolland A, Herbet G, Duffau H. Awake surgery for gliomas within the right inferior parietal lobule: new insights into the functional connectivity gained from stimulation mapping and surgical implications. World Neurosurg. 2018;112:e393–406.
142. Dorfer C, Czech T, Muhlebner-Fahrngruber A, Mert A, Groppel G, Novak K, et al. Disconnective surgery in posterior quadrantic epilepsy: experience in a consecutive series of 10 patients. Neurosurg Focus. 2013;34(6):E10.
143. Yang PF, Mei Z, Lin Q, Pei JS, Zhang HJ, Zhong ZH, et al. Disconnective surgery in posterior quadrantic epilepsy: a series of 12 paediatric patients. Epileptic Disord. 2014;16(3):296–304.
144. Santos MV, Machado HR. Extratemporal disconnective procedures for the treatment of epilepsy in children. Epilepsia. 2017;58:28–34.
145. Olivier A, Boling W Jr. Surgery of parietal and occipital lobe epilepsy. Adv Neurol. 2000;84:533–75.
146. Kim CH, Chung CK, Lee SK, Lee YK, Chi JG. Parietal lobe epilepsy: surgical treatment and outcome. Stereotact Funct Neurosurg. 2004;82(4):175–85.
147. Gleissner U, Kuczaty S, Clusmann H, Elger CE, Helmstaedter C. Neuropsychological results in pediatric patients with epilepsy surgery in the parietal cortex. Epilepsia. 2008;49(4):700–4.
148. Cascino GD, Hulihan JF, Sharbrough FW, Kelly PJ. Parietal lobe lesional epilepsy: electroclinical correlation and operative outcome. Epilepsia. 1993;34(3):522–7.
149. Liava A, Mai R, Cardinale F, Tassi L, Casaceli G, Gozzo F, et al. Epilepsy surgery in the posterior part of the brain. Epilepsy Behav. 2016;64:273–82.

Suggested Reading

Binder DK, Podlogar M, Clusmann H, et al. Surgical treatment of parietal lobe epilepsy. J Neurosurg. 2009;110(6):1170–8.

Binder DK, Von Lehe M, Kral T, et al. Surgical treatment of occipital lobe epilepsy. J Neurosurg. 2008;109(1):57–69.

Cascino GD, Hulihan JF, Sharbrough FW, Kelly PJ. Parietal lobe lesional epilepsy: electroclinical correlation and operative outcome. Epilepsia. 1993;34(3):522–7.

Desai A, Jobst BC, Thadani VM, et al. Stereotactic depth electrode investigation of the insula in the evaluation of medically intractable epilepsy. J Neurosurg. 2011;114(4):1176–86.

Englot DJ, Breshears JD, Sun PP, Chang EF, Auguste KI. Seizure outcomes after resective surgery for extra-temporal lobe epilepsy in pediatric patients. J Neurosurg Pediatr. 2013;12(2):126–33.

Englot DJ, Wang DD, Rolston JD, Shih TT, Chang EF. Rates and predictors of long-term seizure freedom after frontal lobe epilepsy surgery: a systematic review and meta-analysis. J Neurosurg. 2012;116(5):1042–8.

Harward SC, Chen WC, Rolston JD, Haglund MM, Englot DJ. Seizure outcomes in occipital lobe and posterior quadrant epilepsy surgery: a systematic review and meta-analysis. Neurosurgery. 2017;82(3):350–8.

Isnard J, Guenot M, Sindou M, Mauguiere F. Clinical manifestations of insular lobe seizures: a stereo-electroencephalographic study. Epilepsia. 2004;45(9):1079–90.

Jeha LE, Najm I, Bingaman W, Dinner D, Widdess-Walsh P, Luders H. Surgical outcome and prognostic factors of frontal lobe epilepsy surgery. Brain. 2007;130(Pt 2):574–584.17.

Jobst BC, Williamson PD, Thadani VM, et al. Intractable occipital lobe epilepsy: clinical characteristics and surgical treatment. Epilepsia. 2010;51(11):2334–7.

Kasowski HJ, Stoffman MR, Spencer SS, Spencer DD. Surgical management of parietal lobe epilepsy. Adv Neurol. 2003;93:347–56.

Lazow SP, Thadani VM, Gilbert KL, et al. Outcome of frontal lobe epilepsy surgery. Epilepsia. 2012;53(10):1746–55.

Lee SK, Lee SY, Kim KK, Hong KS, Lee DS, Chung CK. Surgical outcome and prognostic factors of cryptogenic neocortical epilepsy. Ann Neurol. 2005;58(4):525–32.

Rolston JD, Deng H, Wang DD, Englot DJ, Chang EF. Multiple subpial transections for medically refractory epilepsy: a disaggregated review of patient-level data. Neurosurgery. 2017;82(5):613–20.

Schramm J, Kral T, Grunwald T, Blümcke I. Surgical treatment for neocortical temporal lobe epilepsy: clinical and surgical aspects and seizure outcome. J Neurosurg. 2001;94(1):33–42.

Schramm J, Kral T, Kurthen M, Blumcke I. Surgery to treat focal frontal lobe epilepsy in adults. Neurosurgery. 2002;51(3):644–54; discussion 654-645.

Spencer D, Nguyen DK, Sivaraju A. Invasive EEG in presurgical evaluation of epilepsy. Treat Epilepsy. 2015:733–55.

Sveinbjornsdottir S, Duncan JS. Parietal and occipital lobe epilepsy: a review. Epilepsia. 1993;34(3):493–521.

Tandon N, Alexopoulos AV, Warbel A, Najm IM, Bingaman WE. Occipital epilepsy: spatial categorization and surgical management. J Neurosurg. 2009;110(2):306–18.

von Lehe M, Wellmer J, Urbach H, Schramm J, Elger CE, Clusmann H. Insular lesionectomy for refractory epilepsy: management and outcome. Brain. 2009;132(Pt 4):1048–56.

Williamson PD, Boon PA, Thadani VM, et al. Parietal lobe epilepsy: diagnostic considerations and results of surgery. Ann Neurol. 1992;31(2):193–201.

Williamson PD, Thadani VM, Darcey TM, Spencer DD, Spencer SS, Mattson RH. Occipital lobe epilepsy: clinical characteristics, seizure spread patterns, and results of surgery. Ann Neurol. 1992;31(1):3–13.

Williamson PD. Frontal lobe seizures. Problems of diagnosis and classification. Adv Neurol. 1992;57:289–309.

Zentner J, Hufnagel A, Pechstein U, Wolf HK, Schramm J. Functional results after resective procedures involving the supplementary motor area. J Neurosurg. 1996;85(4):542–9.

Pediatric Epilepsy

26

Marc A. Prablek, Nisha Giridharan, and Howard L. Weiner

Abbreviations

EEG	Electroencephalography
HH	Hypothalamic hamartoma
LITT	Laser interstitial thermal therapy
MEG	Magnetoencephalography
MRI	Magnetic resonance imaging
PET	Positron emission tomography
RNS	Responsive neurostimulation
sEEG	Stereoelectroencephalography
SPECT	Single-photon emission computed tomography
TS	Tuberous sclerosis

The role of surgery in the management of pediatric epilepsy has expanded greatly within the last several years [1]. This trend has many contributing causes, among which are the consideration of surgery for diseases which were previously managed nonoperatively, the consideration of seizure palliation rather than seizure freedom as a goal of epilepsy surgery, and a growing acceptance of epilepsy surgery in both the medical and lay communities as a safe and effective means of seizure control. Certainly, the increased usage and development of stereotactic guidance and methods of treating various neurologic disorders contributes to this phenomenon as well, as the use of these methods allows for increased surgical access to deep structures of the brain, the use of new treatment modalities for treatment of discrete seizure foci, and the avoidance of large craniotomies for both invasive epilepsy monitoring and eventual treatment measures. In short, effective use of stereotaxy in both the diagnosis and treatment of pediatric epilepsy has facilitated a large amount of growth in this field and expanded the neurosurgical armamentarium with regard to pediatric seizure control.

In current practice, the workup of pediatric epilepsy is comprehensive and multidisciplinary in nature, involving neuropsychiatric evaluations, laboratory and imaging studies, inpatient observation in dedicated epilepsy units, and electroencephalography (EEG) [2, 3]. Broadly speaking, these studies can be divided into Phase 1 (nonsurgical) and Phase 2 (surgical), the latter of which includes invasive placement of electrographic monitoring devices such as subdural grids, strips, and intraparenchymal depth electrodes. Routine Phase 1 studies include thorough documentation of the patient's seizure semiology, neuropsychiatric evaluation, and comprehensive imaging workup consisting of magnetic resonance imaging (MRI), positron emission tomography (PET), single-photon emission

M. A. Prablek (✉) · N. Giridharan
Department of Neurosurgery, Baylor College of Medicine, Houston, TX, USA
e-mail: prablek@bcm.edu

H. L. Weiner
Department of Neurosurgery, Baylor College of Medicine, Houston, TX, USA

Division of Pediatric Neurosurgery, Department of Surgery, Texas Children's Hospital, Houston, TX, USA

N. Pouratian, S. A. Sheth (eds.), *Stereotactic and Functional Neurosurgery*,
https://doi.org/10.1007/978-3-030-34906-6_26

computed tomography (SPECT), noninvasive EEG, and magnetoencephalography (MEG). Even in non-lesional or MRI-negative epilepsy, these other imaging studies may provide valuable clues in localizing potential epileptogenic foci.

The findings of Phase 1 of epilepsy workup form the basis of surgical planning for Phase 2 studies which generally include placement of subdural grids and strips, as well as the placement of intraparenchymal depth electrodes to areas of interest identified during Phase 1. There are several clinical situations in which the use of invasive EEG monitoring is especially helpful. In cases where a patient has a normal MRI but partial epilepsy which localizes the lesion, or in cases where the presumed epileptogenic focus overlaps eloquent cortex, invasive EEG studies can help define the goal extent of resection [3, 4]. Additionally, in patients who have multifocal epilepsy, invasive EEG can help elucidate the contribution of each epileptogenic focus to the patient's semiology. Furthermore, invasive EEG can help correlate the relationship between a presumed seizure focus and a radiographic lesion.

Once the decision is made to pursue invasive EEG recording, a variety of options remain available to achieve this. Traditionally, subdural grids and strips have been placed to record focal areas of suspected epileptogenic activity. Depth electrodes increase the ability to measure the electrical activity of subcortical structures and are especially useful in measuring the electrical activity of, for example, the mesial temporal lobe. These can be placed through open craniotomy or with stereotactic guidance, i.e., stereoelectroencephalography (sEEG).

In particular, stereotactic placement of depth electrodes is of interest in cases where the suspected lesion is located in deep cortical or subcortical areas, where regions of interest are bilateral or would otherwise require multiple operations, and when a more extensive epilepsy network is suspected. Furthermore, sEEG is a useful strategy in a patient without clear suspected lesion on noninvasive workup, if the patient has previously failed craniotomy for subdural grid/depth electrode placement, or failed the subsequent monitoring period [4].

Stereotactic placement of electrodes can be accomplished in a number of ways. A stereotactic frame may be applied to the patient's head to assist in placement of electrodes. Advantages include widespread familiarity with stereotactic frame placement due to common usage in other applications such as deep brain stimulation. Disadvantages include difficult workflow if many trajectories are required. Such an approach would involve resetting frame coordinates for each trajectory, which can be unwieldy and time-consuming. In contrast, the use of robot-assisted stereotaxy allows for more streamlined placement of depth electrodes along multiple trajectories, sometimes up to 16–18. Other advantages include the adaptability of the robot to access a wide variety of approaches and trajectories in the same operation. Disadvantages of this approach include costs associated with the robotic device, as well as potential unfamiliarity of neurosurgeons with maneuvering the robot (Fig. 26.1).

Perhaps the greatest advantage to stereotactic epilepsy monitoring, however, is the potential seamlessness with which the patient can be transitioned from monitoring to treatment. Once suffi-

Fig. 26.1 Representative photo of patient immediately following sEEG placement in the operating room

cient data from the patient's monitoring stay has determined the appropriate site of treatment, the same skull bolts that guided the depth electrodes can be used to guide devices such as responsive neurostimulation (RNS) leads or laser ablation filaments to the desired site. This allows for effective and relatively minimally invasive treatment of epilepsy through closed loop neurostimulation or laser interstitial thermal therapy (LITT) [5–8].

Stereotactic LITT is a novel surgical technique that allows for minimally invasive treatment of focal intracranial lesions [9]. The technique involves using stereotaxy to place a laser fiber into the target tissue, thermally ablating the tissue, and monitoring real-time temperature with MRI thermography during lesioning [9]. The procedure is beneficial in cases where open cranial surgery has a high morbidity rate. Its other advantage is the ability to deliver targeted thermal energy without injury to adjacent cortical and deep structures [10]. Its use in epilepsy was first described in 2012 by Curry et al. for children with lesional, localization-related intractable epilepsy [5]. In this series of five patients, all children achieved seizure freedom at follow-up with no complications [5].

MRI-guided laser interstitial therapy for medically refractory temporal lobe epilepsy syndromes has been published in several case series [5, 11–18]. Historically anterior temporal lobectomies and amygdalohippocampectomies have shown to have good rates of seizure freedom, but are often not undertaken due the possible adverse neurocognitive effects from resecting lateral neocortical temporal structures [12–14]. Stereotactic laser ablation can spare these structures, and patients have reported fewer deficits in naming and facial recognition after laser ablation compared with anterior temporal lobectomies [12]. The rates of seizure freedom in patients with mesial temporal lobe epilepsy undergoing stereotactic laser ablation are high. About 60–70% of patients achieved Engel class I outcomes [5, 11–15, 17, 18]. In extratemporal lobe epilepsy, lesions amenable to MRI-guided laser interstitial therapy include hypothalamic hamartomas, tuberous sclerosis, focal cortical dysplasia, and periventricular nodular heterotopia [6, 9].

Through the use of stereotaxy, and especially stereotactic laser ablation, the indications for surgical management of epilepsy are evolving rapidly. Due to the less invasive nature of epilepsy monitoring and treatment, stereotaxy potentially has a large role in the palliative treatment of epilepsy, cases where the goal of surgery is not necessarily complete seizure control, but rather limiting the most profoundly debilitating seizure events. When the goal of surgery is no longer complete seizure control, minimizing the extent of surgery and craniotomy becomes a stronger consideration, strengthening the case for a stereotactic approach. Furthermore, patients with lesional epilepsy in areas of eloquent cortex or epilepsy related to deep subcortical lesions may be good candidates for LITT, which allows for a more targeted approach for seizure control [19].

A variety of epilepsy syndromes for which epilepsy surgery was not commonly offered now may benefit from management with stereotactic approaches to surgery. In particular, the management of tuberous sclerosis and hypothalamic hamartomas has changed drastically with the development of stereotactic techniques for both diagnostic and treatment measures.

Tuberous Sclerosis

Tuberous sclerosis (TS) is an autosomal dominant neurocutaneous disorder affecting 1 in 6000 to 10,000 live births in which patients develop masses of largely benign nature, including renal angiomyolipomas, cardiac rhabdomyomas, and cutaneous nodules [20]. Intracranial findings in this disease include cortical tubers, subependymal nodules, and subependymal giant cell astrocytomas (SEGAs). These lesions, especially cortical tubers, can be highly epileptogenic, and indeed 80–90% of patients with TS have epilepsy, and 50–80% of these patients have epilepsy refractory to medical therapy [20–23].

Resection of cortical tubers in TS patients has been shown to be effective in terms of seizure control, and so much of the preoperative seizure workup proceeds as described above, utilizing

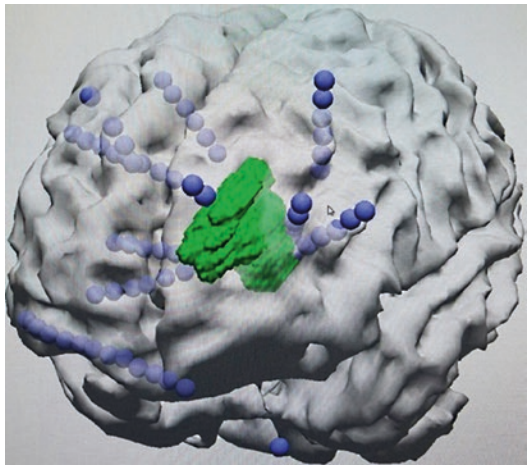

Fig. 26.2 Schematic of sEEG placement in a TS patient. Blue spheres represent EEG contacts, and green-shaded area represents presumed epileptogenic lesion

advanced imaging techniques and video monitoring [21]. Nevertheless, in a significant number of patients, more invasive monitoring is needed. These patients may have inconclusive findings on preoperative imaging and frequently have multiple and bilateral cortical tubers [21]. Additionally, the cortex adjacent to particular tubers can be monitored, as it has been suggested that the epileptogenic focus can be localized to this adjacent cortex rather than simply to the tuber itself, and furthermore that resection of this cortex leads to better seizure control outcomes [24]. In addition to traditional methods of intracranial EEG recording, EEG leads may be placed stereotactically, which allows for less invasive bilateral monitoring, as well as targeted monitoring of multiple cortical tubers and other suspected epileptogenic foci simultaneously (Fig. 26.2).

Once the target area of resection has been identified, the patient can begin the surgical planning process, which is frequently focal tuber resection. As discussed earlier, many patients achieve durable seizure freedom with focal resection alone, with one study reporting about 50% of patients with complete seizure freedom at 5 and 10 years [23]. Moreover, even patients with bilateral lesions may benefit from either resection of a single seizure focus or further iterative craniotomies for seizure control [25, 26].

Nevertheless, patients can benefit tremendously from near-total or even partial seizure control, which significantly improves quality of life [27]. Furthermore, the option of bilateral intracranial monitoring prior to resection, as well as the idea of multiple iterative operations for seizure control, offers a clear indication for the use of stereotactic methods. Utilizing stereotaxy to place multiple electrodes into multiple tubers or cortical areas allows for more extensive pre-resection monitoring, and as mentioned above, the use of stereotaxy to place EEG leads theoretically allows for the use of LITT during the treatment phase to achieve seizure control. Although the use of LITT for the treatment of epilepsy in TS patients has not been extensively studied, some case reports have demonstrated good seizure control, although follow-up data is limited [5].

The advent of stereotactic methods in neurosurgery provides interesting new options in the treatment of childhood epilepsy related to TS. Because of the nature of the disease, many children may have widespread bilateral lesions which require bilateral invasive monitoring, which is much more facile with stereotactic invasive EEG monitoring than with traditional approaches. LITT also offers additional surgical options to patients who may require a more iterative approach to surgical seizure control, limiting the potential morbidity associated with multiple craniotomies or tuber resections.

In this manner, the approach to treating patients with tuberous sclerosis has evolved significantly over the course of decades. Although current standard methods of epilepsy monitoring and focal tuber resection can help many children achieve seizure freedom, the use of stereotactic methods for EEG lead placement as well as LITT as a surgical option in addition or in place of focal tuber resection may offer an expanded number of patients an opportunity for seizure freedom. We hope that with further investigation, further improvements in stereotactic techniques for both monitoring and treatment will further expand the neurosurgical armamentarium in treating this challenging disease.

Hypothalamic Hamartoma

Hypothalamic hamartomas are heterotopic masses with an incidence of about 1 in 200,000 persons, which are composed of neuronal cells and glia arising from the tuber cinereum and floor of the third ventricle [9, 28]. These patients often have a number of cognitive and neuroendocrine deficits including central precocious puberty, behavioral disturbances, and gelastic seizures, which are marked by stereotyped, emotionless bursts of laughter [9].

These seizures can be highly debilitating and are frequently refractory to antiepileptic medications. Furthermore, several studies have demonstrated the intrinsic epileptogenicity of hypothalamic hamartomas, which is often difficult to measure via scalp EEG, but has been measured in several studies by utilizing depth electrodes [29–31].

Due to the harmful nature of the disease and the localization of epileptogenicity to a single seizure focus, open surgical resection of the lesion has traditionally been an attractive treatment option for hypothalamic hamartoma [32]. Pterional, transcallosal, and intraventricular endoscopic approaches were classically described approaches for resecting these lesions; however the morbidity was high with reported complications of endocrine dysfunction, vision changes, memory loss, and hemiparesis [33]. The rate of permanent deficit was about 25% [33–37]. Furthermore, alternate methods of treating HH such as stereotactic radiosurgery (SRS) or endoscopic disconnection surgeries have also been described [32]. These are attractive because of their less invasive nature and relatively good rates of seizure control. Nevertheless, using SRS or performing disconnection surgery still incurs the risk of damage to critical surrounding structures near the lesion, and patients treated with SRS may have an unacceptably long period between completion of therapy and onset of seizure control [32].

Another option for the treatment of epilepsy related to HH is MRI-guided, stereotactic LITT. Utilizing laser ablation allows access to the deeply seated lesion without retraction or destruction of the surrounding tissue [38]. Laser ablation has been shown to be safe and effective for treating hypothalamic hamartomas as there is minimal corridor-related morbidity [38]. Tissue ablation may be imprecise and may require more than one trajectory to successfully ablate the entirety of the lesion, but the morbidity is still considerably less than with open craniotomy procedures [38]. The current evidence for stereotactic laser ablation in these lesions includes several retrospective case series which show 76–86% freedom of gelastic seizures following the procedure [28, 38–41].

Similar to TS, HH represents an epilepsy pathology which has long presented unique challenges to neurosurgical management. As in the treatment of TS, however, stereotactic methods present a minimally invasive and thus attractive paradigm for the treatment of these diseases. Hopefully, stereotaxy continues to yield new diagnostic and treatment modalities for pediatric epilepsy, and our ability to manage these complex patients and conditions continues to expand and improve.

References

1. Dwivedi R, Ramanujam B, Chandra PS, Sapra S, Gulati S, Kalaivani M, et al. Surgery for drug-resistant epilepsy in children. N Engl J Med. 2017; 377(17):1639–47.
2. Lee J, Adelson PD. Neurosurgical management of pediatric epilepsy. Pediatr Clin N Am. 2004;51:441–56.
3. Jayakar P, Gaillard WD, Tripathi M, Libenson MH, Mathern GW, Cross JH, et al. Diagnostic test utilization in evaluation for resective epilepsy surgery in children. Epilepsia. 2014;55(4):507–18.
4. Alomar S, Jones J, Maldonado A, Gonzalez-Martinez J. The stereo-electroencephalography methodology. Neurosurg Clin N Am. 2016;27(1):83–95.
5. Curry DJ, Gowda A, McNichols RJ, Wilfong AA. MR-guided stereotactic laser ablation of epileptogenic foci in children. Epilepsy Behav. 2012;24(4): 408–14.
6. North RY, Raskin JS, Curry DJ. MRI-guided laser interstitial thermal therapy for epilepsy. Neurosurg Clin N Am. 2017;28(4):545–57.
7. Morrell MJ, Halpern C. Responsive direct brain stimulation for epilepsy. Neurosurg Clin N Am. 2016;27(1):111–21.
8. Bandt SK, Leuthardt EC. Minimally invasive neurosurgery for epilepsy using stereotactic MRI guidance. Neurosurg Clin N Am. 2016;27(1):51–8.

9. Buckley RT, Wang AC, Miller JW, Novotny EJ, Ojemann JG. Stereotactic laser ablation for hypothalamic and deep intraventricular lesions. Neurosurg Focus. 2016;41(4):E10.
10. Tovar-Spinoza Z, Carter D, Ferrone D, Eksioglu Y, Huckins S. The use of MRI-guided laser-induced thermal ablation for epilepsy. Child's Nerv Syst. 2013;29(11):2089–94.
11. Dadey DY, Kamath AA, Smyth MD, Chicoine MR, Leuthardt EC, Kim AH. Utilizing personalized stereotactic frames for laser interstitial thermal ablation of posterior fossa and mesiotemporal brain lesions: a single-institution series. Neurosurg Focus. 2016;41(4):E4.
12. Drane DL, Loring DW, Voets NL, Price M, Ojemann JG, Willie JT, et al. Better object recognition and naming outcome with MRI-guided stereotactic laser amygdalohippocampotomy for temporal lobe epilepsy. Epilepsia. 2015;56(1):101–13.
13. Jermakowicz WJ, Kanner AM, Sur S, Bermudez C, D'Haese PF, Kolcun JPG, et al. Laser thermal ablation for mesiotemporal epilepsy: analysis of ablation volumes and trajectories. Epilepsia. 2017;58(5):801–10.
14. Kang JY, Wu C, Tracy J, Lorenzo M, Evans J, Nei M, et al. Laser interstitial thermal therapy for medically intractable mesial temporal lobe epilepsy. Epilepsia. 2016;57(2):325–34.
15. Lewis EC, Weil AG, Duchowny M, Bhatia S, Ragheb J, Miller I. MR-guided laser interstitial thermal therapy for pediatric drug-resistant lesional epilepsy. Epilepsia. 2015;56(10):1590–8.
16. Patel P, Patel NV, Danish SF. Intracranial MR-guided laser-induced thermal therapy: single-center experience with the Visualase thermal therapy system. J Neurosurg. 2016;125(4):853–60.
17. Willie JT, Laxpati NG, Drane DL, Gowda A, Appin C, Hao C, et al. Real-time magnetic resonance-guided stereotactic laser amygdalohippocampotomy for mesial temporal lobe epilepsy. Neurosurgery. 2014;74(6):569–84; discussion 84–5
18. Willie JT, Gross RE. 202 role of repeat ablation to treat seizure recurrence following stereotactic laser amygdalohippocampotomy. Neurosurgery. 2015;62(CN_suppl_1):233–4.
19. Kuo CH, Feroze AH, Poliachik SL, Hauptman JS, Novotny EJ Jr, Ojemann JG. Laser ablation therapy for pediatric patients with intracranial lesions in eloquent areas. World Neurosurg. 2019;121:e191.
20. Overwater IE, Bindels-de Heus K, Rietman AB, Ten Hoopen LW, Vergouwe Y, Moll HA, et al. Epilepsy in children with tuberous sclerosis complex: chance of remission and response to antiepileptic drugs. Epilepsia. 2015;56(8):1239–45.
21. Evans LT, Morse R, Roberts D. Epilepsy surgery in tuberous sclerosis: a review. Neurosurg Focus. 2011;32(3):E5.
22. Romanelli P, Verdecchia M, Rodas R, Seri S, Curatolo P. Epilepsy surgery for tuberous sclerosis. Pediatr Neurol. 2004;31(4):239–47.
23. Liang S, Zhang J, Yang Z, Zhang S, Cui Z, Cui J, et al. Long-term outcomes of epilepsy surgery in tuberous sclerosis complex. J Neurol. 2017;264(6):1146–54.
24. Fallah A, Rodgers SD, Weil AG, Vadera S, Mansouri A, Connolly MB, et al. Resective epilepsy surgery for tuberous sclerosis in children: determining predictors of seizure outcomes in a multicenter retrospective Cohort Study. Neurosurgery. 2015;77(4):517–24; discussion 24
25. Arya R, Tenney JR, Horn PS, Greiner HM, Holland KD, Leach JL, et al. Long-term outcomes of resective epilepsy surgery after invasive presurgical evaluation in children with tuberous sclerosis complex and bilateral multiple lesions. J Neurosurg Pediatr. 2015;15(1):26–33.
26. Weiner HL, Ferraris N, LaJoie J, Miles D, Devinsky O. Epilepsy surgery for children with tuberous sclerosis complex. J Child Neurol. 2004;19:687–9.
27. Curatolo P, Bombardieri R, Jozwiak S. Tuberous sclerosis. Lancet. 2008;372:657–68.
28. Wilfong AA, Curry DJ. Hypothalamic hamartomas: optimal approach to clinical evaluation and diagnosis. Epilepsia. 2013;54(Suppl 9):109–14.
29. Mittal S, Mittal M, Montes JL, Farmer J, Andermann F. Hypothalamic hamartomas. Part 1. Clinical, neuroimaging, and neurophysiological characteristics. Neurosurg Focus. 2013;34(6):1–12.
30. Munari C, Kahane P, Francione S, Hoffmann D, Tassi L, Cusmai R, et al. Role of the hypothalamic hamartoma in the genesis of gelastic fits (a video-stereo-EEG study). Electroencephalogr Clin Neurophysiol. 1995;95(3):154–60.
31. Palmini A, Chandler C, Andermann F, Costa Da Costa J. Resection of the lesion in patients with hypothalamic hamartomas and catastrophic epilepsy. Neurology. 2002;58(9):1338.
32. Mittal S, Mittal M, Montes JL, Farmer J, Andermann F. Hypothalamic hamartomas. Part 2. Surgical considerations and outcome. Neurosurg Focus. 2013;34(6):1–10.
33. Mittal S, Mittal M, Montes JL, Farmer JP, Andermann F. Hypothalamic hamartomas. Part 2. Surgical considerations and outcome. Neurosurg Focus. 2013;34(6):E7.
34. Harvey AS, Freeman JL, Berkovic SF, Rosenfeld JV. Transcallosal resection of hypothalamic hamartomas in patients with intractable epilepsy. Epileptic Disord. 2003;5(4):257–65.
35. Mottolese C, Stan H, Bret P, Berlier P, Lapras C. Hypothalamic hamartoma: the role of surgery in a series of eight patients. Child's Nerv Syst. 2001;17(4–5):229–36. discussion 37-8
36. Ng YT, Rekate HL, Prenger EC, Chung SS, Feiz-Erfan I, Wang NC, et al. Transcallosal resection of hypothalamic hamartoma for intractable epilepsy. Epilepsia. 2006;47(7):1192–202.
37. Polkey CE. Resective surgery for hypothalamic hamartoma. Epileptic Disord. 2003;5(4):281–6.
38. Curry DJ, Raskin J, Ali I, Wilfong AA. MR-guided laser ablation for the treatment of hypothalamic hamartomas. Epilepsy Res. 2018;142:131–4.

39. Kameyama S, Murakami H, Masuda H, Sugiyama I. Minimally invasive magnetic resonance imaging-guided stereotactic radiofrequency thermocoagulation for epileptogenic hypothalamic hamartomas. Neurosurgery. 2009;65(3):438–49. discussion 49
40. Kameyama S, Shirozu H, Masuda H, Ito Y, Sonoda M, Akazawa K. MRI-guided stereotactic radiofrequency thermocoagulation for 100 hypothalamic hamartomas. J Neurosurg. 2016;124(5):1503–12.
41. Xu DS, Chen T, Hlubek RJ, Bristol RE, Smith KA, Ponce FA, et al. Magnetic resonance imaging-guided laser interstitial thermal therapy for the treatment of hypothalamic hamartomas: a retrospective review. Neurosurgery. 2018;83(6):1183–92.

Epilepsy: Neuromodulation

27

Matthew K. Mian and Robert E. Gross

Introduction

Epilepsy afflicts 1% of the population and is resistant to medication in 30–40% of cases [1]. When seizures persist despite adequate trials of at least two first-line antiepileptic drugs, they are deemed "refractory," and additional drugs are unlikely to confer seizure freedom [2, 3]. Patients with refractory epilepsy may be candidates for resective or ablative surgery with curative potential, with long-term seizure-freedom rates of up to 70% [4–7], but epilepsy surgery remains woefully underutilized.

Among patients who are evaluated for surgical candidacy, many are not suitable for destructive procedures, namely, those with poorly defined or multiple foci, a focus in eloquent cortex, and generalized epilepsy and those for whom resection or ablation would be attended by disruptive neuropsychological morbidity. These patients have historically presented a management challenge.

Since the late 1990s, our field has witnessed the approval by the US Food and Drug Administration (FDA) of three neuromodulatory techniques for refractory partial-onset seizures, each involving the application of electric current to the nervous system: vagus nerve stimulation (VNS), responsive neurostimulation (RNS), and thalamic deep brain stimulation (DBS). Each of these approvals was supported by one or more randomized controlled trials, and these devices have expanded the pool of refractory epilepsy patients who can be treated surgically to include many of those with the dilemmas above.

Current epilepsy neuromodulatory therapies are palliative in that they offer a reduction in seizure frequency and mitigation of seizure severity, but they are not applied with curative intent. While a slender minority of neurostimulation patients enjoy long-term seizure freedom, many patients experience a meaningful decrement in seizure frequency. Neurostimulation can have other attendant benefits – often independent of the degree of seizure relief – including enhanced neuropsychological performance, improved quality of life, and attenuated rates of sudden unexpected death in epilepsy (SUDEP).

In this chapter, we will review the rationale, supporting data, operative technique, and postoperative considerations for VNS, RNS, and DBS for partial-onset seizures. We will compare the techniques, highlighting considerations for selecting a therapy for individual patients. Finally, we will conclude with a discussion of off-label application of neurostimulation for generalized epilepsy.

M. K. Mian · R. E. Gross (✉)
Department of Neurosurgery, Emory University, Atlanta, GA, USA
e-mail: rgross@emory.edu

N. Pouratian, S. A. Sheth (eds.), *Stereotactic and Functional Neurosurgery*,
https://doi.org/10.1007/978-3-030-34906-6_27

Vagus Nerve Stimulation

Electrical vagus nerve stimulation (VNS) for arresting seizures was explored in humans as early as the 1880s by James Corning, who applied current transcutaneously [8]. His experiments followed prior efforts for aborting seizures with mechanical compression of the carotid artery. In its current form, VNS is applied in a bipolar manner through a pair of electrodes encircling the mid-cervical segment of the vagus nerve and connected to an infraclavicular pulse generator.

Left vagus nerve stimulation was approved by the FDA in 1997 for the treatment of refractory partial-onset seizures in both adults and children over 12 years of age. Several iterations of a commercial device were developed by Cyberonics, which later merged with an Italian medical device company to form LivaNova.

VNS neurostimulators have offered both a chronic, intermittent stimulation cycle and an on-demand mode triggered by an external magnet that a patient or caregiver can apply as needed to abort a forthcoming or ongoing seizure. In 2015, LivaNova released the AspireSR VNS model, which added a closed-loop mode using a cardiac-based detection algorithm to screen for ictal tachycardia and then deliver abortive stimulation automatically.

Rationale

The left vagus nerve conveys afferents from the viscera to the brain stem. Prior to its application in human epilepsy, studies had established that VNS could abort induced seizures in animal models of epilepsy [9, 10]. The mechanism is possibly related to activation of the locus coeruleus [11]: VNS raises extracellular levels of norepinephrine [12] in a manner that correlates with anti-seizure effects [13]. Further, these effects can be abolished by a lesion of the locus coeruleus [14].

In humans, VNS reduces the frequency of interictal discharges [15–17]. Increases in cerebral blood flow to the thalamus have been associated with successful VNS [18], though there appears to be a time dependence to this phenomenon, as other studies have noted reduced metabolic activity in the medial thalamus in those with effective therapy [19–21].

As with other forms of neurostimulation, the effects of VNS are dynamic in time and probably evolve through more than one mechanism. Some have proposed that VNS may be mediated in part through a blunting of neuroinflammation [22]. VNS does not appear to act via long-term modulation of parasympathetic tone [23], as indices of autonomic function remain stable in patients after VNS.

Evidence and Outcomes

The FDA approval of VNS relied on two clinical trials with similar designs (E03 and E05) in which subjects with partial-onset seizures were implanted and then randomized to either high or low stimulation (presumed therapeutic and subtherapeutic doses, respectively). Vagal stimulation is generally perceptible to patients, so an active placebo arm was necessary to maintain the blind in these trials. The primary outcome was change in seizure frequency.

In the E03 trial (n = 114), there was a significant reduction in seizure frequency in the high- vs low-stimulation arm (24.5% vs 6.1%; p = 0.01) during a 12-week assessment period [24]. Additionally, more patients in the high-stimulation group achieved at least a 50% reduction in seizure frequency (31% vs 13%; p = 0.02). In the E05 trial (n = 199), there was again a greater reduction in seizure frequency among the high-stimulation vs low-stimulation subjects during a 3-month assessment period (27.9% vs 15.2%; p = 0.04) [25].

The anti-seizure effects of VNS are sustained and even increase over time. Open-label extension studies that followed the E03 and E05 pivotal trial patients reported median reductions in seizure frequency of 32% and 45% at 1 year, respectively [26, 27]. A long-term efficacy study involving patients from five clinical trials (n = 454) found median seizure reductions of 35% at 1 year, 44% at 2 years, and 44% at 3 years,

with ≥50% seizure reductions in 36.8% of patients at 1 year, in 43.2% at 2 years, and in 42.7% at 3 years [28]. Data from a large VNS registry revealed median seizure reductions of 56% at 1 year and 62% at 2 years, with ≥50% response rates of 53% at 1 year and 56% at 2 years [29], but these data have the typical limitations associated with registries and are likely to be an overestimation of benefits. Anti-seizure effects among this cohort were consistent against a broad range of seizure subtypes. Smaller series with extended follow-up suggest these effects are sustained long term [30].

Several reports have suggested added benefit of the VNS device's magnet mode. Applying the magnet to avoid or abort a seizure can be a challenge for many patients [31] for a variety of reasons: lack of an aura, rapid ictal alteration of consciousness, occurrence during sleep, and baseline cognitive or physical impairment. Nonetheless, many patients describe a benefit from the magnet, with 28% reporting seizure cessation [32]. A retrospective study from patients in the E03 and E04 studies found that of magnet activations for 9482 seizures, 24% terminated the event and 38% diminished it [33].

Newer VNS models offer automatic triggering of stimulation using a tachycardia detection algorithm. Ictal tachycardia is common, occurring in over 80% of partial-onset seizures in some studies [34–36], and it may even precede electrographic or clinical onset [37, 38]. Initial studies of the closed-loop tachycardia algorithm have suggested it is effective [39] and that it could improve seizure control in patients initially implanted with older VNS models [40].

Technique

VNS implantation is performed under general anesthesia as an outpatient procedure. The procedure is performed on the left, since the right vagus nerve preferentially supplies parasympathetic tone to the sinoatrial node; stimulation on the right therefore risks bradyarrhythmias (although there are isolated case reports of successful right-sided implants in special circumstances [41]). The patient is positioned supine with the neck in slight extension and the arm tucked at the side. A mid-scapular roll can be used to drop the left shoulder away from the field. We do not turn the head.

A 3 cm transverse incision is made in a neck crease crossing over the medial border of the sternocleidomastoid muscle (SCM) and ending just shy of the midline. This incision falls about one third of the distance from the sternal notch to the mastoid. The dermis is undermined above and below the incision.

The platysma is elevated, incised vertically in line with its fibers, and then retracted open. Metzenbaum scissors are spread transversely in the groove medial to the SCM to open up a natural plane that is followed down to the carotid sheath. Small bridging vessels are coagulated and divided. Care is taken to maintain rigorous hemostasis; even modest oozing can obscure the natural tissue plans and also threaten a postoperative neck hematoma.

The carotid artery is palpated medially, and the transverse blunt-tipped retractor is deepened to sweep away the SCM laterally and strap muscles medially. As the exposure is carried into the carotid sheath, the retractor can be further deepened by placing the lateral teeth (always blunt) against the jugular vein itself, if necessary, though care should be taken not to avulse any bridging veins. The vagus nerve can be identified deep in the groove between the carotid artery and the jugular vein (Fig. 27.1). In cases where a candidate nerve is encountered elsewhere, this groove should still be explored to confirm that the candidate nerve is indeed the vagus.

A 3 cm segment of the nerve is delicately dissected circumferentially; there is no need to remove or transgress the epineurium, which may jeopardize the vascular supply to the nerve. A small pulse generator pocket is created either inferior to the clavicle or in the axilla for cosmetic reasons. We make a transverse incision two fingerbreadths beneath the clavicle and two fingerbreadths medial to the deltopectoral groove. A trocar with a sheath is passed subcutaneously from the pocket up to the cervical incision. The electrode is brought into the field and slipped through the sheath.

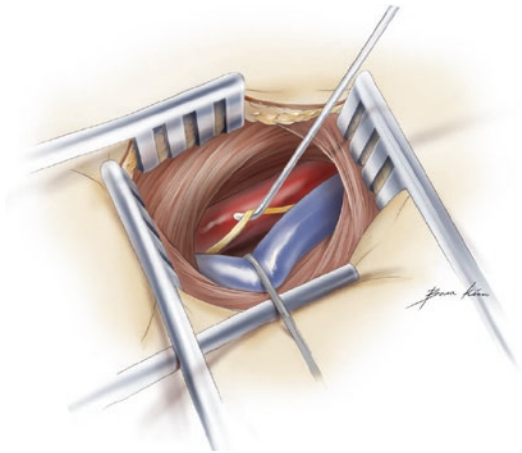

Fig. 27.1 Exposure of the left vagus nerve. The nerve is identified in the carotid sheath in the groove between the carotid artery (medially) and the jugular vein (laterally). (All rights reserved to Emory University, printed with permission)

The stimulating end of the lead includes three coils that encircle the nerve: cathode (distal), anode (middle), and anchor (proximal). Placement of the delicate coils around the nerve is facilitated by an assistant who can elevate and steady the nerve; this is also aided by placing a plastic grid underneath the nerve to isolate it from other soft tissue and to ensure its complete circumferential dissection. Each coil is stretched along its length, set down onto the nerve, and then the two ends are threaded around the nerve in either direction using the affixed strings. We place the anchor first, as it is a longer coil than the cathode or anode and thus less easy to inadvertently displace while wrapping the other coils.

Once all three coils have been placed, the proximal end of the lead is inserted into the pulse generator. An impedance check is performed, and heart rate detection is verified. Note that test stimulation during these steps can rarely provoke bradycardia, so the anesthesia team is alerted prior to testing.

The pulse generator is secured in the pocket with sutures, and the white anchoring tabs are placed along the proximal part of the lead and sutured to the medial face of the sternocleidomastoid or strap muscles. After once again confirming normal impedances, the incisions are closed in layers, culminating in surgical glue on the skin.

Post-op Care and Complications

The stimulator is turned on after a few weeks. We usually begin at a very low current and then ramp up stepwise every few weeks while monitoring for side effects. Common final parameters are 1.5–2.25 mA, 20–30 Hz, 250–500 μs, and cycle of 30 sec on and 3–5 min off, with the magnet activation set at a slightly higher current. Clinical effects are usually apparent after several weeks of stimulation.

Dysphonia during stimulation is common and expected. Other common complaints include hoarseness and cough, which tend to improve with time [28]. Permanent hoarseness is rare. In large VNS series, other adverse events include headache (4–5%), dyspnea (3%), surgical site infection (1–2%), vocal cord paralysis (<1%), and dysphagia (<1%) [28, 30, 42, 43].

Responsive Neurostimulation

Responsive neurostimulation (RNS) was approved by the FDA in 2013 for the treatment of partial-onset seizures with one or two foci in patients at least 18 years of age who had failed two or more antiepileptic drugs. In its current form, a microprocessor (NeuroPace Inc., Mountain View, CA) embedded in the skull performs continuous electrocorticography (ECoG) through up to two depth or strip electrodes implanted at one or two seizure foci and then delivers electrical stimulation to abort seizures using up to three detection algorithms for triggering. Windows of ECoG are stored and then uploaded to an online server periodically by the patient or caregiver; these tracings can then be studied by the patient's clinical team to further tailor detection programs and therapy.

The RNS approach is distinct from VNS and DBS in that it delivers stimulation to the seizure focus itself. RNS permits a greater degree of therapy customization than either VNS or DBS, though this process can be labor-intensive.

Chronic ECoG from RNS has also yielded new insights about epilepsy, including the oscillatory nature of interictal discharges and how it can predict seizure vulnerability [44], and about individual patients, including the presence of unilateral temporal disease among patients who had been previously deemed bitemporal [45] and prediction of whether antiepileptic drug trials are likely to succeed [46].

Rationale

The idea for closed-loop intracranial stimulation emerged in part from observations that delivery of brief electrical pulses could disrupt induced afterdischarges in patients undergoing intracranial seizure monitoring [47]. The mechanisms by which RNS influences seizure propagation remain, however, unclear. Limitations of the device preclude analysis of ECoG during stimulation pulses. Seizure frequency could be reduced through inhibition locally within the seizure focus during stimulation. Prior work has also established that cortical stimulation can disrupt synchrony between brain regions [48], so RNS alternatively could mediate its effects through network desynchronization. Whether the mode of effect is primarily local or network-dependent could have clinical implications regarding the specificity of electrode placement, which remains minimally characterized.

Compared to VNS and DBS, RNS delivers a modest dose of current. VNS and DBS both function largely in open-loop paradigms, delivering stimulation regularly on a duty cycle, commonly 30–60 seconds every 5 min. In contrast, RNS stimulates only briefly (100–200 ms) in response to cortical activity meeting a prespecified threshold for ictal suspicion. Individual patients vary widely in the number of triggers, but in one analysis, most patients triggered 600–2000 times daily, resulting in cumulative stimulation doses of 5 min or less per day [49]. However, these doses are sufficient to achieve seizure control at least on par with VNS and DBS (see below) and also to exert neuromodulatory effects resulting in gradual seizure improvement over time. How this is achieved and whether reduced stimulation dosing has implications for the long-term function of eloquent cortex within or adjacent to ictal zones remains unknown.

Evidence and Outcomes

Experience with externalized closed-loop stimulators piloted during admissions for intracranial monitoring [50, 51] motivated development of the NeuroPace device. The pivotal RNS trial [52] recruited 191 subjects with frequent, disabling partial-onset seizures with either one or two foci. Subjects were implanted and then underwent a 4-week baseline stabilization period, after which they were randomized to blinded active or sham stimulation for 12 weeks. Seizure outcomes were assessed at the end of the blinded phase, and all patients then participated in an open-label extension, receiving stimulation for 2 years.

Both treatment arms experienced an "implantation effect," with a temporary reduction in seizure frequency, although the etiology of this effect, i.e., vs placebo or regression to the mean, is not clear [53]. At the conclusion of the 12-week blinded phase, mean seizure frequency was reduced in the active stimulation arm (37.9% vs 17.3%; $p = 0.01$). Response was unaffected by factors including the location of onset zone (mesial temporal vs neocortical), number of foci, presence of VNS, and prior epilepsy surgery, among others. In the open-label extension where all patients received active stimulation, seizure reductions improved to 44% at 1 year and 53% at 2 years, with a ≥50% response rate of 55% at 2 years. Longer-term follow-up with these patients revealed a plateau effect in seizure reduction hovering at 48–66% in years 3–6 and a ≥50% response rate of ~60%; 23% of patients experienced a seizure-free interval of at least 6 months [54].

Subsequent analyses of the open-label extension patients suggested that degree of response indeed depended on focus location: for those with neocortical onset, median seizure reduction was 70% for the frontal and parietal lobes, 58% for the temporal lobe, and 51% for multilobar

foci [55]. Patients with MRI-visible lesions fared better than those without (77% vs 45% median seizure reduction) [55]. Those with mesial temporal foci, the largest subset of trial patients, experienced a median seizure reduction of 70%, with a responder rate of 66% [56]. The presence of mesial temporal sclerosis did not influence outcome. Neuropsychological profiles disclosed no adverse effects on cognition, affect, or memory; in fact, some patients showed improvements in verbal memory [57]. Quality of life was improved slightly [58].

Technique

Implantation can be performed using a variety of stereotactic techniques. Since the approach varies based on the seizure-onset zone(s) being targeted, we will discuss implantation for one of the most common scenarios – bilateral hippocampal foci.

We implant the depth leads first to avoid the introduction of brain shift by the craniectomy. The leads are introduced either in the MRI suite using the ClearPoint system (MRI Interventions, Irvine, CA), which permits direct visualization of the target and leads, or in the operating room with the ROSA robot (Zimmer Biomet, Warsaw, IN), a stereotactic platform (StarFix, FHC, Bowdoin, ME), or a conventional stereotactic frame. The former method introduces the additional step of traveling with the anesthetized patient from the diagnostic MRI suite to the operating room. We have found that the typical parieto-occipital entry point for the leads can make using a conventional stereotactic head frame a challenge.

In the MRI, the patient is positioned prone. For a robot case, prone positioning mandates skull fiducials for registration, so we typically position the patient supine with the head turned. The latest version of the ROSA robot is generally able to reach the posterior entry sites in this position, but this is important to verify for each case. A trajectory from a parieto-occipital entry is chosen to maximize the number of electrode contacts within the hippocampus. We typically create a small burr hole/craniostomy and anchor the leads with a "dogbone" titanium miniplate rather than with the proprietary burr hole cover. Confirmation of the lead position is verified radiographically with intraoperative MRI or CT. The leads are then tunneled beneath the scalp.

The curvature of the stimulator is suited for placement in the high parietal bone. We make an inverted "U" incision and then map out a craniectomy above the superior temporal line, although this general strategy may need to be altered due to previous surgery. The craniectomy is tailored to the ferrule, which is then anchored to the skull. Care is taken to orient the device such that the fragile leads will not pass beneath the segment of the incision that will be reopened for battery replacement. The device is inserted, and we confirm that impedances are within normal limits and that we can stream live ECoG. The field is irrigated, sprinkled with vancomycin powder, and then closed.

Post-op Care and Complications

Stimulation is activated several weeks postoperatively. Typical final parameters are 1.5–3 mA (usually <3 mA for mesial temporal and <6 mA for neocortical), 200 Hz, 160 μs pulse width, and 100 ms pulse duration [49]. Detection modes and thresholds are patient-specific. The ceiling for the number of stimulations allowed per day is commonly 1000–3000.

In the pivotal RNS trial and extension studies, adverse events included intracranial hemorrhage (5%), implant site pain (15%), headache (11%), and surgical site infection (5–9%) [52, 59, 60]. There was one suicide. In long-term follow-up, there were seven instances of possible, probable, or definite SUDEP [54], yielding a rate that was comparable to that observed for high-risk patients being evaluated for epilepsy surgery. Patients should be reminded that MRI is contraindicated with RNS.

Deep Brain Stimulation of the Anterior Nucleus of the Thalamus

Deep brain stimulation (DBS) of the anterior nucleus of the thalamus (ANT) was approved by the FDA in 2018 for treating adults with focal-onset seizures refractory to three or more

medications. ANT DBS had been in use in Europe since 2010 following publication of the findings of the Medtronic-sponsored double-blind randomized trial, the Stimulation of the Anterior Nuclei of Thalamus for Epilepsy (SANTE) trial, described below. Advantages of ANT DBS over cortical RNS include stereotyped lead placement and stimulator programming, no requirement for patients to upload data, the ability to treat patients with poorly localized foci or more than two foci, and a simpler battery placement and replacement procedure. Owing to its recent approval, however, there is limited long-term outcome data outside of those patients enrolled in the pivotal trial.

Rationale

The ANT is a node in the circuit of Papez [61], which has a role both in supporting emotion and memory and also in initiating and propagating limbic seizures. The ANT comprises the anterior-superior-medial surface of the thalamus and is visible on imaging studies as a bulge into the lateral ventricle (Fig. 27.2). It receives afferents from the mammillary bodies via the mammillothalamic tract (MTT) and then projects widely to cerebral cortex chiefly via the anterior thalamic radiation [62].

Animal studies beginning in the 1940s established that electrical stimulation of the ANT could modulate the synchrony of surface EEG tracings [63, 64], perhaps via activation of inhibitory corticothalamic projections [65]. High-frequency stimulation raised seizure thresholds in both rat [66] and sheep [67] epilepsy models. Further, lesions of the ANT or upstream afferent structures mitigate seizure genesis and propagation [66, 68–71], a finding later supported by a small clinical series in humans [72].

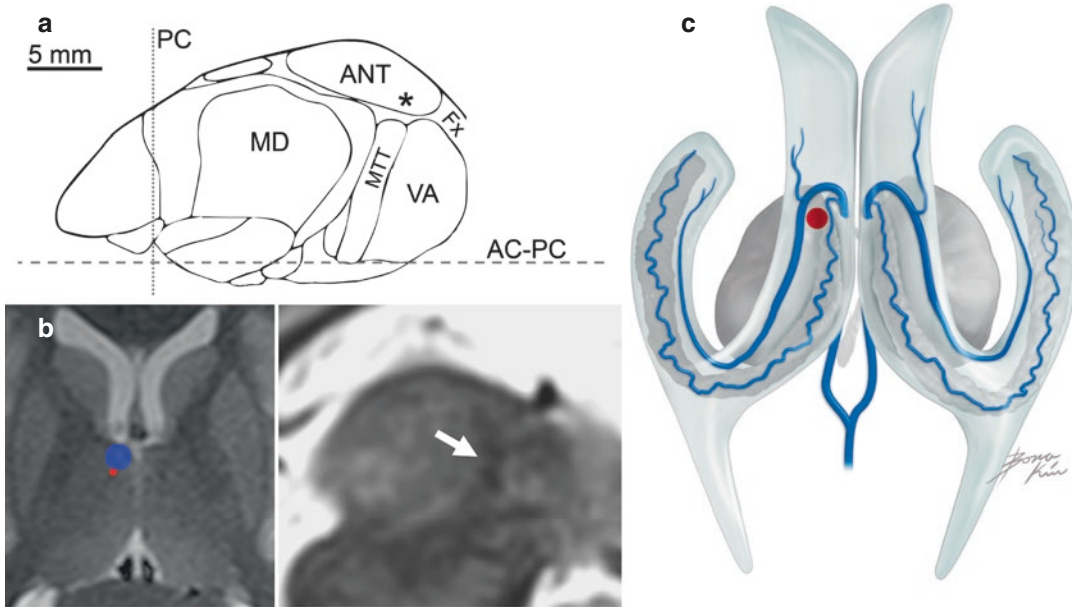

Fig. 27.2 Targeting the ANT. (**a**) Sagittal section through the thalamus 8.2 mm lateral to the midline, adapted from [106]. The ANT lies on the superior surface of the thalamus. The surgical target (∗) is slightly superior and anterior to the ANT-MTT junction. (**b**) Axial T2 (left) and sagittal STIR (right) MRI sections through the ANT. In the axial image, the right ANT and MTT are noted with blue and red circles, respectively. The MTT is visible on sagittal STIR images as a dark band (white arrow). (**c**) Dorsal view of the thalami and surrounding ventricular veins. The ANT (red circle) is draped by the thalamostriate (superiolaterally), superior choroidal (superiomedially), and internal cerebral (inferomedially) veins. All rights reserved to Emory University, printed with permission. Abbreviations: AC anterior commissure, ANT anterior nucleus of the thalamus, Fx fornix, MD mediodorsal nucleus, MTT mammillothalamic tract, PC posterior commissure, VA ventral anterior nucleus

Evidence and Outcomes

The seminal studies of Cooper [73, 74] and later small pilot studies suggesting the tolerability and potential effectiveness of ANT DBS [75, 76] motivated the pivotal SANTE trial [77]. In that trial, 110 subjects with partial-onset seizures were implanted with bilateral ANT DBS and then randomized to 3 months of blinded active or sham stimulation; this was followed by an open-label extension with active stimulation applied in both treatment arms. Stimulation was delivered in a monopolar configuration using the contact most centrally located in the ANT with a fixed schedule with a 1 min on and 5 min off duty cycle. The primary outcome measure was change in seizure frequency from baseline.

At the end of the 3-month blinded phase, the active stimulation arm showed a greater reduction in seizure frequency (40.4% vs 14.5%; $p = 0.002$). After 2 years, there was a 56% median seizure reduction among all participants, with a ≥50% response rate of 54%. Longer-term follow-up showed continued improvement over time, with a mean seizure reduction of 69% and a 68% responder rate at 5 years [78].

In the SANTE trial, self-reports of new-onset depressive symptoms and memory dysfunction were more common in the active stimulation arm, though there were no objective between-group differences detected in mood or cognition [77]. At 7 years, some complaints persisted but were not accompanied by objective neuropsychological declines; by contrast, as a group, subjects actually scored higher in measures of executive function and attention [79].

The anatomy of the circuit of Papez fueled the supposition that patients with frontotemporal or limbic circuit seizures might fare better with ANT DBS than those with onset zones elsewhere. Indeed, there was a suggestion within the SANTE trial that patients with temporal lobe foci responded the best, and a subsequent meta-analysis of eight ANT studies showed a 59% response rate for achieving at least a 70% seizure reduction [80]. Temporal lobe epilepsy patients were overrepresented in the SANTE trial, though, so it is difficult to draw definitive conclusions.

Technique

We perform ANT DBS in two stages: lead insertion and pulse generator implantation. As with RNS, we use one of several approaches to lead insertion, all performed under general anesthesia and all with direct targeting. Because of the direct targeting, we favor lead insertion in the MRI scanner using the ClearPoint system. The ANT can be visualized on T2 and short-tau inversion recovery (STIR) sequences (Fig. 27.2), as well as with the FGATIR sequence [81]. Since placing the leads accurately within the ANT appears critical to outcome [82] and there is yet an unestablished role for either microelectrode recordings or intraoperative test stimulation, we feel that direct confirmation of targeting with intraoperative MRI is the preferred approach. However, the surgery is equally as effectively performed with conventional or platform stereotactic frames, so long as some form of intraoperative radiographic verification is performed. This is ideally done with intraoperative CT scan (i.e., 3D) or with biplanar imaging. It should be noted that solely using lateral radiographs will not detect medial deflections of the DBS lead, which are not uncommon.

Thalamic anatomy varies substantially between patients; thus, indirect targeting with standardized coordinates relative to the anterior or posterior commissure is not appropriate, even though that is how targeting was performed in the SANTE trial. We plot a transventricular approach using entry points roughly at the coronal suture, targeting just anterior to and 1–2 mm above the MTT-ANT junction (Fig. 27.2), which is best visualized on sagittal STIR images. The goal is to place contacts within the ANT itself – not within the MTT. Malposition secondary to deflection off of the ependymal surface of the thalamus is not uncommon; a sharp stylet (but see below) or a long cannula inserted all the way to the target can help avoid this pitfall.

The ANT is defended by veins draped around and over its ependymal surface: the thalamostriate vein supero-laterally, the superior choroidal vein supero-medially, and the internal cerebral vein ventromedially (Fig. 27.2). The surgical target lies near the junction of these veins, but there

is significant variability from patient to patient and from side to side within individual patients. Threading the needle through this venous web can be challenging, and on rare occasions, a safe approach may require a lateral or posterior extraventricular trajectory, though there is some evidence these trajectories are inferior in achieving accurate targeting [83]. Because a posterior approach may mandate prone positioning of the patient, we advise an initial planning session the day before surgery.

Post-op Care and Complications

As with other neurostimulator systems, the device is typically not activated for several weeks. This is in part because impedance around the electrode changes with postoperative edema which, using the FDA-approved constant voltage Medtronic generator, can lead to current fluctuations. Final stimulation parameters are fairly standardized between patients. In the SANTE trial, all patients were initially programmed with a monopolar configuration, 5 V, 145 Hz, 90 μs pulse width, and intermittent stimulation with a duty cycle of 1 min on and 5 min off. One patient in the active treatment arm during the blinded phase had a flurry of over 200 brief partial seizures associated with activation of the device; these resolved with lowering of the stimulation amplitude to 4 V. For this reason, we start at 1–2 V and then increase gradually over several clinic visits.

Adverse events can be divided into those associated with DBS implantation and those associated with ANT stimulation. Regarding the former, in the SANTE trial there were five asymptomatic intracranial hemorrhages (4.5%), in keeping with rates in the literature for DBS lead insertion [84–87]. The 12.7% infection rate (14 participants; device removal needed in 9) was slightly higher than might be expected based on other series [84]. Implant site pain was reported by 10.9% of subjects.

Stimulation-related adverse events in the SANTE trial included induced seizures, paresthesias, depressive symptoms, and memory impairment. Five patients had an episode of status epilepticus: two after device insertion but before activation, one on activation that resolved with reprogramming, one during stimulation that required hospitalization, and one long after stimulation had been discontinued for 1 year. Complaints related to mood and memory were more common in the treatment than sham arm of the trial, but as discussed above these did not translate into verifiable decrements in neuropsychological performance. Patients should be counseled preoperatively regarding these symptoms.

Comparison of Therapies

Though the pivotal trials for VNS, RNS, and ANT DBS enrolled similar patients, any direct comparison of the therapies suffers from the methodological differences between the trials and a lack of head-to-head studies. Long-term seizure reductions and responder rates for VNS are slightly inferior to those for DBS and RNS. At present, there is sparse available data to distinguish DBS and RNS with regard to seizure reduction, seizure freedom, quality of life, neuropsychological outcome, and risk of SUDEP.

Seizure freedom rates are similar between DBS and RNS, with 16% experiencing a 6-month period of seizure freedom with DBS (over a monitoring period of 5 years) vs 23% with RNS (over 7 years) [54, 78]; rates of seizure freedom with VNS are more modest. Quality-of-life improvements are observed for subjects with all three therapies [58, 79, 88–90].

SUDEP remains a major cause of mortality for those with poorly controlled seizures [91], and all three neurostimulation therapies appear to attenuate the risk to a similar degree. Analysis of a large database of patients with VNS revealed an age-adjusted SUDEP rate of 2.47/1000 person-years in years 1–2 after implantation [92] versus 6.3–9.3/1000 person-years among a presumably similar cohort of patients being considered for epilepsy surgery [93]. There was one probable SUDEP death in the SANTE trial during the baseline phase and two definite and one possible

after implantation, yielding a definite/probable rate of 2.9/1000 patient-years. A review of deaths of RNS patients from pivotal trial and post-approval studies identified 1 probable and 4 definite events, corresponding to a definite/probable rate of 2/1000 patient-years [94].

Are these therapies synergistic? In other words, could the effects of VNS, DBS, and RNS be additive in an individual patient? In short, we don't know. In the RNS pivotal trial, 34% of subjects had previously been implanted with VNS, and prior VNS was not found to be associated with RNS treatment response [52]. The small sample size and short assessment period (neuromodulatory effects of these therapies evolve over years) limit the conclusions that can be drawn from these data. In the SANTE trial, explantation of any preexisting VNS system was mandated for trial participation [77], so there are no data on synergistic effects.

At this time, we lack a data-supported framework for informing selection of a therapy. In the absence of data, our decisions routinely boil down to patient-related factors. Frequent seizures arising from outside the circuit of Papez, for example, in primary motor or sensory cortex, are probably best suited to RNS. Poorly characterized multifocality may lend itself to ANT DBS, perhaps preceded by VNS – particularly if a patient is apprehensive about intracranial stimulation. Bitemporal epilepsy patients are candidates for DBS or RNS, with the latter favored if there is a question as to whether there is truly bitemporal disease such that one positive outcome could be to determine that there are only unilateral onsets and thus candidacy for more definitive surgery (i.e., resection or ablation). Patients with a reasonable expectation of needing future MRI scans may not be suitable for RNS, nor are patients with compliance difficulties, such as those unwilling or unable to submit to regular uploads of their data or those for whom travel to frequent RNS programming visits is not feasible. DBS and VNS are more standardized in programming, and therefore do not require follow-up that is quite as intensive. Finally, patient preference regarding the need for craniotomy with RNS needs to be considered, including the subsequent neurostimulator replacements that can predispose to infection or erosion.

Deep Brain Stimulation of the Centromedian Thalamus

Heretofore we have discussed therapy for patients with refractory partial-onset seizures. A common clinical dilemma is the management of patients with poorly controlled primary or symptomatic generalized epilepsy. None of the three aforementioned neurostimulation therapies carries FDA approval for generalized epilepsy. VNS, however, has long been used off-label for generalized epilepsy, and while there are no prospective trials, retrospective review of a large registry has supported its effectiveness [29]. ANT DBS and RNS are both untested in this realm.

DBS of another thalamic target – the centromedian nucleus (CM) – has received attention from groups in Mexico, the UK, South Korea, and Brazil. Limited series have provided evidence for efficacy in generalized epilepsy – particularly for Lennox-Gastaut syndrome (LGS). We have begun offering CM DBS to select adult patients with generalized epilepsy who have exhausted medical therapy and VNS. As such, we provide below a limited discussion of the therapy. To be clear, CM DBS is currently an off-label use in the USA.

Rationale

The CM is regarded as a node in the ascending reticular activating system, which modulates cortical excitability. It has strong projections to the striatum and insula [95], and in primates, it also projects diffusely to neocortex, particularly motor and premotor cortices [96, 97]. Its diffuse cortical projections support the observation that a "recruiting rhythm," with widespread induced cortical synchrony, can be reliably generated with low-frequency CM stimulation. High-frequency CM stimulation, by contrast, is hypothesized to desynchronize cortical activity, providing a putative mechanism for seizure inhibition.

Evidence and Outcomes

Velasco's promising initial report of successful CM stimulation [98] motivated continued investigation by his group and others [99–104], which have documented reductions in EEG spiking and the frequency of generalized tonic-clonic and absence seizures, favorable responses in Lennox-Gastaut syndrome, and inconsistent but generally unfavorable responses in frontal and temporal lobe epilepsy.

There have been three small prospective trials of CM DBS, none of which enrolled exclusively generalized epilepsy patients. In retrospect, the trials suffered from small sample sizes, patient heterogeneity, and methodological and outcome reporting inconsistencies.

In one trial [105], seven patients were enrolled in a double-blind crossover study in which active or sham CM stimulation was delivered for 3 months, followed by a washout period and then a crossover. Stimulation was delivered at a lower intensity than used by the Mexican studies to avoid the potential unblinding associated with paresthesias and for only 2 hours per day. Patients experienced a mean reduction of 30% during the active stimulation arm vs 8% in the sham arm, which was not statistically significant, though dropout of one patient with effective stimulation may have limited statistical power. Generalized seizures were noted to respond more than partial seizures in an open-label extension.

In a second trial [99], 13 patients implanted with CM DBS underwent a 3-month double-blinded stimulation off period after 6, 12, or 9 months of active stimulation. Velasco reported that unblinded active stimulation yielded marked reductions relative to baseline in generalized tonic-clonic seizures, absence seizures, generalized spike-wave discharges, and frontal spikes but no change in complex partial seizures or temporal spikes. However, there was no change in frequency of total number of seizures or of any of the seizure types during the blinded stimulation off period.

Most recently, Valentin [103] reported a study of 11 patients with either generalized or frontal epilepsy implanted and then activated in a single-blinded manner after a washout period. Two patients achieved a seizure-free period lasting >1 year with implantation alone (no stimulation). Of those with symptomatic or idiopathic generalized epilepsy (n = 6), during the 3-month active stimulation period, all had ≥50% improvement in seizure frequency (two of them had been seizure-free from insertion alone); in the long-term extension, five of six had ≥50% improvement in the major seizure frequency, with three of five being seizure-free. Only one of five patients with frontal lobe epilepsy had a ≥50% response during the blind period.

Technique and Post-op Care

We perform CM DBS under general anesthesia with the patient in the operating room in a stereotactic frame. Direct MRI targeting, as we use for ANT, is not useful given inability to directly visualize CM. We have also observed that solely relying on indirect targeting, using atlas-based calculations, is also likely less effective given high patient-to-patient variability in this patient population. Microelectrode recordings have uncertain utility. Intraoperative stimulation testing consists of generating a cortical recruiting, rhythm, which does not require an awake, participating patient. To assess for this rhythm, scalp EEG electrodes are placed around the operative field prior to prepping and draping.

Since the CM is not MRI-visible, we perform indirect targeting using published coordinates and then adjust as needed based on patient anatomy. The CM is a large nucleus; existing data suggest that accurate placement influences outcome [99]. Published targets vary by center, but common coordinates for generalized epilepsy are 10 mm lateral to midline, 0–4 mm anterior to the PC, and 0–1 mm above the AC-PC plane (Fig. 27.3).

We insert both electrodes and then screen for cortical recruiting rhythms. We deliver monopolar stimulation in the form of 6 Hz square waves with 300 μs pulse width for 30 seconds at a time at escalating amplitudes, usually in 1 or 2 V increments. The scalp EEG is screened for a

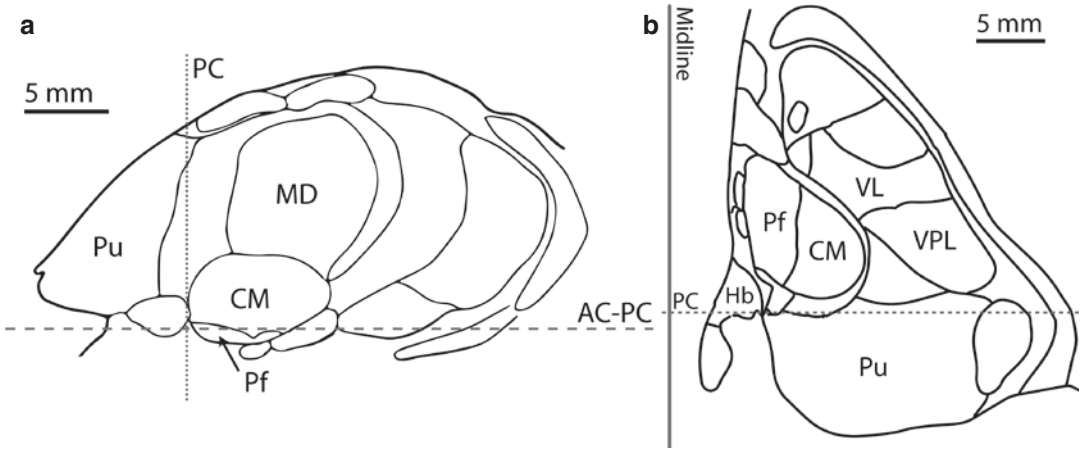

Fig. 27.3 Sagittal (**a**) and axial (**b**) sections through the CM nucleus, adapted from [106]. Sagittal section is 10 mm lateral to midline, and axial section is 2.7 mm dorsal to AC-PC plane. Abbreviations: AC anterior commissure, CM centromedian nucleus, Hb habenula, MD mediodorsal nucleus, PC posterior commissure, Pf parafascicular nucleus, Pu pulvinar, VL ventral lateral nucleus, VPL ventral posterior lateral nucleus

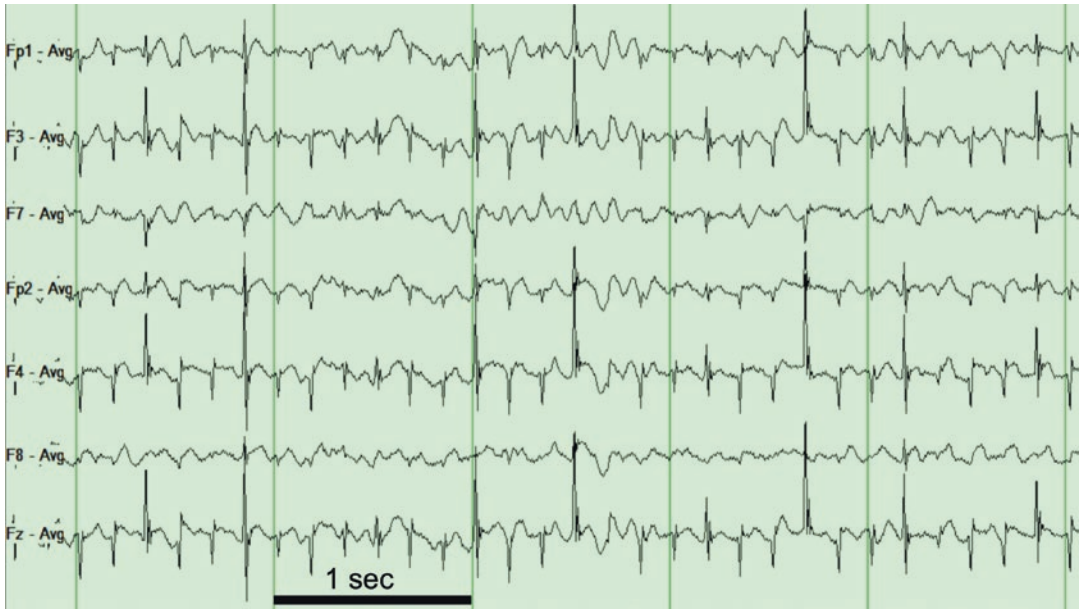

Fig. 27.4 Example intraoperative confirmation of CM targeting with cortical recruiting rhythm. Depicted is a bilateral cortical recruiting rhythm generated by unilateral CM monopolar stimulation, delivered as square waves at 6 Hz, 300 μs pulse width, and up to 6–8 V

recruiting response. A typical finding is the appearance of a low-amplitude and low-frequency (i.e., <6 Hz) rhythm – often in only one hemisphere – at lower stimulus amplitudes that evolves into a more robust 6 Hz high-amplitude signal at higher stimulus amplitudes (Fig. 27.4).

As with ANT DBS, patients are activated after a delay of several weeks. Parameters are incremented slowly. Stimulation is delivered in monopolar mode at 60 Hz and 90 μs pulse width and with a voltage dictated by patient tolerance. It is unclear as yet whether continuous or intermittent stimulation is superior.

References

1. Kwan P, Brodie MJ. Early identification of refractory epilepsy. N Engl J Med. 2000;342(5):314–9.
2. Banerjee PN, Filippi D, Allen HW. The descriptive epidemiology of epilepsy-a review. Epilepsy Res. 2009;85(1):31–45.
3. Beyenburg S, Stavem K, Schmidt D. Placebo-corrected efficacy of modern antiepileptic drugs for refractory epilepsy: systematic review and meta-analysis. Epilepsia. John Wiley & Sons, Ltd (10.1111). 2010;51(1):7–26.
4. Wiebe S, Blume WT, Girvin JP, Eliasziw M, Effectiveness and Efficiency of Surgery for Temporal Lobe Epilepsy Study Group. A randomized, controlled trial of surgery for temporal-lobe epilepsy. N Engl J Med. 2001;345(5):311–8.
5. Engel J, Wiebe S, French J, Sperling M, Williamson P, Spencer D, et al. Practice parameter: temporal lobe and localized neocortical resections for epilepsy: report of the Quality Standards Subcommittee of the American Academy of Neurology, in association with the American Epilepsy Society and the American Association of Neurological Surgeons. Neurology. 2003;60:538–47.
6. Engel J, McDermott MP, Wiebe S, Langfitt JT, Stern JM, Dewar S, et al. Early surgical therapy for drug-resistant temporal lobe epilepsy: a randomized trial. JAMA. 2012;307(9):922–30.
7. Josephson CB, Dykeman J, Fiest KM, Liu X, Sadler RM, Jetté N, et al. Systematic review and meta-analysis of standard vs selective temporal lobe epilepsy surgery. Neurology. Wolters Kluwer Health, Inc. on behalf of the American Academy of Neurology. 2013;80(18):1669–76.
8. Lanska DJ. J.L. Corning and vagal nerve stimulation for seizures in the 1880s. Neurology. 2002;58: 452–9.
9. Woodbury DM, Woodbury JW. Effects of vagal stimulation on experimentally induced seizures in rats. Epilepsia. 1990;31(Suppl 2):S7–19.
10. Zabara J. Inhibition of experimental seizures in canines by repetitive vagal stimulation. Epilepsia. 1992;33(6):1005–12.
11. Devoto P, Flore G, Saba P, Fà M, Gessa GL. Stimulation of the locus coeruleus elicits noradrenaline and dopamine release in the medial prefrontal and parietal cortex. J Neurochem. Wiley/Blackwell (10.1111). 2005;92(2):368–74.
12. Roosevelt RW, Smith DC, Clough RW, Jensen RA, Browning RA. Increased extracellular concentrations of norepinephrine in cortex and hippocampus following vagus nerve stimulation in the rat. Brain Res. 2006;1119(1):124–32.
13. Raedt R, Clinckers R, Mollet L, Vonck K, Tahry El R, Wyckhuys T, et al. Increased hippocampal noradrenaline is a biomarker for efficacy of vagus nerve stimulation in a limbic seizure model. J Neurochem. John Wiley & Sons, Ltd (10.1111). 2011;117(3):461–9.
14. Krahl SE, Clark KB, Smith DC, Browning RA. Locus coeruleus lesions suppress the seizure-attenuating effects of vagus nerve stimulation. Epilepsia. 1998;39(7):709–14.
15. Koo B. EEG changes with vagus nerve stimulation. J Clin Neurophysiol. 2001;18(5):434–41.
16. Kuba R, Guzaninová M, Brázdil M, Novák Z, Chrastina J, Rektor I. Effect of vagal nerve stimulation on interictal epileptiform discharges: a scalp EEG study. Epilepsia. 2002;43(10):1181–8.
17. Wang H, Chen X, Lin Z, Shao Z, Sun B, Shen H, et al. Long-term effect of vagus nerve stimulation on interictal epileptiform discharges in refractory epilepsy. J Neurol Sci. 2009;284(1–2):96–102.
18. Liu W-C, Mosier K, Kalnin AJ, Marks D. BOLD fMRI activation induced by vagus nerve stimulation in seizure patients. J Neurol Neurosurg Psychiatr. BMJ Publishing Group. 2003;74(6):811–3.
19. Henry TR, Votaw JR, Pennell PB, Epstein CM, Bakay RA, Faber TL, et al. Acute blood flow changes and efficacy of vagus nerve stimulation in partial epilepsy. Neurology. 1999;52(6):1166–73.
20. Ring HA, White S, Costa DC, Pottinger R, Dick JP, Koeze T, et al. A SPECT study of the effect of vagal nerve stimulation on thalamic activity in patients with epilepsy. Seizure. 2000;9(6):380–4.
21. Chae J-H, Nahas Z, Lomarev M, Denslow S, Lorberbaum JP, Bohning DE, et al. A review of functional neuroimaging studies of vagus nerve stimulation (VNS). J Psychiatr Res. 2003;37(6):443–55.
22. Borovikova LV, Ivanova S, Zhang M, Yang H, Botchkina GI, Watkins LR, et al. Vagus nerve stimulation attenuates the systemic inflammatory response to endotoxin. Nature. Nature Publishing Group. 2000;405(6785):458–62.
23. Garamendi I, Acera M, Agundez M, Galbarriatu L, Marinas A, Pomposo I, et al. Cardiovascular autonomic and hemodynamic responses to vagus nerve stimulation in drug-resistant epilepsy. Seizure. 2017;45:56–60.
24. The Vagus Nerve Stimulation Study Group. A randomized controlled trial of chronic vagus nerve stimulation for treatment of medically intractable seizures. The Vagus Nerve Stimulation Study Group. Neurology. 1995;45(2):224–30.
25. Handforth A, DeGiorgio CM, Schachter SC, Uthman BM, Naritoku DK, Tecoma ES, et al. Vagus nerve stimulation therapy for partial-onset seizures: a randomized active-control trial. Neurology. 1998;51(1):48–55.
26. Salinsky MC, Uthman BM, Ristanovic RK, Wernicke JF, Tarver WB. Vagus nerve stimulation for the treatment of medically intractable seizures. Results of a 1-year open-extension trial. Vagus Nerve Stimulation Study Group. Arch Neurol. 1996;53(11):1176–80.
27. DeGiorgio CM, Schachter SC, Handforth A, Salinsky M, Thompson J, Uthman B, et al. Prospective long-term study of vagus nerve stimulation for the treatment of refractory seizures. Epilepsia. 2000;41(9):1195–200.

28. Morris GL, Mueller WM. Long-term treatment with vagus nerve stimulation in patients with refractory epilepsy. The Vagus Nerve Stimulation Study Group E01-E05. Neurology. 1999;53(8):1731–5.
29. Englot DJ, Chang EF, Auguste KI. Efficacy of vagus nerve stimulation for epilepsy by patient age, epilepsy duration, and seizure type. Neurosurg Clin N Am. 2011;22(4):443–8–v.
30. Elliott RE, Morsi A, Tanweer O, Grobelny B, Geller E, Carlson C, et al. Efficacy of vagus nerve stimulation over time: review of 65 consecutive patients with treatment-resistant epilepsy treated with VNS > 10 years. Epilepsy Behav. 2011;20(3):478–83.
31. Boon P, Vonck K, Van Walleghem P, D'Havé M, Goossens L, Vandekerckhove T, et al. Programmed and magnet-induced vagus nerve stimulation for refractory epilepsy. J Clin Neurophysiol. 2001;18(5):402–7.
32. Fisher RS, Eggleston KS, Wright CW. Vagus nerve stimulation magnet activation for seizures: a critical review. Acta Neurol Scand. John Wiley & Sons, Ltd (10.1111). 2015;131(1):1–8.
33. Morris GL. A retrospective analysis of the effects of magnet-activated stimulation in conjunction with vagus nerve stimulation therapy. Epilepsy Behav. 2003;4(6):740–5.
34. Jansen K, Lagae L. Cardiac changes in epilepsy. Seizure. 2010;19(8):455–60.
35. Sevcencu C, Struijk JJ. Autonomic alterations and cardiac changes in epilepsy. Epilepsia. John Wiley & Sons, Ltd (10.1111). 2010;51(5):725–37.
36. Eggleston KS, Olin BD, Fisher RS. Ictal tachycardia: the head-heart connection. Seizure. 2014;23(7):496–505.
37. Zijlmans M, Flanagan D, Gotman J. Heart rate changes and ECG abnormalities during epileptic seizures: prevalence and definition of an objective clinical sign. Epilepsia. 2002;43(8):847–54.
38. Leutmezer F, Schernthaner C, Lurger S, Pötzelberger K, Baumgartner C. Electrocardiographic changes at the onset of epileptic seizures. Epilepsia. 2003;44(3):348–54.
39. Fisher RS, Afra P, Macken M, Minecan DN, Bagić A, Benbadis SR, et al. Automatic vagus nerve stimulation triggered by ictal tachycardia: clinical outcomes and device performance–The U.S. E-37 Trial. Neuromodulation. Wiley/Blackwell (10.1111). 2016;19(2):188–95.
40. Hamilton P, Soryal I, Dhahri P, Wimalachandra W, Leat A, Hughes D, et al. Clinical outcomes of VNS therapy with AspireSR® (including cardiac-based seizure detection) at a large complex epilepsy and surgery centre. Seizure. 2018;58:120–6.
41. McGregor A, Wheless J, Baumgartner J, Bettis D. Right-sided vagus nerve stimulation as a treatment for refractory epilepsy in humans. Epilepsia. John Wiley & Sons, Ltd (10.1111). 2005;46(1):91–6.
42. Kuba R, Brázdil M, Kalina M, Procházka T, Hovorka J, Nezádal T, et al. Vagus nerve stimulation: longitudinal follow-up of patients treated for 5 years. Seizure. 2009;18(4):269–74.
43. Ben-Menachem E. Vagus nerve stimulation, side effects, and long-term safety. J Clin Neurophysiol. 2001;18(5):415–8.
44. Baud MO, Kleen JK, Mirro EA, Andrechak JC, King-Stephens D, Chang EF, et al. Multi-day rhythms modulate seizure risk in epilepsy. Nat Commun Nature Publishing Group. 2018;9(1):88.
45. King-Stephens D, Mirro E, Weber PB, Laxer KD, Van Ness PC, Salanova V, et al. Lateralization of mesial temporal lobe epilepsy with chronic ambulatory electrocorticography. Epilepsia. Wiley/Blackwell (10.1111). 2015;56(6):959–67.
46. Skarpaas TL, Tcheng TK, Morrell MJ. Clinical and electrocorticographic response to antiepileptic drugs in patients treated with responsive stimulation. Epilepsy Behav. 2018;83:192–200.
47. Lesser RP, Kim SH, Beyderman L, Miglioretti DL, Webber WR, Bare M, et al. Brief bursts of pulse stimulation terminate afterdischarges caused by cortical stimulation. Neurology. 1999;53(9):2073–81.
48. Sohal VS, Sun FT. Responsive neurostimulation suppresses synchronized cortical rhythms in patients with epilepsy. Neurosurg Clin N Am. 2011;22(4):481. –8–vi
49. Sun FT, Morrell MJ. Closed-loop neurostimulation: the clinical experience. Neurotherapeutics. 2014;11(3):553–63.
50. Kossoff EH, Ritzl EK, Politsky JM, Murro AM, Smith JR, Duckrow RB, et al. Effect of an external responsive neurostimulator on seizures and electrographic discharges during subdural electrode monitoring. Epilepsia. John Wiley & Sons, Ltd (10.1111). 2004;45(12):1560–7.
51. Osorio I, Frei MG, Sunderam S, Giftakis J, Bhavaraju NC, Schaffner SF, et al. Automated seizure abatement in humans using electrical stimulation. Ann Neurol. John Wiley & Sons, Ltd. 2005;57(2):258–268.
52. Morrell MJ, RNS System in Epilepsy Study Group. Responsive cortical stimulation for the treatment of medically intractable partial epilepsy. Neurology. 2011;77(13):1295–304.
53. Sun FT, Arcot Desai S, Tcheng TK, Morrell MJ. Changes in the electrocorticogram after implantation of intracranial electrodes in humans: the implant effect. Clin Neurophysiol. 2018;129(3):676–86.
54. Bergey GK, Morrell MJ, Mizrahi EM, Goldman A, King-Stephens D, Nair D, et al. Long-term treatment with responsive brain stimulation in adults with refractory partial seizures. Neurology. Wolters Kluwer Health, Inc. on behalf of the American Academy of Neurology. 2015;84(8):810–7.
55. Jobst BC, Kapur R, Barkley GL, Bazil CW, Berg MJ, Bergey GK, et al. Brain-responsive neurostimulation in patients with medically intractable seizures arising from eloquent and other neocortical areas. Epilepsia. Wiley/Blackwell (10.1111). 2017;58(6):1005–14.

56. Geller EB, Skarpaas TL, Gross RE, Goodman RR, Barkley GL, Bazil CW, et al. Brain-responsive neurostimulation in patients with medically intractable mesial temporal lobe epilepsy. Epilepsia. 2017;58(6):994–1004.
57. Loring DW, Kapur R, Meador KJ, Morrell MJ. Differential neuropsychological outcomes following targeted responsive neurostimulation for partial-onset epilepsy. Epilepsia. 2015;56(11):1836–44.
58. Meador KJ, Kapur R, Loring DW, Kanner AM, Morrell MJ, RNS® System Pivotal Trial Investigators. Quality of life and mood in patients with medically intractable epilepsy treated with targeted responsive neurostimulation. Epilepsy Behav. 2015;45:242–7.
59. Heck CN, King-Stephens D, Massey AD, Nair DR, Jobst BC, Barkley GL, et al. Two-year seizure reduction in adults with medically intractable partial onset epilepsy treated with responsive neurostimulation: final results of the RNS system pivotal trial. Epilepsia. 2014;55(3):432–41.
60. Bergey GK, Morrell MJ, Mizrahi EM, Goldman A, King-Stephens D, Nair D, et al. Long-term treatment with responsive brain stimulation in adults with refractory partial seizures. Neurology. Lippincott Williams & Wilkins. 2015;84(8):810–7.
61. Papez JW. A proposed mechanism of emotion. Archives of Neurology & Psychiatry. American Medical Association. 1937;38(4):725–743.
62. Child ND, Benarroch EE. Anterior nucleus of the thalamus: functional organization and clinical implications. Neurology. Wolters Kluwer Health, Inc. on behalf of the American Academy of Neurology. 2013;81(21):1869–76.
63. Dempsey E, Morison R. The production of rhythmically recurrent cortical potentials after localized thalamic stimulation. Am J Physiol. 1942;135:293–300.
64. Hunter J, Jasper HH. Effects of thalamic stimulation in unanaesthetised animals: the arrest reaction and petit mal-like seizures, activation patterns and generalized convulsions. Electroencephalogr Clin Neurophysiol Elsevier. 1949;1(1–4):305–24.
65. Molnar GF, Sailer A, Gunraj CA, Cunic DI, Wennberg RA, Lozano AM, et al. Changes in motor cortex excitability with stimulation of anterior thalamus in epilepsy. Neurology. Wolters Kluwer Health, Inc. on behalf of the American Academy of Neurology. 2006;66(4):566–71.
66. Mirski MA, Rossell LA, Terry JB, Fisher RS. Anticonvulsant effect of anterior thalamic high frequency electrical stimulation in the rat. Epilepsy Res. 1997;28(2):89–100.
67. Stypulkowski PH, Giftakis JE, Billstrom TM. Development of a large animal model for investigation of deep brain stimulation for epilepsy. Stereotact Funct Neurosurg Karger Publishers. 2011;89(2):111–22.
68. Mirski MA, Ferrendelli JA. Anterior thalamic mediation of generalized pentylenetetrazol seizures. Brain Res. 1986;399(2):212–23.
69. Mirski MA, Ferrendelli JA. Interruption of the connections of the mammillary bodies protects against generalized pentylenetetrazol seizures in Guinea pigs. J Neurosci. 1987;7(3):662–70.
70. Mirski MA, Fisher RS. Electrical stimulation of the mammillary nuclei increases seizure threshold to pentylenetetrazol in rats. Epilepsia. 1994;35(6):1309–16.
71. Hamani C, Hodaie M, Chiang J, del Campo M, Andrade DM, Sherman D, et al. Deep brain stimulation of the anterior nucleus of the thalamus: effects of electrical stimulation on pilocarpine-induced seizures and status epilepticus. Epilepsy Res. 2008;78(2–3):117–23.
72. Sitnikov AR, Grigoryan YA, Mishnyakova LP. Bilateral stereotactic lesions and chronic stimulation of the anterior thalamic nuclei for treatment of pharmacoresistant epilepsy. Surg Neurol Int. 2018;9(1):137.
73. Cooper IS, Upton AR, Amin I. Reversibility of chronic neurologic deficits. Some effects of electrical stimulation of the thalamus and internal capsule in man. Appl Neurophysiol. 1980;43(3–5):244–58.
74. Cooper IS, Upton AR, Amin I, Garnett S, Brown GM, Springman M. Evoked metabolic responses in the limbic-striate system produced by stimulation of anterior thalamic nucleus in man. Int J Neurol. 1984;18:179–87.
75. Hodaie M, Wennberg RA, Dostrovsky JO, Lozano AM. Chronic anterior thalamus stimulation for intractable epilepsy. Epilepsia. 2002;43(6):603–8.
76. Kerrigan JF, Litt B, Fisher RS, Cranstoun S, French JA, Blum DE, et al. Electrical stimulation of the anterior nucleus of the thalamus for the treatment of intractable epilepsy. Epilepsia. 4 ed. 2004;45(4):346–54.
77. Fisher R, Salanova V, Witt T, Worth R, Henry T, Gross R, et al. Electrical stimulation of the anterior nucleus of thalamus for treatment of refractory epilepsy. Epilepsia. 2010;51(5):899–908.
78. Salanova V, Witt T, Worth R, Henry TR, Gross RE, Nazzaro JM, et al. Long-term efficacy and safety of thalamic stimulation for drug-resistant partial epilepsy. Neurology Lippincott Williams & Wilkins. 2015;84(10):1017–25.
79. Tröster AI, Meador KJ, Irwin CP, Fisher RS, SANTE Study Group. Memory and mood outcomes after anterior thalamic stimulation for refractory partial epilepsy. Seizure. 2017;45:133–41.
80. Chang B, Xu J. Deep brain stimulation for refractory temporal lobe epilepsy: a systematic review and meta-analysis with an emphasis on alleviation of seizure frequency outcome. Childs Nerv Syst. Springer Berlin Heidelberg. 2018;34(2):321–7.
81. Cukiert A, Lehtimäki K. Deep brain stimulation targeting in refractory epilepsy. Cukiert A, Rydenhag

B, editors. Epilepsia. 2nd ed. John Wiley & Sons, Ltd; 2017;58 Suppl 1(Suppl 1):80–4.
82. Lehtimäki K, Möttönen T, Järventausta K, Katisko J, Tähtinen T, Haapasalo J, et al. Outcome based definition of the anterior thalamic deep brain stimulation target in refractory epilepsy. Brain Stimul. 2016;9(2):268–75.
83. Lehtimäki K, Coenen VA, Gonçalves Ferreira A, Boon P, Elger C, Taylor RS, et al. The surgical approach to the anterior nucleus of thalamus in patients with refractory epilepsy: experience from the International Multicenter Registry (MORE). Neurosurgery. 3rd ed. 2019;84(1):141–50.
84. Voges J, Waerzeggers Y, Maarouf M, Lehrke R, Koulousakis A, Lenartz D, et al. Deep-brain stimulation: long-term analysis of complications caused by hardware and surgery–experiences from a single centre. J Neurol Neurosurg Psychiatr. BMJ Publishing Group Ltd. 2006;77(7):868–72.
85. Sansur CA, Frysinger RC, Pouratian N, Fu K-M, Bittl M, Oskouian RJ, et al. Incidence of symptomatic hemorrhage after stereotactic electrode placement. J Neurosurg Am Assoc Neurol Surg. 2007;107(5):998–1003.
86. Tonge M, Ackermans L, Kocabicak E, van Kranen-Mastenbroek V, Kuijf M, Oosterloo M, et al. A detailed analysis of intracerebral hemorrhages in DBS surgeries. Clin Neurol Neurosurg. 2015;139:183–7.
87. Park CK, Jung NY, Kim M, Chang JW. Analysis of delayed intracerebral hemorrhage associated with deep brain stimulation surgery. World Neurosurg. 2017;104:537–44.
88. Ryvlin P, Gilliam FG, Nguyen DK, Colicchio G, Iudice A, Tinuper P, et al. The long-term effect of vagus nerve stimulation on quality of life in patients with pharmacoresistant focal epilepsy: the PuLsE (Open Prospective Randomized Long-term Effectiveness) trial. Epilepsia. John Wiley & Sons, Ltd (10.1111). 2014;55(6):893–900.
89. Loring DW, Kapur R, Meador KJ, Morrell MJ. Differential neuropsychological outcomes following targeted responsive neurostimulation for partial-onset epilepsy. Epilepsia. John Wiley & Sons, Ltd (10.1111). 2015;56(11):1836–44.
90. Englot DJ, Hassnain KH, Rolston JD, Harward SC, Sinha SR, Haglund MM. Quality-of-life metrics with vagus nerve stimulation for epilepsy from provider survey data. Epilepsy Behav. 2017;66:4–9.
91. Tomson T, Sveinsson O, Carlsson S, Andersson T. Evolution over time of SUDEP incidence: a nationwide population-based cohort study. Epilepsia. John Wiley & Sons, Ltd (10.1111). 2018;59(8):e120–4.
92. Ryvlin P, So EL, Gordon CM, Hesdorffer DC, Sperling MR, Devinsky O, et al. Long-term surveillance of SUDEP in drug-resistant epilepsy patients treated with VNS therapy. Epilepsia. John Wiley & Sons, Ltd (10.1111). 2018;59(3):562–72.
93. Ryvlin P, Cucherat M, Rheims S. Risk of sudden unexpected death in epilepsy in patients given adjunctive antiepileptic treatment for refractory seizures: a meta-analysis of placebo-controlled randomised trials. Lancet Neurol. 2011;10(11):961–8.
94. Devinsky O, Friedman D, Duckrow RB, Fountain NB, Gwinn RP, Leiphart JW, et al. Sudden unexpected death in epilepsy in patients treated with brain-responsive neurostimulation. Epilepsia. John Wiley & Sons, Ltd (10.1111). 2018;59(3):555–61.
95. Eckert U, Metzger CD, Buchmann JE, Kaufmann J, Osoba A, Li M, et al. Preferential networks of the mediodorsal nucleus and centromedian-parafascicular complex of the thalamus–a DTI tractography study. Hum Brain Mapp. 2012;33(11):2627–37.
96. Smith Y, Raju DV, Pare J-F, Sidibe M. The thalamostriatal system: a highly specific network of the basal ganglia circuitry. Trends Neurosci. 2004;27(9):520–7.
97. Parent M, Parent A. Single-axon tracing and three-dimensional reconstruction of centre median-parafascicular thalamic neurons in primates. J Comp Neurol. 2005;481(1):127–44.
98. Velasco F, Velasco M, Ogarrio C, Fanghanel G. Electrical stimulation of the centromedian thalamic nucleus in the treatment of convulsive seizures: a preliminary report. Epilepsia. 1987;28(4):421–30.
99. Velasco F, Velasco M, Jiménez F, Velasco AL, Brito F, Rise M, et al. Predictors in the treatment of difficult-to-control seizures by electrical stimulation of the centromedian thalamic nucleus. Neurosurgery. 2000;47(2):295–304. discussion 304–5.
100. Velasco M, Velasco F, Jiménez F, Carrillo-Ruiz JD, Velasco AL, Salín-Pascual R. Electrocortical and behavioral responses elicited by acute electrical stimulation of inferior thalamic peduncle and nucleus reticularis thalami in a patient with major depression disorder. Clin Neurophysiol. 2006;117(2):320–7.
101. Andrade DM, Zumsteg D, Hamani C, Hodaie M, Sarkissian S, Lozano AM, et al. Long-term follow-up of patients with thalamic deep brain stimulation for epilepsy. Neurology. Wolters Kluwer Health, Inc. on behalf of the American Academy of Neurology. 2006;66(10):1571–3.
102. Cukiert A, Burattini JA, Cukiert CM, Argentoni-Baldochi M, Baise-Zung C, Forster CR, et al. Centro-median stimulation yields additional seizure frequency and attention improvement in patients previously submitted to callosotomy. Seizure. 2009;18(8):588–92.
103. Valentín A, García Navarrete E, Chelvarajah R, Torres C, Navas M, Vico L, et al. Deep brain stimulation of the centromedian thalamic nucleus for the treatment of generalized and frontal epilepsies.

Epilepsia. 2nd ed. Wiley/Blackwell (10.1111). 2013;54(10):1823–33.
104. Son B-C, Shon Y-M, Choi J-G, Kim J, Ha S-W, Kim S-H, et al. Clinical outcome of patients with deep brain stimulation of the centromedian thalamic nucleus for refractory epilepsy and location of the active contacts. Stereotact Funct Neurosurg. 2016;94(3):187–97.
105. Fisher RS, Uematsu S, Krauss GL, Cysyk BJ, McPherson R, Lesser RP, et al. Placebo-controlled pilot study of centromedian thalamic stimulation in treatment of intractable seizures. Epilepsia. 1992 Sep;33(5):841–51.
106. Morel, A. (2007). Stereotactic Atlas of the Human Thalamus and Basal Ganglia. CRC Press.

Treatment-Resistant Depression: Deep Brain Stimulation

28

Patricio Riva-Posse and A. Umair Janjua

Introduction

Major depressive disorder (MDD) is a debilitating disease that has a lifetime prevalence of 16% in the US population [1]. It is estimated that MDD causes an economic burden of approximately $83 billion annually due to multiple socioeconomic factors including loss of workdays and productivity [2]. In a nationally representative sample of more than 3000 workers, patients with major depression lost 27.2 workdays per year [3]. Such a debilitating disease brings about a prominent healthcare burden, as suicide is the tenth leading cause of death in the United States, claiming the lives of 47,000 people annually, and ranking as the second leading cause of death for ages 10 to 34.

The current diagnostic criteria within the *Diagnostic and Statistical Manual of Mental Disorders, Fifth Edition* (DSM 5), for MDD include a continuous 2-week period where the patient must exhibit at least five out of nine symptoms (depressed mood, anhedonia, changes in weight/appetite, feelings of guilt, changes in sleep, loss of energy, decreased concentration, psychomotor agitation/retardation, feelings of worthlessness, thoughts of suicide); one symptom must be either depressed mood or anhedonia, and symptoms must be a change from baseline and cause a marked impairment in function while not being associated with other medical causes or a component of other psychiatric illness (i.e., bipolar disorder, schizophrenia) [4]. Identification and treatment of depression has increased in recent decades. The use of antidepressants is more common today than decades past, in part due to increased access to treatment but also due to the introduction of medications that have better side effect profiles and tolerability [5]. The vast majority of oral antidepressant treatments have targeted monoaminergic pathways, namely, serotonin, dopamine, and norepinephrine [6]. Since the discovery of monoamine oxidase inhibitors and tricyclic antidepressants in the 1960s, these neurotransmitters have been the main target of medications intended to treat mood symptomatology. This may explain why there are minimal differences in the efficacy of oral antidepressants [7]. Unfortunately, despite having more options for treatment, the treatment efficacy of these medications is limited, and there are certain patient populations that fail to respond or stop responding to medication. The largest antidepressant clinical trial, STAR-D (Sequenced Treatment Alternatives to Relieve Depression), found only one-third of patients achieved remission after their first antidepressant trial. In addition, further success of achieving remission decreased with

P. Riva-Posse (✉) · A. U. Janjua
Department of Psychiatry and Behavioral Sciences, Emory University School of Medicine, Atlanta, GA, USA
e-mail: privapo@emory.edu

N. Pouratian, S. A. Sheth (eds.), *Stereotactic and Functional Neurosurgery*,
https://doi.org/10.1007/978-3-030-34906-6_28

each additional antidepressant trial, and the likelihood of relapse was higher [8]. Depressed patients with multiple treatment options and ongoing failures have been described as suffering from treatment-resistant depression (TRD). There are several classifications for treatment resistant depression that are usually based on the number and types of treatment failures as well as the duration of the illness [9, 10]. Typically, TRD is defined as failure of two antidepressant treatments with adequate duration, augmentation strategies, and behavioral therapies. Within this population, symptoms are severe, and there is even greater economic, healthcare, mortality, and social burdens [11]. Almost one-third of patients suffering from MDD do not improve after adequate treatments and will be considered as having TRD. About 10% have the more difficult to treat illness, having failed not only multiple medications, but non-pharmacological interventions such as neuromodulation approaches [12]. Patients suffering from depression that is treatment resistant undergo more medication trials and hospitalizations, have higher rates of disability, and have higher rates of suicide [13, 14].

Treatment options beyond oral psychopharmacology include electroconvulsive therapy (ECT), repetitive transcranial magnetic stimulation (rTMS), and, more recently, ketamine and esketamine [15]. ECT has been historically the most effective intervention for TRD and is considered superior to all other treatments of depression, with remission rates of 60–90% reported in clinical trials, depending on the patient population and type of stimulus used [16]. However, the chance of response might be lower in patients with longer depressive episodes and/or who have failed to respond to numerous medications.

Other type of noninvasive neuromodulation involves the delivery of magnetic pulses via rTMS. Multiple meta-analysis show efficacy by stimulation of the dorsolateral prefrontal cortex (DLPFC) [17, 18]. However, rTMS requires daily treatment for up to 6 weeks, while there is much to learn about the optimal treatment parameters. Patients with high levels of treatment resistance are less likely to respond to rTMS [19].

The use of neurosurgery within psychiatry has been in existence since before there were antidepressants [20]. Neurosurgical approaches in psychiatry are considered some of the earliest treatment approaches to TRD. Previous approaches have had various ranges of efficacy (30–70%) with treatments for melancholic features including anterior cingulotomy, stereotactic subcaudate tractotomy, limbic leucotomy, and anterior capsulotomy [21, 22]. Such management fell out of favor due to the possibility of personality and cognitive changes and the fact that interventions were permanent and irreversible. The dawn of psychopharmacology also contributed to a less invasive approach to the treatment of psychiatric disorders.

In recent decades, the insights provided by functional neuroimaging shed light into the functioning of distinct areas of the brain in patients suffering from mood disorders. Additionally, there has been a move toward a conceptualization of neuropsychiatric disorders as dysfunctional brain networks. Functional imaging allowed the progress beyond a static lesion model highlighting the relevance of interconnected nodes and neural circuits in the pathophysiology of depression. Neuroimaging techniques introduced the possibility of identifying the role of different areas of the "mood regulation network" in distinct aspects of the depressive symptomatology [23]. Recognition of these cortical and subcortical nodes, the pathways between them, functional changes observed in pathological states, and mood changes when these areas were targets of surgical ablation for other neuropsychiatric disorders opened the tangible possibility of implementing invasive neurostimulation in the form of deep brain stimulation (DBS). Since its initial reports in 2005, multiple targets have been tried as a therapeutic option for treatment-resistant depression. While the exact mechanism of action of DBS is still unclear, it has become clear that it involves modulation of pathologically functioning circuits.

In the development of this chapter, the rationale for antidepressant treatment with DBS in different targets will be discussed. Anatomical targets include the subcallosal cingulate white matter (SCC), the ventral capsule/ventral striatum or anterior limb of the internal capsule (VC/VS or ALIC), the nucleus accumbens (NAcc), the supero-lateral medial forebrain bundle (MFB),

the inferior thalamic peduncle (ITP), and the lateral habenula (LHb).

Several groups in North America and Europe have explored DBS for depression in these targets with varying results. While the initial publications documenting its potential efficacy go back almost 15 years, the field is still considered to be in its early stages. Considering the prevalence of depression, the levels of treatment resistance, and the continuing high rates of suicide, the total numbers of patients who have received DBS for TRD remains in the low hundreds [24]. The pattern that happened in many of these targets started with initial promising results of open-label trials that were not successfully replicated in randomized, sham-controlled, double-blind studies. There are several reasons that can explain this discordance. Importantly, there may be a number of explanations that are related to study design, patient selection, or lack of clear biomarkers that would define this clinically diverse syndrome. The knowledge base that has been developed in the last decade will likely give the clinical trials that may be conducted in the future a larger chance of success, as several aspects involving neurosurgical refinement of the techniques have advanced, trial design has been critically discussed, and the promise of biomarkers appears closer to be fulfilled.

A historical and chronological discussion will be made, incorporating the basic and translational science behind the selection of targets and the advances in neuroimaging that have allowed improvement in the precision and implantation.

Targets for DBS in Treatment-Resistant Depression

Subcallosal Cingulate White Matter (SCC)

Rationale

The anterior cingulate cortex plays a crucial role in the pathophysiology of depression. The participation of this region has been verified through imaging data (both structural and functional), as well as through physiology. Multiple experiments have described the subcallosal aspect of the anterior cingulate as a critical node in mood regulation networks involved in negative mood and antidepressant treatment response. Unlike other targets for DBS who had been previously studied in ablative surgery or in lesion studies, the subcallosal cingulate cortex did not fit classic "lesion-deficit" expectations. Functional imaging highlights this region as a primary dynamic modulator within a larger, multi-component mood regulation system.

The metabolism in the SCC (studied mostly through positron emission tomography) is positively correlated with depression and anxiety severity [25–27]. When normal controls underwent a sadness induction experiment, increases in blood flow in the area were documented [28]. Patients who responded to antidepressant therapy had a decline in metabolism from an abnormal elevation toward normality [29]. These changes observed in the SCC were not isolated, and other brain region changes in treatment supported the concept of neurocircuitry-based changes in mood states. Resting state functional connectivity between SCC and the thalamus within the default mode network (DMN) is significantly greater in depressed subjects. The length of the depressive episode is positively correlated with functional connectivity in the SCC in depressed subjects [30]. Meta-analytic findings show reliably increased functional connectivity between the DMN and SCC predicting levels of depressive rumination [31, 32].

Clinical Studies

The observations that described the overactivity of the SCC (Brodmann Area 25) and its abnormal connectivity with other brain regions involved in mood regulation in patients with TRD postulated that direct stimulation of that region, via DBS, would lead to a change in the depressive state. With this hypothesis in mind, the high-frequency stimulation of DBS would correct these abnormalities and restore normal mood regulation. A small pilot study of this approach was conducted in six severely treatment-resistant depressed patients (five had failed ECT) in Canada, and four of the six patients responded at 6 months (50% decline in depression severity from baseline), with three of them achieving remission of

symptoms. There was a 71% reduction in the Hamilton Depression Rating Scale [33]. That initial cohort of 6 patients was increased to 20 patients, who were implanted and monitored for antidepressant effects of chronic stimulation. One month after surgery, 35% of patients met criteria for response with 10% of patients in remission. After 6 months, 60% of patients were responders, and 35% met criteria for remission, benefits that were largely maintained at 12 months [34]. Notably, the antidepressant effects of DBS were observed to be maintained. The long-term follow-up of this cohort of patients showed sustained reduction in the mood rating scales. After 1 year of DBS, 62.5% of patients were responders, and the response rate after 2 years was 46%, with 75% response rate after 3 years of stimulation. These patients (as all patients being considered across different targets for DBS) were considered to be the highest level of treatment resistance, having been in the current depressive episode for almost 7 years. All of them had profound occupational impairment prior to surgery (only 10% were employed) and had tried and relapsed after ECT. DBS did not only cause a symptom reduction that was remarkable and sustained, but functional impairment in the areas of physical health and social functioning progressively improved up to the last follow-up visit [35]. No significant stimulation-related adverse events were reported during this follow-up, although two patients died by suicide during depressive relapses.

The initial enthusiasm led the field to attempt to replicate these findings in different centers. In the ensuing years, a number of single and multicenter studies were published, demonstrating comparable degrees of efficacy in open-label designs (Table 28.1). Seventeen patients were implanted at Emory University. This study also included patients with bipolar 2 disorder (7 of the 17 patients). After 6 months of stimulation, the response rate was 41% (7/17) and 92% after 2 years of stimulation (12 of the 17 patients having reached the latter timepoint by the time of publication). Interestingly, there were no differences in response between patients with bipolar disorder and unipolar major depression. There were no side effects related to stimulation, such as mania or cognitive changes [36]. Other centers have described similar outcomes, with many case series [37–40]. Puigdemont et al. reported that in eight patients with severe TRD the 6-month response and remission rates were 87.5% and 37.5%, respectively. These dramatic improvements were sustained after 12 months, with 62.5% response and 50% remission rates. Another group in Germany implanted six subjects and explored acute effects of stimulation but also described long-term antidepressant effects, with two of the six patients in remission of depression after 6 months of stimulation. Importantly, they did not describe side effects secondary to high-voltage stimulation [39]. An early analysis showed promising results of this target, as Berlim et al. looked at four observational studies and found response and remission rates of 36.6% and 16.7%, 53.9% and 24.1%, and 39.9% and 26.3% at follow-up endpoints of 3, 6, and 12 months, respectively [41]. There was an additional multicenter study conducted in three different sites in Canada that implanted 21 patients [37]. Forty-eight percent of patients were responders at 6 months.

An industry-sponsored, multicenter study was conducted, with the initial intention of recruiting 200 patients in the United States. The study was halted after a futility analysis determined that the likelihood of it achieving its primary outcome was low [48]. Ninety patients had been implanted by the time the study was stopped. Its primary outcome was response (≥40% reduction in depression severity from baseline) averaged over months 4–6 of the double-blind phase (24 weeks). Participants were randomized either active ($n = 60$) or sham ($n = 30$) stimulation, and then all participants received active simulation. There was no statistically significant difference in response during the double-blind, sham-controlled phase (12 (20%) patients in the stimulation group vs 5 (17%) patients in the control group). These results were lower than the reports in the prior open-label studies, but interestingly the long-term (open-label) follow-up phase described an increase in response to treatment. The antidepressant effects doubled the initial

Table 28.1 Most relevant deep brain stimulation trials for major depressive disorder

Study	Target	Subjects	Design	Follow-up	Results	Impact
Mayberg et al. (2005) [33]	SCC	6	OLS	6 months	71% reduction in HAM-D; 66% response, 50% remission	First DBS for depression study. Positive clinical results, PET changes in local and remote areas
Lozano et al. (2008) [34]	SCC	20	OLS	1 year	55% response, 33% remission	Showed sustained mood improvement at 1 year
Kennedy et al. (2011) [35]	SCC	20	OLS	3 years	64% response, 43–50% remission	Long-term follow-up is safe and effective
Puigdemont et al. (2012) [42]	SCC	8	OLS	1 year	62.5% response, 50% remission	Second independent study to show efficacy of SCC-DBS
Holtzheimer et al. (2012) [43]	SCC	17	OLS	2 years	41% response at 6 months, 92% response at 2 years (11/12 patients)	Showed long-term efficacy and safety of SCC-DBS
Ramasubbu et al. (2013) [44]	SCC	4	OLS	6 months	50% response	Longer pulse widths may have a role in antidepressive effects
Merkl et al. (2013) [39]	SCC	6	OLS	24–36 weeks	33% response, 33% remission	SCC-DBS causes acute and chronic antidepressant effects
Puigdemont et al. (2015) [45]	SCC	5	COS	6 months	Active phase, 4/5 sustained response; sham phase, 2/5 relapsed	Continuous electrical stimulation is necessary to avoid relapse. Slow return of symptoms
Accolla et al. (2016) [46]	SCC	5	OLS	24 months	20% response	Posterior gyrus rectus is a viable target for DBS in MDD
Riva-Posse et al. (2017) [47]	SCC	11	OLS	1 year	81.8% response, 54% remission	Tractography-based target selection DBS improves outcomes
Holtzheimer et al. (2017) [48]	SCC	90	RCT	6 months in RCT and then open-label follow-up	Response, 20% (active) vs 17% (sham); remission, 5% (active) vs 7% (sham)	Not clinically significant at primary endpoint. Increased response rates over long-term phase (open label)
Merkl et al. (2017) [49]	SCC	8	RCT and then OLS	28–48 months	37.% response at 6 months 51% response (average), 33% remission in long-term follow-up	No clinical significance during double-blind phase (8 weeks); long-term treatment with significant response
Eitan et al. (2017) [50]	SCC	9	RCT-COS	13 months	44% response	Long-term high-frequency stimulation appears to be better than low frequency
Malone et al. (2009) [51]	VC/VS	15	OLS	12 months	53% response; 40% remission	Significant improvement in depressive symptoms

(continued)

Table 28.1 (continued)

Study	Target	Subjects	Design	Follow-up	Results	Impact
Malone et al. (2010) [52]	VC/VS	17	OLS	14–67 months	71% response at last follow-up, 35% remission	Significant improvement in depressive symptoms over long-term follow-up
Dougherty et al. (2015) [53]	VC/VS	30	RCT and then OLS	16 weeks in RCT and then OLS	Response during RCT: 20% (active) vs 14.3% (sham); 20–26.7% response in long-term follow-up	First DBS RCT
Bergfeld et al. (2016) [54]	vALIC	25 (OLS); 16 (COS)	OLS and then RCT-COS	1 year (OLS), 22 weeks (COS)	40% response (OLS phase); 16 COS patients had lower HAM-D (p <0.001) during active DBS	vALIC DBS showed significant decrease of depressive symptoms. Discontinuation of stimulation was followed by return of depression
Bewernick et al. (2012) [55]	NAc	11	OLS	48 months	45% response	Response found in patients with long-term follow-up
Millet et al. (2014) [56]	NAc	4	OLS	6 months	50% response during extended stimulation	NAc is a more promising target than caudate nucleus
Schlaepfer et al. (2013) [57]	MFB	7	OLS	12–33 weeks	86% response, 57.1% remission	Rapid reduction of symptoms within 2 days, response with long-term treatment
Fenoy et al. (2016) [58]	MFB	4	OLS	26 weeks	75% response	Rapid reduction of symptoms within 7 days and response with long-term treatment
Fenoy et al. (2018) [59]	MFB	6	OLS	1 year	80% response (4/5, one withdrawal, one lost to follow-up)	Sustained and durable antidepressant response
Jimenez et al. (2005) [60]	ITP	1	CR	18 weeks	HAM-D scale from 42 to 6, 100% remission	ITP DBS with prominent antidepressant effects
Raymaekers et al. (2017) [61]	ITP vs vALIC	7	COS	3–8 years	Response to ALIC stimulation and ITP 2 suicides	6/7 patients preferred the vALIC
Sartorius et al. (2010) [62]	LHb	1	CR	4 months	Remission	Highlighted antidepressive effects of LHb; cessation of DBS current resulted in the return of depressive symptoms

Legend: *OLS* open-label study, *RCT* randomized controlled trial, *COS* crossover study, *CR* case report, *SCC* subcallosal cingulate, *VC/VS* ventral capsule/ventral striatum, *vALIC* ventral anterior limb of the internal capsule, *NAc* nucleus accumbens, *MFB* medial forebrain bundle, *ITP* inferior thalamic peduncle, *LHb* lateral habenula, *HAM-D* Hamilton Depression Rating Scale

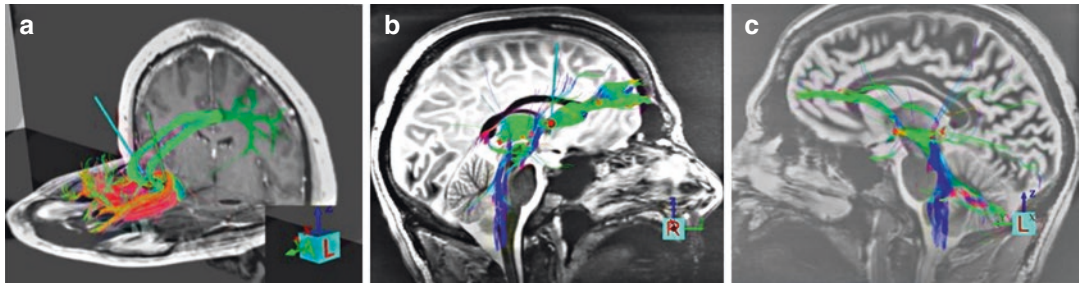

Fig. 28.1 Deterministic tractography imaging of three DBS targets. (**a**) Subcallosal cingulate target. (**b**) Ventral capsule/ventral striatum target. (**c**) Medial forebrain bundle target. (Credit: KiSueng Choi, PhD)

response rates at 18, 24, and 30 months, and half of the patients who were in the study showed a positive effect of chronic DBS. Long-term sustained antidepressant effectiveness has been demonstrated in other groups as well [49]. Stimulation appears to be most effective with high-frequency parameters, and delivery of stimulation needs to be uninterrupted, with return of symptoms over periods of weeks if it were to be stopped [50].

Studies of this kind have multiple possible reasons for failure. Among them, patient selection and study design are common culprits [63]. Neurosurgical stereotactic interventions have a unique source of variability between patients that other studies of antidepressant treatments do not have (except for rTMS): the anatomical precision of the implanted lead turned out to be a key factor in determining response to treatment [64]. The targeting of the SCC for DBS was originally chosen by identifying the anatomical location of metabolic changes seen on positron emission tomography (PET). These imaging techniques lack the precision of high-resolution structural imaging and advanced neuroimaging sequences. Additionally, the SCC is a region of high anatomical variability without clear landmarks identifiable with routine in vivo imaging [65]. There was no difference between responders and non-responders to DBS in the anatomical coordinates that were used as guide for the implantation of the leads [66]. The advantage that open-label studies had then was probably related to the possibility of making contact changes in a trial-and-error approach. Within the confines of predetermined contact and stimulation parameter changes, a blinded trial could not control an essential factor of response. Knowledge of the white matter fibers and the network that were stimulated in the SCC became more apparent when newer methods combining tractography imaging and engineering methods that estimated the volume of activated tissue were combined (Fig. 28.1a) [67]. These findings suggested that small differences in electrode location could generate substantial differences in the directly activated pathways and confirmed widespread network changes associated with DBS-induced antidepressant effects. Activation of a critical mass of a unique combination of cortical, subcortical, and cingulate pathways may be necessary for therapeutic benefit. A retrospective analysis of 17 subjects that had received DBS described that all responders shared a common tractography map [68]. Using models that calculate volume of stimulation with individualized stimulation parameters, each contact had a unique set of white matter fibers. All the DBS responders shared a combination of white matter tracts connecting the SCC to the rest of the cingulate cortex (via the cingulum bundle), bilateral medial frontal cortices (through the forceps minor), subcortical nuclei, and thalamus (via uncinate fasciculus and frontostriatal fibers). Once the pattern was identified in the retrospective analysis, a prospective testing of this hypothesis was conducted. Eleven subjects were implanted using target selection for the DBS that was based on the connectivity map that was present in responders [69]. This approach resulted in a significant increase in the response rate, with 8/11 (72.7%) of patients improving by more than 50% from baseline after 6 months, with an additional

subject becoming a responder at the 12-month timepoint (9/11–81.8% response rate). The "blueprint" was reliably defined and precisely implanted in each of the 11 subjects. Prospective targeting allowed for personalized, patient-specific, target selection. This targeting method confirmed and validated the conceptualization of a network model with the cingulate as a hub, where engagement of remote areas of the depression network is needed for the adequate antidepressant effect. Furthermore, there have been additional reports that confirmed the network model rationale behind the SCC-DBS. Distinct patterns of white matter activation have been found to be related to the intraoperative responses when there are changes in autonomic behavior (heart rate elevation) as well as positive antidepressant responses [70, 71].

Diffusion tractography imaging (DTI) tracts are complex mathematical objects, and the validity of tractography-derived information in clinical settings has yet to be fully established. Better ways of using tractography will involve evolving from a deterministic approach, which is a manual and iterative methodology, to data-driven probabilistic tractography-based targeting [72]. Replication, higher-volume trials, and well-described protocols for target selection will have the task to validate these promising methods [73, 74].

Ventral Capsule/Ventral Striatum (Ventral Anterior Limb of Internal Capsule)

Rationale

The ventral capsule/ventral striatum (VC/VS) also referred to as the ventral anterior limb of the internal capsule (vALIC) has been identified as another target for both depression and anxiety. For many years and still in use, ablative surgery in the form of anterior capsulotomy has been an effective treatment for treatment-refractory obsessive-compulsive disorder (OCD) [75, 76]. With DBS, patients with OCD not only demonstrated improvements in OCD symptoms but also in depression scales after capsulotomy [77]. The findings of improved mood in patients with OCD led to exploration of this target for TRD. While initially replicating the old ablative approach, newer studies have demonstrated that stimulation in different contacts of the DBS leads along the span of the capsule-generated distinct patterns of activation along the cortico-striatal-thalamic-cortical network [78]. Modulation of neural activity with DBS showed increased perfusion based on whether the stimulation was more ventral or dorsal along the lead axis in the VC/VS. Evidence was found that DBS at the most ventral site was associated with clinical changes in depressive symptom severity, but not OCD symptom severity.

Clinical Studies

The surgical technique for VC/VS DBS involves stereotactic anatomic targeting, using high-resolution volumetric magnetic resonance imaging for planning. The anterior limb of the internal capsule and the VS can be easily visualized on T2 and inversion recovery images for direct targeting. Typical coordinates are 4–10 mm lateral to the midline, 3–5 mm ventral to the anterior commissure, and 1–3 mm anterior to the posterior border of the anterior commissure. DBS electrodes are implanted bilaterally through the shaft of the internal capsule with the most ventral aspect in the NAcc [50, 79].

DBS in this region evolved naturally as a way to replicate the "functional lesion" caused by high-frequency stimulation. The first open-label study commented on VC/VS-DBS of 17 TRD patients and found response rates of 53% at 12-month follow-up and 71% at the last follow-up after 14–67 months (and remission in 40%) [50, 51]. Such open-label results were promising, and a multicenter randomized clinical trial was designed with the goal of providing a higher level of evidence supporting this target for treatment in TRD. DBS for OCD had already received a humanitarian device exemption in 2009 [52, 80]. A 16-week, randomized, sham-controlled trial in the United States did not find clinical significance in treatment response rates. Only 3 of the 15 patients randomized to active stimulation (20%) had achieved response, while 2 of the 14 (14.3%) who received sham therapy responded. The

response rates in the open-label phase of 24 months of follow-up were also low, with 20–26.7% achieving response at any time during that period [52].

A different study, designed and conducted in the Netherlands, had better results although they were not directly comparable. The change in the trial was that it had an initial open-label optimization phase that lasted 52 weeks. This open-label phase described a 40% overall response rate in 25 patients. Mean depression scores decreased 28.3% (Hamilton Depression Rating Scale – 17 items) and 30% (Montgomery-Åsberg Depression Rating Scale (MADRS)). Of these 25 patients, 16 (9 responders and 7 non-responders) were entered in a randomized crossover period (active-sham vs. sham-active). All responders had a return of symptoms within less than 2 weeks when stimulation was discontinued [53]. There are reasons to think that different targets may have variable times to have relapse in symptoms when stimulation is stopped [81].

Studies of DBS for OCD in this same target have started to identify neuroimaging techniques such as tractography, identifying certain fibers that are responsible for response in patients (Fig. 28.1b) [82]. In OCD, active stimulation of the capsule fibers closer to the MFB than the anterior thalamic radiations was associated with better treatment outcome ($p = 0.04$; $r^2 = 0.34$). Confirming the differences in tractography imaging and standard anatomical imaging (like in SCC), stimulation sites were largely overlapping and could not differentiate responder status, suggesting response is independent of the anatomically defined electrode position. As discussed earlier, the concept of the optimal target has evolved, from thinking of the target as a coordinate-determined gray or white matter structure to conceiving of the target as "tapping into" a circuit connects to several regions of the symptomatic network [83]. Innovative trial design, introduction of newer imaging methods, and engagement of specific biomarkers, whether physiologic, imaging, or neuropsychological, will continue to elucidate the mechanisms of action of DBS and making this target a viable therapy for patients with TRD.

Nucleus Accumbens

Rationale

The nucleus accumbens (NAcc) has been implicated as a neuromodulation target since the earlier days of this technology [84]. It is known to play key roles in the cognitive processing of motivation, reward (i.e., incentive salience, pleasure, and positive reinforcement), and reinforcement learning [85]. Preclinical animal studies have long described the anti-anhedonic effects of electrical stimulation of the accumbens [86]. In animal models of depression, the reward system is dysfunctional and is reset by chronic administration of an antidepressant [87].

Clinical Studies

While septal stimulation had been conducted many decades ago, the "modern" beginnings of DBS in NAcc started when a group in Germany implanted three patients with severe refractory depression [88]. The three participants improved "immediately" in their depression when the stimulator was on and worsened in all three patients when the stimulator was turned off. Using FDG-PET, significant changes in brain metabolism as a function of the stimulation in frontostriatal networks were observed. The cohort was extended to ten participants. After 1 year of stimulation, half (50%) were responders, and three patients were in remission [89]. Similar PET results were seen in this larger cohort, with decreased metabolism in the subgenual cingulate and in prefrontal regions including orbital prefrontal cortex. DBS in the NAcc also has sustained and durable antidepressant effects, with the same open-label cohort describing response rates of 45% (5 of 11) at 48 [54]. A different group in France implanted four subjects with the intention of doing a pilot multicenter prospective, noncomparative, and open trial. Patients initially received caudate stimulation and, after lack of antidepressant response, accumbens stimulation. This change in the DBS stimulation target caused that three of the four subjects had positive changes in mood [55]. No cognitive or other major adverse effects were reported in either trial [90]. The literature provides promising evidence of NAcc-DBS

being a treatment for TRD; however, small samples have prevented definitive conclusions regarding its antidepressant efficacy.

Medial Forebrain Bundle

Rationale

The MFB is a part of the mesolimbic-mesocortical dopamine reward system [91]. Researchers have hypothesized the role of MFB stimulation as either a pathway to regulate descending glutaminergic fibers from the mPFC to the VTA and modulate dopamine and stimulate cortical brain regions. The MFB has been considered for a long time as an essential structure related to psychobehavioral functioning in both animals and human subjects [92, 93]. There have been descriptions of its function involving affect regulation, as well as the reward-seeking system [94, 95]. The MFB, with its fibers traveling between the ventral tegmental area and the NAcc and structures beyond the reward-seeking system, appears to be involved in the pathophysiology of MDD. Interestingly, while other targets within the reward system (ventral striatum and nucleus accumbens) had already been tried, the difficulties identifying it in standard imaging had delayed its potential target for DBS in depression [96].

Clinical Studies

The surgical technique of DBS in MFB invariably requires of deterministic tractography to individually map the target area (Fig. 28.1c). The original pilot study in Germany assessed safety and efficacy of DBS in MFB in seven patients with TRD [56]. Strikingly, the antidepressant effects were very rapid in their onset, even faster than NAcc previously described. The authors described instant intraoperative antidepressant-like effects such as appetitive motivation. Within the first week of stimulation, patients already had significant improvement, and the response and remission rates were 86% and 57.1%, respectively. The fast response was replicated in a different cohort of four patients implanted in the United Sates. Three of four patients had >50% decrease in depression scores after a week post-stimulation initiation relative to baseline [57]. A notable fact in these two case series is that in the original cohort, the patient who did not respond to DBS had had a minor intracranial hemorrhage in the trajectory of the lead, therefore irreversibly lesioning the intended target of stimulation. In the second cohort described above, the patient that did not respond to DBS had reduced frontal connectivity to the MFB when her DTI was analyzed. Both centers have published their long-term results, and the antidepressant effectiveness is sustained, and the neurocognitive tests did not find changes in cognition or impulsivity [58, 97, 98]. Due to the proximity to oculomotor control areas in the midbrain, strabismus and double vision are the most significant stimulation-related adverse effects of DBS in this target. In a similar manner to the rapid onset of antidepressant effects, there seems to be an abrupt return of depressive symptomatology if stimulation is discontinued [81].

More recently, a clinical study with a randomized controlled onset of stimulation was reported [99]. Sixteen patients were implanted in the MFB and randomized to sham or real stimulation for the initial 2 months after implantation. The study reached its primary outcome at 12 months of stimulation, with all participants responding to DBS and a 56% mean decline in MADRS (50% of patients in remission). This lack of difference at this endpoint highlights the difficulties in trial design for DBS. It would be hard to imagine that a trial with the sustained antidepressant results as these have reported would be due to placebo effects. Patients with TRD usually have little response to antidepressant interventions, and these are usually short lived. But any regulatory agency who would have asked for a sham versus active trial as the primary efficacy outcome would have deemed this study inconclusive. The authors of this trial rightfully comment that slow, careful, and adaptive study development in DBS for depression is appropriate.

Inferior Thalamic Peduncle (ITP)

The ITP is part of the circuit connecting the dorsomedial thalamus and the orbitofrontal cortex [100]. Depression models have shown a dysregulation in this connection [101]. A case report

regarding ITP DBS showed a decrease in depression scores early after surgery and sustained after 8 months of stimulation using high-frequency DBS and very large pulse widths (3.5 V, 450 μs pulse width) [59]. There was a return of depressive symptoms when stimulation was interrupted, and the antidepressant effects were recaptured after stimulation was resumed with sustained effects [102]. One trial attempted to evaluate the difference between stimulation in the internal capsule and the inferior thalamic peduncle. The group consisted of seven patients with TRD who were implanted and underwent blinded crossover periods of 2 months per target. Due to low number of participants, it was not possible to determine superiority of one target over the other. All patients (n = 7) were followed up for at least 3 years (3–8 years) after implantation. Six patients completed the first crossover and five patients completed the second. Two participants died of suicide. Numerically, it appeared as if depression scores were lower for capsule stimulation. Three out of five subjects had response to ITP stimulation. Patients preferred the ALIC/BNST target with no major adverse effects [60]. Further clinical studies are needed to further validate the ITP as a DBS target for depression.

Lateral Habenula

Rationale

The LHb is an epithalamic structure that regulates serotonergic raphe nucleus activity and modulates dopaminergic midbrain functions [103]. Increased activation of the lateral habenular nucleus leads to the downregulation of the serotonergic, noradrenergic, dopaminergic systems and stimulation of the hypothalamic-pituitary-adrenal (HPA) axis [104]. This overactivity in the habenula in depressive states may be counteracted by functional inhibition of the lateral habenula with DBS. The hypothesis is based on the findings of a clinical imaging study examining the habenula after tryptophan depletion and several animal models of depression [86]. The acute antidepressant properties of ketamine (a rapid acting antidepressant) may be mediated through the habenula [105].

Clinical Studies

Despite its promising neurobiological support, there have only been two case reports in the literature [106]. In one case, the authors reported remission of depressive symptoms after 4 months of habenular stimulation. Interestingly, cessation of DBS current resulted in the return of depressive symptoms [61]. Further clinical trials, case series, and studies of comparison between targets are underway to further examine the feasibility as a DBS target.

Conclusions

Psychiatric disorders are complex, with a constellation of symptoms and signs that are manifestations of multiple interconnected relevant circuits (mood, reward, anxiety/fear, homeostasis, cognition, etc.). Functional neurosurgery has been at the forefront of the advances in clinical neurosciences in the last couple of decades. Newer surgical techniques allow for more precise implantation, minimizing complications, and directly monitoring the physiologic changes caused by stimulation in the affected neurocircuitry [107]. The progress in DBS for depression will come not from a single discovery or breakthrough but with a concerted effort by all the parties involved (basic scientists, neurosurgeons, psychiatrists, computational scientists, and biomedical engineering, to name some of them). Identification of biomarkers of illness, response, and change will play a role in the design of more precise targets for engagement [108]. Likewise, this will impact patient selection and trial design. The field of neuromodulation in psychiatry is ripe for interventions that bring hope for many patients with severe, treatment-resistant disorders. The initial enthusiasm generated by small, open-label, and mostly single-center studies was followed by uncertainty when the results of multicenter, randomized, double-blind trials did not replicate the positive results [63, 109]. New ideas and approaches to address these insufficiencies have already been implemented into innovative ongoing trials that will further advance our knowledge in this complex field (NCT01984710, NCT03437928). The entire

field, not only clinicians and scientists but also industry, funding, and regulatory agencies, remains optimistic that better approaches to this problem will eventually deliver the critical answers that many patients need.

References

1. Kessler RC, Berglund P, Demler O, Jin R, Merikangas KR, Walters EE. Lifetime prevalence and age-of-onset distributions of DSM-IV disorders in the National Comorbidity Survey Replication. Arch Gen Psychiatry. 2005;62(6):593–602.
2. Greenberg PE, Kessler RC, Birnbaum HG, Leong SA, Lowe SW, Berglund PA, et al. The economic burden of depression in the United States: how did it change between 1990 and 2000? J Clin Psychiatry. 2003;64(12):1465–75.
3. Kessler RC, Akiskal HS, Ames M, Birnbaum H, Greenberg P, Hirschfeld RM, et al. Prevalence and effects of mood disorders on work performance in a nationally representative sample of U.S. workers. Am J Psychiatry. 2006;163(9):1561–8.
4. American Psychiatric Association. Diagnostic and statistical manual of mental disorders. 5th ed. Washington, D.C.: American Psychiatric Association Publishing; 2013.
5. Pratt LA, Brody DJ, Gu Q. Antidepressant use among persons aged 12 and over: United States, 2011–2014. NCHS Data Brief. 2017(283):1–8.
6. Taylor C, Fricker AD, Devi LA, Gomes I. Mechanisms of action of antidepressants: from neurotransmitter systems to signaling pathways. Cell Signal. 2005;17(5):549–57.
7. Cipriani A, Furukawa TA, Salanti G, Chaimani A, Atkinson LZ, Ogawa Y, et al. Comparative efficacy and acceptability of 21 antidepressant drugs for the acute treatment of adults with major depressive disorder: a systematic review and network meta-analysis. Lancet. 2018;391(10128):1357–66.
8. Trivedi MH, Rush AJ, Wisniewski SR, Nierenberg AA, Warden D, Ritz L, et al. Evaluation of outcomes with citalopram for depression using measurement-based care in STAR∗D: implications for clinical practice. Am J Psychiatry. 2006;163(1):28–40.
9. McIntyre RS, Filteau MJ, Martin L, Patry S, Carvalho A, Cha DS, et al. Treatment-resistant depression: definitions, review of the evidence, and algorithmic approach. J Affect Disord. 2014;156:1–7.
10. Conway CR, George MS, Sackeim HA. Toward an evidence-based, operational definition of treatment-resistant depression: when enough is enough. JAMA Psychiat. 2017;74(1):9–10.
11. Gibson TB, Jing Y, Smith Carls G, Kim E, Bagalman JE, Burton WN, et al. Cost burden of treatment resistance in patients with depression. Am J Manag Care. 2010;16(5):370–7.
12. Holtzheimer PE, Mayberg HS. Stuck in a rut: rethinking depression and its treatment. Trends Neurosci. 2011;34(1):1–9.
13. Amital D, Fostick L, Silberman A, Beckman M, Spivak B. Serious life events among resistant and non-resistant MDD patients. J Affect Disord. 2008;110(3):260–4.
14. Bergfeld IO, Mantione M, Figee M, Schuurman PR, Lok A, Denys D. Treatment-resistant depression and suicidality. J Affect Disord. 2018;235:362–7.
15. Zarate C, Duman RS, Liu G, Sartori S, Quiroz J, Murck H. New paradigms for treatment-resistant depression. Ann N Y Acad Sci. 2013;1292:21–31.
16. UK ECT Review Group. Efficacy and safety of electroconvulsive therapy in depressive disorders: a systematic review and meta-analysis. Lancet. 2003;361(9360):799–808.
17. Lam RW, Chan P, Wilkins-Ho M, Yatham LN. Repetitive transcranial magnetic stimulation for treatment-resistant depression: a systematic review and meta-analysis. Can J Psychiatry. 2008;53(9):621–31.
18. Gaynes BN, Lloyd SW, Lux L, Gartlehner G, Hansen RA, Brode S, et al. Repetitive transcranial magnetic stimulation for treatment-resistant depression: a systematic review and meta-analysis. J Clin Psychiatry. 2014;75(5):477–89. quiz 89
19. Burt T, Lisanby SH, Sackeim HA. Neuropsychiatric applications of transcranial magnetic stimulation: a meta-analysis. Int J Neuropsychopharmacol. 2002;5(1):73–103.
20. Moniz E. Prefrontal leucotomy in the treatment of mental disorders. 1937. Am J Psychiatry. 1994;151(6 Suppl):236–9.
21. Abosch A, Cosgrove GR. Biological basis for the surgical treatment of depression. Neurosurg Focus. 2008;25(1):E2.
22. Volpini M, Giacobbe P, Cosgrove GR, Levitt A, Lozano AM, Lipsman N. The history and future of ablative neurosurgery for major depressive disorder. Stereotact Funct Neurosurg. 2017;95(4):216–28.
23. Williams LM. Precision psychiatry: a neural circuit taxonomy for depression and anxiety. Lancet Psychiatry. 2016;3(5):472–80.
24. Dandekar MP, Fenoy AJ, Carvalho AF, Soares JC, Quevedo J. Deep brain stimulation for treatment-resistant depression: an integrative review of preclinical and clinical findings and translational implications. Mol Psychiatry. 2018;23(5):1094–112.
25. Drevets WC, Bogers W, Raichle ME. Functional anatomical correlates of antidepressant drug treatment assessed using PET measures of regional glucose metabolism. Eur Neuropsychopharmacol. 2002;12(6):527–44.
26. Kennedy SH, Evans KR, Kruger S, Mayberg HS, Meyer JH, McCann S, et al. Changes in regional brain glucose metabolism measured with positron emission tomography after paroxetine treatment of major depression. Am J Psychiatry. 2001;158(6):899–905.

27. Osuch EA, Ketter TA, Kimbrell TA, George MS, Benson BE, Willis MW, et al. Regional cerebral metabolism associated with anxiety symptoms in affective disorder patients. Biol Psychiatry. 2000;48(10):1020–3.
28. Liotti M, Mayberg HS, Brannan SK, McGinnis S, Jerabek P, Fox PT. Differential limbic–cortical correlates of sadness and anxiety in healthy subjects: implications for affective disorders. Biol Psychiatry. 2000;48(1):30–42.
29. Mayberg HS, Brannan SK, Tekell JL, Silva JA, Mahurin RK, McGinnis S, et al. Regional metabolic effects of fluoxetine in major depression: serial changes and relationship to clinical response. Biol Psychiatry. 2000;48(8):830–43.
30. Greicius MD, Flores BH, Menon V, Glover GH, Solvason HB, Kenna H, et al. Resting-state functional connectivity in major depression: abnormally increased contributions from subgenual cingulate cortex and thalamus. Biol Psychiatry. 2007;62(5):429–37.
31. Hamilton JP, Farmer M, Fogelman P, Gotlib IH. Depressive rumination, the default-mode network, and the dark matter of clinical neuroscience. Biol Psychiatry. 2015;78(4):224–30.
32. Dutta A, McKie S, Deakin JF. Resting state networks in major depressive disorder. Psychiatry Res. 2014;224(3):139–51.
33. Mayberg HS, Lozano AM, Voon V, McNeely HE, Seminowicz D, Hamani C, et al. Deep brain stimulation for treatment-resistant depression. Neuron. 2005;45(5):651–60.
34. Lozano AM, Mayberg HS, Giacobbe P, Hamani C, Craddock RC, Kennedy SH. Subcallosal cingulate gyrus deep brain stimulation for treatment-resistant depression. Biol Psychiatry. 2008;64(6):461–7.
35. Kennedy SH, Giacobbe P, Rizvi SJ, Placenza FM, Nishikawa Y, Mayberg HS, et al. Deep brain stimulation for treatment-resistant depression: follow-up after 3 to 6 years. Am J Psychiatry. 2011;168(5):502–10.
36. Moreines JL, McClintock SM, Kelley ME, Holtzheimer PE, Mayberg HS. Neuropsychological function before and after subcallosal cingulate deep brain stimulation in patients with treatment-resistant depression. Depress Anxiety. 2014;31(8):690–8.
37. Lozano AM, Giacobbe P, Hamani C, Rizvi SJ, Kennedy SH, Kolivakis TT, et al. A multicenter pilot study of subcallosal cingulate area deep brain stimulation for treatment-resistant depression. J Neurosurg. 2012;116(2):315–22.
38. Puigdemont D, Perez-Egea R, Portella MJ, Molet J, de Diego-Adelino J, Gironell A, et al. Deep brain stimulation of the subcallosal cingulate gyrus: further evidence in treatment-resistant major depression. Int J Neuropsychopharmacol. 2012;15:121–33.
39. Merkl A, Schneider GH, Schonecker T, Aust S, Kuhl KP, Kupsch A, et al. Antidepressant effects after short-term and chronic stimulation of the subgenual cingulate gyrus in treatment-resistant depression. Exp Neurol. 2013;249:160–8.
40. Ramasubbu R, Anderson S, Haffenden A, Chavda S, Kiss ZH. Double-blind optimization of subcallosal cingulate deep brain stimulation for treatment-resistant depression: a pilot study. J Psychiatry Neurosci. 2013;38(3):120–60.
41. Berlim MT, McGirr A, Van den Eynde F, Fleck MP, Giacobbe P. Effectiveness and acceptability of deep brain stimulation (DBS) of the subgenual cingulate cortex for treatment-resistant depression: a systematic review and exploratory meta-analysis. J Affect Disord. 2014;159:31–8.
42. Puigdemont D, Perez-Egea R, Portella MJ, Molet J, de Diego-Adelino J, Gironell A, et al. Deep brain stimulation of the subcallosal cingulate gyrus: further evidence in treatment-resistant major depression. Int J Neuropsychopharmacol. 2012;15(1):121–33.
43. Holtzheimer PE, Kelley ME, Gross RE, Filkowski MM, Garlow SJ, Barrocas A, et al. Subcallosal cingulate deep brain stimulation for treatment-resistant unipolar and bipolar depression. Arch Gen Psychiatry. 2012;69(2):150–8.
44. Ramasubbu R, Anderson S, Haffenden A, Chavda S, Kiss ZH. Double-blind optimization of subcallosal cingulate deep brain stimulation for treatment-resistant depression: a pilot study. J Psychiatry Neurosci JPN. 2013;38(5):325–32.
45. Puigdemont D, Portella M, Perez-Egea R, Molet J, Gironell A, de Diego-Adelino J, et al. A randomized double-blind crossover trial of deep brain stimulation of the subcallosal cingulate gyrus in patients with treatment-resistant depression: a pilot study of relapse prevention. J Psychiatry Neurosci JPN. 2015;40(4):224–31.
46. Accolla EA, Aust S, Merkl A, Schneider GH, Kuhn AA, Bajbouj M, et al. Deep brain stimulation of the posterior gyrus rectus region for treatment resistant depression. J Affect Disord. 2016;194:33–7.
47. Riva-Posse P, Choi KS, Holtzheimer PE, Crowell AL, Garlow SJ, Rajendra JK, et al. A connectomic approach for subcallosal cingulate deep brain stimulation surgery: prospective targeting in treatment-resistant depression. Mol Psychiatry. 2018;23(4):843–9.
48. Holtzheimer PE, Husain MM, Lisanby SH, Taylor SF, Whitworth LA, McClintock S, et al. Subcallosal cingulate deep brain stimulation for treatment-resistant depression: a multisite, randomised, sham-controlled trial. Lancet Psychiatry. 2017;4(11):839–49.
49. Merkl A, Aust S, Schneider GH, Visser-Vandewalle V, Horn A, Kuhn AA, et al. Deep brain stimulation of the subcallosal cingulate gyrus in patients with treatment-resistant depression: a double-blinded randomized controlled study and long-term follow-up in eight patients. J Affect Disord. 2018;227:521–9.
50. Eitan R, Fontaine D, Benoit M, Giordana C, Darmon N, Israel Z, et al. One year double blind study of high vs low frequency subcallosal cingulate stimulation for depression. J Psychiatr Res. 2018;96:124–34.

51. Malone DA Jr, Dougherty DD, Rezai AR, Carpenter LL, Friehs GM, Eskandar EN, et al. Deep brain stimulation of the ventral capsule/ventral striatum for treatment-resistant depression. Biol Psychiatry. 2009;65(4):267–75.
52. Malone DA Jr. Use of deep brain stimulation in treatment-resistant depression. Cleve Clin J Med. 2010;77(Suppl 3):S77–80.
53. Dougherty DD, Rezai AR, Carpenter LL, Howland RH, Bhati MT, O'Reardon JP, et al. A randomized sham-controlled trial of deep brain stimulation of the ventral capsule/ventral striatum for chronic treatment-resistant depression. Biol Psychiatry. 2015;78(4):240–8.
54. Bergfeld IO, Mantione M, Hoogendoorn ML, Ruhe HG, Notten P, van Laarhoven J, et al. Deep brain stimulation of the ventral anterior limb of the internal capsule for treatment-resistant depression: a randomized clinical trial. JAMA Psychiat. 2016;73(5):456–64.
55. Bewernick BH, Kayser S, Sturm V, Schlaepfer TE. Long-term effects of nucleus accumbens deep brain stimulation in treatment-resistant depression: evidence for sustained efficacy. Neuropsychopharmacology. 2012;37(9):1975–85.
56. Millet B, Jaafari N, Polosan M, Baup N, Giordana B, Haegelen C, et al. Limbic versus cognitive target for deep brain stimulation in treatment-resistant depression: accumbens more promising than caudate. Eur Neuropsychopharmacol. 2014;24(8):1229–39.
57. Schlaepfer TE, Bewernick BH, Kayser S, Madler B, Coenen VA. Rapid effects of deep brain stimulation for treatment-resistant major depression. Biol Psychiatry. 2013;73(12):1204–12.
58. Fenoy AJ, Schulz P, Selvaraj S, Burrows C, Spiker D, Cao B, et al. Deep brain stimulation of the medial forebrain bundle: distinctive responses in resistant depression. J Affect Disord. 2016;203:143–51.
59. Fenoy AJ, Schulz PE, Selvaraj S, Burrows CL, Zunta-Soares G, Durkin K, et al. A longitudinal study on deep brain stimulation of the medial forebrain bundle for treatment-resistant depression. Transl Psychiatry. 2018;8(1):111.
60. Jimenez F, Velasco F, Salin-Pascual R, Hernandez JA, Velasco M, Criales JL, et al. A patient with a resistant major depression disorder treated with deep brain stimulation in the inferior thalamic peduncle. Neurosurgery. 2005;57(3):585–93; discussion −93
61. Raymaekers S, Luyten L, Bervoets C, Gabriels L, Nuttin B. Deep brain stimulation for treatment-resistant major depressive disorder: a comparison of two targets and long-term follow-up. Transl Psychiatry. 2017;7(10):e1251.
62. Sartorius A, Kiening KL, Kirsch P, von Gall CC, Haberkorn U, Unterberg AW, et al. Remission of major depression under deep brain stimulation of the lateral habenula in a therapy-refractory patient. Biol Psychiatry. 2010;67(2):e9–e11.
63. Schlaepfer TE. Deep brain stimulation for major depression-steps on a long and winding road. Biol Psychiatry. 2015;78(4):218–9.
64. Fitzgerald PB, Hoy K, McQueen S, Maller JJ, Herring S, Segrave R, et al. A randomized trial of rTMS targeted with MRI based neuro-navigation in treatment-resistant depression. Neuropsychopharmacology. 2009;34:1255.
65. Dombrowski SM, Hilgetag CC, Barbas H. Quantitative architecture distinguishes prefrontal cortical systems in the rhesus monkey. Cereb Cortex. 2001;11(10):975–88.
66. Hamani C, Mayberg H, Snyder B, Giacobbe P, Kennedy S, Lozano AM. Deep brain stimulation of the subcallosal cingulate gyrus for depression: anatomical location of active contacts in clinical responders and a suggested guideline for targeting. J Neurosurg. 2009;111(6):1209–15.
67. Lujan JL, Chaturvedi A, Choi KS, Holtzheimer PE, Gross RE, Mayberg HS, et al. Tractography-activation models applied to subcallosal cingulate deep brain stimulation. Brain Stimul. 2013;6(5):737–9.
68. Riva-Posse P, Choi KS, Holtzheimer PE, McIntyre CC, Gross RE, Chaturvedi A, et al. Defining critical white matter pathways mediating successful subcallosal cingulate deep brain stimulation for treatment-resistant depression. Biol Psychiatry. 2014;76(12):963–9.
69. Riva-Posse P, Choi KS, Holtzheimer PE, Crowell AL, Garlow SJ, Rajendra JK, et al. A connectomic approach for subcallosal cingulate deep brain stimulation surgery: prospective targeting in treatment-resistant depression. Mol Psychiatry. 2018;23(4):843.
70. Choi KS, Riva-Posse P, Gross RE, Mayberg HS. Mapping the "depression switch" during intraoperative testing of subcallosal cingulate deep brain stimulation. JAMA Neurol. 2015;72(11):1252–60.
71. Riva-Posse P, Inman CS, Choi KS, Crowell AL, Gross RE, Hamann S, et al. Autonomic arousal elicited by subcallosal cingulate stimulation is explained by white matter connectivity. Brain Stimul. 2019;12(3):743–51.
72. Tsolaki E, Espinoza R, Pouratian N. Using probabilistic tractography to target the subcallosal cingulate cortex in patients with treatment resistant depression. Psychiatry Res Neuroimaging. 2017;261:72–4.
73. Noecker AM, Choi KS, Riva-Posse P, Gross RE, Mayberg HS, McIntyre CC. StimVision Software: examples and applications in subcallosal cingulate deep brain stimulation for depression. Neuromodulation. 2018;21(2):191–6.
74. Mavridis IN. Commentary: tractography-activation models applied to subcallosal cingulate deep brain stimulation. Front Neuroanat. 2015;9:148.
75. Ballantine HT Jr, Cassidy WL, Flanagan NB, Marino R Jr. Stereotaxic anterior cingulotomy for neuropsychiatric illness and intractable pain. J Neurosurg. 1967;26(5):488–95.
76. Miguel EC, Lopes AC, McLaughlin NCR, Noren G, Gentil AF, Hamani C, et al. Evolution of gamma knife capsulotomy for intractable obsessive-compulsive disorder. Mol Psychiatry. 2019;24(2):218–40.

77. Greenberg BD, Malone DA, Friehs GM, Rezai AR, Kubu CS, Malloy PF, et al. Three-year outcomes in deep brain stimulation for highly resistant obsessive-compulsive disorder. Neuropsychopharmacology. 2006;31(11):2384–93.
78. Dougherty DD, Chou T, Corse AK, Arulpragasam AR, Widge AS, Cusin C, et al. Acute deep brain stimulation changes in regional cerebral blood flow in obsessive-compulsive disorder. J Neurosurg. 2016;125(5):1087–93.
79. Greenberg BD, Gabriels LA, Malone DA Jr, Rezai AR, Friehs GM, Okun MS, et al. Deep brain stimulation of the ventral internal capsule/ventral striatum for obsessive-compulsive disorder: worldwide experience. Mol Psychiatry. 2010;15(1):64–79.
80. Richardson RM, Ghuman AS, Karp JF. Results of the first randomized controlled trial of deep brain stimulation in treatment-resistant depression. Neurosurgery. 2015;77(2):N23–4.
81. Kilian HM, Meyer DM, Bewernick BH, Spanier S, Coenen VA, Schlaepfer TE. Discontinuation of superolateral medial forebrain bundle deep brain stimulation for treatment-resistant depression leads to critical relapse. Biol Psychiatry. 2019;85(6):e23–e4.
82. Liebrand LC, Caan MWA, Schuurman PR, van den Munckhof P, Figee M, Denys D, et al. Individual white matter bundle trajectories are associated with deep brain stimulation response in obsessive-compulsive disorder. Brain Stimul. 2019;12(2):353–60.
83. Karas PJ, Lee S, Jimenez-Shahed J, Goodman WK, Viswanathan A, Sheth SA. Deep brain stimulation for obsessive compulsive disorder: evolution of surgical stimulation target parallels changing model of dysfunctional brain circuits. Front Neurosci. 2018;12:998.
84. Bishop MP, Elder ST, Heath RG. Intracranial self-stimulation in man. Science. 1963;140(3565):394–6.
85. Floresco SB. The nucleus accumbens: an interface between cognition, emotion, and action. Annu Rev Psychol. 2015;66:25–52.
86. Lim LW, Prickaerts J, Huguet G, Kadar E, Hartung H, Sharp T, et al. Electrical stimulation alleviates depressive-like behaviors of rats: investigation of brain targets and potential mechanisms. Transl Psychiatry. 2015;5:e535.
87. Berton O, McClung CA, Dileone RJ, Krishnan V, Renthal W, Russo SJ, et al. Essential role of BDNF in the mesolimbic dopamine pathway in social defeat stress. Science. 2006;311(5762):864–8.
88. Schlaepfer TE, Cohen MX, Frick C, Kosel M, Brodesser D, Axmacher N, et al. Deep brain stimulation to reward circuitry alleviates anhedonia in refractory major depression. Neuropsychopharmacology. 2008;33(2):368–77.
89. Bewernick BH, Hurlemann R, Matusch A, Kayser S, Grubert C, Hadrysiewicz B, et al. Nucleus accumbens deep brain stimulation decreases ratings of depression and anxiety in treatment-resistant depression. Biol Psychiatry. 2010;67(2):110–6.
90. Grubert C, Hurlemann R, Bewernick BH, Kayser S, Hadrysiewicz B, Axmacher N, et al. Neuropsychological safety of nucleus accumbens deep brain stimulation for major depression: effects of 12-month stimulation. World J Biol Psychiatry. 2011;12(7):516–27.
91. Gálvez JF, Keser Z, Mwangi B, Ghouse AA, Fenoy AJ, Schulz PE, et al. The medial forebrain bundle as a deep brain stimulation target for treatment resistant depression: a review of published data. Prog Neuro-Psychopharmacol Biol Psychiatry. 2015;58:59–70.
92. Coenen VA, Honey CR, Hurwitz T, Rahman AA, McMaster J, Burgel U, et al. Medial forebrain bundle stimulation as a pathophysiological mechanism for hypomania in subthalamic nucleus deep brain stimulation for Parkinson's disease. Neurosurgery. 2009;64(6):1106–14. discussion 14-5
93. Coenen VA, Panksepp J, Hurwitz TA, Urbach H, Madler B. Human medial forebrain bundle (MFB) and anterior thalamic radiation (ATR): imaging of two major subcortical pathways and the dynamic balance of opposite affects in understanding depression. J Neuropsychiatry Clin Neurosci. 2012;24(2):223–36.
94. Panksepp J. Affective neuroscience of the emotional BrainMind: evolutionary perspectives and implications for understanding depression. Dialogues Clin Neurosci. 2010;12(4):533–45.
95. Panksepp J. Affective consciousness: Core emotional feelings in animals and humans. Conscious Cogn. 2005;14(1):30–80.
96. Coenen VA, Schlaepfer TE, Allert N, Madler B. Diffusion tensor imaging and neuromodulation: DTI as key technology for deep brain stimulation. Int Rev Neurobiol. 2012;107:207–34.
97. Bewernick BH, Kayser S, Gippert SM, Switala C, Coenen VA, Schlaepfer TE. Deep brain stimulation to the medial forebrain bundle for depression- long-term outcomes and a novel data analysis strategy. Brain Stimul. 2017;10(3):664–71.
98. Bewernick BH, Kilian HM, Schmidt K, Reinfeldt RE, Kayser S, Coenen VA, et al. Deep brain stimulation of the supero-lateral branch of the medial forebrain bundle does not lead to changes in personality in patients suffering from severe depression. Psychol Med. 2018;48(16):2684–92.
99. Coenen VA, Bewernick BH, Kayser S, Kilian H, Bostrom J, Greschus S, et al. Superolateral medial forebrain bundle deep brain stimulation in major depression: a gateway trial. Neuropsychopharmacology. 2019;44(7):1224–32.
100. Kopell BH, Greenberg BD. Anatomy and physiology of the basal ganglia: implications for DBS in psychiatry. Neurosci Biobehav Rev. 2008;32(3):408–22.
101. Drevets WC. Functional anatomical abnormalities in limbic and prefrontal cortical structures in major depression. Prog Brain Res. 2000;126:413–31.
102. Jimenez F, Nicolini H, Lozano AM, Piedimonte F, Salin R, Velasco F. Electrical stimulation of the inferior thalamic peduncle in the treatment of major

depression and obsessive compulsive disorders. World Neurosurg. 2013;80(3–4):S30.e17–25.
103. Boulos LJ, Darcq E, Kieffer BL. Translating the Habenula-from rodents to humans. Biol Psychiatry. 2017;81(4):296–305.
104. Sartorius A, Henn FA. Deep brain stimulation of the lateral habenula in treatment resistant major depression. Med Hypotheses. 2007;69(6):1305–8.
105. Gass N, Becker R, Reinwald J, Cosa-Linan A, Sack M, Weber-Fahr W, et al. Differences between ketamine's short-term and long-term effects on brain circuitry in depression. Transl Psychiatry. 2019;9(1):172.
106. Geisler S, Trimble M. The lateral habenula: no longer neglected. CNS Spectr. 2008;13(6):484–9.
107. Lozano AM, Lipsman N. Probing and regulating dysfunctional circuits using deep brain stimulation. Neuron. 2013;77(3):406–24.
108. Dougherty DD. Will deep brain stimulation help move precision medicine to the clinic in psychiatry? Biol Psychiatry. 2019;85(9):706–7.
109. Mayberg HS, Riva-Posse P, Crowell AL. Deep brain stimulation for depression: keeping an eye on a moving target. JAMA Psychiat. 2016;73(5):439–40.

Obsessive-Compulsive Disorder: Deep Brain Stimulation

29

Patrick J. Hunt, Xuefeng Zhang, Eric A. Storch, Catherine Catlett Christian, Ashwin Viswanathan, Wayne K. Goodman, and Sameer A. Sheth

Introduction

Obsessive-compulsive disorder (OCD) has a lifetime prevalence of 2–3% [1, 2], confers significant impairment, and frequently presents with complicating comorbidities. Patients with OCD experience obsessions and/or compulsions that cause a loss of productive time (≥1 hour per day and often several hours per day in severely affected patients) and significant distress or impairment. Patient insight is variable [3], which can lead to additional distress/impairment, but can also serve as a useful indicator of treatment outcome.

Although strong evidence for the heritability of OCD has been found [4], no individual genes have been identified [5]. Hypotheses stating that abnormalities in serotonin neurotransmission lead to OCD have been supported by both laboratory and clinical investigations. In addition to aberrant serotonin dynamics, abnormalities in other neurotransmitters are believed to play important roles in the development and progression of OCD. Thus, both selective serotonin reuptake inhibitors (SSRIs) and the tricyclic antidepressant clomipramine are approved by the Food and Drug Administration (FDA) to manage obsessive-compulsive symptoms [6]. In addition, atypical antipsychotics have been found useful for augmentation of SRIs [7].

To understand OCD neuropathology, scientists and clinicians have made tremendous efforts to characterize the brain circuitry in patients with OCD. In the 1980s–1990s, the cortico-striato-thalamo-cortical (CSTC) loop model emerged to describe how these brain regions functionally coordinate efforts to control behavior [8–10]. Various such CSTC loops have been proposed and studied, each responsible for different aspects of motor, emotional, and affective behavior. Within each loop, so-called direct and indirect sub-networks are responsible for promoting and inhibiting the behavior, respectively, such that in the normal state, a homeostatic balance may be achieved. In particular, the CSTC loop including prefrontal cortical regions (Fig. 29.1) may be dysfunctional and hyperactive in OCD patients, leading to an imbalance between the indirect and direct pathways and subsequent uncontrolled obsessions [11, 12]. Other areas of the brain, such as the prefrontal cortex, limbic circuitry,

P. J. Hunt (✉)
Molecular and Human Genetics, Baylor College of Medicine, Houston, TX, USA
e-mail: PJHunt@bcm.edu

X. Zhang
Menninger Department of Psychiatry & Behavioral Sciences, Baylor College of Medicine, Michael E. DeBakey VA Medical Center, Houston, TX, USA

E. A. Storch · C. C. Christian · W. K. Goodman
Menninger Department of Psychiatry & Behavioral Sciences, Baylor College of Medicine, Houston, TX, USA

A. Viswanathan · S. A. Sheth
Department of Neurosurgery, Baylor College of Medicine, Houston, TX, USA

N. Pouratian, S. A. Sheth (eds.), *Stereotactic and Functional Neurosurgery*,
https://doi.org/10.1007/978-3-030-34906-6_29

hypothalamus, and amygdala, may also play critical roles in OCD neuropathology [13, 14]. Most recently, a large meta-analysis has revealed that patients with OCD showed impaired task performance with hyperactivation in bilateral dorsal anterior cingulate cortex, supplementary motor area (SMA), pre-SMA, right anterior insula/frontal operculum (aI/fO), and anterior lateral prefrontal cortex during error processing. In contrast, during inhibitory control, patients with OCD demonstrated hypoactivation in the rostral and ventral anterior cingulate cortex, bilateral thalamus/caudate and parietal lobe, right aI/fO, and medial orbitofrontal cortex (Fig. 29.2). According to this theory, patients with OCD may be trapped in compulsive loops because erroneous OCD behaviors remained uncorrected by the hypoactive inhibitory control network [15]. Thus, this suggested new framework builds off of the original CSTC loop theory.

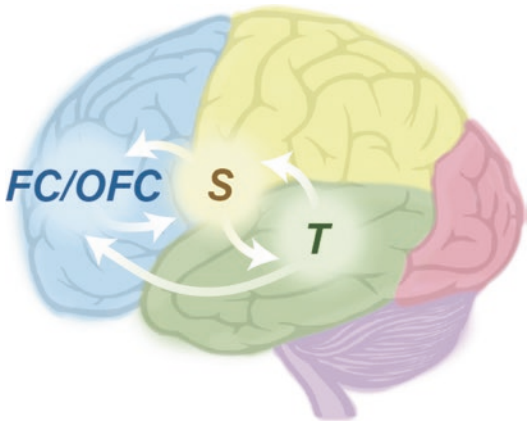

Fig. 29.1 Diagram of the cortico-striatal-thalamic-cortical loop, which connects the orbitofrontal cortex, anterior cingulate cortex, thalamus, and basal ganglia and is traditionally thought to regulate the central pathophysiology of OCD. FC frontal cortex, OFC orbitofrontal cortex, S striatum, T thalamus

Clinical Management of OCD

Cognitive Behavioral Therapy

Cognitive behavioral therapy (CBT) is the first-line psychotherapeutic treatment for OCD and relies primarily on behavioral techniques, namely, exposure and response prevention (ERP) [16]. Although high-fidelity CBT with ERP is highly efficacious for many OCD patients (response rates up to 85%), some patients relapse following therapy, and up to 15% of patients have difficulty tolerating CBT [17]. Therefore, combinations of CBT/ERP with pharmacotherapy are often required for symptom improvement in patients with OCD. Indeed, while CBT monotherapy (when available) is recommended for mild and moderate severity cases, combined treatment is the intervention of choice for more severely affected patients [18].

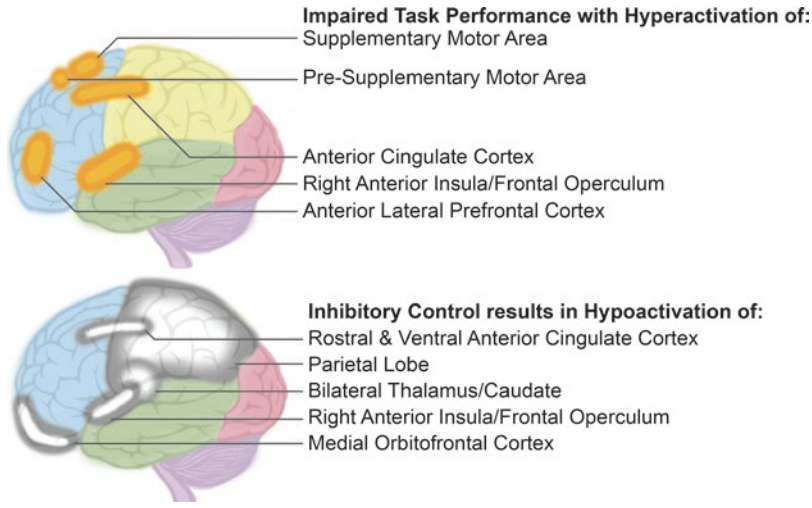

Fig. 29.2 Recent evidence supports dysregulation of multiple brain regions outside of the CSTC loop that result in OCD pathophysiology. Thus, evidence now supports an expanded and more complex etiology of OCD

Pharmacotherapy

To date, the FDA has approved four SSRIs (fluoxetine, fluvoxamine, paroxetine, and sertraline) and the tricyclic antidepressant clomipramine for OCD treatment. Other medications, including escitalopram, venlafaxine, and other SSRIs, are also commonly prescribed to treat OCD. Additionally, a group of antipsychotics, including haloperidol, risperidone, quetiapine, olanzapine, aripiprazole, and ziprasidone, have been used to augment treatment outcomes in OCD patients who respond poorly to SSRIs and clomipramine (Table 29.1). However, conclusions regarding the addition of these antipsychotics remain equivocal [19].

Neuromodulation

In addition to CBT and pharmacotherapy, neuromodulation, including neurosurgery (stereotactic lesion procedures such as anterior capsulotomy or cingulotomy), DBS, and deep transcranial magnetic brain stimulation (dTMS), is an effective intervention in OCD treatment [14, 20–24]. In this chapter, we focus on DBS. Lesion procedures, especially capsulotomy, are still in use today [25] and have certain advantages [20, 26], but we direct the reader to the referenced articles for a full discussion of this surgical option. Similarly, noninvasive deep transcranial magnetic brain stimulation (dTMS), which has been recently approved by the FDA for OCD treatment [27], will not be addressed in this chapter.

Deep Brain Stimulation

Deep brain stimulation has been used for over two decades for treating neurological disorders and, more recently but at a rapidly increasing rate, for psychiatric disorders. DBS for movement disorders such as essential tremor, Parkinson's disease, and dystonia received US FDA approval in the late 1990s and early 2000s, as described in the respective chapters on these topics. The first trial of DBS for OCD was published in 1999, demonstrating the initial promise of this therapy for patients with treatment-resistant OCD [28]. DBS for OCD was approved by the FDA under a Humanitarian Device Exemption (HDE) in 2009 [29]. Since then, a few dozen studies have established a high level of

Table 29.1 Pharmacotherapy used to treat OCD

SSRIs	Tricyclic Antidepressants	Antipsychotics	SNRI
Fluoxetine	Clomipramine	Aripiprazole	Venlafaxine
Fluvoxamine		Haloperidol	
Paroxetine		Olanzapine	
Sertraline		Quetiapine	
Escitalopram		Risperidone	
		Ziprasidone	
Medications approved by the FDA for use in OCD are highlighted			

evidence supporting the efficacy of this therapy for severe, treatment-refractory OCD, as described below in the section on outcomes.

Indications and Contraindications

Determining candidacy for DBS for OCD requires thoughtful deliberation by an experienced, multidisciplinary committee consisting of representatives from psychiatry, psychology, neurosurgery, and, at times, ethics and other disciplines [30]. Patients must demonstrate appropriate primary diagnosis, chronicity, severity, and treatment refractoriness, as well as the lack of other comorbid diagnoses that could interfere with the DBS treatment. Inclusion criteria typically include:

1. Adults with a diagnosis of OCD based on the DSM-5 diagnostic criteria [31].
2. A well-documented chronic history of OCD (duration ≥5 years).
3. Severity, as determined by a Y-BOCS/Y--BOCS-II score ≥28 [32–34].
4. Refractoriness, as determined by failure to achieve adequate and long-lasting symptom control with pharmacotherapy and cognitive behavioral therapy (CBT). Adequate pharmacotherapy typically consists of trials of adequate dose and duration using multiple SSRIs (≥3), clomipramine, and augmentation with antipsychotics (≥2). Adequate CBT consists of a trial (total ≥25 hours) of expert exposure/response prevention (ERP) therapy.
5. Be in good general health with no major medical issues.
6. Have full capacity to understand and comply with instructions and to give full informed and written consent.
7. Have sufficient social support and appropriate expectations regarding treatment outcome.

Common exclusion criteria include:

1. Significant psychiatric comorbidities that could interfere with treatment, such as psychotic or personality disorder.
2. Significant neurological comorbidity, such as major neurocognitive disorder.
3. Significant recent substance abuse.
4. Acute psychiatric safety issues, including imminent risk to harm self or others.
5. Pregnancy.

Procedure

The DBS procedure is performed much like a DBS procedure for any other indication. A volumetric MRI scan with and without contrast is obtained prior to surgery for planning purposes. A high-quality T1-weighted sequence is typically all that is needed to see the required landmarks if one is targeting the region of the ventral portion of the anterior limb of the internal capsule (ALIC). The FGATIR sequence [35] also shows these landmarks very well. There are many nominal targets in this region, but they are likely different names for the same optimal target region, as described below. Because this target region is the one approved under the US FDA HDE, and because most of the published experience is in this target region, we focus on this target here.

The key anatomical landmarks are the anterior commissure (AC), ALIC, ventral striatum (VS), and the fornices. As described below in the outcomes section, the optimal target has empirically moved posteriorly over the course of accumulated clinical experience in the past decade. Today, most groups target within a few mm of the AC in the anterior-posterior (Y) direction. The classical ventral capsule/ventral striatum (VC/VS) or "ventral ALIC" target is approximately 0–2 mm anterior to the AC, whereas the bed nucleus of the stria terminalis (BNST) target is approximately 0–2 mm posterior to the AC (Fig. 29.3). We have used both targets with success, and ongoing work seeks to individualize targeting based on patient-specific white matter pathway reconstruction, as also described below. The superior-inferior (Z) coordinate is usually just below the AC-PC plane for both of these targets. We usually plan for the most ventral contact to be within the gray matter (VS or BNST) and the higher contacts to be in the white matter just

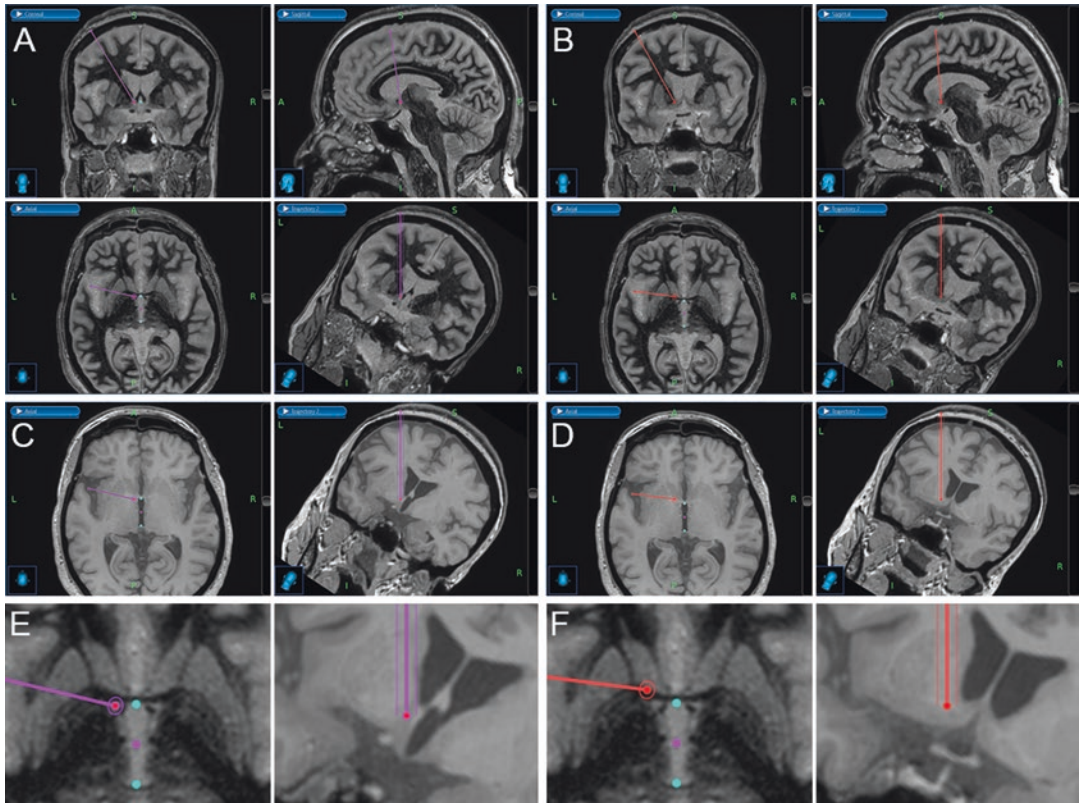

Fig. 29.3 Typical trajectories used for DBS for OCD. Trajectories are shown for BNST (**a**, **c**, **e**, magenta trajectory) and VC/VS targets (**b**, **d**, **f**, red trajectory). (**a**) shows coronal, sagittal, coronal inline and axial views (in clockwise order starting with top left panel) of a typical BNST target on an FGATIR MRI sequence. (**b**) Shows the same for a VC/VS target. (**c**, **d**) Show axial (left) and coronal inline (right) views on a T1 MRI sequence for BNST and VC/VS targets, respectively. (**e**) Shows a zoomed-in view of the BNST target in axial FGATIR (left) and coronal inline T1 (right) sequences. The target lies between the AC anteriorly and the fornix postero-medially. (**f**) Shows the same as (**e**) for the VC/VS target. We typically target the ventral-most contact of the DBS lead in the gray matter (as shown here), with the dorsal contacts in the overlying white matter. Note that only unilateral trajectories are shown here for the sake of clarity, even though plans are typically bilateral

dorsal to it. The medial-lateral (X) coordinate is adjusted to keep the trajectory within the white matter of the capsule. Once the target is set, we choose an entry point that keeps the trajectory aiming down the barrel of the ALIC. We also use a contrast-enhanced sequence to adjust the entry point so that the trajectory does not cross blood vessels.

The stereotactic apparatus is of course the surgeon's choice, whether traditional frame, robotic stereotactic system, skull-mounted frame, or other method. Our practice is to use a traditional frame. We apply the frame in the OR with local anesthesia, sometimes with the aid of light IV sedation. The patient is then positioned in a comfortable, reclined position and sedated under monitored anesthesia. We mark the entry points and plan the incisions. We use two curvilinear incisions designed to prevent the incision from overlying the hardware of the burr hole cover. We prefer two smaller incisions to a single bicoronal incision as the entry points for this target are usually quite lateral on the skull (given the coronal angle of the ALIC; see Fig. 29.3), and thus a single coronal incision would have to be quite long.

We perform a standard opening and awaken the patient. We do not find microelectrode recordings clinically useful for targeting and instead

prefer intraoperative imaging (3D fluoroscopic imaging/CT) to verify the appropriate position of the lead. We routinely perform intraoperative macrocontact stimulation testing through the DBS lead. We find that obtaining a "mirth" response with intraoperative stimulation is an excellent predictor of later clinical improvement [36]. Once both leads are secured, we obtain a final 3D image to verify the lead position prior to ending the procedure. We usually perform the second stage (pulse generator implantation) immediately following lead placement, after repositioning and re-draping, rather than staging the generator as we usually do for movement disorder cases. Most patients go home the following day.

Activation, Programming, and Adjustment of the DBS Device

The process of optimizing stimulation conditions typically takes 6–12 months. For the first 2 months, patients return for follow-up appointments roughly every 2 weeks. Afterward, patients return to follow-up approximately monthly or per protocol if on a clinical trial. Patients may be provided a patient programmer to make small adjustments themselves at home between appointments. However, providing patients this ability is always preceded by thorough education, specific instructions, and demonstration by members of the care team. In the rare event of complete non-response and occurrence of adverse effects, the device may be eventually removed.

During postoperative programming visits, DBS stimulation parameters are adjusted by an experienced psychiatrist with expertise in both OCD and DBS programming. The device is programmed telemetrically using a handheld tablet. As in DBS for movement disorders, the following stimulation parameters can be adjusted: selection of active contact(s) across the leads, amplitude, frequency, and pulse width. As the number of different possible permutations is enormous, programming algorithms built on prior clinical experience are followed to render this task more manageable. Initially, a monopolar survey is conducted with frequency typically set between 130 and 150 Hz at a constant pulse width of 90–150 microseconds. Amplitudes are gradually adjusted as tolerated and guided by bedside assessment of mood/affect, "energy," and anxiety. Acute induction of a mirth response is used to guide programming. However, it is critical not to send the patient home on settings that produce hypomania. Future visits take into account changes in OCD symptom severity as reflected in changes in Y-BOCS scores.

Clinical Efficacy of DBS for OCD

As mentioned above, the first attempt at DBS for OCD was from Nuttin and colleagues in Belgium in the late 1990s [28]. Although outcomes were not measured using the standard Y-BOCS scale, thus making objective quantification difficult, the overall promising results (3/4 patients with beneficial effects) led to dozens more attempts at using and improving DBS for OCD from groups around the world. Here we highlight some of the more influential reports in this field (Table 29.2). We have excluded case reports and small (<5 patients) series.

The majority of studies have targeted the region of the ventral ALIC, albeit using different nomenclature for the targets. Only one study attempted unilateral (right-sided) DBS [37]. This group from Cologne, Germany, targeted the right nucleus accumbens (NAc, a structure within the VS). Following implant, patients were randomized to 3 months of active vs. sham stimulation and then crossed over to serve as their own control. The difference in Y-BOCS score between active and sham stimulation during the blinded phase was insignificant, and therefore the study did not provide substantial support for unilateral DBS.

The remaining studies have been bilateral. The Amsterdam group performed a trial starting with open-label stimulation right after DBS implant, followed 8 months later with a randomized, blinded, sham-controlled discontinuation phase [38]. Overall Y-BOCS scores were lower during active stimulation than during sham, providing evidence favoring the efficacy of DBS. In

Table 29.2 DBS for OCD series

Reference	Target	*N*	Design	Findings	Response rate
Nuttin et al. [28]	ALIC	4	Open-label	3/4 patients showed improvements. Y-BOCS was not used	N/A
Mallet et al. [42]	STN	17	Double-blind, randomized, active vs. sham crossover	Level I evidence for STN DBS, although a lower responder threshold of 25% was used (vs. the typical 35%)	N/A
Huff et al. [37]	Right NAc	10	Double-blind, randomized active vs. sham crossover	At 12 months, average Y-BOCS of the cohort dropped 7 points but no difference between active and sham stimulation	1/10 (10%)
Denys et al. [38]	NAc	16	Open-label, optimization followed by double-blind, randomized, active vs. sham crossover	In stimulated patients compared to sham, an 8.3 point reduction in Y-BOCS was seen. At 2-year follow-up, 9/16 patients were responders	9/16 (56%)
Goodman et al. [40]	VC/VS	6	Double-blind, randomized, staggered onset	No difference between stimulated and sham cohorts. At 1 year, 4/6 patients were responders	4/6 (66%)
Greenberg et al. [41]	VC/VS	26	Open-label	Response rate increased from 28% at 1 month to 62% at last follow-up. The effective target moved posteriorly toward the AC	16/26 (62%)
van den Munckhof et al. [39]	NAc/vALIC	16	Open-label	Of the 9 patients with stimulation to the vALIC, there was a 73% improvement in Y-BOCS. NAc stimulation led to 42% improvement	11/16 (69%)
Luyten et al. [43]	ALIC/BNST	24	Open-label, optimization followed by double-blind, randomized, active vs. sham crossover	Median decrease of 37% in Y-BOCS comparing stim to sham. For the 17/24 patients still using DBS 4 years after implant, a median 66% decrease was seen. 15/24 still demonstrated response at last follow-up. Vicinity to the BNST appeared to improve outcomes	15/24 (63%)
Tyagi et al. [44]	STN + VC/VS	6	Double-blind, randomized, active vs. sham crossover	VC/VS and STN stimulation produced approximately similar reduction in Y-BOCS, but VC/VS stimulation produced a better antidepressant effect	5/6 (83%)

Abbreviations: *ALIC* anterior limb of the internal capsule, *BNST* bed nucleus of the stria terminalis, *DBS* deep brain stimulation, *N/A* not available, *NAc* nucleus accumbens, *STN* subthalamic nucleus, *VC/VS* ventral capsule/ventral striatum, *Y-BOCS* Yale-Brown Obsessive-Compulsive Scale

addition, subsequent imaging analyses of these cases demonstrated that the active contact for these cases was not in the VS per se, but rather in the overlying white matter [39]. These results support the view that the efficacy of this procedure is largely derived from network-wide effects gained by engaging a node within the network, and not solely by local effects in a single brain region.

The Gainesville, FL group reported their results of a double-blind staggered onset study in six patients targeting the VC/VS [40]. During the staggered blind period, there was no difference in Y-BOCS related to timing of the staggered onset, but in the follow-up open-label portion, there was a significant reduction in Y-BOCS.

In the same year, the international, multicenter group led by Brown University reported their results from an open-label trial in 26 patients [41]. Over the course of 3 months of active (unblinded) stimulation, the responder (≥35% Y-BOCS reduction) rate was 50%, and at last follow-up, the responder rate was 61.5%. This study also importantly observed the trend of

using a more posterior target, as mentioned above. Empirical evidence over the course of the study showed that targeting more posteriorly, closer to the AC, produced better results.

A French consortium performed a double-blind, randomized, sham-controlled trial of subthalamic nucleus (STN) DBS in 16 patients [42]. They used a lower criterion of 25% reduction in Y-BOCS for response. Indeed, symptom scores were lower during active than during sham stimulation, providing Level I evidence supporting this target and therapy.

An influential study from the Belgian group that first introduced DBS for OCD used a different trial design, consisting of open-label stimulation for up to 1 year, followed by double-blind, randomized discontinuation in 24 patients [43]. They targeted the BNST, which is even with or just posterior to the AC, as described above and in Fig. 29.3. During the blinded crossover phase, the active group was significantly better than the sham group, again providing Level I evidence in favor of DBS in this target. Similar to the Greenberg study [41], these authors also found that more posteriorly located targets were more effective.

Most recently, the London group performed a double-blind crossover trial in six patients with both VC/VS and STN leads [44]. They found that both targets were effective at reducing Y-BOCS scores more than sham stimulation but that the VC/VS target was better at reducing depressive symptoms in addition to OCD symptoms. Similar to several previous studies, they also found that the most effective contacts were in the white matter of the ventral ALIC and not in the gray matter of the VS.

Risks, Side Effects, and Adverse Events

The risks of DBS for OCD treatment include (1) the common risks of brain surgery, (2) unique stimulation side effects, and (3) device-related complications. DBS requires brain penetration, which carries with it the small but non-zero risk of intracerebral hemorrhage and infection. Within the concatenated cohort of approximately 100 patients in the trials mentioned above, there were 4 asymptomatic hemorrhages and 1 minimally symptomatic hemorrhage. This rate is similar to that reported in a large series of DBS for movement disorders [45]. Wound infections numbered five as well in the OCD studies, again within the range found in the movement disorder DBS literature.

Unique stimulation-related complications in patients with OCD include induction of the following psychiatric symptoms: hypomania or mania, exacerbation or relapse of OCD symptoms, exacerbation of depression and anxiety with increased suicidal ideation and behavior, and transient cognitive dysfunction. Among these conditions, hypomania is the most common side effect of DBS [46] but can be alleviated by adjusting stimulation parameters. Although a higher risk of suicide was reported in OCD patients [47], no completed suicide has been directly linked to DBS in OCD treatment [48].

Future Directions and Conclusion

Ongoing efforts continue to improve the efficacy and adoptability of DBS for OCD. The first one to two decades of its utilization has seen largely empirical changes in stereotactic targeting. More recently, studies are beginning to demonstrate the utility of targeting based on advanced connectomic imaging. We are now entering an age of individualized targeting based on the patient's specific connectivity patterns [44, 49, 50]. Continued efforts in this space will help optimize targeting and therefore improve outcomes.

In addition, recent efforts have focused on improved programming strategies. Unlike in the movement disorder field, programming adjustments may not have an immediate observable effect in the patient. Thus it can be difficult to know how to attribute causality to programming adjustments. Current strategies to handle this challenge include using DBS devices with recording as well as stimulating capabilities. Recording local field potential (LFP) activity from the DBS lead potentially allows measurement of the local "brain state." If a relationship

exists between this electrical brain state and the patient's symptom profile, then an on-board algorithm on the DBS device could be trained to make adjustments automatically, striving to move away from more symptomatic states toward less symptomatic ones. These so-called "adaptive" or "closed-loop" DBS systems have been proposed [51], and clinical trials are underway to develop and test these methodologies (e.g., NCT03184454, NCT03457675).

DBS for OCD has progressed rapidly over its first two decades, and the next decade promises to bring further enhancements. Exchange of information and best practices (regarding individualized targeting, adaptive strategies, etc.) with the movement disorders DBS field will continue fueling improvements. The future of DBS for OCD is not without challenges, however. Widespread adoption continues to increase at a slow pace. In the USA, Europe, and much of the world, the number of sites with sufficient neurosurgical and psychiatric expertise to optimally identify, implant, and manage patients remains small. Expanded education and training in both of these clinical fields on this topic will be critical. Furthermore, there remains little awareness of this option among patients and the general psychiatric community, such that potentially eligible patients often never hear about this option and reach experienced sites. Outreach and public education will therefore also be critical. If current trends continue, however, the future of this therapy remains exciting.

References

1. Regier DA, Narrow WE, Rae DS, Manderscheid RW, Locke BZ, Goodwin FK. The de facto US mental and addictive disorders service system. Epidemiologic catchment area prospective 1-year prevalence rates of disorders and services. Arch Gen Psychiatry. 1993;50:85–94.
2. Ruscio AM, Stein DJ, Chiu WT, Kessler RC. The epidemiology of obsessive-compulsive disorder in the National Comorbidity Survey Replication. Mol Psychiatry. 2010;15:53–63.
3. Foa EB, Kozak MJ, Goodman WK, Hollander E, Jenike MA, Rasmussen SA. DSM-IV field trial: obsessive-compulsive disorder. Am J Psychiatry. 1995;152(1):90–6.
4. Taylor MJ, Martin J, Lu Y, Brikell I, Lundstrom S, Larsson H, Lichtenstein P. Association of genetic risk factors for psychiatric disorders and traits of these disorders in a Swedish Population Twin Sample. JAMA Psychiatry. 2019;76:280.
5. Fernandez TV, Leckman JF, Pittenger C. Genetic susceptibility in obsessive-compulsive disorder. Handb Clin Neurol. 2018;148:767–81.
6. Varigonda AL, Jakubovski E, Bloch MH. Systematic review and meta-analysis: early treatment responses of selective serotonin reuptake inhibitors and clomipramine in pediatric obsessive-compulsive disorder. J Am Acad Child Adolesc Psychiatry. 2016;55:851–9. e852
7. Brakoulias V, Stockings E. A systematic review of the use of risperidone, paliperidone and aripiprazole as augmenting agents for obsessive-compulsive disorder. Expert Opin Pharmacother. 2019;20:47–53.
8. Saxena S, Brody AL, Schwartz JM, Baxter LR. Neuroimaging and frontal-subcortical circuitry in obsessive-compulsive disorder. Br J Psychiatry Suppl. 1998;173:26–37.
9. Alexander GE, DeLong MR, Strick PL. Parallel organization of functionally segregated circuits linking basal ganglia and cortex. Annu Rev Neurosci. 1986;9:357–81.
10. Rauch SL, Jenike MA. Neurobiological models of obsessive-compulsive disorder. Psychosomatics. 1993;34:20–32.
11. Maia TV, Cooney RE, Peterson BS. The neural bases of obsessive-compulsive disorder in children and adults. Dev Psychopathol. 2008;20:1251–83.
12. McGovern RA, Sheth SA. Role of the dorsal anterior cingulate cortex in obsessive-compulsive disorder: converging evidence from cognitive neuroscience and psychiatric neurosurgery. J Neurosurg. 2016;126:132–47.
13. Lapidus KA, Stern ER, Berlin HA, Goodman WK. Neuromodulation for obsessive-compulsive disorder. Neurotherapeutics. 2014;11:485–95.
14. Karas PJ, Lee S, Jimenez-Shahed J, Goodman WK, Viswanathan A, Sheth SA. Deep brain stimulation for obsessive compulsive disorder: evolution of surgical stimulation target parallels changing model of dysfunctional brain circuits. Front Neurosci. 2019;12:998.
15. Norman LJ, Taylor SF, Liu Y, Radua J, Chye Y, De Wit SJ, Huyser C, Karahanoglu FI, Luks T, Manoach D, Mathews C, Rubia K, Suo C, van den Heuvel OA, Yucel M, Fitzgerald K. Error processing and inhibitory control in obsessive-compulsive disorder: a meta-analysis using statistical parametric maps. Biol Psychiatry. 2019;85(9):713.
16. American Psychiatric Association. Practice guideline for the treatment of patients with obsessive-compulsive disorder. Arlington: American Psychiatric Association; 2007. Available online at: http://www.psych.org/psych_pract/treatg/pg/prac_guide.cfm.
17. Foa EB, Liebowitz MR, Kozak MJ, Davies S, Campeas R, Franklin ME, Huppert JD, Kjernisted K,

Rowan V, Schmidt AB, Simpson HB, Tu X. Randomized, placebo-controlled trial of exposure and ritual prevention, clomipramine, and their combination in the treatment of obsessive-compulsive disorder. Am J Psychiatry. 2005;162(1):151–61.
18. Eddy KT, Dutra L, Bradley R, Westen D. A multidimensional meta-analysis of psychotherapy and pharmacotherapy for obsessive-compulsive disorder. Clin Psychol Rev. 2004;24:1011–30.
19. Simpson HB. Pharmacotherapy for obsessive-compulsive disorder in adults. www.uptodate.com ©2019 UpToDate, Inc. and/or its affiliates. Wolters Kluwer Health; 2019.
20. Pepper J, Hariz M, Zrinzo L. Deep brain stimulation versus anterior capsulotomy for obsessive-compulsive disorder: a review of the literature. J Neurosurg. 2015;122:1028–37.
21. Jung HH, Kim CH, Chang JH, Park YG, Chung SS, Chang JW. Bilateral anterior cingulotomy for refractory obsessive-compulsive disorder: long-term follow-up results. Stereotact Funct Neurosurg. 2006;84:184–9.
22. Doshi PK. Surgical treatment of obsessive compulsive disorders: current status. Indian J Psychiatry. 2009;51:216–21.
23. Patel SR, Aronson JP, Sheth SA, Eskandar EN. Lesion procedures in psychiatric neurosurgery. World Neurosurg. 2013;80(3-4):S31.e9–16.
24. Mian MK, Campos M, Sheth SA, Eskandar EN. Deep brain stimulation for obsessive-compulsive disorder: past, present, and future. Neurosurg Focus. 2010;29(2):E10.
25. Lopes AC, Greenberg BD, Pereira CA, Norén G, Miguel EC. Notice of Retraction and Replacement. Lopes et al. Gamma ventral capsulotomy for obsessive-compulsive disorder: a randomized clinical trial. JAMA Psychiatry. 2014;71(9):1066–76. JAMA Psychiatry. 2015;72(12):1258
26. Miguel EC, Lopes AC, McLaughlin NCR, Norén G, et al. Evolution of gamma knife capsulotomy for intractable obsessive-compulsive disorder. Mol Psychiatry. 2019 Feb;24(2):218–40.
27. Blom RM, Figee M, Vulink N, Denys D. Update on repetitive transcranial magnetic stimulation in obsessive-compulsive disorder: different targets. Curr Psychiatry Rep. 2011;13:289–94.
28. Nuttin B, Cosyns P, Demeulemeester H, Gybels J, Meyerson B. Electrical stimulation in anterior limbs of internal capsules in patients with obsessive-compulsive disorder. Lancet. 1999;354(9189):1526.
29. Administration USTFaD. "Humanitarian Device Exemption (HDE) DBS for OCD" Accessdata.fda.gov, https://www.accessdata.fda.gov/scripts/cdrh/cfdocs/cfhde/hde.cfm?id=H050003. 2009.
30. Garnaat SL, Greenberg BD, Sibrava NJ, Goodman WK, Mancebo MC, Eisen JL, Rasmussen SA. Who qualifies for deep brain stimulation for OCD? Data from a naturalistic clinical sample. J Neuropsychiatry Clin Neurosci. 2014;26:81–6.
31. American Psychiatric Association. Obsessive-compulsive and related disorders. In: Diagnostic and statistical manual of mental disorders. 5th ed; 2013. https://doi.org/10.1176/appi.books.9780890425596.
32. Goodman WK, Price LH, Rasmussen SA, Mazure C, Fleischmann RL, Hill CL, Heninger GR, Charney DS. The Yale-Brown obsessive compulsive scale. I. Development, use, and reliability. Arch Gen Psychiatry. 1989 Nov;46(11):1006–11.
33. Goodman WK, Price LH, Rasmussen SA, Mazure C, Delgado P, Heninger GR, Charney DS. The Yale-Brown obsessive compulsive scale. II validity. Arch Gen Psychiatry. 1989 Nov;46(11):1012–6.
34. Storch EA, Rasmussen SA, Price LH, Larson MJ, Murphy TK, Goodman WK. Development and psychometric evaluation of the Yale-Brown obsessive-compulsive scale–second edition. Psychol Assess. 2010 Jun;22(2):223–32.
35. Sudhyadhom A, Haq IU, Foote KD, Okun MS, Bova FJ. A high resolution and high contrast MRI for differentiation of subcortical structures for DBS targeting: the fast gray matter acquisition T1 inversion recovery (FGATIR). NeuroImage. 2009;47(Suppl 2):T44–52.
36. Haq IU, Foote KD, Goodman WG, Wu SS, Sudhyadhom A, Ricciuti N, Siddiqui MS, Bowers D, Jacobson CE, Ward H, Okun MS. Smile and laughter induction and intraoperative predictors of response to deep brain stimulation for obsessive-compulsive disorder. NeuroImage. 2011;54(Suppl 1):S247–55.
37. Huff W, Lenartz D, Schormann M, Lee SH, Kuhn J, Koulousakis A, Mai J, Daumann J, Maarouf M, Klosterkötter J, Sturm V. Unilateral deep brain stimulation of the nucleus accumbens in patients with treatment-resistant obsessive-compulsive disorder: outcomes after one year. Clin Neurol Neurosurg. 2010;112(2):137–43.
38. Denys D, Mantione M, Figee M, van den Munckhof P, Koerselman F, Westenberg H, Bosch A, Schuurman R. Deep brain stimulation of the nucleus accumbens for treatment-refractory obsessive-compulsive disorder. Arch Gen Psychiatry. 2010;67:1061–8.
39. van den Munckhof P, Bosch DA, Mantione MH, Figee M, Denys DA, Schuurman PR. Active stimulation site of nucleus accumbens deep brain stimulation in obsessive-compulsive disorder is localized in the ventral internal capsule. Acta Neurochir Suppl. 2013;117:53–9.
40. Goodman WK, Foote KD, Greenberg BD, Ricciuti N, Bauer R, Ward H, Shapira NA, Wu SS, Hill CL, Rasmussen SA, Okun MS. Deep brain stimulation for intractable obsessive compulsive disorder: pilot study using a blinded, staggered-onset design. Biol Psychiatry. 2010;67(6):535–42.
41. Greenberg BD, Gabriels LA, Malone DA Jr, Rezai AR, et al. Deep brain stimulation of the ventral internal capsule/ventral striatum for obsessive-compulsive disorder: worldwide experience. Mol Psychiatry. 2010;15(1):64–79.
42. Mallet L, Polosan M, Jaafari N, Baup N, et al. STOC Study Group. Subthalamic nucleus stimulation in severe obsessive-compulsive disorder. N Engl J Med. 2008;359(20):2121–34.

43. Luyten L, Hendrickx S, Raymaekers S, Gabriëls L, Nuttin B. Electrical stimulation in the bed nucleus of the stria terminalis alleviates severe obsessive-compulsive disorder. Mol Psychiatry. 2016;21(9):1272–80.
44. Tyagi H, Apergis-Schoute AM, Akram H, Foltynie T, et al. A randomized trial directly comparing ventral capsule and Anteromedial subthalamic nucleus stimulation in obsessive-compulsive disorder: clinical and imaging evidence for dissociable effects. Biol Psychiatry. 2019;85(9):726–34.
45. Fenoy AJ, Simpson RK Jr. Risks of common complications in deep brain stimulation surgery: management and avoidance. J Neurosurg. 2014;120(1):132–9.
46. Greenberg BD, Malone DA, Friehs GM, Rezai AR, Kubu CS, Malloy PF, Salloway SP, Okun MS, Goodman WK, Rasmussen SA. Three-year outcomes in deep brain stimulation for highly resistant obsessive-compulsive disorder. Neuropsychopharmacology. 2006;31:2384–93.
47. Khan A, Leventhal RM, Khan S, Brown WA. Suicide risk in patients with anxiety disorders: a meta-analysis of the FDA database. J Affect Disord. 2002;68:183–90.
48. Naesstrom M, Blomstedt P, Bodlund O. A systematic review of psychiatric indications for deep brain stimulation, with focus on major depressive and obsessive-compulsive disorder. Nord J Psychiatry. 2016;70:483–91.
49. Baldermann JC, Melzer C, Zapf A, Kohl S, Timmermann L, Tittgemeyer M, Huys D, Visser-Vandewalle V, Kühn AA, Horn A, Kuhn J. Connectivity profile predictive of effective deep brain stimulation in obsessive-compulsive disorder. Biol Psychiatry. 2019;85(9):735–43.
50. Liebrand LC, Caan MWA, Schuurman PR, van den Munckhof P, Figee M, Denys D, van Wingen GA. Individual white matter bundle trajectories are associated with deep brain stimulation response in obsessive-compulsive disorder. Brain Stimul. 2019;12(2):353–60.
51. Widge AS, Ellard KK, Paulk AC, Basu I, et al. Treating refractory mental illness with closed-loop brain stimulation: progress towards a patient-specific transdiagnostic approach. Exp Neurol. 2017;287:461–72.

Obsessive-Compulsive Disorder: Lesions

30

Adriel Barrios-Anderson
and Nicole C. R. McLaughlin

Abbreviations

ACC	Anterior cingulate cortex
CSTC	Cortico-striato-thalamo-cortical
DBS	Deep brain stimulation
ERP	Exposure and response prevention
GKRS	Gamma Knife radiosurgery
GVC	Gamma Knife ventral capsulotomy
MDD	Major depressive disorder
MRI	Magnetic resonance imaging
OCD	Obsessive-compulsive disorder
OFC	Orbitofrontal cortex
SSRI	Selective serotonin reuptake inhibitor
YBOCS	Yale-Brown Obsessive Compulsive Scale

Introduction

OCD is one of the most common psychiatric illnesses, affecting approximately 2.3% of the United States population [1]. OCD is classified as an anxiety disorder defined by anxiety-inducing intrusive thoughts or images, called obsessions, accompanied by recurrent compulsive behaviors that often represent an attempt to reduce obsession-mediated anxiety [2, 3]. OCD symptoms can be extremely debilitating with individuals at the higher end of the OCD severity spectrum experiencing nearly constant anxiety due to intrusive, often disturbing thoughts and compulsively completing ritualistic behaviors to the point of self-harm or at the detriment of completing tasks of daily living [4–6]. The World Health Organization has listed OCD as one of the most debilitating illnesses worldwide because of the extreme functional impairment that results from OCD symptoms [4, 7].

Despite significant advances in clinical pharmacotherapy for mental illnesses, there remain a significant number of patients who suffer from medically refractory or intractable illness [8, 9]. By definition, these patients' illnesses do not exhibit significant or sustained responses to conventional pharmacological and cognitive-behavioral therapy [8–10]. In OCD, it is estimated that anywhere from 10% to 20% of the population have medically refractory illness [8, 11]. Unfortunately, this means that a significant number of individuals with OCD do

A. Barrios-Anderson
Psychiatric Neurosurgery Program at Butler Hospital, Providence, RI, USA

N. C. R. McLaughlin (✉)
Psychiatric Neurosurgery Program at Butler Hospital, Providence, RI, USA

Psychiatry and Human Behavior, The Warren Alpert Medical School of Brown University, Providence, RI, USA
e-mail: nicole_mclaughlin@brown.edu

N. Pouratian, S. A. Sheth (eds.), *Stereotactic and Functional Neurosurgery*,
https://doi.org/10.1007/978-3-030-34906-6_30

not achieve sustained improvement, which significantly compromises their quality of life, limits function, and increases the risk of suicide [9, 12, 13]. For a subset of these patients, psychiatric neurosurgical intervention, including neuroablation, has proven useful in reducing symptom severity and improving functional outcomes [3, 8, 14, 15].

Based on the century-old theory that certain psychiatric pathologies can be treated by the removal or destruction of specific brain tissue, modern psychiatric neurosurgical teams employ various technologies to place selective lesions in brain structures implicated in the functional pathology of OCD [16, 17]. Unlike older psychosurgical procedures, modern neuroablative techniques have exhibited an acceptable safety profile, in part due to smaller, more precise lesion placement, and exhibit much-improved efficacy [11].

Prospective and retrospective data indicate that 50–60% of patients undergoing lesion procedures show meaningful improvement in OCD severity, and a subset may show partial improvement [3, 15, 18, 19]. Today, a limited number of specialized centers in the world conduct surgical procedures for intractable OCD [20–22]. The modern neurosurgical repertoire of neuroablative procedures to treat OCD includes subcaudate tractotomy, cingulotomy, limbic leucotomy, and capsulotomy [12, 23, 24].

Patient Selection

Most psychiatric neurosurgery programs consist of an interdisciplinary team of psychiatrists, neuropsychologists, neurosurgeons, neurologists, and often medical ethicists who establish whether patients have truly exhausted all other treatment modalities and would be good candidates for a neuroablative procedure.

The process of patient selection for lesion procedures in OCD is simultaneously one of the most challenging and critical components of care. Most patients that suffer from severe, intractable OCD have comorbid conditions including severe depression, body dysmorphic disorder, generalized anxiety disorder, and personality disorders [5, 9, 12–14]. There is a high rate of depression and suicidal ideation in this population, and patients who qualify for surgery have had many years of severely debilitating illness [3, 8, 14, 22, 25]. Clinicians must, therefore, make every effort to select patients who have completely exhausted all nonsurgical interventions and who are most likely to have a significant, positive response to surgery. Strict criteria have been established by various clinical sites to determine the former; the latter is significantly more challenging to predict.

Patients who are considered for these surgical interventions must meet strict criteria for medical refractoriness and extreme symptom severity. While various psychiatric neurosurgical practices have their own specific established inclusion criteria for surgery, they are very similar in content. In order to qualify, patients must meet criteria for a primary diagnosis of OCD in the very severe range, with significant impairment in global functioning that has persisted for at least 5 years. Numerous validated psychiatric measures are used to evaluate patients; however, the gold-standard measure for OCD severity is the Yale-Brown Obsessive Compulsive Scale (YBOCS), which clinicians use to screen patients and also determine treatment response [26, 27]. Patients must be deemed to have medically refractory illness indicated by medical records indicating multiple failed medication trials with a selective serotonin reuptake inhibitor (SSRI), first-line for OCD, and augmenting medications including antipsychotics as indicated [3, 12, 22]. Further, all patients must have failed to respond to cognitive behavioral therapy including Exposure and Response Prevention (ERP), often in intensive psychiatric treatment [3, 12, 22]. Finally, it is critical that patients can fully provide informed consent and comply with study protocol.

Patients are typically excluded if they are less than 18 years old, and the upper age limit may vary across study sites. Comorbid psychiatric illnesses that may affect a patients' ability to consent or that place a patient at risk of adverse effects such as substance use disorder may be grounds for exclusion and is up to the discretion of the multidisciplinary team. Additionally, mania and other medical or neurologic conditions that

place patients at risk for serious adverse effects (i.e., suicide, psychosis) due to surgery may also disqualify a patient for lesion procedures.

Given a paucity in predictive data analyses for patients undergoing surgery, clinicians must determine which patients may or may not be good candidates for surgery based on their collective judgment. With that said, there are some guidelines and practical considerations that clinicians ought to consider when reviewing individual candidates for neuroablative procedures. Numerous factors such as comorbid psychiatric illness as well as access to follow-up psychiatric care must be assessed for each surgical candidate in order to ensure optimal patient care. Lesion procedures are intended as adjunctive treatments to standard pharmaceuticals and/or ERP, so ensuring that patients are willing and likely to comply with continued psychiatric follow-up after their procedure may be critical for improvement after surgery. Take, for instance, a clinical case, discussed by Spofford and colleagues, of a patient who showed marked improvement and ability to engage with ERP after capsulotomy compared to before [25]. In this case, the patient continued intensive medication and ERP and exhibited an overall 67.6% reduction in OCD symptom severity 3 years after surgery [25]. Additional factors to take into consideration include access to regular psychiatric care and a positive relationship with a psychiatrist or psychiatric treatment facility. Some other factors have been shown in recent analyses to be predictive of improved response to lesion procedures for OCD, including family support, employment, a relatively later age of OCD symptom onset, and even some specific variations in neuroanatomical structure and connectivity [3, 28].

The Neurobiology and Neurocircuitry OCD

Before discussing the specific lesion procedures used by clinicians to treat medically refractory OCD, it is important for clinicians to have an understanding of the current scientific understanding of OCD pathophysiology. The collective experience of fMRI, structural MRI, and diffusion studies underlie the rationale for neurosurgical targets aimed at treating OCD. Studies that have been instrumental in identifying regions and circuits in the brain involved in OCD come from functional neuroimaging experiments which have been done in humans through clinical research studies [12, 29]. Important studies in nonhuman primates have further elucidated specific frontal-subcortical pathways that may be related to changes in surgical treatment. Here we will briefly outline the current model of the neurocircuitry of OCD and discuss some of the studies that have been instrumental in developing the current state of the science.

The current predominant theory explaining the neurobiology of OCD is described as the cortico-striato-thalamo-cortical (CSTC) loop model. This model represents a hypothesized set of interconnected circuits or loops that include the cortex, basal ganglia, thalamus, and amygdala and form functional circuits that are dysfunctional in OCD [30–33]. Two loops, in particular, are thought to be involved in OCD due in large part to the functional and structural imaging findings discussed earlier: the lateral orbitofrontal loop and the anterior cingulate loop [31]. The two loops that have been associated with OCD pathophysiology depicted in Fig. 30.1 are suspected primarily because the regions highlighted in the name of both loops, the OFC and ACC, have been repeatedly implicated in OCD pathology.

These circuits and loops are broadly characterized as either excitatory or inhibitory based upon the types of neurotransmitters released between neurons in those circuits. This is important to note because pervading neuroscientific theory of cortical function implies that a balance between cortical excitation and inhibition is what regulates brain activity and promotes optimal functioning. Researchers have observed elevated activity in the OFC and ACC in OCD patients and have developed a hypothesis for how the circuits may work together in OCD to produce the characteristic hyperactivity or overexcitation in these regions [12, 29, 31]. The two loops or circuits mentioned above work in concert, and OCD symptoms may arise when an aberrant positive feedback loop

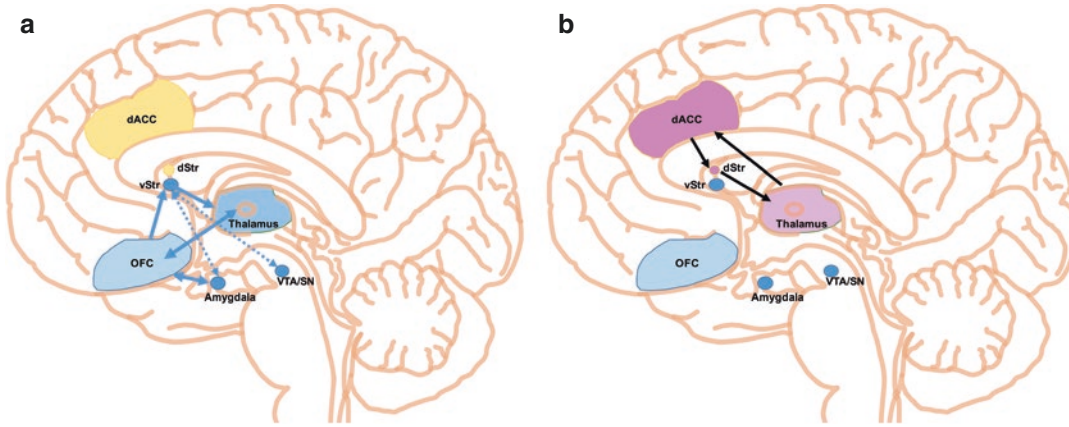

Fig. 30.1 This figure illustrates the two CSTC loops implicated in the pathophysiology of OCD. (**a**) Depicts the loop involving the medial orbitofrontal cortex (OFC) and thalamus as well as secondary structures. This loop is typically associated with assigning value to a particular outcome to facilitate reward learning and forms a positive feedback loop that may underlie OFC hyperactivity in OCD. (**b**) Illustrates the dorsal anterior cingulate cortex (dACC) loop that relays directly with the thalamus and is thought to potentially contribute to perseverative behaviors in OCD compulsions. This figure was illustrated using the Motifolio Drawing Toolkit (Motifolio Inc., MD, USA)

develops in the frontothalamic neuronal pathways leading to inadequately inhibited activity in the OFC and thalamus [31]. Additionally, Papez circuitry, implicated in psychosomatic experience of disturbing feelings and anxiety, which is interconnected with the pathways illustrated in Fig. 30.1, could be improperly activated through OFC connections with the amygdala [31].

Though findings are variable, consistent CTSC abnormalities are found through structural imaging, functional imaging at rest, and functional imaging during provocation. Changes in these regions are also seen after pharmacological and behavioral treatments. OCD symptoms have been correlated through various studies with specific structural brain differences in the orbitofrontal cortex (OFC), anterior cingulate cortex (ACC), and striatum [29]. One large structural MRI study found that in individuals with OCD, OFC gray matter was reduced, increased gray matter was seen in the ventral striatum, and there were changes in ACC volume [29]. Notably, research in structural imaging has been somewhat inconsistent in OCD with studies implicating the same structures but showing opposing volume changes in the aforementioned structures [8, 31].

Functional neuroimaging studies in humans have also supported the CSTC circuit model in OCD. Methods of functional neuroimaging used include two methods of indirectly measuring brain activity, while individuals are conscious and capable of completing tasks: the use of functional MRI (fMRI) to measure blood flow in the brain and positron emission tomography (PET) to measure glucose levels in the brain [12, 29]. In one study using PET, researchers looked at OCD patients at rest and also in a "provoked" condition, where a provocative stimulus such as a contaminated object was used to trigger anxiety in patients [34]. In this study, researchers found that the OFC exhibited increased activation in the OCD group at rest and when provoked [29, 34]. Through similar studies using PET and fMRI, increased activity in the OFC, ACC, and head of the caudate nucleus has been implicated in OCD pathophysiology [29].

The hypothesis that activity in the OFC, ACC, and caudate nucleus is involved in or maybe even be responsible for OCD has been more recently supported by findings indicating that clinical therapies used for OCD may directly affect these circuits. For instance, two recent studies examining the effects of fluvoxamine and cognitive behavioral therapy (two first-line treatments for OCD) on brain activity in OCD patients revealed in both PET and fMRI that changes in frontal

lobe activity, specifically decreased activity in the OFC and increased activity in the posterior cingulate cortex (PCC), were correlated with better treatment response [35, 36].

Additional evidence supporting relevant brain regions comes from evidence from psychiatric neurosurgical procedures. One study that combined the use of functional imaging with deep brain stimulation demonstrated that targeting specific fibers with disruptive stimulation can reduce activity in the OFC [37]. In this experiment, patients at Rhode Island Hospital or Cleveland Clinic Foundation Hospital had electrodes implanted in the anterior limb of the internal capsule the same region targeted in ablative capsulotomy [37]. More recent studies examining the effects of surgical procedures including DBS and anterior cingulotomy have shown that both procedures modulate activity in the OFC and ACC and that those individuals who respond best to treatment show significant changes in the neuroanatomy and neural fiber tracts as measured by MRI and Diffuse Tensor Imaging (DTI), a method for visualizing white matter connectivity in the brain [11, 30, 33, 38–40].

Taken together these findings, all appear to consistently affirm the presence of significant biological mechanism(s) involving the specific brain regions identified through multiple experimental methods and paradigms. These findings have strongly supported the predominant working hypothesis for the functional changes in neural circuitry thought to underlie OCD pathophysiology.

While we have identified some of the circuity involved, the precise neurobiological mechanisms responsible for OCD symptoms remain unclear. Psychiatric neurosurgical work, though initially developed empirically, has helped to support the development of the neurocircuitry model, in part due to the relatively equal response rates of patients with OCD to ablation and stimulation in distinct brain regions [18]. In other words, the subcaudate tractotomy, cingulotomy, limbic leucotomy, and capsulotomy may all target different regions of the brain, but as we will now discuss, each target is thought to play a role in the circuitry that becomes "imbalanced" in OCD, and by removing specific regions of the circuit, OC symptoms may be reduced.

Types of Operations for OCD

As discussed earlier, the following four procedures are used to treat severe, intractable OCD: subcaudate tractotomy, cingulotomy, limbic leucotomy, and capsulotomy. The lesions in these procedures are placed using a stereotactic frame to permit high accuracy in placing lesions [12, 23]. Bilateral lesions are typically placed in the brain regions of interest as previously planned with magnetic resonance imaging (MRI). Procedures can be conducted under local anesthesia with light sedation or under general anesthesia depending on the technique and technology used to place lesions. Lesions are made using various tools including radiation, thermocoagulation, radiofrequency-induced ablation, and laser ablation [41]. Here we will introduce the four lesion procedures, their early development, reports of current methods of use, efficacy, and reported risks associated with the procedure.

Subcaudate Tractotomy

In 1964, Knight and colleagues in London developed the subcaudate tractotomy, a procedure intended to create a bilateral lesion in the substantia innominata, a region inferior to the head of the caudate nucleus [10, 12, 22]. This lesion location is intended to interrupt white matter tracts connecting the orbitofrontal cortex (OFC) to various subcortical regions, white matter tracts that are hyperactive in OCD patients and believed to underlie OCD pathophysiology [12, 29].

This procedure was first successfully achieved by using beta radioactive 90-Yttrium rods that were inserted into the desired brain region in rows, but this method has since been replaced with a thermocoagulation method by which a probe is inserted into burr holes in the skull and heat is used to destroy tissue in the specific area described above[22, 42]. Researchers at the time used X-ray ventriculogram imaging to view the

anatomical target after surgery and relied upon skull sutures and other anatomic landmarks to place the lesion during the operation [12, 42–44].

Two major retrospective studies examining the efficacy of subcaudate tractotomy in treating OCD were published in the early 1970s by Strom-Olsen and Carlisle as well as by Göktepe et al. [12, 22]. In both studies, approximately 50% of 20 or so patients included in the studies were said to have "either completely recovered" or showed "clinical improvement" in their OCD symptoms after a minimum of 1-year follow-up [12]. A more recent review of 1300 patients who underwent psychiatric neurosurgical procedures revealed that 40–60% of patients with OCD showed some improved outcome after subcaudate tractotomy and were able to lead "normal" or "near-normal" lives [8, 12, 23]. A more recent case report has shown improvement in one patient who improved after subcaudate tractotomy using a novel "frameless" stereotactic method [19].

Short-term risks associated with the subcaudate tractotomy include reported hypersomnolence for a few days post-operatively, confusion for 1 month postoperatively, and temporary decline in cognitive function [12]. Serious adverse effects of the procedure include seizures, which occurred in at least 1.6% of cases, and mild personality changes [12]. Presently, this procedure is used infrequently alone.

Cingulotomy

First proposed by Fulton, removal or destruction of the anterior portion of the cingulate gyrus is a procedure that has remained and shown considerable benefit in treating patients with both OCD and major depressive disorder (MDD) [12, 18]. The cingulotomy involves a lesion of the anterior cingulate cortex (ACC) that aims to disrupt afferent and efferent fiber connecting the anterior cingulum, ventral striatum, anterior nuclei, dorsomedial nuclei, and other midline thalamic nuclei. It is one of the most widely used surgical procedures to treat OCD [12, 18, 40]. Whittey and colleagues were the first to show considerable benefit in treating patients with OCD using the cingulotomy with a case report showing 4 out of 5 patients improving in an initial sample [42]. Since the initial validation, the psychiatric neurosurgical team at Massachusetts General Hospital has conducted over 1000 cingulotomies for OCD and depression [12].

As with the subcaudate tractotomy, early lesions were carried out with ventriculography, which has now been replaced with MRI-guided stereotactic ablation methods. The procedure consists of making two to three 1-cm lesions along the anterior cingulate cortex, 7 mm from the midline and 20–25 mm posterior to the frontal horns [10, 12]. Lesions are created by thermocoagulation through approximately 12 mm bilateral burr holes [10, 12, 18]. While stimulation is not typically used during the procedure, local anesthesia may be used to allow for neurologic testing during lesion placement to preserve motor or sensory function, particularly in the lower extremities [10, 12].

Clinical research studies have shown that the cingulotomy can lead to substantial improvement in OCD symptoms [42]. Cingulotomies are considered to be safe procedures for treatment of severe psychiatric illness. Cosgrove and colleagues reported that 800 cingulotomies performed over a 40-year period at Massachusetts General Hospital resulted in no surgically related deaths and only two infections [12, 23]. It is important to note that the 800 cingulotomies performed were not only for OCD but also included MDD, other anxiety disorders, and intractable pain [12, 23]. Nevertheless, the surgical procedure and risks are identical and have proven safe in human patients.

As far as the efficacy of cingulotomies, older studies showed response rates, or rates of improvement in OCD symptoms after surgery, from 25% to 28%; however, more recent retrospective studies of larger patient cohorts have shown that some improvement in symptoms occurs in 60% of surgical cases [8, 10, 23, 42]. In a retrospective analysis of 64 OCD patients, Sheth and colleagues showed that approximately 5 years after cingulotomy 47% of patients experienced ≥35% reduction in OCD severity (measured by YBOCS) and 22% of patients

experienced a 25–34% reduction [18]. Of note, approximately 30 patients in this retrospective analysis underwent a second cingulotomy during the course of their treatment [18]. Comorbid MDD has also been shown to decrease significantly after anterior cingulotomy.

Repeated lesion procedures of the ACC are an appropriate option for patients with OCD that remains refractory after initial cingulotomy. In one retrospective cohort analysis of 31 OCD patients, Bourne and colleagues found that 53% of patients who underwent a repeated cingulotomy or subsequent subcaudate tractotomy exhibited a ≥35% reduction in OCD severity as compared to only 17% of patients who only underwent a single cingulotomy [45].

Short-term postoperative side effects of anterior cingulotomy include urinary incontinence, abulia, headache, nausea, and vomiting. One to nine percent of patients experience intraoperative seizures, with a few of these patients developing subsequent seizure disorders [12, 18].

Limbic Leucotomy

The limbic leucotomy combines both the subcaudate tractotomy and the cingulotomy into one procedure [8, 12, 42]. In the 1970s, Richardson and Kelly developed this procedure with multiple targets including the dorsal cingulate gyrus and the white fiber tracts anterior to the caudate nucleus in the hopes of further improving outcomes of surgery for OCD [12].

This procedure, like the cingulotomy, involved the use of the ventriculogram, and now clinicians utilize MRI images, or more recently intraoperative MRI when available, to visualize the anatomical locations where the lesions will be placed. Historically, this lesion is made by using thermocoagulation, a cryoprobe, or radiofrequency-heated electrodes to ablate the tissue through bilateral burr holes near the dorsal midline of the skull [10, 12, 22]. In 1973 Kelly et al. found that in a group of 49 patients, 89% showed some improvement in OCD symptoms approximately 20 months after surgery based on an unvalidated OCD severity rating system, and Hay and colleagues found a significant reduction in only 38% of their cohort who underwent limbic leucotomy [12]. As discussed earlier, Sheth and colleagues examined the effect of a second procedure after anterior cingulotomy, and for some of the patients observed the second procedure was a subcaudate tractotomy. Based on those data it does appear that addition of the subcaudate tractotomy, creating a limbic leucotomy, increased the number of responders to surgery [18]. The limbic leucotomy is by nature an extensive procedure with multiple lesion locations, which dissuades clinicians from conducting the procedure in a single operation, particularly when either the cingulotomy or subcaudate tractotomy may be effective alone.

Risks associated with the limbic leucotomy include short-term side effects such as headache, lethargy, perseveration, and loss of sphincter control, as well as more serious adverse effects including seizures and long-term or enduring lethargy [12].

Capsulotomy

The capsulotomy was a procedure first performed by Tailarach and colleagues in France and later developed and popularized by Lars Leksell in Sweden in the 1960s as a means of treating OCD [12, 22]. The procedure involves placing a lesion in the anterior limb of the internal capsule in an effort to lesion orbitofrontal and anterior cingulate efferent fibers that pass through the anterior internal capsule, connecting the prefrontal cortex and subcortical nuclei including the dorsomedial thalamus [3, 12].

The capsulotomy was first performed by placing burr holes in the skull and using thermocoagulation to make the lesion in the anterior internal capsule [12]. Early reports of this method suggested that the anterior capsulotomy may prove beneficial in OCD patients with one showing that 71% of patients 35 months after the procedure "were either 'free of symptoms' or 'much improved'" [12, 22]. Leskell and his colleagues conducted the capsulotomy on 116 patients for several indications, including OCD, depression,

and schizophrenia, and found that 50% of patients with obsessional neurosis showed improvement after anterior internal capsulotomy [10, 12].

Leskell and his colleagues also developed a novel method for placing the lesion in the internal capsule using Gamma Knife Radiosurgery (GKRS). GKRS, developed by Lars Leksell, is widely used in neurosurgery to treat intracranial tumors, arteriovenous malformations, and trigeminal neuralgia and neurosurgeons to target intracranial structures with focused gamma radiation from a stereotactic unit [3]. The biologic effect of any individual gamma beam is negligible, and the beam can pass through the skull and brain tissue and only apply focused radiation at the point of focus of multiple beams, allowing clinicians to make a radiosurgical lesion without a craniotomy or burr holes [3, 12]. For over 20 years, GKRS has been used for capsulotomy in a procedure known as the Gamma Knife Ventral Capsulotomy (GVC), a procedure that can be completed in the outpatient setting [3, 12, 14].

GVC has been shown to be efficacious in treating medically refractory OCD, with one prospective cohort study of 55 patients showing significant improvement (≥35% reduction in YBOCS) in 56% of patients [3]. In this study, Rasmussen and colleagues placed two bilateral lesions in the anterior internal capsule 8–10 mm rostral to the posterior border of the anterior commissure [3]. Of note, comorbid MDD and generalized anxiety severity were also significantly reduced in capsulotomy patients [3]. Rück and colleagues found in a long-term follow-up of 25 OCD patients that 48% of patients showed ≥35% reduction in YBOCS from 4 to 17 years after surgery, and patients showed a reduction in depression severity [46]. In this study, the clinicians included data from patients who underwent GVC and thermocoagulation and found no significant differences in outcome [46].

One randomized, double-blinded, placebo-controlled trial was conducted by Lopes and colleagues at the University of São Paulo on 16 patients who were randomized to receive either active or inactive GVC for severe OCD. Participants were unblinded after 12 months, and those who were randomized to the placebo group were given the option to undergo GVC. Unfortunately, the clinical trial was terminated early, because the cobalt sources for the gamma knife equipment began to decay rapidly, compromising the safety of the participants [14, 47]. After 12 months, the median YBOCS was lower for the GVC group compared to placebo, but with only 2 responders in the GVC group and none in the placebo group, the absolute difference in GVC effect compared to placebo was not statistically significant [14]. While preliminary, this study represented the first blinded, randomized control trial for a neuroablative psychiatric neurosurgical procedure and supported the GVC as safe and efficacious interventions in severe, intractable OCD.

More recently, Kim and colleagues at Yonsei University College of Medicine in South Korea reported success using focused ultrasound to target and ablate fibers in the anterior internal capsule [48]. MRI-guided, focused ultrasound is a method of thermal neuroablation that applies high power sonication to neural tissue. In a case series of 11 OCD patients treated with MRI-guided focused ultrasound, Kim and colleagues reported that after a two-year follow-up, 6 patients experienced >35% reduction in OCD severity and no serious, permanent adverse outcomes [48]. The application of MRI-guided focused ultrasound for neuroablative procedures in OCD is promising because, like GKRS, the procedure is noninvasive and has the additional benefit of avoiding adverse effects associated with radiation. Further research on the application of focused ultrasound in this area is critical to assess the side effects, efficacy, and long-term sequelae of this procedure [48].

Short-term reported risks associated with capsulotomy include nausea, vomiting, and headache, confusion, and incontinence [3, 12]. Researchers have noted a few isolated cases of cerebral cyst formation and radiation necrosis in patients who underwent GVC at various institutions, which is a reported risk of GKRS for arteriovenous malformation of 1.6–3.6% [3, 12, 14, 47, 49, 50].

Postoperative Care

Immediate postsurgical monitoring is critical and dependent upon the surgical intervention. Special care should be given to avoid or reduce the damaging effects of adverse events associated with nearly all lesion procedures including headache, seizures, lethargy, and weakness. Surgical management should also be tailored to the specific intervention and technology used to place the lesions (i.e., monitoring cerebral edema and cyst formation in GVC).

Long-term, postsurgical psychiatric treatment for OCD should be planned prior to surgery, and clinicians should make every effort to coordinate follow-up psychiatric care with their own psychiatric neurosurgical research teams as well as referring physician and clinicians that are able to provide long-term psychiatric care including ERP therapy and medication management for patients. As mentioned earlier, this patient population experiences disabling OCD symptoms, significant comorbid mental illness burden, and limited functional capacity, placing patients at an extremely high risk of self-harm as well as mental and physical decline, particularly if there is no symptom reduction. Numerous follow-up studies have shown that postsurgical reduction in OCD symptom severity often takes months to years, which means that patients are just as vulnerable with severe disease for a significant amount of time postoperatively [14, 25, 41, 51, 52].

Optimizing and Improving Surgical Outcome

While the existing neurosurgical procedures have shown significant capacity for treating patients with OCD for whom all other treatment modalities have failed, there is still room for improving patient outcomes and mitigating adverse events associated with surgery. Uncovering changes in clinical practice that can improve neurosurgical treatment for patients with intractable OCD is an active area of research that must examine myriad factors including patient utilization and access to follow-up care, pharmaceutical management of OCD, and optimization and development of emerging technology.

In order to improve outcome and reduce risk, it is critical that the above procedures are conducted at specialized institutions with interdisciplinary teams to manage both the procedural and the long-term follow-up care of patients. In a 5-year retrospective database review, Rück and colleagues uncovered that in 70 OCD patients treated with capsulotomy, the mortality rate was 41% at 5 years after surgery, approximately 10% of which were due to suicide [52]. Further, after capsulotomy, 75% of OCD patients were on high doses of psychotropic medications, and 84% had been admitted at some point during their 5 years to intensive inpatient psychiatric treatment [52]. These data serve as a reminder that the patients who undergo surgery for OCD are extremely ill, and even after positive responses to surgical intervention, patients may have poor long-term outcomes relative to the general population due to the severity of their illness. However, it should also be noted that more current procedures may use smaller, more targeted lesions, leading to a reduced side effect burden.

Continued psychiatric care and follow-up are critical for patients, however, neuroablative procedures that create permanent lesions do not inherently require the same specialized follow-up for treatment that medication, therapy, and neurostimulation procedures often require. However, ensuring that patients have access to and receive continued care for their OCD and other comorbid psychiatric conditions is critical to improving outcomes in this patient population [3, 25, 52].

Developing novel technology/techniques and adjusting our use of existing technology to conduct neuroablative procedures for OCD is another critical component to improving patient outcomes. Take, for instance, GVC, while a promising procedure with limited side effects, the risks of placing a radiosurgical lesion are not negligible, so adjustment of radiation dose, alternative methods of ablation, or other solutions could be used to preserve the beneficial effects of the lesion

while preventing the incidence of these serious adverse events. This same principle applies to all the existing procedures, and psychiatric neurosurgical research groups are actively involved in uncovering techniques, adjustments, and medical interventions that can benefit patients.

Further clinical research is critical to attempt to compare and contrast the existing neurosurgical techniques, an area of research that has been severely limited by the lack of clinical trials and small sample sizes of these studies. One recent study by Brown and colleagues aimed to compare the efficacy of anterior internal capsulotomy and dorsal anterior cingulotomy through a systematic review of published observational studies. By examining outcomes of ten studies, the research team was able to assess the observational findings of 193 patients who underwent either capsulotomy or cingulotomy and found that overall the full response rate of capsulotomy was 54% and 42% for cingulotomy [15]. In addition, the rate of serious adverse events appeared to be greater in capsulotomy than cingulotomy, 21.4% and 5.2%, respectively [15]. However, the observational nature of these studies prevented a systematic review and direct comparison for differences between the studies so the authors determined that the data indicated both were similarly efficacious and safe [15].

More studies employing innovative study design and/or statistical methods are needed to uncover answers in the existing data that is limited by small sample sizes and significant confounding variables as well as to design studies that allow researchers to gain as much information as possible. Studies examining predictive factors of outcome, nonsurgical aspects of care that improve outcome, and the neurobiological basis and functional pathophysiology of OCD are all critical to improving the care of patients with this devastating disease.

Conclusions

For patients with significantly severe OCD that is refractory to psychopharmaceutical and cognitive behavioral therapy, psychiatric neurosurgical procedures are safe, well-established, and efficacious adjunctive treatment modalities for OCD in the subset of patients for whom they are appropriate.

In the advent of novel technological advances such as DBS for the neurosurgical treatment of OCD, lesion procedures remain an important therapeutic consideration. First, it is important to note that current DBS protocols for OCD are designed to work very similarly to lesions in that they create a disruption, albeit reversible in DBS, in many of the same white fiber tracts as lesion procedures. The primary target of DBS for OCD is the ventral capsule/ventral striatum, which is the same target region of the anterior capsulotomy, and data suggests that significant improvement in OCD symptom severity is seen in 40–61% of patients [3, 6, 11, 12, 15, 41, 49]. Notably, the efficacy of lesion procedures and DBS are strikingly similar, making lesion procedures a comparable approach to treat medically refractory OCD. Furthermore, there are additional considerations in the management of DBS such as regular follow-up with a team specialized in DBS application and settings for OCD, follow-up procedures to replace batteries, adverse effects due to stimulation, and the lifetime cost of treatment [15]. Some of these factors may make lesion procedures a better practical option for some patients who may, for instance, not live near a specialized site that can monitor stimulation parameters or who have a history of inconsistent engagement in psychiatric treatment.

Today, neuroablative procedures are used to treat severe, intractable OCD at a few specialized sites in the world with multidisciplinary teams of psychiatrists, neuropsychologists, and neurosurgeons. These procedures are based on the hypothesis that overactivation of certain CSTC fiber tracts in the brain underlies OCD pathophysiology, and selective disruption of these pathways can modulate them and treat OCD symptoms. In order to navigate treating patients with severe OCD using neurosurgical intervention, clinicians employ careful, detailed protocols for patient selection and screening, utilize various techniques to carry out detailed surgical ablation procedures, and conduct extensive follow-up care and monitoring.

The armamentarium available to clinicians to effectively and safely treat psychiatric illness is greater than it ever has been, and this is espe-

cially true for the neurosurgical treatment of severe, intractable OCD. With numerous options for safe and effective lesion procedures in addition to novel methods of stimulation, clinicians and patients have a variety of similarly effective options to choose from, and this choice may allow for the freedom to optimize and personalize patient care. With that being said, limited data of factors that impact surgical outcome and comparative studies among lesion procedures makes it difficult to distinguish which course of treatment might be best. In addition, our understanding of the neurobiological basis of OCD is still growing, with clinical interventions such as lesion procedures showing efficacy despite a limited understanding as to why ablation of certain neural fibers is effective. Gaining a clearer understanding of how current neuroablative interventions for OCD work will serve to simultaneously improve patient care and uncover the neurophysiologic basis of the maladaptive neural circuitry of one of the most debilitating psychiatric diseases.

References

1. Ruscio AM, Stein DJ, Chiu WT, Kessler RC. The epidemiology of obsessive-compulsive disorder in the National Comorbidity Survey Replication. Mol Psychiatry. 2010;15:53–63.
2. Rasmussen SA, Eisen JL. Treatment strategies for chronic and refractory obsessive-compulsive disorder. J Clin Psychiatry. 1997;58 Suppl 13:9–13.
3. Rasmussen SA, Noren G, Greenberg BD, Marsland R, McLaughlin NC, Malloy PJ, et al. Gamma ventral capsulotomy in intractable obsessive-compulsive disorder. Biol Psychiatry. 2018;84:355.
4. de Haan S, Rietveld E, Stokhof M, Denys D. The phenomenology of deep brain stimulation-induced changes in OCD: an enactive affordance-based model. Front Hum Neurosci. 2013;7:653.
5. de Haan S, Rietveld E, Stokhof M, Denys D. Effects of deep brain stimulation on the lived experience of obsessive-compulsive disorder patients: in-depth interviews with 18 patients. PLoS One. 2015;10:e0135524.
6. Kohl S, Schönherr DM, Luigjes J, Denys D, Mueller UJ, Lenartz D, et al. Deep brain stimulation for treatment-refractory obsessive compulsive disorder: a systematic review. BMC Psychiatry. 2014;14:214.
7. Heyman I, Mataix-Cols D, Fineberg NA. Obsessive-compulsive disorder. BMJ. 2006;333(7565):424–9.
8. Greenberg BD, Price LH, Rauch SL, Friehs G, Noren G, Malone D, et al. Neurosurgery for intractable obsessive-compulsive disorder and depression: critical issues. Neurosurg Clin N Am. 2003;14:199–212.
9. Ferrão YA, Shavitt RG, Bedin NR, de Mathis ME, Carlos Lopes A, Fontenelle LF, et al. Clinical features associated to refractory obsessive–compulsive disorder. J Affect Disord. 2006;94:199–209.
10. Cosgrove GR, Rauch SL. Psychosurgery – Neurosurgical Service – Massachusetts General Hospital. Neurosurgery Massachusetts General Hospital. 2005.
11. McLaughlin NCR, Stewart C, Greenberg BD. Deep brain stimulation for obsessive-compulsive disorder and major depressive disorder. In: Psychiatric neurotherapeutics. New York: Springer New York; 2016. p. 141–63.
12. Greenberg BD, Rauch SL, Haber SN. Invasive circuitry-based neurotherapeutics: stereotactic ablation and deep brain stimulation for OCD. Neuropsychopharmacology. 2010;35:317–36.
13. Fernandez de la Cruz L, Rydell M, Runeson B, D'Onofrio BM, Brander G, Ruck C, et al. Suicide in obsessive-compulsive disorder: a population-based study of 36 788 Swedish patients. Mol Psychiatry. 2017;22(11):1626–32.
14. Lopes AC, Greenberg BD, Canteras MM, Batistuzzo MC, Hoexter MQ, Gentil AF, et al. Gamma ventral capsulotomy for obsessive-compulsive disorder. JAMA Psychiat. 2014;71:1066.
15. Brown LT, Mikell CB, Youngerman BE, Zhang Y, McKhann GM, Sheth SA. Dorsal anterior cingulotomy and anterior capsulotomy for severe, refractory obsessive-compulsive disorder: a systematic review of observational studies. J Neurosurg. 2016;124:77–89.
16. Manjila S, Rengachary S, Xavier AR, Parker B, Guthikonda M. Modern psychosurgery before Egas Moniz: a tribute to Gottlieb Burckhardt. Neurosurg Focus. 2008;25(1):E9. https://doi.org/10.3171/FOC/2008/25/7/E9.
17. El-Hai J. The lobotomist: a maverick medical genius and his tragic quest to rid the world of mental illness. BMJ. 2005;330:1275.
18. Sheth SA, Neal J, Tangherlini F, Mian MK, Gentil A, Cosgrove GR, et al. Limbic system surgery for treatment-refractory obsessive-compulsive disorder: a prospective long-term follow-up of 64 patients. J Neurosurg. 2013;118(3):491–7.
19. Woerdeman PA, Willems PW, Noordmans HJ, Berkelbach van der Sprenkel JW, van Rijen PC. Frameless stereotactic subcaudate tractotomy for intractable obsessive-compulsive disorder. Acta Neurochir. 2006;148(6):633–7; discussion 7
20. Anderson CA, Arciniegas DB. Neurosurgical interventions for neuropsychiatric syndromes. Curr Psychiatry Rep. 2004;6:355–63.
21. Feldman RP, Alterman RL, Goodrich JT. Contemporary psychosurgery and a look to the future. J Neurosurg. 2001;95:944–56.
22. Jenike MA, Rauch SL, Baer L, Rasmussen SA. Neurosurgical treatment of obsessive-compulsive disorder. In: Jenike MA, Baer L, Minichiello WE, editors. Obsessive-compulsive disorders: practical management. St. Louis: Mosby; 1998. p. 592–610.

23. Shah DB, Pesiridou A, Baltuch GH, Malone DA, O'Reardon JP. Functional neurosurgery in the treatment of severe obsessive compulsive disorder and major depression: overview of disease circuits and therapeutic targeting for the clinician. Psychiatry (Edgmont). 2008;5:24–33.
24. Doshi PK. Surgical treatment of obsessive compulsive disorders: current status. Indian J Psychiatry. 2009;51:216–21.
25. Spofford CM, McLaughlin NCR, Penzel F, Rasmussen SA, Greenberg BD. OCD behavior therapy before and after gamma ventral capsulotomy: case report. Neurocase. 2014;20:42–5.
26. Goodman WK, Price LH, Rasmussen SA, Mazure C, Fleischmann RL, Hill CL, et al. The Yale-Brown obsessive compulsive scale. Arch Gen Psychiatry. 1989;46:1006.
27. López-Pina JA, Sánchez-Meca J, López-López JA, Marín-Martínez F, Núñez-Núñez RM, Rosa-Alcázar AI, et al. The Yale-Brown obsessive compulsive scale: a reliability generalization meta-analysis. Assessment. 2015;22:619–28.
28. Banks GP, Mikell CB, Youngerman BE, Henriques B, Kelly KM, Chan AK, et al. Neuroanatomical characteristics associated with response to dorsal anterior cingulotomy for obsessive-compulsive disorder. JAMA Psychiat. 2015;72(2):127–35.
29. Ahmari SE, Dougherty DD. Dissecting OCD circuits: from animal models to targeted treatments. Depress Anxiety. 2015;32:550–62.
30. McGovern RA, Sheth SA. Role of the dorsal anterior cingulate cortex in obsessive-compulsive disorder: converging evidence from cognitive neuroscience and psychiatric neurosurgery. J Neurosurg. 2017;126:132–47.
31. Kopell BH, Greenberg B, Rezai AR. Deep brain stimulation for psychiatric disorders. J Clin Neurophysiol. 2004;21:51–67.
32. Kopell BH, Rezai AR. The continuing evolution of psychiatric neurosurgery. CNS Spectr. 2000;5:20–31.
33. Wichmann T, DeLong MR. Deep brain stimulation for neurologic and neuropsychiatric disorders. Neuron. 2006;52:197–204.
34. Rauch SL, Savage CR, Alpert NM, Fischman AJ, Jenike MA. The functional neuroanatomy of anxiety: a study of three disorders using positron emission tomography and symptom provocation. Biol Psychiatry. 1997;42:446–52.
35. Nakao T, Nakagawa A, Yoshiura T, Nakatani E, Nabeyama M, Yoshizato C, et al. Brain activation of patients with obsessive-compulsive disorder during neuropsychological and symptom provocation tasks before and after symptom improvement: a functional magnetic resonance imaging study. Biol Psychiatry. 2005;57:901–10.
36. Rauch S, Shin LM, Dougherty DD, Alpert NM, Fischman AJ, Jenike MA. Predictors of fluvoxamine response in contamination-related obsessive compulsive disorder a PET symptom provocation study. Neuropsychopharmacology. 2002;27:782–91.
37. Rauch SL, Dougherty DD, Malone D, Rezai A, Friehs G, Fischman AJ, et al. A functional neuroimaging investigation of deep brain stimulation in patients with obsessive–compulsive disorder. J Neurosurg. 2006;104:558–65.
38. Szeszko PR, Ardekani BA, Ashtari M, Malhotra AK, Robinson DG, Bilder RM, et al. White matter abnormalities in obsessive-compulsive disorder. Arch Gen Psychiatry. 2005;62:782.
39. Hartmann CJ, Lujan JL, Chaturvedi A, Goodman WK, Okun MS, McIntyre CC, et al. Tractography activation patterns in dorsolateral prefrontal cortex suggest better clinical responses in OCD DBS. Front Neurosci. 2016;9:519.
40. Sheth SA, Ogas P, Eskandar EN. Future of neurosurgery. In: Psychiatric neurotherapeutics. New York: Springer New York; 2016. p. 209–20.
41. Greenberg BD, Gabriels LA, Malone DA, Rezai AR, Friehs GM, Okun MS, et al. Deep brain stimulation of the ventral internal capsule/ventral striatum for obsessive-compulsive disorder: worldwide experience. Mol Psychiatry. 2010;15:64–79.
42. Rasmussen S, Greenberg B, Mindus P, Friehs G, Noren G. Neurosurgical approaches to intractable obsessive-compulsive disorder. CNS Spectr. 2000;5(11):23–34.
43. Knight G. Bifrontal stereotaxic tractotomy in the substantia innominata: an experience of 450 cases. In: Hitchcock E, Laitinen L, Vaernet K, editors. Psychosurgery. Springfield: Charles C Thomas; 1972. p. 267–77.
44. Newcombe R. The lesion in stereotactic subcaudate tractotomy. Br J Psychiatry. 1975;6:478–81.
45. Bourne SK, Sheth SA, Neal J, Strong C, Mian MK, Cosgrove GR, et al. Beneficial effect of subsequent lesion procedures after nonresponse to initial cingulotomy for severe, treatment-refractory obsessive-compulsive disorder. Neurosurgery. 2013;72(2):196–202; discussion
46. Ruck C, Karlsson A, Steele JD, Edman G, Meyerson BA, Ericson K, et al. Capsulotomy for obsessive-compulsive disorder: long-term follow-up of 25 patients. Arch Gen Psychiatry. 2008;65(8):914–21.
47. Miguel EC, Lopes AC, McLaughlin NCR, Noren G, Gentil AF, Hamani C, et al. Evolution of gamma knife capsulotomy for intractable obsessive-compulsive disorder. Mol Psychiatry. 2019;24(2):218–40.
48. Kim SJ, Roh D, Jung HH, Chang WS, Kim CH, Chang JW. A study of novel bilateral thermal capsulotomy with focused ultrasound for treatment-refractory obsessive-compulsive disorder: 2-year follow-up. J Psychiatry Neurosci. 2018;43(4):170188.
49. Interview with Dr. Benjamin Greenberg, (2017).
50. Camprodon JA, Rauch SL, Greenberg BD, Dougherty DD. Psychiatric neurotherapeutics: contemporary surgical and device-based treatments. Totowa: Humana Press; 2016. p. 230.
51. Garnaat SL, Boisseau CL, Yip A, Sibrava NJ, Greenberg BD, Mancebo MC, et al. Predicting course of illness in patients with severe obsessive compulsive disorder. J Clin Psychiatry. 2015;76:e1605–10.
52. Ruck C, Larsson JK, Mataix-Cols D, Ljung R. A register-based 13-year to 43-year follow-up of 70 patients with obsessive-compulsive disorder treated with capsulotomy. BMJ Open. 2017;7(5):e013133.

Gilles de la Tourette Syndrome: Deep Brain Stimulation

31

Michael H. Pourfar and Alon Y. Mogilner

Introduction

The history of the neurosurgical treatment of Gilles de la Tourette syndrome (TS) – whether via lesioning or stimulation – has been predicated on the notion that intervention at key nodes can improve disorder-specific circuit abnormalities. One major, unresolved question at the time of this writing is what or which are the key surgical nodes in TS, a question that is particularly challenging given the variable, multifaceted nature of TS, which often includes prominent obsessive-compulsive and attention-deficit behaviors alongside the hyperkinetic motor and vocal tic behaviors. Historically, as we shall review, surgical approaches have often targeted regions classically associated either with the presumed compulsive nature of tics akin to targets used for OCD (e.g., cingulum and anterior limb of the internal capsule) or regions more commonly associated with hyperkinetic movement disorders (e.g., the motor thalamus and posteroventral globus pallidus). Over time, subregions within the thalamus and pallidum, areas that represent a kind of crossroads between motor and limbic function, have emerged as stereotactic targets of choice, namely, the anteromedial globus pallidus and the dorsomedial thalamus. These two areas will receive the greater focus of our attention but not to the exclusion of other still-utilized targets.

The TS Network

A basic understanding of the underlying circuit-based abnormalities in TS provides a useful platform for better understanding the surgical history. The cause or causes of TS are currently unknown. Genetics clearly plays a role in many cases with particular interest focusing on the role of single nucleotide polymorphisms, but the exact genetic underpinning has yet to be identified [1, 2]. Subtle neuropathological abnormalities have been reported (e.g., changes in caudate and thalamic volumes) but not consistently [3, 4]. What has been repeatedly observed, however, is a difference in regional brain metabolism supporting a circuit-based pathophysiology or, more specifically, a cortico-striato-thalamo-cortical (CSTC) abnormality [5]. In this model, simplified for our present purposes, aberrant activation of striatal neurons with inhibitory connections to GPi/SN leads to disinhibition of thalamocortical projections. The result is an imbalance of the normal promotion of voluntary movements that leads to unwanted, specific motor patterns manifesting as tics. The prominent striatal role is supported

M. H. Pourfar · A. Y. Mogilner (✉)
Department of Neurosurgery, NYU Langone Medical Center, New York, NY, USA
e-mail: alon.mogilner@nyumc.org

N. Pouratian, S. A. Sheth (eds.), *Stereotactic and Functional Neurosurgery*,
https://doi.org/10.1007/978-3-030-34906-6_31

by the symptomatic improvement following dopamine blocking and depleting therapies (the mainstay of medical management for decades) as well as evidence supporting metabolic "normalization" following successful surgical intervention [6].

Surgical History

The first contemporary references to surgical intervention for TS involved anecdotal reports of patients who underwent frontal lobotomies and leukotomies in the 1950s (Stevens 1955; Baker 1960) often for treatment of comorbid psychiatric symptoms. Beginning in the 1960s, the medial thalamus – which was noted to have degenerated following these more indiscriminate procedures – was more specifically targeted for TS [7]. Cooper, an early pioneer of stereotactic lesioning for movement disorders, targeted the ventrolateral thalamus with some reported success, followed soon after by Dieckmann and Hassler who, drawing from their prior experience lesioning patients with OCD, theorized that tics were a form of "motor obsessional phenomena" [8]. They targeted the medial thalamus with a fairly extensive lesion that involved the rostral interlaminar, ventro-oralis, and centromedian-parafascicular nuclei. They reported improvement of 70–100% in 3 patients and, interestingly for the pre-DBS era, noted different symptomatic responses when testing stimulation frequencies prior to lesioning. Their approach, with its reported good results and safety outcomes, would provide a roadmap for the earliest DBS interventions some 35 years later and can thus be seen as an important landmark. At the time, however, they shared company with a variety of other approaches that included dentotomies, limbic leukotomies, and anterior cingulotomies [9, 10]. From the 1950s through the 1980s, approximately 65 cases were reported involving lesioning of these and other targets thought to be involved in the TS network. Reports often provided limited information on the precise location of the lesion and results generally lacked specifics in terms of pre/post tic evaluations. Furthermore, complications in the pre-DBS era were often considerable ranging from debilitating dysarthria (a not infrequent complication of bilateral thalamic lesioning), dystonia, ataxia, and hemiplegia [7, 11]. Interestingly, the data (limited though it is) suggested that targeting the cingulum, which was seen to be effective for OCD, was less effective for motor tics, suggesting that TS and OCD, while sharing many features, are not necessarily amenable to the same intervention [10]. The era of DBS, starting in the late 1980s, saw a rekindling of interest in possible surgical intervention for TS even if the ideal target remained a matter of conjecture. Targeting possibilities seemed to broaden rather than narrow with anecdotal reports of tics improving following STN DBS in a patient with Parkinson's and TS, and following GPI DBS for patients with dystonia and TS [12, 13]. The first reported case of DBS specifically for TS was in 1999 by Vandewalle, who targeted Hassler's aforementioned centromedian thalamic region and described the tics at 1 year as "abolished" [14]. Since that time, approximately 200 DBS cases, often as part of small case series, have been reported using as many as nine stereotactic targets, though largely focused on medial thalamic subregions, pallidal subregions, and the anterior limb of the internal capsule. Optimal candidates, optimal targets, and optimal programming approaches remain topics of debate with consensus being further hampered by the relatively small patient population requiring surgical intervention. Nevertheless, results continue to support the potential for improvement, sometimes dramatic and lasting, in properly selected patients as shall be discussed below.

Candidate Selection

Consensus guidelines for patient selection were proposed in 2006 and slightly revised in 2015 [15, 16]. Being a surgical procedure with its attendant risks (as discussed below), candidates should have sufficient burden from their TS and should have tried the commonly prescribed medications before being considered. The Yale Global Tic Severity Scale Score (YGTSS), which grades

motor and vocal tics based on a number of variables with maximal score of 50 (or 100 if including the 50-point impairment score), is often used as a proxy of severity. The latest consensus guidelines suggest a score of 35/50 being indicative of sufficiently severe TS to warrant surgical. While this is not unreasonable, it should be borne in mind that the score cannot entirely stratify potential risk of harm from tics and, being report-based, can over- or underestimate severity at any given point in time. For example, a single, forceful neck-jerking tic that poses a risk for cervical myelopathy might result in a relatively low YGTSS in the absence of other more complex tics. Conversely, an individual could have a large variety of complex motor and vocal tics, all on the milder side and not impacting quality of life greatly despite a high YGTSS score. Therefore, understanding the risk of harm and impairment from tics is more important than a particular number, and this is now also acknowledged in the consensus algorithm. Although the evidence for various specific medications in treatment of TS is often weak, standard of care includes trials of alpha-adrenergic agents, dopamine blocking, and/or depleting medications. Not every medication within these classes needs to be tried, but clearly, treatment by an experienced TS specialist familiar with appropriate options is required before a patient is deemed medically refractory. In addition to medications, there is good evidence that cognitive behavioral therapy or habit reversal therapy is helpful to some TS patients and should be pursued prior to DBS. From a practical standpoint, it is not always easy to identify experienced cognitive behavioral specialists, insurance coverage can be challenging, and evidence for its efficacy in the most severe TS cases is lacking, but given the possibility for benefit, every effort to connect patients with a behavioral therapist prior to DBS should be undertaken.

The appropriate minimum age at which surgery be considered has been a matter of debate. TS often naturally wanes in early adulthood and so performing brain surgery on a minor who might improve with time alone has been viewed with some apprehension. In the initial proposed algorithm from the Tourette Syndrome Association [15], the suggested minimum age was 25, at which point the likelihood of natural attenuation was assumed diminishing. Arguing against this conservative approach was the contention that severe TS in younger patients could be associated with significant physical and psychosocial disability, and thus performing an intervention earlier could have a meaningful long-term impact. The revised TSA algorithm [16] took a more nuanced stand, recommending that surgery only be considered in patients under 18 in cases where a multidisciplinary team and local ethic committee reviews the circumstances of a given case and weighs the relative risks and benefits. Our current approach, particularly given the lack of FDA approval for the indication at present, is to have all cases reviewed by a multidisciplinary committee not involved in the case with the addition of a pediatric specialist for patients under 18 and, though not absolute, will generally not perform surgery in patients under 16.

TS often keeps company with other neuropsychiatric and behavioral symptoms including depression, anxiety, OCD, and ADHD. The response to these does not always follow suit even following successful reduction in tic severity (OCD, for example, is common and sometimes improves alongside tics but can remain unchanged or even worsen despite improvement in tics in some cases). It is thus helpful to understand how much of a potential candidate's quality of life is impaired by tics and ideally select those whose benefit would not be undercut by significant, persistent depression or OCD. Optimizing and understanding comorbid factors prior to surgery and often working as part of a multispecialty team are vital to optimal outcomes. A particular emphasis on identifying suicidal or addictive behaviors that could potentially worsen following DBS (especially if results are not as positive as hoped for) is of paramount importance. Along these lines, framing patient expectations is a very important part of candidate selection. As will be detailed below, outcomes are variable and nonresponders difficult to predict prospectively, so patients should understand the potential for no or minimal improvement. Thoughtfully consider whether a patient's expectations are realistic.

In summary, a reasonable candidate is an otherwise healthy individual with a clear diagnosis of TS who has failed an adequate trial of medications and behavioral therapy as assessed by an experienced specialist and has significant impairment resulting chiefly if not exclusively from the motor and/or vocal tics with reasonable expectations and understanding of the possible outcomes and risks.

The Surgical Targets

The recent publication by international Tourette Syndrome Deep Brain Stimulation Public Database and Registry [17], pooling case data from multiple centers and reporting on 185 patients, reports the most common surgical as the centromedian thalamic region (57.1%), followed by the anterior globus pallidus internus (25.2%), posterior GPi (15.3%), and the anterior limb of the internal capsule (2.5%). There is currently insufficient evidence to suggest which target affords the most clinical benefit, as no significant difference in outcome was noted between targets.

Surgical Technique

As in DBS for the more common movement disorders (PD, ET, dystonia), the surgical technique varies from center to center. Challenges unique to the TS population include a relatively young patient age, as well as the potential for an increased rate of surgical complications due to the presence of self-mutilatory and/or OCD behavior in a substantial fraction of these patients [18]. While the authors' surgical target (medial thalamus, described as CM/Pf/Voi depending on the publication) has remained the same over our 10-year experience, we have modified our technique due to both our own clinical experience as well as the introduction of adjunctive technology.

Staging Our preference is to perform the surgery in a staged fashion, with simultaneous bilateral cranial lead placement as an inpatient procedure, followed by generator placement 1–2 weeks later as an outpatient.

Choice of generator We have moved from placing bilateral single-channel devices to dual channel rechargeable devices, given the aforementioned young patient age as well as the real-world experience of insurance company denials of generator replacement surgery, despite having approved the initial implantation.

Anesthetic technique For lead placement, we have utilized both the traditional method of awake/conscious sedation surgery with agents such as propofol and dexmedetomidine, which provides the opportunity for both microelectrode recording and macrostimulation to assess for both clinical efficacy and side effects. Given the severe and violent tics experienced by many of our patients resulting in difficulty with maintaining an appropriate level of conscious sedation, combined with the introduction of intraoperative CT, we have begun to perform all our of lead placement surgeries under general anesthesia, with anesthetic techniques that still allow for microelectrode recording. We utilize frame-based stereotaxis with MRI-CT fusion, with the MRI scan performed in the weeks prior to surgery under general anesthesia. CT scanning is performed following frame placement for the purposes of stereotactic target calculation and after each lead is placed to confirm lead placement.

Surgical targeting The choice of target, by definition, determines the method used for anatomic target identification. Whereas the pallidal and capsular targets can be visualized on MRI, individual thalamic nuclei including the centromedian region remain difficult if not impossible to target directly, and thus indirect anterior-posterior commissure-based targeting remains the primary targeting method. Our thalamic coordinates are 5 mm lateral to midline, 4 mm posterior to the midcommissural point, and on the AC-PC plane ($Z = 0$). These coordinates reflect the location of the electrode tip, which

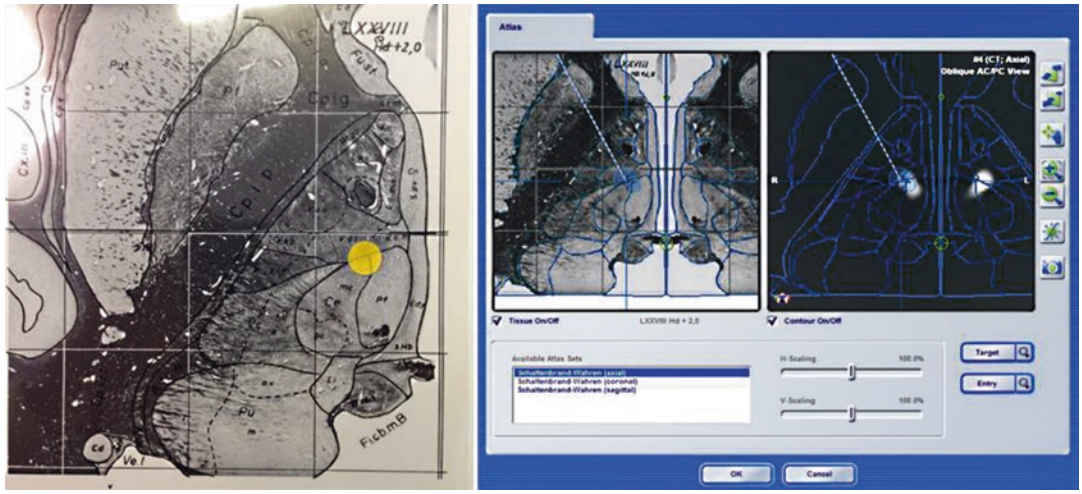

Fig. 31.1 Image from the Schaltenbrand and Wahren stereotactic atlas, axial slice at 2.0 mm above the AC-PC plane. The yellow marker represents the average area of stimulation as calculated using the postoperative imaging studies. This point corresponds to the calculated average area of stimulation in our series. (From Dowd et al. [19]. Reprinted with permission from Journal of Neurosurgery)

Fig. 31.2 AP skull X-ray demonstrating the lateral approach angle to the medial CM thalamic target

corresponds to Hassler's substantia periventricularis (Spv). The deepest (most ventral) contact is rarely used, and the actual locus of stimulation in our experience maps to the junction of the Voi/CmPf [19] (Fig. 31.1). For this rather medial target, lateral approach angles (usually over 30 degrees in the coronal plane), are necessary. Sagittal angles are similar to those traditionally used for the Vim thalamic and STN targets, from 50 to 70 degrees posterior in the sagittal plane (Fig. 31.2).

Microelectrode Recording and Macrostimulation

Our findings during microelectrode recording (MER) of the medial thalamus are similar to those reported in the literature [20]. We have found that the cessation of thalamic bursting activity can be useful to identify the laterality of the trajectory. Thalamic bursting cells are usually encountered until the microelectrode tip exits the thalamus and enters the SPv, approximately 2 mm above the target. Loss of thalamic activity earlier in the trajectory suggests a medial deviation, and continued thalamic activity closer to target suggests the opposite, namely, a lateral offset.

As the medial thalamus is distant from the corticospinal tracts as well as the medial lemniscus, motor and sensory effects are not seen with macrostimulation. In awake patients, ventral stimulation can result in a subjective complaint of dizziness. Whereas direct tic suppression is

difficult to confirm intraoperatively, stimulation slightly dorsal to the tip will, in some patients, elicit a sensation of "calmness."

Outcomes

A pithy distillation of TS outcomes across numerous studies would be to state that approximately 50% of patients improve about 50%. A more rigorous examination of the data, however, leads to a far more nuanced and cautious assessment of the results along with greater awareness of the imperfections and limitations of the relatively small and variable data. The vast majority of the reported outcomes derive from small, retrospective, non-blinded, non-placebo-controlled case series. Different age ranges, different rating scales, different brain targets, different stimulation paradigms, and different follow-up periods make it hard to glean a clear picture let alone make convincing comparisons across different studies. Despite these important caveats, reported outcomes from approximately 200 patients (at time of this writing), including a handful of small, randomized trials and published meta-analyses, allow for some general remarks. Rather than delving into the details of each small case series, we will highlight an illustrative few that will hopefully provide context for better understanding of some pooled analyses.

Thalamic DBS for TS

As mentioned above, the medial thalamus was an early target for TS in the pre-DBS era and was the first dedicated target for DBS in 1999 with Vandewalle reporting a 72–90% reduction in tic severity in 3 patients at up to 72 months follow-up [14, 21, 22]. The thalamus has subsequently remained the most common target but where precisely within the medial thalamus is targeted has varied across different centers. For example, the Milan-Bergamot group, with the largest thalamic case series published to date, targeted approximately 2 mm anterior to Vandewalle's target and reported a 24–72% improvement in the YGTSS in 18 patients at up to 18 months follow-up [23]. Interestingly, while the tic reduction was highly statistically significant, there was a surprising lack of concordance between patient and physician perceptions of outcome in nearly half the cases. This disconnect speaks perhaps to the complexity of issues TS patients deal with that are not captured by a tic-related rating scale. Our group reported results in 13 patients who had undergone medial thalamic DBS and found a 50% reduction at last follow-up (ranging from 6 months to 5 years [19]. Closer inspection of the improvement on a case-by-case basis revealed a separation between marked responders and mild to minimal responders with no clear prospectively differentiating features. Notably, all subjects including those with less robust YGTSS reductions reported that they would repeat the procedure knowing what they know now. Two blinded, crossover studies highlight, in part, the challenges of performing such studies in this patient population. Maciunas et al. performed a double-blind, randomized stimulation versus sham stimulation study in 5 patients over 4 weeks followed by open, unblinded stimulation for 3 months [24]. A video assessment, which was selected as the primary outcome, did demonstrate significant overall improvement comparing stimulation versus non-stimulation, but the YGTSS, selected as a secondary outcome, did not reach significance perhaps in part due to the small number and in part perhaps related to varying overall outcomes with 3 of 5 patients demonstrating a more robust improvement. No clear factors appeared to distinguish the responders from the 2 nonresponders. Ackermans et al. also undertook a blinded study but faced recruitment challenges with only 8 subjects over 4 years and only 6 who completed 1 year follow-up with a randomized OFF versus ON assessment at 3 months [25]. At 3 months there was a 37% improvement ON versus OFF stimulation (though not statistically significant) with a 49% improvement at 1 year, again with varying individual degrees of improvement. Despite improvement, all patients reported a sense of diminished energy and visual complaints without associated, objective findings on examination.

Pallidal DBS for TS

Pallidal DBS results are likewise chiefly derived from case series. A small double-blind trial of 3 patients implanted with both pallidal and thalamic electrodes suggested a greater response to pallidal stimulation at 20–60 months follow-up compared with thalamic or thalamic and pallidal together [26]. Though generalizing from a small study is difficult, it did generate increased interest in pallidal stimulation. As with the medial thalamus, targeting has varied with some centers using the traditional posteroventral "motor" target and others using a more anteromedial target with some studies including a mix of the two. One of the largest case series involving both pallidal targets (though predominantly the anteromedial target) involved 15 patients, 13 of whom successfully completed a double-blind, crossover trial of on versus off stimulation evaluations for two three-month periods followed by open-label on stimulation follow-up of up to 36 months [27]. Improvement during the blinded phase was modest and not statistically significant, but open-labeled follow-up demonstrated a 40% improvement in the YGTSS with associated improvements in quality of life scales. Martinez-Torres et al. also reported a mixed cohort of anteromedial and posteroventral GPI DBS in 5 patients and found variable degrees of improvement, slightly more robust with the anteromedial target compared with the posteroventral [28]. In an open-label series of 17 patients targeting the anteromedial GPI, Sachdev et al. reported a mean reduction of 54% in the YGTSS in patients followed up to 46 months with 12 of the 17 improving over 50% and all but one reporting some perceived benefit [29]. Eleven of the 17 also reported some improvement in their OCD symptoms.

Other Targets for TS (ALIC, STN)

The anterior limb of the internal capsule is the approved target for OCD, and as TS shares obsessive/compulsive features, it is perhaps not surprising that it has been used to treat TS as well. The majority of ALIC reports for TS are limited to single case reports [30–33]. The small numbers make generalizable conclusions difficult particularly as results have varied from worsening of tics [30] to dramatic reduction of tics and OCD [33]. In one open-label case report, a patient received a 25% improvement in YGTSS global severity following ALIC but experienced apathy or hypomania with adjustments. Following a lead fracture, the ALIC electrodes were replaced with medial thalamic electrodes resulting in a 50% overall improvement without stimulation-associated mood issues despite considerably higher stimulation parameters [34]. The STN is another potential if seldom utilized contender in the busy field of potential TS targets. Stimulation of the STN, often preferred for Parkinson's, has been reported to improve OCD [35] and, in a single case report, improved tics in a patient suffering from both PD and TS [13].

Meta-Analyses

Two recent reports, one a meta-analysis based on review of the published literature and another a meta-analysis of data from the International Deep Brain Stimulation Registry and Database for Tourette Syndrome [17, 36], convey a broader sense of the outcomes to date. Baldermann et al. reviewed 57 articles consisting of 156 cases, 78 being thalamic, 64 being pallidal, and 9 ALIC [36]. Median age at time of surgery was 30 (15–60) with a mean improvement 53% (mainly derived from changes in YGTSS from median 83 to 35). Reduction in motor tics was about equivalent to reduction in vocal tics at 39% and 40%, respectively, with >50% of patients improving by >50%. In comparing outcomes across targets, they found the median YGTSS improvement following thalamic DBS to be 48% compared with Gpi-pl at 58%, Gpi-am at 55%, and ALIC at 44%. OCD scores, measured using the YBOCS, had a mean improvement of 31% (median 16 to 11) and were similar across targets. There was a trend toward more improvement in younger patients, but no particular target was unequivocally superior nor were any determining factors

identifiable in terms of separating responders from nonresponders. The DBS Registry and Database encompasses the pooled data from 31 actively involved DBS centers across 9 countries and recently reported 12-month data on 163 patients (many of whom are also included in the aforementioned meta-analysis). In terms of demographics, the population was 72% male with a mean age at surgery 29.5 (youngest being 13). Fifty-seven percent received thalamic stimulation, while 25% received anterior pallidal, 15% posterior pallidal, and 3% ALIC. The pooled improvement in the YGTSS was 44.1% with vocal responding slightly more than motor tics. Most improvement was obtained by 6 months and maintained at 1 year, and no significant differences were clearly perceived between targets though the most robust improvement compared with baseline was noted in the anterior pallidal cohort though not to a point where any clear recommendations could be made in regard to preferred target selection.

Complications

Although the risk of serious adverse events following DBS at experienced centers is low, it has been repeatedly noted that the risk of complications appear to be higher in the TS population compared with indications such as Parkinson's disease [19, 23, 29]. Reasons for this may include the presence of obsessive behaviors such as picking at incision sites or compulsive twiddling of the pulse generator resulting in infection or hardware malfunction (both of which occurred in our patient cohort and required hardware removal without lasting sequelae) [37]. Serious intraoperative complications at experienced centers appear to be relatively uncommon and were reported as 1.3% in the International TS DBS Registry. A thalamic hemorrhage at the lead tip in one patient resulted in a gaze palsy [25]. Postoperative infections and hardware malfunctions likewise appear to be more common in TS, reported as occurring in 2.5% of patients in the Registry. Servello, in reviewing all DBS cases, reported a higher incidence of infectious complication in patients who received DBS for TS [18]. It does not appear that a particular target is inherently more or less risk-prone. As many TS patients receive DBS at a relatively young age, the compounded risk of long-term indwelling hardware and IPG replacements also needs consideration. Stimulation-related complications – though generally reversible – are not infrequent in TS. The TS Registry reported as many as 30% of patients experiencing a stimulation-related side effect, perhaps not surprising given the high stimulation parameters used in some patients. Thalamic stimulation has been associated with a subjective feeling of decreased energy and visual disturbances [25] despite a lack of objective neuroophthalmological findings. Dysarthria and paresthesias are also frequent though, again, typically amenable to reprogramming. Higher anxiety levels have occasionally been associated with anterior GPI stimulation [38] as has worsening of mood, impulsivity, and imbalance [29]. Although OCD has often improved or remained unchanged following DBS for TS, there have been thalamic and pallidal cases were OCD has worsened despite an improvement in tics [19, 23].

Caveats and Conclusions

Despite the heterogeneous nature of the data, mainly derived from small case series with varying targets, methodologies, and outcome measures, there is a collective sense that DBS is an often (if variably) effective treatment option for refractory TS. Few of the studies allow for a conclusive determination as to what constitutes the best target, optimal stimulation parameters, or the most likely responders. These remain major limitations in our present understanding. Further hampering a clinical consensus is the relatively small number of patients requiring DBS, making a large multicenter, blinded study difficult to accomplish. The best means forward appears to be aggregated data as is being undertaken by the International Registry, which continues to publish outcomes data in hopes of providing a clearer picture. At this point, the authors feel safe stating that there is ample case-based evidence to warrant

consideration of DBS for severe medication refractory TS targeting either the globus pallidus or median thalamus. However, the variable degree of response – including possibility of non-response – along with the higher incidence of complications needs to be explicitly explained to prospective candidates, particularly to potentially more vulnerable younger patients. Ideally, continued thoughtful and systematic collection of pre- and postsurgical data will allow for a more straightforward assessment of DBS's place in the armamentarium.

References

1. Scharf JM, Yu D, Mathews CA, Neale BM, Stewart SE, Fagerness JA, et al. Genome-wide association study of Tourette's syndrome. Mol Psychiatry. 2013;18(6):721–8.
2. Mufford M, Cheung J, Jahanshad N, van der Merwe C, Ding L, Groenewold N, et al. Concordance of genetic variation that increases risk for tourette syndrome and that influences its underlying neurocircuitry. Transl Psychiatry. 2019;9(1):120.
3. Greene DJ, Williams Iii AC, Koller JM, Schlaggar BL, Black KJ, The Tourette Association of America Neuroimaging C. Brain structure in pediatric Tourette syndrome. Mol Psychiatry. 2017;22(7):972–80.
4. Peterson BS, Thomas P, Kane MJ, Scahill L, Zhang H, Bronen R, et al. Basal ganglia volumes in patients with Gilles de la Tourette syndrome. Arch Gen Psychiatry. 2003;60(4):415–24.
5. Pourfar M, Feigin A, Tang CC, Carbon-Correll M, Bussa M, Budman C, et al. Abnormal metabolic brain networks in Tourette syndrome. Neurology. 2011;76(11):944–52.
6. Jo HJ, McCairn KW, Gibson WS, Testini P, Zhao CZ, Gorny KR, et al. Global network modulation during thalamic stimulation for Tourette syndrome. Neuroimage Clin. 2018;18:502–9.
7. Babel TB, Warnke PC, Ostertag CB. Immediate and long term outcome after infrathalamic and thalamic lesioning for intractable Tourette's syndrome. J Neurol Neurosurg Psychiatry. 2001;70(5):666–71.
8. Hassler R, Dieckmann G. Stereotaxic treatment of tics and inarticulate cries or coprolalia considered as motor obsessional phenomena in Gilles de la Tourette's disease. Rev Neurol (Paris). 1970;123(2):89–100.
9. Beckers W. Gilles de la Tourette's disease based on five own observations. Arch Psychiatr Nervenkr (1970). 1973;217(2):169–86.
10. Kurlan R, Kersun J, Ballantine HT Jr, Caine ED. Neurosurgical treatment of severe obsessive-compulsive disorder associated with Tourette's syndrome. Mov Disord. 1990;5(2):152–5.
11. Asam U, Karrass W. Gilles de la Tourette syndrome and psychosurgery. Acta Paedopsychiatr. 1981;47(1):39–48.
12. Hwynn N, Tagliati M, Alterman RL, Limotai N, Zeilman P, Malaty IA, et al. Improvement of both dystonia and tics with 60 Hz pallidal deep brain stimulation. Int J Neurosci. 2012;122(9):519–22.
13. Martinez-Torres I, Hariz MI, Zrinzo L, Foltynie T, Limousin P. Improvement of tics after subthalamic nucleus deep brain stimulation. Neurology. 2009;72(20):1787–9.
14. Vandewalle V, van der Linden C, Groenewegen HJ, Caemaert J. Stereotactic treatment of Gilles de la Tourette syndrome by high frequency stimulation of thalamus. Lancet. 1999;353(9154):724.
15. Mink JW, Walkup J, Frey KA, Como P, Cath D, Delong MR, et al. Patient selection and assessment recommendations for deep brain stimulation in Tourette syndrome. Mov Disord. 2006;21(11):1831–8.
16. Schrock LE, Mink JW, Woods DW, Porta M, Servello D, Visser-Vandewalle V, et al. Tourette syndrome deep brain stimulation: a review and updated recommendations. Mov Disord. 2015;30(4):448–71.
17. Martinez-Ramirez D, Jimenez-Shahed J, Leckman JF, Porta M, Servello D, Meng FG, et al. Efficacy and safety of deep brain stimulation in Tourette syndrome: the international Tourette syndrome deep brain stimulation public database and registry. JAMA Neurol. 2018;75:353.
18. Servello D, Sassi M, Gaeta M, Ricci C, Porta M. Tourette syndrome (TS) bears a higher rate of inflammatory complications at the implanted hardware in deep brain stimulation (DBS). Acta Neurochir. 2011;153(3):629–32.
19. Dowd RS, Pourfar M, Mogilner AY. Deep brain stimulation for Tourette syndrome: a single-center series. J Neurosurg. 2018;128:596–604.
20. Bour LJ, Ackermans L, Foncke EM, Cath D, van der Linden C, Visser Vandewalle V, et al. Tic related local field potentials in the thalamus and the effect of deep brain stimulation in Tourette syndrome: report of three cases. Clin Neurophysiol. 2015;126(8):1578–88.
21. Visser-Vandewalle V, Temel Y, Boon P, Vreeling F, Colle H, Hoogland G, et al. Chronic bilateral thalamic stimulation: a new therapeutic approach in intractable Tourette syndrome. Report of three cases. J Neurosurg. 2003;99(6):1094–100.
22. Visser-Vandewalle V, Kuhn J. Deep brain stimulation for Tourette syndrome. Handb Clin Neurol. 2013;116:251–8.
23. Porta M, Servello D, Zanaboni C, Anasetti F, Menghetti C, Sassi M, et al. Deep brain stimulation for treatment of refractory Tourette syndrome: long-term follow-up. Acta Neurochir. 2012;154(11):2029–41.
24. Maciunas RJ, Maddux BN, Riley DE, Whitney CM, Schoenberg MR, Ogrocki PJ, et al. Prospective randomized double-blind trial of bilateral thalamic deep brain stimulation in adults with Tourette syndrome. J Neurosurg. 2007;107(5):1004–14.

25. Ackermans L, Duits A, van der Linden C, Tijssen M, Schruers K, Temel Y, et al. Double-blind clinical trial of thalamic stimulation in patients with Tourette syndrome. Brain. 2011;134(Pt 3):832–44.
26. Welter ML, Mallet L, Houeto JL, Karachi C, Czernecki V, Cornu P, et al. Internal pallidal and thalamic stimulation in patients with Tourette syndrome. Arch Neurol. 2008;65(7):952–7.
27. Kefalopoulou Z, Zrinzo L, Jahanshahi M, Candelario J, Milabo C, Beigi M, et al. Bilateral globus pallidus stimulation for severe Tourette's syndrome: a double-blind, randomised crossover trial. Lancet Neurol. 2015;14(6):595–605.
28. Martinez-Fernandez R, Zrinzo L, Aviles-Olmos I, Hariz M, Martinez-Torres I, Joyce E, et al. Deep brain stimulation for Gilles de la Tourette syndrome: a case series targeting subregions of the globus pallidus internus. Mov Disord. 2011;26(10):1922–30.
29. Sachdev PS, Mohan A, Cannon E, Crawford JD, Silberstein P, Cook R, et al. Deep brain stimulation of the antero-medial globus pallidus interna for Tourette syndrome. PLoS One. 2014;9(8):e104926.
30. Burdick A, Foote KD, Goodman W, Ward HE, Ricciuti N, Murphy T, et al. Lack of benefit of accumbens/capsular deep brain stimulation in a patient with both tics and obsessive-compulsive disorder. Neurocase. 2010;16(4):321–30.
31. Flaherty AW, Williams ZM, Amirnovin R, Kasper E, Rauch SL, Cosgrove GR, et al. Deep brain stimulation of the anterior internal capsule for the treatment of Tourette syndrome: technical case report. Neurosurgery. 2005;57(4 Suppl):E403; discussion E
32. Kuhn J, Lenartz D, Huff W, Mai JK, Koulousakis A, Maarouf M, et al. Transient manic-like episode following bilateral deep brain stimulation of the nucleus accumbens and the internal capsule in a patient with Tourette syndrome. Neuromodulation. 2008;11(2):128–31.
33. Neuner I, Podoll K, Lenartz D, Sturm V, Schneider F. Deep brain stimulation in the nucleus accumbens for intractable Tourette's syndrome: follow-up report of 36 months. Biol Psychiatry. 2009;65(4):e5–6.
34. Shields DC, Cheng ML, Flaherty AW, Gale JT, Eskandar EN. Microelectrode-guided deep brain stimulation for Tourette syndrome: within-subject comparison of different stimulation sites. Stereotact Funct Neurosurg. 2008;86(2):87–91.
35. Mallet L, Polosan M, Jaafari N, Baup N, Welter ML, Fontaine D, et al. Subthalamic nucleus stimulation in severe obsessive-compulsive disorder. N Engl J Med. 2008;359(20):2121–34.
36. Baldermann JC, Kohl S, Visser-Vandewalle V, Klehr M, Huys D, Kuhn J. Deep brain stimulation of the ventral capsule/ventral striatum reproducibly improves symptoms of body dysmorphic disorder. Brain Stimul. 2016;9(6):957–9.
37. Pourfar M, Budman C, Mogilner A. A case of deep brain stimulation in Tourette's complicated by Twiddler's syndrome. Mov Disord Clin Pract. 2015;2(2):192.
38. Cannon E, Silburn P, Coyne T, O'Maley K, Crawford JD, Sachdev PS. Deep brain stimulation of anteromedial globus pallidus interna for severe Tourette's syndrome. Am J Psychiatry. 2012;169(8):860–6.

Chronic Pain: Neuromodulation

32

Zoe E. Teton and Ahmed M. Raslan

Introduction

Chronic pain affects 1 in 5 people in the United States and is the most common complaint of those seeking medical care [1]. This has a crippling effect on individuals and their ability to provide for themselves and their families and represents a 500 million dollar economic toll from both medical treatment and loss of productivity [2]. In the wake of an aging baby boomer generation, as well as an opioid epidemic that has left thousands of lives lost, finding and utilizing effective solutions to treat chronic pain is of the utmost importance [3].

While there is a paucity of evidence supporting opioid efficacy in the management of chronic pain, continued prevalence puts an additional onus on expanding the pain physician's armamentarium to include various neuromodulatory techniques as potential treatment options [4]. There are many pain pathway targets available to the neurosurgeon attempting to treat chronic pain – from the peripheral nerve and the dorsal root through the spinal cord and midbrain to the thalamus and cerebral cortex [5]. Despite a multitude of potential targets, therapeutic efficacy is highly variable, and the popularity of particular procedures has continued to transform over the years [2, 6].

An overview of the most common neuromodulatory techniques used to treat chronic pain, by neurosurgeons, is presented and discussed.

Pharmacologic

Intrathecal Opioid Pumps

The use of intrathecal pumps in the treatment of intractable pain was first described in the early 1980s and introduced a novel pathway to administer analgesic medications, one that rendered morphine administration with 400 times the potency of subcutaneously administered opioid [7]. Despite this benefit, intrathecal opioid delivery did not become particularly widespread in part due to lack of research and in part due to unease surrounding the administration of opioids via a pump and the subsequent complications that could arise [8]. However, a 2016 meta-analysis on the use of intrathecal morphine in spine surgery patients examined 8 randomized controlled trials (RCTs) involving nearly 400 patients and found that postoperative morphine use was significantly lower in the 24 hours following surgery with comparable levels of pain relief [9]. A German group of investigators sought to examine the long-term use of intrathecal therapy to evaluate efficacy, side effects, and

Z. E. Teton · A. M. Raslan (✉)
Department of Neurological Surgery, Oregon Health & Science University, Portland, OR, USA
e-mail: raslana@ohsu.edu

N. Pouratian, S. A. Sheth (eds.), *Stereotactic and Functional Neurosurgery*,
https://doi.org/10.1007/978-3-030-34906-6_32

degree of dose escalation [8]. In their review of 36 patients with a mean duration of over 11 years of intrathecal opioid delivery, they demonstrated significant pain relief that was maintained at longest follow-up. They also reported a benefit in speech, mobility, and improved functional scores on anxiety/depression scales. Mean morphine dose increased from 1 mg/day to 4.6 mg/day, which was in line with a previous study that reported an average annual dose increase of 12% in intrathecal opioid users. Side effects were similar to oral opioid administration and included obstipation (58%), fatigue (36%), sexual dysfunction (33%), and urinary retention (30%) [8]. Intrathecal opioids have been used most extensively among cancer patients where efficacy rates are considerably higher with up to 77% reporting long-term pain relief with the use of intrathecal analgesia [7].

Intracerebroventricular Opioids

The use of intracerebroventricular (ICV) opioid administration has become increasingly rare and is now generally reserved for palliative treatment of otherwise refractory cancer pain [10]. The infusion device itself is small, relatively simple to install and use, and ultimately provides an opportunity for certain hospice patients to transition from hospital to home while maintaining quality of life. A review on ICV opioid use in 2011 described the onset of action to be about 20–40 minutes with the analgesic effect lasting anywhere from 12–16 hours depending on the dose and reported minimal complaints of respiratory depression or constipation [10].

Stimulation

Spinal Cord Stimulation

The most commonly utilized neurosurgical treatment for chronic pain is the spinal cord stimulator (discussed in detail in Chap. 13). Initially introduced in the late 1960s, spinal cord stimulation (SCS) did not become popular until the 1980s and was officially approved by the US Food and Drug Administration (FDA) to treat chronic pain in the trunk, arms, or legs in 1989 [11, 12]. Today, approximately 34,000 spinal cord stimulators are implanted each year and account for over two-thirds of all neuromodulatory procedures [12]. Three factors are important when evaluating SCS – efficacy, indications, and cost-effectiveness.

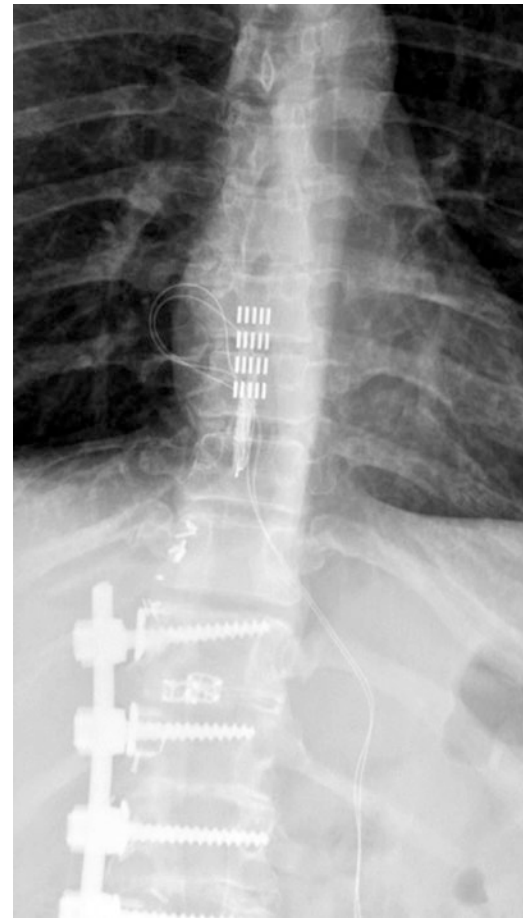

Fig. 32.1 Fluoroscopy demonstrating placement of SCS percutaneous leads

Traditionally, SCS is thought to work by generating a small electrical current in the epidural space of the spinal cord that replaces the pain that patients feel with a mild tingling or paresthesia [4]. The leads are either electrodes placed percutaneously into the epidural space (Fig. 32.1) or paddles placed surgically via laminotomy (Fig. 32.2). Generally, patients will undergo a

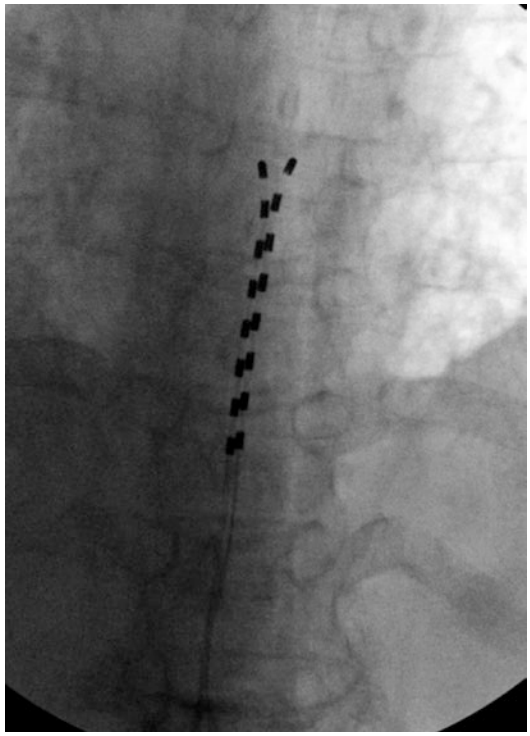

Fig. 32.2 Fluoroscopy demonstrating placement of SCS paddle electrode

trial stimulator placement with an external power source to determine level of efficacy before undergoing subcutaneous, surgical placement of an implantable pulse generator [13].

Spinal cord stimulation is particularly useful for treating mixed neuropathic with either nociceptive or radicular pain and is popular as it provides a minimally invasive, relatively safe, and reversible treatment option for patients [4]. Stimulators are programmed based on different parameters. This makes configuration more complex, but has the potential to increase use, as newer variations are explored. The amplitude, pulse width, and frequency of neurostimulation can vary, and each change introduces a new set of variables that need to be adjusted (and studied) separately. Frequencies range from low (<5 Hz) to high (up to 1400 Hz), though conventional parameters consist of 40–60Hz of tonic stimulation [14–16].

A SCS meta-analysis was published in 2016 and examined the efficacy of SCS for the treatment of chronic spinal pain. It included 6 RCTs, 3 of which were efficacy trials, while 3 were stimulation trials [11]. The authors determined that there was significant (Level I to II) evidence for the use of SCS for lumbar failed back surgery syndrome (FBSS), while only moderate (Level II to III) evidence for high frequency stimulation, but ultimately reported that SCS for each indication studied was cost-effective. This was in line with a large meta-analysis previously conducted in 2014 that included 74 studies for a total of over 3000 patients with chronic back and leg pain (CBLP), the majority of which were due to FBSS [17]. The authors determined that 53% of patients will experience at least a 50% reduction in pain with a mean follow-up period of 2 years. While there had previously been suggestion in the literature that SCS was more effective for leg predominant CBLP, this study did not find a difference [13].

This was echoed in a review by the National Institute for Health and Care Excellence (NICE) in the United Kingdom that examined 11 RCTs, 8 of which were aimed at treating ischemic pain, while 3 were aimed at treating neuropathic pain [18]. The group ultimately recommended SCS as a cost-effective treatment for medically refractory, chronic neuropathic pain conditions, such as FBSS, though were unable to draw conclusions with regard to the utility of SCS for ischemic pain.

Newer and potentially more promising stimulation patterns such as ultra-high-frequency SCS up to 10 kHz (HF10-SCS) and burst stimulation (short bursts of electrical impulses followed by a quiescent period) are rising in popularity due to their "paresthesia-free" nature and higher efficacy rates. There is class I evidence to support the effectiveness of initial and long-term use of HF10-SCS therapy for treatment of back and leg pain [16, 19]. Additionally, there is class I evidence to support the use of Burst-DR® therapy for back and leg pain [20]. Two reviews published by the same group in 2018 examined these new modalities and found that both HF10-SCS and burst stimulation demonstrated superior long-term efficacy in the treatment of CLBP compared to traditional SCS [15, 16, 21].

A relatively recently discovered therapy that falls under the umbrella of SCS is dorsal root ganglion stimulation (DRGS). It provides an alternative treatment option for patients with chronic regional pain syndrome (CPRS) and other forms of neuropathic pain with roughly equal efficacy rates [22]. A randomized, comparative trial examining DRGS vs. SCS in the treatment of CRPS found higher treatment success rates in the DRGS population 3 months post-surgery (81% vs 55%, $p < 0.001$) [23]. Complication rates were similar between the two groups with implantable pulse generator (IPG) pocket pain (10%) and pain at the incision site (8%) being the most common within the DRGS group.

Complications for SCS are generally mild, though rates are high and are reported as 30–40% [4]. Usually, these are hardware related and include lead fracture (5–9%) and lead migration (0–27%). Biological complications (infection, allergic reaction, pain, hematoma, etc.) occur at lower rates, with infection being the most common, observed in 3–8% of cases [4].

Peripheral Nerve Stimulation

Peripheral nerve stimulation is another neuromodulatory option to treat chronic pain with its most common application being occipital nerve stimulation (ONS) for occipital neuralgia. Details of outcomes of PNS for facial pain are provided in more detail in Chap. 14 and briefly described here. Occipital neuralgia is an uncommon cause of occipital headaches, characterized by intermittent, shooting pains in the distribution of the greater, lesser, or third occipital nerves [24]. There are few studies on the use of ONS for occipital neuralgia treatment, but efficacy rates are documented as high as 85% (17/20) in some series with relatively minor complications [25]. The Congress of Neurological Surgeons (CNS) published a systematic review and evidence-based guideline in response to the question, "Is ONS an effective treatment option for medically refractory occipital neuralgia?" with nine studies meeting the inclusion criteria [26]. They did note that the sample size was limited as only patients with medically refractory occipital neuralgia were examined and concluded with Level III evidence that ONS should be considered as a treatment option in this patient cohort. Complications were most commonly infection (up to 29%) and lead migration (up to 10%).

Peripheral trigeminal nerve stimulation has emerged in recent years to aid in the treatment of peripheral trigeminal neuropathic pain [27]. Data on use, however, is even rarer than its occipital counterpart. In one of the larger case series on the topic ($n = 10$), peripheral nerve stimulation (PNS) was found to provide at least 50% pain relief in 70% of patients with 80% of patients indicating they were mostly or completely satisfied with the treatment overall with a mean follow-up period of over 2 years [28]. Complications requiring reoperation were high, however, and totaled nearly a third of patients.

Deep Brain Stimulation

Since peak use in the 1970s, deep brain stimulation (DBS) use for chronic pain treatment has been on the decline, in large part due to the many variations in targets and surgical technique, which clouds the interpretation of individual study efficacy measurements [29]. Deep brain stimulation for pain is most commonly used for central post-stroke pain, atypical facial pain, and brachial plexus injury, as well as a certain subset of patients that have failed SCS [2].

Multiple target use over time, with heterogeneous indications for treatment, leads to cessation of a major DBS trial in the USA, and therefore, DBS is currently not covered by insurance or FDA approved for treatment of pain [30]. Current DBS use and research for pain is conducted in Europe. An Oxford Group contributed substantially to current worldwide knowledge about use of DBS in treating chronic pain. The group had initially led the effort of dual thalamic (VPL/VPM) and periventricular gray and periaqueductal gray PAG/PVG stimulation [31]. Later, they switched their approach to anterior cingulate cortex (ACC) stimulation

with encouraging long-term results, although with unexpected complications of seizure induction [32, 33].

A review by Bittar et al. concluded that DBS was more effective for nociceptive pain with success rates as high as 80% and less so for deafferentation pain where the highest success in any study was reported at 67%. This difference was significant across the 6 studies reviewed [29]. A review in 2015 concluded that DBS for pain has been shown to be effective in several case series though lamented that clinical trials are required to demonstrate this effect more robustly [5].

Motor Cortex Stimulation

Motor cortex stimulation (MCS) is a potential alternative for the alleviation of central pain [29]. Stimulation of the motor cortex in the treatment of neuropathic pain is thought to work by the inhibition of thalamic sensory neurons that have become hyperactive as a result of deafferentation [6, 34]. Motor cortex stimulation involves the implantation of epidural electrodes over the motor cortex via a frontoparietal craniotomy. The hope was that this less invasive approach to cranial neuromodulation would show comparable pain relief rates to DBS though comparison studies are lacking [2]. While this neuromodulation technique has been in place since the early 1990s, its use remains very limited due to highly variable efficacy rates among individuals and the lack of standardized stimulation thresholds [34–36]. A meta-analysis in 2009 reported on outcomes from 210 patients and found that 55% experienced a good response to MCS (pain relief of at least 40–50%), and this was maintained out to 1 year for 45% of the 152 patients that could be contacted [37]. Complications included seizures in the early postoperative period (12%), infections (5.7%), and hardware complications (5.1%). However, none of the studies included were blinded or controlled, and a significant placebo effect is described with as many as 35% of patients describing pain relief despite their stimulator not being turned on during the trial period [37]. Patient selection is of paramount importance in these cases with neurogenic pain generally showing better response than nociceptive pain and with higher success rates in facial pain (68%) as compared to central pain (54%) [6, 34, 37].

Conclusion

Chronic pain is a debilitating condition that lacks a straightforward treatment regimen. While the neurosurgeon does have a multitude of options at their disposal to aid in treatment, research into each option is difficult to interpret due to heterogeneity in reporting paradigms, individual's subjective experience of pain, and the inherent variability in the procedures themselves. However, for the well-selected patient with otherwise intractable pain, neuromodulation represents an effective option to alleviate suffering. Further study should be aimed at conducting larger scale, RCTs to answer the question of efficacy, and complication rates for each treatment modality.

References

1. Dahlhamer J, Lucas J, Zelaya C, et al. Prevalence of chronic pain and high-impact chronic pain among adults — United States, 2016. Morb Mortal Wkly Rep. 2018;67:1001–6.
2. Farrell SM, Green A, Aziz T. The current state of deep brain stimulation for chronic pain and its context in other forms of neuromodulation. Brain Sci. 2018;8(8):158.
3. Clark DJ, Schumacher MA. America's opioid epidemic: supply and demand considerations. Anesth Analg. 2017;125(5):1667–74.
4. Verrills P, Sinclair C, Barnard A. A review of spinal cord stimulation systems for chronic pain. J Pain Res. 2016;9:481–92.
5. Boccard SG, Pereira EA, Aziz TZ. Deep brain stimulation for chronic pain. J Clin Neurosci. 2015;22(10):1537–43.
6. Raslan AM, McCartney S, Burchiel KJ. Management of chronic severe pain: cerebral neuromodulatory and neuroablative approaches. Acta Neurochir Suppl. 2007;97(Pt 2):17–26.
7. Textor LH. CE: intrathecal pumps for managing cancer pain. Am J Nurs. 2016;116(5):36–44.
8. Kleinmann B, Wolter T. Intrathecal opioid therapy for non-malignant chronic pain: a long-term perspective. Neuromodulation. 2017;20(7):719–26.

9. Pendi A, Acosta FL, Tuchman A, et al. Intrathecal morphine in spine surgery: a meta-analysis of randomized controlled trials. Spine (Phila Pa 1976). 2017;42(12):E740–e747.
10. Raffa RB, Pergolizzi JV Jr. Intracerebroventricular opioids for intractable pain. Br J Clin Pharmacol. 2012;74(1):34–41.
11. Grider JS, Manchikanti L, Carayannopoulos A, et al. Effectiveness of spinal cord stimulation in chronic spinal pain: a systematic review. Pain Physician. 2016;19(1):E33–54.
12. Simon Thomson M, FRCA, FIPP, FFPMRCA. Spinal cord stimulation: its role in managing chronic disease symptoms. 2016. https://www.neuromodulation.com/assets/documents/Fact_Sheets/fact_sheet_spinal_cord_stimulation.pdf. Accessed 10 Dec 2018.
13. Dones I, Levi V. Spinal cord stimulation for neuropathic pain: current trends and future applications. Brain Sci. 2018;8(8):138.
14. Miller JP, Eldabe S, Buchser E, Johanek LM, Guan Y, Linderoth B. Parameters of spinal cord stimulation and their role in electrical charge delivery: a review. Neuromodulation. 2016;19(4):373–84.
15. Chakravarthy K, Richter H, Christo PJ, Williams K, Guan Y. Spinal cord stimulation for treating chronic pain: reviewing preclinical and clinical data on paresthesia-free high-frequency therapy. Neuromodulation. 2018;21(1):10–8.
16. Kapural L, Yu C, Doust MW, et al. Novel 10-kHz high-frequency therapy (HF10 therapy) is superior to traditional low-frequency spinal cord stimulation for the treatment of chronic back and leg pain: the SENZA-RCT randomized controlled trial. Anesthesiology. 2015;123(4):851–60.
17. Taylor RS, Desai MJ, Rigoard P, Taylor RJ. Predictors of pain relief following spinal cord stimulation in chronic back and leg pain and failed back surgery syndrome: a systematic review and meta-regression analysis. Pain Pract. 2014;14(6):489–505.
18. Simpson EL, Duenas A, Holmes MW, Papaioannou D, Chilcott J. Spinal cord stimulation for chronic pain of neuropathic or ischaemic origin: systematic review and economic evaluation. Health Technol Assess. 2009;13(17):iii, ix–x, 1–154.
19. Kapural L, Yu C, Doust MW, et al. Comparison of 10-kHz high-frequency and traditional low-frequency spinal cord stimulation for the treatment of chronic back and leg pain: 24-month results from a multicenter, randomized, controlled pivotal trial. Neurosurgery. 2016;79(5):667–77.
20. Deer T, Slavin KV, Amirdelfan K, et al. Success using neuromodulation with BURST (SUNBURST) study: results from a prospective, randomized controlled trial using a novel burst waveform. Neuromodulation. 2018;21(1):56–66.
21. Chakravarthy K, Kent AR, Raza A, Xing F, Kinfe TM. Burst spinal cord stimulation: review of preclinical studies and comments on clinical outcomes. Neuromodulation. 2018;21(5):431–9.
22. Liem L. Stimulation of the dorsal root ganglion. Prog Neurol Surg. 2015;29:213–24.
23. Deer TR, Levy RM, Kramer J, et al. Dorsal root ganglion stimulation yielded higher treatment success rate for complex regional pain syndrome and causalgia at 3 and 12 months: a randomized comparative trial. Pain. 2017;158(4):669–81.
24. Dougherty C. Occipital neuralgia. Curr Pain Headache Rep. 2014;18(5):411.
25. Keifer OP Jr, Diaz A, Campbell M, Bezchlibnyk YB, Boulis NM. Occipital nerve stimulation for the treatment of refractory occipital neuralgia: a case series. World Neurosurg. 2017;105:599–604.
26. Sweet JA, Mitchell LS, Narouze S, et al. Occipital nerve stimulation for the treatment of patients with medically refractory occipital neuralgia: congress of neurological surgeons systematic review and evidence-based guideline. Neurosurgery. 2015;77(3):332–41.
27. Feletti A, Santi GZ, Sammartino F, Bevilacqua M, Cisotto P, Longatti P. Peripheral trigeminal nerve field stimulation: report of 6 cases. Neurosurg Focus. 2013;35(3):E10.
28. Johnson MD, Burchiel KJ. Peripheral stimulation for treatment of trigeminal postherpetic neuralgia and trigeminal posttraumatic neuropathic pain: a pilot study. Neurosurgery. 2004;55(1):135–41; discussion 141-132.
29. Bittar RG, Kar-Purkayastha I, Owen SL, et al. Deep brain stimulation for pain relief: a meta-analysis. J Clin Neurosci. 2005;12(5):515–9.
30. Coffey RJ. Deep brain stimulation for chronic pain: results of two multicenter trials and a structured review. Pain Med. 2001;2(3):183–92.
31. Owen SL, Green AL, Stein JF, Aziz TZ. Deep brain stimulation for the alleviation of post-stroke neuropathic pain. Pain. 2006;120(1–2):202–6.
32. Boccard SG, Pereira EA, Moir L, et al. Deep brain stimulation of the anterior cingulate cortex: targeting the affective component of chronic pain. Neuroreport. 2014;25(2):83–8.
33. Boccard SGJ, Prangnell SJ, Pycroft L, et al. Long-term results of deep brain stimulation of the anterior cingulate cortex for neuropathic pain. World Neurosurg. 2017;106:625–37.
34. Ostergard T, Munyon C, Miller JP. Motor cortex stimulation for chronic pain. Neurosurg Clin N Am. 2014;25(4):693–8.
35. Ivanishvili Z, Poologaindran A, Honey CR. Cyclization of motor cortex stimulation for neuropathic pain: a prospective, randomized, blinded trial. Neuromodulation. 2017;20(5):497–503.
36. Radic JA, Beauprie I, Chiasson P, Kiss ZH, Brownstone RM. Motor cortex stimulation for neuropathic pain: a randomized cross-over trial. Can J Neurol Sci. 2015;42(6):401–9.
37. Fontaine D, Hamani C, Lozano A. Efficacy and safety of motor cortex stimulation for chronic neuropathic pain: critical review of the literature. J Neurosurg. 2009;110(2):251–6.

Chronic Pain: Lesions

33

Patrick J. Karas and Ashwin Viswanathan

Introduction

For most patients with chronic pain, neuromodulation or intrathecal drug delivery is the best approach for the management of their pain. However, for patients in whom neuromodulation is not appropriate or does not lead to effective pain control, ablative techniques remain an important alternative. Moreover, cranial and spinal ablations are both relevant and important techniques for treatment of medically refractory cancer pain. Cordotomy, the interruption of the spinothalamic tract, and myelotomy, the interruption of the dorsal column visceral pain pathway, can be performed percutaneously or through open surgery via laminectomy. Cingulotomy, the lesioning of the anterior cingulate cortex, is a useful approach for patients who suffer from a significant affective component of pain. Ablative techniques offer the advantages of immediate pain relief, do not require routine medical visits for maintenance of an implanted device, and have greater cost efficacy as compared to neuromodulation alternatives. In this chapter, we will review cordotomy, myelotomy, and cingulotomy for the treatment of intractable pain.

P. J. Karas · A. Viswanathan (✉)
Department of Neurosurgery, Baylor College of Medicine, Houston, TX, USA
e-mail: ashwinv@bcm.edu

Cordotomy

Cordotomy is an established technique and multiple approaches to lesioning the spinothalamic tract have been explored. Open cervical or thoracic cordotomy with mechanical sectioning of the spinal cord, as well percutaneous approaches using radiofrequency ablation, are commonly used. CT-guided cordotomy, pioneered by Kanpolat, has made cordotomy significantly safer and more effective. Two important large neurosurgical series of CT-guided cordotomy have been published. In one, a prospective study of 41 patients who underwent cordotomy, 80% of patients had no pain postoperatively and for 1 month post-procedure [1]. In the patients surviving at 6 months post-procedure, 32% had no pain, while another 48% percent had partial satisfactory pain relief. Similarly, Kanpolat achieved significant improvement in pain intensity from mean 7.6 preoperatively to mean 1.3 postoperatively in a series of 207 cordotomies [2]. When Kanpolat reported his subset of 108 patients with lung cancer, 89% of patients had no pain postoperatively.

More recently, Viswanathan and colleagues performed a prospective randomized crossover trial in which patients with medically refractory pain were randomized to undergo cordotomy versus continued comprehensive palliative care [3]. Significant improvement in pain intensity was seen in patients randomized to cordotomy, while

N. Pouratian, S. A. Sheth (eds.), *Stereotactic and Functional Neurosurgery*,
https://doi.org/10.1007/978-3-030-34906-6_33

those randomized to continued palliative care had no further pain improvement. In addition, most patients randomized to continued palliative care elected to crossover to cordotomy. After surgery all of these patients also had dramatic pain improvements.

Indications

Cordotomy is an effective treatment for nociceptive cancer pain. Nociceptive pain is caused by direct tissue involvement from the tumor. We highly recommend that high cervical cordotomy should only be performed unilaterally in order to avoid interrupting the adjacent reticulospinal tracts bilaterally. Disruption of both reticulospinal tracts can lead to central hypoventilation syndrome (Ondine's curse), which has been reported after bilateral high cervical cordotomy [4, 5]. Because the spinothalamic fibers decussate, the effect of a cordotomy begins on pain arising 2–5 segments below the targeted spinal level. Therefore C1–2 percutaneous cordotomy usually decreases pain arising at C5 or C6 dermatomes and below.

While cordotomy is extremely effective for nociceptive pain, the effect on neuropathic pain is mixed. In our experience, cordotomy is much less effective for pain associated with complete deafferentation. Most pain conditions associated with cancer have both nociceptive and neuropathic pain components. Because of this hybrid pain phenotype, we have experienced some variability in pain outcomes with cordotomy [6]. While the neuropathic pain component is partially responsible for this variability, incomplete ablation of the spinothalamic tract likely also plays a role.

Intraprocedural Imaging Considerations

A significant body of literature was generated performing cordotomy with standalone fluoroscopy. Modernly, three-dimensional intraoperative imaging techniques allow for safer and more accurate targeting, leading to even better pain control outcomes. Two main imaging modalities are commonly used. Conventional CT with myelography, available either in a diagnostic radiology suit or in the operating room, provides excellent imaging and visualization of the spinal cord, and scanning is very fast. A movable table within the CT scanner greatly facilitates moving the patient quickly in and out of the scanner to adjust the needle position. The O-arm (Medtronic) is an intraoperative imaging technique with increasing availability in the United States. The O-arm allows for x-ray during advancement of the spinal needle instead of performing short segment CT scans. While O-arm allows for time saving and lower radiation dose during needle insertion as compared to conventional CT, the O-arm does not allow short segment scans limited to a narrow working area such as the C1-C2 region. Each O-arm spine acquires complete cervical spine junction images. The myelogram quality obtained with O-arm is not as clear as conventional CT, though it is adequate for cordotomy. Endoscopy is a third technique for performing cordotomy, described in detail by Fonoff and colleagues [7].

Surgical Techniques

A preoperative cranial CT scan must be obtained prior to cordotomy to rule out a mass lesion which could lead to herniation during the C1–2 spinal puncture. We perform cordotomy in the diagnostic CT scanning area. A lumbar puncture is performed for injection of intrathecal contrast to perform a cervical myelogram. After injection of intrathecal contrast, the patient is placed in Trendelenburg for 15–20 minutes allowing for contrast distribution prior to CT scan.

It is helpful for an anesthesiologist to assist with pain control during the procedure, particularly since cordotomy patients have severe pain at baseline. We recommend light intravenous sedation via intermittent propofol boluses added to a baseline continuous infusion. The needle entry point for cordotomy is approximately 1 cm inferior and posterior to the tip of the mastoid.

A small amount of lidocaine (1%) is used to anesthetize the skin. A cervical spine CT scan centered at the C1–2 area is obtained, and the skin-to-dura distance is measured on the scan. This distance is marked on the 20-guage spinal needle included in the disposable percutaneous cordotomy electrode kit (LCED, Boston Scientific). The 20-gauge needle is then advanced from the entry point toward the C1–2 interspace. During needle advancement, multiple short CT scans are obtained, centered around the needle, in order to direct the needle along the correct trajectory toward the dura and anterior half of the spinal cord (Fig. 33.1). If targeting lower extremity pain, the spinal needle should be directed to slightly anterior to the midline (in anterior-posterior direction) of spinal cord. If targeting upper extremities or trunk, the needle should be directed more anteriorly by 1–2 mm. Using image guidance, the needle tip is advanced through the dura into the CSF. The needle stylet is then replaced with the LCED electrode. Tactile feel, impedance measurement, and imaging are then used to direct the electrode. Impedance measurement of the electrode will measure a few hundred Ohms (<300 Ω) when in CSF. This will increase significantly to a range of several hundred Ohms (300–500 Ω) when the electrode touches and begins to penetrate the cervical spinal cord pia. A clear tactile feeling is noticeable when the electrode enters the spinal cord, along with a dramatic increase in impedance to greater than 700 Ω. At this point, another CT scan is obtained to confirm the location of the RF electrode within the spinal cord. If necessary, the electrode can be withdrawn until it is positioned within the radiographically expected location of the spinothalamic tract.

To determine the exact location of the electrode within the sensory and motor tracts, intraoperative physiological testing is performed after placement of the electrode. Sensory testing is performed at 100 Hz and a 0.1 msec pulse width, while motor testing is performed at 2 Hz and a 0.1 msec pulse width. Sedation must be stopped prior to testing so that the patient is communicative. Sensory testing is performed to ensure physiological presence within the spinothalamic tract – sensory sensation should cover the same distribution as the targeted painful

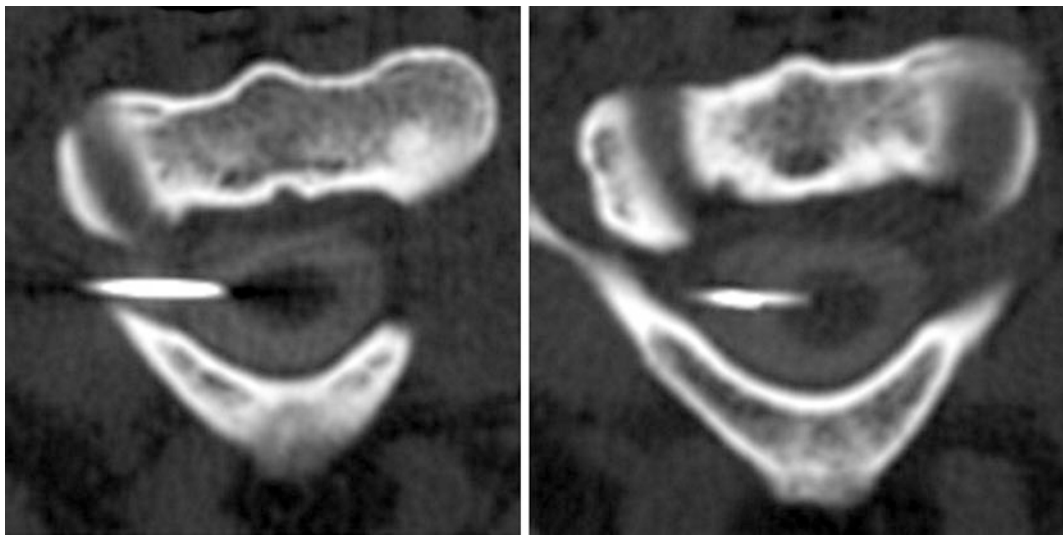

Fig. 33.1 Short segment CT scans (after intrathecal myelogram contrast injection) are taken at the C1-C2 interspace to guide the trajectory of the percutaneous radiofrequency ablation needle. The needle should be advanced perpendicularly to the floor, targeted to the anterior half of the spinal cord just anterior to the anterior-posterior plane midline. CT should be obtained after entering the thecal sac (left) and also after entering the pia prior to sensory/motor testing and radiofrequency ablation (right). (From Viswanathan [6]. Reprinted with permission from Elsevier Books)

lesions. Patients will often report feeling warmth. Sensory stimulation can be conducted up to 1 V, but responses are often elicited at much lower voltage (e.g., 0.2 V). Testing for motor contractions is also performed up to 1 V stimulation to indicate a safe distance from the corticospinal tract.

After confirmation of electrode placement in the desired radiological and physiological location, lesioning is performed. Additional anesthesia is not required during lesioning because ablation of the spinothalamic tract is not painful. Our practice is to create two lesions at 80 °C for 60 seconds in order to achieve adequate ablation for cordotomy. Under-lesioning will lead to inadequate or transient pain relief. It is important to test for new hypesthesia between lesions. If the patient does not have decreased pinprick sensation, an additional lesion may be needed. Adequate cordotomy should produce moderate hypalgesia.

Complications

Overall, cordotomy is a very safe procedure. Additional safety is provided by CT guidance. Risks from the insertion of the spinal needle through the cervical dura and pia are very small. In our experience of over 70 cordotomies, we have never had a complication attributable to needle insertion or radiofrequency electrode insertion, even when the pia was penetrated multiple times as necessary to map the spinothalamic tract somatotopy and achieve the optimal electrode location.

However, the radiofrequency ablation can cause complications. Inadequate, excessive, or misplaced lesions are the primary source of complications in cordotomy. Experience and judgment must be used to obtain an optimal balance between aggressive lesioning to achieve durable pain outcome while maintaining safety and avoiding undesired side effects due to excessive or misplaced lesioning. We have moved toward performing two lesions at 80 °C for 60 seconds each, largely because these parameters have provided adequate ablation of the spinothalamic target while minimizing side effects from excessive lesioning. In select cases, we create three lesions at 80 °C for 60 seconds each; however, increasing the number of spinal cord ablations also increases the risk of creating moderate to severe dysesthesia which can be uncomfortable to patients. Bothersome dysesthesias are extremely unlikely to result from two lesions at 70 °C for 60 seconds.

Ipsilateral motor weakness from ablation of the nearby lateral corticospinal tract is a possible, though rare, complication. Using CT guidance to ensure the needle is anterior to the midline of the spinal cord in the anterior-posterior plane helps to prevent this complication. Additionally, if motor stimulation up to 1 V (at 2 Hz and 0.1 msec pulse width) does not elicit motor contractions, a post ablation motor deficit is extremely unlikely. If placing the radiofrequency electrode at the midpoint of the spinal cord is necessary to achieve adequate lesioning of the spinothalamic tract based on sensory stimulation mapping, transient motor weakness may result. In our series of 70 patients, transient ipsilateral lower extremity weakness occurred in 2–6% of cases. The leg weakness was minimal, with patients maintaining at least 4/5 strength and continuing to walk with a walker. The weakness improved uniformly by 3 weeks postoperatively.

In addition to motor weakness, complications of cordotomy include bothersome dysesthesias, seen in 2% of our series. While respiratory complications have traditionally been associated with cordotomy (from ablation of the diaphragmatic reticulospinal tract), we have not seen a case of respiratory complications in the era of CT-guided cordotomy. Similarly, other serious neurological injuries are exceedingly rare using a CT-guided approach.

Data from more than 300 CT-guided cordotomies has been published across multiple series in the literature [1–3]. In Raslan's 2008 series of 41 patients who underwent cordotomy, no patients had new postoperative neurological deficits. Kanpolat's 2009 series of 207 cordotomies reported 5 cases (2.4%) of new transient weakness and 5 cases (2.4%) of temporary ataxia. All weakness and ataxia symptoms resolved by

3 weeks after surgery. Dysesthesias causing significant discomfort to patients occur in approximately 2% of cases. No other major morbidities have been reported in modern series.

Myelotomy

Myelotomy describes a broad range of techniques including interrupting either the anterolateral system commissural fibers [8] or the midline visceral pain pathway fibers, or sometimes both. From here on out, we use the term myelotomy to signify the interruption of the medial dorsal column visceral pain transmission fibers. Midline myelotomy is most useful in patients who have intractable visceral pain, usually from malignancy, localized to the abdominal or pelvic region.

Multiple different surgical techniques can be used to perform myelotomy. Open midline myelotomy [9], percutaneous myelotomy either performed with stereotactic [10, 11] or CT guidance [12], and punctate midline myelotomy [13] are all well described and acceptable methods. Armour introduced the midline commissural myelotomy in 1927 [14], and Hitchcock performed the first stereotactic percutaneous myelotomy in 1968. To perform Hitchcock's stereotactic percutaneous myelotomy, the patient is seated with head held flexed in a stereotactic headframe. A puncture in the midline atlanto-occipital membrane is used to perform a myelogram and visualized the spinal cord. Hitchcock used a spark gap diathermy machine, creating a spinal commissure lesion [10]. After this procedure, Hitchcock remarked on the far greater pain relief seen in his patients compared to what was expected if only lesioning the commissural fibers; his observations support previous hypotheses of alternative spinal pathways for visceral pain.

Our understanding of the midline dorsal column visceral pain pathway has been bolstered by several preclinical studies. Cell bodies in the nucleus proprius and spinal grey matter dorsal to the central canal receive primary afferents from the dorsal visceral pain pathway. The axons then synapse in the nucleus gracilis after ascending ipsilaterally in the midline of the dorsal columns [15–18].

Surgical Techniques

Modernly, myelotomy is performed via three techniques: open punctate myelotomy, percutaneous radiofrequency myelotomy, and percutaneous mechanical myelotomy [19].

Open Limited Myelotomy

Open punctate myelotomy, a technique initially described by Nauta [13, 20] and others [21–23] is performed under general anesthesia with patients positioned prone on the operating table. Surgical level is localized using fluoroscopy, keeping in mind that surgery interrupts the ascending pain pathway. The T3 or T4 level is generally used for upper abdominal pain, and T6 to T8 levels are used for patients with perineal pain. A wide single level thoracic laminectomy is performed allowing for visualization of the bilateral root entry zone. Such a wide laminectomy is not destabilizing in the thoracic spine since this region is stabilized by the ribcage. Bilateral root entry zone visualization is important as it aids in localization of the midpoint of the spinal cord. The dura is opened in the midline and is retracted with sutures. The midline dorsal vein is preserved with mobilization if necessary to view the dorsal median sulcus. The midline pia is then coagulated with bipolar electrocautery, and a 16-gauge angiocatheter is used to create the lesions. Bilateral lesions should be 5 mm deep and extend 0.5 mm from the midline. In order to create lesions to the desired depth, the outer catheter sheath of the angiocatheter assembly should be cut to expose only 5 mm of the tip of the needle (Fig. 33.2). At each location, the angiocatheter is inserted into the pia four times, rotating the needle by 90 degrees between each lesion. After creation of satisfactory lesions, hemostasis is obtained using thrombin-soaked Gelfoam, and the dura is closed with a running suture. Patients can be mobilized safely on the evening of surgery.

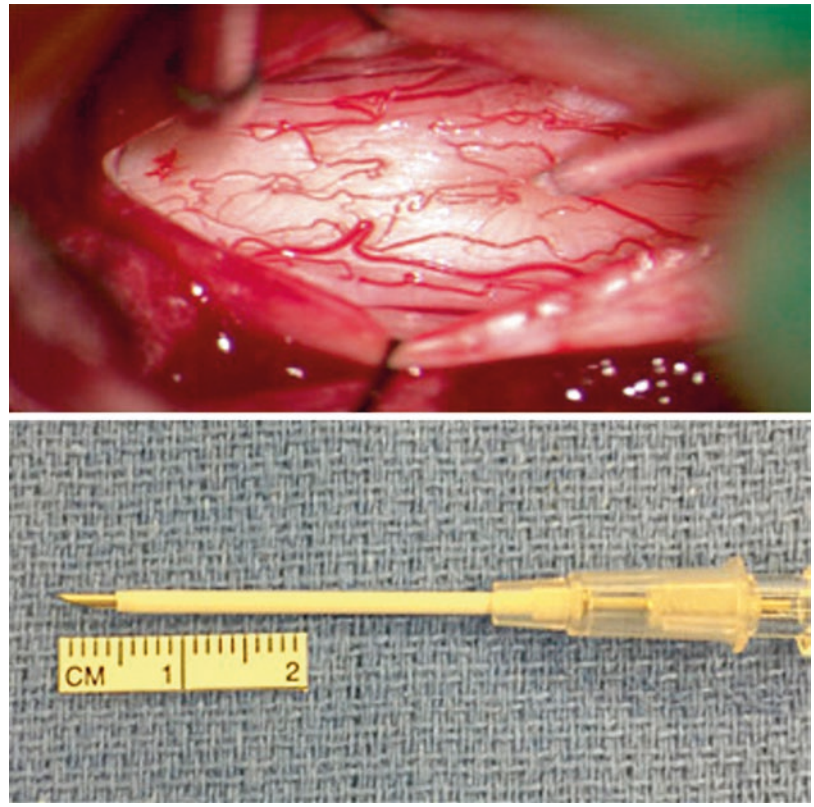

Fig. 33.2 Interoperative image of lesioning in open mechanical myelotomy (top). The midline of the dorsal spinal cord is exposed, and 5 mm deep bilateral lesions are made 0.5 mm from midline with an angiocatheter. The outer sheath of the angiocatheter is trimmed to expose 5 mm of the needle tip to ensure accurate lesion depth (bottom). (From Viswanathan [6]. Reprinted with permission from Elsevier Books)

Percutaneous Radiofrequency Lesioning

Percutaneous radiofrequency lesions can be performed both at the occiput-C1 level and in the thoracic spine. We use a custom 0.46 mm diameter 26G radiofrequency electrode (Boston Scientific, CA), larger than the 0.33 mm cordotomy electrode, given Kanpolat's better reported experiences using a larger diameter radiofrequency electrode for myelotomy [12]. First, the spinal cord is visualized with myelogram, and the patient is positioned prone with head flexed. For occiput-C1 myelotomy, the space between the occiput and C1 is targeted with intraoperative CT guidance. Using a posterior approach, a spinal needle is advanced aiming toward the midline of the spinal cord (Fig. 33.3). After puncturing dura, the needle stylet is removed, and a radiofrequency electrode is introduced into the spinal cord parenchyma. The radiofrequency electrode is targeted toward the antero-posterior midpoint of the spinal cord, and impedance measurements confirm placement of the electrode into the spinal cord parenchyma. Sensory stimulation is used to confirm correct placement, eliciting lower limb paresthesias at an amplitude less than 0.2 V (100 Hz, 100 μs). Two 60-second radiofrequency ablations at 70 °C to 80 °C are performed. Analogously, this same procedure can be performed at an appropriate thoracic level.

Percutaneous Mechanical Lesioning

We perform percutaneous mechanical myelotomy similar to as described by Vilela Filho [24], though we prefer contrast myelogram over air myelography. The patient is positioned prone and a spinal myelogram is performed. Intraoperative CT guidance aids in localization of the correct spinal level. A cerebrospinal fluid tap is performed with a 16-gauge angiocatheter assembly, taking care to maintain a midline trajectory of the needle. Under CT-guidance, the angiocatheter needle is then introduced into the spinal cord parenchyma. One penetration of the posterior

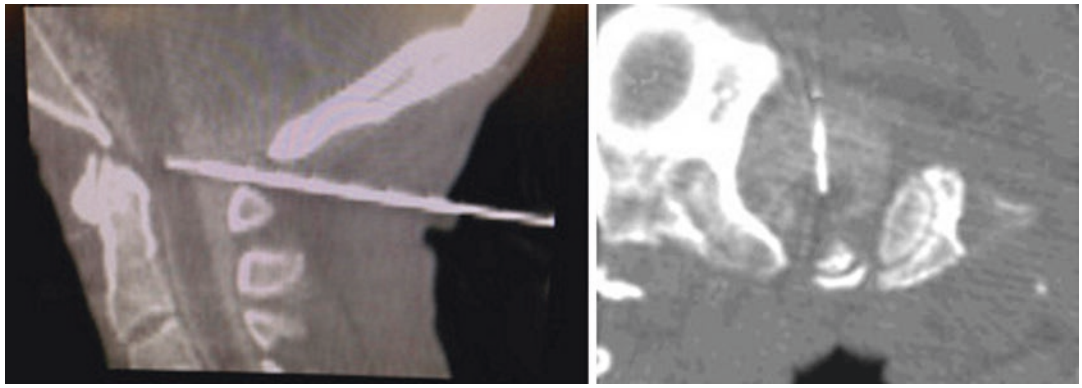

Fig. 33.3 Sagittal interoperative CT of posterior approach occiput-C1 percutaneous radiofrequency myelotomy. Note the trajectory and depth of the spinal needle and radiofrequency electrode (left). The midline trajectory is strictly maintained, with guidance provided by axial CT (right). (From Viswanathan [6]. Reprinted with permission from Elsevier Books)

midline spinal cord to 5 mm depth is performed and confirmed by CT.

Complications

Open myelotomy is safe, with motor complications being extremely rare. Motor and sensory monitoring can be a useful adjunct to prevent complication; however, the main precaution remains to take caution and remain in the midline of the spinal cord. Image guidance percutaneous techniques have a similarly low rate of motor complications, largely thanks to the distance of the corticospinal tract from the midline of the spinal cord.

Transient dorsal column dysfunction can occur given that lesions are created between the dorsal columns. Such symptoms present tingling, coolness, or as decreased proprioception. While noticeable, these symptoms are generally well tolerated by patients and eventually resolve without intervention.

Cingulotomy

Cingulotomy is the creation of lesions where the cingulum white matter bundle passes the grey matter of the anterior cingulate gyrus. The development and use of anterior cingulotomy for pain was derived from anterior cingulectomy procedures, originally used in the mid twentieth century as an alternative to frontal lobotomy. The cingulotomy procedure arose as less invasive procedures were developed in the 1940s and 1950s with advances in stereotaxy, which Ballantine applied in the 1960s to create cingulate lesions at the Massachusetts General Hospital [25]. This enabled cingulotomy to yield beneficial outcomes in psychiatric patients without creating significant adverse effects seen with cingulectomy or lobectomy. Early patients undergoing cingulotomy over the next several decades had decreased dependency on pain medications after surgery. The first series reporting cingulotomy for the treatment of refractory chronic pain was by Foltz and White in 1968 [26], and since then numerous case series have illustrated the efficacy of anterior cingulotomy in alleviating pharmacologically intractable severe chronic pain.

The rising popularity of neuromodulation alternatives, including spinal cord stimulators and implanted chronic pain pumps, has led to decreasing use of anterior cingulotomy in recent decades. Modern practices generally reserve cingulotomy as second or third line surgical treatment after failure of non-lesional interventions [27]. Cingulotomy may be considered as first line surgical intervention in some scenarios. Patients too cachectic or nutritionally depleted to tolerate foreign body implantation, patients with end-stage malignancy with very short life expectancy,

and patients who do not want a foreign body implantation or for whom device management is too burdensome may benefit from anterior cingulotomy prior to consideration of neuromodulation. Patients with a large affective component of chronic pain may also benefit from consideration of anterior cingulotomy prior to neuromodulation, as cingulotomy has greater effect on reducing psychological and affective components of chronic pain.

The etiology of intractable chronic pain is diverse. Chronic pain is commonly stratified as cancer-related (e.g., treatment-related neuropathic pain or tumor infiltration) or non-cancer-related (e.g., chronic lower back pain, diabetic neuropathy, post-traumatic neuropathic pain, atypical facial pain, phantom pain). The broad spectrum of etiologies results in diverse presentations of patients being evaluated for surgical intervention. Chronic pain refractory to previous treatment, particularly if contraindicated for a neuromodulation procedure or with a psychologic component to the pain, should be considered for anterior cingulotomy [28].

Decision Making

The anterior cingulate cortex plays an important role in the affective dimension of pain, defined as the psychological unpleasantness associated with a painful sensation. Modulation of the response to pain in the anterior cingulate with lesioning seems to provide relief by altering the perception of pain [29]. This occurs through long-term potentiation of anterior cingulate excitatory synapses in response to painful stimulus. The potentiation can even continue despite the absence of continued input from the peripheral nervous system. In this way the anterior cingulate cortex is intimately tied to generation and perception of chronic pain.

Surgical Technique

Radiofrequency ablation (RFA) and laser interstitial thermal therapy (LITT) are the most commonly used modern techniques for surgical ablation of the anterior cingulate cortex. RFA, a well-established technique for lesioning the central nervous system, is a fast and inexpensive technique that can be performed with the patient awake allowing the surgeon to monitor the patient for potential complications prior to creating permanent lesions. LITT is a newer, more expensive technique but allows surgeons to monitor the size and location of the lesions in near real time with MR thermometry. LITT must be performed under general anesthesia in an MRI machine.

For both RFA and LITT, the anterior cingulate lesion is planned and localized using an anatomic thin cut stereotactic magnetic resonance image (MRI) scan obtained prior to surgery. The anterior cingulate is located just adjacent to the midline sagittal plane of the brain, partially circumscribing the corpus callosum.

The specific approach to targeting varies by surgeon preference, generally based on anatomy as opposed to a standardized coordinate system. General targets are centered in a coronal plane 20 mm posterior to the tip of the frontal horn of the lateral ventricle, 10 mm lateral from midline, and 1–2 mm above the roof of the lateral ventricle. The exact target is adjusted based on the preoperative imaging. There is some debated about the best anterior-posterior target, varying in the literature from 17.5 to 37.5 mm posterior to the anterior tip of the frontal horn of the lateral ventricle. Sharim and Pouratian showed with a meta-analysis that more anterior lesions, closer to 17.5 mm posterior to the anterior border of the lateral ventricles, led to better outcomes compared to more posterior lesion placement [30]. Improved outcomes with more anteriorly placed lesions were also shown by Steele and colleagues in another series of patients with intractable depression treated by cingulotomy [31]. For both RFA and LITT, after completion of the first lesion, a second lesion can be created along the same trajectory by withdrawing the lesioning device by 10 mm and creating a second lesion.

To perform RFA ablation, skin incision and bilateral burr holes are placed based on the planned stereotactic trajectories. Dura is opened just prior to placing the RFA probe, and care taken to minimize CSF loss. Excessive CSF loss

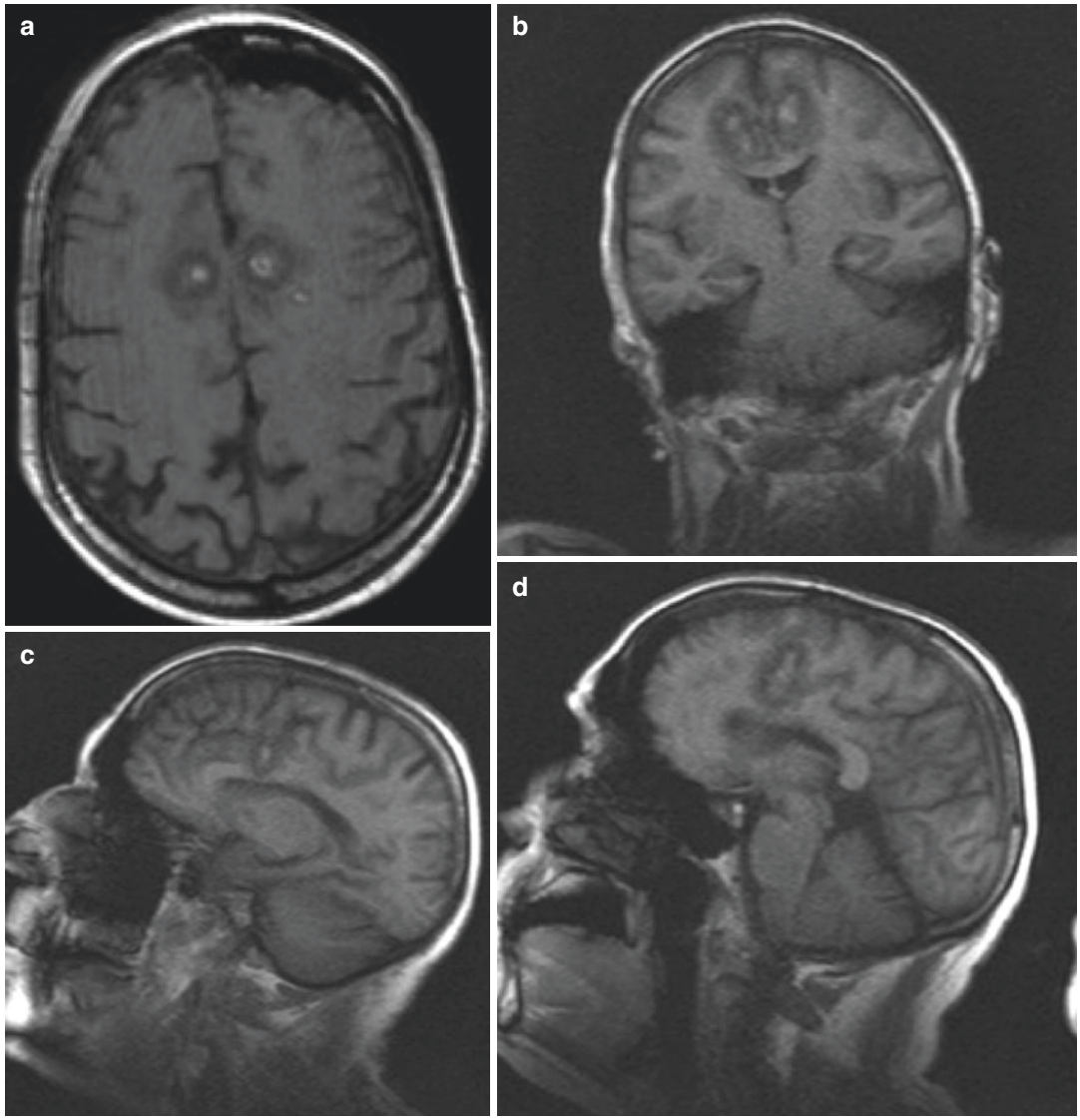

Fig. 33.4 Postoperative MRI showing location of radiofrequency cingulotomy for medically refractory pain. (**a**) axial, (**b**) coronal, (**c**) parasagittal, and sagittal (**d**). (From Viswanathan et al. [27]. Reprinted with permission from the Journal of Neurosurgery)

can lead to brain shift and loss of stereotactic accuracy. Sulci and superficial vascular structures are avoided to minimize the chance of perioperative intracranial hemorrhage. A RF probe with 10 mm exposed tip is used for lesioning. After placing the probe to target, it is heated to 80 °C for 90 seconds. A second more dorsal lesion is created along the same trajectory by withdrawing the RFA probe by 10 mm and reheating just as for the first lesion. A postoperative MRI can be obtained to confirm lesion location and size (Fig. 33.4).

LITT has more recently been used to perform anterior cingulotomy and has the advantage of near real-time MR thermography monitoring of the lesion size. As reported by Patel and colleagues [32], the laser cannula/fiber assembly is first placed to target using standard percutaneous stereotactic techniques. A skull-mounted anchor bolt is used to secure the cannula/fiber assembly.

The patient, still under general anesthesia, is then taken to the MRI scanner. MRI thermography measures the temperature surrounding the laser tip every 2–8 seconds within the chosen field of view. Estimates of irreversible and reversible thermal damage are calculated over the course of the ablation to provide estimates of the total size of the lesion. A gadolinium post-contrast T1 MRI is performed after completion of the ablation to document the extent of the lesion and screen for any associated intracranial hemorrhage.

Post-ablation, patients are monitored overnight in an inpatient unit and discharged on postoperative day 1. A steroid taper over 1–2 weeks is prudent to prevent extensive edema around the lesions.

Complications

The most common side effects include nausea, headache, vomiting, and confusion. If present, these usually resolve within days after surgery and can often be temporized by a steroid taper and mild analgesics. Urinary incontinence and gait difficulty is more rare but also generally resolves over time, thought to be secondary to peri-ablation edema involving the adjacent micturition and lower extremity motor areas adjacent to the cingulate. Seizures and intracranial hemorrhage are less common, occurring in <5% of cases. Personality changes (e.g., flat affect), new psychiatric symptoms (e.g., paranoid ideations), and executive function impairment (e.g., attention, visual-processing, or simple motor skill) are also documented but rare. These symptoms generally resolve by 12 months after ablation. Rare but permanent cognitive side effects, including difficulty with spontaneous word production, objection construction, and focused attention, have been documented.

Outcomes

Sharim and Pouratian reviewed 224 surgical cases across 11 studies of patients undergoing anterior cingulotomy for intractable chronic pain. These studies included both cases involving cancer-related pain in addition to non-cancer-related pain [30]. In total, 67% (n = 149) reported significant pain relief in the immediate postoperative period. Interestingly, populations of patients with cancer-related and non-cancer-related pain did not show significantly different responses. Sustained pain relief at 12 months after surgery was achieved in 65% (n = 53 of 82) of patients; however, the majority of the cancer-related pain cohort was not included in this follow-up secondary to disease-related death (cancer n = 6 of 9; non-cancer n = 47 of 73 sustained relief). Ten patients underwent reoperations, for which 8 achieved significant or improved pain relief compared to the initial ablation. Four of 6 (67%) of these patients with follow-up past 1 month maintained significant pain relief.

A second meta-analysis by Agarwal and colleagues showed pain improvement of 50–100% on pain assessment scales across 41 patients [33]. Again, these outcomes were comparable between cancer-related and non-cancer-related cohorts.

While its use has decreased in the past decade with the rising popularity of neuromodulation, anterior cingulotomy remains a safe and effective surgery for the treatment of treatment-resistant chronic pain. Anterior cingulotomy remains a viable option for patient's refractory to neuromodulation, as well as in populations for which device-based therapies are not appropriate. In particular, anterior cingulotomy should be considered in patients with a significant affective component to their pain. The psychological side of pain is difficult to address with current neuromodulation approaches and may be more effectively treated with anterior cingulotomy.

Conclusion

Both intracranial and spinal ablative techniques are useful for the management of medically intractable pain. Though consideration should be given to non-lesional approaches, ablation can provide an immediate benefit with no ongoing device management. Advances in imaging have made these techniques more precise and safer. As

the level of evidence increases for these techniques, broader adoption of these techniques will be facilitated.

References

1. Raslan AM. Percutaneous computed tomography-guided radiofrequency ablation of upper spinal cord pain pathways for cancer-related pain. Neurosurgery. 2008;62(3 Suppl 1):226–33; discussion 233-4.
2. Kanpolat Y, Ugur HC, Ayten M, Elhan AH. Computed tomography-guided percutaneous cordotomy for intractable pain in malignancy. Oper Neurosurg. 2009;64(3 Suppl):ons187–94.
3. Viswanathan A, Vedantam A, Hess KR, Ochoa J, Dougherty PM, Reddy AS, et al. Minimally invasive cordotomy for refractory cancer pain: a randomized controlled trial. Oncologist. 2019;24(7):):e590–6. https://doi.org/10.1634/theoncologist.2018-0570.
4. Krieger AJ, Rosomoff HL. Sleep-induced apnea. 1. A respiratory and autonomic dysfunction syndrome following bilateral percutaneous cervical cordotomy. J Neurosurg. 1974;40(2):168–80.
5. Nannapaneni R, Behari S, Todd NV, Mendelow AD. Retracing "Ondine's curse". Neurosurgery. 2005;57(2):354–63.
6. Viswanathan A. Spinal ablation for cancer pain (cordotomy and myelotomy). In: Burchiel KJ, Raslan AM, editors. Functional neurosurgery and neuromodulation. St. Louis: Elsevier; 2019. p. 63–8.
7. Fonoff ET, de Oliveira YSA, Lopez WOC, Alho EJL, Lara NA, Teixeira MJ. Endoscopic-guided percutaneous radiofrequency cordotomy. J Neurosurg. 2010;113(3):524–7.
8. Šourek K. Commissural myelotomy. J Neurosurg. 1969;31(5):524–7.
9. Gildenberg PL, Hirshberg RM. Limited myelotomy for the treatment of intractable cancer pain. J Neurol Neurosurg Psychiatry. 1984;47(1):94–6.
10. Hitchcock E. Stereotactic cervical myelotomy. J Neurol Neurosurg Psychiatry. 1970;33(2):224–30.
11. Schvarcz JR. Stereotactic extralemniscal myelotomy. J Neurol Neurosurg Psychiatry. 1976;39(1):53–7.
12. Kanpolat Y, Savas A, Caglar S, Akyar S. Computerized tomography-guided percutaneous extralemniscal myelotomy. Neurosurg Focus. 1997;2(1):e5.
13. Nauta HJ, Soukup VM, Fabian RH, Lin JT, Grady JJ, Williams CG, et al. Punctate midline myelotomy for the relief of visceral cancer pain. J Neurosurg. 2000;92(2 Suppl):125–30.
14. Armour D. Lettsomian lecture on the surgery of the spinal cord and its membranes. Lancet. 1927;209(5405):691–8.
15. Brogan SE, Sindt J, Viswanathan A. Interventional pain therapies. In: Ballantyne JC, Fishman Scott M, Rathmell JP, editors. Bonica's management of pain. 5th ed. Philadelphia: Wolters Kluwer Health; 2019.
16. Al-Chaer ED, Lawand NB, Westlund KN, Willis WD. Pelvic visceral input into the nucleus gracilis is largely mediated by the postsynaptic dorsal column pathway. J Neurophysiol. 1996;76(4):2675–90.
17. Wang Y, Wu J, Lin Q, Nauta H, Yue Y, Fang L. Effects of general anesthetics on visceral pain transmission in the spinal cord. Mol Pain. 2008;4:50.
18. Willis WD, Al-Chaer ED, Quast MJ, Westlund KN. A visceral pain pathway in the dorsal column of the spinal cord. Proc Natl Acad Sci. 1999;96(14):7675–9.
19. Vedantam A, Koyyalagunta D, Bruel BM, Dougherty PM, Viswanathan A. Limited midline myelotomy for intractable visceral pain: surgical techniques and outcomes. Neurosurgery. 2018;83(4):783–9.
20. Nauta HJW, Hewitt E, Westlund KN, Willis WD. Surgical interruption of a midline dorsal column visceral pain pathway. J Neurosurg. 1997;86(3):538–42.
21. Hong D, Andrén-Sandberg A. Punctate midline myelotomy: a minimally invasive procedure for the treatment of pain in inextirpable abdominal and pelvic cancer. J Pain Symptom Manag. 2007;33(1):99–109.
22. Hwang S-L, Lin C-L, Lieu A-S, Kuo T-H, Yu K-L, Ou-Yang F, et al. Punctate midline myelotomy for intractable visceral pain caused by hepatobiliary or pancreatic cancer. J Pain Symptom Manag. 2004;27(1):79–84.
23. Kim YS, Kwon SJ. High thoracic midline dorsal column myelotomy for severe visceral pain due to advanced stomach cancer. Neurosurgery. 2000;46(1):85–90; discussion 90-2.
24. Vilela Filho O, Araujo MR, Florencio RS, Silva MA, Silveira MT. CT-guided percutaneous punctate midline myelotomy for the treatment of intractable visceral pain: a technical note. Stereotact Funct Neurosurg. 2001;77(1–4):177–82.
25. Ballantine HT, Cassidy WL, Flanagan NB, Marino R. Stereotaxic anterior cingulotomy for neuropsychiatric illness and intractable pain. J Neurosurg. 1967;26(5):488–95.
26. Foltz EL, White LE. The role of rostral cingulumotomy in "pain" relief. Int J Neurol. 1968;6(3–4):353–73.
27. Viswanathan A, Harsh V, Pereira EAC, Aziz TZ. Cingulotomy for medically refractory cancer pain. Neurosurg Focus. 2013;35(3):E1.
28. Hunt PJ, Karas PJ, Viswanathan A, Sheth SA. Cingulotomy for intractable pain. In: Sagher O, Levin E, Pilitsis J, editors. Pain neurosurgery (neurosurgery by example). New York: Oxford University Press; 2019.
29. Wang G-C, Harnod T, Chiu T-L, Chen K-P. Effect of an anterior Cingulotomy on pain, cognition, and sensory pathways. World Neurosurg. 2017;102:593–7.
30. Sharim J, Pouratian N. Anterior cingulotomy for the treatment of chronic intractable pain: a systematic review. Pain Physician. 2016;19(8):537–50.
31. Steele JD, Christmas D, Eljamel MS, Matthews K. Anterior cingulotomy for major depression: clinical outcome and relationship to lesion characteristics. Biol Psychiatry. 2008;63(7):670–7.

32. Patel NV, Agarwal N, Mammis A, Danish SF. Frameless stereotactic magnetic resonance imaging-guided laser interstitial thermal therapy to perform bilateral anterior cingulotomy for intractable pain: feasibility, technical aspects, and initial experience in 3 patients. Oper Neurosurg (Hagerstown, Md). 2015;11(Suppl 2): 17–25; discussion 25.
33. Agarwal N, Choi PA, Shin SS, Hansberry DR, Mammis A. Anterior cingulotomy for intractable pain. Interdiscip Neurosurg. 2016;6:80–3.

Cluster Headache: Deep Brain Stimulation

34

Harith Akram and Ludvic Zrinzo

Introduction

Cluster headache (CH) is a facial pain disorder that falls under the umbrella of trigeminal autonomic cephalalgias (TACs). The International Classification of Headache Disorders-III (ICHD-III) describes CH attacks as "severe, strictly unilateral pain which is orbital, supraorbital, temporal or in any combination of these sites, lasting 15–180 minutes and occurring from once every other day to eight times a day. The pain is associated with ipsilateral conjunctival injection; lacrimation; nasal congestion; rhinorrhoea; forehead and facial sweating; miosis, ptosis and/or eyelid oedema; and/or restlessness or agitation" [1]. Although the attacks are described as "strictly unilateral", it is not uncommon for these attacks to switch sides [2, 3]. CH is often considered as "the worst pain known to man". The pain severity has been described as a "hot red poker piercing the eye" and as being "worse than giving birth" in those who have experienced both kinds of pain. CH has also been referred to as "suicide headache" due to the high risk of suicide associated with it [2, 4]. When CH attacks occur for more than 1 year without a remission, or with remissions lasting less than 3 months, it is defined as chronic cluster headache (CCH). Around 10–15% of sufferers have CCH as opposed to the episodic variety [5].

Diagnostic Criteria of Cluster Headache [1]

A. At least five attacks fulfilling criteria B–D
B. Severe or very severe unilateral orbital, supraorbital and/or temporal pain lasting 15–180 minutes (when untreated)
C. Either or both of the following:
   1. At least one of the following symptoms or signs, ipsilateral to the headache:
      - Conjunctival injection and/or lacrimation
      - Nasal congestion and/or rhinorrhoea
      - Eyelid oedema
      - Forehead and facial sweating
      - Miosis and/or ptosis
   2. Sense of restlessness or agitation
D. Occurring with a frequency between one every other day and eight per day
E. Not better accounted for by another ICHD-III diagnosis

CH has a prevalence of 0.2%, usually affecting young adults with a clear male predominance [6–8]. The majority of sufferers respond to standard medical therapy with acute treatments to

H. Akram (✉) · L. Zrinzo
Unit of Functional Neurosurgery, UCL Queen Square Institute of Neurology and the National Hospital for Neurology and Neurosurgery, London, UK
e-mail: harith.akram@ucl.ac.uk

N. Pouratian, S. A. Sheth (eds.), *Stereotactic and Functional Neurosurgery*,
https://doi.org/10.1007/978-3-030-34906-6_34

treat attacks and prophylactic treatments to prevent attacks or reduce their frequency and severity. Evidence-based acute treatments are high-flow oxygen (100% at 7–15 L/min), subcutaneous sumatriptan injections and nasal triptans. Prophylactic treatments include verapamil, lithium, methysergide, topiramate, gabapentin, melatonin and valproate [9].

Other TACs consist of paroxysmal hemicrania (PH), short-lasting unilateral neuralgiform headache attacks, short-lasting unilateral neuralgiform headache attacks with conjunctival injection and tearing (SUNCT), short-lasting unilateral neuralgiform headache attacks with cranial autonomic symptoms (SUNA) and hemicrania continua (HC) [1].

Pathophysiology of Cluster Headache

The underlying pathophysiology in cluster headache (CH) is not fully understood [10–17]. Attacks often involve a nociceptive (facial pain in the trigeminal nerve's ophthalmic distribution) and a parasympathetic component (tearing, redness, nasal discharge, etc.).

Though the exact trigger site in the brain for CH attacks is not clear, the hypothalamus has been implicated in the disease process [18–22], and pathological activation of the trigeminoparasympathetic brainstem reflex is thought to be responsible for simultaneous activation of trigeminal nerve and craniofacial parasympathetic nerve fibres, respectively, leading to the characteristic ipsilateral cranial pain and autonomic features [15, 23]. The periodicity of individual attacks, the relapsing-remitting course and the seasonal recurrence of headache bouts are all suggestive of possible hypothalamic role in CH [2, 15]. This has been supported by neuroendocrinological studies [18, 19] as well as neuroimaging studies [20, 21]. Occasionally, cranial sympathetic dysfunction can occur as a secondary event caused by parasympathetically mediated internal carotid artery dilatation in the cavernous sinus.

Neuromodulation in the Treatment of Cluster Headache

Although the majority of patients respond to medical treatments, a small but significant number prove intractable to medical therapies. For these patients, neuromodulation, whether peripheral, central or both, may present a last resort treatment option. Peripheral neuromodulation is less invasive than central neuromodulation and should be considered first. This is delivered either through chronic stimulation of the greater occipital nerves (bilaterally) using two subcutaneous electrodes connected to an implantable pulse generator (IPG) [24] or through intermittent sphenopalatine ganglion (SPG) stimulation using a submucosal, oral implant with electrodes in the sphenopalatine fossa [25, 26]. Occipital nerve stimulation (ONS) and SPG stimulation for CH are thought to work by activating the trigeminocervical complex (TCC) [27, 28]. Central neuromodulation may be carried out in select patients where peripheral neuromodulation has failed or is not available. This treatment is more invasive and is delivered through ipsilateral (or bilateral) chronic, high-frequency deep brain stimulation (DBS) in the ventral tegmental area (VTA). This target has also been described as "the posterior hypothalamic region" although, strictly speaking, anatomically it lies behind the posterior border of the hypothalamus proper in the midbrain tegmentum [29].

Rationale for Ventral Tegmental Area (VTA) DBS in the Treatment of Cluster Headache

In 1998, a positron emission tomography (PET) study during acute cluster attacks reported increased activation in the posterior hypothalamic region ipsilateral to the headache attacks (although we now know that the maximal activation was centred over the ventral tegmental area as previously highlighted). Subsequent neuroimaging studies also pointed to increased activity and neuronal density in the same region [20–22,

29, 30]. The finding led to the first deep brain stimulation procedure using this target in 2001 with attacks disappearing within 48 hours of starting stimulation [30].The first series of patients with CH treated with DBS in 5 patients was later reported in 2003, and subsequently a cohort of DBS in 19 patients was reported in 2013 [31, 32]. Incidentally, the brain region used for DBS had been previously described as a surgical target by Sano et al. for stereotactic lesions in 51 patients with pathologically aggressive behaviour [33]. A similar target has also been used in DBS trials for the treatment of depression [34]. To date, different centres have published data on over 120 patients with DBS for medically intractable CCH with varying response rate but an overall good efficacy and safety record with the exception of one fatal intracerebral haemorrhage during a microelectrode-guided procedure [3, 31–33, 36–42].

A randomized controlled trial of DBS in chronic cluster headache was carried out by Fontaine et al. in 2009. Eleven patients received either stimulation or placebo "sham stimulation" following surgery for 1 month only with a crossover design separated by a 1-week washout period. No significant difference between placebo and therapy effects was seen. Nonetheless, the open-label 10-month extension (reported in the same paper) showed a clear and significant improvement with 6 out of the 11 patients responding to the chronic stimulation leading to a reduction of >50% in the weekly frequency of attacks. In fact, 3 out of the 11 patients receiving DBS were pain-free at the end of follow-up [35]. This is not surprising as most prospective, open-label studies have shown that longer periods of stimulation are required before a significant improvement is achieved; moreover, in the case of a long-lasting implantation "stun" effect, sham stimulation is likely to show a degree of improvement from baseline thus making the comparison meaningless [3].

Chronic, high-frequency deep brain stimulation (DBS) in the VTA has been shown to be a safe and effective treatment modality for patients with refractory chronic cluster headache (CCH) in several prospective studies [3, 30, 31, 36–40]. Leads are implanted ipsilateral to the cluster headache symptoms, and bilateral lead implantation is recommended in patients with side-alternating cluster headache.

Patient Selection, Surgical Procedure and DBS Programming

A multi-disciplinary approach to selecting suitable patients for surgery is essential. Patients who fulfil the ICHD-III diagnostic criteria for CCH and who have been experiencing highly disabling, medically refractory symptoms for at least 2 years and who have no contraindications to stereotactic surgery are considered suitable. In our practice, patients are classified as medically intractable if they fail adequate trials of at least five of the following seven drugs: verapamil, lithium, methysergide, topiramate, melatonin, gabapentin and valproate. A failed trial is defined as an unsatisfactory response, side effects, intolerance or contraindication to the use of the agent [41].Patients should be considered for ONS and SPG stimulation prior to DBS. Neuropsychological evaluations and MRI brain scans are performed to rule out cognitive impairment, brain lesions or significant brain atrophy prior to the MDT assessment.

An MRI-guided and MRI-verified approach, without microelectrode recording, is recommended for lead implantation [3, 42, 43]. A fatality linked to the use of microelectrode recording in DBS for CH has been previously reported [36]. Surgery can be safely carried out asleep under general anaesthesia [3]. In awake patients, however, intraoperative testing with macrostimulation can elicit transient tachycardia, raised blood pressure, vertical diplopia and a feeling of "panic" or "impending doom" with higher voltages. These effects tend to be reproducible across patients. The anatomical target is in the ipsilateral ventral tegmental area. In patients with a history of bilateral attacks (side-switching), bilateral surgery is advised. In our practice, the location for the deepest contact is defined on a T2-weighted

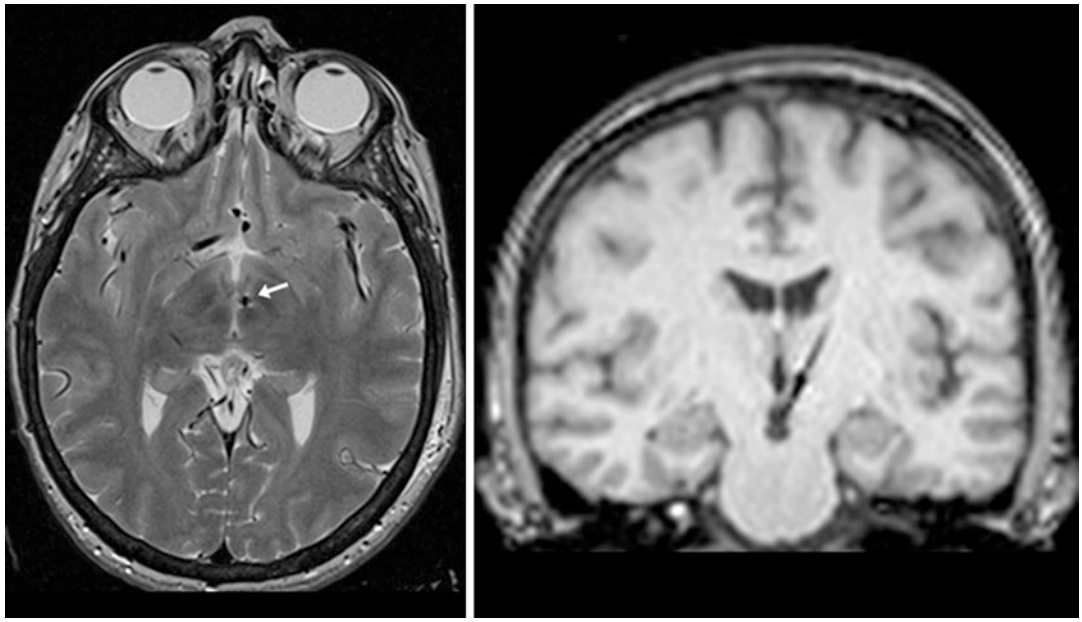

Fig. 34.1 DBS lead location in the left VTA on axial (left) and coronal (right) MRI slices. (From Akram et al. [3]. Reprinted with permission from Wolters Kluwer Health, Inc)

stereotactic MR image at an axial level immediately above the mammillary bodies, anteromedial to the hypointense red nucleus and posterolateral to the hypointense mammillothalamic tract. Immediately after lead implant, lead location is verified with a stereotactic MRI scan (Fig. 34.1) in patients without ONS. Stereotactic CT scan can also be performed in patients to confirm lead location. The lead is then connected to a single- or dual-channel implantable pulse generator (IPG) implanted in the infra-clavicular region on the same day of lead implantation or at a later date, as a staged procedure.

It is not uncommon for some patients to experience an implantation "stun effect" postoperatively. This can be sustained for several weeks during which attacks improve without any stimulation. DBS programming is conducted to define optimal stimulation parameters once the stun effect has resolved, or otherwise a week or two after surgery to allow for the oedema around the leads to settle in patients with no stun effect. No strong evidence exists for the optimal stimulation frequency and pulse width. Early reports described using a frequency of 180 Hz and a pulse width of 60 μs [30, 31]. Voltage is adjusted according to self-limiting side effects (diplopia, vertigo, oscillopsia and ophthalmoplegia) in single or multiple steps, depending on the patient.

Measuring the Burden of Headache and the Response to Treatment

The "objective" measurement of chronic pain remains a challenge in clinical practice. Patient-reported scores are often used but, as CH is episodic, attacks can be measured in terms of severity, frequency and duration. Traditionally, change in headache severity and/ or frequency but not attack duration has been used to describe the response to treatment. This may not represent the real response that patients subjectively experience. An alternative, more meaningful measure of symptom severity can be applied using the headache load (HAL) measure. This is calculated from the sum total of the product of attack severity (on a verbal rating scale) multiplied by attack duration (i.e. $\sum$ [severity on the verbal rating scale] × [duration in hours]) for each cluster attack occurring over a 2-week period [3]. Though the International Headache Society

guidelines for cluster headache clinical trials advocate a reduction of 50% in headache frequency as a marker for treatment response [44], it is our experience that patients who achieve a significant improvement in only one of the variables can be extremely satisfied with the therapy provided. For example, a patient with six attacks of 1-hour duration per day with severity of 8/10 who, after DBS, then experiences five attacks of 1-hour per day with a 2/10 severity will not be a responder in terms of headache frequency but is certainly a responder in terms of headache load and overall disease burden. We therefore consider patients to be responders after sustaining a reduction in HAL of ≥30%. This threshold is deemed meaningful in line with the Initiative on Methods, Measurement, and Pain Assessment in Clinical Trials (IMMPACT) guidelines and is in keeping with similar thresholds for response to drug trials [45]. Other outcome measures that can be useful in determining a response to treatment are the reduction in medications and disability, mood and quality of life scales as well as patient-reported percentage of improvement [3].

Reported Improvement Following DBS

In one of the largest, open-label prospective studies, MRI-guided and MRI-verified DBS of the ventral tegmental area in 21 patients (follow-up range 1–5 years) was shown to be a safe and effective procedure in patients with chronic cluster headache whose symptoms were refractory to other treatments. Symptomatic improvement was sustained over time and was accompanied by significant improvements in a number of quality of life scales [3].

At the final follow-up point, there was a 50% overall improvement in the median headache frequency and a 30% improvement in the median headache severity. The HAL improved by 79% from baseline at the 1-year follow-up point and by 68% at the final follow-up point. DBS appeared to have a greater beneficial effect on headache attack frequency than on attack severity, although both attributes improved. The percentage of patients who had at least 30% reduction in median frequency and median severity of attacks at the final follow-up point was 62% and 43%, respectively. The percentage of patients who had at least 30% reduction in headache load was 81% at the final follow-up point. The monthly triptan intake of the group as a whole also dropped by 57%. Using current UK costing estimates [46], this was calculated to be a saving of £8291.15 a month for the 21 patients or around £395 a month per patient on triptans alone.

In this study, a number of quality of life, disability and mood outcome measures improved significantly from baseline (the Migraine Disability Assessment Score [MIDAS] [47], the Headache Impact Test-6 [HIT-6] [47], Summary Measures of the Physical Scale [SF36-PCS] and EuroQol [EQ-5D]). The largest improvement was seen in MIDAS (median 79%) at 12 months and in the SF36-PCS (median 13%) at 6 months (Fig. 34.2).

Over the whole cohort, four patients (19%) did not show any response to DBS. This lack of response in some patients has also been reported in other studies in spite of well-positioned DBS electrodes [48]. This might suggest a yet unidentified pathological process that renders these patients refractory to DBS. Further work into structural and functional connectivity of this patient group may reveal underlying differences between responders and non-responders, improving patient selection and outcome of DBS in cluster headache [3].

Endoventricular DBS of the Third Ventricle for the Treatment of Chronic CH

In a proof of concept, seven patients were implanted with a single DBS lead laid on the floor of the posterior third ventricle. All patients had medically intractable chronic CH. One patient had bilateral attacks. Targeting utilized preoperative MRI merged with stereotactic, intraoperative contrast ventriculography. The target coordinates were 0 for the "x", 6 mm behind the mid-commissural point for the "y" and 1–3 mm

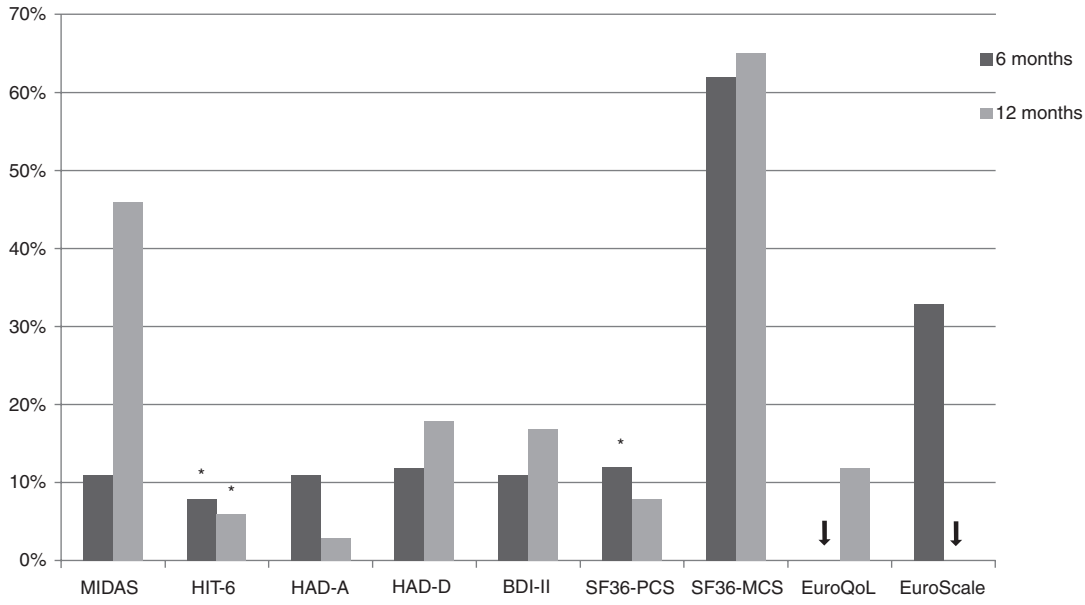

Fig. 34.2 Improvement in quality of life, disability and mood. ∗: *p value ≤ 0.05. P values are Bonferroni corrected; they represent individual tests at each time point relative to baseline (number of comparisons = 2 for tests at 6 and 12 months).* Median percentage of improvement in quality of life (SF36, EuroQol), disability (MIDAS, HIT6) and mood (HADS-A, HADS-D). MIDAS Migraine Disability Assessment Score, HIT6 Headache Impact-6, HADS-A, HADS-D Hospital Anxiety and Depression Scale, BDI-II Beck Depression Inventory II, SF36-PCS Short Form 36 Physical Component Summary, SF36-MCS Short Form 36 Mental Component Summary. (From Akram et al. [3]. Reprinted with permission from Wolters Kluwer Health, Inc)

below the commissural plane for the "z" coordinate, according to the depth of the third ventricular floor [49].

The surgical procedure involves frame-based stereotactic insertion of a guide tube, using a robotic arm, into the lateral ventricle. The DBS lead is then advanced along the trajectory towards the entry of the foramen of Monro. Once in the third ventricle, the stylet is removed, bent and reintroduced under fluoroscopic control, in order to place the electrode on the medial part of the floor of the posterior third ventricle. The location is then verified using postoperative CT and 1.5 T MRI scan. In this study, the stimulation amplitude ranged from 0.9 to 2.3 V. Some patients had monopolar whilst others had bipolar stimulation modes [49]. Improvement in the frequency of attacks emerged within 3 months of stimulation. At the 12-month follow-up point, three patients were in complete remission, two had 90% improvement and one had 75% improvement. One out of seven patients did not show significant improvement. Interestingly, most patients showed an improvement in the hospital-acquired depression scores (HAD-D) but not the anxiety scores (HAD-A). This was attributed to possible stimulation spread to the medial forebrain bundle, a structure currently being investigated in the treatment of depression [50]. One patient needed to have the lead repositioned 3 months after surgery due to lead migration. All patients reported stimulation-related "trembling vision" with conjugated, rapid, circular movement of the eyes. This seems to settle with stimulation parameters adjustment. All patients also reported hemifacial autonomic attacks described as warm sensations with tearing ipsilateral to the site of the CH. Two patients experienced significant weight change (−14 kg and +5 kg) explained by change in exercise levels for the first and improvement in mood and appetite for the second patient. One patient experienced "a sensation of well-being during the first trial of stimulation, mainly at 60 Hz, with a pleasant feeling of pressure to sleep" [49].

In general, endoventricular DBS for chronic cluster headache appears to be feasible and to have a good efficacy and safety profile. Having said that, this remains a small pilot study and more data are required to support this approach which provides an alternative means of delivering stimulation to the posterior hypothalamic region/ventral tegmental area [49].

Optimal VTA-DBS Target and CH Network

The exact mode of action of DBS for CH and the neural networks involved remain poorly understood. Furthermore, the optimal stimulation site is yet to be identified [29–32, 36–38, 48]. Activation of the trigeminal nerve and ganglion has been demonstrated with hypothalamic stimulation [51], possibly mediated by the trigeminohypothalamic tract (THT) described in human and non-human studies [52–54].

The first patient [30] and patient series [31] to undergo DBS for CCH had the target in what was termed the hypothalamic grey. The target in this area, which is referred to here as the VTA, is not readily demarcated. This is due to three factors; firstly, the target has to be identified using surrounding landmarks on MRI (e.g. the red nucleus, the mammillothalamic tract); secondly, the stimulation amplitude (reaching ups of 4 Amp) covers a comparatively large brain tissue area around the active DBS contact, hence allowing some leeway in targeting accuracy; and thirdly, PET studies are subject to misalignment during the co-registration process, potentially introducing a spatial error [52]. This has been reflected in the discrepancy in the reported coordinates of activation with another PET study [53] and with a functional MRI study [54]. The original target's coordinates were 2 mm lateral to the midline, 6 mm behind the mid-commissural point (MCP) and 8 mm below the AC-PC [30]. This is the same area identified in an earlier PET study [20]. The target was then modified to 2 mm lateral to the midline, 3 mm posterior and 5 mm below the MCP [31]. This last "Franzini" target has been generally adopted in the other surgical series [48, 55, 56]. A study of ten patients with CCH implanted with unilateral DBS leads using Franzini's target employed postoperative AC-PC coordinates of the active DBS contact centres, projected on the Schaltenbrand atlas [57] and a three-dimensional 4.7 Tesla MRI atlas of the diencephalon-mesencephalic junction atlas to identify the anatomical location of the effective DBS electrodes [48]. Five patients responded to treatment. The mean coordinates of the active contacts in the responders were 3 mm lateral, 3.5 mm posterior and 3.3 mm below the MCP. The study, however, did not find a statistically significant difference between the responder and non-responder groups. The authors pointed out the limitation from the method used to localize the contacts, i.e. projection of AC-PC coordinates on atlases [48].

In a study of seven patients with medically refractory CCH treated with VTA-DBS surgery, probabilistic maps of activation around DBS contacts were used to identify the optimal stimulation site. These maps were correlated with outcome after 1 year of surgery. Detailed, state-of-the-art diffusion MRI was used to map-out the structural connectivity of the DBS target in six out of the seven patients who were deemed responders [58].

The responders' average activation volume lay in the ventral tegmental area in the area between the red nucleus and the mammillothalamic tract. The cluster predictive of improvement in HAL lay in the superior, posterior and lateral portion of the group average activation volume (6 mm lateral, 2 mm posterior and 1 mm inferior to the MCP). The activation volume for the non-responder lay outside the efficacy cluster (Fig. 34.3) [58].

The group average probabilistic tractography streamlines, generated from individual responders DBS activation volume, are shown in Fig. 34.4. Anteriorly, the streamlines traverse the hypothalamus and then split into two pathways: an inferolateral pathway towards the mesial temporal lobe and amygdalar complex, possibly via the amygdalofugal pathway, and an anterosuperior pathway towards the prefrontal area via the anterior limb of the internal capsule.

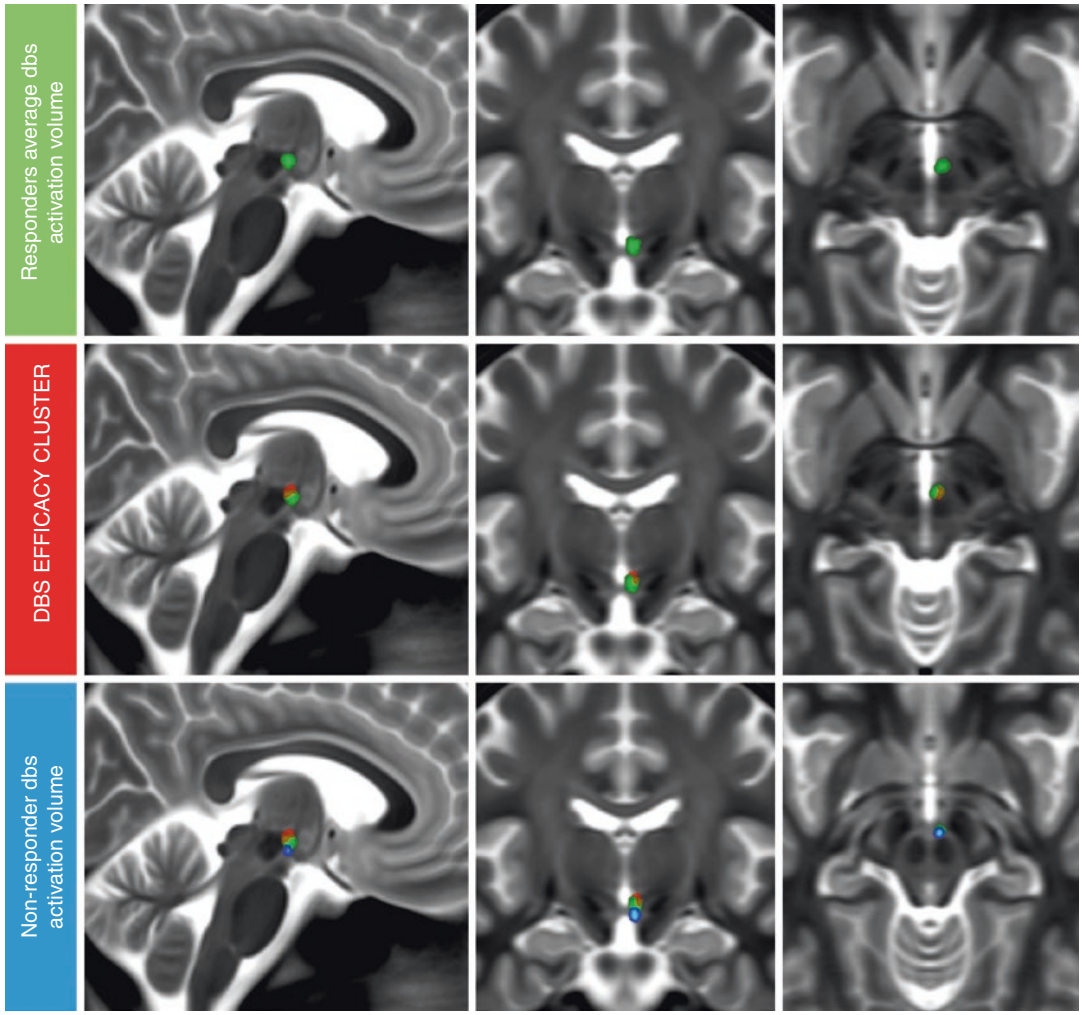

Fig. 34.3 Average DBS activation volume (green) with DBS efficacy cluster (red) and activation volume for the non-responder (blue). (From Akram et al. [58]. Reprinted with permission from Wolters Kluwer Health, Inc)

Posteriorly, the streamlines run medial to the red nucleus towards the periaqueductal grey and then caudally through the pons and upper medulla in a dorso-lateral position towards the trigeminal tract and nuclei [58].

The difficulty in explaining the mechanism of action of DBS in CH is partly caused by the lack of a definitive understanding of the pathophysiological process itself [59, 60]. Some authors suggest that simple local blockade of the "posterior hypothalamic grey" or VTA activity is not a likely mechanism for improvement in headache. However, this does not explain the micro-lesion or "stun" effect some patients experience with complete abolition of attacks for a few days or even weeks following DBS lead implantation alone, suggesting disruption of pathological neural activity in the region [3, 15, 59]. Paradoxically, there is often a latency in achieving maximal DBS efficacy that has been seen across several studies, including our own. Increased threshold for cold pain at the site of the first trigeminal branch ipsilateral to the stimulated side in chronically stimulated patients could be caused by modulation of the anti-nociceptive system [61]; however, a generic anti-nociceptive effect does not explain why DBS is effective for the trigeminal autonomic cephalalgias but not "atypical

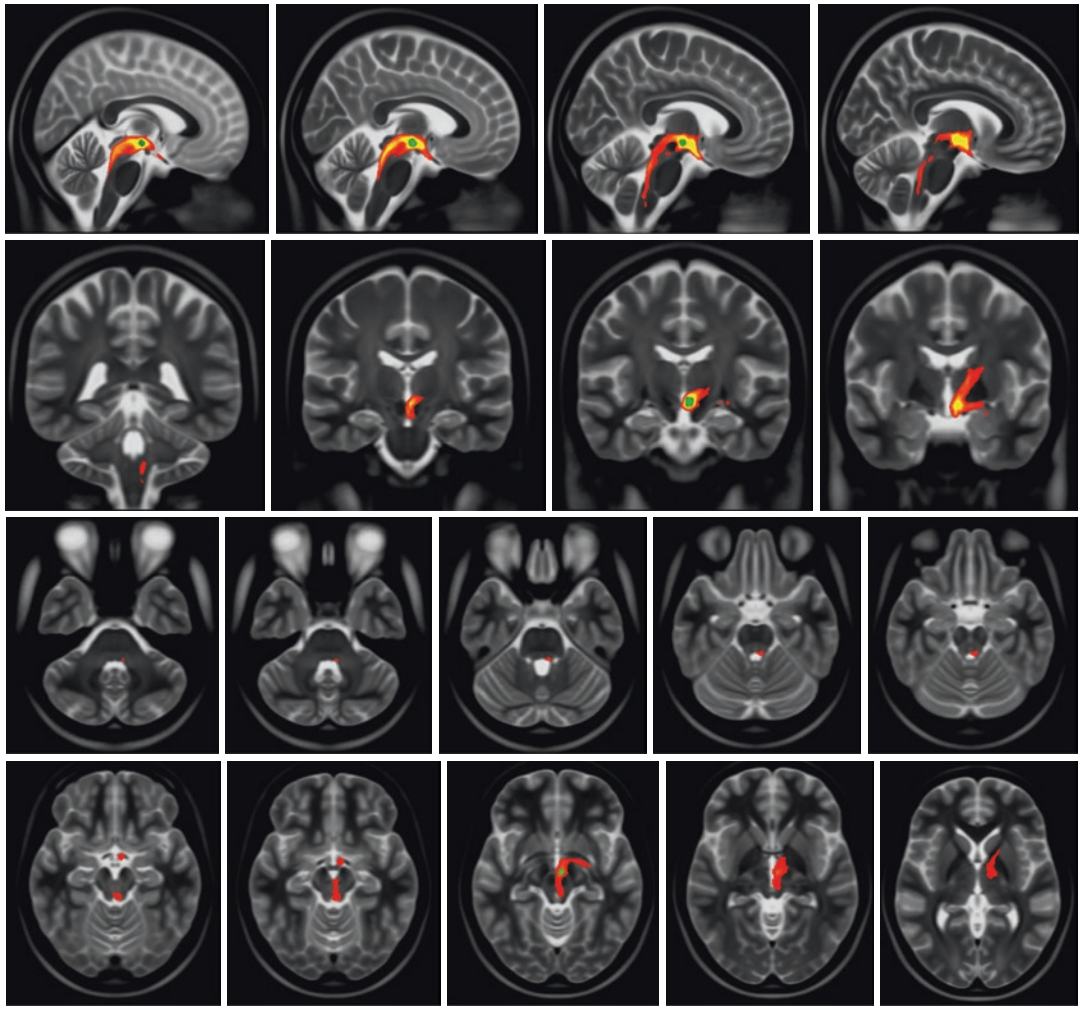

Fig. 34.4 Group average probabilistic tractography streamlines (red-yellow) with group average DBS tissue activation volume (green). (From Akram et al. [58]. Reprinted with permission from Wolters Kluwer Health, Inc)

facial pain" [15, 59, 60, 62]. DBS has been shown to modulate a complex network of pain-processing areas [51]. Stimulation induced local activation around the active DBS contact as well as distant activation in the ipsilateral thalamus, the somatosensory cortex and precuneus, the anterior cingulate cortex and the ipsilateral trigeminal nucleus and ganglion, coupled with deactivation in the middle temporal gyrus, posterior cingulate cortex, inferior temporal gyrus bilaterally and contralateral anterior insula [51]. The activation in the trigeminal system however does not seem to provoke CH pain attacks or the typical sensations that commonly accompany trigeminal activation [51]. This connection between the posterior hypothalamus and the trigeminal system has been previously observed following injection of the neuropeptide orexin B into the "posterior hypothalamic region" of the rat which increased spontaneous activity in the caudal trigeminal nucleus (with discharges persisting for several minutes) and heightened responses in the nucleus to dural stimulation and noxious thermal stimulation of the face [63].

The connection between the trigeminal system and the hypothalamus is crucial in integrating somatosensory and visceral information (e.g. innervation from cranial skin, intracranial

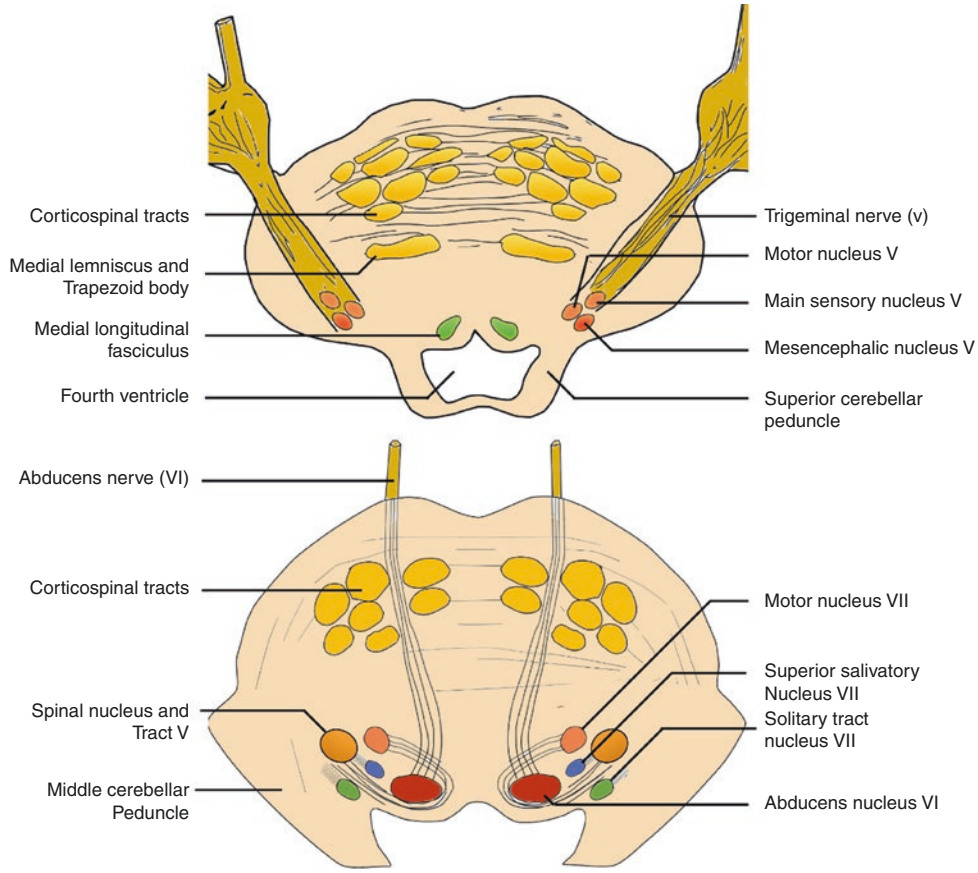

Fig. 34.5 Illustration showing two cross-sections in the pons at the level of the trigeminal nerve, main sensory and mesencephalic trigeminal nuclei (top) and spinal trigeminal nucleus and tract, superior salivatory nucleus and solitary tract (bottom). (From Akram et al. [58]. Reprinted with permission from Wolters Kluwer Health, Inc)

blood vessels and meninges) with endocrine and autonomic responses [64]. Single-unit recording and antidromic microstimulation techniques in rats have established a direct two-way connection between the posterior hypothalamus and the spinal trigeminal nucleus through the THT [64].

Other brainstem nuclei have neurons that respond to noxious and innocuous somatosensory and visceral stimulation [65–69]. These nuclei also give efferents to the hypothalamus, such as the parabrachial nuclei [70–72], nucleus of the solitary tract [73, 74], periaqueductal grey [75–78] and caudal ventrolateral medulla [79, 80], suggesting that somatosensory signals reach the hypothalamus through several polysynaptic pathways [64].

This tractography study shows that the DBS activated area, posterior to the hypothalamus, in the ventral tegmentum lies on a tract that connects the hypothalamus, prefrontal and mesial temporal regions anteriorly with brainstem areas in the proximity of the parabrachial nuclei, nucleus of the solitary tract and periaqueductal grey and ending in the region of the trigeminal nucleus and tract and the superior salivatory nucleus (SSN) (Figs. 34.4 and 34.5).

Although this finding does not explain the mechanism of action of DBS, it confirms the relevance of the target site by means of its connections to anatomically relevant brainstem areas. One possibility is by exerting a top-down antinociceptive effect, whilst another possibility is by modulation of the trigeminal parasympathetic

reflex, commonly activated in primary headache disorders [81] and which is thought to mediate the cranial autonomic symptoms in CH [82]. This pathway can be triggered by hypodermic capsaicin injection in the first trigeminal nerve division area [83] as well as a variety of trigeminal nociceptive triggers [60]. Nociceptive trigeminal activation, in the first division of the trigeminal nerve, is relayed into the spinal trigeminal nucleus and the C1/C2 dorsal horns (i.e. the trigemino-cervical complex or TCC) [84] which have a reflex connection to the SSN in the pons [85]. The output is then carried via the parasympathetic pathway of the facial nerve, through the geniculate ganglion within the greater superficial petrosal nerve [86] to the sphenopalatine ganglion (SPG) [60, 87].

It must be noted, however, that the pain and the autonomic phenomenon can at times occur independently [23] especially in patients taking preventive medications, suggesting either anatomically separate pathways albeit partly or different activation thresholds mediating these two features [5, 54, 87].

References

1. Headache Classification Committee of the International Headache Society (IHS). The International Classification of Headache Disorders, 3rd edition. Cephalalgia. 2018;38(1):1–211.
2. Donnet A, Lanteri-Minet M, Guegan-Massardier E, Mick G, Fabre N, Geraud G, et al. Chronic cluster headache: a French clinical descriptive study. J Neurol Neurosurg Psychiatry. 2007;78(12):1354–8.
3. Akram H, Miller S, Lagrata S, Hyam J, Jahanshahi M, Hariz M, et al. Ventral tegmental area deep brain stimulation for refractory chronic cluster headache. Neurology. 2016;86(18):1676–82.
4. Rothrock J. Cluster: a potentially lethal headache disorder. Headache. 2006;46(2):327.
5. May A. Cluster headache: pathogenesis, diagnosis, and management. Lancet. 2005;366(9488):843–55.
6. Leroux E, Ducros A. Cluster headache. Orphanet J Rare Dis. 2008;3(1):20.
7. Russell MB. Epidemiology and genetics of cluster headache. Lancet Neurol. 2004;3(5):279–83.
8. Bahra A, May A, Goadsby PJ. Cluster headache: a prospective clinical study with diagnostic implications. Neurology. 2002;58(3):354–61.
9. May A, Leone M, Afra J, Linde M, Sándor PS, Evers S, et al. EFNS guidelines on the treatment of cluster headache and other trigeminal-autonomic cephalalgias. Eur J Neurol. Blackwell Publishing Ltd;. 2006;13:1066–77.
10. de Tommaso M, Vecchio E. Primary headaches and trigeminal neuralgia: neuropathic pain yes or not? Evidences from neurophysiological procedures. Expert Rev Neurother. 2013;13(9):1031–9.
11. Goadsby PJ. Trigeminal autonomic cephalalgias. Continuum (Minneap Minn). 2012;18(4):883–95.
12. Holle D, Obermann M. Cluster headache and the hypothalamus: causal relationship or epiphenomenon? Expert Rev Neurother. 2011;11(9):1255–63.
13. Waldenlind E, Sjöstrand C. Pathophysiology of cluster headache and other trigeminal autonomic cephalalgias. Handb Clin Neurol. Elsevier;. 2010;97:389–411.
14. Holland PR. Modulation of trigeminovascular processing: novel insights into primary headache disorders. Cephalalgia. 2009;29 Suppl 3:1–6.
15. Leone M, Bussone G. Pathophysiology of trigeminal autonomic cephalalgias. Lancet Neurol. 2009;8(8):755–64.
16. Bussone G. Cluster headache: from treatment to pathophysiology. Neurol Sci. 2008;29(S1):1–6.
17. Nardone R, Ausserer H, Bratti A, Covi M, Lochner P, Marth R, et al. Trigemino-cervical reflex abnormalities in patients with migraine and cluster headache. Headache. 2008;48(4):578–85.
18. Waldenlind E, Gustafsson SA, Ekbom K, Wetterberg L. Circadian secretion of cortisol and melatonin in cluster headache during active cluster periods and remission. J Neurol Neurosurg Psychiatry. BMJ Group;. 1987;50(2):207–13.
19. Leone M, Bussone G. A review of hormonal findings in cluster headache. Evidence for hypothalamic involvement. Cephalalgia. 1993;13(5):309–17.
20. May A, Bahra A, Büchel C, Frackowiak RS, Goadsby PJ. Hypothalamic activation in cluster headache attacks. Lancet. 1998;352(9124):275–8.
21. May A, Ashburner J, Büchel C, McGonigle DJ, Friston KJ, Frackowiak RS, et al. Correlation between structural and functional changes in brain in an idiopathic headache syndrome. Nat Med. 1999;5(7):836–8.
22. Cutrer FM. Functional imaging in primary headache disorders. Headache. 2008;48(5):704–6.
23. Goadsby PJ, Lipton RB. A review of paroxysmal hemicranias, SUNCT syndrome and other short-lasting headaches with autonomic feature, including new cases. Brain. 1997;120(Pt 1):193–209.
24. Goadsby PJ, Bartsch T, Dodick DW. Occipital nerve stimulation for headache: mechanisms and efficacy. Headache. 2008;48(2):313–8.
25. Goadsby PJ. Sphenopalatine (pterygopalatine) ganglion stimulation and cluster headache: new hope for ye who enter here. Cephalalgia. SAGE Publications;. 2013;33(10):813–5.
26. Jürgens TP, May A. Role of sphenopalatine ganglion stimulation in cluster headache. Curr Pain Headache Rep. 2014;18(7):433.

27. Bartsch T, Goadsby PJ. Stimulation of the greater occipital nerve induces increased central excitability of dural afferent input. Brain. 2002;125(Pt 7): 1496–509.
28. Wolter T, Kaube H. Spinal cord stimulation in cluster headache. Curr Pain Headache Rep. 2013;17(5):324.
29. Matharu MS, Zrinzo L. Deep brain stimulation in cluster headache: hypothalamus or midbrain tegmentum? Curr Pain Headache Rep. 2010;14(2):151–9.
30. Leone M, Franzini A, Bussone G. Stereotactic stimulation of posterior hypothalamic gray matter in a patient with intractable cluster headache. N Engl J Med. 2001;345(19):1428–9.
31. Franzini A, Ferroli P, Leone M, Broggi G. Stimulation of the posterior hypothalamus for treatment of chronic intractable cluster headaches: first reported series. Neurosurgery. 2003;52(5):1095–101.
32. Leone M, Franzini A, Cecchini AP, Bussone G. Success, failure, and putative mechanisms in hypothalamic stimulation for drug-resistant chronic cluster headache. Pain. 2013;154(1):89–94.
33. Sano K, Mayanagi Y, Sekino H, Ogashiwa M, Ishijima B. Results of stimulation and destruction of the posterior hypothalamus in man. J Neurosurg. 1970;33(6):689–707.
34. Schlaepfer TE, Bewernick BH, Kayser S, Mädler B, Coenen VA. Rapid effects of deep brain stimulation for treatment-resistant major depression. Biol Psychiatry. 2013;73(12):1204–12.
35. Fontaine D, Lazorthes Y, Mertens P, Blond S, Géraud G, Fabre N, et al. Safety and efficacy of deep brain stimulation in refractory cluster headache: a randomized placebo-controlled double-blind trial followed by a 1-year open extension. J Headache Pain. 2009;11(1):23–31.
36. Schoenen J. Hypothalamic stimulation in chronic cluster headache: a pilot study of efficacy and mode of action. Brain. 2005;128(4):940–7.
37. Magis D, Schoenen J. Advances and challenges in neurostimulation for headaches. Lancet Neurol. 2012;11(8):708–19.
38. Clelland CD, Zheng Z, Kim W, Bari A, Pouratian N. Common cerebral networks associated with distinct deep brain stimulation targets for cluster headache. Cephalalgia. 2014;34(3):224–30.
39. Schoenen J, Jensen RH, Lantéri-Minet M, Láinez MJA, Gaul C, Goodman AM, et al. Stimulation of the sphenopalatine ganglion (SPG) for cluster headache treatment. Pathway CH-1: a randomized, sham-controlled study. Cephalalgia. 2013;33(10): 816–30.
40. Fontaine D, Vandersteen C, Magis D, Lantéri-Minet M. Neuromodulation in cluster headache. Adv Tech Stand Neurosurg. Cham: Springer International Publishing;. 2015;42(Chapter 1):3–21.
41. Goadsby PJ, Schoenen J, Ferrari MD, Silberstein SD, Dodick D. Towards a definition of intractable headache for use in clinical practice and trials. Cephalalgia. SAGE Publications;. 2006;26(9):1168–70.
42. Foltynie T, Zrinzo L, Martinez-Torres I, Tripoliti E, Petersen E, Holl E, et al. MRI-guided STN DBS in Parkinson's disease without microelectrode recording: efficacy and safety. J Neurol Neurosurg Psychiatry. 2011;82(4):358–63.
43. Holl EM, Petersen EA, Foltynie T, Martinez-Torres I, Limousin P, Hariz MI, et al. Improving targeting in image-guided frame-based deep brain stimulation. Neurosurgery. 2010;67:ons437–47.
44. Lipton RB, Micieli G, Russell D, Solomon S, Tfelt-Hansen P, Waldenlind E. Guidelines for controlled trials of drugs in cluster headache. Cephalalgia. 1995;15:452–62.
45. Dworkin RH, Turk DC, Wyrwich KW, Beaton D, Cleeland CS, Farrar JT, et al. Interpreting the clinical importance of treatment outcomes in chronic pain clinical trials: IMMPACT recommendations. J Pain. 2008;9(2):105–21.
46. Joint Formulary Committee. British National Formulary (online). London: BMJ Group and Pharmaceutical Press; 2015. http://www.medicinescomplete.com. Accessed March 2015.
47. Kosinski M, Bayliss MS, Bjorner JB, Ware JE, Garber WH, Batenhorst A, et al. A six-item short-form survey for measuring headache impact: the HIT-6. Qual Life Res. 2003;12(8):963–74.
48. Fontaine D, Lanteri-Minet M, Ouchchane L, Lazorthes Y, Mertens P, Blond S, et al. Anatomical location of effective deep brain stimulation electrodes in chronic cluster headache. Brain. 2010;133(4):1214–23.
49. Chabardes S, Carron R, Seigneuret E, Torres N, Goetz L, Krainik A, et al. Endoventricular deep brain stimulation of the third ventricle: proof of concept and application to cluster headache. Neurosurgery. 2016;79(6):806–15.
50. Coenen VA, Sajonz B, Reisert M, Bostroem J, Bewernick B, Urbach H, et al. Tractography-assisted deep brain stimulation of the superolateral branch of the medial forebrain bundle (slMFB DBS) in major depression. Neuroimage Clin. 2018;20:580–93.
51. May A. Hypothalamic deep brain stimulation in positron emission tomography. J Neurosci. 2006;26(13):3589–93.
52. Bailey DL, Townsend DW, Valk PE, Maisey MN. Positron emission tomography: Springer; 2006. 1 p.
53. Sprenger T, Boecker H, Tölle TR, Bussone G, May A, Leone M. Specific hypothalamic activation during a spontaneous cluster headache attack. Neurology. 2004;62(3):516–7.
54. Morelli N, Pesaresi I, Cafforio G, Maluccio MR, Gori S, Di Salle F, et al. Functional magnetic resonance imaging in episodic cluster headache. J Headache Pain. 2008;10(1):11–4.
55. Starr PA, Barbaro NM, Raskin NH, Ostrem JL. Chronic stimulation of the posterior hypothalamic region for cluster headache: technique and 1-year results in four patients. J Neurosurg. 2007;106(6):999–1005.
56. Bartsch T, Pinsker MO, Rasche D, Kinfe T, Hertel F, Diener HC, et al. Hypothalamic deep brain stimula-

tion for cluster headache: experience from a new multicase series. Cephalalgia. 2008;28(3):285–95.
57. Schaltenbrand G, Wahren W, Hassler R. Atlas for stereotaxy of the human brain. Stuttgart: Thieme Medical Publishers; 1977. 1 p.
58. Akram H, Miller S, Lagrata S, Hariz M, Ashburner J, Behrens T, et al. Optimal deep brain stimulation site and target connectivity for chronic cluster headache. Neurology. 2017;89(20):2083–91.
59. May A. Hypothalamic deep-brain stimulation: target and potential mechanism for the treatment of cluster headache. Cephalalgia. 2008;28(7):799–803.
60. Eller M, Goadsby PJ. Trigeminal autonomic cephalalgias. Oral Dis. 2016;22(1):1–8.
61. Jürgens TP, Leone M, Proietti-Cecchini A, Busch V, Mea E, Bussone G, et al. Hypothalamic deep-brain stimulation modulates thermal sensitivity and pain thresholds in cluster headache. Pain. 2009;146(1–2):84–90.
62. Broggi G, Franzini A, Leone M, Bussone G. Update on neurosurgical treatment of chronic trigeminal autonomic cephalalgias and atypical facial pain with deep brain stimulation of posterior hypothalamus: results and comments. Neurol Sci. 2007;28(S2):S138–45.
63. Bartsch T, Levy MJ, Knight YE, Goadsby PJ. Differential modulation of nociceptive dural input to [hypocretin] orexin A and B receptor activation in the posterior hypothalamic area. Pain. 2004;109(3):367–78.
64. Malick A, Strassman RM, Burstein R. Trigeminohypothalamic and reticulohypothalamic tract neurons in the upper cervical spinal cord and caudal medulla of the rat. J Neurophysiol. 2000;84(4):2078–112.
65. Bernard JF, Besson JM. The spino(trigemino)pontoamygdaloid pathway: electrophysiological evidence for an involvement in pain processes. J Neurophysiol. 1990;63(3):473–90.
66. Kannan H, Osaka T, Kasai M, Okuya S, Yamashita H. Electrophysiological properties of neurons in the caudal ventrolateral medulla projecting to the paraventricular nucleus of the hypothalamus in rats. Brain Res. 1986;376(2):342–50.
67. Pan B, Castro-Lopes JM, Coimbra A. Central afferent pathways conveying nociceptive input to the hypothalamic paraventricular nucleus as revealed by a combination of retrograde labeling and c-fos activation. J Comp Neurol. 1999;413(1):129–45.
68. Person RJ. Somatic and vagal afferent convergence on solitary tract neurons in cat: electrophysiological characteristics. NSC. 1989;30(2):283–95.
69. Zhang X, Fogel R, Renehan WE. Physiology and morphology of neurons in the dorsal motor nucleus of the vagus and the nucleus of the solitary tract that are sensitive to distension of the small intestine. J Comp Neurol. 1992;323(3):432–48.
70. Cechetto DF, Standaert DG, Saper CB. Spinal and trigeminal dorsal horn projections to the parabrachial nucleus in the rat. J Comp Neurol. 1985;240(2):153–60.
71. Saper CB, Loewy AD. Efferent connections of the parabrachial nucleus in the rat. Brain Res. 1980;197(2):291–317.
72. Slugg RM, Light AR. Spinal cord and trigeminal projections to the pontine parabrachial region in the rat as demonstrated with Phaseolus vulgaris leucoagglutinin. J Comp Neurol. 1994;339(1):49–61.
73. Menétrey D, Basbaum AI. Spinal and trigeminal projections to the nucleus of the solitary tract: a possible substrate for somatovisceral and viscerovisceral reflex activation. J Comp Neurol. 1987;255(3):439–50.
74. Ricardo JA, Koh ET. Anatomical evidence of direct projections from the nucleus of the solitary tract to the hypothalamus, amygdala, and other forebrain structures in the rat. Brain Res. 1978;153(1):1–26.
75. Beitz AJ. The organization of afferent projections to the midbrain periaqueductal gray of the rat. NSC. 1982;7(1):133–59.
76. Eberhart JA, Morrell JI, Krieger MS, Pfaff DW. An autoradiographic study of projections ascending from the midbrain central gray, and from the region lateral to it, in the rat. J Comp Neurol. 1985;241(3):285–310.
77. Lima D, Coimbra A. Morphological types of spinomesencephalic neurons in the marginal zone (lamina I) of the rat spinal cord, as shown after retrograde labelling with cholera toxin subunit B. J Comp Neurol. 1989;279(2):327–39.
78. Liu RP. Laminar origins of spinal projection neurons to the periaqueductal gray of the rat. Brain Res. 1983;264(1):118–22.
79. Lima D, Mendes-Ribeiro JA, Coimbra A. The spino-latero-reticular system of the rat: projections from the superficial dorsal horn and structural characterization of marginal neurons involved. NSC. 1991;45(1):137–52.
80. Sawchenko PE, Swanson LW. Central noradrenergic pathways for the integration of hypothalamic neuroendocrine and autonomic responses. Science. 1981;214(4521):685–7.
81. Goadsby PJ. Lacrimation, conjunctival injection, nasal symptoms... cluster headache, migraine and cranial autonomic symptoms in primary headache disorders – what's new? J Neurol Neurosurg Psychiatry. 2009;80(10):1057–8.
82. May A, Goadsby PJ. The trigeminovascular system in humans: pathophysiologic implications for primary headache syndromes of the neural influences on the cerebral circulation. J Cereb Blood Flow Metab. SAGE Publications;. 1999;19(2):115–27.
83. Frese A, Evers S, May A. Autonomic activation in experimental trigeminal pain. Cephalalgia. 2003;23(1):67–8.
84. Goadsby PJ, Hoskin KL. The distribution of trigeminovascular afferents in the nonhuman primate brain Macaca nemestrina: a c-fos immunocytochemical study. J Anat. Wiley-Blackwell;. 1997;190(Pt 3):367–75.

85. Knight YE, Classey JD, Lasalandra MP, Akerman S, Kowacs F, Hoskin KL, et al. Patterns of fos expression in the rostral medulla and caudal pons evoked by noxious craniovascular stimulation and periaqueductal gray stimulation in the cat. Brain Res. 2005;1045(1–2):1–11.
86. Goadsby PJ, Lambert GA, Lance JW. Effects of locus coeruleus stimulation on carotid vascular resistance in the cat. Brain Res. 1983;278(1–2):175–83.
87. Goadsby PJ. Pathophysiology of cluster headache: a trigeminal autonomic cephalgia. Lancet Neurol. 2002;1(4):251–7.

Part V

Diseases and Targets

35

Developing New Indications: Strategies and Hurdles to Discovery

Robert W. Bina and Jean-Philippe Langevin

Developing New Indications

As we search for new indications and seek for answers to the perplexing problems of cognitive or behavioral circuitopathies with little objective criteria, we must look to our strengths to navigate the difficulties.

In reviewing the history of neurostimulation for essential tremor (ET) and Parkinson's disease (PD), we can identify several reasons explaining the success of those neuromodulation applications. First, there is an objective measure of efficacy directly linked to neurostimulation: when stimulated, tremor disappears and rigidity improves. Another critical piece in the success of neurostimulation for these movement disorders has been the existence of three clearly defined surgical targets. The serendipitous, curative effect of ligating the anterior choroidal artery gave us the initial anatomical location [1]. This information was more precisely delineated by anatomic and surgical studies of these patients and more recently further refined by functional neuroimaging studies.

One of the major challenges with several new possible indications, such as psychiatric disorders, is that the definitions are largely clinical – the diseases are defined and differentiated by symptom clusters – and there are no clear objective imaging or metabolic criteria to diagnose them and differentiate them from each other [2]. In order to successfully approach these conditions, we would need to redefine them in terms of "circuitopathies" and dysfunctional networks. We must look back to the development of our current indications with the use of emerging neurobiology, behavioral neuroscience, and technology with a strong ethical leash to proceed into developing and expanding new indications.

When studying recent advances in neuromodulation, three main strategies emerge in the identification of new targets: (1) translation of previous lesioning targets to neuromodulation, (2) network-based modeling of the condition, and (3) use of animal models to test specific targets.

Translation of Lesioning Targets to Neuromodulation

Movement Disorder

The use of deep brain stimulation (DBS) in Parkinson's disease represents the first example

R. W. Bina
Division of Neurosurgery, Banner University Medical Center, Tucson, AZ, USA

J.-P. Langevin (✉)
Department of Neurosurgery, David Geffen School of Medicine at UCLA, Los Angeles, CA, USA

Neurosurgery Service, Greater Los Angeles VA Healthcare System, Los Angeles, CA, USA
e-mail: Jlangevin@mednet.ucla.edu

N. Pouratian, S. A. Sheth (eds.), *Stereotactic and Functional Neurosurgery*,
https://doi.org/10.1007/978-3-030-34906-6_35

of translation of lesioning to neuromodulation. The first discovery that the tremor associated with Parkinson's disease could be treated with a brain lesion came as the result of a serendipitous treatment of a patient who had concurrent aneurysm and PD [1]. This single case led to a glut of lesional surgeries in PD patients. The targets for pallidotomy and for thalamotomy were identified and refined [3, 4]. Prior to the introduction of carbidopa-levodopa, thermal and radiation lesions were the mainstay of tremor therapy. After the dopaminergic medication treatments didn't have the hoped-for longevity, returning to lesions to supplement medical therapy was an easy shift because the efficacy of lesioning was already established.

The introduction of adaptable, transferrable technology into medicine proved to be perfect soil for the fertilization of a new treatment [5]. Benabid et al. [6, 7] placed electrodes in the ventralis intermedius (VIM) for patients with ET and PD with clinical results comparable to lesional procedures. High-frequency stimulation was used to predict the effects of lesion, and with the advent of cardiac pacemaker, it was possible to use the stimulation chronically instead of performing the lesion.

The benefits of DBS have been illuminated since its introduction and will be briefly restated here – reversible, plastic, adaptable, and transferable. These characteristics, along with the efficacy of symptomatic control, have led to a resurrection of interest in the use of DBS to treat other brain circuitopathies. Two important strategies to identify potential targets for focal neuromodulation include (1) translation of lesional target to DBS and (2) target selection driven by network-based model of the condition.

Obsessive-Compulsive Disorder

Treating psychiatric disease with neurosurgery has a long history [8] which is mostly benign but has, at times, veered into ethical conundra [9–13]. Alleviating the suffering of patients with debilitating psychiatric symptoms has been the aim of largely well-intentioned surgeons through lobotomy, lesions of specific nuclei, or tractotomy [13]. Ballantine started a long cohort study lesioning the anterior capsule in patients with severe, intractable psychiatric symptoms and chronic pain [14]. The outcomes of this 198-patient cohort study from 1962 to 1987 are informative for the development and solidification of new indications. The target was the same across all patients, regardless of symptomatic presentation. Schizophrenia and personality disorder patients remained largely intractable to surgical therapy, but 18/32 (56%) of the patients diagnosed with obsessive-compulsive disorder as defined by the American Psychiatric Association's (APA) Diagnostic and Statistical Manual III (DMS III) had clinically significant improvement.

In comparable studies of obsessive-compulsive disorder (OCD) patients refractory to standard therapies published by Mindus [15] for capsulotomy and by Jenike [16] and Baer [17] for cingulotomy, outcomes were similar. 45% of capsulotomy patients had a 35% or greater symptom reduction and 44% of the cingulotomy patients had a similar symptom outcome.

DBS of the bilateral anterior limbs of the internal capsule was reported as an effective treatment for refractory OCD by Nuttin and colleagues in 1999 [18] with a follow-up series in 2003 [19]. The scientific and philosophical underpinnings of this study were borne out of the efficacy of DBS for movement disorders [19] and the lesional procedures performed for OCD. Patients were carefully selected and underwent rigorous post-operative blinded symptom evaluation using standardized symptom scales including the Yale-Brown Obsessive Compulsive Scale (Y-BOCS), in cross-over stimulated and non-stimulated states. Although there were limited numbers of patients in the study (six total in the initial report and two more in a supplemental update), other reports have supported the findings and have further refined the target [20–22].

Other examples exist where the application of DBS derives from clinical experience with lesional treatment. For instance, Lipsman et al. [23] reviewed a total of 17 case reports of AN patients treated with prefrontal leucotomy with unstandardized reporting of results; there was a trend toward clinical benefits in these disparate

cases. These lesional studies have guided the target nuclei for DBS trials for AN [23–25]. In addition, the application of lateral hypothalamic (LH) DBS for obesity was largely based on observation of weight loss in animals after LH lesioning [26].

Developing Network-Based Models

Major Depressive Disorder

Several studies have recently focused on the description of the networks implicated in specific conditions. Functional neuroimaging under symptomatic conditions has provided clinicians and researchers with specific targets for modulation. For example, in AN patients exposed to high-calorie foods, fMRI indicates activation in a wide variety of limbic structures including the medial orbitofrontal cortex and anterior cingulate cortex. In PTSD patients exposed to war imagery, the amygdala is activated [27]. These fMRI findings are corroborated with fluorodeoxyglucose (FDG) positron emission tomography (PET) [28, 29]. The work on DBS for depression presents a clear example of target selection driven by network-based model. Based on PET findings, Mayberg et al. [30] proposed the involvement of Brodmann area 25 (BA-25) in patients who have tried and failed multiple medical therapies for major depressive disorder (MDD). BA-25, implicated in feelings of sadness and sustained dysphoria, is located in the subgenual cingulate cortex and is hyperactive in MDD. Patients that respond to medical and other therapies for MDD show a reduction in PET activity of BA-25. This finding led to the hypothesis supporting the 2005 publication by Mayberg and Lozano of their pilot work in which DBS electrodes were implanted into the subcallosal cingulate for patients with treatment refractory MDD [22]. Since BA-25 was active during symptomatic episodes and quiet in periods of improvement, it lent itself well as a DBS target. The results of that trial were heartening for the patients with the debilitating disease with reduction in depressive symptoms of at least 40% in four of the six patient cohorts. Unfortunately, a larger trial was stopped early as a result of the futility analysis [31]. Despite being disappointing, these results inspired investigators to further refine the area 25 target using diffusion tensor imaging (DTI) in conjunction with fMRI [32–35]. These studies have demonstrated the utility of studying DTI data in relation to neurostimulation outcomes to gain a network perspective of the therapy. For instance, patients with good outcomes with DBS for depression had undergone stimulation at the convergence of the forceps minor and the cingulum bundle. These findings highlight the importance of considering the entire network when modulating a target.

Animal Models to Test New Targets

Long have animal models provided significant insight into the neuroscience underlying human psychiatric and psychological disease [36, 37]. Animal models can serve as an in vivo confirmation of a network-based concept. The success of DBS for movement disorders is due in part to the reproducible effects MTPT has on rodents [3, 4].

The neurocircuitry of addiction in rodents has been well-studied with clear evidence pointing to the nucleus accumbens core, the ventral tegmental area, and the mesolimbic pathway [34–43] as critical nodes in a diffuse network. The translation to humans is due to the high degree of evolutionary conservation of reward circuitry in mammals. These animal models are the base on which human ablational studies in opiate addiction [44–46] and neuromodulation studies for alcoholism [47–50] have been conducted. They also underlie ongoing trials in Germany and China [51].

Similar to reward circuitry, fear circuitry also has a high degree of fidelity among mammals [52, 53]. This evolutionary conservation has been instrumental in using rodent models of PTSD [54] to refine the ongoing investigations of neuromodulation by DBS in this disease [55–57]. DBS electrodes in the basolateral portion of the amygdala have reduced PTSD symptoms in two implanted patients [55] (unpublished data).

Obesity researchers have also turned to animal models to study potential targets. These models have been used to study caloric intakes, weight loss, and physiological and biochemical hemostasis while receiving DBS therapy [20, 21].

Challenges to Innovation

Despite intense work in the field and the deployment of various robust strategies to identify new targets, the outcomes in human trials are modest. The initial results of Mayberg and Lozano's work [22, 58] were promising. Similarly, there has been great success in small trials of neuromodulation for OCD [59, 60], for alcoholism [47, 50], and for AN [25]. However, the disappointing results of the BROADEN trial [31] have raised questions in regard to the value of smaller early feasibility trial. The cost associated with large trials is significant and the potential economic benefit has thus far remained questionable. Examination of the failure of the BROADEN trial should inform the design and reporting of future trials. First, as mentioned in the BROADEN report, the time frame for results may be limited in diseases which don't have well-established patterns [61].The modulation of neural circuits may help restore proper information processing quickly, but functional outcomes may take longer to improve. For instance, a patient undergoing the fixation of an unstable spinal fracture may not demonstrate significant functional improvement immediately post-operatively until significant time is allowed for neural recovery and physical therapy. Similarly, the time lag for improvement in cognitive dysfunction and psychiatric conditions is likely a function of the severity and the duration of the illness. Second, the programming of the device itself can pose a challenge to progress. Since there is not always direct feedback from the patient's symptoms, it is unclear how to select the optimal parameters of stimulation. There is no direct indication that the programming parameters are optimally engaging the target neurocircuit. As a result, a lot of programming algorithms have relied on a trial and error strategy where the device is programmed to subjective improvement in certain dimensions (i.e., mood, anxiety level) and the effects are verified over time. This strategy is not as efficient as programming performed optimally to a specific biomarker of target engagement with subsequent clinical follow-up.

The success of future clinical trials depends in large part on successfully navigating these obstacles. A few emerging strategies may help move the field forward. In particular, the search for neural biomarker and the use of closed-loop DBS systems have shown some promises.

New Strategies for Innovation

The Necessity of Biomarkers

Looking at the strengths and successes of DBS for movement disorders can inform how to proceed in developing new indications for neuromodulation through DBS and other modalities in the future. The measurable, objective, symptom biomarker of tremor standardizes efficacy measurements. The clear, concisely mapped brain motor network affected in movement disorders makes study and therapeutic hypotheses easy to test and easy to interpret. However, several conditions lack overt marker of network engagement and clinical response.

For example, clinical improvement following the onset of neuromodulation in psychiatry takes a long time and does not follow a linear path. Neuromodulation may normalize the activity of the network, but the patients still need to change their behavior based on modified function to notice the improvement and then learn from this experience to alter future decisions. For instance, OCD patients undergoing DBS could only realize the improvement if they attempt exposing themselves to their fear to see if the compulsion is still present. Psychometric scores are unlikely to improve until this internal work is performed. In addition, as more benign exposures are cleared, the patient is likely to attempt more substantial real-life exposures leading to temporary failures and worsening in the scores. In summary, after

the onset of successful network modulation, patients need psychotherapy to discover their new abilities and to learn strategies to handle new life challenges. This time of transformation is clinically volatile and the psychometric scores are unlikely to present an accurate perspective of future improvements. In this sense, accurate biomarkers are necessary to confirm network engagement and help predict future outcome based on current network activity. The ideal biomarker would be one that tracks network activity in real time and correlates to symptomatic deficits. This would be akin to following ongoing EMG activity in the paralyzed muscles of a spinal cord injury patient undergoing a novel treatment. Although clinically the patient would go through periods of relapse from exhaustion, fluctuations in motivation, and exacerbation of medical conditions, the EMG could more accurately track the progressive increase in muscle fiber recruitment predicting gradual improvement over time.

Electrophysiological signals are a natural candidate for this type of biomarker in psychiatric conditions. Hypothetically, an electrophysiological signal could monitor the frequency and intensity of responses relevant to specific disorders: fear, avoidance, self-depreciation, drug craving, food craving, and cognitive performance. The existence of such biomarkers has been suggested in experiments studying fear responses in animal models. For example, preclinical studies using classical fear conditioning paradigms in animal models have reported the existence of recordable electrophysiological signals from the basolateral amygdala (BLA) that predict exposure to a reminder and subsequent fear response. During acquisition, the animal is presented with a positive conditioned stimulus (CS+), paired with a noxious stimulus such as a foot shock (the unconditioned stimulus, US) and a negative conditioned stimulus (CS−) that remains unpaired. During testing, the animal is presented with CS+ and CS− without the US while LFPs are recorded from the BLA. Cats exposed to foot shock (US) show a sustained increase in BLA neuronal firing and synchrony that peaks 30–50 min after exposure [53]. Rodents presented with CS+ showed an increase in the BLA local field potential (LFP) power in the low-gamma range (25–40 Hz) [62]. Stujenske et al. [63] recorded LFPs from the BLA, the mPFC, and the vHPC after classical fear conditioning. The BLA recordings revealed a theta power increase at about 6 Hz following exposure to the aversive CS+ [63]. This theta power increase is a particularly robust electrophysiological signal of fear state and it has been described in several other studies [64–67]. It is also possible to study specific oscillations from one nucleus in relation to the occurrence of another oscillation in a remote nucleus using phase-amplitude coupling analysis. When one nucleus is exerting influence on the activity of a remote nucleus, we theoretically find that high-frequency oscillations of the receiving nucleus align to the phase of slow oscillations of the influencing nucleus (i.e., the phase of the slow oscillation from the influencing nucleus determines when the fast oscillation in the receiving nucleus will occur). In fear conditioning, it has been suggested that the origin of the slow theta oscillation determines the ultimate behavioral response (fear vs. extinction). When the theta oscillation originates from the prefrontal cortex, the animal exhibits extinction, but when the theta originates from the BLA, a strong fear response is expected. As such, the theta power increase in the BLA and the associated theta-fast gamma coupling are described as the "neural signatures" of enhanced fear state [63] (i.e., hypervigilance).

Similarly, a putative biomarker has been identified in obesity. Mice exposed to different diets exhibit a significant increase in power in delta range field potentials prior to the consumption of high-fat diet but not prior to regular chow. Furthermore, stimulation triggered in response to the occurrence of this biomarker led to a reduction in hyperphagia in the mouse model [68].

These findings represent only examples of the existence of neural biomarkers underpinning symptomatic states. These types of critical neural signatures could be identified for each specific condition to track network engagement and disease fluctuations during the course of therapy. The introduction of new technologies that allow simultaneous recording and therapy for humans

with implanted devices will facilitate this quest for biomarkers.

Deploying New Technologies: Virtual Reality and Closed-Loop DBS

Virtual reality (VR) can enrich the content and the specificity of neural recordings. In animals, VR has been used to expose rodents to controlled environmental cues linked to a treadmill activity while the animal's head is fixated in a frame to permit whole cell neuronal recording (for review, Lee and Brecht [69]). These recordings have shed light on the neural mechanisms underlying the fluctuations in membrane potential of place cells as the animal goes through a place field [70]. In humans, VR has been used to study the effects of neuromodulation on spatial memory. Epilepsy patients undergoing depth electrode recordings are completing a task where they are asked to navigate to different locations in a virtual environment. The patients were found to have improved performance with stimulation of the entorhinal cortex but not the hippocampus, at the time of the acquisition. The stimulation triggered theta-phase resetting which is thought to facilitate learning [71].

The emergence of closed-loop DBS systems can also help with the identification of neural biomarkers. One such commercially available system is the responsive neurostimulation device (RNS, NeuroPace) used to modulate intractable epilepsy [72–74]. In those patients, the closed-loop RNS system detects pre-defined epileptiform discharges (i.e., the biomarker) and responds by emitting an electrical signal to abort upcoming seizures. The system also helps to track the severity of the illness over time by recording and compiling abnormal neural discharges on a monthly basis. The clinician can then track the outcome of a treatment (medication or neuromodulation) by following the frequency and intensity of the epileptiform discharges. A similar strategy could theoretically be employed in other conditions once specific biomarkers are identified and shown to correlate with symptomatic events. One advantage of an implantable system is that the biomarker recordings can be collected live under laboratory symptom-provoking conditions and also during real-life symptomatic phases. For example, Aghajan et al. [75] recorded hippocampal activity in freely moving patients and demonstrated an increase in the power of theta oscillations during movement compared to immobility. In this instance, the theta power could be seen as a biomarker of movement. Other manufacturers are developing similar implants. For example, Medtronic is expected to release a revised version of the Activa PC + S with the capability of on-demand stimulation in response to specific detections. In theory, the device should allow investigators to record neural activity in patients who have previously undergone DBS implant and now need a pulse generator replacement.

These recordings might also lend much needed credence to the largely subjective disease severity scales. In particular, neural activity could be collected during the symptomatic episodes of the patient. In addition, the biomarkers could be tracked over time in relation to the clinical fluctuations of the underlying condition.

Conclusion

Neuromodulation is confronting the future and expansion of its own utility. The perfect storm of history, technology, and anatomy of movement disorders[4] established the efficacy of the therapy, but the hoped-for broad applicability to brain circuit diseases remains shy. Despite using every available tool, results have been slow to materialize. The traditional approaches to neuromodulation innovation have relied on the translation of lesioning targets and the development of disease models using a combination of functional neuroimaging data, network modeling, and confirmation with animal models. Emerging approaches to innovation have, in part, focused on the identification of neural markers of disease states and the application of immersive technology in neuromodulation. As these strategies are deployed in a range of ailments, we will acquire the necessary data to challenge our current models of the conditions and further our knowledge.

References

1. Cooper IS. Ligation of the anterior choroidal artery for involuntary movements; parkinsonism. Psychiatry Q. 1953;27(2):317–9.
2. Association AP. Diagnostic and statistical manual of mental disorders: DSM-5. Washington, DC: American Psychiatric Association; 2013.
3. Duker AP, Espay AJ. Surgical treatment of Parkinson disease: past, present, and future. Neurol Clin. 2013;31(3):799–808.
4. Gardner J. A history of deep brain stimulation: technological innovation and the role of clinical assessment tools. Soc Stud Sci. 2013;43:707–28. © The Author(s) 2013.
5. Baier RR, Gardner RL, Coleman EA, Jencks SF, Mor V, Gravenstein S. Shifting the dialogue from hospital readmissions to unplanned care. Am J Manag Care. 2013;19(6):450–3.
6. Benabid AL, Pollak P, Louveau A, Henry S, de Rougemont J. Combined (thalamotomy and stimulation) stereotactic surgery of the VIM thalamic nucleus for bilateral Parkinson disease. Appl Neurophysiol. 1987;50(1–6):344–6.
7. Benabid AL, Wallace B, Mitrofanis J, et al. Therapeutic electrical stimulation of the central nervous system. C R Biol. 2005;328(2):177–86.
8. Stone JL. Dr. Gottlieb Burckhardt–the pioneer of psychosurgery. J Hist Neurosci. 2001;10(1):79–92.
9. O'Neal CM, Baker CM, Glenn CA, Conner AK, Sughrue ME. Dr. Robert G. Heath: a controversial figure in the history of deep brain stimulation. Neurosurg Focus. 2017;43(3):E12.
10. Heath RG. Pleasure and brain activity in man. Deep and surface electroencephalograms during orgasm. J Nerv Ment Dis. 1972;154(1):3–18.
11. Heath RG, Monroe RR, Mickle WA. Stimulation of the amygdaloid nucleus in a schizophrenic patient. Am J Psychiatry. 1955;111(11):862–3.
12. Nudeshima J, Taira T. A brief note on the history of psychosurgery in Japan. Neurosurg Focus. 2017;43(3):E13.
13. Patel SR, Aronson JP, Sheth SA, Eskandar EN. Lesion procedures in psychiatric neurosurgery. World Neurosurg. 2013;80(3–4):S31.e39–16.
14. Ballantine HT Jr, Bouckoms AJ, Thomas EK, Giriunas IE. Treatment of psychiatric illness by stereotactic cingulotomy. Biol Psychiatry. 1987;22(7):807–19.
15. Mindus P, Rasmussen SA, Lindquist C. Neurosurgical treatment for refractory obsessive-compulsive disorder: implications for understanding frontal lobe function. J Neuropsychiatry Clin Neurosci. 1994;6(4):467–77.
16. Jenike MA, Baer L, Ballantine T, et al. Cingulotomy for refractory obsessive-compulsive disorder. A long-term follow-up of 33 patients. Arch Gen Psychiatry. 1991;48(6):548–55.
17. Baer L, Rauch SL, Ballantine HT Jr, et al. Cingulotomy for intractable obsessive-compulsive disorder. Prospective long-term follow-up of 18 patients. Arch Gen Psychiatry. 1995;52(5):384–92.
18. Nuttin B, Cosyns P, Demeulemeester H, Gybels J, Meyerson B. Electrical stimulation in anterior limbs of internal capsules in patients with obsessive-compulsive disorder. Lancet. England;. 1999;354:1526.
19. Nuttin BJ, Gabriels LA, Cosyns PR, et al. Long-term electrical capsular stimulation in patients with obsessive-compulsive disorder. Neurosurgery. 2003;52(6):1263–72; discussion 1272–1264.
20. Melega WP, Lacan G, Gorgulho AA, Behnke EJ, De Salles AA. Hypothalamic deep brain stimulation reduces weight gain in an obesity-animal model. PLoS One. 2012;7(1):e30672.
21. Torres N, Chabardes S, Piallat B, Devergnas A, Benabid AL. Body fat and body weight reduction following hypothalamic deep brain stimulation in monkeys: an intraventricular approach. Int J Obes. 2012;36(12):1537–44.
22. Mayberg HS, Lozano AM, Voon V, et al. Deep brain stimulation for treatment-resistant depression. Neuron. 2005;45(5):651–60.
23. Lipsman N, Woodside B, Lozano AM. Evaluating the potential of deep brain stimulation for treatment-resistant anorexia nervosa. Handb Clin Neurol. 2013;116:271–6.
24. Lipsman N, Woodside DB, Giacobbe P, et al. Subcallosal cingulate deep brain stimulation for treatment-refractory anorexia nervosa: a phase 1 pilot trial. Lancet. 2013;381(9875):1361–70.
25. Lipsman N, Lam E, Volpini M, et al. Deep brain stimulation of the subcallosal cingulate for treatment-refractory anorexia nervosa: 1 year follow-up of an open-label trial. Lancet Psychiatry. 2017;4(4):285–94.
26. Ho AL, Sussman ES, Zhang M, et al. Deep brain stimulation for obesity. Cureus. 2015;7(3):e259.
27. Etkin A, Wager TD. Functional neuroimaging of anxiety: a meta-analysis of emotional processing in PTSD, social anxiety disorder, and specific phobia. Am J Psychiatry. 2007;164(10):1476–88.
28. Whiting AC, Oh MY, Whiting DM. Deep brain stimulation for appetite disorders: a review. Neurosurg Focus. 2018;45(2):E9.
29. Shin LM, Orr SP, Carson MA, et al. Regional cerebral blood flow in the amygdala and medial prefrontal cortex during traumatic imagery in male and female Vietnam veterans with PTSD. Arch Gen Psychiatry. 2004;61(2):168–76.
30. Mayberg HS, Liotti M, Brannan SK, et al. Reciprocal limbic-cortical function and negative mood: converging PET findings in depression and normal sadness. Am J Psychiatry. 1999;156(5):675–82.
31. Holtzheimer PE, Husain MM, Lisanby SH, et al. Subcallosal cingulate deep brain stimulation for treatment-resistant depression: a multisite, randomised, sham-controlled trial. Lancet Psychiatry. 2017;4(11):839–49.
32. Lujan JL, Chaturvedi A, Choi KS, et al. Tractography-activation models applied to subcallosal cingulate deep brain stimulation. Brain Stimul. 2013;6(5):737–9.

33. Riva-Posse P, Choi KS, Holtzheimer PE, et al. Defining critical white matter pathways mediating successful subcallosal cingulate deep brain stimulation for treatment-resistant depression. Biol Psychiatry. 2014;76(12):963–9.
34. Howell B, Choi KS, Gunalan K, Rajendra J, Mayberg HS, McIntyre CC. Quantifying the axonal pathways directly stimulated in therapeutic subcallosal cingulate deep brain stimulation. Hum Brain Mapp. 2019;40(3):889–903.
35. Riva-Posse P, Choi KS, Holtzheimer PE, et al. A connectomic approach for subcallosal cingulate deep brain stimulation surgery: prospective targeting in treatment-resistant depression. Mol Psychiatry. 2018;23(4):843–9.
36. Ahmari SE, Dougherty DD. Dissecting OCD circuits: from animal models to targeted treatments. Depress Anxiety. 2015;32(8):550–62.
37. Nestler EJ. Is there a common molecular pathway for addiction? Nat Neurosci. 2005;8(11):1445–9.
38. Wang J, Bina RW, Wingard JC, Terwilliger EF, Hammer RP Jr, Nikulina EM. Knockdown of tropomyosin-related kinase B receptor expression in the nucleus accumbens shell prevents intermittent social defeat stress-induced cross-sensitization to amphetamine in rats. Eur J Neurosci. 2014;39(6):1009–17.
39. Koob GF, Volkow ND. Neurocircuitry of addiction. Neuropsychopharmacology. 2010;35(1):217–38.
40. Luthi A, Luscher C. Pathological circuit function underlying addiction and anxiety disorders. Nat Neurosci. 2014;17(12):1635–43.
41. Luigjes J, van den Brink W, Feenstra M, et al. Deep brain stimulation in addiction: a review of potential brain targets. Mol Psychiatry. 2012;17(6):572–83.
42. Wang J, Bastle RM, Nikulina EM. VTA BDNF enhances social stress-induced compulsive cocaine bingeing. Oncotarget. 2017;8:5668–9.
43. Volkow ND, Wang GJ, Fowler JS, Tomasi D. Addiction circuitry in the human brain. Annu Rev Pharmacol Toxicol. 2012;52:321–36.
44. Gao G, Wang X, He S, et al. Clinical study for alleviating opiate drug psychological dependence by a method of ablating the nucleus accumbens with stereotactic surgery. Stereotact Funct Neurosurg. 2003;81(1–4):96–104.
45. Li N, Wang J, Wang XL, et al. Nucleus accumbens surgery for addiction. World Neurosurg. 2013;80(3–4):S28.e29–19.
46. Orellana C. Controversy over brain surgery for heroin addiction in Russia. Lancet Neurol. England;. 2002;1:333.
47. Voges J, Muller U, Bogerts B, Munte T, Heinze HJ. Deep brain stimulation surgery for alcohol addiction. World Neurosurg. 2013;80(3–4):S28.e21–31.
48. Muller UJ, Sturm V, Voges J, et al. Successful treatment of chronic resistant alcoholism by deep brain stimulation of nucleus accumbens: first experience with three cases. Pharmacopsychiatry. 2009;42(6):288–91.
49. Muller UJ, Voges J, Steiner J, et al. Deep brain stimulation of the nucleus accumbens for the treatment of addiction. Ann N Y Acad Sci. 2013;1282:119–28.
50. Muller UJ, Sturm V, Voges J, et al. Nucleus accumbens deep brain stimulation for alcohol addiction - safety and clinical long-term results of a pilot trial. Pharmacopsychiatry. 2016;49(4):170–3.
51. Clinical Trials. https://clinicaltrials.gov/ct2/show/NCT01245075; https://clinicaltrials.gov/ct2/show/NCT02282072. Accessed 2 Jan 2019; 2019.
52. Tovote P, Fadok JP, Luthi A. Neuronal circuits for fear and anxiety. Nat Rev Neurosci. 2015;16(6):317–31.
53. Pelletier JG, Likhtik E, Filali M, Pare D. Lasting increases in basolateral amygdala activity after emotional arousal: implications for facilitated consolidation of emotional memories. Learn Mem. 2005;12(2):96–102.
54. Stidd DA, Vogelsang K, Krahl SE, Langevin JP, Fellous JM. Amygdala deep brain stimulation is superior to paroxetine treatment in a rat model of posttraumatic stress disorder. Brain Stimul. 2013;6(6):837–44.
55. Langevin JP, De Salles AA, Kosoyan HP, Krahl SE. Deep brain stimulation of the amygdala alleviates post-traumatic stress disorder symptoms in a rat model. J Psychiatr Res. 2010;44(16):1241–5.
56. Langevin JP. The amygdala as a target for behavior surgery. Surg Neurol Int. 2012;3(Suppl 1):S40–6.
57. Langevin JP, Chen JW, Koek RJ, et al. Deep brain stimulation of the basolateral amygdala: targeting technique and electrodiagnostic findings. Brain Sci. 2016;6(3)
58. Lozano AM, Mayberg HS, Giacobbe P, Hamani C, Craddock RC, Kennedy SH. Subcallosal cingulate gyrus deep brain stimulation for treatment-resistant depression. Biol Psychiatry. 2008;64(6):461–7.
59. Greenberg BD, Malone DA, Friehs GM, et al. Three-year outcomes in deep brain stimulation for highly resistant obsessive-compulsive disorder. Neuropsychopharmacology. 2006;31(11):2384–93.
60. Raymaekers S, Vansteelandt K, Luyten L, et al. Long-term electrical stimulation of bed nucleus of stria terminalis for obsessive-compulsive disorder. Mol Psychiatry. 2017;22(6):931–4.
61. Widge AS, Deckersbach T, Eskandar EN, Dougherty DD. Deep brain stimulation for treatment-resistant psychiatric illnesses: what has gone wrong and what should we do next? Biol Psychiatry. 2016;79(4):e9–10.
62. Fenton GE, Spicer CH, Halliday DM, Mason R, Stevenson CW. Basolateral amygdala activity during the retrieval of associative learning under anesthesia. Neuroscience. 2013;233:146–56.
63. Stujenske JM, Likhtik E, Topiwala MA, Gordon JA. Fear and safety engage competing patterns of theta-gamma coupling in the basolateral amygdala. Neuron. 2014;83(4):919–33.
64. Likhtik E, Stujenske JM, Topiwala MA, Harris AZ, Gordon JA. Prefrontal entrainment of amygdala activity signals safety in learned fear and innate anxiety. Nat Neurosci. 2014;17(1):106–13.

65. Popa D, Duvarci S, Popescu AT, Lena C, Pare D. Coherent amygdalocortical theta promotes fear memory consolidation during paradoxical sleep. Proc Natl Acad Sci U S A. 2010;107(14):6516–9.
66. Seidenbecher T, Laxmi TR, Stork O, Pape HC. Amygdalar and hippocampal theta rhythm synchronization during fear memory retrieval. Science. 2003;301(5634):846–50.
67. Pare D, Collins DR. Neuronal correlates of fear in the lateral amygdala: multiple extracellular recordings in conscious cats. J Neurosci. 2000;20(7):2701–10.
68. Wu H, Miller KJ, Blumenfeld Z, et al. Closing the loop on impulsivity via nucleus accumbens delta-band activity in mice and man. Proc Natl Acad Sci U S A. 2018;115(1):192–7.
69. Lee AK, Brecht M. Elucidating neuronal mechanisms using intracellular recordings during behavior. Trends Neurosci. 2018;41(6):385–403.
70. Harvey CD, Collman F, Dombeck DA, Tank DW. Intracellular dynamics of hippocampal place cells during virtual navigation. Nature. 2009;461(7266):941–6.
71. Suthana N, Haneef Z, Stern J, et al. Memory enhancement and deep-brain stimulation of the entorhinal area. N Engl J Med. 2012;366(6):502–10.
72. Fountas KN, Smith JR. A novel closed-loop stimulation system in the control of focal, medically refractory epilepsy. Acta Neurochir Suppl. 2007;97(Pt 2):357–62.
73. Morrell MJ. Responsive cortical stimulation for the treatment of medically intractable partial epilepsy. Neurology. 2011;77(13):1295–304.
74. Sprengers M, Vonck K, Carrette E, Marson AG, Boon P. Deep brain and cortical stimulation for epilepsy. Cochrane Database Syst Rev. 2017;7:Cd008497.
75. M Aghajan Z, Schuette P, Fields TA, et al. Theta oscillations in the human medial temporal lobe during real-world ambulatory movement. Curr Biol. 2017;27(24):3743–3751.e3743.

36

Imaging: Patient Selection, Targeting, and Outcome Biomarkers

Vibhor Krishna, Nicole A. Young, and Francesco Sammartino

With over three decades of experience in clinical applications of deep brain stimulation (DBS), three critical predictors of successful outcomes have emerged : precise stereotactic targeting of the stimulation target [1, 2], systematic stimulation titration [3], and selection of appropriate candidates [4, 5]. Therefore, significant effort should be focused on further refining these processes. This effort has been bolstered because recent investigations uncovered the mechanisms underlying DBS efficacy, specifically via the network modulation framework. Initially, the "functional lesion" hypothesis was proposed to explain the efficacy of DBS [6, 7] because high-frequency stimulation (HFS) decreased local neuronal firing rates [8, 9] and DBS-induced clinical effects were similar to lesioning and muscimol injections [10–12]. This effect is presumably mediated by depolarization block, inactivation of voltage-dependent channels [13], functional deafferentation [8, 9], or synaptic inhibition [14]. However, DBS has both short- and long-term clinical effects that are not fully explained by a functional lesion; for example, stimulation-induced parkinsonian tremor arrest is immediate [15], while bradykinesia and gait improvement may take longer [16]. Similarly, phasic dystonic symptoms improve within hours to days, while tonic movements take a few months to improve [17–19]. Additionally, the functional lesion hypothesis does not explain DBS efficacy in both hypokinetic (rigidity and bradykinesia) and hyperkinetic (tremor, dystonia, or dyskinesia) movement disorders [20–22]. These observations have led us to believe that clinical improvement with DBS likely involves a combination of therapeutic mechanisms. In addition to local effects, DBS modulates activity in distant but interconnected brain regions (or brain networks), through the stimulation of axonal tracts within the field of stimulation [23]. Functional neuroimaging and direct neuronal recordings have allowed us to observe distinct local and network-level effects of DBS [24–26]. Diagnostic modalities like scalp electroencephalogram (EEG;[27, 28]), magnetoencephalogram (MEG; [29]), transcranial magnetic stimulation [30], positron emission tomography (PET; [31]), and single positron emission tomography [32] have contributed toward the emerging evidence of network effects of DBS.

V. Krishna (✉)
Departments of Neurosurgery and Neuroscience, Center for Neuromodulation, The Ohio State University, Columbus, OH, USA
e-mail: Vibhor.Krishna@osumc.edu

N. A. Young
Department of Neuroscience, The Ohio State University Wexner Medical Center, Columbus, OH, USA

F. Sammartino
Center for Neuromodulation, The Ohio State University, Columbus, OH, USA

N. Pouratian, S. A. Sheth (eds.), *Stereotactic and Functional Neurosurgery*,
https://doi.org/10.1007/978-3-030-34906-6_36

Overall, the network modulation framework represents a paradigm shift in our approach to patient care and research. In this chapter, we discuss three major implications of integrating this approach: (1) identification of therapeutic zones using tractography, (2) optimization of stimulation parameters to address patient-specific network dysfunction, and (3) improved patient selection based on markers for network dysfunction in addition to clinical phenotypes. These implications are discussed in separate sections and include the current progress being made, as well as potential future developments, in these three areas.

Identification of Therapeutic Zones Using Tractography

It is generally accepted that precise stereotactic targeting is associated with excellent surgical outcomes [1, 2, 33]. The most immediate application for the network modulation framework involves the visualization of specific brain networks for stereotactic targeting [34]. For this purpose, diffusion tensor imaging (DTI), or tractography, is the most appropriate technique to non-invasively delineate the white matter tracts in the brain [35]. The tensor calculation is based on a voxel-wise analysis of degree and direction of restriction (or anisotropy) of water molecules in the extracellular matrix. The principal determinant of this diffusion anisotropy is the laminar organization of cell membranes and myelin sheaths [36]. Typically, the anisotropy is higher in white matter (>0.2) than in gray matter (<0.2). The anatomical connections reconstructed by the propagation of calculated tensor across distant brain regions are commonly referred to as structural connectivity, in contrast with functional connectivity, which is derived from functional magnetic resonance imaging (fMRI; [35]). Structural connectivity has been shown to correlate well with the anatomy in the region of white matter tracts [37], but the interpretation of structural connectivity from regions of interests (ROIs) within gray matter is more complex. Overall, the large projection axons are still the major determinant of anisotropy within gray matter [36, 38]. Therefore, structural connectivity within gray matter represents the major afferent and efferent connections and is clinically relevant for (1) identifying gray matter nuclei with extensive network connectivity ("nodes") and (2) developing imaging biomarkers for surgical targeting to modulate their activity with DBS.

The computation of the tensor can be performed using either probabilistic or deterministic tractography. Probabilistic tractography methods estimate the probability of structural connectivity at each voxel and are better suited for investigations designed to gain mechanistic insights or discover novel pathways [39, 40]. From its initial implementation (Fiber Assignment by Continuous Tracking [FACT] algorithm;[41]) to the newer methods that take into consideration the problem of crossing fibers [42], deterministic tractography performs tracking based on the estimation of the principal direction of eigenvector at each voxel. This approach is useful for clinical applications because of its ease of use, clinical approval, and integration with current stereotactic targeting software [43]. Although higher-order tractography models (e.g., high angular resolution diffusion imaging [HARDI]) address some of the shortcomings of traditional DTI models [44], their implementation for clinical use is not yet established. The diffusion tensor (DT) model characterizes the orientation dependence of the diffusion probability density function (pdf) of the water molecules. An important limitation of the DT model is the Gaussian diffusion assumption, which implies that there can only be a single fiber population per voxel. At the resolution of DTI acquisitions, this is an important problem since many voxels have low anisotropy index due to non-Gaussian diffusion from multiple fibers crossing, branching, fanning, or in a bottleneck. Thus, tractography algorithms based on the DT model can follow false tracts due to diffusion profiles that are prolate or prematurely stop in regions of isotropic tensors. New higher-resolution acquisition techniques such as diffusion spectrum imaging (DSI), HARDI, and Q-ball imaging (QBI) have been proposed to estimate the orientation distribution function (ODF) of water molecules and overcome the limitations of the DT model. These algorithms deal with the

non-Gaussian diffusion process and reconstruct spherical functions with potentially multiple maxima aligned with the underlying fiber populations. Overall, the availability of multi-core computers has ignited the quest for more advanced models of diffusivity to tackle the shortcomings of "classic" DT algorithms, especially in patients with neurodegeneration or malignant white matter infiltration (e.g., glial neoplasms). The primary benefit of these non-parametric algorithms is their ability to model multiple fibers in each voxel, which is of paramount interest in neurosurgery and neuroscience in general. The approach developed by Yeh et al. proposes a solution for inappropriate fiber termination and partial volume problems by using an ODF-based index scaled with spin density information [45]. In an in vivo study, this group showed that the newly developed diffusion metric, quantitative anisotropy (QA), had less noise, and the QA-aided tractography had better spatial resolution than the fractional anisotropy [FA]-aided or the generalized fractional anisotropy [GFA]-aided tractography. In addition, this new non-parametric diffusion algorithm models the diffusivity of free water in each voxel, which can be removed to improve the signal in areas with partial volume effect (e.g., edema, neurodegeneration). Our group has recently demonstrated that a metric based on this approach, restricted diffusion imaging [46], outperformed conventional tensor-based metrics like FA and MD in delineating long-term microstructural changes after focused ultrasound thalamotomy [47]. Among the various algorithms for deterministic tractography, the streamline algorithm has high specificity (low false-positive rate), making it particularly useful for stereotactic targeting [40].

Tractography markers for efficacious DBS stimulation are now being investigated. For example, Klein et al. compared the structural connectivity of therapeutic versus non-therapeutic ventral intermediate medial (VIM) DBS contacts using probabilistic tractography [48]; they concluded that therapeutic DBS contacts had significant cerebellar (dentate nucleus) and motor cortex connectivity in contrast to the cerebellar (hemispheric) and premotor connectivity of the non-efficacious contacts. Similar conclusions have been drawn from studies in PD patients with subthalamic nucleus (STN) DBS, where the hyperdirect pathway is proposed to be the imaging marker associated with efficacious stimulation [49, 50].

Based on these observations of tractography correlates of clinical outcomes, a tractography-based VIM targeting method was recently published for tremor surgery [43, 51]. Currently, neurosurgeons rely on formulaic methods because the VIM nucleus is not visible on the conventional 1.5 T or 3 T magnetic resonance imaging (MRI; [52]). For this reason, improved visualization of this therapeutic target with tractography has the potential to improve clinical outcomes. To maximize the anatomical accuracy of this method for clinical application, the scan acquisition and pre-processing steps were optimized. In this method, the lateral and posterior borders of the VIM were first visualized by tracking the pyramidal tract (PT) and medial lemniscus (ML) using streamline tractography (StealthViz, Medtronic Inc., Minneapolis, MN; Fig. 36.1).

These tracks are important to avoid PT- and ML-related side effects (contractions and motor paralysis and paresthesias and sensory deficits, respectively). In the next step, a VIM ROI was created in relation to the borders (at a safe distance of 3 mm each from the PT and ML). The size of the ROI was kept constant at $4 \times 4 \times 6$ mm to match the dimensions of the human VIM. If the VIM ROI overlapped with the anatomical VIM, it was structurally connected to the ipsilateral motor cortex (M1) and both ipsilateral and contralateral cerebellum (specifically, the dentate nucleus). This method was found to be accurate for prospective stereotactic targeting of the VIM, and the short-term tremor control outcomes were satisfactory.

With increasing application of powerful preclinical techniques like optogenetics, we will develop a better understanding of therapeutic networks of clinical interest that mediate therapeutic efficacy, as well as those that cause undesirable side effects [17, 53–57]. Translational applications of this research, coupled with the development of electrode designs with current steering capabilities (i.e., the electrode design allows

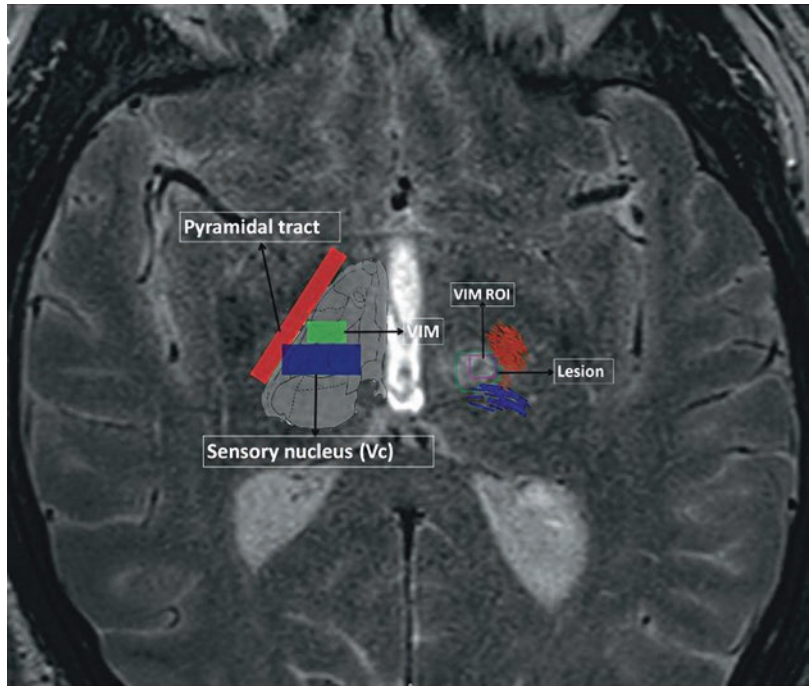

Fig. 36.1 The methodology for VIM nucleus targeting using DTI-based identification of the "safety" margins (PT and ML tracks). (From Krishna et al. [112]. Reprinted with permission from Oxford University Press)

directing the spread of electrical current in a particular direction), will be important to optimize outcomes and minimize stimulation-associated side effects. The next generation of implantable electrodes [58] incorporates multiple microelectrode contacts, rather than a few macroelectrode contacts, to increase the surface area for stimulation delivery and potentially activate more neural elements in their proximity [59]. Although multiple-source current steering will help shape electrical fields to optimize benefits [60], it also poses a significant challenge for stimulation titration and programming. In the next section, we discuss the incorporation of network dynamics for efficient DBS titration.

Optimization of Stimulation Parameters to Address Patient-Specific Network Dysfunction

The current understanding of DBS-mediated network modulation is derived from data collected from post-processed scalp EEG [61–64] or invasive intracranial recordings [53, 65–69]. Recently, de Hemptinne and colleagues investigated the network-level effects of STN DBS using electrocorticography from the motor cortex [70, 71]. STN stimulation reduced the phase amplitude coupling between beta (13–30 Hz) and broadband gamma (50–200 Hz) oscillations in the primary motor cortex (M1). Crucially, this reduction in beta-broadband gamma coupling was concurrent with improvement in Parkinsonian motor symptoms. These observations underscore the importance of incorporating the network-level effects of DBS in the design of a closed-loop system [72]. By individualizing therapy, this approach may allow for stimulation at lower amplitude or duration for better therapeutic effects, as well as prolonged battery life. Other approaches for closed-loop design include feedback from local neuronal signals [73, 74] or patients' clinical state by measuring peripheral activity [17, 67, 68, 75–84]. A closed-loop stimulation system will eventually emerge based on the overall feasibility of designs (surgical risks associated with additional electrodes for measuring cortical activity, technological challenges of incorporating the necessary computational power.) and clinical usefulness.

In addition to physiology, functional neuroimaging can also improve the understanding of network integration of implanted DBS electrodes. Probabilistic tractography is ideal for this application because it provides objective estimates of structural connectivity [35]. Based on the modeling of current spread in vivo [85–87], realistic models of the volume of tissue activated (VTA) can be created and used as a seed for probabilistic tractography by fitting a Bayesian model of fiber distribution at each voxel [88]. The different patterns of connectivity generated can be input into an automated pipeline to simulate different settings and predict the likelihood of stimulation-related clinical efficacy and side effects in advance of stimulation titration (Fig. 36.2).

Our group has recently shown that a machine-learning classifier trained on the connectivity fingerprint associated with each stimulation-induced acute clinical effect (ACE) was able to rank STN DBS contacts solely based on the associated connections. The efficacious contact predicted by this algorithm matched with the contact being stimulated in the long-term (1 year) [89]. Active investigations are underway to define the clinical correlates of structural connectivity for clinical effects associated with acute and chronic stimulation (Fig. 36.3). This approach, by itself, may not be sufficient for finer stimulation titration; therefore, a complementary line of research to investigate stimulation-induced network modulation in real time is important.

fMRI is increasingly being used to define network dysfunction in neurological and psychiatric disorders [90, 91], but patients with DBS implants cannot undergo 3 T MRI due to electrode heating safety concerns [92, 93]. Functional connectivity studies in DBS ON and OFF conditions in the 1.5 T MRI environment provide initial insights into DBS-mediated network modulation [94, 95]; however, 3 T MRI remains the modality of choice for the non-invasive study of brain networks due to better image resolution than 1.5 T [96]. Although there have been several recent animal investigations delineating changes in functional connectivity under DBS ON and OFF conditions, human studies are strikingly lacking [97–99]. The first human safety study of 3 T MRI in PD patients with externalized bilateral DBS electrodes was published by Phillips et al. in 2006 [24]. A more recent study confirmed the safety of 3 T MRI with a fully implanted DBS system in the OFF condition [100]. More safety studies of 3 T imaging in patients with an implanted DBS system are needed to discover the fMRI correlates of various stimulation parameters. This transformative research may allow us to develop an objective fMRI-based feedback metric to optimize stimulation parameters and potentially improve clinical outcomes. As we learn more about the network-based predictors of outcomes after DBS, we can extend this knowledge to inform patient selection, as discussed in the next section.

Improved Patient Selection Based on Network Dynamics

Although the clinical effects of DBS are often dramatic, the consistency and durability of clinical improvement remain variable [101, 102]. Among the predictors of outcomes, the selection of appropriate patients is most important [4]. For this reason, the possibility of patient selection with objective measures of network dynamics remains the most promising and potentially transformative application of the network modulation framework.

Network dysfunction in neurodegenerative diseases presents with the development of pathological rhythms due to loss of neurons, inadequate neurotransmitter modulation, etc. [103, 104]. Similar evidence of network dysfunction is beginning to emerge for psychiatric disorders [62, 105]. Although abnormal connectivity has been investigated with conventional scalp EEG, more recent studies have acquired invasive neural recordings and functional neuroimaging, and these methods have played an increasing role in defining disorders [105, 106]. As discussed earlier, the two imaging-based parameters of interest are structural connectivity, reflecting direct axonal projections, and functional connectivity, as a surrogate of coordinated neuronal activity mediated by neural oscillations. Functional stud-

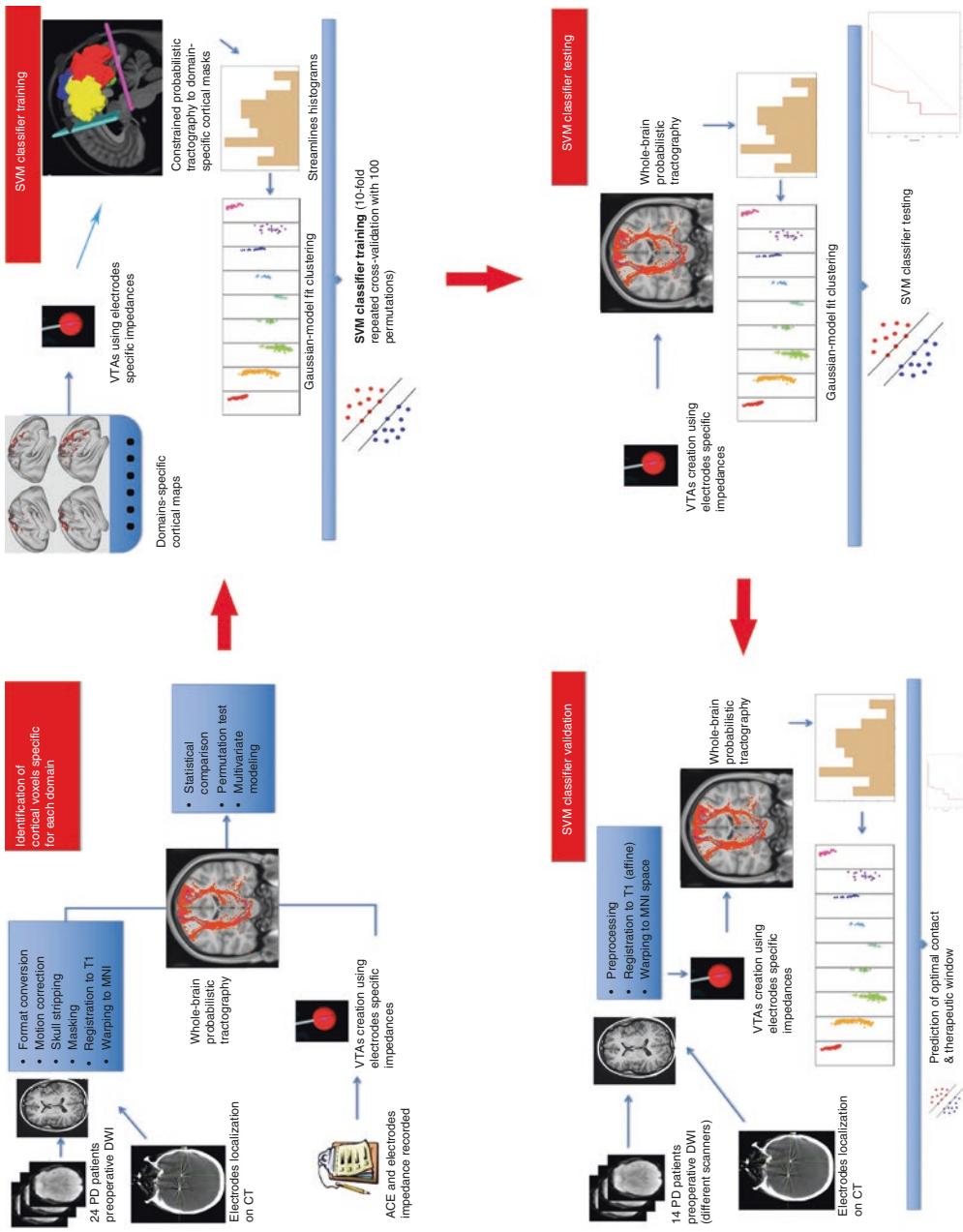

Fig. 36.2 Illustration of the automated machine-learning pipeline for STN DBS contact selection based solely on connectivity.(From Krishna et al. [89]. Reprinted with permission from John Wiley and Sons)

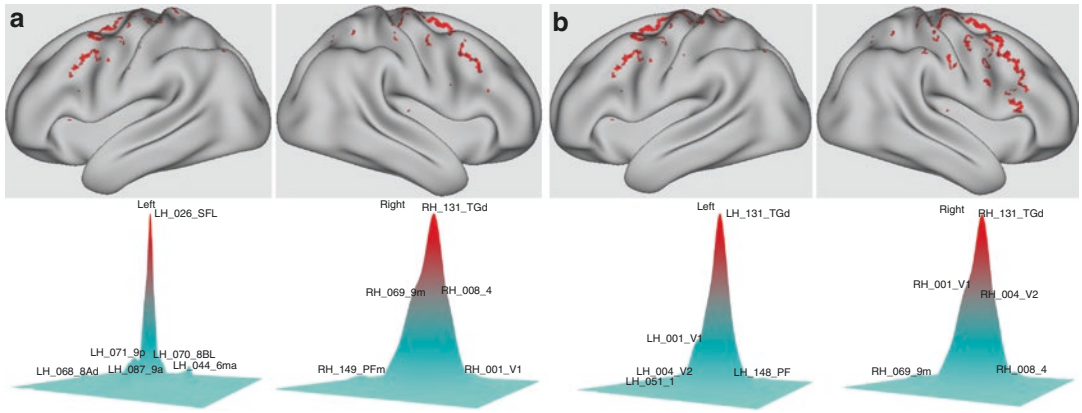

Fig. 36.3 Summary of cortical voxels associated with efficacy. (**a**) Improvements in rigidity, bradykinesia, and tremor and side effects (**b**) sensory, motor, and visual. (From Krishna et al. [89]. Reprinted with permission from John Wiley and Sons)

ies, especially using 3 T MRI, will be an essential tool to non-invasively estimate network dynamics in the human brain [23, 65, 90, 97]. The blood oxygen level-dependent (BOLD) signals measured by functional MRI are also thought to correlate with local field potential activity [107]. In addition to the network dynamics in resting state, transient perturbation of the network of interest with non-invasive approaches like transcranial magnetic stimulation, coupled with EEG or fMRI, can be investigated for potentially screening patients for invasive neuromodulation. Similarly, the stimulation capabilities of low-frequency focused ultrasound could also be used to study network dynamics with transient therapeutic neuromodulation since this technology has the capability of targeting deep brain structures [108].

Although DTI has been primarily used to visualize structural connectivity in the brain, a quantitative assessment of water diffusion with FA and diffusivity (axial and radial) can be a marker of microstructural integrity and neuronal degeneration [109]. The changes in diffusion metrics are disease- and network-specific; for example, in amyotrophic lateral sclerosis, the FA is significantly lower in the internal capsule, peduncles, pons, and pyramids in comparison to controls [110]. Similarly, the FA changes in essential tremor are most pronounced in the dentate nucleus and superior cerebellar peduncles [111]. The eventual screening modality may involve a combination of different estimates of both structural and functional network connectivity.

Conclusion

DBS has been proven to be highly efficacious in Parkinson's disease, essential tremor, dystonia, and obsessive-compulsive disorder. Recent evidence demonstrates that the pathology of neural networks underlies many neurological and psychiatric disorders and that restoration of these networks to a more "normal" state with DBS can improve clinical symptoms. It is increasingly clear that the stimulation of critical nodes within specific brain networks improves clinical symptoms without reversing the underlying pathology. This modulation of brain networks is mediated by axonal stimulation and resetting pathological oscillation. Integration of the network modulation framework in DBS clinical practice has significant implications for the field, such as in the identification of therapeutic zones with tractography. Future investigations may begin by characterizing the network dysfunction associated with a specific symptom (or a symptom complex) within the overall clinical syndrome. The identification of specific network dysfunction will then allow (a) a critical analysis of the potential therapeutic targets, (b) identification of titratable

markers of network dysfunction for objective feedback, and, eventually, (c) discovery of the most efficient parameters for closed-loop stimulation.

References

1. Sammartino F, Krishna V, King NK, Bruno V, Kalia S, Hodaie M, et al. Sequence of electrode implantation and outcome of deep brain stimulation for Parkinson's disease. J Neurol Neurosurg Psychiatry. 2016;87(8):859–63.
2. Papavassiliou E, Rau G, Heath S, Abosch A, Barbaro NM, Larson PS, et al. Thalamic deep brain stimulation for essential tremor: relation of lead location to outcome. Neurosurgery. 2004;54(5):1120–30; discussion 9–30.
3. Okun MS, Tagliati M, Pourfar M, Fernandez HH, Rodriguez RL, Alterman RL, et al. Management of referred deep brain stimulation failures: a retrospective analysis from 2 movement disorders centers. Arch Neurol. 2005;62(8):1250–5.
4. Bronstein JM, Tagliati M, Alterman RL, Lozano AM, Volkmann J, Stefani A, et al. Deep brain stimulation for Parkinson disease: an expert consensus and review of key issues. Arch Neurol. 2011;68(2):165.
5. Filkowski MM, Mayberg HS, Holtzheimer PE. Considering eligibility for studies of deep brain stimulation for treatment-resistant depression: insights from a clinical trial in unipolar and bipolar depression. J ECT. 2016;32(2):122–6.
6. Benazzouz A, Gross C, Feger J, Boraud T, Bioulac B. Reversal of rigidity and improvement in motor performance by subthalamic high-frequency stimulation in MPTP-treated monkeys. Eur J Neurosci. 1993;5(4):382–9.
7. Benazzouz A, Piallat B, Pollak P, Benabid AL. Responses of substantia nigra pars reticulata and globus pallidus complex to high frequency stimulation of the subthalamic nucleus in rats: electrophysiological data. Neurosci Lett. 1995;189(2):77–80.
8. Meissner W, Leblois A, Hansel D, Bioulac B, Gross CE, Benazzouz A, et al. Subthalamic high frequency stimulation resets subthalamic firing and reduces abnormal oscillations. Brain. 2005;128(Pt 10):2372–82.
9. Filali M, Hutchison WD, Palter VN, Lozano AM, Dostrovsky JO. Stimulation-induced inhibition of neuronal firing in human subthalamic nucleus. Exp Brain Res. 2004;156(3):274–81.
10. Pahapill PA, Levy R, Dostrovsky JO, Davis KD, Rezai AR, Tasker RR, et al. Tremor arrest with thalamic microinjections of muscimol in patients with essential tremor. Ann Neurol. 1999;46(2):249–52.
11. Lozano AM, Lang AE, Galvez-Jimenez N, Miyasaki J, Duff J, Hutchinson WD, et al. Effect of GPi pallidotomy on motor function in Parkinson's disease. Lancet. 1995;346(8987):1383–7.
12. Schuurman PR, Bosch DA, Bossuyt PM, Bonsel GJ, van Someren EJ, de Bie RM, et al. A comparison of continuous thalamic stimulation and thalamotomy for suppression of severe tremor. N Engl J Med. 2000;342(7):461–8.
13. Beurrier C, Bioulac B, Audin J, Hammond C. High-frequency stimulation produces a transient blockade of voltage-gated currents in subthalamic neurons. J Neurophysiol. 2001;85(4):1351–6.
14. Zucker RS, Regehr WG. Short-term synaptic plasticity. Annu Rev Physiol. 2002;64:355–405.
15. Hristova A, Lyons K, Troster AI, Pahwa R, Wilkinson SB, Koller WC. Effect and time course of deep brain stimulation of the globus pallidus and subthalamus on motor features of Parkinson's disease. Clin Neuropharmacol. 2000;23(4):208–11.
16. Fasano A, Deuschl G. Therapeutic advances in tremor. Mov Disord. 2015;30(11):1557–65.
17. Udupa K, Chen R. The mechanisms of action of deep brain stimulation and ideas for the future development. Prog Neurobiol. 2015;133:27–49.
18. Udupa K, Ghahremani A, Chen R. Are we close to the advent of closed loop deep brain stimulation in Parkinson's disease? Mov Disord. 2015;30(10):1326.
19. Lee JY, Deogaonkar M, Rezai A. Deep brain stimulation of globus pallidus internus for dystonia. Parkinsonism Relat Disord. 2007;13(5):261–5.
20. Marsden CD, Obeso JA. The functions of the basal ganglia and the paradox of stereotaxic surgery in Parkinson's disease. Brain. 1994;117(Pt 4):877–97.
21. Vitek JL. Deep brain stimulation: how does it work? Cleve Clin J Med. 2008;75 Suppl 2:S59–65.
22. McCairn KW, Iriki A, Isoda M. Common therapeutic mechanisms of pallidal deep brain stimulation for hypo- and hyperkinetic movement disorders. J Neurophysiol. 2015;114(4):2090–104.
23. van Hartevelt TJ, Cabral J, Deco G, Moller A, Green AL, Aziz TZ, et al. Neural plasticity in human brain connectivity: the effects of long term deep brain stimulation of the subthalamic nucleus in Parkinson's disease. PLoS One. 2014;9(1):e86496.
24. Phillips MD, Baker KB, Lowe MJ, Tkach JA, Cooper SE, Kopell BH, et al. Parkinson disease: pattern of functional MR imaging activation during deep brain stimulation of subthalamic nucleus--initial experience. Radiology. 2006;239(1):209–16.
25. Rezai AR, Lozano AM, Crawley AP, Joy ML, Davis KD, Kwan CL, et al. Thalamic stimulation and functional magnetic resonance imaging: localization of cortical and subcortical activation with implanted electrodes. Technical note. J Neurosurg. 1999;90(3):583–90.
26. Lee KH, Chang SY, Roberts DW, Kim U. Neurotransmitter release from high-frequency stimulation of the subthalamic nucleus. J Neurosurg. 2004;101(3):511–7.
27. Ashby P, Paradiso G, Saint-Cyr JA, Chen R, Lang AE, Lozano AM. Potentials recorded at the scalp by stimulation near the human subthalamic nucleus. Clin Neurophysiol. 2001;112(3):431–7.

28. Silberstein P, Pogosyan A, Kuhn AA, Hotton G, Tisch S, Kupsch A, et al. Cortico-cortical coupling in Parkinson's disease and its modulation by therapy. Brain. 2005;128(Pt 6):1277–91.
29. Litvak V, Eusebio A, Jha A, Oostenveld R, Barnes GR, Penny WD, et al. Optimized beamforming for simultaneous MEG and intracranial local field potential recordings in deep brain stimulation patients. NeuroImage. 2010;50(4):1578–88.
30. Kuriakose R, Saha U, Castillo G, Udupa K, Ni Z, Gunraj C, et al. The nature and time course of cortical activation following subthalamic stimulation in Parkinson's disease. Cereb Cortex (New York, NY: 1991). 2010;20(8):1926–36.
31. Ko JH, Tang CC, Eidelberg D. Brain stimulation and functional imaging with fMRI and PET. Handb Clin Neurol. 2013;116:77–95.
32. Paschali A, Constantoyannis C, Angelatou F, Vassilakos P. Perfusion brain SPECT in assessing motor improvement after deep brain stimulation in Parkinson's disease. Acta Neurochir. 2013;155(3):497–505.
33. Hamel W, Köppen JA, Alesch F, Antonini A, Barcia JA, Bergman H, et al. Targeting of the subthalamic nucleus for deep brain stimulation: a survey among Parkinson disease specialists. World Neurosurg. 2017;99:41–6.
34. Accolla EA, Herrojo Ruiz M, Horn A, Schneider GH, Schmitz-Hubsch T, Draganski B, et al. Brain networks modulated by subthalamic nucleus deep brain stimulation. Brain. 2016;139(Pt 9):2503–15.
35. Mori S, Zhang J. Principles of diffusion tensor imaging and its applications to basic neuroscience research. Neuron. 2006;51(5):527–39.
36. Beaulieu C. The basis of anisotropic water diffusion in the nervous system – a technical review. NMR Biomed. 2002;15(7–8):435–55.
37. Jbabdi S, Lehman JF, Haber SN, Behrens TE. Human and monkey ventral prefrontal fibers use the same organizational principles to reach their targets: tracing versus tractography. J Neurosci. 2013;33(7):3190–201.
38. Krishna V, Sammartino F, Yee P, Mikulis D, Walker M, Elias G, et al. Diffusion tensor imaging assessment of microstructural brainstem integrity in Chiari malformation Type I. J Neurosurg. 2016;125(5):1112–9.
39. Behrens TEJ, Johansen-Berg H, Woolrich MW, Smith SM, Wheeler-Kingshott CAM, Boulby PA, et al. Non-invasive mapping of connections between human thalamus and cortex using diffusion imaging. Nat Neurosci. 2003;6(7):750–7.
40. Thomas C, Ye FQ, Irfanoglu MO, Modi P, Saleem KS, Leopold DA, et al. Anatomical accuracy of brain connections derived from diffusion MRI tractography is inherently limited. Proc Natl Acad Sci U S A. 2014;111(46):16574–9.
41. Mori S, Crain BJ, Chacko VP, van Zijl PC. Three-dimensional tracking of axonal projections in the brain by magnetic resonance imaging. Ann Neurol. 1999;45(2):265–9.
42. Taylor PA, Saad ZS. FATCAT: (an efficient) Functional and Tractographic Connectivity Analysis Toolbox. Brain Connect. 2013;3(5):523–35.
43. Sammartino F, Krishna V, King NK, Lozano AM, Schwartz ML, Huang Y, et al. Tractography-based ventral intermediate nucleus targeting: novel methodology and intraoperative validation. Mov Disord. 2016;31(8):1217–25.
44. Descoteaux M. High angular resolution diffusion imaging (HARDI). In: Webster JG, editor. Wiley encyclopedia of electrical and electronics engineering. Hoboken, NJ: Wiley; 2015.
45. Yeh F-C, Verstynen TD, Wang Y, Fernández-Miranda JC, W-YIJPo T. Deterministic diffusion fiber tracking improved by quantitative anisotropy. PLoS One. 2013;8(11):e80713.
46. Yeh F-C, Wedeen VJ, W-YIJItomi T. Generalized ${q} $-Sampling. Imaging. 2010;29(9):1626–35.
47. Sammartino F, Yeh F-C, VJNC K. Longitudinal analysis of structural changes following unilateral focused ultrasound thalamotomy. Neuroimage Clin. 2019;22:101754.
48. Klein JC, Barbe MT, Seifried C, Baudrexel S, Runge M, Maarouf M, et al. The tremor network targeted by successful VIM deep brain stimulation in humans. Neurology. 2012;78(11):787–95.
49. Vanegas-Arroyave N, Lauro PM, Huang L, Hallett M, Horovitz SG, Zaghloul KA, et al. Tractography patterns of subthalamic nucleus deep brain stimulation. Brain. 2016;139(Pt 4):1200–10.
50. Oswal A, Beudel M, Zrinzo L, Limousin P, Hariz M, Foltynie T, et al. Deep brain stimulation modulates synchrony within spatially and spectrally distinct resting state networks in Parkinson's disease. Brain. 2016;139(5):1482–96.
51. King NK, Krishna V, Basha D, Elias G, Sammartino F, Hodaie M, et al. Microelectrode recording findings within the tractography-defined ventral intermediate nucleus. J Neurosurg. 2017;126(5):1669–75.
52. Abosch A, Yacoub E, Ugurbil K, Harel N. An assessment of current brain targets for deep brain stimulation surgery with susceptibility-weighted imaging at 7 tesla. Neurosurgery. 2010;67(6):1745–56; discussion 56.
53. Hammond C, Ammari R, Bioulac B, Garcia L. Latest view on the mechanism of action of deep brain stimulation. Mov Disord. 2008;23(15):2111–21.
54. Wagle Shukla A, Moro E, Gunraj C, Lozano A, Hodaie M, Lang A, et al. Long-term subthalamic nucleus stimulation improves sensorimotor integration and proprioception. J Neurol Neurosurg Psychiatry. 2013;84(9):1020–8.
55. Chen R, Udupa K. Measurement and modulation of plasticity of the motor system in humans using transcranial magnetic stimulation. Mot Control. 2009;13(4):442–53.
56. Ogura M, Nakao N, Nakai E, Uematsu Y, Itakura T. The mechanism and effect of chronic electrical stimulation of the globus pallidus for treatment of Parkinson disease. J Neurosurg. 2004;100(6):997–1001.

57. Benazzouz A, Hallett M. Mechanism of action of deep brain stimulation. Neurology. 2000;55(12 Suppl 6):S13–6.
58. Pollo C, Kaelin-Lang A, Oertel MF, Stieglitz L, Taub E, Fuhr P, et al. Directional deep brain stimulation: an intraoperative double-blind pilot study. Brain. 2014;137(Pt 7):2015–26.
59. Arcot Desai S, Gutekunst CA, Potter SM, Gross RE. Deep brain stimulation macroelectrodes compared to multiple microelectrodes in rat hippocampus. Front Neuroeng. 2014;7:16.
60. Timmermann L, Jain R, Chen L, Maarouf M, Barbe MT, Allert N, et al. Multiple-source current steering in subthalamic nucleus deep brain stimulation for Parkinson's disease (the VANTAGE study): a non-randomised, prospective, multicentre, open-label study. Lancet Neurol. 2015;14(7):693–701.
61. Baker KB, Montgomery EB Jr, Rezai AR, Burgess R, Luders HO. Subthalamic nucleus deep brain stimulus evoked potentials: physiological and therapeutic implications. Mov Disord. 2002;17(5):969–83.
62. Bahramisharif A, Mazaheri A, Levar N, Richard Schuurman P, Figee M, Denys D. Deep brain stimulation diminishes cross-frequency coupling in obsessive-compulsive disorder. Biol Psychiatry. 2016;80(7):e57–8.
63. Zumsteg D, Lozano AM, Wennberg RA. Mesial temporal inhibition in a patient with deep brain stimulation of the anterior thalamus for epilepsy. Epilepsia. 2006;47(11):1958–62.
64. Zumsteg D, Lozano AM, Wieser HG, Wennberg RA. Cortical activation with deep brain stimulation of the anterior thalamus for epilepsy. Clin Neurophysiol. 2006;117(1):192–207.
65. Duchin Y, Abosch A, Yacoub E, Sapiro G, Harel N. Feasibility of using ultra-high field (7 T) MRI for clinical surgical targeting. PLoS One. 2012;7(5):e37328.
66. Lenglet C, Abosch A, Yacoub E, De Martino F, Sapiro G, Harel N. Comprehensive in vivo mapping of the human basal ganglia and thalamic connectome in individuals using 7T MRI. PLoS One. 2012;7(1):e29153.
67. Ho AL, Sussman ES, Zhang M, Pendharkar AV, Azagury DE, Bohon C, et al. Deep brain stimulation for obesity. Cureus. 2015;7(3):e259.
68. Sankar T, Chakravarty MM, Bescos A, Lara M, Obuchi T, Laxton AW, et al. Deep brain stimulation influences brain structure in Alzheimer's disease. Brain Stimul. 2015;8(3):645–54.
69. McIntyre CC, Savasta M, Walter BL, Vitek JL. How does deep brain stimulation work? Present understanding and future questions. J Clin Neurophysiol. 2004;21(1):40–50.
70. de Hemptinne C, Swann NC, Ostrem JL, Ryapolova-Webb ES, San Luciano M, Galifianakis NB, et al. Therapeutic deep brain stimulation reduces cortical phase-amplitude coupling in Parkinson's disease. Nat Neurosci. 2015;18(5):779–86.
71. Swann NC, Hemptinne CD, Miocinovic S, Qasim S, Ostrem JL, Galifianakis NB, et al. Chronic multisite brain recordings from a totally implantable bidirectional neural interface: experience in 5 patients with Parkinson's disease. J Neurosurg. 2018;128(2):605–16.
72. Rosin B, Slovik M, Mitelman R, Rivlin-Etzion M, Haber SN, Israel Z, et al. Closed-loop deep brain stimulation is superior in ameliorating parkinsonism. Neuron. 2011;72(2):370–84.
73. Wozny TA, Lipski WJ, Alhourani A, Kondylis ED, Antony A, Richardson RM. Effects of hippocampal low-frequency stimulation in idiopathic non-human primate epilepsy assessed via a remote-sensing-enabled neurostimulator. Exp Neurol. 2017;294:68–77.
74. Tinkhauser G, Pogosyan A, Little S, Beudel M, Herz DM, Tan H, et al. The modulatory effect of adaptive deep brain stimulation on beta bursts in Parkinson's disease. Brain. 2017;140(4):1053–67.
75. Lipsman N, Neimat JS, Lozano AM. Deep brain stimulation for treatment-refractory obsessive-compulsive disorder: the search for a valid target. Neurosurgery. 2007;61(1):1–11; discussion −3.
76. Lipsman N, Giacobbe P, Lozano AM. Deep brain stimulation in obsessive-compulsive disorder: neurocircuitry and clinical experience. Handb Clin Neurol. 2013;116:245–50.
77. Foffani G, Priori A. Deep brain stimulation in Parkinson's disease can mimic the 300 Hz subthalamic rhythm. Brain. 2006;129(Pt 12):e59; author reply e60.
78. Deniau JM, Degos B, Bosch C, Maurice N. Deep brain stimulation mechanisms: beyond the concept of local functional inhibition. Eur J Neurosci. 2010;32(7):1080–91.
79. Benabid AL, Krack PP, Benazzouz A, Limousin P, Koudsie A, Pollak P. Deep brain stimulation of the subthalamic nucleus for Parkinson's disease: methodologic aspects and clinical criteria. Neurology. 2000;55(12 Suppl 6):S40–4.
80. Visanji NP, Kamali Sarvestani I, Creed MC, Shams Shoaei Z, Nobrega JN, Hamani C, et al. Deep brain stimulation of the subthalamic nucleus preferentially alters the translational profile of striatopallidal neurons in an animal model of Parkinson's disease. Front Cell Neurosci. 2015;9:221.
81. Tekriwal A, Baltuch G. Deep brain stimulation: expanding applications. Neurol Med Chir. 2015;55:861.
82. Jha A, Litvak V, Taulu S, Thevathasan W, Hyam JA, Foltynie T, et al. Functional connectivity of the pedunculopontine nucleus and surrounding region in Parkinson's disease. Cereb Cortex (New York, NY: 1991). 2017;27(1):54–67.
83. Blumenfeld Z, Koop MM, Prieto TE, Shreve LA, Velisar A, Quinn EJ, et al. Sixty-hertz stimulation improves bradykinesia and amplifies subthalamic low-frequency oscillations. Mov Disord. 2017;32(1):80–8.
84. Malekmohammadi M, Herron J, Velisar A, Blumenfeld Z, Trager MH, Chizeck HJ, et al. Kinematic adaptive deep brain stimulation for resting tremor in Parkinson's disease. Mov Disord. 2016;31(3):426–8.

85. McIntyre CC, Mori S, Sherman DL, Thakor NV, Vitek JL. Electric field and stimulating influence generated by deep brain stimulation of the subthalamic nucleus. Clin Neurophysiol. 2004;115(3):589–95.
86. McIntyre CC, Grill WM, Sherman DL, Thakor NV. Cellular effects of deep brain stimulation: model-based analysis of activation and inhibition. J Neurophysiol. 2004;91(4):1457–69.
87. Madler B, Coenen VA. Explaining clinical effects of deep brain stimulation through simplified target-specific modeling of the volume of activated tissue. AJNR Am J Neuroradiol. 2012;33(6):1072–80.
88. Behrens TE, Woolrich MW, Jenkinson M, Johansen-Berg H, Nunes RG, Clare S, et al. Characterization and propagation of uncertainty in diffusion-weighted MR imaging. Magn Reson Med. 2003;50(5):1077–88.
89. Vibhor Krishna M, Sammartino F, Rabbania Q, Changizi B, Agrawal P, Deogaonkar M, Knopp M, Young N, Rezai A. Connectivity-based approach for selection of optimal deep brain stimulation contacts: a feasibility study. Ann Clin Transl Neurol. 2019;6(7):1142–50.
90. Raichle ME. Two views of brain function. Trends Cogn Sci. 2010;14(4):180–90.
91. Fox MD, Buckner RL, Liu H, Chakravarty MM, Lozano AM, Pascual-Leone A. Resting-state networks link invasive and noninvasive brain stimulation across diverse psychiatric and neurological diseases. Proc Natl Acad Sci U S A. 2014;111(41):E4367–75.
92. Sharan A, Rezai AR, Nyenhuis JA, Hrdlicka G, Tkach J, Baker K, et al. MR safety in patients with implanted deep brain stimulation systems (DBS). Acta Neurochir Suppl. 2003;87:141–5.
93. Henderson JM, Tkach J, Phillips M, Baker K, Shellock FG, Rezai AR. Permanent neurological deficit related to magnetic resonance imaging in a patient with implanted deep brain stimulation electrodes for Parkinson's disease: case report. Neurosurgery. 2005;57(5):E1063; discussion E.
94. Figee M, Luigjes J, Smolders R, Valencia-Alfonso CE, van Wingen G, de Kwaasteniet B, et al. Deep brain stimulation restores frontostriatal network activity in obsessive-compulsive disorder. Nat Neurosci. 2013;16(4):386–7.
95. Kahan J, Urner M, Moran R, Flandin G, Marreiros A, Mancini L, et al. Resting state functional MRI in Parkinson's disease: the impact of deep brain stimulation on 'effective' connectivity. Brain. 2014;137(Pt 4):1130–44.
96. Blow N. Functional neuroscience: how to get ahead in imaging. Nature. 2009;458(7240):925–8.
97. Min HK, Ross EK, Lee KH, Dennis K, Han SR, Jeong JH, et al. Subthalamic nucleus deep brain stimulation induces motor network BOLD activation: use of a high precision MRI guided stereotactic system for nonhuman primates. Brain Stimul. 2014;7(4):603–7.
98. Gibson WS, Ross EK, Han SR, Van Gompel JJ, Min HK, Lee KH. Anterior thalamic deep brain stimulation: functional activation patterns in a large animal model. Brain Stimul. 2016;9(5):770–3.
99. Ross EK, Kim JP, Settell ML, Han SR, Blaha CD, Min HK, et al. Fornix deep brain stimulation circuit effect is dependent on major excitatory transmission via the nucleus accumbens. NeuroImage. 2016;128:138–48.
100. Sammartino F, Krishna V, Sankar T, Fisico J, Kalia SK, Hodaie M, et al. 3-Tesla MRI in patients with fully implanted deep brain stimulation devices: a preliminary study in 10 patients. J Neurosurg. 2016;127(4):892–8.
101. Shih LC, LaFaver K, Lim C, Papavassiliou E, Tarsy D. Loss of benefit in VIM thalamic deep brain stimulation (DBS) for essential tremor (ET): how prevalent is it? Parkinsonism Relat Disord. 2013;19(7):676–9.
102. Houeto JL, Bejjani PB, Damier P, Staedler C, Bonnet AM, Pidoux B, et al. Failure of long-term pallidal stimulation corrected by subthalamic stimulation in PD. Neurology. 2000;55(5):728–30.
103. Voytek B, Knight RT. Dynamic network communication as a unifying neural basis for cognition, development, aging, and disease. Biol Psychiatry. 2015;77(12):1089–97.
104. Nimmrich V, Draguhn A, Axmacher N. Neuronal network oscillations in neurodegenerative diseases. NeuroMolecular Med. 2015;17(3):270–84.
105. Deisseroth K. Circuit dynamics of adaptive and maladaptive behaviour. Nature. 2014;505(7483):309–17.
106. Fornito A, Zalesky A, Breakspear M. The connectomics of brain disorders. Nat Rev Neurosci. 2015;16(3):159–72.
107. Bentley WJ, Li JM, Snyder AZ, Raichle ME, Snyder LH. Oxygen level and LFP in task-positive and task-negative areas: bridging BOLD fMRI and electrophysiology. Cereb Cortex. 2016;26(1):346–57.
108. Legon W, Sato TF, Opitz A, Mueller J, Barbour A, Williams A, et al. Transcranial focused ultrasound modulates the activity of primary somatosensory cortex in humans. Nat Neurosci. 2014;17(2):322–9.
109. Mac Donald CL, Dikranian K, Bayly P, Holtzman D, Brody D. Diffusion tensor imaging reliably detects experimental traumatic axonal injury and indicates approximate time of injury. J Neurosci. 2007;27(44):11869–76.
110. Toosy AT. Diffusion tensor imaging detects corticospinal tract involvement at multiple levels in amyotrophic lateral sclerosis. J Neurol Neurosurg Psychiatry. 2003;74(9):1250–7.
111. Nicoletti G, Manners D, Novellino F, Condino F, Malucelli E, Barbiroli B, et al. Diffusion tensor MRI changes in cerebellar structures of patients with familial essential tremor. Neurology. 2010;74(12):988–94.
112. Krishna V, Sammartino F, Agrawal P, Changizi BK, Bourekas E, Knopp MV, Rezai A. Prospective tractography-based targeting for improved safety of focused ultrasound thalamotomy. Neurosurgery. 2019;84(1):160–8.

The Design of Clinical Studies for Neuromodulation

37

Wael F. Asaad, Peter M. Lauro, and Shane Lee

Introduction

The more we understand about the electrophysiology and circuits underlying neuropsychiatric disease, the greater the possibility that focal neuromodulation will be a viable therapeutic strategy. Although the administration of drugs can certainly be a form of neuromodulation, we draw a distinction between chemically targeted and anatomically targeted forms of neural systems manipulation and will use the term "neuromodulation" to refer here specifically to the latter.

Compared to the systemic delivery of drugs, anatomically based neuromodulation strategies are not limited by the existing distributions of molecular targets. While there may be disease entities that are strictly defined by a small number of reversible molecular derangements, there are others—stroke and traumatic brain or spine injury being the most notable—where the pathology does not conform to existing cellular and molecular boundaries. Other diseases, such as epilepsy, may in some cases begin as a circumscribed molecular derangement, but additional circuits may be recruited over time in a manner that does not respect the boundaries of the inciting pathologic entity [1, 2]. In such cases, a treatment approach is required that addresses the resulting neural dysfunction in a manner that is tailored to the type and extent of circuit pathology and that is not limited by the naturally occurring distributions of molecular targets. Parenthetically, while new molecular targets might be introduced in an anatomically targeted manner for interaction with systemically administered medications (e.g., designer receptors for designer drugs), such a strategy would be subject to many of the considerations discussed here.

Of course, current neuromodulation strategies often require invasive techniques and, like systemically administered medications, are likely to have limited specificity at the target as well as poorly defined, extended effects at adjacent, upstream, and downstream sites. Nevertheless, the promise of spatially targeted neuromodulation techniques is ever-increasing anatomical and functional specificity beyond that provided by nature's endowment of the brain with particular molecules in particular distributions.

W. F. Asaad (✉)
Neurosurgery, Neuroscience, and the Carney Institute for Brain Science, Brown University Alpert Medical School and the Norman Prince Neurosciences Institute of Rhode Island Hospital, Providence, RI, USA
e-mail: wfasaad@alum.mit.edu

P. M. Lauro
Department of Neuroscience, Warren Alpert Medical School, Brown University, Providence, RI, USA

S. Lee
Neurosurgery, Neuroscience, and the Carney Institute for Brain Science, Brown University and the Norman Prince Neurosciences Institute of Rhode Island Hospital, Providence, RI, USA

N. Pouratian, S. A. Sheth (eds.), *Stereotactic and Functional Neurosurgery*,
https://doi.org/10.1007/978-3-030-34906-6_37

The process of designing and testing new neuromodulation strategies shares some features with the development of drug-based therapies, but a focus on neuromodulation also introduces novel factors into the process that may be challenges and/or opportunities. Here, we will examine the common and distinctive considerations of clinical studies that seek to investigate potential neuromodulatory approaches to nervous system dysfunction. While the primary hope of all such investigations is to establish the potential or actual clinical utility of a given interventional strategy, the reality is that such studies are more likely ultimately to fail than to succeed in achieving the primary therapeutic endpoint. With this in mind, the design of a clinical investigation must be optimized not only to maximize the probability of success but also to learn as much from failure as from success, so that future endeavors are able to build solidly upon new knowledge in a step-wise and ultimately fruitful manner.

Defining the Scope and Power of a Study

There have been relatively few sufficiently large-scale, prospective, double-blinded, controlled neuromodulation trials (Table 37.1). The expensive nature of neuromodulation therapies—whether due to the cost of implanted devices (e.g., deep brain stimulation systems), therapeutic delivery systems (e.g., focused ultrasound), adjunct neuroimaging, or simply the neurosurgical procedures and related hospitalization—undoubtedly raises the threshold for conducting these studies. Few are therefore willing to invest the time, effort, and funds required to conduct such trials without robustly convincing, smaller-scale, preliminary studies. Even studies that are designed ostensibly as feasibility and safety studies will often be evaluated on the basis of likely efficacy in order to justify the cost of proceeding to the next phase of trials, regardless of whether that justification is assessed by government, industry, academic, or philanthropic interests. Unfortunately, this tendency—to use underpowered studies as a basis to move forward, or not, with larger, more definitive trials to assess clinical efficacy—may in fact add more noise than signal to the process of identifying and pursuing potentially useful therapies. This is because negative results are potentially falsely negative due to the underpowered nature of the preliminary studies, but even positive results may be falsely positive depending on the number of conditions tested and the unknown, underlying proportion of truly effective treatment conditions.

As an example, suppose a DBS feasibility study were designed to assess the effects of high- vs. low-frequency stimulation at a particular target for intractable, debilitating obsessive-compulsive disorder, and the endpoints evaluated were reduction of obsessions and/or compulsions. The study was calculated to have a positive predictive power of 0.8 and results were to be accepted as statistically significant at $p < 0.05$. Suppose further that the unknown, true effect of DBS at this target for this condition was that only low-frequency stimulation would be effective and only for obsessions but not compulsions. Therefore, the proportion of true-positive effects in this trial would be 1/4. Overall, then, what is the likelihood the results of this trial would reflect the underlying reality? A true positive would be revealed in 80% of cases. However, because only one in four conditions assessed was truly effective, a false positive would be detected in 14.3% of cases (resulting from the application of an alpha level of 0.05 to the three ineffective conditions). Therefore, combining the false-negative rate (20%) and the false-positive rate (14.3%) results in a trial that produces results that are misaligned with reality with a probability approaching 1/3 (less than the simple sum of 0.20 and 0.143 because these events are not mutually exclusive, so some outcomes would overlap). This is, in essence, an extrapolation of the multiple-comparisons problem to clinical trials that cannot know in advance this so-called base-rate of true-positive effects across the tested conditions.

These concerns regarding the overall validity of a result are especially relevant in the case of early clinical studies that, although explicitly directed toward establishing only feasibility or safety, nevertheless will often include an efficacy

Table 37.1 A non-exhaustive list of major neuromodulation clinical trials enrolling at least 15 subjects, conducted in a prospective, randomized fashion. The last column, success, relates to successful achievement of the primary outcome

Name of study	*n*	Design	Primary outcomes	Success?
Movement disorders				
Pallidal Deep-Brain Stimulation in Primary Generalized or Segmental Dystonia [3]	40	All patients implanted with DBS in GPi, randomized to active or sham stimulation (no stimulation delivered) for 3 months, followed by 3–6 months of open-label treatment	Burke-Fahn-Marsden Dystonia Rating Scale change from baseline to 3 months	Yes
STN-Stimulation Versus Best Medical Treatment in Advanced PD [4]	156	Unblinded 1:1 randomization to stimulation or best medical management	Parkinson's Disease Questionnaire (PDQ-39, quality of life), Unified Parkinson's Disease Rating Scale (UPDRS-III), baseline to 6 months	Yes
Subthalamic Nucleus Versus Globus Pallidus Bilateral Deep Brain Stimulation for Advanced Parkinson's Disease (NSTAPS Study) [5]	128	Patients 1:1 randomized to STN vs. GPi DBS; patients and assessors blinded to target	Baseline to 12 months: AMC Linear Disability Score (ALDS), Reliable Change Index (RCI), MINI-International Neuropsychiatric Interview (MINI), UPDRS	No
A Comparison of Best Medical Therapy and Deep Brain Stimulation of Subthalamic Nucleus and Globus Pallidus for the Treatment of Parkinson's Disease [6]	255	Patients 1:1 randomized to best medical therapy or DBS, DBS patients additionally randomized/split to GPi or STN; motor evaluation performed by blinded neurologists	Baseline to 6 months: Time spent in the "ON" state w/o dyskinesias (by motor diaries)	Yes
CSP #468 Phase II – A Comparison of Best Medical Therapy and Deep Brain Stimulation of Subthalamic Nucleus and Globus Pallidus for the Treatment of Parkinson's Disease [7]	299	Patients 1:1 randomized to STN or GPi target; DBS neurologists blinded to target	Baseline to 24 months: change in UPDRS-III	No
ExAblate Transcranial MR Guided Focused Ultrasound for the Treatment of Essential Tremors [8]	76	Patients 3:1 randomized to unilateral HIFU thalamotomy or sham procedure	Clinical Rating Scale for Tremor and the Quality of Life in Essential Tremor Questionnaire at 3 months post-op	Yes
Study of AAV-GAD Gene Transfer into the Subthalamic Nucleus for Parkinson's Disease [9]	45	Patients 1:1 randomized to sham surgery or AAV2-GAD infusions	UPDRS part III at 6 months post-op	Yes
Double-Blind, Multicenter, Sham Surgery Controlled Study of CERE-120 in Subjects with Idiopathic Parkinson's Disease [10]	51	Patients 1:1 randomized to AAV2-NRTN infusions or sham surgery	UPDRS part III at 15 months post-op	No
Randomized controlled trial of Intraputamenal Glial Cell Line-Derived Neurotrophic Factor Infusion in Parkinson Disease [11]	34	Patients 1:1 randomized to glial cell line-derived neurotrophic factor or saline infusion	UPDRS part III at 6 months post-op	No

(continued)

Table 37.1 (continued)

Name of study	*n*	Design	Primary outcomes	Success?
Psychiatric disorders				
Subcallosal Cingulate Deep Brain Stimulation for Treatment-Resistant Depression: A Multisite, Randomized, Sham-Controlled Trial [12]	90	All patients implanted with DBS in bilateral subcallosal cingulate white matter, randomized to 6 months of active ($n = 60$) or sham ($n = 30$) DBS, followed by 6 months of open-label DBS	> = 40% reduction in depression severity from baseline	No
A Randomized Sham-Controlled Trial of Deep Brain Stimulation of the Ventral Capsule/Ventral Striatum for Chronic Treatment-Resistant Depression [13]	30	All implanted in ventral capsule/ventral striatum, 1:1 randomized to active versus sham DBS treatment in a blinded fashion for 16 weeks, then open-label phase	> = 50% improvement on Montgomery-Åsberg Depression Rating Scale from baseline at 16 weeks	No
STOC Study: Subthalamic Nucleus Stimulation in Severe Obsessive-Compulsive Disorder [14]	17	Patients 1:1 randomized to ON-OFF or OFF-ON stimulation, 3 months each with a 1-month washout period in the middle, double-blind	Yale-Brown Obsessive Compulsive Scale at the end of two 3-month periods	Yes
Radiosurgical Treatment for Obsessive-Compulsive Disorder [15]	16	Patients 1:1 randomized to gamma ventral capsulotomy or sham surgery. Patients blinded for 1 year post-op	Yale-Brown Obsessive Compulsive Scale at 1 year post-op	No
ADvance Trial: Deep Brain Stimulation of the Fornix for Early, Probable Alzheimer's Disease [16]	42	All implanted in fornix, 1:1 randomized to active and sham stimulation for first 12 months, all patients active the following year	ADAS-Cog (Alzheimer's Disease Assessment Scale-Cognitive Component), Clinical Dementia Rating Sum of Boxes, cerebral glucose metabolism measured with PET	No
Deep Brain Stimulation of the Nucleus Accumbens in Treatment-Refractory Patients with Obsessive-Compulsive Disorder [17]	16	All patients implanted, stimulated for 8 months, 1-month double-blind (2 weeks on stimulation, 2 weeks off stimulation)	Yale-Brown Obsessive Compulsive Scale at each 2-week double-blind interval	Yes
Deep Brain Stimulation of the Ventral Anterior Limb of the Internal Capsule for Depression [18]	25	All patients implanted, 16 randomized to OFF then ON vs. ON then OFF (cross-over design, each phase lasting 2–3 weeks)	>50% reduction in Hamilton-D 17-item scale	Yes
Epilepsy				
A Randomized, Controlled Trial of Surgery for Temporal-Lobe Epilepsy [19]	80	Patients 1:1 randomized to surgery or best medical therapy	Freedom from seizures that impair awareness of self and surroundings	Yes
RNS System Pivotal Trial: Responsive Neurostimulation for Epilepsy [20]	191	All patients implanted to 1 or 2 foci; patients 1:1 randomized to active or sham stimulation 1 month post-op; evaluated 3 months later	Seizure frequency	Yes
Radiosurgery Versus Open Surgery for Mesial Temporal Lobe Epilepsy: The Randomized, Controlled ROSE Trial [21]	58	Patients 1:1 randomized to stereotactic radiosurgery or anterior temporal lobectomy; evaluating neurologists were blinded to procedure	Self-reporting of seizure frequency between 25 and 36 months post-op	Yes

Table 37.1 (continued)

Name of study	*n*	Design	Primary outcomes	Success?
A Multicenter, Prospective Pilot Study of Gamma Knife Radiosurgery for Mesial Temporal Lobe Epilepsy: Seizure Response, Adverse Events, and Verbal Memory [22]	30	Patients 1:1 randomized to 20 or 24Gy targeting the amygdala, hippocampus, and parahippocampal gyrus	Self-reporting of seizure frequency at 36 months post-op	Yes
SANTE: Stimulation of the Anterior Nucleus of the Thalamus for Epilepsy [23]	110	All implanted in anterior nucleus of thalamus, 1:1 assigned to active or no stimulation for first 3 months, months 4–13 were unblinded	Reduction in monthly seizure rate after 3 months	Yes
Spine				
Spinal Cord Stimulation versus Repeated Lumbosacral Spine Surgery for Chronic Pain: A Randomized, Controlled Trial [24]	60	Patients 1:1 randomized to lumbosacral spine reoperation or spinal cord stim	> = 50% pain relief, patient satisfaction, reoperation at 6 months	Yes
Spinal Cord Stimulation Versus Conventional Medical Management for Neuropathic Pain: A Multicentre Randomised Controlled Trial in Patients with Failed Back Surgery Syndrome [25]	100	Patients 1:1 randomized to spinal cord stim or conventional medical management (patients not blinded)	> = 50% leg pain relief at 6 months	Yes
Comparison of 10-kHz High-Frequency and Traditional Low-Frequency Spinal Cord Stimulation for the Treatment of Chronic Back and Leg Pain [26]	198	Patients 1:1 randomized to conventional spinal cord stim (~50 Hz) or 10 kHz spinal cord stim	> = 50% back pain reduction, no stimulation-related neurological deficit at 3 months	Yes
Intrathecal Baclofen for Severe Spinal Spasticity [27]	20	Patients received 2x3-day alternating trials of saline or baclofen	Muscle tone with Ashworth score at end of baclofen 3-day period	Yes
Stroke				
Everest Trial: Epidural Electrical Stimulation for Stroke Rehabilitation [28]	164	Patients 2:1 randomized to implanted epidural motor cortex stimulation or control (no sham surgery); all patients underwent same schedule of rehabilitation; evaluating clinicians were blinded to treatment	Upper-extremity Fugl-Meyer (UEFM) and Arm Motor Ability Test (AMAT) at 4 weeks post-rehabilitation	No

endpoint. For that purpose, they typically have relatively low power and might explore a wider range of parameters and outcomes to assess the broader potential of a particular therapeutic strategy. Despite their statistical and structural limitations, these studies are often evaluated for a "signal" of benefit, and decisions to proceed with larger trials may hinge upon these early efficacy results even if that is explicitly not the main purpose of those studies. Nevertheless, a clear understanding of the statistical limitations of these smaller, early-stage studies may suggest that the combined likelihood of false positives and false negatives is sufficiently high that putting too much emphasis on any result related to an underpowered, over-explored endpoint may be not much more reliable than flipping a coin.

From a statistical perspective, therefore, limiting the number of manipulations tested and the number of outcome measures assessed is desirable. However, in the field of neuromodulation, especially when applying electrical stimulation,

this approach seems intuitively too restrictive: Given the large space of potential stimulation parameters and the complex, multi-dimensional nature of neuropsychiatric disease, selecting a small subset of protocols and outcomes may feel akin to blind spearfishing, whereas what we would like to do, ideally, is cast a wide net to discover a useful therapy.

Because ablation procedures have fewer degrees of freedom (i.e., no stimulation parameters to adjust), these interventions may seem a simpler and potentially more powerful neuromodulation technique in the context of clinical trials and may serve to guide and constrain the later development of stimulation techniques that build upon those lesion results. Nevertheless, lesions cannot capture the full set of effects achievable with various stimulation protocols, so one might be misled by false negatives if relying exclusively on predicate lesion studies to attempt neurostimulation. Furthermore, lesions, like electrical stimulation, vary in anatomical specificity and reproducibility; post-hoc analyses assessing outcomes as a function of exact lesion size or position, for example, will therefore be subject to similar potential multiple-comparisons problems.

To limit the multiplicity of parameters related to the delivery and assessment of an investigational therapy, a neuromodulation study must be built upon a sound scientific premise. For example, if a particular neuroanatomical pathway is hypothesized to mediate a specific dysfunction such that its modulation might mitigate a related symptom, computational analysis such as finite element modeling of electrical fields and neuronal responses might yield a narrow set of stimulation parameters to be tested in order to produce the desired circuit effect (e.g., CENTURY-S, NCT02881151; ADvance II, NCT03622905). This, of course, presumes that at least the type and direction of the desired neural response are understood. In other words, should the target or pathway be driven, inhibited, or recruited in some other manner to generate plasticity or release modulatory chemical factors? If this question cannot be answered with reasonable confidence, it may be a sign the planned study is premature.

One potentially interesting approach to sifting through the enormous space of potential neuromodulation protocols (e.g., electrical stimulation sites and patterns) is to include an exploratory phase within the trial design, during which the goal is to achieve some effect on a well-defined biomarker hypothesized to mediate the intended therapeutic effect. For example, if fronto-medial theta power is proposed to influence depression [29], a flexible trial design could be implemented in which stimulation is "tuned" to produce the desired modulation of theta in that region within each patient, and that empirically determined pattern of stimulation is then delivered continuously in the next phase of the trial to assess efficacy. This sort of adaptive trial design, when conducted according to a rigorously pre-specified plan, may accelerate progress toward a useful neuromodulation therapy [30].

Clarifying the Therapeutic Model

All studies implicitly or explicitly propose a particular causal structure to underlie potential interactions between variables, including the experimental manipulation, the outcome measures, and additional associated factors. While classical statistical methods were developed in a tradition devoid of causality, work over the last 30 years has revealed the importance of designing studies and conducting analyses within a sound framework of putative causal interactions to minimize bias [31]. Constructing an explicit causal diagram for the proposed therapeutic model may therefore provide useful clarity for the design of an appropriate study (Fig. 37.1). Such a diagram would lay bare the logic of the proposed investigation to facilitate a critical analysis of the plausibility of the scientific premise. Furthermore, this diagram would clearly identify mediating and confounding factors, such that the former might be used to derive secondary outcome measures while the latter are addressed with appropriate controls in design or analysis.

To highlight the importance of the proposed causal model in experimental design, suppose a nonrandomized, prospective pilot study is conducted to assess the effect of a novel

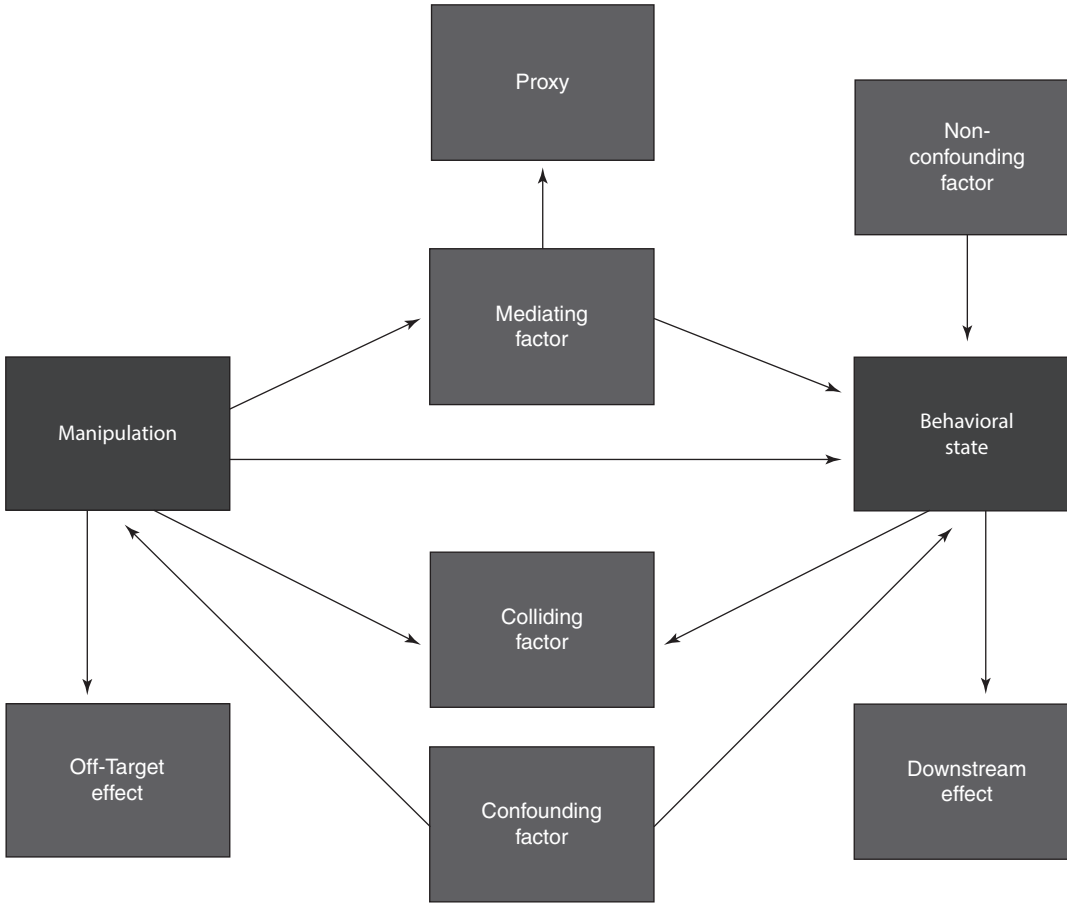

Fig. 37.1 A causal diagram depicting the types of variables that may be present in any particular neuromodulation trial design. A randomized trial, by assigning the experimental manipulation in a stochastic fashion that is not subject to any causal inputs other than the "flip of a coin," in principle removes the possibility of confounding factors. Whether this is true in practice, of course, depends on the size of the studied population and the distributions of characteristics across groups; a happenstance clustering of particular features, such as age, gender, disease severity or subtype, etc., can undermine the randomization. Mediating factors are causally related to the treatment effect, whereas their proxies are related to that effect only insofar as they directly correspond to those mediating factors themselves; secondary outcomes reporting proxies of mediating factors are therefore valid only to the extent of that correspondence. Note that downstream effects can be used as proxies for the behavioral outcomes, subject to the same type of constraint. Colliding factors are present when a factor has multiple potential causes, and here are depicted as caused by both the manipulation and the assessed outcome (behavioral state). In nonrandomized, observational studies, these are often mistaken for confounding factors, and post-hoc stratification of outcomes by "controlling for" these factors can result in spurious correlations between hypothesized treatment and effect [32]. Note that this sort of "collision" also occurs at the behavioral outcome, resulting from causal inputs via the manipulation and non-confounding factors. Stratification of outcomes to assess relationships among potentially relevant experimental variables can result in spurious correlations between the manipulation and these non-confounding factors, similar to the situation with colliding factors, because behavioral state is, here, technically a colliding factor as well

neurostimulation strategy for a particular neuropsychiatric condition. All patients undergo stimulation and are followed so their outcomes can be compared to pre-operative baselines. Overall, a non-significant positive therapeutic trend is observed. To determine if there might be a subgroup of responders, patients expressing a putative biomarker that is postulated to enable or mediate the therapeutic effect—perhaps a particular neural rhythm or metabolic neuroimaging alteration—undergo a subgroup analysis. In other words, this biomarker is hypothesized to be

caused by the therapy and itself to be the cause of the beneficial behavioral effect. However, suppose instead that, while stimulation does indeed tend to increase the expression of this biomarker, patients who happen to show improvements (e.g., due to placebo effects or other study activities) will also tend to show this biomarker independent of stimulation. In other words, observation of this biomarker may result from stimulation and/or from behavioral change, so it is in fact a colliding factor rather than a mediating one (as per Fig. 37.1). In this post-hoc analysis, even though there may be no causal pathway from stimulation to behavioral outcome, spurious associations between these can nevertheless be observed: if the threshold biomarker level used to select the subgroup is chosen such that either the stimulation or the behavioral response may be sufficient to cross it, a spurious negative correlation can be observed; if, however, the threshold is selected such that the combined (independent) influences of the stimulation and behavioral response are more likely to produce a supra-threshold level, then a spurious positive correlation between stimulation and behavioral outcome can be observed. In each case, the false association is termed a collider bias and results from the application of a threshold that screens out a group of non-stimulated *and* non-responding patients (in a manner analogous to Berkson's paradox [33]) in the context of a "true" causal link between the biomarker and behavioral outcome that is inverted with respect to the proposed therapeutic model.

This is but one of many possible examples that can demonstrate the variety of structural pitfalls related to designing and conducting clinical studies. Therefore, explicit elaboration of the proposed therapeutic model underlying a given experimental design and rigorous validation of the hypothesized causal steps within that model will decrease the likelihood of inferential errors.

Selecting Outcome Measures

The primary endpoint, or outcome measure, is ideally a thing of clear, undeniable value to quality and/or length of life. Unfortunately, there are relatively few real-world examples where endpoints are so simple, especially in the context of complex neuropsychiatric disease. For example, a new treatment that reduces a patient's depression according to standard scales (e.g., MADRS or HAM-D) but fails to improve overall social and economic function could be regarded as a success or failure, depending on one's viewpoint. Part of the confusion arises from the fact that those standard scales are, fundamentally, surrogate rather than true endpoints. A true primary endpoint would reflect what a patient desires from a therapy (leaving aside the thorny issues that arise when patients are unable to convey those desires or when they lack insight into their own needs). However, such desires will be heterogeneous and poorly quantifiable, so the use of surrogate measures is in fact the rule rather than the exception. In other words, our goal is to improve the lives of our patients, however they may imagine that improvement in the context of their illnesses ("I want to be able to do my woodworking again"), but a clinical study must necessarily homogenize individual variation through the selection or design of appropriate surrogate measures. In many domains, particular surrogates have, for better or worse, become accepted standards for assessing therapeutic success (e.g., UPDRS in Parkinson's disease).

Despite the fact that surrogate endpoints are far more common than typically appreciated, there exists debate surrounding their proper use [34]. This debate is related to the use of surrogates for the final outcome measure (a surrogate for a surrogate, in the framework presented here) and typically arises from the misconception that a viable surrogate outcome is simply any outcome that correlates well with the "true" outcome [35]. However, an ideal surrogate measure is one that fully predicts the effect of a treatment on the true outcome and may in fact deterministically mediate the effect of treatment on that outcome. In practice, there are many available analytical methods to assess the validity of a proposed surrogate, each with particular strengths, weaknesses, and ideal application scenarios [36].

When secondary outcomes are fashioned in order to support the causal chain of a particular

therapeutic model, the informative value of a trial can be greatly enhanced [37]. If, for example, both the primary and mediating secondary outcomes are met, the validity of a successful primary outcome is rendered more plausible. Conversely, when both primary and secondary outcomes are not achieved, one learns that either the therapeutic model is simply incorrect, or the model is correct but a failure to engage early mechanisms prevented the success of the primary outcome. Meanwhile, failed secondary outcomes with successful primary outcomes suggest the model is incorrect, or perhaps the primary outcome's success was spurious. Lastly, a failed primary outcome with successful mediating secondary outcomes suggests the therapeutic model may be incomplete or incorrect, or perhaps the failed primary outcome represented a false negative. For those with experience writing computer code, this process is akin to debugging a function by reporting out the intermediate states of key variables as the code runs.

Designing Appropriate Control Conditions

Unlike most drug trials, neuromodulation trials cannot simply administer a placebo to a control group. Rather, the "placebo" in the case of many surgical trials is typically some sort of sham procedure [38]. Neurosurgical neuromodulation presents the possibility of additional forms of control: The control condition could take the form of sham surgery in lesion and infusion studies, placebo delivery in infusion studies, or maintaining some group of implanted patients in a blinded, non-stimulated state in neurostimulation studies. The latter can take the form of delayed-start or withdrawal protocols, or crossover designs.

Neurosurgical sham studies, in particular, are fraught with difficulties. Aside from the basic concern that some patients will undergo an invasive procedure that cannot be expected to provide any benefit beyond a likely transient placebo effect, the threshold regarding what constitutes "too little" or "too much" in a sham procedure is difficult to determine. For example, in a lesion study, if a sham lesion involved inserting a radiofrequency or laser probe directly into the target structure, one could argue that a micro-lesion effect may persist and mimic to some degree the actual lesion, and therefore this is not a true control, but a partial treatment. Conversely, if the probe is not inserted fully to target, those control patients will have less of the transient effects of probe insertion at the target (e.g., due to edema) and so will not represent a true control that differs only in the actual creation of a lesion; any improvement observed in the treatment group, especially if transient, could therefore reflect these "insertion effects."

The AAV2-GAD study [9, 39] to assess the efficacy of gene therapy delivered to the subthalamic nucleus of patients with Parkinson's disease is an example of a sham-controlled drug infusion study which engendered some disagreement related to the limited extent of sham surgery employed. The control procedure involved a partial thickness burr hole without the insertion of the drug delivery catheter into the brain. This study was criticized for the lack of any possibility of a micro-lesion effect, which is commonly observed at this target in DBS surgery. Much of the criticism arose from the fact that infusion studies, unlike lesion studies, have the opportunity to perform a more rigorous control procedure, in which all patients undergo catheter placement and infusion, but controls receive only vehicle. A difference in effect can therefore more cleanly be ascribed to the putatively active compound. Practically speaking, however, it was almost certainly better from the perspective of fulfilling enrollment requirements to tell patients that, were they randomized to the control procedure, nothing would be inserted or infused into the brain; yet even this limited sham procedure might be regarded as too much by some patients [40].

More recently, the availability of focused ultrasound (FUS) may offer the potential for more acceptable sham procedures, as in the pivotal trial of FUS for essential tremor (ET) [8]. In that trial, no ultrasound energy was delivered to the control patients, who nevertheless underwent

a head-shave, targeting scans, and in-scanner physical testing. However, to the extent that patients might have understood that FUS creates immediate lesions and that thalamotomy should be associated with improvements in tremor, this sham procedure may not have been truly blinded given the strong precedents and expectations. The only variable being tested, really, was whether the FUS device can indeed produce a sufficiently accurate thalamotomy lesion, and at least some patients would likely have presumed there was enough evidence of this technical capability to run the trial in the first place.

From a regulatory perspective, this trial was sufficient to garner FDA approval for this method of treating medically intractable ET. From a clinical perspective, however, the primary question patients now ask is whether FUS or DBS is the "better" treatment, however they define that term. To many in the field, given that FUS can produce focal lesions and given the knowledge that VIM thalamotomy is an effective lesion procedure for ET, the success of this trial in simply reducing tremor was not surprising or of primary interest. Rather, assessments of effect size and durability, as well as of related complications (e.g., dysarthria, ataxia, persistent paresthesias, etc.), as compared to other neurosurgical treatments, particularly DBS, were the main concerns. One might therefore argue that once the technical capabilities of the FUS device have been established, given the known efficacy of thalamotomy for ET more generally, a sham-controlled trial of FUS thalamotomy was not likely to be very informative, and what was really needed was a comparison with other methods of surgically treating ET. In situations where the baseline efficacy of a particular lesion procedure remains uncertain (e.g., psychiatric disease, where randomized, sham-controlled lesion studies are rare and sometimes indeterminate [15]), this approach might have been more valuable. For ET, should a head-to-head trial of DBS vs. FUS have been performed, and could it have been performed in a rigorous fashion to examine both the baseline efficacy of the new procedure and to compare it to the existing DBS option? Should FUS have been compared to other lesion procedures, rather than to a sham procedure or to DBS? Furthermore, practically speaking, who would pay for such a head-to-head comparison? In many ways, the executed trial was the simplest and cleanest, even though the most pressing clinical questions were not directly addressed. For now, meta-analyses of separate trials are the only available means of comparison [41].

The lesson here is that the "ideal" control may depend on one's perspective. From an industry or commercial viewpoint, the simplest design to achieve regulatory approval is desirable. From a scientific standpoint, however, the comparison between treatment and control groups should inform clinically relevant decisions. These goals do not necessarily align in every case.

Neurostimulation trials may, in many respects, be the simplest to control. Many recent studies have employed the strategy of implanting every subject and then comparing "OFF" to "ON" conditions, whether that is between subjects (e.g., staggered start or withdrawal of active stimulation in one group) or within subjects (cross-over design). Which of these methods to employ may depend on the type of benefit the stimulation is anticipated to provide. For example, if neurostimulation is expected to provide a simple symptomatic benefit (e.g., tremor reduction), a cross-over design may be ideal, because each patient serves as her/his own control (in addition to being able to compare ON and OFF conditions across patients); if there is a benefit, all patients can eventually be placed in the ON state once the trial is complete. Alternatively, if stimulation is predicted to provide a disease-modifying benefit, particularly one that may accumulate with time, then it may be worthwhile to follow patients for longer durations and avoid turning the system off once it has been turned on. In this case, a delayed start paradigm might be more optimal, because the group that is initially ON can continue to be monitored for cumulative effect on disease progression over time (rather than have them ON then OFF then later back ON which could potentially start the accumulation process over again), as was done in the ADvance trial of fornix DBS for Alzheimer's disease [16, 42].

Any of these neurostimulation study designs assumes, for the sake of blinding, that the patients cannot distinguish the ON vs. OFF states. For this reason, it may be worthwhile including a formal experiment in these studies in which patients are challenged in a two-alternative forced-choice paradigm to distinguish whether the stimulator is active or inactive at different settings. This could serve as an important guide to determine which settings are consistent with the goal of double-blinded ON vs. OFF assessments.

Selecting Anatomical Targets

Identifying the optimal anatomical target(s) is a core problem in neuromodulation studies, and the factors involved in this decision are at least as diverse as the conditions to be treated. Here, general principles that may be relevant across a broad range of studies are considered.

Ideally, there should be evidence of a causal link between activity in the target structure or pathway and disease manifestations. Nevertheless, co-variance of activity at the target and disease expression may be helpful when grounded in a well-supported circuit model; even if an area is downstream of those brain regions that directly cause symptom expression, there is the possibility of a retrograde influence of electrical stimulation, for example. Whether retrograde, anterograde, or on-target stimulation is more effective or specific is likely to vary by target and disease.

In principle, a combination of these approaches (e.g., multi-site stimulation to affect multiple nodes in a targeted circuit) could augment efficacy or specificity of a particular stimulation effect; one could imagine that specificity should be enhanced if a lower level of stimulation were applied to multiple nodes in a single network, such that local off-target effects would be reduced, but the effective perturbation applied to that system would nonetheless reflect an approximate sum of that applied to the individual sites. Lesions, of course, may be synergistic as well. For example, combined cingulotomy and subcaudate tractotomy—the so-called limbic leukotomy—appeared to benefit OCD patients who had previously undergone only cingulotomy without significant improvement [43].

This notion that neuromodulation targets are properly networks rather than individual anatomical sites has gained increasing attention and acceptance, especially within the realm of epilepsy surgery [44–47]. While epilepsy may be somewhat an outlier in terms of the strength and coherence of the underlying neural activity, the premise that any behavior, be it normal or symptomatic, arises from the concerted activity of a distributed set of connected neural structures is not controversial [48]. What is not known is whether addressing multiple nodes for neuromodulation will consistently improve therapeutic outcomes, or whether there are cases where single targets are not only sufficient but perhaps optimal. In some cases, there may be a direct relationship between the complexity of disease manifestations and the corresponding size of the optimal target network. For example, most "functional" neurosurgeons have probably wondered if combined STN and GPi DBS in Parkinson's disease might provide synergistic benefits, given the incomplete overlap between the sets of therapeutic benefits observed at each target [5, 49–51]. Perhaps this strong degree of therapeutic overlap itself is reflective of the monosynaptic relationship between these target structures. A corollary of the idea that distributed neuromodulation may benefit multiple dimensions of a disease state may be that the span of benefit across dimensions is related to the network distance (number of synapses) and strength of connectivity between targeted sites.

The degrees of freedom that any particular neuroanatomical target affords—that is, the number of distinct dimensions of behavior that can be differentially modified—may be related to its place in the phylogenetic hierarchy. In other words, more complex behaviors evolved more recently and are likely mediated by more recently appearing structures. Thus brainstem stimulation of ascending neuromodulatory systems may function as a fairly simple gain control on certain aspects of arousal, attention, reinforcement, or decision thresholds [52–55], whereas cortical

stimulation would be expected to produce more complex effects on particular domains of behavior. In fact, given the significant heterogeneity of responses seen in the cortex, especially areas such as the prefrontal cortex where single neurons heterogeneously encode complicated mixtures of task-specific features [56], addressing the full space of information processing available at those sites is likely to require much more fine-scale control of specific cortical columns or layers than is currently possible, though there is certainly interest in developing that capability (e.g., by companies such as Neuralink and Kernel).

White matter targets provide a means to address a potentially wide area of cortex (or other connected structures) within a small volume. Ventral internal capsule lesions or stimulation is one example of this approach, in which the goal is to modify the functioning of the orbitofrontal cortex broadly in patients with intractable, debilitating obsessive-compulsive disorder [57]. Such a strategy, however, necessarily gives up hope of achieving precise behavioral effects with a high degree of specificity. Nonetheless, nonspecific effects over a broad domain of behavior may in fact be what are needed for therapeutic effect in some disease states. Conversely, the apparently limited cognitive sequelae of white matter lesions, particularly within the frontal lobes, can seem quite surprising. Cingulotomy, ventral capsulotomy, and subcaudate tractotomy generally result in relatively subtle cognitive changes [58–63] and may even improve performance in some cognitive domains [64]; these likely reflect the distributed complexity and plasticity of the frontal lobes, as well as the potential ability of information to be routed around the lesion (e.g., while a capsulotomy severs many subcortical orbitofrontal connections, cortico-cortical connections are left intact). However, whether this serves as some simple gain control on the overall function of that region or instead is affecting some subtle aspect of its function in a general manner is unknown (e.g., in capsulotomy, does the orbitofrontal cortex simply have less access to reinforcement mechanisms via the cortical-basal ganglia-thalamic-cortical loop, but it nevertheless retains the ability to process information from other cortical areas much as it had before?).

These considerations reveal that our ability to identify optimal neuroanatomical targets for neuromodulation in specific disorders is limited in large part by our rudimentary understanding of circuit-level disease mechanisms and a nascent understanding of normal systems-level function in the relevant brain areas. Even once a candidate target is identified, the manner in which its activity is to be modified poses yet another significant challenge. Is the goal to block activity to mimic lesion-type benefits? Is the goal to normalize rhythms that serve as "carrier" signals for effective neural processing? Is stimulation intended to "bridge" damaged or dysfunctional circuits, as in many brain-machine interface projects? What types of stimulation will achieve the desired neural effects? These questions, though beyond the scope of this discussion, are clearly central to the development of new neuromodulation therapies.

Selecting Patients

Two factors are highly relevant to defining the most appropriate patient population for neuromodulation within a selected disease entity: included patients should represent a relatively prevalent and typical form of the disease, and those patients should represent a stage or manifestation of the disease that is amenable to modification, either symptomatically or pathophysiologically. In addition, selection criteria should ideally be fairly straightforward to deploy, such that if the neuromodulation therapy were found to be effective, continued success in broader application would not be limited by lack of necessary tools to identify appropriate patients (e.g., ultra-high-field MRI, expensive and sparsely available molecular testing, etc.) or by complex patient selection protocols that yield a mismatch between the studied population and the actually utilized population.

In PD, for example, it is well-known that patients who are beyond a certain stage of disease

progression are ill-suited for DBS [65]; the motor benefits are unlikely to improve overall quality of life significantly because dementia and other non-motor factors have become the major problems, and DBS may even exacerbate dementia directly. So the extent to which the disease in such patients is "modifiable," especially from the motor perspective, is limited. The "ADvance" trial of fornix DBS for Alzheimer's disease was designed with the premise that earlier intervention would lead to better outcomes, so patients with mild, "probable" Alzheimer's dementia were recruited [16]. This study, however, included patients with early-onset dementia who were atypical of the overall disease state. Post-hoc analyses suggested these patients may have negatively biased the DBS effect (though of course such post-hoc analyses are to be viewed with caution given the large number of potential comparisons that can be applied after-the-fact). The ensuing phase of that trial, therefore, raised the minimum age of entry to be better aligned with the typical Alzheimer's population (ADvance II: NCT03622905).

Three major studies of DBS for depression have been conducted, one targeting the subcallosal cingulate [12], another targeting the ventral striatum and ventral portion of the anterior limb of the internal capsule [13], and a third targeting a similar region of the anterior limb of the internal capsule [18]. The former two trials failed to achieve overall efficacy endpoints, although there were individual cases where positive treatment effects were clearly evident (e.g., in which sudden re-emergence of symptoms was found to be related to an unappreciated depletion of the pulse generator battery). These failures are possibly attributable to incomplete specification of the anatomical target, which therefore varied by patient [66], as well as to suboptimal patient selection. Meanwhile, patients were enrolled based upon the diagnosis of depression according to guidelines in the Diagnostic and Statistical Manual (DSM), which applies a checklist of fungible diagnostic criteria, summing the number of checked items to surpass a somewhat arbitrary threshold. Therefore, patients with different constellations of symptoms may be assigned the same overall diagnostic label. Importantly, patients with depression are known to manifest symptoms in particular clusters that may have distinct neurobiological mechanisms [67]. Therefore, subtype heterogeneity may have confounded the results of these depression studies. This type of phenomenon has been observed in OCD, where particular subtypes (e.g., "hoarders") appear less likely to benefit from capsulotomy [68]. For these reasons, if subgroups are known to exist but there is no a priori hypothesis regarding which ones are likely to benefit, adequately powering the study for pre-specified sub-group analyses may be a worthwhile effort, or limiting the study to a particular subgroup might be considered.

The notion that DSM disease categories may be insufficient to capture distinct neuropathological entities has led to the movement to characterize behavior according to traits that are potentially more fundamental as seen from a neural systems perspective. Specifically, the US National Institutes of Health "Research Domain Criteria" (RDoC) framework views behavior through the lens of six domains (positive valence, negative valence, cognitive systems, social processes, arousal/regulatory systems, and sensorimotor systems). Each domain contains constructs that focus on particular functions (e.g., sensitivity to reward and ability to use reward for learning, in the case of positive valence systems). Behavioral performance on a battery of tasks that assess these functions is hypothesized to be a more sensitive and specific classifier of neuropsychological function than traditional criteria [69]. While the particular tasks employed to assess these functions are not nearly as standardized or validated as common clinical tools (i.e., DSM categories, standard scales, and routine neuropsychological tests), the promise of this "first principles" approach to behavior is that neuropsychiatric disease might be defined according to underlying mechanisms, and this would certainly be more desirable for neuromodulation trials.

Determining Frequency and Duration of Follow-Up

Neuromodulation studies, like all clinical trials, must balance a desire for frequent and long-term follow-up with practical considerations such as burden on patients, cost, and timely reporting of results. In many cases, patients will travel long distances to participate in these studies, and so the financial and logistical hurdles resulting from frequent, ongoing follow-up can be significant. Nevertheless, there is a clear need to maximize data collection to benefit the overall reliability of results.

Most neuromodulation studies include some set of behavioral assessments at pre-specified intervals. In light of the high variability of behavioral performance even within subjects across sessions, days, and months, more frequent measurement will serve to reduce noise. Because the power of a study is inversely related to the variability of the measurements, to the extent that more accurate assessments of individual subjects are obtainable (e.g., taken as the average over more frequent estimates), it may be possible to use this increased signal to noise as a means to counterbalance the number of subjects required for the study. There may in fact be an overall cost savings because additional assessments of patients who have already undergone an expensive neuromodulation-related procedure are almost certainly less expensive than performing more procedures on additional patients, even if travel, housing, and other related expenses are required.

Because many neuromodulation therapies show gradual symptomatic responses, a sufficient duration of follow-up can be critical to the proper evaluation of a new approach. One prominent example of an inadequate duration to primary endpoint leading to apparent therapeutic failure is the SANTE trial of thalamic DBS for epilepsy [23]. Here, seizure reduction at the pre-specified 3-month endpoint did not reach the threshold for success, so FDA approval was not immediately obtained. Nevertheless, clear improvements in seizure burden were observed at 6 months and beyond [70]. Eventually, based upon these extended data, regulatory approval was granted. Like epilepsy, dystonia and OCD are also known to exhibit gradually improving responses to neuromodulation with time [71, 72], so future trials are likely to benefit by keeping these examples in mind when scheduling final endpoints.

Planning for Post-protocol Patient Care

Neurostimulation studies are distinct in that subjects are implanted with complicated electronic devices that are often intended to be permanent. When a study ends, these devices nonetheless remain. These devices may require ongoing maintenance (replacement of implanted batteries, replacement or repair of wireless charging equipment, etc.). If a study has succeeded and regulatory approval is granted, long-term care may not be a problem. More likely, however, when a study fails, the status of ongoing care for the device may become uncertain with respect to the responsible parties and the cost.

While one might presume naively that a failed trial should not provide any reason to continue support for an ineffective device, patients often feel differently. In some cases, there truly are individual patients who are receiving benefit from the implanted device; in such cases, withdrawal of device support after a patient has undergone the risks and troubles of having the device implanted and participating in the study could be viewed as unethical. Yet even if there is no clear evidence that a patient is receiving benefit, many patients will perceive benefit—whether through the filter of a placebo effect or because they are truly experiencing something not captured in the study protocol—or they may at least continue to hold onto the hope of benefit. In these cases, many might conclude the most ethical course of action is to continue device support. Even warning patients during the consent process that if the study fails device support will not continue may not be a sufficient means to avoid this ethical responsibility because, at the very least, there may in fact be a real individual benefit.

Committing to and budgeting for long-term device support is therefore the best approach, whenever possible. Device manufacturers have been generally helpful in providing continued support after a failed trial. Insurance companies tend to be more heterogeneous in their willingness to pay for related procedures, but often this is possible if a clinical team is sufficiently persistent and able to work through the logistical hurdles. Depending on the extent to which this becomes a more widespread problem as the number of neuromodulation trials increases, perhaps competitors within academia and industry would be willing to work together to expand the field as a whole by creating a fund, fed by a tax on individual trials, to support at least the medical costs incurred by ongoing device maintenance when other means to cover those costs (insurance or philanthropy) are unavailable.

Conclusions

The advancement of neuromodulation will be driven by successful clinical studies. The success of these studies, however, does not hinge upon solely the achievement of the primary therapeutic goals, but rather derives equally from their ability to deliver confident answers to well-posed questions. We should realistically expect most trials to fail in achieving their predicted therapeutic outcomes; if that were not the case, it would reflect a lack of ambition to overcome the most difficult and pressing problems faced by individuals with neuropsychiatric disease. Designing trials that are just as informative in failure as they are in success is necessary to ensure progress in the field as well as to justify the risks undertaken by the brave and pioneering patients who enroll in these studies.

Trials embarked upon too early, without sufficient rationale, not only expose patients to potentially unnecessary risks but also threaten overall progress. Likewise, a well-reasoned neuromodulation strategy examined via a suboptimal study design may fail to reveal the truth of that strategy. Although interest in neuromodulation has expanded greatly as technological ability and neuroscientific knowledge have improved, there is nevertheless a finite set of resources, both in terms of economic and human capital, to apply toward sufficiently intensive and large-scale studies. Therefore, optimizing trial design by heeding the positive and negative lessons of those studies preceding is essential to realize the brightest future of neuromodulation.

References

1. Teskey GC, Monfils MH, VandenBerg PM, Kleim JA. Motor map expansion following repeated cortical and limbic seizures is related to synaptic potentiation. Cereb Cortex. 2002;12:98–105.
2. van Rooyen F, Young NA, Larson SE, Teskey GC. Hippocampal kindling leads to motor map expansion. Epilepsia. 2006;47:1383–91.
3. Kupsch A, Benecke R, Muller J, Trottenberg T, Schneider GH, et al. Pallidal deep-brain stimulation in primary generalized or segmental dystonia. N Engl J Med. 2006;355:1978–90.
4. Deuschl G, Schade-Brittinger C, Krack P, Volkmann J, Schäfer H, et al. A randomized trial of deep-brain stimulation for Parkinson's disease. N Engl J Med. 2006;355:896–908.
5. Odekerken VJJ, van Laar T, Staal MJ, Mosch A, Hoffmann CFE, et al. Subthalamic nucleus versus globus pallidus bilateral deep brain stimulation for advanced Parkinson's disease (NSTAPS study): a randomised controlled trial. Lancet Neurol. 2013;12:37–44.
6. Weaver FM, Follett K, Stern M, Hur K, Harris C, et al. Bilateral deep brain stimulation vs best medical therapy for patients with advanced Parkinson disease: a randomized controlled trial. JAMA. 2009;301:63–73.
7. Follett KA, Weaver FM, Stern M, Hur K, Harris CL, et al. Pallidal versus subthalamic deep-brain stimulation for Parkinson's disease. N Engl J Med. 2010;362:2077–91.
8. Elias WJ, Lipsman N, Ondo WG, Ghanouni P, Kim YG, et al. A randomized trial of focused ultrasound thalamotomy for essential tremor. N Engl J Med. 2016;375:730–9.
9. LeWitt PA, Rezai AR, Leehey MA, Ojemann SG, Flaherty AW, et al. AAV2-GAD gene therapy for advanced Parkinson's disease: a double-blind, sham-surgery controlled, randomised trial. Lancet Neurol. 2011;10:309–19.
10. Marks WJ Jr, Bartus RT, Siffert J, Davis CS, Lozano A, et al. Gene delivery of AAV2-neurturin for Parkinson's disease: a double-blind, randomised, controlled trial. Lancet Neurol. 2010;9:1164–72.
11. Lang AE, Gill S, Patel NK, Lozano A, Nutt JG, et al. Randomized controlled trial of intraputamenal

glial cell line-derived neurotrophic factor infusion in Parkinson disease. Ann Neurol. 2006;59:459–66.
12. Holtzheimer PE, Husain MM, Lisanby SH, Taylor SF, Whitworth LA, et al. Subcallosal cingulate deep brain stimulation for treatment-resistant depression: a multisite, randomised, sham-controlled trial. Lancet Psychiatry. 2017;4:839–49.
13. Dougherty DD, Rezai AR, Carpenter LL, Howland RH, Bhati MT, et al. A randomized sham-controlled trial of deep brain stimulation of the ventral capsule/ventral striatum for chronic treatment-resistant depression. Biol Psychiatry. 2015;78:240–8.
14. Mallet L, Polosan M, Jaafari N, Baup N, Welter ML, et al. Subthalamic nucleus stimulation in severe obsessive-compulsive disorder. N Engl J Med. 2008;359:2121–34.
15. Lopes AC, Greenberg BD, Canteras MM, Batistuzzo MC, Hoexter MQ, et al. Gamma ventral capsulotomy for obsessive-compulsive disorder: a randomized clinical trial. JAMA Psychiat. 2014;71:1066–76.
16. Lozano AM, Fosdick L, Chakravarty MM, Leoutsakos JM, Munro C, et al. A phase II study of fornix deep brain stimulation in mild Alzheimer's disease. J Alzheimers Dis. 2016;54:777–87.
17. Denys D, Mantione M, Figee M, van den Munckhof P, Koerselman F, et al. Deep brain stimulation of the nucleus accumbens for treatment-refractory obsessive-compulsive disorder. Arch Gen Psychiatry. 2010;67:1061–8.
18. Bergfeld IO, Mantione M, Hoogendoorn ML, Ruhe HG, Notten P, et al. Deep brain stimulation of the ventral anterior limb of the internal capsule for treatment-resistant depression: a randomized clinical trial. JAMA Psychiat. 2016;73:456–64.
19. Wiebe S, Blume WT, Girvin JP, Eliasziw M, Group EaEoSfTLES. A randomized, controlled trial of surgery for temporal-lobe epilepsy. N Engl J Med. 2001;345:311–8.
20. Heck CN, King-Stephens D, Massey AD, Nair DR, Jobst BC, et al. Two-year seizure reduction in adults with medically intractable partial onset epilepsy treated with responsive neurostimulation: final results of the RNS System Pivotal trial. Epilepsia. 2014;55:432–41.
21. Barbaro NM, Quigg M, Ward MM, Chang EF, Broshek DK, et al. Radiosurgery versus open surgery for mesial temporal lobe epilepsy: the randomized, controlled ROSE trial. Epilepsia. 2018;59:1198–207.
22. Barbaro NM, Quigg M, Broshek DK, Ward MM, Lamborn KR, et al. A multicenter, prospective pilot study of gamma knife radiosurgery for mesial temporal lobe epilepsy: seizure response, adverse events, and verbal memory. Ann Neurol. 2009;65:167–75.
23. Fisher R, Salanova V, Witt T, Worth R, Henry T, et al. Electrical stimulation of the anterior nucleus of thalamus for treatment of refractory epilepsy. Epilepsia. 2010;51:899–908.
24. North RB, Kidd DH, Farrokhi F, Piantadosi SA. Spinal cord stimulation versus repeated lumbosacral spine surgery for chronic pain: a randomized, controlled trial. Neurosurgery. 2005;56:98–106; discussion 06–7.
25. Kumar K, Taylor RS, Jacques L, Eldabe S, Meglio M, et al. Spinal cord stimulation versus conventional medical management for neuropathic pain: a multicentre randomised controlled trial in patients with failed back surgery syndrome. Pain. 2007;132:179–88.
26. Kapural L, Yu C, Doust MW, Gliner BE, Vallejo R, et al. Novel 10-kHz high-frequency therapy (HF10 therapy) is superior to traditional low-frequency spinal cord stimulation for the treatment of chronic back and leg pain: the SENZA-RCT randomized controlled trial. Anesthesiology. 2015;123:851–60.
27. Penn RD, Savoy SM, Corcos D, Latash M, Gottlieb G, et al. Intrathecal baclofen for severe spinal spasticity. N Engl J Med. 1989;320:1517–21.
28. Brown JA, Lutsep HL, Weinand M, Cramer SC. Motor cortex stimulation for the enhancement of recovery from stroke: a prospective, multicenter safety study. Neurosurgery. 2006;58:464–73.
29. Broadway JM, Holtzheimer PE, Hilimire MR, Parks NA, Devylder JE, et al. Frontal theta cordance predicts 6-month antidepressant response to subcallosal cingulate deep brain stimulation for treatment-resistant depression: a pilot study. Neuropsychopharmacology. 2012;37:1764–72.
30. Chow SC. Adaptive clinical trial design. Annu Rev Med. 2014;65:405–15.
31. Mansournia MA, Higgins JP, Sterne JA, Hernan MA. Biases in randomized trials: a conversation between trialists and epidemiologists. Epidemiology. 2017;28:54–9.
32. Pearl J. An introduction to causal inference. Int J Biostat. 2010;6:Article 7.
33. Porta M, Vineis P, Bolumar F. The current deconstruction of paradoxes: one sign of the ongoing methodological "revolution". Eur J Epidemiol. 2015;30:1079–87.
34. Weintraub WS, Luscher TF, Pocock S. The perils of surrogate endpoints. Eur Heart J. 2015;36:2212–8.
35. Alonso A, Van der Elst W, Molenberghs G, Buyse M, Burzykowski T. On the relationship between the causal-inference and meta-analytic paradigms for the validation of surrogate endpoints. Biometrics. 2015;71:15–24.
36. Molenberghs G, Burzykowski T, Alonso A, Assam P, Tilahun A, Buyse M. A unified framework for the evaluation of surrogate endpoints in mental-health clinical trials. Stat Methods Med Res. 2010;19:205–36.
37. Landau S, Emsley R, Dunn G. Beyond total treatment effects in randomised controlled trials: baseline measurement of intermediate outcomes needed to reduce confounding in mediation investigations. Clin Trials. 2018;15:247–56.
38. Probst P, Grummich K, Harnoss JC, Huttner FJ, Jensen K, et al. Placebo-controlled trials in surgery: a systematic review and meta-analysis. Medicine (Baltimore). 2016;95:e3516.
39. Niethammer M, Tang CC, LeWitt PA, Rezai AR, Leehey MA, et al. Long-term follow-up of

a randomized AAV2-GAD gene therapy trial for Parkinson's disease. JCI Insight. 2017;2:e90133.
40. Cohen PD, Isaacs T, Willocks P, Herman L, Stamford J, et al. Sham neurosurgical procedures: the patients' perspective. Lancet Neurol. 2012;11:1022.
41. Harary M, Segar DJ, Hayes MT, Cosgrove GR. Unilateral thalamic deep brain stimulation versus focused ultrasound thalamotomy for essential tremor. World Neurosurg, vol. 126; 2019. p. e144.
42. Leoutsakos J-MS, Yan H, Anderson WS, Asaad WF, Baltuch G, et al. Deep brain stimulation targeting the fornix for mild Alzheimer dementia (the ADvance trial): a two year follow-up including results of delayed activation. J Alzheimers Dis. 2018;64:597–606.
43. Bourne SK, Sheth SA, Neal J, Strong C, Mian MK, et al. Beneficial effect of subsequent lesion procedures after nonresponse to initial cingulotomy for severe, treatment-refractory obsessive-compulsive disorder. Neurosurgery. 2013;72:196–202; discussion 02.
44. Bartolomei F, Lagarde S, Wendling F, McGonigal A, Jirsa V, et al. Defining epileptogenic networks: contribution of SEEG and signal analysis. Epilepsia. 2017;58:1131–47.
45. Bernhardt BC, Bonilha L, Gross DW. Network analysis for a network disorder: the emerging role of graph theory in the study of epilepsy. Epilepsy Behav. 2015;50:162–70.
46. Laxpati NG, Kasoff WS, Gross RE. Deep brain stimulation for the treatment of epilepsy: circuits, targets, and trials. Neurotherapeutics. 2014;11:508–26.
47. Spencer SS. Neural networks in human epilepsy: evidence of and implications for treatment. Epilepsia. 2002;43:219–27.
48. Stam CJ. Modern network science of neurological disorders. Nat Rev Neurosci. 2014;15:683–95.
49. Baizabal-Carvallo JF, Roze E, Aya-Kombo M, Romito L, Navarro S, et al. Combined pallidal and subthalamic nucleus deep brain stimulation in secondary dystonia-parkinsonism. Parkinsonism Relat Disord. 2013;19:566–8.
50. Boel JA, Odekerken VJJ, Schmand BA, Geurtsen GJ, Cath DC, et al. Cognitive and psychiatric outcome 3 years after globus pallidus pars interna or subthalamic nucleus deep brain stimulation for Parkinson's disease. Parkinsonism Related Disord. 2016;33:90–5.
51. Weaver FM, Follett KA, Stern M, Luo P, Harris CL, et al. Randomized trial of deep brain stimulation for Parkinson disease: thirty-six-month outcomes. Neurology. 2012;79:55–65.
52. Avery MC, Krichmar JL. Neuromodulatory systems and their interactions: a review of models, theories, and experiments. Front Neural Circuits. 2017;11:108.
53. Carter ME, Yizhar O, Chikahisa S, Nguyen H, Adamantidis A, et al. Tuning arousal with optogenetic modulation of locus coeruleus neurons. Nat Neurosci. 2010;13:1526–33.
54. Lee SH, Dan Y. Neuromodulation of brain states. Neuron. 2012;76:209–22.
55. Lin SC, Brown RE, Hussain Shuler MG, Petersen CC, Kepecs A. Optogenetic dissection of the basal forebrain neuromodulatory control of cortical activation, plasticity, and cognition. J Neurosci. 2015;35:13896–903.
56. Rigotti M, Barak O, Warden MR, Wang X-J, Daw ND, et al. The importance of mixed selectivity in complex cognitive tasks. Nature. 2013;497(7451):585–90.
57. Rasmussen SA, Norén G, Greenberg BD, Marsland R, McLaughlin NC, et al. Gamma ventral capsulotomy in intractable obsessive-compulsive disorder. Biol Psychiatry. 2018;84(5):355–64.
58. Kartsounis LD, Poynton A, Bridges PK, Bartlett JR. Neuropsychological correlates of stereotactic subcaudate tractotomy. A prospective study. Brain. 1991;114(Pt6):2657–73.
59. Nyman H, Andreewitch S, Lundback E, Mindus P. Executive and cognitive functions in patients with extreme obsessive-compulsive disorder treated by capsulotomy. Appl Neuropsychol. 2001;8:91–8.
60. Ochsner KN, Kosslyn SM, Cosgrove GR, Cassem EH, Price BH, et al. Deficits in visual cognition and attention following bilateral anterior cingulotomy. Neuropsychologia. 2001;39:219–30.
61. Ridout N, O'Carroll RE, Dritschel B, Christmas D, Eljamel M, Matthews K. Emotion recognition from dynamic emotional displays following anterior cingulotomy and anterior capsulotomy for chronic depression. Neuropsychologia. 2007;45:1735–43.
62. Subramanian L, Bracht T, Jenkins P, Choppin S, Linden DE, et al. Clinical improvements following bilateral anterior capsulotomy in treatment-resistant depression. Psychol Med. 2017;47:1097–106.
63. Williams ZM, Bush G, Rauch SL, Cosgrove GR, Eskandar EN. Human anterior cingulate neurons and the integration of monetary reward with motor responses. Nat Neurosci. 2004;7:1370–5.
64. Batistuzzo MC, Hoexter MQ, Taub A, Gentil AF, Cesar RC, et al. Visuospatial memory improvement after gamma ventral capsulotomy in treatment refractory obsessive-compulsive disorder patients. Neuropsychopharmacology. 2015;40:1837–45.
65. Daniels C, Krack P, Volkmann J, Pinsker MO, Krause M, et al. Risk factors for executive dysfunction after subthalamic nucleus stimulation in Parkinson's disease. Mov Disord. 2010;25:1583–9.
66. Riva-Posse P, Choi KS, Holtzheimer PE, Crowell AL, Garlow SJ, et al. A connectomic approach for subcallosal cingulate deep brain stimulation surgery: prospective targeting in treatment-resistant depression. Mol Psychiatry. 2018;23:843–9.
67. Drysdale AT, Grosenick L, Downar J, Dunlop K, Mansouri F, et al. Resting-state connectivity biomarkers define neurophysiological subtypes of depression. Nat Med. 2017;23:28–38.
68. Gentil AF, Lopes AC, Dougherty DD, Rück C, Mataix-Cols D, et al. Hoarding symptoms and prediction of poor response to limbic system surgery for treatment-refractory obsessive-compulsive disorder. J Neurosurg. 2014;121:123–30.

69. Cuthbert BN, Insel TR. Toward the future of psychiatric diagnosis: the seven pillars of RDoC. BMC Med. 2013;11:126.
70. Salanova V, Witt T, Worth R, Henry TR, Gross RE, et al. Long-term efficacy and safety of thalamic stimulation for drug-resistant partial epilepsy. Neurology. 2015;84:1017–25.
71. Kupsch A, Tagliati M, Vidailhet M, Aziz T, Krack P, et al. Early postoperative management of DBS in dystonia: programming, response to stimulation, adverse events, medication changes, evaluations, and troubleshooting. Mov Disord. 2011;26 Suppl 1:S37–53.
72. Rasmussen SA, Noren G, Greenberg BD, Marsland R, McLaughlin NC, et al. Gamma ventral capsulotomy in intractable obsessive-compulsive disorder. Biol Psychiatry. 2018;84:355–64.

Registries and Big Data

38

Douglas Kondziolka

Stereotactic and functional neurosurgery is well suited for registry development. The field has a long history of surgical investigation and innovation based on data collection and reporting. We translate the findings of neurobiology or tissue biology into real surgeries for patients to preserve or improve function. Surgeries are commonly guided precisely using mathematical principles and computer support. In our procedures, we collect ample information that is clinical, imaging-based, neurophysiological, electrical, or physical. We have standardized scoring systems to measure disability, disease, and outcome. All of these elements are well suited to registry use. And due to standardization, many elements are already suited for automated uploading into data collection systems.

Big data is the use of large amounts of data collected for one purpose and used for another. In our own field, we are slowly getting to this use. However, for truly meaningful utility, the data sets need to be very big and the questions asked of this data focused and relevant. Using a national insurance sample of CPT codes is a frequent tool reflected in the scientific literature over the past decade or so. Meaningful? Sometimes. These samples can inform about demographics, some outcomes, length of stay, and other concerns. Perhaps one can glean why a hospital stay was longer, if the patient was coded to have had an infection. But the questions you may want to know from such data are often elusive. Was a surgery more frequently performed simply due to surgeon preference or surgeon training? These databases are relatively easy to mine. Interestingly, it is uncommon that authors provide data from their own institution on a topic, which they have with high fidelity, to compare or benchmark with national data. If they care enough about the topic, why do they not share their own experience? Well, one answer is that takes much more work.

Optimally, we want to collect data elements that we value, collect a lot of it, and get it into big data range. The Society of Thoracic Surgeons (STS) has long had a large surgical registry. The American Board of Neurological Surgery (ABNS) has launched its POST system (Practice and Outcomes of Surgical Therapies) as part of the neurosurgeon credentialing and board certification process. This system will collect a set number of cases and outcomes, *with images*, from newly practicing neurosurgeons, evaluated and audited by the ABNS. From approximately 200 candidate neurosurgeons per year, up to 30,000 cases will be collected annually. The database will become the largest of its kind. The purpose is to help the ABNS evaluate individual surgeons for board certification. The ABNS represents the public and the specialty, and this

D. Kondziolka (✉)
Department of Neurosurgery, NYU Langone Health, New York, NY, USA

Department of Radiation Oncology, New York University, New York, NY, USA
e-mail: douglas.kondziolka@nyumc.org

N. Pouratian, S. A. Sheth (eds.), *Stereotactic and Functional Neurosurgery*,
https://doi.org/10.1007/978-3-030-34906-6_38

system works to understand practice dynamics, disease states, and complication rates. It will help the ABNS understand its own credentialing practices and help to improve them. It also makes elements of the oral examination more candidate-relevant and more efficient. This is the *primary* purpose of POST data. Although not its primary intent, the collected data could potentially be used for as a "big data" resource. That might be to inform neurosurgical education and training and foster other investigations (e.g., what is the incidence of durotomy following lumbar disk herniation; how do surgeons actually manage chronic subdural hematomas; since images are collected, what percentage of resected meningiomas are small in volume (i.e., <3 cc); and what is the spectrum of time from diagnosis to deep brain stimulation surgery in patients with Parkinson's disease?). These are big data questions.

What Needs to Be Done

Registry development takes work. A lot of work, time, and expense. If done at your own institution, it will certainly take some form of information sciences support. If built for multicenter use to allow faster and large collected data sets, it will likely need a corporate partner, funding agency, or other stakeholders. One might refer to this as "somebody else who cares." The first stereotactic radiosurgery registry, designed for both local or global use, was developed by four neurosurgeons at the University of Pittsburgh (Kondziolka, Lunsford, Niranjan, Kano), with the input of clinicians at other centers who shared their research databases and the support of software engineers at Elekta (Sunnyvale, CA) [1, 2]. A second radiosurgery registry was developed by Brainlab (Munich, Germany) also working with clinicians [3]. Both were sought after by the NeuroPoint Alliance (NPA), on behalf of the American Association of Neurological Surgeons, to create a United States-based radiosurgery registry. Radiosurgery is an interesting field to study, because it involves so many different elements of neurosurgical practice – benign and malignant tumors, vascular malformations, and functional disorders. The initial goal was to collect data on 30,000 patients in 3 years, focusing only on tumors. This was not achieved. Institutional legal concerns about data sharing, software installation and training, and finding people at each site to "actually do the work" were just some components of the delay. Eventually only data from the Brainlab Quentry system was used, despite the fact that the majority of cases in the first year came from our center at NYU using the Elekta system. Some but not all data fields had been matched. This is not to be critical. Brainlab is to be commended for their continued support of this important project. High-fidelity registry development is labor intensive. But the pay-off can be great.

Current Use of a Large Registry

As of this writing, we have over 3200 stereotactic radiosurgery cases in our prospective registry. This is not yet big data and probably not yet large data. But it is already powerful and growing. Table 38.1 shows NYU's current use of this registry.

Physicians desire tools that allow them to collect useful medical information efficiently and to use that information for a diverse set of tasks. These could include practice assessments, payor-required reporting requirements, data benchmarking, and research [4, 5]. The perceived or measured quality of our practice will be based on the data that we document. Thus, it is increasingly important that practices maintain their own databases that can be coupled with useful analytical tools. In some departments this may not be a priority because it can be inefficient and time consuming.

Registries in other medical specialties that have collected large amounts of data from multiple institutions are known to have changed medical practice. For example, the groundbreaking findings on cardiovascular disease reported from the 5209 patients in the Framingham study 50 years ago demonstrated the power of patient registries [6]. Despite these triumphs in an era

Table 38.1 Stereotactic radiosurgery registry at New York University

Function		Description
Data	Surgery entry	During each case at point of care
	Follow-up	During outpatient clinic or point of care, or when notified
Patient information		Used during clinic appointments for past care information – better/faster than electronic health record
Patient teaching		Live outcomes data shown to patients in the office
Research		Data fields mined/spreadsheets populated for multicenter projects
		Analytics as requested (same day) for any question
Research topic		Analytics to assess how much data has been collected for a specific proposed topic
Research graphics		Selected automatic statistics built (Kaplan-Meier curves)
		Standardized display for pre- and post-data in grading systems
Hospital administration		Case numbers, geocoded demographics, and referral patterns
Auditing		Performed by staff and students. Missing data elements checked biannually and entered from medical records
Support		NYU information sciences

before the personal computer, the tool of the large-scale clinical registry in neurosurgery remained surprisingly underutilized until the last decade. Other fields have been quicker to adopt registry technology including cardiothoracic surgery in the 1990s [7]. The developers of this registry identified six essential components, one of which is the use of a common language and nomenclature. We strongly agree with this assessment and currently adopt the standardized nomenclature developed by the working group tasked with standardizing terminology at the 16th International Leksell Gamma Knife Society Meeting in Sydney, Australia [8]. We also recognize the importance of support from a multinational subspecialty organization such as endorsement of the National Adult Cardiac Database by the Society of Thoracic Surgeons [9]. We used our registry to contribute data to another registry project endorsed by both the American Society for Radiation Oncology (ASTRO) and the American Association of Neurological Surgeons (AANS).

Once fully developed and standardized, the incorporation of data specific to diseases and patients will allow us to study outcomes in new ways. How does an audiogram change after radiosurgery when one accounts for patient age, total radiosurgery dose, rate of radiation delivery, and tumor volume? How does the hormone receptor subtype of a breast cancer brain metastasis correlate with the presence of peritumoral inflammation before radiosurgery and how this process improves or worsens after radiosurgery? If one collects all these data elements prospectively, the questions can be answered in seconds. However, these are not obvious questions to ask using traditional data collection techniques, mainly because the high-level question was formulated once some data was already collected (requiring the collection of more data that can take weeks or months). Our past and present literature broadly describes outcomes according to traditional clinical questions. New science using big data tools will allow us to probe data, ask new questions, and provide new discovery. Some examples already utilized in other fields of research include data mining, machine learning, geocoding, and new forms of graphic presentation [10–12].

Challenges and Limitations

The maintenance and collection of good-quality data is challenging. Data fields were created that described the patients and their diseases, followed the logical flow of a clinical visit, and defined clinical and imaging outcomes together with any related management. We used accepted definitions of disease parameters and validated rating scales. Some free text entry was necessary but avoided whenever possible due to the lack of standardization and of appropriate binning on the web-based display. The challenge was to collect comprehensive data that would eliminate the

need to use a separate clinical chart and yet not collect so many fields as to make the data entry process overwhelming and laborious. We aimed for data entry at the point of care to improve recording accuracy and were disciplined enough to achieve this in the vast majority of cases at all centers.

The lessons learned from developing this database highlighted that quality control is essential. During the test phase of the first 300 patients, clinical data were entered by only one person to test consistency and system reliability. Demographic data were entered by an administrative assistant and then checked by the surgeon. Nevertheless, errors occurred. Errors at data entry (via entering an incorrect decimal point or choosing the wrong selection on a scroll-down menu) were corrected by a separate review prior to saving the record. For both local and shared use, auditing of data will be paramount. For multicenter studies, proof of data fidelity by evaluating a subset of records against another archive (i.e., hospital EMR) should be part of study design and considered when budgeting time and resources.

Another challenge associated with prospective registries is ensuring the security of protected health information. Security features have been incorporated into our system to allow a specific set of privileges for each user. This could prevent errors from less experienced users. These include a "read-only" setting that allows the users the ability to view data but not to enter or change a record, a "standard user" setting allowing the creation and editing of the patient record, and database administrators who have the ability to create new users and edit privileges. All centers and individual users must meet the regulatory requirements of institutional and national agencies [13]. As this pertains to data sharing, it is important to know that protected health information, even when de-identified, is not allowed by all countries. One must check this and not assume that participation will be easy. This will be one obstacle to participation in large-scale studies, which could affect outcomes based on disease or cultural differences related to management and follow-up.

Potential Obstacles and Regulatory Considerations

Once ready for productive use, the maintenance of such a registry is almost as challenging as the inception. Constant periodic reviews by data stewards are key to ensure the data, at its core, are pristine. When an academic institution decides to undertake such an initiative, it is important that clinicians and information technology personnel are constantly collaborating so that the data are not only useful but also underline the proper policies, procedures, and compliance.

Asher et al. describe the regulatory issues important in the creation and use of large-scale registries for local or national use [13]. There are several surgical quality of care registries, including those maintained by the American College of Surgeons and the Society of Thoracic Surgeons. The National Neurosurgery Quality and Outcomes Database (N2QOD) was launched with an initial focus on spinal surgery. As described in their report, the new overlap between human subjects, research, and quality improvement efforts has strong implications on registry design [4].

In the current iteration, the registry we designed for stereotactic radiosurgery is what I describe as "research grade" [2]. We hoped to collect almost all important data elements for any project and limit the external work required from the electronic medical record or other sources. Research is therefore under the rubric of human subjects research. Patient privacy and data control fall under the supervision of an institution's local IRB. The ability to obtain a waiver of informed consent is key to maximizing data collection and reducing bias, since those who are willing to provide consent often comprise a unique, highly motivated patient population. Each center's IRB will have to decide if the registry is simply a quality improvement project and IRB review can be waived, or a research study requiring either informed consent or a consent waiver. Dokholyan et al. review the issues when clinical and administrative databases are conjoined [14]. Clearly data collection poses no direct physical risk to individual patients. HIPAA

compliance and patient protections already in place for clinical care or research must be followed regardless. The N2QOD clearly describes its activities as "not primarily intended to serve as a research initiative" and that the primary purpose of participation is "for health care operations, defined by HIPAA to include quality assessment and improvement activities, including outcomes evaluations" [13]. Registry developers and users would value additional clarity on this topic from federal legislators.

National Data Sampling

Utilizing national or statewide databases for neurosurgical research has become popular. With the data already organized, digitized, and available, access to such data and time for analysis is low cost and, if you know how to find it, efficient. Databases that are based on pragmatic, real-world care are able to describe a particular topic in areas such as demographics, treatments, complications, outcomes, and economic indicators (typically charges as opposed to costs). Geographic and socioeconomic variation in disease and care patterns can also be studied. And these data sets can be large, making them more suited to statistical evaluations [15].

However, a major concern is the reporting of research using ready-made databases that were not designed by neurosurgeons for the study of neurosurgical diseases. In many instances, these were not even designed for research [15]. Within neurosurgery, warnings have been offered via editorials and articles [16–19]. Kestle identified a number of major limitations, such as the data source, coding issues, linkages, confounders, definitions, and data validation [16].

One of the most serious weaknesses is data integrity. Investigators at the University of Calgary compared chart documentation and administrative data for patients who underwent carotid endarterectomy [20]. They reviewed 2061 charts and found that only 43% were well documented, and furthermore, poorly documented hospital charts directly translated into invalid administrative data. Another group of investigators compared readmission rates from the University HealthSystem Consortium (UHC, recently renamed Vizient) to their prospectively maintained department database in order to determine if all coded readmissions should be considered a clinically relevant readmission for the purposes of quality reporting [21]. Based on their review, they recommended exclusion of 25% of the UHC-designated readmissions cases due to clinical irrelevance (i.e., rescheduled or staged procedures, unrelated to the index procedure).

Bohl et al. and Lawson et al. undertook comparisons of two large databases (NIS vs. NSQIP and CMS claims vs. NSQIP, respectively) and found different rates of coded events and low positive predictive values between the two data sets [22, 23]. Other reported database inaccuracies for neurosurgical diseases or procedures are tethered cord release surgery coding, indications for lumbar fusion, complications in lumbar diskectomies, classification of spinal column and spinal cord injury, and coding of the presence and degree of obesity in spine surgery patients [15]. Some data elements are captured accurately, such as patient death. However many others remain problematic. And of course, for surgery, *why* someone has a procedure is rarely ever included. So while big databases may be able to provide precise results, such results may be inaccurate [24].

If you were conducting a retrospective review at your own institution, you would be highly focused on the decision of which data points to collect, the actual data gathering, and concomitant quality control (i.e., data integrity). These are time consuming. Interestingly, most authors do not include data from their own center as a comparison. For example, only three of the publications reviewed by Oravec et al. included comparative data from either the primary or senior author's own institution, including the studies by Woodworth et al. and Amin et al. noted earlier, as well as one other publication that compared institutional data with data from the Nationwide Inpatient Sample in order to validate a novel subarachnoid scoring system [15, 21, 25]. In other words, most investigators that used external data did not try to answer the same question with internal data.

With big database research, the hypothesis can only stem from what data is available. Using national or state databases, neurosurgical researchers are forced to ask questions that have debatable relevance or interest to other neurosurgeons. Often follow-up outcomes are short term. In general, the captured fields may be better suited to answer more superficial questions regarding quality, insurance payments, complications, or outcomes, but are unable to take into account the specific details of a neurosurgical procedure, that are most relevant to surgeons and readers. Thus, efforts to create meaningful registries must focus on the specific data fields to be collected. They should be as comprehensive as possible, but at the same time not too burdensome to preclude data collection.

In the last decade, our journals have published increasing numbers of articles from big external database analyses. Reports are sometimes considered to be accepted as authoritative and accurate. They can be statistically powerful, but are they meaningful? We as surgeons know what we want to know. We are also wary of conclusions that stem from data with missing information elements. This has led some to use the quote "garbage in, gospel out," first coined in the field of computing science as a warning to avoid blindly believing an outcome when the collected data was questionable [26].

The Future

The value of registries, while still underutilized and in development in neurosurgery, remains largely unproven. Although we are committed to the value of data collection for our own analyses and research, we remain concerned that outside entities (i.e., payors) may use registries for payment approval or denial. Already we are aware of some intermediaries who may refuse to pay for patients not entered into "approved registries." Who will approve and fund a big data registry? Will this be a national organization, a government office, or some other group? Will a new registry "industry" be created, similar to that associated with the electronic medical record? Clearly the initial purpose, design, and implementation of any registry require careful thought, planning, execution, and oversight.

Text from the electronic medical record could be used to auto-populate some fields, but this will likely require change in the way text is entered primarily so that it could be understood and sorted. Second, three-dimensional patient treatment images in a format that can be seamlessly integrated into a hospital's diagnostic imaging software (DICOM or DICOM-RT) should be acquired for archival and analytic purposes. We need tools that fuse images from planning and follow-up, measure target response in an automated or assisted fashion, and then record it. Third, we need sophisticated analytical tools to probe registry data in different ways using numerical or textual filters. Randomly selecting data from within a registry is one tool to reduce bias. Natural language processors could also work within this registry to suggest clinical follow-up or create predictive analytics on an individual case, based on interrogation of the entire data set. The future of big data research in medicine will rely on the integration of new database technology that can pool data from various sources, provide rapidly accessible analytics, and provide efficient mechanisms for data validation and maintenance of quality.

References

1. Berkowitz O, Kondziolka D, Bissonette D, Niranjan A, Kano H, Lunsford LD. The evolution of a clinical registry during 25 years of experience with Gamma Knife radiosurgery in Pittsburgh. Neurosurg Focus. 2013;34(1):E4.
2. Kondziolka D, Cooper BT, Lunsford LD, Silverman JS. Development, implementation and use of a local and global clinical registry for stereotactic radiosurgery. Big Data. 2015;3(2):80–9. https://doi.org/10.1089/big.2014.0069.
3. Sheehan JP, Grills I, Chiang V, Dong H, Berg A, Warnick R, Kondziolka D, Kavanaugh B. Quality of life outcomes for brain metastasis patients treated with stereotactic radiosurgery: pre-procedural predictive factors from a prospective national registry. J Neurosurg. 2018:1–7. https://doi.org/10.3171/2018.8.JNS181599.

4. McGirt MJ, Speroff T, Dittus RS, Harrell FE Jr, Asher AL. The National Neurosurgery Quality and Outcomes Database (N2QOD): general overview and pilot-year project description. Neurosurg Focus. 2013;34(1):E6.
5. Selden NR, Ghogawala Z, Harbaugh RE, Litvack ZN, McGirt MJ, Asher AL. The future of practice science: challenges and opportunities for neurosurgery. Neurosurg Focus. 2013;34(1):E8.
6. Kannel WB, Schwartz MJ, McNamara PM. Blood pressure and risk of coronary heart disease: the Framingham study. Dis Chest. 1969;56(1):43–52.
7. Clark RE. The Society of Thoracic Surgeons National Database status report. Ann Thorac Surg. 1994;57(1):20–6.
8. Torrens M, Chung C, Chung HT, Hanssens P, Jaffray D, Kemeny A, et al. Standardization of terminology in stereotactic radiosurgery: Report from the Standardization Committee of the International Leksell Gamma Knife Society: special topic. J Neurosurg. 2014;121 Suppl:2–15.
9. Shahian DM, Edwards F, Grover FL, Jacobs JP, Wright CD, Prager RL, et al. The Society of Thoracic Surgeons National Adult Cardiac Database: a continuing commitment to excellence. J Thorac Cardiovasc Surg. 2010;140(5):955–9.
10. Hassani H, Saporta G, Silva E. Data mining and official statistics: the past, present and future. Big Data. 2014;2(1):34–43.
11. Kondziolka D, Nawn D, Zimmerman B, Sochats K. Knowledge network for authoring, reviewing, editing, searching, and using scientific or other credible information. Disrupt Sci Technol. 2012;1(1):3–10.
12. Schell K, Puri C, Mahler P, Dukatz C. Teaching an old log new tricks with machine learning. Big Data. 2014;2(1):7–11.
13. Asher AL, McGirt MJ, Glassman SD, Groman R, Resnick DK, Mehrlich M, et al. Regulatory considerations for prospective patient care registries: lessons learned from the National Neurosurgery Quality and Outcomes Database. Neurosurg Focus. 2013;34(1):E5.
14. Dokholyan RS, Muhlbaier LH, Falletta JM, Jacobs JP, Shahian D, Haan CK, et al. Regulatory and ethical considerations for linking clinical and administrative databases. Am Heart J. 2009;157(6):971–82.
15. Oravec C, Motiwala M, Reed K, Kondziolka D, Barker FG, Michael LM, Klimo P. Big data research in neurosurgery: a critical look at this popular new study design. Neurosurgery. 2017;82:728–46.
16. Kestle JR. Administrative database research. J Neurosurg. 2015;122:441–2.
17. Sampson JH, Lad SP, Herndon JE 2nd, Starke RM, Kondziolka D. SEER insights. J Neurosurg. 2014;120:297–8.
18. Sarda S, Moore MK, Chern JJ. Letter to the editor: readmission and reoperation after shunt surgery. J Neurosurg Pediatr. 2015;15(5):544–5.
19. Brockmeyer D. Editorial: does it pass the sniff test? Mining the NSQIP-P database for neurosurgical diseases. J Neurosurg Pediatr. 2016;18(4):413–5.
20. So L, Beck CA, Brien S, et al. Chart documentation quality and its relationship to the validity of administrative data discharge records. Health Informatics J. 2010;16(2):101–13.
21. Amin BY, Tu TH, Schairer WW, et al. Pitfalls of calculating hospital readmission rates based on nonvalidated administrative data sets: presented at the 2012 Joint Spine Section Meeting: clinical article. J Neurosurg Spine. 2013;18:134–8.
22. Bohl DD, Russo GS, Basques BA, et al. Variations in data collection methods between national databases affect study results: a comparison of the nationwide inpatient sample and national surgical quality improvement program databases for lumbar spine fusion procedures. J Bone Joint Surg Am. 2014;96(23):e193.
23. Lawson EH, Louie R, Zingmond DS, Brook RH, Hall BL, Han L, Rapp M, Ko CY. A comparison of clinical registry versus administrative claims data for reporting of 30-day surgical complications. Ann Surg. 2012;256(6):973–81.
24. Grimes DA. Epidemiologic research with administrative databases: red herrings, false alarms and pseudoepidemics. Hum Reprod. 2015;30:1749–52.
25. Woodworth GF, Baird CJ, Garces-Ambrossi G, Tonascia J, Tamargo RJ. Inaccuracy of the administrative database: comparative analysis of two databases for the diagnosis and treatment of intracranial aneurysms. Neurosurgery. 2009;65:251–6.
26. Grimes DA. Epidemiologic research using administrative databases: garbage in, garbage out. Obstet Gynecol. 2010;116:1018–9.

Index

N. Pouratian, S. A. Sheth (eds.), *Stereotactic and Functional Neurosurgery*,
https://doi.org/10.1007/978-3-030-34906-6